ASSEMBLY OF THE PHOTOSYSTEM II MEMBRANE-PROTEIN COMPLEX OF OXYGENIC PHOTOSYNTHESIS

EDITED BY: Julian J. Eaton-Rye and Roman Sobotka

PUBLISHED IN: Frontiers in Plant Science

frontiers Research Topics

frontiers

ISSN 1664-8714
ISBN 978-2-88945-233-0
DOI 10.3389/978-2-88945-233-0

About Frontiers

Frontiers is more than just an open-access publisher of scholarly articles: it is a pioneering approach to the world of academia, radically improving the way scholarly research is managed. The grand vision of Frontiers is a world where all people have an equal opportunity to seek, share and generate knowledge. Frontiers provides immediate and permanent online open access to all its publications, but this alone is not enough to realize our grand goals.

Frontiers Journal Series

The Frontiers Journal Series is a multi-tier and interdisciplinary set of open-access, online journals, promising a paradigm shift from the current review, selection and dissemination processes in academic publishing. All Frontiers journals are driven by researchers for researchers; therefore, they constitute a service to the scholarly community. At the same time, the Frontiers Journal Series operates on a revolutionary invention, the tiered publishing system, initially addressing specific communities of scholars, and gradually climbing up to broader public understanding, thus serving the interests of the lay society, too.

Dedication to Quality

Each Frontiers article is a landmark of the highest quality, thanks to genuinely collaborative interactions between authors and review editors, who include some of the world's best academicians. Research must be certified by peers before entering a stream of knowledge that may eventually reach the public - and shape society; therefore, Frontiers only applies the most rigorous and unbiased reviews.
Frontiers revolutionizes research publishing by freely delivering the most outstanding research, evaluated with no bias from both the academic and social point of view.
By applying the most advanced information technologies, Frontiers is catapulting scholarly publishing into a new generation.

What are Frontiers Research Topics?

Frontiers Research Topics are very popular trademarks of the Frontiers Journals Series: they are collections of at least ten articles, all centered on a particular subject. With their unique mix of varied contributions from Original Research to Review Articles, Frontiers Research Topics unify the most influential researchers, the latest key findings and historical advances in a hot research area! Find out more on how to host your own Frontiers Research Topic or contribute to one as an author by contacting the Frontiers Editorial Office: **researchtopics@frontiersin.org**

ASSEMBLY OF THE PHOTOSYSTEM II MEMBRANE-PROTEIN COMPLEX OF OXYGENIC PHOTOSYNTHESIS

Topic Editors:
Julian J. Eaton-Rye, University of Otago, New Zealand
Roman Sobotka, Institute of Microbiology, Czech Academy of Sciences and University of South Bohemia, Czechia

Maple leaves.
Photo by Rémi Walle, Unsplash

Photosystem II is a 700-kDa membrane-protein super-complex responsible for the light-driven splitting of water in oxygenic photosynthesis. The photosystem is comprised of two 350-kDa complexes each made of 20 different polypeptides and over 80 co-factors. While there have been major advances in understanding the mature structure of this photosystem many key protein factors involved in the assembly of the complex do not appear in the holoenzyme. The mechanism for assembling this super-complex is a very active area of research with newly discovered

assembly factors and subcomplexes requiring characterization. Additionally the ability to split water is inseparable from light-induced photodamage that arises from radicals and reactive O_2 species generated by Photosystem II chemistry. Consequently, to sustain water splitting, a "self repair" cycle has evolved whereby damaged protein is removed and replaced so as to extend the working life of the complex. Understanding how the biogenesis and repair processes are coordinated is among several important questions that remain to be answered. Other questions include: how and when are the inorganic cofactors inserted during the assembly and repair processes and how are the subcomplexes protected from photodamage during assembly? Evidence has also been obtained for Photosystem II biogenesis centers in cyanobacteria but do these also exist in plants? Do the molecular mechanisms associated with Photosystem II assembly shed fresh light on the assembly of other major energy-transducing complexes such as Photosystem I or the cytochrome b_6/f complex or indeed other respiratory complexes? The contributions to this Frontiers in Plant Science Research Topic are likely to reveal new details applicable to the assembly of a range of membrane-protein complexes, including aspects of self-assembly and solar energy conversion that may be applied to artificial photosynthetic systems. In addition, a deeper understanding of Photosystem II assembly — particularly in response to changing environmental conditions — will provide new knowledge underpinning photosynthetic yields which may contribute to improved food production and long-term food security.

Citation: Eaton-Rye, J. J., Sobotka, R., eds. (2017). Assembly of the Photosystem II Membrane-Protein Complex of Oxygenic Photosynthesis. Lausanne: Frontiers Media. doi: 10.3389/978-2-88945-233-0

Table of Contents

07 ***Editorial: Assembly of the Photosystem II Membrane-Protein Complex of Oxygenic Photosynthesis***
Julian J. Eaton-Rye and Roman Sobotka

1. Evolutionary origins and photoactivation

11 ***Reconstructing the Origin of Oxygenic Photosynthesis: Do Assembly and Photoactivation Recapitulate Evolution?***
Tanai Cardona

27 ***Photoactivation: The Light-Driven Assembly of the Water Oxidation Complex of Photosystem II***
Han Bao and Robert L. Burnap

40 ***Structural Coupling of Extrinsic Proteins with the Oxygen-Evolving Center in Photosystem II***
Kentaro Ifuku and Takumi Noguchi

2. Pigment biosynthesis and lipids

51 ***Synthesis of Chlorophyll-Binding Proteins in a Fully Segregated Δ*ycf54 *Strain of the Cyanobacterium* Synechocystis *PCC 6803***
Sarah Hollingshead, Jana Kopečná, David R. Armstrong, Lenka Bučinská, Philip J. Jackson, Guangyu E. Chen, Mark J. Dickman, Michael P. Williamson, Roman Sobotka and C. Neil Hunter

66 ***Mutation of Gly195 of the ChlH Subunit of Mg-chelatase Reduces Chlorophyll and Further Disrupts PS II Assembly in a Ycf48-Deficient Strain of* Synechocystis *sp. PCC 6803***
Tim S. Crawford, Julian J. Eaton-Rye and Tina C. Summerfield

77 ***Carotenoids Assist in Cyanobacterial Photosystem II Assembly and Function***
Tomas Zakar, Hajnalka Laczko-Dobos, Tunde N. Toth and Zoltan Gombos

84 ***Multiple Impacts of Loss of Plastidic Phosphatidylglycerol Biosynthesis on Photosynthesis during Seedling Growth of Arabidopsis***
Koichi Kobayashi, Kaichiro Endo and Hajime Wada

3. Photosystem II assembly factors

96 ***Identification and Roles of Photosystem II Assembly, Stability, and Repair Factors in Arabidopsis***
Yan Lu

123 ***Functional Update of the Auxiliary Proteins PsbW, PsbY, HCF136, PsbN, TerC and ALB3 in Maintenance and Assembly of PSII***
Magdalena Plöchinger, Serena Schwenkert, Lotta von Sydow, Wolfgang P. Schröder and Jörg Meurer

136 ***The Role of Slr0151, a Tetratricopeptide Repeat Protein from* Synechocystis *sp. PCC 6803, during Photosystem II Assembly and Repair***
Anna Rast, Birgit Rengstl, Steffen Heinz, Andreas Klingl and Jörg Nickelsen

148 ***Photosystem II Repair and Plant Immunity: Lessons Learned from Arabidopsis Mutant Lacking the THYLAKOID LUMEN PROTEIN 18.3***
Sari Järvi, Janne Isojärvi, Saijaliisa Kangasjärvi, Jarkko Salojärvi, Fikret Mamedov, Marjaana Suorsa and Eva-Mari Aro

161 ***Critical Assessment of Protein Cross-Linking and Molecular Docking: An Updated Model for the Interaction Between Photosystem II and Psb27***
Kai U. Cormann, Madeline Möller and Marc M. Nowaczyk

4. Assembly and maintenance of Photosystem II

175 ***The Use of Advanced Mass Spectrometry to Dissect the Life-Cycle of Photosystem II***
Daniel A. Weisz, Michael L. Gross and Himadri B. Pakrasi

200 ***Testing the Role of the N-Terminal Tail of D1 in the Maintenance of Photosystem II in Tobacco Chloroplasts***
Franck Michoux, Niaz Ahmad, Zheng-Yi Wei, Erica Belgio, Alexander V. Ruban and Peter J. Nixon

209 ***Insights into the Cyanobacterial Deg/HtrA Proteases***
Otilia Cheregi, Raik Wagner and Christiane Funk

223 ***The RNA Structure of* cis*-acting Translational Elements of the Chloroplast* psbC *mRNA in* Chlamydomonas reinhardtii**
Mir Munir A. Rahim, Frederic Vigneault and William Zerges

236 ***The Roles of Cytochrome* b_{559} *in Assembly and Photoprotection of Photosystem II Revealed by Site-Directed Mutagenesis Studies***
Hsiu-An Chu and Yi-Fang Chiu

5. Environmental influences

243 ***Iron–Nutrient Interactions within Phytoplankton***
Hanan Schoffman, Hagar Lis, Yeala Shaked and Nir Keren

255 ***A Two-Component Regulatory System in Transcriptional Control of Photosystem Stoichiometry: Redox-Dependent and Sodium Ion-Dependent Phosphoryl Transfer from Cyanobacterial Histidine Kinase Hik2 to Response Regulators Rre1 and RppA***
Iskander M. Ibrahim, Sujith Puthiyaveetil and John F. Allen

267 ***Environmental pH and the Requirement for the Extrinsic Proteins of Photosystem II in the Function of Cyanobacterial Photosynthesis***
Jaz N. Morris, Julian J. Eaton-Rye and Tina C. Summerfield

275 ***Effect of Light Acclimation on the Organization of Photosystem II Super- and Sub-Complexes in* Arabidopsis thaliana**
Ludwik W. Bielczynski, Gert Schansker and Roberta Croce

6. Methodological and technical considerations

287 ***Photosystem II Assembly from Scratch***
Thilo Rühle and Dario Leister

292 ***Strain of Synechocystis PCC 6803 with Aberrant Assembly of Photosystem II Contains Tandem Duplication of a Large Chromosomal Region***
Martin Tichý, Martina Bečková, Jana Kopečná, Judith Noda, Roman Sobotka and Josef Komenda

302 ***Chloramphenicol Mediates Superoxide Production in Photosystem II and Enhances Its Photodamage in Isolated Membrane Particles***
Ateeq Ur Rehman, Sandeesha Kodru and Imre Vass

307 ***Isolation of Plant Photosystem II Complexes by Fractional Solubilization***
Patrycja Haniewicz, Davide Floris, Domenica Farci, Joanna Kirkpatrick, Maria C. Loi, Claudia Büchel, Matthias Bochtler and Dario Piano

frontiers in Plant Science

EDITORIAL
published: 26 May 2017
doi: 10.3389/fpls.2017.00884

Editorial: Assembly of the Photosystem II Membrane-Protein Complex of Oxygenic Photosynthesis

Julian J. Eaton-Rye[1]* *and Roman Sobotka*[2,3]

[1] Department of Biochemistry, University of Otago, Dunedin, New Zealand, [2] Laboratory of Photosynthesis, Center Algatech, Institute of Microbiology, Czech Academy of Sciences, Třeboň, Czechia, [3] Faculty of Science, University of South Bohemia, České Budějovice, Czechia

Keywords: ***Arabidopsis thaliana***, **cyanobacteria,** ***Chlamydomonas reinhardtii***, **biogenesis, photodamage, Photosystem II, photosynthesis,** ***Synechocystis*** **sp. PCC 6803**

Editorial on the Research Topic

Assembly of the Photosystem II Membrane-Protein Complex of Oxygenic Photosynthesis

OPEN ACCESS

Edited by:
Marinus Pilon,
Colorado State University,
United States

Reviewed by:
Marinus Pilon,
Colorado State University,
United States
Tanai Cardona,
Imperial College London,
United Kingdom

***Correspondence:**
Julian J. Eaton-Rye
julian.eaton-rye@otago.ac.nz

Specialty section:
This article was submitted to Plant Cell Biology, a section of the journal Frontiers in Plant Science

Received: *21 March 2017*
Accepted: *11 May 2017*
Published: *26 May 2017*

Citation:
Eaton-Rye JJ and Sobotka R (2017) Editorial: Assembly of the Photosystem II Membrane-Protein Complex of Oxygenic Photosynthesis. Front. Plant Sci. 8:884. doi: 10.3389/fpls.2017.00884

Photosystem II (PS II) catalyses the light-driven splitting of water at the start of the photosynthetic electron transport chain found in the thylakoid membranes of plants, algae and cyanobacteria (Barber, 2016; Vinyard and Brudvig, 2017). The mature photosystem is dimeric and able to form super-complexes with a range of pigment-binding antenna proteins found across the different phyla (Shen, 2015; Ago et al., 2016; Wei et al., 2016). The highest resolution X-ray-derived crystal structure of PS II is from the thermophilic cyanobacterium *Thermosynechococcus vulcanus* where each monomer is composed of 20 protein subunits and more than 80 cofactors as well as over a 1,000 bound water molecules (Umena et al., 2011; Suga et al., 2015). The precise arrangement of redox co-factors, pigments and other organic and inorganic co-factors is the product of multiple ordered processes requiring spatial and temporal coordination and the participation of numerous protein assembly factors (Nickelsen and Rengstl, 2013).

In this Frontiers Research Topic 25 articles have been collected under six different sections addressing different aspects of PS II assembly. The first section contains three contributions covering the **Evolutionary origins and photoactivation** of PS II. The first of these by Cardona considers the origin of the PS II reaction center D1 and D2 proteins that bind the majority of the PS II redox active cofactors, he also considers afresh the origin of the two chlorophyll-binding proximal antenna proteins, CP43 and CP47 as well as the origins of the additional membrane-spanning low-molecular-weight subunits of the photosystem. Finally this first article considers the events leading to the origin of the Mn_4CaO_5 cluster of the oxygen-evolving complex that catalyzes water splitting. An in-depth treatment of the assembly of the Mn_4CaO_5 cluster then follows in the review by Bao and Burnap and the final article in this section by Ifuku and Noguchi discusses the roles of the lumenal PS II subunits that provide a proteinaceous cap for the oxygen-evolving complex.

Each PS II monomer contains 35 chlorophylls, two pheophytins, 11 β-carotenes as well as over 20 lipids (Umena et al., 2011). So far, however, it is not clear how the synthesis of potentially phototoxic chlorophyll molecules is coordinated with the synthesis of chlorophyll-binding PS II subunits. A mechanistic explanation of pigment insertion into PS II proteins is also not available. Section 2 of the topic, **Pigment biosynthesis and lipids**, includes examples of how chlorophyll synthesis and the presence of other pigments and lipids are integral to the ordered assembly of PS II centers. The report by Hollingshead et al. establishes that restricting *de novo* chlorophyll

biosynthesis, in this case by modulating Mg-protoporphyrin IX methyl ester cyclase activity, affects synthesis of the PS II subunits CP43 and CP47 along with Photosystem I (PS I) but no other chlorophyll-containing proteins, including D1 and D2. A similar alteration in chlorophyll production was achieved by Crawford et al. who introduced a targeted mutation into Mg-chelatase, the enzyme responsible for the first-committed step of chlorophyll biosynthesis. Crawford et al. found that restricting chlorophyll availability in a cyanobacterial strain lacking the Ycf48 assembly factor increased the severity of removing this protein. The results of Hollingshead et al. and Crawford and colleagues indicate a different mode of chlorophyll loading into the D1 and D2 subunits than into other chlorophyll-binding proteins and suggest a role for assembly factors in chlorophyll insertion or turnover. Also in section 2, Zakar et al. review the different roles of carotenes and xanthophylls in cyanobacterial PS II assembly and function and finally the report by Kobayashi et al. concludes this section by showing that plastidic phosphatidylglycerol is required for PS II function in *Arabidopsis thaliana*. It is known that the absence of this lipid in cyanobacterial thylakoids affects electron transfer between Q_A and Q_B, the primary and secondary quinone electron acceptors of PS II, respectively (Gombos et al., 2002). Interestingly, Kobayashi et al. demonstrate that the absence of phosphatidylglycerol in *A. thaliana* also disrupts energy transfer from the antenna to PS II and increases the susceptibility of PS II to photodamage induced by red light.

To date over 30 polypeptides have been identified as PS II assembly factors that participate in biogenesis but are not present in the mature complex. These include kinases, phosphatases, transporters and proteases in addition to those acting as chaperones (Järvi et al., 2015). Currently, an explanation of the exact function of any of these factors in the PSII-assembling machinery is missing and undoubtedly many more factors remain to be discovered (Nickelsen and Rengstl, 2013). In the section **Photosystem II assembly factors**, the review by Lu considers the molecular functions of the many proteins that influence PS II assembly and its repair following photodamage in *A. thaliana*. The next article by Plochinger et al. focuses on the PsbW, PsbY, HCF136, PsbN, TerC, and ALB3 proteins, although among these proteins, PsbY is, in fact, present in the final holoenzyme (Shen, 2015). How thylakoid membrane biogenesis and PS II assembly processes are coordinated is also an area of keen interest (Nickelsen et al., 2011). The report by Rast et al. addresses this topic by investigating the function of the Slr0151 tetratricopeptide repeat protein on thylakoid ultrastructure during PS II assembly and repair in the cyanobacterium *Synechocystis* sp. PCC 6803. Adding to the complexity of PS II assembly are examples where assembly factors appear to have more than one role. The thylakoid lumenal protein TLP18.3 (Psb32 in cyanobacteria) has been shown to influence the repair cycle (Sirpiö et al., 2007) but when Järvi et al. investigated the function of TLP18.3 during fluctuating light in *A. thaliana*, the absence of this protein disrupted expression of genes involved in plant defense processes such that *tlp18.3* plants exhibited stunted growth. The Psb27 protein may also have a dual role influencing biogenesis of both PS I and PS II, although its major contribution appears to be on PS II assembly (Komenda et al., 2012a). The report by Cormann et al. presents new data supporting an interaction of Psb27 with CP43 [as reported by Komenda et al. (2012a) and Liu et al. (2011)] as well as interactions with CP47 and the C-termini of both D1 and D2. The results of Cormann et al. suggest a binding site for Psb27 that is occupied by the lumenal PsbV protein in the mature complex of cyanobacterial PS II.

The existence of two distinct assembly pathways: *de novo* biogenesis and the specialized cycle to repair photodamaged photosystems, is a unique property of PS II (Mulo et al., 2012). Photodamage is an inevitable consequence of the oxidative chemistry of water splitting and is chiefly caused by reactive oxygen species generated both by electron transfer and energy transfer processes (Vass, 2012). The location of these pathways within the thylakoid membrane system and extent to which they may share intermediate complexes, as well as auxiliary assembly factors, remains to be established but may in fact differ between cyanobacteria and algae and potentially between lower and higher plants (Komenda et al., 2012b). Section 4 contains several papers dealing with the **Assembly and maintenance of Photosystem II**. Weisz et al. review recent developments in mass spectrometry that are increasingly contributing to the characterization of the individual PS II sub-complexes that participate in assembly and turnover during biogenesis, photodamage and repair. Michoux et al. analyze the impact of truncating the N-terminal tail of the D1 protein in tobacco. This truncation led to the loss of PS II super-complexes and dimeric complexes in the thylakoid membrane but unlike *Synechocystis* sp. PCC 6803, where the N-terminus of D1 has been shown to be involved in the degradation of photodamaged PS II by FtsH complexes (Komenda et al., 2007), the data from Michoux et al. indicate that tobacco has additional compensatory pathways for regulating D1 turnover when the N-terminus of D1 is removed. It is also known that the Deg1 protease is involved in the repair cycle in *A. thaliana* [for a mechanism see (Kley et al., 2011)] and the paper by Cheregi et al. provides a perspective on the roles of Deg/HtrA proteases in cyanobacteria. A number of assembly factors participate in assembly steps directly or in concert with transcriptional or translational control. In eukaryotes, nuclear factors are required in the regulation of gene expression for plastid-encoded PS II proteins. Working with *Chlamydomonas reinhardtii,* Munir et al. report the role of the nuclear gene *TBC1* in regulating the plastid *psbC* gene that encodes CP43.

Absorption of photons by intermediate pre-assembly complexes is likely to impair biogenesis via the production of reactive oxygen species. This is an important topic that has not yet received the full attention it deserves. It has long been recognized, however, that cytochrome b_{559}, an essential component of the PS II reaction center, may function in a protective side branch pathway for electron transport (Rutherford et al., 2012). The last contribution in this section is a mini review by Chu and Chiu focused on the roles of this cytochrome in PS II assembly and photoprotection.

A broad spectrum of environmental factors influence biogenesis and turnover of PS II and four examples are presented in section 5, **Environmental influences**. In the first contribution, Schoffman et al. review the impact of iron on the availability of several macro and micro nutrients utilized in energy transduction and biochemical catalysis in phytoplankton. On a different tack, both chloroplasts and mitochondria retain genomes encoding certain proteins belonging to bioenergetic protein complexes (Allen and Martin, 2016). The chloroplast sensor kinase CSK in *A. thaliana* has been shown to regulate plastid gene expression in response to the redox status of the electron transport chain (Puthiyaveetil et al., 2008). In the report by Ibrahim et al. the cyanobacterial homolog of CSK is shown to exhibit redox dependent, and Na^+ ion dependent, phosphoryl group transfer to two response regulators and this pathway is proposed to control photosystem stoichiometry. Environmental factors other than light may impact on PS II performance by influencing the thylakoid lumen. It has been observed that several cyanobacterial mutants lacking different combinations of extrinsic PS II proteins are not photoautotrophic at pH 7.5 and their PS II assembly is impaired; however, the cells are photoautotrophic at pH 10 (Summerfield et al., 2013). The perspective provided by Morris et al. discusses possible mechanisms for coupling the environmental pH to the regulation of PS II assembly and activity in mutants lacking specific PS II lumenal proteins. Finally in this section, Bielczynski et al. report the effect of high light on antenna organization and show that acclimation to high light in *A. thaliana* results in a reduction in functional antenna size that exceeds the actual reduction of antenna proteins. In addition, the authors observed an increase in light-harvesting complex II (LHCII) monomers in plants acclimated to high light but they did not observe a corresponding change in the LHCII trimer to monomer ratio during short exposures to light stress.

The final section of this Research Topic has been reserved for papers offering **Methodological and technical considerations**. In the opening opinion piece of this section Rühle and Leister argue for a synthetic biological approach to building PS II using a cyanobacterial chassis that could identify the minimal suite of proteins to assemble a functional photosystem. The research report by Tichý et al. highlights the genome flexibility of *Synechocystis* sp. PCC 6803 during laboratory cultivation and demonstrates that even large chromosomal rearrangements are possible. This study shows that it is essential to establish that the correct control strain is being compared to when analyzing cyanobacterial mutants. In the perspective from Rehman et al. the authors demonstrate that the antibioitic chloramphenicol can accept electrons from PS II and transfer them to oxygen giving rise to superoxide production. Chloramphenicol has been widely used in photodamage studies to separate effects on the rate of damage from effects on recovery due to protein synthesis. This study therefore suggests that caution must be exercised when interpreting photodamage studies in the presence of chloramphenicol. The final contribution by Haniewicz et al. presents a protocol for isolating different PS II populations in thylakoid membranes from tobacco and emphasizes the ability to obtain high yields of PS II-LHCII super-complexes.

CONCLUDING COMMENT

Oxygenic photosynthesis first evolved ∼3 billion years ago resulting in the transition from an anaerobic to an aerobic atmosphere (Lyons et al., 2014). This led to the protective ozone layer and the advent of aerobic respiration that paved the way for the formation and success of the eukaryotic cell (Martin et al., 2015). The chemistry of PS II is therefore responsible for almost all of our planet's biodiversity; however, as noted above, this fundamental process comes with a cost. The oxidative chemistry of water splitting inescapably produces reactive oxygen species and radicals that damage PS II and require the photosynthetic machinery to be continually renewed (Vass, 2012; Nishiyama and Murata, 2014). As the examples in this Research Topic show, in addition to *de novo* biogenesis, PS II possesses a self-healing cycle leading to the rate of repair keeping pace with the rate of light-induced photodamage. Environmental conditions, such as extreme temperatures or excessive light levels, can tip the balance such that repair cannot keep up with damage leading to reduced photosynthetic yields (Murata et al., 2007). A deeper understanding of how plants repair PS II to prolong the lifetime of the enzyme will provide new approaches to the design of hardier crop plants. Alongside this, studies of PS II biogenesis will deepen our understanding of how the catalytic oxygen-evolving center is assembled and provide novel insight into the origin and evolution of oxygenic photosynthesis. These avenues of research will also inform the design of biomimetic systems for the production of hydrogen fuel and electrons from water (Blankenship et al., 2011; Najafpour et al., 2016). Current projections of population growth indicate we will reach 8.5 billion by 2,030 and exceed 11 billion by 2,100 (United Nations, 2015). Research into the assembly of PS II will directly contribute to our food and energy security and benefit these future generations.

AUTHOR CONTRIBUTIONS

JE initiated this research topic. For the editorial both authors reviewed all Research Topic articles. JE wrote the first draft and JE and RS revised and prepared the final version. Both authors approved it for publication.

ACKNOWLEDGMENTS

This work was made possible by funding from the Department of Biochemistry, Otago University to JE, RS was supported by the projects Algatech-Plus (MSMT LO1416) and Algamic (CZ 1.05/2.1.00/19.0392) provided by the Czech Ministry of Education, Youth and Sport.

REFERENCES

Ago, H., Adachi, H., Umena, Y., Tashiro, T., Kawakami, K., Kamiya, N., et al. (2016). Novel features of eukaryotic Photosystem II revealed by its crystal structure analysis from a red alga. *J. Biol. Chem.* 291, 5676–5687. doi: 10.1074/jbc.M115.711689

Allen, J. F., and Martin, W. F. (2016). Why have organelles retained genomes? *Cell Systems* 2, 71–72. doi: 10.1016/j.cels.2016.02.007

Barber, J. (2016). Photosystem II: the water splitting enzyme of photosynthesis and the origin of oxygen in our atmosphere. *Q. Rev. Biophys.* 49:e14. doi: 10.1017/s0033583516000123

Blankenship, R. E., Tiede, D. M., Barber, J., Brudvig, G. W., Fleming, G., Ghirardi, M., et al. (2011). Comparing photosynthetic and photovoltaic efficiencies and recognizing the potential for improvement. *Science* 332, 805–808. doi: 10.1126/science.1200165

Gombos, Z., Varkonyi, V., Hagio, M., Iwaki, M., Kovács, L., Masamoto, K., et al. (2002). Phosphatidylglycerol requirement for the function of electron acceptor QB in the Photosystem II reaction center. *Biochemistry* 41, 3796–3802. doi: 10.1021/bi011884h

Järvi, S., Suorsa, M., and Aro, E.-M. (2015). Photosystem II repair in plant chloroplasts—regulation, assisting proteins and shared components with Photosystem II biogenesis. *Biochim. Biophys. Acta* 1847, 900–909. doi: 10.1016/j.bbabio.2015.01.006

Kley, J., Schmidt, B., Boyanov, B., Stolt-Bergner, P. C., Kirk, R., Ehrmann, M., et al. (2011). Structural adaptation of the plant protease Deg1 to repair Photosystem II during light exposure. *Nat. Struct. Mol. Biol.* 18, 728–731. doi: 10.1038/nsmb.2055

Komenda, J., Knoppová, J., Kopečná, J., Sobotka, R., Halada, P., Yu, J., et al. (2012a). The Psb27 assembly factor binds to the CP43 complex of Photosystem II in the cyanobacterium Synechocystis sp. PCC 6803. *Plant Physiol.* 158, 476–486. doi: 10.1104/pp.111.184184

Komenda, J., Sobotka, R., and Nixon, P. J. (2012b). Assembling and maintaining the Photosystem II complex in chloroplasts and cyanobacteria. *Curr. Opin. Plant Biol.* 15, 245–251. doi: 10.1016/j.pbi.2012.01.017

Komenda, J., Tichy, M., Prášil, O., Knoppová, J., Kuviková, S., de Vries, R., et al. (2007). The exposed N-terminal tail of the D1 subunit is required for rapid D1 degradation during Photosystem II repair in Synechocystis sp. PCC 6803. *Plant Cell* 19, 2839–2854. doi: 10.1105/tpc.107.053868

Liu, H., Huang, R. Y.-C., Chen, J., Gross, M. L., and Pakrasi, H. B. (2011). Psb27, a transiently associated protein, binds to the chlorophyll binding protein CP43 in Photosystem II assembly intermediates. *Proc. Natl. Acad. Sci. U.S.A.* 108, 18536–18541. doi: 10.1073/pnas.1111597108

Lyons, T. W., Reinhard, C. T., and Planavsky, N. J. (2014). The rise of oxygen in Earth's early ocean and atmosphere. *Nature* 506, 307–315. doi: 10.1038/nature13068

Martin, W. F., Garg, S., and Zimorski, V. (2015). Endosymbiotic theories for eukaryotic origin. *Phil. Trans. R. Soc. B* 370:20140330. doi: 10.1098/rstb.2014.0330

Mulo, P., Sakurai, I., and Aro, E.-M. (2012). Strategies for psbA gene expression in cyanobacteria, green algae and higher plants: from transcription to PSII repair. *Biochim. Biophys. Acta* 1817, 247–257. doi: 10.1016/j.bbabio.2011.04.011

Murata, N., Takahashi, S., Nishiyama, Y., and Allakhversiev, S. I. (2007). Photoinhibition of Photosystem II under environmental stress. *Biochim. Biophys. Acta* 1767, 414–421. doi: 10.1016/j.bbabio.2006.11.019

Najafpour, M. M., Renger, G., Holyńska, M., Moghaddam, A. N., Aro, E.-M., Carpentier, R., et al. (2016). Manganese compounds as water-oxidizing catalysts: From the natural water-oxidizing complex to nanosized manganese oxide structures. *Chem. Rev.* 116, 2886–2936. doi: 10.1021/acs.chemrev.5b00340

Nickelsen, J., and Rengstl, B. (2013). Photosystem II assembly: from cyanobacteria to plants. *Annu. Rev. Plant Biol.* 64, 609–635. doi: 10.1146/annurev-arplant-050312-120124

Nickelsen, J., Rengstl, B., Stengel, A., Schottkowski, M., Soll, J., and Ankele, E. (2011). Biogenesis of the cyanobacterial thylakoid membrane system—an update. *FEMS Microbiol. Lett.* 315, 1–5. doi: 10.1111/j.1574-6968.2010.02096.x

Nishiyama, Y., and Murata, N. (2014). Revised scheme for the mechanism of photoinhibition and its application to enhance the abiotic stress tolerance of the photosynthetic machinery. *Appl. Microbiol. Biotechnol.* 98, 8777–8796. doi: 10.1007/s00253-014-6020-0

Puthiyaveetil, S., Kavanagh, T. A., Cain, P., Sullivan, J. A., Newell, C. A., Gray, J. C., et al. (2008). The ancestral symbiont sensor kinase CSK links photosynthesis with gene expression in chloroplasts. *Proc. Natl. Acad. Sci. U.S.A.* 105, 10061–10066. doi: 10.1073/pnas.0803928105

Rutherford, A. W., Osyczka, A., and Rappaport, F. (2012). Back-reactions, short-circuits, leaks and other energy wasteful reactions in biological electron transfer: Redox tuning to survive life in O2. *FEBS Lett.* 586, 603–616. doi: 10.1016/j.febslet.2011.12.039

Shen, J.-R. (2015). The structure of Photosystem, II, and the mechanism of water oxidation in photosynthesis. *Annu. Rev. Plant Biol.* 66, 23–48. doi: 10.1146/annurev-arplant-050312-120129

Sirpiö, S., Allahverdiyeva, Y., Suorsa, M., Paakkarinen, V., Vainonen, J., Battchikova, N., et al. (2007). TLP18.3, a novel thylakoid lumen protein regulating photosystem II repair cycle. *Biochem. J.* 406, 415–425. doi: 10.1042/BJ20070460

Suga, M., Akita, F., Hirata, K., Ueno, G., Murakami, H., Nakajima, Y., et al. (2015). Native structure of Photosystem II at 1.95 Å resolution viewed by femtosecond X-ray pulses. *Nature* 517, 99–103. doi: 10.1038/nature13991

Summerfield, T. C., Crawford, T. S., Young, R. D., Chua, J. P. S., Macdonald, R. L., Sherman, L. A., et al. (2013). Environmental pH affects photoautotrophic growth of Synechocystis sp. PCC 6803 strains carrying mutations in the lumenal proteins of PSII. *Plant Cell Physiol.* 54, 859–874. doi: 10.1093/pcp/pct036

Umena, Y., Kawakami, K., Shen, J.-R., and Kamiya, N. (2011). Crystal structure of oxygen-evolving Photosystem II at a resolution of 1.9 Å. *Nature* 473, 55–60. doi: 10.1038/nature09913

United Nations (2015). *World Population Prospects: The 2015 Revision, Key Findings and Advance Tables. Department of Economic and Social Affairs, Population Division*, Working paper No. ESA/P/WP.241, United Nations.

Vass, I. (2012). Molecular mechanisms of photodamage in the photosystem II complex. *Biochim. Biophys. Acta* 1817, 209–217. doi: 10.1016/j.bbabio.2011.04.014

Vinyard, D. J., and Brudvig, G. W. (2017). Progress towards a molecular mechanism of water oxidation in Photosystem, II. *Annu. Rev. Phys. Chem.* 68, 101–116. doi: 10.1146/annurev-physchem-052516-044820

Wei, X., Su, X., Cao, P., Liu, X., Chang, W., Li, M., et al. (2016). Spinach Photosystem II-LHCII supercomplex at 3.2 Å resolution. *Nature* 534, 69–74. doi: 10.1038/nature18020

Conflict of Interest Statement: The authors declare that the research was conducted in the absence of any commercial or financial relationships that could be construed as a potential conflict of interest.

frontiers in Plant Science

HYPOTHESIS AND THEORY
published: 02 March 2016
doi: 10.3389/fpls.2016.00257

Reconstructing the Origin of Oxygenic Photosynthesis: Do Assembly and Photoactivation Recapitulate Evolution?

Tanai Cardona *

Department of Life Sciences, Imperial College London, London, UK

Due to the great abundance of genomes and protein structures that today span a broad diversity of organisms, now more than ever before, it is possible to reconstruct the molecular evolution of protein complexes at an incredible level of detail. Here, I recount the story of oxygenic photosynthesis or how an ancestral reaction center was transformed into a sophisticated photochemical machine capable of water oxidation. First, I review the evolution of all reaction center proteins in order to highlight that Photosystem II and Photosystem I, today only found in the phylum Cyanobacteria, branched out very early in the history of photosynthesis. Therefore, it is very unlikely that they were acquired via horizontal gene transfer from any of the described phyla of anoxygenic phototrophic bacteria. Second, I present a new evolutionary scenario for the origin of the CP43 and CP47 antenna of Photosystem II. I suggest that the antenna proteins originated from the remodeling of an entire Type I reaction center protein and not from the partial gene duplication of a Type I reaction center gene. Third, I highlight how Photosystem II and Photosystem I reaction center proteins interact with small peripheral subunits in remarkably similar patterns and hypothesize that some of this complexity may be traced back to the most ancestral reaction center. Fourth, I outline the sequence of events that led to the origin of the Mn_4CaO_5 cluster and show that the most ancestral Type II reaction center had some of the basic structural components that would become essential in the coordination of the water-oxidizing complex. Finally, I collect all these ideas, starting at the origin of the first reaction center proteins and ending with the emergence of the water-oxidizing cluster, to hypothesize that the complex and well-organized process of assembly and photoactivation of Photosystem II recapitulate evolutionary transitions in the path to oxygenic photosynthesis.

Keywords: oxygenic photosynthesis, anoxygenic photosynthesis, photosystem, reaction center, water oxidation, photoactivation, photoassembly

OPEN ACCESS

Edited by:
Julian Eaton-Rye, University of Otago, New Zealand

Reviewed by:
Anthony William Larkum, University of Technology, Sydney, Australia
Martin Hohmann-Marriott, Norwegian University of Science and Technology, Norway

***Correspondence:**
Tanai Cardona
t.cardona@imperial.ac.uk

Specialty section:
This article was submitted to Plant Cell Biology, a section of the journal Frontiers in Plant Science

Received: *13 November 2015*
Accepted: *16 February 2016*
Published: *02 March 2016*

Citation:
Cardona T (2016) Reconstructing the Origin of Oxygenic Photosynthesis: Do Assembly and Photoactivation Recapitulate Evolution? Front. Plant Sci. 7:257. doi: 10.3389/fpls.2016.00257

EVOLUTION OF REACTION CENTER PROTEINS

Photochemical reaction centers are thought to have originated only once in the domain Bacteria. This is because currently there are no described strains in the domain Archaea with photosynthesis based on protein complexes containing chlorophyll or bacteriochlorophyll (Hohmann-Marriott and Blankenship, 2011). At the other end of the tree of life, eukaryotic algae and plants obtained

photosynthesis via endosymbiosis of Cyanobacteria (Gould et al., 2008; Parfrey et al., 2010). Within Bacteria, there are currently seven phyla known to have strains with reaction centers, these are: Cyanobacteria, Chloroflexi, Firmicutes, Chlorobi, Proteobacteria, and those recently found in Acidobacteria (Bryant et al., 2007; Tsukatani et al., 2012) and Gemmatimonadetes (Zeng et al., 2014, 2015). Just a while ago, it was suggested that the phylum Actinobacteria might have been ancestrally capable of photosynthesis (Gupta and Khadka, 2016), as some strains in this phylum seem to have a vestigial chlorophyll synthesis pathway. Although a consensus on the type of bacteria in which photochemical reaction centers originated is lacking, it is understood that both Type I and Type II reaction centers have a common origin. This conclusion is supported by the structural similarities of the core proteins, the relative positions of the pigments in the reaction center, and commonalities in the first photochemical steps during charge separation (Olson and Pierson, 1987; Nitschke and Rutherford, 1991; Cardona et al., 2012; Cardona, 2015). Furthermore, it is also clear that oxygenic photosynthesis originated in a lineage of bacteria that was ancestral to the phylum Cyanobacteria (Cardona et al., 2015), as Photosystem II is exclusively found within members of this group and was only transferred to photosynthetic eukaryotes at a later stage.

The story of photosynthesis began early in the history of life. When exactly? It is not yet known with certainty. Organic carbon found in rocks 3.8 billion years old has some signatures of possible photoautotrophy (Rosing, 1999; Nisbet and Fowler, 2014). It is generally accepted that photosynthesis was well established from at least 3.5 billion years ago (Butterfield, 2015; Knoll, 2015). Evidence is growing for a redox-stratified ocean 3.2–3.0 billion years ago, suggestive of some oxygenic photosynthesis (Crowe et al., 2013; Planavsky et al., 2014; Satkoski et al., 2015) and it is likely that Cyanobacteria were already flourishing around the Great Oxygenation Event 2.4 billion years ago (Lyons et al., 2014). But, is the molecular evolution of the photochemical machinery consistent with the geochemical record? Could photochemical reaction centers and chlorophyll synthesis have emerged as early as 3.8 billion years ago? And if they did, what does it imply for the earliest forms of life? Could the water-oxidizing complex of Photosystem II have really appeared already 3.2 billion years ago?

Based on functional and structural homology, and in combination with phylogenetic analysis, it is possible to deduce several stages in the history of photosynthesis with reasonable confidence. I will introduce now a slightly unconventional notation that will facilitate the accurate description of these evolutionary stages (**Figure 1**); or simply put, I will give names to key ancestral reaction center proteins. This will help to highlight the correct position of Photosystem II within the entire diversity of reaction center proteins. Nevertheless, I will only and exclusively use this notation to refer to evolutionary transitions.

All reaction center proteins have a common origin (Olson, 1981; Nitschke and Rutherford, 1991; Sadekar et al., 2006; Cardona, 2015). This means that the evolutionary history of all reaction center proteins can be traced back to a single ancestral protein at the dawn of photosynthesis. I will refer to this primordial reaction center protein as **A** in **Figure 1**. It is worth noting here that the appearance of the first reaction center capable of photochemistry and made of protein **A** already implies a long and complex evolutionary process. This is because the earliest evolutionary stages required the origin of a complete pathway for pigment synthesis coupled to the emergence of the first reaction center protein that could be assembled into a functional photochemical machine. At a later stage and driven by as yet unknown evolutionary pressures, the ancestral reaction center diverged into two new forms. One form was ancestral to all Type I reaction centers and a second form was ancestral to all Type II reaction centers.

All Type I reaction center proteins share among each other significantly more sequence and structural homology than with any Type II protein. In other words, they share a more recent common ancestor with each other than with any Type II. The same is true the other way around, all Type II reaction center proteins share among each other significantly more sequence and structural homology than with any Type I protein, so they descended from a common Type II ancestral protein. I will refer to the ancestral Type I reaction center as $\mathbf{I_1}$ and the ancestral Type II reaction center as $\mathbf{II_1}$(**Figure 1**). The subscript indicates that they are one transitional step away from **A**. This "transitional step" may represent a gene duplication event, horizontal gene transfer within ancestral populations of bacteria, or speciation. The evolutionary path from the primordial reaction center to the ancestral forms of Type I and Type II reaction centers was also very complex; very drastic genetic and structural rearrangements are required to explain their current differences. However, a detailed description of these changes is outside the scope of the present paper, but I have discussed some of these before (Cardona, 2015 and reference therein). In here, it should suffice to say that an ancestral reaction center, by some mechanism, gave rise to two new types. At this point it is tempting to ask: was the primordial protein **A**, Type I or Type II? This question is perhaps unanswerable. But a better question to ask is, what traits present in Type I and Type II reaction centers today were also present in the most ancestral reaction center? I will highlight a few of these conserved traits between the two types throughout the text below.

The early divergence of Type I and Type II reaction center is clear from sequence and structural comparisons; see Sadekar et al. (2006) for example. This straight-forward, often overlooked, early divergence of reaction center types helps solve one of the longest-standing questions on the origin of photosynthesis. In which of the groups of phototrophic bacteria did photosynthesis first evolve? Did it evolve in the phylum Chlorobi or Chloroflexi, or within the Heliobacteriaceae family of Firmicutes, or perhaps in Cyanobacteria? The answer is: none of them. This is because the known groups of phototrophs are crown groups and none of them carry the ancestral protein **A**, nor $\mathbf{I_1}$, nor $\mathbf{II_1}$. The groups of bacteria that carried these ancestral proteins belong to stem groups, very likely no longer part of the current biodiversity and extinct for several billion years.

At a later stage, protein $\mathbf{II_1}$ diverged into two new distinct reaction center proteins: I will refer to these as $\mathbf{D0_2}$ and $\mathbf{K_2}$. $\mathbf{D0_2}$ is ancestral to both D1 and D2, the core subunits of Photosystem II found only in the phylum Cyanobacteria. $\mathbf{K_2}$ is ancestral to

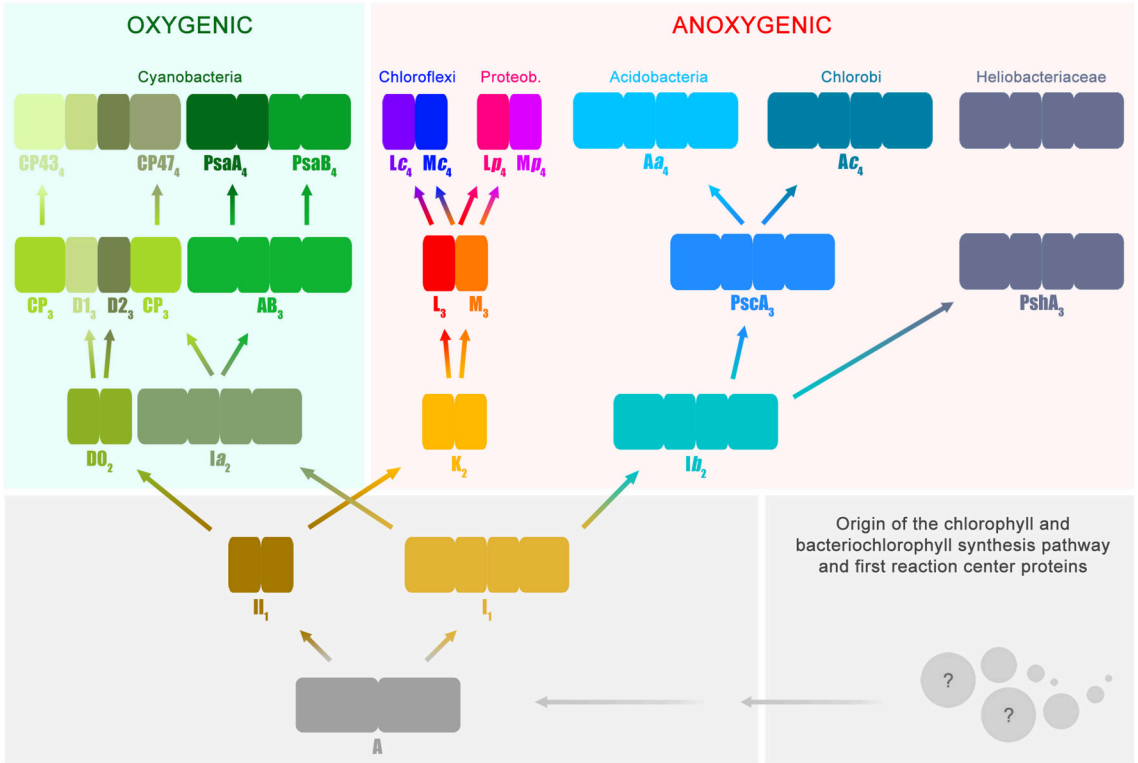

FIGURE 1 | Evolutionary relations of reaction center proteins. This scheme is based on the well-known phylogenetic relationships of reaction center proteins, which I have reviewed in detail before (Cardona, 2015). At the bottom right, the spheres with question marks represent the earliest evolutionary events that led to the evolution of the chlorophyll and bacteriochlorophyll synthesis pathway and the first reaction center proteins. It has been suggested that reaction center proteins might have originated from single-helix pigment-binding proteins (Allen and Vermaas, 2010) or from proteins related to the respiratory Cytochrome *b* proteins (Xiong and Bauer, 2002). Both hypotheses merit further consideration. The ancestral reaction center protein **A** gave rise to two new classes of proteins ancestral to Type I ($\mathbf{I_1}$) and II ($\mathbf{II_1}$), respectively. It is highly likely that these early stages of reaction center evolution occurred at a time well before the radiation of modern bacterial forms. Therefore, it is difficult to envision the mechanisms by which the ancestral reaction center evolved into two new forms and the evolutionary forces that aided such divergence. The subscript indicates transitional stages away from ancestral protein **A**. Both $\mathbf{I_1}$ and $\mathbf{II_1}$ separated into two new classes of proteins, one lineage led to the evolution of Photosystem I and II, employed in oxygenic photosynthesis and today only found in the phylum Cyanobacteria and photosynthetic eukaryotes. The other lineage led to the type of reaction center proteins employed by anoxygenic phototrophic bacteria. Type I reaction centers (longer rectangles) are characterized by having 11 transmembrane helices: the first 6 helices are the antenna domain in charge of light harvesting and the last 5 helices are the reaction center domain in charge of photochemistry. In Type II reaction centers (smaller rectangles) the first 6 helices are missing, and only the reaction center domain is found, the last 5 helices. Photosystem II is unique because it is associated with antenna proteins, the CP43 and CP47 subunits, which originated from a Type I reaction center. The nature of the ancestral reaction center protein **A** is uncertain, was it more like a Type I or Type II reaction center? Did it have an iron-sulfur cluster or a non-heme iron? Did it have an antenna domain or was this fused later with a reaction center protein to make the first Type I reaction centers? At the moment, from the existing structural and sequence data, it is not possible to answer these questions with certainty. Reaction center **A** probably had some traits from each reaction center type and also some unique traits no longer present in reaction center proteins today.

both L and M, the core subunits of anoxygenic Type II reaction centers. Using the subscript to denote the transitional stages away from the primordial protein **A**, then D1 and D2 are equivalent to $\mathbf{D1_3}$ and $\mathbf{D2_3}$, because they are predated consecutively by $\mathbf{D0_2}$, $\mathbf{II_1}$, and **A**. Similarly, the ancestral L and M are equivalent to $\mathbf{L_3}$ and $\mathbf{M_3}$. However, unlike D1 and D2, L and M undergo another evolutionary transition. As two new phyla of bacteria containing an anoxygenic Type II reaction center appeared, the phylum Chloroflexi and the phylum Proteobacteria, L and M diverged. Therefore, the L and M found in phototrophic members of the phylum Chloroflexi form a well-defined subgroup and the L and M found in phototrophic members of the phylum Proteobacteria form a different subgroup (Deisenhofer et al., 1984; Ovchinnikov et al., 1988a,b; Beanland, 1990; Cardona, 2015). I will thus refer to the set found in Chloroflexi as $\mathbf{Lc_4}$ and $\mathbf{Mc_4}$ and to the set found in Proteobacteria as $\mathbf{Lp_4}$ and $\mathbf{Mp_4}$. In relatively recent evolutionary time, some bacteria belonging to the phylum Gemmatimonadetes obtained a Type II reaction center via horizontal gene transfer from a gammaproteobacterium (Zeng et al., 2014, 2015). It is also possible that some bacteria from the phylum Firmicutes, of the genus *Alkalibacterium*, obtained Type II reaction centers from a gammaproteobacterium (Perreault et al., 2008), but this needs experimental verification.

Now, the last common ancestor of the phylum Cyanobacteria had already $\mathbf{D1_3}$ and $\mathbf{D2_3}$ because the earliest diverging strains of the genus *Gloeobacter* have a standard Photosystem II. It follows then that the phototrophic organism that carried the ancestral $\mathbf{D0_2}$ protein is not part of the current diversity and

predated the last common ancestor of the phylum Cyanobacteria. In a similar way, all phototrophic members of the phylum Proteobacteria carry well-defined **L*p*$_4$** and **M*p*$_4$** suggesting that all L and M subunits found in photorophic Alpha-, Beta-, and Gammaproteobacteria originated from those in an ancestral proteobacterium carrying **L*p*$_4$** and **M*p*$_4$**, already distinct from **L*c*$_4$** and **M*c*$_4$**. The same reasoning applies to Chloroflexi. Following along the same lines, the organism that contained the anoxygenic Type II reaction center composed of the ancestral proteins **L$_3$** and **M$_3$** is not part of the current described biodiversity. The existence of this ancestral bacterium must predate the arrival of phototrophy to the phylum Chloroflexi and the phylum Proteobacteria. In consequence, it is impossible that Cyanobacteria obtained Type II reaction center proteins via horizontal gene transfer from a phototroph of the phylum Chloroflexi or Proteobacteria. The evolutionary relationship among Type II reaction center proteins excludes any scenario where D1 and D2 originated from **L*p*$_4$**, **M*p*$_4$**, **L*c*$_4$**, **M*c*$_4$**, or their ancestral forms **L$_3$** and **M$_3$**. This clearly shows that Photosystem II and anoxygenic Type II reaction centers have followed independent evolutionary pathways since the earliest stages of photosynthesis. So, even though Photosystem II looks, at first glance, a lot more sophisticated than anoxygenic Type II reaction centers; the complex itself retains uncanny ancestral characteristics. Some of these will be described further below. The relationship between Photosystem II and anoxygenic Type II reaction centers is fundamental to understand the origin of oxygenic photosynthesis, because some of the protein motifs required to coordinate the Mn_4CaO_5 cluster might have been inherited from the ancestral Type II reaction center protein, **II$_1$**.

In parallel to the evolution of Type II reaction centers, the ancestral protein to all Type I reaction center proteins, **I$_1$**, also diversified into two forms: **I*a*$_2$** and **I*b*$_2$**. On the one hand, **I*a*$_2$** gave rise to two new reaction center proteins, named in **Figure 1** as **AB$_3$** and **CP$_3$**. The former is ancestral to both Photosystem I reaction center proteins, PsaA and PsaB; and the latter is ancestral to the antenna proteins of Photosystem II, CP47 and CP43. In this case, this set of proteins is four transitional stages away from the primordial reaction center protein **A**, and therefore they can be written as **PsaA$_4$**, **PsaB$_4$**, **CP47$_4$**, and **CP43$_4$**. Like D1 and D2, these set of proteins are found exclusively within today's cyanobacterial diversity. The detailed evolution of the CP47 and CP43 antenna proteins will be discussed in the next section.

On the other hand, **I*b*$_2$** is ancestral to all Type I reaction center proteins present only in anoxygenic phototrophic bacteria. **I*b*$_2$** gave rise to two new proteins: **PshA$_3$** that today is only found in the family Heliobacteriaceae of the phylum Firmicutes and **PscA$_3$**. In turn, **PscA$_3$** undergoes another evolutionary transition as the phylum Chlorobi and Acidobacteria diversified. Thus, I shall call them **A*c*$_4$** for Chlorobi and **A*a*$_4$** for Acidobacteria. The **A*c*$_4$** and **A*a*$_4$** reaction center proteins share a common ancestor, **PscA$_3$**, but they are phylogenetically distinct from each other displaying unique sequence variations and structural characteristics (Bryant et al., 2007; Tsukatani et al., 2012). Thus, it cannot be said that the reaction center from Acidobacteria was obtained via horizontal gene transfer from a phototrophic bacterium belonging to the phylum Chlorobi, or vice versa.

Comparable to Type II, the evolutionary relations of Type I reaction center proteins exclude the possibility that Cyanobacteria obtained Photosystem I from a bacterium of the phylum Chlorobi, Acidobacteria, or from a heliobacterium. This is because **PsaA$_4$** and **PsaB$_4$** are predated by **AB$_3$**, and not **A*a*$_4$**, **A*c*$_4$**, or **PshA$_3$**. In other words, **A*a*$_4$**, **A*c*$_4$**, and **PshA$_3$** share among each other significantly more sequence and structural homology than with **PsaA$_4$**, **PsaB$_4$**, or with **CP43$_4$** and **CP47$_4$**. The last common ancestor of **A*a*$_4$**, **A*c*$_4$**, and **PshA$_3$** is **I*b*$_2$** (**Figure 1**), and accordingly it can be concluded that the organism that had **I*b*$_2$** must have existed before the evolutionary radiation that gave origin to the bacteria containing **PscA$_3$** and **PshA$_3$** at a later evolutionary stage. This implies that the reaction center proteins that gave rise to Photosystem I and the antenna proteins of Photosystem II also started to diverge very early during the evolution of photosynthesis, in a similar fashion to Type II reaction center proteins.

EVOLUTION OF THE CP43 AND CP47 SUBUNITS AND THEIR INTERACTION WITH D1 AND D2

The evolution of the antenna proteins of Photosystem II has not been dealt with in as much detail as the core reaction center proteins. Mostly because it is assumed that the CP43 and CP47 subunits of Photosystem II originated from the division or truncation of a gene encoding a Type I reaction center protein, thus leaving only the first six transmembrane helices of the antenna domain (Mix et al., 2005). Nonetheless, a thorough examination of the antenna proteins and the way they are connected with the reaction center core opens a new window to the fascinating evolutionary events that were at play during the early stages of photosynthesis.

The CP43 and CP47 proteins are connected with D1 and D2 via two peripheral chlorophyll *a* molecules known as Chl_Z and Chl_D, also referred to as $ChlZ_{D1}$ and $ChlZ_{D2}$. The chlorophylls are coordinated by D1-H118 and D2-H117 (**Figures 3A,B**) and mediate excitation energy transfer from the CP43 and CP47 antenna to the reaction center core (Lince and Vermaas, 1998; Vasil'ev and Bruce, 2000). From an evolutionary standpoint, the connection of the antenna with the core proteins is of particular importance because homologous peripheral chlorophylls are also present in Photosystem I coordinated by homologous histidine ligands. Sequence comparisons show that this histidine is also present in PshA and the PscA of the Chlorobi and are likely to coordinate a bacteriochlorophyll molecule in order to mediate excitation transfer from the antenna domain to the core domain (Baymann et al., 2001; Cardona, 2015). The presence of these peripheral pigments in Type I reaction centers proteins and in Photosystem II, as well as the remaining sequence identity in this region of the core proteins, strongly suggest that they were present in the primordial reaction center protein, **A** (**Figure 1**). In other words, the peripheral chlorophylls of Photosystem II, Chl_Z, and Chl_D, are ancestral traits retained since the origin of the first

reaction centers. It suggests that the primordial Type II reaction center made of protein **II$_1$**—at the dawn of photosynthesis—was interacting closely with the antenna domain of a Type I reaction center protein. This is consistent with two distinct reaction centers side-by-side, in the same membrane, early during the evolution of photosynthesis in at least some ancestral phototrophic bacteria predating the origin of water oxidation, and likely as well, the diversification of most phyla containing phototrophic bacteria today. The idea of two reaction centers evolving within the same organisms has been hypothesized before; see for example Olson (1981) or Allen (2005). In addition, recent genomic and phylogenetic analyses have provided some support to this as well (Sousa et al., 2013; Cardona, 2015; Harel et al., 2015).

The origin of water oxidation mandates the presence of both types of reaction centers within the same bacterium. Not just because of the energetic requirements of shuttling electrons from water to $NADP^+$, but also because the CP43 antenna protein of Photosystem II, which originated from a Type I reaction center protein, is involved in the coordination of the water-oxidizing complex. Residue E354 of the CP43 coordinates Mn3 and Mn2 of the Mn_4CaO_5 cluster and R357 offers a hydrogen bond to O2 and O4 (Ferreira et al., 2004; Umena et al., 2011), see **Figure 2**. Site-directed mutants of these two residues show a severe impairment of the water oxidation cycle and fail to grow photoautotrophically (Ananyev et al., 2005; Hwang et al., 2007; Strickler et al., 2008; Shimada et al., 2009; Service et al., 2011). In addition to this, both CP43 and CP47 play important roles in water and proton access into or out of the cluster (Umena et al., 2011; Linke and Ho, 2013). This close interaction between the antenna proteins and the water-oxidizing complex is possible thanks to a large extrinsic lumenal domain between the 5th and 6th transmembrane helices of both the CP47 and CP43 proteins (**Figure 3**). The extrinsic domain has about 130 amino acids in CP43 and about 190 in CP47, in both cases showing remarkable structural similarities (Kamiya and Shen, 2003). The assumption that the CP43 and CP47 proteins originated from a fission or truncation of a Type I reaction center gene presupposes that the extrinsic domain originated as a sequence insertion on the ancestral antenna protein, denoted **CP$_3$** in **Figure 1**. This is because no such extrinsic domain is present in the antenna part of any of the Type I reaction center proteins described to date. However, in-depth sequence and structural comparisons reveal that the antenna proteins of Photosystem II most likely emerged from the remodeling of an entire Type I reaction center protein and not from a partial gene duplication (**Figures 3F–J**). While the first five transmembrane helices are indeed homologous between the antenna and the reaction center proteins; the 6th helix in Type I reaction centers (helix F) is homologous to an alpha-helix in CP43 and CP47 located outside the membrane, in the extrinsic domain, and follows immediately after the 5th helix (**Figures 3F–J**). In this way, what was thought to be the 6th transmembrane helix of CP43 and CP47, actually corresponds to the 10th helix (J) in Type I reaction centers. Consequently, the CP43 and CP47 proteins originated from an entire Type I reaction center protein that, over time, underwent a transformation, where the entire region spanning the 6th to the 9th transmembrane helices (F to I) protruded outside the membrane. This change could have been triggered by relatively few mutations such that the 6th helix became unstable within the membrane. Hypothetically, the changes could have enhanced energy transfer to the ancestral Type II reaction center by allowing a better docking of the antenna domain with the Type II core and thus conferred a selective advantage. At the same time, the extrinsic domain was now free to interact with the donor side of the early D1 and D2 proteins fostering perhaps the oxidation of aqueous Mn(II) and the origin of the Mn_4CaO_5 cluster.

Similar structural changes have been accomplished in site-directed mutants, where the insertion of a transmembrane helix or the topology of a membrane protein is radically altered by a single or few amino acid substitutions (Hessa et al., 2007; Seppälä et al., 2010). Some membrane proteins that undergo similar dramatic topological changes under physiological conditions have been described before (Von Heijne, 2006). What is more, these kind of evolutionary transitions are not completely foreign to photosynthesis. For example, the PsbO subunit of Photosystem II, which is located outside the membrane toward the lumen, might have originated from an outer-membrane protein related to porins (De Las Rivas and Barber, 2004; Iverson, 2006). Also, the FMO light-harvesting complex found in Chlorobi and Acidobacteria is proposed to have originated from the refolding of PscA (Olson and Raymond, 2003).

THE ANCIENT RECRUITMENT OF ADDITIONAL PROTEIN SUBUNITS

One big difference between Photosystem II and anoxygenic Type II reaction centers is that Photosystem II is made of many protein subunits. In addition to D1, D2, and the antenna proteins, it requires at least 13 extra proteins as seen in the crystal structures (Zouni et al., 2001; Kamiya and Shen, 2003). The entire collection of subunits can vary from species to species and from Cyanobacteria to photosynthetic eukaryotes (Pagliano et al., 2013): it includes the Cytochrome b_{559}, a range of small membrane proteins located at the periphery of the complex (**Figure 4**), added to the extrinsic polypeptides that shield and stabilize the Mn_4CaO_5 cluster. Like Photosystem II, Photosystem I is also adorned with a range of peripheral small subunits (Jordan et al., 2001; Mazor et al., 2014, 2015). A structural comparison of Photosystem II and Photosystem I shows that the peripheral small subunits are arranged around the core proteins in a strikingly similar pattern (**Figures 4G,H**). In Photosystem II, the Cytochrome b_{559} (PsbE and PsbF) together with PsbJ, which in total make three transmembrane helices, are located perpendicular to the Q_A-Fe^{2+}-Q_B axis. At an equivalent position in Photosystem I the PsaL subunit binds the core proteins perpendicular to A_{1A}-F_X-A_{1B}: PsaL has three transmembrane helices. At the opposite side of the Q_A-Fe^{2+}-Q_B axis in Photosystem II, there are three single-helix subunits PsbL, PsbM, and PsbT making a three-helix bundle. In Photosystem I, PsaJ, and PsaF are found at an equivalent position. While PsaJ has a single transmembrane helix, PsaF has two helices. Although, the second helix of PsaF does not span the entirety

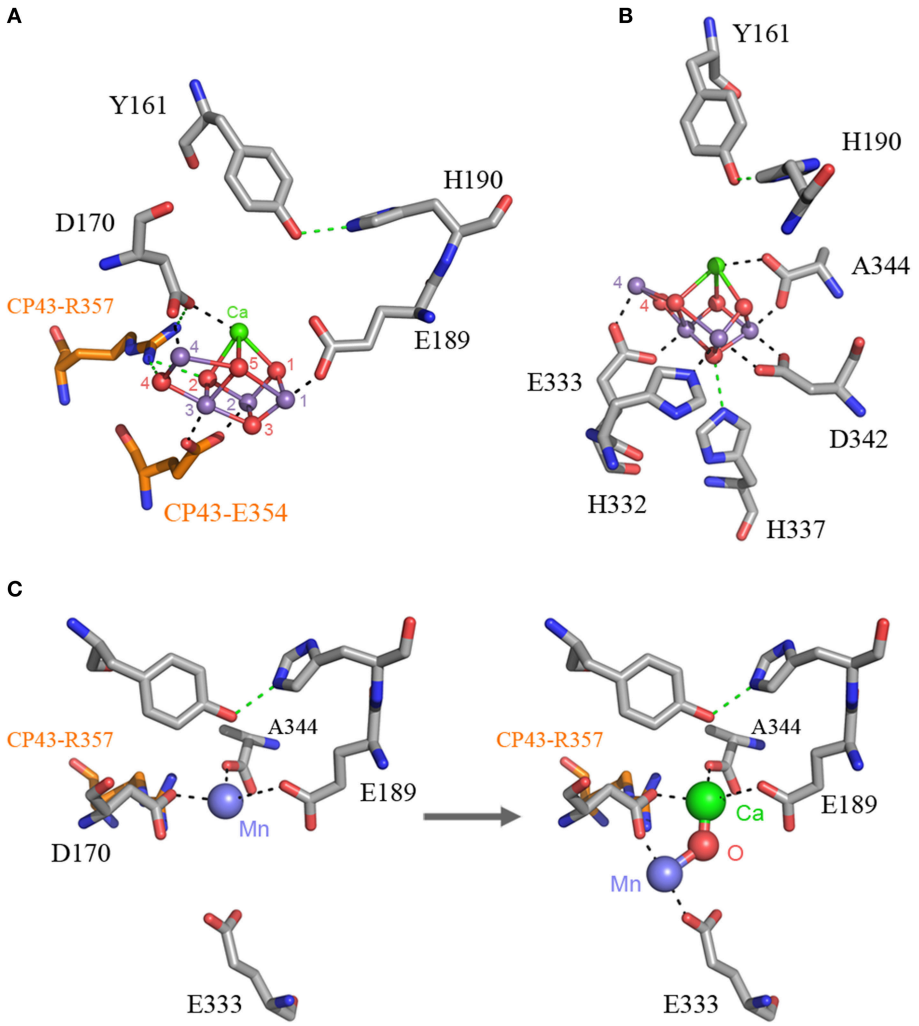

FIGURE 2 | The Mn_4CaO_5 cluster of Photosystem II as resolved in the crystal structure by Umena et al. (2011), PDB ID: 3WU2. Panel **(A)** shows the cluster coordinated by the inner ligands D170 and E189 and the ligands provided by the CP43 subunit, E354, and R357. Panel **(B)** shows the ligands provided from the C-terminus of the D1 protein. Panel **(C)** shows a proposal for the high-affinity Mn binding site based on evolutionary grounds and supported by mutagenesis and spectroscopy (see text). After oxidation of the first Mn(II) to Mn(III), which might occur concomitantly with the deprotonation of a ligating water molecule, Ca^{2+} binds. The binding of Ca^{2+} shifts the initially bound Mn(III) to a position similar to that of Mn4 in the intact cluster.

of the membrane, because it is bent in the middle (Jordan et al., 2001; Mazor et al., 2014, 2015). Interestingly, the homodimeric reaction center found in phototrophic Chlorobi is known to bind two Cytochrome c_{551} proteins. Cytochrome c_{551} has three transmembrane helices and it is the direct electron donor to P840 (Oh-oka et al., 1995). It can be predicted that each Cytochrome c_{551} binds symmetrically to the reaction center in a position equivalent to that of Cytochrome b_{559}-PsbJ and PsbLMT in Photosystem II, or PsaL and PsaFJ in Photosystem I. In fact, this is the only position where Cytochrome c_{551} could bind so that the cytoplasmic domain, which contains the heme, can be positioned near P840 on the periplasmic side of the membrane. This location is also consistent with recent cross-linking experiments done with isolated reaction centers (He et al., 2014). Are these incredible cases of molecular convergent evolution or was the ancestral reaction center to Photosystem I and Photosystem II more complex than previously anticipated? I should reiterate here that the ancestral reaction center to Photosystem I and Photosystem II is the primordial reaction center **A**, ancestral to all reaction centers (**Figure 1**).

D1 and D2 are distinguished from the L and M subunits by the presence of three additional protein segments (Cardona, 2015), these are: (1) an extension of the amino acid sequence in between the 1st and 2nd transmembrane helices (**Figures 4A–D**); (2) an extension between the 4th and 5th transmembrane helices; and (3) an extension beyond the 5th transmembrane helix at the C-terminus. These three differences are tied to the functional and structural differences between the anoxygenic Type II reaction center and Photosystem II (Cardona, 2015). These three protein segments are present in both D1 and D2, suggesting that they

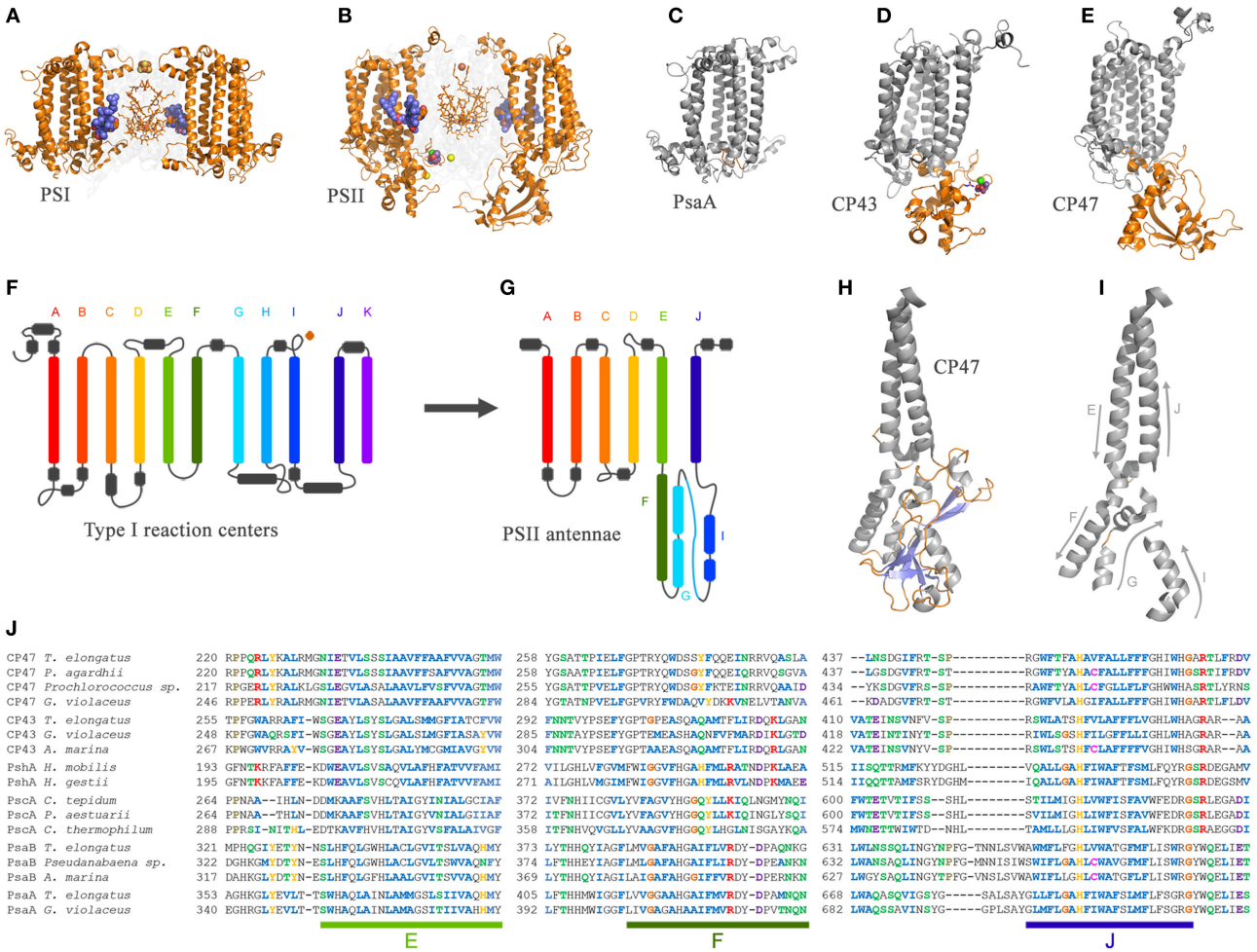

FIGURE 3 | Comparison of the antenna domain of Photosystem I reaction center proteins and the antenna proteins of Photosystem II from the crystal structures PDB ID: 1JB0 and 3WU2 from *Thermosynechococcus* spp., respectively. (A,B) highlight the core antenna of Photosystem I and II respectively (orange). Blue spheres highlight the conserved peripheral chlorophylls that allow excitation energy transfer from the core antenna to the reaction center, named Chl_Z and Chl_D in Photosystem II. **(C–E)** highlight the differences between the antenna domain of the PsaA subunit of Photosystem I with that of the CP43 and CP47, respectively. Note that the extrinsic domain is absent in PsaA. Panels **(F,G)** show and schematic representation of a Type I reaction center and a Photosystem II antenna protein. The alpha-helices have been color coded to show the homologous positions. Panels **(H,I)** show detail of the folding pattern of the extrinsic domain from the CP47 subunit. Panel **(J)** shows a sequence alignment of all Type I reaction center proteins including the CP47 and CP43 subunits. Only three fragments are shown for clarity, those corresponding to transmembrane helices E, F, and J in Type I reaction centers and their respective matching sequences in the antenna proteins of Photosystem II. The sequence alignment was performed using Clustal Omega that applies a Hidden Markov Model-based algorithm (Sievers et al., 2011). The full alignment is available on request.

must have been in the ancestral protein to both, identified as **$D0_2$** in **Figure 1**, before the evolution of the Mn_4CaO_5 cluster. From these three segments, the extension between the 1st and 2nd transmembrane helices is essential for the binding of some of the small subunits of Photosystem II (**Figure 4**). In D1, this loop provides a binding site to PsbI and PsbL. In D2 the loop provides a binding site to the Cytochrome b_{559} and PsbX. It appears that this segment's main function is to provide a site for protein-protein interactions with additional subunits. It follows then that before the origin of water oxidation and before the divergence of D1 and D2, the nascent Photosystem II was already interacting with additional protein subunits of some sort, which are not found in anoxygenic phototrophs containing Type II reaction centers. In fact, like D1 and D2, PsaA and PsaB also have an extension of the protein sequence in between the equivalent transmembrane helices 7th and 8th (homologous to 1st and 2nd in Type II) that interacts with PsaL and PsaFJ, see **Figure 4**. Additionally, in the cross-linking experiment mentioned above, the PscA subunit from the reaction center of *Chlorobaculum tepidum* cross-linked with the Cytochrome c_{551} via a lysine also found in between the 7th and 8th helices (He et al., 2014). All in all, it is a strong indication that the primordial reaction center **A** was interacting with membrane bound proteins, regardless of their original function.

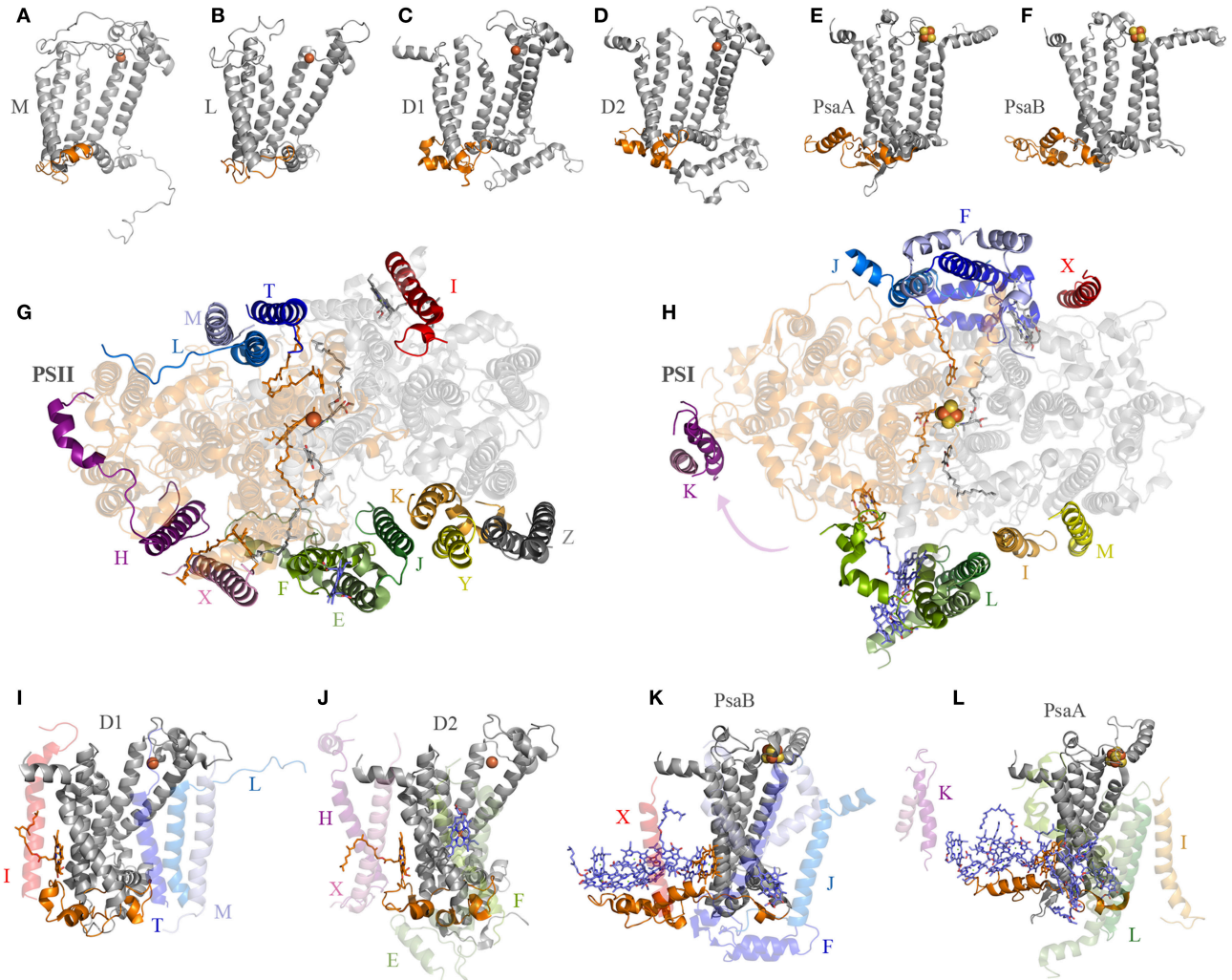

FIGURE 4 | Interaction of reaction center proteins and the small peripheral subunits. Panels **(A–F)** show the reaction center proteins of the anoxygenic Type II reaction center of *Blastochloris viridis* (M and L, PDB ID: 2PRC), *Thermosynechococcus vulcanus* (D1 and D2, PDB ID: 3WU2), and *Thermosynechococcus elongatus* (PsaA and PsaB, core domain only, PDB ID: 1JB0). The orange colored cartoon highlights the protein segment found between the 1st and 2nd transmembrane helices of the core proteins (7th and 8th in Photosystem I). Panels **(G,H)** show the position of the peripheral subunits of Photosystem II and Photosystem I. Panels **(I–L)** show the interaction of the core proteins with some of the small subunits and nearby pigments.

ORIGIN OF THE Mn_4CaO_5 CLUSTER

Several hypotheses regarding the origin of the Mn_4CaO_5 cluster have been proposed before. One of them suggested that the tetramanganese cluster evolved from the interaction of an anoxygenic Photosystem II with a manganese catalase (Raymond and Blankenship, 2008). In this case, the dinuclear Mn cluster of catalase was somehow transferred to Photosystem II. An interaction with a second catalase, should have donated the second pair of Mn ions. A second hypothesis proposed that the cluster originated from natural Mn oxide precipitates present in the ocean (Sauer and Yachandra, 2002). A third hypothesis proposed that the ancestral Photosystem II used bicarbonate as the direct electron donor before the use of water, and this was complexed with Mn (Dismukes et al., 2001). Fortunately, with the great surge in genomic and structural data from Cyanobacteria, it is now possible to reconstruct the origin of the catalytic cluster at a level of detail uncommon for other metalloenzymes. Phylogenetic and structural analysis of the D1 protein of Photosystem II showed that some of them appeared to have diverged at different stages during the evolution of the Mn_4CaO_5 cluster (Cardona et al., 2015). The different types of D1, listed from the earliest to the latest diverging groups, are:

- An atypical D1 sequence found in the genome of *Gloeobacter kilaueensis* JS-1 (Saw et al., 2013; Cardona et al., 2015)
- Group 1: a type of D1 associated with chlorophyll *f*-producing cyanobacteria, also known as super-rogue D1 (Murray, 2012; Gan et al., 2014)

- Group 2: a type of D1 expressed in the night or in darkness, also known as rogue D1 or sentinel D1 (Murray, 2012; Wegener et al., 2015)
- Group 3: a type of D1 expressed under low-oxygen conditions, also known as D1' (Summerfield et al., 2008; Sicora et al., 2009)
- Group 4: the dominant form of D1 expressed under normal conditions and found in all Cyanobacteria and photosynthetic eukaryotes. This group also includes the so-called "high-light" forms of D1.

The common trait of the earliest evolving forms of D1, including the unusual sequence from *Gloeobacter kilaueensis*, Group 1, and Group 2, is that all of them are missing ligands to the Mn_4CaO_5 cluster (Murray, 2012; Cardona et al., 2015). I will call these forms of early evolving D1, "atypical sequences" or "atypical D1 forms." On the other hand, the latest evolving D1 forms, those of Group 3 and Group 4, have a complete set of ligands to the cluster. I will refer to these two groups as "standard sequences" or "standard D1 forms." It is therefore tempting to suggest that when the atypical sequences appeared for the first time, the Mn_4CaO_5 cluster had not evolved yet to its standard form. Only the standard form of D1, those of Group 4, has been characterized in detail. Unfortunately, the function of all other forms of D1 remains quite poorly understood and somewhat mysterious, but they might confer advantages under particular environmental circumstances, such as under anaerobic conditions (Wegener et al., 2015) or challenging light conditions (Gan et al., 2014). It is important to note that the function of these early evolving D1 forms now might not be the same as when they first evolved.

The D1 protein of Photosystem II provides seven ligands to the Mn_4CaO_5 cluster. These can be divided in two groups: (1) D170 and E189, which are located in the CD loop between the 3rd and 4th helix; and (2) the ligands located in the C-terminal lumenal extension beyond the 5th transmembrane helix, H332, E333, H337, D342, and A344. Then, how did the ligand sphere around the Mn_4CaO_5 cluster evolve? The first ligand to have appeared was a glutamate at position equivalent to aspartate 170 (D170) of the crystal structures from *Thermosynechococcus vulcanus* (**Figure 2**). This is because there is a glutamate at this position in both the L and M subunits of the Chloroflexi and in the M of the Proteobacteria. There is also a glutamate at this position in some of the early branching forms of the D1 protein, see **Figure 5** and Cardona et al. (2015). This suggests that the ancestral Type II reaction center protein, $\mathbf{II_1}$, probably had a glutamate at this position.

The ancestral Type II reaction center protein is also likely to have had a C-terminal extension after the 5th transmembrane helix that folded into an alpha-helix located near the donor side (Cardona, 2015). This is because the L subunit found in strains of the genus *Roseiflexus* and in some Proteobacteria also have a C-terminal extension that share sequence homology with the terminal alpha-helix present in D1 and D2. Surprisingly, all the Type I reaction center sequences found in phototrophic Chlorobi also have a C-terminal extension that is predicted to fold into an alpha-helix. It raises the intriguing possibility that a C-terminal alpha-helical extension is a trait original from the primordial reaction center **A**.

Based on these comparisons, it can be deduced that the ancestral Type II reaction center protein, $\mathbf{II_1}$, already had some of the basic components that at a later stage would become essential in the coordination of the Mn_4CaO_5 cluster: a glutamtate at position 170 and an alpha-helical domain extension at the C-terminus. I should reiterate here that $\mathbf{II_1}$ is ancestral not only to D1 and D2, but also to L and M, and therefore the ancestral bacterium that carried this protein almost certainly existed before the phyla Cyanobacteria, Chloroflexi, or Proteobacteria came into existence.

As I discussed before, the ancestral Type II reaction center protein, $\mathbf{II_1}$, diverged into two new forms: $\mathbf{D0_2}$ and $\mathbf{K_2}$. In the evolutionary transition from $\mathbf{II_1}$ to $\mathbf{D0_2}$, in a lineage that would later give rise to the phylum Cyanobacteria, a new feature was gained. This is the tyrosine-histidine pair located at positions homologous to 161 and 190 of the D1 in the crystal structures (Umena et al., 2011). These have been retained in all D1 sequences as the Y_Z-H190 pair and in D2 as Y_D-H189. Thus, a triad made of Tyr-Glu-His was formed in $\mathbf{D0_2}$ and it probably helped maintain the correct folding of the protein via a network of hydrogen bonds (**Figure 5**). A similar triad has evolved independently in the M subunit of bacteria of the genus *Blastochloris*, but rather than having a tyrosine at a position equivalent to 161, it has a histidine, making a pair with a tyrosine nearby. That triad in the M subunit of *Blastochloris* has no redox role and it seems to be only of structural importance. At this stage the Type II reaction center made of $\mathbf{D0_2}$ was still anoxygenic, but the triad was already present in both monomers of the reaction center. Then a major evolutionary transition occurred to the organism containing $\mathbf{D0_2}$ that changed the chemistry of the reaction center. This evolutionary innovation allowed the reaction center to oxidize the tyrosine in the triad upon charge separation, resulting in the formation of the tyrosyl radical. In other words, the oxidizing power of the "special pair" cation, $P^{\bullet+}$, increased.

The redox potential of $P_{D1}^{\bullet+}/P_{D1}$ in standard Photosystem II is around 1200 mV (Rappaport et al., 2002; Ishikita et al., 2006), the redox potential of $Y_Z^{\bullet}/Y_Z$ is calculated to be near 970 mV and that of $Y_D^{\bullet}/Y_D$ near 760 mV (Vass and Styring, 1991). If we assume that the potential for $P^{\bullet+}/P$ in the ancestral Photosystem II before water oxidation was similar to that in Chloroflexi or Proteobacteria, which is measured to be between 360 (Bruce et al., 1982; Collins et al., 2009) and 500 mV (Moss et al., 1991; Williams et al., 1992), respectively. Then, the potential of $P^{\bullet+}/P$ in the ancestral Photosystem II had to increase by about 300–400 mV to at least be able to oxidize a tyrosine with the properties of Y_D. In fact, a mutant reaction center from *Rhodobacter sphaeroides* with the potential of $P870^{\bullet+}/P870$ up-shifted to at least 800 mV can oxidize a tyrosine (Kalman et al., 1999) and exogenous Mn(II) (Thielges et al., 2005). Then how did $P^{\bullet+}$ become so oxidizing in the ancestral Photosystem II before water oxidation was possible?

Ishikita et al. (2006) calculated the influence of cofactors and protein charges on the redox potential of P_{D1}. In comparison with the anoxygenic Type II reaction center from *Rhodobacter sphaeroides*, the use of chlorophyll *a* instead of

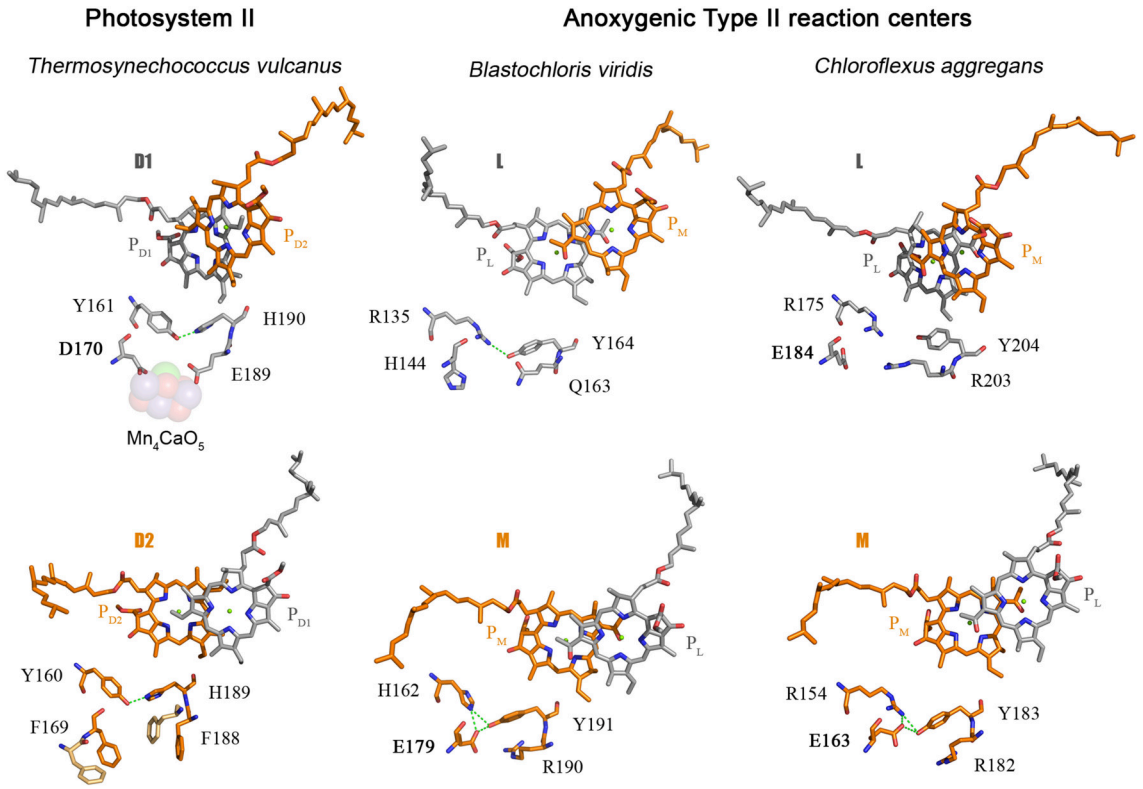

FIGURE 5 | Comparison of the electron donor sides of Type II reaction centers from *Thermosynechococcus vulcanus* (PDB ID: 3WU2), with those from *Blastochloris viridis* (PDB ID: 1JB0), and *Chloroflexus aggregans*. The highlighted residues are at strictly homologous positions as determined by sequence and structural comparisons; the variation in number is due to the fact that different reaction center proteins are of different sizes in different strains of bacteria. The L and M from *Chloroflexus aggregans* are homology models made with the SWISS-MODEL service, automated mode, using the structure of the *Blastochloris viridis* reaction center as a template.

bacteriochlorophyll *a* contributes 160 mV. Up to 200 mV are attributed to the effect from atomic charges and the protein dielectric volume of the antenna proteins and the small subunits. The presence of the Mn_4CaO_5 cluster up-shifts the potential another 200 mV. Finally, the side chains around P_{D1} tune down the potential by about −135 mV; see Cardona et al. (2012) for a full discussion. If we consider that the ancestral Photosystem II made of $\mathbf{D0_2}$ started with a low potential special pair, then just the acquisition of the antenna proteins and some additional peripheral subunits, combined with the use of chlorophyll instead of bacteriochlorophyll, could have up-shifted the potential by at least 360 mV, possibly more. This could have been enough to trigger the oxidation of the tyrosine located on both sides of the reaction center coupled to Mn(II) oxidation. The presence of glutamate near the tyrosine implies that upon oxidation of Mn(II) to Mn(III), the carboxyl side-chain of E170 could have coordinated and partially stabilized the metal. In this scenario, aqueous Mn(II) seems like a plausible electron donor to photosynthesis in an ancestral bacterium prior to the evolution of proper water oxidation. What is more, the initial oxidation and binding of Mn could have pushed the potential of $P^{\bullet+}/P$ even further up, allowing additional oxidation steps or the binding of extra Mn ions. From this evolutionary perspective, it is therefore unnecessary to invoke a catalase or naturally occurring inorganic Mn oxide precipitates as precursors to the Mn_4CaO_5 cluster. It is also unnecessary to suggest that bicarbonate was a transitional direct electron donor before water. Aqueous Mn(II) might have been the direct electron donor once tyrosine oxidation was possible, followed in time, by water.

The second ligand to evolve was glutamate at position 189. The earliest evolving form of D1, the atypical sequence of *Gloeobacter kilaueensis*, only has a glutamate at position 189 and lacks all other ligands. This sequence is unique among D1 proteins because it has retained numerous ancestral traits (Cardona et al., 2015). In particular, the C-terminal alpha-helix looks like D2 and has retained some residues conserved in D2, but no longer in any other D1. In addition, none of the ligands at the C-terminus are present. Judging by the predicted structural similarities with the C-terminus of D2 and its phylogenetic position, it is highly likely that at the evolutionary stage when this sequence branched out, these ligands had not appeared yet. This implies that glutamate 170 and 189 predated the appearance of the ligands at the C-terminus. Another clue about the origin of the first ligands is found within D2: unlike D1, both glutamate ligands changed to phenylalanines (F169 and F188) and their presence impedes the binding of metals near Y_D-H189. No such

phenylalanines are present in any other Type II reaction center protein and therefore it seems they evolved to minimize the possibility of metal oxidation on the D2 side. This suggests that a glutamate at position 189 was also likely in **D0$_2$** and was lost in D2 on the path to heterodimerization of the reaction center.

The existence of an ancestral homodimeric Photosystem II capable of oxidizing manganese in each monomer has been hypothesized before (Rutherford and Nitschke, 1996; Rutherford and Faller, 2003; Williamson et al., 2011; Fischer et al., 2015). While the molecular evidence is somewhat compelling; it is not possible to tell with certainty whether such a reaction center could assemble a metal center of some sort or not, such as a mononuclear or dinuclear Mn cluster. If that early catalytic cluster did exist, it is also very difficult to deduce what kind of chemistry it carried out and whether it could have performed some partial water oxidation, even if inefficiently. Hypothetically, this early photosystem could have trapped at least two Mn atoms, which could have been oxidized sequentially from Mn(II) to Mn(IV) and thereby accumulating four positive charges. During photoactivation experiments, in the absence of Ca^{2+}, oxidation of Mn(II) to Mn(III) occurs for several turnovers without the trapping of any Mn(IV); however, in mutants where D170 was changed to E170, as in the ancestral photosystem, Mn(II) was trapped and oxidized to Mn(IV) and possibly even as a dinuclear Mn_2(IV,IV) complex (Campbell et al., 2000). It was suggested that E170 could provide a Mn binding site with a less positive reduction potential for the Mn(III)/Mn(IV) couple (Campbell et al., 2000). In addition, if Mn is complexed with bicarbonate this could lower its redox potential below 700 mV making it accessible to the early reaction center (Kozlov et al., 1997; Dismukes et al., 2001). It is not inconceivable that the early Photosystem II, before the divergence of D1 and D2, may have been able to assemble a simpler catalytic cluster. This early cluster could plausibly catalyze the partial oxidation of water to peroxide or, alternatively, the inefficient oxidation of water to oxygen.

At this stage the ligands at the C-terminus started to evolve. In the diversity of D1 proteins some of these ligands start to appear for the first time in Group 1 and Group 2 forms, suggesting that such ligands were never present in the equivalent D2 side. The appearance of the ligands at the C-terminus may have been selected in order to retain the metals near Y_Z-H190: at first so that the cluster could be reassembled more quickly, and later to retain the cluster for several turnovers before falling apart. At this stage, oxygen concentrations in the environment or within the cell were likely extremely low. Thus, the formation of reactive oxygen species would have been also very low and so the high turnover rates of D1, as seen in standard Photosystem II today, were probably not needed. However, as water oxidation became more efficient and optimized, so photoprotective mechanisms should have become more sophisticated and specialized.

It is likely that any transitional Mn cluster and its early chemistry could have benefited from controlled deprotonation reactions, as the formation of di-μ-hydroxo or di-μ-oxo bridges might have resulted in the release of protons (Dau and Haumann, 2008). In fact, the atypical sequence from *Gloeobacter kilaueensis* and Group 1 D1 sequences have what appear to be proton exit pathways via the Y_Z-H190 and toward the lumen. The proton pathways, both at the donor and acceptor side, start to resemble those in standard forms of D1 only in Group 2, even though these sequences lack ligands at the C-terminus. At the evolutionary stage that led to Group 1 and Group 2 sequences branching out, it is possible that a more sophisticated cluster already existed. Group 2 sequences can be found having either E170 or D170, so at some point in the evolutionary transition from Group 1 to Group 3, D170 is preferred over E170, possibly to optimize the shape of the cluster (Cardona et al., 2015).

Group 3 D1 sequences, or the low-oxygen form of D1, have all of the features required for water oxidation and a Photosystem II carrying this type of D1 can assemble a cluster and oxidize water (Sugiura et al., 2012). An experimental characterization of Photosystem II carrying one of these forms of D1 showed that the complex seemed to be slightly impaired at certain stages during the catalytic cycle, at least when tested under ambient oxygenic concentrations (Sugiura et al., 2012). It is possible that this type of D1 was predominantly in use when the oxygen concentrations in the environment and within the cell were still very low. The transition from Group 3 to Group 4 might have consisted only of fine-tuning the core of Photosystem II to run in a more oxidizing environment.

ASSEMBLY INTERMEDIATES OF PHOTOSYSTEM II MAY REPRESENT EVOLUTIONARY TRANSITIONS

Levy et al. (2008) suggested that the evolution of multiprotein complexes can be viewed as the sequential assembly of these complexes over a long period of time. From this perspective the starting point in the evolution of oxygenic photosynthesis is a simple anoxygenic Type II reaction center and culminates with the complex water-oxidizing enzyme we know today, with each new layer of complexity built upon the other. The implication of this is that the key evolutionary transitions that led to the appearance of water oxidation may be preserved in the assembly of the protein complex and in the process of photoactivation of the Mn_4CaO_5 cluster.

The assembly of Photosystem II is modular and a highly organized process (Komenda et al., 2012; Nickelsen and Rengstl, 2013). At the earliest stage of assembly, the D1 protein binds PsbI and separately D2 binds the Cytochrome b_{559}. Then these two modules come together to make what looks like a primitive reaction center, composed of the two core subunits, a cytochrome, a small subunit, and devoid of antenna proteins, the Mn_4CaO_5 cluster, and the extrinsic polypeptides (Komenda et al., 2004; Dobáková et al., 2007). I have shown now how the earliest Type II reaction center made of **II$_1$** was probably interacting with additional subunits of some sort via a protein extension located between the 1st and 2nd transmembrane helix, which in Photosystem II serves as the place for protein-protein interactions with—specifically—PsbI and the Cytochrome b_{559}. Once the early reaction center made of **D0$_2$** developed a special pair capable of oxidizing tyrosine, it is expected that the oxidation of Mn becomes possible. Somewhat intriguingly, it has been suggested that at this early stage of assembly, Mn is

preloaded into the system via an assembly factor termed PratA in Cyanobacteria (Stengel et al., 2012). This occurs before the C-terminus of D1 is completely processed, suggesting that at this stage complete photoactiavtion is not possible. This early stage in biogenesis could mimic an ancestral metal-binding photosystem before the origin of the tetramanganese cluster.

Separately, CP43 forms a subcomplex with at least PsbK and PsbZ; and CP47 makes a subcomplex with PsbH, PsbL, and PsbT. The antenna subcomplexes then bind to the D1-D2-Cytochrome b_{559}-PsbI reaction center to form a complete Photosystem II monomer (Sugimoto and Takahashi, 2003; Boehm et al., 2011), but still lacking the completely assembled cluster. Only after this stage can photoactivation of the Mn_4CaO_5 cluster occur. Plausibly mirroring evolution, the Mn_4CaO_5 cluster could have only evolved after the antenna proteins were associated with the reaction center, as the CP43 protein provides ligands to the cluster. I have also mentioned how Photosystem I binds numerous additional subunits that interact with the reaction center in a way very similar to Photosystem II. It is possible then, that many of these subunits were recruited quite early during the origin of the first reaction centers. If the antenna proteins of Photosystem II evolved from a Type I reaction center protein that was interacting with additional subunits, then it is not surprising that CP43 and CP47 bind a series of small polypeptides even before associating with D1 and D2. Upon photoactivation and relatively late in biogenesis, the extrinsic polypeptides bind the lumenal side of Photosystem II to isolate and stabilize the Mn_4CaO_5 cluster.

The first ligand to the Mn_4CaO_5 cluster to have evolved was likely a glutamate at position 170, followed by glutamate 189. This is paralleled during the process of photoactivation, as the first Mn(II) is oxidized to Mn(III) and bound to the high-affinity Mn binding site, known to be in part provided by D170 (Nixon and Diner, 1992; Campbell et al., 2000; Asada and Mino, 2015). The oxidation of Mn(II) to Mn(III) is accompanied by a deprotonating event of one of the ligating water molecules (Dasgupta et al., 2008). This is considered to be the first intermediate, which is unstable until the binding of Ca^{2+} followed by an uncharacterized conformational change (Tamura and Cheniae, 1987; Tamura et al., 1989; Chen et al., 1995; Tyryshkin et al., 2006). Beside D170 being part of the high affinity binding site, Dasgupta et al. (2007) suggested that the first bound Mn may also be coordinated by a N-donor ligand and speculated to be H332 or H337. Because these two histidines are too far from D170 to bind the same Mn, doubt was cast on the role of D170 as part of the high-affinity binding site (Becker et al., 2011). However, from an evolutionary perspective one would expect the first Mn to be bound by D170 and E189. If this is true, it can be predicted that the high-affinity binding site is located in a position near to the Ca^{2+} in the fully assembled cluster. In this position the first bound Mn is coordinated by D170, E189, and A344; the N-donor ligand detected by electron spin echo envelope modulation spectroscopy may be due to the presence of R357 from the CP43 subunit (**Figure 2C**). Although, R357 might appear counterintuitive as a N-donor ligand, arginine-metal interactions are not uncommon in metalloproteins; and arginine is known to ligate Mn in arginase (Di Costanzo et al., 2006). This position is not completely inconsistent with the distance measured by Asada and Mino (2015) using pulsed electron-electron double resonance spectroscopy considering that in the absence of the cluster the ligand sphere should be somewhat shifted. It is also consistent with a six-coordinate tetragonally-elongated or a five-coordinate square-pyramidal geometry as measured using EPR (Campbell et al., 2000). Upon Ca^{2+} binding, the uncharacterized conformational change is due to Ca^{2+} shifting the position of Mn and taking its correct position. Mn(III) then moves to a position similar to that of Mn4 in the crystal structure, where it is coordinated by D170 and E333. This is also consistent with the work by Cohen et al. (2007) that showed E333 mutants were impaired in the binding of the first

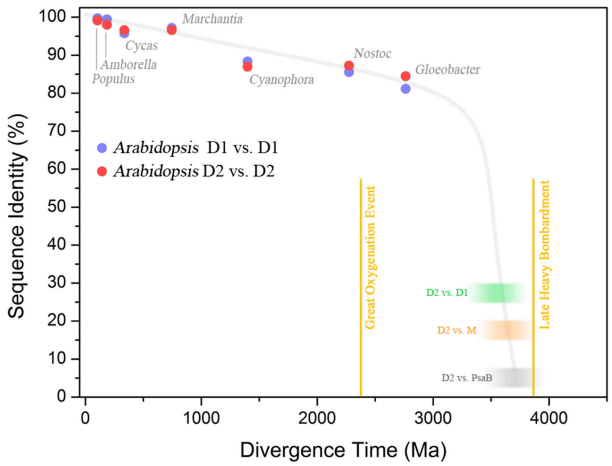

FIGURE 6 | Sequence identity of Photosystem II reaction center proteins as a function of time. The blue dots show the percentage of sequence identity between the D1 protein sequence of *Arabidopsis thaliana* compared to that in other organisms. The red dots show the percentage of sequence identity of D2. The green blurred box shows the level of sequence identity between D1 and D2 of *Arabidopsis* and the blur represents uncertainty. The orange box shows the sequence identity of D2 compared to the M subunit of *Chloroflexus aurantiacus*. The gray box shows the sequence identity of D2 compared to the PsaB subunit of Photosystem I from *Thermosynechococcus elongatus*. This was calculated by overlaying the 3D structures of D2 and PsaB proteins and counting the conserved residues (the identity is below 5%), see Cardona (2015). The plot shows that D1 and D2 have been changing at an almost constant rate since the Great Oxygenation Event (GOE) around 2.4 billion years ago. It also highlights that the events that led to the divergence of Type I from Type II reaction centers (gray box), the anoxygenic from oxygenic Type II reaction centers (orange box), and D1 from D2 (green box), must have occurred very early in the history of life. It is also likely that these early events in the evolution of photosynthesis probably occurred relatively fast after the origin of the first reaction center protein. The divergence times in plant evolution were taken from Clarke et al. (2011). The time for *Cyanophora paradoxa*, representing the origin of plastids, was assumed to be in between 1.1 and 1.5 Ga (Butterfield, 2000; Yoon et al., 2004). The time for *Nostoc* sp. PCC 7120, representing the origin of heterocystous Cyanobacteria, was assumed to have occurred after the GOE (Golubic et al., 1995; Tomitani et al., 2006). The divergence of the genus *Gloeobacter violaceus* sp. PCC 7421 was assumed to have occurred before the GOE. The divergence time for D1/D2, D2/M, and D2/PsaB are hypothetical, but in order to explain the origin and diversification of photosynthesis within the age constraints of planet Earth, very fast rates of evolution are needed at the earliest stages. It suggests that the earliest stages of Photosystem II evolution, such as the divergence of D1 and D2, might have occurred soon after the origin of photochemical reaction centers.

Mn. After the binding and oxidation of Mn(II) to Mn(III), and the subsequent binding of Ca^{2+}, a second Mn(II) is oxidized to Mn(III), which quickly leads to a fully assembled Mn_4CaO_5 cluster. Unfortunately, the fast events after the binding of the second Mn remain to be characterized; however, the evidence for an intermediary photoactivation step made of two Mn and involving at least D170 and E333 seems to be strong (Dasgupta et al., 2008; Becker et al., 2011).

CONCLUDING REMARKS

How long did it take for the ancestral Photosystem II to evolve the Mn_4CaO_5 cluster? Let us remember that the ancestral reaction center made of a double $\mathbf{D0_2}$ could have performed some kind of metal-centered catalysis and even perhaps some inefficient water oxidation. An answer to this question can be calculated by modeling the rates of evolution of D1 and D2 from the known phylogenetic relationships of Cyanobacteria and photosynthetic eukaryotes. Assuming that the last common ancestor of Cyanobacteria lived before the Great Oxygenation Event (2.4 billion years ago); then, the D1 and D2 divergence may have started more than a billion years before it. Even such early dates require rates of D1 and D2 evolution almost two orders of magnitude higher than those observed since the last common ancestor to the phylum Cyanobacteria.

Consider the following example. The standard D1 protein of *Gloeobacter violaceus* and *Arabidopsis thaliana* share 81.6% sequence identity. *Gloeobacter* and *Arabidopsis* are separated by more than two billion years of evolution. In contrast, the D1 and D2 proteins of *Gloeobacter* share between each other only 33.3% identity over the entire length of the sequences, while the D1 and D2 of *Arabidopsis* share 25.7% identity. *Gloeobacter* is the earliest branching genus of Cyanobacteria and it is reasonable to think that it branched out before the Great Oxygenation Event (Criscuolo and Gribaldo, 2011; Schirrmeister et al., 2013; Shih et al., 2013). This implies that when *Gloeobacter* branched out D1 and D2 were already highly divergent. If we assume a constant rate of evolution, the divergence time for D1 and D2 would be placed well before the formation of the planet, which makes no sense (**Figure 6**). Now, when modeling the evolution of reaction center proteins, not only do we need to account for the D1 and D2 divergence, but also the divergence of the LM-branch of Type II reaction center proteins, and the divergence of Type I reaction centers; all of which predated the split of D1 and D2 (**Figure 1**). It becomes necessary to invoke very fast rates of evolution during the early stages of photosynthesis. One might think that the reason why D1 and D2 are evolving so slowly is because water oxidation places a penalty on mutation rates; therefore, one would expect that the anoxygenic reaction center proteins are evolving faster than Photosystem II proteins. In comparison, the L and M of *Chloroflexus aurantiacus* share 24.7% identity between each other and those of *Blastochloris viridis* share 21.9% and are also evolving at a slow rate, albeit just slightly faster than D1 and D2. This is assuming that the phylum Chloroflexi and the phylum Proteobacteria had already appeared, at the very least, around the time of the Great Oxygenation Event. Thus, at that time, they should have carried highly divergent L and M characteristic of their own phylum. If we take into account the large phylogenetic distance among reaction center proteins and their rates of evolution, then the appearance of reaction center proteins around 3.8 billion years ago is likely. Not only that, but if the ancestral Photosystem II before the split of D1 and D2 could have carried out some inefficient water oxidation, then primordial forms of oxygenic phototrophic bacteria 3.2 billion years ago, or before, is perfectly feasible. A detailed analysis on the evolutionary rates of reaction center proteins will be published elsewhere.

There are two main implications derived from the discussions in here. First, if photosynthesis is an ancient process originating 3.8–3.5 billion years ago, this should place its origin near the root or at the root of the bacterial tree of life. It means that photochemical reaction centers were crucial in the development of bacterial bioenergetics systems and were not just merely appended to it. The second ramification is the massive loss of phototrophy throughout the bacterial tree of life, regardless of how pervasive horizontal gene transfer has been. Unlike the trees for Rubisco (Tabita et al., 2008), Nitrogenase-like proteins (Raymond et al., 2004), or Cytochrome bc_1/b_6f complexes (Nitschke et al., 2010), which are quite leafy; the trees of reaction center proteins look like a London Plane tree after the end of the winter: very long branches and only a few leaves left. The long branches summed to relatively slow rates of evolution suggest that the vast majority of phototrophs have gone extinct and that many still remain to be discovered.

AUTHOR CONTRIBUTIONS

The author confirms being the sole contributor of this work and approved it for publication.

ACKNOWLEDGMENTS

The financial support of an Imperial College London Junior Research Fellowship and the Biotechnology and Biological Sciences Research Council (Grant BB/K002627/1) is gracefully acknowledged. I thank Prof. A. William Rutherford, Prof. Peter J. Nixon, Dr. James MacDonald, Dr. Jianfeng Yu, Dr. Andrea Fantuzzi, Shengxi Shao, and two anonymous reviewers for valuable feedback, discussions, and corrections.

REFERENCES

Allen, J. F., and Vermaas, W. (2010). "Evolution of photosynthesis," in *Encyclopedia of Life Sciences (els)*, (Chichester: John Wiley & Sons, Ltd). Available online at: http://jfallen.org/publications/pdf/Allen_2010_ELS.pdf

Allen, J. F. (2005). A redox switch hypothesis for the origin of two light reactions in photosynthesis. *FEBS Lett.* 579, 963–968. doi: 10.1016/j.febslet.2005.01.015

Ananyev, G., Nguyen, T., Putnam-Evans, C., and Dismukes, G. C. (2005). Mutagenesis of CP43-arginine-357 to serine reveals new evidence for (bi)carbonate functioning in the water-oxidizing complex of Photosystem II. *Photochem. Photobiol. Sci.* 4, 991–998. doi: 10.1039/b507519j

Asada, M., and Mino, H. (2015). Location of the high-affinity Mn^{2+} site in Photosystem II detected by peldor. *J. Phys. Chem. B* 119, 10139–10144. doi: 10.1021/acs.jpcb.5b03994

Baymann, F., Brugna, M., Mühlenhoff, U., and Nitschke, W. (2001). Daddy, where did (PS)I come from? *Biochim. Biophys. Acta* 1507, 291–310. doi: 10.1016/S0005-2728(01)00209-2

Beanland, T. J. (1990). Evolutionary relationships between Q-type photosynthetic reaction centers - hypothesis-testing using parsimony. *J. Theor. Biol.* 145, 535–545. doi: 10.1016/S0022-5193(05)80487-4

Becker, K., Cormann, K. U., and Nowaczyk, M. M. (2011). Assembly of the water-oxidizing complex in Photosystem II. *J. Photochem. Photobiol. B* 104, 204–211. doi: 10.1016/j.jphotobiol.2011.02.005

Boehm, M., Romero, E., Reisinger, V., Yu, J., Komenda, J., Eichacker, L. A., et al. (2011). Investigating the early stages of Photosystem II assembly in *Synechocystis* sp. PCC 6803 isolation of CP47 and CP43 complexes. *J. Biol. Chem.* 286, 14812–14819. doi: 10.1074/jbc.M110.207944

Bruce, B. D., Fuller, R. C., and Blankenship, R. E. (1982). Primary photochemistry in the facultatively aerobic green photosynthetic bacterium *Chloroflexus aurantiacus*. *Proc. Natl. Acad. Sci. U.S.A.* 79, 6532–6536. doi: 10.1073/pnas.79.21.6532

Bryant, D. A., Costas, A. M. G., Maresca, J. A., Chew, A. G. M., Klatt, C. G., Bateson, M. M., et al. (2007). Candidatus *Chloracidobacterium thermophilum*: an aerobic phototrophic acidobacterium. *Science* 317, 523–526. doi: 10.1126/science.1143236

Butterfield, N. J. (2000). Bangiomorpha pubescens n. gen., n. sp.: implications for the evolution of sex, multicellularity, and the Mesoproterozoic/Neoproterozoic radiation of eukaryotes. *Paleobiology* 26, 386–404. doi: 10.1666/0094-8373(2000)026<0386:BPNGNS>2.0.CO;2

Butterfield, N. J. (2015). Proterozoic photosynthesis – A critical review. *Paleontology* 58, 953–972. doi: 10.1111/pala.12211

Campbell, K. A., Force, D. A., Nixon, P. J., Dole, F., Diner, B. A., and Britt, R. D. (2000). Dual-mode PER detects the initial intermediate in photoassembly of the Photosystem II Mn cluster: the influence of amino acid residue 170 of the D1 polypeptide on Mn coordination. *J. Am. Chem. Soc.* 122, 3754–3761. doi: 10.1021/ja000142t

Cardona, T., Murray, J. W., and Rutherford, A. W. (2015). Origin and evolution of water oxidation before the last common ancestor of the cyanobacteria. *Mol. Biol. Evol.* 32, 1310–1328. doi: 10.1093/molbev/msv024

Cardona, T., Sedoud, A., Cox, N., and Rutherford, A. W. (2012). Charge separation in Photosystem II: a comparative and evolutionary overview. *Biochim. Biophys. Acta* 1817, 26–43. doi: 10.1016/j.bbabio.2011.07.012

Cardona, T. (2015). A fresh look at the evolution and diversification of photochemical reaction centers. *Photosyn. Res.* 126, 111–134. doi: 10.1007/s11120-014-0065-x

Chen, C., Kazimir, J., and Cheniae, G. M. (1995). Calcium modulates the photoassembly of Photosystem II (Mn)4-clusters by preventing ligation of nonfunctional high-valency states of manganese. *Biochemistry* 34, 13511–13526. doi: 10.1021/bi00041a031

Clarke, J. T., Warnock, R. C. M., and Donoghue, P. C. J. (2011). Establishing a time-scale for plant evolution. *New Phytol.* 192, 266–301. doi: 10.1111/j.1469-8137.2011.03794.x

Cohen, R. O., Nixon, P. J., and Diner, B. A. (2007). Participation of the C-terminal region of the D1-polypeptide in the first steps in the assembly of the Mn_4Ca cluster of Photosystem II. *J. Biol. Chem.* 282, 7209–7218. doi: 10.1074/jbc.M606255200

Collins, A. M., Xin, Y., and Blankenship, R. E. (2009). Pigment organization in the photosynthetic apparatus of *Roseiflexus castenholzii*. *Biochim. Biophys. Acta* 1787, 1050–1056. doi: 10.1016/j.bbabio.2009.02.027

Criscuolo, A., and Gribaldo, S. (2011). Large-scale phylogenomic analyses indicate a deep origin of primary plastids within cyanobacteria. *Mol. Biol. Evol.* 28, 3019–3032. doi: 10.1093/molbev/msr108

Crowe, S. A., Dossing, L. N., Beukes, N. J., Bau, M., Kruger, S. J., Frei, R., et al. (2013). Atmospheric oxygenation three billion years ago. *Nature* 501, 535–538. doi: 10.1038/nature12426

Dasgupta, J., Ananyev, G. M., and Dismukes, G. C. (2008). Photoassembly of the water-oxidizing complex in Photosystem II. *Coordin. Chem. Rev.* 252, 347–360. doi: 10.1016/j.ccr.2007.08.022

Dasgupta, J., Tyryshkin, A. M., and Dismukes, G. C. (2007). ESEEM spectroscopy reveals carbonate and an N-donor protein-ligand binding to Mn^{2+} in the photoassembly reaction of the Mn_4Ca cluster in Photosystem II. *Angew. Chem. Int. Edit.* 46, 8028–8031. doi: 10.1002/anie.200702347

Dau, H., and Haumann, M. (2008). The manganese complex of Photosystem II in its reaction cycle—Basic framework and possible realization at the atomic level. *Coordin. Chem. Rev.* 252, 273–295. doi: 10.1016/j.ccr.2007.09.001

De Las Rivas, J., and Barber, J. (2004). Analysis of the structure of the PsbO protein and its implications. *Photosyn. Res.* 81, 329–343. doi: 10.1023/B:PRES.0000036889.44048.e4

Deisenhofer, J., Epp, O., Miki, K., Huber, R., and Michel, H. (1984). X-ray structure analysis of a membrane protein complex electron density map at 3 Å resolution and a model of the chromophores of the photosynthetic reaction center from *Rhodopseudomonas viridis*. *J. Mol. Biol.* 180, 385–398. doi: 10.1016/S0022-2836(84)80011-X

Di Costanzo, L., Flores, L. V. Jr, and Christianson, D. W. (2006). Stereochemistry of guanidine-metal interactions: implications for L-arginine-metal interactions in protein structure and function. *Proteins* 65, 637–642. doi: 10.1002/prot.21127

Dismukes, G. C., Klimov, V. V., Baranov, S. V., Kozlov, Y. N., DasGupta, J., and Tyryshkin, A. (2001). The origin of atmospheric oxygen on earth: the innovation of oxygenic photosynthesis. *Proc. Natl. Acad. Sci. U.S.A.* 98, 2170–2175. doi: 10.1073/pnas.061514798

Dobáková, M., Tichy, M., and Komenda, J. (2007). Role of the PsbI protein in Photosystem II assembly and repair in the cyanobacterium *Synechocystis* sp. PCC 6803. *Plant Physiol.* 145, 1681–1691. doi: 10.1104/pp.107.107805

Ferreira, K. N., Iverson, T. M., Maghlaoui, K., Barber, J., and Iwata, S. (2004). Architecture of the photosynthetic oxygen-evolving center. *Science* 303, 1831–1838. doi: 10.1126/science.1093087

Fischer, W. W., Hemp, J., and Johnson, J. E. (2015). Manganese and the evolution of photosynthesis. *Origins Life Evol. B* 45, 351–357. doi: 10.1007/s11084-015-9442-5

Gan, F., Zhang, S., Rockwell, N. C., Martin, S. S., Lagarias, J. C., and Bryant, D. A. (2014). Extensive remodeling of a cyanobacterial photosynthetic apparatus in far-red light. *Science* 345, 1312–1317. doi: 10.1126/science.1256963

Golubic, S., Sergeev, V. N., and Knoll, A. H. (1995). Mesoproterozoic archaeoellipsoides: akinetes of heterocystous cyanobacteria. *Lethaia* 28, 285–298. doi: 10.1111/j.1502-3931.1995.tb01817.x

Gould, S. B., Waller, R. R., and McFadden, G. I. (2008). Plastid evolution. *Annu. Rev. Plant Biol.* 59, 491–517. doi: 10.1146/annurev.arplant.59.032607.092915

Gupta, R. S., and Khadka, B. (2016). Evidence for the presence of key chlorophyll-biosynthesis-related proteins in the genus *Rubrobacter* (phylum Actinobacteria) and its implications for the evolution and origin of photosynthesis. *Photosyn. Res.* 127, 201–218. doi: 10.1007/s11120-015-0177-y

Harel, A., Karkar, S., Cheng, S., Falkowski, P. G., and Bhattacharya, D. (2015). Deciphering primordial cyanobacterial genome functions from protein network analysis. *Curr. Biol.* 25, 628–634. doi: 10.1016/j.cub.2014.12.061

He, G., Zhang, H., King, J. D., and Blankenship, R. E. (2014). Structural analysis of the homodimeric reaction center complex from the photosynthetic green sulfur bacterium *Chlorobaculum tepidum*. *Biochemistry* 53, 4924–4930. doi: 10.1021/bi5006464

Hessa, T., Meindl-Beinker, N. M., Bernsel, A., Kim, H., Sato, Y., Lerch-Bader, M., et al. (2007). Molecular code for transmembrane-helix recognition by the Sec61 translocon. *Nature* 450, 1026–1030. doi: 10.1038/nature06387

Hohmann-Marriott, M. F., and Blankenship, R. E. (2011). Evolution of photosynthesis. *Annu. Rev. Plant Biol.* 62, 515–548. doi: 10.1146/annurev-arplant-042110-103811

Hwang, H. J., Dilbeck, P., Debus, R. J., and Burnap, R. L. (2007). Mutation of arginine 357 of the CP43 protein of Photosystem II severely impairs the catalytic S-state cycle of the H_2O oxidation complex. *Biochemistry* 46, 11987–11997. doi: 10.1021/bi701387b

Ishikita, H., Saenger, W., Biesiadka, J., Loll, B., and Knapp, E. W. (2006). How photosynthetic reaction centers control oxidation power in chlorophyll pairs P680, P700, and P870. *Proc. Natl. Acad. Sci. U.S.A.* 103, 9855–9860. doi: 10.1073/pnas.0601446103

Iverson, T. M. (2006). Evolution and unique bioenergetic mechanisms in oxygenic photosynthesis. *Curr. Opin. Chem. Biol.* 10, 91–100. doi: 10.1016/j.cbpa.2006.02.013

Jordan, P., Fromme, P., Witt, H. T., Klukas, O., Saenger, W., and Krauss, N. (2001). Three-dimensional structure of cyanobacterial Photosystem I at 2.5 Å resolution. *Nature* 411, 909–917. doi: 10.1038/35082000

Kalman, L., Lobrutto, R., Allen, J. P., and Williams, J. C. (1999). Modified reaction centres oxidize tyrosine in reactions that mirror Photosystem II. *Nature* 402, 696–699. doi: 10.1038/45300

Kamiya, N., and Shen, J. R. (2003). Crystal structure of oxygen-evolving Photosystem II from *Thermosynechococcus vulcanus* at 3.7 Å resolution. *Proc. Natl. Acad. Sci. U.S.A.* 100, 98–103. doi: 10.1073/pnas.0135651100

Knoll, A. H. (2015). Paleobiological perspectives on early microbial evolution. *Cold Spring Harb. Perspect. Biol.* 7:a018093. doi: 10.1101/cshperspect.a018093

Komenda, J., Reisinger, V., Müller, B. C., Dobáková, M., Granvogl, B., and Eichacker, L. A. (2004). Accumulation of the D2 protein is a key regulatory step for assembly of the Photosystem II reaction center complex in *Synechocystis* PCC 6803. *J. Biol. Chem.* 279, 48620–48629. doi: 10.1074/jbc.M405725200

Komenda, J., Sobotka, R., and Nixon, P. J. (2012). Assembling and maintaining the Photosystem II complex in chloroplasts and cyanobacteria. *Curr. Opin. Plant Biol.* 15, 245–251. doi: 10.1016/j.pbi.2012.01.017

Kozlov, Y. N., Kazakova, A. A., and Klimov, V. V. (1997). Changes in the redox-potential and catalase activity of Mn^{2+} ions during formation of Mn-bicarbonate complexes. *Membr. Cell Biol.* 11, 115–120.

Levy, E. D., Boeri Erba, E., Robinson, C. V., and Teichmann, S. A. (2008). Assembly reflects evolution of protein complexes. *Nature* 453, 1262–1265. doi: 10.1038/nature06942

Lince, M. T., and Vermaas, W. (1998). Association of His117 in the D2 protein of Photosystem II with a chlorophyll that affects excitation-energy transfer efficiency to the reaction center. *Eur. J. Biochem.* 256, 595–602. doi: 10.1046/j.1432-1327.1998.2560595.x

Linke, K., and Ho, F. M. (2013). Water in Photosystem II: structural, functional and mechanistic considerations. *Biochim. Biophys. Acta* 1837, 14–32. doi: 10.1016/j.bbabio.2013.08.003

Lyons, T. W., Reinhard, C. T., and Planavsky, N. J. (2014). The rise of oxygen in earth's early ocean and atmosphere. *Nature* 506, 307–315. doi: 10.1038/nature13068

Mazor, Y., Borovikova, A., and Nelson, N. (2015). The structure of plant Photosystem I super-complex at 2.8 Å resolution. *Elife* 4:e07433. doi: 10.7554/eLife.07433

Mazor, Y., Nataf, D., Toporik, H., and Nelson, N. (2014). Crystal structures of virus-like Photosystem I complexes from the mesophilic cyanobacterium *Synechocystis* PCC 6803. *Elife* 3:e01496. doi: 10.7554/eLife.01496

Mix, L. J., Haig, D., and Cavanaugh, C. M. (2005). Phylogenetic analyses of the core antenna domain: investigating the origin of Photosystem I. *J. Mol. Evol.* 60, 153–163. doi: 10.1007/s00239-003-0181-2

Moss, D. A., Leonhard, M., Bauscher, M., and Mäntele, W. (1991). Electrochemical redox titration of cofactors in the reaction center from *Rhodobacter sphaeroides*. *FEBS Lett.* 283, 33–36. doi: 10.1016/0014-5793(91)80547-G

Murray, J. W. (2012). Sequence variation at the oxygen-evolving centre of Photosystem II: a new class of 'rogue' cyanobacterial D1 proteins. *Photosyn. Res.* 110, 177–184. doi: 10.1007/s11120-011-9714-5

Nickelsen, J., and Rengstl, B. (2013). Photosystem II assembly: from cyanobacteria to plants. *Annu. Rev. Plant Biol.* 64, 609–635. doi: 10.1146/annurev-arplant-050312-120124

Nisbet, E. G., and Fowler, C. F. R. (2014). "The early history of life," in *Treatise on Geochemistry,* 2nd Edn. eds K. D. M. McConnaghay and W. H. Schlesinger (Amsterdam: Elsevier Science), 1–42.

Nitschke, W., and Rutherford, A. W. (1991). Photosynthetic reaction centers - variations on a common structural theme. *Trends Biochem. Sci.* 16, 241–245. doi: 10.1016/0968-0004(91)90095-D

Nitschke, W., van Lis, R., Schoepp-Cothenet, B., and Baymann, F. (2010). The "green" phylogenetic clade of rieske/cytb complexes. *Photosyn. Res.* 104, 347–355. doi: 10.1007/s11120-010-9532-1

Nixon, P. J., and Diner, B. A. (1992). Aspartate-170 of the Photosystem II reaction center polypeptide D1 is involved in the assembly of the oxygen-evolving manganese cluster. *Biochemistry* 31, 942–948. doi: 10.1021/bi00118a041

Oh-oka, H., Kamei, S., Matsubara, H., Iwaki, M., and Itoh, S. (1995). Two molecules of cytochrome *c* function as the electron donors to P840 in the reaction center complex isolated from a green sulfur bacterium, *Chlorobium tepidum*. *FEBS Lett.* 365, 30–34. doi: 10.1016/0014-5793(95)00433-A

Olson, J. M., and Pierson, B. K. (1987). Origin and evolution of photosynthetic reaction centers. *Origins Life Evol. B* 17, 419–430. doi: 10.1007/BF02386479

Olson, J. M., and Raymond, J. (2003). The FMO protein is related to PscA in the reaction center of green sulfur bacteria. *Photosyn. Res.* 75, 277–285. doi: 10.1023/A:1023998000396

Olson, J. M. (1981). Evolution of photosynthetic reaction centers. *BioSystems.* 14, 89–94. doi: 10.1016/0303-2647(81)90024-1

Ovchinnikov, Y. A., Abdulaev, N. G., Shmuckler, B. E., Zargarov, A. A., Kutuzov, M. A., Telezhinskaya, I. N., et al. (1988a). Photosynthetic reaction centre of *Chloroflexus aurantiacus*. Primary structure of M-subunit. *FEBS Lett.* 232, 364–368. doi: 10.1016/0014-5793(88)80770-1

Ovchinnikov, Y. A., Abdulaev, N. G., Zolotarev, A. S., Shmukler, B. E., Zargarov, A. A., Kutuzov, M. A., et al. (1988b). Photosynthetic reaction centre of *Chloroflexus aurantiacus* I. Primary structure of L-subunit. *FEBS Lett.* 231, 237–242. doi: 10.1016/0014-5793(88)80739-7

Pagliano, C., Saracco, G., and Barber, J. (2013). Structural, functional and auxiliary proteins of Photosystem II. *Photosyn. Res.* 116, 167–188. doi: 10.1007/s11120-013-9803-8

Parfrey, L. W., Grant, J., Tekle, Y. I., Lasek-Nessel-Quist, E., Morrison, H. G., Sogin, L. M., et al. (2010). Broadly sampled multigene analyses yield a well-resolved eukaryotic tree of life. *Syst. Biol.* 59, 518–533. doi: 10.1093/sysbio/syq037

Perreault, N. N., Greer, C. W., Andersen, D. T., Tille, S., Lacrampe-Couloume, G., Lollar, B. S., et al. (2008). Heterotrophic and autotrophic microbial populations in cold perennial springs of the high arctic. *Appl. Environ. Microbiol.* 74, 6898–6907. doi: 10.1128/AEM.00359-08

Planavsky, N. J., Asael, D., Hofmann, A., Reinhard, C. T., Lalonde, S. V., Knudsen, A., et al. (2014). Evidence for oxygenic photosynthesis half a billion years before the great oxidation event. *Nat. Geosci.* 7, 283–286. doi: 10.1038/ngeo2122

Rappaport, F., Guergova-Kuras, M., Nixon, P. J., Diner, B. A., and Lavergne, J. (2002). Kinetics and pathways of charge recombination in Photosystem II. *Biochemistry* 41, 8518–8527. doi: 10.1021/bi025725p

Raymond, J., and Blankenship, R. E. (2008). The origin of the oxygen-evolving complex. *Coord. Chem. Rev.* 252, 377–383. doi: 10.1016/j.ccr.2007.08.026

Raymond, J., Siefert, J. L., Staples, C. R., and Blankenship, R. E. (2004). The natural history of nitrogen fixation. *Mol. Biol. Evol.* 21, 541–554. doi: 10.1093/molbev/msh047

Rosing, M. T. (1999). ^{13}C-depleted carbon microparticles in >3700-Ma sea-floor sedimentary rocks from west Greenland. *Science* 283, 674–676. doi: 10.1126/science.283.5402.674

Rutherford, A. W., and Faller, P. (2003). Photosystem II: evolutionary perspectives. *Philos. Trans. R. Soc. B Biol. Sci.* 358, 245–253. doi: 10.1098/rstb.2002.1186

Rutherford, A. W., and Nitschke, W. (1996). "Photosystem II and the quinone-iron-containing reaction centers," in *Origin and Evolution of Biological Energy Conversion,* ed H. Baltscheffsky (New York, NY: VCH), 143–175.

Sadekar, S., Raymond, J., and Blankenship, R. E. (2006). Conservation of distantly related membrane proteins: photosynthetic reaction centers share a common structural core. *Mol. Biol. Evol.* 23, 2001–2007. doi: 10.1093/molbev/msl079

Satkoski, A. M., Beukes, N. J., Li, W., Beard, B. L., and Johnson, C. M. (2015). A redox-stratified ocean 3.2 billion years ago. *Earth Planet. Sci. Lett.* 430, 43–53. doi: 10.1016/j.epsl.2015.08.007

Sauer, K., and Yachandra, V. K. (2002). A possible evolutionary origin for the Mn_4 cluster of the photosynthetic water oxidation complex from natural MnO_2 precipitates in the early ocean. *Proc. Natl. Acad. Sci. U.S.A.* 99, 8631–8636. doi: 10.1073/pnas.132266199

Saw, J. H. W., Schatz, M., Brown, M. V., Kunkel, D. D., Foster, J. S., Shick, H., et al. (2013). Cultivation and complete genome sequencing of *Gloeobacter kilaueensis* sp. nov., from a lava cave in *Kilauea caldera,* Hawai'i. *PLoS ONE* 8:e76376. doi: 10.1371/journal.pone.0076376

Schirrmeister, B. E., de Vos, J. M., Antonelli, A., and Bagheri, H. C. (2013). Evolution of multicellularity coincided with increased diversification of

cyanobacteria and the great oxidation event. *Proc. Natl. Acad. Sci. U.S.A.* 110, 1791–1796. doi: 10.1073/pnas.1209927110

Seppälä, S., Slusky, J. S., Lloris-Garcerá, P., Rapp, M., and Von Heijne, G. (2010). Control of membrane protein topology by a single C-terminal residue. *Science* 328, 1698–1700. doi: 10.1126/science.1188950

Service, R. J., Yano, J., McConnell, I., Hwang, H. J., Niks, D., Hille, R., et al. (2011). Participation of glutamate-354 of the CP43 polypeptide in the ligation of manganese and the binding of substrate water in Photosystem II. *Biochemistry* 50, 63–81. doi: 10.1021/bi1015937

Shih, P. M., Wu, D., Latifi, A., Axen, S. D., Fewer, D. P., Talla, E., et al. (2013). Improving the coverage of the cyanobacterial phylum using diversity-driven genome sequencing. *Proc. Natl. Acad. Sci. U.S.A.* 110, 1053–1058. doi: 10.1073/pnas.1217107110

Shimada, Y., Suzuki, H., Tsuchiya, T., Tomo, T., Noguchi, T., and Mimuro, M. (2009). Effect of a single-amino acid substitution of the 43 kDa chlorophyll protein on the oxygen-evolving reaction of the cyanobacterium *Synechocystis* sp. PCC 6803: analysis of the Glu354Gln mutation. *Biochemistry* 48, 6095–6103. doi: 10.1021/bi900317a

Sicora, C. I., Ho, F. M., Salminen, T., Styring, S., and Aro, E. M. (2009). Transcription of a "silent" cyanobacterial *psbA* gene is induced by microaerobic conditions. *Biochim. Biophys. Acta* 1787, 105–112. doi: 10.1016/j.bbabio.2008.12.002

Sievers, F., Wilm, A., Dineen, D. G., Gibson, T. J., Karplus, K., Li, W., et al. (2011). Fast, scalable generation of high-quality protein multiple sequence alignments using Clustal Omega. *Mol. Syst. Biol.* 7, 539. doi: 10.1038/msb.2011.75

Sousa, F. L., Shavit-Grievink, L., Allen, J. F., and Martin, W. F. (2013). Chlorophyll biosynthesis gene evolution indicates photosystem gene duplication, not photosystem merger, at the origin of oxygenic photosynthesis. *Genome Biol. Evol.* 5, 200–216. doi: 10.1093/gbe/evs127

Stengel, A., Gügel, I. L., Hilger, D., Rengstl, B., Jung, H., and Nickelsen, J. (2012). Initial steps of Photosystem II *de novo* assembly and preloading with manganese take place in biogenesis centers in *Synechocystis*. *Plant Cell* 24, 660–675. doi: 10.1105/tpc.111.093914

Strickler, M. A., Hwang, H. J., Burnap, R. L., Yano, J., Walker, L. M., Service, R. J., et al. (2008). Glutamate-354 of the CP43 polypeptide interacts with the oxygen-evolving Mn_4Ca cluster of Photosystem II: a preliminary characterization of the Glu354Gln mutant. *Philos. Trans. R. Soc. B Biol. Sci.* 363, 1179–1187. doi: 10.1098/rstb.2007.2213

Sugimoto, I., and Takahashi, Y. (2003). Evidence that the PsbK polypeptide is associated with the Photosystem II core antenna complex CP43. *J. Biol. Chem.* 278, 45004–45010. doi: 10.1074/jbc.M307537200

Sugiura, M., Ogami, S., Kusumi, M., Un, S., Rappaport, F., and Boussac, A. (2012). Environment of TyrZ in Photosystem II from *Thermosynechococcus elongatus* in which PsbA2 is the D1 protein. *J. Biol. Chem.* 287, 13336–13347. doi: 10.1074/jbc.M112.340323

Summerfield, T. C., Toepel, J., and Sherman, L. A. (2008). Low-oxygen induction of normally cryptic *psbA* genes in cyanobacteria. *Biochemistry* 47, 12939–12941. doi: 10.1021/bi8018916

Tabita, F. R., Satagopan, S., Hanson, T. E., Kreel, N. E., and Scott, S. S. (2008). Distinct form I, II, III, and IV Rubisco proteins from the three kingdoms of life provide clues about Rubisco evolution and structure/function relationships. *J. Exp. Bot.* 59, 1515–1524. doi: 10.1093/jxb/erm361

Tamura, N., and Cheniae, G. (1987). Photoactivation of the water-oxidizing complex in Photosystem II membranes depleted of Mn and extrinsic proteins. 1. Biochemical and kinetic characterization. *Biochim. Biophys. Acta* 890, 179–194. doi: 10.1016/0005-2728(87)90019-3

Tamura, N., Inoue, Y., and Cheniae, G. M. (1989). Photoactivation of the water-oxidizing complex in Photosystem II membranes depleted of Mn, Ca and extrinsic proteins. 2. Studies on the functions of Ca^{2+}. *Biochim. Biophys. Acta* 976, 173–181. doi: 10.1016/S0005-2728(89)80227-0

Thielges, M., Uyeda, G., Cámara-Artigas, A., Kálmán, L., Williams, J. C., and Allen, J. P. (2005). Design of a redox-linked active metal site: manganese bound to bacterial reaction centers at a site resembling that of Photosystem II. *Biochemistry* 44, 7389–7394. doi: 10.1021/bi050377n

Tomitani, A., Knoll, A. H., Cavanaugh, C. M., and Ohno, T. (2006). The evolutionary diversification of cyanobacteria: molecular-phylogenetic and paleontological perspectives. *Proc. Natl. Acad. Sci. U.S.A.* 103, 5442–5447. doi: 10.1073/pnas.0600999103

Tsukatani, Y., Romberger, S. P., Golbeck, J. H., and Bryant, D. A. (2012). Isolation and characterization of homodimeric Type-I reaction center complex from *candidatus Chloracidobacterium thermophilum*, an aerobic chlorophototroph. *J. Biol. Chem.* 287, 5720–5732. doi: 10.1074/jbc.M111.323329

Tyryshkin, A. M., Watt, R. K., Baranov, S. V., Dasgupta, J., Hendrich, M. P., and Dismukes, G. C. (2006). Spectroscopic evidence for Ca^{2+} involvement in the assembly of the Mn_4Ca cluster in the photosynthetic water-oxidizing complex. *Biochemistry* 45, 12876–12889. doi: 10.1021/bi061495t

Umena, Y., Kawakami, K., Shen, J. R., and Kamiya, N. (2011). Crystal structure of oxygen-evolving Photosystem II at a resolution of 1.9 Å. *Nature* 473, 55–60. doi: 10.1038/nature09913

Vasil'ev, S., and Bruce, D. (2000). Picosecond time-resolved fluorescence studies on excitation energy transfer in a histidine 117 mutant of the D2 protein of Photosystem II in *Synechocystis* 6803. *Biochemistry* 39, 14211–14218. doi: 10.1021/bi000476v

Vass, I., and Styring, S. (1991). pH-dependent charge equilibria between tyrosine-D and the S states in Photosystem II. Estimation of relative midpoint redox potentials. *Biochemistry* 30, 830–839. doi: 10.1021/bi00217a037

Von Heijne, G. (2006). Membrane-protein topology. *Nat. Rev. Mol. Cell Biol.* 7, 909–918. doi: 10.1038/nrm2063

Wegener, K. M., Nagarajan, A., and Pakrasi, H. B. (2015). An atypical *psbA* gene encodes a sentinel D1 protein to form a physiologically relevant inactive Photosystem II complex in cyanobacteria. *J. Biol. Chem.* 290, 3764–3774. doi: 10.1074/jbc.M114.604124

Williams, J. C., Alden, R. G., Murchison, H. A., Peloquin, J. M., Woodbury, N. W., and Allen, J. P. (1992). Effects of mutations near the bacteriochlorophylls in reaction centers from *Rhodobacter sphaeroides*. *Biochemistry* 31, 11029–11037. doi: 10.1021/bi00160a012

Williamson, A., Conlan, B., Hillier, W., and Wydrzynski, T. (2011). The evolution of Photosystem II: insights into the past and future. *Photosynth. Res.* 107, 71–86. doi: 10.1007/s11120-010-9559-3

Xiong, J., and Bauer, C. E. (2002). A cytochrome *b* origin of photosynthetic reaction centers: an evolutionary link between respiration and photosynthesis. *J. Mol. Biol.* 322, 1025–1037. doi: 10.1016/S0022-2836(02)00822-7

Yoon, H. S., Hackett, J. D., Ciniglia, C., Pinto, G., and Bhattacharya, D. (2004). A molecular timeline for the origin of photosynthetic eukaryotes. *Mol. Biol. Evol.* 21, 809–818. doi: 10.1093/molbev/msh075

Zeng, Y., Selyanin, V., Lukes, M., Dean, J., Kaftan, D., Feng, F., et al. (2015). Characterization of the microaerophilic, bacteriochlorophyll *a*-containing bacterium *Gemmatimonas phototrophica* sp. nov., and emended descriptions of the genus *Gemmatimonas* and *Gemmatimonas aurantiaca*. *Int. J. Syst. Evol. Microbiol.* 65, 2410–2419. doi: 10.1099/ijs.0.000272

Zeng, Y., Feng, F., Medová, H., Dean, J., and Koblížek, M. (2014). Functional Type 2 photosynthetic reaction centers found in the rare bacterial phylum Gemmatimonadetes. *Proc. Natl. Acad. Sci. U.S.A.* 111, 7795–7800. doi: 10.1073/pnas.1400295111

Zouni, A., Witt, H. T., Kern, J., Fromme, P., Krauss, N., Saenger, W., et al. (2001). Crystal structure of Photosystem II from synechococcus elongatus at 3.8 Å resolution. *Nature* 409, 739–743. doi: 10.1038/35055589

Conflict of Interest Statement: The author declares that the research was conducted in the absence of any commercial or financial relationships that could be construed as a potential conflict of interest.

frontiers in Plant Science

REVIEW
published: 03 May 2016
doi: 10.3389/fpls.2016.00578

Photoactivation: The Light-Driven Assembly of the Water Oxidation Complex of Photosystem II

Han Bao and Robert L. Burnap *

Department of Microbiology and Molecular Genetics, Oklahoma State University, Stillwater, OK, USA

Photosynthetic water oxidation is catalyzed by the Mn_4CaO_5 cluster of photosystem II. The assembly of the Mn_4O_5Ca requires light and involves a sequential process called photoactivation. This process harnesses the charge-separation of the photochemical reaction center and the coordination environment provided by the amino acid side chains of the protein to oxidize and organize the incoming manganese ions to form the oxo-bridged metal cluster capable of H_2O-oxidation. Although most aspects of this assembly process remain poorly understood, recent advances in the elucidation of the crystal structure of the fully assembled cyanobacterial PSII complex help in the interpretation of the rich history of experiments designed to understand this process. Moreover, recent insights on the structure and stability of the constituent ions of the Mn_4CaO_5 cluster may guide future experiments. Here we consider the literature and suggest possible models of assembly including one involving single Mn^{2+} oxidation site for all Mn but requiring ion relocation.

Keywords: photosystem II, water oxidation, manganese, oxygen evolution, photoactivation, EPR, oxo bridge

OPEN ACCESS

Edited by:
Roman Sobotka, Czech Academy of Sciences, Czech Republic

Reviewed by:
Peter Julian Nixon, Imperial College London, UK
Charles Yocum, University of Michigan, USA

***Correspondence:**
Robert L. Burnap
rob.burnap@okstate.edu

Specialty section:
This article was submitted to Plant Cell Biology, a section of the journal Frontiers in Plant Science

Received: *19 February 2016*
Accepted: *14 April 2016*
Published: *03 May 2016*

Citation:
Bao H and Burnap RL (2016) Photoactivation: The Light-Driven Assembly of the Water Oxidation Complex of Photosystem II. Front. Plant Sci. 7:578. doi: 10.3389/fpls.2016.00578

INTRODUCTION

A decline in the photosynthetic activity of oxygenic photosynthetic organisms due to light stress has been described as photoinhibition (Björkman, 1981; Osmond, 1981; Powles and Björkman, 1981; Ohad et al., 1984). The primary damage occurs within the reaction center of Photosystem II (PSII). It is distinct from the concurrent oxidative damage to the machinery of protein synthesis, which compounds the problem since *de novo* protein synthesis is necessary for the replacement of damaged PSII proteins (Adir et al., 2003; Lupínková and and Komenda, 2004; Nishiyama et al., 2004; Edelman and Mattoo, 2008). The precise mechanism of PSII photoinhibition *in vivo* remains under debate (Adir et al., 2003; Edelman and Mattoo, 2008; Vass and Cser, 2009). Despite this uncertainty, it is evident that the D1 reaction center protein is the primary target for photodamage and this leads to an increased turnover rate of D1, in comparison to other PSII proteins, upon exposure to high light intensities (Ohad et al., 1984). To cope with light stress, all oxygenic photosynthetic organisms have developed protective mechanisms both to minimize the effects of exposure to excess light and to efficiently repair the damage when it occurs. Overall, the efficiency of photosynthetic electron transfer decreases markedly only when the rate of damage exceeds the rate of repair. A crucial phase of the *de novo* biogenesis of PSII, as well as the damage repair process, is the assembly of the Mn_4CaO_5 complex. This involves the oxidative assembly of Mn^{2+} and Ca^{2+} ions into the coordination environment of the PSII water-oxidation complex (WOC) in a light-driven

process called photoactivation (for previous reviews, see Ono, 2001; Burnap, 2004; Dismukes et al., 2005).

PSII DAMAGE AND D1 REPLACEMENT

Replacement of Damaged D1

The entire process of PSII damage-repair cycle can be described as follows: (i) damage occurring to PSII, (ii) signaling of this damage, (iii) monomerization of PSII dimer and partial disassembly of PSII monomer, (iv) degradation of D1 and insertion of a newly synthesized D1 into PSII sub-complex, and (v) reassembly of holoenzyme and photoactivation of the Mn_4CaO_5 cluster (Aro et al., 1993; Koivuniemi et al., 1995; Nixon et al., 2005; **Figure 1**). We briefly outline some features of the overall PSII assembly and repair process to place the assembly of the Mn_4CaO_5 cluster in context. For more comprehensive information the reader is advised to examine several recent review articles (Nixon et al., 2010; Becker et al., 2011; Nickelsen and Rengstl, 2013; Heinz et al., 2016).

Monomerization of dimeric PSII has been suggested to result from the detachment or rearrangement of PsbO, one of three luminal extrinsic subunits of PSII (Nixon et al., 2010). The basis of this assessment is the failure to accumulate dimeric PSII in a mutant of *Synechocystis* sp. PCC 6803 (hereafter *Synechocystis* 6803) lacking PsbO (Komenda et al., 2010). In plants and green algae, it has also been proposed that PSII core phosphorylation might trigger disassembly of PSII dimer to form monomer by acting alone or in conjunction with PsbO (Puthiyaveetil and Kirchhoff, 2013). Detachment of CP43 from PSII monomer leads to the formation of so-called RC47 complex which is a pivotal sub-complex for further replacement of damaged D1 during PSII repair (Komenda et al., 2005). Given the fact that PsbO functions as PSII manganese-stabilizing protein and CP43 participates with D1 in ligating the Mn_4CaO_5 cluster, it is conceivable that photodamage to Mn_4CaO_5 cluster might cause the detachment of these two subunits. It is also interesting to note that the assembly and disassembly of the Mn_4O_5Ca regulates the coupling of the phycobilisome to the cyanobacterial PSII reaction center such that centers without an intact metal cluster are not efficiently coupled with respect to energy transfer from the phycobilisome (Hwang et al., 2008).

Radioactive pulse-chase experiments (Komenda and Barber, 1995) showed that translation inhibitors slow D1 degradation, suggesting that D1 degradation and new D1 synthesis are synchronized. Increased turnover of D1 could be a generalized response to damage-promoting light conditions, with all D1 copies prone to increased probability of replacement or there could be a specific targeting mechanism that replaces only damaged D1 copies. Intuitively, a targeting mechanism seems more likely. However, despite good circumstantial evidence, direct evidence for the specific targeting of PSII centers with damaged D1 has not been obtained, mainly because it is technically difficult to separately track damaged and undamaged forms of D1 through the replacement process. Recently, targeting has been inferred from experiments where cells are allowed to express two alternative forms of the D1 protein in the same cell, with one wild-type form and the other a light-sensitive form. The analysis indicates that only the light-sensitive version of D1 and not the wild-type version is turned over very rapidly (Nagarajan and Burnap, 2014).

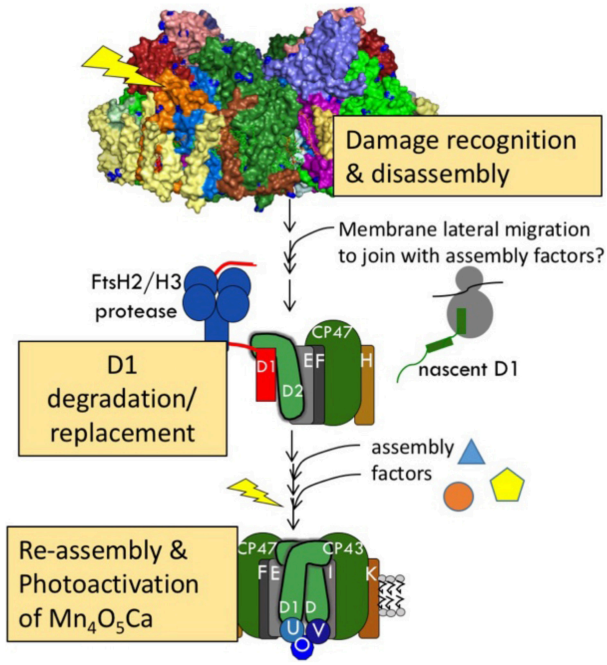

FIGURE 1 | Schematic repair pathway for photodamaged PSII. The process can be divided into the three main phases: (1) damage recognition and partial disassembly of photodamage PSII complexes, (2) D1 degradation and replacement, and (3) reassembly of the subunits and light-driven assembly (photoactivation) of the Mn_4O_5Ca metal cluster.

FtsH proteases play an important role in degradation of damaged D1 during PSII repair (Mann et al., 2000; Bailey et al., 2002; Silva et al., 2003). Mutants lacking FtsH proteases display impaired D1 degradation and thus accumulate damaged D1 (Bailey et al., 2002; Silva et al., 2003; Komenda et al., 2006; Kato et al., 2009). Additionally, the AAA-type protease, FtsH is crucial for the degradation of D1 protein (Silva et al., 2003; Nixon et al., 2005). Without it efficient repair ceases. How newly synthesized D1 subunit is integrated into the RC47 sub-complex is still a matter of debate. Studies in chloroplasts have led to the conclusion that D1 replacement occurs co-translationally (Zhang et al., 1999, 2000). Following initiation of *psbA* mRNA translation, nascent D1 protein is targeted to the thylakoid membrane by the chloroplast signal recognition particle (cpSRP54) and then released after interacting with a putative SRP receptor (Zhang and Aro, 2002). It was demonstrated that cpSRP54 can be efficiently crosslinked to nascent D1 chains that are still attached to ribosomes (Nilsson et al., 1999; Nilsson and van Wijk, 2002). Polypeptide chain elongation of the docked complex results in precursor D1 (pD1, see below) insertion into the thylakoid translocation channel (cpSecY) (Zhang et al., 2001). During translocation, the transmembrane domains of nascent pD1 appear to interact with existing PSII sub-complexes containing D2, PsbI, and

cytochrome b_{559}, CP47, but lacking CP43 (van Wijk et al., 1996, 1997; Zhang and Aro, 2002) and subsequently incorporate into PSII complex. Pulse-labeling studies indicated that this association already exists before the synthesis of the pD1 protein is complete (Zhang et al., 1999, 2000).

There is still uncertainty about where the repair of damaged PSII takes place and it is worth noting that PSII assembly for repair and PSII *de novo* assembly appear to involve distinct PSII assembly pathways (reviewed in Heinz et al., 2016). Regions of connection between the plasma membrane and thylakoid membrane appear to be sites of PSII assembly (Klinkert et al., 2004; Schottkowski et al., 2009; Nickelsen et al., 2011; Stengel et al., 2012; Heinz et al., 2016). These studies have led to the suggestion that regions of the thylakoid membrane are differentiated by being specifically enriched in assembly proteins, which are designated PratA-defined membranes (PDMs) being especially relevant to the photoassembly of the Mn_4CaO_5 as discussed below. The idea of localized region of the thylakoid membrane enriched in assembly factors fits with the report that FtsH proteins are localized in thylakoids (Komenda et al., 2006; Krynická et al., 2014) in distinct patches that are less enriched in chlorophyll (Sacharz et al., 2015). Thus, from an ultrastructural perspective, a reasonable working hypothesis is that the repair processes, including photoactivation, are located in discreet regions of the thylakoid enriched in the factors facilitating reassembly.

Processing of the D1 Carboxy Terminus

D1 protein is synthesized in a precursor form (pD1) with a carboxyl-terminal extension (C-terminal) whose length and sequence vary among different organisms (Diner et al., 1988b; Seibert et al., 1989; Nixon et al., 1992; Anbudurai et al., 1994; Shestakov et al., 1994; Ivleva et al., 2000; Zhang and Aro, 2002). The pD1 protein is subsequently cleaved on the carboxyl side of residue Ala344, resulting in the removal of the extension (Nixon and Diner, 1992; Nixon et al., 1992), which is carried out by carboxy terminal protease (CtpA), which is dedicated to this post-translational processing (Diner et al., 1988a; Seibert et al., 1989; Nixon et al., 1992; Taguchi et al., 1995; Trost et al., 1997; Ivleva et al., 2000). In plants, an extension consisting of 9 residues is cleaved in a single proteolytic step, whereas in *Synechocystis* 6803 a 16 amino acid extension is removed in two steps (Komenda et al., 2007; Satoh and Yamamoto, 2007). Although the extension is not essential for assembly of functional PSII complex (Nixon et al., 1992; Satoh and Yamamoto, 2007), it is required for optimal photosynthetic performance implying that it might plays an important role in PSII repair (Diner, 2001). For example, *Synechocystis* mutants lacking the C-terminal extension exhibit decreased fitness and are more susceptible to photodamage (Ivleva et al., 2000; Kuviková et al., 2005). D1 maturation is a prerequisite for assembly of the Mn_4CaO_5 cluster (Diner et al., 1991; Nixon et al., 1992) and binding of the PSII extrinsic proteins (Roose and Pakrasi, 2004), thus is essential for oxygen evolution activity (Taylor et al., 1988). The extension must be cleaved before the Mn_4CaO_5 cluster can be functionally assembled (Nixon et al., 1992; Anbudurai et al., 1994; Komenda et al., 2007), suggesting the C-terminus of the mature D1 polypeptide is involved in assembly of the Mn_4CaO_5 cluster. In recent X-ray structures (Umena et al., 2011), Ala344 is shown to coordinate the Mn(2) and the Ca atom of Mn_4CaO_5 through its backbone α-carboxyl moiety. These assignments are consistent with mutational analysis that had originally led to this suggestion (Diner et al., 1991; Nixon et al., 1992)

Accessory Proteins for PSII Assembly and Repair

Numerous accessory proteins are being discovered to have roles in the assembly, maturation and repair of the PSII complex (Shestakov et al., 1994; Inagaki et al., 2001; Yamamoto, 2001; Kashino et al., 2002; Silva et al., 2003; Roose and Pakrasi, 2004; Keren et al., 2005; Chen et al., 2006; Komenda et al., 2006; Nowaczyk et al., 2006; Park et al., 2007). All full accounting of these is beyond the scope of this review and for the most recent summary of the numerous assembly factors the reader should consult (Heinz et al., 2016). Biochemical approaches (e.g., Nowaczyk et al., 2006; Mamedov et al., 2007) and genetic analyses (e.g., Klinkert et al., 2004; Liu et al., 2011b), have led to the identification of proteins facilitating the assembly of PSII that could be of specific relevance to the process of photoactivation, most notably, PratA and Psb27. Deletion of *pratA* results in a dramatic decrease in the accumulation of PSII in *Synechocystis* and a defect in the processing of the D1 C-terminus by CtpA. Moreover, PratA interacts with the D1 C-terminus and may bind Mn^{2+} possibly facilitating the assembly of the Mn_4O_5Ca (Klinkert et al., 2004; Schottkowski et al., 2009). Psb27 is found to bind to forms of the PSII complex thought to represent assembly and/or disassembly intermediates (Roose and Pakrasi, 2004; Nowaczyk et al., 2006; Mamedov et al., 2007; Liu et al., 2011a,b) and deletion of the protein affects photoactivation of the complex (Roose and Pakrasi, 2007). Thus, Psb27 and PratA are especially good candidates for facilitating photoactivation of the Mn_4CaO_5. Indeed, there is good reason to believe that the published *in vitro* assembly experiments are missing assembly cofactors, which may explain why the yield of active PSII centers produced by *in vitro* photoactivation of Mn_4CaO_5 clusters by biochemical methods is invariably lower than intact cells as discussed below.

MECHANISM OF PHOTOACTIVATION

Coordinating Residues of Mn_4CaO_5 Cluster

According to 1.9 Å PSII crystal structure (Umena et al., 2011), Mn_4O_5Ca cluster coordinated by one nitrogen ligand from D1-His332 and six carboxylate ligands from D1-Asp170, D1-Glu189, D1-Glu333, D1-Asp342, D-Ala344, CP43-Glu354 (**Figure 2**). Three of them, D1-Glu333, D1-Asp342, and CP43-Glu354, form μ–carboxylate bridges between Mn (Mn(1)–Mn(2) (Asp342), Mn(2)–Mn(3) (CP43-Glu354), and Mn(3)–Mn(4) (Glu333)). D1-Asp170 and the C-terminal carboxylate group of D1-Ala344 bridge Ca with Mn(4) and Mn(2), respectively. The Mn(4) has been referred to as the "dangler manganese" (Peloquin et al., 2000) because it is located outside the semi-cubic cluster formed by the other four metals of the cluster, Ca, Mn(1), Mn(2), and Mn(3). Both D1-Glu189 and D1-His332 serve as monodentate

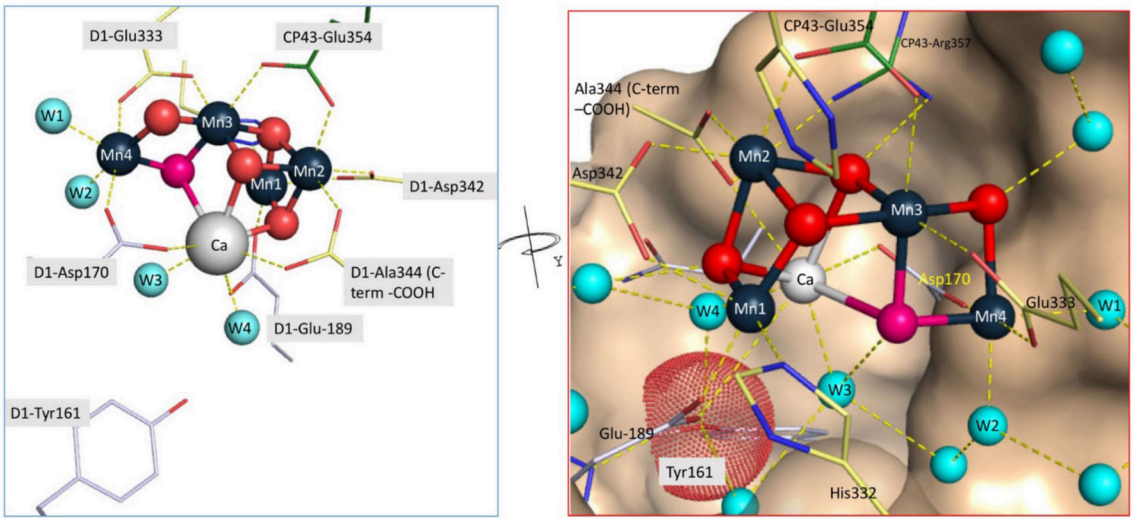

FIGURE 2 | Coordination environment of the assembled Mn_4CaO_5 H_2O-oxidation complex of PSII. The high affinity site of Mn^{2+} binding and photooxidation during the initial phase of the assembly process minimally involves D1-Asparate170 (Nixon and Diner, 1992; Campbell et al., 2000) located in the vicinity of Mn4 in the final complex. The initial state of the complex for photoassembly appears to involve the binding of one Mn^{2+} at the high affinity site (Ono and Mino, 1999) together with one Ca^{2+} ion that modulates the ligand environment of the Mn^{2+} possibly via the formation of a bridging water or hydroxide, although the presence of the Ca^{2+} does not appreciably change the binding affinity of the Mn^{2+} at the high affinity site (Tyryshkin et al., 2006). The C-terminal polypeptide backbone carboxylate of D1-Alanine344, which is available only following proteolytic cleavage of the precursor form of the D1 protein (pD1), is also critical for the assembly process, although it too does not markedly alter the binding of Mn^{2+} at the high affinity site (Nixon et al., 1992; Cohen et al., 2007). Figures developed upon 3D coordinates (PDB 4UB6) of the published X-ray diffraction model (Umena et al., 2011).

ligands to Mn(1). The D1-Asp170 plays an especially crucial role during the assembly process since it helps form the so-called "high affinity site" involved in the initial photooxidation of Mn^{2+} (Nixon and Diner, 1992).

Two-Quantum Model of Photoactivation

The assembly of the metals of the Mn_4O_5Ca requires light to induce charge separation to oxidize and strongly bind the Mn ions. It is important to note that the assembly is an oxidative process that involves removal of electrons from the Mn ions and the formation of oxo-bridges between the metals of the cluster with the bridging oxygen atoms (shown in red, **Figure 2**) derived from water molecular coordinated to the metal ions. The oxidative assembly utilizes the same light-driven charge separation events within the photochemical reaction center that subsequently drive photosynthetic electron transfer in the fully functional enzyme. Apart from the definition of the Mn-binding site characteristics and some very well-defined kinetic features that govern the development of H_2O-oxidation activity, photoactivation remains poorly understood. The quantum efficiency of photoactivation is very low, typically in the range of ∼1%, which is much lower than for photosynthetic water oxidation in the assembled PSII (>90%) even in intact systems (Cheniae and Martin, 1971a,b; Cheniae and Martin, 1972; Radmer and Cheniae, 1971; Ono and Inoue, 1982, 1983). The kinetic model of photoactivation, termed as "two-quantum series model" (Radmer and Cheniae, 1971), was originally observed during photoactivation as a function of either light intensity or flash interval using fixed numbers of Xe light flashes (Cheniae and Martin, 1971a,b; Cheniae and Martin, 1972; Radmer and Cheniae, 1971). These pioneering studies showed that the quantum efficiency for photoactivation is low at low light intensities, reached a maximum at intermediate intensities, and were again low at high light intensities. Equivalently, the quantum efficiency is low when saturating, single turnover flashes are given at long intervals, maximum at intermediate flash frequencies (∼1 per second), and were again low when the flashes are given with short intervals between flashes. From these features, Cheniae derived a minimal model, the so-called two-quantum model that postulated the light-induced Mn assembly with at least one unstable chemical intermediate as depicted in **Figure 3**. The first photoevent involves the high quantum yield photooxidation of a single Mn^{2+} to Mn^{3+} ion (Ono and Mino, 1999) at the unique high affinity Mn-binding site (see below). The resultant Mn^{3+} species (B) can spontaneously convert to C in the dark with a 100–150 mshalf-time, with a kinetic constant designated k_R in the scheme in **Figure 3**. A second quantum of light must be absorbed to convert the nascent complex into the first stable intermediate D as shown in **Figure 3** as C⇒D. The formation of a labile intermediate, $t_{1/2}$ ∼1–2 s, accounted for the optimum in light intensity or, alternatively, flash frequency, utilized for the assembly process. Photoactivation using saturating single turnover flashes is optimal with flash spacing of ∼1 s, which is enough time to allow the dark rearrangement to occur (k_R), but short enough to minimize the decay of the intermediate(s). If, however, the flash interval is too long, the second flash is not in time to trap forward progress and the reactants decay (k_{D1}, K_{D2}, **Figure 3**).

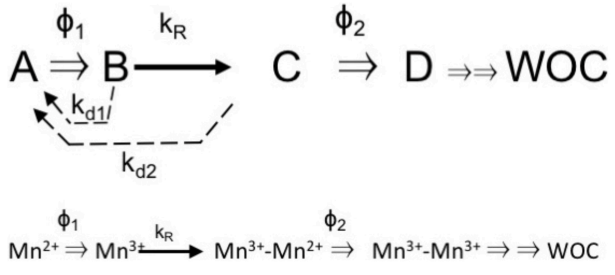

FIGURE 3 | Kinetic scheme of basic two-quantum mechanism. Double arrows indicate light-activated processes with the quantum efficiencies Φ_1 and Φ_2 representing the first and second photooxidative events in the assembly sequence, k_R representing the still ill-defined "dark" rearrangement, and k_{D1}, k_{D2} representing the decay of intermediates. After the initial two Mn are photoligated, subsequent Mn appear to be added with high quantum yield.

The molecular nature of the process occurring during this dark rearrangement period (B→C) is not clear, and its understanding is key to understanding the overall molecular mechanism. After the initial two Mn are photoligated, subsequent Mn appear to be added with high quantum yield.

Of the many examples providing experimental support for the two quantum mechanism, perhaps the most striking are the experiments of Miyao, which showed a minimal two quantum requirement in an experiment where as few as five flashes restored nearly 20% of the maximal activity (Miyaotokutomi and Inoue, 1992). This amounts to several percent assembly per flash, which is remarkable given that the typical per flash yield is often on the order of 1% or even lower. That experiment and others also showed that the instability of the intermediates could be minimized by preventing the back-reaction of the electrons from the acceptor side of the PSII reaction center (Miyao and Inoue, 1991; Miyaotokutomi and Inoue, 1992). This also fits with another early result showing that the intermediates of assembly are highly sensitive to reductant (Ono and Inoue, 1987) and fits with the concept that the formation of state C (eligible for utilizing the second quantum) occurs with low frequency and/or once formed, the quantum yield of photooxidation of the second Mn^{2+} occurs with low quantum yield (also see Miller and Brudvig, 1989, for relevant model).

It has been speculated the rearrangement (k_R) involves a protein conformational change required for the binding and subsequent photooxidation of the second Mn^{2+} (Chen et al., 1995a; Ananyev and Dismukes, 1996b; Qian et al., 1999; Burnap, 2004). However, if (B→C) is indeed a protein structural change, then it is unlikely a large scale conformational rearrangement since carboxy terminal ligands are already close to high affinity site ligand D1-Asp170 during the first photooxidation (A⇒B) (Cohen et al., 2007). Also, whether the dark unstable intermediate is B or C (or both) remains unresolved. Given this uncertainty, **Figure 3** shows both decays are possible (k_{D1} and k_{D2}) (Miller and Brudvig, 1989). The development of a highly sensitive and fast Clark-type oxygen electrode (Ananyev and Dismukes, 1996b) led to the assignment of additional photoactivation intermediates and has provided alternative parameter estimates for the kinetic components (Ananyev and Dismukes, 1996a,b, 1997; Zaltsman et al., 1997; Baranov et al., 2000, 2004). At the same time, the use of this apparatus makes comparisons difficult because to the different illumination regimes. Most of the original experiments utilized single turnover Xe flashes for actinic illumination. In contrast, the photoactivation studies using the fast Clark-type oxygen electrode employed 30 ms red LED pulses promote optimum yields of assembled center (Ananyev and Dismukes, 1996b). This relatively long duration of the LED light pulses allows greater mixing of different assembly states because of the possibility of having multiple "hits" per center per pulse. That said, the 30 ms duration of the pulse is relatively short with respect to the $t_{1/2}$ ~150 ms of the B→C rearrangement and therefore the majority of those centers in the initial state that were excited (i.e., those undergoing A⇒B), will not be ready to utilize the second quantum and would thus the LED pulse would be effectively similar to a single turnover flash distributed in time over the population of centers. Variations and refinements of the original two-quantum model have been advanced based upon alternative techniques for illumination and O_2 detection during photoactivation (Miller and Brudvig, 1989; Meunier et al., 1995; Ananyev and Dismukes, 1996b; Zaltsman et al., 1997; Hwang and Burnap, 2005). The multiflash experiments of Hwang and Burnap (2005) using staggered Xe single turnover flashes revealed a new kinetic intermediate, more rapid rearrangement, although where it is in the sequence could not be established owing to high miss factor (low quantum efficiency) and the associated de-phasing of the assembly during the flash induced assembly process.

Are the Complicated "Two-Quantum" Kinetics Of Photoactivation an Artifact of *In vitro* Experimental Procedures?

Many of the insights into the mechanism, including the nature of the cofactor requirements, were from experiments performed *in vitro* using biochemical techniques, including detergent solublization, that yield simplified PSII preparations. Such preparations allowed a range of information from the better definition of the affinity constants for the cofactors (Tamura and Cheniae, 1986, 1987; Miller and Brudvig, 1989; Tamura et al., 1989; Ananyev and Dismukes, 1996a,b, 1997; Zaltsman et al., 1997; Baranov et al., 2000, 2004) to the comparative efficiency of artificial electron acceptors (Miyao and Inoue, 1991; Miyaotokutomi and Inoue, 1992). However, the most efficient *in vitro* protocols explicitly involve the remove of extrinsic proteins or involve procedures that would also cause the loss of extrinsic proteins, although the authors may not have evaluated the degree to which this loss may have occurred. Importantly, the simplified preparations also likely lack the multiple assembly factors that are now identified. Since photoactivation is a low quantum yield process, even *in vivo,* it has been important for technical reasons to maximize the *in vitro* efficiency to estimate its kinetic parameters. For example, a Mn^{2+} concentration dependence assays require modest increments in yield, which can only be experimentally distinguished if the procedures provide materials with sufficiently high rates of O_2 evolution to allow

discrimination beyond to envelope of experimental errors. Thus, in the development of the procedures, removal of the extrinsic proteins provided researchers with a system that satisfied these requirements. The mutational loss of the extrinsic proteins increases the quantum efficiency of photoactivation (Burnap et al., 1996; Shen et al., 1998) as do mutations that weaken the binding of the extrinsic proteins (Qian et al., 1997, 1999). This appears to be due greater access of the Mn^{2+} ions to their site of photooxidation on the donor side of PSII (Chu et al., 1994a). However, this begs the question of how much the "natural" physiological kinetics are distorted by the loss of the extrinsic proteins and what other factors that might be removed or inactivated in the process. Indeed, it is almost certain that important assembly factors may have been absent in many of the defining photoactivation experiments. From this standpoint, it is clear that the *in vitro* photoactivation experiments have been decidedly non-physiological. Then what are the implications for the kinetics that have defined the mechanism to date? Here it is worth noting that the basic two quantum mechanism was first discovered using intact cells and chloroplasts. This includes experiments in samples that were not extracted with chemical reductant to remove the Mn_4O_5Ca. For example, these include using intact chloroplasts from leaves grown under intermittent light to promote de-etiolation, but remaining un-photoactivated (Ono and Inoue, 1982, 1983) and cyanobacterial cells grown under conditions of Mn-deficiency, and dark grown (with glucose) *Chlorella* cells (Cheniae and Martin, 1973). These samples are likely have the full complement of extrinsic proteins and assembly factors. Similarly, the extraction of whole cyanobacterial cells and chloroplasts with the hydroxylamine probably preserves many if not most assembly factors as operational. This probably explains the fact that nearly 100% of PSII centers become reactivated by photoactivation in these more intact preparations, but *in vitro* preparations typically have considerably lower total yields. The more "physiological" preparations still exhibit (1) low quantum efficiency and (2) the requirement for optimal flash spacing. However, inspection of data involving dark grown *Chlorella* indicates that photoactivation occurs more quickly, although optimal flash spacing is still required. Clearly, the role of assembly factors needs to be further pursued. One might imagine in this case that a closely associated assembly factor, like PratA, provides Mn^{2+} ions at critical times during the formation of intermediates and thereby mitigates potential losses due to intermediate decay. Except for one instance where the Psb27 mutant was analyzed (Roose and Pakrasi, 2007), a careful side-by-side comparisons of photoactivation in mutants and wild-type remain to be performed.

High Affinity Binding Site

Biochemical preparations of PSII that have been depleted of their Mn_4O_5Ca have been used to test the binding affinity for Mn^{2+}. The principal finding is that a single binding site, termed the high affinity site, dominates the kinetics. The dissociation constant for Mn^{2+} at this site is estimated to be in the range of 0.1–2 μM (Hsu et al., 1987; Diner, 2001) and is strongly pH dependent (pK_a 6–7) (Ono and Mino, 1999). As described below, these are accurate, but essentially, non-equilibrium assays. In one of the few examples of an estimate of the true equilibrium binding constant, a significantly higher value of 40–50 μM was estimated. In this case, binding was allowed to occur in the dark and the samples were frozen to −20°C, where diffusion was eliminated and an EPR binding photoxoidation signal could be detected, thereby giving a "snapshot" of the amount of photooxidizable Mn^{2+} bound at equilibrium (Tyryshkin et al., 2006). Notably, the binding affinity was found to be independent of the binding of Ca^{2+}. Almost all other assays have been performed utilizing the ability of Mn^{2+} to donate electrons to photochemically generated $Y_Z^{\bullet}$. Therefore, the high affinity site has been largely defined biochemically based upon the combination of affinity *and* the ability to be photooxidized by $Y_Z^{\bullet}$ during charge separation, rather that equilibrium binding assays alone (see older review Debus, 1992, for still up-to-date discussion). -This high affinity/efficient oxidation site remains intact in the mutant without processing of D1 carboxy terminus (Nixon et al., 1992), although subtle differences in the affinity characteristics of these mutants are observed when the biphasic kinetics of the binding/oxidation are fully taken into account (Cohen et al., 2007). On the other hand, the access of Mn^{2+} to this site is significantly increased in the carboxyterminal processing mutants as well as mutants lacking extrinsic proteins (Chu et al., 1994a; Semin et al., 2015). Mutagenesis of D1-Asp170 has shown that the residue clearly has the strongest effect upon on the affinity of Mn^{2+} and the ability to assemble a fully functional Mn_4CaO_5 cluster (Boerner et al., 1992; Diner and Nixon, 1992; Nixon and Diner, 1992; Chu et al., 1994b; Whitelegge et al., 1995; Campbell et al., 2000; Cohen et al., 2007). This is consistent with the crystal structures of PSII (Umena et al., 2011; Suga et al., 2015), which have shown that Asp170 is a ligand to the Mn(4) of assembled (intact) Mn_4CaO_5 cluster (**Figure 2**). Notably, the other carboxyl O of the D1-Asp170 side chain provides a monodentate ligand to the adjacent Ca^{2+} ion of the assembled cluster, which probably relates to the Ca^{2+} requirement photoactivation, as discussed below. Other residues, notably the other main amino acid ligand to Mn(4), D1-Glu333 affect the affinity characteristics of the high affinity binding site, but none as decisively as mutations of D1-Asp170 (Cohen et al., 2007).

D1-Glu333 is a ligand to Mn(4) presumptive the first photo-oxidized Mn^{2+} at the high affinity binding site (Umena et al., 2011). In all mutants of Glu333, substantial fractions of PSII complexes lack photooxidizable Mn ions *in vivo* (Chu et al., 1995), showing that Glu333 influences the assembly or stability of the Mn_4CaO_5 cluster. Nevertheless, mutations of Glu333 do not display the large changes in Mn^{2+} affinity compared to D1-Asp170 mutations, at least as measured using single turn-over methods to assay affinity (Nixon and Diner, 1994; Cohen et al., 2007). One possibility to accommodate these observations is that Glu333 provides some coordination of Mn^{2+} ions at the high affinity site, but play an even greater role in the subsequent assembly process. Pulsed electron-electron double resonance (PELDOR) experiments have recently provided the evidence to support this hypothesis that the high-affinity Mn^{2+} site is located at the position denoted by Mn(4) in the crystal

structure and the first photooxidized Mn^{2+} bound to the apo-WOC is coordinated with axial ligands Asp170 and Glu333 in the D1 protein (Asada and Mino, 2015). These results thus substantiate and extend the initial assessments of the high affinity site based upon site-directed mutagenesis, yet deepen the puzzle about the seeming modest influence this axial ligand has to the affinity/photooxidation characteristics of the site. For the C-terminal residues D1-Ala344, neither mutations in the C-terminal region of D1 nor the processing of the C-terminal extension (Ala344stop and Ser345Pro mutants) has a large influence on the ability to bind and oxidize the first Mn^{2+} in the assembly of the cluster (Nixon et al., 1992). These observations indicate that these C-terminal residues do not participate in the coordination of the first bound Mn, though they certainly must contribute to the coordination of those bound later on in the assembly process (Diner, 2001). In the recent crystal structure of PS II, His337 residue is sufficiently close to Mn_4CaO_5 cluster and engage in H-bonding interactions with the μ_3-oxo bridge connecting Mn(1), Mn(2), and Mn(3) (Umena et al., 2011).

Trapping Intermediates of Photoassembly

Britt and coworkers (Campbell et al., 2000) provided the first direct EPR spectral evidence for the initial photooxidized intermediate formed at the high affinity site in *Synechocystis* 6803 PSII core complexes. Conventional perpendicular-mode EPR in X-band is used to detect spin transitions in half integer spin systems which satisfy the selection rules $\Delta M_s = \pm 1$. Accordingly, the first light induced Mn^{3+} species, due to the integer spin $S = 2$ of Mn^{3+}, is an EPR-silent species for perpendicular polarization EPR spectroscopy at X-band frequencies. X-band parallel polarization EPR spectroscopy, however, can be used to investigate integral spin systems with $S \geq 1$ where the spin transitions satisfy the selection rules $\Delta M_s = \pm 2$ and higher. This latter technique is therefore well-suited to examine the coordination environment of this Mn^{3+} intermediate (high spin $S = 2$). A six-line signal with a hyperfine splitting of ∼45 G that was only visible in parallel mode. This signal clearly arises from Mn^{3+} as it closely resembles that observed for Mn^{3+} in superoxide dismutase (Campbell et al., 1999). The parallel mode EPR spectrum of this photooxidation species consists of six well-resolved transitions split by a relatively small ^{55}Mn hyperfine coupling (44 G). The Mn^{3+} parallel mode EPR signal gives an axial zero-field splitting value of $D \approx -2.5$ cm^{-1} and a rhombic zero-field splitting value of $|E| \approx 0.269$ cm^{-1}. The negative D value for this d^4 ion is indicative of either an octahedral Mn^{3+} geometry or a five-coordinate square-pyramidal Mn^{3+} geometry. In contrast to wild-type, a different parallel polarization EPR signal of Mn^{3+} ion without a resolved hyperfine structure was observed in Asp170His mutant, suggesting a modified coordination environment of Mn^{3+}. In the case of Asp170Glu mutant, instead of a parallel mode Mn^{3+} signal, a perpendicular mode signal generated by Mn^{4+} ion was detectable (Campbell et al., 2000), which indicates an impact of glutamate on the redox property of the photo-oxidized Mn^{2+} ion. As noted previously (Hoganson et al., 1989), coordination by oxo anions as would have effect of lowering the redox potential of the Mn^{2+} ion into the range that the oxidizing potential of $Y_Z^{\bullet}$.

The weak EPR signal found by Dismukes et al. in the dark apo-PSII samples upon binding of Mn^{2+} in the absence of Ca^{2+} is characterized by six-line ^{55}Mn hyperfine structure and $g_{effe} = 8.3$, which indicates a high-spin electronic ground state ($S = 5/2$) of Mn^{2+} bound in a low-symmetry environment (Ananyev and Dismukes, 1997). This signal is likely arise from a Mn^{2+} bound in the high-affinity site. Dismukes et al. (Ananyev et al., 1999) later suggested using competitive inhibition studies that the first species that initiated photoactivation (Ananyev et al., 1999) is hydroxide of Mn^{2+}, $[MnOH]^+$, bound to the apo-WOC at high affinity site. Subsequent work by the same group would provide evidence that the hydroxide formation was modulated by Ca^{2+} (Tyryshkin et al., 2006).

Role of Ca^{2+} and the Ca^{2+} Bound Intermediate

Ca^{2+} is an indispensable cofactor of the water-splitting Mn_4CaO_5 cluster. As noted in the previous section, biophysical studies attempting to trap early intermediates showed that Ca^{2+} exerts pronounced, and possibly physiologically significant effects upon the structure of Mn ions undergoing photooxidation at the high affinity site. However, from the biochemical perspective, the roles of Ca^{2+} ion in the process of photoactivation *initially* appeared contradictory: A requirement for Ca^{2+} in photoactivation was also noted using cyanobacterial preparations (Pistorius and Schmid, 1984). Ono and Inoue (1983) proposed that photoactivation occurs in one stage with Ca^{2+} essential for the assembly process itself using isolated intact chloroplasts depleted of Mn. According to the one-stage model the first-order rate constant for the assembly of O_2-evolving centers is dependent on the extent of occupancy of both Mn^{2+} and Ca^{2+} bound to their specific binding sites during photoactivation. Later experiments seemed to indicate that the Ca^{2+}-binding site is "created" during the photoassembly (Shinohara et al., 1992). For example, Tamura and Cheniae (1987) found that only light and Mn^{2+} were essential for Mn re-ligation to the apo-WOC-PSII, but Ca^{2+} addition was required for maximal expression of water oxidation activity by the photoligated Mn. In other words, it appeared that Ca^{2+} was not required for proper assembly, but was needed as a cofactor that readily diffused into its site of action after the assembly of the Mn cluster was completed and, once in place, activated its catalytic function. However, this conclusion was later modified to account for the complicating effects of the artificial electron acceptor used in the assay (Chen et al., 1995a). Ultimately, it was thus concluded that Ca^{2+} is indeed absolutely required *during* the assembly of functional clusters, not simply being added in after assembly (Chen et al., 1995a). The same work provides what may be another important clue about the role of Ca^{2+}. It was found that photoactivation of PSII membranes in the absence of Ca^{2+} led to the formation of inactive PSII with more than four Mn ion per PSII center (5–10 non-functional Mn per PSII). Thus, when Ca^{2+} is left out of the photoactivation medium, binding and photooxidation of many more Mn^{2+} to the apo-WOC-PSII protein occurs, but no O_2 evolution activity is observable (Chen et al., 1995a). Manganese bound

in this way could be released with reductant indicating that it was bound oxidatively, but it clearly cannot bind to specific protein binding sites. Instead, probably resembles amorphous oxides which are multinucleate metal-oxo deposits produced by inorganic processes (Sauer and Yachandra, 2002). This suggests that one role for Ca^{2+} is to guide assembly or simply block Mn^{2+} oxidation at the Ca^{2+} site, which prevents "inappropriately assembled" Mn (Chen et al., 1995a). Interestingly, mutants that are defective in processing the D1 carboxy terminus also seem to assemble centers with excess Mn (Seibert et al., 1989). Recent X-ray crystallographic studies (Umena et al., 2011) provides a structural explanation for the Seibert result. The PSII structure reveals that mature D1 C-terminal residue Ala344 ligate the Ca^{2+} and Mn(2) of Mn_4CaO_5 cluster, thus without the availability of the mature C-terminus Ala344, Ca^{2+} cannot bind and the destructive photoligation of Mn^{2+} to inappropriate sites can proceed. Additionally, competition between Ca^{2+} and Mn^{2+} for each other's binding sites has been indicated by many studies (Cheniae and Martin, 1971b; Radmer and Cheniae, 1971; Ono and Inoue, 1983; Tamura and Cheniae, 1987; Miller and Brudvig, 1989; Chen et al., 1995a,b; Ananyev and Dismukes, 1996a; Zaltsman et al., 1997). Since Sr^{2+} can substitute of Ca^{2+} in PSII *in vivo*, albeit with impaired H_2O-oxidation activity (Boussac et al., 2004), it would be interesting to see how photoactivation occurs with this substitution. However, only limited information is currently available (Ananyev et al., 2001).

The effect of Ca^{2+} on the formation of the first photoactivation intermediate, corresponding to a photooxidized mononuclear Mn^{3+} species bound to apo-WOC-PSII, was investigated by EPR spectroscopy (Tyryshkin et al., 2006). In the absence of Ca^{2+}, the Mn^{3+} species was found to be generated as two forms in a pH-dependent equilibrium: an EPR-invisible low-pH form and an EPR-visible high-pH form. Note, these spectra of Mn^{3+} species were acquired in parallel mode and EPR invisible vs. visible is attributable to changes in the influences in ligand environment rather than the spin state selection rules noted above. The conversion between the visible and invisible forms occurs by deprotonation of an ionizable ligand bound to Mn^{3+}, postulated to be a H_2O molecule: $[Mn^{3+}(OH_2)] \leftrightarrow [Mn^{3+}(OH^-)]$. The EPR-visible high-pH form exhibits a strong pH effect (pH 6.5–9) on Mn^{3+} spectral parameters, including the rhombicity (δ) derived from center field position (g_{eff}), the ^{55}Mn hyperfine coupling (A_Z), and the signal intensity. A pH-induced protein conformational change was proposed to account for the observed significant changes in the symmetry of the ligand field at the Mn^{3+} site. On the other hand, the EPR-detectable Mn^{3+} induced in the presence of Ca^{2+}, exhibits a greatly weakened pH dependence of its ligand-field symmetry with reduced variation of rhombicity δ and ^{55}Mn hyperfine coupling $A_Z$in the pH range of 6.5–9.0. Moreover, the addition of Ca^{2+} moves both g_{eff} and A_Z to a range of values observed at alkaline pH $\geq$ 9 without added Ca^{2+}, indicating that Ca^{2+} binding exerts an influence on the coordination shell of Mn^{3+} species equivalent to the alkaline pH effect in the absence of Ca^{2+}. Therefore, it was proposed that Ca^{2+} binding induces a second ionization of the bridging hydroxo ligand bound to Mn^{3+} resulting in the formation of a bridging oxide ion ($[Mn^{3+}(OH^-)\text{-}Ca^{2+}] \leftrightarrow [Mn^{3+}(O^{2-})\text{-}Ca^{2+}]$). The proton ionization of the water ligand is postulated to be controlled by a nearby base B^-, which serves as an immediate proton acceptor with a pK_a that depends upon the occupancy of the Ca^{2+} effector site. Looking at the current crystal structure and assuming a similar, although almost certainly not identical, spatial configuration of the Ca and Mn, the inferred oxo bridge would join these ions with D1-Asp170, Glu333 and the carboxyl terminus in proximity of one another.

Other Inorganic Cofactors

There is a long debated role of inorganic carbon in photosynthetic water oxidation. Recently, it has been demonstrate that bicarbonate (HCO_3^-) can act as a mobile acceptor and transporter of protons produced by photosynthetic water oxidation PSII (Koroidov et al., 2014). Bicarbonate also seem to have an impact on photoassembly of Mn_4CaO_5 cluster (reviewed in Dasgupta et al., 2008). The proposed roles of bicarbonate in facilitating assembly of Mn_4CaO_5 cluster during PSII repair include acceleration of the binding and photooxidation of the first Mn^{2+} at the high affinity Mn site, putatively by increase the location concentration of Mn^{2+} and even direct ligation to Mn^{2+} (Baranov et al., 2000, 2004; Dasgupta et al., 2007). Bicarbonate has been found not an essential constituent of the WOC of PSII based on the most recent PSII crystal structure (Umena et al., 2011), making the direct ligation seem unlikely. However, this does not necessarily mean that the possibility of a weakly bound HCO_3^- at the donor side affecting the PSII repair has been excluded. It is also important to note that high concentrations of Cl^- also enhance photoactivation *in vitro*, but this appears to be an effect distinct from the known effects on the activation of the photosynthetic water oxidation catalytic activity. Instead, it more likely relates to the stabilization of the Mn_4CaO_5 in the absence of the extrinsic proteins in the studied photoactivation reactions (Miyao and Murata, 1985; Miyaotokutomi and Inoue, 1992). The catalytic activation properties of Cl^- are likely to be exerted indirectly upon water and/or proton movement during H_2O-oxidation given it binding locations in the second ligation sphere of the assembled Mn_4O_5Ca.

Possible Models of Assembly

Although the two-quantum model remains solidly at the foundation of our understanding of photoactivation, the molecular mechanisms that give rise to these kinetic features remain almost completely unresolved. A crucial question is what molecular processes gives rise to the so-called dark rearrangement. As discussed, consistent models would require occupancy of the high affinity site by Mn^{2+} and the presence Ca^{2+} at a nearby site, and the Ca^{2+} probably needs to be present during the initial photooxidation of the Mn^{2+}. This first photooxidation (A⇒B) likely occurs with high quantum efficiency, yet the photooxidation of the second Mn^{2+} (C⇒D) occurring after the rearrangement occurs with low quantum efficiency. There are essentially two general alternative hypotheses accounting for the low quantum yield of C⇒D that

depend, in part, on the nature of the rearrangement. First, the rearrangement after A⇒B forms a binding site for the second Mn^{2+} that is not optimal for electron transfer to $Y_Z^{\bullet}$, perhaps because it is further away from the high affinity site and because of this, charge recombination effectively competes with the low probability of photooxidation of the second Mn^{2+} at the new site. Please note that the charge recombination may actually be the 'rearrangement' and could be important for removing mis-assembled clusters (Hwang et al., 2007). Second, the rearrangement is again a slow process, but this time leads to formation of efficient site for Mn^{2+} photooxidation, but its initial product, the first Mn^{3+} fails to convert efficiently into a stable chemical product. This could happen if, for example, a requisite oxo bridge forms inefficiently and the new Mn^{3+} diffuses away or is re-reduced. Based upon the finding that the C-terminus of D1 is already in a conformation close to the final configuration in the fully assembled enzyme (Cohen et al., 2007), then the dark rearrangement is unlikely to be a major rearrangement of the D1 polypeptide backbone. With this constraint, we imagine these two alternative assembly mechanisms as follows. One alternative is that the slow rearrangement corresponds to slow oxo bridge formation chemistry that is kinetically very sluggish, occurring with the rate constant k_R after the initial photooxidation. Further, once the first Mn^{3+} is produced at the high affinity site, the new binding site for the second Mn^{2+} is at a more distal site where the quantum yield of its photooxidation lower. In this case, the first Mn^{3+} at the high affinity site is already engaged oxo linkage with the Ca^{2+} (Tyryshkin et al., 2006) and one of its other coordination positions occupied by a water must deprotonate to form a stable linkage with the second Mn^{2+}. According to this hypothesis, the slow formation of the second oxo corresponds to k_R and the low quantum yield of C⇒D is due to the more distal location from $Y_Z^{\bullet}$. However, one problem with this model is that each of the subsequent two Mn additions would seem to have to also occur with low quantum yields, since the high affinity site remains occupied. However, these later photoligations are thought to occur with high quantum efficiency, although the evidence even for that remains sparse. A second alternative to a primarily protein rearrangement is a rearrangement of the ions. As mentioned above, the high affinity site has been largely defined biochemically based upon the combination of affinity *and* the ability to be photooxidized by $Y_Z^{\bullet}$ during charge separation. Perhaps the high affinity site remains the site of oxidation for each of the photooxidations for the assembly reactions and the resultant Mn^{3+} ions migrate to their final locations. In this model, the relocation of the Mn ion, vacating the high affinity site, and its coordination into its new site accounts for the "dark rearrangement." However, the dissociation of the Mn^{3+} dissociates from its initial binding and oxidation site presents a problem because of the likely increase in ligand field stabilization energy. This would not be a problem for Mn^{2+}, which has no associated LFSE. On the other hand, Mn^{3+} should bind with a substantially higher affinity owing to the acquisition of LFSE in the higher oxidation state. There may be meahisms to alleviate this problem such as a redox disproportionation of bound Mn^{3+}-Mn^{2+} to (Mn^{2+}-Mn^{3+} so the original Mn^{3+} is now weakly bound (no LFSE) and can exchange to another site. The EPR observations consistent with oxo bridge formation Ca^{2+} ion accompanying the photooxidation of Mn^{2+} ions at the high affinity site suggest a templating function for Ca^{2+} during assembly. Based upon the crystal structure, the Ca^{2+} would be captured between D1-Asp170 and the carboxyterminal carboxylate of the D1 protein. As noted, there is good evidence that Ca^{2+} binding induces a second ionization of the bridging hydroxo ligand bound to Mn^{3+} resulting in the formation of a bridging oxide ion ($[Mn^{3+}(OH^{-})\text{-}Ca^{2+}] \leftrightarrow [Mn^{3+}(O^{2-})\text{-}Ca^{2+}]$) (Tyryshkin et al., 2006). If the Mn^{3+} leaves the high affinity site, then Ca^{2+} may tether the new Mn with an oxo (or hydroxo) bridge and facilitate the movement to the next site. Moreover, the water molecules coordinated Ca^{2+} may be provided as the substrate for additional μ-oxo bridge formation. In this way, Ca^{2+} functions in a manner similar to proposals for its role in catalytic water oxidation and substrate exchange though the positioning of coordinated waters (Vrettos et al., 2001; Hillier and Wydrzynski, 2008; Rappaport et al., 2011; Cox and Messinger, 2013). According to electrostatic calculations, there are substantial differences in the redox potentials for each of the four spatially distributed Mn ions of the assembled Mn_4CaO_5 cluster due to their specific coordination and large electrostatic environments (Amin et al., 2015). Based upon these electrostatic calculations of Amin et al. (2015), it is likely that Mn^{3+} ions are thermodynamically more stable at coordination positions elsewhere within the partially assembled cluster in comparison to their primary site of oxidation at the high affinity site. It also fits with a variety of biochemical studies showing that one pair of Mn ions, presumably a binuclear di-μ-oxo bridged unit, in the assembled cluster is more stable and has different accessibility to external reductants than the other pair (Frankel and Bricker, 1989; Mei and Yocum, 1991, 1992; Riggs et al., 1992). In this model, the rearrangement time may correspond to the relocation of the first Mn^{3+} ion to exit the high affinity site and relocate to another site, perhaps guided via a nascent oxo with the Ca^{2+}.

AUTHOR CONTRIBUTIONS

HB researched the topic and wrote the initial draft of the manuscript. RB added materialand made figures, performed additional research and edited the draft.

FUNDING

The work was generously funded by a grant form the National Science Foundation (MCB-1244586).

ACKNOWLEDGMENTS

The authors thank Dr. Aparna Nagarajan for providing the initial sketch of **Figure 1**. We also thank reviewer 2 for the pointing out the issue with our proposed rearrangement model regarding ligand field stabilization energy and suggesting redox disproportionation as a possible mechanism. The work was funded by the National Science Foundation MCB-1244586.

REFERENCES

Adir, N., Zer, H., Shochat, S., and Ohad, I. (2003). Photoinhibition - a historical perspective. *Photosyn. Res.* 76, 343–370. doi: 10.1023/A:1024969518145

Amin, M., Vogt, L., Szejgis, W., Vassiliev, S., Brudvig, G. W., Bruce, D., et al. (2015). Proton-coupled electron transfer during the S-state transitions of the oxygen-evolving complex of photosystem II. *J. Phys. Chem. B.* 119, 7366–7377. doi: 10.1021/jp510948e

Ananyev, G. M., and Dismukes, G. C. (1996a). Assembly of the tetra Mn site of photosynthetic water oxidation by photoactivation: Mn stoichiometry and detection of a new intermediate. *Biochemistry* 35, 4102–4109. doi: 10.1021/bi952667h

Ananyev, G. M., and Dismukes, G. C. (1996b). High-resolution kinetic studies of the reassembly of the tetra-manganese cluster of photosynthetic water oxidation: proton equilibrium, cations, and electrostatics. *Biochemistry* 35, 14608–14617. doi: 10.1021/bi960894t

Ananyev, G. M., and Dismukes, G. C. (1997). Calcium induces binding and formation of a spin-coupled dimanganese(II,II) center in the apo-water oxidation complex of photosystem II as precursor to the functional tetra-Mn/Ca cluster. *Biochemistry* 36, 11342–11350. doi: 10.1021/bi970626a

Ananyev, G. M., Murphy, A., Abe, Y., and Dismukes, G. C. (1999). Remarkable affinity and selectivity for Cs+ and uranyl (UO_2^{2+}) binding to the manganese site of the apo-water oxidation complex of photosystem II. *Biochemistry* 38, 7200–7209. doi: 10.1021/bi990023u

Ananyev, G. M., Zaltsman, L., Vasko, C., and Dismukes, G. C. (2001). The inorganic biochemistry of photosynthetic oxygen evolution/water oxidation. *Biochim. Biophys. Acta* 1503, 52–68. doi: 10.1016/S0005-2728(00)00215-2

Anbudurai, P. R., Mor, T. S., Ohad, I., Shestakov, S. V., and Pakrasi, H. B. (1994). The ctpA gene encodes the C-terminal processing protease for the D1 protein of the photosystem II reaction center complex. *Proc. Natl. Acad. Sci. U.S.A.* 91, 8082–8086. doi: 10.1073/pnas.91.17.8082

Aro, E. M., Virgin, I., and Andersson, B. (1993). Photoinhibition of photosystem II. Inactivation, protein damage and turnover. *Biochim. Biophys. Acta* 1143, 113–134. doi: 10.1016/0005-2728(93)90134-2

Asada, M., and Mino, H. (2015). Location of the High-Affinity $Mn^{(2+)}$ Site in Photosystem II Detected by PELDOR. *J. Phys. Chem. B* 119, 10139–10144. doi: 10.1021/acs.jpcb.5b03994

Bailey, S., Thompson, E., Nixon, P. J., Horton, P., Mullineaux, C. W., Robinson, C., et al. (2002). A critical role for the Var2 FtsH homologue of Arabidopsis thaliana in the photosystem II repair cycle *in vivo*. *J. Biol. Chem.* 277, 2006–2011. doi: 10.1074/jbc.M105878200

Baranov, S. V., Ananyev, G. M., Klimov, V. V., and Dismukes, G. C. (2000). Bicarbonate accelerates assembly of the inorganic core of the water- oxidizing complex in manganese-depleted photosystem II: a proposed biogeochemical role for atmospheric carbon dioxide in oxygenic photosynthesis. *Biochemistry* 39, 6060–6065. doi: 10.1021/bi992682c

Baranov, S. V., Tyryshkin, A. M., Katz, D., Dismukes, G. C., Ananyev, G. M., and Klimov, V. V. (2004). Bicarbonate is a native cofactor for assembly of the manganese cluster of the photosynthetic water oxidizing complex. Kinetics of reconstitution of O_2 evolution by photoactivation. *Biochemistry* 43, 2070–2079. doi: 10.1021/bi034858n

Becker, K., Cormann, K. U., and Nowaczyk, M. M. (2011). Assembly of the water-oxidizing complex in photosystem II. *J. Photochem. Photobiol. B. Biol.* 104, 204–211. doi: 10.1016/j.jphotobiol.2011.02.005

Björkman, O. (1981). "Responses to different quantum flux densities," in *Physiological Plant Ecology I: Responses to the Physical Environment*, eds O. L. Lange, P. S. Nobel, C. B. Osmond and H. Ziegler (Berlin; Heidelberg: Springer), 57–107. doi: 10.1007/978-3-642-68090-8_4

Boerner, R. J., Nguyen, A. P., Barry, B. A., and Debus, R. J. (1992). Evidence from directed mutagenesis that aspartate 170 of the D1 polypeptide influences the assembly and-or stability of the manganese cluster in the photosynthetic water-splitting complex. *Biochemistry* 31, 6660–6672. doi: 10.1021/bi00144a005

Boussac, A., Rappaport, F., Carrier, P., Verbavatz, J. M., Gobin, R., Kirilovsky, D., et al. (2004). Biosynthetic Ca^{2+}/Sr^{2+} exchange in the photosystem II oxygen evolving enzyme of *Thermosynechococcus elongatus*. *J. Biol. Chem.* 279, 22809–22819. doi: 10.1074/jbc.M401677200

Burnap, R. L. (2004). D1 protein processing and Mn cluster assembly in light of the emerging photosystem II structure. *Phys. Chem. Chem. Phys.* 6, 4803–4809. doi: 10.1039/b407094a

Burnap, R. L., Qian, M., and Pierce, C. (1996). The manganese-stabilizing protein (MSP) of photosystem II modifies the *in vivo* deactivation and photoactivation kinetics of the H_2O-oxidation complex in *Synechocystis* sp. PCC6803. *Biochemistry* 35, 874–882. doi: 10.1021/bi951964j

Campbell, K. A., Force, D. A., Nixon, P. J., Dole, F., Diner, B. A., and Britt, R. D. (2000). Dual-mode EPR detects the initial intermediate in photoassembly of the photosystem II Mn cluster: the influence of amino acid residue 170 of the D1 polypeptide on Mn coordination. *Biochemistry* 122, 3754–3761. doi: 10.1021/ja000142t

Campbell, K. A., Yikilmaz, E., Grant, C. V., Gregor, W., Miller, A.-F., and Britt, R. D. (1999). Parallel polarization EPR characterization of the Mn(III) center of oxidized manganese superoxide dismutase. *J. Am. Chem. Soc.* 121, 4714–4715. doi: 10.1021/ja9902219

Chen, C., Kazimir, J., and Cheniae, G. M. (1995a). Calcium modulates the photoassembly of photosystem II (Mn)4 clusters by preventing ligation of nonfunctional high valency states of manganese. *Biochemistry* 34, 13511–13526.

Chen, G. X., Blubaugh, D. J., Homann, P. H., Golbeck, J. H., and Cheniae, G. M. (1995b). Superoxide contributes to the rapid inactivation of specific secondary donors of the photosystem II reaction center during photodamage of manganese depleted photosystem II membranes. *Biochemistry* 3470, 2317–2332. doi: 10.1021/bi00007a028

Chen, H., Zhang, D., Guo, J., Wu, H., Jin, M., Lu, Q., et al. (2006). A Psb27 homologue in Arabidopsis thaliana is required for efficient repair of photodamaged photosystem II. *Plant Mol. Biol.* 61, 567–575. doi: 10.1007/s11103-006-0031-x

Cheniae, G. M., and Martin, I. F. (1971a). Effects of hydroxylamine on photosystem II. I. Factors affecting the decay of O_2 evolution. *Plant Physiol.* 47, 568–575. doi: 10.1104/pp.47.4.568

Cheniae, G. M., and Martin, I. F. (1971b). Photoactivation of the manganese catalyst of O_2 evolution. I. Biochemical and kinetic aspects. *Biochim. Biophys. Acta* 253, 167–181. doi: 10.1016/0005-2728(71)90242-8

Cheniae, G. M., and Martin, I. F. (1972). Effects of hydroxylamine on photosystem II. II Photoreversal of the NH_2OH destruction of O_2 evolution. *Plant Physiol.* 50, 87–94. doi: 10.1104/pp.50.1.87

Cheniae, G. M., and Martin, I. F. (1973). Absence of oxygen-evolving capacity in dark-grown *Chlorella*: the photoactivation of oxygen evolving centers. *Photochem. Photobiol.* 17, 441–459. doi: 10.1111/j.1751-1097.1973.tb06378.x

Chu, H.-A., Nguyen, A. P., and Debus, R. J. (1994a). Site-directed mutagenesis of photosynthetic oxygen evolution: increased binding or photooxidation of manganese in the absence of the extrinsic 33-kDa polypeptide *in vivo*. *Biochemistry* 33, 6150–6157. doi: 10.1021/bi00186a014

Chu, H.-A., Nguyen, A. P., and Debus, R. J. (1994b). Site-directed mutagenesis of photosynthetic oxygen evolution: instability or inefficient assembly of the manganese cluster *in vivo*. *Biochemistry* 33, 6137–6149. doi: 10.1021/bi00186a013

Chu, H. A., Nguyen, A. P., and Debus, R. J. (1995). Amino acid residues that influence the binding of manganese or calcium to photosystem II. 2. The carboxy terminal domain of the D1 polypeptide. *Biochemistry* 3496, 5859–5882. doi: 10.1021/bi00017a017

Cohen, R. O., Nixon, P. J., and Diner, B. A. (2007). Participation of the C-terminal region of the D1-polypeptide in the first steps in the assembly of the Mn4Ca cluster of photosystem II. *J. Biol. Chem.* 282, 7209–7218. doi: 10.1074/jbc.M606255200

Cox, N., and Messinger, J. (2013). Reflections on substrate water and dioxygen formation. *Biochim. Biophys. Acta* 1827, 1020–1030. doi: 10.1016/j.bbabio.2013.01.013

Dasgupta, J., Ananyev, G. M., and Dismukes, G. C. (2008). Photoassembly of the water-oxidizing complex in photosystem II. *Coord. Chem. Rev.* 252, 347–360. doi: 10.1016/j.ccr.2007.08.022

Dasgupta, J., Tyryshkin, A. M., and Dismukes, G. C. (2007). ESEEM spectroscopy reveals carbonate and an N-donor protein-ligand binding to Mn^{2+} in the photoassembly reaction of the Mn4Ca cluster in photosystem II. *Angew. Chem. Int. Ed Engl.* 46, 8028–8031. doi: 10.1002/anie.200702347

Debus, R. J. (1992). The manganese and calcium ions of photosynthetic oxygen evolution. *Biochim. Biophys. Acta* 1102, 269–352. doi: 10.1016/0005-2728(92)90133-M

Diner, B. A. (2001). Amino acid residues involved in the coordination and assembly of the manganese cluster of photosystem II. Proton-coupled electron transport of the redox-active tyrosines and its relationship to water oxidation. *Biochim. Biophys. Acta* 1503, 147–163. doi: 10.1016/S0005-2728(00)00220-6

Diner, B. A., and Nixon, P. J. (1992). The rate of reduction of oxidized redox-active tyrosine, Z^+, by exogenous Mn^{2+} Is slowed in a site-directed mutant, at aspartate 170 of polypeptide D1 of photosystem II, inactive for photosynthetic oxygen evolution. *Biochim. Biophys. Acta* 1101, 134–138. doi: 10.1016/0005-2728(92)90196-9

Diner, B. A., Nixon, P. J., and Farchaus, J. W. (1991). Site-directed mutagenesis of photosynthetic reaction centers. *Curr. Opin. Struct. Biol.* 1, 546–554. doi: 10.1016/S0959-440X(05)80076-4

Diner, B. A., Ries, D. F., Cohen, B. N., and Metz, J. G. (1988a). Carboxyl-terminal processing of polypeptide D of the photosystem II reaction center of Scenedesmus obliquus is necessary for the assembly of the oxygen-evolving complex. *J. Biol. Chem.* 263, 8972–8980.

Diner, B. A., Ries, D. F., Cohen, B. N., and Metz, J. G. (1988b). COOH-terminal processing of polypeptide D1 of the photosystem II reaction center of *Scenedesmus obliquus* is necessary for the assembly of the oxygen-evolving complex. *J. Biol. Chem.* 263, 8972–8980.

Dismukes, C. G., Ananyev, G., and Watt, R. (2005). "Photo-assembly of the catalytic manganese cluster," in *Photosystem II*, eds T. Wydrzynski, K. Satoh, and J. Freeman (Dordrecht: Springer), 609–626.

Edelman, M., and Mattoo, A. K. (2008). D1-protein dynamics in photosystem II: the lingering enigma. *Photosyn. Res.* 98, 609–620. doi: 10.1007/s11120-008-9342-x

Frankel, L. K., and Bricker, T. M. (1989). Epitope mapping of the monoclonal antibody FAC2 on the apoprotein of Cpa-1 in photosystem II. *FEBS Lett.* 257, 279–282. doi: 10.1016/0014-5793(89)81552-2

Heinz, S., Liauw, P., Nickelsen, J., and Nowaczyk, M. (2016). Analysis of photosystem II biogenesis in cyanobacteria. *Biochim. Biophy. Acta* 1857, 274–287. doi: 10.1016/j.bbabio.2015.11.007

Hillier, W., and Wydrzynski, T. (2008). O^{18}-Water exchange in photosystem II: substrate binding and intermediates of the water splitting cycle. *Coord. Chem. Rev.* 252, 306–317. doi: 10.1016/j.ccr.2007.09.004

Hoganson, C. W., Ghanotakis, D. F., Babcock, G. T., and Yocum, C. F. (1989). Manganese ion reduces redox activated tyrosine in manganese-depleted photosystem II preparations. *Photosyn. Res.* 22, 285–294. doi: 10.1007/BF00048306

Hsu, B. D., Lee, J. Y., and Pan, R. L. (1987). The high-affinity binding-site for manganese on the oxidizing side of photosystem-Ii. *Biochim. Biophys. Acta* 890, 89–96. doi: 10.1016/0005-2728(87)90072-7

Hwang, H. J., and Burnap, R. L. (2005). Multiflash experiments reveal a new kinetic phase of photosystem II manganese cluster assembly in *Synechocystis* sp PCC6803 *in vivo*. *Biochemistry* 44, 9766–9774. doi: 10.1021/bi050069p

Hwang, H. J., McLain, A., Debus, R. J., and Burnap, R. L. (2007). Photoassembly of the manganese cluster in mutants perturbed in the high affinity Mn-binding site of the H_2O-oxidation complex of photosystem II. *Biochemistry* 46, 13648–13657. doi: 10.1021/bi700761v

Hwang, H. J., Nagarajan, A., McLain, A., and Burnap, R. L. (2008). Assembly and disassembly of the photosystem II manganese cluster reversibly alters the coupling of the reaction center with the light-harvesting phycobilisome. *Biochemistry* 47, 9747–9755. doi: 10.1021/bi800568p

Inagaki, N., Maitra, R., Satoh, K., and Pakrasi, H. B. (2001). Amino acid residues that are critical for *in vivo* catalytic activity of CtpA, the carboxyl-terminal processing protease for the D1 protein of photosystem II. *J. Biol. Chem.* 14, 14. doi: 10.1074/jbc.M102600200

Ivleva, N. B., Shestakov, S. V., and Pakrasi, H. B. (2000). The carboxyl-terminal extension of the precursor D1 protein of photosystem II is required for optimal photosynthetic performance of the cyanobacterium *Synechocystis* sp. PCC 6803. *Plant Physiol.* 124, 1403–1412. doi: 10.1104/pp.124.3.1403

Kashino, Y., Lauber, W. M., Carroll, J. A., Wang, Q., Whitmarsh, J., Satoh, K., et al. (2002). Proteomic analysis of a highly active photosystem II preparation from the cyanobacterium *Synechocystis* sp. PCC 6803 reveals the presence of novel polypeptides. *Biochemistry* 41, 8004–8012. doi: 10.1021/bi026012+

Kato, Y., Miura, E., Ido, K., Ifuku, K., and Sakamoto, W. (2009). The variegated mutants lacking chloroplastic FtsHs are defective in D1 degradation and accumulate reactive oxygen species. *Plant Physiol.* 151, 1790–1801. doi: 10.1104/pp.109.146589

Keren, N., Ohkawa, H., Welsh, E. A., Liberton, M., and Pakrasi, H. B. (2005). Psb29, a conserved 22-kD protein, functions in the biogenesis of Photosystem II complexes in *Synechocystis* and Arabidopsis. *Plant Cell* 17, 2768–2781. doi: 10.1105/tpc.105.035048

Klinkert, B., Ossenbühl, F., Sikorski, M., Berry, S., Eichacker, L., and Nickelsen, J. (2004). PratA, a periplasmic tetratricopeptide repeat protein involved in biogenesis of photosystem II in *Synechocystis* sp. PCC 6803. *J. Biol. Chem.* 279, 44639–44644. doi: 10.1074/jbc.M405393200

Koivuniemi, A., Aro, E. M., and Andersson, B. (1995). Degradation of the D1- and D2-proteins of photosystem II in higher plants is regulated by reversible phosphorylation. *Biochemistry* 34, 16022–16029. doi: 10.1021/bi00049a016

Komenda, J., and Barber, J. (1995). Comparison of *psbO* and *psbH* deletion mutants of *Synechocystis* PCC 6803 indicates that degradation of D1 protein is regulated by the QB site and dependent on protein synthesis. *Biochemistry* 34, 9625–9631. doi: 10.1021/bi00029a040

Komenda, J., Barker, M., Kuviková, S., de Vries, R., Mullineaux, C. W., Tichy, M., et al. (2006). The FtsH protease slr0228 is important for quality Control of photosystem II in the thylakoid membrane of *Synechocystis* sp. PCC 6803. *J. Biol. Chem.* 281, 1145–1151. doi: 10.1074/jbc.M503852200

Komenda, J., Knoppová, J., Krynická, V., Nixon, P. J., and Tichý, M. (2010). Role of FtsH2 in the repair of Photosystem II in mutants of the cyanobacterium *Synechocystis* PCC 6803 with impaired assembly or stability of the $CaMn_4$ cluster. *Biochim. Biophys. Acta* 1797, 566–575. doi: 10.1016/j.bbabio.2010.02.006

Komenda, J., Kuviková, S., Granvogl, B., Eichacker, L. A., Diner, B. A., and Nixon, P. J. (2007). Cleavage after residue Ala352 in the C-terminal extension is an early step in the maturation of the D1 subunit of Photosystem II in *Synechocystis* PCC 6803. *Biochim. Biophys. Acta* 1767, 829–837. doi: 10.1016/j.bbabio.2007.01.005

Komenda, J., Tichý, M., and Eichacker, L. A. (2005). The PsbH protein is associated with the inner antenna CP47 and facilitates D1 processing and incorporation into PSII in the cyanobacterium *Synechocystis* PCC 6803. *Plant Cell Physiol.* 46, 1477–1483. doi: 10.1093/pcp/pci159

Koroidov, S., Shevela, D., Shutova, T., Samuelsson, G., and Messinger, J. (2014). Mobile hydrogen carbonate acts as proton acceptor in photosynthetic water oxidation. *Proc. Natl. Acad. Sci. U.S.A.* 111, 6299–6304. doi: 10.1073/pnas.1323277111

Krynická, V., Tichý, M., Krafl, J., Yu, J., Kana, R., Boehm, M., et al. (2014). Two essential FtsH proteases control the level of the Fur repressor during iron deficiency in the cyanobacterium *Synechocystis* sp. PCC 6803. *Mol. Microbiol.* 94, 609–624. doi: 10.1111/mmi.12782

Kuviková, S., Tichý, M., and Komenda, J. (2005). A role of the C-terminal extension of the photosystem II D1 protein in sensitivity of the cyanobacterium *Synechocystis* PCC 6803 to photoinhibition. *Photochem. Photobiol. Sci.* 4, 1044–1048. doi: 10.1039/b506059a

Liu, H., Huang, R. Y., Chen, J., Gross, M. L., and Pakrasi, H. B. (2011a). Psb27, a transiently associated protein, binds to the chlorophyll binding protein CP43 in photosystem II assembly intermediates. *Proc. Natl. Acad. Sci. U.S.A.* 108, 18536–18541. doi: 10.1073/pnas.1111597108

Liu, H., Roose, J. L., Cameron, J. C., and Pakrasi, H. B. (2011b). A genetically tagged Psb27 protein allows purification of two consecutive photosystem II (PSII) assembly intermediates in *Synechocystis* 6803, a cyanobacterium. *J. Biol. Chem.* 286, 24865–24871. doi: 10.1074/jbc.M111.246231

Lupinkova, L., and Komenda, J. (2004). Oxidative modifications of the Photosystem II D1 protein by reactive oxygen species: from isolated protein to cyanobacterial cells. *Photochem. Photobiol.* 79, 152–162. doi: 10.1111/j.1751-1097.2004.tb00005.x

Mamedov, F., Nowaczyk, M. M., Thapper, A., Rogner, M., and Styring, S. (2007). Functional characterization of monomeric photosystem II core preparations from *Thermosynechococcus elongatus* with or without the Psb27 protein. *Biochemistry* 46, 5542–5551. doi: 10.1021/bi7000399

Mann, N. H., Novac, N., Mullineaux, C. W., Newman, J., Bailey, S., and Robinson, C. (2000). Involvement of an FtsH homologue in the assembly of functional

photosystem I in the cyanobacterium *Synechocystis* sp. PCC 6803. *FEBS Lett.* 479, 72–77. doi: 10.1016/S0014-5793(00)01871-8

Mei, R., and Yocum, C. F. (1991). Calcium retards NH_2OH inhibition of O_2 evolution activity by stabilization of Mn^{2+} binding to Photosystem II. *Biochemistry* 30, 7863–7842. doi: 10.1021/bi00245a025

Mei, R., and Yocum, C. F. (1992). Comparative properties of hydroquinone and hydroxylamine reduction of the Ca^{2+}stablilized O_2-evolving complex of photosystem II: reductant-dependent Mn^{2+} formation and activity inhibition. *Biochemistry* 31, 8449–8454. doi: 10.1021/bi00151a009

Meunier, P. C., Burnap, R. L., and Sherman, L. A. (1995). Modelling of the S-state mechanism and Photosystem II manganese photoactivation in cyanobacteria. *Photosyn. Res.* 47, 61–76. doi: 10.1007/BF00017754

Miller, A. F., and Brudvig, G. W. (1989). Manganese and calcium requirements for reconstitution of oxygen evolution activity in manganese-depleted photosystem II membranes. *Biochemistry* 28, 8181–8190. doi: 10.1021/bi00446a033

Miyao, M., and Inoue, Y. (1991). An improved procedure for photoactivation of photosynthetic oxygen evolution - effect of artificial electron-acceptors on the photoactivation yield of NH_2OH -treated wheat photosystem II membranes. *Biochim. Biophys. Acta* 1056, 47–56. doi: 10.1016/S0005-2728(05)80071-4

Miyao, M., and Murata, N. (1985). The Cl- effect on photosynthetic oxygen evolution: interaction of Cl- with 18-kDa, 24-kDa and 33-kDa proteins. *FEBS Lett.* 180, 303–308. doi: 10.1016/0014-5793(85)81091-7

Miyaotokutomi, M., and Inoue, Y. (1992). Improvement by benzoquinones of the quantum yield of photoactivation of photosynthetic oxygen evolution - direct evidence for the 2-quantum mechanism. *Biochemistry* 31, 526–532. doi: 10.1021/bi00117a032

Nagarajan, A., and Burnap, R. L. (2014). Parallel expression of alternate forms of psbA2 gene provides evidence for the existence of a targeted D1 repair mechanism in *Synechocystis* sp. PCC 6803. *Biochim. Biophys. Acta* 1837, 1417–1426. doi: 10.1016/j.bbabio.2014.02.022

Nickelsen, J., and Rengstl, B. (2013). Photosystem II assembly: from cyanobacteria to plants. *Annu. Rev. Plant Biol.* 64, 609–635. doi: 10.1146/annurev-arplant-050312-120124

Nickelsen, J., Rengstl, B., Stengel, A., Schottkowski, M., Soll, J., and Ankele, E. (2011). Biogenesis of the cyanobacterial thylakoid membrane system–an update. *FEMS Microbiol. Lett.* 315, 1–5. doi: 10.1111/j.1574-6968.2010.02096.x

Nilsson, R., Brunner, J., Hoffman, N. E., and van Wijk, K. J. (1999). Interactions of ribosome nascent chain complexes of the chloroplast- encoded D1 thylakoid membrane protein with cpSRP54. *EMBO J.* 18, 733–742. doi: 10.1093/emboj/18.3.733

Nilsson, R., and van Wijk, K. J. (2002). Transient interaction of cpSRP54 with elongating nascent chains of the chloroplast-encoded D1 protein; 'cpSRP54 caught in the act'. *FEBS Lett.* 524, 127–133. doi: 10.1016/S0014-5793(02)03016-8

Nishiyama, Y., Allakhverdiev, S. I., Yamamoto, H., Hayashi, H., and Murata, N. (2004). Singlet oxygen inhibits the repair of photosystem II by suppressing the translation elongation of the D1 protein in *Synechocystis* sp. PCC 6803. *Biochemistry* 43, 11321–11330. doi: 10.1021/bi036178q

Nixon, P. J., Barker, M., Boehm, M., de Vries, R., and Komenda, J. (2005). FtsH-mediated repair of the photosystem II complex in response to light stress. *J. Exp. Bot.* 56, 357–363. doi: 10.1093/jxb/eri021

Nixon, P. J., and Diner, B. A. (1992). Aspartate 170 of the photosystem II reaction center polypeptide D1 is involved in the assembly of the oxygen evolving manganese cluster. *Biochemistry* 31, 942–948. doi: 10.1021/bi00118a041

Nixon, P. J., and Diner, B. A. (1994). Analysis of water oxidation mutants constructed in the cyanobacterium *Synechocystis* sp. PCC 6803. *Biochem. Soc. Trans.* 22, 338–343. doi: 10.1042/bst0220338

Nixon, P. J., Michoux, F., Yu, J., Boehm, M., and Komenda, J. (2010). Recent advances in understanding the assembly and repair of photosystem II. *Ann. Bot.* 106, 1–16. doi: 10.1093/aob/mcq059

Nixon, P. J., Trost, J. T., and Diner, B. A. (1992). Role of the carboxy terminus of polypeptide D1 in the assembly of a functional water oxidizing manganese cluster in photosystem II of the cyanobacterium *Synechocystis* sp. PCC 6803: assembly requires a free carboxyl group at C terminal position 344. *Biochemistry* 31, 10859–10871. doi: 10.1021/bi00159a029

Nowaczyk, M. M., Hebeler, R., Schlodder, E., Meyer, H. E., Warscheid, B., and Rögner, M. (2006). Psb27, a cyanobacterial lipoprotein, is involved in the repair cycle of photosystem II. *Plant Cell* 18, 3121–3131. doi: 10.1105/tpc.106.042671

Ohad, I., Kyle, D. J., and Arntzen, C. J. (1984). Membrane protein damage and repair: removal and replacement of inactivated 32-kilodalton polypeptides in chloroplast membranes. *J. Cell Biol.* 99, 481–485. doi: 10.1083/jcb.99.2.481

Ono, T. (2001). Metallo-radical hypothesis for photoassembly of (Mn)4-cluster of photosynthetic oxygen evolving complex. *Biochim. Biophys. Acta* 1503, 40–51. doi: 10.1016/S0005-2728(00)00226-7

Ono, T. A., and Inoue, Y. (1982). Photoactivation of the water oxidation system in isolated intact chloroplasts prepared from wheat triticum-aestivum leaves grown under intermittent flash illumination. *Plant Physiol.* 69, 1418–1422. doi: 10.1104/pp.69.6.1418

Ono, T. A., and Inoue, Y. (1983). Requirement of divalent cations for photoactivation of the latent water oxidation system in intact chloroplasts from flashed leaves. *Biochim. Biophys. Acta* 723, 191–201. doi: 10.1016/0005-2728(83)90119-6

Ono, T. A., and Inoue, Y. (1987). Reductant-sensitive intermediates involved in multi-quantum process of photoactivation of latent oxygen-evolving system. *Plant Cell Physiol.* 28, 1293–1300.

Ono, T. A., and Mino, H. (1999). Unique binding site for Mn^{2+} ion responsible for reducing an oxidized Y_Z tyrosine in manganese-depleted photosystem II membranes. *Biochemistry* 38, 8778–8785. doi: 10.1021/bi982949s

Osmond, C. B. (1981). Photorespiration and photoinhibition. *Biochim. Biophys. Acta* 639, 77–98. doi: 10.1016/0304-4173(81)90006-9

Park, S., Khamai, P., Garcia-Cerdan, J. G., and Melis, A. (2007). REP27, a tetratricopeptide repeat nuclear-encoded and chloroplast- localized protein, functions in D1/32-kD reaction center protein turnover and photosystem II repair from photodamage. *Plant Physiol.* 143, 1547–1560. doi: 10.1104/pp.107.096396

Peloquin, J. M., Campbell, K. A., Randall, D. W., Evanchik, M. A., Pecoraro, V. L., Armstrong, W. H., et al. (2000). 55Mn ENDOR of the S2-state multiline EPR signal of photosystem II: implications on the structure of the tetranuclear Mn cluster. *J. Am. Chem. Soc.* 122, 10926–10942. doi: 10.1021/ja002104f

Pistorius, E. K., and Schmid, G. H. (1984). Effect of Mn^{2+} and Ca^{2+} on O_2 evolution and on the variable fluorescence yield associated with Photosystem II in preparations of Anacystis nidulans. *FEBS Lett.* 171, 173–178. doi: 10.1016/0014-5793(84)80482-2

Powles, S. B., and Björkman, O. (1981). Photoinhibition of photosynthesis: effect on chlorophyll fluorescence at 77K in intact leaves and in chloroplast membranes of Nerium oleander. *Planta* 156, 97–107. doi: 10.1007/BF00395424

Puthiyaveetil, S., and Kirchhoff, H. (2013). A phosphorylation map of the photosystem II supercomplex C2S2M2. *Front. Plant Sci.* 4:459. doi: 10.3389/fpls.2013.00459

Qian, M., Al-Khaldi, S. F., Putnam-Evans, C., Bricker, T. M., and Burnap, R. L. (1997). Photoassembly of the photosystem II (Mn)4 cluster in site directed mutants impaired in the binding of the manganese stabilizing protein. *Biochemistry* 36, 15244–15252.

Qian, M., Dao, L., Debus, R. J., and Burnap, R. L. (1999). Impact of mutations within the putative Ca^{2+}-binding lumenal interhelical a-b loop of the photosystem II D1 protein on the kinetics of photoactivation and H_2O-oxidation in *Synechocystis* sp. PCC6803. *Biochemistry* 38, 6070–6081. doi: 10.1021/bi982331i

Radmer, R., and Cheniae, G. M. (1971). Photoactivation of the manganese catalyst of O_2 evolution. II. A two quantum mechanism. *Biochim. Biophys. Acta* 253, 182–186. doi: 10.1016/0005-2728(71)90243-X

Rappaport, F., Ishida, N., Sugiura, M., and Boussac, A. (2011). Ca^{2+} determines the entropy changes associated with the formation of transition states during water oxidation by Photosystem II. *Energy Environ. Sci.* 4, 2520–2524. doi: 10.1039/c1ee01408k

Riggs, P. J., Mei, R., Yocum, C. F., and Penner, H. J. E. (1992). Reduced derivatives of the manganese cluster in the photosynthetic oxygen-evolving complex. *J. Am. Chem. Soc.* 114, 10650–10651. doi: 10.1021/ja00052a079

Roose, J. L., and Pakrasi, H. B. (2004). Evidence that D1 processing is required for manganese binding and extrinsic protein assembly into photosystem II. *J. Biol. Chem.* 279, 45417–45422. doi: 10.1074/jbc.M408458200

Roose, J. L., and Pakrasi, H. B. (2007). The PSB27 protein facilitates manganese cluster assembly in photosystem II. *J. Biol. Chem.* 44, 45417–45422. doi: 10.1074/jbc.M408458200

Sacharz, J., Bryan, S. J., Yu, J., Burroughs, N. J., Spence, E. M., Nixon, P. J., et al. (2015). Sub-cellular location of FtsH proteases in the cyanobacterium *Synechocystis* sp. PCC 6803 suggests localised PSII repair zones in the thylakoid membranes. *Mol. Microbiol.* 96, 448–462. doi: 10.1111/mmi.12940

Satoh, K., and Yamamoto, Y. (2007). The carboxyl-terminal processing of precursor D1 protein of the photosystem II reaction center. *Photosyn. Res.* 94, 203–215. doi: 10.1007/s11120-007-9191-z

Sauer, K., and Yachandra, V. K. (2002). A possible evolutionary origin for the Mn-4 cluster of the photosynthetic water oxidation complex from natural MnO_2 precipitates in the early ocean. *Proc. Natl. Acad. Sci. U.S.A.* 99, 8631–8636. doi: 10.1073/pnas.132266199

Schottkowski, M., Gkalympoudis, S., Tzekova, N., Stelljes, C., Schünemann, D., Ankele, E., et al. (2009). Interaction of the periplasmic PratA factor and the PsbA (D1) protein during biogenesis of photosystem II in *Synechocystis* sp. PCC 6803. *J. Biol. Chem.* 284, 1813–1819. doi: 10.1074/jbc.M806116200

Seibert, M., Tamura, N., and Inoue, Y. (1989). Lack of photoactivation capacity in scenedesmus-obliquus Lf-1 results from loss of half the high-affinity manganese-binding site - relationship to the unprocessed D1 protein. *Biochim. Biophys. Acta* 974, 185–191. doi: 10.1016/S0005-2728(89)80371-8

Semin, B. K., Podkovirina, T. E., Davletshina, L. N., Timofeev, K. N., Ivanov, I.I, and Rubin, A. B. (2015). The extrinsic PsbO protein modulates the oxidation/reduction rate of the exogenous Mn cation at the high-affinity Mn-binding site of Mn-depleted PSII membranes. *J. Bioenerg. Biomembr.* 47, 361–367. doi: 10.1007/s10863-015-9618-8

Shen, J. R., Qian, M., Inoue, Y., and Burnap, R. L. (1998). Functional characterization of *Synechocystis* sp. PCC 6803 delta psbU and delta psbV mutants reveals important roles of cytochrome c-550 in cyanobacterial oxygen evolution. *Biochemistry* 37, 1551–1558. doi: 10.1021/bi971676i

Shestakov, S. V., Anbudurai, P. R., Stanbekova, G. E., Gadzhiev, A., Lind, L. K., and Pakrasi, H. B. (1994). Molecular cloning and characterization of the ctpA gene encoding a carboxyl terminal processing protease. Analysis of a spontaneous photosystem II deficient mutant strain of the cyanobacterium *Synechocystis* sp. PCC 6803. *J. Biol. Chem.* 269, 19354–19359.

Shinohara, K., Ono, T. A., and Inoue, Y. (1992). Photoactivation of oxygen-evolving enzyme in dark-grown pine cotyledons relationship between assembly of photosystem II proteins and integration of manganese and calcium. *Plant Cell Physiol.* 33, 281–289.

Silva, P., Thompson, E., Bailey, S., Kruse, O., Mullineaux, C. W., Robinson, C., et al. (2003). FtsH is involved in the early stages of repair of photosystem II in *Synechocystis* sp PCC 6803. *Plant Cell* 15, 2152–2164. doi: 10.1105/tpc.012609

Stengel, A., Gügel, I. L., Hilger, D., Rengstl, B., Jung, H., and Nickelsen, J. (2012). Initial steps of photosystem II *de novo* assembly and preloading with manganese take place in biogenesis centers in *Synechocystis*. *Plant Cell* 24, 660–675. doi: 10.1105/tpc.111.093914

Suga, M., Akita, F., Hirata, K., Ueno, G., Murakami, H., Nakajima, Y., et al. (2015). Native structure of photosystem II at 1.95 A resolution viewed by femtosecond X-ray pulses. *Nature* 517, 99–103. doi: 10.1038/nature13991

Taguchi, F., Yamamoto, Y., and Satoh, K. (1995). Recognition of the structure around the site of cleavage by the carboxyl terminal processing protease for D1 precursor protein of the photosystem II reaction center. *J. Biol. Chem.* 270, 10711–10716.

Tamura, N., and Cheniae, G. (1987). Photoactivation of the water-oxidizing complex in photosystem II membranes depleted of Mn and extrinsic proteins. I. Biochemical and kinetic characterization. *Biochim. Biophys. Acta* 890, 179–194. doi: 10.1016/0005-2728(87)90019-3

Tamura, N., and Cheniae, G. M. (1986). Requirements for the photoligation of Mn^{2+} in PSII membranes and the expression of water-oxidizing activity of the polynuclear Mn-catalyst. *Feder. Eur. Biochem. Soc. Lett.* 200, 231–236. doi: 10.1016/0014-5793(86)80544-0

Tamura, N., Inoue, Y., and Cheniae, G. (1989). Photoactivation of the water-oxidizing complex in photosystem II membranes depleted of Mn, Ca, and extrinsic proteins. II. Studies on the function of Ca^{2+}. *Biochim. Biophys. Acta* 976, 173–181. doi: 10.1016/S0005-2728(89)80227-0

Taylor, M. A., Nixon, P. J., Todd, C. M., Barber, J., and Bowyer, J. R. (1988). Characterisation of the D1 protein in a photosystem II mutant (LF-1) of Scenedesmus obliquus blocked on the oxidising side Evidence supporting non-processing of D1 as the cause of the lesion. *FEBS Lett.* 235, 109–116. doi: 10.1016/0014-5793(88)81243-2

Trost, J. T., Chisholm, D. A., Jordan, D. B., and Diner, B. A. (1997). The D1 C-terminal processing protease of photosystem II from *Scenedesmus obliquus*. Protein purification and gene characterization in wild type and processing mutants. *J. Biol. Chem.* 272, 20348–20356. doi: 10.1074/jbc.272.33.20348

Tyryshkin, A. M., Watt, R. K., Baranov, S. V., Dasgupta, J., Hendrich, M. P., and Dismukes, G. C. (2006). Spectroscopic evidence for Ca^{2+} involvement in the assembly of the Mn_4Ca cluster in the photosynthetic water-oxidizing complex. *Biochemistry* 45, 12876–12889. doi: 10.1021/bi061495t

Umena, Y., Kawakami, K., Shen, J. R., and Kamiya, N. (2011). Crystal structure of oxygen-evolving photosystem II at a resolution of 1.9 Ångstrom. *Nature* 473, U55–U65. doi: 10.1038/nature09913

van Wijk, K. J., Andersson, B., and Aro, E. M. (1996). Kinetic resolution of the incorporation of the D1 protein into photosystem II and localization of assembly intermediates in thylakoid membranes of spinach chloroplasts. *J. Biol. Chem.* 271, 9627–9636. doi: 10.1074/jbc.271.16.9627

van Wijk, K. J., Roobol-Boza, M., Kettunen, R., Andersson, B., and Aro, E. M. (1997). Synthesis and assembly of the D1 protein into photosystem II: processing of the C terminus and identification of the initial assembly partners and complexes during photosystem II repair. *Biochemistry* 36, 6178–6186. doi: 10.1021/bi962921l

Vass, I., and Cser, K. (2009). Janus-faced charge recombinations in photosystem II photoinhibition. *Trends Plant Sci.* 14, 200–205. doi: 10.1016/j.tplants.2009.01.009

Vrettos, J. S., Limburg, J., and Brudvig, G. W. (2001). Mechanism of photosynthetic water oxidation: combining biophysical studies of photosystem II with inorganic model chemistry. *Biochim. Biophys. Acta* 1503, 229–245. doi: 10.1016/S0005-2728(00)00214-0

Whitelegge, J. P., Koo, D., Diner, B. A., Domian, I., and Erickson, J. M. (1995). Assembly of the Photosystem II oxygen evolving complex is inhibited in psbA site directed mutants of Chlamydomonas reinhardtii. Aspartate 170 of the D1 polypeptide. *J. Biol. Chem.* 270, 225–235. doi: 10.1074/jbc.270.1.225

Yamamoto, Y. (2001). Quality control of photosystem ii. *Plant Cell Physiol.* 42, 121–128. doi: 10.1093/pcp/pce022

Zaltsman, L., Ananyev, G. M., Bruntrager, E., and Dismukes, G. C. (1997). Quantitative kinetic model for photoassembly of the photosynthetic water oxidase from its inorganic constituents: requirements for manganese and calcium in the kinetically resolved steps. *Biochemistry* 36, 8914–8922. doi: 10.1021/bi970187f

Zhang, L., and Aro, E. M. (2002). Synthesis, membrane insertion and assembly of the chloroplast-encoded D1 protein into photosystem II. *FEBS Lett.* 512, 13–18. doi: 10.1016/S0014-5793(02)02218-4

Zhang, L., Paakkarinen, V., Suorsa, M., and Aro, E. M. (2001). A SecY homologue is involved in chloroplast-encoded D1 protein biogenesis. *J. Biol. Chem.* 276, 37809–37814. doi: 10.1074/jbc.M105522200

Zhang, L., Paakkarinen, V., van Wijk, K. J., and Aro, E. M. (1999). Co-translational assembly of the D1 protein into photosystem II. *J. Biol. Chem.* 274, 16062–16067. doi: 10.1074/jbc.274.23.16062

Zhang, L., Paakkarinen, V., van Wijk, K. J., and Aro, E. M. (2000). Biogenesis of the chloroplast-encoded D1 protein: regulation of translation elongation, insertion, and assembly into photosystem II. *Plant Cell* 12, 1769–1782. doi: 10.1105/tpc.12.9.1769

Conflict of Interest Statement: The authors declare that the research was conducted in the absence of any commercial or financial relationships that could be construed as a potential conflict of interest.

frontiers in Plant Science

REVIEW
published: 05 February 2016
doi: 10.3389/fpls.2016.00084

Structural Coupling of Extrinsic Proteins with the Oxygen-Evolving Center in Photosystem II

Kentaro Ifuku[1] and Takumi Noguchi[2]*

[1] *Graduate School of Biostudies, Kyoto University, Kyoto, Japan,* [2] *Graduate School of Science, Nagoya University, Aichi, Japan*

Photosystem II (PSII), which catalyzes photosynthetic water oxidation, is composed of more than 20 subunits, including membrane-intrinsic and -extrinsic proteins. The PSII extrinsic proteins shield the catalytic Mn_4CaO_5 cluster from the outside bulk solution and enhance binding of inorganic cofactors, such as Ca^{2+} and Cl^-, in the oxygen-evolving center (OEC) of PSII. Among PSII extrinsic proteins, PsbO is commonly found in all oxygenic organisms, while PsbP and PsbQ are specific to higher plants and green algae, and PsbU, PsbV, CyanoQ, and CyanoP exist in cyanobacteria. In addition, red algae and diatoms have unique PSII extrinsic proteins, such as PsbQ′ and Psb31, suggesting functional divergence during evolution. Recent studies with reconstitution experiments combined with Fourier transform infrared spectroscopy have revealed how the individual PSII extrinsic proteins affect the structure and function of the OEC in different organisms. In this review, we summarize our recent results and discuss changes that have occurred in the structural coupling of extrinsic proteins with the OEC during evolutionary history.

Keywords: extrinsic proteins, FTIR, oxygen-evolving complex, photosystem II, photosynthetic electron transport

OPEN ACCESS

Edited by:
Julian Eaton-Rye, University of Otago, New Zealand

Reviewed by:
Terry Michael Bricker, Louisiana State University and A&M College, USA
Marc M. Nowaczyk, Ruhr University Bochum, Germany

****Correspondence:***
Kentaro Ifuku
ifuku@kais.kyoto-u.ac.jp

Specialty section:
This article was submitted to Plant Cell Biology, a section of the journal Frontiers in Plant Science

Received: *14 November 2015*
Accepted: *17 January 2016*
Published: *05 February 2016*

Citation:
Ifuku K and Noguchi T (2016) Structural Coupling of Extrinsic Proteins with the Oxygen-Evolving Center in Photosystem II. Front. Plant Sci. 7:84. doi: 10.3389/fpls.2016.00084

INTRODUCTION

Photosystem II (PSII) is a key protein complex involved in light-energy conversion reactions in photosynthesis. PSII converts light energy into the electrochemical potential energy required to split water into H^+, electrons, and molecular oxygen (Debus, 1992). The PSII complex is composed of more than 20 subunits, with CP47, CP43, D1, D2, Cyt b_{559} α- and β-subunits, and PsbI comprising the reaction center complex (Satoh, 2008). In addition, a number of small peripheral subunits stabilize the PSII core (Pagliano et al., 2013). Recent X-ray structural analysis of the cyanobacterial PSII complex has revealed the location of most subunits, pigments, and redox cofactors (Ferreira et al., 2004; Guskov et al., 2009; Umena et al., 2011; Suga et al., 2015). In PSII, light excitation of the primary donor P680, comprising a special pair of chlorophyll (Chl) *a*, results in electron transfer to a nearby pheophytin, followed by electron transfer to the acceptor quinones (Q_A and Q_B). The resulting cation radical of $P680^+$ receives electrons via a redox-active tyrosine of D1, Y_Z, from the Mn_4CaO_5 cluster. The Mn_4CaO_5 cluster converts two water molecules into one molecular oxygen and four protons through a light-driven cycle consisting of five intermediates called S_i states ($i = 0$–4; McEvoy and Brudvig, 2006). Among them, the S_1 state is the most dark-stable, and flash illumination advances each S_i state ($i = 0$–3) to the next S_{i+1} state. Molecular oxygen is released during the S_3–S_4–S_0 transition after the transient S_4 state (Vinyard et al., 2013).

The mechanism of water oxidation and the subunit structure of the PSII core are highly conserved across oxygenic photosynthetic organisms ranging from cyanobacteria to flowering plants, while the composition of the extrinsic subunits of PSII surrounding the catalytic Mn_4CaO_5 cluster has undergone a large evolutionary change (Bricker et al., 2012; Ifuku, 2015; **Figure 1**). Green eukaryotes including higher plants and green algae have a set of three extrinsic proteins — PsbO, PsbP, and PsbQ — that bind to the lumenal surface of PSII. In cyanobacterial PSII, PsbV, and PsbU are present instead of PsbP and PsbQ (Shen and Inoue, 1993). Furthermore, cyanobacteria have PsbP and PsbQ homologs (CyanoP and CyanoQ, respectively; Kashino et al., 2002; Thornton et al., 2004), but these proteins are not yet included in the current crystal structures. Furthermore, there are multiple homologs of PsbP and PsbQ in the chloroplast thylakoid lumen and some of them play important roles in the assembly and stability of various thylakoid membrane complexes including PSII, PSI, and the chloroplast NADH dehydrogenase-like complex (Ifuku et al., 2008, 2010, 2011a; Bricker et al., 2013; Ifuku, 2014). These facts suggest that PsbP and PsbQ proteins in green plants have evolved from their cyanobacterial homologs, where considerable genetic and functional modifications have occurred to generate the present eukaryotic forms.

In red algae and diatoms, PsbQ′, a 20-kDa homolog of CyanoQ, is bound to PSII as an extrinsic subunit in addition to PsbO, PsbU, and PsbV (Ohta et al., 2003). Diatoms possess an additional specific extrinsic subunit, Psb31 (Okumura et al., 2008), and recent structural analysis suggests that Psb31 might be a homolog of PsbQ (Nagao et al., 2013). Although high-resolution structures of individual PSII extrinsic subunits have been reported for eukaryotes (Calderone et al., 2003; Ifuku et al., 2004; Balsera et al., 2005; Kopecky et al., 2012; Cao et al., 2015), their binding sites and topologies have not been determined because crystallographic information derived from prokaryotic cyanobacterial PSII cannot be fully applied to eukaryotic PSII.

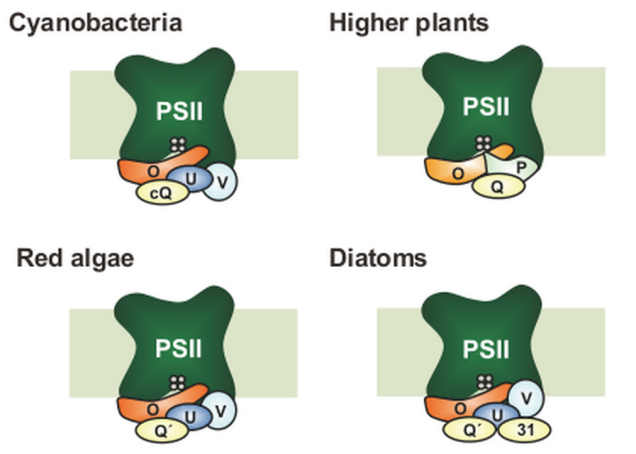

FIGURE 1 | Differences in subunit composition of the extrinsic proteins of photosystem II (PSII). Only PsbO (O) has remained in all photosynthetic organisms. In higher plants, PsbV (V) and PsbU (U) were lost, while PsbP (P) and PsbQ (Q) have been derived from CyanoP (cP) and CyanoQ (cQ), respectively. Green algal PSII is basically similar to that in higher plants, whereas green-algal PsbQ is more similar to PsbQ′ (not shown). CyanoP has been excluded from the model, because its stable association with PSII is still unclear. In red algae and diatoms, PsbQ′ (Q′) has developed from CyanoQ; in addition, Psb31 (31) is found in diatoms. These models do not show the exact location and interaction of the PSII extrinsic subunits.

A number of reviews have been published about function, structure, and evolution of PSII extrinsic proteins in various photosynthetic organisms (Roose et al., 2007b; Enami et al., 2008; Ifuku et al., 2008, 2011b; Bricker and Frankel, 2011; Bricker et al., 2012; Ifuku, 2014, 2015). In this review, we focus on the structural coupling of extrinsic proteins with the oxygen-evolving center (OEC) in different photosynthetic organisms, which has been investigated by reconstitution experiments combined with light-induced Fourier transform infrared (FTIR) difference spectroscopy (Tomita et al., 2009; Ido et al., 2012; Uno et al., 2013; Nishimura et al., 2014; Nagao et al., 2015). This technique can detect the structural changes in the OEC in the S-state transitions, including the changes in the secondary structures of polypeptide main chains, amino acid side chains, and hydrogen bond networks of proteins and water molecules (Noguchi, 2007, 2015; Debus, 2015). The results of FTIR are evaluated in light of the current knowledge on the subunit interactions in PSII and also discussed in terms of the changes that occurred during evolution.

HIGHER PLANTS

Functions of Extrinsic Proteins in PSII, Briefly

The molecular functions of the extrinsic proteins in higher plants have been intensively analyzed by release-reconstitution experiments using PSII-enriched membrane preparations (BBY membranes; Berthold et al., 1981). Briefly, PsbO is most strongly bound to PSII and stabilizes the Mn cluster (Kuwabara et al., 1985). PsbP is involved in Ca^{2+} and Cl^- retention in PSII (Ghanotakis et al., 1984a), and PsbQ participates primarily in Cl^- retention (Akabori et al., 1984; Miyao and Murata, 1985). In addition, PsbP and PsbQ have a role in protecting the Mn cluster from reductants in the bulk solution (Ghanotakis et al., 1984b). It is reasonable that PsbO, commonly found in PSII in all oxygenic photosynthetic organisms, is essential for the accumulation and assembly of PSII *in planta* (Murakami et al., 2002; Yi et al., 2005). In addition, genetic studies using knockdown or knockout plants have suggested that PsbP, but not PsbQ, is essential for the oxygen-evolving activity of PSII *in vivo* (Ifuku et al., 2005b; Yi et al., 2007), suggesting that the development of the PsbP protein as an extrinsic subunit would be the crucial event for PSII function during evolution (Ido et al., 2009; Ifuku et al., 2011b). PsbQ is reported to be required for PSII stability under prolonged low-light conditions (Yi et al., 2006).

It was suggested that PsbP and PsbQ also play an important role in stabilizing the architecture of the PSII-light-harvesting complex (LHC) II supercomplexes in higher plants (Ifuku et al., 2011b). PsbP knockdown by RNAi caused a severe decrease in the levels of PSII-LHCII supercomplexes, whereas

the amounts of unattached LHCII trimers and minor LHCs were significantly increased (Ido et al., 2009). Similarly, the abundance of PSII-LHCII supercomplexes decreased in mutants lacking PsbQ and/or PsbR (Allahverdiyeva et al., 2013). PsbR is another subunit, mostly extrinsic and specifically found in green plants, which stabilizes the binding of PsbP (Suorsa et al., 2006; Allahverdiyeva et al., 2007; Liu et al., 2009). Furthermore, depletion of PsbQ and/or PsbR affects short-term regulatory mechanisms such as state transitions and non-photochemical quenching (Allahverdiyeva et al., 2013). These observations are relevant to the chemical-crosslinking study showing the interaction of PsbP and PsbQ with a minor antenna protein CP26 and the inner core antenna CP43 (Ido et al., 2014).

Structural Coupling with the OEC

The importance of PsbP in structural coupling with the OEC has been suggested by *in vitro* reconstitution studies combined with FTIR measurements (Tomita et al., 2009). PSII membranes depleted of PsbP and PsbQ by NaCl washing showed clear changes in amide I bands (1700-1600 cm^{-1}; C=O stretches of backbone amides), which reflect structural changes in polypeptide main chains, in S_2-minus-S_1 FTIR difference spectra (**Figure 2**), whereas no appreciable changes were observed in the bands of carboxylate and imidazole groups, which arise from ligands or the immediate surroundings of the Mn_4CaO_5 cluster. Further depletion of PsbO by $CaCl_2$ washing did not induce further changes (**Figure 2**). The original amide I features were recovered by reconstitution of the NaCl-washed PSII membranes with a recombinant PsbP heterologously expressed in *Escherichia coli*, and the same recovery was observed with ^{13}C-labeled PsbP (Tomita et al., 2009). These results indicate that the PsbP protein, but not PsbQ or PsbO, affects the protein conformation around the Mn_4CaO_5 cluster in the intrinsic proteins without changing the immediate interactions of the Mn_4CaO_5 cluster in the OEC.

It should be noted that controversial data have recently been reported stating that the removal of PsbP and PsbQ from the PSII core preparations of spinach showed no significant effect on the S_2-minus-S_1 spectrum (Offenbacher et al., 2013). However, the control spectrum in this report showed an amide I feature typical of PsbP-depleted PSII: lower and higher intensities at the 1668 and 1686 cm^{-1} peaks, respectively (**Figure 2**). We thus speculate that the control PSII sample was actually depleted of PsbP and PsbQ during FTIR measurement, possibly by the presence of potassium ferricyanide in addition to 20 mM $CaCl_2$.

The structural coupling of PsbP with the OEC has been studied by truncation and site-directed mutagenesis. **Table 1** summarizes the results of our reconstitution-FTIR experiments, while **Figure 3** shows the amide I region of the FTIR double difference (untreated-minus-treated) spectra. The positions of mutated amino-acid residues are indicated in the cartoon model of the spinach PsbP structure reported recently (Cao et al., 2015; (**Figure 4**). Overall, the abilities of mutated PsbPs to restore the structural changes around the OEC correlate well with the oxygen-evolving activity reconstituted by each PsbP species. This strongly suggests the tight structural coupling of PsbP with the OEC in higher plant PSII.

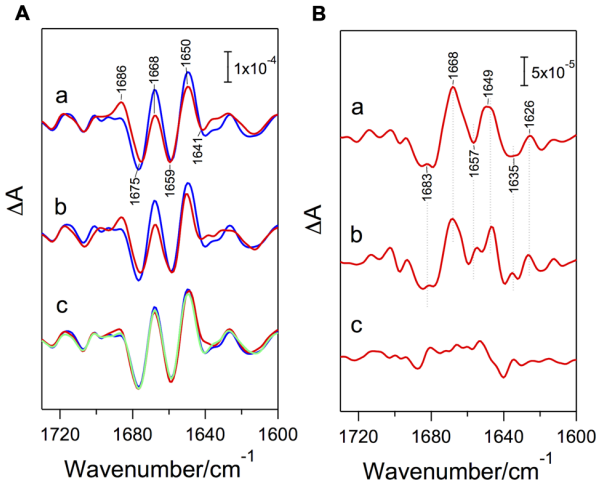

FIGURE 2 | (A) Amide I region of the S_2-minus-S_1 FTIR difference spectra (red lines) of NaCl-washed (a), $CaCl_2$-washed (b), and NaCl-washed, PsbP-reconstituted (c) PSII membranes in comparison with the spectrum of untreated PSII membranes (blue lines). A green line in (c) is the spectrum of PSII reconstituted with ^{13}C-labeled PsbP. **(B)** Double-difference spectra between the S_2-minus-S_1 spectra of treated and untreated PSII samples. (a) untreated-*minus*-NaCl-washed PSII; (b) untreated-*minus*-$CaCl_2$-washed PSII; (c) untreated-*minus*-NaCl-washed, PsbP-reconstituted PSII. Reproduced from Tomita et al. (2009).

TABLE 1 | Effects of various PsbP mutations on structural coupling with the oxygen-evolving center (OEC).

PsbP	[a]O_2 activity	[b]Binding to PSII	[c]FTIR	Reference
Wild-type (spinach)	++++	++++	○	Tomita et al., 2009
Δ9	++	+++	n.d.	Miyao et al., 1988; Ifuku et al., 2008
Δ15	–	–	×	Ifuku et al., 2005a; Tomita et al., 2009; Kakiuchi et al., 2012
Δ19	–	–	n.d.	Ifuku and Sato, 2002
K160A	++	+++	×	Nishimura et al., 2014
K143A	++	+++	×	
R48A	++	+++	Δ	
K143A/R48A	+	+	n.d.	
K143A/K160A/R48A	–	–	n.d.	
K11A	++++	+++	n.d.	
K13A	++++	+++	n.d.	
H144A	+	++++	×	Ido et al., 2012
D165V	++++	++++	○	
E177V	++++	++++	n.d.	
H144A/D165V	++++	++++	○	

[a]*O_2-evolving activities were measured in buffer depleted of Ca^{2+} and Cl^-. The activity restored by binding of mutant PsbP is indicated by the number of plus signs (+). A minus sign (–) indicates no recovery.* [b]*Binding to PSII was estimated by imaging SDS-PAGE gels. The binding affinity of mutant PsbP to PSII is indicated by the number of plus signs (+). A minus sign (–) indicates no binding to PSII.* [c]*Recovery of the amide I bands in the S_2-minus-S_1 FTIR difference spectra, which were measured in the presence of Ca^{2+} and Cl^-. ○, full recovery; Δ, partial recovery; ×, no recovery; n.d., not determined.*

Noticeably, reconstitution with Δ15-PsbP, in which the 15 N-terminal residues were truncated, did not restore the amide I bands, indicating that the interaction of the N-terminal region

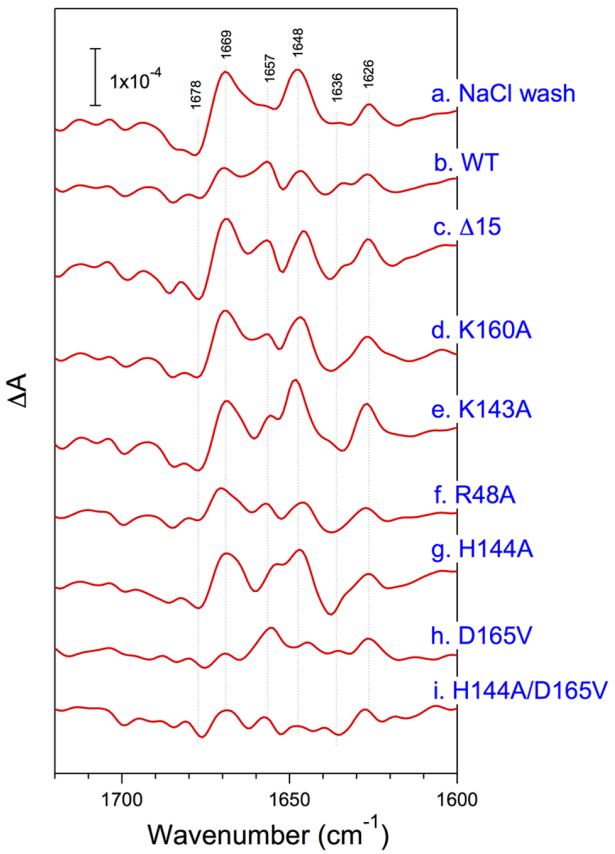

FIGURE 3 | Amide I region of untreated-minus-treated double difference spectra of the $S_2Q_A^-$-minus-S_1Q_A FTIR spectra of PSII membranes from spinach. PSII membranes were NaCl-washed (a) and then reconstituted with WT- (b), Δ15- (c), K160A- (d), K142A- (e), R48A- (f), H144A- (g), D165V- (h), and H144A/D165V- (i) PsbP. Reproduced from Ido et al. (2012), Kakiuchi et al. (2012), and Nishimura et al. (2014).

would be responsible for inducing the conformational changes around the OEC (Tomita et al., 2009). In fact, Δ15-PsbP did not restore the Ca^{2+} and Cl^- retention ability upon rebinding to PSII (Ifuku and Sato, 2002). It was found that additional binding of PsbQ partly restores the ability of Δ15-PsbP to induce the proper conformational changes and activate oxygen evolution in the OEC (Kakiuchi et al., 2012). These facts suggest that the N-terminal region of PsbP is not essential but may have a function in recruiting PsbP to the proper binding site to induce the conformational changes. PsbQ would have an auxiliary role in supporting PsbP binding and function in higher plants.

The central αβα structure of PsbP in its C-terminal domain is also important for the interaction with PSII to induce the conformational change in the OEC. The PsbP surface has a basic region consisting of conserved Arg48, Lys143, and Lys160, and the mutations of R48A, K143A, and K160A result in lower binding affinity with PSII, and double and triple mutation of those residues severely diminishes their binding to PSII (Nishimura et al., 2014). Even when a saturating amount of protein is used for the reconstitution, the R48A, K143A, and K160A proteins cannot restore the rate of oxygen evolution fully at low chloride concentrations. The results of FTIR were consistent with the above finding, showing that these mutated proteins are not able to induce the normal conformational change around the Mn cluster during the S_1-to-S_2 transition. The above observations suggest that the basic surface of PsbP is involved in the electrostatic interaction with the PSII complex. This binding topology of PsbP is further supported by a recent study using synchrotron radiolysis of water to further define buried surface regions by modification with $OH^{\cdot}$ (Mummadisetti et al., 2014).

We also investigated the role of the structure around His-144 and Asp-165 in the C-terminal domain of PsbP, which is suggested to be a metal binding site in PsbP (Ido et al., 2012). PsbP with an H144A mutation shows a reduced ability to retain Cl^- anions in PSII, whereas the D165V mutation does not affect PsbP function. In FTIR, PsbP-H144A could not restore proper interaction with PSII inducing the conformational change around the Mn cluster during the S_1-to-S_2 transition. Consistently, mutations of K166A and K170A near His144 are suggested to affect the PsbP binding to PSII (Tohri et al., 2004). Unexpectedly, the H144A/D165V double mutation suppresses the defect caused by H144A mutation. Presumably, His-144 and Asp-165 form a salt bridge and H144A mutation would disrupt this bridge and liberate Asp-165, inhibiting the proper PsbP-PSII interaction. These residues therefore have a role other than metal binding. The recently observed crystal structure of spinach PsbP suggests an additional binding site for Mn^{2+} coordinated by Asp-98 (Cao et al., 2015). The authors speculated that Mn-binding in this site may induce conformational change of PsbP during the PSII damage–repair cycle. However, PsbPs of some plant species, such as *Arabidopsis* and cucumber, have Ala-98 instead of Asp-98. To discuss the physiological importance of the metal binding site observed in the crystal structures, it is necessary to evaluate the exact metal binding constant for each binding site. Further characterization of mutated PsbP proteins *in vivo* will provide conclusive results.

Interaction within the PSII Supercomplex

The historical model of the organization of the extrinsic subunits in higher plants is that PsbO binds directly to the PSII core, followed by PsbP binding to PsbO, and then PsbQ binding to PsbP or PsbO. However, recent studies using chemical cross-linking combined with mass spectrometry suggest the direct interactions of PsbP and PsbQ with membrane-intrinsic PSII subunits. Using the zero-length cross-linker 1-ethyl-3-(3-diethylaminopropyl) carbodiimide (EDC), interactions between PsbP and PsbE and between PsbP and PsbR were detected (Ido et al., 2012, 2014). In addition, PsbP and PsbQ were further linked to the CP26 and CP43 light-harvesting proteins. Furthermore, the cross-linked sites between PsbP:Ala-1 and PsbE:Glu-57, PsbP:Lys-27 and PsbR:Asp-22, and PsbP:Lys-174 and CP26:Glu-96 were identified by tandem mass spectrometry. The above information allows us to evaluate the binding manner of extrinsic proteins in the PSII supercomplex in higher plants (Ido et al., 2014) in light of the FTIR studies.

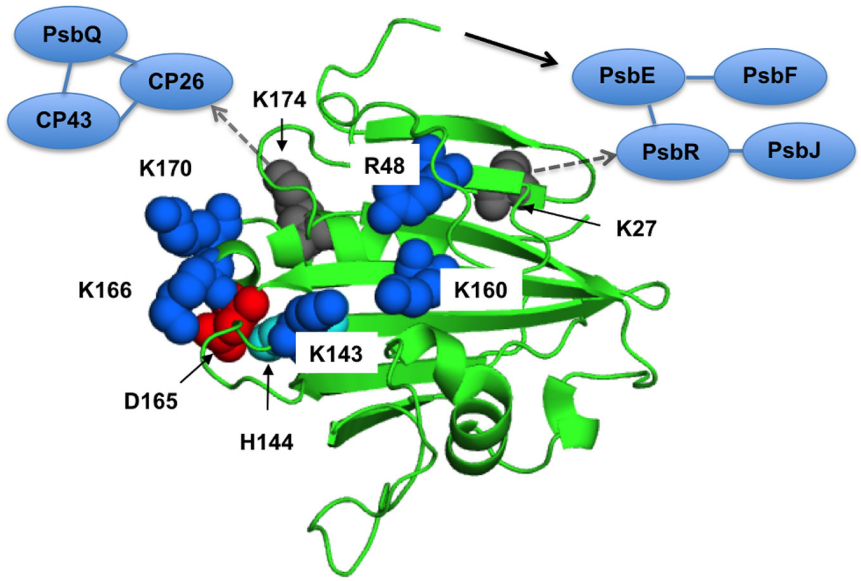

FIGURE 4 | The proposed interaction surface of the extrinsic PsbP protein with the PSII core. The basic amino-acid residues important for the structural coupling with the OEC are labeled and shown as blue sphere models in a spinach PsbP crystal structure (PDB ID: 4RTI, Cao et al., 2015). Asp-165 and His-144, shown as red and cyan spheres, make a salt bridge required for the proper interaction with PSII (Ido et al., 2012). Lys-27 and Lys-174, shown as gray spheres, are suggested to interact with PsbR and CP26, respectively (Ido et al., 2014). A black arrow indicates the N-terminal sequence of PsbP extended to interact with PsbE. Interactions around CP26 and PsbR are also schematically indicated. See text for detail.

The possible candidates for the polypeptide chains affected by PsbP during the S_1 to S_2 transition are those interacting with the Mn_4CaO_5 cluster and Cl^- ions via ligation or direct hydrogen bonding. In the cyanobacterial PSII core complex, the Mn_4CaO_5 cluster and one Cl^- ion interact with a number of residues in the C-terminal region of the D1 protein, as well as the Glu-354 and Arg-357 of the CP43 proteins (Umena et al., 2011). In addition, another Cl^- ion is coordinated by Lys-317 on the D2 protein (Kawakami et al., 2009). These two Cl^- bindings are suggested to be important for the coordination structure of the Mn_4CaO_5 cluster and/or for proposed proton channels, thereby keeping the OEC fully active (Pokhrel et al., 2013; Suzuki et al., 2013). Our cross-linking study suggested that PsbP may change the structure of CP43 to induce structural changes around the OEC (Ido et al., 2014). Alternatively, interaction of the N-terminal region of PsbP with PsbE and PsbR, and possibly PsbJ, may affect the structure of D2 by inducing changes around the Cl^- binding site. This binding manner of PsbP may be similar to that of PsbV in cyanobacterial systems, as has been suggested in recent reviews (Bricker et al., 2015; Ifuku, 2015).

It should be noted that a later study using a cross-linker bis-sulfosuccinimidyl suberate (BS3), which has a spacer length of 11.4 Å, has proposed another binding model of PsbP and PsbQ in higher plants' PSII (Mummadisetti et al., 2014). Cross-linking by BS3 failed to detect an interaction between extrinsic and intrinsic PSII proteins, while it indicated that the N-terminal 15-amino-acid residue domain of PsbP was in close proximity ($\leq$11.4 Å) to the C-terminal region of PsbP. Assuming that PsbP and PsbQ are located near the interface between CP43 and CP26, the N-terminal sequence of PsbP should extend toward PsbE (Ido et al., 2012, 2014); however, this model was unsupported by BS3 crosslinking experiments. Attempts to reconcile this discrepancy have been made in the recent reviews by Ifuku (2015). High-resolution structural analysis is required to reveal the detailed extrinsic lumenal relationships in the PSII-LHCII supercomplex.

OTHER EUKARYOTIC ALGAE

Red Algae

Red algae have PsbV, PsbU, and PsbQ′ in addition to the common PsbO. Enami et al. (1998) performed reconstitution of the PSII core complexes of *Cyanidium caldarium* with these extrinsic proteins in various combinations. PsbO and PsbQ′ were independently bound to PSII, whereas PsbV and PsbU required binding of PsbO and could fully bind only in the presence of both PsbO and PsbQ′. The O_2-evolution activity was recovered step by step in the course of reconstitution (**Figure 5B**, blue bars). Uno et al. (2013) examined the effect of rebinding the extrinsic proteins to the core complexes of *C. caldarium* on the OEC protein conformation by S_2-minus-S_1 FTIR measurements. The vibrations of carboxylate groups were virtually unchanged even by removal of all extrinsic proteins, indicating that the interactions of the Mn_4CaO_5 cluster were not affected by extrinsic proteins. By contrast, amide I and II bands, reflecting changes in polypeptide main chains, were significantly altered by the removal and rebinding of extrinsic proteins (**Figure 5A**). The extent of the recovery of the amide I and II bands by reconstitution with extrinsic proteins

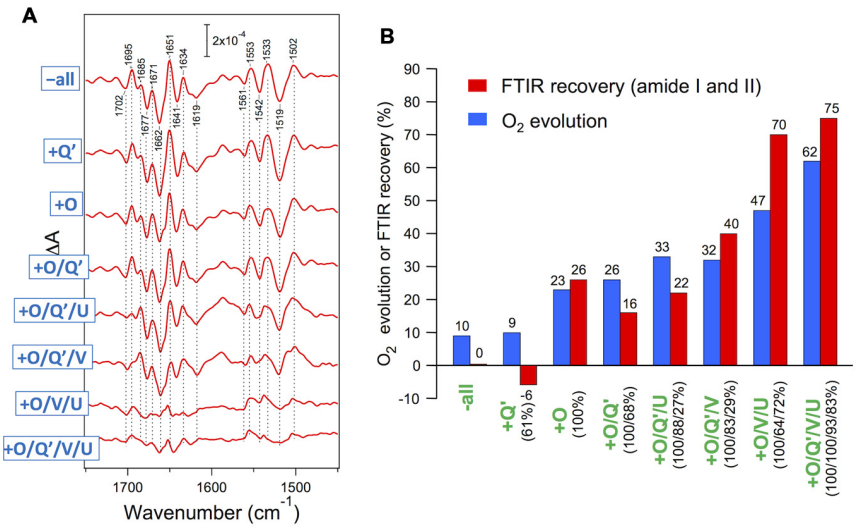

FIGURE 5 | (A) Recovery of amide I and II bands in FTIR spectra upon reconstitution of PSII core complexes of *Cyanidium caldarium* with extrinsic proteins. Double difference spectra between the S_2-minus-S_1 FTIR difference spectra of reconstituted and untreated PSII samples are shown. The samples involved 10 mM $CaCl_2$. **(B)** Comparison of the recovery of the FTIR amide I and II bands (red bars) with that of O_2 evolution (blue bars: taken from Enami et al., 1998) upon reconstitution with extrinsic proteins. The amounts of reconstituted extrinsic proteins are indicated as figures in parentheses. O_2 evolution was measured in the presence of 50 mM $CaCl_2$ (Enami et al., 1998). Reproduced from Uno et al. (2013).

(**Figure 5B**, red bars) correlated well with that of O_2-evolution activity (blue bars), revealing a direct relationship of the protein conformation of the OEC with its activity. It was shown that PsbV binding mainly contributed to the restoration of the protein conformation of the OEC, resembling the function of PsbP in higher plants. PsbU seemed to support the proper binding of PsbV, which is analogous to PsbQ in higher plants. These facts support a model proposed by Ido et al. (2014), in which PsbP in higher plant PSII occupies a position roughly similar to that occupied by PsbV in the cyanobacterial crystal structure (Ifuku, 2015). Crystallization and preliminary X-ray diffraction analysis have already been reported (Adachi et al., 2009), so that the structure of red algal PSII will be available in the near future.

Diatoms

Diatom PSII contains a fifth extrinsic protein, Psb31, in addition to the four red algal-type extrinsic proteins. Psb31 is suggested to have originated via a secondary endosymbiosis event (Nagao et al., 2013). Reconstitution experiments using proteins from a centric diatom, *Chaetoceros gracilis*, have suggested that Psb31 binds directly to PSII intrinsic proteins. Noticeably, PSII reconstituted with Psb31 alone can partially restore oxygen-evolving activity in the absence of PsbO, suggesting that Psb31 has a novel and specific function in diatom PSII. Analysis of the crystal structure of Psb31 has revealed a four-helix bundled structure showing partial structural similarity with PsbQ family proteins (Nagao et al., 2013). Thus, two copies of PsbQ-like proteins with different binding and functional properties seem to be present as extrinsic subunits in the diatom PSII. A further study using FTIR is required to elucidate the structural coupling of those extrinsic proteins with the OEC in diatoms. Crystallization and preliminary X-ray diffraction analysis of the diatom PSII complex have not yet been reported.

CYANOBACTERIA

Molecular Functions of Extrinsic Proteins, Briefly

The crystal structure of PSII from *Thermosynechococcus vulcanus* (Umena et al., 2011) shows the location and interaction of cyanobacterial PSII extrinsic subunits PsbO, PsbU, and PsbV on the lumenal surface of PSII. Each extrinsic protein has multiple interactions with both membrane-intrinsic and -extrinsic subunits of PSII, affecting the stabilization of the complex as a whole. In brief, PsbO interacts with CP43, CP47, D1, D2, and PsbU subunits, PsbU interacts with CP47, PsbO, and PsbV, and PsbV interacts with CP43, D1, D2, and PsbU. Detailed information about the amino acid residues involved in these interactions have been summarized by Bricker et al. (2012). Although none of these proteins provide a ligand to the catalytic Mn_4CaO_5 cluster, they have critical roles: they protect the metal cluster from reductants outside the PSII complex and optimize the required ionic environments, such as those of Ca^{2+} and Cl^-, in the OEC. The functions of each PSII extrinsic subunit have been intensively studied by deletion mutagenesis of cyanobacterial cells (Seidler, 1996; Bricker et al., 2012). It is of note that crystal structures and theoretical calculations suggest another role of the extrinsic proteins — namely, the maintenance of access channels for

substrate water to the Mn_4CaO_5 cluster and exit channels for the products (molecular oxygen and protons; Linke and Ho, 2014; Vogt et al., 2015). A number of amino acid residues in the extrinsic proteins have been predicted to be associated with these channels, but their actual roles still need to be investigated experimentally.

Structural Coupling with the OEC

Nagao et al. (2015) recently reported the FTIR measurements of S_2-minus-S_1 difference spectra using PSII core complexes from *T. elongatus* reconstituted with its extrinsic proteins, PsbO, PsbV, and PsbU. Under the condition of low-concentration $CaCl_2$ (5 mM), the spectral intensity was mostly lost when all the extrinsic proteins were removed, whereas the intensity in the carboxylate region was fully recovered by the binding of PsbO, revealing the significant role of PsbO in stabilizing the Mn_4CaO_5 cluster at a low $CaCl_2$ concentration. Even at a high $CaCl_2$ concentration (100 mM), amide I bands were significantly affected by removal of all the extrinsic proteins, indicative of the protein conformational changes in the OEC (**Figure 6**). The bands largely recovered when PsbO was bound, and further stepwise recoveries were observed by the binding of PsbV and then PsbU. Thus, in cyanobacteria, the binding of PsbO seems mainly to determine the conformation of the OEC. PsbV and PsbU induced the recovery of specific amide I bands, and hence it was suggested that these extrinsic proteins affected different regions of polypeptide chains from those affected by PsbO. PsbO and PsbV have multiple interactions with different membrane-intrinsic subunits of PSII. This makes it difficult to assign the exact polypeptide regions affected by PsbO and PsbV during the S_1-to-S_2 transition. Nevertheless, the recoveries of the OEC protein conformation were very consistent with those of O_2-evolution activity upon reconstitution with extrinsic proteins reported by Shen and Inoue (1993), suggesting again the correlation between the OEC activity and its protein conformation.

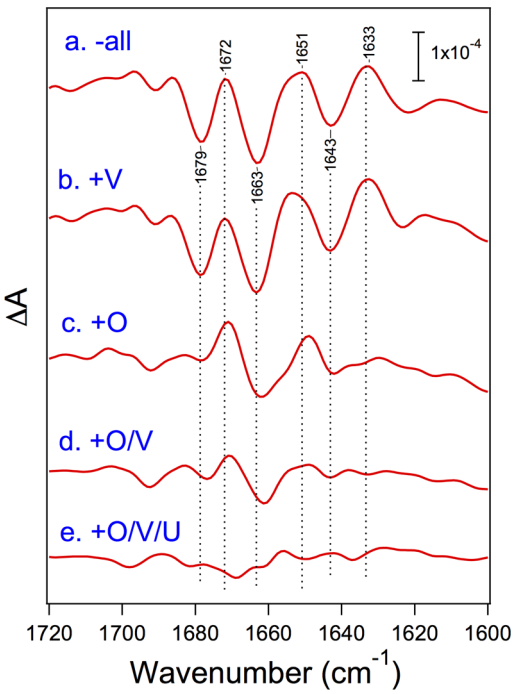

FIGURE 6 | Amide I region of the untreated-minus-treated double-difference spectra of the S_2-minus-S_1 difference spectra of the PSII core complexes from cyanobacterium *Thermosynechococcus elongatus*. PSII core complexes were depleted of all the extrinsic proteins **(a)** and then reconstituted with PsbV **(b)**, PsbO **(c)**, PsbO/V **(d)**, and PsbO/V/U **(e)**. The samples involved 100 mM $CaCl_2$. Reproduced from Nagao et al. (2015).

CyanoP and CyanoQ

It has been known that cyanobacteria have ancestral homologs of eukaryotic PsbP and PsbQ, CyanoP, and CyanoQ (De Las Rivas et al., 2004). Their involvement in Ca^{2+} and Cl^- retention has been suggested (Thornton et al., 2004; Aoi et al., 2014), however, they are not included in current crystal structures of PSII from thermophilic cyanobacteria (Umena et al., 2011). CyanoQ is reported to bind PSII tightly and to optimize oxygen evolution (Roose et al., 2007a), and a recent study using chemical cross-linking suggests that CyanoQ is closely associated with PsbO and CP47 proteins in *Synechocystis* sp. PCC 6803 (Liu et al., 2014). Furthermore, two molecules of CyanoQ may interact at the interface of the PSII dimers, indicating that CyanoQ, together with PsbO, is important for PSII dimer stability (Liu et al., 2014). Binding of multiple CyanoQ copies to the PSII assembly intermediates without PsbU and PsbV was recently reported (Liu et al., 2015). Similarly, interaction of CyanoP with the binding site in PSII, which is occupied by the PsbO subunit in mature PSII complexes, was suggested (Cormann et al., 2014). These facts suggest that localizations of CyanoP and CyanoQ in cyanobacterial PSII would be largely different form those of PsbP and PsbQ in higher plant PSII. It is likely that both CyanoP and CyanoQ have auxiliary functions in regulating and stabilizing the association of the extrinsic subunits with the PSII core.

FUNCTIONAL CHANGES DURING EVOLUTION

Cyanobacteria are thought to be an ancestor of chloroplasts in both the red lineage involving red algae and diatoms and the green lineage involving green algae and higher plants. Reconstitution and FTIR studies mentioned above showed that PsbO, PsbV, and PsbP are mainly responsible for determining the protein conformation of the OEC in cyanobacteria (Nagao et al., 2015), red algae (Uno et al., 2013), and higher plants (Tomita et al., 2009), respectively. The FTIR results obtained so far are summarized in a schematic diagram of the relationship between the OEC conformation and the binding of the extrinsic proteins (**Figure 7**). The protein conformation of the OEC detected by FTIR amide I bands directly correlated with O_2-evolution activity in all the cases. It probably regulates the binding of

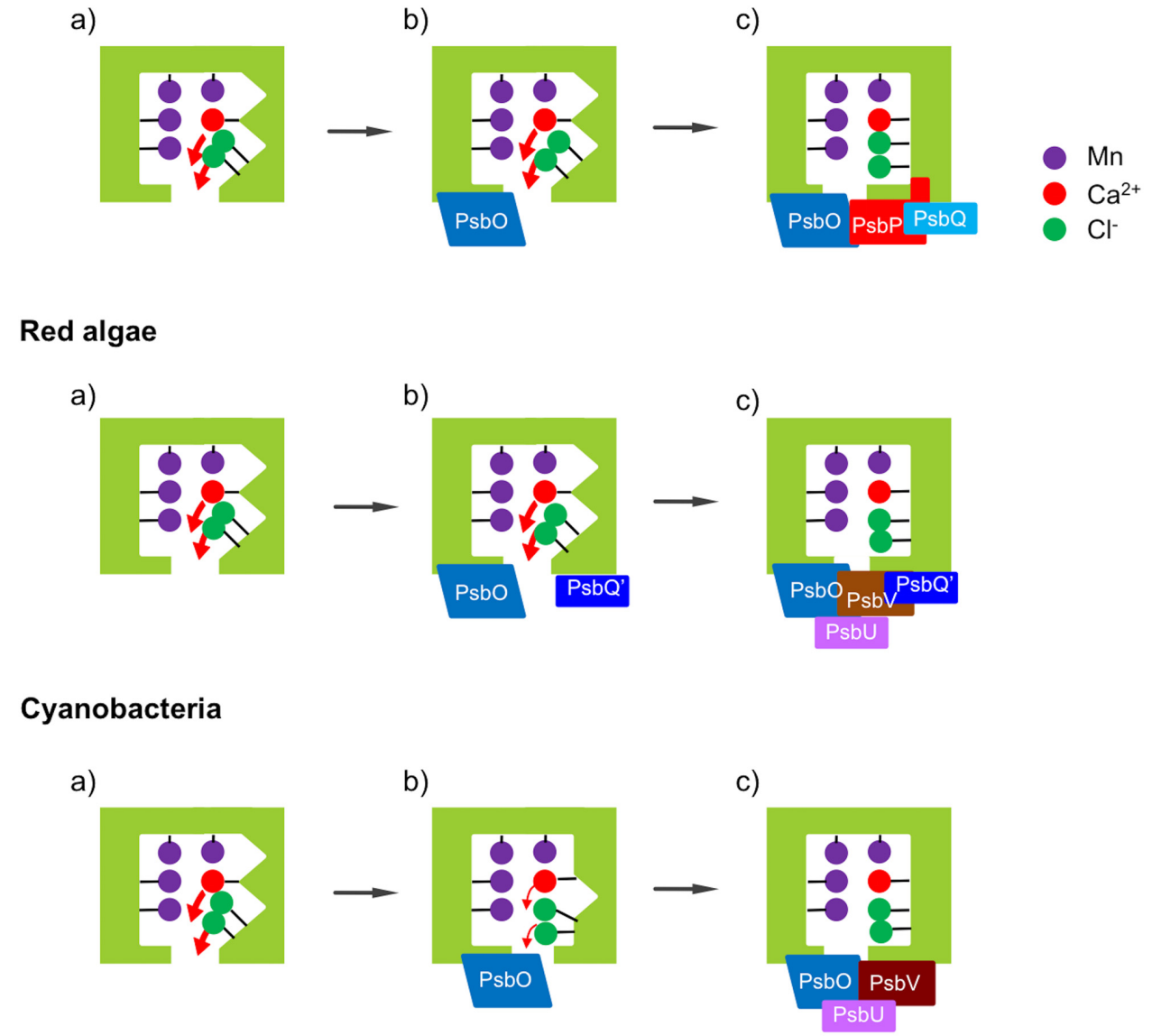

FIGURE 7 | Schematic view of the effects of the extrinsic proteins on the protein conformation of the OEC in different photosynthetic organisms. (a) Upon depletion of all the extrinsic proteins, the protein conformation of the OEC is significantly altered. **(b)** Binding of PsbO does not restore the structure of the OEC in higher plants and red algae, but largely restores it in cyanobacteria. **(c)** Further binding of PsbP can restore the structure of the OEC mostly in higher plants, while both PsbV and PsbU are required for full recovery in red algae and cyanobacteria. PsbQ and PsbQ′ function to stabilize the binding of PsbP and PsbV, respectively.

Ca^{2+} and Cl^{-} ions in the OEC by changing the dissociation constants and/or the energy barrier in releasing and binding reactions.

It is interesting that although PsbO was conserved in all oxyphototrophs, its function was not fully conserved and the function of regulating the OEC conformation was transferred to PsbV and PsbP in the red and green lineages, respectively, during evolution. This suggests that PsbP and PsbQ did not simply replace the functions of PsbV and PsbU, necessitating a substantial reconsideration of historical concepts regarding the evolution of the extrinsic subunits of PSII. PsbO undoubtedly keeps the important function of stabilizing the Mn_4CaO_5 cluster in all species. It is possible that PsbV or PsbP took over the specific function of the regulation of protein conformations from PsbO to realize a more delicate control over the O_2-evolving reaction without the destruction of the Mn_4CaO_5 cluster. By contrast, the function of PsbU in cyanobacteria as supporting the binding of PsbV seems to remain in red algae but be transferred to PsbQ, which stabilizes the binding of PsbP, in higher plants (Kakiuchi et al., 2012). It has been

reported that CyanoQ in cyanobacterial PSII also stabilizes the PsbV binding to PSII, thereby contributing to the protection of the catalytic Mn cluster of the OEC (Kashino et al., 2006). Interestingly, PsbQ′ in red algal PSII is required for the stable binding of PsbV (Enami et al., 1998). Presumably, the molecular functions of CyanoQ, PsbQ′, and PsbQ are partly conserved during evolution, while the interacting partner has changed from PsbV to PsbP. Further studies will reveal how the variations of PSII extrinsic proteins confer functional differences to PSII, presumably by fine tuning of the light-induced charge separation and the OEC reactivity, and how they affect the processes of the assembly and repair of the entire PSII complex.

AUTHOR CONTRIBUTIONS

All authors listed, have made substantial, direct and intellectual contribution to the work, and approved it for publication.

ACKNOWLEDGMENTS

This work was supported in part by JST PRESTO (to KI), by JSPS KAKENHI (grant no. 26660087 to KI; 24000018 and 25291033 to TN), and MEXT KAKENHI (grant no. 24107003 to TN).

REFERENCES

Adachi, H., Umena, Y., Enami, I., Henmi, T., Kamiya, N., and Shen, J. R. (2009). Towards structural elucidation of eukaryotic photosystem II: purification, crystallization and preliminary X-ray diffraction analysis of photosystem II from a red alga. *Biochim. Biophys. Acta* 1787, 121–128. doi: 10.1016/j.bbabio.2008.11.004

Akabori, K., Imaoka, A., and Toyoshima, Y. (1984). The role of lipids and 17-kDa protein in enhancing the recovery of O_2 evolution in cholate-treated thylakoid membranes. *FEBS Lett.* 173, 36–40. doi: 10.1016/0014-5793(84)81012-1

Allahverdiyeva, Y., Mamedov, F., Suorsa, M., Styring, S., Vass, I., and Aro, E. M. (2007). Insights into the function of PsbR protein in *Arabidopsis thaliana*. *Biochim. Biophys. Acta* 1767, 677–685. doi: 10.1016/j.bbabio.2007.01.011

Allahverdiyeva, Y., Suorsa, M., Rossi, F., Pavesi, A., Kater, M. M., Antonacci, A., et al. (2013). *Arabidopsis* plants lacking PsbQ and PsbR subunits of the oxygen-evolving complex show altered PSII super-complex organization and short-term adaptive mechanisms. *Plant J.* 75, 671–684. doi: 10.1111/tpj.12230

Aoi, M., Kashino, Y., and Ifuku, K. (2014). Function and association of CyanoP in photosystem II of *Synechocystis* sp. PCC 6803. *Res. Chem. Intermed.* 40, 3209–3217. doi: 10.1007/s11164-014-1827-y

Balsera, M., Arellano, J. B., Revuelta, J. L., de las Rivas, J., and Hermoso, J. A. (2005). The 1.49 Å resolution crystal structure of PsbQ from photosystem II of *Spinacia oleracea* reveals a PPII structure in the N-terminal region. *J. Mol. Biol.* 350, 1051–1060. doi: 10.1016/j.jmb.2005.05.044

Berthold, D. A., Babcock, G. T., and Yocum, C. F. (1981). A highly resolved, oxygen-evolving photosystem II preparation from spinach thylakoid membranes. *FEBS Lett.* 134, 231–234. doi: 10.1016/0014-5793(81)80608-4

Bricker, T. M., and Frankel, L. K. (2011). Auxiliary functions of the PsbO, PsbP, and PsbQ proteins of higher plant Photosystem II: a critical analysis. *J. Photochem. Photobiol. B* 104, 165–178. doi: 10.1016/j.jphotobiol.2011.01.025

Bricker, T. M., Mummadisetti, M. P., and Frankel, L. K. (2015). Recent advances in the use of mass spectrometry to examine structure/function relationships in photosystem II. *J. Photochem. Photobiol. B* 152, 227–246. doi: 10.1016/j.jphotobiol.2015.08.031

Bricker, T. M., Roose, J. L., Fagerlund, R. D., Frankel, L. K., and Eaton-Rye, J. J. (2012). The extrinsic proteins of Photosystem II. *Biochim. Biophys. Acta* 1817, 121–142. doi: 10.1016/j.bbabio.2011.07.006

Bricker, T. M., Roose, J. L., Zhang, P., and Frankel, L. K. (2013). The PsbP family of proteins. *Photosynth. Res.* 116, 235–250. doi: 10.1007/s11120-013-9820-7

Calderone, V., Trabucco, M., Vujicić, A., Battistutta, R., Giacometti, G. M., Andreucci, F., et al. (2003). Crystal structure of the PsbQ protein of photosystem II from higher plants. *EMBO Rep.* 4, 900–905. doi: 10.1038/sj.embor.embor923

Cao, P., Xie, Y., Li, M., Pan, X., Zhang, H., Zhao, X., et al. (2015). Crystal structure analysis of extrinsic PsbP protein of photosystem II reveals a manganese-induced conformational change. *Mol. Plant* 8, 664–666. doi: 10.1016/j.molp.2015.01.002

Cormann, K. U., Bartsch, M., Rögner, M., and Nowaczyk, M. M. (2014). Localization of the CyanoP binding site on photosystem II by surface plasmon resonance spectroscopy. *Front. Plant Sci.* 5:595. doi: 10.3389/fpls.2014.00595

Debus, R. J. (1992). The manganese and calcium ions of photosynthetic oxygen evolution. *Biochim. Biophys. Acta* 1102, 269–352. doi: 10.1016/0005-2728(92)90133-M

Debus, R. J. (2015). FTIR studies of metal ligands, networks of hydrogen bonds, and water molecules near the active site Mn_4CaO_5 cluster in Photosystem II. *Biochim. Biophys. Acta* 1847, 19–34. doi: 10.1016/j.bbabio.2014.07.007

De Las Rivas, J., Balsera, M., and Barber, J. (2004). Evolution of oxygenic photosynthesis: genome-wide analysis of the OEC extrinsic proteins. *Trends Plant Sci.* 9, 18–25. doi: 10.1016/j.tplants.2003.11.007

Enami, I., Kikuchi, S., Fukuda, T., Ohta, H., and Shen, J. R. (1998). Binding and functional properties of four extrinsic proteins of photosystem II from a red alga, *Cyanidium caldarium*, as studied by release-reconstitution experiments. *Biochemistry* 37, 2787–2793. doi: 10.1021/bi9724624

Enami, I., Okumura, A., Nagao, R., Suzuki, T., Iwai, M., and Shen, J. R. (2008). Structures and functions of the extrinsic proteins of photosystem II from different species. *Photosynth. Res.* 98, 349–363. doi: 10.1007/s11120-008-9343-9

Ferreira, K. N., Iverson, T. M., Maghiaoui, K., Barber, J., and Iwata, S. (2004). Architecture of the photosynthetic oxygen-evolving center. *Science* 303, 1831–1838. doi: 10.1126/science.1093087

Ghanotakis, D. F., Topper, J. N., Babcock, G. T., and Yocum, C. F. (1984a). Water-soluble 17 and 23 kDa polypeptides restore oxygen evolution activity by creating a high-affinity binding site for Ca^{2+} on the oxidizing side of Photosystem II. *FEBS Lett.* 170, 169–173. doi: 10.1016/0014-5793(84)81393-9

Ghanotakis, D. F., Topper, J. N., and Youcum, C. F. (1984b). Structural organization of the oxidizing side of photosystem II. Exogenous reductants reduce and destroy the Mn-complex in photosystems II membranes depleted of the 17 and 23 kDa polypeptides. *Biochim. Biophys. Acta* 767, 524–531. doi: 10.1016/0005-2728(84)90051-3

Guskov, A., Kern, J., Gabdulkhakov, A., Broser, M., Zouni, A., and Saenger, W. (2009). Cyanobacterial photosystem II at 2.9-Å resolution and the role of quinones, lipids, channels and chloride. *Nat. Struct. Mol. Biol.* 16, 334–342. doi: 10.1038/nsmb.1559

Ido, K., Ifuku, K., Yamamoto, Y., Ishihara, S., Murakami, A., Takabe, K., et al. (2009). Knockdown of the PsbP protein does not prevent assembly of the dimeric PSII core complex but impairs accumulation of photosystem II supercomplexes in tobacco. *Biochim. Biophys. Acta* 1787, 873–881. doi: 10.1016/j.bbabio.2009.03.004

Ido, K., Kakiuchi, S., Uno, C., Nishimura, T., Fukao, Y., Noguchi, T., et al. (2012). The conserved His-144 in the PsbP protein is important for the interaction between the PsbP N-terminus and the Cyt b_{559} subunit of photosystem II. *J. Biol. Chem.* 287, 26377–26387. doi: 10.1074/jbc.M112.385286

Ido, K., Nield, J., Fukao, Y., Nishimura, T., Sato, F., and Ifuku, K. (2014). Cross-linking evidence for multiple interactions of the PsbP and PsbQ proteins in a higher plant photosystem II supercomplex. *J. Biol. Chem.* 289, 20150–20157. doi: 10.1074/jbc.M114.574822

Ifuku, K. (2014). The PsbP and PsbQ family proteins in the photosynthetic machinery of chloroplasts. *Plant Physiol. Biochem.* 81, 108–114. doi: 10.1016/j.plaphy.2014.01.001

Ifuku, K. (2015). Localization and functional characterization of the extrinsic subunits of photosystem II: an update. *Biosci. Biotechnol. Biochem.* 79, 1223–1231. doi: 10.1080/09168451.2015.1031078

Ifuku, K., Endo, T., Shikanai, T., and Aro, E. M. (2011a). Structure of the chloroplast NADH dehydrogenase-like complex: nomenclature for nuclear-encoded subunits. *Plant Cell Physiol.* 52, 1560–1568. doi: 10.1093/pcp/pcr098

Ifuku, K., Ido, K., and Sato, F. (2011b). Molecular functions of PsbP and PsbQ proteins in the photosystem II supercomplex. *J. Photochem. Photobiol. B* 104, 158–164. doi: 10.1016/j.jphotobiol.2011.02.006

Ifuku, K., Ishihara, S., and Sato, F. (2010). Molecular functions of oxygen-evolving complex family proteins in photosynthetic electron flow. *J. Integr. Plant Biol.* 52, 723–734. doi: 10.1111/j.1744-7909.2010.00976.x

Ifuku, K., Ishihara, S., Shimamoto, R., Ido, K., and Sato, F. (2008). Structure, function, and evolution of the PsbP protein family in higher plants. *Photosynth. Res.* 98, 427–437. doi: 10.1007/s11120-008-9359-1

Ifuku, K., Nakatsu, T., Kato, H., and Sato, F. (2004). Crystal structure of the PsbP protein of photosystem II from *Nicotiana tabacum*. *EMBO Rep.* 5, 362–367. doi: 10.1038/sj.embor.7400113

Ifuku, K., Nakatsu, T., Shimamoto, R., Yamamoto, Y., Ishihara, S., Kato, H., et al. (2005a). Structure and function of the PsbP protein of photosystem II from higher plants. *Photosynth. Res.* 84, 251–255. doi: 10.1007/s11120-004-7160-3

Ifuku, K., Yamamoto, Y., Ono, T. A., Ishihara, S., and Sato, F. (2005b). PsbP protein, but not PsbQ protein, is essential for the regulation and stabilization of photosystem II in higher plants. *Plant Physiol.* 139, 1175–1184. doi: 10.1104/pp.105.068643

Ifuku, K., and Sato, F. (2002). A truncated mutant of the extrinsic 23-kDa protein that absolutely requires the extrinsic 17-kDa protein for Ca^{2+} retention in photosystem II. *Plant Cell Physiol.* 43, 1244–1249. doi: 10.1093/pcp/pcf136

Kakiuchi, S., Uno, C., Ido, K., Nishimura, T., Noguchi, T., Ifuku, K., et al. (2012). The PsbQ protein stabilizes the functional binding of the PsbP protein to photosystem II in higher plants. *Biochim. Biophys. Acta* 1817, 1346–1351. doi: 10.1016/j.bbabio.2012.01.009

Kashino, Y., Inoue-Kashino, N., Roose, J. L., and Pakrasi, H. B. (2006). Absence of the PsbQ protein results in destabilization of the PsbV protein and decreased oxygen evolution activity in cyanobacterial photosystem II. *J. Biol. Chem.* 281, 20834–20841. doi: 10.1074/jbc.M603188200

Kashino, Y., Lauber, W. M., Carroll, J. A., Wang, Q., Whitmarsh, J., Satoh, K., et al. (2002). Proteomic analysis of a highly active photosystem II preparation from the cyanobacterium *Synechocystis* sp. PCC 6803 reveals the presence of novel polypeptides. *Biochemistry* 41, 8004–8012. doi: 10.1021/bi026012+

Kawakami, K., Umena, Y., Kamiya, N., and Shen, J.-R. (2009). Location of chloride and its possible functions in oxygen-evolving photosystem II revealed by X-ray crystallography. *Proc. Natl. Acad. Sci. U.S.A.* 106, 8567–8572. doi: 10.1073/pnas.0812797106

Kopecky, V. Jr., Kohoutova, J., Lapkouski, M., Hofbauerova, K., Sovova, Z., Ettrichova, O., et al. (2012). Raman spectroscopy adds complementary detail to the high-resolution X-ray crystal structure of photosynthetic PsbP from *Spinacia oleracea*. *PLoS ONE* 7:e46694. doi: 10.1371/journal.pone.0046694

Kuwabara, T., Miyao, M., Murata, T., and Murata, N. (1985). The function of 33-kDa protein in the photosynthetic oxygen-evolution system studied by reconstitution experiments. *Biochim. Biophys. Acta* 806, 283–289. doi: 10.1016/0005-2728(85)90107-0

Linke, K., and Ho, F. M. (2014). Water in Photosystem II: structural, functional and mechanistic considerations. *Biochim. Biophys. Acta* 1837, 14–32. doi: 10.1016/j.bbabio.2013.08.003

Liu, H., Frankel, L. K., and Bricker, T. M. (2009). Characterization and complementation of a psbR mutant in *Arabidopsis thaliana*. *Arch. Biochem. Biophys.* 489, 34–40. doi: 10.1016/j.abb.2009.07.014

Liu, H., Weisz, D. A., and Pakrasi, H. B. (2015). Multiple copies of the PsbQ protein in a cyanobacterial photosystem II assembly intermediate complex. *Photosynth. Res.* 126, 375–383. doi: 10.1007/s11120-015-0123-z

Liu, H., Zhang, H., Weisz, D. A., Vidavsky, I., Gross, M. L., and Pakrasi, H. B. (2014). MS-based cross-linking analysis reveals the location of the PsbQ protein in cyanobacterial photosystem II. *Proc. Natl. Acad. Sci. U.S.A.* 111, 4638–4643. doi: 10.1073/pnas.1323063111

McEvoy, J. P., and Brudvig, G. W. (2006). Water-splitting chemistry of photosystem II. *Chem. Rev.* 106, 4455–4483. doi: 10.1021/cr02 04294

Miyao, M., Fujimura, Y., and Murata, N. (1988). Partial degradation of the extrinsic 23-kDa protein of the Photosystem II complex of spinach. *Biochim. Biophys. Acta* 936, 465–474. doi: 10.1016/0005-2728(88)90024-2

Miyao, M., and Murata, N. (1985). The Cl^- effect on photosynthetic oxygen evolution: interaction of Cl^- with 18-kDa, 24-kDa and 33-kDa proteins. *FEBS Lett.* 180, 303–308. doi: 10.1016/0014-5793(85)81091-7

Mummadisetti, M. P., Frankel, L. K., Bellamy, H. D., Sallans, L., Goettert, J. S., Brylinski, M., et al. (2014). Use of protein cross-linking and radiolytic footprinting to elucidate PsbP and PsbQ interactions within higher plant Photosystem II. *Proc. Natl. Acad. Sci. U.S.A.* 111, 16178–16183. doi: 10.1073/pnas.1415165111

Murakami, R., Ifuku, K., Takabayashi, A., Shikanai, T., Endo, T., and Sato, F. (2002). Characterization of an *Arabidopsis thaliana* mutant with impaired *psbO*, one of two genes encoding extrinsic 33-kDa proteins in photosystem II. *FEBS Lett.* 523, 138–142. doi: 10.1016/S0014-5793(02)02963-0

Nagao, R., Suga, M., Niikura, A., Okumura, A., Koua, F. H., Suzuki, T., et al. (2013). Crystal structure of Psb31, a novel extrinsic protein of photosystem II from a marine centric diatom and implications for its binding and function. *Biochemistry* 52, 6646–6652. doi: 10.1021/bi400770d

Nagao, R., Tomo, T., and Noguchi, T. (2015). Effects of extrinsic proteins on the protein conformation of the oxygen-evolving center in cyanobacterial photosystem II as revealed by Fourier transform infrared spectroscopy. *Biochemistry* 54, 2022–2031. doi: 10.1021/acs.biochem.5b00053

Nishimura, T., Uno, C., Ido, K., Nagao, R., Noguchi, T., Sato, F., et al. (2014). Identification of the basic amino acid residues on the PsbP protein involved in the electrostatic interaction with photosystem II. *Biochim. Biophys. Acta* 1837, 1447–1453. doi: 10.1016/j.bbabio.2013.12.012

Noguchi, T. (2007). Light-induced FTIR difference spectroscopy as a powerful tool toward understanding the molecular mechanism of photosynthetic oxygen evolution. *Photosynth. Res.* 91, 59–69. doi: 10.1007/s11120-007-9137-5

Noguchi, T. (2015). Fourier transform infrared difference and time-resolved infrared detection of the electron and proton transfer dynamics in photosynthetic water oxidation. *Biochim. Biophys. Acta* 1847, 35–45. doi: 10.1016/j.bbabio.2014.06.009

Offenbacher, A. R., Polander, B. C., and Barry, B. A. (2013). An intrinsically disordered photosystem II subunit, PsbO, provides a structural template and a sensor of the hydrogen-bonding network in photosynthetic water oxidation. *J. Biol. Chem.* 288, 29056–29068. doi: 10.1074/jbc.M113.487561

Ohta, H., Suzuki, T., Ueno, M., Okumura, A., Yoshihara, S., Shen, J. R., et al. (2003). Extrinsic proteins of photosystem II: an intermediate member of PsbQ protein family in red algal PS II. *Eur. J. Biochem.* 270, 4156–4163. doi: 10.1046/j.1432-1033.2003.03810.x

Okumura, A., Nagao, R., Suzuki, T., Yamagoe, S., Iwai, M., Nakazato, K., et al. (2008). A novel protein in Photosystem II of a diatom *Chaetoceros gracilis* is one of the extrinsic proteins located on lumenal side and directly associates with PSII core components. *Biochim. Biophys. Acta* 1777, 1545–1551. doi: 10.1016/j.bbabio.2008.09.004

Pagliano, C., Saracco, G., and Barber, J. (2013). Structural, functional and auxiliary proteins of photosystem II. *Photosynth. Res.* 116, 167–188. doi: 10.1007/s11120-013-9803-8

Pokhrel, R., Service, R. J., Debus, R. J., and Brudvig, G. W. (2013). Mutation of lysine 317 in the D2 subunit of photosystem II alters chloride binding and proton transport. *Biochemistry* 52, 4758–4773. doi: 10.1021/bi301700u

Roose, J. L., Kashino, Y., and Pakrasi, H. B. (2007a). The PsbQ protein defines cyanobacterial Photosystem II complexes with highest activity and stability. *Proc. Natl. Acad. Sci. U.S.A.* 104, 2548–2553. doi: 10.1073/pnas.0609337104

Roose, J. L., Wegener, K. M., and Pakrasi, H. B. (2007b). The extrinsic proteins of Photosystem II. *Photosynth. Res.* 92, 369–387. doi: 10.1007/s11120-006-9117-1

Satoh, K. (2008). Protein-pigments and the photosystem II reaction center: a glimpse into the history of research and reminiscences. *Photosynth. Res.* 98, 33–42. doi: 10.1007/s11120-008-9348-4

Seidler, A. (1996). The extrinsic polypeptides of Photosystem II. *Biochim. Biophys. Acta* 1277, 35–60. doi: 10.1016/S0005-2728(96)00102-8

Shen, J. R., and Inoue, Y. (1993). Binding and functional properties of two new extrinsic components, cytochrome *c*-550 and a 12-kDa protein, in cyanobacterial photosystem II. *Biochemistry* 32, 1825–1832. doi: 10.1021/bi00058a017

Suga, M., Akita, F., Hirata, K., Ueno, G., Murakami, H., Nakajinra, Y., et al. (2015). Native structure of photosystem II at 1.95 Å resolution viewed by femtosecond X-ray pulses. *Nature* 517, 99–103. doi: 10.1038/nature13991

Suorsa, M., Sirpiö, S., Allahverdiyeva, Y., Paakkarinen, V., Mamedov, F., Styring, S., et al. (2006). PsbR, a missing link in the assembly of the oxygen-evolving complex of plant photosystem II. *J. Biol. Chem.* 281, 145–150. doi: 10.1074/jbc.M510600200

Suzuki, H., Yu, J., Kobayashi, T., Nakanishi, H., Nixon, P. J., and Noguchi, T. (2013). Functional roles of D2-Lys317 and the interacting chloride ion in the water oxidation reaction of photosystem II as revealed by fourier transform infrared analysis. *Biochemistry* 52, 4748–4757. doi: 10.1021/bi301699h

Thornton, L. E., Ohkawa, H., Roose, J. L., Kashino, Y., Keren, N., and Pakrasi, H. B. (2004). Homologs of plant PsbP and PsbQ proteins are necessary for regulation of photosystem II activity in the cyanobacterium *Synechocystis* 6803. *Plant Cell* 16, 2164–2175. doi: 10.1105/tpc.104.023515

Tohri, A., Dohmae, N., Suzuki, T., Ohta, H., Inoue, Y., and Enami, I. (2004). Identification of domains on the 23 kDa protein possibly involved in electrostatic interaction with the extrinsic 33 kDa protein in spinach photosystem II. *Eur. J. Biochem.* 271, 962–971. doi: 10.1111/j.1432-1033.2004.03998.x

Tomita, M., Ifuku, K., Sato, F., and Noguchi, T. (2009). FTIR evidence that the PsbP extrinsic protein induces protein conformational changes around the oxygen-evolving Mn cluster in photosystem II. *Biochemistry* 48, 6318–6325. doi: 10.1021/bi9006308

Umena, Y., Kawakami, K., Shen, J.-R., and Kamiya, N. (2011). Crystal structure of oxygen-evolving photosystem II at a resolution of 1.9 Å. *Nature* 473, 55–60. doi: 10.1038/nature09913

Uno, C., Nagao, R., Suzuki, H., Tomo, T., and Noguchi, T. (2013). Structural coupling of extrinsic proteins with the oxygen-evolving center in red algal photosystem II as revealed by light-induced FTIR difference spectroscopy. *Biochemistry* 52, 5705–5707. doi: 10.1021/bi4009787

Vinyard, D. J., Ananyev, G. M., and Dismukes, G. C. (2013). Photosystem II: the reaction center of oxygenic photosynthesis. *Annu. Rev. Biochem.* 82, 577–606. doi: 10.1146/annurev-biochem-070511-100425

Vogt, L., Vinyard, D. J., Khan, S., and Brudvig, G. W. (2015). Oxygen-evolving complex of Photosystem II: an analysis of second-shell residues and hydrogen-bonding networks. *Curr. Opin. Chem. Biol.* 25C, 152–158. doi: 10.1016/j.cbpa.2014.12.040

Yi, X., Hargett, S. R., Frankel, L. K., and Bricker, T. M. (2006). The PsbQ protein is required in *Arabidopsis* for photosystem II assembly/stability and photoautotrophy under low light conditions. *J. Biol. Chem.* 281, 26260–26267. doi: 10.1074/jbc.M603582200

Yi, X., Hargett, S. R., Liu, H., Frankel, L. K., and Bricker, T. M. (2007). The PsbP protein is required for photosystem II complex assembly/stability and photoautotrophy in *Arabidopsis thaliana*. *J. Biol. Chem.* 282, 24833–24841. doi: 10.1074/jbc.M705011200

Yi, X., McChargue, M., Laborde, S., Frankel, L. K., and Bricker, T. M. (2005). The manganese-stabilizing protein is required for photosystem II assembly/stability and photoautotrophy in higher plants. *J. Biol. Chem.* 280, 16170–16174. doi: 10.1074/jbc.M501550200

Conflict of Interest Statement: The authors declare that the research was conducted in the absence of any commercial or financial relationships that could be construed as a potential conflict of interest.

frontiers in Plant Science

ORIGINAL RESEARCH
published: 17 March 2016
doi: 10.3389/fpls.2016.00292

Synthesis of Chlorophyll-Binding Proteins in a Fully Segregated Δ*ycf54* Strain of the Cyanobacterium *Synechocystis* PCC 6803

*Sarah Hollingshead[1,2], Jana Kopečná[3], David R. Armstrong[1], Lenka Bučinská[3,4], Philip J. Jackson[1,5], Guangyu E. Chen[1], Mark J. Dickman[5], Michael P. Williamson[1], Roman Sobotka[3,4] and C. Neil Hunter[1]**

[1] Department of Molecular Biology and Biotechnology, University of Sheffield, Sheffield, UK, [2] Sir William Dunn School of Pathology, University of Oxford, Oxford, UK, [3] Institute of Microbiology, Centre Algatech, Academy of Sciences of the Czech Republic, Třeboň, Czech Republic, [4] Faculty of Science, University of South Bohemia, České Budějovice, Czech Republic, [5] ChELSI Institute, Department of Chemical and Biological Engineering, University of Sheffield, Sheffield, UK

OPEN ACCESS

Edited by:
John Love,
University of Exeter, UK

Reviewed by:
Peter Jahns,
University of Düsseldorf, Germany
Caiji Gao,
The Chinese University of Hong Kong, China

***Correspondence:**
C. Neil Hunter
c.n.hunter@sheffield.ac.uk

Specialty section:
This article was submitted to Plant Cell Biology, a section of the journal Frontiers in Plant Science

Received: *09 November 2015*
Accepted: *23 February 2016*
Published: *17 March 2016*

Citation:
Hollingshead S, Kopečná J, Armstrong DR, Bučinská L, Jackson PJ, Chen GE, Dickman MJ, Williamson MP, Sobotka R and Hunter CN (2016) Synthesis of Chlorophyll-Binding Proteins in a Fully Segregated Δycf54 Strain of the Cyanobacterium Synechocystis PCC 6803. Front. Plant Sci. 7:292. doi: 10.3389/fpls.2016.00292

In the chlorophyll (Chl) biosynthesis pathway the formation of protochlorophyllide is catalyzed by Mg-protoporphyrin IX methyl ester (MgPME) cyclase. The Ycf54 protein was recently shown to form a complex with another component of the oxidative cyclase, Sll1214 (CycI), and partial inactivation of the *ycf54* gene leads to Chl deficiency in cyanobacteria and plants. The exact function of the Ycf54 is not known, however, and further progress depends on construction and characterization of a mutant cyanobacterial strain with a fully inactivated *ycf54* gene. Here, we report the complete deletion of the *ycf54* gene in the cyanobacterium *Synechocystis* 6803; the resulting Δ*ycf54* strain accumulates huge concentrations of the cyclase substrate MgPME together with another pigment, which we identified using nuclear magnetic resonance as 3-formyl MgPME. The detection of a small amount (∼13%) of Chl in the Δ*ycf54* mutant provides clear evidence that the Ycf54 protein is important, but not essential, for activity of the oxidative cyclase. The greatly reduced formation of protochlorophyllide in the Δ*ycf54* strain provided an opportunity to use ^{35}S protein labeling combined with 2D electrophoresis to examine the synthesis of all known Chl-binding protein complexes under drastically restricted *de novo* Chl biosynthesis. We show that although the Δ*ycf54* strain synthesizes very limited amounts of photosystem I and the CP47 and CP43 subunits of photosystem II (PSII), the synthesis of PSII D1 and D2 subunits and their assembly into the reaction centre (RCII) assembly intermediate were not affected. Furthermore, the levels of other Chl complexes such as cytochrome b_6f and the HliD–Chl synthase remained comparable to wild-type. These data demonstrate that the requirement for *de novo* Chl molecules differs completely for each Chl-binding protein. Chl traffic and recycling in the cyanobacterial cell as well as the function of Ycf54 are discussed.

Keywords: Ycf54, *Synechocystis* 6803, chlorophyll, photosystem II, protochlorophyllide, Mg-protoporphyrin IX methylester cyclase

INTRODUCTION

Chlorophylls (Chl) and Chl binding proteins are essential components of the photosynthetic apparatus. Together they act as principal light harvesting and energy transforming cofactors in photosynthetic organisms, as demonstrated by the structures of both photosystem I (PSI) and photosystem II (PSII; Jordan et al., 2001; Zouni et al., 2001; Umena et al., 2011). It is likely that at least for large Chl-binding subunits of PSI (PsaA, PsaB) and PSII (CP43, CP47) Chl molecules must be inserted into these proteins co-translationally as a prerequisite for correct protein folding (Chua et al., 1976; Eichacker et al., 1996; Müller and Eichacker, 1999; Chidgey et al., 2014). As demonstrated recently using a cyanobacterial Δ*chlL* mutant, which is unable to synthesize Chl in the dark, the availability of *de novo* Chl molecules is ultimately essential for synthesis of all central subunits of both photosystems (Kopečná et al., 2013). Nonetheless, there are unexplained aspects of the assembly of PSII subunits, such as the particular sensitivity of the CP47 subunit to the lack of *de novo* Chl (Dobáková et al., 2009; Kopečná et al., 2015).

The Chls are a group of modified tetrapyrrole molecules distinguished by their fifth isocyclic or E ring, the geranylgeranyl/phytol moiety esterified at C17 and a centrally chelated magnesium ion. The isocyclic ring arises from the cyclisation of the methyl-propionate side-chain at C-13 to the C-15 bridge carbon between rings C and D. In oxygenic phototrophs this biosynthetic reaction is catalyzed by the oxidative Mg-protoporphyrin IX monomethyl ester cyclase (MgPME-cyclase), which incorporates atmospheric oxygen into the $C13^1$ carbonyl group (Porra et al., 1996). Although studied in some detail, the enzyme responsible for the aerobic cyclisation reaction remains the least understood in the Chl biosynthesis pathway. The first gene identified as encoding an oxidative cyclase component was the *Rubrivivax gelatinosus acsF* (aerobic cyclisation system iron containing protein) locus (Pinta et al., 2002). Subsequently, AcsF homologs have been identified in all studied oxygenic photosynthetic organisms (Boldareva-Nuianzina et al., 2013).

The Ycf54 protein (12.1 kDa) has been shown recently to interact with the AcsF homolog Sll1214 (hereafter CycI; Peter et al., 2009) in the cyanobacterium *Synechocystis* PCC 6803 (hereafter *Synechocystis*; Hollingshead et al., 2012). Demonstrations that partial elimination of Ycf54 strongly impairs the formation of PChlide and causes Chl deficiency in both cyanobacteria and plants (Albus et al., 2012; Hollingshead et al., 2012) led to speculations that this protein is a catalytic subunit of the MgPME cyclase (Bollivar et al., 2014). Here, we clarify this issue by achieving the complete deletion of the *ycf54* gene in *Synechocystis*. Although the Chl content in this strain was very low, the MgPME-cyclase was apparently active, which demonstrated that the Ycf54 protein is not an essential subunit of the MgPME cyclase. On the other hand, the mutant contained a very low level of CycI and lacked a high-mass complex associated with the light-dependent PChlide oxidoreductase enzyme (POR). The greatly limited formation of PChlide in the *ycf54* mutant provided an opportunity to assess the sensitivity of assembly pathways for all known Chl-proteins in cyanobacteria to the availability of *de novo* Chl. Interestingly, the deletion of the *ycf54* gene almost abolished the synthesis of PsaA/B subunits and PSII antennas CP47 and CP43, whereas the accumulation of other Chl-proteins showed little or no defects.

EXPERIMENTAL PROCEDURES

Growth Conditions

Synechocystis strains were grown photomixotrophically in a rotary shaker under low light conditions (5 μmol photons m^{-2} s^{-1}) at 30°C in liquid BG11 medium (Rippka et al., 1979) supplemented with 10 mM TES-KOH (pH 8.2) and 5 mM glucose.

Construction of the Δ*ycf54 Synechocystis* Strain

In order to disrupt open reading frame *slr1780* (*ycf54*), we prepared a construct for replacing the most this gene (bp 64–276) by a Zeocin resistance cassette. The sequences up- and down-stream (∼300 bp) of the *ycf54* gene were amplified with the relevant primers and fusion PCR in conjunction with megaprimers (Ke and Madison, 1997) were used to anneal these either side of the Zeocin resistance cassette. The resulting PCR product was transformed into the GT-W *Synechocystis* substrain (Bečková et al., submitted) and transformants were selected on a BG11 agar plate containing 2 μg ml^{-1} Zeocin. Complete segregation was achieved by sequentially doubling the concentration of antibiotic to a final concentration of 32 μg ml^{-1} Zeocin.

Cell Absorption Spectra and Determination of Chl Content

Absorption spectra of whole cells were measured at room temperature using a Shimadzu UV-3000 spectrophotometer (Kyoto, Japan). To determine Chl levels, pigments were extracted from cell pellets (2 ml, OD_{750} = ∼0.5) with 100% methanol and the Chl concentration was determined spectroscopically (Porra et al., 1989).

Analysis of Pigments by HPLC

Pigments were extracted from equal quantities of cells by the method described in Canniffe et al. (2013) and separated on a Phenomenex Aqua C_{18} reverse phase column (5 μM particle size, 125 Å pore size, 250 mm × 4.6 mm) at a flow rate of 1 ml min^{-1}. 3-formyl-MgPME was purified on a Fortis Universil C_{18} reverse phase column (5 μM particle size, 125 Å pore size, 150 mm × 10 mm) at a flow rate of 3.5 ml min^{-1}. Reverse phase columns were run using a method modified from Sobotka et al. (2011). Solvents A and B were 350 mM ammonium acetate pH 6.9/30% methanol (v/v) and 100% methanol, respectively. Pigments were

eluted over a linear gradient of 65 to 75% buffer A over 35 min.

Purification of 3-Formyl-MgPME for NMR Analysis

Pigments were extracted by phase partitioning from 6 L of Δ*ycf54* culture grown to an $OD_{750\,nm}$ 1.2. One volume of diethyl ether was added to two volumes of cell culture in a separation funnel and the diethyl ether phase containing 3-formyl-MgPME was separated from the cell culture. Pigments were extracted from the cell culture three times. The diethyl ether was removed by rotary evaporation and the extracted pigments were re-suspended in a small volume of HPLC grade methanol. After centrifugation at 15,000 × *g* for 10 min, 3-formyl-MgPME was purified by preparative HPLC. Ammonium acetate was removed from the HPLC purified 3-formyl-MgPME by solid-phase extraction on DSC-18 reverse-phase columns (Supelco). Solvents C, D, and E were QH_2O, 50% methanol (v/v) and 100% methanol, respectively. After equilibration of the column with 1.0 ml solvent D, the purified 3-formyl-MgPME, diluted 1/3 with QH_2O, was loaded and allowed to enter the column by gravity flow. The column was washed with 1 ml solvent C, then 1 ml solvent D to remove the ammonium acetate. The pigment was eluted into a glass vial with 300 μl methanol. The purified pigment was completely dried in a vacuum centrifuge and stored at –20°C.

NMR Assignment of 3-Formyl-MgPME

The dried pigment from HPLC was re-suspended in 500 μl methanol-d4 (Sigma), centrifuged to remove any insoluble pigment, transferred to a 5 mm NMR tube and sealed. All NMR experiments were carried out on a Bruker Avance DRX 600 instrument equipped with a cryoprobe at an acquisition temperature of 298 K.

The one-dimensional selective Nuclear Overhauser Enhancement (NOE) experiments were recorded using a double pulsed field gradient spin echo selective NOE experiment (Stott et al., 1995) using an 80 ms 180° Gaussian pulse for the selective excitation and a 1 s mixing time, acquiring 1024 transients at each saturation frequency. The Total Correlation Spectroscopy (TOCSY) experiment was recorded using a 45 ms spin lock at a power of 8.3 kHz. Two carbon Heteronuclear Single Quantum Correlation (HSQC) experiments were recorded with carbon offsets of 60 and 140 ppm.

2D Electrophoresis, Immunodetection, and Protein Radiolabeling

Membrane and soluble protein fractions were isolated from 50 ml of cells at $OD_{750\,nm}$ ~0.4 according to Dobáková et al. (2009) using buffer A (25 mM MES/NaOH, pH 6.5, 5 mM $CaCl_2$, 10 mM $MgCl_2$, 20% glycerol). Isolated membrane complexes (0.25 mg/ml Chl) were solubilized in buffer A containing 1% *n*-dodecyl-β-D-maltoside.

To assess protein levels by immunodetection, the protein content of *Synechocystis* lysates was quantified spectroscopically (Kalb and Bernlohr, 1977), separated by SDS-PAGE (Novagen) and transferred to a nitrocellulose membrane. The membranes were probed with specific primary antibodies and then with secondary antibodies conjugated to horseradish peroxidise (Sigma). The primary antibodies used in this study were raised in rabbits as described in Hollingshead et al. (2012), with the exception of CHL27 (anti-CycI), which was purchased from Agrisera (Sweden).

Two-dimensional clear-native electrophoresis was performed essentially as described in Kopečná et al. (2013). Proteins separated in the gel were stained either by Coomassie Blue, or Sypro Orange, followed by transfer onto a PVDF membrane. Membranes were incubated with specific primary antibodies, and then with a secondary antibody conjugated with horseradish peroxidase (Sigma).

Radioactive pulse labeling of the proteins in cells was performed using a mixture of [^{35}S]Met and [^{35}S]Cys (Translabel; MP Biochemicals). After 30 min incubation of cells with labeled amino-acids, the solubilized membranes isolated from radiolabelled cells were separated by 2D-electrophoresis. The stained 2D gel was finally exposed to a phosphor-imager plate, which was scanned by Storm (GE Healthcare) to visualize labeled protein spots.

Relative Quantification of FLAG-CycI and Captured Proteins in Pulldown Assays

Pulldown assays using N-terminal FLAG-tagged CycI as bait, with both wild-type (WT) and Δ*ycf54* backgrounds, were carried out according to Hollingshead et al. (2012). FLAG eluates were concentrated to 100 μl using Amicon Ultra 0.5 ml 3 kDa MWCO ultrafiltration devices (Millipore). The proteins were then precipitated, reduced and *S*-alkylated according to Zhang et al. (2015). Proteolytic digestion was carried out with 1:25 w/w (enzyme:substrate) pre-mixed trypsin/Lys-C (1 μg/μL, Promega, mass spectrometry grade) at 37°C for 2 h. The samples were then diluted with 75 μl 100 mM Tris-HCl, pH 8.5, 10 mM $CaCl_2$ and the digestion allowed to proceed for a further 18 h at 37°C. After the addition of 5μl 10% TFA, the samples were desalted using C_{18} spin columns (Thermo Fisher) and analyzed by nano-flow liquid chromatography (Ultimate 3000 RSLCnano system, Dionex) coupled to a mass spectrometer (Maxis UHR-TOF, Bruker or Q Exactive HF Orbitrap, Thermo Scientific). For Maxis data, mass spectra were internally calibrated with the lock-mass ion at m/z 1221.9906 then converted to MGF format using a script provided by Bruker. Q Exactive data-files were converted to MGFs using MSConvert[1]. Protein identification was carried out by searching against the *Synechocystis* PCC 6803 proteome database (release date 02-08-2015, 3507 entries[2] using Mascot Daemon v. 2.5.1 running with Mascot Server v. 2.5 (Matrix Science), specifying trypsin as the enzyme in the search parameters and allowing for one missed cleavage. *S*-carbamidomethyl-cysteine and methionine oxidation were selected as fixed and variable modifications, respectively. MS and MS/MS tolerances were set to 0.01 Da and false discovery rates determined by searching of a decoy database composed of reversed protein sequences. The data-files and search results have

[1] www.proteowizard.sourceforge.net

[2] www.uniprot.org/proteomes/UP000001425

been uploaded to the ProteomeXchange Consortium[3] via the PRIDE partner repository (identifier DOI 10.6019/PXD003149).

Electron Microscopy

Wild-type and Δ*ycf54* cells were harvested in the log phase by centrifugation. Cell pellets were loaded into 200 μm deep specimen carriers (Leica Microsystems), pre-treated with 1% lecithin in chloroform and cryo-immobilized by high-pressure freezing using EM PACT2 (Leica Microsystems). Freeze-substitution was carried out as described by van de Meene et al. (2006) using an automatic freeze substitution unit (EM ASF, Leica). Samples were then infiltrated with graded series (1:2, 1:1, 2:1) of Spurr-acetone mixture (6–8 h for each), twice with 100% Spurr's resin (SPI Supplies) and finally embedded in fresh resin. The polymerization was performed at 60°C for 48 h. Ultra-thin 70 nm sections were cut on ultramicrotome (UCT, Leica), collected on formvar-coated copper grids and stained with uranyl acetate (5 min) and lead citrate (3 min). Grids were viewed with a JEOL 1010 transmission electron microscope operating at 80 kV equipped with a Mega View III camera (SIS GmbH).

RESULTS

Ycf54 Is Not Essential for Activity of MgPME Cyclase

In our previous report (Hollingshead et al., 2012) we described a *ycf54*$^{-}$ *Synechocystis* strain harboring an insertion of the Erythromycin resistance cassette in the *ycf54* gene. Although prolonged attempts to fully segregate the mutant allele into all copies of the chromosome were unsuccessful, the phenotype of the partially segregated strain was informative nevertheless, and it exhibited an obvious defect in PChlide formation. However, the capability of *Synechocystis* cells to tolerate deletions of important genes also depends on the 'WT' substrain used. For instance, a previous attempt to inactivate *gun4*, another gene crucial for Chl biosynthesis, was achieved in the non-motile *Synechocystis* GT-P substrain but it failed in the motile PCC-M (compare Wilde et al., 2004; Sobotka et al., 2008). Thus, in order to obtain a fully segregated *ycf54* mutant, we prepared a new construct for replacement of the *ycf54* gene and transformed GT-P, GT-S, GT-W and PCC-M substrains; the GT-P substrain has been used in our previous work (Hollingshead et al., 2012). Interestingly, the *ycf54* deletion readily segregated in the GT-W substrain (**Figure 1A**) under low light (5 μmol photons.m^{-2}.s^{-1}) and photomixotrophic conditions; all attempts to segregate the *ycf54* deletion in other substrains failed (not shown). For the purposes of the work reported here the GT-W substrain is designated as the WT; a detailed analysis of GT-P and GT-W including genome sequencing is presented elsewhere in this issue (Bečková et al., submitted).

The fully segregated Δ*ycf54* strain did not grow photoautotrophically, although supplementation of the growth medium with glucose made photomixotrophic growth possible at light intensities up to 100 μmol photons.m^{-2}.s^{-1}. Examination of the absorption spectra from cells normalized for optical density at 750 nm (OD_{750}), shows that the Chl absorbance maxima at 439 and 679 nm and the carotenoid absorbance maximum at 494 nm are severely depleted in Δ*ycf54*, whilst the absorbance maximum of the phycobiliproteins at 624 nm remains unchanged when compared to the WT (**Figure 1B**). Mutant cells contained only about 13% of WT Chl (**Figure 1B**) and the whole cell spectrum showed a large absorbance peak at 422 nm, indicating a substantial accumulation of MgPME (**Figure 1B**) (Hollingshead et al., 2012).

Identification of the Chl Precursors that Accumulate in the Δ*ycf54* Mutant

Previously we reported that Chl biosynthesis in a partially segregated *ycf54*$^{-}$ mutant was blocked at the MgPME cyclase step, which causes accumulation of high levels of MgPME, the substrate of the cyclase, and lesser levels of an unknown pigment with a Soret peak at 433 nm (Hollingshead et al., 2012). To examine the photosynthetic precursor pigments present in Δ*ycf54*, methanol extracts from low light grown cells were separated by HPLC (**Figure 2A**). As with *ycf54*$^{-}$, Δ*ycf54* synthesized high levels of MgPME and lesser levels of the unknown pigment. Given that the Soret band of this pigment is situated between the Soret peaks of MgPME at 416 nm and PChlide at 440 nm (**Figure 2B**) we proposed that it could be an intermediate of the cyclase reaction.

Nuclear magnetic resonance spectroscopy was used to determine the identity and structure of this unknown pigment, which was extracted by diethyl ether/water phase partitioning from the medium of Δ*ycf54* cells grown under very low light conditions. This pigment was purified to homogeneity by preparative HPLC. The one-dimensional ^{1}H spectrum (**Figure 3A**) shows the reasonable degree of purity of the pigment, with impurities indicated by an asterisk; the signals downfield of 5 ppm represent minor contaminants and methanol, whilst the impurity signals upfield of 5 ppm represent solvents, including water. Signals from the unknown pigment were assigned using a combination of ^{1}H TOCSY, gradient-selected 1D NOE, and natural abundance ^{13}C HSQC spectra.

NOE experiments were carried out with selective saturation of all proton peaks downfield from 3 ppm in order to identify protons with through-space correlation (**Figure 3A**). To cover the full range of ^{13}C shifts, two ^{13}C HSQC spectra were run with ^{13}C offsets of 60 ppm and 140 ppm. Many of the signals have ^{1}H and ^{13}C chemical shifts similar in frequency to those from MgPME (**Figure 3B**), with the expected TOCSY and NOE connectivities, and can therefore be assigned straightforwardly. The ^{13}C HSQC spectra (**Figure 3C**) confirmed the assignments of the four meso protons and the five methyl groups (with the four imidazole methyls having ^{13}C shifts of around 10 ppm and the propionate methyl having a shift of 50 ppm). The signals from the 3-vinyl protons were absent, but there is a new signal with ^{1}H and ^{13}C shifts of 11.6 and 190 ppm, respectively, which can only come from an aldehyde. This

[3]http://proteomecentral.proteomexchange.org

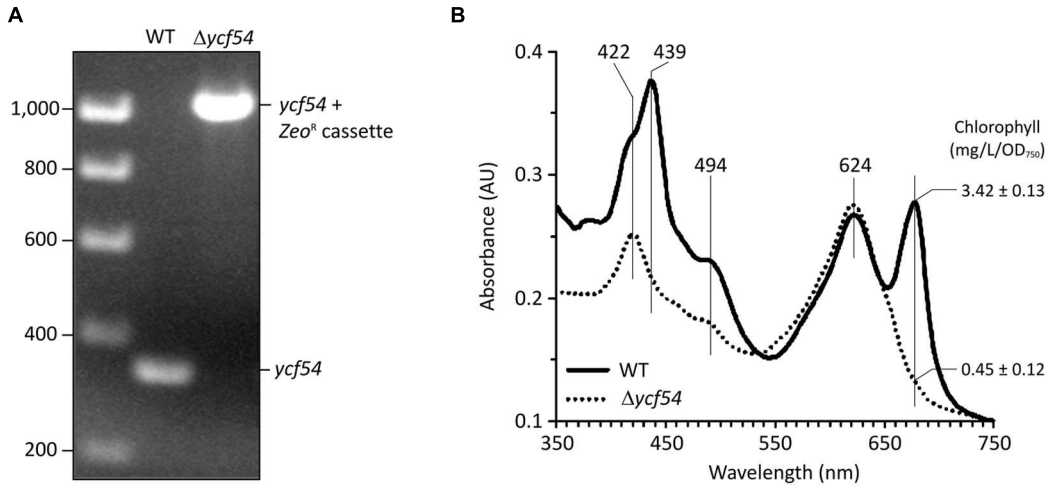

FIGURE 1 | Deletion of the *ycf54* gene in *Synechocystis* and the whole-cell spectra the resulting Δ*ycf54* strain. (A) PCR amplification of the *slr1780* (*ycf54*) region to confirm full segregation of the Zeocin resistance cassette. WT, wild-type. **(B)** Whole cell absorbance spectra of *Synechocystis* whole cells grown photomixotrophically under low light conditions. Chl *a* is represented by the 682-nm peak, and phycobiliproteins are represented by the 625-nm peak. Spectra were measured with cells at a similar optical density ($OD_{750\ nm}$ = ∼0.3) and normalized to light scattering at 750 nm.

signal has NOEs to both the 5-meso and 2-methyl protons, both of which were shifted downfield, and no through-bond connectivity in the TOCSY, verifying that this was a 3-formyl group which had replaced the 3-vinyl group of the MgPME. The NMR data are compiled, together with details of the acquisition parameters, in Supplementary Table 1, including Supplementary Figures S1–S3. Further confirmation that this signal represents a 3-formyl group comes from the ^{1}H-NMR spectra of Chl *d* (Fukusumi et al., 2012), which has a clear signal at ∼11.5 assigned as the 3-formyl group. Thus, the unknown pigment is magnesium 3-formyl-protoporphyrin IX monomethyl ester (**Figure 2D**).

Effects of Removal of Ycf54 on Other Chl Biosynthesis Enzymes

In order to investigate levels of Chl biosynthetic enzymes, and to verify the loss of Ycf54 in the Δ*ycf54* mutant, lysates from WT and Δ*ycf54* cells were fractionated into membrane and soluble components. The appearance of the cell lysate fractions (**Figure 4A**) reflects their pigment composition; the WT whole cell lysate and membrane fractions are green, and in Δ*ycf54* whole cell lysate and membrane fractions are blue and orange, respectively, because of the near-absence of Chl. A western blot of each of these extracts was probed with antibodies raised against a wide range of Chl biosynthesis enzymes (**Figure 4B**). The immunoblot probed with the antibody to Ycf54 shows this protein is distributed evenly between the soluble and insoluble fractions and is not detected in Δ*ycf54*, confirming the full segregation of this mutant. The absence of Ycf54 is also accompanied by a decrease in CycI and geranylgeranyl reductase (ChlP) and increased relative levels of the Mg-chelatase subunits ChlI and ChlD, although no change was detected in the levels of ChlH (**Figure 4B**).

Mass spectrometry was used to quantify the effects of *ycf54* deletion, in terms of the ability of CycI to associate with partner proteins *in vivo*. Pulldown assays with FLAG-tagged CycI are already known to retrieve Ycf54 from cell extracts (Hollingshead et al., 2012), so this experiment was repeated using FLAG- CycI in a Δ*ycf54* background. The amounts of PChlide oxidoreductase (POR), 3,8-divinyl (proto)chorophyllide reductase (DVR) and ChlP captured in pulldown assays by FLAG- CycI/WT and FLAG-CycI in Δ*ycf54* were compared by mass spectrometry. Proteins extracted from FLAG eluates were digested with a combination of endoproteinase LysC and trypsin and the peptide fragments analyzed by nanoLC-MS/MS. The captured proteins were quantified relative to the CycI bait as shown in **Figure 5**. Captured POR levels had decreased significantly in the Δ*ycf54* strain while DVR was reduced to an undetectable level. ChlP was only just detectable in one Δ*ycf54* replicate and relative to CycI by three orders of magnitude in the other two.

Lack of PChlide Impairs Synthesis of PsaA/B and Inner PSII Antennae but the Accumulation of Other Chl-Binding Proteins Is Not Affected

To evaluate the effects of greatly reduced Chl on the photosystems in Δ*ycf54* compared to the WT, photosynthetic membranes isolated from an equal biomass were gently solubilized with β-DDM and the membrane complexes were resolved by clear native electrophoresis (CN-PAGE), followed by SDS-PAGE in the second dimension. The resulting 2D CN/SDS-PAGE (**Figure 6A**) showed that Δ*ycf54* has drastically reduced levels of both photosystems, whilst the levels of other abundant membrane complexes such as ATP synthase, NADH:ubiquinone oxidoreductase and the cytochrome b_6f complex (shown by the western blot) are comparable between the two strains.

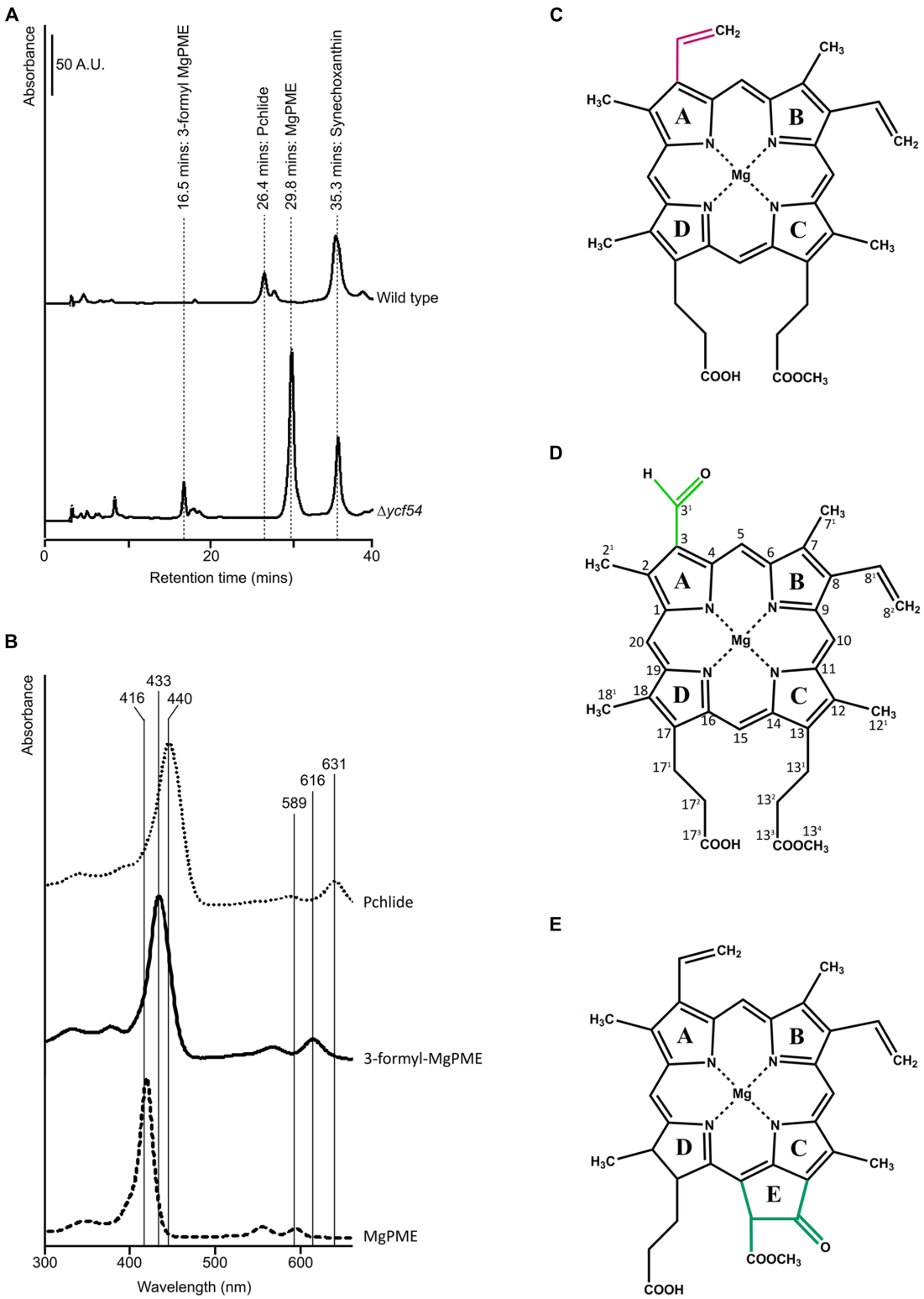

FIGURE 2 | HPLC analyses of pigments from WT and Δ*ycf54* cells. (A) Polar pigments were extracted with 80% methanol containing 0.2% (v/v) ammonium from an equal volume of cells at an $OD_{750\ nm}$ = ~0.7 and analyzed on a Phenomenex C_{18} column. Separation of precursors was detected by a diode array detector set to 432 nm, the Soret peak of 3-formyl MgPME, which is observed in Δ*ycf54* cells. The elution times of the pigments of interest are indicated. **(B)** Absorbance spectra of MgPME, PChlide and 3-formyl-MgPME, **(C)** Mg-protoporphyrin IX monomethyl ester (MgPME), **(D)** Mg-3-formyl-protoporphyrin IX monomethyl ester (3-formyl-MgPME), **(E)** protochlorophyllide (PChlide).

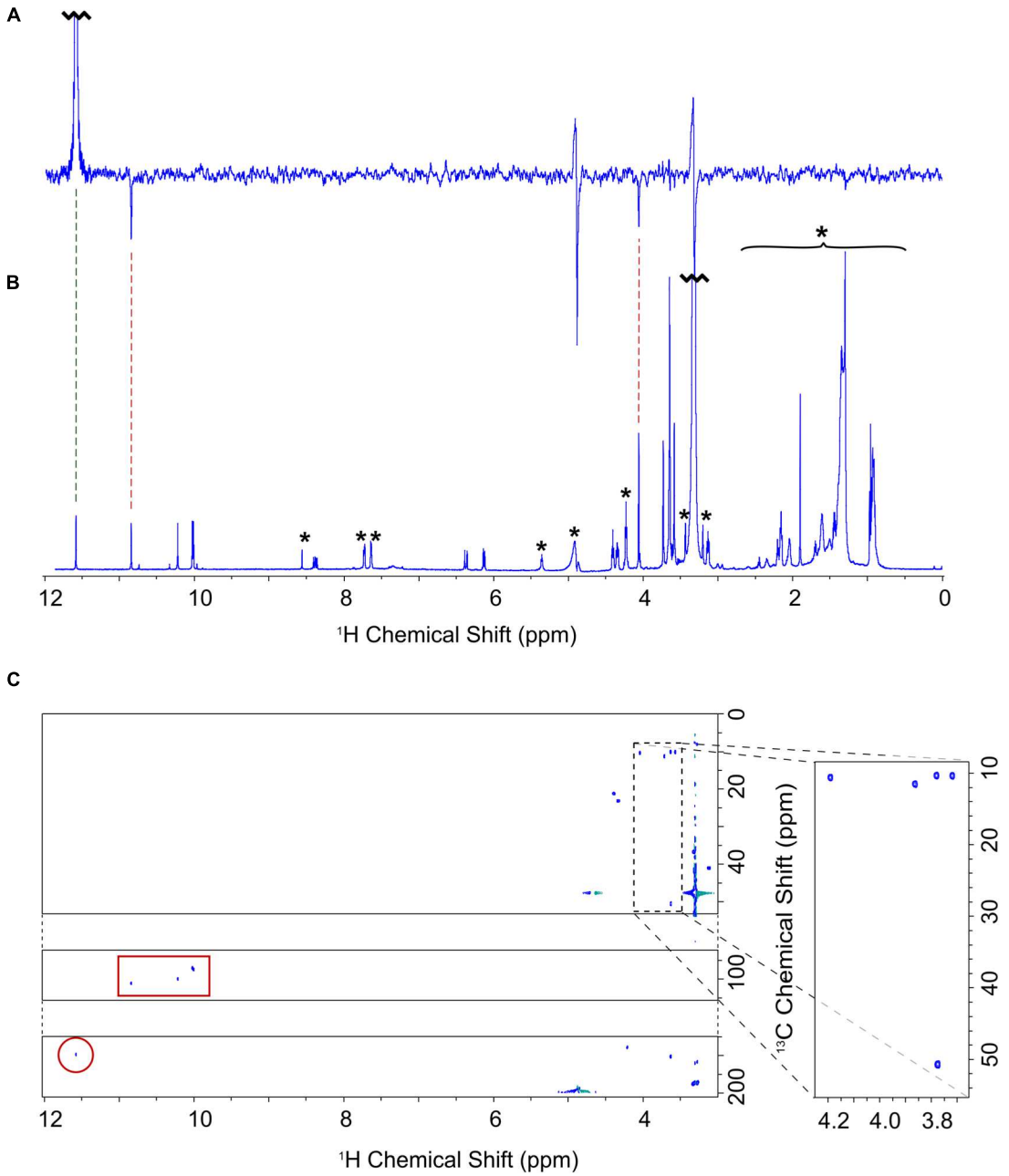

FIGURE 3 | NMR assignment of the A432 pigment accumulating in the Δ*ycf54* strain. (A) One dimensional selective NOE spectrum of 3-formyl-MgPME, selectively pulsed at 11.60 ppm (selectively exciting proton 3^1). Negative signals indicate NOE cross signal with protons 5 and 2^1 at 10.86 and 4.07 ppm, respectively. **(B)** ^{1}H-NMR spectrum of 3-formyl-MgPME. Signals marked with an asterisk are either solvent signals (methanol, water) or impurities (e.g., column matrix). **(C)** ^{13}C-HSQC spectrum for 3-formyl-MgPME. The carbon axis is split for clarity. The dashed box indicates methyl signals, expanded on the right. The red box indicates signals from meso protons. The red circle indicates a 3^1 aldehyde signal.

Interestingly, although the fully assembled PSII complexes in the mutant were barely detectable, this strain still accumulated relatively high levels of unassembled CP43 (**Figure 6A**). This observation suggests a block in formation of the early PSII assembly intermediates, which precedes attachment of the CP43 module and finalization of PSII reaction center core assembly (Komenda et al., 2004).

PSII assembly occurs in a stepwise fashion from four preassembled modules. These consist of one large Chl binding subunit (D1, D2, CP47, or CP43) in addition to several low molecular mass membrane polypeptides, bound pigments and other co-factors (Komenda et al., 2012). Assembly is initiated via the association of D1 and D2 to form the intermediate complex RCII* Knoppová et al. (2014), next the CP47 assembly

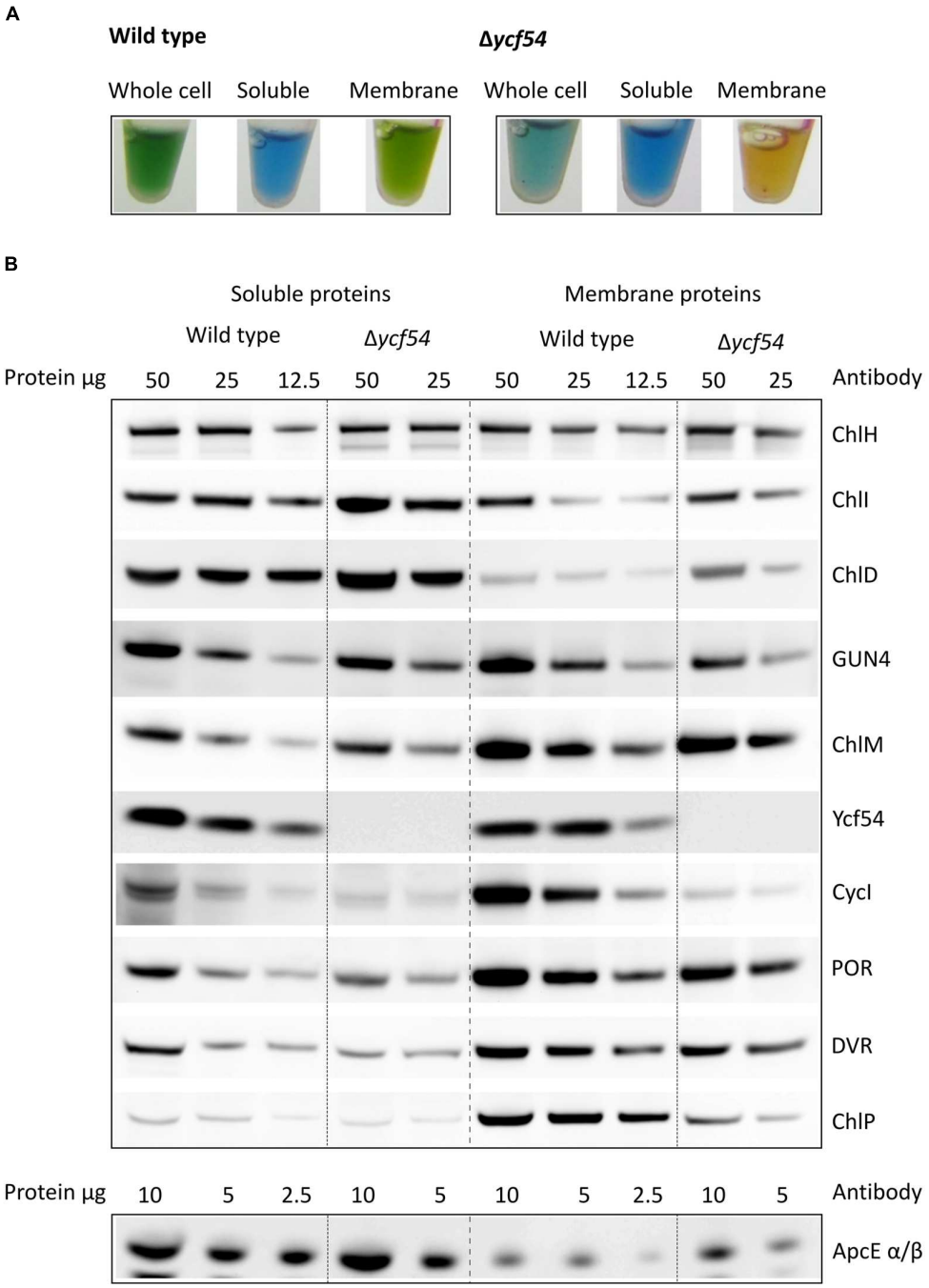

FIGURE 4 | Levels of Chl biosynthesis enzymes in WT and Δ*ycf54* cells. (A) Photographs of the whole cell, soluble and solubilized membrane lysate fractions, illustrating the changes in pigmentation between WT and Δ*ycf54*. **(B)** Western blot analysis of the soluble and membrane fractions from WT and Δ*ycf54 Synechocystis* strains. Samples of known protein concentration were separated by SDS-electrophoresis and transferred to a nitrocellulose membrane, which was probed with antibodies to the magnesium chelatase subunits (ChlH, ChlI, ChlD, and GUN4), CycI (CHL27), Mg-protoporphyrin IX methyltransferase (ChlM), Ycf54, PChlide oxidoreductase (POR), 3,8-divinyl (proto)chorophyllide reductase (DVR), geranylgeranyl reductase (ChlP). Detection of phycobiliprotein ApcE α/β served as a loading control.

module is attached, forming RC47, and finally mature PSII is formed by addition of the CP43 module (Boehm et al., 2011, 2012), attachment of the lumenal extrinsic proteins, and light-driven assembly of the oxygen-evolving Mn_4CaO_5 complex (Komenda et al., 2008; Nixon et al., 2010). To further investigate the perturbations in PSII assembly, the levels of individual PSII assembly sub-complexes were ascertained by 2D gel electrophoresis and immunodetection (**Figure 6B**). To assess

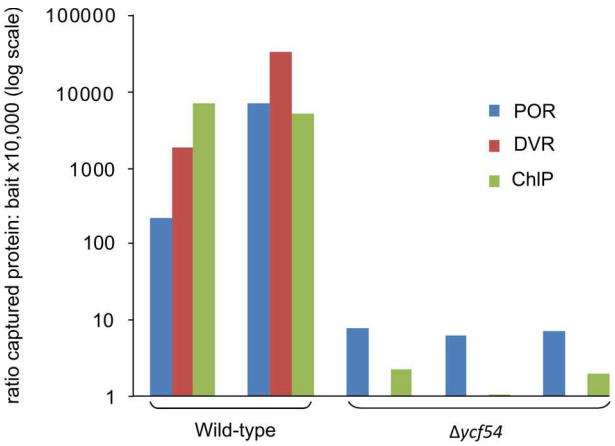

FIGURE 5 | Relative quantification of CycI, POR, DVR, and ChlP in FLAG-CycI pulldowns against WT and Δ*ycf54* backgrounds, using mass spectrometry. The bait and captured proteins in FLAG-CycI elutes were identified by mass spectrometry and database searching as described in Materials and Methods. For each analysis, a representative tryptic peptide ion was extracted from the full scan spectra as follows: CycI, AILEEFR, m/z 439.24, 2+; POR, VADELGFPK, m/z 488.26, 2+; DVR (Slr1923), VNKPTLSPNLSVLEEVEK, 666.03 3+; ChlP, AGIETYLFER, 599.81, 2+.

accumulation of the RCII* complex, the immunoblot was probed with antibodies raised against the RCII* components D1, Ycf39, and HliD (Knoppová et al. (2014). **Figure 6B** shows that the level of RCII* is unaffected by the large reduction in cellular Chl levels in the Δ*ycf54* mutant. Next, we investigated if PSII maturation was blocked at CP47 attachment and formation of RC47, by probing the blots with antibodies raised against HliA, a specific component of the CP47 assembly module (Promnares et al., 2006). We found that HliA, and hence the CP47 assembly module, was readily detectable in WT, but could not be detected in Δ*ycf54* (**Figure 6B**), indicating that low Chl abundance in Δ*ycf54* is impairing accumulation of the CP47 assembly module.

Our FLAG-pulldown experiments show that the interactions between CycI, POR, and DVR are significantly reduced in the Δ*ycf54* strain (**Figure 5**), therefore we compared the co-migration of these enzymes on a 2D gel (**Figure 6C**). Evident in the WT is a putative high-mass complex of ∼400 kDa (highlighted by the green box), which contains both CycI and POR; this complex was not detectable in the mutant (**Figure 6C**). Interestingly, our 2D gel shows that levels of Chl synthase, ChlG, HliD, and Ycf39, components of a chlorophyll biosynthetic/membrane insertase assembly complex (Chidgey et al., 2014), are unaffected in the Δ*ycf54* mutant (**Figure 6C**).

To understand the flux of photosystem biogenesis, we used ^{35}S pulse radio-labeling coupled with 2D CN/SDS-PAGE (**Figure 7**; a Coomassie stained gel is provided as Supplementary Figure S4), to compare the levels of protein synthesis between the WT and Δ*ycf54* mutant. As demonstrated in **Figure 7**, the ability of Δ*ycf54* to synthesize the Chl-binding PSI subunits PsaA/B is limited and synthesis of CP47 and CP43 subunits is hardly detectable even though 3-times more Δ*ycf54* protein was loaded onto the gel (See Supplementary Figure S4 for overexposed signal of the CP47). In contrast, there were comparable levels of synthesis of the PSII reaction center core subunits D1 and D2 in the WT and Δ*ycf54* strains. This observation, coupled with the data from our 2D-immunoblot (**Figure 6B**), shows that the D1 and D2 subunits are rapidly assembled into RCII* in Δ*ycf54*, but given the lack of assembled PSII complexes, these RCII* are presumably rapidly degraded in the mutant. Interestingly, in the mutant the unassembled CP43 was still detectable on the stained gel, which contrasted to virtually zero level of unassembled CP47 (**Figures 6A,B** and **7**; Supplementary Figure S4). This observation indicates that both synthesis and stability of the CP47 are impaired in the mutant, whereas the structurally similar CP43 antenna can still accumulate though the synthesis is also very weak (Supplementary Figure S4). Taken together, our data suggest that the depleted levels of *de novo* Chl in Δ*ycf54* specifically hinder the synthesis of PSI and the inner antennae of the PSII. However, given different stability of CP47 and CP43, it is the lack of CP47 protein that blocks assembly of RC47 and thus PSII maturation, sensitizing the PSII assembly pathway to the availability of *de novo* Chl.

Lack of *De Novo* Chl Affects Ultrastructure of Δ*ycf54* Cells

In order to investigate the effects of removal of 87% of the cellular Chl on the ultrastructure of Δ*ycf54* cells, electron microscopy of negatively stained thin cell sections was performed. Electron micrographs are shown in **Figure 8**. In the WT the thylakoids are observed as parallel stacks of two to five membranes that closely follow the contour of the cell membrane (**Figures 8A–C**), but no such organized thylakoid membranes are visible in micrographs of the Δ*ycf54* mutant (**Figures 8B–D**). Instead, membrane-like structures are dispersed throughout the cytoplasm of the cell. These results suggest key role of photosystems in the formation of the highly ordered thylakoid structures.

DISCUSSION

The MgPME-cyclase is the least understood component in the Chl biosynthetic pathway, and current knowledge of the individual components of the MgPME-cyclase had been limited to homologs of the *Rubrivivax gelatinosus* AcsF protein. Previous work identified two genes in *Synechocystis*, *sll1214*, and *sll1874*, as *acsF* homologs, which encode a membrane associated component of the MgPME-cyclase (Minamizaki et al., 2008; Peter et al., 2009). AcsF and its homologs contain a putative di-iron site and are thus viewed as the true catalytic subunit of the MgPME-cyclase (Tottey et al., 2003). The discovery of another gene, *ycf54*, that plays an important role in cyclase activity (Albus et al., 2012; Hollingshead et al., 2012) showed that other components are required, but so far it is not possible to assign a catalytic or assembly-related function to the Ycf54 protein. Further work on the role of Ycf54 required a fully segregated Δ*ycf54* mutant, which is reported herein.

In our efforts to construct a fully segregated Δ*ycf54* mutant, we discovered it was only possible to completely delete the *ycf54* gene in one specific substrain of *Synechocystis* (GT-W).

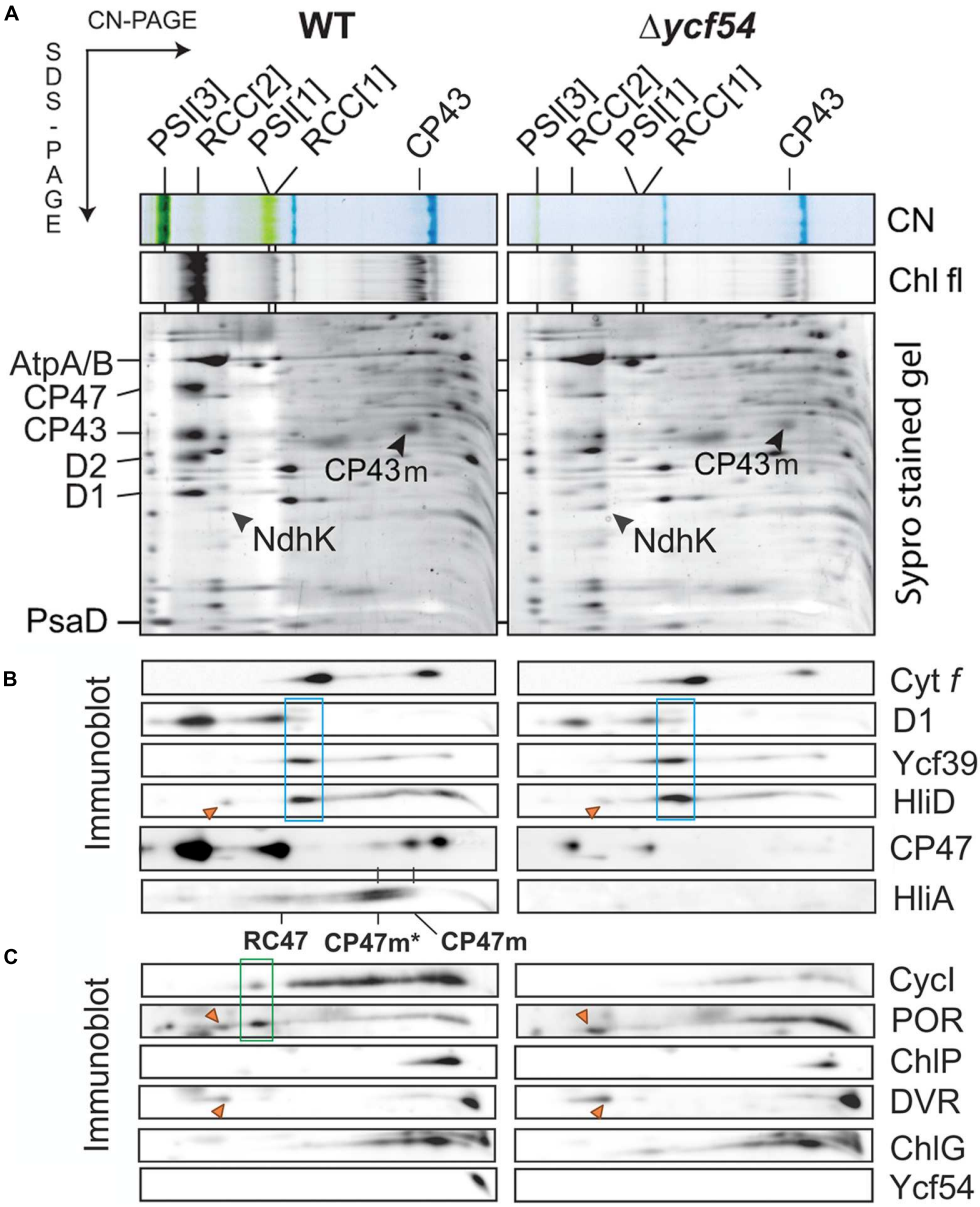

FIGURE 6 | 2D gel-electrophoresis of membrane complexes isolated from WT and Δ*ycf54* cells, followed by immunodetection of PSII assembly complexes and enzymes involved in Chl biosynthesis. (A) Membrane proteins were separated by 4–14% CN-PAGE, and then in the second dimension by 12–20% SDS-PAGE. The loading corresponds to the same number of cells. The SDS gel was stained by Sypro Orange, blotted and the cytochrome *f* visualized by heme *f* peroxidase activity. Chl fluorescence emitted by PSII and by unassembled CP43 (Chl fl) was detected by Fuji LAS 4000 after excitation by blue light. Designation of complexes is: PSI[3] and PSI[1], trimeric and monomeric PSI, respectively; RCC[2] and RCC[1], dimeric and monomeric PSII core complexes, respectively. **(B)** Immunodetection of PSII assembly complexes. RCII* complex (boxed in blue) was detected using D1, Ycf39, and HliD antibodies. The positions of the CP47 assembly module CP47m, and CP47m associated with High-Light-Inducible proteins HliA/B (CP47m*), are indicated. The HliA signal also marks the position of the PSII core complex lacking CP43 (RC47). **(C)** Immunodetection of Ycf54 proteins and enzymes involved in Chl biosynthesis in the membrane fraction separated by 2D electrophoresis. Highlighted by the green box is a putative high-mass complex (~400 kDa) containing CycI and POR; this complex is not detectable in the mutant. Orange triangles indicate unspecific cross-reactions with a subunit of the NDH complex. ChlG is Chl-synthase; other enzymes are designated as in **Figure 2**.

One possible explanation for this finding was elucidated by analysis of the GT-W genome, which contains a long (~100 kbp) chromosomal duplication that covers one hundred genes, including *cycI (sll1214*; Bečková et al., submitted). This chromosomal duplication is not present in any of the other *Synechocystis* substrains for which a genome sequence is available (Kanesaki et al., 2012; Trautmann et al., 2012). Given the duplication of *cycI* in GT-W, it is likely that *cycI* expression is

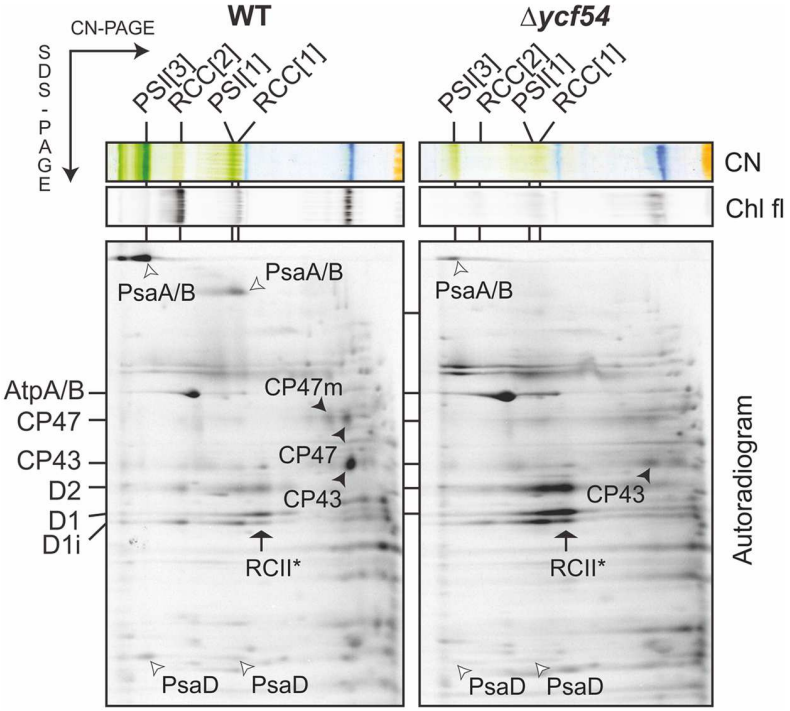

FIGURE 7 | Synthesis of the Chl-binding proteins in the Δ*ycf54* strain. WT and mutant cells were radiolabeled with [^{35}S]Met/Cys mixture using a 30-min pulse. Isolated membrane proteins were separated by CN-PAGE on a 4–14% linear gradient gel, and another 12–20% SDS-electrophoresis was used for the second dimension. For Δ*ycf54* membrane proteins three-times more cells were loaded than for the control to obtain a detectable signal for weakly labeled proteins (PsaA/B). The 2D gels were stained with Coomassie Blue (the stained gel is shown as Supplementary Figure S4) then dried, and the labeled proteins were then detected by a phosphorimager (Autorad). Protein complexes are designated as in **Figure 6**.

increased in this strain. A very low level of CycI is a hallmark of the strains in which we partially or completely inactivated the *ycf54* gene. Thus, we hypothesize that the doubled expression of the *sll1214* gene coding for CycI may suppress the lethality of inactivating the *ycf54* gene. This hypothesis is in agreement with our observation that in the absence of Ycf54 the CycI cyclase component is destabilized (**Figures 4** and **5**) and the remaining CycI content is probably very close to a threshold essential for viability.

Analysis of the pigments that accumulate in the Δ*ycf54* mutant could provide clues regarding the role of the Ycf54 protein, and a previous analysis showed that the partially segregated *ycf54* mutant accumulates MgPME, the substrate of the cyclase. In addition, there was an unknown pigment (**Figure 2**) that was suggested to be an intermediate in the cyclase reaction (Hollingshead et al., 2012), on the basis that the 433 nm Soret absorbance peak falls between the Soret peaks of the cyclase substrate MgPME (416 nm) and the PChlide product (440 nm). Similarly, early work with greening cucumber cotyledons had found pigments with emission maxima between 434 and 436 nm, proposed to be biosynthetic intermediates between MgPME and PChlide (Rebeiz et al., 1975). Identification of the unknown pigment as Mg-3-formyl-PME suggests that this pigment is not an intermediate in the cyclase reaction, as it is highly unlikely that this would produce a Chl pigment modified at the C3 position. Rather, Mg-3-formyl-PME bears a striking resemblance to Chl *d*, the major light harvesting pigment found in the cyanobacterium *Acaryochloris marina* (Miyashita et al., 1996). The pathway and reaction mechanism of Chl *d* biosynthesis in *Acaryochloris marina* have not yet been elucidated but, based on the genome sequence, Chl *d* is thought to be derived from Chl *a* (Swingley et al., 2008). Previously, Chl *d* has been synthesized in low yields in aqueous acetone from Chl *a* by treatment with papain (Koizumi et al., 2005) and peroxide (Aoki et al., 2011) and in much higher yields from Chl *a* incubated with thiophenol and acetic acid in tetrahydrofuran (Fukusumi et al., 2012). Given the high accumulation of MgPME in Δ*ycf54*, it is likely that reactive oxygen species, including peroxide, convert the MgPME 3-vinyl group, leading to the formation of Mg-3-formyl-PME.

The identification of Mg-3-formyl-PME as an oxidation product of the substrate rather than a catalytic intermediate is not consistent with a catalytic role for Ycf54 in the MgPME-cyclase complex. However, the hypothesis by Hollingshead et al. (2012) that Ycf54 plays a role in the assembly or stabilization of the catalytic MgPME-cyclase enzyme complex remains valid. By using FLAG-CycI as bait in pulldown assays, combined with quantitative MS analysis, we demonstrated that the absence of Ycf54 affects formation of a complex between CycI and enzymes further down the pathway (POR, DVR, and ChlP). In particular, the almost complete absence of DVR in the pulldown from the Δ*ycf54* strain provides a strong evidence that Ycf54 facilitates formation of such a complex; in contrast to POR and ChlP the

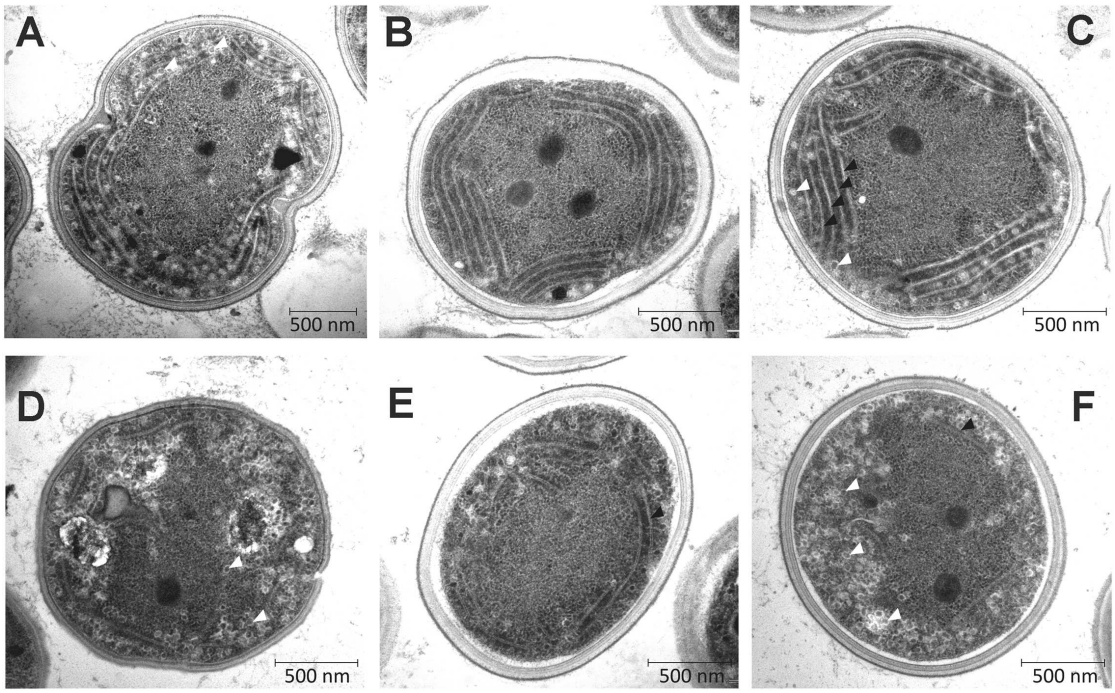

FIGURE 8 | Transmission electron micrographs of WT and Δ*ycf54* cells. Ultrathin sections from *Synechocystis* WT **(A–C)** and Δ*ycf54* cells **(D–F)** grown photomixotrophically under low light conditions. White arrows indicate thylakoid membranes and white triangles indicate glycogen granules.

stability of DVR in the mutant does not seem to be compromised and thus this result cannot be explained by a hypothetical fast degradation of this enzyme during pulldown assay. Indeed, the present data also provide evidence for an interaction between Cycl1 and POR, DVR, and ChlP, which aligns well with data obtained by Kauss et al. (2012) who performed pulldown experiments with the *Arabidopsis* FLU protein. These analyses found that FLU forms a complex with CHL27, the *Arabidopsis* AcsF homolog, PORB, PORC, and ChlP. In *Synechocystis* at least, it appears that Ycf54 plays no direct catalytic role, and that it is important for the formation and maintenance of a Chl biosynthetic complex, with disruption of this complex possibly triggering degradation of CycI and consequently Chl deficiency. However, a wider role for Ycf54 in governing the whole pathway appears to be excluded by the lack of effect of the Δ*ycf54* on components of the ChlG-HliD-Ycf39 complex that operates at the end of the pathway. This complex likely coordinates Chl delivery to the membrane-intrinsic apparatus for insertion and translocation of apoproteins of the photosynthetic apparatus (Chidgey et al., 2014). It is notable that although the CycI is almost exclusively associated with the membrane fraction under moderate light conditions Ycf54 is distributed equally between membrane and soluble fractions (**Figure 4B**). It is not known whether membrane-bound or soluble Ycf54 is critical for the CycI stability but there is a possibility that dissociation of Ycf54 from a membrane-bound assembly of CycI, POR, and DVR enzymes triggers degradation of CycI. Such a mechanism might regulate CycI activity at post-translational level and allow the cell to respond quickly to fluctuations in the environment.

Deletion of the *ycf54* gene generated a *Synechocystis* strain with very low levels of Chl, facilitating our studies on the cellular effects of a greatly lowered flux down the Chl biosynthetic pathway. It has long been known that photosystem biosynthesis requires Chl (Mullet et al., 1990; Eichacker et al., 1992; Müller and Eichacker, 1999), so we took advantage of the low Chl levels in the Δ*ycf54* mutant to investigate the effects of Chl depletion on the synthesis and assembly of the photosystems. Although the levels of some Chl biosynthesis enzymes are altered in the Δ*ycf54* mutant the ChlG-HliD-Ycf39 complex is unaffected, allowing the effects of reduced flux down the Chl pathway on Chl binding proteins to be investigated without disrupting ChlG-HliD-Ycf39 interactions with the YidC/Alb3 insertase and the consequent synthesis of nascent photosystem polypeptides. In addition, we were able to investigate the accumulation of "minor" Chl binding proteins, including cytochrome b_6f (Kurisu et al., 2003), the Hli proteins (Staleva et al., 2015) and the Chl-synthase complex (Chidgey et al., 2014). Our findings show that whilst the Chl binding proteins PsaA/B and CP47 are highly sensitive to cellular Chl levels, the accumulation of CP43 and "minor" Chl binding proteins, including cytochrome b_6f, is robust under Chl limiting conditions.

PSI is the main sink for *de novo* Chl (Kopečná et al., 2013); our results (**Figure 7**) show that synthesis of the core PSI subunits PsaA/B is impaired in the absence of Ycf54, i.e., under *de novo* Chl limiting conditions, suggesting that *Synechocystis* is unable to recycle Chl molecules released from degraded complexes for the synthesis of new PSI complexes. In comparison, the dependence of PSII biogenesis on the availability of *de novo* Chl

modules appears to be more complex, as previous studies show Chl molecules are re-cycled during PSII synthesis and repair (Kopečná et al., 2013, 2015) via re-phytylation of chlorophyllide (Vavilin and Vermaas, 2007). The PSII complex assembles in a modular fashion, starting with the association of D1 and D2 assembly modules, to form the RCII* complex. This is followed by attachment of a CP47 module, then a CP43 module, then the lumenal extrinsic proteins and the oxygen-evolving Mn_4CaO_5 complex (reviewed in Komenda et al., 2012). Despite the large decrease in cellular Chl levels in Δ*ycf54*, all components of the RCII* complex are synthesized in adequate amounts and assembled. We hypothesize that synthesis of the RCII* complex is enabled by the continuous recycling of a relatively stable pool of Chl molecules made available during the RCII* assembly/degradation cycle. Evidence that RCII* contains Chl as well pheophytin, carotenoids and heme cofactors has been shown previously (Knoppová et al., 2014). We cannot exclude the possibility that in the Δ*ycf54* mutant there is a pool of the RCII* complex that lacks Chl. However, we did not observe any shift of electrophoretic mobility even for the ^{35}S labeled RCII* that would indicate presence of a hypothetical Chl-less RCII*. Furthermore, Δ*ycf54* contains some functional PSII complexes, which requires that at least some RCII* with cofactors has to be synthesized en route to the fully assembled PSII.

Our findings also show that CP43 can accumulate as an unassembled module in Δ*ycf54* even though the synthesis is very limited (**Figures 6A** and **7**). In contrast, CP47 seems to be unstable in Δ*ycf54*, which suggests that CP47 is the *de novo* Chl sensitive component of PSII biogenesis. This observation is consistent with previous work on the accumulation of PSII subunits in Δ*por* (Kopečná et al., 2013) and Δ*gun4* (Sobotka et al., 2008) mutants, disrupted in the PChlide reduction and Mg-chelatase steps, respectively. As also seen for Δ*ycf54*, the Δ*por* and Δ*gun4* strains accumulate the PSII core complex RCII* and the PSII antenna CP43, but CP47 synthesis is not observed (Sobotka et al., 2008; Kopečná et al., 2013). It is not currently known why CP47 is more sensitive to the availability of *de novo* Chl than the similar CP43 subunit, although it has been recently observed that the newly synthesized CP43, but not CP47, subunit is attached to a PSI complex (Kopečná et al., 2015). We tentatively speculate that the situation in the mutant leads frequently to the synthesis of aberrant CP47 lacking one or more Chl molecules. The synthesis of CP43 might be less error-prone because Chl molecules bound to the periphery of PSI could be used for the assembly of this complex.

In summary, the role of Ycf54 in the MgPME-cyclase complex has been elucidated further. This work shows that whilst Ycf54 is required for stabilization of Cyc1, the known catalytic component of the MgPME-cyclase, the protein itself is unlikely to play a key catalytic role in the formation of the fifth isocyclic ring. Furthermore, Ycf54 does not appear to be directly implicated in Chl phytolation or Chl insertion into proteins. The construction of a Δ*ycf54* mutant has provided a useful tool to investigate the effects of reduced *de novo* Chl on the biosynthesis of cyanobacterial Chl binding proteins, highlighting the differing requirements for Chl exhibited by proteins within the PSI and PSII light harvesting complexes that bind this pigment. Insights into the catalytic cycle of the MgPME-cyclase remain elusive and further work is required to determine the exact molecular mechanisms of this enzyme.

AUTHOR CONTRIBUTIONS

SH, JK, DA, LB, PJ, and GC performed the research; MD, MW, RS, and CNH designed the experiments, and SH, DA, PJ, MD, MW, RS, and CNH wrote the paper.

ACKNOWLEDGMENTS

SH, PJ, CNH, and MD gratefully acknowledge financial support from the Biotechnology and Biological Sciences Research Council (BBSRC UK), award numbers BB/G021546/1 and BB/M000265/1. MD acknowledges support from the Biotechnology and Biological Sciences Research Council (UK; BB/M012166/1). CNH was also supported by Advanced Award 338895 from the European Research Council. SH was supported by a doctoral studentship from the University of Sheffield. GC and DA were supported by a BBSRC doctoral studentship. JK, LB, and RS were supported by project 14-13967S of the Czech Science Foundation, and by the National Programme of Sustainability I (LO1416).

SUPPLEMENTARY MATERIAL

The Supplementary Material for this article can be found online at: http://journal.frontiersin.org/article/10.3389/fpls.2016.00292

REFERENCES

Albus, C. A., Salinas, A., Czarnecki, O., Kahlau, S., Rothbart, M., Thiele, W., et al. (2012). LCAA, a novel factor required for magnesium protoporphyrin monomethylester cyclase accumulation and feedback control of aminolevulinic acid biosynthesis in Tobacco. *Plant Physiol.* 160, 1923–1939. doi: 10.1104/pp.112.206045

Aoki, K., Itoh, S., Furukawa, H., Nakazato, M., Iwamoto, K., Shiraiwa, Y., et al. (2011). "Enzymatic and non-enzymatic conversion of Chl a to Chl d," in *Proceedings of the 5th Asia and Oceania Conference on Photobiology*, Nara.

Boehm, M., Romero, E., Reisinger, V., Yu, J., Komenda, J., Eichacker, L. A., et al. (2011). Investigating the early stages of Photosystem II assembly in *Synechocystis* sp PCC 6803: isolation of CP47 and CP43 complexes. *J. Biol. Chem.* 286, 14812–14819. doi: 10.1074/jbc.M110.207944

Boehm, M., Yu, J., Reisinger, V., Bečková, M., Eichacker, L. A., Schlodder, E., et al. (2012). Subunit composition of CP43-less photosystem II complexes of *Synechocystis* sp PCC 6803: implications for the assembly and repair of photosystem II. *Philos. Trans. R. Soc. B Biol. Sci.* 367, 3444–3454. doi: 10.1098/rstb.2012.0066

Boldareva-Nuianzina, E. N., Bláhová, Z., Sobotka, R., and Koblížek, M. (2013). Distribution and origin of oxygen-dependent and oxygen-independent forms of Mg-protoporphyrin monomethylester cyclase among phototrophic *proteobacteria*. *Appl. Environ. Microbiol.* 79, 2596–2604. doi: 10.1128/AEM.00104-13

Bollivar, D., Braumann, I., Berendt, K., Gough, S. P., and Hansson, M. (2014). The Ycf54 protein is part of the membrane component of Mg-protoporphyrin IX monomethyl ester cyclase from barley (*Hordeum vulgare* L.). *FEBS J.* 281, 2377–2386. doi: 10.1111/febs.12790

Canniffe, D. P., Jackson, P. J., Hollingshead, S., Dickman, M. J., and Hunter, C. N. (2013). Identification of an 8-vinyl reductase involved in bacteriochlorophyll biosynthesis in *Rhodobacter sphaeroides* and evidence for the existence of a third distinct class of the enzyme. *Biochem. J.* 450, 397–405. doi: 10.1042/BJ20121723

Chidgey, J. W., Linhartová, M., Komenda, J., Jackson, P. J., Dickman, M. J., Canniffe, D. P., et al. (2014). A cyanobacterial chlorophyll synthase-HliD complex associates with the Ycf39 protein and the YidC/Alb3 insertase. *Plant Cell* 26, 1267–1279. doi: 10.1105/tpc.114.124495

Chua, N. H., Blobel, G., Siekevitz, P., and Palade, G. E. (1976). Periodic variations in the ratio of free to thylakoid-bound chloroplast ribosomes during the cell cycle of *Chlamydomonas reinhardtii*. *J. Cell Biol.* 71, 497–514. doi: 10.1083/jcb.71.2.497

Dobáková, M., Sobotka, R., Tichý, M., and Komenda, J. (2009). Psb28 protein is involved in the biogenesis of the photosystem II inner antenna CP47 (PsbB) in the cyanobacterium *Synechocystis* sp. PCC 6803. *Plant Physiol.* 149, 1076–1086. doi: 10.1104/pp.108.130039

Eichacker, L., Paulsen, H., and Rüdiger, W. (1992). Synthesis of chlorophyll a regulates translation of chlorophyll a apoproteins P700, CP47, CP43 and D2 in barley etioplasts. *Eur. J. Biochem.* 205, 17–24. doi: 10.1111/j.1432-1033.1992.tb16747.x

Eichacker, L. A., Helfrich, M., Rüdiger, W., and Muller, B. (1996). Stabilization of chlorophyll a-binding apoproteins P700, CP47, CP43, D2, and D1 by chlorophyll a or Zn-pheophytin a. *J. Biol. Chem.* 271, 32174–32179. doi: 10.1074/jbc.271.50.32174

Fukusumi, T., Matsuda, K., Mizoguchi, T., Miyatake, T., Ito, S., Ikeda, T., et al. (2012). Non-enzymatic conversion of chlorophyll-a into chlorophyll-d in vitro: a model oxidation pathway for chlorophyll-d biosynthesis. *FEBS Lett.* 586, 2338–2341. doi: 10.1016/j.febslet.2012.05.036

Hollingshead, S., Kopečná, J., Jackson, P. J., Canniffe, D. P., Davison, P. A., Dickman, M. J., et al. (2012). Conserved chloroplast open-reading frame ycf54 is required for activity of the magnesium protoporphyrin monomethylester oxidative cyclase in *Synechocystis* PCC 6803. *J. Biol. Chem.* 287, 27823–27833. doi: 10.1074/jbc.M112.352526

Jordan, P., Fromme, P., Witt, H. T., Klukas, O., Saenger, W., and Krauss, N. (2001). Three-dimensional structure of cyanobacterial photosystem I at 2.5 Å resolution. *Nature* 411, 909–917. doi: 10.1038/35082000

Kalb, V. F., and Bernlohr, R. W. (1977). A new spectrophotometric assay for protein in cell extracts. *Anal. Biochem.* 82, 362–371. doi: 10.1016/0003-2697(77)90173-7

Kanesaki, Y., Shiwa, Y., Tajima, N., Suzuki, M., Watanabe, S., Sato, N., et al. (2012). Identification of substrain-specific mutations by massively parallel whole-genome resequencing of *Synechocystis* sp. PCC 6803. *DNA Res.* 19, 67–79. doi: 10.1093/dnares/dsr042

Kauss, D., Bischof, S., Steiner, S., Apel, K., and Meskauskiene, R. (2012). FLU, a negative feedback regulator of tetrapyrrole biosynthesis, is physically linked to the final steps of the Mg++-branch of this pathway. *FEBS Lett.* 586, 211–216. doi: 10.1016/j.febslet.2011.12.029

Ke, S. H., and Madison, E. L. (1997). Rapid and efficient site-directed mutagenesis by single-tube 'megaprimer' PCR method. *Nucleic Acids Res.* 25, 3371–3372. doi: 10.1093/nar/25.16.3371

Knoppová, J., Sobotka, R., Tichý, M., Yu, J., Koník, P., Halada, P., et al. (2014). Discovery of a chlorophyll binding protein complex involved in the early steps of photosystem II assembly in *Synechocystis*. *Plant Cell* 26, 1200–1212. doi: 10.1105/tpc.114.123919

Koizumi, H., Itoh, Y., Hosoda, S., Akiyama, M., Hoshino, T., Shiraiwa, Y., et al. (2005). Serendipitous discovery of Chl d formation from Chl a withpapain. *Sci. Technol. Adv. Mater.* 6, 551–557. doi: 10.1016/j.stam.2005.06.022

Komenda, J., Nickelsen, J., Tichý, M., Prášil, O., Eichacker, L. A., and Nixon, P. J. (2008). The cyanobacterial homologue of HCF136/YCF48 is a component of an early photosystem II assembly complex and is important for both the efficient assembly and repair of photosystem II in *Synechocystis* sp PCC 6803. *J. Biol. Chem.* 283, 22390–22399. doi: 10.1074/jbc.M801917200

Komenda, J., Reisinger, V., Müller, B. C., Dobáková, M., Granvogl, B., and Eichacker, L. A. (2004). Accumulation of the D2 protein is a key regulatory step for assembly of the photosystem II reaction center complex in *Synechocystis* PCC 6803. *J. Biol. Chem.* 279, 48620–48629. doi: 10.1074/jbc.M405725200

Komenda, J., Sobotka, R., and Nixon, P. J. (2012). Assembling and maintaining the Photosystem II complex in chloroplasts and cyanobacteria. *Curr. Opin. Plant Biol.* 15, 245–251. doi: 10.1016/j.pbi.2012.01.017

Kopečná, J., Pilný, J., Krynická, V., Tomèala, A., Kis, M., Gombos, Z., et al. (2015). Lack of phosphatidylglycerol inhibits chlorophyll biosynthesis at multiple sites and limits chlorophyllide reutilization in *Synechocystis* sp. Strain PCC 6803. *Plant Physiol.* 169, 1307–1317. doi: 10.1104/pp.15.01150

Kopečná, J., Sobotka, R., and Komenda, J. (2013). Inhibition of chlorophyll biosynthesis at the protochlorophyllide reduction step results in the parallel depletion of Photosystem I and Photosystem II in the cyanobacterium *Synechocystis* PCC 6803. *Planta* 237, 497–508. doi: 10.1007/s00425-012-1761-4

Kurisu, G., Zhang, H. M., Smith, J. L., and Cramer, W. A. (2003). Structure of the cytochrome b6f complex of oxygenic photosynthesis: tuning the cavity. *Science* 302, 1009–1014. doi: 10.1126/science.1090165

Minamizaki, K., Mizoguchi, T., Goto, T., Tamiaki, H., and Fujita, Y. (2008). Identification of two homologous genes, chlAI and chlAII, that are differentially involved in isocyclic ring formation of chlorophyll a in the cyanobacterium *Synechocystis* sp PCC 6803. *J. Biol. Chem.* 283, 2684–2692. doi: 10.1074/jbc.M708954200

Miyashita, H., Ikemoto, H., Kurano, N., Adachi, K., Chihara, M., and Miyachi, S. (1996). Chlorophyll d as a major pigment. *Nature* 383, 402. doi: 10.1038/383402a0

Müller, B., and Eichacker, L. A. (1999). Assembly of the D1 precursor in monomeric photosystem II reaction center precomplexes precedes chlorophyll a-triggered accumulation of reaction center II in barley etioplasts. *Plant Cell* 11, 2365–2377. doi: 10.2307/3870961

Mullet, J. E., Klein, P. G., and Klein, R. R. (1990). Chlorophyll regulates accumulation of the plastid encoded chlorophyll apoprotein CP43 and apoprotein D1 by increasing apoprotein stability. *Proc. Natl. Acad. Sci. U.S.A.* 87, 4038–4042. doi: 10.1073/pnas.87.11.4038

Nixon, P. J., Michoux, F., Yu, J., Boehm, M., and Komenda, J. (2010). Recent advances in understanding the assembly and repair of photosystem II. *Ann. Bot.* 106, 1–16. doi: 10.1093/aob/mcq059

Peter, E., Salinas, A., Wallner, T., Jeske, D., Dienst, D., Wilde, A., et al. (2009). Differential requirement of two homologous proteins encoded by sll1214 and sll1874 for the reaction of Mg protoporphyrin monomethylester oxidative cyclase under aerobic and micro-oxic growth conditions. *Biochim. Biophys. Acta* 1787, 1458–1467. doi: 10.1016/j.bbabio.2009.06.006

Pinta, V., Picaud, M., Reiss-Husson, F., and Astier, C. (2002). *Rubrivivax gelatinosus* acsF (previously orf358) codes for a conserved, putative binuclear-iron-cluster-containing protein involved in aerobic oxidative cyclization of Mg-protoporphyrin IX monomethylester. *J. Bacteriol.* 184, 746–753. doi: 10.1128/JB.184.3.746-753.2002

Porra, R., Thompson, W., and Kriedemann, P. (1989). Determination of accurate extinction coefficients and simulataneous equations for assaying chlorophylls a and b extracted with four different solvents: verification of the concentration of chlorophyll standards by atomic absorption spectroscopy. *Biochim. Biophys. Acta* 975, 384–389. doi: 10.1016/S0005-2728(89)80347-0

Porra, R. J., Schafer, W., Gadon, N., Katheder, I., Drews, G., and Scheer, H. (1996). Origin of the two carbonyl oxygens of bacteriochlorophyll alpha – Demonstration of two different pathways for the formation of ring E in *Rhodobacter sphaeroides* and *Roseobacter denitrificans*, and a common hydratase mechanism for 3-acetyl group formation. *Eur. J. Biochem.* 239, 85–92. doi: 10.1111/j.1432-1033.1996.0085u.x

Promnares, K., Komenda, J., Bumba, L., Nebesarova, J., Vacha, F., and Tichy, M. (2006). Cyanobacterial small chlorophyll-binding protein ScpD (HliB) is located on the periphery of photosystem II in the vicinity of PsbH and CP47 subunits. *J. Biol. Chem.* 281, 32705–32713. doi: 10.1074/jbc.M606360200

Rebeiz, C. A., Mattheis, J. R., Smith, B. B., Rebeiz, C., and Dayton, D. F. (1975). Chloroplast biogenesis. Biosynthesis and accumulation of Mg-protoprophyrin IX monoester and longer wavelength metalloporphyrins by greening cotyledons. *Arch. Biochem. Biophys.* 166, 446–465. doi: 10.1016/0003-9861(75)90408-7

Rippka, R., Deruelles, J., Waterbury, J., Herdman, M., and Stanier, R. (1979). Generic assignments, strain histories and properties of pure cultures of cyanobacteria. *Microbiology* 111, 1–61. doi: 10.1099/00221287-111-1-1

Sobotka, R., Duerhring, U., Komenda, J., Peter, E., Gardian, Z., Tichy, M., et al. (2008). Importance of the cyanobacterial GUN4 protein for chlorophyll metabolism and assembly of photosynthetic complexes. *J. Biol. Chem.* 283, 25794–25802. doi: 10.1074/jbc.M803787200

Sobotka, R., Tichy, M., Wilde, A., and Hunter, C. N. (2011). Functional assignments for the carboxyl-terminal domains of the ferrochelatase from *Synechocystis* PCC 6803: the CAB domain plays a regulatory role, and region II is essential for catalysis. *Plant Physiol.* 155, 1735–1747. doi: 10.1104/pp.110.167528

Staleva, H., Komenda, J., Shukla, M. K., Šlouf, V., Kaòa, R., Polívka, T., et al. (2015). Mechanism of photoprotection in the cyanobacterial ancestor of plant antenna proteins. *Nat. Chem. Biol.* 11, 287–291. doi: 10.1038/nchembio.1755

Stott, K., Stonehouse, J., Keeler, J., Hwang, T., and Shaka, A. (1995). Excitation sculpting in high-resolution nuclear magnetic resonance spectroscopy: application to selective NOE experiments. *J. Am. Chem. Soc.* 117, 4199–4200. doi: 10.1021/ja00119a048

Swingley, W. D., Chen, M., Cheung, P. C., Conrad, A. L., Dejesa, L. C., Hao, J., et al. (2008). Niche adaptation and genome expansion in the chlorophyll d-producing cyanobacterium *Acaryochloris marina*. *Proc. Natl. Acad. Sci. U.S.A.* 105, 2005–2010. doi: 10.1073/pnas.0709772105

Tottey, S., Block, M. A., Allen, M., Westergren, T., Albrieux, C., Scheller, H. V., et al. (2003). *Arabidopsis* CHL27, located in both envelope and thylakoid membranes, is required for the synthesis of protochlorophyllide. *Proc. Natl. Acad. Sci. U.S.A.* 100, 16119–16124. doi: 10.1073/pnas.2136793100

Trautmann, D., Voss, B., Wilde, A., Al-Babili, S., and Hess, W. R. (2012). Microevolution in cyanobacteria: re-sequencing a motile substrain of *Synechocystis* sp. PCC 6803. *DNA Res.* 19, 435–448. doi: 10.1093/dnares/dss024

Umena, Y., Kawakami, K., Shen, J. R., and Kamiya, N. (2011). Crystal structure of oxygen-evolving photosystem II at a resolution of 1.9 Å. *Nature* 473, 55–60. doi: 10.1038/nature09913

van de Meene, A. M., Hohmann-Marriott, M. F., Vermaas, W. F., and Roberson, R. W. (2006). The three-dimensional structure of the cyanobacterium *Synechocystis* sp. PCC 6803. *Arch. Microbiol.* 184, 259–270.

Vavilin, D., and Vermaas, W. (2007). Continuous chlorophyll degradation accompanied by chlorophyllide and phytol reutilization for chlorophyll synthesis in *Synechocystis* sp PCC 6803. *Biochim. Biophys. Acta* 1767, 920–929. doi: 10.1016/j.bbabio.2007.03.010

Wilde, A., Mikolajczyk, S., Alawady, A., Lokstein, H., and Grimm, B. (2004). The gun4 gene is essential for cyanobacterial porphyrin metabolism. *FEBS Lett.* 571, 119–123. doi: 10.1016/j.febslet.2004.06.063

Zhang, H., Liu, H., Blankenship, R. E., and Gross, M. L. (2015). Isotope-encoded carboxyl group footprinting for mass spectrometry-based protein conformational studies. *J. Am. Soc. Mass Spectrom.* 27, 178–181. doi: 10.1007/s13361-015-1260-5

Zouni, A., Witt, H. T., Kern, J., Fromme, P., Krauss, N., Saenger, W., et al. (2001). Crystal structure of photosystem II from *Synechococcus elongatus* at 3.8 Å resolution. *Nature* 409, 739–743. doi: 10.1038/35055589

Conflict of Interest Statement: The authors declare that the research was conducted in the absence of any commercial or financial relationships that could be construed as a potential conflict of interest.

frontiers in Plant Science

ORIGINAL RESEARCH
published: 20 July 2016
doi: 10.3389/fpls.2016.01060

Mutation of Gly195 of the ChlH Subunit of Mg-chelatase Reduces Chlorophyll and Further Disrupts PS II Assembly in a Ycf48-Deficient Strain of *Synechocystis* sp. PCC 6803

*Tim S. Crawford[1,2], Julian J. Eaton-Rye[1] and Tina C. Summerfield[2]**

[1] Department of Biochemistry, University of Otago, Dunedin, New Zealand, [2] Department of Botany, University of Otago, Dunedin, New Zealand

Biogenesis of the photosystems in oxygenic phototrophs requires co-translational insertion of chlorophyll *a*. The first committed step of chlorophyll *a* biosynthesis is the insertion of a Mg^{2+} ion into the tetrapyrrole intermediate protoporphyrin IX, catalyzed by Mg-chelatase. We have identified a *Synechocystis* sp. PCC 6803 strain with a spontaneous mutation in *chlH* that results in a Gly195 to Glu substitution in a conserved region of the catalytic subunit of Mg-chelatase. Mutant strains containing the ChlH Gly195 to Glu mutation were generated using a two-step protocol that introduced the *chlH* gene into a putative neutral site in the chromosome prior to deletion of the native gene. The Gly195 to Glu mutation resulted in strains with decreased chlorophyll *a*. Deletion of the PS II assembly factor Ycf48 in a strain carrying the ChlH Gly195 to Glu mutation did not grow photoautotrophically. In addition, the ChlH-G195E:ΔYcf48 strain showed impaired PS II activity and decreased assembly of PS II centers in comparison to a ΔYcf48 strain. We suggest decreased chlorophyll in the ChlH-G195E mutant provides a background to screen for the role of assembly factors that are not essential under optimal growth conditions.

Keywords: ChlH, Ycf48, chlorophyll biosynthesis, PS II, *Synechocystis*

OPEN ACCESS

Edited by:
Qingfang He,
University of Arkansas at Little Rock, USA

Reviewed by:
Robert L. Burnap,
Oklahoma State University–Stillwater, USA
Gaozhong Shen,
Pennsylvania State University, USA

****Correspondence:***
Tina C. Summerfield
tina.summerfield@otago.ac.nz

Specialty section:
This article was submitted to Plant Cell Biology, a section of the journal Frontiers in Plant Science

Received: *29 April 2016*
Accepted: *06 July 2016*
Published: *20 July 2016*

Citation:
Crawford TS, Eaton-Rye JJ and Summerfield TC (2016) Mutation of Gly195 of the ChlH Subunit of Mg-chelatase Reduces Chlorophyll and Further Disrupts PS II Assembly in a Ycf48-Deficient Strain of Synechocystis sp. PCC 6803. Front. Plant Sci. 7:1060. doi: 10.3389/fpls.2016.01060

INTRODUCTION

In oxygenic photosynthesis Photosystem II (PS II) and Photosystem I (PS I) catalyze the conversion of light energy into the chemical energy that is required for carbon fixation. The reaction center (RC) and core antenna proteins of both PS II and PS I require the co-translational insertion of chlorophyll *a* for correct folding (Eichacker et al., 1996; Sobotka, 2014; Yang et al., 2015). In addition, the co-ordinated production of chlorophyll and chlorophyll-binding proteins is essential to prevent the accumulation of potentially detrimental unbound chlorophyll and chlorophyll precursors. Although a large proportion of newly synthesized chlorophyll *a* is associated with PS I, the assembly of PS II and chlorophyll biosynthesis are synchronized (He and Vermaas, 1998). There are 70 chlorophyll *a* molecules in the PS II pigment-protein complex along with at least 20 protein subunits and additional cofactors (Umena et al., 2011; Shen, 2015). Assembly of PS II involves the formation of four pre-complexes, each containing one of the four chlorophyll *a*-binding proteins

that are found in the mature complex: D1 and D2 that form the RC, and CP43 and CP47 that function as a core antenna (Boehm et al., 2011). The pre-complexes are assembled, beginning with the association of the D1- and D2-containing modules, to form larger assembly intermediates and finally the mature photosystem (Komenda et al., 2012). In addition, the D1 subunit is the site of light-induced photo-oxidative damage and a repair cycle enables the removal and replacement of damaged D1 to maintain PS II activity (Komenda et al., 2012). Part of this repair cycle involves the removal of chlorophyll *a* from damaged D1, as well as insertion of chlorophyll *a* into new D1 subunits (Yao et al., 2012).

The chlorophyll *a* biosynthesis pathway is comprised of at least 15 enzymatic steps, many of which are shared with the biosynthetic pathway for heme (Sobotka, 2014; Fujita et al., 2015). The first dedicated step in the synthesis of chlorophyll *a* is the insertion of Mg^{2+} into protoporphyrin IX (PP IX) to form Mg-PP IX; this reaction is catalyzed by Mg-chelatase (Jensen et al., 1996). This represents a branch point that contributes to the regulation of tetrapyrrole biosynthesis by controlling the partitioning of precursor molecules such as PP IX into different biosynthetic pathways (Shepherd et al., 2005). Mg-chelatase is a large protein complex consisting of three different subunits CHLI, CHLD, and CHLH. Both CHLI and CHLD form hexamers that associate with a single catalytic CHLH subunit (Wang and Grimm, 2015). The corresponding ChlH protein in cyanobacteria is comprised of an N-terminal 'head' domain and a larger domain that forms a hollow, cage-like structure that binds porphyrin and a similar domain organization is expected in plant CHLH (Qian et al., 2012; Chen et al., 2015). Regulation of the Mg-chelatase enzyme occurs through association of the CHLH subunit with the GUN4 protein, in an interaction that stimulates enzyme activity (Larkin et al., 2003; Sobotka et al., 2008). In addition, in plants, CHLH is involved in plastid-nuclear signaling and in cyanobacteria ChlH has a regulatory role as an anti-sigma factor, binding to the RNA polymerase sigma factor SigE in the light (Mochizuki et al., 2001; Osanai et al., 2009). Two mutant lines of *Arabidopsis thaliana* with mutations in *CHLH* have been described: the Pro to Leu mutation in *cch* plants corresponds to the Pro595 residue in ChlH from the cyanobacterium *Synechocystis* sp. PCC 6803 (hereafter *Synechocystis* 6803) and the Ala to Val substitution in the *gun5* mutant corresponds to the Ala942 residue. Both Pro595 and Ala942 are located in the central cage-like structure of the protein and may interfere with the chelation reaction due to spatial hindrance (Chen et al., 2015). In *A. thaliana* these mutations caused reductions in chlorophyll levels of ∼70 and ∼30% in the *cch* and *gun5* mutants, respectively (Mochizuki et al., 2001).

Re-sequencing of *Synechocystis* 6803 has shown genetic differences have arisen between wild-type sub-strains under laboratory conditions (Jones, 2014). This occurrence of spontaneous mutations has produced several mutations in a sub-strain, GT-O2, including in the *chlH* gene (Morris et al., 2014). The mutation in *chlH* results in a Gly195 to Glu amino acid substitution in a conserved region of the ChlH protein. The GT-O2 strain was able to grow photoautotrophically, although at a slightly slower rate and reaching a lower $OD_{730\ nm}$ compared to its parental strain, GT-O1 (Morris et al., 2014). In this report, we show the construction and characterization of *Synechocystis* 6803 strains carrying this ChlH Gly195 to Glu mutation. In addition, we investigated the impact of impairing biogenesis of PS II in the ChlH mutant by deleting the assembly factor Ycf48. We selected the Ycf48 protein [HCF136 in *A. thaliana* and the first assembly factor discovered (Meurer et al., 1998)] because it is transiently associated with the D1 pre-complex during assembly and repair of PS II. This factor binds to the D1 precursor polypeptide (pD1) and stabilizes formation of the RC II complex containing the D1 and D2 pre-complex modules (Komenda et al., 2008; Mabbitt et al., 2014). We hypothesized that deletion of Ycf48 in a strain where chlorophyll *a* supply is reduced may impact on both PS II biogenesis and the PS II repair cycle.

MATERIALS AND METHODS

Synechocystis 6803 Growth Conditions and Construction of Mutant Strains

Strains of *Synechocystis* 6803 were maintained on BG-11 medium agar plates supplemented with 5 mM glucose, 20 μM atrazine, 10 mM TES-NaOH (pH 8.2), 0.3% sodium thiosulfate and appropriate antibiotics. Liquid cultures were grown photoautotrophically or photomixotrophically (with 5 mM glucose) in BG-11 liquid medium with appropriate antibiotics, as previously described (Eaton-Rye, 2011; Summerfield et al., 2013).

Generation of *chlH* mutants was performed in two steps. Amplicons were generated using overlap-extension PCR (Bryskin and Matsumura, 2010), in which most of the *slr0168* gene was deleted and replaced by a spectinomycin-resistance cassette (Supplementary Figures S1A,B). The *slr0168* gene site has been used as a neutral site for integration of genes into the chromosome previously with no reported effect on phenotype (Kunert et al., 2000). A HindIII restriction site was introduced into the 5′ end of the spectinomycin-resistance cassette using PCR. This amplicon was ligated into pGEM-T Easy and the resulting Δ*slr0168*:specR plasmid was transformed into wild-type *Synechocystis* 6803 (GT-O1) to create the Δ*slr0168* neutral site control strain (Supplementary Figure S1B). The *slr1055* (*chlH*) gene was amplified from the GT-O1 and GT-O2 wild types (Morris et al., 2014), using primers designed to introduce HindIII restriction sites at the 5′ and 3′ ends of the amplicons (Supplementary Table S1). These amplicons and the Δ*slr0168*:specR plasmid, were digested with HindIII and ligated to produce the ChlH-G195G:specR and ChlH-G195E:specR plasmids, respectively. The resultant plasmids were transformed into *Synechocystis* 6803 strains (GT-O1 or GT-O2) to introduce either the unmodified *chlH* (in the GT-O1:G195G and GT-O2:E195G strains) or the mutant *chlH* gene (in the GT-O1:G195E and GT-O2:E195E strains) into the putative neutral site (Supplementary Figure S1). In the second step, a Δ*chlH* plasmid was constructed using overlap-extension

PCR in which a chloramphenicol-resistance cassette was located between the sequences up- and downstream of the native *chlH* gene (Supplementary Figures S1C,D). This plasmid was transformed into the strains which contained a copy of the *chlH* gene in the neutral site to produce strains which each contained only one copy of *chlH,* either the GT-O1 (Gly195) or GT-O2 (Gly195 to Glu) variant. A summary of the mutants created in this study is presented in **Table 1**.

Construction of the Δ*ycf48* (Δ*slr2034*) plasmid has been described previously (Jackson et al., 2014); this plasmid was transformed into the GT-O1:G195G and GT-O1:G195E strains to produce the GT-O1:G195G:ΔYcf48 and GT-O1:G195E:ΔYcf48 strains, respectively. Colony PCR and sequencing were used to confirm the mutant genotypes as appropriate (data not shown).

Physiological Measurements

Photoautotrophic growth, whole-cell absorption spectra, oxygen evolution, and chlorophyll *a* fluorescence analyses were performed as previously described (Crawford et al., 2016). Cells grown photomixotrophically to mid-exponential phase were washed and re-suspended to an optical density at 730 nm ($OD_{730\ nm}$) of 1.5 in BG-11 supplemented with 25 mM HEPES-NaOH (pH 7.5) for physiological measurements. Chlorophyll *a* was quantified by extraction in methanol and measurement at 663 nm (MacKinney, 1941). Low-temperature (77 K) fluorescence emission spectroscopy was performed using sodium fluorescein as an internal standard as previously described (Crawford et al., 2016). Traces were normalized to the fluorescein emission maxima at 505 nm.

Protein Analyses

For analysis of PS II assembly, thylakoid membranes were isolated from photomixotrophically grown cultures, solubilized with β-dodecylmaltoside and separated by blue-native polyacrylamide gel electrophoresis (BN-PAGE) as previously described (Crawford et al., 2016). Proteins were transferred to polyvinylidene fluoride (PVDF) membranes for 1 h at 25 V in the presence of 0.1% SDS, and were subjected to immunodetection using antibodies to PS II and PS I core protein subunits (Jackson and Eaton-Rye, 2015).

RESULTS

A Strain with an Altered Whole-Cell Spectrum Had Accumulated Several Mutations Including a *chlH* Mutation Changing Residue Gly195 to Glu

Comparison of two strains in our laboratories, GT-O1 and GT-O2, showed differences in whole-cell absorption spectra. Both strains exhibited absorption maxima at 625 nm, as well as at 435 and 685 nm, corresponding to phycobilins and chlorophyll *a*, respectively (**Figure 1A**). The GT-O2 strain exhibited a reduction in the peaks at 435 nm and 685 nm corresponding to chlorophyll *a* absorbance but not the 625 nm phycobilin peak (**Figure 1A**). Six unique genome sequence variants are present in the GT-O2 strain compared to GT-O1 cells (Morris et al., 2014). These are predicted to result in amino acid changes in five proteins: the long-chain fatty acid CoA ligase, FadD (Slr1609, Arg641 to Gln); the serine metalloprotease, HtrA/DegP (Slr1204, frameshift after amino acid 66 of 452); hypothetical protein Slr0154 (Ser307 to Phe); the histidine kinase, Hik8 (Sll0750, Arg65 to Cys), and the Mg-chelatase catalytic subunit, ChlH (Slr1055, Gly195 to Glu). The Mg-chelatase enzyme catalyzes the first committed step in chlorophyll *a* biosynthesis, therefore the ChlH Gly195 to Glu mutation was a candidate for the decreased absorbance of chlorophyll *a* in the GT-O2 wild type.

The ChlH Gly195 residue is located in the α6 helix of the N-terminal 'head' domain I (**Figure 1B**; Supplementary Figure S2). This Gly195 residue was conserved in ChlH proteins representing all five sections of cyanobacteria, and is part of a conserved protein region (**Figure 1C**). Although chiefly monomeric in solution, the crystal structure of ChlH obtained by Chen et al. (2015) indicated that this protein can form a dimer, and that interactions occur exclusively between the N-terminal domain I and the domain V of opposing monomers (Supplementary Figure S2). Dimerization of ChlH subunits is mediated by polar interactions, including six hydrogen bonds and a salt bridge between the Glu199 and Lys1018 residues of opposing monomers. The Gly195 residue is in close proximity to Glu199 (Supplementary Figure S2); the Glu199 residue is conserved in many cyanobacteria, but is substituted for an Asp in the cyanobacterium *Gloeobacter violaceus* PCC 7421. The Lys1018 residue was found in the aligned cyanobacterial ChlH protein sequences except that of *G. violaceus* PCC 7421 (**Figure 1D**).

TABLE 1 | Strains of *Synechocystis* sp. PCC 6803 used in this study.

Strain	Background	Insertion at neutralsite (*slr0168*)	Gene at native *chlH* site (*slr1055*)	Reference
GT-O1	–	–	*chlH* (G195)	Morris et al., 2014
GT-O2	–	–	*chlH* (E195)	Morris et al., 2014
Δ*slr0168*	GT-O1	$spec^R$	*chlH* (G195)	This study
GT-O1:G195G	GT-O1	*chlH* (G195) + $spec^R$	cam^R (Δ*chlH*)	This study
GT-O1:G195E	GT-O1	*chlH* (E195) + $spec^R$	cam^R (Δ*chlH*)	This study
GT-O2:E195G	GT-O2	*chlH* (G195) + $spec^R$	cam^R (Δ*chlH*)	This study
GT-O2:E195E	GT-O2	*chlH* (E195) + $spec^R$	cam^R (Δ*chlH*)	This study

$spec^R$ and cam^R refer to spectinomycin-resistance and chloramphenicol-resistance cassettes, respectively.

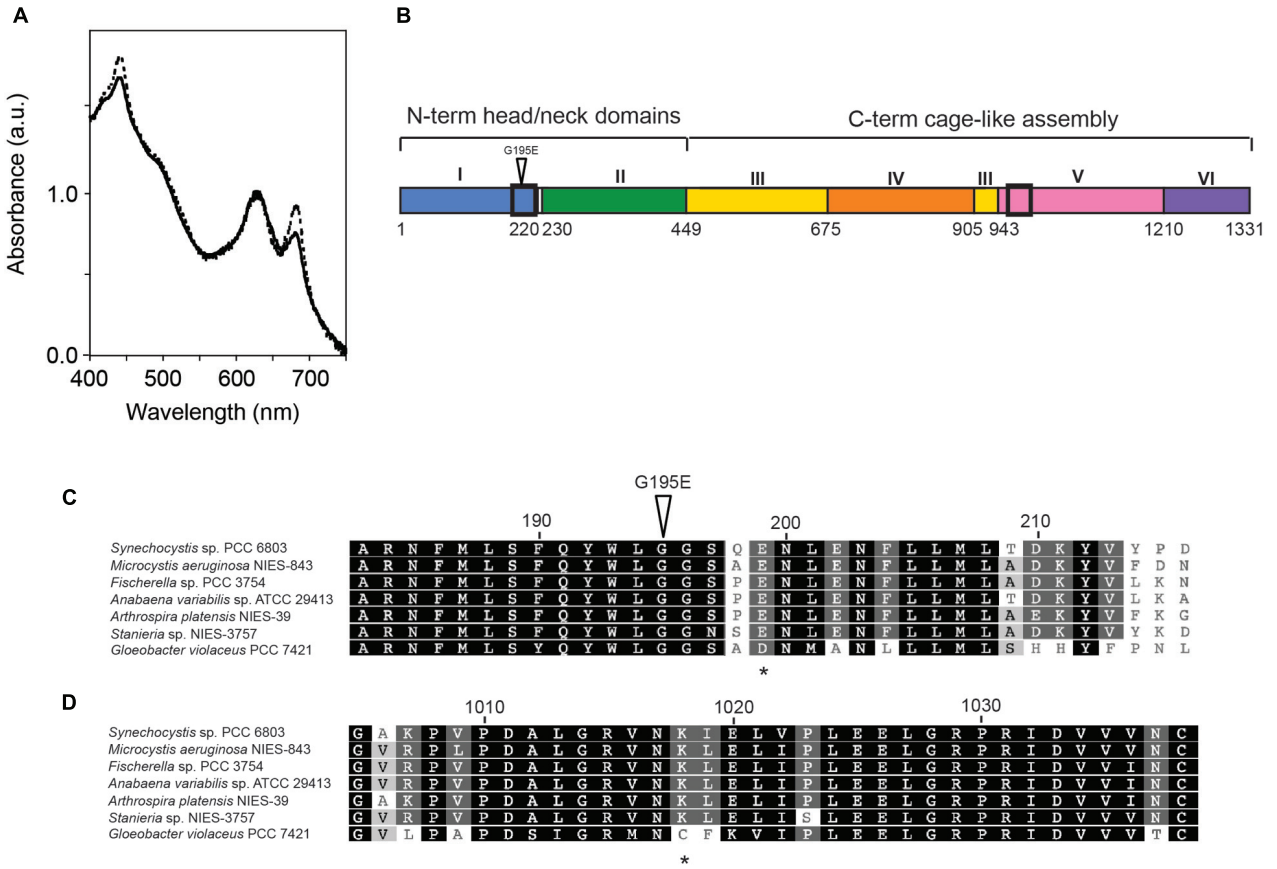

FIGURE 1 | The *Synechocystis* sp. PCC 6803 GT-O2 strain has an altered whole-cell absorption spectrum and contains a *chlH* mutation resulting in a Gly195 to Glu amino acid substitution. (A) Whole-cell absorption spectra of the GT-O1 (dotted line) and GT-O2 cells (solid line) grown photoautotrophically to mid-exponential phase in 40 $\mu E.m^{-2}.s^{-1}$ constant white light. Spectra representative of three independent biological replicates are shown normalized to the phycobilin absorption maxima at 625 nm. **(B)** Schematic representation showing the domains of the ChlH subunit of the Mg-chelatase enzyme from *Synechocystis* sp. PCC 6803. Black boxes indicate the positions of the sections expanded in **(C,D)**, and the position of the Gly195-Glu mutation is indicated by an inverted triangle (Chen et al., 2015). **(C,D)** Amino acid sequence alignment of sections of domain I **(C)** or domain V **(D)** of cyanobacterial ChlH proteins. Amino acids are numbered according to the ChlH protein of *Synechocystis* sp. PCC 6803. The position of the Gly195 to Glu mutation present in the GT-O2 strain is indicated by an inverted triangle, and the positions of the Glu199 and Lys1018 residues, which form the inter-monomer salt bridge contact, are indicated by asterisks.

Generation of Mutations in *chlH* with a Two-Step Process Involving Insertion into the Putative Neutral Site at *slr0168*

To determine the effect of the ChlH Gly195 to Glu mutation *in vivo,* a copy of either the unmodified gene (encoding Gly195) or mutant *chlH* gene (encoding the Gly195 to Glu mutation) was introduced at a putative neutral site (*slr0168*) in the *Synechocystis* 6803 genome (Kunert et al., 2000). A spectinomycin-resistance cassette inserted downstream of the *chlH* gene enabled selection (**Figure 2A**). Once the introduced *chlH* gene had been fully segregated, the native gene was deleted and a chloramphenicol-resistance cassette was inserted in place of this copy of *chlH* (**Figure 2B**). This method was used to generate strains containing only the GT-O1 copy of *chlH,* encoding Gly195, in both the GT-O1 and GT-O2 backgrounds. Similarly, strains were generated containing only the GT-O2 copy of *chlH*, encoding the Gly195 to Glu substitution, in both the GT-O1 or GT-O2 backgrounds. Mutants in the GT-O2 background enabled us to determine the impact of restoring the Gly195 to this background, as well as, including an additional control strain where the Glu195 was introduced into ChlH in the neutral site. The sequences of the oligonucleotides used for the construction and verification of these strains are in Table S1. In addition, a Δ*slr0168* control strain was produced which contained only the spectinomycin-resistance cassette in the neutral site and which retained the native *chlH* gene at its wild-type locus.

A Mutation That Changes ChlH Residue 195 from Gly to Glu Altered the Whole-Cell Spectrum

The whole-cell spectra of the GT-O1 wild type and Δ*slr0168* control strain were similar (data not shown). Introduction of unmodified *chlH,* under its own promoter, to produce the GT-O1:G195G strain using the *slr0168* site resulted in a whole-cell

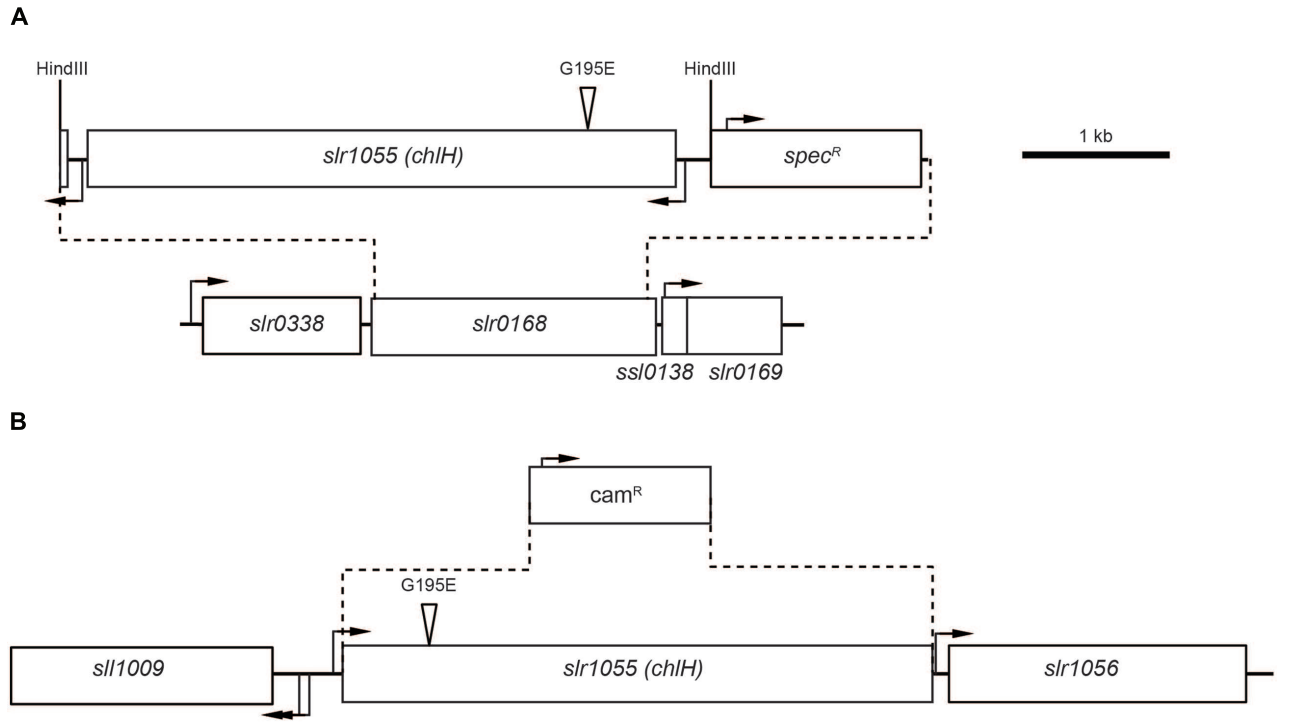

FIGURE 2 | Construction of the *chlH* mutant strains of *Synechocystis* sp. PCC 6803. (A) Genomic structure of the *chlH* insertion into the *slr0168* neutral site region of the chromosome. Dotted lines indicate the replacement of *slr0168* with a sequence containing either the unmodified *chlH* gene or the copy encoding the Gly195 to Glu substitution (amplified from the GT-O1 or GT-O2 strains, respectively) and a spectinomycin-resistance cassette. The boxes represent predicted ORFs and transcriptional start sites, based on data published in Kopf et al. (2014), are indicated by black arrows. The position of the Gly195 to Glu substitution is indicated by a triangle, and the introduced HindIII site in the spectinomycin-resistance cassette into which the amplified *chlH* genes were ligated is indicated. **(B)** Genomic structure of the *slr1055* (*chlH*) region in the *chlH* mutant strains. Dotted lines indicate the deletion of the *chlH* ORF and its replacement with a chloramphenicol-resistance cassette. For a more detailed explanation of this process see Supplementary Information and Supplementary Figure S1.

spectrum similar to that observed with GT-O1 cells, whereas introduction of the ChlH Gly195 to Glu mutation to produce the GT-O1:G195E strain resulted in decreased chlorophyll *a* absorption at both the 435 and 685 nm maxima compared to the GT-O1 strain (**Figure 3A**). Conversely, the introduction of unmodified *chlH* into the GT-O2 background resulted in the GT-O2:E195G strain which had increased chlorophyll *a* maxima that were similar to the GT-O1 wild type (cf. **Figures 1A** and **3B**). In addition, the GT-O2:E195G strain showed an increased absorption in the 475–520 nm range compared to the GT-O2:E195E strain suggesting elevated carotenoid levels. Furthermore, the spectrum of the GT-O2:E195E strain was similar to spectra from the GT-O2 and GT-O1:G195E strains, suggesting that the presence of the Gly195 to Glu variant in ChlH results in a decrease in chlorophyll *a* absorbance (**Figures 1A** and **3A,B**). The quantification of methanol-extracted chlorophyll *a* showed that the Gly195 to Glu mutation in ChlH resulted in a ∼35–40% reduction of chlorophyll *a* accumulation in the GT-O2 and the GT-O1:G195E and GT-O2:E195E strains, in comparison to the GT-O1 and the GT-O1:G195G and GT-O2:E195G strains in samples normalized to an $OD_{730\ nm}$ of 1.0 (**Figure 3C**). The Gly195 to Glu mutation had little effect on the rate of photoautotrophic growth of the GT-O1:G195E strain, although these cells reached a slightly lower final $OD_{730\ nm}$ in stationary phase (**Figure 4A**); this is consistent with that observed in the GT-O2 wild type (Morris et al., 2014). The photoautotrophic growth of the Δ*slr0168* control strain was indistinguishable from the GT-O1 wild type and the GT-O1:G195G strain (data not shown). Using flow cytometry and electron microscopy we did not detect any difference in size between strains containing Gly195 or Glu195 (data not shown), therefore the $OD_{730\ nm}$ should represent a similar cell number in all strains compared.

Introduction of the ChlH Gly195 to Glu Mutation Abolished Photoautotrophic Growth in a ΔYcf48 Strain

Formation of mature PS II is a multistep process involving the co-ordinated assembly of several intermediate complexes that require the insertion of chlorophyll *a*. The Ycf48 assembly factor is associated with the RC pre-complex; however, the absence of this factor does not completely block PS II assembly (Komenda et al., 2008; Jackson et al., 2014; Sobotka, 2014). We determined whether deletion of Ycf48 in a strain with reduced chlorophyll *a* would impact on PS II biogenesis and the PS II repair cycle. Deletion of Ycf48 resulted in reduced photoautotrophic growth, with a decrease in the final $OD_{730\ nm}$ reached in stationary phase from 1.43 ± 0.02 in the GT-O1:G195G background to

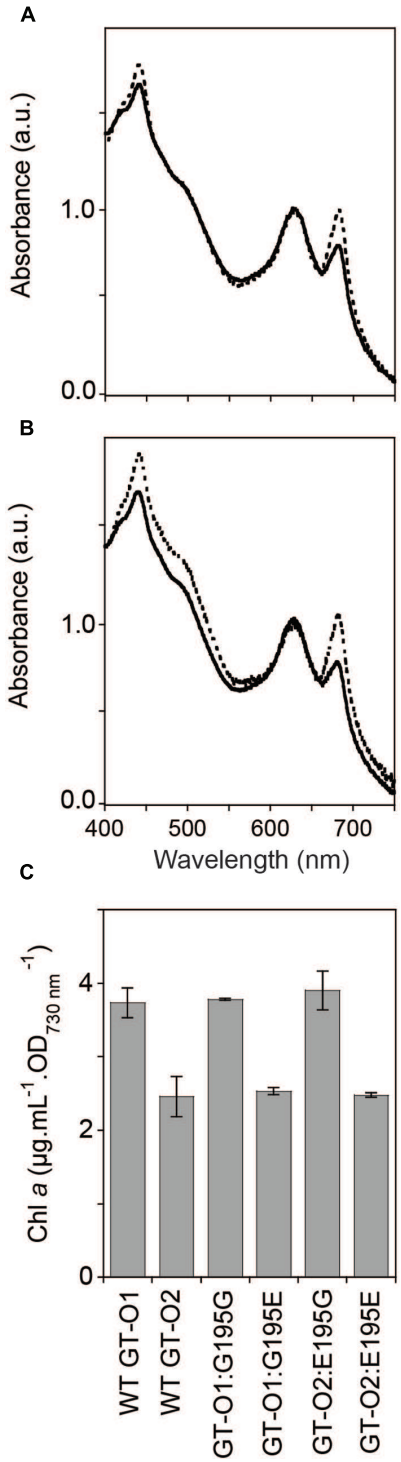

FIGURE 3 | Pigment composition of the *chlH* mutant strains of *Synechocystis* sp. PCC 6803. Cells were grown photoautotrophically to mid-exponential phase in BG-11 (25 mM HEPES-NaOH, pH 7.5). **(A)** Whole-cell absorption spectra of the GT-O1:G195G (dotted line) and GT-O1:G195E strains (solid line). **(B)** Whole-cell absorption spectra of the GT-O2:E195G (dotted line) and GT-O2:E195E strains (solid line). Spectra representative of three independent biological replicates are shown

(Continued)

FIGURE 3 | Continued

normalized to the phycobilin absorption maxima at 625 nm. **(C)** Levels of chlorophyll *a* in photoautotrophically grown cells, determined by measuring the absorbance of methanol-extracted chlorophyll at 663 nm. The data shown are the mean [Chl *a*] per optical density of 1.0 at 730 nm ± the standard error of the mean (SEM) from three independent biological replicates.

0.40 ± 0.04 for the GT-O1:G195G:ΔYcf48 strain (**Figure 4A**); this is consistent with other ΔYcf48 strains characterized (Komenda et al., 2008; Jackson et al., 2014; Jackson and Eaton-Rye, 2015). However, deletion of Ycf48 from the GT-O1:G195E mutant resulted in a strain that reached an $OD_{730\ nm}$ of only 0.1 ± 0.02 under photoautotrophic growth conditions, indicating increased sensitivity of cells to the absence of this PS II assembly factor when the ChlH Gly195 to Glu mutation is present.

Whole-cell absorption spectra of photomixotrophically grown cells showed a slight decrease in the 685 nm absorption of chlorophyll *a* in the GT-O1:G195E strain relative to the GT-O1:G195G strain, when normalized to the absorbance at 435 nm (**Figure 4B**). The GT-O1:G195G:ΔYcf48 mutant had a whole-cell absorption spectrum with decreased absorption maxima at 625 and 685 nm compared to the GTO1:G195G strain. The GT-O1:G195E:ΔYcf48 strain's whole-cell spectrum was the most altered, exhibiting a decreased 685 nm maxima and an increased carotenoid shoulder compared to the GT-O1:G195G:ΔYcf48 strain (**Figure 4B**). Levels of chlorophyll *a* measured for each strain at the same $OD_{730\ nm}$ showed a 16% decrease in the GT-O1:G195E strain relative to the GT-O1:G195G strain (**Figure 4C**). Deletion of Ycf48 resulted in a small decrease in chlorophyll *a* levels in the GT-O1:G195G:ΔYcf48 strain, whereas in a GT-O1:G195E:ΔYcf48 strain there was a ∼26% decrease in chlorophyll *a* compared to the GT-O1:G195G strain.

Oxygen Evolution and Variable Chlorophyll *a* Fluorescence Induction Were Reduced in the GT-O1:G195E:ΔYcf48 Mutant

Oxygen evolution was measured in mixotrophically grown cultures. The rates of oxygen evolution were similar in the GT-O1:G195E and GT-O1:G195G strains, when measured in the presence of 15 mM bicarbonate (measuring whole-chain electron transport) or 200 μM of the artificial quinone 2,5-dimethyl-1,4-benzoquinone (DMBQ) (measuring PS II-specific electron transport) (**Figure 4D**). In the GT-O1:G195G:ΔYcf48 strain, oxygen evolution was decreased, to 89 ± 12 and 71 ± 5% of the GT-O1:G195G strain in the presence of bicarbonate and DMBQ, respectively. Removal of Ycf48 in a ChlH-G195E background resulted in rates of oxygen evolution that were reduced, to 38 ± 1 and 17 ± 3% of the rates for the GT-O1:G195G strain in the presence of bicarbonate and DMBQ, respectively.

The activity of the acceptor side of PS II was analyzed by measuring variable chlorophyll *a* fluorescence induction. Fluorescence induction transients of the GT-O1:G195G and GT-O1:G195E strains differed by only a slightly decreased P level in the latter (**Figure 4E**). It was previously reported that

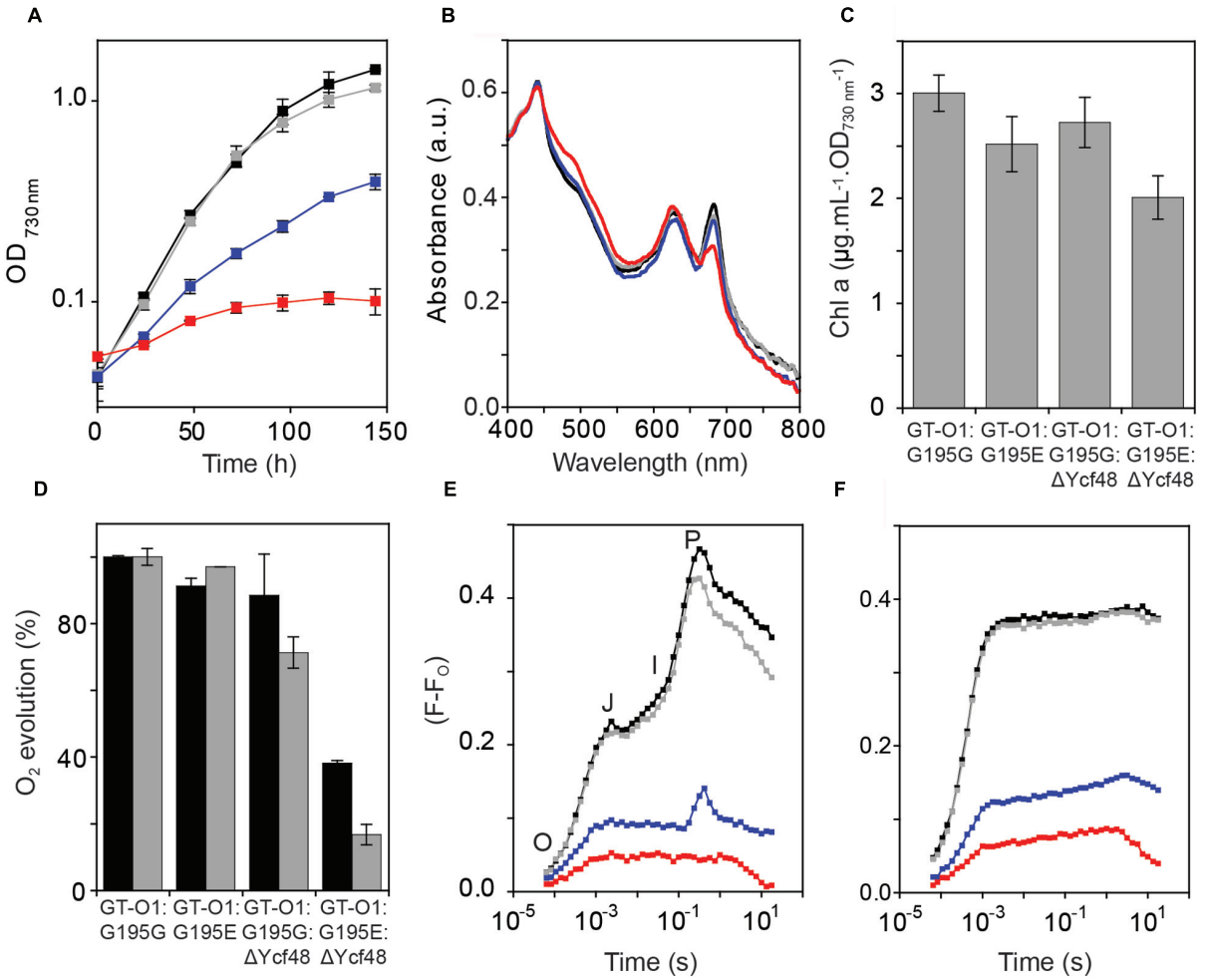

FIGURE 4 | Phenotype of the ChlH-ΔYcf48 mutant strains of *Synechocystis* sp. PCC 6803. The strains were: GT-O1:G195G: black; GT-O1:G195E: gray; GT-O1:G195G:ΔYcf48: blue; GT-O1:G195E:ΔYcf48: red. **(A)** Photoautotrophic growth of the ChlH mutants in unbuffered BG-11 liquid media. Cultures were incubated in constant white light at an intensity of 40 $\mu E.m^{-2}.s^{-1}$ at 30°C, and their optical density at 730 nm was measured every 24 h. The data are the mean $OD_{730\ nm}$ ± the SEM. **(B)** Whole-cell absorption spectra of photomixotrophically grown strains. Representative spectra are shown, normalized to the absorption maxima at 435 nm. **(C)** Levels of chlorophyll *a* in photomixotrophically-grown cells, determined by measuring the absorbance of methanol-extracted chlorophyll at 663 nm. The data shown are the mean [Chl *a*] per optical density of 1.0 at 730 nm ± the SEM. **(D)** Oxygen evolution of strains was measured in the presence of either 15 mM $NaHCO_3$ (black) or 200 µM DMBQ and 1 mM $K_3Fe(CN)_6$ (gray) as electron acceptors. Data shown are the mean rate of oxygen evolution over the 1st minute of actinic illumination ± the SEM. Rates are shown as a percentage of that measured in the GT-O1:G195G strain (278 and 293 µmol O_2.mg $Chl^{-1}.h^{-1}$ in the presence of bicarbonate and DMBQ, respectively). **(E,F)** Room temperature chlorophyll *a* fluorescence induction of strains, measured with a 455 nm measuring pulse in the absence **(E)** or presence **(F)** of 40 µM DCMU. The O (origin), J, I (inflections), and P (peak) features of the fluorescence transient are indicated. Representative traces are shown normalized to the same initial fluorescence level (F_O).

removal of Ycf48 resulted in a considerable decrease in the variable fluorescence level and this was observed in the GT-O1:G195G:ΔYcf48 strain (Jackson et al., 2014). The variable fluorescence induction of the GT-O1:G195E:ΔYcf48 strain was further reduced compared to the GT-O1:G195G:ΔYcf48 strain and did not display an I-P rise (**Figure 4E**). In the presence of 40 µM 3-(3,4-dichlorophenyl)-1,1-dimethylurea (DCMU), which blocks electron transfer beyond Q_A of PS II, variable fluorescence was similar in the GT-O1:G195G and GT-O1:G195E strains, reduced in the GT-O1:G195G:Ycf48 strain and further decreased in the GT-O1:G195E:ΔYcf48 strain (**Figure 4F**). Variable fluorescence in the presence of DCMU provides an indication of the numbers of assembled PS II centers and these data are consistent with decreased centers in both strains lacking Ycf48, with the lowest number of centers in the GT-O1:G195E:ΔYcf48 strain.

The 77 K Fluorescence Emission Spectra Were Altered in the GT-O1:G195E:ΔYcf48 Mutant

Reduced PS II-specific oxygen evolution and variable fluorescence in the GT-O1:G195G:ΔYcf48 and the GT-O1:G195E:ΔYcf48 strains are consistent with decreased numbers

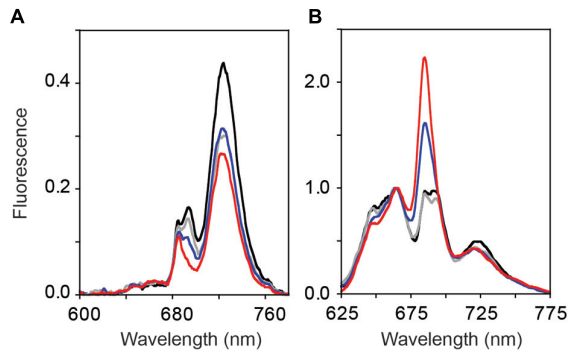

FIGURE 5 | Low-temperature (77 K) fluorescence emission spectra of the ChlH mutant strains of *Synechocystis* sp. PCC 6803. Photomixotrophically grown cells of the GT-O1:G195G (black), GT-O1:G195E (gray), GT-O1:G195G:ΔYcf48 (blue) and GT-O1:G195E:ΔYcf48 strains (red) were excited with either a 440 nm **(A)** or 580 nm excitation light **(B)**. Representative spectra are shown normalized to either the 505 nm emission maximum of a 250 nM sodium fluorescein internal standard **(A)** or the 665 nm phycocyanin emission **(B)**.

of assembled PS II centers in these strains. Low-temperature (77 K) fluorescence emission spectroscopy was performed on photomixotrophically grown cultures using 250 nM sodium fluorescein as an internal standard. Introduction of the ChlH Gly195 to Glu mutation had little effect on the 685 and 695 nm fluorescence emission in the GT-O1:G195E strain with a 440 nm excitation light (**Figure 5A**). The 685 nm emission peak is attributed to unassembled pre-complexes and the CP43 core antenna protein, while the emission at 695 nm arises from the CP47 core antenna and is indicative of fully assembled PS II RCs (Boehm et al., 2011; D'Haene et al., 2015). The fluorescence emission maximum observed at 725 nm originates from PS I, and this was decreased by ∼35% in the GT-O1:G195E strain compared with the GT-O1:G195G strain when spectra were normalized to the emission maximum of fluorescein at 505 nm (**Figure 5A**). A similar decrease in the emission at 725 nm was observed in the GT-O1:G195G:ΔYcf48 strain and this strain also displayed a decreased emission at 685 nm with a further decrease at 695 nm. This is consistent with impaired assembly and/or repair of PS II in the absence of Ycf48; however, the decrease in fluorescence emission from PS I suggests an additional effect on PS I assembly due to the removal of this assembly factor. Deletion of Ycf48 in a ChlH-G195E background resulted in a complete absence of the 695 nm emission in the GT-O1:G195E:ΔYcf48 strain, suggesting a decreased number of PS II centers; this strain also showed a decreased PS I emission maxima at 725 nm, compared to the GT-O1:G195G:ΔYcf48 strain.

Steady-state phycobilisome-coupled energy transfer was assessed by low-temperature emission spectra following excitation at 580 nm. When normalized to the fluorescence emission maximum at 665 nm, little difference was observed between the emission spectra of the GT-O1:G195G and GT-O1:G195E strains, except for a slight decrease in the 725 nm emission originating from PS I in the latter, consistent with the decrease in PS I emissions observed in 440 nm-excited cells (**Figure 5B**). In the GT-O1:G195G:ΔYcf48 strain, an increase in the fluorescence emission at 685 nm was observed; this emission originates from the ApcE terminal emitter of the phycobilisome antenna and indicates an increased level of uncoupled phycobilisomes in this strain (Shen et al., 1993; Jackson et al., 2014). This emission was further increased in the GT-O1:G195E:ΔYcf48 strain, and both this and the GT-O1:G195G:ΔYcf48 strains displayed the decreased PS I emission seen in the GT-O1:G195E strain.

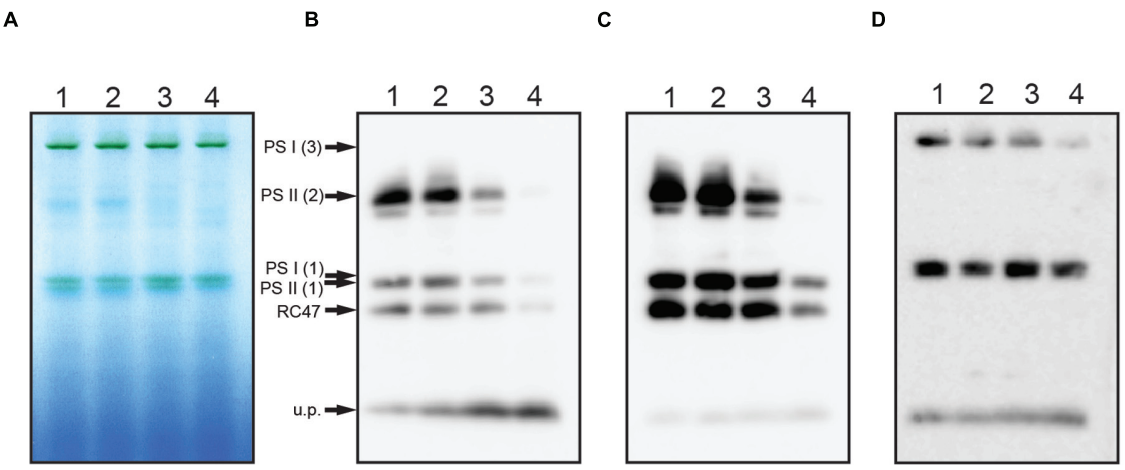

FIGURE 6 | Assembly of PS II and PS I complexes in the ChlH mutant strains of *Synechocystis* sp. PCC 6803. Thylakoid membranes, isolated from photomixotrophically grown cultures, were solubilized with 1.0% β-D-dodecylmaltoside and 25 μg protein equivalent separated on 3–12% NativePAGE gel **(A)**. Proteins were transferred to PVDF membranes and subjected to immunodetection using antibodies to the D1 **(B)** or D2 subunits of PS II **(C)**, or the PsaA subunit of PS I **(D)**. Lanes: 1: GT-O1:G195G; 2: GT-O1:G195E; 3: GT-O1:G195G:ΔYcf48; 4: GT-O1:G195E:ΔYcf48. Putative photosystem multimers and assembly intermediates are indicated by arrows: PS I (3): trimeric PS I; PS II (2): dimeric PS II; PS I (1) and PS II (1): monomeric PS I and PS II, respectively; RC47: CP43-less PS II repair/assembly intermediate; u.p., Unassembled protein.

BN-PAGE Confirmed PS II and PS I Assembly was Altered in the GT-O1:G195E:ΔYcf48 Mutant

To further analyze the PS II complexes in the ChlH mutant strains, thylakoid membranes were analyzed using BN-PAGE and western blotting. In the GT-O1:G195G and GT-O1:G195E strains, the D1 and D2 core subunits were detected at similar levels in dimeric and monomeric PS II complexes, and in a CP43-less assembly/repair intermediate, RC47 (**Figures 6B,C**). In the GT-O1:G195G:ΔYcf48 strain the D1 and D2 proteins detected in PS II dimers and monomers were reduced, and the unassembled D1 slightly increased. However, only low levels of PS II monomers and only trace amounts of dimers were detected in the GT-O1:G195E:ΔYcf48 strain, consistent with the very low levels of PS II activity, while a low level of the RC47 complex was present. In addition, an antibody to the PsaA subunit of PS I revealed that the ratio of PS I monomers to trimers in the GT-O1:G195G:ΔYcf48 appeared to increase and that trimers were greatly reduced or destabilized in the GT-O1:G195E:ΔYcf48 mutant (**Figure 6D**).

DISCUSSION

A Strain with the ChlH Gly195 to Glu Mutation has Less Chlorophyll *a*

The ChlH subunit of Mg-chelatase catalyzes the first committed step in chlorophyll *a* biosynthesis and is involved in the regulation of gene expression in cyanobacteria (Jensen et al., 1996; Osanai et al., 2009). Commensurate with the importance of ChlH, segregation of gene-targeted knockouts has not been successful (Kong and Xu, 2002). Instead we have used a two-step approach to construct mutant strains with an inactivated *chlH* locus but which contain a *chlH* gene, expressed from a neutral site and encoding either an unmodified ChlH protein or the Gly195 to Glu variant. Characterization of these mutants revealed that introduction of the Gly195 to Glu mutation decreased the accumulation of chlorophyll *a*, with a more pronounced decrease in photoautotrophically grown cells compared to mixotrophically grown cultures. Our approach is readily applicable to the *in vivo* study of other targeted mutants in *chlH* from *Synechocystis* 6803.

The ChlH-Pro595 to Leu variant (equivalent to the substitution in the *A. thaliana cch* mutant) and the ChlH-Ala942 to Val change (equivalent to the substitution in the *A. thaliana gun5* mutant) have both been studied in the *Synechocystis* ChlH subunit *in vitro* (Davison and Hunter, 2011). In the *cch* and *gun5* mutants the observed reduction in chlorophyll was attributed to defective Mg-PP IX synthesis (Mochizuki et al., 2001). Likewise, *in vitro* characterization of the recombinant *Synechocystis* 6803 ChlH proteins showed both mutations abolished Mg-chelatase activity; however, Mg-chelatase activity was partially restored with the addition of the Gun4 protein (Davison and Hunter, 2011). The crystal structure of *Synechocystis* ChlH reveals that Pro595 and Ala942 are in the central cage-like structure of the protein that houses the catalytic site (Chen et al., 2015). However, while the Gly195 to Glu substitution in our *Synechocystis* 6803 ChlH-G195E strains also resulted in reduced chlorophyll *a*, the Gly195 residue is not in the catalytic cage-like domain. Therefore it is not clear whether the reduction in chlorophyll *a* in our mutants is caused by impaired catalytic activity or by an indirect mechanism. The proximity of Gly195 to the inter-dimeric salt bridge formed by Glu199 and Lys1018 might mean the Gly195 to Glu substitution could affect the formation and stability of the ChlH dimer; however, the physiological relevance of the ChlH dimer in chlorophyll *a* biosynthesis is unknown. In addition, the residues involved in salt bridge formation were not conserved in all cyanobacteria.

Combining the ChlH-Gly195 to Glu Mutation in a ΔYcf48 Strain Abolishes Photoautotrophic Growth

During PS II biogenesis and repair Ycf48 is transiently associated with pD1-containing pre-complexes prior to D1 processing and subsequent formation of the RC47 assembly intermediate (Komenda et al., 2007, 2008, 2012). In this study when the absence of Ycf48 was combined with the ChlH Gly195 to Glu mutation, the resultant double mutant showed limited photoautotrophic growth, a decreased level of PS II activity and a decrease in levels of assembled PS II dimers, monomers and the RC47 assembly intermediate compared with the GT-O1:G195G:ΔYcf48 strain (**Figures 4–6**). We also observed that PS I assembly was destabilized in our GT-O1:G195E:ΔYcf48 strain, perhaps as an indirect consequence of perturbing nascent PS II assembly and repair complexes. A similar effect on PS I assembly in an *A. thaliana* mutant lacking HCF136 – the homolog of Ycf48 – has also been reported (Plücken et al., 2002).

Given the close relationship between chlorophyll biosynthesis and the assembly and repair of PS II (Vavilin et al., 2007; Yao et al., 2012; Chidgey et al., 2014; Knoppová et al., 2014) and PS I (Kopečná et al., 2013; Hollingshead et al., 2016) manipulating the supply of chlorophyll may reveal novel roles for assembly factors of both PS II and PS I as seen in our GT-O1:G195E:ΔYcf48 strain.

AUTHOR CONTRIBUTIONS

TC performed the experiments and wrote the first draft of the manuscript. TS and JE-R designed the experiments, wrote, and edited the manuscript.

SUPPLEMENTARY MATERIAL

The Supplementary Material for this article can be found online at: http://journal.frontiersin.org/article/10.3389/fpls.2016.01060

REFERENCES

Boehm, M., Romero, E., Reisinger, V., Yu, J., Komenda, J., Eichacker, L. A., et al. (2011). Investigating the early stages of Photosystem II assembly in *Synechocystis* sp. PCC 6803: isolation of CP47 and CP43 complexes. *J. Biol. Chem.* 286, 14812–14819. doi: 10.1074/jbc.M110.207944

Bryskin, A. V., and Matsumura, I. (2010). Overlap extension PCR cloning: a simple and reliable way to create recombinant plasmids. *Biotechniques* 48, 463–465. doi: 10.2144/000113418

Chen, X., Pu, H., Fang, Y., Wang, X., Zhao, S., Lin, Y., et al. (2015). Crystal structure of the catalytic subunit of magnesium chelatase. *Nat. Plants* 1, 15125–15129. doi: 10.1038/nplants.2015.125

Chidgey, J. W., Linhartová, M., Komenda, J., Jackson, P. J., Dickman, M. J., Canniffe, D. P., et al. (2014). A cyanobacterial chlorophyll synthase-HliD complex associates with the Ycf39 protein and the YidC/Alb3 insertase. *Plant Cell* 26, 1–14. doi: 10.1105/tpc.114.124495

Crawford, T. S., Hanning, K. R., Chua, J. P. S., Eaton-Rye, J. J., and Summerfield, T. S. (2016). Comparison of D1′- and D1-containing PS II reaction centre complexes under different environmental conditions in *Synechocystis* sp. PCC 6803. *Plant Cell Environ.* 39, 1715–1726. doi: 10.1111/pce.12738

D'Haene, S. E., Sobotka, R., Bučinská, L., Dekker, J. P., and Komenda, J. (2015). Interaction of the PsbH subunit with a chlorophyll bound to histidine 114 of CP47 is responsible for the red 77K fluorescence of Photosystem II. *Biochim. Biophys. Acta* 1847, 1327–1334. doi: 10.1016/j.bbabio.2015.07.003

Davison, P. A., and Hunter, C. N. (2011). Abolition of magnesium chelatase activity by the *gun5* mutation and reversal by Gun4. *FEBS Lett.* 585, 183–186. doi: 10.1016/j.febslet.2010.11.037

Eaton-Rye, J. J. (2011). Construction of gene interruptions and gene deletions in the cyanobacterium *Synechocystis* sp. strain PCC 6803. *Methods Mol. Biol.* 684, 295–312. doi: 10.1007/978-1-60761-925-3_22

Eichacker, L. A., Helfrich, M., Rüdiger, W., and Muller, B. (1996). Stabilization of chlorophyll *a*-binding apoproteins P700, CP47, CP43, D2, and D1 by chlorophyll *a* or Zn-pheophytin *a*. *J. Biol. Chem.* 271, 32174–32179. doi: 10.1074/jbc.271.50.32174

Fujita, Y., Tsujimoto, R., and Aoki, R. (2015). Evolutionary aspects and regulation of tetrapyrrole biosynthesis in cyanobacteria under aerobic and anaerobic environments. *Life* 5, 1172–1203. doi: 10.3390/life5021172

He, Q., and Vermaas, W. (1998). Chlorophyll *a* availability affects psbA translation and D1 precursor processing in vivo in *Synechocystis* sp. PCC 6803. *Proc. Natl. Acad. Sci. U.S.A.* 95, 5830–5835. doi: 10.1073/pnas.95.10.5830

Hollingshead, S., Kopečná, J., Armstrong, D. R., Bučinská, L., Jackson, P. J., Chen, G. E., et al. (2016). Synthesis of chlorophyll-binding proteins in a fully segregated Δ*ycf54* strain of the cyanobacterium *Synechocystis* sp. PCC 6803. *Front. Plant Sci.* 7:292. doi: 10.3389/fpls.2016.00292

Jackson, S. A., and Eaton-Rye, J. J. (2015). Characterization of a *Synechocystis* sp. PCC 6803 double mutant lacking the CyanoP and Ycf48 proteins of Photosystem II. *Photosynth. Res.* 124, 217–229. doi: 10.1007/s11120-015-0122-0

Jackson, S. A., Hervey, J. R. D., Dale, A. J., and Eaton-Rye, J. J. (2014). Removal of both Ycf48 and Psb27 in *Synechocystis* sp. PCC 6803 disrupts Photosystem II assembly and alters Q_A^- oxidation in the mature complex. *FEBS Lett.* 588, 3751–3760. doi: 10.1016/j.febslet.2014.08.024

Jensen, P. E., Gibson, L. C., Henningsen, K. W., and Hunter, C. N. (1996). Expression of the *chlI*, *chlD*, and *chlH* genes from the cyanobacterium *Synechocystis* PCC6803 in *Escherichia coli* and demonstration that the three cognate proteins are required for magnesium-protoporphyrin chelatase activity. *J. Biol. Chem.* 271, 16662–16667. doi: 10.1074/jbc.271.28.16662

Jones, P. R. (2014). Genetic instability in cyanobacteria - an elephant in the room? *Front. Bioeng. Biotechnol.* 2:12. doi: 10.3389/fbioe.2014.00012

Knoppová, J., Sobotka, R., Tichy, M., Yu, J., Konik, P., Halada, P., et al. (2014). Discovery of a chlorophyll binding protein complex involved in the early steps of Photosystem II assembly in *Synechocystis*. *Plant Cell* 26, 1200–1212. doi: 10.1105/tpc.114.123919

Komenda, J., Kuviková, S., Granvogl, B., Eichacker, L. A., Diner, B. A., and Nixon, P. J. (2007). Cleavage after residue Ala352 in the C-terminal extension is an early step in the maturation of the D1 subunit of Photosystem II in *Synechocystis* PCC 6803. *Biochim. Biophys. Acta* 1767, 829–837. doi: 10.1016/j.bbabio.2007.01.005

Komenda, J., Nickelsen, J., Tichý, M., Prášil, O., Eichacker, L. A., and Nixon, P. J. (2008). The cyanobacterial homologue of HCF136/YCF48 is a component of an early Photosystem II assembly complex and is important for both the efficient assembly and repair of Photosystem II in *Synechocystis* sp. PCC 6803. *J. Biol. Chem.* 283, 22390–22399. doi: 10.1074/jbc.M801917200

Komenda, J., Sobotka, R., and Nixon, P. J. (2012). Assembling and maintaining the Photosystem II complex in chloroplasts and cyanobacteria. *Curr. Opin. Plant Biol.* 15, 245–251. doi: 10.1016/j.pbi.2012.01.017

Kong, R., and Xu, X. (2002). Three-piece-ligation PCR and application in disruption of chlorophyll synthesis genes in *Synechocystis* sp. PCC 6803. *Curr. Microbiol.* 44, 241–245. doi: 10.1007/s00284-001-0032-6

Kopečná, J., Sobotka, R., and Komenda, J. (2013). Inhibition of chlorophyll biosynthesis at the protochlorophyllide reduction step results in the parallel depletion of Photosystem I and Photosystem II in the cyanobacterium *Synechocystis* PCC 6803. *Planta* 237, 497–508. doi: 10.1007/s00425-012-1761-4

Kopf, M., Kähn, S., Scholz, I., Matthiesen, J. K. F., Hess, W. R., and Voß, B. (2014). Comparative analysis of the primary transcriptome of *Synechocystis* sp. PCC 6803. *DNA Res.* 21, 537–539. doi: 10.1093/dnares/dsu018

Kunert, A., Hagemann, M., and Erdmann, N. (2000). Construction of promoter probe vectors for *Synechocystis* sp. PCC 6803 using the light-emitting reporter systems Gfp and LuxAB. *J. Microbiol. Methods* 41, 185–194. doi: 10.1016/S0167-7012(00)00162-7

Larkin, R. M., Alonso, J. M., Ecker, J. R., and Chory, J. (2003). GUN4, a regulator of chlorophyll synthesis and intracellular signaling. *Science* 299, 902–906. doi: 10.1126/science.1079978

Mabbitt, P. D., Wilbanks, S. M., and Eaton-Rye, J. J. (2014). Structure and function of the hydrophilic Photosystem II assembly proteins: Psb27, Psb28 and Ycf48. *Plant Physiol. Biochem.* 81, 96–107. doi: 10.1016/j.plaphy.2014.02.013

MacKinney, G. (1941). Absorption of light by chlorophyll solutions. *J. Biol. Chem.* 140, 315–322.

Meurer, J., Plücken, H., Kowallik, K. V., and Westhoff, P. (1998). A nuclear-encoded protein of prokaryotic origin is essential for the stability of Photosystem II in *Arabidopsis thaliana*. *EMBO J.* 17, 5286–5297. doi: 10.1093/emboj/17.18.5286

Mochizuki, N., Brusslan, J. A., Larkin, R., Nagatani, A., and Chory, J. (2001). *Arabidopsis* genomes uncoupled 5 (GUN5) mutant reveals the involvement of Mg-chelatase H subunit in plastid-to-nucleus signal transduction. *Proc. Natl. Acad. Sci. U.S.A.* 98, 2053–2058. doi: 10.1073/pnas.98.4.2053

Morris, J. N., Crawford, T. S., Jeffs, A., Stockwell, P. A., Eaton-Rye, J. J., and Summerfield, T. C. (2014). Whole genome re-sequencing of two "wild-type" strains of the model cyanobacterium *Synechocystis* sp. PCC 6803. *N. Z. J. Bot.* 52, 36–47. doi: 10.1080/0028825X.2013.846267

Osanai, T., Imashimizu, M., Seki, A., Sato, S., Tabata, S., and Imamura, S. (2009). ChlH, the H subunit of the Mg-chelatase, is an anti-sigma factor for SigE in *Synechocystis* sp. PCC 6803. *Proc. Natl. Acad. Sci. U.S.A.* 106, 6860–6865. doi: 10.1073/pnas.0810040106

Plücken, H., Müller, B., Grohmann, D., Westhoff, P., and Eichacker, L. A. (2002). The HCF136 protein is essential for assembly of the Photosystem II reaction center in *Arabidopsis thaliana*. *FEBS Lett.* 532, 85–90. doi: 10.1016/S0014-5793(02)03634-7

Qian, P., Marklew, C. J., Davison, P. A., Brindley, A. A., Söderberg, C., Al-karadaghi, S., et al. (2012). Structure of the cyanobacterial magnesium chelatase H subunit determined by single particle reconstruction and small-angle X-ray scattering. *J. Biol. Chem.* 287, 4946–4956. doi: 10.1074/jbc.M111.308239

Shen, G., Boussiba, S., and Vermaas, W. F. J. (1993). *Synechocystis* sp PCC 6803 strains lacking Photosystem I and phycobilisome function. *Plant Cell* 5, 1853–1863. doi: 10.1105/tpc.5.12.1853

Shen, J.-R. (2015). The structure of Photosystem II and the mechanism of water oxidation in photosynthesis. *Annu. Rev. Plant Biol.* 66, 23–48. doi: 10.1146/annurev-arplant-050312-120129

Shepherd, M., McLean, S., and Hunter, C. N. (2005). Kinetic basis for linking the first two enzymes of chlorophyll biosynthesis. *FEBS J.* 272, 4532–4539. doi: 10.1111/j.1742-4658.2005.04873.x

Sobotka, R. (2014). Making proteins green: biosynthesis of chlorophyll-binding proteins in cyanobacteria. *Photosynth. Res.* 119, 223–232. doi: 10.1007/s11120-013-9797-2

Sobotka, R., Dühring, U., Komenda, J., Peter, E., Gardian, Z., Tichy, M., et al. (2008). Importance of the cyanobacterial Gun4 protein for chlorophyll metabolism and assembly of photosynthetic complexes. *J. Biol. Chem.* 283, 25794–25802. doi: 10.1074/jbc.M803787200

Summerfield, T. C., Crawford, T. S., Young, R. D., Chua, J. P. S., MacDonald, R. L., Sherman, L. A., et al. (2013). Environmental pH affects photoautotrophic growth of *Synechocystis* sp. PCC 6803 strains carrying mutations in the lumenal proteins of PS II. *Plant Cell Physiol.* 54, 859–874. doi: 10.1093/pcp/pct036

Umena, Y., Kawakami, K., Shen, J.-R., and Kamiya, N. (2011). Crystal structure of oxygen-evolving Photosystem II at a resolution of 1.9 Å. *Nature* 473, 55–60. doi: 10.1038/nature09913

Vavilin, D., Yao, D., and Vermaas, W. (2007). Small Cab-like proteins retard degradation of Photosystem II-associated chlorophyll in *Synechocystis* sp. PCC 6803. *J. Biol. Chem.* 282, 37660–37668. doi: 10.1074/jbc.M707133200

Wang, P., and Grimm, B. (2015). Organization of chlorophyll biosynthesis and insertion of chlorophyll into the chlorophyll-binding proteins in chloroplasts. *Photosynth. Res.* 126, 189–202. doi: 10.1007/s11120-015-0154-5

Yang, H., Liu, J., Wen, X., and Lu, C. (2015). Molecular mechanism of Photosystem I assembly in oxygenic organisms. *Biochim. Biophys. Acta* 1847, 838–848. doi: 10.1016/j.bbabio.2014.12.011

Yao, D. C. I., Brune, D. C., Vavilin, D., and Vermaas, W. F. J. (2012). Photosystem II component lifetimes in the cyanobacterium *Synechocystis* sp. strain PCC 6803: small Cab-like proteins stabilize biosynthesis intermediates and affect early steps in chlorophyll synthesis. *J. Biol. Chem.* 287, 682–692. doi: 10.1074/jbc.M111.320994

Conflict of Interest Statement: The authors declare that the research was conducted in the absence of any commercial or financial relationships that could be construed as a potential conflict of interest.

frontiers in Plant Science

MINI REVIEW
published: 10 March 2016
doi: 10.3389/fpls.2016.00295

Carotenoids Assist in Cyanobacterial Photosystem II Assembly and Function

*Tomas Zakar, Hajnalka Laczko-Dobos, Tunde N. Toth and Zoltan Gombos**

Laboratory of Plant Lipid Function and Structure, Institute of Plant Biology, Biological Research Centre, Hungarian Academy of Sciences, Szeged, Hungary

Carotenoids (carotenes and xanthophylls) are ubiquitous constituents of living organisms. They are protective agents against oxidative stresses and serve as modulators of membrane microviscosity. As antioxidants they can protect photosynthetic organisms from free radicals like reactive oxygen species that originate from water splitting, the first step of photosynthesis. We summarize the structural and functional roles of carotenoids in connection with cyanobacterial Photosystem II. Although carotenoids are hydrophobic molecules, their complexes with proteins also allow cytoplasmic localization. In cyanobacterial cells such complexes are called orange carotenoid proteins, and they protect Photosystem II and Photosystem I by preventing their overexcitation through phycobilisomes (PBS). Recently it has been observed that carotenoids are not only required for the proper functioning, but also for the structural stability of PBSs.

Keywords: carotenoids, Photosystem II, cyanobacteria, *Synechocystis*, phycobilisomes, xanthophylls

OPEN ACCESS

Edited by:
Julian Eaton-Rye, University of Otago, New Zealand

Reviewed by:
Shigeru Itoh, Nagoya University, Japan
Kinga Klodawska, Jagiellonian University, Poland

****Correspondence:***
Zoltan Gombos
gombos.zoltan@gmail.com

Specialty section:
This article was submitted to Plant Cell Biology, a section of the journal Frontiers in Plant Science

Received: *21 October 2015*
Accepted: *24 February 2016*
Published: *10 March 2016*

Citation:
Zakar T, Laczko-Dobos H, Toth TN and Gombos Z (2016) Carotenoids Assist in Cyanobacterial Photosystem II Assembly and Function. Front. Plant Sci. 7:295. doi: 10.3389/fpls.2016.00295

ROLES OF CAROTENOIDS IN MODULATING PHOTOSYNTHETIC AND CYTOPLASMIC MEMBRANES OF CYANOBACTERIA

Carotenoids as Protective Agents

Carotenoids are a group of pigments that play multiple structural and functional roles. They are molecules with conjugated double bonds, which allow them to participate in photosynthetic functions (Gruszecki and Strzalka, 2005). In cyanobacteria the most abundant carotenoids are carotenes (e.g., β-carotene) and various types of xanthophylls (synechoxanthin, canthaxanthin, caloxanthin, echinenone, myxoxanthophyll, nostoxanthin, zeaxanthin), which are oxygenated derivates of the carotenes (Takaichi and Mochimaru, 2007; Domonkos et al., 2013; Kusama et al., 2015; Toth et al., 2015).

Carotene and xanthophyll molecules are indispensable components of both cytoplasmic and thylakoidal membranes of cyanobacteria. However, β-carotene is the only carotenoid, which was localized in PSII by X-ray crystallography (Loll et al., 2005; Umena et al., 2011). As an extremly hydrophobic molecule, β-carotene forms complexes with proteins, thereby functioning as a bridge between various proteins involved in photosynthetic processes. In thylakoid membranes a protective role of β-carotene was demonstrated as a scavenger of singlet oxygen (Packer et al., 1981).

Abbreviations: CP43, chlorophyll-protein complex 43; CP47, chlorophyll-protein complex 47; FRP, fluorescence recovery protein; NPQ, non-photochemical quenching; OCP, photoactive orange carotenoid protein; PBS, phycobilisome; PSI and PSII, Photosystem I and II; RC47, reaction center 47; ROS, reactive oxygen species; *Synechocystis, Synechocystis* sp. PCC6803.

In contrast to β-carotene, xanthophylls have not been localized unambiguously. Their presence in the photosystems is expected, and has been demonstrated by various biophysical and biochemical methods (Van der Weij-de Wit et al., 2007; Domonkos et al., 2009). Nevertheless the binding of xanthophylls to membrane proteins has not yet been demonstrated. In the membranes they are positioned in a way that their hydrophilic part faces the aqueous phase.

Free carotenes and xanthophylls occupy the hydrophobic region of membrane bilayers. Accordingly, it was predicted that xanthophylls rigidify membranes, whereas β-carotene and echinenon have a neutral or fluidizing effect (Gruszecki and Strzalka, 2005).

Although the scavenging character of xanthophylls is stronger than that of β-carotene (Steiger et al., 1999; Domonkos et al., 2013), neither their localization nor their exact scavenging role has been elucidated yet. Xanthophylls are found mainly in cytoplasmic membranes (Masamoto and Furukawa, 1997; Masamoto et al., 1999). A recent review has summarized the protective mechanism of carotenoids and other putative protective functions against ROS, which are produced by PSII of photosynthesis that mediates light-driven oxidation of water and the release of molecular oxygen (Derks et al., 2015).

Carotenes and Xanthophylls Affect Membrane Viscosity

Due to their influence on membrane properties, the xanthopylls are also important in the adaptation to various temperature conditions. Low growth temperatures induce enhanced synthesis of xanthophylls and, consequently, the xanthophyll content of thylakoid membranes is increased to compensate for elevated lipid desaturation. Instead of increasing membrane microviscosity, enhanced xanthophyll content alters membrane dynamics by allowing a tighter arrangement of fatty acyl moieties. The observed discrepancy could be explained by an apparent increase of very rigid, myxoxanthophyll-related lipids in the thylakoid membranes (Varkonyi et al., 2002).

Presence of Enzymes of Carotenoid Biosynthesis in Cytoplasmic Membrane

More recent research has shown that cytoplasmic membranes contain some biosynthetic enzymes specific for the biosynthesis of echinenone and β-carotene. The CrtQ (zeta-carotene desaturase) and CrtO (beta-carotene ketolase) enzymes involved in carotenoid synthesis are localized in cytoplasmic membranes (Zhang et al., 2015). This would mean that echinenone and precursors of β-carotene are more abundant in cytoplasmic membranes than in thylakoids. Cytoplasmic membranes contain higher amounts of carotenoids than thylakoid membranes, which results in a more pronounced modulation of their membrane fluidity.

Despite the relatively low carotenoid content of the thylakoid membrane, these compounds are indispensable for photosynthetic processes. They not only affect the membrane structure, but also influence the oligomerization of proteins, thereby modulating photosynthetic functions.

THE EFFECT OF CAROTENOIDS ON THE ARCHITECTURE AND VARIOUS FUNCTIONS OF PHOTOSYSTEM II COMPLEXES

Structure

X-ray crystallography revealed that in thylakoid membranes the main carotene (β-carotene) localizes in the photosynthetic reaction centers (Loll et al., 2005; Umena et al., 2011). These results revealed that a PSII complex contains 11 β-carotene molecules. Xanthophylls could not be localized unambiguously. The importance of carotenoids in maintaining the stability and functioning of PSII was demonstrated in a carotenoid-deficient mutant strain (Sozer et al., 2010).

The completely carotenoid deficient Δ*crtH/B* or Δ*crtB* mutants of *Synechocystis* sp. PCC 6803 (hereafter *Synechocystis*) are devoid of active PSII reaction centers. These strains do not show oxygen-evolving activity (Sozer et al., 2010; Toth et al., 2015). The cells have reduced translation for a number of genes encoding PSII proteins and hence do not assemble active PSII complexes. They are capable of synthesizing only a limited amount of CP47, which is crucial for the formation of dimeric PSII complexes, but CP43 synthesis is almost completely blocked. The lack of these protein subunits prevents the formation of functional PSII complexes. This is the reason why we think that carotenoids are indispensable components of PSII.

Complete loss of carotenoids prevents the proper assembly of PSII (**Figure 1**), and such cells contain almost exclusively CP43-less oligomers. They show reduced PSII fluorescence, which originates from PSII components that are unable to integrate into a fully functional complex. In the carotenoid-less mutant Δ*crtB* we observed the accumulation of fluorescence-emitting spots with long lifetime close to the cell walls (Toth et al., 2015, Supplementary Figures). This could indicate that PSII biogenesis is blocked and incomplete adducts remain localized at the thylakoid-organizing complexes. This is in good agreement with an earlier observation of dysfunctional thylakoid membrane systems in a carotenoid-deficient mutant (Nickelsen et al., 2011). The PSII structure of *Thermosynechococcus elongatus*, deduced from X-ray crystallographic data (Guskov et al., 2009) shows the presence of various protein subunits and cofactors, such as carotenoids, in the dimeric form of reaction centers (**Figure 1A**). The structure of the imagined carotenoid-less PSII is presented in **Figure 1B**. However, the reaction center in Δ*crtB* cells contains almost exclusively CP43-less oligomers. Radioactive labeling demonstrated limited synthesis of inner PSII antennae, CP47 and, particularly, CP43. The lack of CP43 resulted in the formation of the RC47 pre-assembly complex (Komenda et al., 2012), demonstrating that carotenoid deficiency results in low levels of partially assembled reaction center complexes. These cells show reduced fluorescence originating from the remaining chlorophyll-protein complexes that are unable to integrate into a complex (Sozer et al., 2010; Toth et al., 2015).

Carotenoids, together with chlorophylls, are also necessary for the translation and stabilization of photosynthetic reaction center apoproteins in the green alga *Chlamydomonas reinhardtii*,

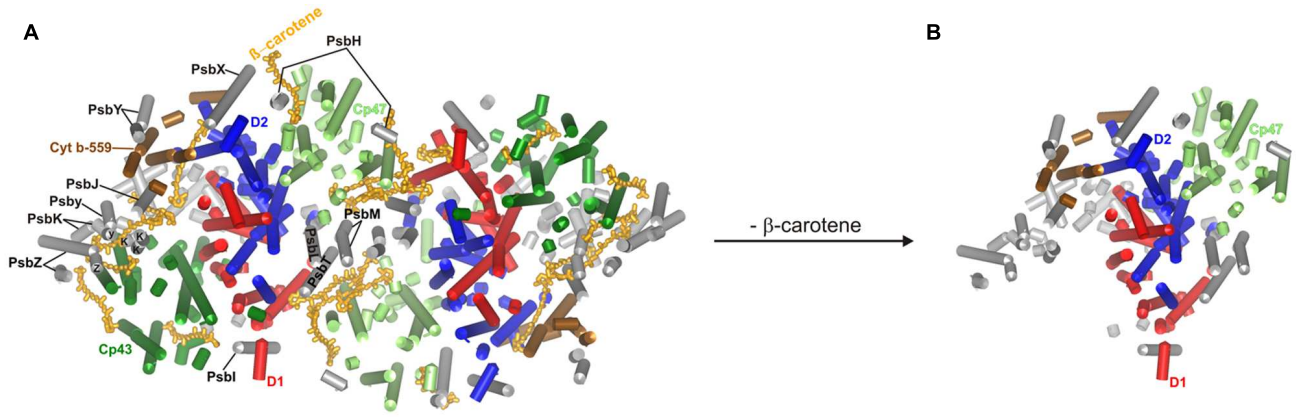

FIGURE 1 | Structure of the PSII complex deduced from X-ray crystallographic data (PDB files: 3BZ1 and 3BZ2). The PSII supercomplex in wild type **(A)** and assumed PSII structure in carotenoid-deficient **(B)** *Thermosynechococcus elongatus*.

however, they do not regulate the transcription of reaction center apoproteins (Herrin et al., 1992).

Our recent results suggest some structural function of xanthophylls in stabilizing PSII, as well as its dimeric complexes in *Synechocystis* (Toth et al., 2015). Carotenoids are essential mediators of interactions between PSII monomers, highlighting the role of neutral lipids, which can regulate the equilibrium between dimerization and dissociation (Guskov et al., 2009).

Accordingly, carotenoids are indispensable constituents of the photosynthetic apparatus, being essential not only for antioxidative protection but also for the productive synthesis and accumulation of photosynthetic proteins and, especially, those of the PSII antenna subunits.

Function

Carotenoids, due to their light harvesting (Stamatakis et al., 2014) and photoprotective capacity (Schafer et al., 2005; Sozer et al., 2010), are indispensable for the function of the photosynthetic apparatus, and particularly in that of PSII. Under low light conditions carotenoids can provide more efficient light absorption (Koyama et al., 1996; Bode et al., 2009). By contrast, when cyanobacteria are exposed to high light, excess energy needs to be reduced to avoid photoinhibition damage to the photosystems (Powles, 1984; Aro et al., 1993, 2005). Carotenoids can exert protection by dissipating excess energy as heat, a phenomenon called NPQ, or by scavenging ROS.

The activity of light-damaged PSII is efficiently restored by a repair system, therefore photoinhibition occurs only when the rate of inactivation exceeds that of repair. In order to understand the mechanism by which carotenoids protect the cells under light stress it would be necessary to study the two processes of photoinhibition, photodamage and repair, separately (Nishiyama and Murata, 2014).

Photosystem II complexes are very sensitive not only to strong light but also to a wide range of abiotic stress effects, such as low and high temperatures, UV-B exposure, drought, and high concentration of salts (Takahashi and Murata, 2008). These stress factors ultimately lead to oxidative stress. Recently it has been shown that Δ*sigCDE*, a group 2 σ factor mutant of *Synechocystis*, is more sensitive to oxidative stress, but also more resistant to the photoinhibition of PSII. In this mutant an up-regulation of photoprotective carotenoids was observed, but it has been suggested that the resistance to light damage of PSII and the overall tolerance to oxidative stress are distinct in cyanobacteria, and their mechanisms are different (Hakkila et al., 2014).

In order to study the specific role of different carotenoids in cyanobacteria a wide range of carotenoid-deficient mutants were generated. Studies with various xanthophyll mutants of *Synechococcus* sp. PCC 7002 indicate that xanthophylls contribute to protection against photo-oxidative stress (Zhu et al., 2010). Similarly *Synechocystis* mutants lacking almost all xanthophylls (Δ*crtRO*) were sensitized to photodamage only under high light conditions (Schafer et al., 2005), whereas under normal illumination charge separation in PSII seemed unaffected (Toth et al., 2015). Recently it has been shown that zeaxanthin and echinenon protect the repair part of the PSII recovery cycle from photoinhibition by decreasing the level of singlet oxygen that inhibits protein synthesis (Kusama et al., 2015).

The removal of all β-carotene and xanthophylls from *Synechocystis* (Δ*crtH/B* and Δ*crtB* mutants) causes more severe effects. These strains are extremely light sensitive and they can grow only in the dark under light-activated heterotrophic conditions, without detectable oxygen evolution (Sozer et al., 2010). Time-resolved fluorescence (streak camera) measurements of these mutant cells also indicate inactive PSII (Toth et al., 2015).

In PSII reaction centers there are at least two redox active β-carotenes (Telfer et al., 2003). Recently it has been shown that one of the two so-called redox active carotenoids, Car_{D2}, plays a role in photoprotection. Site-directed mutations around the binding pocket of Car_{D2} in *Synechocystis* cells revealed the importance of β-carotenes in the initiation of secondary electron transfer processes, which occurs when water oxidation is inhibited (Shinopoulos et al., 2014).

In addition to the role of carotenoids as constituents of membrane-embedded PSII, they also have crucial functions in the formation of protein complexes, the so-called photoactive orange carotenoid proteins. A recent study has elucidated the dual role of carotenoids in OCP, namely the protection of photosystems by quenching excess energy, and also the capacity of quenching singlet oxygen formed during the light reactions (Sedoud et al., 2014). Using an OCP-deficient mutant it has been shown that OCP-related thermal dissipation protects the repair of PSII during photoinhibition (Kusama et al., 2015). Although it is clear that carotenoids are the principal actors in energy dissipation, the mechanism of this process is poorly understood. Staleva et al. (2015) pointed out a new function of carotenoids associated with proteins. They have shown that *Synechocystis* HliD, a Hlips (high light-inducible proteins) family protein, binds chlorophyll *a* and β-carotene with a 3:1 ratio. The photoprotective role of this carotenoid-binding protein was demonstrated by femtosecond spectroscopy, showing that energy dissipation is achieved via direct energy transfer from a chlorophyll *a* Qy state to the β-carotene S1 state (Staleva et al., 2015).

Currently global changes in the environment can generate a multitude of stress factors, such as high or low temperatures, high light or UV-B radiation, etc. This underlines the importance of the evolutionary role of carotenoids and the mechanisms by which they can contribute to the survival of various organisms under extreme conditions.

HOW DO CAROTENOIDS AFFECT THE STRUCTURE AND PROCESSES OF PHYCOBILISOMES OF CYANOBACTERIAL PHOTOSYSTEM II COMPLEXES?

Structure

Cyanobacteria have special light-harvesting complexes, PBSs, which can absorb light in a wide spectral range. In addition to PBS, carotenoids can function as accessory pigments to widen the range of absorption. PBSs are comprised of rods attached to a core complex that is directly linked to PSII. In *Synechocystis* the rods contain phycocyanin, which can harvest long wavelength light and transfer its energy to the allophycocynin core, which then transduces it directly to the PSII reaction center (Maccoll and Guard-Friar, 1986). In the reaction center the main pigment is chlorophyll *a*, whereas in the PBS the chromophore is phycocyanobilin or some other, structurally related pigment.

In the PBS structure the presence of β-carotene or xanthophylls has not yet been demonstrated. Surprisingly, in carotenoid-less Δ*crtB* cells a large amount of unconnected phycocyanin units has been observed (Toth et al., 2015). Density gradient centrifugation revealed that most of the assembled core complexes had shorter rods than those of the wild type. In this mutant PSI is in monomeric form, only a negligible amount of PSII is formed, and CP43 is mostly detached from PSII. Schematic structures of the photosynthetic complexes, as well as images of the sucrose density gradient-separated PBS components of wild-type *Synechocystis* and its carotenoid-less Δ*crtB* mutant are shown in **Figure 2**.

It seems that carotenoids are required for the assembly or maintenance of the complete PBS structure (Toth et al., 2015), suggesting a direct or indirect effect of carotenoids on the structure and functions of this complex (Toth et al., 2015).

Light-Harvesting Process

Cyanobacterial carotenoid-proteins play an important role in photoprotection (Kerfeld et al., 2003; Kerfeld, 2004). One of these, the water-soluble OCP, has been structurally characterized and has recently emerged as a key player in cyanobacterial photoprotection (Sedoud et al., 2014). OCP was first described by David Krogmann more than 25 years ago (Holt and Krogmann, 1981). Highly conserved homologs of the gene encoding the 34 kDa OCP are present in most of the known cyanobacterial genomes.

The carotenoid composition of the OCP isolated from wild-type cells is as follows: 60% echinenone, 30% keto-carotenoid

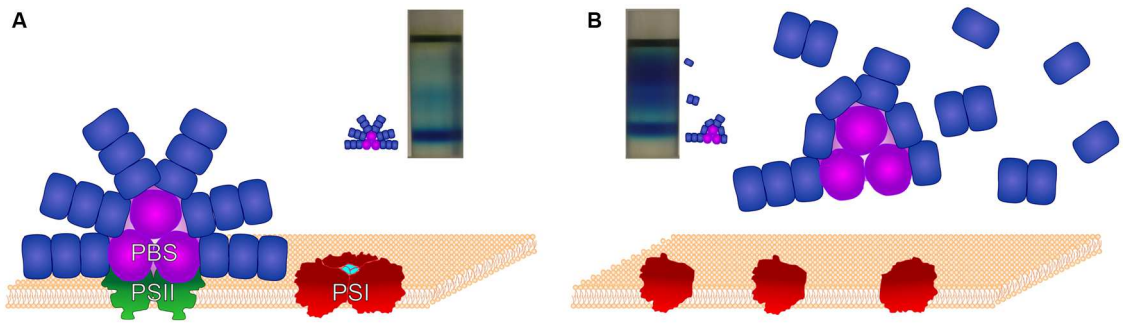

FIGURE 2 | The structures of PBS and the photosynthetic reaction centers in wild-type *Synechocystis* and its Δ*crtB* carotenoid-less mutant. Schematic figure showing the assembled supercomplexes and the positions of their constituents following separation by stepwise sucrose density gradient centrifugation. **(A)**: Fully assembled functional supercomplexes of wild-type cells with entire PBS, dimeric PSII and trimerized PSI. **(B)**: Monomeric PSI and partially assembled PBS of the Δ*crtB* mutant. In these cells only a negligible amount of PSII is formed.

3′-hydroxyechinenone, and 10% zeaxanthin (Sedoud et al., 2014). The energy collected by the PBS is rapidly transferred from rods to the core, and subsequently to membrane-embedded reaction centers of PSII or PSI.

Photoactive orange carotenoid protein is a photoactive protein. Illumination of OCP by strong blue-green light induces changes in its carotenoid, converting the inactive orange dark form (OCPo) into an active red form (OCPr). In OCPo, 3′-hydroxyechinenone is in all-trans configuration. In OCPr, it is also in all-trans configuration, but its apparent conjugation length increases, resulting in a less distorted, more planar structure. Fourier transform infrared spectra showed that these changes in the carotenoid induce conformational changes in the protein, leading to a less rigid helical structure and a compaction of the β-sheet. These changes in OCP are essential for the induction of the photoprotective mechanism. Only OCPr is capable of binding to the PBSs, inducing fluorescence quenching and the photoprotective mechanism (Wilson et al., 2012).

In contrast to photosynthetic eukaryotes, photoprotection in cyanobacteria is not induced by transthylakoid ΔpH or excitation pressure on PSII. Instead, intense blue–green light (400–550 nm) induces quenching of PSII fluorescence that is reversible in minutes, even in the presence of translation inhibitors (El Bissati et al., 2000). Fluorescence spectra and the study of NPQ mechanism in PBS- and PSII-mutants of *Synechocystis* indicate that this mechanism involves a specific decrease in the fluorescence emission of PBSs, as well as a decrease of energy transfer from PBS to the reaction centers (Scott et al., 2006; Wilson et al., 2006). The site of the quenching appears to be the core of the PBS (Scott et al., 2006; Wilson et al., 2006; Rakhimberdieva et al., 2007).

The action spectrum of PBS fluorescence quenching resembles the absorption spectrum of cyanobacterial carotenoids. In the absence of OCP, strong white or blue–green light-induced NPQ was completely inhibited in *Synechocystis*. As a consequence, OCP-deficient cells are more sensitive to light stress. Moreover, the action spectrum of cyanobacterial NPQ (Rakhimberdieva et al., 2004) exactly matches the absorption spectrum of the carotenoid, 3′-hydroxyechinenone (Polivka et al., 2005) in the OCP. OCP is now known to be specifically involved in the PBS -associated NPQ and not in the other mechanisms affecting the levels of fluorescence, such as state transitions or D1 damage (Wilson et al., 2006; Zhang et al., 2014). Electron microscopic studies using immunogold labeling revealed that the majority of OCP is localized in the inter-thylakoidal cytoplasmic region, on the PBS side of the membrane (Wilson et al., 2006). The interaction between the OCP and the PBSs and thylakoids was corroborated by the presence of OCP in the PBS-associated membrane fraction (Wilson et al., 2006, 2007). In *Synechocystis*, OCP is constitutively expressed, and it is present even in mutants that lack PBSs (Wilson et al., 2007). Stress conditions (high light, salt stress, iron starvation) increase levels of the OCP transcript and proteins (Hihara et al., 2001; Kanesaki et al., 2002; Fulda et al., 2006; Wilson et al., 2007). All known OCP-like genes of cyanobacteria are transcriptionally active and the NPQ mechanism is inducible by blue light. This suggests that the OCP-based photoprotective mechanism is widespread in cyanobacteria (Boulay et al., 2008).

Fluorescence recovery protein is known to be involved in photoprotection and restoration of full light-harvesting capacity. FRP is needed for the recovery of full antenna capacity when light intensity decreases (Boulay et al., 2010). FRP interacts with the activated OCP and accelerates its deactivation and detachment from the PBS (Boulay et al., 2010; Gwizdala et al., 2011), although the details of these processes have not yet been elucidated (Zhang et al., 2014).

Carotenoid containing OCP molecules have an essential role in cyanobacterial photoprotection by binding to the PBS.

CONCLUSION

Carotenoids are important for multiple PSII functions, as they are not only required for its activity but also participate in the light-harvesting process. They act as pigments, which can increase the spectral range, and can also protect against over-excitation and oxidative side products. It has been shown that β-carotene is essential for the assembly of PSII and the PSI trimer, whereas xanthophylls can stabilize them. The influence of OCP on the light-harvesting capacity of PBS and the requirement of carotenoids for the proper assembly and function of this complex highlight important additional roles of not only β-carotene, but also of the xanthophylls in cyanobacterial photosynthesis. Further studies are required to elucidate the exact mechanisms by which carotenoids influence the structure and function of PSII and the PBS, and how they contribute to the protection of the photosynthetic processes.

AUTHOR CONTRIBUTIONS

The authors of this mini-review equally contributed to its concept and design. The tasks were assigned as follows: TZ contributed to all chapters and had a key role in formulating the review. HL-D wrote a chapter, critically read and corrected the entire manuscript, and adjusted it to the required format. TT prepared the figures, the list of references, and gave advice on the text. ZG provided the general concept and design, and also contributed to a chapter.

ACKNOWLEDGMENTS

This work was supported by grants K108411 and PD108551 from the Hungarian Scientific Research Fund, and a bilateral project between the science academies of the Czech Republic and Hungary (HU/2013/06). The authors are thankful to Miklós Szekeres for reading and correcting the manuscript and to Mihály Kis for his help in preparing the figures.

REFERENCES

Aro, E. M., Suorsa, M., Rokka, A., Allahverdiyeva, Y., Paakkarinen, V., Saleem, A., et al. (2005). Dynamics of photosystem II: a proteomic approach to thylakoid protein complexes. *J. Exp. Bot.* 56, 347–356. doi: 10.1093/jxb/eri041

Aro, E. M., Virgin, I., and Andersson, B. (1993). Photoinhibition of Photosystem II – Inactivation, protein damage and turnover. *Biochim. Biophys. Acta* 1143, 113–134. doi: 10.1016/0005-2728(93)90134-2

Bode, S., Quentmeier, C. C., Liao, P. N., Hafi, N., Barros, T., Wilk, L., et al. (2009). On the regulation of photosynthesis by excitonic interactions between carotenoids and chlorophylls. *Proc. Natl. Acad. Sci. U.S.A.* 106, 12311–12316. doi: 10.1073/pnas.0903536106

Boulay, C., Abasova, L., Six, C., Vass, I., and Kirilovsky, D. (2008). Occurrence and function of the orange carotenoid protein in photoprotective mechanisms in various cyanobacteria. *Biochim. Biophys. Acta* 1777, 1344–1354. doi: 10.1016/j.bbabio.2008.07.002

Boulay, C., Wilson, A., D'haene, S., and Kirilovsky, D. (2010). Identification of a protein required for recovery of full antenna capacity in OCP-related photoprotective mechanism in cyanobacteria. *Proc. Natl. Acad. Sci. U.S.A.* 107, 11620–11625. doi: 10.1073/pnas.1002912107

Derks, A., Schaven, K., and Bruce, D. (2015). Diverse mechanisms for photoprotection in photosynthesis. Dynamic regulation of photosystem II excitation in response to rapid environmental change. *Biochim. Biophys. Acta* 1847, 468–485. doi: 10.1016/j.bbabio.2015.02.008

Domonkos, I., Kis, M., Gombos, Z., and Ughy, B. (2013). Carotenoids, versatile components of oxygenic photosynthesis. *Prog. Lipid Res.* 52, 539–561. doi: 10.1016/j.plipres.2013.07.001

Domonkos, I., Malec, P., Laczko-Dobos, H., Sozer, O., Klodawska, K., Wada, H., et al. (2009). Phosphatidylglycerol depletion induces an increase in myxoxanthophyll biosynthetic activity in *Synechocystis* PCC 6803 Cells. *Plant Cell Phys.* 50, 374–382. doi: 10.1093/pcp/pcn204

El Bissati, K., Delphin, E., Murata, N., Etienne, A. L., and Kirilovsky, D. (2000). Photosystem II fluorescence quenching in the cyanobacterium *Synechocystis* PCC 6803: involvement of two different mechanisms. *Biochim. Biophys. Acta* 1457, 229–242. doi: 10.1016/S0005-2728(00)00104-3

Fulda, S., Mikkat, S., Huang, F., Huckauf, J., Marin, K., Norling, B., et al. (2006). Proteome analysis of salt stress response in the cyanobacterium *Synechocystis* sp. strain PCC 6803. *Proteomics* 6, 2733–2745. doi: 10.1002/pmic.200500538

Gruszecki, W. I., and Strzalka, K. (2005). Carotenoids as modulators of lipid membrane physical properties. *Biochim. Biophys. Acta* 1740, 108–115. doi: 10.1016/j.bbadis.2004.11.015

Guskov, A., Kern, J., Gabdulkhakov, A., Broser, M., Zouni, A., and Saenger, W. (2009). Cyanobacterial photosystem II at 2.9-angstrom resolution and the role of quinones, lipids, channels and chloride. *Nat. Struct. Mol. Biol.* 16, 334–342. doi: 10.1038/nsmb.1559

Gwizdala, M., Wilson, A., and Kirilovsky, D. (2011). In vitro reconstitution of the cyanobacterial photoprotective mechanism mediated by the orange carotenoid protein in *Synechocystis* PCC 6803. *Plant Cell* 23, 2631–2643. doi: 10.1105/tpc.111.086884

Hakkila, K., Antal, T., Rehman, A. U., Kurkela, J., Wada, H., Vass, I., et al. (2014). Oxidative stress and photoinhibition can be separated in the cyanobacterium *Synechocystis* sp. PCC 6803. *Biochim. Biophys. Acta* 1837, 217–225. doi: 10.1016/j.bbabio.2013.11.011

Herrin, D. L., Battey, J. F., Greer, K., and Schmidt, G. W. (1992). Regulation of chlorophyll apoprotein expression and accumulation – Requirements for carotenoids and chlorophyll. *J. Biol. Chem.* 267, 8260–8269.

Hihara, Y., Kamei, A., Kanehisa, M., Kaplan, A., and Ikeuchi, M. (2001). DNA microarray analysis of cyanobacterial gene expression during acclimation to high light. *Plant Cell* 13, 793–806. doi: 10.1105/tpc.13.4.793

Holt, T. K., and Krogmann, D. W. (1981). A carotenoid-protein from cyanobacteria. *Biochim. Biophys. Acta* 637, 408–414. doi: 10.1016/0005-2728(81)90045-1

Kanesaki, Y., Suzuki, I., Allakhverdiev, S. I., Mikami, K., and Murata, N. (2002). Salt stress and hyperosmotic stress regulate the expression of different sets of genes in *Synechocystis* sp. PCC 6803. *Biochem. Biophys. Res. Commun.* 290, 339–348. doi: 10.1006/bbrc.2001.6201

Kerfeld, C. A. (2004). Water-soluble carotenoid proteins of cyanobacteria. *Arch. Biochem. Biophys.* 430, 2–9. doi: 10.1016/j.abb.2004.03.018

Kerfeld, C. A., Sawaya, M. R., Brahmandam, V., Cascio, D., Ho, K. K., Trevithick-Sutton, C. C., et al. (2003). The crystal structure of a cyanobacterial water-soluble carotenoid binding protein. *Structure* 11, 55–65. doi: 10.1016/S0969-2126(02)00936-X

Komenda, J., Sobotka, R., and Nixon, P. J. (2012). Assembling and maintaining the photosystem II complex in chloroplasts and cyanobacteria. *Curr. Opin. Plant Biol.* 15, 245–251. doi: 10.1016/j.pbi.2012.01.017

Koyama, Y., Kuki, M., Andersson, P. O., and Gillbro, T. (1996). Singlet excited states and the light-harvesting function of carotenoids in bacterial photosynthesis. *Photochem. Photobiol.* 63, 243–256. doi: 10.1111/j.1751-1097.1996.tb03021.x

Kusama, Y., Inoue, S., Jimbo, H., Takaichi, S., Sonoike, K., Hihara, Y., et al. (2015). Zeaxanthin and echinenone protect the repair of photosystem II from inhibition by singlet oxygen in *Synechocystis* sp. PCC 6803. *Plant Cell Physiol.* 56, 906–916. doi: 10.1093/pcp/pcv018

Loll, B., Kern, J., Saenger, W., Zouni, A., and Biesiadka, J. (2005). Towards complete cofactor arrangement in the 3.0 angstrom resolution structure of photosystem II. *Nature* 438, 1040–1044. doi: 10.1038/nature04224

Maccoll, R., and Guard-Friar, D. (1986). *Phycobiliproteins*. Boca Raton, FL: CRC Press.

Masamoto, K., and Furukawa, K. (1997). Accumulation of zeaxanthin in cells of the cyanobacterium, *Synechococcus* sp. strain PCC 7942 grown under high irradiance. *J. Plant Physiol.* 151, 257–261. doi: 10.1093/pcp/pcu199

Masamoto, K., Zsiros, O., and Gombos, Z. (1999). Accumulation of zeaxanthin in cytoplasmic membranes of the cyanobacterium *Synechococcus* sp. strain PCC 7942 grown under high light condition. *J. Plant Physiol.* 155, 136–138. doi: 10.1016/S0176-1617(99)80155-2

Nickelsen, J., Rengstl, B., Stengel, A., Schottkowski, M., Soll, J., and Ankele, E. (2011). Biogenesis of the cyanobacterial thylakoid membrane system – an update. *FEMS Microbiol. Lett.* 315, 1–5. doi: 10.1111/j.1574-6968.2010.02096.x

Nishiyama, Y., and Murata, N. (2014). Revised scheme for the mechanism of photoinhibition and its application to enhance the abiotic stress tolerance of the photosynthetic machinery. *Appl. Microbiol. Biotechnol.* 98, 8777–8796. doi: 10.1007/s00253-014-6020-0

Packer, J. E., Mahood, J. S., Mora-Arellano, V. O., Slater, T. F., Willson, R. L., and Wolfenden, B. S. (1981). Free radicals and singlet oxygen scavengers: reaction of a peroxy-radical with beta-carotene, diphenyl furan and 1,4-diazobicyclo (2,2,2)-octane. *Biochem. Biophys. Res. Commun.* 98, 901–906. doi: 10.1016/0006-291X(81)91196-7

Polivka, T., Kerfeld, C. A., Pascher, T., and Sundstrom, V. (2005). Spectroscopic properties of the carotenoid 3′-hydroxyechinenone in the orange carotenoid protein from the cyanobacterium *Arthrospira maxima*. *Biochemistry* 44, 3994–4003. doi: 10.1021/bi047473t

Powles, S. B. (1984). Photoinhibition of photosynthesis induced by visible-light. *Annu. Rev. Plant Physiol. Plant Mol. Biol.* 35, 15–44. doi: 10.1146/annurev.pp.35.060184.000311

Rakhimberdieva, M. G., Stadnichuk, I. N., Elanskaya, T. V., and Karapetyan, N. V. (2004). Carotenoid-induced quenching of the phycobilisome fluorescence in photosystem II-deficient mutant of *Synechocystis* sp. *FEBS Lett.* 574, 85–88. doi: 10.1016/j.febslet.2004.07.087

Rakhimberdieva, M. G., Vavilin, D. V., Vermaas, W. F., Elanskaya, I. V., and Karapetyan, N. V. (2007). Phycobilin/chlorophyll excitation equilibration upon carotenoid-induced non-photochemical fluorescence quenching in phycobilisomes of the *Synechocystis* sp. PCC 6803. *Biochim. Biophys. Acta* 1767, 757–765. doi: 10.1016/j.bbabio.2006.12.007

Schafer, L., Vioque, A., and Sandmann, G. (2005). Functional in situ evaluation of photo synthesis-protecting carotenoids in mutants of the cyanobacterium *Synechocystis* PCC 6803. *J. Photochem. Photobiol. B Biol.* 78, 195–201. doi: 10.1016/j.jphotobiol.2004.11.007

Scott, M., Mccollum, C., Vasilev, S., Crozier, C., Espie, G. S., Krol, M., et al. (2006). Mechanism of the down regulation of photosynthesis by blue light in the cyanobacterium *Synechocystis* sp. PCC 6803. *Biochemistry* 45, 8952–8958. doi: 10.1021/bi060767p

Sedoud, A., Lopez-Igual, R., Rehman, A. U., Wilson, A., Perreau, F., Boulay, C., et al. (2014). The cyanobacterial photoactive orange carotenoid protein is an excellent singlet oxygen quencher. *Plant Cell* 26, 1781–1791. doi: 10.1105/tpc.114.123802

Shinopoulos, K. E., Yu, J., Nixon, P. J., and Brudvig, G. W. (2014). Using site-directed mutagenesis to probe the role of the D2 carotenoid in the secondary electron-transfer pathway of photosystem II. *Photosynth. Res.* 120, 141–152. doi: 10.1007/s11120-013-9793-6

Sozer, O., Komenda, J., Ughy, B., Domonkos, I., Laczko-Dobos, H., Malec, P., et al. (2010). Involvement of carotenoids in the synthesis and assembly of protein subunits of photosynthetic reaction centers of *Synechocystis* sp. PCC 6803. *Plant Cell Physiol.* 51, 823–835. doi: 10.1093/pcp/pcq031

Staleva, H., Komenda, J., Shukla, M. K., Slouf, V., Kana, R., Polivka, T., et al. (2015). Mechanism of photoprotection in the cyanobacterial ancestor of plant antenna proteins. *Nat. Chem. Biol.* 11, 287–U296. doi: 10.1038/Nchembio.1755

Stamatakis, K., Tsimilli-Michael, M., and Papageorgiou, G. C. (2014). On the question of the light-harvesting role of beta-carotene in photosystem II and photosystem I core complexes. *Plant Physiol. Biochem.* 81, 121–127. doi: 10.1016/j.plaphy.2014.01.014

Steiger, S., Schafer, L., and Sandmann, G. (1999). High-light-dependent upregulation of carotenoids and their antioxidative properties in the cyanobacterium *Synechocystis* PCC 6803. *J. Photochem. Photobiol. B Biol.* 52, 14–18. doi: 10.1016/S1011-1344(99)00094-9

Takahashi, S., and Murata, N. (2008). How do environmental stresses accelerate photoinhibition? *Trends Plant Sci.* 13, 178–182. doi: 10.1016/j.tplants.2008.01.005

Takaichi, S., and Mochimaru, M. (2007). Carotenoids and carotenogenesis in cyanobacteria: unique ketocarotenoids and carotenoid glycosides. *Cell. Mol. Life Sci.* 64, 2607–2619. doi: 10.1007/s00018-007-7190-z

Telfer, A., Frolov, D., Barber, J., Robert, B., and Pascal, A. (2003). Oxidation of the two beta-carotene molecules in the photosystem II reaction center. *Biochemistry* 42, 1008–1015. doi: 10.1021/bi026206p

Toth, T. N., Chukhutsina, V., Domonkos, I., Knoppova, J., Komenda, J., Kis, M., et al. (2015). Carotenoids are essential for the assembly of cyanobacterial photosynthetic complexes. *Biochim. Biophys. Acta* 1847, 1153–1165. doi: 10.1016/j.bbabio.2015.05.020

Umena, Y., Kawakami, K., Shen, J. R., and Kamiya, N. (2011). Crystal structure of oxygen-evolving photosystem II at a resolution of 1.9 angstrom. *Nature* 473, 55–65. doi: 10.1038/nature09913

Van der Weij-de Wit, C. D., Ihalainen, J. A., Van De Vijver, E., D'haene, S., Matthijs, H. C., Van Grondelle, R., et al. (2007). Fluorescence quenching of IsiA in early stage of iron deficiency and at cryogenic temperatures. *Biochim. Biophys. Acta* 1767, 1393–1400. doi: 10.1016/j.bbabio.2007.10.001

Varkonyi, Z., Masamoto, K., Debreczeny, M., Zsiros, O., Ughy, B., Gombos, Z., et al. (2002). Low-temperature-induced accumulation of xanthophylls and its structural consequences in the photosynthetic membranes of the cyanobacterium *Cylindrospermopsis raciborskii*: an FTIR spectroscopic study. *Proc. Natl. Acad. Sci. U.S.A.* 99, 2410–2415. doi: 10.1073/pnas.042698799

Wilson, A., Ajlani, G., Verbavatz, J. M., Vass, I., Kerfeld, C. A., and Kirilovsky, D. (2006). A soluble carotenoid protein involved in phycobilisome-related energy dissipation in cyanobacteria. *Plant Cell* 18, 992–1007. doi: 10.1105/tpc.105.040121

Wilson, A., Boulay, C., Wilde, A., Kerfeld, C. A., and Kirilovsky, D. (2007). Light-induced energy dissipation in iron-starved cyanobacteria: roles of OCP and IsiA proteins. *Plant Cell* 19, 656–672. doi: 10.1105/tpc.106.045351

Wilson, A., Gwizdala, M., Mezzetti, A., Alexandre, M., Kerfeld, C. A., and Kirilovsky, D. (2012). The essential role of the N-terminal domain of the orange carotenoid protein in cyanobacterial photoprotection: importance of a positive charge for phycobilisome binding. *Plant Cell* 24, 1972–1983. doi: 10.1105/tpc.112.096909

Zhang, H., Liu, H., Niedzwiedzki, D. M., Prado, M., Jiang, J., Gross, M. L., et al. (2014). Molecular mechanism of photoactivation and structural location of the cyanobacterial orange carotenoid protein. *Biochemistry* 53, 13–19. doi: 10.1021/bi401539w

Zhang, L., Selao, T. T., Selstam, E., and Norling, B. (2015). Subcellular localization of carotenoid biosynthesis in *Synechocystis* sp. PCC 6803. *PLoS ONE* 10:e0130904. doi: 10.1371/journal.pone.0130904

Zhu, Y., Graham, J. E., Ludwig, M., Xiong, W., Alvey, R. M., Shen, G., et al. (2010). Roles of xanthophyll carotenoids in protection against photoinhibition and oxidative stress in the cyanobacterium *Synechococcus* sp. strain PCC 7002. *Arch. Biochem. Biophys.* 504, 86–99. doi: 10.1016/j.abb.2010.07.007

Conflict of Interest Statement: The authors declare that the research was conducted in the absence of any commercial or financial relationships that could be construed as a potential conflict of interest.

frontiers in Plant Science

ORIGINAL RESEARCH
published: 21 March 2016
doi: 10.3389/fpls.2016.00336

Multiple Impacts of Loss of Plastidic Phosphatidylglycerol Biosynthesis on Photosynthesis during Seedling Growth of Arabidopsis

Koichi Kobayashi[1], *Kaichiro Endo*[1] *and Hajime Wada*[1,2]*

[1] Department of Life Sciences, Graduate School of Arts and Sciences, The University of Tokyo, Tokyo, Japan, [2] Core Research for Evolutional Science and Technology, Japan Science and Technology Agency, Tokyo, Japan

Phosphatidylglycerol (PG) is the only major phospholipid in the thylakoid membrane in cyanobacteria and plant chloroplasts. Although PG accounts only for ∼10% of total thylakoid lipids, it plays indispensable roles in oxygenic photosynthesis. In contrast to the comprehensive analyses of PG-deprived mutants in cyanobacteria, *in vivo* roles of PG in photosynthesis during plant growth remain elusive. In this study, we characterized the photosynthesis of an *Arabidopsis thaliana* T-DNA insertional mutant (*pgp1-2*), which lacks plastidic PG biosynthesis. In the *pgp1-2* mutant, energy transfer from antenna pigments to the photosystem II (PSII) reaction center was severely impaired, which resulted in low photochemical efficiency of PSII. Unlike in the wild type, in *pgp1-2*, the PSII complexes were susceptible to photodamage by red light irradiation. Manganese ions were mostly dissociated from protein systems in *pgp1-2*, with oxygen-evolving activity of PSII absent in the mutant thylakoids. The oxygen-evolving complex may be disrupted in *pgp1-2*, which may accelerate the photodamage to PSII by red light. On the acceptor side of the mutant PSII, decreased electron-accepting capacity was observed along with impaired electron transfer. Although the reaction center of PSI was relatively active in *pgp1-2* compared to the severe impairment in PSII, the cyclic electron transport was dysfunctional. Chlorophyll fluorescence analysis at 77K revealed that PG may not be needed for the self-organization of the macromolecular protein network in grana thylakoids but is essential for the assembly of antenna-reaction center complexes. Our data clearly show that thylakoid glycolipids cannot substitute for the role of PG in photosynthesis during plant growth.

Keywords: phosphatidylglycerol, photosynthesis, thylakoid membrane lipid, chloroplast, photosystem I, photosystem II, electron transport, photodamage

OPEN ACCESS

Edited by:
Julian Eaton-Rye, University of Otago, New Zealand

Reviewed by:
Norihiro Sato, Tokyo University of Pharmacy and Life Sciences, Japan
Yuichiro Takahashi, Okayama University, Japan

***Correspondence:**
Hajime Wada
hwada@bio.c.u-tokyo.ac.jp

Specialty section:
This article was submitted to Plant Cell Biology, a section of the journal Frontiers in Plant Science

Received: *19 December 2015*
Accepted: *04 March 2016*
Published: *21 March 2016*

Citation:
Kobayashi K, Endo K and Wada H (2016) Multiple Impacts of Loss of Plastidic Phosphatidylglycerol Biosynthesis on Photosynthesis during Seedling Growth of Arabidopsis. Front. Plant Sci. 7:336. doi: 10.3389/fpls.2016.00336

INTRODUCTION

The thylakoid lipid bilayer formed by amphipathic glycerolipids serves as a matrix embedded with photosynthesis protein–cofactor complexes forming the electron transport chain. The lipid composition of the thylakoid membrane is highly conserved among cyanobacteria and plant chloroplasts, with glycolipids as major constituents (Mizusawa and Wada, 2012). The only major phospholipid in the thylakoid membrane is phosphatidylglycerol (PG), an anionic lipid with a

negative charge in the phosphoglyceryl head group attached to the diacylglycerol backbone. Although PG accounts only for ∼10 mol% of total thylakoid lipids, this lipid has crucial roles in oxygenic photosynthesis, as described later.

In addition to having a role as building blocks of the thylakoid membrane, lipids serve as structural components of membrane protein complexes to support their structure and function. Many lipid molecules are present in photosystem I (PSI) and PSII complexes. Crystallography analysis of the PSII dimer complex from *Thermosynechococcus vulcanus* at 1.9-Å resolution identified 20 lipid molecules per monomer in the structure; 5 molecules were PG, which were buried near the reaction center with their head groups facing the cytoplasmic side (Umena et al., 2011). In the PSII complex, 3 PGs were located around the primary electron acceptor (Q_A) binding site, one was present at the interface between D1 and CP43 and the other was located near the secondary electron acceptor (Q_B) binding site. In the crystal structure of the PSI complex from *Thermosynechococcus elongatus* at 2.5-Å resolution, 4 lipid molecules were assigned per monomer, and 3 of the 4 molecules were PG (Jordan et al., 2001). One of the 3 PG molecules was located near the reaction center, and the other 2 located between the PsaB and PsaX subunits and near the monomer–monomer interface of the trimeric PSI complex, respectively. Moreover, x-ray crystallography analysis of the light-harvesting complex I (LHCI)-PSI complex from pea at 2.8 Å identified 6 PG molecules in addition to 4 molecules of other thylakoid lipids; 3 PGs were found in the PSI core and another 3 were in the LHCI complex (Qin et al., 2015). PG is also structurally involved in LHCII; in LHCII crystal structures from spinach at 2.7 Å (Liu et al., 2004) and pea at 2.5 Å (Standfuss et al., 2005), one PG molecule was buried at the monomer-monomer interface with the *trans*-Δ^3-hexadecenoic acid at the *sn*-2 position penetrating the deep binding pocket of the trimer.

The role of PG in photosynthesis was initially examined in phospholipase-treated thylakoid membranes in which PG was specifically degraded. Elimination of up to 70% of the original PG from pea thylakoid membranes disrupted electron transport in PSII without decreasing PSI activity (Jordan et al., 1983; Droppa et al., 1995). Moreover, the PSII dimer from spinach (Kruse et al., 2000) and LHCII trimers from pea (Nussberger et al., 1993) were dissociated into monomers by phospholipase A_2 treatment, which suggests a requirement of PG for the structural organization of the PSII-LHCII complex. Likewise, phospholipase A_2 treatment to thylakoid membranes from *Arabidopsis thaliana* inhibited the PSII electron transport at both donor and acceptor sides and disassembled the PSII–LHCII complexes into PSII and LHCII monomers (Kim et al., 2007).

Reverse genetic approaches have greatly contributed to unraveling the functions of PG in oxygenic photosynthesis. Both in plants and cyanobacteria, PG is synthesized from phosphatidic acid through PG phosphate (PGP) as an intermediate (Mizusawa and Wada, 2012). In *Synechocystis* sp. PCC 6803 (hereafter *Synechocystis* 6803), a mutant of the *pgsA* gene encoding PGP synthase was made and characterized to study the role of PG (Hagio et al., 2000). The mutant was unable to synthesize PG but could grow photoautotrophically with PG exogenously supplemented to the growth media. After deprivation of PG from the growth media, the photosynthetic activity of the *pgsA* mutant rapidly decreased with concomitant decrease of PG content, mainly due to the severely impaired PSII function. In the mutant, deprivation of PG inhibited electron transport from Q_A to Q_B (Gombos et al., 2002; Itoh et al., 2012) and destabilized the Mn cluster of the oxygen-evolving complex by dissociating extrinsic proteins (PsbO, PsbV, and PsbU) from the PSII core (Sakurai et al., 2007). The activity of PSI was decreased in *pgsA* as well but only after a longer period of PG deficiency (Domonkos et al., 2004). Long-term PG deprivation induced accumulation of PSI monomer with a decrease in PSI trimer, which is consistent with the existence of a PG molecule in the monomer-monomer interface of PSI from *T. elongatus* (Jordan et al., 2001).

In higher plants, PG is synthesized in plastids, mitochondria, and endoplasmic reticula (ER) membranes (Wada and Murata, 2007). In *A. thaliana*, two isoforms of PGP synthase (PGP1 and PGP2) have been identified; PGP1 is dual localized to plastids and mitochondria (Babiychuk et al., 2003), whereas PGP2 is in the ER (Tanoue et al., 2014). Knockout mutations of PGP1 decreased PG content in leaves by ∼80% from wild-type levels and impaired thylakoid membrane development in chloroplasts (Hagio et al., 2002; Babiychuk et al., 2003). In a T-DNA insertional PGP1 knockout mutant (*pgp1-2*), amounts of PSI and PSII core proteins were substantially decreased with strong transcriptional downregulation of photosynthesis-associated genes (Kobayashi et al., 2015). The photochemical efficiency of PSII was greatly decreased in *pgp1-2*, and further depletion of PG in the mutant by phosphate starvation caused complete loss of the PSII activity (Kobayashi et al., 2015). Despite the severe perturbation of chloroplast functions in *pgp1-2*, the morphology of mitochondria was similar to that in the wild type (Hagio et al., 2002; Babiychuk et al., 2003). A double knockout mutant of PGP1 and PGP2 (*pgp1-2 pgp2*) has an embryonic lethal phenotype with complete loss of PG biosynthesizing activity (Tanoue et al., 2014), so PG biosynthesis by PGP2 at the ER can complement the loss of PGP1 activity in mitochondria but not in chloroplasts in the *pgp1-2* mutant.

Studies in phospholipase-treated thylakoid membranes of plants and in cyanobacterial mutants deficient in PG biosynthesis have elucidated a special requirement of PG for photochemical and electron transport reactions particularly in PSII, as described earlier. Meanwhile, some parts of the PG functions can be substituted by sulfoquinovosyldiacylglycerol (SQDG), another anionic lipid in the thylakoid membrane (Güler et al., 1996; Essigmann et al., 1998; Yu and Benning, 2003). Moreover, as suggested by no or negligible photosynthetic defects in a PGP1 point mutant (*pgp1-1*) with an 80% reduction in the PGP1 activity (Xu et al., 2002; Yu and Benning, 2003), the effect of reduced PG content on photosynthesis may be alleviated to some extent by fine-tuning the photosynthetic systems and lipid metabolism during plant growth. By contrast, the effect of severe loss of plastidic PG biosynthesis on photosynthesis during plant growth is largely unknown.

To gain deep insight into *in vivo* effects of PG biosynthesis on photosynthetic machinery during plant growth, we examined the activity and functionality of photosynthetic components in the PGP1-knockout *pgp1-2* mutant.

MATERIALS AND METHODS

Plant Materials and Growth Conditions

The wild type and *pgp1-2* mutant (the KG10062 line; Hagio et al., 2002) were the Columbia ecotype of *A. thaliana*. Surface-sterilized seeds were cold-treated at 4°C for 3 days in the dark before germination. Unless otherwise stated, plants were grown on Murashige and Skoog medium (adjusted to pH 5.7 with KOH) containing 3% (w/v) sucrose solidified with 0.8% (w/v) agar in plates at 23°C under continuous white light (15 μmol photon m^{-2} s^{-1}). Wild-type and *pgp1-2* plants were grown in a growth chamber (CLE-303, Tomy Seiko, Tokyo) for 14 and 21 days, respectively, to equalize their developmental stages.

Pigment Determination

Lipophilic pigments were extracted with 80% (v/v) acetone from leaves or thylakoid membrane fractions, and debris was removed by centrifugation at 10,000 × *g* for 5 min. The absorbance of the supernatant at 720, 663.2, 646.8, 645, and 470 nm was measured by using the V-730 BIO spectrophotometer (JASCO, Tokyo). The chlorophyll (chl *a* and *b*) and carotenoid contents were determined as described in Melis et al. (1987) and Lichtenthaler (1987), respectively.

Imaging Analysis of Chlorophyll Fluorescence

Seedlings grown on agar plates were dark-incubated for 15 min before measurement. Minimum chlorophyll fluorescence (Fo) and maximum quantum yield of PSII (Fv/Fm) were determined under a saturating pulse with the IMAGING-PAM MAXI chlorophyll fluorometer and the ImagingWin software (Heinz Walz, Effeltrich, Germany). Lowest intensity of measuring light was used to minimize the photosynthetic effect of measuring light.

Photochemical Efficiency Analysis under Light

Photochemical efficiency of PSII under actinic light in leaves was determined with the JUNIOR-PAM chlorophyll fluorometer and the WinControl-3 software (Heinz Walz). Light-response curves of effective quantum yield of PSII (Y_{II}) and quantum yield of non-regulated energy dissipation (Y_{NO}) were determined as described in Kobayashi et al. (2013b). To determine the contribution of photoinhibition-related non-photochemical quenching (qI) to total non-photochemical quenching (qN), leaves dark-adapted for 15 min were exposed to light stress (125 μmol photon m^{-2} s^{-1}) for 10 min and total qN was measured at the end of the light stress. After relaxation of the rapidly reversible qN component with additional dark treatment for 15 min, the remaining qN component was determined as qI.

Measurement of Red-Light Induced Photoinhibition

Leaves detached from seedlings were vacuum-infiltrated with 150 mM sorbitol containing 0 or 1 mg/ml lincomycin and incubated under dim light at room temperature for 3 h. Then leaves were illuminated with or without red LED light (660 nm peak wavelength) (VBL-SL150-RB, Valore, Kyoto, Japan) for 1 h. Red light intensity was measured with the LI-250A light meter and the LI-190SA quantum sensor (LI-COR, Lincoln, USA). Fv/Fm in illuminated leaves was measured with the JUNIOR-PAM fluorometer under lowest measuring light intensity after incubation in darkness for 15 min.

Electron Paramagnetic Resonance (EPR) Spectroscopy

Seedlings were incubated in a growth chamber at 23 or 45°C for 16 h before measurement. EPR spectra from Mn^{2+} were directly obtained from fresh leaves placed in a quartz EPR tube (Tokyo Chemical Industry, Tokyo) with a JES-TE300 X-band (9.2 GHz) spectrometer (JEOL, Tokyo) at room temperature. Measurement conditions were frequency = ∼9.18 GHz, power = ∼1.0 mW, center field = 325 mT, sweep width = 50 mT, sweep time = 4 min, modulation width = 2 mT, amplitude = 500–1000, time constant = 0.3 s. Signal intensity was normalized with fresh weight of leaf samples.

Measurement of Fast-Induction Kinetics of Chlorophyll Fluorescence in Leaves

Leaves were treated with or without 40 μM 3-(3,4-dichlorophenyl)-1,1-dimethylurea (DCMU) in 150 mM sorbitol by vacuum infiltration, followed by dark-incubation for 5 min. Chlorophyll fluorescence transients in leaves were measured in a logarithmic time series between 30 μs and 20 s after the onset of strong actinic light (1650 μmol photon m^{-2} s^{-1}) with a light-emitting diode pump-probe spectrometer (JTS-10, BioLogic, Claix, France).

Measurement of Decay Kinetics of Chlorophyll Fluorescence in Thylakoid Membrane Fractions

Thylakoid membrane fractions of 5 μg/ml chlorophyll concentration were prepared under dim light as described in Allahverdiyeva et al. (2007), but with skipping the washing step with a low osmotic buffer. When required, 40 μM DCMU or 400 μM 1,4-benzoquinone (BQ) was added to the thylakoid fraction. We confirmed that 0.1 % (v/v) ethanol and 1% (v/v) dimethyl sulfoxide, the solvents used to dissolve DCMU and BQ, respectively, did not affect the kinetics. Decay kinetics of chlorophyll fluorescence following a single saturation flash was measured between 0.2 ms and 60 s with the FL3500 fluorometer (Photon Systems Instruments, Brno, Czech). Because small artificial signals were recorded even in the blank sample containing only water, they are subtracted from data as background noises. Fv/Fm values of thylakoid samples were calculated from the minimum (Fo) and maximum (Fm) yields of chlorophyll fluorescence measured before and just after the saturating excitation, respectively.

Chlorophyll Fluorescence Analysis in Thylakoid Membranes at 77K

To prepare stacked thylakoid fractions, seedlings were homogenized in a cold grinding buffer (0.4 M sucrose, 5 mM

$MgCl_2$, 10 mM NaCl, 2 mM EDTA, 2 g/L bovine serum albumin, 2 g/L ascorbic acid, HEPES-NaOH, pH 7.5) under dim light. The homogenates were filtered through a single layer of Miracloth (Merck Millipore, Darmstadt, Germany). After centrifugation at 6000 × *g* for 4 min at 4°C, the pellet was resuspended in a cold resuspension buffer (0.4 M sucrose, 5 mM $MgCl_2$, 10 mM NaCl, HEPES-NaOH, pH 7.5) to obtain 1 μg/ml chlorophyll-containing membrane fractions. To prepare unstacked thylakoids, $MgCl_2$ and NaCl were eliminated from both the grinding buffer and resuspension buffer. A restacked membrane fraction was obtained by adding 5 mM $MgCl_2$ and 10 mM NaCl in a final concentration to the unstacked thylakoid samples, followed by incubation for 1 h at 4°C.

Fluorescence emission spectra of chlorophyll proteins at 77K were obtained from thylakoid membrane fractions in liquid nitrogen by using the RF-5300PC spectrofluorometer (Shimadzu, Kyoto, Japan) under 435- nm excitation.

Measurement of Oxygen-Evolving Activity in Thylakoid Membrane Fractions

Thylakoid membranes were prepared as described in Allahverdiyeva et al. (2007). Steady-state rate of oxygen evolution from thylakoids was measured as 23°C with a Clark-type oxygen electrode (Hansatech, King's Lynn, UK) using 1 mM 2, 6-dimethyl-1, 4-benzoquinone (DMBQ) under saturating white light.

P700 Absorbance Measurement

The light-response curves corresponding to the different redox states of P700 were determined in a batch of leaves at room temperature by measuring the absorbance change at 830–875 nm as a reference with a Dual-PAM-100 (Heinz Walz). Maximum P700 change (Pm) was determined under a saturating far-red light irradiation for 20 s without saturation pulse flash, because saturation pulses caused small artificial signals unaffected by both DCMU and methylviologen (MV) treatments, which was significant in the case of the *pgp1-2* leaves emitting only low signals. The minimum P700 level (Po) in the absence of light was taken as the baseline and the steady-state P700 level (P) was recorded under actinic light. Using these values the ratio of oxidized $P700^+$ to total P700 under a given light treatment was calculated as (P-Po)/(Pm-Po). When required, 40 μM DCMU was used to block electron transfer from PSII.

P700 oxidation-reduction kinetics in leaves was measured by absorbance changes at 705 nm under a weak far-red excitation with the JTS-10 spectrometer (BioLogic). When required, leaf samples were treated with 1 mM MV by vacuum infiltration before measurement to block cyclic electron transport around PSI.

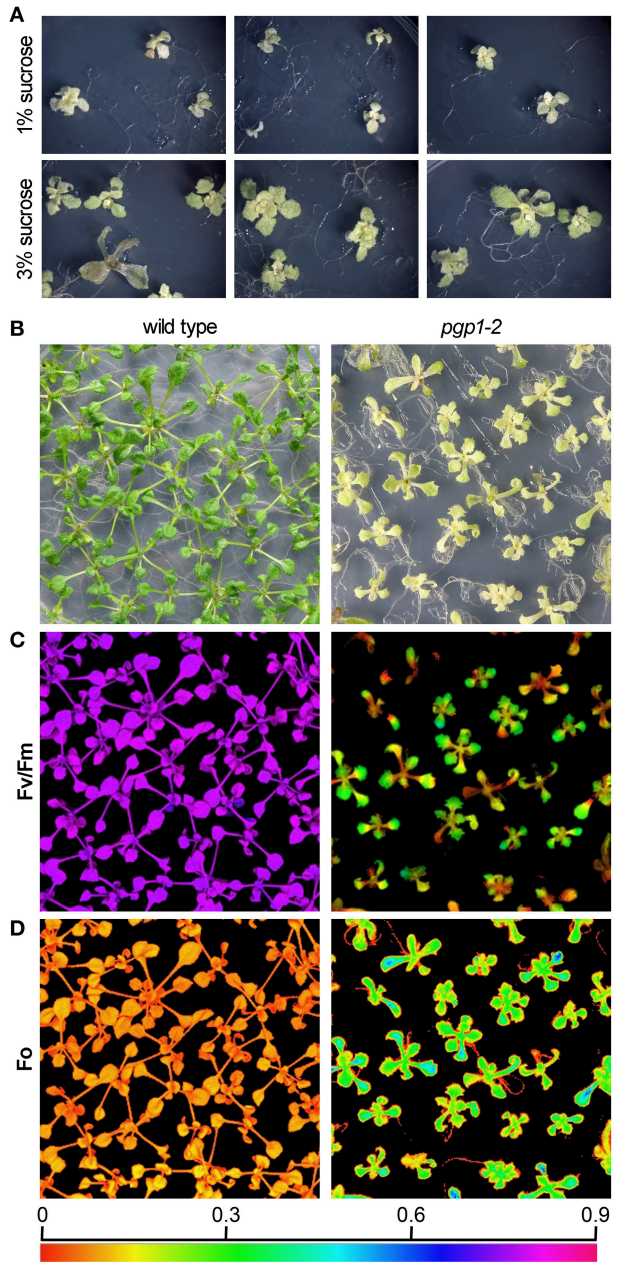

FIGURE 1 | Images of growth and photosynthesis of *pgp1-2* mutant plants in the presence of 3% sucrose. (A) Growth phenotypes of *pgp1-2* seedlings grown for 21 days on agar media containing 1 or 3% sucrose. **(B)** Comparison of growth of 21-days-old *pgp1-2* seedlings with 14-days-old wild type. **(C,D)** Images of **(C)** maximum quantum yield (Fv/Fm) and **(D)** minimum chlorophyll fluorescence (Fo) in dark-adapted seedlings. Seedlings were the same as shown in **(B)** for both wild type and *pgp1-2* plants. The color in **(C,D)** represents the value of each parameter in the color scale.

RESULTS

Impaired Photosynthesis with Decreased Chlorophyll Content in *pgp1-2*

The *pgp1-2* mutant requires exogenous sugars for growth (Hagio et al., 2002). This mutant showed better growth with supplementation of 3% (w/v) sucrose than with 1% sucrose in the growth medium (**Figure 1A**). Even in the presence of 3% sucrose, the growth of *pgp1-2* was slower than that of wild type; 21-days-old *pgp1-2* seedlings were at a growth stage similar to that of 14-days-old wild-type plants (**Figure 1B**). Decreasing

TABLE 1 | Pigment composition in the first and second leaves of seedlings.

	Chl *a* nmol g^{-1} FW	Chl *b* nmol g^{-1} FW	Carotenoids μg g^{-1} FW	Chl *a*/*b* mol/mol	Chl *a*/Carotenoids mmol/g
Wild type	2276.6 ± 117.1	734.2 ± 37.0	463.8 ± 27.0	3.10 ± 0.01	4.91 ± 0.22
pgp1-2	60.6 ± 2.4	28.1 ± 0.9	26.6 ± 0.6	2.16 ± 0.06	2.28 ± 0.12

Values are mean ± SD (n = 4). Chl, chlorophyll.

TABLE 2 | PSII activity in isolated thylakoid membranes.

	Fo (a.u.)	Fm (a.u.)	Fv/Fm	O_2 evolution
Wild type	0.073 ± 0.009	0.266 ± 0.031	0.727 ± 0.006	190 ± 16
pgp1-2	0.326 ± 0.031	0.385 ± 0.045	0.151 ± 0.024	22 ± 4

Thylakoid membrane samples corresponding to 5 μg chlorophyll ml^{-1} were used for both plants. Values are mean ± SD (n = 8 for fluorescence analysis and 3 for O_2 evolution). Fo, minimum yield; Fm, maximum yield; Fv/Fm, maximum quantum yield of PSII. The steady-state rates of O_2 evolution (μmol O_2 mg chlorophyll^{-1} h^{-1}) was measured in the presence of 1 mM DMBQ.

light intensity from about 15 μmol photon m^{-2} s^{-1} to < 5 μmol photon m^{-2} s^{-1} did not alleviate the impaired leaf development, whereas stronger light intensity (∼75 μmol photon m^{-2} s^{-1}) damaged the *pgp1-2* seedlings (Supplemental Figure 1). Thus, we compared 21-days-old *pgp1-2* seedlings with 14-days-old wild-type seedlings under the 3% sucrose condition with 15 μmol photon m^{-2} s^{-1} continuous light for further experiments.

We previously reported that the *pgp1-2* mutation substantially decreased chlorophyll accumulation (Kobayashi et al., 2015). As represented by the pale yellow-green leaf color, chlorophyll content in the first and second true leaves of the *pgp1-2* mutant was only 3% of wild-type levels on a fresh weight basis even under the growth condition with 3% sucrose (**Table 1**). Carotenoid content was also substantially decreased in *pgp1-2* leaves. In the mutant, ratios of chl *a* to chl *b* and to carotenoids were decreased as compared with the wild type (**Table 1**), which suggests greater decrease of photosystem reaction centers than light-harvesting antennas in *pgp1-2*.

Unlike in the wild type, in the *pgp1-2* mutant, chloroplast development in leaves is non-uniform and is limited around vascular tissues in leaves (Hagio et al., 2002; Kobayashi et al., 2015). To examine a spatial pattern of photosynthetic activity in the *pgp1-2* mutant, we determined Fv/Fm in whole seedlings using an imaging pulse amplitude modulation fluorometer (**Figure 1C**). Consistent with our previous analysis that *pgp1-2* plants had reduced Fv/Fm levels in leaves (Kobayashi et al., 2015), the mutant showed very low Fv/Fm values in whole seedlings, with particularly low signals around the shoot apical meristem and petioles. The low Fv/Fm was attributed to high Fo values representing large emission of chlorophyll fluorescence in the dark-adapted state (**Figure 1D**). The higher Fo with lower Fv/Fm in *pgp1-2* mutant than the wild type was also confirmed in thylakoid membrane samples by single-turnover flash-induced chlorophyll fluorescence measurement (**Table 2**). These data suggest that PG deficiency globally occurs in photosynthetic membranes and limits the photosynthetic electron transfer in the *pgp1-2* mutant.

PG Deficiency in *pgp1-2* Plants Increases the Light Susceptibility

To further characterize the functionality of photosynthetic machinery in the *pgp1-2* mutant, we analyzed the quantum yield of PSII (Y_{II}) and non-regulated energy dissipation (Y_{NO}) under increased actinic light intensity. Both wild-type and *pgp1-2* leaves showed a gradual decrease in Y_{II} in response to increased light intensity (**Figure 2A**). The Y_{II} values were substantially lower in the *pgp1-2* mutant than the wild type mainly due to the decreased intrinsic photochemical efficiency of PSII represented by low Fv/Fm (**Figure 1C**). Meanwhile, Y_{NO} values were consistently higher in *pgp1-2* plants than the wild type under all ranges of light intensity (**Figure 2B**). The higher proportion of light energy dissipation in a non-regulated form (Y_{NO}) implies loss of photoprotective mechanisms in the *pgp1-2* mutant (Kramer et al., 2004). Although the level of non-photochemical quenching (qN) was similar in the *pgp1-2* mutant and the wild type, the proportion of the photoinhibitory component (qI) to total qN was substantially higher in the mutant; in fact, most of the qN was attributed to the qI component in the mutant (**Figure 2C**).

To investigate the photoinhibition mechanism in *pgp1-2* plants, we illuminated leaves with various intensities of red light in the presence or absence of lincomycin, an inhibitor of protein synthesis in chloroplasts, for 1 h and then measured Fv/Fm values in the leaves after dark adaptation for 15 min (**Figure 3**). In wild-type leaves, Fv/Fm was only slightly decreased in response to increased red light intensities even in the presence of lincomycin. The data were consistent with observations that red light has little photoinhibitory effect on undamaged leaves (Ohnishi et al., 2005; Sarvikas et al., 2006; Takahashi et al., 2010). By contrast, in the absence of lincomycin, Fv/Fm was strongly decreased in *pgp1-2* leaves in response to increased red light intensity, and the decrease was further enhanced by lincomycin treatment. These data indicate that photoinhibition of PSII is strongly enhanced particularly in the damage process in *pgp1-2* mutant.

Oxygen-Evolving Activity of PSII is Abolished in *pgp1-2*

In the *Synechocystis* 6803 *pgsA* mutant, the Mn cluster of the oxygen-evolving complex is destabilized by PG deprivation with the extrinsic proteins being dissociated from the PSII complex (Sakurai et al., 2007). To examine the state of Mn in *pgp1-2* cells

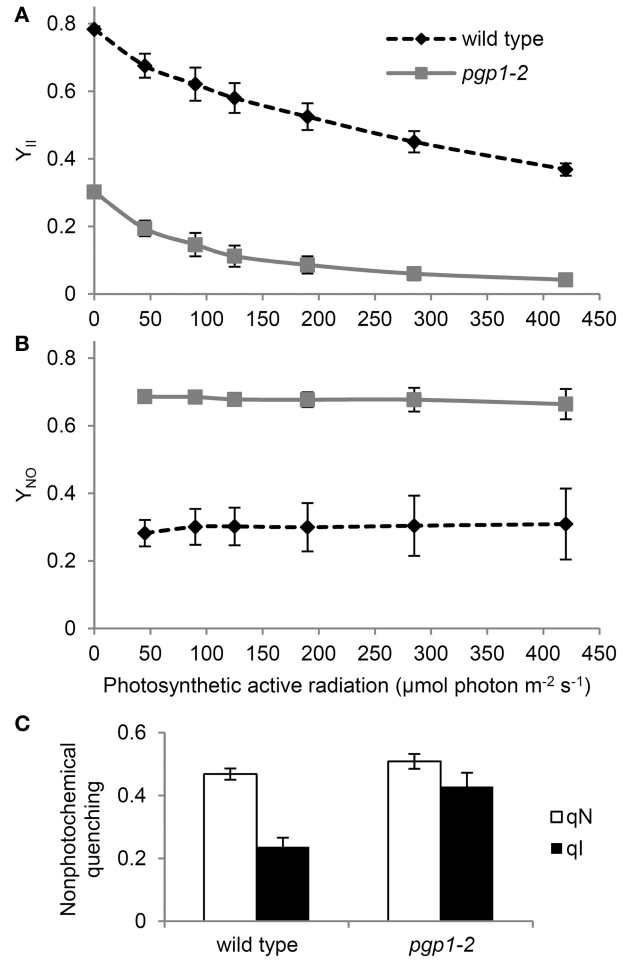

FIGURE 2 | Photosynthetic parameters of wild-type and *pgp1-2* seedlings. (A,B) Light-response curves of **(A)** effective quantum yield of PSII (Y_{II}) and **(B)** quantum yield of non-regulated energy dissipation (Y_{NO}). **(C)** Contribution of photoinhibition (qI) to total non-photochemical quenching (qN) under 125 μmol photon m^{-2} s^{-1} photosynthetic active radiation. Data are mean ± SE from 3 independent experiments.

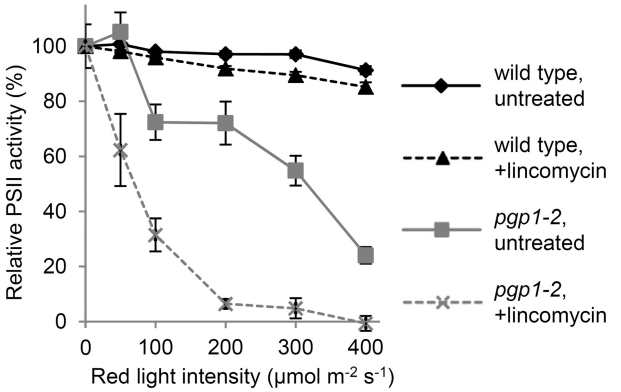

FIGURE 3 | Photoinhibition of Photosystem II (PSII) activity under red-light irradiation. Maximum quantum yield of PSII (Fv/Fm) was determined as a measure of PSII activity after red light irradiation for 1 h. Before red light irradiation, leaves were treated with or without lincomycin for 3 h. Data are mean ± SE from 8 independent experiments.

in vivo, we performed EPR spectroscopic analysis in intact leaves (**Figure 4**). The feature of the EPR-spectrum of protein-unbound Mn^{2+} is its sextet signals (Morsy and Khaled, 2002). In wild-type seedlings incubated at 23°C, no clear sextet lines from Mn^{2+} were detected. However, Mn^{2+} signals emerged with incubation at 45°C. Thus, in the wild type, most Mn^{2+} ions are integrated into protein systems but are dissociated from the complexes by heat treatment. In *pgp1-2* seedlings, fine sextet lines of Mn^{2+} were detected even at 23°C, so Mn^{2+} ions exist as a free form in the *pgp1-2* seedlings.

To directly determine the PSII activity in the *pgp1-2* mutant, oxygen-evolving activity was measured in the thylakoid membrane fraction in the presence of the artificial electron acceptor DMBQ (**Table 2**). Consistent with the result in the *Synechocystis* 6803 *pgsA* mutant, oxygen-evolving activity was almost abolished in the *pgp1-2* mutant.

Energy Transfer from Antenna Pigments to the PSII Reaction Center is Severely Impaired in *pgp1-2* Mutant

To evaluate electron transport activity in the *pgp1-2* mutant, we analyzed the induction kinetics of chlorophyll fluorescence in leaves in a logarithmic time series (**Figure 5**). The wild-type leaves showed a slow polyphasic increase of chlorophyll fluorescence after actinic light irradiation, which is explained by a stepwise retardation of the photosynthetic electron flow from primary photochemical reactions in PSII to later reduction processes at the acceptor side of PSI (Krause, 1991). In the presence of DCMU, which inhibits electron transport from Q_A to Q_B, chlorophyll fluorescence rapidly peaked because reoxidation of Q_A^- was inhibited. In *pgp1-2* leaves, chlorophyll fluorescence quickly increased in the absence of DCMU. In the presence of DCMU, fluorescence increase was further accelerated, although the fluorescence decreased after peaking at about 5 ms. Very fast increase of chlorophyll fluorescence in the *pgp1-2* mutant suggests that the electron-transfer capability of PSII is very limited in the mutant. In *pgp1-2* leaves, particularly in the presence of DCMU, continuous irradiation of strong actinic light might severely damage PSII complexes and cause strong quenching of chlorophyll fluorescence.

Different Characteristics of Electron Transfer at the PSII Acceptor Side between *pgp1-2* and *Synechocystis* 6803 *pgsA* Mutant

In the *Synechocystis* 6803 *pgsA* mutant, PG deprivation strongly impairs electron transfer from Q_A to Q_B, particularly in the presence of artificial electron acceptors such as BQ (Hagio et al., 2000; Gombos et al., 2002; Itoh et al., 2012). To ascertain whether this also occurs in the *pgp1-2* mutant, we analyzed decay of single flash-induced chlorophyll fluorescence in thylakoid membrane fractions from wild-type and *pgp1-2* leaves (**Figure 6**). The decay

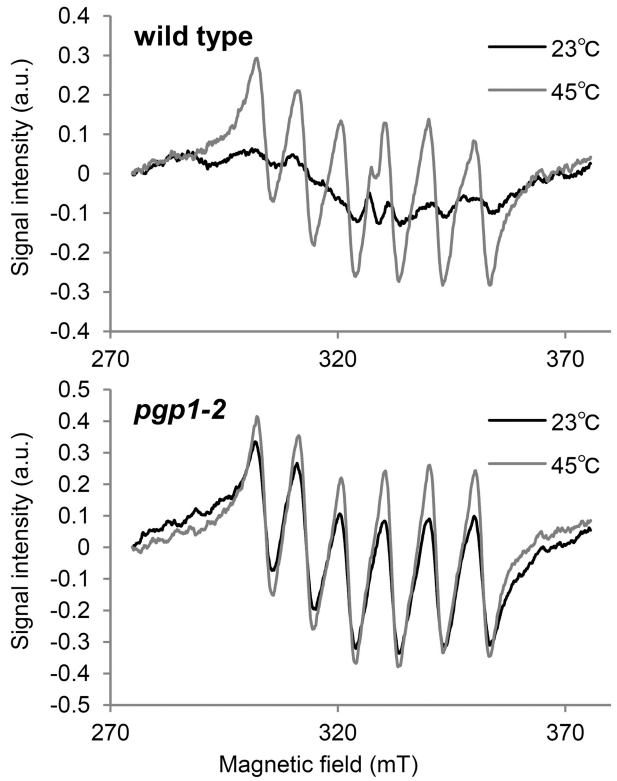

FIGURE 4 | Electron paramagnetic resonance spectra of Mn^{2+} in leaves incubated for 23 or 45°C for 16 h. Signal intensity was normalized to fresh weight of the samples. Data are means from 3 independent experiments.

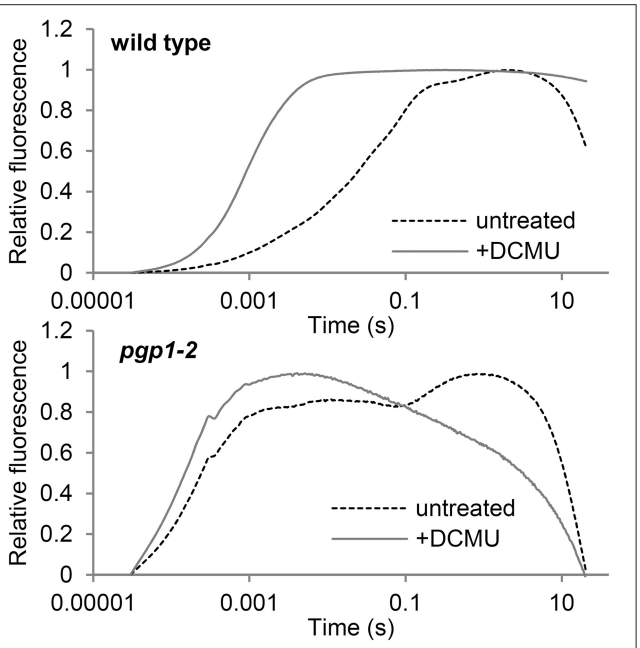

FIGURE 5 | Transient fluorescence induction kinetics of chlorophyll in leaves treated with or without DCMU. Data are means from 3 independent experiments.

profiles reflect reoxidation kinetics of Q_A, which can be divided into 3 processes (Krause, 1991): (1) fast fluorescence decay (< 1 ms) related to the electron transfer from Q_A^- to a plastoquinone bound to the Q_B pocket; (2) middle exponential decay (∼2 ms) related to the reoxidation of Q_A^- by a plastoquinone molecule moving from the plastoquinone pool to the empty Q_B pocket; and (3) slow decay (∼1 s) related to reoxidation of Q_A^- by charge recombination with donor-side components.

In the absence of BQ, fluorescence decay was slower for the *pgp1-2* mutant than the wild type through the fast to the middle phase (**Figure 6A**), which suggests that reoxidation of Q_A^- by Q_B and the plastoquinone pool is impaired in *pgp1-2* thylakoids. In the wild type, BQ treatment accelerated the decay of chlorophyll fluorescence particularly in the middle phase (**Figure 6B**). In *pgp1-2* leaves, the fluorescence decay was almost unchanged by BQ treatment, which contrasted with the strong impairment of Q_A^- reoxidation with BQ supplementation in the *pgsA* mutant (Itoh et al., 2012). In **Figure 6C**, the variable fluorescence decays with similar kinetics in wild type and the *pgp1-2* mutant. The slow fluorescence decay in the DCMU-treated sample mainly resulted from charge recombination between Q_A^- and the donor-side components. These data suggest that charge recombination with the donor-side components is not notably affected in the mutant but reoxidation of Q_A^- at the acceptor side is retarded independently of the effect of artificial quinones.

Cyclic Electron Flow around PSI is Dysfunctional in the *pgp1-2* Mutant

To assess whether the PSI activity is also affected by the *pgp1-2* mutation, we examined the redox state of the primary electron donor chlorophyll (P700) of the PSI reaction center under increased actinic light intensity (**Figure 7A**). In the presence of DCMU, P700 in both wild-type and *pgp1-2* leaves was mostly oxidized even under low actinic light conditions because of the blockage of electron transfer from PSII by DCMU. In the absence of DCMU, P700 in wild-type leaves was highly reduced under low actinic light mainly by linear electron transfer from PSII but was gradually oxidized in response to increased light intensity. By contrast, P700 in *pgp1-2* leaves was highly oxidized under low actinic light irradiation in the absence of DCMU. The data suggest that the electron donation from PSI to the acceptor side is more active than electron supply to PSI from the donor side.

To further assess the functionality of PSI in the *pgp1-2* mutant, kinetics of P700 oxidation by far-red light irradiation was measured in leaves by monitoring absorbance at 705 nm in the presence or absence of 1 mM MV (**Figure 7B**). MV with this high concentration efficiently accepts electrons from all PSI and thus abolishes the cyclic electron flow around PSI. In wild-type leaves treated with MV, rapid oxidation of P700 was observed as was reported previously (Joliot and Joliot, 2005). However, in the absence of MV, kinetics of P700 oxidation was slowed, which indicates reinjection of electrons to P700 via the cyclic pathway. In the *pgp1-2* leaves, P700 oxidation kinetics were similar with and without MV. The data suggest that cyclic electron flow is impaired in the *pgp1-2* mutant. Moreover, as compared with

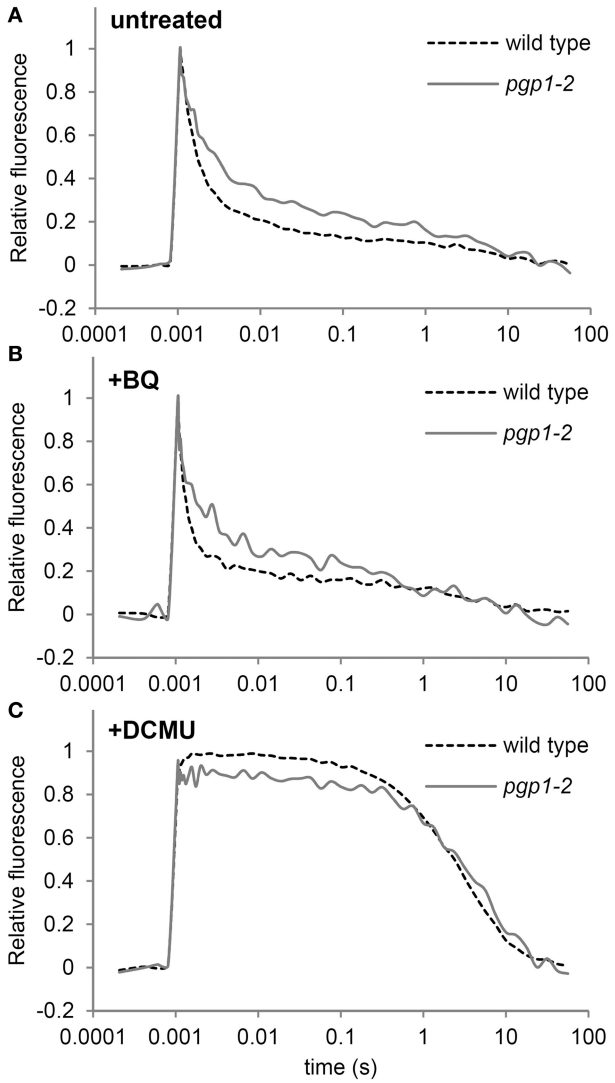

FIGURE 6 | Q_A^- reoxidation kinetics following a single saturating flash in thylakoid membrane fractions. Fluorescence decay kinetics of chlorophyll were measured **(A)** in the absence or **(B)** presence of 1,4-benzoquinone (BQ) and **(C)** DCMU. Thylakoid membrane samples corresponding to 5 μg/ml chlorophyll were used for all measurements. Data are means from 4 independent experiments.

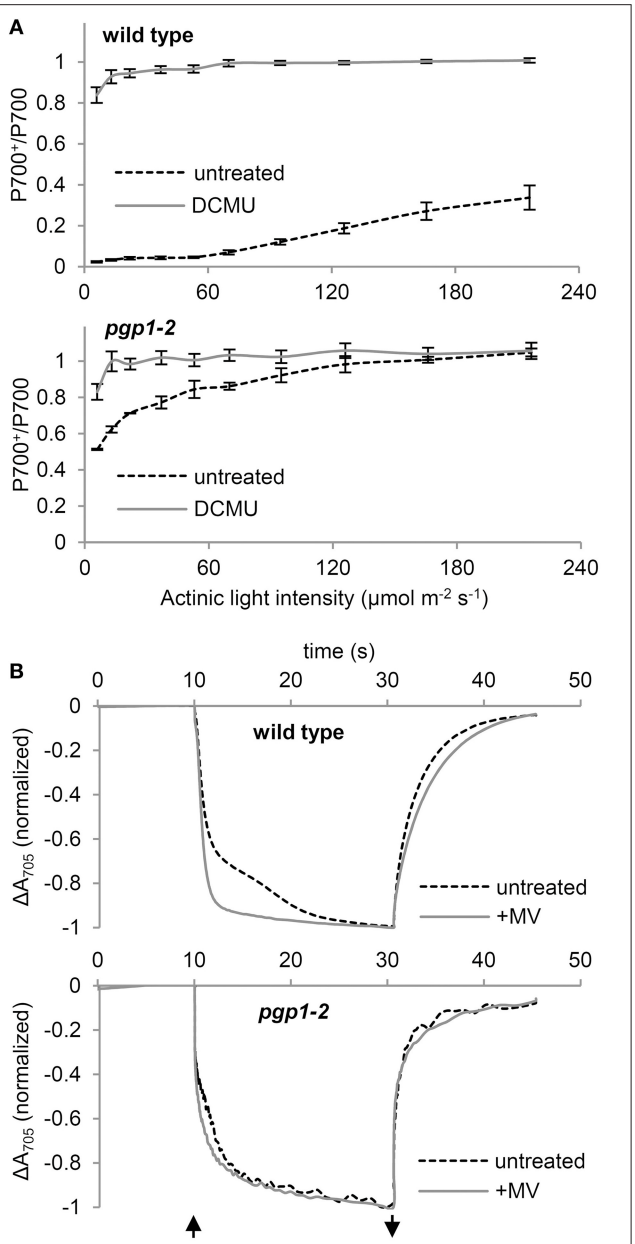

FIGURE 7 | P700 oxidation kinetics in leaf samples. (A) Light-response curve of P700 oxidation in the absence or presence of DCMU. **(B)** P700 oxidation-reduction kinetics in response to far-red light irradiation in the absence or presence of 1 mM methylviologen (MV). The upward and downward arrows represent the start and end of far-red light illumination, respectively.

wild-type leaves treated with MV, P700 oxidation kinetics were slower in MV-treated *pgp1-2* leaves.

PG Deficiency in *pgp1-2* Plants Perturbs Interaction between Antenna Complexes and Reaction Centers

Thylakoid membrane lipids greatly affect energetic interactions between reaction centers and antenna complexes. In fact, chlorophyll fluorescence at 77K, which reflects interaction states of photosystem–antenna complexes and structural organization of thylakoids (Krause, 1991; Andreeva et al., 2003; Kirchhoff et al., 2007), was remarkably changed in mutants defective in thylakoid lipid biosynthesis, including the *pgp1-2* mutant (Härtel et al., 1997; Kobayashi et al., 2013a, 2015). To gain insight into the effect of the lack of PG on protein arrangement in the thylakoid membrane, we examined the effect of cations on membrane organization in the *pgp1-2* mutant by measuring chlorophyll fluorescence spectra at 77K (**Figure 8**). The thylakoid membrane fraction from wild-type leaves showed two major peaks at 682 nm from the PSII-LHCII complex and at 731 nm from the PSI-LHCI complex. In the presence of cations (NaCl and $MgCl_2$), LHCII was tightly connected with PSII in stacked

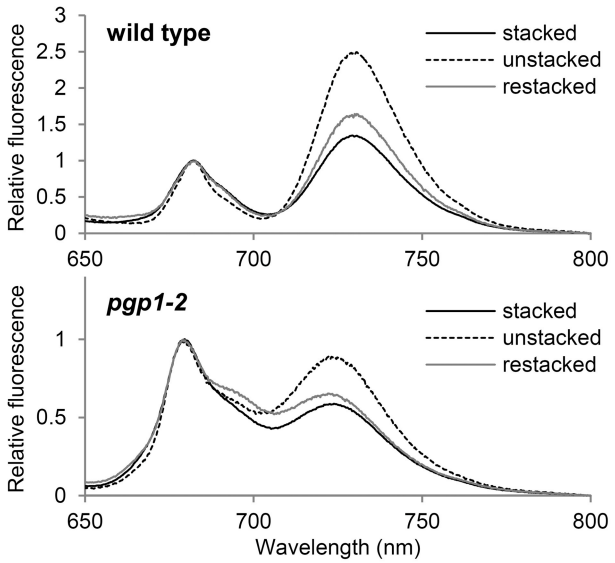

FIGURE 8 | Chlorophyll fluorescence spectra at 77K in the thylakoid membrane fraction (1 μg/ml chlorophyll). Stacked and unstacked samples were prepared with or without 5 mM $MgCl_2$ and 10 mM NaCl, respectively. Restacked membranes were prepared by incubating unstacked thylakoid samples with 5 mM $MgCl_2$ and 10 mM NaCl for 1 h.

grana regions (Kirchhoff et al., 2007), which resulted in high fluorescence emission from the PSII complexes (**Figure 8**). Depletion of cations in the buffer induced unstacking of the grana thylakoids and caused a spillover of excitation energy from LHCII to PSI as indicated by increased fluorescence emission from the PSI complex. Supplementation of cations to unstacked thylakoids induced restacking and decreased the emission from PSI probably due to a reduced energetic connection between PSI and LHCII (Kirchhoff et al., 2007).

As reported previously (Kobayashi et al., 2015), in *pgp1-2* thylakoids, emissions from PSII and PSI were both blue-shifted to 679 and 724 nm, respectively, which implies dissociation of antenna complexes from each reaction center. As observed in wild-type samples, fluorescence emission from PSI relative to that from PSII was increased in the *pgp1-2* mutant by preparing thylakoids in the absence of cations but was decreased with the addition of cations to the membrane samples (**Figure 8**). The changes in energy distribution between PSII and PSI did not accompany notable shifts of peak wavelength, which suggests that global rearrangement of the thylakoid membrane environment does not affect an intrinsic structure of photosystem core-antenna complexes in the mutant.

DISCUSSION

Pleiotropic Effects of the *pgp1-2* Mutation on Photosynthetic Activities in the Thylakoid Membrane

In this study, the *pgp1-2* mutant, which lacks the ability to synthesize PG in plastids (Hagio et al., 2002), showed various defects in photochemical and electron transport activities in the thylakoid membrane. The very high Fo levels in the mutant (**Figure 1D** and **Table 2**) suggest that the energy transfer from antenna pigments to the open PSII reaction center is severely impaired, which results in loss of absorbed energy as fluorescence and decreased PSII photochemical efficiency. Dissociation of light-harvesting antenna complexes from the PSII core complex (**Figure 8**) may cause the energetic disconnection between the reaction center and antenna complexes in the mutant. Because high Fo is observed in mutants deficient in PSII (Meurer et al., 1996; Shikanai et al., 1999), PSII core components may be largely deficient in the *pgp1-2* mutant as suggested in the lack of oxygen evolution (**Table 2**). Upon illumination, chlorophyll fluorescence from the mutant PSII immediately reached nearly the maximal level (**Figure 5**), which reflects very small electron-accepting capacity of Q_A and the plastoquinone pool. Consistent with a larger decrease in reaction center proteins than that in LHC proteins in *pgp1-2* seedlings (Kobayashi et al., 2015), the mutant showed lower ratio of chl *a* to chl *b* and to carotenoids (**Table 1**), which may explain in part the decreased PSII capacity in *pgp1-2* plants. In addition, accumulation of oxidized P680, the primary electron donor of PSII, with the dysfunctional oxygen-evolving complex may inhibit repeated photochemical reactions in the mutant, thereby causing a rapid rise of chlorophyll fluorescence from the antenna systems. In the presence of DCMU, chlorophyll fluorescence from *pgp1-2* leaves was strongly quenched soon after peaking (**Figure 5**). Interestingly, similar kinetic profiles were observed in spinach monomeric PSII core complexes incubated with PG or SQDG in the absence of DCMU (Kansy et al., 2014). Excessive imbalance in the thylakoid lipid composition with more or less anionic lipids may strongly perturb the intrinsic PSII electron transport.

In vitro biochemical analysis demonstrated that degradation of phospholipids in the pea thylakoid membrane did not decrease PSI activity (Jordan et al., 1983). Moreover, in the *Synechocystis* 6803 *pgsA* mutant, decreased PSI activity was observed only after a longer period of PG deprivation (>2 weeks; Domonkos et al., 2004). These data suggest less importance for PG in the function of PSI. Indeed, compared to the crucial defects of the mutant PSII, PSI seemed relatively active in *pgp1-2* plants (**Figure 7A**). Considering the high structural stability of PSI, the interaction of PG molecules with PSI core proteins may be stronger than with PSII, so the effect of PG deprivation may be primarily observed in the PSII function. However, kinetic analysis of P700 oxidation showed that the cyclic electron pathway is dysfunctional in the *pgp1-2* mutant (**Figure 7B**). Moreover, the P700 oxidation kinetics in the presence of MV was slower in the mutant than the wild type, which may be attributed to an enhanced charge recombination within the PSI reaction center and/or inefficient energy transfer from the LHCI as suggested in the 77K chlorophyll fluorescence (**Figure 8**). X-ray crystallographic analyses revealed that PG molecules are structural components of the PSI complex in both cyanobacteria (*T. elongatus*; Jordan et al., 2001) and plants (*Pisum sativum*; Qin et al., 2015). Therefore, PG in the PSI complex, which may be resistant to phospholipase treatments (Jordan et al., 1983) and short-term PG deprivation (Domonkos et al., 2004), may also play an important role in the PSI activity.

In *pgp1-2*, the PGP2 isoform is functional in ER (Tanoue et al., 2014). Although total PG content is substantially decreased in the mutant (Hagio et al., 2002; Kobayashi et al., 2015), whether PGP2 can provide a significant amount of PG for chloroplasts remains undetermined. We previously reported that phosphate starvation further decreased total PG levels in *pgp1-2* mutant, which resulted in complete loss of Fv/Fm despite of accumulation of thylakoid membrane glycolipids (Kobayashi et al., 2015). Thus, PG produced by PGP2 may be partially transported into chloroplasts and support the marginal photosynthetic activity in *pgp1-2* plants, but further depletion of PG by phosphate starvation may completely abolish the PSII photochemical activity.

The *pgp1-2* Mutation Caused Strong Photodamage

The impaired energy transfer from antenna pigments to the PSII reaction center and decreased electron-accepting capacity of PSII plastoquinones could increase non-photochemical dissipation of light energy within the antenna system. The very high Y_{NO} levels in *pgp1-2* mutant (**Figure 2B**) represent enhanced dissipation of absorbed light energy as a non-regulated form of fluorescence or heat, which indicates limited photoprotective capacity in the mutant. In fact, the non-photochemical quenching in the *pgp1-2* mutant was predominantly caused by photoinhibition of PSII (**Figure 2C**), which is consistent with the *pgp1-2* PSII being very susceptible to photodamage under red light irradiation (**Figure 3**).

Recent studies have proposed that photodamage to PSII occurs in two steps: first, the Mn cluster of oxygen-evolving complex is damaged by UV or blue light presumably via direct excitation of Mn, and second, the photochemical reaction center of PSII is inactivated by photosynthetically active light absorbed by chlorophyll (Tyystjärvi, 2008; Murata et al., 2012). Irradiation of red light alone has little effect on the PSII photoinhibition in the wild type, as was reported previously (Ohnishi et al., 2005; Sarvikas et al., 2006; Takahashi et al., 2010), but it strongly inactivated the PSII photochemical reaction in the *pgp1-2* mutant (**Figure 3**). As suggested by the dissociation of Mn^{2+} ions from protein systems in the mutant leaves (**Figure 4**) and lack of oxygen-evolving activity in the thylakoids from the mutant (**Table 2**), the Mn cluster in *pgp1-2* mutant may be dysfunctional, so the mutant PSII may be susceptible to red light. The finding in *Synechocystis* 6803 that PG is required for the stabilization of the Mn cluster in the oxygen-evolving complex (Sakurai et al., 2007) supports this hypothesis. Because the effects of the *pgp1-2* mutation on photosynthesis were pleiotropic, other defects such as impaired photochemical reactions or acceptor-side limitations might also be responsible for photoinhibition of the mutant PSII.

The severe defects in leaf development with reduced mesophyll cells in *pgp1-2* plants (Hagio et al., 2002; Kobayashi et al., 2015) may be explained in part by photodamage of developing chloroplasts. Indeed, the growth of *pgp1-2* seedlings was damaged under continuous 75 μmol photon m^{-2} s^{-1} light (Supplemental Figure 1). However, the development of *pgp1-2* leaves was perturbed even under dim light (<5 μmol photon m^{-2} s^{-1}), which suggests a specific role of PG synthesized in chloroplasts in leaf development.

Effect of the *pgp1-2* Mutation on the Acceptor Side of PSII

In *Synechocystis* 6803, deprivation of PG caused impaired electron transport from Q_A^- to Q_B, and the impairment was further enhanced by BQ treatment (Gombos et al., 2002; Itoh et al., 2012). Retarded electron transfer at the acceptor side of PSII was also observed in the *pgp1-2* thylakoids (**Figure 6A**), consistent with the reports that phospholipase treatment inhibits electron transport at the Q_B site in thylakoid membranes isolated from plant leaves (Droppa et al., 1995; Kim et al., 2007). However, unlike in the *pgsA* mutant, in *pgp1-2* leaves, BQ treatment did not inhibit Q_A reoxidation in thylakoids. In *Synechocystis* 6803, PG deficiency may change the structure around the Q_B site so that it becomes inactivated by BQ (Itoh et al., 2012). Furthermore, with site-directed mutations in the *Synechocystis* 6803 D1 protein disrupting interactions with PG around the Q_A binding site, the Q_B-related site was sensitive to BQ-mediated inactivation, which suggests PG molecules near the Q_A site are important for the function of the Q_B site (Endo et al., 2015). Therefore, the mode of interaction between PG and proteins in the PSII reaction center may differ between *A. thaliana* and *Synechocystis* 6803, although both organisms require PG to maintain the function of the acceptor side of PSII.

Involvement of PG in Organization of Antenna-Core Complexes of Photosystems

Biochemical approaches with phospholipases have revealed the importance of PG for the assembly of PSII-LHCII complexes. Phospholipase A_2 treatments disassembled the spinach PSII dimer into monomers (Kruse et al., 2000), pea LHCII trimers into monomers (Nussberger et al., 1993), and *A. thaliana* PSII-LHCII complexes into PSII and LHCII monomers (Kim et al., 2007). Consistent with these findings, the *pgp1-2* thylakoids at 77K emitted chlorophyll fluorescence at ∼680 nm (**Figure 8**), which suggests accumulation of free LHCII uncoupled from PSII. Furthermore, 77K fluorescence emission at ∼723 nm suggests dissociation of LHCI from the PSI core, which may cause slower P700 oxidation in the presence of MV by far-red light in *pgp1-2* mutant than the wild type (**Figure 7B**). In the crystal structure of the pea PSI-LHCI complex, 3 PG molecules were identified in LHCI in addition to one PG molecule locating between LHCI and the PSI core (Qin et al., 2015). Thus, PG molecules in the complex may be involved in the association of PSI with LHCI.

Formation of the supramolecular networks of photosystems in grana thylakoids is self-organized and the balance between negative thylakoid surface charges and cations such as Mg^{2+} would play a crucial role (Kirchhoff et al., 2007). Low salt conditions cause an intermixing and randomization of the protein complex along with unstacking of the grana thylakoids, presumably by electrostatic repulsion of negative thylakoid surface charges. Such changes increase spillover of excitation energy from the PSII antenna system to the PSI (**Figure 8**; Kirchhoff et al., 2007). Incubation of the unstacked thylakoids

with cations induces restacking of grana and rearrangement of PSII-LHCII supercomplexes, which leads to reduced energy spillover from PSII to PSI (**Figure 8**). As in wild-type thylakoids, *pgp1-2* thylakoids show an increase and decrease in the fluorescence emission from PSI in response to elimination and re-addition of cations, respectively. Thus, PG may not be needed for the self-organization of macromolecular protein networks formed in stacked grana thylakoids, although it is essential for the intrinsic assembly of antenna complexes with photosystem reaction centers. These results are consistent with the observation that enhanced biosynthesis of glycolipids including SQDG by phosphate starvation caused extensive stacking of the thylakoid membrane in the *pgp1-2* mutant but could not induce association of LHC antennas with PS core complexes (Kobayashi et al., 2015).

We previously reported that the amount of PS core proteins was decreased more strongly than that of LHC proteins in *pgp1-2* plants, although downregulation of genes encoding PS core proteins (*psaA* and *psbA*) was weaker than that of *LHC* genes (*LHCA4* and *LHCB6*; Kobayashi et al., 2015). Considering the importance of PG for the assembly of PS-LHC complexes, PG in chloroplasts may be required for stabilizing the core proteins during translation or post-translational assembly in complexes.

CONCLUSION

Loss of plastidic PG biosynthesis by the *pgp1-2* mutation caused severely impaired electron transfer both in donor and acceptor sides of PSII and energetic uncoupling between PSII and LHCII, which would cause strong photodamage to PSII and presumably affected leaf development in part. Functionality of PSI was also affected by the mutation. By contrast, an 80% reduction in the PGP1 activity in *pgp1-1* mutant caused no remarkable defects in photochemical and electron transport activities, although it decreased chlorophyll content and mesophyll cell number (Xu et al., 2002; Yu and Benning, 2003). Thus, in the *pgp1-1* mutant, photosynthetic efficiency may be maintained by fine-tuning the quality and quantity of photosynthetic components to the reduced PG content and by increasing another anionic lipid, SQDG, to substitute for some functions of PG. However, in the *pgp1-2* mutant, the stress with critical loss of PG in chloroplasts might exceed the homeostatic capacity of plants and cause fatal damage to photosynthetic machinery directly and indirectly.

AUTHOR CONTRIBUTIONS

HW directed the study. KK and HW designed the experiments. KK and KE performed the experiments and analyzed the data. KK wrote the manuscript.

ACKNOWLEDGMENTS

We thank Dr. Krishna K. Niyogi, Department of Plant and Microbial Biology, University of California, Berkeley, for providing access to equipment for photosynthetic measurements and valuable comments. We thank Dr. Atsushi Okazawa, Graduate School of Arts and Sciences, The University of Tokyo, for a technical support in the EPR analysis. This work was supported by Grants-in-Aid for Scientific Research on Priority Areas (No. 24770055 and 26711016).

SUPPLEMENTARY MATERIAL

The Supplementary Material for this article can be found online at: http://journal.frontiersin.org/article/10.3389/fpls.2016.00336

REFERENCES

Allahverdiyeva, Y., Mamedov, F., Suorsa, M., Styring, S., Vass, I., and Aro, E. M. (2007). Insights into the function of PsbR protein in *Arabidopsis thaliana*. *Biochim. Biophys. Acta.* 1767, 677–685. doi: 10.1016/j.bbabio.2007.01.011

Andreeva, A., Stoitchkova, K., Busheva, M., and Apostolova, E. (2003). Changes in the energy distribution between chlorophyll–protein complexes of thylakoid membranes from pea mutants with modified pigment content. I. Changes due to the modified pigment content. *J. Photochem. Photobiol. B Biol.* 70, 153–162. doi: 10.1016/S1011-1344(03)00075-7

Babiychuk, E., Müller, F., Eubel, H., Braun, H.-P., Frentzen, M., and Kushnir, S. (2003). *Arabidopsis* phosphatidylglycerophosphate synthase 1 is essential for chloroplast differentiation, but is dispensable for mitochondrial function. *Plant J.* 33, 899–909. doi: 10.1046/j.1365-313X.2003.01680.x

Domonkos, I., Malec, P., Sallai, A., Kovács, L., Itoh, K., Shen, G., et al. (2004). Phosphatidylglycerol is essential for oligomerization of photosystem I reaction center. *Plant Physiol.* 134, 1471–1478. doi: 10.1104/pp.103.037754

Droppa, M., Horváth, G., Hideg, É., and Farkas, T. (1995). The role of phospholipids in regulating photosynthetic electron transport activities: Treatment of thylakoids with phospholipase C. *Photosynth. Res.* 46, 287–293. doi: 10.1007/BF00020442

Endo, K., Mizusawa, N., Shen, J.-R., Yamada, M., Tomo, T., Komatsu, H., et al. (2015). Site-directed mutagenesis of amino acid residues of D1 protein interacting with phosphatidylglycerol affects the function of plastoquinone Q_B in photosystem II. *Photosynth. Res.* 126, 385–397. doi: 10.1007/s11120-015-0150-9

Essigmann, B., Güler, S., Narang, R. A., Linke, D., and Benning, C. (1998). Phosphate availability affects the thylakoid lipid composition and the expression of *SQD1*, a gene required for sulfolipid biosynthesis in *Arabidopsis thaliana*. *Proc. Natl. Acad. Sci. U.S.A.* 95, 1950–1955.

Gombos, Z., Várkonyi, Z., Hagio, M., Iwaki, M., Kovács, L., Masamoto, K., et al. (2002). Phosphatidylglycerol requirement for the function of electron acceptor plastoquinone Q_B in the photosystem II reaction center. *Biochemistry* 41, 3796–3802. doi: 10.1021/bi011884h

Güler, S., Seeliger, A., Härtel, H., Renger, G., and Benning, C. (1996). A null mutant of *Synechococcus* sp. PCC7942 deficient in the sulfolipid sulfoquinovosyl diacylglycerol. *J. Biol. Chem.* 271, 7501–7507.

Hagio, M., Gombos, Z., Várkonyi, Z., Masamoto, K., Sato, N., Tsuzuki, M., et al. (2000). Direct evidence for requirement of phosphatidylglycerol in photosystem II of photosynthesis. *Plant Physiol.* 124, 795–804. doi: 10.1104/pp.124.2.795

Hagio, M., Sakurai, I., Sato, S., Kato, T., Tabata, S., and Wada, H. (2002). Phosphatidylglycerol is essential for the development of thylakoid membranes in *Arabidopsis thaliana*. *Plant Cell Physiol.* 43, 1456–1464. doi: 10.1093/pcp/pcf185

Härtel, H., Lokstein, H., Dörmann, P., Grimm, B., and Benning, C. (1997). Changes in the composition of the photosynthetic apparatus in the galactolipid-deficient *dgd1* mutant of *Arabidopsis thaliana*. *Plant Physiol.* 115, 1175–1184.

Itoh, S., Kozuki, T., Nishida, K., Fukushima, Y., Yamakawa, H., Domonkos, I., et al. (2012). Two functional sites of phosphatidylglycerol for regulation of reaction of plastoquinone Q_B in photosystem II. *Biochim. Biophys. Acta* 1817, 287–297. doi: 10.1016/j.bbabio.2011.10.002

Joliot, P., and Joliot, A. (2005). Quantification of cyclic and linear flows in plants. *Proc. Natl. Acad. Sci. U.S.A.* 102, 4913–4918. doi: 10.1073/pnas.0501268102

Jordan, B. R., Chow, W., and Baker, A. J. (1983). The role of phospholipids in the molecular organisation of pea chloroplast membranes. Effect of phospholipid depletion on photosynthetic activities. *Biochim. Biophys. Acta* 725, 77–86. doi: 10.1016/0005-2728(83)90226-8

Jordan, P., Fromme, P., Witt, H. T., Klukas, O., Saenger, W., and Krauss, N. (2001). Three-dimensional structure of cyanobacterial photosystem I at 2.5 Å resolution. *Nature* 411, 909–917. doi: 10.1038/35082000

Kansy, M., Wilhelm, C., and Goss, R. (2014). Influence of thylakoid membrane lipids on the structure and function of the plant photosystem II core complex. *Planta* 240, 781–796. doi: 10.1007/s00425-014-2130-2

Kim, E.-H., Razeghifard, R., Anderson, J. M., and Chow, W. S. (2007). Multiple sites of retardation of electron transfer in Photosystem II after hydrolysis of phosphatidylglycerol. *Photosynth. Res.* 93, 149–158. doi: 10.1007/s11120-006-9126-0

Kirchhoff, H., Haase, W., Haferkamp, S., Schott, T., Borinski, M., Kubitscheck, U., et al. (2007). Structural and functional self-organization of Photosystem II in grana thylakoids. *Biochim. Biophys. Acta* 1767, 1180–1188. doi: 10.1016/j.bbabio.2007.05.009

Kobayashi, K., Fujii, S., Sato, M., Toyooka, K., and Wada, H. (2015). Specific role of phosphatidylglycerol and functional overlaps with other thylakoid lipids in *Arabidopsis* chloroplast biogenesis. *Plant Cell Rep.* 34, 631–642. doi: 10.1007/s00299-014-1719-z

Kobayashi, K., Narise, T., Sonoike, K., Hashimoto, H., Sato, N., Kondo, M., et al. (2013a). Role of galactolipid biosynthesis in coordinated development of photosynthetic complexes and thylakoid membranes during chloroplast biogenesis in *Arabidopsis*. *Plant J.* 73, 250–261. doi: 10.1111/tpj.12028

Kobayashi, K., Sasaki, D., Noguchi, K., Fujinuma, D., Komatsu, H., Kobayashi, M., et al. (2013b). Photosynthesis of root chloroplasts developed in *Arabidopsis* lines overexpressing GOLDEN2-LIKE transcription factors. *Plant Cell Physiol.* 54, 1365–1377. doi: 10.1093/pcp/pct086

Kramer, D. M., Johnson, G., Kiirats, O., and Edwards, G. E. (2004). New fluorescence parameters for the determination of Q_A redox state and excitation energy fluxes. *Photosynth. Res.* 79, 209–218. doi: 10.1023/B:PRES.0000015391.99477.0d

Krause, G. H. (1991). Chlorophyll fluorescence and photosynthesis: the basics. *Annu. Rev. Plant Physiol. Plant Mol. Biol.* 42, 313–349.

Kruse, O., Hankamer, B., Konczak, C., Gerle, C., Morris, E., Radunz, A., et al. (2000). Phosphatidylglycerol is involved in the dimerization of photosystem II. *J. Biol. Chem.* 275, 6509–6514. doi: 10.1074/jbc.275.9.6509

Lichtenthaler, H. K. (1987). Chlorophylls and carotenoids: pigments of photosynthetic biomembranes. *Methods Enzymol.* 148, 350–382. doi: 10.1016/0076-6879(87)48036-1

Liu, Z., Yan, H., Wang, K., Kuang, T., Zhang, J., Gui, L., et al. (2004). Crystal structure of spinach major lightharvesting complex at 2.72 Å resolution. *Nature* 428, 287–292. doi: 10.1038/nature02373

Melis, A., Spangfort, M., and Andersson, B. (1987). Light-absorption and electron transport balance between photosystem II and photosystem I in spinach chloroplasts. *Photochem. Photobiol.* 45, 129–136.

Meurer, J., Meierhoff, K., and Westhoff, P. (1996). Isolation of high-chlorophyll-fluorescence mutants of *Arabidopsis thaliana* and their characterisation by spectroscopy, immunoblotting and Northern hybridisation. *Planta* 49, 385–396.

Mizusawa, N., and Wada, H. (2012). The role of lipids in photosystem II. *Biochim. Biophys. Acta* 1817, 194–208. doi: 10.1016/j.bbabio.2011.04.008

Morsy, M. A., and Khaled, M. M. (2002). Novel EPR characterization of the antioxidant activity of tea leaves. *Spectrochim. Acta A* 58, 1271–1277. doi: 10.1016/S1386-1425(01)00716-8

Murata, N., Allakhverdiev, S. I., and Nishiyama, Y. (2012). The mechanism of photoinhibition *in vivo*: re-evaluation of the roles of catalase, a-tocopherol, non-photochemical quenching, and electron transport. *Biochim. Biophys. Acta* 1817, 1127–1133. doi: 10.1016/j.bbabio.2012.02.020

Nussberger, S., Dörr, K., Wang, D. N., and Kühlbrandt, W. (1993). Lipid-protein interactions in crystals of plant light-harvesting complex. *J. Mol. Biol.* 234, 347–356. doi: 10.1006/jmbi.1993.1591

Ohnishi, N., Allakhverdiev, S. I., Takahashi, S., Higashi, S., Watanabe, M., Nishiyama, Y., et al. (2005). Two-step mechanism of photodamage to photosystem II: step 1 occurs at the oxygen-evolving complex and step 2 occurs at the photochemical reaction center. *Biochemistry* 44, 8494–8499. doi: 10.1021/bi047518q

Qin, X., Suga, M., Kuang, T., and Shen, J.-R. (2015). Structural basis for energy transfer pathways in the plant PSI-LHCI supercomplex. *Science* 348, 989–995. doi: 10.1126/science.aab0214

Sakurai, I., Mizusawa, N., Ohashi, S., Kobayashi, M., and Wada, H. (2007). Effects of the lack of phosphatidylglycerol on the donor side of photosystem II. *Plant Physiol.* 144, 1336–1346. doi: 10.1104/pp.107.098731

Sarvikas, P., Hakala, M., Pätsikkä, E., Tyystjärvi, T., and Tyystjärvi, E. (2006). Action spectrum of photoinhibition in leaves of wild type and *npq1-2* and *npq4-1* mutants of *Arabidopsis thaliana*. *Plant Cell Physiol.* 47, 391–400. doi: 10.1093/pcp/pcj006

Shikanai, T., Munekage, Y., Shimizu, K., Endo, T., and Hashimoto, T. (1999). Identification and characterization of *Arabidopsis* mutants with reduced quenching of chlorophyll fluorescence. *Plant Cell Physiol.* 40, 1134–1142.

Standfuss, J., Terwisscha van Scheltinga, A. C., Lamborghini, M., and Kühlbrandt, W. (2005). Mechanisms of photoprotection and nonphotochemical quenching in pea light-harvesting complex at 2.5 Å resolution. *EMBO J.* 24, 919–928. doi: 10.1038/sj.emboj.7600585

Takahashi, S., Milward, S. E., Yamori, W., Evans, J. R., Hillier, W., and Badger, M. R. (2010). The solar action spectrum of photosystem II damage. *Plant Physiol.* 153, 988–993. doi: 10.1104/pp.110.155747

Tanoue, R., Kobayashi, M., Katayama, K., Nagata, N., and Wada, H. (2014). Phosphatidylglycerol biosynthesis is required for the development of embryos and normal membrane structures of chloroplasts and mitochondria in *Arabidopsis*. *FEBS Lett.* 588, 1680–1685. doi: 10.1016/j.febslet.2014.03.010

Tyystjärvi, E. (2008). Photoinhibition of Photosystem II and photodamage of the oxygen evolving manganese cluster. *Coord. Chem. Rev.* 252, 361–376. doi: 10.1016/j.ccr.2007.08.021

Umena, Y., Kawakami, K., Shen, J.-R., and Kamiya, N. (2011). Crystal structure of oxygen-evolving photosystem II at a resolution of 1.9 Å. *Nature* 473, 55–60. doi: 10.1038/nature09913

Wada, H., and Murata, N. (2007). The essential role of phosphatidylglycerol in photosynthesis. *Photosynth. Res.* 92, 205–215. doi: 10.1007/s11120-007-9203-z

Xu, C., Härtel, H., Wada, H., Hagio, M., Yu, B., Eakin, C., et al. (2002). The *pgp1* mutant locus of *Arabidopsis* encodes a phosphatidylglycerolphosphate synthase with impaired activity. *Plant Physiol.* 129, 594–604. doi: 10.1104/pp.002725

Yu, B., and Benning, C. (2003). Anionic lipids are required for chloroplast structure and function in *Arabidopsis*. *Plant J.* 36, 762–770. doi: 10.1046/j.1365-313X.2003.01918.x

Conflict of Interest Statement: The authors declare that the research was conducted in the absence of any commercial or financial relationships that could be construed as a potential conflict of interest.

frontiers in Plant Science

REVIEW
published: 16 February 2016
doi: 10.3389/fpls.2016.00168

Identification and Roles of Photosystem II Assembly, Stability, and Repair Factors in Arabidopsis

Yan Lu *

Department of Biological Sciences, Western Michigan University, Kalamazoo, MI, USA

Photosystem II (PSII) is a multi-component pigment-protein complex that is responsible for water splitting, oxygen evolution, and plastoquinone reduction. Components of PSII can be classified into core proteins, low-molecular-mass proteins, extrinsic oxygen-evolving complex (OEC) proteins, and light-harvesting complex II proteins. In addition to these PSII subunits, more than 60 auxiliary proteins, enzymes, or components of thylakoid protein trafficking/targeting systems have been discovered to be directly or indirectly involved in *de novo* assembly and/or the repair and reassembly cycle of PSII. For example, components of thylakoid-protein-targeting complexes and the chloroplast-vesicle-transport system were found to deliver PSII subunits to thylakoid membranes. Various auxiliary proteins, such as PsbP-like (Psb stands for PSII) and light-harvesting complex-like proteins, atypical short-chain dehydrogenase/reductase family proteins, and tetratricopeptide repeat proteins, were discovered to assist the *de novo* assembly and stability of PSII and the repair and reassembly cycle of PSII. Furthermore, a series of enzymes were discovered to catalyze important enzymatic steps, such as C-terminal processing of the D1 protein, thiol/disulfide-modulation, peptidylprolyl isomerization, phosphorylation and dephosphorylation of PSII core and antenna proteins, and degradation of photodamaged PSII proteins. This review focuses on the current knowledge of the identities and molecular functions of different types of proteins that influence the assembly, stability, and repair of PSII in the higher plant *Arabidopsis thaliana*.

Keywords: Photosystem II assembly, Photosystem II stability, Photosystem II repair, *Arabidopsis thaliana*, identification and roles

OPEN ACCESS

Edited by:
Julian Eaton-Rye,
University of Otago, New Zealand

Reviewed by:
Biswapriya Biswavas Misra,
University of Florida, USA
Peter Julian Nixon,
Imperial College London, UK

***Correspondence:**
Yan Lu
yan.1.lu@wmich.edu

Specialty section:
This article was submitted to Plant Cell Biology, a section of the journal Frontiers in Plant Science

Received: *18 November 2015*
Accepted: *31 January 2016*
Published: *16 February 2016*

Citation:
Lu Y (2016) Identification and Roles of Photosystem II Assembly, Stability, and Repair Factors in Arabidopsis. Front. Plant Sci. 7:168. doi: 10.3389/fpls.2016.00168

INTRODUCTION

Photosystem II (PSII) is a multi-subunit pigment-protein complex found in thylakoid membranes of oxygenic photosynthetic organisms, including cyanobacteria, algae, and plants (Nickelsen and Rengstl, 2013; Järvi et al., 2015). Driven by light, PSII catalyzes electron transfer from water to plastoquinone. Therefore, PSII is also known as a water-plastoquinone oxidoreductase. Proteomics, X-ray crystallography, and single-particle electron cryo-microscopy studies revealed that PSII components include core proteins, low-molecular-mass (LMM, i.e., <10 kDa) proteins, extrinsic oxygen-evolving complex (OEC) proteins, and light-harvesting complex (LHC) proteins (da Fonseca et al., 2002; Kashino et al., 2002; Liu et al., 2004; Aro et al., 2005; Nield and Barber, 2006; Umena et al., 2011; Suga et al., 2015). Except for some minor differences in the composition of LMM proteins, the core of PSII is conserved from cyanobacteria to land plants

(Umena et al., 2011; Nickelsen and Rengstl, 2013). Proteins that form the PSII core complex in land plants include PSII reaction center core proteins D1 and D2 (i.e., PsbA and PsbD; Psb stands for PSII), core antenna proteins CP43 and CP47 (i.e., PSII chlorophyll proteins of 43 and 47 kDa, also known as PsbC and PsbB, respectively), cytochrome b_{559} subunits alpha and beta (i.e., PsbE and PsbF), and LMM proteins PsbH, PsbI, PsbJ, PsbK, PsbL, PsbM, PsbR, PsbTc (chloroplast-encoded PSII protein T), PsbTn (nuclear-encoded PSII protein T), PsbW, PsbX, PsbY, and PsbZ (Nickelsen and Rengstl, 2013). Due to the loss of PsbU and PsbV during green plant evolution, cyanobacterial OEC has PsbO, PsbP, PsbQ, PsbU, and PsbV subunits but land plant OEC only contains PsbO, PsbP, and PsbQ subunits (Thornton et al., 2004; Bricker et al., 2012). The PSII-light-harvesting antenna in cyanobacteria is made of phycobilisomes, which are attached to the cytoplasmic side of PSII (Liu et al., 2005). The PSII-light-harvesting antenna (i.e., light-harvesting complex II, abbreviated as LHCII) in land plants is an integral membrane complex. LHCII contains three major trimeric PSII light-harvesting chlorophyll *a*/*b*-binding (LHCB) proteins LHCB1, LHCB2, and LHCB3 and three minor monomeric LHCB proteins LHCB4, LHCB5, and LHCB6 (Jansson, 1999; Liu et al., 2004). In addition to PSII subunits, more than 60 auxiliary proteins or enzymes have been found to be involved in the assembly, stability, and repair of PSII complexes (Nixon et al., 2010; Nickelsen and Rengstl, 2013; Järvi et al., 2015). This article focuses on the identification and roles of different types of proteins that influence the assembly, stability, and repair of PSII in the higher plant *Arabidopsis thaliana*.

Abbreviations: ALB3, Albino3; BN-PAGE, blue native-polyacrylamide gel electrophoresis; CP43, Photosystem II chlorophyll protein of 43 kDa, also known as PsbC; CP47, Photosystem II chlorophyll protein of 47 kDa, also known as PsbB; CPRabA5e, chloroplast Rab GTPase A5e; cpFtsY, filamentation temperature sensitive protein Y; cpSec, chloroplast secretory; cpSecA, cpSecE, cpSecY, chloroplast secretory translocase A, E, and Y; cpSRP, chloroplast signal recognition particle; cpSRP43 and cpSRP54, chloroplast Signal Recognition Particle protein of 43 and 54 kDa; cpTat, chloroplast twin-arginine translocation; cpTatC, chloroplast twin-arginine translocation protein C; CtpA1 and CtpA2, C-terminal processing peptidases A 1 and 2; CYO1, Shiyou 1 (Shiyou means cotyledon in Japanese), also known as SCO2; CYP20-3, 20-kDa cyclophilin 3; CYP38, cyclophilin of 38 kDa; Cyt b_{559}, cytochrome b_{559}; Deg1; Deg2, Deg5, Deg7, and Deg8, Degradation-of-periplasmic-proteins proteases 1, 2, 5, 7, and 8; FKBP20-2, 20-kDa FK506 (tacrolimus)-binding protein; ELIP1 and ELIP2, early light-induced proteins 1 and 2; FtsH1, FtsH2, FtsH5, FtsH6, FtsH8, FtsH9, FtsH11, and FtsH12, filamentation temperature sensitive proteins H 1, 2, 5, 6, 8, 9, 11, and 12; FtsH2 and FtsH5 are also known as VAR2 and VAR1, respectively; fug1, fu-gaeri1; GTPase, GTP hydrolase; HCF106, HCF136, HCF173, HCF243, and HCF244, High Chlorophyll Fluorescence 106, 136, 173, 243, and 244; HHL1, Hypersensitive to High Light 1; HLIP, high-light-induced protein; LHCII, light-harvesting complex II; LHCB1, LHCB2, LHCB3, LHCB4, LHCB5, and LHCB6, Photosystem II light-harvesting chlorophyll *a*/*b*-binding proteins 1, 2, 3, 4, 5, and 6; LHCP, light-harvesting chlorophyll *a*/*b*-binding protein; LIL3:1 and LIL3:2, light-harvesting-like proteins 3:1 and 3:2; LMM, low molecular mass; LPA1, LPA2, LPA3, and LPA19, Low Photosystem II Accumulation 1, 2, 3, and 19; LPA1 is also known as PratA; LQY1, Low Quantum Yield of Photosystem II 1; LTO1, Lumen Thiol Oxidoreductase 1; MET1, Mesophyll-Enriched Thylakoid protein 1; MPH1, Maintenance of Photosystem II under High light 1; OEC, oxygen-evolving complex; OHP1 and OHP2, one-helix proteins 1 and 2; PAM68, Photosynthesis Affected Mutant 68; PBCP, Photosystem II core phosphatase; PBF1, Photosystem Biogenesis Factor 1; pD1, precursor D1; PDI6, Protein Disulfide Isomerase 6, also known as PDIL1-2; PDIase, protein disulfide isomerase; PDIL1-2, Protein Disulfide Isomerase-Like 1-2, also known as PDI6; PPH1, Protein Phosphatase 1; PPIase, Peptidylprolyl Isomerase; PPL1 and PPL2, PsbP-Like proteins 1 and 2; PratA, Processing-associated tetratricopeptide repeat protein A, also known as LPA1; PSI, Photosystem I; PSII, Photosystem II; Psa, Photosystem II; PsaH and PsaK, Photosystem I proteins H and K; Psb, Photosystem II; PSB28, PSB29, and PSB33, Photosystem II proteins 28, 29 and 33; PSB29 is also known as THF1; PsbA, PsbB, PsbC, PsbD, PsbE, PsbF, PsbH, PsbI, PsbJ, PsbK, PsbL, PsbM, PsbN, PsbO, PsbP, PsbQ, PsbR, PsbT, PsbU, PsbV, PsbW, PsbX, PsbY, PsbZ, Photosystem II protein A, B, C, D, E, F, H, I, J, K, L, M, N, O, P, Q, R, T, U, V, W, X, Y and Z; PsbA, PsbB, PsbC, and PsbD are also known as D1, CP47, CP43, and D2; PsbE and PsbF are also known as cytochrome b_{559} subunit alpha and beta, respectively; PsbN is also known as PBF1; PsbO, PsbP, and PsbQ are also known as the 33-, 23-, and 17-kDa protein of the oxygen-evolving complex, respectively; PsbTc, chloroplast-encoded Photosystem II protein T; PsbTn, nuclear-encoded PSII protein T; RC, minimal reaction-center complex which lacks CP47 and CP43; RC47a and RC 47b, reaction-center complexes that contain CP47 but lack CP43; RBD1, rubredoxin 1; RNAi, RNA interference; SCO2, Snowy Cotyledon 2, also known as CYO1; SCP, small chlorophyll-binding-like protein; SDR, short-chain dehydrogenase/reductase; SRP, signal recognition particle; STN7 and STN8, state transition 7 and 8; ROC4, rotamase cyclophilin 4; SEP3.1 and SEP3.2, stress-enhanced protein 3.1 and 3.2; TerC, Tellurite-resistance protein C; T-DNA, transfer DNA; TAP38, Thylakoid-Associated Phosphatase of 38 kDa; THA4, Thylakoid Assembly 4; THF1, Thylakoid Formation 1, also known as PSB29; TLP18.3 and TLP40, Thylakoid Lumen Proteins of 18.3 and 40 kDa; TPR, tetratricopeptide repeat; TRX, thioredoxin; VAR1 and VAR2, Yellow Variegated 1 and 2, also known as FtsH5 and FtsH2, respectively; VIPP1, Vesicle-Inducing Protein in Plastids 1; YCF48, hypothetical chloroplast reading frame number 48.

DE NOVO ASSEMBLY OF PSII

De novo (Latin for "anew" or "from the beginning") PSII assembly is a sequential and highly coordinated process. The principal steps were revealed by the use of radioactive pulse-chase experiments, two-dimensional blue native/sodium dodecyl sulfate-polyacrylamide gel electrophoresis, and subsequent proteomics and mass spectrometry analysis (Aro et al., 2005; Rokka et al., 2005; Boehm et al., 2012a). *De novo* PSII assembly in higher plants include: (1) assembly of the precursor D1-PsbI (pD1-PsbI) and D2-cytochrome b_{559} (D2-Cyt b_{559}) precomplexes, (2) assembly of the minimal reaction-center complex (RC), which lacks CP47 and CP43, (3) assembly of the reaction-center complex (RC47a) that contains CP47 but lacks CP43, (4) incorporation of LMM subunits, such as PsbH, PsbM, PsbT, and PsbR, to form RC47b, (5) incorporation of CP43, along with LMM subunit PsbK, to form the OEC-less PSII monomer, (6) assembly of the OEC and additional LMM subunits, such as PsbW and PsbZ, to form the PSII core monomer, and (7) dimerization and formation of the PSII-LHCII supercomplex (**Figure 1**; Rokka et al., 2005; Nixon et al., 2010; Komenda et al., 2012a; Nickelsen and Rengstl, 2013). A similar pathway exists in cyanobacteria, algae, and lower plants, suggesting that the core components of PSII and the assembly process of PSII complexes are conserved (Nixon et al., 2010; Komenda et al., 2012a; Nickelsen and Rengstl, 2013). From cyanobacteria to green algae to land plants, the initial assembly steps of photosynthetic complexes appear to be spatially separated from sites of active photosynthesis (Nickelsen and Rengstl, 2013). For instance, in *Chlamydomonas reinhardtii*, initial steps of *de novo* PSII assembly occur in discrete regions near the pyrenoid, called translation zones (Uniacke and Zerges, 2007).

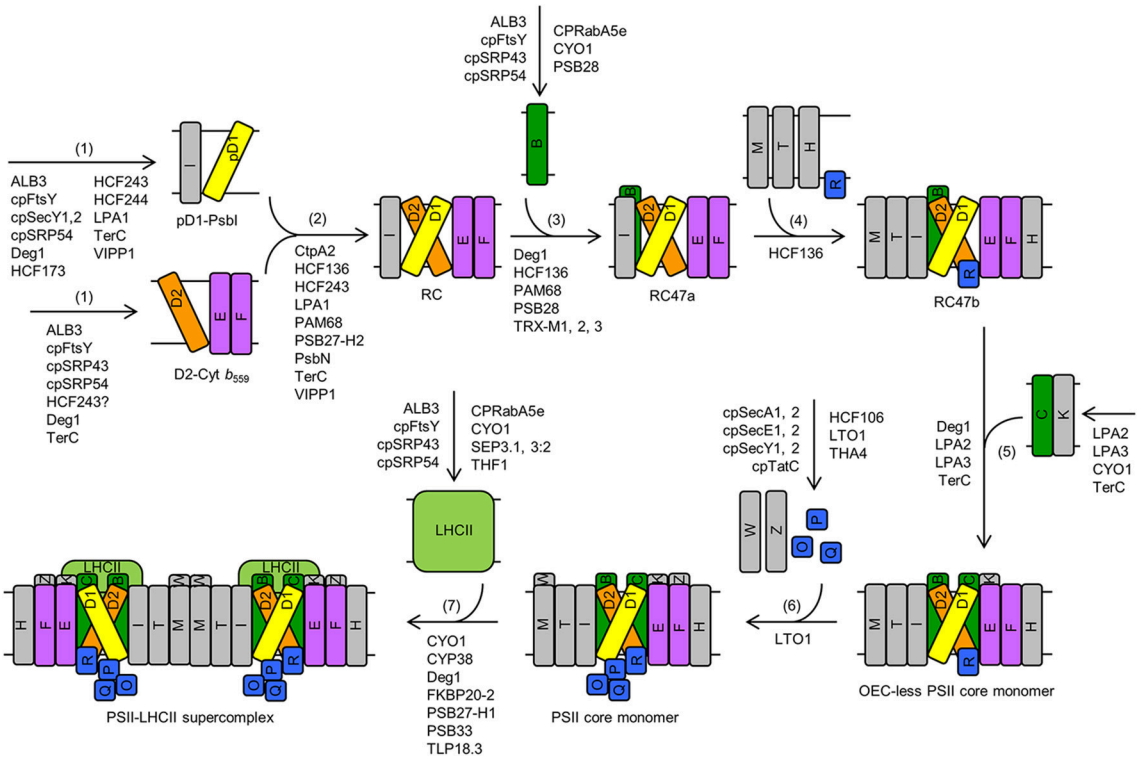

FIGURE 1 | *De novo* assembly of PSII in Arabidopsis. The major steps include: (1) assembly of precursor D1-PsbI (pD1-PsbI) and D2-cytochrome b_{559} (D2-Cyt b_{559}) precomplexes, (2) assembly of the minimal reaction-center complex (RC), which lacks CP47 and CP43, (3) assembly of the reaction-center complex (RC47a) that contains CP47 but lacks CP43, (4) incorporation of LMM subunits, such as PsbH, PsbM, PsbT, and PsbR, to form RC47b, (5) incorporation of CP43, along with LMM subunit PsbK, to form the OEC-less PSII core monomer, (6) assembly of the oxygen-evolving complex (OEC) and additional LMM subunits, such as PsbW and PsbZ, to form the PSII core monomer, and (7) dimerization and formation of the PSII-light-harvesting complex II (LHCII) supercomplex. Proteins that are involved in these steps are listed. Although RBD1 promotes PSII assembly and/or PSII stability, it is not depicted in this figure because it is not clear which step(s) of *de novo* PSII assembly this protein is involved in. Letters (B, C, D1, D2, E, F, H, I, K, M, O, P, Q, R, T, W, Z) in rectangles represent PSII proteins PsbB (i.e., CP47), PsbC (i.e., CP43), D1, D2, PsbE, PsbF, PsbH, PsbI, PsbK, PsbM, PsbO, PsbP, PsbQ, PsbR, PsbT, PsbW, and PsbZ, respectively. Abbreviations: D2-Cyt b_{559}, D2-cytochrome b_{559} precomplex; LHCII, light-harvesting complex II; OEC, oxygen-evolving complex; pD1, precursor D1; pD1-PsbI, precursor D1-PsbI precomplex; PSII, Photosystem II; RC, PSII minimal reaction-center complex; RC47a, PSII reaction-center complex with CP47, without PsbM, PsbH, PsbT, or PsbR; RC47b, PSII reaction-center complex with CP47, PsbM, PsbH, PsbT, and PsbR. For simplicity, only one name is shown for proteins with multiple names (e.g., "THF1" for THF1/PSB29).

Assembly of LHCII is recently thought to initiate on the chloroplast envelope in developing chloroplasts and on thylakoid membranes in developed chloroplasts (Tanz et al., 2012; Khan et al., 2013). LHCII assembly on the chloroplast envelope consists of four major steps: (1) partial insertion of LHCP (light-harvesting chlorophyll *a*/*b*-binding protein) apoproteins into the inner chloroplast envelope, (2) binding of chlorophyll to reach a stable conformation in the membrane, (3) insertion of the rest of the protein domains, and (4) further pigment binding and protein assembly into a fully assembled pigment-protein complex (Hoober et al., 2007; Dall'Osto et al., 2015). The pigment-protein complexes on the inner chloroplast envelope can be transferred to thylakoid membranes via the chloroplast-vesicle-transport system, the primary source of lipids and proteins for developing thylakoids in young chloroplasts (Tanz et al., 2012; Khan et al., 2013; Karim et al., 2014). In developed chloroplasts, LHCP proteins are primarily transported and integrated into thylakoid membranes via the chloroplast signal recognition particle (cpSRP) pathway (Cline and Dabney-Smith, 2008; Albiniak et al., 2012; Dall'Osto et al., 2015).

DAMAGE, REPAIR, AND REASSEMBLY OF PSII

The PSII repair cycle is a sequential process as well. The major steps in higher plants include: (1) high-light-induced phosphorylation, damage, and disassembly of the PSII-LHCII supercomplex and the PSII core dimer in grana stacks, (2) lateral migration of the PSII core monomer to stroma-exposed thylakoid membranes, (3–5) dephosphorylation, partial disassembly of the PSII core monomer, and degradation of photodamaged D1, (6) synthesis and reassembly of new D1, (7) re-incorporation of CP43, (8) re-attachment of OEC, (9) migration of the PSII core monomer back to grana stacks, and (10) dimerization into PSII core dimers and reformation of PSII-LHCII

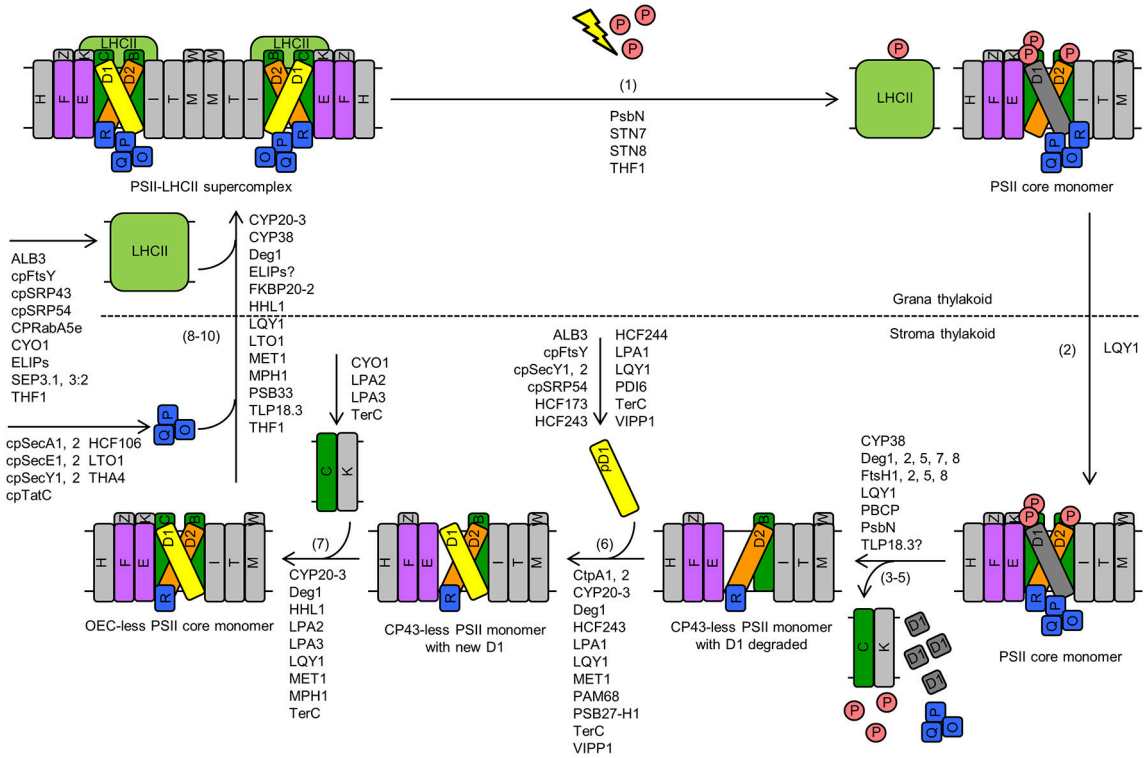

FIGURE 2 | Damage, repair, and reassembly of PSII in Arabidopsis. The major steps include: (1) high-light-induced phosphorylation, damage, and disassembly of the PSII-LHCII supercomplex and the PSII core dimer in grana stacks, (2) lateral migration of the PSII core monomer to stroma-exposed thylakoid membranes, (3–5) dephosphorylation, partial disassembly of the PSII core monomer, and degradation of photodamaged D1, (6) synthesis and reassembly of new D1, (7) re-incorporation of CP43, (8) reattachment of OEC, (9) migration of the PSII core monomer back to grana stacks, and (10) dimerization into PSII core dimers and reformation of PSII-LHCII supercomplexes. Proteins that are involved in these steps are listed. Although PPL1 might be involved in PSII repair, it is not depicted in this figure because it is not clear which step(s) of PSII repair this protein is involved in. Letters (B, C, D1, D2, E, F, H, I, K, M, O, P, Q, R, T, W, Z) in rectangles represent PSII proteins PsbB (i.e., CP47), PsbC (i.e., CP43), D1, D2, PsbE, PsbF, PsbH, PsbI, PsbK, PsbM, PsbO, PsbP, PsbQ, PsbR, PsbT, PsbW, and PsbZ, respectively. The letter P in a circle represents phosphate. The yellow lightning bolt represents light. Abbreviations: LHCII, light-harvesting complex II; OEC, oxygen-evolving complex; pD1, precursor D1; PSII, Photosystem II. For simplicity, only one name is shown for proteins with multiple names (e.g., "THF1" for THF1/PSB29).

supercomplexes (**Figure 2**; Mulo et al., 2008; Järvi et al., 2015).

PROTEINS THAT INFLUENCE THE ASSEMBLY, STABILITY, AND REPAIR OF PSII

Assistance from a series of protein factors is required for the assembly, stability, and repair of PSII (**Figures 1**, **2**; Mulo et al., 2008; Nickelsen and Rengstl, 2013; Järvi et al., 2015). The types of protein factors include: (1) components of thylakoid-protein-targeting complexes; (2) components of the chloroplast-vesicle-transport system, (3) PSII subunit-like proteins, e.g., PsbP-like and LHCP-like proteins, (4) atypical short-chain dehydrogenase/reductase (SDR) family proteins, (5) C-terminal D1 processing endopeptidases, (6) tetratricopeptide repeat (TPR) proteins, (7) thiol/disulfide-modulating proteins, (8) peptidylprolyl isomerases (PPIases), (9) protein kinases, (10) protein phosphatases, (11) FtsH (filamentation temperature sensitive protein H) proteases, (12) Deg (Degradation of periplasmic proteins) proteases, and (13) other auxiliary proteins with unique or unknown domain compositions (**Table 1**). As discussed below, many proteins that are involved in *de novo* PSII assembly also play roles in the repair and reassembly cycle of PSII.

Some of these factors, such as components of the thylakoid-protein-targeting complexes and the chloroplast-vesicle-transport system, are not specific for the assembly, stability, or repair of PSII. However, because thylakoid protein targeting and chloroplast vesicle transport are essential for translocation and accumulation of thylakoid membrane/lumen proteins, and because most of PSII subunits and assembly, stability, and repair factors are thylakoid membrane/lumen proteins, these two types of protein factors are included in this article.

Components of Thylakoid-Protein-Targeting Complexes

Four thylakoid transport and integration pathways have been identified to date (Cline and Dabney-Smith, 2008; Albiniak et al., 2012). The cpSRP pathway and an unusual pathway that

TABLE 1 | Summary of proteins that influence the assembly, stability, and repair of PSII in Arabidopsis.

Name	Gene locus in *Synechocystis* sp. PCC 6803[a]	Gene locus in Arabidopsis[b]	Full-length Size (kDa)	Mature size (kDa)	Location	Protein classification	Function	References[c]
cpSRP43	–	At2g47450	41	35	CS	Thylakoid protein targeting: cpSRP translocase	Insertion and assembly of PSII proteins such as D1, D2, and CP47, and LHCII subunits	Henry et al., 2007; Schunemann, 2007; Cline and Dabney-Smith, 2008; Albiniak et al., 2012
cpSRP54	slr1531	At5g03940	61	53	CS	Thylakoid protein targeting: cpSRP translocase	Insertion and assembly of PSII proteins such as D1, D2, and CP47, and LHCII subunits	Henry et al., 2007; Schunemann, 2007; Cline and Dabney-Smith, 2008; Albiniak et al., 2012; Walter et al., 2015
cpFtsY	slr2102	At2g45770	40	36	CS, TM	Thylakoid protein targeting: cpSRP translocase	Insertion and assembly of PSII proteins such as D1, D2, and CP47, and LHCII subunits	Henry et al., 2007; Schunemann, 2007; Cline and Dabney-Smith, 2008; Albiniak et al., 2012; Walter et al., 2015
ALB3	slr1471	At2g28800	50	45	TM	Thylakoid protein targeting: cpSRP translocase	Insertion and assembly of PSII proteins such as D1, D2, and CP47, and LHCII subunits	Pasch et al., 2005; Henry et al., 2007; Ma et al., 2007; Schunemann, 2007; Cline and Dabney-Smith, 2008; Walter et al., 2015
cpSecA1	sll0616	At4g01800	117	111	CS, TM	Thylakoid protein targeting: cpSec translocase	Insertion and assembly of PSII proteins such as PsbO	Cline and Theg, 2007; Schunemann, 2007; Cline and Dabney-Smith, 2008; Albiniak et al., 2012
cpSecA2		At1g21650	203	203	CS, TM	Thylakoid protein targeting: cpSec translocase	Insertion and assembly of PSII proteins such as PsbO	Cline and Theg, 2007; Schunemann, 2007; Cline and Dabney-Smith, 2008; Albiniak et al., 2012
cpSecE1	ssl3335	At4g14870	19	15	TM	Thylakoid protein targeting: cpSec translocase	Insertion and assembly of PSII proteins such as PsbO	Cline and Theg, 2007; Schunemann, 2007; Cline and Dabney-Smith, 2008; Albiniak et al., 2012
cpSecE2		At4g38490	17	12	TM	Thylakoid protein targeting: cpSec translocase	Insertion and assembly of PSII proteins such as PsbO	Cline and Theg, 2007; Schunemann, 2007; Cline and Dabney-Smith, 2008; Albiniak et al., 2012
cpSecY1	sll1814	At2g18710	59	51	TM	Thylakoid protein targeting: cpSec translocase	Insertion and assembly of PSII proteins such as D1 and PsbO	Cline and Theg, 2007; Henry et al., 2007; Schunemann, 2007; Cline and Dabney-Smith, 2008; Albiniak et al., 2012; Walter et al., 2015
cpSecY2		At2g31530	65	61	TM	Thylakoid protein targeting: cpSec translocase	Insertion and assembly of PSII proteins such as D1 and PsbO	Cline and Theg, 2007; Henry et al., 2007; Schunemann, 2007; Cline and Dabney-Smith, 2008; Albiniak et al., 2012; Walter et al., 2015
Tha4	slr1046	At5g28750	16	14	TM	Thylakoid protein targeting: cpTat translocase	Insertion and assembly of PSII proteins such as PsbP and PsbQ	Cline and Theg, 2007; Schunemann, 2007; Cline and Dabney-Smith, 2008; Albiniak et al., 2012

(Continued)

TABLE 1 | Continued

Name	Gene locus in *Synechocystis* sp. PCC 6803[a]	Gene locus in Arabidopsis[b]	Full-length Size (kDa)	Mature size (kDa)	Location	Protein classification	Function	References[c]
HCF106	slr1046	At5g52440	28	19	TM	Thylakoid protein targeting: cpTat translocase	Insertion and assembly of PSII proteins such as PsbP and PsbQ	Cline and Theg, 2007; Schunemann, 2007; Cline and Dabney-Smith, 2008; Albiniak et al., 2012
cpTatC	sll0194	At2g01110	37	34	TM	Thylakoid protein targeting: cpTat translocase	Insertion and assembly of PSII proteins such as PsbP and PsbQ	Cline and Theg, 2007; Schunemann, 2007; Cline and Dabney-Smith, 2008; Albiniak et al., 2012
CPRabA5e	–	At1g05810	29	24	CS, TM	Chloroplast vesicle transport	Transport of PSII proteins such as LHCB1, LHCB3, and CP47, to and from thylakoids	Karim et al., 2014; Karim and Aronsson, 2014
CYO1/ SCO2	–	At3g19220	21	17	TM	Chloroplast vesicle transport; thiol/disulfide-modulating protein	Chloroplast and thylakoid biogenesis; folding and transport of cysteine-containing proteins such as CP43, CP47, and LHCB1; stability of PSI-LHCI and PSII-LHCII supercomplexes	Shimada et al., 2007; Albrecht et al., 2008; Muranaka et al., 2012; Tanz et al., 2012
THF1/ PSB29	sll1414	At2g20890	34	27	CE, CS, TM	Chloroplast vesicle transport	Thylakoid biogenesis; dynamics of PSII-LHCII supercomplexes	Wang et al., 2004; Keren et al., 2005; Huang et al., 2006, 2013; Shi et al., 2012; Yamatani et al., 2013
TerC	–	At5g12130	42	34	TM	Chloroplast vesicle transport	Thylakoid biogenesis; co-translational insertion of PSII proteins such as D1, D2, and CP43	Kwon and Cho, 2008; Schneider et al., 2014
VIPP1	sll0617	At1g65260	36	32	ICE, TM	Chloroplast vesicle transport	Thylakoid biogenesis; transport and/or co-translational insertion of photosynthetic proteins such as D1	Kroll et al., 2001; Zhang et al., 2012; Zhang and Sakamoto, 2012; Walter et al., 2015
PPL1	sll1418	At3g55330	26	18	TL	PSII subunit-like: PsbP-like	PSII repair	Ishihara et al., 2007
ELIP1	–	At3g22840	20	16	TM	PSII subunit-like: LHCP-like	Binding of chlorophyll and/or stability of pigment-binding proteins and complexes during photoinhibition?	Hutin et al., 2003; Casazza et al., 2005; Heddad et al., 2006; Rossini et al., 2006
ELIP2	–	At4g14690	20	16	TM	PSII subunit-like: LHCP-like	Binding of chlorophyll and/or stability of pigment-binding proteins and complexes during photoinhibition?	Hutin et al., 2003; Casazza et al., 2005; Heddad et al., 2006; Rossini et al., 2006
SEP3.1/ LIL3:1	–	At4g17600	29	25	TM	PSII subunit-like: LHCP-like	Anchoring geranylgeranyl reductase to thylakoid membranes; stabilizing LHCII	Tanaka et al., 2010; Takahashi et al., 2014; Lohscheider et al., 2015

(Continued)

TABLE 1 | Continued

Name	Gene locus in *Synechocystis* sp. PCC 6803[a]	Gene locus in Arabidopsis[b]	Full-length Size (kDa)	Mature size (kDa)	Location	Protein classification	Function	References[c]
SEP3.2/ LIL3:2	–	At5g47110	29	24	TM	PSII subunit-like: LHCP-like	Anchoring geranylgeranyl reductase to thylakoid membranes; stabilizing LHCII	Tanaka et al., 2010; Takahashi et al., 2014; Lohscheider et al., 2015
HCF173	sll1218	At1g16720	66	57	CS, TM	atypical SDR	Translational initiation of the *psbA* mRNA	Schult et al., 2007; Link et al., 2012
HCF244	slr0399	At4g35250	44	38	TM	atypical SDR	Translational initiation of the *psbA* mRNA	Link et al., 2012
CtpA1	slr0008	At3g57680	56	47	TL	C-terminal processing peptidase	C-terminal processing of D1 under high light	Yamamoto et al., 2001; Yin et al., 2008
CtpA2		At4g17740	56	46	TL	C-terminal processing peptidase	C-terminal processing of D1	Yamamoto et al., 2001; Che et al., 2013
LPA1/ PratA	slr2048	At1g02910	50	47	TM	TPR	Biogenesis and assembly of the D1 protein	Peng et al., 2006
MET1	–	At1g55480	37	30	TM	TPR	Supercomplex formation in PSII repair	Ishikawa et al., 2005a; Bhuiyan et al., 2015
LQY1	–	At1g75690	16	12	TL	Thiol/disulfide-modulating protein	Dissembly, folding, and/or reassembly of cysteine-containing PSII subunits and complexes and/or D1 synthesis and turnover, during PSII repair	Lu, 2011; Lu et al., 2011
PDI6/ PDIL1-2	–	At1g77510	56	54	CS	Thiol/disulfide-modulating protein	Regulation of D1 synthesis	Houston et al., 2005; Wittenberg et al., 2014
TRX-M1	slr0623	At1g03680	20	14	CS	Thiol/disulfide-modulating protein	Assembly of CP47 into PSII	Cain et al., 2009; Wang et al., 2013
TRX-M2		At4g03520	20	13	CS	Thiol/disulfide-modulating protein	Assembly of CP47 into PSII	Cain et al., 2009; Wang et al., 2013
TRX-M4		At3g15360	21	13	CS	Thiol/disulfide-modulating protein	Assembly of CP47 into PSII	Cain et al., 2009; Wang et al., 2013
LTO1	slr0565	At4g35760	40	35	TM	Thiol/disulfide-modulating protein	Disulfide bond formation in PsbO	Feng et al., 2011; Karamoko et al., 2011; Lu et al., 2013
RBD1	slr2033	At1g54500	22	16	TM	Thiol/disulfide-modulating protein	PSII assembly and stability	Calderon et al., 2013

(Continued)

TABLE 1 | Continued

Name	Gene locus in *Synechocystis* sp. PCC 6803[a]	Gene locus in Arabidopsis[b]	Full-length Size (kDa)	Mature size (kDa)	Location	Protein classification	Function	References[c]
CYP20-3/ROC4	slr1251	At3g62030	34	23	CS	PPIase	Repair and reassembly of PSII under high light; redox regulation during stress acclimation	Lippuner et al., 1994; Cai et al., 2008; Dominguez-Solis et al., 2008; Park et al., 2013; Speiser et al., 2015
CYP38/ TLP40	sll0408	At3g01480	48	38-40	TL	PPIase	Inhibiting dephosphorylation of PSII subunits during the PSII repair; conversion of PSII core monomers to PSII supercomplexes	Fulgosi et al., 1998; Vener et al., 1999; Rokka et al., 2000; Fu et al., 2007; Sirpiö et al., 2008; Vasudevan et al., 2012
FKBP20-2	slr1761	At3g60370	27	20	TM, TL	PPIase	Formation of PSII-LHCII supercomplexes under normal and high light	Lima et al., 2006
STN7	–	At1g68830	63	59	TM	Protein kinase	Phosphorylation of LHCII; phosphorylation of D1, D2, CP43, and PsbH under low light	Bellafiore et al., 2005; Bonardi et al., 2005; Tikkanen et al., 2008; Pesaresi et al., 2011; Tikkanen and Aro, 2012
STN8	–	At5g01920	55	50	TM	Protein kinase	Phosphorylation of D1, D2, CP43, and PsbH	Bonardi et al., 2005; Tikkanen et al., 2008; Pesaresi et al., 2011; Tikkanen and Aro, 2012; Nath et al., 2013
PBCP	–	At2g30170	32	30	CS, TM	Protein phosphatase	Dephosphorylation of D1, D2, CP43, and PsbH	Samol et al., 2012
TLP18.3	sll1390	At1g54780	31	18	TL, TM	Protein phosphatase	D1 degradation and PSII dimerization; dephosphorylation of PSII core proteins (e.g., D1 and D2)	Sirpiö et al., 2007; Wu et al., 2011
PPH1/ TAP38	–	At4g27800	43	41	TM	Protein phosphatase	Dephosphorylation of LHCII	Pribil et al., 2010; Shapiguzov et al., 2010; Pesaresi et al., 2011
FtsH1	slr1390, slr0228, slr1604, sll1463[d]	At1g50250	77	71	TM	FtsH protease	Degradation of photodamaged D1	Sakamoto et al., 2003; Yu et al., 2004, 2005; Zaltsman et al., 2005b
FtsH2/ VAR2		At2g30950	74	69	TM	FtsH protease	Chloroplast biogenesis; thylakoid formation; degradation of photodamaged D1	Bailey et al., 2002; Sakamoto et al., 2002, 2003; Yu et al., 2004, 2005; Zaltsman et al., 2005a,b; Kato et al., 2007, 2009, 2012; Wagner et al., 2011
FtsH5/ VAR1		At5g42270	75	69	TM	FtsH protease	Chloroplast biogenesis; thylakoid formation; degradation of photodamaged D1	Sakamoto et al., 2002, 2003; Yu et al., 2004, 2005; Zaltsman et al., 2005b; Kato et al., 2009; Wagner et al., 2011

(Continued)

TABLE 1 | Continued

Name	Gene locus in *Synechocystis* sp. PCC 6803[a]	Gene locus in Arabidopsis[b]	Full-length Size (kDa)	Mature size (kDa)	Location	Protein classification	Function	References[c]
FtsH6		At5g15250	77	69	TM	FtsH protease	Degradation of LHCII during high-light acclimation and senescence?	Sakamoto et al., 2003; Yu et al., 2004; Zelisko et al., 2005; Wagner et al., 2011
FtsH8		At1g06430	73	69	TM	FtsH protease	Degradation of photodamaged D1	Sakamoto et al., 2003; Yu et al., 2004, 2005; Zaltsman et al., 2005b; Wagner et al., 2011
FtsH11		At5g53170	89	82	C(TM?), IMM	FtsH protease	Thermoprotection of the photosynthetic apparatus	Sakamoto et al., 2003; Yu et al., 2004; Urantowka et al., 2005; Chen et al., 2006b; Wagner et al., 2011
Deg1	slr1204, sll1679, sll1427[e]	At3g27925	47	42	TL, TM,	Deg protease	Degradation of plastocyanin and PsbO, and photodamaged D1; integration of newly synthesized PSII subunits such as D1, D2, CP43, and CP47, into PSII complexes	Chassin et al., 2002; Huesgen et al., 2005; Kapri-Pardes et al., 2007; Sun et al., 2010b; Schuhmann and Adamska, 2012
Deg2		At2g47940	67	59	CS, TM	Deg protease	Stress-induced degradation of LHCB6; a minor protease in *in vivo* degradation of photodamaged D1	Haubühl et al., 2001; Huesgen et al., 2005, 2006; Luciński et al., 2011b; Schuhmann and Adamska, 2012
Deg5		At4g18370	35	32	TL, TM	Deg protease	Degradation of photodamaged D1; wound-induced degradation of PsbF	Huesgen et al., 2005; Sun et al., 2007; Luciński et al., 2011a; Kato et al., 2012; Schuhmann and Adamska, 2012
Deg7		At3g03380	120	120?	CS, TM	Deg protease	Degradation of photodamaged D1, D2, CP43, and CP47	Huesgen et al., 2005; Sun et al., 2010a; Schuhmann et al., 2011; Schuhmann and Adamska, 2012
Deg8		At5g39830	47	45	TL, TM	Deg protease	Degradation of photodamaged D1	Huesgen et al., 2005; Sun et al., 2007; Kato et al., 2012; Schuhmann and Adamska, 2012
HCF243	–	At3g15095	76	67	TM	Other[f]	Biogenesis, C-terminal processing, and assembly of D1; possibly biogenesis of D2	Zhang et al., 2011
PSB27-H1	slr1645	At1g03600	19	12	TL, TM	Other	C-terminal processing of D1 during PSII repair?	Chen et al., 2006a; Wei et al., 2010; Dietzel et al., 2011; Shi et al., 2012; Mabbitt et al., 2014
PSB27-H2/ LPA19		At1g05385	22	15	TL, TM	Other	C-terminal processing during *de novo* PSII assembly	Wei et al., 2010; Shi et al., 2012; Mabbitt et al., 2014

(Continued)

TABLE 1 | Continued

Name	Gene locus in *Synechocystis* sp. PCC 6803[a]	Gene locus in Arabidopsis[b]	Full-length Size (kDa)	Mature size (kDa)	Location	Protein classification	Function	References[c]
HCF136	slr2034	At5g23120	44	38	TL	Other	Assembly of PSII reaction-center complexes such as RC, RC47a, and RC47b	Meurer et al., 1998; Plücken et al., 2002; Mabbitt et al., 2014
PAM68	sll0933	At4g19100	24	20	TM	Other	Conversion of PSII minimal reaction-center complexes into larger PSII assembly intermediates; C-terminal processing of D1	Armbruster et al., 2010
PsbN/ PBF1	smr0009	AtCg00700	4.7	4.7	TM	Other	Assembly of PSII minimal reaction-center complexes; regulation of PSII core and antenna protein phosphorylation	Krech et al., 2013; Torabi et al., 2014
PSB28	sll1398	At4g28660	22	14	TL	Other	Biogenesis of chlorophyll-binding proteins such as CP47, PsaA, and PsaB	Jung et al., 2008; Shi et al., 2012; Mabbitt et al., 2014
LPA2	–	At5g51545	20	~20	TM	Other	Synthesis and assembly of CP43	Ma et al., 2007; Cai et al., 2010
LPA3	–	At1g73060	40	34	CS, TM	Other	Synthesis and assembly of CP43	Cai et al., 2010
PSB33	–	At1g71500	32	25	TM	Other	Association of LHCII with PSII	Fristedt et al., 2015
HHL1	–	At1g67700	26	18	TM	Other	Reassembly of PSII core monomers and PSII-LHCII supercomplexes during PSII repair	Jin et al., 2014
MPH1	–	At5g07020	24	20	TM	Other	Assembly and/or stability of PSII core monomers and higher order PSII complexes under high light	Liu and Last, 2015a,b

C, chloroplast; CE, chloroplast envelope; CS, chloroplast stroma; ICE, inner chloroplast envelope; IMM, inner mitochondria membranes; TL, thylakoid lumen; TM, thylakoid membranes.

[a] The gene loci in Synechocystis sp. PCC 6803 are included in this table only to distinguish between factors that are conserved in cyanobacteria and land plants and factors that are found in land plants but not in cyanobacteria. The hyphen indicates that the corresponding factor is either absent or not yet found in Synechocystis sp. PCC 6803.

[b] This article focuses on the identification and roles of PSII assembly, stability, and repair factors in Arabidopsis; therefore the gene loci for factors in other land plants are not listed in this table.

[c] Detailed descriptions of factors involved in the assembly, stability, and repair of PSII in cyanobacteria can be found in Nickelsen and Rengstl (2013). Therefore, references for factors in cyanobacteria are not listed in this table.

[d] The Synechocystis sp. PCC 6803 genome contains four FtsH genes. Because there is no straightforward one-to-one correspondence between the 12 Arabidopsis FtsH genes and four cyanobacterial FtsH genes, the four cyanobacterial FtsH loci are listed together.

[e] The Synechocystis sp. PCC 6803 genome contains three Deg genes. Because there is no straightforward one-to-one correspondence between the 16 Arabidopsis Deg genes and three cyanobacterial Deg genes, the three cyanobacterial Deg loci are listed together.

[f] Factors that do not fall in the 12 well-defined classifications (see Section Proteins that influence the assembly, stability, and repair of PSII) are classified as "other proteins" that influence the assembly, stability, and repair of PSII.

requires none of the known targeting apparatus are responsible for translocating thylakoid membrane proteins. LHCPs are translocated via the cpSRP pathway that requires the action of cpSRP43 (chloroplast Signal Recognition Particle protein of 43 kDa), cpSRP54 (cpSRP protein of 54 kDa), cpFtsY (chloroplast filamentation temperature sensitive protein Y), and ALB3 (Albino3) (**Figures 1**, **2**). ALB3 was found to interact with PSII subunits D1, D2, and CP47 (Ossenbühl et al., 2004; Pasch et al., 2005; Göhre et al., 2006), consistent with the function of the cpSRP pathway in translocating PSII proteins such as D1, D2, and CP47 (**Figures 1**, **2**). Most of the remaining thylakoid membrane proteins are inserted by the unusual pathway that requires none of the known targeting apparatus. The cpSecA-cpSecYE (cpSec means chloroplast secretory) pathway and the chloroplast twin-arginine translocation (cpTat) pathway are responsible for translocation of lumenal proteins. In Arabidopsis, each cpSec component is encoded by two genes (**Table 1**). The cpTat pathway has three components: Thylakoid Assembly 4 (THA4), High Chlorophyll Fluorescence 106 (HCF106), and cpTat protein C (cpTatC) (Albiniak et al., 2012). PsbO and plastocyanin are substrates of the cpSec pathway while PsbP and PsbQ are substrates of the cpTat pathway (**Figures 1**, **2**; Albiniak et al., 2012). Like their bacterial counterparts, components of the cpSRP and cpSec pathways may act in a modular fashion (Cline and Theg, 2007; Henry et al., 2007). For instance, cpSRP54 was identified in co-translational D1 insertion intermediates, along with cpSecY (chloroplast secretory translocase Y) and chloroplast ribosomes (Cline and Theg, 2007; Henry et al., 2007). Consistent with this finding, Walter et al. (2015) reported that cpSecY forms a complex with VIPP1 (Vesicle-Inducing Protein in Plastids 1) and cpSec components ALB3, cpFtsY, and cpSRP54 during co-translational integration of D1 (**Figures 1**, **2**). How different thylakoid membrane and lumenal proteins, including components of PSII complexes, are transported and integrated into thylakoids by the above-mentioned thylakoid-protein-targeting complexes can be found in a number of reviews (Schunemann, 2007; Cline and Dabney-Smith, 2008; Albiniak et al., 2012).

Components of the Putative Chloroplast-Vesicle-Transport System

PSII is located in the thylakoid membranes of oxygenic photosynthetic organisms; therefore thylakoid membrane biogenesis is essential to PSII assembly (Nickelsen and Zerges, 2013; Rast et al., 2015). It has been suggested that thylakoids could develop from invaginations of the inner envelope membrane via a vesicle-based transfer process and these vesicles are thought as a method of transporting lipids and proteins to and from thylakoids (Hoober et al., 1991; Westphal et al., 2001, 2003; Charuvi et al., 2012; Karim and Aronsson, 2014; Rast et al., 2015). Chloroplast vesicles are typically not observed when vesicular transport from the inner chloroplast envelope to thylakoids is continuous at ambient temperature (Morré et al., 1991). When vesicular transport is blocked by low temperature, chloroplast vesicles accumulate (Morré et al., 1991). A number of proteins have been implicated as part of the chloroplast-vesicle-transport system, including CPRabA5e (chloroplast Rab GTPase A5e), CYO1/SCO2 (Shiyou 1/Snowy Cotyledon 2), THF1/PSB29 (Thylakoid Formation 1/PSII protein 29), TerC (Tellurite-resistance protein C), and VIPP1 (Karim and Aronsson, 2014; Rast et al., 2015).

CPRabA5e is a small Rab GTPase targeted to the chloroplast stroma and thylakoid membranes (Karim et al., 2014). Transfer DNA (T-DNA) insertions in the *CPRabA5e* gene cause a reduced amount of grana thylakoids in Arabidopsis leaves (Karim et al., 2014). After pre-incubation at 4°C, the *cprabA5e* mutants have larger plastoglobules and an increased number of small vesicles, compared to the wild type. CPRabA5e was found to interact with a number of photosynthetic proteins, including PSI subunits H2 and K (PsaH2 and PsaK; Psa stands for Photosystem I), the PSII core subunit CP47, and LHCB proteins LHCB1 and LHCB3 (Karim et al., 2014). These findings led to the hypothesis that CPRabA5e is involved in transport of photosynthetic proteins, such as LHCB1, LHCB3, and CP47 (**Figures 1**, **2**), to developing thylakoids in young chloroplasts via vesicles (Karim et al., 2014).

CYO1/SCO2 is a zinc-finger-domain-containing thylakoid membrane protein with protein disulfide isomerase (PDI) activity (Shimada et al., 2007; Albrecht et al., 2008; Muranaka et al., 2012; Tanz et al., 2012). A loss-of-function mutation in the *CYO1/SCO2* gene results in globularly or normally shaped plastids with very big vesicles in Arabidopsis cotyledons (Tanz et al., 2012). A closer look at normally shaped chloroplasts from mutant cotyledons showed that small vesicles emerged from the inner chloroplast envelope, even at ambient temperature. These vesicles were not observed in chloroplasts from wild-type cotyledons used in the same study. These observations suggest that vesicular transport from the inner chloroplast envelope to developing thylakoids is blocked in the cotyledons of mutant seedlings and that the chloroplast-vesicle-transport system is important for thylakoid biogenesis rather than damage or programmed degradation of the thylakoid membrane system. CYO1/SCO2 was found to interact with PSI core subunits PsaA and PsaB, PSII core subunits CP43 and CP47, and LHCB1 (Muranaka et al., 2012; Tanz et al., 2012) and to co-migrate with Photosystem I-light-harvesting complex I (PSI-LHCI) and PSII-LHCII supercomplexes in blue native-polyacrylamide gel electrophoresis (BN-PAGE) (Shimada et al., 2007). Therefore, it is conceivable that CYO1/SCO2 participates in transport of photosynthetic proteins, such as CP43, CP47, and LHCB1 (**Figures 1**, **2**), to and from thylakoids via chloroplast vesicles in cotyledons (Tanz et al., 2012). The association of CYO1/SCO2 with PSI-LHCI and PSII-LHCII supercomplexes also begs the question whether this protein has a role in stabilizing these supercomplexes (**Figures 1**, **2**).

THF1/PSB29 is a coiled-coil-domain-containing protein targeted to the chloroplast envelope, chloroplast stroma, and thylakoid membranes (Wang et al., 2004; Huang et al., 2006). The *thf1/psb29* knockout mutant of Arabidopsis has a variegated phenotype in cotyledons and true leaves and the chloroplasts in the yellow sectors of *thf1/psb29* leaves lack normal thylakoids and accumulate chloroplast vesicles (Wang et al., 2004; Keren et al., 2005; Zhang et al., 2009). These data led to the hypothesis that THF1/PSB29 is required for organizing chloroplast vesicles

into mature thylakoids (Wang et al., 2004). THF1/PSB29 was thought to be involved in maintaining levels of FtsHs in plants because D1, a substrate of FtsHs, was found to be more stable in the *thf1/psb29* mutant than in the wild type (Zhang et al., 2009). However, it was later found that the stay-green phenotype of the *thf1/psb29* mutant is not due to reduced FtsH protease activity, because *ftsh2/var2* (*var2* stands for *yellow variegated 2*) leaves turn yellow much faster than wild-type and *thf1/psb29* leaves during dark-induced senescence (Huang et al., 2013). THF1/PSB29 was found to interact with all six LHCB proteins (Huang et al., 2013); therefore it is possible that LHCB proteins are transported to thylakoid membranes via direct interaction with THF1/PSB29 (**Figures 1**, **2**). In addition, it was proposed that THF1/PSB29 regulates the dynamics of PSII-LHCII supercomplexes during high-light stress and leaf senescence (**Figure 2**; Huang et al., 2013; Yamatani et al., 2013). The THF1/PSB29-deficient mutants of Arabidopsis and rice (*Oryza sativa*) also have a stay-green phenotype in pathogen-infected and dark-induced senescent leaves (Huang et al., 2013; Yamatani et al., 2013). In dark- and high-light-treated *thf1/psb29* Arabidopsis leaves, PSII-LHCII supercomplexes are highly unstable but a type of PSII-LHCII megacomplexes is retained (Huang et al., 2013). Consistent with a role in regulating the dynamics of PSII-LHCII supercomplexes, THF1/PSB29 was found to co-migrate with trimeric and monomeric LHCII in BN-PAGE (Huang et al., 2013).

TerC is an integral thylakoid membrane protein with eight transmembrane helices (Kwon and Cho, 2008; Schneider et al., 2014). T-DNA insertions in the *TerC* gene caused a pigment-deficient and seedling-lethal phenotype in Arabidopsis (Kwon and Cho, 2008; Schneider et al., 2014). This is accompanied with a substantial reduction or complete loss of thylakoid membranes and over-accumulation of chloroplast vesicles. Therefore, TerC was considered to be invloved in thylakoid biogenesis and vesicle transport (Kwon and Cho, 2008). To further analyze the function of TerC, Schneider et al. (2014) generated an artifical microRNA-based knockdown allele *amiR-TerC* in Arabidopsis and found that the severe phenotype of the T-DNA mutants is likely due to the subsantaially reduced rates of synthesis and insertion of PSII proteins. In line with these observations, TerC was found to interact with PSII proteins D1, D2, and CP43 as well as PSII assembly factors ALB3, LPA1/PratA (Low PSII Accumulation 1/Processing-associated tetratricopeptide repeat protein A), LPA2 (Low PSII Accumulation 2), and PAM68 (Photosynthesis Affected Mutant 68) (Schneider et al., 2014). Taken together, it is reasonable to propose that TerC is also invloved in co-translational insertion of PSII proteins (e.g., D1, D2, and CP43) into thylakoid membranes, in colaboration with other PSII assembly factors (**Figures 1**, **2**; Schneider et al., 2014).

VIPP1 is homologous to the phage shock protein A in *Escherichia coli*, which is induced under various stress environments (Karim and Aronsson, 2014). VIPP1 is targeted to the inner chloroplast envelope and thylakoid membranes (Kroll et al., 2001). The *vipp1* knockdown and knockout mutants of Arabidopsis are pigment-deficient and semi-lethal (i.e., unable to grow photoautotrophically) (Kroll et al., 2001; Zhang et al., 2012; Zhang and Sakamoto, 2012). Chloroplasts from the *vipp1* knockout and knockdown mutants are defective in thylakoid membrane formation and vesicle budding from inner envelope membranes. In addition, *vipp1* mutant chloroplasts are swollen due to damage in the chloroplast envelope and increases in the osmotic pressure in the chloroplast stroma (Zhang et al., 2012; Zhang and Sakamoto, 2012). VIPP1 was recently found in co-translational D1 insertion intermediates isolated from thylakoid membranes of pea (*Pisum sativum*) leaves, along with cpSecY, ALB3, cpFtsY, and cpSRP54 (Walter et al., 2015). Therefore, VIPP1 was proposed as a multifunctional protein that is involved in chloroplast vesicular transport, thylakoid biogenesis, and co-translational insertion of photosynthetic proteins (**Figure 1**).

PSII Subunit-Like Proteins, e.g., PsbP-Like and LHCP-Like Proteins

Five PSII subunit-like proteins, including one PsbP-like protein and four LHCP-like proteins, have been implicated to be involved in the assembly, stability, and/or repair of PSII complexes or subunits. PsbP-like proteins are in the same family as PsbP proteins (Bricker et al., 2013; Ifuku, 2014). Unlike PsbP proteins, whose primary function is water splitting and oxygen evolution, PsbP-like proteins are not part of the OEC. Arabidopsis has two PsbP-like proteins: PPL1 and PPL2 (**Table 1**). A T-DNA insertion in the *PPL1* gene led to increased sensitivity to high light and delayed recovery after photoinhibition (Ishihara et al., 2007). These data suggest that PPL1 is required for efficient repair of photodamaged PSII. Although PPL1 has not been shown to be associated with PSII in higher plants, its cyanobacterial homolog cyanoP (ssl1418) has been shown to be loosely associated with PSII and possess the same beta-sandwich fold and a well-conserved zinc-binding site as PsbP in higher plants (Ishikawa et al., 2005b; Summerfield et al., 2005; Michoux et al., 2010, 2014; Jackson et al., 2012). Further studies are needed to investigate the precise function of PPL1 in PSII repair. Unlike PPL1, PPL2 is required for the accumulation of chloroplast NAD(P)H dehydrogenase complex (Ishihara et al., 2007); therefore the function of PPL2 is not discussed in this review.

LHCP-like proteins are in the same superfamily as LHCPs (Heddad et al., 2012). Unlike LHCPs, whose primary function is light-harvesting, most LHCP-like proteins are involved in chlorophyll- and carotenoid-binding, assembly and stability of chlorophyll-protein complexes, and/or photoprotection. LHCP-like proteins can be classified into three subfamilies: three-helix, early light-induced proteins (ELIPs), two-helix, stress-enhanced proteins (SEPs), and one-helix, high-light-induced, small chlorophyll-binding-like proteins (OHPs/HLIPs/SCPs). ELIPs are restricted to green algae and land plants, SEPs are ubiquitously present in photosynthetic eukaryotes, OHP1 exists in cyanophages, cyanobacteria, and photosynthetic eukaryotes, and OHP2 exists in eukaryotes. The Arabidopsis genome encodes two ELIPs, six SEPs, and two OHPs (Heddad et al., 2012).

ELIPs appear to be associated with PSII under standard conditions in pea plants; they become associated with monomeric and trimeric LHCII under high light in Arabidopsis

(Adamska and Kloppstech, 1991; Heddad et al., 2006). Heddad et al. (2006) showed that the relative amounts of ELIP transcripts and proteins increase as the light intensity increases. It was therefore proposed that ELIPs may be involved in photoprotection by binding free chlorophyll released during degradation of pigment-binding proteins or by stabilizing the assembly of pigment-binding proteins during photoinhibition (Adamska and Kloppstech, 1991; Hutin et al., 2003). The potential function of ELIPs in stabilizing LHCII and PSII-LHCII supercomplexes under light stress is included in **Figure 2**. However, *elip1* and *elip2* single knockout mutants and the *elip1 elip2* double knockout mutant have a similar phenotype and light sensitivity as the wild-type Arabidopsis plants (Casazza et al., 2005; Rossini et al., 2006). Additional studies are needed to dissect the exact functions of ELIP proteins.

Among the six SEPs in Arabidopsis, the functions of SEP3.1/LIL3:1 (SEP stands for stress-enhanced protein; LIL stands for light-harvesting-like protein) and SEP3.2/LIL3:2 have been extensively studied (Tanaka et al., 2010; Takahashi et al., 2014; Lohscheider et al., 2015; Mork-Jansson et al., 2015). The anti-sense *sep3.1/lil3:1* mutant and the *sep3.1/lil3:1 sep3.2/lil3:2* double knockout mutant are deficient in chlorophyll and α-tocopherol biosynthesis (Tanaka et al., 2010; Lohscheider et al., 2015). The deficiency is due to a substantial reduction in the amount of chlorophyll and α-tocopherol biosynthetic enzyme geranylgeranyl reductase. In line with these findings, SEP3.1/LIL3:1 and SEP3.2/LIL3:2 were found to interact with geranylgeranyl reductase and their transmembrane domain was found to be important for the interaction (Tanaka et al., 2010; Takahashi et al., 2014). Therefore, SEP3.1/LIL3:1 and SEP3.2/LIL3:2 were proposed to be involved in chlorophyll and tocopherol biosynthesis by anchoring and stabilizing geranylgeranyl reductase to thylakoid membranes. In addition, SEP3.1/LIL3:1 and SEP3.2/LIL3:2 were found to accumulate with increasing light irradiance and they are associated with subcomplexes of LHCII (Lohscheider et al., 2015). Thus, it is also possible that SEP3.1/LIL3:1 and SEP3.2/LIL3:2 may function in stabilizing LHCII (**Figures 1**, **2**).

The *OHP* genes have an expression pattern similar to the *ELIP* and *SEP* genes, whose expression is up-regulated upon high light (Mulo et al., 2008; Heddad et al., 2012). The function of OHP1 is not yet known, but OHP2 was showed to be associated with PSI under low or high light and was therefore proposed to play a role in photoprotection of PSI (Andersson et al., 2003). Recently, a cyanobacterial OHP family protein was found to bind chlorophyll *a* and β-carotene and possess an energy-dissipative conformation, suggesting that OHP family proteins may have a photoprotective role (Staleva et al., 2015).

Atypical SDR Family Proteins

Classic SDR family proteins have an intact cofactor-binding site (TGXXGXXG) and an intact catalytic tetrad (NSYK), which are required for their SDR activity (Persson et al., 2009). Unlike classic SDR family proteins, atypical SDR family proteins have no known enzyme activity because they have an altered glycine-rich cofactor-binding site and partially or completely lack the signature catalytic tetrad (Link et al., 2012). Two atypical SDR family proteins have been found to be important for PSII: HCF173 (High Chlorophyll Fluorescence 173) and HCF244 (High Chlorophyll Fluorescence 244) (Schult et al., 2007; Link et al., 2012; Chidgey et al., 2014; Knoppová et al., 2014). Compared to HCF244, HCF173 is ∼200 amino acids longer and its SDR domain is fragmented into two regions. HCF173 and HCF244 have the same subcellular localization: they are both predominantly associated with chloroplast membranes, with a small fraction located in the chloroplast stroma. Loss-of-function mutations in the *HCF173* or *HCF244* gene result in similar defects in Arabidopsis: a drastic reduction in D1 synthesis, inability to accumulate PSII subunits, substantial decreases in PSII activity, and a complete loss of photoautotrophy (Schult et al., 2007; Link et al., 2012). The *hcf173* and *hcf244* single mutants are able to grow on sucrose-supplemented media but they are pale green and much smaller than the wild type (Link et al., 2012). Polysome association experiments demonstrated that these defects are caused by reduced translation initiation of the *psbA* transcript (Schult et al., 2007; Link et al., 2012). The decrease in translation initiation is accompanied by a reduction in *psbA* mRNA stability. The *hcf173 hcf244* double mutant grown on sucrose-supplemented media is smaller than the single mutants, suggesting that simultaneous loss of HCF173 and HCF244 has an additive effect (Link et al., 2012). The function of HCF173 and HCF244 in translation initiation of the *psbA* transcript is included in **Figures 1**, **2**. Some SDR family proteins, such as dihydrolipoamide acetyltransferases, glyceraldehyde-3-phosphate dehydrogenase, and lactate dehydrogenase, have evolved the capacity to bind RNA (Hentze, 1994; Nagy et al., 2000; Pioli et al., 2002; Bohne et al., 2013). Therefore, it is possible that HCF173 and HCF244 may act as RNA-binding proteins and facilitate translation initiation of the *psbA* mRNA (Link et al., 2012).

C-terminal Processing Peptidases

The PSII reaction-center protein D1 is often synthesized in the precursor form (pD1), with a C-terminal extension of 8–16 amino acids (Nixon et al., 1992; Anbudurai et al., 1994; Liao et al., 2000). In plants, this C-terminal extension is cleaved in a single step by C-terminal processing peptidase A (CtpA) at an early step of *de novo* PSII assembly or at the reassembly step of PSII repair (**Figures 1**, **2**). CtpAs are serine endopeptidases with a serine/lysine catalytic dyad (Anbudurai et al., 1994; Liao et al., 2000; Yamamoto et al., 2001). Recombinant spinach (*Spinacia oleracea*) CtpA exhibited efficient proteolytic activity toward thylakoid membrane-embedded pD1 (Yamamoto et al., 2001). Arabidopsis has three CtpAs in the thylakoid lumen and the functions of CtpA1 and CtpA2 have been studied (Yin et al., 2008; Che et al., 2013).

Under normal growth conditions, T-DNA insertions in the Arabidopsis *CtpA1* gene do not cause changes to plant growth and morphology, PSII activity, or thylakoid membrane complex formation (Yin et al., 2008). Under high light, the *ctpA1* mutant displays retarded growth, accelerated D1 turnover, as well as increased photosensitivity and delayed recovery of PSII activity. Therefore, CtpA1 was proposed to be involved in D1 protein C-terminal processing in the PSII repair cycle (**Figure 2**).

Unlike the *ctpA1* mutant, the T-DNA mutant of the Arabidopsis *CtpA2* gene is lethal under normal light but is viable in sucrose-supplemented media under low light (Che et al., 2013). The viable *ctpA2* mutant displays a complete loss of the mature D1 protein, reduced levels of other PSII core proteins, a severely decreased level of PSII supercomplexes, and a substantial reduction or complete loss of PSII activity. pD1 and other PSII subunits in the viable *ctpA2* mutant are present in PSII monomers and PSII dimers but absent in PSII supercomplexes. These data suggest that CtpA2 is indispensible for C-terminal processing of D1 (**Figure 1**), which in itself is essential for *de novo* PSII assembly. A weak allele expressing ∼2% of the wild-type level of CtpA2 appears to be normal under normal light but displays stunted growth and over-accumulation of pD1 under elevated light (Che et al., 2013). These data suggest that CtpA2 is also involved in C-terminal processing of D1 during high-light-induced PSII repair (**Figure 2**).

TPR Proteins

The TPR is a 34-amino acid repeated motif that ubiquitously exits among all organisms (Ishikawa et al., 2005a). Two TPR proteins have been found to be involved in PSII assembly and/or repair: LPA1/PratA and MET1 (Mesophyll-Enriched Thylakoid protein 1) (Ishikawa et al., 2005a; Peng et al., 2006; Bhuiyan et al., 2015).

LPA1/PratA is an intrinsic thylakoid membrane protein with two tandem TPR motifs and a double-pass transmembrane domain (Klinkert et al., 2004; Peng et al., 2006). T-DNA insertions in the Arabidopsis *LPA1/PratA* gene result in reduced growth, pale-green leaves, reduced PSII activity, reduced amounts of PSII proteins, reduced synthesis of D1 and D2, increased turnover of PSII core subunits D1, D2, CP43, and CP47, and inefficient assembly of PSII (Peng et al., 2006). The transcript levels of genes encoding PSII core subunits are unchanged in the mutants. LPA1/PratA was found to directly interact with D1 in a split-ubiquitin yeast-two-hybrid assay. These data suggest that LPA1/PratA has a role in biogenesis and assembly of D1 (**Figures 1**, **2**). Consistent with this hypothesis, LPA1/PratA was identified in thylakoid-membrane-associated ribosome nascent chain fractions (Peng et al., 2006).

MET1 has an N-terminal PDZ domain and a C-terminal TPR motif, which are conserved across green algae and land plants (Ishikawa et al., 2005a; Bhuiyan et al., 2015). MET1 is peripherally attached to thylakoid membranes on the stromal side and it is enriched in stroma lamellae (Bhuiyan et al., 2015). T-DNA insertions in the Arabidopsis *MET1* gene do not cause obvious changes to the accumulation and assembly state of the photosynthetic apparatus under normal light (Bhuiyan et al., 2015). Under fluctuating light, the *met1* mutants demonstrate reduced growth, decreased PSII efficiency, a near-complete loss of PSII-LHCII supercomplexes, and increased amounts of unassembled CP43. Loss of MET1 also causes increased photosensitivity of PSII activity and an accelerated rate of D1 turnover under high light. MET1 was found to co-migrate with a series of PSII subcomplexes, such as PSII dimers, PSII core monomers, CP43-less PSII monomers, and PSII reaction-center complexes (i.e., RC, RC47a, and RC47b), in BN-PAGE. Therefore, MET1 was proposed to be involved in supercomplex formation during PSII repair (**Figure 2**). In line with this hypothesis, MET1 was found to interact with the stromal loops of PSII core subunits CP43 and CP47 (Bhuiyan et al., 2015).

Thiol/Disulfide-Modulating Proteins

Thiol/disulfide modulation is important for regulating photosynthetic processes (Järvi et al., 2013; Karamoko et al., 2013). Three types of thiol/disulfide-modulating proteins have been found to be involved in the assembly, stability, function, and repair of PSII: protein disulfide isomerases (PDIases), protein disulfide reducing proteins, and protein thiol oxidizing proteins.

As mentioned above, thylakoid membrane protein CYO1/SCO2 was found to play a role in chloroplast and thylakoid biogenesis and vesicular transport of photosynthetic proteins to developing thylakoids in cotyledons (Shimada et al., 2007; Albrecht et al., 2008; Tanz et al., 2012). CYO1/SCO2 has a C_4-type zinc-finger domain with two conserved CXXCXGXG repeats, the signature domain for PDIase activity (Shimada et al., 2007). Recombinant CYO1/SCO2 is able to catalyze reduction of protein disulfide bonds and oxidative renaturation of reduced and denatured protein substrates, indicating that CYO1/SCO2 is a PDIase (Shimada et al., 2007). CYO1/SCO2 was found to interact with PsaA, PsaB, CP47, CP43, and LHCB1 (Muranaka et al., 2012; Tanz et al., 2012). These five CYO1/SCO2-interacting proteins contain cysteine in the hydrophobic region(s). Therefore, CYO1/SCO2 may also participate in folding of cysteine-containing PSI and PSII subunits (**Figures 1**, **2**), by forming transient disulfide bonds with its protein substrates via the CXXC motif (Jessop et al., 2007; Feige and Hendershot, 2011).

LQY1 (Low Quantum Yield of PSII 1) is another thylakoid membrane protein with PDIase activity. Full-length LQY1 has a chloroplast transit peptide, a transmembrane domain, and a C-terminal C_4-type zinc-finger domain with four conserved CXXCXGXG repeats (Lu et al., 2011). Recombinant LQY1 is able to catalyze oxidative renaturation of reduced and denatured protein substrates and reductive renaturation of oxidized protein substrates. T-DNA insertions in the Arabidopsis *LQY1* gene cause reduced efficiency of PSII photochemistry, increased sensitivity to high light, and increased accumulation of reactive oxygen species under high light. The *lqy1* mutants were found to accumulate fewer PSII-LHCII supercomplexes and have altered rates of high-light-induced D1 turnover and re-synthesis. The *lqy1* mutant phenotype can be suppressed by complementation of *lqy1* mutants with the wild-type *LQY1* gene (Lu, 2011). LQY1 is associated with the PSII core monomer and the CP43-less PSII monomer (a marker for ongoing PSII repair and reassembly) and it is most abundant in stroma-exposed thylakoid membranes, where important steps of PSII repair occurs (Lu et al., 2011). Under high light, LQY1 associated with PSII monomers increases at the expense of free LQY1 and LQY1 associated with smaller PSII complexes. Immunoprecipitation analysis showed that LQY1 interacts with PSII core subunits

CP47 and CP43, which contain three and four conserved cysteine residuals, respectively. Therefore, it was proposed that LQY1 is involved in PSII repair (Lu, 2011; Lu et al., 2011). It is possible that LQY1 participates in dissembly, folding, and/or reassembly of cysteine-containing PSII subunits and complexes and/or regulates D1 synthesis and turnover during PSII repair (**Figure 2**). These hypotheses require further investigation.

PDI6/PDIL1-2 (Protein Disulfide Isomerase 6/Protein Disulfide Isomerase-Like 1-2) contains two redox-active thioredoxin domains (with the WCGHC active site), two redox-inactive thioredoxin-like domains, and a C-terminal endoplasmic reticulum retention signal KDEL (Houston et al., 2005; Wittenberg et al., 2014). PDI6/PDIL1-2 is dual-targeted to chloroplasts and the endoplasmic reticulum; chloroplast–targeted PDI6 is located in the stroma (Wittenberg et al., 2014). Similar to CYO1/SCO2 and LQY1, recombinant PDI6/PDIL1-2 is capable of catalyzing oxidative renaturation of reduced and denatured protein substrates. Compared to wild-type Arabidopsis, the *pdi6-1* and *pdi6-2* knockdown mutants display increased resistance to high light, reduced photoinhibition, and an accelerated rate of D1 synthesis (Wittenberg et al., 2014). Therefore, it was proposed that PDI6/PDIL1-2 may function as an attenuator of D1 synthesis during PSII repair (**Figure 2**).

Thioredoxins are small proteins that contain a redox-active thioredoxin domain with the WCGHC active site (Cain et al., 2009). As enzymes, thioredoxins are active in the reduced form and are able to reduce disulfide bonds in protein substrates (Cain et al., 2009). Thioredoxins are important for regulating thiol/disulfide homeostasis inside chloroplasts (Cain et al., 2009). Three M-type thioredoxins (TRX-M1, M2, and M4) have been found to be involved in PSII biogenesis in chloroplasts (Wang et al., 2013). TRX-M1, M2, and M4 are associated with minor PSII assembly intermediate subcomplexes and they interact with PSII core subunits D1, D2, and CP47. Simultaneous inactivation of the three Arabidopsis *TRX-M* genes causes pale-green leaves, reduced PSII activity, decreased accumulation of PSII complexes, and increased accumulation of reactive oxygen species. PSII core proteins D1 and CP47 were found to be able to form redox-sensitive intermolecular disulfide bonds and concurrent loss of the three M-type thioredoxins interrupts the redox status of these PSII core subunits. According to these results, Wang et al. (2013) proposed that the three TRX-M proteins may assist incorporation of CP47 into PSII core complexes (**Figure 1**).

In addition to PDIases and thioredoxins, a new type of proteins has been found to regulate thiol/disulfide homeostasis and they mainly act as oxidases by converting free thiols on protein substrates into disulfide bridges. One example is Lumen Thiol Oxidoreductase 1 (LTO1), a thylakoid membrane protein with an integral-membrane vitamin K epoxide reductase domain and a soluble disulfide-bond A oxidoreductase-like domain (Feng et al., 2011; Karamoko et al., 2011; Lu et al., 2013). Each of the two domains contains four conserved cysteine residues (a pair of cysteine residues in the CXXC motif and another pair of separate cysteine residues), which are critical for the disulfide-bond-forming activity of LTO1 (Feng et al., 2011). According to membrane topology analysis, Feng et al. (2011) proposed that the eight conserved cysteine residues are positioned on the lumenal side of thylakoid membranes. This led to the hypothesis that LTO1 is involved in formation of the intramolecular disulfide bond in PsbO (**Figures 1**, **2**), which is located on the lumenal side of thylakoid membranes (Karamoko et al., 2011). Consistent with this hypothesis, LTO1 was found to interact with PsbO1 and PsbO2 and catalyze formation of intramolecular disulfide bonds in recombinant PsbO (Karamoko et al., 2011). In line with these observations, the amounts of PsbO, PsbQ, and PsbQ are substantially reduced in the LTO1-deficient Arabidopsis mutants and the mutants display reduced efficiency of PSII photochemistry, increased accumulation of reactive oxygen species, a smaller plant size, and delayed growth (Karamoko et al., 2011; Lu et al., 2013).

RBD1 (rubredoxin 1) is a small iron-containing protein with a C-terminal transmembrane domain and a rubredoxin domain with two redox-active CXXC motifs (Calderon et al., 2013). Homologs of RBD1 have been found in thylakoid membranes but not plasma membranes of cyanobacteria and in thylakoid membranes of green algae and land plants (Shen et al., 2002; Calderon et al., 2013). The *rbd1* knockout mutants in the cyanobacterium *Synechocystis* sp. PCC 6803, the green alga *Chlamydomonas reinhardtii*, and the higher plant Arabidopsis display a substantial reduction or complete loss of PSII activity and photoautotrophy (Calderon et al., 2013). The amounts of PSII core subunits, such as D1, D2, and CP47, are reduced by 40–90% in these mutants while other components of the photosynthetic apparatus, such as PSI, cytochrome b_6f complex, and ATP synthase, are not affected. Based on these data, Calderon et al. (2013) proposed that RBD1 is required for the assembly and/or stability of PSII in oxygenic photosynthetic organisms. Further studies are needed to dissect the precise function of RBD1.

PPIases

Peptide bonds to proline have *cis* and *trans* conformations (Fischer et al., 1998; Ingelsson et al., 2009). Therefore, folding of proteins such as PSII subunits often involves *cis-trans* proline isomerization, which is catalyzed by PPIases (He et al., 2004; Romano et al., 2004; Ingelsson et al., 2009). Three PPIase families have been established according to their immunosuppressant ligand specificity: cyclophilins (CYPs), FK506 (tacrolimus)-binding proteins (FKBPs), and parvulins (Fischer et al., 1998; He et al., 2004; Ingelsson et al., 2009). Two CYPs and one FKBP have been found to be important for the assembly, stability, and/or repair of PSII (Järvi et al., 2015).

CYP20-3/ROC4 (20-kDa cyclophilin 3/rotamase cyclophilin 4) is localized in the chloroplast stroma (Lippuner et al., 1994). The Arabidopsis T-DNA insertion mutant of CYP20-3/ROC4 has a normal phenotype and normal PSII function under ambient light (Cai et al., 2008). Under high light, PSII in the *cyp20-3/roc4* mutant exhibits increased photosensitivity and delayed recovery, which caused growth retardation and leaf yellowing. Under high light, D1 degradation is not affected in the mutant but repair and reassembly of photodamaged PSII is impaired. According to the *cyp20-3/roc4* mutant phenotype, Cai et al. (2008) proposed that CYP20-3/ROC4 is involved in repair and reassembly of PSII under high light (**Figure 2**). The

PPIase activity of CYP20-3/ROC4 makes it a good candidate for catalyzing correct folding of PSII proteins during the repair process of PSII. CYP20-3/ROC4 was also reported to link light and redox signals to cysteine biosynthesis and stress acclimation (Dominguez-Solis et al., 2008; Park et al., 2013; Speiser et al., 2015).

CYP38/TLP40 (cyclophilin of 38 kDa/Thylakoid Lumen Protein of 40 kDa) is predominantly confined in the lumen of non-appressed thylakoids (Fulgosi et al., 1998). Full-length CYP38/TLP40 has a bipartite thylakoid lumen targeting transit peptide, a leucine zipper, a phosphatase-binding module, an acid region for protein-protein interaction, and a C-terminal cyclophilin-type PPIase domain (Fulgosi et al., 1998; Sirpiö et al., 2008). CYP38/TLP40 isolated from spinach leaves demonstrates *in vivo* PPIase activity and co-purification with a thylakoid membrane phosphatase (Fulgosi et al., 1998; Vener et al., 1999). In addition, it was reported that CYP38/TLP40 could be released from thylakoid membranes to the thylakoid lumen upon heat stress and the release is associated with activation of dephosphorylation of PSII subunits in thylakoid membranes (Rokka et al., 2000). Therefore, it was proposed that CYP38/TLP40 acts as a phosphatase inhibitor and regulates dephosphorylation of PSII subunits during PSII repair (**Figure 2**). Consistent with this hypothesis, T-DNA insertions in the Arabidopsis *CYP38/TLP40* gene cause increased phosphorylation of PSII core subunits and increased photosensitivity of PSII activity (Fu et al., 2007; Sirpiö et al., 2008). In addition, CYP38/TLP40 was found to interact with CP47 through its cyclophilin domain (Vasudevan et al., 2012). Dephosphorylation of PSII subunits during light acclimation is carried out by a type 2C protein phosphatase called PSII core phosphatase (PBCP) (Samol et al., 2012). Further studies are needed to investigate whether CYP38/TLP40 interacts with PBCP and inhibits its phosphatase activity. The *cyp38/tlp40* mutants display retarded growth, pale-green leaves, increased accumulation of PSII monomers, and decreased accumulation of PSII supercomplexes, even under low or ambient light (Fu et al., 2007; Sirpiö et al., 2008). In addition, CYP38/TLP40 was found to co-migrate with PSII core monomers in BN-PAGE (Sirpiö et al., 2008). Therefore, it is likely that CYP38 also functions in conversion of PSII core monomers into higher order PSII complexes (**Figures 1**, **2**).

FKBP20-2 (20-kDa FK506-binding protein 2) is located in the thylakoid lumen (Lima et al., 2006). Recombinant FKBP20-2 demonstrates PPIase activity and the C-terminus of FKBP20-2 has a unique pair of cysteine residues which can be reduced by thioredoxin. T-DNA insertions in the Arabidopsis *FKBP20-2* gene cause smaller plant sizes, reduced chlorophyll contents, stunted growth, reduced PSII activity, increased accumulation of PSII monomers and PSII dimers, and decreased accumulation of PSII supercomplexes under normal light conditions (Lima et al., 2006). Under higher light, the difference in PSII activity between the mutant and the wild type is more pronounced. According to the mutant phenotype, Lima et al. (2006) proposed that FKBP20-2 functions in formation of PSII-LHCII supercomplexes under normal and high light (**Figures 1**, **2**).

Protein Kinases

Multiple studies have shown that high light induces phosphorylation of PSII core proteins, such as D1, D2, CP43, and PsbH (Rintamaki et al., 1997; Vener et al., 2001), which facilitates migration of photodamaged PSII complexes from grana stacks to stroma lamellae (Tikkanen et al., 2008; Goral et al., 2010). Two serine/threonine protein kinases were found to be localized the thylakoid membranes: STN7 (state transition 7) and STN8 (state transition 8) (Bellafiore et al., 2005; Bonardi et al., 2005; Nath et al., 2013). Light-induced phosphorylation of PSII core proteins is carried out by STN8, and to a lesser degree under low light also by STN7 (**Figure 2**; Bonardi et al., 2005; Tikkanen et al., 2008; Nath et al., 2013). The primary role of STN7 is phosphorylation of LHCII proteins, which leads to displacement of LHCII from PSII to PSI (Bellafiore et al., 2005). Phosphorylation of PSII core proteins promotes unfolding of grana stacks and migration of photodamaged PSII complexes from grana stacks to stroma-exposed thylakoids. This allows easier access of membrane or membrane-associated proteases and co-translational integration of D1 and therefore facilitates repair of photodamaged PSII complexes and proteins (Bonardi et al., 2005; Tikkanen et al., 2008; Khatoon et al., 2009; Goral et al., 2010; Herbstová et al., 2012; Tikkanen and Aro, 2012).

Protein Phosphatases

While the migration of photodamaged PSII complexes is assisted by phosphorylation of PSII core proteins, dephosphorylation of D1 is necessary for efficient turnover of photodamaged D1 in stroma lamellae (Järvi et al., 2015). Two chloroplast protein phosphatases, PBCP and TLP18.3 (Thylakoid Lumen Protein of 18.3 kDa), have demonstrated *in vivo* or *in vitro* phosphatase activity toward PSII core proteins (Sirpiö et al., 2007; Wu et al., 2011; Samol et al., 2012). PBCP is a type 2C protein phosphatase predominantly found in the chloroplast stroma, with a minor fraction associated with thylakoid membranes (Samol et al., 2012). Compared to wild-type Arabidopsis, the PBCP-deficient mutants display delayed dephosphorylation of PSII core proteins (D1, D2, CP43, and PsbH) and normal dephosphorylation of LHCII proteins, upon exposure to far-red light, which favors PSI excitation and dephosphorylation of thylakoid proteins (Samol et al., 2012). Samol et al. (2012) concluded that PBCP is required for efficient dephosphorylation of PSII core proteins (**Figure 2**).

TLP18.3 is a thylakoid membrane protein with the N-terminal domain of unknown function located in the thylakoid lumen (Sirpiö et al., 2007). It was originally identified as an auxiliary protein involved in dimerization of PSII monomers and degradation of photodamaged D1 (**Figures 1**, **2**). The TLP18.3-deficient Arabidopsis mutants do not show a clear visual phenotype under normal growth conditions but exhibit retarded growth under fluctuating light (Sirpiö et al., 2007), suggesting that TLP18.3 is more important to PSII repair than to *de novo* PSII assembly. Compared to the wild type, the TLP18.3-deficient mutants have fewer PSII dimers and more PSI monomers under normal and fluctuating light. In addition, the rate of high-light-induced D1 turnover is ∼50% slower in

the TLP18.3-deficient mutants. Consistent with its dual roles in dimerization of PSII monomers, which occurs in grana stacks, and degradation of photodamaged D1, which takes place in stroma lamellae, TLP18.3 was found evenly distributed between grana stacks and stroma lamellae (Sirpiö et al., 2007). It was later found that the domain of unknown function in TLP18.3 possesses acid phosphatase activity toward synthetic phosphorylated oligopeptides that resemble the phosphorylation sites of PSII core proteins D1 and D2 (Wu et al., 2011). However, how the acid phosphatase activity of TLP18.3 is related to the role of TLP18.3 in PSII assembly and repair is still not clear (**Figure 2**): the phosphorylation sites of D1 are exposed to the stroma side while the acid phosphatase domain of TLP18.3 is located in the thylakoid lumen.

Dephosphorylation of LHCII proteins, such as LHCB1 and LHCB2, is carried out by PPH1/TAP38 (Protein Phosphatase 1/Thylakoid-Associated Phosphatase of 38 kDa) (Pribil et al., 2010; Shapiguzov et al., 2010). PPH1/TAP38 is a type 2C protein phosphatase with a C-terminal single-pass transmembrane domain; it is predominantly located in stroma lamellae and grana margins, where active dephosphorylation of LHCII and PSII core proteins occurs. Loss-of-function mutations in the Arabidopsis *PPH1/TAP38* gene causes decreased dephosphorylation of LHCII while overexpression of PPH1/TAP38 enhances dephosphorylation of LHCII (Pribil et al., 2010; Shapiguzov et al., 2010). The phosphorylation status of PSII core proteins is largely unaffected in the *pph1/tap38* mutants, suggesting that the primary function of PPH1/TAP38 is dephosphorylation of LHCII proteins. Recombinant PPH1/TAP38 is able to dephosphorylate LHCII directly, in an *in vitro* assay (Pribil et al., 2010). Reversible phosphorylation of LHCII is important for the movement of LHCII between PSII and PSI, according to the changes in the spectral composition of incident light. Therefore, the catalytic activities of LHCII kinase STN7 and phosphatase PPH1/TAP38 are important for balancing the light absorption capacity between PSI and PSII (Pesaresi et al., 2011).

FtsH Proteases

FtsH proteases are ubiquitous ATP-dependent, zinc metalloendopeptidases (Yu et al., 2004). FtsHs typically consist of an N-terminal double-pass transmembrane domain, an ATPase domain, and a C-terminal zinc-binding site. Crystal structures of the ATPase domain of bacterial FtsHs and single-particle electron cryo-microscopy analysis of cyanobacterial FtsHs showed that FtsHs exist as ringlike hexamers (Krzywda et al., 2002; Niwa et al., 2002; Boehm et al., 2012b). Bacteria contain one *FtsH* gene and the FtsH protein forms homohexamers while cyanobacteria and eukaryotes have multiple *FtsH* genes and the FtsH proteins form heterohexamers (Mann et al., 2000; Krzywda et al., 2002; Niwa et al., 2002; Zaltsman et al., 2005b; Boehm et al., 2012b). The Arabidopsis genome encodes 12 FtsH proteases; eight FtsHs (FtsH1, FtsH2/VAR2, FtsH5/VAR1—FtsH9, and FtsH12; VAR1 stands for Yellow Variegated 1) were verified experimentally to be chloroplast-targeted; FtsH11 was showed to be dual targeted to the chloroplast (possible thylakoid membranes) and the inner mitochondria membrane (Chen et al., 2000; Takechi et al., 2000; Sakamoto et al., 2002, 2003; Urantowka et al., 2005). FtsH2/VAR2 and FtsH5/VAR1 were found to be localized to thylakoid membranes, with their catalytic domain facing the stromal side of the membrane (Chen et al., 2000; Sakamoto et al., 2003). Among the nine chloroplast- or dual-targeted FtsHs, the functions of FtsH1, FtsH2/VAR2, FtsH5/VAR1, FtsH6, FtsH8, and FtsH11 have been explored experimentally. FtsH and Deg proteases have been known to be involved in degradation of photodamaged D1. Early *in vitro* studies suggested that this is a two-step process including the initial cleavage at the stromal DE loop via Deg2 and the subsequent removal of the N-terminal fragment by FtsHs (Lindahl et al., 1996, 2000; Spetea et al., 1999; Haubühl et al., 2001). It was later proposed that FtsHs play a more important role than Deg proteases in D1 turnover (Silva et al., 2003; Nixon et al., 2005, 2010; Huesgen et al., 2009; Kato et al., 2012; Komenda et al., 2012a).

Loss-of-function mutations in the Arabidopsis *FtsH2/VAR2* or *FtsH5/VAR1* gene cause variegated leaves (Sakamoto et al., 2002, 2003; Yu et al., 2004, 2005; Zaltsman et al., 2005a,b; Kato et al., 2007, 2009, 2012; Wagner et al., 2011). The green sectors in the *ftsh2/var2* or *ftsh5/var1* mutants are formed by cells with normal chloroplasts and the white leaf sectors are formed by viable cells with undifferentiated plastids (Chen et al., 2000; Sakamoto et al., 2002; Kapri-Pardes et al., 2007). These data suggest that FtsH2/VAR2 and FtsH5/VAR1 are required for chloroplast biogenesis and thylakoid formation (Chen et al., 2000; Sakamoto et al., 2002; Zaltsman et al., 2005a,b; Kapri-Pardes et al., 2007).

Compared to wild-type leaves, the green leaf sectors of the *ftsh2/var2* or *ftsh5/var1* mutants demonstrate increased photosensitivity and delayed recovery of PSII activity (Zaltsman et al., 2005a,b). Chloroplasts in the green sectors of the *ftsh2/var2* or *ftsh5/var1* mutants accumulate fewer PSII supercomplexes, more PSII subcomplexes, and more reactive oxygen species than wild-type chloroplasts (Kato et al., 2009). These observations are due to the proteolytic activity of FtsHs toward photodamaged D1 (Bailey et al., 2002; Kato et al., 2009). Because the variegated phenotype complicates biochemical analyses, Kato et al. (2009) used another mutation, *fu-gaeri1* (*fug1*), to suppress leaf variegation, and generated the non-variegated *ftsh2/var2 fug1* and *ftsh5/var1 fug1* plants. Compared to the *fug1* single mutant, photodamaged D1 is not replaced in the *ftsh2/var2 fug1* and *ftsh5/var1 fug1* mutants, under different light intensities. Taken together, these data show that FtsH2/VAR2 and FtsH5/VAR1 play an important role at the early stage of D1 turnover and not just in the subsequent removal of D1 degradation products (**Figure 2**; Bailey et al., 2002; Kato et al., 2009).

The phenotypes observed in the *ftsh2/var2* or *ftsh5/var1* mutants are absent in the *ftsh1*, *ftsh6*, *ftsh8*, and *ftsh11* single mutants under normal or high-light conditions (Sakamoto et al., 2003; Zaltsman et al., 2005b; Chen et al., 2006b; Wagner et al., 2011). These findings suggest that FtsH2/VAR2 and FtsH5/VAR1 play a dominant role in chloroplast biogenesis, thylakoid formation, and PSII repair (Sakamoto et al., 2003). Phylogenetic analysis showed that *FtsH1* and *FtsH5* are two duplicated genes (subunit type A), so are *FtsH2* and *FtsH8* (subunit type B) (Yu et al., 2004, 2005; Zaltsman et al., 2005b).

The phenotype of the *ftsh2/var2* mutant can be restored by overexpression of *FtsH8*; the *ftsh2/var2 ftsh8* double mutant is infertile; and the *ftsh1 ftsh5/var1* double mutant resembles the *ftsh2/var2 ftsh8* double mutant (Yu et al., 2004; Zaltsman et al., 2005b). These data suggest that FtsH1 and FtsH5/VAR1 are interchangeable, so are FtsH2/VAR2 and FtsH8, and that the presence of two types of FtsH subunits is necessary for chloroplast biogenesis, thylakoid formation, and PSII repair (**Figure 2**; Zaltsman et al., 2005b).

FtsH6 was reported to participate in degradation of LHCII in Arabidopsis leaves during high-light acclimation and senescence (Zelisko et al., 2005). Using an *in vitro* degradation system (i.e., isolated thylakoid membranes), Zelisko et al. (2005) showed that, compared to the wild type, the *ftsh6* knockout mutant has reduced degradation of LHCB1 after high-light acclimation and reduced degradation of LHCB3 after dark-induced senescence. However, *in vivo* degradation of LHCII proteins does not appear to be impaired in the *ftsh6* knockout mutants (Wagner et al., 2011). Under various conditions, including high-light acclimation and dark-induced senescence, the abundances of LHCB1 and LHCB3 in the *ftsh6* knockout mutants are not statistically different from those in the wild type. Further investigation is needed to understand the precise role of FtsH6.

FtsH11 was reported to be critical in thermoprotection of the photosynthetic apparatus (Chen et al., 2006b; Wagner et al., 2011). When exposed to temperatures above 30°C, which are permissive for wild-type Arabidopsis, the growth and development of the *ftsh11* mutants is arrested (Chen et al., 2006b). Compared to the wild type under the same high-temperature treatment, the *ftsh11* mutants have reduced levels of chlorophyll and reduced PSII activity. Consistent with the hypothesis that FtsH11 is involved in thermotolerance, the expression of the *FtsH11* gene is up-regulated by high temperature (Chen et al., 2006b).

Deg Proteases

Deg proteases are ubiquitous ATP-independent, serine endopeptidases (Schuhmann and Adamska, 2012). The Arabidopsis genome encodes 16 Deg proteases, five of which are peripherally attached to thylakoid membranes: two (Deg2 and Deg7) on the stroma side and three (Deg1, Deg5, and Deg8) on the lumenal side (Huesgen et al., 2005; Schuhmann and Adamska, 2012). These five chloroplast-localized Deg proteases have been proposed to be involved in degradation of photodamaged D1 (Schuhmann and Adamska, 2012). In addition to the trypsin-like protease domain, most Deg proteases, such as Deg1, Deg2, Deg7, and Deg8, have at least one PDZ domain for protein-protein interactions. It is conceivable that these chloroplast-localized PDZ domain-containing Deg proteases may act as chaperones and function in assembly of the photosynthetic apparatus (Sun et al., 2010b; Schuhmann and Adamska, 2012).

Arabidopsis RNA interference (RNAi) lines of Deg1 have a smaller plant size, increased sensitivity of PSII activity to high light, and increased accumulation of non-degraded (and presumably photodamaged) D1 (Kapri-Pardes et al., 2007). The RNAi lines display decreased accumulation of the 16- and 5.2-kDa C-terminal degradation products of D1, which correspond to the cleavage products at the lumenal CD loop, and immediately after the transmembrane helix E, respectively. The addition of recombinant Deg1 into inside-out thylakoid membranes isolated from the Deg1-deficient plants induces formation of the 5.2-kDa C-terminal degradation product of D1. These data suggest that Deg1 is involved in degradation of photodamaged D1 (specifically, the cleavage at the lumenal CD loop immediately downstream of the transmembrane helix E) in PSII repair (**Figure 2**; Kapri-Pardes et al., 2007). Unfortunately, D1 turnover was not assessed in Deg1 RNAi lines. Deg1 is capable of degrading lumenal proteins plastocyanin and PsbO, suggesting that Deg1 may also acts as a general purpose endopeptidase in the thylakoid lumen (Chassin et al., 2002).

Because Deg1 has a PDZ domain for protein-protein interactions, Sun et al. (2010b) investigated whether Deg1 functions as a chaperone during assembly of PSII complexes (Sun et al., 2010b). Deg1 was found to co-migrate with D1 in BN-PAGE and pull down D1, D2, CP43, and CP47 in an immunoprecipitation assay. Recombinant Deg1 has the ability to fold reduced and denatured protein substrates in the presence of both reduced and oxidized glutathione. The RNAi lines of Deg1 display reduced accumulation of PSII complexes and normal accumulation of other photosynthetic complexes. In addition, assembly of newly synthesized PSII subunits into PSII dimers and PSII supercomplexes is hindered in the RNAi lines, although synthesis of the corresponding proteins in chloroplasts is not impaired. Based on these results, Sun et al. (2010b) proposed that Deg1 also acts as a chaperone and functions in the integration of newly synthesized PSII subunits, such as D1, D2, CP43, and CP47, into PSII complexes (**Figures 1**, **2**). However, these experimental data do not rule out the possibility that Deg1 is directly involved in degradation of these PSII subunits.

Deg2 has a PDZ domain and a short hydrophobic segment, in addition to the trypsin-like protease domain (Haubühl et al., 2001). Recombinant Deg2 demonstrates proteolytic activity toward photodamaged D1 and is able to produce the 23-kDa N-terminal and the 10-kDa C-terminal degradation products, which correspond to the cleavage products at the stromal DE loop (Haubühl et al., 2001). Although recombinant Deg2 is proteolytically active, the *deg2* knockout mutants have the same plant morphology, PSII activity, and D1 turnover rate as wild-type Arabidopsis, under normal or elevated light (Huesgen et al., 2006). Therefore, it was proposed that Deg2 functions as a minor protease in *in vivo* degradation of photodamaged D1 (**Figure 2**). Deg2 was also reported to be involved in stress-induced degradation of LHCB6 (Luciński et al., 2011b).

Deg5 and Deg8 form heterohexamers and the Deg5-to-Deg8 ratio is ∼1:1 (Sun et al., 2007). Deg5 is ∼120 amino acids shorter than Deg1 and Deg8 and it does not contain any PDZ domain (Schuhmann and Adamska, 2012). Although Deg8 has a PDZ domain, it shows no chaperone activity (i.e., PDIase activity)

toward reduced and denatured protein substrates (Sun et al., 2010b). Recombinant Deg8 demonstrates proteolytic activity toward photodamaged D1 and is able to produce the 16-kDa N-terminal and the 18-kDa C-terminal degradation products, which correspond to the cleavage products at the lumenal CD loop (Sun et al., 2007). Although only recombinant Deg8 is proteolytically active, the *deg5* and *deg8* single knockout mutants of Arabidopsis both display impaired degradation of newly synthesized D1 and the impairment is more pronounced in the *deg5 deg8* double mutant (Sun et al., 2007). The defect in D1 turnover in the mutants is reflected in PSII activity. PSII in the *deg5* and *deg8* single mutants exhibits increased sensitivity to high light and the sensitivity is more obvious in the *deg5 deg8* double mutant. Under normal light, the two single mutants and the double mutant have a normal phenotype. Based on these data, Sun et al. (2007) proposed that Deg5 and Deg8 act as heterohexameric endopeptidases and cleave photodamaged D1 at the lumenal CD loop during PSII repair (**Figure 2**). Deg5 has also been reported to be involved in wounding-related disposal of PsbF (Luciński et al., 2011a).

Deg7 (1097 amino acids at full length) is twice as long as most Deg proteases; it has two trypsin-like protease domains (one active and one degenerated) and four PDZ domains (three active and one degenerated) (Schuhmann et al., 2011). The domain composition suggests that Deg7 is the result of a whole-gene duplication event followed by subsequent degeneration (Schuhmann et al., 2011). Deg7 forms homotrimers and the oligomerization is mediated through the degenerated protease domain (Schuhmann et al., 2011). Recombinant Deg7 demonstrates proteolytic activity toward photodamaged D1, D2, CP43, and CP47 (Sun et al., 2010a). Compared to wild-type Arabidopsis, the *deg7* null mutant displays retarded growth, reduced PSII activity, and reduced degradation of PSII core proteins D1, D2, CP43, and CP47 under high light. However, under normal light, there is no apparent difference in plant growth or morphology between the *deg7* mutant and the wild type. These data suggest that Deg7 is involved in cleavage of photodamaged PSII core proteins D1, D2, CP47, and CP43 from the stroma side during PSII repair (**Figure 2**; Sun et al., 2010a).

HCF243, PSB27-H1, and PSB27-H2/LPA19 in Biogenesis, C-Terminal Processing, and/or Assembly of D1

HCF243 (High Chlorophyll Fluorescence 243) is an intrinsic thylakoid membrane protein with no recognizable domain or motif (Zhang et al., 2011). A loss-of-function mutation in the Arabidopsis *HCF243* gene causes substantial reductions in accumulation of PSII core subunits (D1, D2, CP43, and CP47) and assembly of PSII complexes (Zhang et al., 2011). Unlike PSII core subunits, the amounts of extrinsic PSII subunits, PSII antenna proteins, and other non-PSII thylakoid membrane proteins are hardly affected in the *hcf243* mutant. In line with these observations, PSII activity is dramatically reduced in the *hcf243* mutant and the mutant has pale-green leaves and a much smaller plant size than the wild type. Pulse-labeling experiments indicated that these defects are caused by the severely reduced synthesis of D1 and to a lesser degree of D2 (Zhang et al., 2011). Indeed, the *hcf243* mutant over-accumulates pD1, the D1 precursor with an unprocessed C-terminus. HCF243 was also found to interact with D1 *in vivo* (Zhang et al., 2011). These data suggest that HCF243 is involved in biogenesis, processing, and assembly of D1 and possible biogenesis of D2 as well (**Figures 1**, **2**).

PSB27s (PSII protein 27s) are thylakoid lumen proteins peripherally attached to thylakoid membranes (Chen et al., 2006a; Wei et al., 2010). Cyanobacterial Psb27 was found to facilitate assembly of the OEC manganese and plays a role in PSII repair (Nowaczyk et al., 2006; Liu et al., 2011a,b; Komenda et al., 2012b). The Arabidopsis genome encodes two PSB27s: PSB27-H1 and PSB27-H2/LPA19 (LPA19 stands for Low PSII Accumulation 19). Under normal light, the PSII protein composition is not changed and PSII activity is only slightly reduced in the Arabidopsis T-DNA insertion mutant of PSB27-H1 (Chen et al., 2006a; Dietzel et al., 2011). However, the *psb27-H1* mutant has reduced amounts of PSII-LHCII supercomplexes, suggesting that PSB27-H1 is required for the formation and stability of PSII-LHCII supercomplexes (**Figure 1**; Dietzel et al., 2011). Under high light, PSII activity and the amount of D1 decrease much faster in the *psb27-H1* mutant than in the wild type. In addition, the *psb27-H1* mutant displays delayed recovery of PSII activity after photoinhibition, suggesting that PSB27-H1 is involved in the repair cycle of photodamaged PSII. Unlike *psb27-H1*, the *psb27-H2/lpa19* mutants of Arabidopsis have pale-green leaves, a smaller plant size, and reduced PSII activity even under normal light conditions (Wei et al., 2010). Pulse-labeling experiments showed that C-terminal processing of D1 is impaired in the *psb27-H2/lpa19* null mutants. PSB27-H2/LPA19 was found to specifically interact with the soluble C-terminus of precursor and mature D1. It was concluded that PSB27-H2/LPA19 functions in C-terminal processing of D1 (**Figure 1**; Wei et al., 2010).

HCF136, PAM68, and PsbN/PBF1 in Assembly OF PSII Reaction Complexes

HCF136 (High Chlorophyll Fluorescence 136) is a lumenal protein found in stroma lamellae; it contains no recognizable domain or motif (Meurer et al., 1998). The cyanobacterial homolog of HCF136, YCF48 (hypothetical chloroplast reading frame number 48), was found to interact with pD1, and to a lesser degree, partially processed and unassembled D1, but not with mature and unassembled D1 or D2, in a split-ubiquitin yeast-two-hybrid assay (Komenda et al., 2008). In addition, higher-plant HCF136 was found to be associated with the PSII precomplex D2-Cyt b_{559} and PSII reaction-center complexes RC, RC47a, and RC47b (Plücken et al., 2002). The HCF136-deficient Arabidopsis mutant is able to accumulate PSI and cytochrome b_6f complex proteins, but unable to accumulate PSII proteins, perform PSII activity, or grow photoautotrophically (Meurer et al., 1998; Plücken et al., 2002). Pulse-labeling studies showed that the *hcf136* mutant is defective in biogenesis of PSII minimal reaction-center complexes, not in biosynthesis

of PSII proteins (Meurer et al., 1998; Plücken et al., 2002). Therefore, it was proposed that HCF136 is involved in assembly of PSII reaction-center complexes such as RC, RC47a, and RC47b (**Figure 1**). Consistent with this hypothesis, HCF136 was found to interact with another PSII assembly factor, PAM68 (Armbruster et al., 2010).

PAM68 in vascular plants is an integral thylakoid membrane protein with an acidic domain and a double-pass transmembrane domain (Armbruster et al., 2010). PAM68 was found to be associated with LMM complexes that are formed at an early step of PSII assembly (Armbruster et al., 2010). These complexes contain D1, D2, and LPA1/PratA, which may correspond to PSII minimal reaction-center complexes. PAM68 was found to interact with a number of PSII core subunits (D1, D2, CP43, CP47, PsbH, and PsbI) and PSII assembly factors (ALB3, HCF136, and LPA1/PratA, and LPA2). The PAM68-deficient Arabidopsis mutants have pale-green leaves, drastically reduced PSII activity, and severely retarded growth, under normal growth conditions. Consistent with these observations, the *pam68* mutants have severely reduced amounts of PSII core subunits, and they over-accumulate PSII reaction-center complexes at the expense of higher order PSII complexes. PAM68 was therefore proposed to be necessary for converting PSII minimal reaction-center complexes into larger PSII complexes (**Figure 1**; Armbruster et al., 2010). The *pam68* mutants were also found to over-accumulate pD1 (Armbruster et al., 2010), suggesting that PAM68 is also necessary for efficient C-terminal processing of D1 (**Figures 1**, **2**).

PsbN is a small thylakoid membrane protein encoded by the plastid genome (Krech et al., 2013; Torabi et al., 2014). It was originally thought as a PSII subunit (Ikeuchi et al., 1989); however, two recent studies showed that PsbN is not a PSII subunit, but an assembly factor of PSII (Krech et al., 2013; Torabi et al., 2014). Thus, Krech et al. (2013) proposed a new name, Photosystem Biogenesis Factor 1 (PBF1) for this protein. Tobacco (*Nicotiana tabacum*) homoplastomic Δ*psbN/pbf1* mutants have pale-green leaves and slow autotrophic growth (Krech et al., 2013). Pulse-labeling and two-dimensional gel electrophoresis showed that formation of PSII precomplexes, e.g., pD1-PsbI and D2-Cyt b_{559}, is not affected in the Δ*psbN/pbf1* mutants but assembly of PSII minimal reaction-center complexes and higher order PSII complexes is hampered (Torabi et al., 2014). It was concluded that PsbN/PBF1 is involved in formation of PSII minimal reaction-center complexes (**Figure 1**). The Δ*psbN/pbf1* mutants are extremely sensitive to light, even at relatively low light and PSII in the Δ*psbN/pbf1* mutants is unable to recover from photoinhibition (Torabi et al., 2014). These data indicate that PsbN/PBF1 may also function in PSII repair, which occurs in stroma lamellae. Consistent with this hypothesis, PsbN was found to be predominantly located in stroma lamellae (Torabi et al., 2014). Loss of PsbN changes the phosphorylation status of PSII core proteins and LHCII proteins, which is important for the migration of photodamaged PSII complexes from grana stacks to stroma-exposed thylakoids, and for balancing the light absorption capacity between PSI and PSII, respectively. Therefore, it is possible that PsbN is involved in PSII repair by regulating the phosphorylation status of PSII core proteins and LHCII proteins (**Figure 2**).

PSB28 in Biogenesis of Chlorophyll-Binding Proteins Such as CP47, PsaA, and PsaB

PSB28 (PSII protein 28) is a small protein predominantly localized in the stroma/cytoplasm (Shi et al., 2012). In *Synechocystis* sp. PCC 6803, a small fraction of Psb28 was found to be associated with unassembled CP47, RC47, and PSII monomers at the stroma side (Dobáková et al., 2009; Boehm et al., 2012a). Deletion of this protein in *Synechocystis* sp. PCC 6803 cause a decreased amount of unassembled CP47 and increased amounts of PSII minimal reaction-center complexes and unassembled D1 (Dobáková et al., 2009). In addition, the Δ*psb28* mutant exhibits reduced synthesis of CP47 and PsaA/PsaB heterodimers. Therefore, Psb28 was considered to function in biogenesis and assembly of chlorophyll-containing proteins such as CP47, PsaA, and PsaB in cyanobacteria (Dobáková et al., 2009). Little is known about the role of PSB28 in photosynthetic eukaryotes except that PSB28 does exist in higher plants and that the absence of PSB28 results in a pale-green phenotype in rice (Jung et al., 2008; Mabbitt et al., 2014). However, because PSB28 is evolutionary conserved, it is reasonable to predict that PSB28 in higher plants may also function in biogenesis and assembly of chlorophyll-containing proteins such as CP47 (**Figure 1**).

LPA2 and LPA3 in Synthesis and Assembly of CP43

LPA2 is a small intrinsic thylakoid membrane protein with a C-terminal double-pass transmembrane domain (Ma et al., 2007). LPA3 (Low PSII Accumulation 3) is a chloroplast protein without any transmembrane domain or any other recognizable domain or motif. However, sub-chloroplast fractionation revealed that LPA3 could be located in chloroplast stroma or associated with thylakoid membranes (Cai et al., 2010). Although LPA2 and LPA3 are not homologous, they were identified as two auxiliary proteins assisting incorporation of CP43 into PSII via interaction with cpSRP translocase ALB3 (Ma et al., 2007; Cai et al., 2010). LPA2 and LPA3 were found to interact with CP43, ALB3, and each other (Cai et al., 2010). Pulse-labeling experiments showed that assembly from CP43-less reaction-center complexes to PSII monomers and formation of PSII-LHCII supercomplexes are distinctively slower in the *lpa2* and *lpa3* single mutants than in wild-type Arabidopsis (Ma et al., 2007; Cai et al., 2010). Synthesis of CP43 is greatly reduced in the *lpa2* and *lpa3* single mutants while synthesis of other PSII core subunits D1, D2, and CP47 is comparable between the single mutants and the wild type (Ma et al., 2007; Cai et al., 2010). LPA2 and LPA3 appear to be functional redundant because the *lpa2 lpa3* double mutant has no detectable amounts of D1, D2, CP43, and CP47 and is seedling-lethal. Taken together, LPA2 and LPA3 were proposed to be involved in synthesis and assembly of CP43 (**Figures 1**, **2**; Ma et al., 2007; Cai et al., 2010).

PSB33 in Association of LHCII with PSII

PSB33 (PSII protein 33) is a thylakoid membrane protein with an N-terminal Rieske-type domain exposed to the stroma side, a double-pass transmembrane domain, and a C-terminal partial chlorophyll-binding domain (Fristedt et al., 2015). PSB33 was found to co-migrate with PSII-LHCII supercomplexes, PSII dimers, PSII monomers, and CP43-less PSII monomers in BN-PAGE (Fristedt et al., 2015). Loss-of-function mutations in the Arabidopsis *PSB33* gene cause reduced amounts of PSII-LHCII supercomplexes, and increased amounts of PSII dimers, lower state transition, lower non-photochemical quenching, increased photosensitivity, and retarded growth (Fristedt et al., 2015). According to these data, Fristedt et al. (2015) proposed that PSB33 may mediate the association of LHCII with PSII core complexes (**Figure 1**) and balance the light absorption capacity between PSII and PSI. It is likely that PSB33 also functions in attaching LHCII to PSII during reassembly of repaired PSII (**Figure 2**), because the defect in PSII activity in the *psb33* mutants is more pronounced under higher light (Fristedt et al., 2015).

HHL1 and MPH1 in Protection of PSII from Photodamage

HHL1 (Hypersensitive to High Light 1) is a thylakoid membrane protein with a single-pass transmembrane domain, and a C-terminal partial von Willebrand factor type A domain, which is known to mediate protein-protein interactions (Jin et al., 2014). Under high light, the HHL1-deficient mutants have lower efficiency of PSII photochemistry, lower amounts of PSII core subunits and PSII-LHCII supercomplexes, and higher amounts of reactive oxygen species, than wild-type Arabidopsis (Jin et al., 2014). Many of these defects become milder under normal light. Therefore, it was proposed that HHL1 is involved in the repair and reassembly cycle of photodamaged PSII. Consistent with this hypothesis, HHL1 was found in both grana stacks and stroma lamellae, and PSII core subunits in thylakoid membranes isolated from HHL1-deficient plants were found to be less stable than those isolated from wild-type plants (Jin et al., 2014). Jin et al. (2014) also observed *in vivo* and *in vitro* interaction between HHL1 and LQY1, another protein involved in PSII repair. Because the majority of HHL1 is associated with PSII core monomers, it is likely that HHL1 "collaborates" with LQY1 and assists the reassembly of PSII core monomers and PSII-LHCII supercomplexes during PSII repair (**Figure 2**). In line with this hypothesis, the *hhl1 lqy1* double mutant is more sensitive to high light than the single mutants (Jin et al., 2014).

MPH1 (Maintenance of PSII under High light 1) is a proline-rich intrinsic thylakoid membrane protein with a single-pass transmembrane domain; it is present in grana stacks, grana margins, and stroma lamellae (Liu and Last, 2015a,b). Under normal light, PSII activity and the composition of PSII complexes in MPH1-deficient mutants are similar to those in wild-type Arabidopsis. Under high light, the *mph1* mutants have lower efficiency of PSII photochemistry, and lower amounts of PSII-LHCII supercomplexes, PSII dimers, and PSII core monomers, than the wild type. Therefore, it was proposed that MPH1 has a role in protection and/or stabilization of PSII under high light (Liu and Last, 2015a,b). Consistent with this hypothesis, MPH1 was found to change its association under different light intensities: under normal light, the majority of MPH1 is associated with PSII core monomers; under high light, the majority of MPH1 becomes associated with PSII-LHCII supercomplexes (Liu and Last, 2015a). Because of the interactions between MPH1 and different PSII complexes under different light irradiance and the reductions in the amounts of PSII monomers and higher order PSII complexes, it is likely that MPH1 is involved in the assembly and/or stability of PSII core monomers and higher order PSII complexes under high light (**Figure 2**).

CONCLUDING REMARKS

Photosynthesis directly or indirectly provides chemical energy for nearly all life forms on earth. Due to the importance of photosynthesis, the structure, biogenesis, and maintenance of the photosynthetic apparatus have long been one of the major focuses of research. The combination of proteomics, X-ray crystallography, and single-particle electron cryo-microscopy approaches has led to a comprehensive understanding of the structure and subunit composition of PSII. In addition, significant progresses have been made in the identification and functional studies of protein factors that are involved in *de novo* assembly and/or the repair and reassembly cycle of PSII. The inclusion of thylakoid protein trafficking/targeting systems and enzymes that catalyze important enzymatic steps, along with various assembly/stability factors allows a more comprehensive view of recent advances in this field. However, additional efforts are in great need to (1) dissect the precise functions of understudied assembly/stability factors or enzymes; and (2) build a protein interactome network that would provide a systems view of the interplay among different assembly/stability factors, enzymes, thylakoid protein trafficking/targeting systems, PSII assembly and repair complexes, and PSII subunits.

AUTHOR CONTRIBUTIONS

This review was written entirely by YL.

ACKNOWLEDGMENTS

This work was supported by the US National Science Foundation Grant MCB-1244008.

REFERENCES

Adamska, I., and Kloppstech, K. (1991). Evidence for an association of the early light-inducible protein (ELIP) of pea with Photosystem II. *Plant Mol. Biol.* 16, 209–223. doi: 10.1007/BF00020553

Albiniak, A. M., Baglieri, J., and Robinson, C. (2012). Targeting of lumenal proteins across the thylakoid membrane. *J. Exp. Bot.* 63, 1689–1698. doi: 10.1093/jxb/err444

Albrecht, V., Ingenfeld, A., and Apel, K. (2008). *Snowy cotyledon 2*: the identification of a zinc finger domain protein essential for chloroplast development in cotyledons but not in true leaves. *Plant Mol. Biol.* 66, 599–608. doi: 10.1007/s11103-008-9291-y

Anbudurai, P. R., Mor, T. S., Ohad, I., Shestakov, S. V., and Pakrasi, H. B. (1994). The *ctpA* gene encodes the C-terminal processing protease for the D1 protein of the Photosystem II reaction center complex. *Proc. Natl. Acad. Sci. U.S.A.* 91, 8082–8086. doi: 10.1073/pnas.91.17.8082

Andersson, U., Heddad, M., and Adamska, I. (2003). Light stress-induced one-helix protein of the chlorophyll *a*/*b*-binding family associated with Photosystem I. *Plant Physiol.* 132, 811–820. doi: 10.1104/pp.102.019281

Armbruster, U., Zühlke, J., Rengstl, B., Kreller, R., Makarenko, E., Ruhle, T., et al. (2010). The *Arabidopsis* thylakoid protein PAM68 is required for efficient D1 biogenesis and Photosystem II assembly. *Plant Cell* 22, 3439–3460. doi: 10.1105/tpc.110.077453

Aro, E.-M., Suorsa, M., Rokka, A., Allahverdiyeva, Y., Paakkarinen, V., Saleem, A., et al. (2005). Dynamics of Photosystem II: a proteomic approach to thylakoid protein complexes. *J. Exp. Bot.* 56, 347–356. doi: 10.1093/jxb/eri041

Bailey, S., Thompson, E., Nixon, P. J., Horton, P., Mullineaux, C. W., Robinson, C., et al. (2002). A critical role for the Var2 FtsH homologue of *Arabidopsis thaliana* in the Photosystem II repair cycle *in vivo*. *J. Biol. Chem.* 277, 2006–2011. doi: 10.1074/jbc.M105878200

Bellafiore, S., Barneche, F., Peltier, G., and Rochaix, J. D. (2005). State transitions and light adaptation require chloroplast thylakoid protein kinase STN7. *Nature* 433, 892–895. doi: 10.1038/nature03286

Bhuiyan, N. H., Friso, G., Poliakov, A., Ponnala, L., and van Wijk, K. J. (2015). MET1 is a thylakoid-associated TPR protein involved in Photosystem II supercomplex formation and repair in *Arabidopsis*. *Plant Cell* 27, 262–285. doi: 10.1105/tpc.114.132787

Boehm, M., Yu, J., Krynicka, V., Barker, M., Tichy, M., Komenda, J., et al. (2012b). Subunit organization of a *Synechocystis* hetero-oligomeric thylakoid FtsH complex involved in Photosystem II repair. *Plant Cell* 24, 3669–3683. doi: 10.1105/tpc.112.100891

Boehm, M., Yu, J., Reisinger, V., Beckova, M., Eichacker, L. A., Schlodder, E., et al. (2012a). Subunit composition of CP43-less Photosystem II complexes of *Synechocystis* sp. PCC 6803: implications for the assembly and repair of Photosystem II. *Phil. Trans. R. Soc. B* 367, 3444–3454. doi: 10.1098/rstb.2012.0066

Bohne, A.-V., Schwarz, C., Schottkowski, M., Lidschreiber, M., Piotrowski, M., Zerges, W., et al. (2013). Reciprocal regulation of protein synthesis and carbon metabolism for thylakoid membrane biogenesis. *PLoS Biol.* 11:e1001482. doi: 10.1371/journal.pbio.1001482

Bonardi, V., Pesaresi, P., Becker, T., Schleiff, E., Wagner, R., Pfannschmidt, T., et al. (2005). Photosystem II core phosphorylation and photosynthetic acclimation require two different protein kinases. *Nature* 437, 1179–1182. doi: 10.1038/nature04016

Bricker, T., Roose, J. L., Zhang, P., and Frankel, L. (2013). The PsbP family of proteins. *Photosynth. Res.* 116, 235–250. doi: 10.1007/s11120-013-9820-7

Bricker, T. M., Roose, J. L., Fagerlund, R. D., Frankel, L. K., and Eaton-Rye, J. J. (2012). The extrinsic proteins of Photosystem II. *Biochim. Biophys. Acta* 1817, 121–142. doi: 10.1016/j.bbabio.2011.07.006

Cai, W., Ma, J., Chi, W., Zou, M., Guo, J., Lu, C., et al. (2010). Cooperation of LPA3 and LPA2 is essential for Photosystem II assembly in *Arabidopsis*. *Plant Physiol.* 154, 109–120. doi: 10.1104/pp.110.159558

Cai, W., Ma, J., Guo, J., and Zhang, L. (2008). Function of ROC4 in the efficient repair of photodamaged Photosystem II in *Arabidopsis*. *Photochem. Photobiol.* 84, 1343–1348. doi: 10.1111/j.1751-1097.2008.00448.x

Cain, P., Hall, M., Schröder, W. P., Kieselbach, T., and Robinson, C. (2009). A novel extended family of stromal thioredoxins. *Plant Mol. Biol.* 70, 273–281. doi: 10.1007/s11103-009-9471-4

Calderon, R. H., García-Cerdán, J. G., Malnoë, A., Cook, R., Russell, J. J., Gaw, C., et al. (2013). A Conserved rubredoxin is necessary for Photosystem II accumulation in diverse oxygenic photoautotrophs. *J. Biol. Chem.* 288, 26688–26696. doi: 10.1074/jbc.M113.487629

Casazza, A. P., Rossini, S., Rosso, M. G., and Soave, C. (2005). Mutational and expression analysis of ELIP1 and ELIP2 in *Arabidopsis thaliana*. *Plant Mol. Biol.* 58, 41–51. doi: 10.1007/s11103-005-4090-1

Charuvi, D., Kiss, V., Nevo, R., Shimoni, E., Adam, Z., and Reich, Z. (2012). Gain and loss of photosynthetic membranes during plastid differentiation in the shoot apex of *Arabidopsis*. *Plant Cell* 24, 1143–1157. doi: 10.1105/tpc.111.094458

Chassin, Y., Kapri-Pardes, E., Sinvany, G., Arad, T., and Adam, Z. (2002). Expression and characterization of the thylakoid lumen protease DegP1 from *Arabidopsis*. *Plant Physiol.* 130, 857–864. doi: 10.1104/pp.007922

Che, Y., Fu, A., Hou, X., McDonald, K., Buchanan, B. B., Huang, W., et al. (2013). C-terminal processing of reaction center protein D1 is essential for the function and assembly of Photosystem II in *Arabidopsis*. *Proc. Natl. Acad. Sci. U.S.A.* 110, 16247–16252. doi: 10.1073/pnas.1313894110

Chen, H., Zhang, D., Guo, J., Wu, H., Jin, M., Lu, Q., et al. (2006a). A Psb27 homologue in *Arabidopsis thaliana* is required for efficient repair of photodamaged Photosystem II. *Plant Mol. Biol.* 61, 567–575. doi: 10.1007/s11103-006-0031-x

Chen, J., Burke, J. J., Velten, J., and Xin, Z. (2006b). FtsH11 protease plays a critical role in *Arabidopsis* thermotolerance. *Plant J.* 48, 73–84. doi: 10.1111/j.1365-313X.2006.02855.x

Chen, M., Choi, Y., Voytas, D. F., and Rodermel, S. (2000). Mutations in the *Arabidopsis VAR2* locus cause leaf variegation due to the loss of a chloroplast FtsH protease. *Plant J.* 22, 303–313. doi: 10.1046/j.1365-313x.2000.00738.x

Chidgey, J. W., Linhartová, M., Komenda, J., Jackson, P. J., Dickman, M. J., Canniffe, D. P., et al. (2014). A cyanobacterial chlorophyll synthase-HliD complex associates with the Ycf39 protein and the YidC/Alb3 insertase. *Plant Cell* 26, 1267–1279. doi: 10.1105/tpc.114.124495

Cline, K., and Dabney-Smith, C. (2008). Plastid protein import and sorting: different paths to the same compartments. *Curr. Opin. Plant Biol.* 11, 585–592. doi: 10.1016/j.pbi.2008.10.008

Cline, K., and Theg, S. (2007). "The Sec and Tat protein translocation pathways in chloroplasts," in *The Enzymes: Molecular Machines Involved in Protein Transport across Cellular Membranes*, eds R. E. Dalbey, C. M. Koehler, and F. Tamanoi (Waltham, MA: Academic Press), 463–492.

da Fonseca, P., Morris, E. P., Hankamer, B., and Barber, J. (2002). Electron crystallographic study of Photosystem II of the cyanobacterium *Synechococcus elongatus*. *Biochemistry* 41, 5163–5167. doi: 10.1021/bi0120650

Dall'Osto, L., Bressan, M., and Bassi, R. (2015). Biogenesis of light harvesting proteins. *Biochim. Biophys. Acta* 1847, 861–871. doi: 10.1016/j.bbabio.2015.02.009

Dietzel, L., Bräutigam, K., Steiner, S., Schüffler, K., Lepetit, B., Grimm, B., et al. (2011). Photosystem II supercomplex remodeling serves as an entry mechanism for state transitions in *Arabidopsis*. *Plant Cell* 23, 2964–2977. doi: 10.1105/tpc.111.087049

Dobáková, M., Sobotka, R., Tichy, M., and Komenda, J. (2009). Psb28 protein is involved in the biogenesis of the Photosystem II inner antenna CP47 (PsbB) in the cyanobacterium *Synechocystis* sp. PCC 6803. *Plant Physiol.* 149, 1076–1086. doi: 10.1104/pp.108.130039

Dominguez-Solis, J. R., He, Z. Y., Lima, A., Ting, J., Buchanan, B. B., and Luan, S. (2008). A cyclophilin links redox and light signals to cysteine biosynthesis and stress responses in chloroplasts. *Proc. Natl. Acad. Sci. U.S.A.* 105, 16386–16391. doi: 10.1073/pnas.0808204105

Feige, M. J., and Hendershot, L. M. (2011). Disulfide bonds in ER protein folding and homeostasis. *Curr. Opin. Cell Biol.* 23, 167–175. doi: 10.1016/j.ceb.2010.10.012

Feng, W.-K., Wang, L., Lu, Y., and Wang, X.-Y. (2011). A protein oxidase catalysing disulfide bond formation is localized to the chloroplast thylakoids. *FEBS J.* 278, 3419–3430. doi: 10.1111/j.1742-4658.2011.08265.x

Fischer, G., Tradler, T., and Zarnt, T. (1998). The mode of action of peptidyl prolyl *cis*/*trans* isomerases *in vivo*: binding vs. catalysis. *FEBS Lett.* 426, 17–20. doi: 10.1016/S0014-5793(98)00242-7

Fristedt, R., Herdean, A., Blaby-Haas, C. E., Mamedov, F., Merchant, S. S., Last, R. L., et al. (2015). PHOTOSYSTEM II PROTEIN33, a protein conserved

in the plastid lineage, is associated with the chloroplast thylakoid membrane and provides stability to Photosystem II supercomplexes in *Arabidopsis*. *Plant Physiol.* 167, 481–492. doi: 10.1104/pp.114.253336

Fu, A., He, Z. Y., Cho, H. S., Lima, A., Buchanan, B. B., and Luan, S. (2007). A chloroplast cyclophilin functions in the assembly and maintenance of Photosystem II in *Arabidopsis thaliana*. *Proc. Natl. Acad. Sci. U.S.A.* 104, 15947–15952. doi: 10.1073/pnas.0707851104

Fulgosi, H., Vener, A. V., Altschmied, L., Herrmann, R. G., and Andersson, B. (1998). A novel multi-functional chloroplast protein: identification of a 40 kDa immunophilin-like protein located in the thylakoid lumen. *EMBO J.* 17, 1577–1587. doi: 10.1093/emboj/17.6.1577

Göhre, V., Ossenbühl, F., Crèvecoeur, M., Eichacker, L. A., and Rochaix, J.-D. (2006). One of two Alb3 proteins is essential for the assembly of the photosystems and for cell survival in *Chlamydomonas*. *Plant Cell* 18, 1454–1466. doi: 10.1105/tpc.105.038695

Goral, T. K., Johnson, M. P., Brain, A. P., Kirchhoff, H., Ruban, A. V., and Mullineaux, C. W. (2010). Visualizing the mobility and distribution of chlorophyll proteins in higher plant thylakoid membranes: effects of photoinhibition and protein phosphorylation. *Plant J.* 62, 948–959. doi: 10.1111/j.1365-313x.2010.04207.x

Haubühl, K., Andersson, B., and Adamska, I. (2001). A chloroplast DegP2 protease performs the primary cleavage of the photodamaged D1 protein in plant Photosystem II. *EMBO J.* 20, 713–722. doi: 10.1093/emboj/20.4.713

He, Z., Li, L., and Luan, S. (2004). Immunophilins and parvulins. Superfamily of peptidyl prolyl isomerases in *Arabidopsis*. *Plant Physiol.* 134, 1248–1267. doi: 10.1104/pp.103.031005

Heddad, M., Engelken, J., and Adamska, I. (2012). "Light stress proteins in viruses, cyanobacteria and photosynthetic eukaryota," in *Photosynthesis*, eds J. J. Eaton-Rye, B. C. Tripathy, and T. D. Sharkey (Dordrecht: Springer), 299–317.

Heddad, M., Norén, H., Reiser, V., Dunaeva, M., Andersson, B., and Adamska, I. (2006). Differential expression and localization of early light-induced proteins in *Arabidopsis*. *Plant Physiol.* 142, 75–87. doi: 10.1104/pp.106.081489

Henry, R., Goforth, R., and Schunemann, D. (2007). "Chloroplast SRP/FtsY and Alb3 in protein integration into the thylakoid membrane," in *The Enzymes: Molecular Machines Involved in Protein Transport across Cellular Membranes*, eds R. E. Dalbey, C. M. Koehler, and F. Tamanoi (Waltham, MA: Academic Press), 493–521.

Hentze, M. W. (1994). Enzymes as RNA-binding proteins: a role for (di)nucleotide-binding domains? *Trends Biochem. Sci.* 19, 101–103. doi: 10.1016/0968-0004(94)90198-8

Herbstová, M., Tietz, S., Kinzel, C., Turkina, M. V., and Kirchhoff, H. (2012). Architectural switch in plant photosynthetic membranes induced by light stress. *Proc. Natl. Acad. Sci. U.S.A.* 109, 20130–20135. doi: 10.1073/pnas.1214265109

Hoober, J. K., Boyd, C. O., and Paavola, L. G. (1991). Origin of thylakoid membranes in *Chlamydomonas reinhardtii y-1* at 38°C. *Plant Physiol.* 96, 1321–1328. doi: 10.1104/pp.96.4.1321

Hoober, J. K., Eggink, L. L., and Chen, M. (2007). Chlorophylls, ligands and assembly of light-harvesting complexes in chloroplasts. *Photosynth. Res.* 94, 387–400. doi: 10.1007/s11120-007-9181-1

Houston, N. L., Fan, C., Xiang, Q.-Y., Schulze, J.-M., Jung, R., and Boston, R. S. (2005). Phylogenetic analyses identify 10 classes of the protein disulfide isomerase family in plants, including single-domain protein disulfide isomerase-related proteins. *Plant Physiol.* 137, 762–778. doi: 10.1104/pp.104.056507

Huang, J., Taylor, J. P., Chen, J. G., Uhrig, J. F., Schnell, D. J., Nakagawa, T., et al. (2006). The plastid protein THYLAKOID FORMATION1 and the plasma membrane G-protein GPA1 interact in a novel sugar-signaling mechanism in *Arabidopsis*. *Plant Cell* 18, 1226–1238. doi: 10.1105/tpc.105.037259

Huang, W., Chen, Q., Zhu, Y., Hu, F., Zhang, L., Ma, Z., et al. (2013). *Arabidopsis* thylakoid formation 1 is a critical regulator for dynamics of PSII-LHCII complexes in leaf senescence and excess light. *Mol. Plant* 6, 1673–1691. doi: 10.1093/mp/sst069

Huesgen, P. F., Schuhmann, H., and Adamska, I. (2005). The family of Deg proteases in cyanobacteria and chloroplasts of higher plants. *Physiol. Plant.* 123, 413–420. doi: 10.1111/j.1399-3054.2005.00458.x

Huesgen, P. F., Schuhmann, H., and Adamska, I. (2006). Photodamaged D1 protein is degraded in *Arabidopsis* mutants lacking the Deg2 protease. *FEBS Lett.* 580, 6929–6932. doi: 10.1016/j.febslet.2006.11.058

Huesgen, P. F., Schuhmann, H., and Adamska, I. (2009). Deg/HtrA proteases as components of a network for Photosystem II quality control in chloroplasts and cyanobacteria. *Res. Microbiol.* 160, 726–732. doi: 10.1016/j.resmic.2009.08.005

Hutin, C., Nussaume, L., Moise, N., Moya, I., Kloppstech, K., and Havaux, M. (2003). Early light-induced proteins protect *Arabidopsis* from photooxidative stress. *Proc. Natl. Acad. Sci. U.S.A.* 100, 4921–4926. doi: 10.1073/pnas.0736939100

Ifuku, K. (2014). The PsbP and PsbQ family proteins in the photosynthetic machinery of chloroplasts. *Plant Physiol. Biochem.* 81, 108–114. doi: 10.1016/j.plaphy.2014.01.001

Ikeuchi, M., Koike, H., and Inoue, Y. (1989). N-terminal sequencing of low-molecular-mass components in cyanobacterial Photosystem II core complex: two components correspond to unidentified open reading frames of plant chloroplast DNA. *FEBS Lett.* 253, 178–182. doi: 10.1016/0014-5793(89)80954-8

Ingelsson, B., Shapiguzov, A., Kieselbach, T., and Vener, A. V. (2009). Peptidyl prolyl isomerase activity in chloroplast thylakoid lumen is a dispensable function of immunophilins in *Arabidopsis thaliana*. *Plant Cell Physiol.* 50, 1801–1814. doi: 10.1093/pcp/pcp122

Ishihara, S., Takabayashi, A., Ido, K., Endo, T., Ifuku, K., and Sato, F. (2007). Distinct functions for the two PsbP-like proteins PPL1 and PPL2 in the chloroplast thylakoid lumen of *Arabidopsis*. *Plant Physiol.* 145, 668–679. doi: 10.1104/pp.107.105866

Ishikawa, A., Tanaka, H., Kato, C., Iwasaki, Y., and Asahi, T. (2005a). Molecular characterization of the *ZKT* gene encoding a protein with PDZ, K-Box, and TPR motifs in *Arabidopsis*. *Biosci. Biotechnol. Biochem.* 69, 972–978. doi: 10.1271/bbb.69.972

Ishikawa, Y., Schroder, W. P., and Funk, C. (2005b). Functional analysis of the PsbP-like protein (sll1418) in *Synechocystis* sp. PCC 6803. *Photosynth. Res.* 84, 257–262. doi: 10.1007/s11120-005-0477-8

Jackson, S. A., Hinds, M. G., and Eaton-Rye, J. J. (2012). Solution structure of CyanoP from *Synechocystis* sp. PCC 6803: new insights on the structural basis for functional specialization amongst PsbP family proteins. *Biochim. Biophys. Acta* 1817, 1331–1338. doi: 10.1016/j.bbabio.2012.02.032

Jansson, S. (1999). A guide to the Lhc genes and their relatives in *Arabidopsis*. *Trends Plant Sci.* 4, 236–240. doi: 10.1016/S1360-1385(99)01419-3

Järvi, S., Gollan, P. J., and Aro, E.-M. (2013). Understanding the roles of the thylakoid lumen in photosynthesis regulation. *Front. Plant Sci.* 4:434. doi: 10.3389/fpls.2013.00434

Järvi, S., Suorsa, M., and Aro, E.-M. (2015). Photosystem II repair in plant chloroplasts—Regulation, assisting proteins and shared components with Photosystem II biogenesis. *Biochim. Biophys. Acta* 1847, 900–909. doi: 10.1016/j.bbabio.2015.01.006

Jessop, C. E., Chakravarthi, S., Garbi, N., Hämmerling, G. J., Lovell, S., and Bulleid, N. J. (2007). ERp57 is essential for efficient folding of glycoproteins sharing common structural domains. *EMBO J.* 26, 28–40. doi: 10.1038/sj.emboj.7601505

Jin, H., Liu, B., Luo, L., Feng, D., Wang, P., Liu, J., et al. (2014). HYPERSENSITIVE TO HIGH LIGHT1 interacts with LOW QUANTUM YIELD OF PHOTOSYSTEM II1 and functions in protection of Photosystem II from photodamage in *Arabidopsis*. *Plant Cell* 26, 1213–1229. doi: 10.1105/tpc.113.122424

Jung, K.-H., Lee, J., Dardick, C., Seo, Y.-S., Cao, P., Canlas, P., et al. (2008). Identification and functional analysis of light-responsive unique genes and gene family members in rice. *PLoS Genet.* 4:e1000164. doi: 10.1371/journal.pgen.1000164

Kapri-Pardes, E., Naveh, L., and Adam, Z. (2007). The thylakoid lumen protease Deg1 is involved in the repair of Photosystem II from photoinhibition in *Arabidopsis*. *Plant Cell* 19, 1039–1047. doi: 10.1105/tpc.106.046573

Karamoko, M., Cline, S., Redding, K., Ruiz, N., and Hamel, P. P. (2011). Lumen Thiol Oxidoreductase1, a disulfide bond-forming catalyst, is required for the assembly of Photosystem II in *Arabidopsis*. *Plant Cell* 23, 4462–4475. doi: 10.1105/tpc.111.089680

Karamoko, M., Gabilly, S., and Hamel, P. P. (2013). Operation of trans-thylakoid thiol-metabolizing pathways in photosynthesis. *Front. Plant Sci.* 4:476. doi: 10.3389/fpls.2013.00476

Karim, S., Alezzawi, M., Garcia-Petit, C., Solymosi, K., Khan, N. Z., Lindquist, E., et al. (2014). A novel chloroplast localized Rab GTPase protein CPRabA5e is involved in stress, development, thylakoid biogenesis and vesicle transport in *Arabidopsis*. *Plant Mol. Biol.* 84, 675–692. doi: 10.1007/s11103-013-0161-x

Karim, S., and Aronsson, H. (2014). The puzzle of chloroplast vesicle transport – involvement of GTPases. *Front. Plant Sci.* 5:472. doi: 10.3389/fpls.2014.00472

Kashino, Y., Lauber, W. M., Carroll, J. A., Wang, Q. J., Whitmarsh, J., Satoh, K., et al. (2002). Proteomic analysis of a highly active Photosystem II preparation from the cyanobacterium *Synechocystis* sp. PCC 6803 reveals the presence of novel polypeptides. *Biochemistry* 41, 8004–8012. doi: 10.1021/bi026012+

Kato, Y., Miura, E., Ido, K., Ifuku, K., and Sakamoto, W. (2009). The variegated mutants lacking chloroplastic FtsHs are defective in D1 degradation and accumulate reactive oxygen species. *Plant Physiol.* 151, 1790–1801. doi: 10.1104/pp.109.146589

Kato, Y., Miura, E., Matsushima, R., and Sakamoto, W. (2007). White leaf sectors in *yellow variegated2* are formed by viable cells with undifferentiated plastids. *Plant Physiol.* 144, 952–960. doi: 10.1104/pp.107.099002

Kato, Y., Sun, X., Zhang, L., and Sakamoto, W. (2012). Cooperative D1 degradation in the Photosystem II repair mediated by chloroplastic proteases in *Arabidopsis*. *Plant Physiol.* 159, 1428–1439. doi: 10.1104/pp.112.199042

Keren, N., Ohkawa, H., Welsh, E. A., Liberton, M., and Pakrasi, H. B. (2005). Psb29, a conserved 22-kD protein, functions in the biogenesis of Photosystem II complexes in *Synechocystis* and *Arabidopsis*. *Plant Cell* 17, 2768–2781. doi: 10.1105/tpc.105.035048

Khan, N. Z., Lindquist, E., and Aronsson, H. (2013). New putative chloroplast vesicle transport components and cargo proteins revealed using a bioinformatics approach: an *Arabidopsis* model. *PLoS ONE* 8:e59898. doi: 10.1371/journal.pone.0059898

Khatoon, M., Inagawa, K., Pospisil, P., Yamashita, A., Yoshioka, M., Lundin, B., et al. (2009). Quality control of Photosystem II: Thylakoid unstacking is necessary to avoid further damage to the D1 protein and to facilitate D1 degradation under light stress in spinach thylakoids. *J. Biol. Chem.* 284, 25343–25352. doi: 10.1074/jbc.M109.007740

Klinkert, B., Ossenbuhl, F., Sikorski, M., Berry, S., Eichacker, L., and Nickelsen, J. (2004). PratA, a periplasmic tetratricopeptide repeat protein involved in biogenesis of Photosystem II in *Synechocystis* sp. PCC 6803. *J. Biol. Chem.* 279, 44639–44644. doi: 10.1074/jbc.M405393200

Knoppová, J., Sobotka, R., Tich, M., Yu, J., Konik, P., Halada, P., et al. (2014). Discovery of a chlorophyll binding protein complex involved in the early steps of Photosystem II assembly in *Synechocystis*. *Plant Cell* 26, 1200–1212. doi: 10.1105/tpc.114.123919

Komenda, J., Knoppová, J., Kopečná, J., Sobotka, R., Halada, P., Yu, J., et al. (2012b). The Psb27 assembly factor binds to the CP43 complex of Photosystem II in the cyanobacterium *Synechocystis* sp. PCC 6803. *Plant Physiol.* 158, 476–486. doi: 10.1104/pp.111.184184

Komenda, J., Nickelsen, J., Tich, M., Prášil, O., Eichacker, L. A., and Nixon, P. J. (2008). The cyanobacterial homologue of HCF136/YCF48 is a component of an early Photosystem II assembly complex and is important for both the efficient assembly and repair of Photosystem II in *Synechocystis* sp. PCC 6803. *J. Biol. Chem.* 283, 22390–22399. doi: 10.1074/jbc.M801917200

Komenda, J., Sobotka, R., and Nixon, P. J. (2012a). Assembling and maintaining the Photosystem II complex in chloroplasts and cyanobacteria. *Curr. Opin. Plant Biol.* 15, 245–251. doi: 10.1016/j.pbi.2012.01.017

Krech, K., Fu, H.-Y., Thiele, W., Ruf, S., Schöttler, M. A., and Bock, R. (2013). Reverse genetics in complex multigene operons by co-transformation of the plastid genome and its application to the open reading frame previously designated *psbN*. *Plant J.* 75, 1062–1074. doi: 10.1111/tpj.12256

Kroll, D., Meierhoff, K., Bechtold, N., Kinoshita, M., Westphal, S., Vothknecht, U. C., et al. (2001). *VIPP1*, a nuclear gene of *Arabidopsis thaliana* essential for thylakoid membrane formation. *Proc. Natl. Acad. Sci. U.S.A.* 98, 4238–4242. doi: 10.1073/pnas.061500998

Krzywda, S., Brzozowski, A. M., Verma, C., Karata, K., Ogura, T., and Wilkinson, A. J. (2002). The crystal structure of the AAA domain of the ATP-dependent protease FtsH of *Escherichia coli* at 1.5 Å resolution. *Structure* 10, 1073–1083. doi: 10.1016/S0969-2126(02)00806-7

Kwon, K.-C., and Cho, M. H. (2008). Deletion of the chloroplast-localized *AtTerC* gene product in *Arabidopsis thaliana* leads to loss of the thylakoid membrane and to seedling lethality. *Plant J.* 55, 428–442. doi: 10.1111/j.1365-313X.2008.03523.x

Liao, D. I., Qian, J., Chisholm, D. A., Jordan, D. B., and Diner, B. A. (2000). Crystal structures of the Photosystem II D1 C-terminal processing protease. *Nat. Struct. Biol.* 7, 749–753. doi: 10.1038/78973

Lima, A., Lima, S., Wong, J. H., Phillips, R. S., Buchanan, B. B., and Luan, S. (2006). A redox-active FKBP-type immunophilin functions in accumulation of the Photosystem II supercomplex in *Arabidopsis thaliana*. *Proc. Natl. Acad. Sci. U.S.A.* 103, 12631–12636. doi: 10.1073/pnas.0605452103

Lindahl, M., Spetea, C., Hundal, T., Oppenheim, A. B., Adam, Z., and Andersson, B. (2000). The thylakoid FtsH protease plays a role in the light-induced turnover of the Photosystem II D1 protein. *Plant Cell* 12, 419–432. doi: 10.1105/tpc.12.3.419

Lindahl, M., Tabak, S., Cseke, L., Pichersky, E., Andersson, B., and Adam, Z. (1996). Identification, characterization, and molecular cloning of a homologue of the bacterial FtsH protease in chloroplasts of higher plants. *J. Biol. Chem.* 271, 29329–29334. doi: 10.1074/jbc.271.46.29329

Link, S., Engelmann, K., Meierhoff, K., and Westhoff, P. (2012). The atypical short-chain dehydrogenases HCF173 and HCF244 are jointly involved in translational initiation of the *psbA* mRNA of *Arabidopsis*. *Plant Physiol.* 160, 2202–2218. doi: 10.1104/pp.112.205104

Lippuner, V., Chou, I. T., Scott, S. V., Ettinger, W. F., Theg, S. M., and Gasser, C. S. (1994). Cloning and characterization of chloroplast and cytosolic forms of cyclophilin from *Arabidopsis thaliana*. *J. Biol. Chem.* 269, 7863–7868.

Liu, H., Huang, R. Y.-C., Chen, J., Gross, M. L., and Pakrasi, H. B. (2011b). Psb27, a transiently associated protein, binds to the chlorophyll binding protein CP43 in Photosystem II assembly intermediates. *Proc. Natl. Acad. Sci. U.S.A.* 108, 18536–18541. doi: 10.1073/pnas.1111597108

Liu, H., Roose, J. L., Cameron, J. C., and Pakrasi, H. B. (2011a). A genetically tagged Psb27 protein allows purification of two consecutive Photosystem II (PSII) assembly intermediates in *Synechocystis* 6803, a cyanobacterium. *J. Biol. Chem.* 286, 24865–24871. doi: 10.1074/jbc.M111.246231

Liu, J., and Last, R. L. (2015a). A land plant-specific thylakoid membrane protein contributes to Photosystem II maintenance in *Arabidopsis thaliana*. *Plant J.* 82, 731–743. doi: 10.1111/tpj.12845

Liu, J., and Last, R. L. (2015b). MPH1 is a thylakoid membrane protein involved in protecting Photosystem II from photodamage in land plants. *Plant Signal. Behav.* 10:e1076602. doi: 10.1080/15592324.2015.1076602

Liu, L.-N., Chen, X.-L., Zhang, Y.-Z., and Zhou, B.-C. (2005). Characterization, structure and function of linker polypeptides in phycobilisomes of cyanobacteria and red algae: an overview. *Biochim. Biophys. Acta* 1708, 133–142. doi: 10.1016/j.bbabio.2005.04.001

Liu, Z., Yan, H., Wang, K., Kuang, T., Zhang, J., Gui, L., et al. (2004). Crystal structure of spinach major light-harvesting complex at 2.72 Å resolution. *Nature* 428, 287–292. doi: 10.1038/nature02373

Lohscheider, J. N., Rojas-Stutz, M. C., Rothbart, M., Andersson, U., Funck, D., Mendgen, K., et al. (2015). Altered levels of LIL3 isoforms in *Arabidopsis* lead to disturbed pigment-protein assembly and chlorophyll synthesis, chlorotic phenotype and impaired photosynthetic performance. *Plant Cell Environ.* 38, 2115–2127. doi: 10.1111/pce.12540

Lu, Y. (2011). The occurrence of a thylakoid-localized small zinc finger protein in land plants. *Plant Signal. Behav.* 6, 1181–1185. doi: 10.4161/psb.6.12.18022

Lu, Y., Hall, D. A., and Last, R. L. (2011). A small zinc finger thylakoid protein plays a role in maintenance of Photosystem II in *Arabidopsis thaliana*. *Plant Cell* 23, 1861–1875. doi: 10.1105/tpc.111.085456

Lu, Y., Wang, H.-R., Li, H., Cui, H.-R., Feng, Y.-G., and Wang, X.-Y. (2013). A chloroplast membrane protein LTO1/AtVKOR involving in redox regulation and ROS homeostasis. *Plant Cell Rep.* 32, 1427–1440. doi: 10.1007/s00299-013-1455-9

Luciński, R., Misztal, L., Samardakiewicz, S., and Jackowski, G. (2011a). Involvement of Deg5 protease in wounding-related disposal of PsbF apoprotein. *Plant Physiol. Biochem.* 49, 311–320. doi: 10.1016/j.plaphy.2011.01.001

Luciński, R., Misztal, L., Samardakiewicz, S., and Jackowski, G. (2011b). The thylakoid protease Deg2 is involved in stress-related degradation of the Photosystem II light-harvesting protein Lhcb6 in *Arabidopsis thaliana*. *New Phytol.* 192, 74–86. doi: 10.1111/j.1469-8137.2011.03782.x

Ma, J., Peng, L., Guo, J., Lu, Q., Lu, C., and Zhang, L. (2007). LPA2 is required for efficient assembly of Photosystem II in *Arabidopsis thaliana*. *Plant Cell* 19, 1980–1993. doi: 10.1105/tpc.107.050526

Mabbitt, P. D., Wilbanks, S. M., and Eaton-Rye, J. J. (2014). Structure and function of the hydrophilic Photosystem II assembly proteins: Psb27, Psb28 and Ycf48. *Plant Physiol. Biochem.* 81, 96–107. doi: 10.1016/j.plaphy.2014.02.013

Mann, N. H., Novac, N., Mullineaux, C. W., Newman, J., Bailey, S., and Robinson, C. (2000). Involvement of an FtsH homologue in the assembly of functional Photosystem I in the cyanobacterium *Synechocystis* sp. PCC 6803. *FEBS Lett.* 479, 72–77. doi: 10.1016/S0014-5793(00)01871-8

Meurer, J., Plücken, H., Kowallik, K. V., and Westhoff, P. (1998). A nuclear-encoded protein of prokaryotic origin is essential for the stability of Photosystem II in *Arabidopsis thaliana*. *EMBO J.* 17, 5286–5297. doi: 10.1093/emboj/17.18.5286

Michoux, F., Boehm, M., Bialek, W., Takasaka, K., Maghlaoui, K., Barber, J., et al. (2014). Crystal structure of CyanoQ from the thermophilic cyanobacterium *Thermosynechococcus elongatus* and detection in isolated Photosystem II complexes. *Photosynth. Res.* 122, 57–67. doi: 10.1007/s11120-014-0010-z

Michoux, F., Takasaka, K., Boehm, M., Nixon, P. J., and Murray, J. W. (2010). Structure of CyanoP at 2.8 Å: implications for the evolution and function of the PsbP subunit of Photosystem II. *Biochemistry* 49, 7411–7413. doi: 10.1021/bi1011145

Mork-Jansson, A. E., Gargano, D., Kmiec, K., Furnes, C., Shevela, D., and Eichacker, L. A. (2015). Lil3 dimerization and chlorophyll binding in *Arabidopsis thaliana*. *FEBS Lett.* 589, 3064–3070. doi: 10.1016/j.febslet.2015.08.023

Morré, D. J., Selldén, G., Sundqvist, C., and Sandelius, A. S. (1991). Stromal low temperature compartment derived from the inner membrane of the chloroplast envelope. *Plant Physiol.* 97, 1558–1564. doi: 10.1104/pp.97.4.1558

Mulo, P., Sirpiö, S., Suorsa, M., and Aro, E. M. (2008). Auxiliary proteins involved in the assembly and sustenance of Photosystem II. *Photosynth. Res.* 98, 489–501. doi: 10.1007/s11120-008-9320-3

Muranaka, A., Watanabe, S., Sakamoto, A., and Shimada, H. (2012). *Arabidopsis* cotyledon chloroplast biogenesis factor CYO1 uses glutathione as an electron donor and interacts with PSI (A1 and A2) and PSII (CP43 and CP47) subunits. *J. Plant Physiol.* 169, 1212–1215. doi: 10.1016/j.jplph.2012.04.001

Nagy, E., Henics, T., Eckert, M., Miseta, A., Lightowlers, R. N., and Kellermayer, M. (2000). Identification of the NAD(+)-binding fold of glyceraldehyde-3-phosphate dehydrogenase as a novel RNA-binding domain. *Biochem. Biophys. Res. Commun.* 275, 253–260. doi: 10.1006/bbrc.2000.3246

Nath, K., Poudyal, R. S., Eom, J.-S., Park, Y. S., Zulfugarov, I. S., Mishra, S. R., et al. (2013). Loss-of-function of OsSTN8 suppresses the Photosystem II core protein phosphorylation and interferes with the Photosystem II repair mechanism in rice (*Oryza sativa*). *Plant J.* 76, 675–686. doi: 10.1111/tpj.12331

Nickelsen, J., and Rengstl, B. (2013). Photosystem II assembly: from cyanobacteria to plants. *Annu. Rev. Plant Biol.* 64, 609–635. doi: 10.1146/annurev-arplant-050312-120124

Nickelsen, J., and Zerges, W. (2013). Thylakoid biogenesis has joined the new era of bacterial cell biology. *Front. Plant Sci.* 4:458. doi: 10.3389/fpls.2013.00458

Nield, J., and Barber, J. (2006). Refinement of the structural model for the Photosystem II supercomplex of higher plants. *Biochim. Biophys. Acta* 1757, 353–361. doi: 10.1016/j.bbabio.2006.03.019

Niwa, H., Tsuchiya, D., Makyio, H., Yoshida, M., and Morikawa, K. (2002). Hexameric ring structure of the ATPase domain of the membrane-integrated metalloprotease FtsH from *Thermus thermophilus* HB8. *Structure* 10, 1415–1423. doi: 10.1016/S0969-2126(02)00855-9

Nixon, P. J., Barker, M., Boehm, M., de Vries, R., and Komenda, J. (2005). FtsH-mediated repair of the Photosystem II complex in response to light stress. *J. Exp. Bot.* 56, 357–363. doi: 10.1093/jxb/eri021

Nixon, P. J., Michoux, F., Yu, J., Boehm, M., and Komenda, J. (2010). Recent advances in understanding the assembly and repair of Photosystem II. *Ann. Bot.* 106, 1–16. doi: 10.1093/aob/mcq059

Nixon, P. J., Trost, J. T., and Diner, B. A. (1992). Role of the carboxy terminus of polypeptide D1 in the assembly of a functional water-oxidizing manganese cluster in Photosystem II of the cyanobacterium *Synechocystis* sp. PCC 6803: assembly requires a free carboxyl group at C-terminal position 344. *Biochemistry* 31, 10859–10871. doi: 10.1021/bi00159a029

Nowaczyk, M. M., Hebeler, R., Schlodder, E., Meyer, H. E., Warscheid, B., and Rögner, M. (2006). Psb27, a cyanobacterial lipoprotein, is involved in the repair cycle of Photosystem II. *Plant Cell* 18, 3121–3131. doi: 10.1105/tpc.106.042671

Ossenbühl, F., Göhre, V., Meurer, J., Krieger-Liszkay, A., Rochaix, J.-D., and Eichacker, L. A. (2004). Efficient assembly of Photosystem II in *Chlamydomonas reinhardtii* requires Alb3.1p, a homolog of *Arabidopsis* ALBINO3. *Plant Cell* 16, 1790–1800. doi: 10.1105/tpc.023226

Park, S. W., Li, W., Viehhauser, A., He, B., Kim, S., Nilsson, A. K., et al. (2013). Cyclophilin 20-3 relays a 12-oxo-phytodienoic acid signal during stress responsive regulation of cellular redox homeostasis. *Proc. Natl. Acad. Sci. U.S.A.* 110, 9559–9564. doi: 10.1073/pnas.1218872110

Pasch, J. C., Nickelsen, J., and Schünemann, D. (2005). The yeast split-ubiquitin system to study chloroplast membrane protein interactions. *Appl. Microbiol. Biotechnol.* 69, 440–447. doi: 10.1007/s00253-005-0029-3

Peng, L. W., Ma, J. F., Chi, W., Guo, J. K., Zhu, S. Y., Lu, Q. T., et al. (2006). LOW PSII ACCUMULATION1 is involved in efficient assembly of Photosystem II in *Arabidopsis thaliana*. *Plant Cell* 18, 955–969. doi: 10.1105/tpc.105.037689

Persson, B., Kallberg, Y., Bray, J. E., Bruford, E., Dellaporta, S. L., Favia, A. D., et al. (2009). The SDR (short-chain dehydrogenase/reductase and related enzymes) nomenclature initiative. *Chem. Biol. Interact.* 178, 94–98. doi: 10.1016/j.cbi.2008.10.040

Pesaresi, P., Pribil, M., Wunder, T., and Leister, D. (2011). Dynamics of reversible protein phosphorylation in thylakoids of flowering plants: the roles of STN7, STN8 and TAP38. *Biochim. Biophys. Acta* 1807, 887–896. doi: 10.1016/j.bbabio.2010.08.002

Pioli, P. A., Hamilton, B. J., Connolly, J. E., Brewer, G., and Rigby, W. F. (2002). Lactate dehydrogenase is an AU-rich element-binding protein that directly interacts with AUF1. *J. Biol. Chem.* 277, 35738–35745. doi: 10.1074/jbc.M204002200

Plücken, H., Müller, B., Grohmann, D., Westhoff, P., and Eichacker, L. A. (2002). The HCF136 protein is essential for assembly of the Photosystem II reaction center in *Arabidopsis thaliana*. *FEBS Lett.* 532, 85–90. doi: 10.1016/S0014-5793(02)03634-7

Pribil, M., Pesaresi, P., Hertle, A., Barbato, R., and Leister, D. (2010). Role of plastid protein phosphatase TAP38 in LHCII dephosphorylation and thylakoid electron flow. *PLoS Biol.* 8:e1000288. doi: 10.1371/journal.pbio.1000288

Rast, A., Heinz, S., and Nickelsen, J. (2015). Biogenesis of thylakoid membranes. *Biochim. Biophys. Acta* 1847, 821–830. doi: 10.1016/j.bbabio.2015.01.007

Rintamaki, E., Salonen, M., Suoranta, U. M., Carlberg, I., Andersson, B., and Aro, E. M. (1997). Phosphorylation of light-harvesting complex II and Photosystem II core proteins shows different irradiance-dependent regulation *in vivo*: application of phosphothreonine antibodies to analysis of thylakoid phosphoproteins. *J. Biol. Chem.* 272, 30476–30482. doi: 10.1074/jbc.272.48.30476

Rokka, A., Aro, E.-M., Herrmann, R. G., Andersson, B., and Vener, A. V. (2000). Dephosphorylation of Photosystem II reaction center proteins in plant photosynthetic membranes as an immediate response to abrupt elevation of temperature. *Plant Physiol.* 123, 1525–1536. doi: 10.1104/pp.123.4.1525

Rokka, A., Suorsa, M., Saleem, A., Battchikova, N., and Aro, E. M. (2005). Synthesis and assembly of thylakoid protein complexes: multiple assembly steps of Photosystem II. *Biochem. J.* 388, 159–168. doi: 10.1042/BJ20042098

Romano, P. G., Horton, P., and Gray, J. E. (2004). The *Arabidopsis* cyclophilin gene family. *Plant Physiol.* 134, 1268–1282. doi: 10.1104/pp.103.022160

Rossini, S., Casazza, A. P., Engelmann, E. C. M., Havaux, M., Jennings, R. C., and Soave, C. (2006). Suppression of both ELIP1 and ELIP2 in *Arabidopsis* does not affect tolerance to photoinhibition and photooxidative stress. *Plant Physiol.* 141, 1264–1273. doi: 10.1104/pp.106.083055

Sakamoto, W., Tamura, T., Hanba-Tomita, Y., Sodmergen, and Murata, M. (2002). The *VAR1* locus of *Arabidopsis* encodes a chloroplastic FtsH and is responsible for leaf variegation in the mutant alleles. *Genes Cells* 7, 769–780. doi: 10.1046/j.1365-2443.2002.00558.x

Sakamoto, W., Zaltsman, A., Adam, Z., and Takahashi, Y. (2003). Coordinated regulation and complex formation of YELLOW VARIEGATED1 and YELLOW VARIEGATED2, chloroplastic FtsH metalloproteases involved in the repair cycle of Photosystem II in *Arabidopsis* thylakoid membranes. *Plant Cell* 15, 2843–2855. doi: 10.1105/tpc.017319

Samol, I., Shapiguzov, A., Ingelsson, B., Fucile, G., Crèvecoeur, M., Vener, A. V., et al. (2012). Identification of a Photosystem II phosphatase

involved in light acclimation in *Arabidopsis*. *Plant Cell* 24, 2596–2609. doi: 10.1105/tpc.112.095703

Schneider, A., Steinberger, I., Strissel, H., Kunz, H.-H., Manavski, N., Meurer, J., et al. (2014). The *Arabidopsis* Tellurite resistance C protein together with ALB3 is involved in Photosystem II protein synthesis. *Plant J.* 78, 344–356. doi: 10.1111/tpj.12474

Schuhmann, H., and Adamska, I. (2012). Deg proteases and their role in protein quality control and processing in different subcellular compartments of the plant cell. *Physiol. Plant.* 145, 224–234. doi: 10.1111/j.1399-3054.2011.01533.x

Schuhmann, H., Mogg, U., and Adamska, I. (2011). A new principle of oligomerization of plant DEG7 protease based on interactions of degenerated protease domains. *Biochem. J.* 435, 167–174. doi: 10.1042/BJ20101613

Schult, K., Meierhoff, K., Paradies, S., Toller, T., Wolff, P., and Westhoff, P. (2007). The nuclear-encoded factor HCF173 is involved in the initiation of translation of the *psbA* mRNA in *Arabidopsis thaliana*. *Plant Cell* 19, 1329–1346. doi: 10.1105/tpc.106.042895

Schunemann, D. (2007). Mechanisms of protein import into thylakoids of chloroplasts. *Biol. Chem.* 388, 907–915. doi: 10.1515/BC.2007.111

Shapiguzov, A., Ingelsson, B., Samol, I., Andres, C., Kessler, F., Rochaix, J. D., et al. (2010). The PPH1 phosphatase is specifically involved in LHCII dephosphorylation and state transitions in *Arabidopsis*. *Proc. Natl. Acad. Sci. U.S.A.* 107, 4782–4787. doi: 10.1073/pnas.0913810107

Shen, G., Zhao, J., Reimer, S. K., Antonkine, M. L., Cai, Q., Weiland, S. M., et al. (2002). Assembly of Photosystem I: I. Inactivation of the *rubA* gene encoding a membrane-associated rubredoxin in the cyanobacterium *Synechococcus* sp. PCC 7002 causes a loss of Photosystem I activity. *J. Biol. Chem.* 277, 20343–20354. doi: 10.1074/jbc.M201103200

Shi, L.-X., Hall, M., Funk, C., and Schröder, W. P. (2012). Photosystem II, a growing complex: updates on newly discovered components and low molecular mass proteins. *Biochim. Biophys. Acta* 1817, 13–25. doi: 10.1016/j.bbabio.2011.08.008

Shimada, H., Mochizuki, M., Ogura, K., Froehlich, J. E., Osteryoung, K. W., Shirano, Y., et al. (2007). *Arabidopsis* cotyledon-specific chloroplast biogenesis factor CYO1 is a protein disulfide isomerase. *Plant Cell* 19, 3157–3169. doi: 10.1105/tpc.107.051714

Silva, P., Thompson, E., Bailey, S., Kruse, O., Mullineaux, C. W., Robinson, C., et al. (2003). FtsH is involved in the early stages of repair of Photosystem II in *Synechocystis* sp. PCC 6803. *Plant Cell* 15, 2152–2164. doi: 10.1105/tpc.012609

Sirpiö, S., Allahverdiyeva, Y., Suorsa, M., Paakkarinen, V., Vainonen, J., Battchikova, N., et al. (2007). TLP18.3, a novel thylakoid lumen protein regulating Photosystem II repair cycle. *Biochem. J.* 406, 415–425. doi: 10.1042/BJ20070460

Sirpiö, S., Khrouchtchova, A., Allahverdiyeva, Y., Hansson, M., Fristedt, R., Vener, A. V., et al. (2008). AtCYP38 ensures early biogenesis, correct assembly and sustenance of Photosystem II. *Plant J.* 55, 639–651. doi: 10.1111/j.1365-313X.2008.03532.x

Speiser, A., Haberland, S., Watanabe, M., Wirtz, M., Dietz, K. J., Saito, K., et al. (2015). The significance of cysteine synthesis for acclimation to high light conditions. *Front. Plant Sci.* 5:776. doi: 10.3389/fpls.2014.00776

Spetea, C., Hundal, T., Lohmann, F., and Andersson, B. (1999). GTP bound to chloroplast thylakoid membranes is required for light-induced, multienzyme degradation of the Photosystem II D1 protein. *Proc. Natl. Acad. Sci. U.S.A.* 96, 6547–6552. doi: 10.1073/pnas.96.11.6547

Staleva, H., Komenda, J., Shukla, M. K., Slouf, V., Kana, R., Polivka, T., et al. (2015). Mechanism of photoprotection in the cyanobacterial ancestor of plant antenna proteins. *Nat. Chem. Biol.* 11, 287–291. doi: 10.1038/nchembio.1755

Suga, M., Akita, F., Hirata, K., Ueno, G., Murakami, H., Nakajima, Y., et al. (2015). Native structure of Photosystem II at 1.95 Å resolution viewed by femtosecond X-ray pulses. *Nature* 517, 99–103. doi: 10.1038/nature13991

Summerfield, T., Winter, R., and Eaton-Rye, J. (2005). Investigation of a requirement for the PsbP-like protein in *Synechocystis* sp. PCC 6803. *Photosynth. Res.* 84, 263–268. doi: 10.1007/s11120-004-6431-3

Sun, X., Fu, T., Chen, N., Guo, J., Ma, J., Zou, M., et al. (2010a). The stromal chloroplast Deg7 protease participates in the repair of Photosystem II after photoinhibition in *Arabidopsis*. *Plant Physiol.* 152, 1263–1273. doi: 10.1104/pp.109.150722

Sun, X., Ouyang, M., Guo, J., Ma, J., Lu, C., Adam, Z., et al. (2010b). The thylakoid protease Deg1 is involved in Photosystem-II assembly in *Arabidopsis thaliana*. *Plant J.* 62, 240–249. doi: 10.1111/j.1365-313X.2010.04140.x

Sun, X., Peng, L., Guo, J., Chi, W., Ma, J., Lu, C., et al. (2007). Formation of DEG5 and DEG8 complexes and their involvement in the degradation of photodamaged Photosystem II reaction center D1 protein in *Arabidopsis*. *Plant Cell* 19, 1347–1361. doi: 10.1105/tpc.106.049510

Takahashi, K., Takabayashi, A., Tanaka, A., and Tanaka, R. (2014). Functional analysis of light-harvesting-like protein 3 (LIL3) and its light-harvesting chlorophyll-binding motif in *Arabidopsis*. *J. Biol. Chem.* 289, 987–999. doi: 10.1074/jbc.M113.525428

Takechi, K., Sodmergen, Murata, M., Motoyoshi, F., and Sakamoto, W. (2000). The *YELLOW VARIEGATED (VAR2)* locus encodes a homologue of FtsH, an ATP-dependent protease in *Arabidopsis*. *Plant Cell Physiol.* 41, 1334–1346. doi: 10.1093/pcp/pcd067

Tanaka, R., Rothbart, M., Oka, S., Takabayashi, A., Takahashi, K., Shibata, M., et al. (2010). LIL3, a light-harvesting-like protein, plays an essential role in chlorophyll and tocopherol biosynthesis. *Proc. Natl. Acad. Sci. U.S.A.* 107, 16721–16725. doi: 10.1073/pnas.1004699107

Tanz, S. K., Kilian, J., Johnsson, C., Apel, K., Small, I., Harter, K., et al. (2012). The SCO2 protein disulphide isomerase is required for thylakoid biogenesis and interacts with LHCB1 chlorophyll a/b binding proteins which affects chlorophyll biosynthesis in *Arabidopsis* seedlings. *Plant J.* 69, 743–754. doi: 10.1111/j.1365-313X.2011.04833.x

Thornton, L. E., Ohkawa, H., Roose, J. L., Kashino, Y., Keren, N., and Pakrasi, H. B. (2004). Homologs of plant PsbP and PsbQ proteins are necessary for regulation of Photosystem II activity in the cyanobacterium *Synechocystis* 6803. *Plant Cell* 16, 2164–2175. doi: 10.1105/tpc.104.023515

Tikkanen, M., and Aro, E. M. (2012). Thylakoid protein phosphorylation in dynamic regulation of Photosystem II in higher plants. *Biochim. Biophys. Acta* 1817, 232–238. doi: 10.1016/j.bbabio.2011.05.005

Tikkanen, M., Nurmi, M., Kangasjärvi, S., and Aro, E. M. (2008). Core protein phosphorylation facilitates the repair of photodamaged Photosystem II at high light. *Biochim. Biophys. Acta* 1777, 1432–1437. doi: 10.1016/j.bbabio.2008.08.004

Torabi, S., Umate, P., Manavski, N., Plöchinger, M., Kleinknecht, L., Bogireddi, H., et al. (2014). PsbN is required for assembly of the Photosystem II reaction center in *Nicotiana tabacum*. *Plant Cell* 26, 1183–1199. doi: 10.1105/tpc.113.120444

Umena, Y., Kawakami, K., Shen, J. R., and Kamiya, N. (2011). Crystal structure of oxygen-evolving Photosystem II at a resolution of 1.9 Å. *Nature* 473, 55–U65. doi: 10.1038/nature09913

Uniacke, J., and Zerges, W. (2007). Photosystem II assembly and repair are differentially localized in *Chlamydomonas*. *Plant Cell* 19, 3640–3654. doi: 10.1105/tpc.107.054882

Urantowka, A., Knorpp, C., Olczak, T., Kolodziejczak, M., and Janska, H. (2005). Plant mitochondria contain at least two *i*-AAA-like complexes. *Plant Mol. Biol.* 59, 239–252. doi: 10.1007/s11103-005-8766-3

Vasudevan, D., Fu, A., Luan, S., and Swaminathan, K. (2012). Crystal structure of *Arabidopsis* cyclophilin38 reveals a previously uncharacterized immunophilin fold and a possible autoinhibitory mechanism. *Plant Cell* 24, 2666–2674. doi: 10.1105/tpc.111.093781

Vener, A. V., Harms, A., Sussman, M. R., and Vierstra, R. D. (2001). Mass spectrometric resolution of reversible protein phosphorylation in photosynthetic membranes of *Arabidopsis thaliana*. *J. Biol. Chem.* 276, 6959–6966. doi: 10.1074/jbc.M009394200

Vener, A. V., Rokka, A., Fulgosi, H., Andersson, B., and Herrmann, R. G. (1999). A cyclophilin-regulated PP2A-like protein phosphatase in thylakoid membranes of plant chloroplasts. *Biochemistry* 38, 14955–14965. doi: 10.1021/bi990971v

Wagner, R., Aigner, H., Pruzinska, A., Jankanpaa, H. J., Jansson, S., and Funk, C. (2011). Fitness analyses of *Arabidopsis thaliana* mutants depleted of FtsH metalloproteases and characterization of three FtsH6 deletion mutants exposed to high light stress, senescence and chilling. *New Phytol.* 191, 449–458. doi: 10.1111/j.1469-8137.2011.03684.x

Walter, B., Hristou, A., Nowaczyk, M. M., and Schunemann, D. (2015). *In vitro* reconstitution of co-translational D1 insertion reveals a role of the cpSec-Alb3 translocase and Vipp1 in Photosystem II biogenesis. *Biochem. J.* 468, 315–324. doi: 10.1042/BJ20141425

Wang, P., Liu, J., Liu, B., Feng, D., Da, Q., Shu, S., et al. (2013). Evidence for a role of chloroplastic m-type thioredoxins in the biogenesis of Photosystem

II in *Arabidopsis*. *Plant Physiol.* 163, 1710–1728. doi: 10.1104/pp.113.228353

Wang, Q., Sullivan, R. W., Kight, A., Henry, R. L., Huang, J., Jones, A. M., et al. (2004). Deletion of the chloroplast-localized *Thylakoid formation1* gene product in *Arabidopsis* leads to deficient thylakoid formation and variegated leaves. *Plant Physiol.* 136, 3594–3604. doi: 10.1104/pp.104.049841

Wei, L., Guo, J., Ouyang, M., Sun, X., Ma, J., Chi, W., et al. (2010). LPA19, a Psb27 homolog in *Arabidopsis thaliana*, facilitates D1 protein precursor processing during PSII biogenesis. *J. Biol. Chem.* 285, 21391–21398. doi: 10.1074/jbc.M110.105064

Westphal, S., Soll, J., and Vothknecht, U. C. (2001). A vesicle transport system inside chloroplasts. *FEBS Lett.* 506, 257–261. doi: 10.1016/S0014-5793(01)02931-3

Westphal, S., Soll, J., and Vothknecht, U. C. (2003). Evolution of chloroplast vesicle transport. *Plant Cell Physiol.* 44, 217–222. doi: 10.1093/pcp/pcg023

Wittenberg, G., Levitan, A., Klein, T., Dangoor, I., Keren, N., and Danon, A. (2014). Knockdown of the *Arabidopsis thaliana* chloroplast protein disulfide isomerase 6 results in reduced levels of photoinhibition and increased D1 synthesis in high light. *Plant J.* 78, 1003–1013. doi: 10.1111/tpj.12525

Wu, H. Y., Liu, M. S., Lin, T. P., and Cheng, Y. S. (2011). Structural and functional assays of AtTLP18.3 identify its novel acid phosphatase activity in thylakoid lumen. *Plant Physiol.* 157, 1015–1025. doi: 10.1104/pp.111.184739

Yamamoto, Y., Inagaki, N., and Satoh, K. (2001). Overexpression and characterization of carboxyl-terminal processing protease for precursor D1 protein: regulation of enzyme-substrate interaction by molecular environments. *J. Biol. Chem.* 276, 7518–7525. doi: 10.1074/jbc.M008877200

Yamatani, H., Sato, Y., Masuda, Y., Kato, Y., Morita, R., Fukunaga, K., et al. (2013). *NYC4*, the rice ortholog of *Arabidopsis THF1*, is involved in the degradation of chlorophyll – protein complexes during leaf senescence. *Plant J.* 74, 652–662. doi: 10.1111/tpj.12154

Yin, S., Sun, X., and Zhang, L. (2008). An *Arabidopsis ctpA* homologue is involved in the repair of Photosystem II under high light. *Chin. Sci. Bull.* 53, 1021–1026. doi: 10.1007/s11434-008-0153-4

Yu, F., Park, S., and Rodermel, S. R. (2004). The *Arabidopsis* FtsH metalloprotease gene family: interchangeability of subunits in chloroplast oligomeric complexes. *Plant J.* 37, 864–876. doi: 10.1111/j.1365-313X.2003.02014.x

Yu, F., Park, S., and Rodermel, S. R. (2005). Functional redundancy of AtFtsH metalloproteases in thylakoid membrane complexes. *Plant Physiol.* 138, 1957–1966. doi: 10.1104/pp.105.061234

Zaltsman, A., Feder, A., and Adam, Z. (2005a). Developmental and light effects on the accumulation of FtsH protease in *Arabidopsis* chloroplasts – implications for thylakoid formation and Photosystem II maintenance. *Plant J.* 42, 609–617. doi: 10.1111/j.1365-313X.2005.02401.x

Zaltsman, A., Ori, N., and Adam, Z. (2005b). Two types of FtsH protease subunits are required for chloroplast biogenesis and Photosystem II repair in *Arabidopsis*. *Plant Cell* 17, 2782–2790. doi: 10.1105/tpc.105.035071

Zelisko, A., Garcia-Lorenzo, M., Jackowski, G., Jansson, S., and Funk, C. (2005). AtFtsH6 is involved in the degradation of the light-harvesting complex II during high-light acclimation and senescence. *Proc. Natl. Acad. Sci. U.S.A.* 102, 13699–13704. doi: 10.1073/pnas.0503472102

Zhang, D., Zhou, G., Liu, B., Kong, Y., Chen, N., Qiu, Q., et al. (2011). *HCF243* encodes a chloroplast-localized protein involved in the D1 protein stability of the *Arabidopsis* Photosystem II complex. *Plant Physiol.* 157, 608–619. doi: 10.1104/pp.111.183301

Zhang, L., Kato, Y., Otters, S., Vothknecht, U. C., and Sakamoto, W. (2012). Essential role of VIPP1 in chloroplast envelope maintenance in *Arabidopsis*. *Plant Cell* 24, 3695–3707. doi: 10.1105/tpc.112.103606

Zhang, L., and Sakamoto, W. (2012). Possible function of VIPP1 in thylakoids: protection but not formation? *Plant Signal. Behav.* 8:e22860. doi: 10.4161/psb.22860

Zhang, L., Wei, Q., Wu, W., Cheng, Y., Hu, G., Hu, F., et al. (2009). Activation of the heterotrimeric G protein alpha-subunit GPA1 suppresses the ftsh-mediated inhibition of chloroplast development in *Arabidopsis*. *Plant J.* 58, 1041–1053. doi: 10.1111/j.1365-313X.2009.03843.x

Conflict of Interest Statement: The author declares that the research was conducted in the absence of any commercial or financial relationships that could be construed as a potential conflict of interest.

frontiers in Plant Science

REVIEW
published: 07 April 2016
doi: 10.3389/fpls.2016.00423

Functional Update of the Auxiliary Proteins PsbW, PsbY, HCF136, PsbN, TerC and ALB3 in Maintenance and Assembly of PSII

Magdalena Plöchinger[1†], Serena Schwenkert[2†], Lotta von Sydow[3†], Wolfgang P. Schröder[3†] and Jörg Meurer[1†]*

[1] Department Biologie I, Molekularbiologie der Pflanzen (Botanik), Ludwig-Maximilians-Universität, Planegg-Martinsried, Germany, [2] Department Biologie I, Biochemie und Physiologie der Pflanzen, Ludwig-Maximilians-Universität, Planegg-Martinsried, Germany, [3] Umeå Plant Science Center and Department of Chemistry, Umeå University, Umeå, Sweden

Assembly of Photosystem (PS) II in plants has turned out to be a highly complex process which, at least in part, occurs in a sequential order and requires many more auxiliary proteins than subunits present in the complex. Owing to the high evolutionary conservation of the subunit composition and the three-dimensional structure of the PSII complex, most plant factors involved in the biogenesis of PSII originated from cyanobacteria and only rarely evolved *de novo*. Furthermore, in chloroplasts the initial assembly steps occur in the non-appressed stroma lamellae, whereas the final assembly including the attachment of the major LHCII antenna proteins takes place in the grana regions. The stroma lamellae are also the place where part of PSII repair occurs, which very likely also involves assembly factors. In cyanobacteria initial PSII assembly also occurs in the thylakoid membrane, in so-called thylakoid centers, which are in contact with the plasma membrane. Here, we provide an update on the structures, localisations, topologies, functions, expression and interactions of the low molecular mass PSII subunits PsbY, PsbW and the auxiliary factors HCF136, PsbN, TerC and ALB3, assisting in PSII complex assembly and protein insertion into the thylakoid membrane.

Keywords: PSII photosystem II, cytochrome b559, assembly, low molecular mass proteins, *Arabidopsis*

OPEN ACCESS

Edited by:
Julian Eaton-Rye, University of Otago, New Zealand

Reviewed by:
Kentaro Ifuku, Kyoto University, Japan
Yasuhiro Kashino, University of Hyogo, Japan

***Correspondence:**
Wolfgang P. Schröder
wolfgang.schroder@chem.umu.se

†The first three authors contributed equally to this paper and the work is the result of an equal collaboration between the laboratories of the last two authors.

Specialty section:
This article was submitted to Plant Cell Biology, a section of the journal Frontiers in Plant Science

Received: *15 December 2015*
Accepted: *18 March 2016*
Published: *07 April 2016*

Citation:
Plöchinger M, Schwenkert S, von Sydow L, Schröder WP and Meurer J (2016) Functional Update of the Auxiliary Proteins PsbW, PsbY, HCF136, PsbN, TerC and ALB3 in Maintenance and Assembly of PSII. Front. Plant Sci. 7:423. doi: 10.3389/fpls.2016.00423

INTRODUCTION

Photosynthesis converts sunlight energy into chemical energy and takes place in chloroplasts and cyanobacteria. This process is fundamental for life on our planet and starts with the excitation of electrons in the multi-subunit and pigment-containing photosystem (PS) II complex. PSII has a molecular mass of more than 600 kDa and comprises more than 30 protein subunits, pigments and cofactors, such as Ca^{2+}, Cl^{-} and different oxidation states of Fe and Mn. Our current knowledge about the function, structure and components of PSII is quite comprehensive, yet still little is known about how the complex assembles or disassembles for repair and even less regarding how its function is fine-tuned for optimal performance under fast and ever changing light and temperature conditions as well as varying water availability. For optimal flexibility the PSII complex requires a set of auxiliary proteins which assist in quenching of excited states, electron flow, assembly, repair and stability. Previous genetic and biochemical work provided insights into these processes.

Abbreviations: Cyt, cytochrome; PSII, photosystem II.

So far, more than 30 auxiliary (see recent reviews; Shi et al., 2012; Nickelsen and Rengstl, 2013) components have been identified that bind at least transiently to the complex by interacting with individual proteins and/or protein sub complexes to optimize PSII function and assembly.

In this review we present an update on the latest findings of two possible structural and four auxiliary proteins which we have been studying. Information about the proteins is summarized in **Table 1**. PsbW is required for the PSII homodimerization and the function of the PsbY proteins still remains to be solved. PsbN and HCF136 are required for heterodimerization of PSII reaction center in the stroma lamellae, whereas TerC and ALB3 act on translation and/or incorporation of proteins into PSII and other thylakoid membrane complexes.

PsbW

Discovery, Localization and Topology of PsbW

The nuclear encoded PsbW protein was first discovered in spinach chloroplasts and found to contain a long bipartite transit peptide directing it to the thylakoid lumen (Lorković et al., 1995). The mature PsbW protein (formerly 6.1 kDa protein) is composed of 54 amino acids and predicted to have one transmembrane α-helix (Lorković et al., 1995; Hagman et al., 1997). The PsbW protein has been found to be highly conserved in algae such as *Chlamydomonas reinhardtii* (Bishop et al., 1999) and higher plants, but is absent in cyanobacteria (see Shi and Schröder, 2004 for a discussion on this). The localization of the PsbW protein within the PSII complex has not been unambiguously determined. The original analysis (Lorković et al., 1995; Hagman et al., 1997) placed the protein in or close to the PSII reaction center. Meanwhile, two other studies (Rokka et al., 2005; Granvogl et al., 2008) propose a connection to the Lhcb proteins. As the protein is absent in cyanobacteria the present crystal structures of PSII cannot give any suggestions to where the protein is located and the solution to this question has to await high resolution crystal structures from higher plants or algae.

Functional Aspects of the PsbW Protein

The PsbW protein has several unique features which point to an important function in PSII. Firstly, it was shown that the PsbW protein is degraded under photoinhibitory conditions, i.e., high light treatments, to the same extent as the D1 protein of the PSII reaction center (Hagman et al., 1997). *Arabidopsis thaliana* (hereafter *Arabidopsis*) plants with reduced amounts of PsbW showed decreased levels of PSII core proteins and functional PSII complexes (Shi et al., 2000). Using *in vitro* translated PsbW protein in combination with BN-PAGE it was shown that the newly imported PsbW protein was assembled rapidly into dimeric PSII supercomplexes and that the negatively charged N-terminus of PsbW was crucial for this, as a recombinant form with an uncharged N-terminus did not incorporate into PSII (Thidholm et al., 2002). These findings were further corroborated using T-DNA insertion knock-out PsbW *Arabidopsis* plants (García-Cerdán et al., 2011). It was shown that the loss of PsbW destabilizes the supramolecular organization of PSII and no PSII-LHCII supercomplexes could be detected. The absence of "normal" PSII macroorganization leads to a decrease of the maximum PSII quantum yield, changed core protein phosphorylation and faster redox changes of the PQ pool (García-Cerdán et al., 2011). Thus, formation of the supramolecular organization of PSII seems to optimize the functions of the complex. Based on these analyses, it was suggested that PsbW is located close to the minor antennae of the PSII complex, which would explain that the PsbW protein is associated with the PSII reaction center and the LHC complex. Presumably, the PsbW protein is important for the assembly and/or stability of the PSII-LHCII supercomplexes in the grana regions of the thylakoid membrane.

PsbY

Discovery, Localization and Topology of PsbY

The PsbY protein was originally isolated and reported to be associated with PSII in tobacco and spinach (Gau et al., 1995). It is thought to exhibit a manganese requiring L-arginine metabolizing activity. Genomic inspections and alignments of the PsbY amino acid sequence revealed that the protein is present in all photosynthetic plants, in some algal chloroplasts (formerly *ycf32*) and also in various cyanobacteria (Sml0007) (Gau et al., 1998). In higher plants, PsbY is nuclear encoded and targeted to the thylakoids. The unique locus encodes two homologous products (PsbY-1 and PsbY-2) with molecular masses of 4.7 and 4.9 kDa, respectively. *In vitro* protein import analysis supports these predictions (Mant and Robinson, 1998; Thompson et al., 1999). The gene fusion is most probably a result of an intragenic duplication which occurred during

TABLE 1 | Summary of auxiliary proteins associated with PS II discussed in this update.

Protein	Other designations	Gene *Arabidopsis*	Size (kDa) *Arabidopsis*	Location	Function
PsbW	T6B20.8	At2g30570	6.1	Grana, thylakoid membrane	PSII supracomplex formation
PsbY1/PsbY2	*YCF32*	At1g67740	4.7/4.9	PSII complex	Unclear at present
PsbN	*ORF43*	AtC00700	4.7	Stroma lamellae	heterodimeric PSII RC assembly
HCF136	*YCF48*	At5g23120	37	Thylakoid lumen	heterodimeric PSII RC assembly
TerC	PDE149 ATTERC	At5g12130	42	Integral thylakoid protein	Insertion of thylakoid membrane proteins
ALB3	ALBINO3	At2g28800	44,5	Integral thylakoid protein	Insertion of thylakoid membrane proteins

endosymbiosis as in cyanobacterial species only one *psbY* gene exists. Immunological studies using a peptide specific antibody directed against the C-terminal part of PsbY-2 (NILQPALNQINKMRSGD) failed to identify a protein with a molecular mass of around 10 kDa corresponding to a protein fusion including both PsbY-1 and PsbY-2. Instead a single band of approximately 5 kDa was detected, corresponding to a cleaved PsbY product. Mass spectrometry in barley (*Hordeum vulgare*) revealed that PsbY-1 was absent in etioplasts and chloroplasts, while PsbY-2 appeared with high signal intensity (Plöscher et al., 2009). Taking all this together, PsbY-2 also seems to be the major product in barley and probably also in *Arabidopsis*.

Functional Aspects of the PsbY Protein in Photosystem II

Co-expression analysis of the *psbY* gene showed that its expression is similar to other nuclear genes encoding PSII components and that it grouped close to genes encoding PsbO, PsbQ, PsbS and PsbTn, pointing toward a function in PSII (Shi et al., 2012). Interestingly, PsbY was missing in some of the early PSII structures (Ferreira et al., 2004; Kawakami et al., 2007). Furthermore, in the crystal structures of PSII from *Thermosynechococcus elongatus* the PsbY protein was located on the outside of the PSII complex in close connection with Cyt b_{559} (Zouni et al., 2001; Ferreira et al., 2004; Loll et al., 2005; Kawakami et al., 2007) and in close proximity to PsbE and PsbF, two low molecular mass proteins sharing a heme group and forming Cyt b_{559} (Guskov et al., 2009; Umena et al., 2011) (**Figure 1**). Thus, a direct interaction of PsbY with Cyt b_{559} seems possible. Cyt b_{559} is suggested to take part in the cyclic electron flow around PSII together with pheophytin, Q_A and Q_B, in order to protect PSII against photoinhibition (Barber and De Las Rivas, 1993; Kropacheva et al., 2003). Cyt b_{559} is found in three redox potential forms: low potential (LP), intermediate potential (IP), and high potential (HP). Interconversion between them is believed to be important for the photoprotection of the complex. However, the exact mechanism by which Cyt b_{559} is switching between the three potential forms is unclear at present. A number of possibilities for the interconversions were discussed, among them a change in the orientation of the axial histidine ligands (histidine residues from PsbE and PsbF) and a change in the polarity of the heme environment or in the coordination of the heme (Kaminskaya et al., 2007). An oxygen reductase activity (LP), superoxide oxidase activity (IP to HP), superoxide reductase activity (HP to IP) and plastoquinol oxidase activity (HP) were discussed to be involved in the different forms or conversions (Pospíšil, 2012). Indications of an additional quinone site apart from Q_A and Q_B was suggested (Kruk and Strzalka, 2001; Kaminskaya et al., 2007), which initially was believed to function as a switch for the different redox potential states of Cyt b_{559} (Kruk and Strzalka, 2001). Recently, this site was included in the crystal structure of PSII (Guskov et al., 2009; Lambreva et al., 2014), as the Q_C pocket between Cyt b_{559} and PsbJ. A detailed study of this quinone concluded that it does not have the characteristics needed to influence the redox potential of Cyt b_{559} (Guskov et al., 2009). The presence of an additional quinone, Q_D, was also suggested (Kaminskaya and Shuvalov, 2013). However, Q_D has not been found in any of the numerous crystal structures presenting PSII, possibly due to a location outside of Cyt b_{559}. The probability of Q_D residing in very close vicinity to PsbY is rather high and perhaps the evolutionary conserved tryptophan (Q109 and Q181 for *PsbY-1* and *PsbY-2*, respectively) could serve as a ligand for this quinone. Another possible function of PsbY is to stabilize the binding of PsbE and PsbF to the heme group by providing a shelter for Cyt b_{559} from oxidizing compounds.

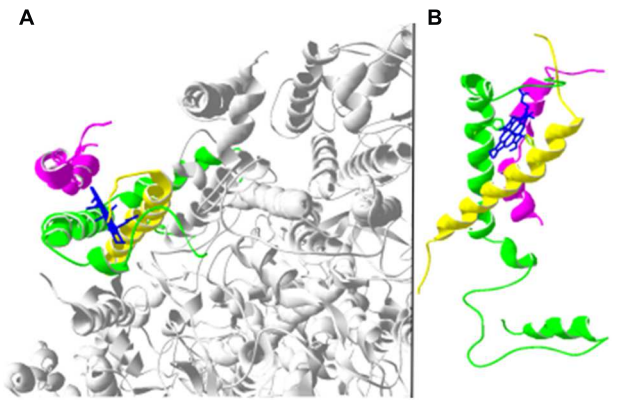

FIGURE 1 | Structure of the PSII complex from *T. vulcanus* (Pdb id: 4il6 [3]) generated by Swiss-pdb viewer program. (A) Overview of PSII in the Cytb_{559} area. Low molecular mass proteins: PsbE (green), PsbF (yellow) and PsbY (magenta). The heme group is shown in blue and PSII core in gray. **(B)** Close-up of PsbE, PsbF, and PsbY proteins showing ligands and the heme.

HCF136

Expression, Localization and Structure of the HCF136 Protein

Unlike structural components of the photosynthetic apparatus, the HCF136 protein accumulates already in etiolated *Arabidopsis* seedlings, indicating an important role for HCF136 during the early stages of chloroplast development. Its expression level increases upon illumination in parallel with the appearance of constituent PSII subunits and the biogenesis of the first PSII complexes (Meurer et al., 1998). After its synthesis in the cytosol, plant HCF136 containing a bipartite transit sequence is imported into the chloroplast lumen by the Tat pathway (Meurer et al., 1998; Hynds et al., 2000). The mature HCF136 protein attaches to the stroma lamellae, the place where early PSII biogenesis and repair takes place. Therefore, a function of HCF136 as a constituent subunit of PSII could be excluded (Meurer et al., 1998). Association with the thylakoid membrane may occur via a conserved hydrophobic patch formed by 18 N-terminal amino acids and/or via interaction with other proteins. However, the rest of the lumenal protein is hydrophilic, harboring no predicted transmembrane domains (Meurer et al., 1998). The

cyanobacterial HCF136 homolog named YCF (hypothetical chloroplast open reading frame) 48 is targeted to the thylakoid lumen in a Sec-dependent manner in *Synechocystis* sp. PCC 6803 (hereafter *Synechocystis)* (Hynds et al., 2000). Interestingly, a smaller amount of the protein resides in the PratA-defined membrane (PDM), a specialized membrane region of the thylakoids, where early steps of PSII biogenesis are thought to take place in cyanobacteria (Schottkowski et al., 2009; Rengstl et al., 2011).

The elucidation of the X-ray crystal structure of YCF48 from *Thermosynechococcus elongatus* revealed that the protein displays the shape of a β-propeller (Mabbitt et al., 2014) (deposited at http://pdbj.org/, PDB: 2XBG, Michoux et al., unpublished). It is built up by seven blade-shaped beta-sheets which are radially arranged, building up a central pore (Mabbitt et al., 2014) (**Figure 2**). Moreover, HCF136 of many eukaryotes is predicted to harbor an additional highly conserved internal stretch of 19 amino acids (Meurer et al., 1998) protruding between the 3rd and 4th blade of the propeller (**Figure 2**). Such propeller architecture has been reported to enable specific protein–protein interactions all around the formed funnel (Chen et al., 2011).

Evolution and Gene Context of the Cyanobacterial HCF136 Homolog

In cyanobacteria, *YCF48* is often embedded into a gene cluster associated with PSII. It is located downstream of the rubredoxin *rubA* gene and upstream of the *psbE-F-L-J* gene cluster. RubA is associated with PSII core complexes and required for the accumulation of this complex (Wastl et al., 2000; Calderon et al., 2013). PsbE and PsbF encode for the two Cyt b_{559} subunits of PSII. PsbL and PsbJ also encode low-molecular-weight proteins of PSII which are required for stability and functional forward electron transport within PSII by affecting Q_B binding site properties (Ohad et al., 2004). The arrangement and composition of these genes is highly conserved in cyanobacteria, implying a possible functional correlation. Nevertheless, there are a few exceptions concerning the conserved arrangement of these genes: *YCF48* still resides next to *rubA* but is physically separated from the *psbE-F-L-J* gene cluster in *Synechococcus* sp. Ja-2-3B'a, *Synechococcus* sp. Ja-3-3Ab and *Thermosynechococcus elongatus BP-1* whereas the arrangement has been subject to duplication and gene loss in *Acayochloris marina* (Calderon et al., 2013). Interestingly, no functional homologs of *YCF48* and *rubA* could be found in the recently discovered cyanobacteria UCYN-A which lacks PSII (Zehr et al., 2008). HCF136 is still encoded in the plastomes or cyanelles of the glaucocystophycean alga *Cyanophora paradoxa* upstream of the *psbE-F-L-J* gene cluster but was transferred into the nuclear genome most likely before divergence of the green and red lineages during endosymbiosis (Meurer et al., 1998). The HCF136 protein is present in all organisms performing oxygenic photosynthesis.

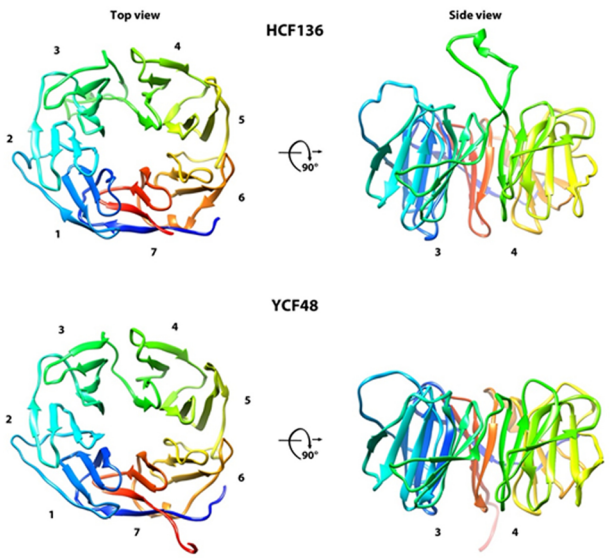

FIGURE 2 | Predicted structure of the mature HCF136 in chloroplasts and YCF48 in cyanobacteria. The structure of HCF136 in *Arabidopsis* (C-score 0.81 ± 0.09) and *Thermosynechococcus elongatus* strain BP-1 (C-score 0.92 ± 0.06) was calculated by I-Tasser (Yang et al., 2015) and is shown from the top and the side view demonstrating the position of the additional loop in the chloroplast form.

HCF136/YCF48 Functions in Stabilization of pD1, Formation of the PSII Reaction Center and Presumably PSII Repair

A mutant screen based on the identification of *high chlorophyll fluorescence* (*hcf*) phenotypes led to the discovery of HCF136, the first identified assembly factor for PSII in plants (Meurer et al., 1998). Different from most knock outs of PSII assembly factors, homozygous *Arabidopsis hcf136* mutants were seedling lethal and could only survive on sucrose-containing medium, caused by their inability to accumulate PSII complexes. Consequently, they suffered from photooxidative stress even under very low light conditions and displayed a pale phenotype (Meurer et al., 1998). Transcription and translation of PSII genes and proteins in the mutant were comparable to the wild type, suggesting that PSII proteins are synthesized normally but are rapidly degraded (Meurer et al., 1998). As a secondary effect and depending on the light intensity, the mutants lacking HCF136 also accumulated lower amounts of PSI proteins; however, the PSI complexes present were functional (Plücken et al., 2002). *In vivo* labeling experiments revealed that newly translated D1 proteins are inserted into the thylakoid membrane and that the formation of the heterodimeric PSII reaction center, built up by the connection of the pre-D2-Cytb_{559}-precomplex (pre-D2) and the pD1-PsbI precomplex (pre-D1) is the first blocked step in PSII biogenesis in *hcf136* mutants. Consequently, this leads to the accumulation of radiolabelled PSII core proteins in the free protein fraction and precomplexes, proving that HCF136 is essentially required for the assembly, stability and/or repair of the heterodimeric PSII RC complex in *Arabidopsis* (Meurer et al., 1998; Plücken et al., 2002).

Interestingly, the removal of YCF48 in *Synechococcus* sp. PCC 7002 did not result in any obvious phenotypical changes

and PSII accumulated normally (Shen et al., 2002). In contrast, inactivation of the *YCF48* gene in *Synechocystis* affected PSII and pigmentation but led to milder phenotypical defects as compared to the *Arabidopsis hcf136* mutant (Meurer et al., 1998; Komenda et al., 2008). In contrast to *hcf136* in *Arabidopsis*, the *ycf48* strain was able to grow photoautotrophically albeit its growth was severely slowed as compared to the "wild type strain" (Komenda et al., 2008). At present, it remains unclear if there are discrepancies between different strains and species concerning the function of HCF136/YCF48. However, the function of YCF48 in *Synechococcus* sp. PCC 7002 and presumably other cyanobacteria becomes probably more important under conditions which require fast repair of PSII, such as heat or high light which induce damage of PSII.

In vivo labeling analysis revealed that the assembly of the PSII reaction center is also the first step of PSII biogenesis, which is impaired in the *ycf48 Synechocystis* mutant, in line with the observed effects in the corresponding plant mutant. However, the cyanobacterial *ycf48* deletion mutant was still able to assemble higher order PSII complexes, though more slowly, contrasting with their complete absence in the chloroplast (Plücken et al., 2002; Komenda et al., 2008). As a consequence, free PSII core proteins and corresponding precomplexes accumulated in both phylogenetic lineages (Meurer et al., 1998; Plücken et al., 2002; Komenda et al., 2008). Additionally, the absence of YCF48 led to a severe reduction in the levels of the cyanobacterial precursor forms of D1 (pD1 and iD1) and their availability for fast-turnover of D1 after photodamage (Komenda et al., 2008). Native gel analysis showed that the plant HCF136 co-migrated predominantly with PSII precomplexes up to the PSII reaction center, but very little amounts could still be observed in the regions of the RC47 precomplex, the PSII monomer and dimer, whereas YCF48 could only be detected up to the PSII reaction center in cyanobacteria (Plücken et al., 2002; Komenda et al., 2008). In line with these results, an interaction of YCF48 with unassembled pD1 and iD1 could be observed in split ubiquitin assays in cyanobacteria (Komenda et al., 2008). Altogether, these observations strongly suggest that plant HCF136 and its cyanobacterial homolog play a specific role in the stabilization of newly synthesized pD1 and/or subsequent dimerization of pre-D1 and pre-D2 to form the PSII reaction center and are also involved in PSII repair after photoinhibition (Meurer et al., 1998; Plücken et al., 2002; Komenda et al., 2008).

Interaction Partners of HCF136/YCF48 and Assembly of PSII

HCF136/YCF48 interacts with another PSII assembly factor, namely PAM68/Sll0933 in *Arabidopsis* and *Synechocystis*, respectively (Armbruster et al., 2010; Rengstl et al., 2013). In contrast to the dual localization of YCF48 in cyanobacterial thylakoid membranes and PDMs, Sll0933 resides only in the thylakoid membrane and has been proposed to be relevant for the conversion of the PSII reaction center complex into the RC47 complex and into larger PSII complexes (Rengstl et al., 2011, 2013). Nevertheless, several lines of evidence exist that both proteins interact with each other in an at least transiently formed intermediate PSII complex. In the absence of Sll0933, YCF48 was found to co-migrate with smaller complexes and its distribution shifted toward the PDMs (Rengstl et al., 2011). Moreover, a strong reciprocal dependency between the protein levels of YCF48 and Sll0933 and their reduction in the absence of D1 further reinforce a direct link between the two proteins (Rengstl et al., 2011). YCF48 has also been reported to interact with a Hyper Conserved Protein (PSHCP) of unknown function which was found recently in marine picocyanobacteria. This protein is specific for this clade and conserved to 100% (Whidden et al., 2014). Apart from its interaction with YCF48, PSHCP is also associated to the 50S ribosomal protein L2 and PsaD, pointing to a direct connection of protein synthesis and PS biogenesis via PSHCP (Whidden et al., 2014) and suggesting insertion of thylakoid proteins *in statu nascendi* in *Prochlorococcus* and marine *Synechococcus* species. However, the precise molecular mechanisms underlying PSII assembly, the exact role of HCF136/YCF48 and other PSII assembly factors and the complicated network between them remain elusive to a large part. Current knowledge suggests the following scenario for the early steps of PSII biogenesis: Simultaneously with the co-translational insertion of pD1 into the membrane, it is provided with recycled chlorophyll via the YCF39-Hlip complex in cyanobacteria (Nickelsen and Rengstl, 2013; Chidgey et al., 2014; Knoppová et al., 2014). Afterwards pD1 is loaded with Mn^{2+} by PratA (probably by LPA1 in plants) and builds up the pre-D1 complex together with PsbI (Nickelsen and Rengstl, 2013). HCF136/YCF48 subsequently binds to pD1 in the lumen and assists in the formation of the PSII reaction center by connecting the pre-D1 and pre-D2 complexes (Komenda et al., 2008; Nickelsen and Rengstl, 2013). This step also requires PsbN located on the stromal side in chloroplasts (Torabi et al., 2014). All these early steps of PSII assembly are thought to take place in PDMs in cyanobacteria and in the stroma lamellae in chloroplasts (Danielsson et al., 2006; Rengstl et al., 2011; Nickelsen and Rengstl, 2013). The RC complex connected at least to YCF48 moves subsequently toward the thylakoid membrane where the pre-CP47 complex containing PAM68/Sll0933 waits to be associated (Rengstl et al., 2011). YCF48 and the YCF39-Hlip complex are thought to be released upon the formation of the so-called RC47 complex (Komenda et al., 2008; Knoppová et al., 2014). It is conceivable, that YCF48, Sll0933 and the YCF39-Hlip complex work in a concerted manner together with factors responsible for chlorophyll synthesis to ensure that production of harmful reactive oxygen species is avoided and that pigments are inserted properly into the PSII complex to achieve functional PSII complexes (Rengstl et al., 2011; Chidgey et al., 2014; Knoppová et al., 2014).

PsbN

Discovery, Localization and Topology of PsbN

The *psbN* gene was originally identified in liverwort and named ORF43 (Kohchi et al., 1988) before the protein was

renamed erroneously as PSII subunit PsbN based on N-terminal sequencing of PSII complex proteins of *Synechococcus vulcanus* (Ikeuchi et al., 1989). It then turned out that the identified N-terminus protein did not belong to PsbN but to PsbTc (Kashino et al., 2002a). Moreover, the PsbN protein could not be found associated to PSII complexes in any proteomic or crystal structure analysis (Gomez et al., 2002; Kashino et al., 2002a,b; Guskov et al., 2009; Plöscher et al., 2009; Umena et al., 2011). This all disputed the assumptions that PsbN is a constituent subunit of PSII.

Only recently, it could be shown, that PsbN does not co-localize with PSII complexes in the grana core but accumulates in the stroma lamella and is – if at all – only transiently associated to other complexes or proteins (Torabi et al., 2014). Taken together, this provides evidence that PsbN is not a constituent subunit of PSII. Instead, a detailed functional characterization of transplastomic Δ*psbN* tobacco mutants revealed its function as the only plastid-encoded PSII assembly factor known so far (Torabi et al., 2014).

PsbN is a conserved plastid encoded low-molecular-weight protein of approximately 5 kDa corresponding to 43 amino acids in most photosynthetic organisms. The N-terminus of PsbN forms an α-helical anchor located in the stroma lamellae. Only a few N-terminal amino acids are expected to extend into the lumen. The stromal exposed C-terminus is predicted to be linked by a flexible spacer who might confer dynamic movability to the C-terminus. Due to its high conservation, the hydrophilic C-terminus is thought to represent the main functional part of PsbN (Torabi et al., 2014).

Gene Context and Expression of *PsbN*

In most cyanobacteria, the *psbN* gene resides next to *psbH* on the opposite strand and represents one of the few genes that were never integrated successfully into the nuclear genome of any photosynthetic organism during evolution (Mayes and Barber, 1991; Race et al., 1999). Instead, the plastid *psbN* gene is expressed from the strand opposite of the highly conserved *psbB* gene cluster, residing in the intergenic region between *psbTc* and *psbH* of all vascular plants (Stoppel and Meurer, 2013). The transcription of *psbN* depends on the plastid-encoded RNA polymerase (PEP) and is regulated by the sigma factor SIG3 in *Arabidopsis* (Zghidi et al., 2007). Hence, the expression of *psbN* might influence the processing of the *psbT-psbH* intercistronic RNA by enabling double-strand specific cleavage (Chevalier et al., 2015). Additionally, it was hypothesized that read-through transcription of *psbN* potentially could lead to the production of antisense RNA resulting in translational inactivation and protection of the *psbTc* mRNA (Zghidi et al., 2007; Zghidi-Abouzid et al., 2011). The accumulation of *psbN* mRNA was shown to be photoresponsive. However, the effect of light differs between pea and wheat seedlings concerning the abundance of the *psbN* transcript. In pea, *psbN* mRNA was absent in etiolated seedlings but enhanced transcript accumulation occurred upon illumination (Kohchi et al., 1988). In contrast, *psbN* mRNA decreased slightly during greening in wheat seedlings (Kawaguchi et al., 1992). In *Arabidopsis*, PsbN seems to play an important role already during early development, since significant amounts of PsbN protein were detected in etiolated seedlings, which strongly increased after the onset of light much before the appearance of the constituent subunits of the photosynthetic complexes. PsbN levels decreased again after 24 h to reach a constant plateau in the light (Torabi et al., 2014). The tobacco 5′ UTR of *psbN* harbors two processing sites which were reported to be crucial for the translation rate of *psbN* mRNA *in vitro* and therefore could offer an explanation for the *in vivo* fluctuations of *psbN* transcript and protein levels observed in different species (Kuroda and Sugiura, 2014).

PsbN is Required for Early PSII Assembly and Repair

Three different *psbN* knock-out plants have been generated in *Nicotiana tabacum* via plastid transformation to reveal the function of its gene product. Two *psbN* knock-out plants were generated by inserting a resistance cassette in forward (Δ*psbN*-F) and reverse (Δ*psbN*-R) orientation into the *psbN* gene to estimate potential side effects of the transcriptional direction of the transgene on the transcription of the adjacent genes within the *psbB* operon (Torabi et al., 2014). To overcome possible secondary effects induced by the insertion, a Δ*psbN* mutant was created by a new co-transformation approach replacing the natural *psbN* gene by a mutated *psbN* allele harboring a frameshift mutation and simultaneously integrating a selection marker into a neutral insertion site further away from the *psbB* operon (Krech et al., 2013). All three homoplastomic tobacco mutants were somehow able to grow photoautotrophically but were extremely light sensitive and retarded in growth even when grown on sucrose supplemented medium. The mutants reached maturity solely under very low light intensities (Krech et al., 2013; Torabi et al., 2014) and they were not able to recover from photoinhibition efficiently (Torabi et al., 2014). Spectroscopic measurements revealed that the mutant plants displayed essentially similar deficiencies in terms of severely impaired PSII activity and intactness leading to a diminished electron transport toward PSI (Torabi et al., 2014). The lack of PsbN led to drastic deficiencies of PSII proteins and, presumably as a secondary effect, a slight reduction of PSI protein levels (Krech et al., 2013; Torabi et al., 2014) even though translation of photosynthetic transcripts was not impaired (Torabi et al., 2014). Detailed biochemical analysis showed that the efficient formation of the dimeric PSII reaction center is obviously the first step during PSII complex assembly in which PsbN plays a crucial role. The lack of PsbN protein had no effect on the formation of intermediate precomplexes (pre-D1, pre-D2, pre-CP43 and pre-CP47), these complexes even transiently accumulated in the mutants. The assembly of the dimeric PSII reaction center was, however, very ineffective, leading to a reduced abundance of all higher order PSII complexes (Torabi et al., 2014).

Interestingly, although translation of PSI reaction center proteins were comparable to the wild type, the *psbN* mutants assembled higher order PSI complexes much faster. This very likely represents a secondary effect due to an altered thylakoid structure in Δ*psbN*. In conclusion, PsbN specifically functions as an authentic assembly factor already during early PSII biogenesis

and is also involved in the PSII repair cycle (Torabi et al., 2014). Whether PsbN acts on its own or in transient association with other proteins assisting the assembly process remains to be shown.

A *psbH psbN* double mutant in *Synechocystis* did not exhibit a visibly deteriorated phenotype compared to mutant strains lacking solely PsbH (Mayes et al., 1993) suggesting that PsbN is not essential for PSII assembly in this cyanobacterial species. Nevertheless, it is reasonable to assume that the cyanobacterial PsbN fulfills the same or a similar function in PSII assembly as its counterpart in higher plants, in accordance with its highly conserved C-terminus (Torabi et al., 2014). However, a more detailed investigation of a cyanobacterial *psbN* single mutant would be required to definitively determine the function of PsbN in this clade. Especially the lack of low-molecular-weight proteins in cyanobacterial mutants often leads to more relieved phenotypes in comparison with their eukaryotic counterparts, arguing for the presence of compensatory mechanisms and a greater flexibility of cyanobacteria in terms of environmental and genetic modifications in cyanobacteria (Shi and Schröder, 2004). On the other hand, the chloroplast could have evolved a sensitive protein complex quality control system, which includes heat shock proteins, chaperones and the proteolytic action of proteases to remove not properly assembled or destroyed structures (Malnoë et al., 2014). This may explain the dispensability of other PSII assembly factors, such as HCF136 and PsbN, in cyanobacterial species in contrast to the chloroplast system (Meurer et al., 1998; Shen et al., 2002; Komenda et al., 2008).

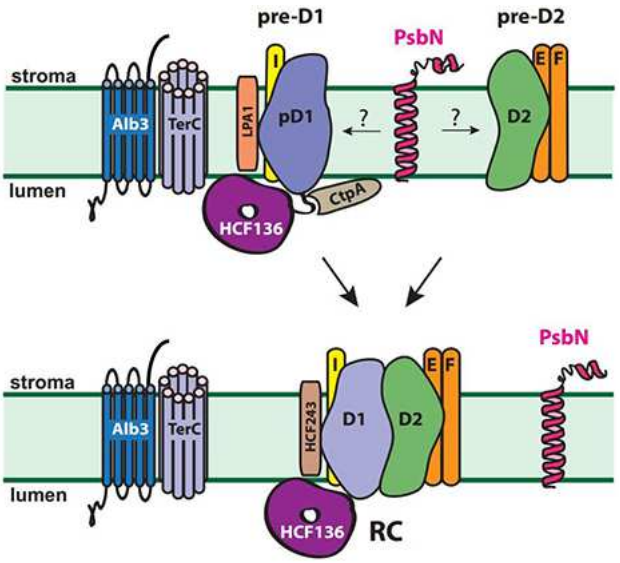

FIGURE 3 | Role of factors required for early assembly of the heterodimeric PSII reaction center complex in chloroplasts. Proposed interactions of CtpA, LPA1, HCF243 and HCF136 are shown. The interaction of PsbN with PSII precomplexes and/or other assembly factors remains to be elucidated. HCF136 assists on the lumenal side of the stroma lamellae and presumably the functional C-terminus of PsbN on the stromal side in the heterodimerisation of pre-D1 and pre-D2 to form the PSII reaction center (RC). ALB3 and TerC are required for efficient post- and co-translational insertion of proteins into the PSII complex (see **Figure 4**).

PsbN and HCF136 Assist the Formation of the PSII RC on Opposite Sides of the Membrane

Strikingly, PsbN and HCF136 have many main features in common. For instance, they share their specific function in PSII reaction center assembly, their conservation during evolution and their localization in the loosely packed stroma lamellae (Meurer et al., 1998; Plücken et al., 2002; Torabi et al., 2014). Moreover, different from knock-outs of most other PSII assembly factors, *hcf136* and *psbN* mutant lines both exhibit a severely impaired growth and photosynthetic performance and both proteins exhibit a crucial role already during very early assembly of PSII (Meurer et al., 1998; Torabi et al., 2014). This hypothesis is further supported by their early appearance in etiolated seedlings and similar light–induced expression pattern (Meurer et al., 1998; Torabi et al., 2014). The formation of PSII precomplexes occurs at a normal rate and the PSI complex assembly is even accelerated, whereas the formation of the heterodimeric PSII reaction center is the first step which is impaired in PSII assembly in both mutants (Plücken et al., 2002; Torabi et al., 2014). In contrast to the lumenal localization of HCF136, the conserved and presumably functional C-terminus of PsbN resides on the opposite side of the membrane (**Figure 3**). This renders a direct physical interaction of both proteins rather unlikely (Plücken et al., 2002; Torabi et al., 2014). However, all the shared characteristics indicate that both assembly factors function in a concerted manner to enable the formation of the PSII reaction center. They also demonstrate that factors for the assembly of the PSII complex are required on both sides of the thylakoid membrane.

TerC

Discovery and Localization of the TerC Protein

TerC is an ancient gene and most probably originates from prokaryotic ancestors. The nuclear-encoded *Arabidopsis* tellurite resistance C protein (AtTerC) is an integral thylakoid membrane protein with a molecular mass of 37 kDa, which shares its conserved TerC domain with a bacterial gene product, TerC, which is involved in conferring resistance to the highly toxic element tellurium (Jobling and Ritchie, 1987, 1988). An initial study analyzing AtTerC knock-out mutants revealed that the protein is essential for chloroplast biogenesis, since the mutants are highly pigment-deficient and seedling lethal (Kwon and Cho, 2008). Electron microscopy was used to analyse the transition from proplastids to chloroplasts and revealed that AtTerC is indispensable for formation of the prolamellar body prior to light exposure as well as for thylakoid formation after illumination. Consequently, thylakoid membrane complexes are lacking entirely (Kwon and Cho, 2008). Grown under lower light conditions, a minor amount of LHCPs was accumulating

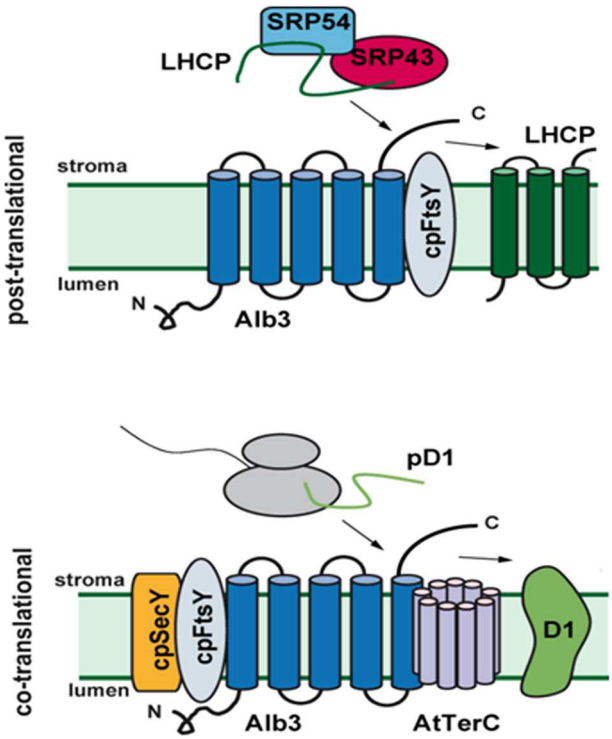

FIGURE 4 | Role of ALB3 and AtTerC in protein insertion into the thylakoid membrane. ALB3 functions in the insertion of the nuclear-encoded LHCPs, which are post-translationally targeted by the soluble SRP transit-complex **(upper)**. Co-translational integration of chloroplast-encoded proteins is also mediated by ALB3, which thereby acts in concert with TerC, cpSecY and cpFtsY **(lower)**.

and PSII assembly factors, such as ALB3, PAM68, LPA1 and LPA2 were detectable (Schneider et al., 2014). It was speculated that AtTerC might either be involved in the translocation or insertion of thylakoid membrane proteins, the attachment of polysomes to the membrane or even during the arrangement of lipids from the non-bilayer to the bilayer lipid phase (Kwon and Cho, 2008). A recent study utilized an mRNAi knock-down mutant in addition to the null-mutant to further investigate the function of AtTerC (Schneider et al., 2014). Although Kwon and Cho demonstrated that neither the transcription nor association of mRNA with ribosomes is responsible for the lack of accumulation of plastome-encoded proteins, Schneider et al. (2014) could show that the synthesis of PSII subunits is severely affected in knock-out as well as knock-down mutants. Moreover, complementation of the *terc* mutant with a C-terminally GFP-tagged AtTerC fusion protein could only partially rescue the phenotype, indicating an interference with AtTerC function caused by altering the C-terminus of the protein. Intriguingly, AtTerC could interact with ALB3 *in vivo*, suggesting that the two proteins may function in concert during the co-translational insertion of plastome-encoded subunits. Split-ubiquitin assays further showed an additional direct interaction with the PSII subunits D1, D2 and CP43 as well as with LPA1 and PAM68, all together indicating that TerC may function in several steps of PSII assembly, but is especially indispensable during the early formation of the PSII reaction center (Schneider et al., 2014).

Origin and Proposed Function of TerC in Bacteria

Tellurite-resistance-genes have been identified in *Escherichia coli* and other bacteria, where they are part of the *ter* operon, containing the *terZABCDEF* genes (Anantharaman et al., 2012). However, the exact mode of function of these gene products in tellurite resistance has remained enigmatic over the past decades. In addition to tellurite resistance, some gene products of the *ter* operon also play a role in resistance to other xenobiotics, colicines and bacteriophages. In this respect *terBCD* and *E* seem to be specifically required for tellurite resistance (Taylor et al., 2002), whereas *terDC* and *Z* have a more general function and disrupt all resistance mechanisms (Whelan et al., 1995). Upon contact with tellurite it was observed that black crystals are formed and studies in *Pseudomonas* cells (*P. putida* BS228 and *P. aeruginosa* ML4262) suggested that these are secreted from the cells via vesicle budding from the outer membrane (Suzina et al., 1995). TerC domains from all organisms commonly share 7 transmembrane domains (8 are predicted for AtTerC) (Kwon and Cho, 2008; Anantharaman et al., 2012). In these hydrophobic domains several conserved charged residues are found and it was speculated that these residues could provide an anionic surface within the membrane, thus functioning as a pore or as a binding site for metals (Anantharaman et al., 2012). In some putative bacterial transport proteins, the TerC domain is linked to the CorC_HlyC motif presumably involved in magnesium and/or cobalt efflux (UniProt: Q3A573). The CorC_HlyC motif is also found at the C terminus of some Na^+/H^+ antiporters indicating a function of TerC in modulating transport of ion substrates. This is a feature that might also play a crucial role for protein insertion into the thylakoid membrane and it will, thus, be exciting to unravel the exact role of AtTerC during these processes in the future. Since counterparts of any of the other *ter* gene products could not be found in the genome of *Arabidopsis* the function of TerC might have diverged and is not related to ion transport in chloroplasts.

ALB3

Characteristics of the YidC/Oxa1/ALB3 Protein Family

ALB3 was initially identified by Sundberg et al. (1997) due to the isolation of an *Arabidopsis* mutant showing an albinotic and seedling lethal phenotype (Sundberg et al., 1997). The ALB3 is a thylakoid-membrane protein with a molecular mass 40–45 kDa and is related to the protein insertases YidC and Oxa1 that are located in the bacterial plasma membrane and the inner membrane of mitochondria, respectively (see Hennon et al., 2015 for a recent review). Together they comprise the YidC/Oxa1/ALB3 protein family, which is more conserved on a structural level than on a primary sequence level and

most representatives possess five membrane-spanning regions (Saller et al., 2012). Specificity their substrate recruitment is most likely conferred by their varying C-termini, which differ in length and structure and thus provide the prerequisite for an either co- or post-translational mode of action. Both YidC and Oxa1 are necessary for the insertion of protein components of the respiratory complexes, whereas ALB3 substrates are thylakoid-membrane proteins. Notably, bacterial, chloroplast and mitochondrial proteins were frequently observed to functionally complement each other, thus suggesting a widely conserved insertion mechanism (Jiang et al., 2002; Preuss et al., 2005; Benz et al., 2009). Recently, the first crystal structure of YidC from *Bacillus halodurans* could be solved in which the five transmembrane regions were found to form a positively charged hydrophilic cavity, which is closed from the extracellular side of the membrane, but opening to the cytoplasm and the lipid bilayer (Kumazaki et al., 2014).

SRP-Mediated Post-translational LHCP Insertion Mechanism

Following the initial identification and characterization of the *alb3* mutant in *Arabidopsis*, a model proposing a function of ALB3 in the membrane insertion of light-harvesting complex proteins (LHCPs) was rapidly established (Moore et al., 2000; Woolhead et al., 2001). LHCPs associated with both, PSI and PSII, are exclusively encoded in the nucleus and need to be post-translationally targeted to the chloroplast and the thylakoid membrane. Hence, the chloroplast has gained a unique signal recognition particle (SRP) system, involving the chloroplast specific cpSRP43 and the GTPase cpSRP54, the latter which, although it is evolutionary conserved, lacks the typical RNA component (Schünemann et al., 1998). After import and processing of the LHCP precursors a conserved DPLG motif in the third transmembrane helix of the LHCPs binds to an ankyrin repeat in cpSRP43. Together with cpSRP54, which in turn interacts with chromodomains of cpSRP43, a transit-complex is formed (Hermkes et al., 2006; Stengel et al., 2008). To target this soluble transit-complex to the thylakoid membrane a receptor protein is required, which is represented by cpFtsY, a protein related to the bacterial homolog of the SRP receptor, FtsY. The LHCPs are thought to be transferred to ALB3 prior to their insertion since cpFtsY was shown to directly interact with ALB3 (Moore et al., 2003; Asakura et al., 2008). Moreover, an association of cpSRP43 and ALB3 has been observed and investigated in further detail (Bals et al., 2010; Falk et al., 2010; Falk and Sinning, 2010; Lewis et al., 2010; Dünschede et al., 2011). ALB3 exposes its extended intrinsically disordered C-terminal domain into the stroma, which adopts an alpha helical fold upon interaction with cpSRP43 (Falk et al., 2010). The C-terminus comprises four positively charged motifs (I–IV), and two models for the interaction with cpSRP43 have been suggested. On the one hand, motifs II and IV were identified as important binding determinates (Falk et al., 2010). On the other hand, Dünschede et al. (2011) suggested a model of ALB3 forming a dimeric pore with motif II and a membrane embedded region being involved in cpSRP binding (Dünschede et al., 2011). Moreover, a mutant expressing a truncated ALB3 protein lacking motifs III and IV did not show a significant effect in LHCP accumulation, although the C-terminus seems to be important for ALB3 stability in a light-dependent manner (Urbischek et al., 2015). Possibly, cpSRP43 is initially captured by an interaction with motif IV, but the insertion into the membrane requires other domains of ALB3 and the exact mechanism remains to be elucidated.

SEC-Mediated Post-translational LHCP Insertion Mechanism

In contrast to this unique SRP-mediated post-translational LHCP insertion mechanism, the related proteins YidC and Oxa1 are also involved in co-translational protein insertion. YidC can act in concert with the SecY translocon in bacteria, and Oxa1 interacts with ribosomes, thus integrating mitochondrial encoded proteins in a co-translational manner. Considering the severe albinotic phenotype of *ALB3* mutants and the reduced levels of all thylakoid membrane complexes in the mutant, an essential role in co-translational protein insertion of ALB3 is feasible. Chloroplasts contain an evolutionary conserved, but minimalized Sec system, which is suggested to transport proteins post-translationally into the thylakoid lumen (Albiniak et al., 2012). However, cpSecY also interacts with chloroplast ribosomes, was found in the vicinity of D1 elongation intermediates and cpSecY maize mutants display a severe loss of thylakoid membranes (Roy and Barkan, 1998; Zhang et al., 2001). Although LHCP insertion was shown to be independent of cpSecY, it could be demonstrated that at least a portion of ALB3 is associated with cpSecY (Klostermann et al., 2002; Benz et al., 2009).

Interaction Partners of ALB3

More recently, D1 insertion intermediates could be co-precipitated with ALB3, FtsY, cpSRP54 and Vipp1 (Walter et al., 2015a). Nevertheless, cpSRP54 mutants display only a mild phenotype, arguing against a prominent role of cpSRP54 in co-translational D1 insertion (Amin et al., 1999; Walter et al., 2015b). FtsY, in contrast, seems to be more important since severe defects especially during the PSII repair cycle were observed in the cpFtsY mutant (Walter et al., 2015b). In addition, split-ubiquitin assays showed an interaction of ALB3 with the chloroplast-encoded PSII subunits D1, D2, CP43 as well as with the PSI subunit PsaA and the ATP synthase subunit CF_O-III, strengthening a role of ALB3 in the co-translational insertion of several chloroplast-encoded proteins, in addition to D1 (Pasch et al., 2005). Moreover, D1 synthesis and PSII complex assembly were found to depend on ALB3 protein levels, albeit being independent of motifs III and IV in the C-terminal domain (Urbischek et al., 2015). The co-translational mechanism is likely to be corroborated by a number of auxiliary factors in addition to ALB3 and interestingly ALB3 has been found to interact with a number of proteins involved in the biogenesis of PSII, such as LPA2 and LPA3 and TerC (see below) (Ma et al., 2007; Cai et al., 2010; Schneider et al., 2014) (**Figure 4**). Future studies will be required to understand their mode of function on a molecular level.

Conserved Function and Homologs of ALB3

In addition to ALB3 in *Arabidopsis*, studies in the green algae *Chlamydomonas reinhardtii* and the cyanobacterium *Synechocystis* have indicated a function of ALB3 in co-translational D1 insertion. In *Chlamydomonas reinhardtii* two ALB3 orthologs are found, ALB3.1 and ALB3.2. Both are found in one complex and depletion of ALB3.1 results in a clear impairment in LHCP accumulation. However, an RNAi strain of ALB3.2 showed impaired biogenesis of PSI and PSII, suggesting complementary functions for the two orthologs in post- and co-translational protein insertion (Bellafiore et al., 2002; Ossenbühl et al., 2004; Göhre et al., 2006). The *Synechocystis* encodes only for a single ALB3 ortholog, designated Srl1471. Equipment of Srl1471 with a C-terminal tag resulted in a reduced D1 insertion into the membrane and a lower assembly into PSII complexes in the Srl1471 mutant (Spence et al., 2004; Ossenbühl et al., 2006).

In *Arabidopsis*, a second homolog of the YidC/ALB3/Oxa1 family has been identified in chloroplasts (Gerdes et al., 2006). In contrast to ALB3, ALB4 mutants only show a mild phenotype with retarded growth. ALB4 was shown to play a role in CF_1-CF_O-ATP synthase assembly and stabilization (Benz et al., 2009). Although ALB4 lacks the C-terminal extension, recent studies analyzing double mutants suggest that ALB4 participates in the ALB3-mediated protein insertion pathway possibly restricted to specific substrates, such as Cyt *f* and the Rieske protein (Trösch et al., 2015).

OUTLOOK AND SUMMARY

The inner core of PSII contains more than 20 structural proteins which bind all cofactors and are able to perform light absorption, electron transfer and oxygen evolution. To date more than 30 auxiliary proteins have been identified (see recent reviews; Shi et al., 2012; Nickelsen and Rengstl, 2013; Järvi et al., 2015) and many more are to be expected by avant-garde biochemical and genetic approaches, allowing to discern between secondary and primary effects in corresponding mutants. This means that the auxiliary proteins of the PSII complex are outnumbering the structural proteins by a factor of two to three. It will be an extremely challenging task to elucidate how these auxiliary proteins keep PSII in an optimal state to efficiently perform photosynthesis under changing environmental conditions. Of special interest will be to understand if these auxiliary proteins function individually in series or in assembled complexes in a concerted way and how they are coordinated in order to promote PSII function. Future studies will elucidate whether they form dynamic complexes which change their compositions according to the requirement of the plant cell. Furthermore, the sequential attachment of most of the intriguingly numerous low-molecular-mass subunits remains to be solved. Moreover, almost nothing is known regarding the incorporation of cofactors and the protein factors involved in those processes. To understand the function and to unravel the complicated network of auxiliary proteins will be a major task for scientists in the field of photosynthesis for the next decade.

AUTHOR CONTRIBUTIONS

All authors listed, have made substantial, direct and intellectual contribution to the work, and approved it for publication.

ACKNOWLEDGMENTS

This work was supported by Umeå University (to LvS and WS), Carl Trygger Foundation (to WS), by the Strong Research Environment Solar Fuels (Umeå University) and the Artificial Leaf Project Umeå (K and A Wallenberg foundation) and the German Research Council (DFG, SFB1035, project A4 to SS and DFG, ME1794/7 to JM).

REFERENCES

Albiniak, A. M., Baglieri, J., and Robinson, C. (2012). Targeting of lumenal proteins across the thylakoid membrane. *J. Exp. Bot.* 63, 1689–1698. doi: 10.1093/jxb/err444

Amin, P., Sy, D. A., Pilgrim, M. L., Parry, D. H., Nussaume, L., and Hoffman, N. E. (1999). *Arabidopsis* mutants lacking the 43- and 54-kilodalton subunits of the chloroplast signal recognition particle have distinct phenotypes. *Plant Physiol.* 121, 61–70. doi: 10.1104/pp.121.1.61

Anantharaman, V., Iyer, L. M., and Aravind, L. (2012). Ter-dependent stress response systems: novel pathways related to metal sensing, production of a nucleoside-like metabolite, and DNA-processing. *Mol. Biosyst.* 8, 3142–3165. doi: 10.1039/c2mb25239b

Armbruster, U., Zühlke, J., Rengstl, B., Kreller, R., Makarenko, E., Rühle, T., et al. (2010). The *Arabidopsis* thylakoid protein PAM68 is required for efficient D1 biogenesis and photosystem II assembly. *Plant Cell* 22, 3439–3460. doi: 10.1105/tpc.110.077453

Asakura, Y., Kikuchi, S., and Nakai, M. (2008). Non-identical contributions of two membrane-bound cpSRP components, cpFtsY and Alb3, to thylakoid biogenesis. *Plant J.* 56, 1007–1017. doi: 10.1111/j.1365-313X.2008.03659.x

Bals, T., Dünschede, B., Funke, S., and Schünemann, D. (2010). Interplay between the cpSRP pathway components, the substrate LHCP and the translocase Alb3: an in vivo and in vitro study. *FEBS Lett.* 584, 4138–4144. doi: 10.1016/j.febslet.2010.08.053

Barber, J., and De Las Rivas, J. (1993). A functional model for the role of cytochrome b559 in the protection against donor and acceptor side photoinhibition. *Proc. Natl. Acad. Sci. U.S.A.* 90, 10942–10946. doi: 10.1073/pnas.90.23.10942

Bellafiore, S., Ferris, P., Naver, H., Göhre, V., and Rochaix, J. D. (2002). Loss of Albino3 leads to the specific depletion of the light-harvesting system. *Plant Cell* 14, 2303–2314. doi: 10.1105/tpc.003442

Benz, M., Bals, T., Gügel, I. L., Piotrowski, M., Kuhn, A., Schünemann, D., et al. (2009). Alb4 of *Arabidopsis* promotes assembly and stabilization of a non chlorophyll-binding photosynthetic complex, the CF1CF0-ATP synthase. *Mol. Plant* 2, 1410–1424. doi: 10.1093/mp/ssp095

Bishop, C. L., Cain, A. J., Purton, S., and Nugent, J. H. A. (1999). Molecular cloning and sequence analysis of the *Chlamydomonas reinhardtii* nuclear gene encoding the photosystem II subunit PsbW (Accession No. AF170026). *Plant Physiol.* 121:313.

Cai, W., Ma, J., Chi, W., Zou, M., Guo, J., Lu, C., et al. (2010). Cooperation of LPA3 and LPA2 is essential for photosystem II assembly in *Arabidopsis*. *Plant Physiol.* 154, 109–120. doi: 10.1104/pp.110.159558

Calderon, R. H., García-Cerdán, J. G., Malnoë, A., Cook, R., Russell, J. J., Gaw, C., et al. (2013). A conserved rubredoxin is necessary for photosystem II accumulation in diverse oxygenic photoautotrophs. *J. Biol. Chem.* 288, 26688–26696. doi: 10.1074/jbc.M113.487629

Chen, C. K., Chan, N. L., and Wang, A. H. (2011). The many blades of the beta-propeller proteins: conserved but versatile. *Trends Biochem. Sci.* 36, 553–561. doi: 10.1016/j.tibs.2011.07.004

Chevalier, F., Ghulam, M. M., Rondet, D., Pfannschmidt, T., Merendino, L., and Lerbs-Mache, S. (2015). Characterization of the psbH precursor RNAs reveals a precise endoribonuclease cleavage site in the psbT/psbH intergenic region that is dependent on psbN gene expression. *Plant Mol. Biol.* 88, 357–367. doi: 10.1007/s11103-015-0325-y

Chidgey, J. W., Linhartová, M., Komenda, J., Jackson, P. J., Dickman, M. J., Canniffe, D. P., et al. (2014). A cyanobacterial chlorophyll synthase-HliD complex associates with the Ycf39 protein and the YidC/Alb3 insertase. *Plant Cell* 26, 1267–1279. doi: 10.1105/tpc.114.124495

Danielsson, R., Suorsa, M., Paakkarinen, V., Albertsson, P. A., Styring, S., Aro, E. M., et al. (2006). Dimeric and monomeric organization of photosystem II. Distribution of five distinct complexes in the different domains of the thylakoid membrane. *J. Biol. Chem.* 281, 14241–14249. doi: 10.1074/jbc.M600634200

Dünschede, B., Bals, T., Funke, S., and Schünemann, D. (2011). Interaction studies between the chloroplast signal recognition particle subunit cpSRP43 and the full-length translocase Alb3 reveal a membrane-embedded binding region in Alb3 protein. *J. Biol. Chem.* 286, 35187–35195. doi: 10.1074/jbc.M111.250746

Falk, S., Ravaud, S., Koch, J., and Sinning, I. (2010). The C terminus of the Alb3 membrane insertase recruits cpSRP43 to the thylakoid membrane. *J. Biol. Chem.* 285, 5954–5962. doi: 10.1074/jbc.M109.084996

Falk, S., and Sinning, I. (2010). The C terminus of Alb3 interacts with the chromodomains 2 and 3 of cpSRP43. *J. Biol. Chem.* 285, le25–le26. doi: 10.1074/jbc.L110.160093

Ferreira, K. N., Iverson, T. M., Maghlaoui, K., Barber, J., and Iwata, S. (2004). Architecture of the photosynthetic oxygen-evolving center. *Science* 303, 1831–1838. doi: 10.1126/science.1093087

García-Cerdán, J. G., Kovács L. L., Tóth, T., Kereïche S., Aseeva, E., Boekema, E. J., et al. (2011). The PsbW protein stabilizes the supramolecular organization of photosystem II in higher plants. *Plant J.* 65, 368–381. doi: 10.1111/j.1365-313X.2010.04429.x

Gau, A. E., Thole, H. H., and Pistorius, E. K. (1995). Isolation and partial characterization of a manganese requiring l-arginine metabolizing enzyme being present in photosystem II complexes of spinach and tobacco. *Z. Naturforsch.* 50:14.

Gau, A. E., Thole, H. H., Sokolenko, A., Altschmied, L., Hermann, R. G., and Pistorius, E. K. (1998). PsbY, a novel manganese-binding, low-molecular-mass protein associated with photosystem II. *Mol. Gen. Genet.* 260, 56–68. doi: 10.1007/s004380050870

Gerdes, L., Bals, T., Klostermann, E., Karl, M., Philippar, K., Hünken, M., et al. (2006). A second thylakoid membrane-localized Alb3/OxaI/YidC homologue is involved in proper chloroplast biogenesis in *Arabidopsis thaliana*. *J. Biol. Chem.* 281, 16632–16642. doi: 10.1074/jbc.M513623200

Göhre, V., Ossenbühl, F., Crèvecoeur, M., Eichacker, L. A., and Rochaix, J. D. (2006). One of two alb3 proteins is essential for the assembly of the photosystems and for cell survival in *Chlamydomonas*. *Plant Cell* 18, 1454–1466. doi: 10.1105/tpc.105.038695

Gomez, S. M., Nishio, J. N., Faull, K. F., and Whitelegge, J. P. (2002). The chloroplast grana proteome defined by intact mass measurements from liquid chromatography mass spectrometry. *Mol. Cell. Proteomics* 1, 46–59. doi: 10.1074/mcp.M100007-MCP200

Granvogl, B., Zoryan, M., Plöscher, M., and Eichacker, L. A. (2008). Localization of 13 one-helix integral membrane proteins in photosystem II subcomplexes. *Anal. Biochem.* 383, 279–288. doi: 10.1016/j.ab.2008.08.038

Guskov, A., Kern, J., Gabdulkhakov, A., Broser, M., Zouni, A., and Saenger, W. (2009). Cyanobacterial photosystem II at 2.9-Å resolution and the role of quinones, lipids, channels and chloride. *Nat. Struct. Mol. Biol.* 16, 334–342. doi: 10.1038/nsmb.1559

Hagman, A., Shi, L. X., Rintamäki, E., Andersson, B., and Schröder, W. P. (1997). The nuclear-encoded PsbW protein subunit of photosystem II undergoes light-induced proteolysis. *Biochemistry* 36, 12666–12671. doi: 10.1021/bi970685o

Hennon, S. W., Soman, R., Zhu, L., and Dalbey, R. E. (2015). YidC/Alb3/Oxa1 family of insertases. *J. Biol. Chem.* 290, 14866–14874. doi: 10.1074/jbc.R115.638171

Hermkes, R., Funke, S., Richter, C., Kuhlmann, J., and Schünemann, D. (2006). The alpha-helix of the second chromodomain of the 43 kDa subunit of the chloroplast signal recognition particle facilitates binding to the 54 kDa subunit. *FEBS Lett.* 580, 3107–3111. doi: 10.1016/j.febslet.2006.04.055

Hynds, P. J., Plücken, H., Westhoff, P., and Robinson, C. (2000). Different lumen-targeting pathways for nuclear-encoded versus cyanobacterial/plastid-encoded Hcf136 proteins. *FEBS Lett.* 467, 97–100. doi: 10.1016/S0014-5793(00)01129-7

Ikeuchi, M., Koike, H., and Inoue, Y. (1989). N-terminal sequencing of low-molecular-mass components in cyanobacterial photosystem II core complex. Two components correspond to unidentified open reading frames of plant chloroplast DNA. *FEBS Lett.* 253, 178–182. doi: 10.1016/0014-5793(89)80954-8

Järvi, S., Suorsa, M., and Aro, E. M. (2015). Photosystem II repair in plant chloroplasts–Regulation, assisting proteins and shared components with photosystem II biogenesis. *Biochim. Biophys. Acta* 1847, 900–909. doi: 10.1016/j.bbabio.2015.01.006

Jiang, F., Yi, L., Moore, M., Chen, M., Rohl, T., Van Wijk, K. J., et al. (2002). Chloroplast YidC homolog Albino3 can functionally complement the bacterial YidC depletion strain and promote membrane insertion of both bacterial and chloroplast thylakoid proteins. *J. Biol. Chem.* 277, 19281–19288. doi: 10.1074/jbc.M110857200

Jobling, M. G., and Ritchie, D. A. (1987). Genetic and physical analysis of plasmid genes expressing inducible resistance of tellurite in *Escherichia coli*. *Mol. Gen. Genet.* 208, 288–293. doi: 10.1007/BF00330455

Jobling, M. G., and Ritchie, D. A. (1988). The nucleotide sequence of a plasmid determinant for resistance to tellurium anions. *Gene* 66, 245–258. doi: 10.1016/0378-1119(88)90361-7

Kaminskaya, O., Shuvalov, V. A., and Renger, G. (2007). Evidence for a novel quinone-binding site in the photosystem II (PS II) complex that regulates the redox potential of cytochrome b559. *Biochemistry* 46, 1091–1105. doi: 10.1021/bi0613022

Kaminskaya, O. P., and Shuvalov, V. A. (2013). Biphasic reduction of cytochrome b559 by plastoquinol in photosystem II membrane fragments: evidence for two types of cytochrome b559/plastoquinone redox equilibria. *Biochim. Biophys. Acta* 1827, 471–483. doi: 10.1016/j.bbabio.2013.01.007

Kashino, Y., Koike, H., Yoshio, M., Egashira, H., Ikeuchi, M., Pakrasi, H. B., et al. (2002a). Low-molecular-mass polypeptide components of a photosystem II preparation from the thermophilic cyanobacterium *Thermosynechococcus vulcanus*. *Plant Cell Physiol.* 43, 1366–1373. doi: 10.1093/pcp/pcf168

Kashino, Y., Lauber, W. M., Carroll, J. A., Wang, Q., Whitmarsh, J., Satoh, K., et al. (2002b). Proteomic analysis of a highly active photosystem II preparation from the cyanobacterium *Synechocystis* sp. *PCC* 6803 reveals the presence of novel polypeptides. *Biochemistry* 41, 8004–8012.

Kawaguchi, H., Fukuda, I., Shiina, T., and Toyoshima, Y. (1992). Dynamical behavior of psb gene transcripts in greening wheat seedlings. I. Time course of accumulation of the pshA through psbN gene transcripts during light-induced greening. *Plant Mol. Biol.* 20, 695–704. doi: 10.1007/BF00046454

Kawakami, K., Iwai, M., Ikeuchi, M., Kamiya, N., and Shen, J. R. (2007). Location of PsbY in oxygen-evolving photosystem II revealed by mutagenesis and X-ray crystallography. *FEBS Lett.* 581, 4983–4987. doi: 10.1016/j.febslet.2007.09.036

Klostermann, E., Droste Gen Helling, I., Carde, J. P., and Schünemann, D. (2002). The thylakoid membrane protein ALB3 associates with the cpSecY-translocase in *Arabidopsis thaliana*. *Biochem. J.* 368, 777–781. doi: 10.1042/BJ20021291

Knoppová, J., Sobotka, R., Tichý, M., Yu, J., Konik, P., Halada, P., et al. (2014). Discovery of a chlorophyll binding protein complex involved in the early steps of photosystem II assembly in *Synechocystis*. *Plant Cell* 26, 1200–1212. doi: 10.1105/tpc.114.123919

Kohchi, T., Yoshida, T., Komano, T., and Ohyama, K. (1988). Divergent mRNA transcription in the chloroplast psbB operon. *EMBO J.* 7, 885–891.

Komenda, J., Nickelsen, J., Tichý, M., Prásil, O., Eichacker, L. A., and Nixon, P. J. (2008). The cyanobacterial homologue of HCF136/YCF48 is a component of an early photosystem II assembly complex and is important for both the efficient

assembly and repair of photosystem II in *Synechocystis* sp. PCC 6803. *J. Biol. Chem.* 283, 22390–22399. doi: 10.1074/jbc.M801917200

Krech, K., Fu, H. Y., Thiele, W., Ruf, S., Schöttler, M. A., and Bock, R. (2013). Reverse genetics in complex multigene operons by co-transformation of the plastid genome and its application to the open reading frame previously designated psbN. *Plant J.* 75, 1062–1074. doi: 10.1111/tpj.12256

Kropacheva, T. N., Feikema, W. O., Mamedov, F., Feyziyev, Y., Styring, S., and Hoff, A. J. (2003). Spin conversion of cytochrome b559 in photosystem II induced by exogenous high potential quinone. *Chem. Phys.* 294, 471–482. doi: 10.1016/s0301-0104(03)00327-6

Kruk, J., and Strzalka, K. (2001). Redox changes of cytochrome b559 in the presence of plastoquinones. *J. Biol. Chem.* 276, 86–91. doi: 10.1074/jbc.M003602200

Kumazaki, K., Chiba, S., Takemoto, M., Furukawa, A., Nishiyama, K., Sugano, Y., et al. (2014). Structural basis of Sec-independent membrane protein insertion by YidC. *Nature* 509, 516–520. doi: 10.1038/nature13167

Kuroda, H., and Sugiura, M. (2014). Processing of the 5′-UTR and existence of protein factors that regulate translation of tobacco chloroplast psbN mRNA. *Plant Mol. Biol.* 86, 585–593. doi: 10.1007/s11103-014-0248-z

Kwon, K. C., and Cho, M. H. (2008). Deletion of the chloroplast-localized AtTerC gene product in *Arabidopsis thaliana* leads to loss of the thylakoid membrane and to seedling lethality. *Plant J.* 55, 428–442. doi: 10.1111/j.1365-313X.2008.03523.x

Lambreva, M. D., Russo, D., Polticelli, F., Scognamiglio, V., Antonacci, A., Zobnina, V., et al. (2014). Structure/function/dynamics of photosystem II plastoquinone binding sites. *Curr. Protein Pept. Sci.* 15, 285–295. doi: 10.2174/1389203715666140327104802

Lewis, N. E., Marty, N. J., Kathir, K. M., Rajalingam, D., Kight, A. D., Daily, A., et al. (2010). A dynamic cpSRP43-Albino3 interaction mediates translocase regulation of chloroplast signal recognition particle (cpSRP)-targeting components. *J. Biol. Chem.* 285, 34220–34230. doi: 10.1074/jbc.M110.160093

Loll, B., Kern, J., Saenger, W., Zouni, A., and Biesiadka, J. (2005). Towards complete cofactor arrangement in the 3.0 Å resolution structure of photosystem II. *Nature* 438, 1040–1044. doi: 10.1038/nature04224

Lorković, Z. J., Schröder, W. P., Pakrasi, H. B., Irrgang, K. D., Herrmann, R. G., and Oelmüller, R. (1995). Molecular characterization of PsbW, a nuclear-encoded component of the photosystem II reaction center complex in spinach. *Proc. Natl. Acad. Sci. U.S.A.* 92, 8930–8934. doi: 10.1073/pnas.92.19.8930

Ma, J., Peng, L., Guo, J., Lu, Q., Lu, C., and Zhang, L. (2007). LPA2 is required for efficient assembly of photosystem II in *Arabidopsis thaliana*. *Plant Cell* 19, 1980–1993. doi: 10.1105/tpc.107.050526

Mabbitt, P. D., Wilbanks, S. M., and Eaton-Rye, J. J. (2014). Structure and function of the hydrophilic Photosystem II assembly proteins: Psb27, Psb28 and Ycf48. *Plant Physiol. Biochem.* 81, 96–107. doi: 10.1016/j.plaphy.2014.02.013

Malnoë, A., Wang, F., Girard-Bascou, J., Wollman, F. A., and de Vitry, C. (2014). Thylakoid FtsH protease contributes to photosystem II and cytochrome b6f remodeling in *Chlamydomonas reinhardtii* under stress conditions. *Plant Cell* 26, 373–390. doi: 10.1105/tpc.113.120113

Mant, A., and Robinson, C. (1998). An *Arabidopsis* cDNA encodes an apparent polyprotein of two non-identical thylakoid membrane proteins that are associated with photosystem II and homologous to algal ycf32 open reading frames. *FEBS Lett.* 423, 183–188. doi: 10.1016/S0014-5793(98)00089-1

Mayes, S. R., and Barber, J. (1991). Primary structure of the psbN-psbH-petC-petA gene cluster of the cyanobacterium *Synechocystis* PCC 6803. *Plant Mol. Biol.* 17, 289–293. doi: 10.1007/BF00039508

Mayes, S. R., Dubbs, J. M., Vass, I., Hideg, E., Nagy, L., and Barber, J. (1993). Further characterization of the psbH locus of *Synechocystis* sp. PCC 6803: inactivation of psbH impairs QA to QB electron transport in photosystem 2. *Biochemistry* 32, 1454–1465. doi: 10.1021/bi00057a008

Meurer, J., Plücken, H., Kowallik, K. V., and Westhoff, P. (1998). A nuclear-encoded protein of prokaryotic origin is essential for the stability of photosystem II in *Arabidopsis thaliana*. *EMBO J.* 17, 5286–5297. doi: 10.1093/emboj/17.18.5286

Moore, M., Goforth, R. L., Mori, H., and Henry, R. (2003). Functional interaction of chloroplast SRP/FtsY with the ALB3 translocase in thylakoids: substrate not required. *J. Cell Biol.* 162, 1245–1254. doi: 10.1083/jcb.200307067

Moore, M., Harrison, M. S., Peterson, E. C., and Henry, R. (2000). Chloroplast Oxa1p homolog albino3 is required for post-translational integration of the light harvesting chlorophyll-binding protein into thylakoid membranes. *J. Biol. Chem.* 275, 1529–1532. doi: 10.1074/jbc.275.3.1529

Nickelsen, J., and Rengstl, B. (2013). Photosystem II assembly: from cyanobacteria to plants. *Annu. Rev. Plant Biol.* 64, 609–635. doi: 10.1146/annurev-arplant-050312-120124

Ohad, I., Dal Bosco, C., Herrmann, R. G., and Meurer, J. (2004). Photosystem II proteins PsbL and PsbJ regulate electron flow to the plastoquinone pool. *Biochemistry* 43, 2297–2308. doi: 10.1021/bi0348260

Ossenbühl, F., Göhre, V., Meurer, J., Krieger-Liszkay, A., Rochaix, J. D., and Eichacker, L. A. (2004). Efficient assembly of photosystem II in *Chlamydomonas reinhardtii* requires Alb3.1p, a homolog of *Arabidopsis* ALBINO3. *Plant Cell* 16, 1790–1800. doi: 10.1105/tpc.023226

Ossenbühl, F., Inaba-Sulpice, M., Meurer, J., Soll, J., and Eichacker, L. A. (2006). The *Synechocystis* sp. PCC 6803 oxa1 homolog is essential for membrane integration of reaction center precursor protein pD1. *Plant Cell* 18, 2236–2246. doi: 10.1105/tpc.106.043646

Pasch, J. C., Nickelsen, J., and Schünemann, D. (2005). The yeast split-ubiquitin system to study chloroplast membrane protein interactions. *Appl. Microbiol. Biotechnol.* 69, 440–447. doi: 10.1007/s00253-005-0029-3

Plöscher, M., Granvogl, B., Zoryan, M., Reisinger, V., and Eichacker, L. A. (2009). Mass spectrometric characterization of membrane integral low molecular weight proteins from photosystem II in barley etioplasts. *Proteomics* 9, 625–635. doi: 10.1002/pmic.200800337

Plücken, H., Müller, B., Grohmann, D., Westhoff, P., and Eichacker, L. A. (2002). The HCF136 protein is essential for assembly of the photosystem II reaction center in *Arabidopsis thaliana*. *FEBS Lett.* 532, 85–90. doi: 10.1016/S0014-5793(02)03634-7

Pospíšil, P. (2012). Molecular mechanisms of production and scavenging of reactive oxygen species by photosystem II. *Biochim. Biophys. Acta* 1817, 218–231. doi: 10.1016/j.bbabio.2011.05.017

Preuss, M., Ott, M., Funes, S., Luirink, J., and Herrmann, J. M. (2005). Evolution of mitochondrial oxa proteins from bacterial YidC. Inherited and acquired functions of a conserved protein insertion machinery. *J. Biol. Chem.* 280, 13004–13011. doi: 10.1074/jbc.M414093200

Race, H. L., Herrmann, R. G., and Martin, W. (1999). Why have organelles retained genomes? *Trends Genet.* 15, 364–370. doi: 10.1016/S0168-9525(99)01766-7

Rengstl, B., Knoppová, J., Komenda, J., and Nickelsen, J. (2013). Characterization of a *Synechocystis* double mutant lacking the photosystem II assembly factors YCF48 and Sll0933. *Planta* 237, 471–480. doi: 10.1007/s00425-012-1720-0

Rengstl, B., Oster, U., Stengel, A., and Nickelsen, J. (2011). An intermediate membrane subfraction in cyanobacteria is involved in an assembly network for Photosystem II biogenesis. *J. Biol. Chem.* 286, 21944–21951. doi: 10.1074/jbc.M111.237867

Rokka, A., Suorsa, M., Saleem, A., Battchikova, N., and Aro, E. M. (2005). Synthesis and assembly of thylakoid protein complexes: multiple assembly steps of photosystem II. *Biochem. J.* 388, 159–168. doi: 10.1042/BJ20042098

Roy, L. M., and Barkan, A. (1998). A SecY homologue is required for the elaboration of the chloroplast thylakoid membrane and for normal chloroplast gene expression. *J. Cell Biol.* 141, 385–395. doi: 10.1083/jcb.141.2.385

Saller, M. J., Wu, Z. C., de Keyzer, J., and Driessen, A. J. (2012). The YidC/Oxa1/Alb3 protein family: common principles and distinct features. *Biol. Chem.* 393, 1279–1290. doi: 10.1515/hsz-2012-0199

Schneider, A., Steinberger, I., Strissel, H., Kunz, H. H., Manavski, N., Meurer, J., et al. (2014). The *Arabidopsis* Tellurite resistance C protein together with ALB3 is involved in photosystem II protein synthesis. *Plant J.* 78, 344–356. doi: 10.1111/tpj.12474

Schottkowski, M., Gkalympoudis, S., Tzekova, N., Stelljes, C., Schünemann, D., Ankele, E., et al. (2009). Interaction of the periplasmic PratA factor and the PsbA (D1) protein during biogenesis of photosystem II in *Synechocystis* sp. PCC 6803. *J. Biol. Chem.* 284, 1813–1819. doi: 10.1074/jbc.M806116200

Schünemann, D., Gupta, S., Persello-Cartieaux, F., Klimyuk, V. I., Jones, J. D., Nussaume, L., et al. (1998). A novel signal recognition particle targets light-harvesting proteins to the thylakoid membranes. *Proc. Natl. Acad. Sci. U.S.A.* 95, 10312–10316. doi: 10.1073/pnas.95.17.10312

Shen, G., Zhao, J., Reimer, S. K., Antonkine, M. L., Cai, Q., Weiland, S. M., et al. (2002). Assembly of photosystem I. I. Inactivation of the rubA gene encoding a membrane-associated rubredoxin in the cyanobacterium *Synechococcus* sp.

PCC 7002 causes a loss of photosystem I activity. *J. Biol. Chem.* 277, 20343–20354. doi: 10.1074/jbc.M201103200

Shi, L. X., Hall, M., Funk, C., and Schröder, W. P. (2012). Photosystem II, a growing complex: updates on newly discovered components and low molecular mass proteins. *Biochim. Biophys. Acta* 1817, 13–25. doi: 10.1016/j.bbabio.2011.08.008

Shi, L. X., Lorković, Z. J., Oelmüller, R., and Schröder, W. P. (2000). The low molecular mass PsbW protein is involved in the stabilization of the dimeric photosystem II complex in *Arabidopsis thaliana*. *J. Biol. Chem.* 275, 37945–37950. doi: 10.1074/jbc.M006300200

Shi, L. X., and Schröder, W. P. (2004). The low molecular mass subunits of the photosynthetic supracomplex, photosystem II. *Biochim. Biophys. Acta* 1608, 75–96. doi: 10.1016/j.bbabio.2003.12.004

Spence, E., Bailey, S., Nenninger, A., Møller, S. G., and Robinson, C. (2004). A homolog of Albino3/OxaI is essential for thylakoid biogenesis in the cyanobacterium *Synechocystis* sp. PCC6803. *J. Biol. Chem.* 279, 55792–55800. doi: 10.1074/jbc.M411041200

Stengel, K. F., Holdermann, I., Cain, P., Robinson, C., Wild, K., and Sinning, I. (2008). Structural basis for specific substrate recognition by the chloroplast signal recognition particle protein cpSRP43. *Science* 321, 253–256. doi: 10.1126/science.1158640

Stoppel, R., and Meurer, J. (2013). Complex RNA metabolism in the chloroplast: an update on the psbB operon. *Planta* 237, 441–449. doi: 10.1007/s00425-012-1782-z

Sundberg, E., Slagter, J. G., Fridborg, I., Cleary, S. P., Robinson, C., and Coupland, G. (1997). ALBINO3, an *Arabidopsis* nuclear gene essential for chloroplast differentiation, encodes a chloroplast protein that shows homology to proteins present in bacterial membranes and yeast mitochondria. *Plant Cell* 9, 717–730. doi: 10.1105/tpc.9.5.717

Suzina, N. E., Duda, V. I., Anisimova, L. A., Dmitriev, V. V., and Boronin, A. M. (1995). Cytological aspects of resistance to potassium tellurite conferred on *Pseudomonas* cells by plasmids. *Arch. Microbiol.* 163, 282–285. doi: 10.1007/BF00393381

Taylor, D. E., Rooker, M., Keelan, M., Ng, L. K., Martin, I., Perna, N. T., et al. (2002). Genomic variability of O islands encoding tellurite resistance in enterohemorrhagic *Escherichia coli* O157:H7 isolates. *J. Bacteriol.* 184, 4690–4698. doi: 10.1128/JB.184.17.4690-4698.2002

Thidholm, E., Lindström, V., Tissier, C., Robinson, C., Schröder, W. P., and Funk, C. (2002). Novel approach reveals localisation and assembly pathway of the PsbS and PsbW proteins into the photosystem II dimer. *FEBS Lett.* 513, 217–222. doi: 10.1016/S0014-5793(02)02314-1

Thompson, S. J., Robinson, C., and Mant, A. (1999). Dual signal peptides mediate the signal recognition particle/Sec-independent insertion of a thylakoid membrane polyprotein, PsbY. *J. Biol. Chem.* 274, 4059–4066. doi: 10.1074/jbc.274.7.4059

Torabi, S., Umate, P., Manavski, N., Plöchinger, M., Kleinknecht, L., Bogireddi, H., et al. (2014). PsbN is required for assembly of the photosystem II reaction center in *Nicotiana tabacum*. *Plant Cell* 26, 1183–1199. doi: 10.1105/tpc.113.120444

Trösch, R., Töpel, M., Flores-Pérez, U., and Jarvis, P. (2015). Genetic and physical interaction studies reveal functional similarities between ALBINO3 and ALBINO4 in *Arabidopsis*. *Plant Physiol.* 169, 1292–1306. doi: 10.1104/pp.15.00376

Umena, Y., Kawakami, K., Shen, J. R., and Kamiya, N. (2011). Crystal structure of oxygen-evolving photosystem II at a resolution of 1.9 *Å*. *Nature* 473, 55–60. doi: 10.1038/nature09913

Urbischek, M., Nick von Braun, S., Brylok, T., Gügel, I. L., Richter, A., Koskela, M., et al. (2015). The extreme Albino3 (Alb3) C terminus is required for Alb3 stability and function in *Arabidopsis thaliana*. *Planta* 242, 733–746. doi: 10.1007/s00425-015-2352-y

Walter, B., Hristou, A., Nowaczyk, M. M., and Schünemann, D. (2015a). In vitro reconstitution of co-translational D1 insertion reveals a role of the cpSec-Alb3 translocase and Vipp1 in photosystem II biogenesis. *Biochem. J.* 468, 315–324. doi: 10.1042/BJ20141425

Walter, B., Pieta, T., and Schünemann, D. (2015b). *Arabidopsis thaliana* mutants lacking cpFtsY or cpSRP54 exhibit different defects in photosystem II repair. *Front. Plant Sci.* 6:250. doi: 10.3389/fpls.2015.00250

Wastl, J., Duin, E. C., Iuzzolino, L., Dörner, W., Link, T., Hoffmann, S., et al. (2000). Eukaryotically encoded and chloroplast-located rubredoxin is associated with photosystem II. *J. Biol. Chem.* 275, 30058–30063. doi: 10.1074/jbc.M004629200

Whelan, K. F., Colleran, E., and Taylor, D. E. (1995). Phage inhibition, colicin resistance, and tellurite resistance are encoded by a single cluster of genes on the IncHI2 plasmid R478. *J. Bacteriol.* 177, 5016–5027.

Whidden, C. E., DeZeeuw, K. G., Zorz, J. K., Joy, A. P., Barnett, D. A., Johnson, M. S., et al. (2014). Quantitative and functional characterization of the hyper-conserved protein of *Prochlorococcus* and marine *Synechococcus*. *PLoS ONE* 9:e109327. doi: 10.1371/journal.pone.0109327

Woolhead, C. A., Thompson, S. J., Moore, M., Tissier, C., Mant, A., Rodger, A., et al. (2001). Distinct Albino3-dependent and -independent pathways for thylakoid membrane protein insertion. *J. Biol. Chem.* 276, 40841–40846. doi: 10.1074/jbc.M106523200

Yang, J., Yan, R., Roy, A., Xu, D., Poisson, J., and Zhang, Y. (2015). The I-TASSER suite: protein structure and function prediction. *Nat. Methods* 12, 7–8.

Zehr, J. P., Bench, S. R., Carter, B. J., Hewson, I., Niazi, F., Shi, T., et al. (2008). Globally distributed uncultivated oceanic N2-fixing cyanobacteria lack oxygenic photosystem II. *Science* 322, 1110–1112. doi: 10.1126/science.1165340

Zghidi, W., Merendino, L., Cottet, A., Mache, R., and Lerbs-Mache, S. (2007). Nucleus-encoded plastid sigma factor SIG3 transcribes specifically the psbN gene in plastids. *Nucleic Acids Res.* 35, 455–464. doi: 10.1093/nar/gkl1067

Zghidi-Abouzid, O., Merendino, L., Buhr, F., Malik Ghulam, M., and Lerbs-Mache, S. (2011). Characterization of plastid psbT sense and antisense RNAs. *Nucleic Acids Res.* 39, 5379–5387. doi: 10.1093/nar/gkr143

Zhang, L., Paakkarinen, V., Suorsa, M., and Aro, E. M. (2001). A SecY homologue is involved in chloroplast-encoded D1 protein biogenesis. *J. Biol. Chem.* 276, 37809–37814. doi: 10.1074/jbc.M105522200

Zouni, A., Witt, H. T., Kern, J., Fromme, P., Krauss, N., Saenger, W., et al. (2001). Crystal structure of photosystem II from *Synechococcus* elongatus at 3.8 Å resolution. *Nature* 409, 739–743. doi: 10.1038/35055589

Conflict of Interest Statement: The authors declare that the research was conducted in the absence of any commercial or financial relationships that could be construed as a potential conflict of interest.

frontiers in Plant Science

ORIGINAL RESEARCH
published: 03 May 2016
doi: 10.3389/fpls.2016.00605

The Role of Slr0151, a Tetratricopeptide Repeat Protein from *Synechocystis* sp. PCC 6803, during Photosystem II Assembly and Repair

*Anna Rast[1], Birgit Rengstl[1], Steffen Heinz[1], Andreas Klingl[2] and Jörg Nickelsen[1]**

[1] Molekularbiologie der Pflanzen, Biozentrum der Ludwig-Maximilians-Universität München, Planegg-Martinsried, Germany,
[2] Pflanzliche Entwicklungsbiologie, Biozentrum der Ludwig-Maximilians-Universität München, Planegg-Martinsried, Germany

The assembly and repair of photosystem II (PSII) is facilitated by a variety of assembly factors. Among those, the tetratricopeptide repeat (TPR) protein Slr0151 from *Synechocystis* sp. PCC 6803 (hereafter *Synechocystis*) has previously been assigned a repair function under high light conditions (Yang et al., 2014). Here, we show that inactivation of *slr0151* affects thylakoid membrane ultrastructure even under normal light conditions. Moreover, the level and localization of Slr0151 are affected in a variety of PSII-related mutants. In particular, the data suggest a close functional relationship between Slr0151 and Sll0933, which interacts with Ycf48 during PSII assembly and is homologous to PAM68 in *Arabidopsis thaliana*. Immunofluorescence analysis revealed a punctate distribution of Slr0151 within several different membrane types in *Synechocystis* cells.

Keywords: *Synechocystis*, biogenesis center, TPR protein, photosystem II, thylakoid membrane

OPEN ACCESS

Edited by:
Julian Eaton-Rye,
University of Otago, New Zealand

Reviewed by:
Yan Lu,
Western Michigan University, USA
Simon Andrew Jackson,
University of Otago, New Zealand

***Correspondence:**
Jörg Nickelsen
joerg.nickelsen@lrz.uni-muenchen.de

Specialty section:
This article was submitted to Plant Cell Biology, a section of the journal Frontiers in Plant Science

Received: *19 February 2016*
Accepted: *19 April 2016*
Published: *03 May 2016*

Citation:
Rast A, Rengstl B, Heinz S, Klingl A and Nickelsen J (2016) The Role of Slr0151, a Tetratricopeptide Repeat Protein from Synechocystis sp. PCC 6803, during Photosystem II Assembly and Repair. Front. Plant Sci. 7:605. doi: 10.3389/fpls.2016.00605

INTRODUCTION

The ability of plastid-bearing organisms to perform oxygenic photosynthesis was inherited from an ancient cyanobacterium about 2.4 billion years ago. In present-day cyanobacteria, the photosynthetic electron transport chain (PET) is embedded in an internal membrane system made up of thylakoids (Hohmann-Marriott and Blankenship, 2011). The PET is fueled by electrons originating from the water-splitting complex within PSII, which is therefore considered to be the heart of photosynthesis. Recently, the structural analysis of PSII has revealed detailed insights into the architecture and working mode of its Mn_4CaO_5 cluster, where water is oxidized and molecular oxygen is released (Umena et al., 2011; Kupitz et al., 2014; Suga et al., 2015).

Overall, PSII comprises at least 20 protein subunits as well as numerous organic and inorganic co-factors. All these components have to be assembled in a strictly coordinated manner in both time and space. The emerging picture indicates that the assembly process is initiated at specialized, biogenic thylakoid membrane (TM) regions and proceeds step-wise until the active PSII super-complex is formed as part of photosynthetically active thylakoids (Komenda et al., 2012; Nickelsen and Rengstl, 2013; Nickelsen and Zerges, 2013; Rast et al., 2015).

In the cyanobacterium *Synechocystis* sp. PCC 6803 (hereafter *Synechocystis*), the initial steps in *de novo* PSII assembly have been proposed to take place at biogenesis centers (BC) where the

thylakoids converge on the plasma membrane (PM; van de Meene et al., 2006; Schottkowski et al., 2009a; Stengel et al., 2012; Nickelsen and Rengstl, 2013). The precise architecture of BCs is not yet fully understood; however, they are characterized by the accumulation of the PSII assembly factor PratA, which delivers Mn to the precursor of the D1 reaction-center protein (pD1; Stengel et al., 2012). The C-terminal extension of pD1 is then processed by the protease CtpA (Anbudurai et al., 1994; Zak et al., 2001; Komenda et al., 2007). Concomitantly, the first detectable PSII assembly intermediate, i.e., the reaction-center complex (RC), is formed by the attachment of the D2-Cyt b_{559} module which is aided by the assembly factor Ycf48, a homolog of Hcf136 from *Arabidopsis thaliana* (Komenda et al., 2004, 2008). Via the interaction of Ycf48 with the PAM68-homolog Sll0933, the inner core antenna proteins CP47 and CP43 bind successively to the RC complex, forming a PSII monomer that still lacks the lumenal subunits of the oxygen-evolving complex (OEC; Komenda et al., 2004; Rengstl et al., 2013). Finally, the OEC is built with the help of the assembly factors CyanoP and Psb27, yielding a fully functional PSII monomer (Nowaczyk et al., 2006; Becker et al., 2011; Komenda et al., 2012; Cormann et al., 2014).

Moreover, due to its susceptibility to photodamage, PSII needs to be repaired about every 30 min (Prasil et al., 1992; Mulo et al., 1998). In this process, PSII is disassembled by removing the PsbO, PsbV, PsbU, and CyanoQ subunits, followed by CP43 (Mulo et al., 2012; Mabbitt et al., 2014). Damaged D1 protein is then degraded by the FtsH2/H3 protease complex (Silva et al., 2003; Komenda et al., 2006; Boehm et al., 2012; Mabbitt et al., 2014) and replaced by newly synthesized D1, which is co-translationally inserted into the complex. Next, CP43 re-attaches and functional PSII is restored (Zhang et al., 1999; Komenda et al., 2008; Mulo et al., 2012; Mabbitt et al., 2014).

As outlined above, recent years have seen the discovery of many accessory factors that are involved in catalyzing distinct PSII assembly/repair steps. Many of these have been found to belong to the so-called family of TPR (tetratricopeptide repeat) proteins (Heinz et al., 2016; Rast et al., 2015). TPR proteins represent solenoid-like, "scaffold" proteins which are distributed throughout all kingdoms of life (for a recent review see Bohne et al., 2016). Typically, a TPR domain consists of multiple copies (3–16) of a degenerate motif which comprises 34 amino acids forming two amphipathic α-helices. The crystal structure of TPR domains revealed that these form right-handed superhelices that serve as a platform for protein–protein interactions (Blatch and Lässle, 1999; D'Andrea and Regan, 2003). TPR proteins have been implicated in a variety of functions during the biogenesis of TMs, including chloroplast protein import, gene expression and chlorophyll (Chl) synthesis, as well as PSII and PSI assembly (Bohne et al., 2016). In total, the *Synechocystis* genome encodes 29 TPR proteins (Bohne et al., 2016). These include Ycf3 and Ycf37, which have been shown to facilitate PSI assembly. The TPR protein Pitt (light-dependent protochlorophyllide oxidoreductase interacting TPR protein) interacts with POR (light-dependent protochlorophyllide oxidoreductase) and regulates Chl synthesis (Schottkowski et al., 2009b; Rengstl et al., 2011). For cyanobacterial PSII assembly, the above-mentioned TPR protein PratA plays an important role and recently the protein Slr0151 has been shown to be involved in the PSII repair cycle (Yang et al., 2014).

The *slr0151* gene is part of the *slr0144-slr0151* operon, which codes for eight proteins (Kopf et al., 2014; Yang et al., 2014). This operon was first discovered in the course of a microarray analysis in which expression of the cluster was down-regulated under iron-depleted conditions and during oxidative stress (Singh et al., 2004). The authors hypothesized that the gene cluster is involved in PSI assembly (Singh et al., 2004), and indeed a second study found Slr0151 to be associated with PSI complexes (Kubota et al., 2010). Others, however, have pointed to connections between Slr0151 and PSII (Wegener et al., 2008; Yang et al., 2014). Thus, Wegener et al. (2008) referred to the proteins encoded by the *slr0144-slr0151* operon as PSII assembly proteins (Pap) because they stabilize PSII intermediates. Furthermore, these authors showed that the entire *pap* operon is up-regulated upon loss of any of the lumenal proteins CyanoP, PsbV, and CyanoQ (Wegener et al., 2008). In a *slr0151*$^-$ mutant, however, the expression of the other *pap* genes was not affected (Yang et al., 2014). In addition, experimental evidence has been provided that links Slr0151 to the PSII repair cycle, and yeast two-hybrid and pulldown analyses have revealed that Slr0151 interacts directly with both CP43 and D1 (Yang et al., 2014). In this study, we further characterize the function and subcellular localization of Slr0151.

MATERIALS AND METHODS

Construction and Growth of Strains

Synechocystis wild-type and mutant strains were grown on solid or in liquid BG-11 medium at 30°C at a continuous photon irradiance of 30 μmol photons m^{-2} s^{-1}. The insertion mutant *slr0151*$^-$ was generated by PCR amplification of the wild-type *slr0151* gene with the oligonucleotides 0151/5 ATGATGGAAAATCAAGTTAATGA and 0151/3 TTAACCAAATAGGTTAGCTGC as primers, and subsequent cloning of the resulting fragment into the pDrive vector (Qiagen). The fragment was cut from pDrive and inserted into Bluescript pKS vector via the restriction enzymes SalI and PstI of both multiple cloning sites. A kanamycin-resistance cassette was then inserted into its unique HindIII restriction site, and wild-type cells were transformed with the construct as described. For complementation of the *slr0151*$^-$ mutant, the *slr0151* gene (including its own promoter) was PCR-amplified with oligonucleotides 0151/5b CTCGAGTGATGAGTTTTTTTAGCTCTA and 0151/3b CTCGAGAACTGGAGTTTTAACCAAA, and cloned into the single XhoI site in the vector pVZ321, which replicates autonomously in *Synechocystis* 6803 (Zinchenko et al., 1999). Transfer of this construct into *slr0151*$^-$ via conjugation was performed as described (Zinchenko et al., 1999). Construction of the mutant lines *psbA*$^-$ (*TD41*), (Nixon et al., 1992), *ctpA*$^-$ (Rengstl et al., 2011), *pratA*$^-$ (Klinkert et al., 2004), *psbB*$^-$ (Eaton-Rye and Vermaas, 1991), *ycf48*$^-$ (Komenda et al., 2008), *sll0933*$^-$ (Armbruster et al., 2010), *psb27*$^-$ (Komenda et al.,

2012), and *pitt*$^{-}$ (Schottkowski et al., 2009b) was described previously.

Antibody Production and Western Analysis

For production of the αSlr0151 antibody, the *slr0151* reading frame without the N-terminal transmembrane region (amino acid positions 62 to 320) was PCR-amplified using oligonucleotides TH0151a GGATCCGAATTCCA TTTGTTTAACCGTAAGCAGTT and TH0151b GTCGACTT AACCAAATAGGTTAGCTGCGGT. The resulting DNA fragment was inserted into the pDrive vector (Qiagen), sequenced and further subcloned into the BamHI and SalI restriction sites of the expression vector pGex-4T-1. Expression of the GST fusion protein in *Escherichia coli* BL21 and its affinity purification on Glutathione-Sepharose 4B (GE Healthcare) were performed according to the manufacturers' instructions. Polyclonal antiserum was raised in rabbits (Biogenes). Protein preparation from *Synechocystis* 6803 and western analyses were carried out as previously reported (Wilde et al., 2001).

Isolation of Total Cell Protein, Membrane Fractionation, and Western Analysis

Isolation of whole-cell protein, two-step membrane fractionation via consecutive sucrose-density gradients, and western analyses were carried out as described previously (Wilde et al., 2001; Schottkowski et al., 2009a,b; Rengstl et al., 2011). Apart from αSlr0151, the primary antibodies used in this study have been described earlier, i.e., αD1 (Schottkowski et al., 2009b), αD2 (Klinkert et al., 2004), αPratA (Klinkert et al., 2004), αYcf48 (Rengstl et al., 2011), αPitt (Schottkowski et al., 2009a), αPOR (Schottkowski et al., 2009a), αYidC (Ossenbühl et al., 2006), αSll0933 (Armbruster et al., 2010), or were purchased from Agrisera (Vännäs, Sweden), i.e., αCP43, αCP47, αRbcL. Western blots were quantified using AIDA software (version 3.52.046). For each experiment, the respective RbcL signal served as internal loading control. Quantifications are based on at least three independent experiments. Mean and standard deviation were calculated for the protein levels and Student's *t*-test was performed to verify statistical significant differences between wild-type and *slr0151*$^{-}$.

Transmission Electron Microscopy

Synechocystis cells (*slr0151*$^{-}$ mutant and wild-type) were harvested in mid-log phase by centrifugation at 5000 *g* and adjusted to an $OD_{750\,nm} = 3$ in BG-11. Aliquots (2 µl) of the cell suspension were high-pressure frozen at 2100 bar (Leica HPM 100) in HPF gold platelets (Leica Microsystems, Vienna, Austria) and stored in liquid nitrogen (Rachel et al., 2010; Klingl et al., 2011). The cryofixed cells were then freeze-substituted (Leica EM AFS2) at −90°C with 2% osmium tetroxide and 0.2% uranyl acetate in pure acetone. Freeze substitution was carried out at −90°C for 20 h, −60°C for 8 h, −30°C for 8 h, with a heating time of 1 h between each step, and then held at 0°C for 3 h. Samples were washed three times with pure, ice-cold acetone followed by infiltration with Epon resin (Fluka, Buchs, Switzerland). After polymerization for 72 h at 63°C, ultrathin sections were cut, and post-stained with lead citrate (Reynolds, 1963). Transmission electron microscopy was carried out at 80 kV either on a Zeiss EM 912 or on a Fei Morgagni 268 electron microscope (FEI). Data analysis was carried out with the Fiji ImageJ software.

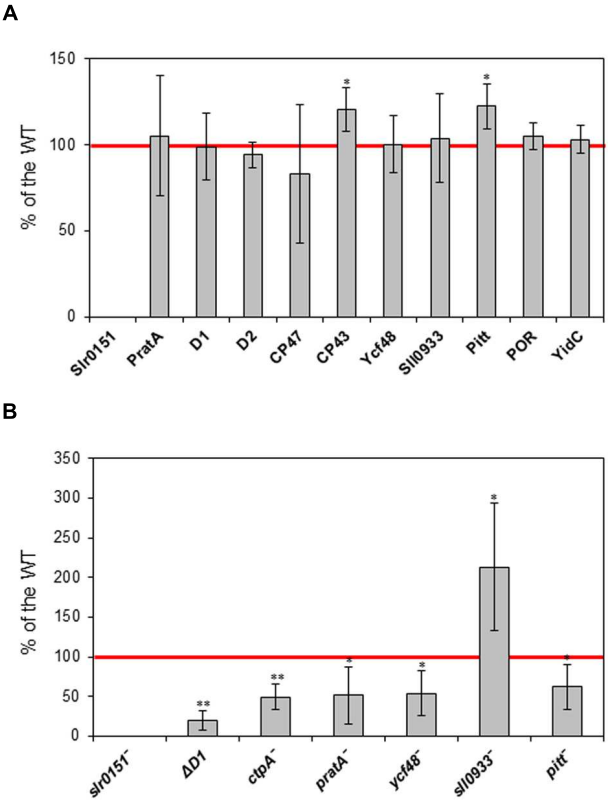

FIGURE 1 | Steady-state levels of the indicated PSII-related proteins in the *slr0151*$^{-}$ mutant (A) and of Slr0151 in the indicated PSII mutants (B). Each value is expressed relative to that in the wild type. Total cell proteins were isolated, fractionated by SDS-PAGE, blotted onto nitrocellulose membranes and detected immunologically. Signals were quantified with AIDA software (version 3.52.046) after densitometrical scanning. Values plotted are means ± SD of at least three independent experiments. Significance according to Student's *t*-test with an error probability of 5 and 1% is indicated by one and two asterisks, respectively.

Immunofluorescence and Fluorescence Microscopy

Synechocystis cells were harvested in mid-log phase by centrifugation at 5000 *g* and adjusted to an $OD_{750\,nm} = 3$ in PBS (140 mM NaCl, 2.7 mM KCl, 10 mM Na_2HPO_4, 1.8 mM KH_2PO_4; pH 7.4). The cells were fixed with 2% formaldehyde (35%, for Histology, Roth) in PBS for 20 min at 30°C on a shaker, then washed twice with PBS-T (PBS supplemented with 0.05% Tween-20). For permeabilization, the cells were incubated with PBS-T for 2 min × 3 min on an overhead rotor. All subsequent steps were performed in

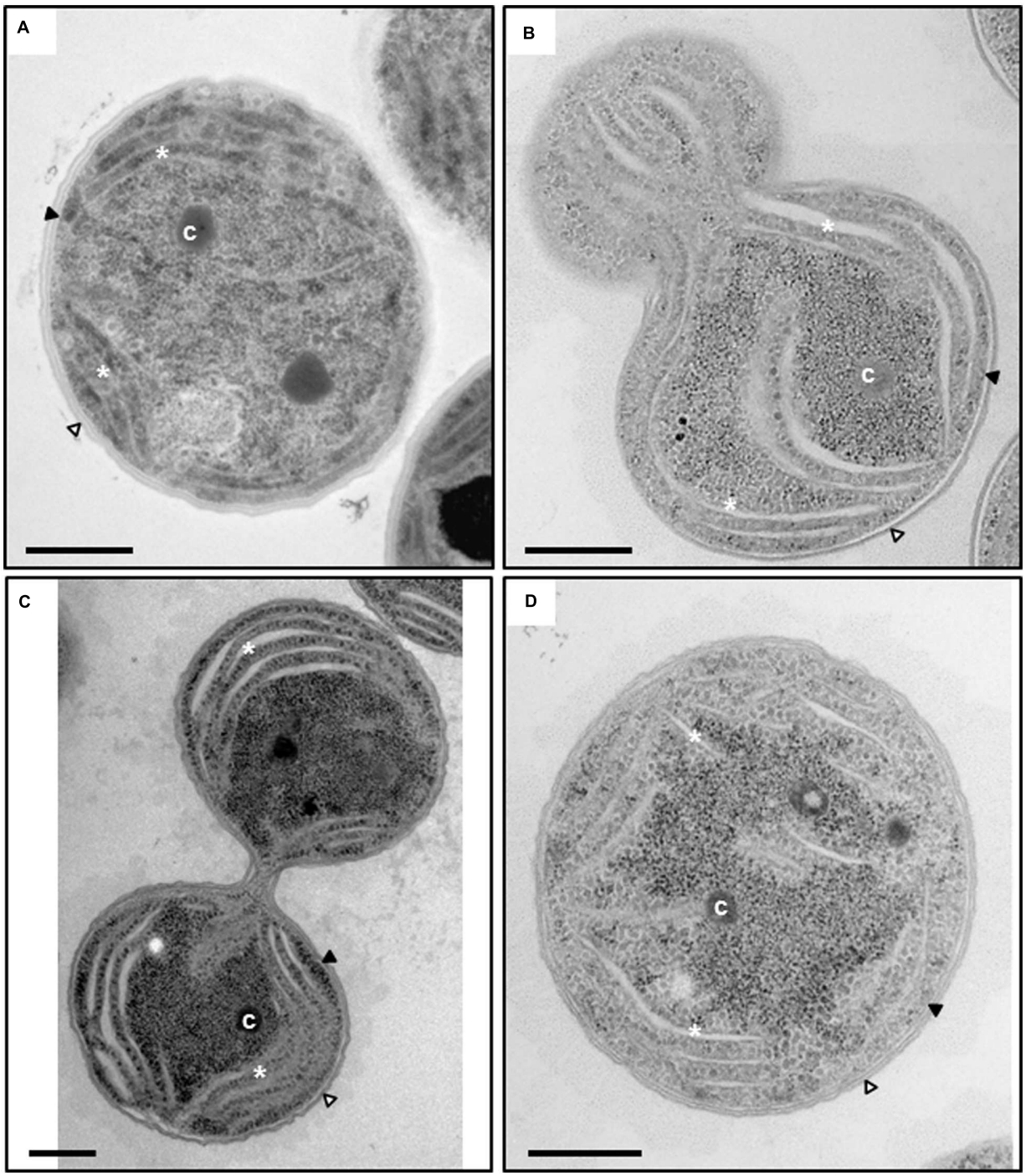

FIGURE 2 | Transmission electron microscopy of wild-type *Synechocystis* (A) and *slr0151*$^{-}$ mutant cells (B–D). Different stages during the cell division of the *slr0151*$^{-}$ strain are shown; early stage of the cell division **(B)**, late stage of cell division right before cytokinesis **(C)** and non-dividing single cell **(D)**. Intracellular components are labeled: Outer membrane (white arrowhead), plasma membrane (black arrowhead), thylakoids (white asterisks) and carboxysome (c). Bars = 500 nm.

the dark. The cells were applied to poly-L-lysine-coated glass slides (Sigma) and incubated for 30 min to allow them to settle, then incubated with blocking buffer (5% non-fat milk powder in PBS-T) for 20 min. The slides were incubated for 3 h with the first antibody (αSlr0151 and αRbcL, diluted 1:500 in blocking buffer, then washed for 3 min × 3 min by incubating them with PBS-T and rinsing the solution off the slide. The secondary HRP-conjugated goat anti-rabbit

antibody (Sigma) was labeled with Alexa 488 (Alexa Fluor Dyes, Life Technologies, ThermoFisher Scientific) according the manufacturer's instruction. The slides were incubated with the labeled secondary antibody (diluted 1:2000 in blocking buffer) for 1 h. The slides were washed twice with PBS-T and twice with PBS-G (PBS supplemented with 10 mM glycine) to minimize background fluorescence due to non-labeled fluorophores. The slides were then dried and each was covered with a drop of FluorSave^{TM} Reagent (Calbiochem, Merck Millipore) and a coverslip. Next day, the coverslip was sealed with nail polish. Fluorescence was imaged using a Delta Vision Elite (GE Healthcare, Applied Precision) equipped with Insight SSI^{TM} illumination and a CoolSNAP_HQ2 CCD camera. Cells were imaged with a 100× oil PSF U-Plan S-Apo 1.4 objective. The four-color standard set InsightSSI module (code number: 52-852113-003, GE Healthcare, Applied Precision) was used for imaging. Alexa488 was excited with the FITC/GFP excitation filter (461–489 nm) and emission was detected with the FITC/GFP emission filter (501–549 nm). Chlorophyll autofluorescence was excited with the TRITC/Cy3-filter (528–555 nm) and emission was detected with the TRITC/Cy3 filter (574–619 nm). Images were analyzed using the Fiji ImageJ software.

RESULTS

Molecular *slr0151*$^{-}$ Phenotype

The *slr0151* open reading frame in *Synechocystis* encodes a protein of 320 amino acids, which contains two consecutive TPR domains comprising positions 185–218 and 219–252 (analyzed with TPRpred; Yang et al., 2014; Bohne et al., 2016). It has previously been shown that Slr0151 is an intrinsic membrane protein which forms part of a high-molecular-weight complex (Yang et al., 2014).

To analyze the function of Slr0151, we disrupted its cloned reading frame by inserting a kanamycin-resistance cassette into the unique HindIII site 425 bp downstream of the start codon (**Supplementary Figure S1A**). After transformation of wild-type (WT) cells with this construct, the transformants were tested for complete segregation by PCR analysis (**Supplementary Figure S1B**). The complete absence of the Slr0151 protein in the *slr0151*$^{-}$ mutant was verified by western analysis using an αSlr0151 antibody (**Supplementary Figure S1C**). Like the previously described *slr0151*$^{-}$ mutant, the mutant strain described in this study exhibited a high light (800 μmol photons m^{-2} s^{-1}) sensitive phenotype (Yang et al., 2014). Moreover, and also in agreement with the previous report, less pronounced effects were observed under normal lighting conditions (30 μmol photons m^{-2} s^{-1}). These effects included moderately reduced photoautotrophic growth and oxygen production rates (Yang et al., 2014). Together, these findings suggest that, like other PSII assembly factors such as Ycf48 or Psb27, Slr0151 might be involved in both PSII assembly and repair (Komenda et al., 2012; Rengstl et al., 2013; Mabbitt et al., 2014; Jackson and Eaton-Rye, 2015).

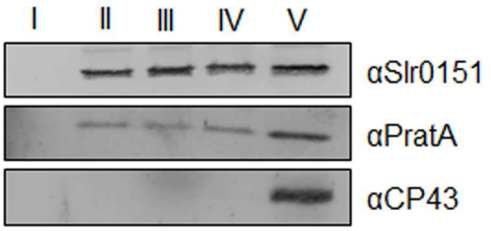

FIGURE 3 | Membrane localization of Slr0151. Sucrose step-gradient centrifugation was used to separate membrane types from wild-type *Synechocystis* cells. Fraction II corresponds to the plasma membrane (PM) and fraction V contains pratA-defined biogenic membranes (PDMs) + thylakoid membrane (TMs). For fractions I–IV 10% of the total volume of each fraction was loaded, while only 0.2% of fraction V was analyzed (Schottkowski et al., 2009a).

To explore this possibility further, the levels of various photosynthetic subunits and PSII biogenesis factors accumulated in the *slr0151*$^{-}$ strain under normal growth conditions were analyzed. Almost all analyzed proteins showed no significant differences relative to WT, except CP43 and Pitt had increased levels in the mutant (**Figure 1A**; **Supplementary Figure S2A**). Conversely, however, levels of Slr0151 were significantly altered in different PSII assembly mutants (**Figure 1B**; **Supplementary Figure S2B**). In the Δ*D1* mutant, in which all three copies of the *psbA* gene are inactivated, Slr0151 was reduced to only 20% of its wild-type level (Nixon et al., 1992). The *ctpA*$^{-}$ mutant lacking the C-terminal processing protease for pD1 accumulated only 50% as much Slr0151 as did wild-type cells (Anbudurai et al., 1994). In the PSII assembly factor mutants *pratA*$^{-}$, *ycf48*$^{-}$, and *pitt*$^{-}$ (Klinkert et al., 2004; Komenda et al., 2008; Schottkowski et al., 2009b) amounts of Slr0151 reached 52, 53, and 62% of the wild-type level, respectively. In sharp contrast, however, more than twice the WT level of Slr0151 was detected in *sll0933*$^{-}$, which lacks the cyanobacterial homolog of the *Arabidopsis* PSII assembly factor PAM68. This suggests a functional relationship between Slr0151 and Sll0933, despite the fact that levels of the latter were unchanged in the *slr0151*$^{-}$ mutant (**Figure 1**; **Supplementary Figure S2**). To test if this relationship relies on a physical interaction of both factors, we performed co-immunoprecipitation experiments. However, no interaction between Slr0151 and Sll0933 were detected under the applied conditions suggesting that they do not form parts of a stable complex *in vivo*.

Ultrastructure of *slr0151*$^{-}$ Cells

In order to gain more insight into the subcellular consequences of *slr0151* inactivation, the ultrastructure of the mutant was visualized by transmission electron microscopy (**Figure 2**). In *slr0151*$^{-}$ cells grown at normal light intensities, the thylakoids appeared to be less densely packed and thylakoid lumina were swollen when compared to the wild-type (**Figure 2**). Lumen diameters ranged from 4 to 91 nm in the mutant, whereas the values for wild-type thylakoids fell within the 5- to 9-nm range, as previously observed (**Figure 2**; van de Meene et al., 2006). Thus,

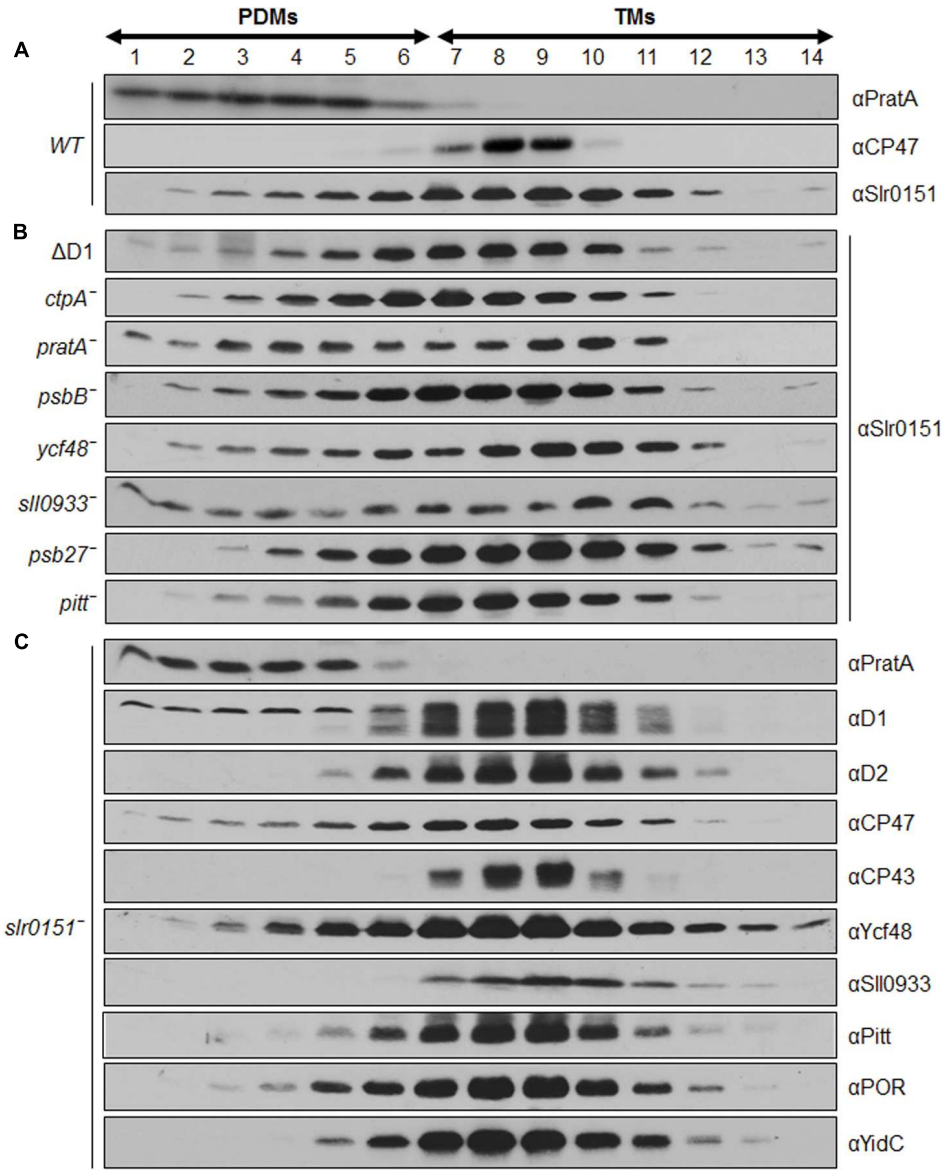

FIGURE 4 | Distribution of Slr0151 between PDMs and TMs. (A) Wild-type fraction V (see **Figure 3**) was centrifuged on linear sucrose gradients in order to separate wild-type PDMs from TMs. **(B)** Distribution of Slr0151 between PDMs and TMs in the indicated PSII mutants. **(C)** Distribution of various PSII-related proteins in *slr0151*⁻ cells. The part of the gradient from 20 to 60% sucrose was apportioned into 14 fractions, which were analyzed by immunoblotting using the antibodies indicated on the right. Fractions 1–6 represent PDMs, and fractions 7–14 represent TMs. To facilitate comparison between gradients, sample volumes were normalized to the volume of fraction 7 that contained 40 μg of protein.

in addition to PSII assembly/repair, Slr0151 deficiency appears to affect TM organization.

Localization of Slr0151 and PSII-Related Factors in Membrane Subfractions

Slr0151 has previously been reported to localize to both the PM and TMs, based on a combined sucrose density/two-phase partitioning approach (Yang et al., 2014). Alternatively, cyanobacterial membranes can be fractionated into PM and TMs via a sucrose step gradient, and the latter can be further fractionated into PratA-defined biogenic membranes (PDMs) and photosynthetically active thylakoids on a second, linear sucrose gradient (Schottkowski et al., 2009a; Heinz et al., 2016). When the distribution of Slr0151 in membrane subfractions was followed by applying the latter technique, the protein was accordingly detected in both PM and TM fractions (**Figure 3**). Further fractionation of thylakoids then revealed that Slr0151 is found in both PDMs and TMs, indicating that the protein is broadly distributed throughout the cell (**Figure 4A**). Since Slr0151 accumulation was affected in several PSII-related mutants, we next analyzed its TM distribution in the various

mutant backgrounds (**Figures 2B** and **4B**). In most cases, Slr0151 distribution followed the wild-type pattern. The only exceptions were the *pratA*$^{-}$ and *sll0933*$^{-}$ mutants (**Figures 4A,B**). In these strains, a shift of Slr0151-containing material toward the less dense PDM fractions was observed (**Figures 4A,B**). This again suggested a functional relationship between Slr0151 and the PAM68 homolog Sll0933 and, furthermore, a connection to the biogenic PratA-defined region at the periphery of the cell.

When the distribution of several PSII-related proteins was monitored in a *slr0151*$^{-}$ background, no significant effects were seen (**Figure 4C**; Rengstl et al., 2011). The only alteration in membrane distribution concerned CP47. This is usually

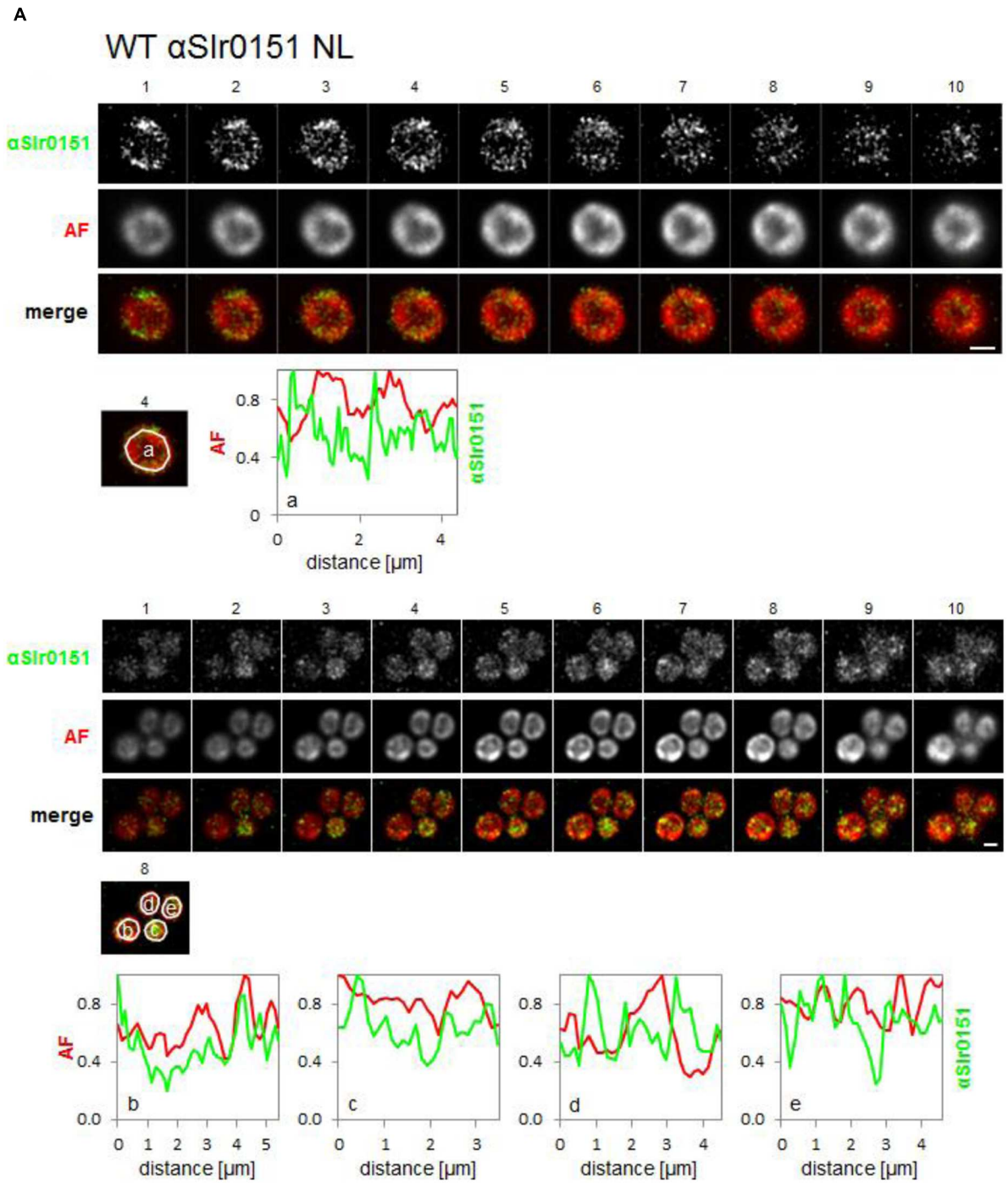

FIGURE 5 | Continued

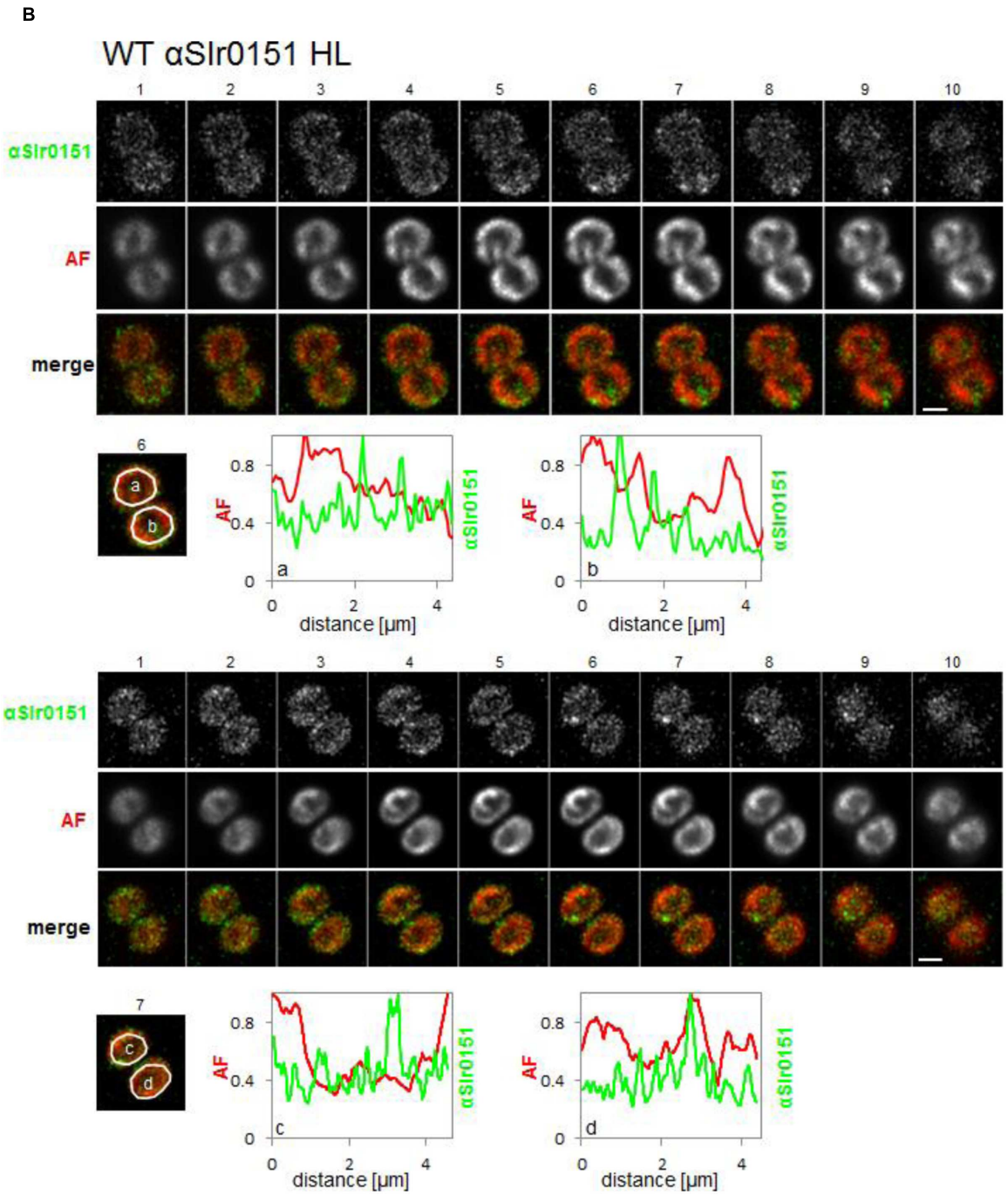

FIGURE 5 | Continued

seen exclusively in TMs, but accumulates to some extent in PDM fractions in the absence of Slr0151 (**Figures 4A,C**). However, Slr0151 localization was not affected in a *psbB*$^{-}$ mutant (**Figure 4B**). Taken together, these data revealed a broad membrane distribution of Slr0151 and further confirmed its relationship to PSII assembly/repair. The distribution Slr0151 in the WT is almost identical to the distribution of Ycf48 which has been shown to be involved in assembly and repair of PSII.

Localization of Slr0151 via Immunofluorescence

To obtain a more comprehensive view of the subcellular localization of Slr0151, we next performed immunofluorescence (IF) analyses with affinity-purified αSlr0151, in combination with an Alexa488-labeled secondary antibody. Fluorescence was recorded by wide-field microscopy followed by deconvolution.

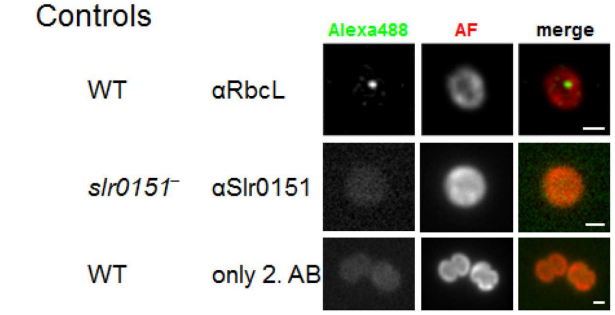

FIGURE 5 | Subcellular localization of Slr0151 by immunofluorescence analysis of wild-type *Synechocystis* cells. Cells grown under normal light conditions **(A)** and cells that had been exposed to high light for 1 h **(B)** were treated with αSlr0151 antibody and detected with an Alexa-488-coupled secondary antibody. The constituent subpanels show Z-montages (200 nm spacing) of each separate channel as well as the merged channel. The line plots of relative fluorescence signals are derived from scans of the area defined by the white circle around the indicated cells, and correspond to the *Z*-slice number of the analyzed slice (given at the top). **(C)** For controls, cells were grown under normal conditions. In the upper row, *Synechocystis* wild-type cells were immunostained with αRbcL and visualized with Alexa-488 coupled secondary antibody. In the middle row, *slr0151*$^-$ mutant cells have been treated with the αSlr0151 antibody followed by Alexa-488-coupled secondary antibody. In the bottom row, wild-type cells were probed with Alexa-488-coupled secondary antibody alone. AF, autofluorescence of chlorophyll; scale bar 1 μm.

In **Figure 5**, Z-montages from different cells are shown that display sequential slices from the Z-stack to provide a better 3D representation of whole cell volumes. Overall, Slr0151 IF signals in wild-type cells grown under normal light conditions were unevenly distributed, with frequent spot-like concentrations. These partly coincided with the Chl autofluorescence of the thylakoids, but were also detected in regions with low Chl fluorescence, i.e., in the PM at the cell periphery and in thylakoid convergence zones close to the PM. Interestingly, fluorescence signals were also visible in Chl-less central regions of the cells, where fewer thylakoid lamellae tend to traverse the cytoplasm (**Figure 5A**). Thus, the fluorescence signal is in accordance with the observations from membrane fraction analysis, i.e., that Slr0151 is located in the PM, and in PDMs and TMs. In addition, these data provide evidence that Slr0151 is found in punctate concentrations within the membrane, reminiscent of the previously described distribution of FtsH2-GFP signals, which are thought to label PSII repair zones (Sacharz et al., 2015). Similar to FtsH-GFP signals, Slr0151 IF patterns were unchanged after a 1-h exposure to high light, suggesting that an enhanced requirement for PSII repair does not provoke any substantial reorganization of Slr0151 localization (**Figure 5B**; Sacharz et al., 2015).

Control experiments included the omission of the specific αSlr0151 antibody, and analysis of the *slr0151*$^-$ mutant, which displayed at most diffuse background signals (**Figure 5C**). Moreover, we used an αRbcL antibody as a control for a non-membrane protein that gives rise to fluorescence labeling of carboxysomes from *Synechocystis* (Cameron et al., 2013).

DISCUSSION

Yang et al. (2014) demonstrated that the TPR protein Slr0151 is involved in the repair of PSII in *Synechocystis* cultures grown at high light. Prompted by the finding that a milder phenotype can be observed under normal lighting conditions, we have carried out a further investigation of the effects of loss of Slr0151 in that context. In particular, our data suggest a functional relationship between Slr0151 and the PSII assembly factor Sll0933, a homolog of the PAM68 protein from *A. thaliana*, which has been shown to play a role in the conversion of RC complexes into larger PSII pre-complexes by facilitating attachment of the inner antenna proteins (**Figure 1B**; Armbruster et al., 2010; Rengstl et al., 2013).

In agreement with the idea that Slr0151 is involved in the transition to larger PSII pre-complexes, reduced amounts of the RC47 complex have previously been detected in *slr0151*$^-$ cells grown under high light (Yang et al., 2014). Moreover, the direct interaction of Slr0151 with CP43 and D1, as well as the unusual membrane distribution of CP47 in PDMs in the *slr0151*$^-$ background, suggest a role for Slr0151 in the transition from RC complexes to PSII monomers (**Figure 4C**; Yang et al., 2014). Interestingly, PDM-localized CP47 fractions have also been observed in a *ctpA*$^-$ mutant, which further supports the idea that Slr0151 acts during the transition from the RC47 complex to the PSII monomer lacking the OEC (Rengstl et al., 2011). Ycf48 is involved in the formation of the RC complex during assembly and repair of PSII (Komenda et al., 2008; Rengstl et al., 2011). Interestingly, it is distributed like Slr0151 in membrane fractionation experiments (**Figure 4**). This might suggest that a broad membrane distribution of PSII related proteins is characteristic for factors being involved in both PSII assembly and repair. Taken together, these findings confirm a PSII-related function for Slr0151, and demonstrate that, even under normal lighting conditions, distinct molecular phenotypes are detectable upon inactivation of Slr0151.

This is further underlined by the altered ultrastructure of thylakoids, i.e., looser membrane packing and increased lumen volume, seen in the *slr0151*$^-$ mutant grown in normal light. Swollen lumina of thylakoids have been observed before in WT cells grown at 0.5 μmol photons m^{-2} s^{-1} and in WT and mutants with different depletions of carotenoids grown in the dark with 10 min of light per day (Van de Meene et al., 2012; Toth et al., 2015). Recently, a study using inelastic neutron scattering on living *Synechocystis* WT cells investigated the membrane dynamics of thylakoids during light and dark periods (Stingaciu et al., 2016). The authors showed that the TM in *Synechocystis* is less flexible in the light as compared to dark conditions due to formation of the photosynthetic proton gradient across the TMs. Therefore, it appears possible that distorted photosynthesis or an absence of the structural function

of Slr0151 itself causes swollen thylakoids in the *slr0151*$^-$ mutant. Such a structural role would also be in line with the observed broader membrane distribution of Slr0151. Taken together, we propose that Slr0151 – like other PSII assembly factors such as CtpA, Ycf48 and Psb27 – is involved in both PSII assembly and repair (Nowaczyk et al., 2006; Komenda et al., 2007; Nickelsen and Rengstl, 2013; Jackson et al., 2014; Mabbitt et al., 2014). The suggested involvement of Slr0151 in both processes is also consistent with the fact that the RC47 complex represents the point of convergence between them.

Slr0151 is an intrinsic membrane protein that does not accumulate in the cytoplasm (Yang et al., 2014; data not shown). Indeed, it can be found in a variety of specialized membrane domains. Previously, Slr0151 was detected in the PM as well as in the thylakoids of *Synechocystis* (Huang et al., 2002; Yang et al., 2014). This distribution was confirmed by our membrane fraction experiments (**Figures 3** and **4**). In addition, substantial amounts of Slr0151 were observed in PDMs, which are localized at sites where thylakoids converge upon the PM. According to rough estimates based on densitometrical signal analysis, approximately 2% of total cellular Slr0151 is found in PMs and 25 and 70% in PDMs and TMs, respectively. IF analyses confirmed this overall distribution and revealed frequent punctate concentrations of Slr0151 in all membrane types (**Figure 5**). Intriguingly, a similar localization pattern has been observed for GFP-tagged FtsH2, the protease which degrades damaged D1 protein during PSII repair. The GFP signal co-localized with the Chl autofluorescence and showed patches of increased intensity within as well as between thylakoids at their peripheral convergence sites (Sacharz et al., 2015). The same patterns were maintained under high light conditions for both Slr0151 and FtsH2 (Sacharz et al., 2015). Thus, these data, together with the observation that the synthesis of D1 following photodamage is affected by Slr0151 inactivation (Yang et al., 2014), are consistent with a role of Slr0151 during repair. Furthermore, IF analysis has shown that some Slr0151 is concentrated in thylakoids that traverse the cell center. Whether this reflects any distinct functional role of these regions remains to be discovered.

This work reveals new aspects of the function of the TPR protein Slr0151, i.e., its involvement in PSII assembly in addition to its previously described role in PSII repair. The fact that PSII assembly takes place in BCs does not exclude the possibility that repair and assembly of PSII are co-localized in those regions. Since several steps of assembly and repair involve the same assembly/repair factors as well as some assembly and assembly repair intermediates (Schottkowski et al., 2009a; Rengstl et al., 2011; Stengel et al., 2012). Therefore, the current findings suggest a close relationship between PSII assembly and repair, with regard to the factors involved and their subcellular distribution (Nickelsen and Rengstl, 2013; Mabbitt et al., 2014).

AUTHOR CONTRIBUTIONS

AR, BR, SH, AK, and JN designed the research. AR, BR, and SH performed the research. AR and JN perpared the article.

FUNDING

This work was supported by funding from the Deutsche Forschungsgemeinschaft for Research Unit FOR2092 (Ni390/9-1).

ACKNOWLEDGMENTS

We thank Jürgen Soll for providing αYidC antibody, Marc Bramkamp for help with the Delta Vision and Silvia Dobler for technical assistance. Furthermore, we thank Paul Hardy for critical reading of the manuscript.

SUPPLEMENTARY MATERIAL

The Supplementary Material for this article can be found online at: http://journal.frontiersin.org/article/10.3389/fpls.2016.00605

FIGURE S1 | Generation of the *Synechocystis slr0151*$^-$ mutant. **(A)** Construction of the insertional *slr0151*$^-$ mutant. **(B)** PCR-based segregation analysis of the *Synechocystis slr0151*$^-$ mutant [primer locations are indicated by black arrows in **(A)**]. **(C)** Levels of Slr0151 protein detected with αSlr0151 antiserum in the wild-type (WT), *slr0151*$^-$ mutant and the complemented *slr0151*$^-$ strain (*re-slr0151*$^-$). RbcL served as the loading control.

FIGURE S2 | Protein levels in the *slr0151*$^-$ mutant and of Slr0151 in various PSII mutants. Representative western blots from the protein level analysis shown in **Figure 1**. Total proteins were isolated from the respective line and analyzed via SDS-PAGE and western blot. 30 μg were loaded for 100% wild type and each mutant. The quantification of at least three independent experiments is summarized in **Figure 1**. The RbcL signal served as internal standard for relative quantification. **(A)** Protein levels of the indicated PSII subunits and PSII-related proteins in the *slr0151*$^-$ mutant. Wild-type and mutant samples were analyzed on the same gel. However, signals from unrelated samples, which were loaded in between, were excised. **(B)** Representative western analysis of Slr0151 in various PSII mutants.

REFERENCES

Anbudurai, P. R., Mor, T. S., Ohad, I., Shestakov, S. V., and Pakrasi, H. B. (1994). The ctpA gene encodes the C-terminal processing protease for the D1 protein of the photosystem II reaction center complex. *Proc. Natl. Acad. Sci. U.S.A.* 91, 8082–8086. doi: 10.1073/pnas.91.17.8082

Armbruster, U., Zuhlke, J., Rengstl, B., Kreller, R., Makarenko, E., Rühle, T., et al. (2010). The *Arabidopsis* thylakoid protein PAM68 is required for efficient D1 biogenesis and photosystem II assembly. *Plant Cell* 22, 3439–3460. doi: 10.1105/tpc.110.077453

Becker, K., Cormann, K. U., and Nowaczyk, M. M. (2011). Assembly of the water-oxidizing complex in photosystem II. *J. Photochem. Photobiol. B Biol.* 104, 204–211. doi: 10.1016/j.jphotobiol.2011.02.005

Blatch, G. L., and Lässle, M. (1999). The tetratricopeptide repeat: a structural motif mediating protein-protein interactions. *Bioessays* 21, 932–939. doi: 10.1002/(SICI)1521-1878(199911)21:11<932::AID-BIES5>3.3.CO;2-E

Boehm, M., Yu, J., Krynicka, V., Barker, M., Tichy, M., Komenda, J., et al. (2012). Subunit organization of a *Synechocystis* hetero-oligomeric thylakoid FtsH complex involved in photosystem II repair. *Plant Cell* 24, 3669–3683. doi: 10.1098/rstb.2012.0066

Bohne, A. V., Schwenkert, S., Grimm, B., and Nickelsen, J. (2016). Roles of tetratricopeptide repeat proteins in piogenesis of the photosynthetic apparatus. *Int. Rev. Cell Mol. Biol.* 324, 187–227. doi: 10.1016/bs.ircmb.2016.01.005

Cameron, J. C., Wilson, S. C., Bernstein, S. L., and Kerfeld, C. A. (2013). Biogenesis of a bacterial organelle: the carboxysome assembly pathway. *Cell* 155, 1131–1140. doi: 10.1016/j.cell.2013.10.044

Cormann, K. U., Bartsch, M., Rogner, M., and Nowaczyk, M. M. (2014). Localization of the CyanoP binding site on photosystem II by surface plasmon resonance spectroscopy. *Front. Plant Sci.* 5:595. doi: 10.3389/fpls.2014.00595

D'Andrea, L. D., and Regan, L. (2003). TPR proteins: the versatile helix. *Trends Biochem. Sci.* 28, 655–662. doi: 10.1016/j.tibs.2003.10.007

Eaton-Rye, J. J., and Vermaas, W. F. (1991). Oligonucleotide-directed mutagenesis of psbB, the gene encoding CP47, employing a deletion mutant strain of the cyanobacterium *Synechocystis* sp. PCC 6803. *Plant Mol. Biol.* 17, 1165–1177. doi: 10.1007/BF00028733

Heinz, S., Liauw, P., Nickelsen, J., and Nowaczyk, M. (2016). Analysis of photosystem II biogenesis in cyanobacteria. *Biochim. Biophys. Acta* 1857, 274–287. doi: 10.1016/j.bbabio.2015.11.007

Hohmann-Marriott, M. F., and Blankenship, R. E. (2011). Evolution of photosynthesis. *Annu. Rev. Plant Biol.* 62, 515–548. doi: 10.1146/annurev-arplant-042110-103811

Huang, F., Parmryd, I., Nilsson, F., Persson, A. L., Pakrasi, H. B., Andersson, B., et al. (2002). Proteomics of *Synechocystis* sp. strain PCC 6803: identification of plasma membrane proteins. *Mol. Cell. Proteomics* 1, 956–966. doi: 10.1074/mcp.M200043-MCP200

Jackson, S. A., and Eaton-Rye, J. J. (2015). Characterization of a *Synechocystis* sp. PCC 6803 double mutant lacking the CyanoP and Ycf48 proteins of Photosystem II. *Photosynth. Res.* 124, 217–229. doi: 10.1007/s11120-015-0122-0

Jackson, S. A., Hervey, J. R., Dale, A. J., and Eaton-Rye, J. J. (2014). Removal of both Ycf48 and Psb27 in *Synechocystis* sp. PCC 6803 disrupts Photosystem II assembly and alters Q(A)(-) oxidation in the mature complex. *FEBS Lett.* 588, 3751–3760. doi: 10.1016/j.febslet.2014.08.024

Klingl, A., Moissl-Eichinger, C., Wanner, G., Zweck, J., Huber, H., Thomm, M., et al. (2011). Analysis of the surface proteins of *Acidithiobacillus ferrooxidans* strain SP5/1 and the new, pyrite-oxidizing *Acidithiobacillus* isolate HV2/2, and their possible involvement in pyrite oxidation. *Arch. Microbiol.* 193, 867–882. doi: 10.1007/s00203-011-0720-y

Klinkert, B., Ossenbuhl, F., Sikorski, M., Berry, S., Eichacker, L., and Nickelsen, J. (2004). PratA, a periplasmic tetratricopeptide repeat protein involved in biogenesis of photosystem II in *Synechocystis* sp. PCC 6803. *J. Biol. Chem.* 279, 44639–44644. doi: 10.1074/jbc.M405393200

Komenda, J., Barker, M., Kuvikova, S., De Vries, R., Mullineaux, C. W., Tichy, M., et al. (2006). The FtsH protease slr0228 is important for quality control of photosystem II in the thylakoid membrane of *Synechocystis* sp. PCC 6803. *J. Biol. Chem.* 281, 1145–1151. doi: 10.1074/jbc.M503852200

Komenda, J., Knoppova, J., Kopecna, J., Sobotka, R., Halada, P., Yu, J., et al. (2012). The Psb27 assembly factor binds to the CP43 complex of photosystem II in the cyanobacterium *Synechocystis* sp. PCC 6803. *Plant Physiol.* 158, 476–486. doi: 10.1016/j.pbi.2012.01.017

Komenda, J., Nickelsen, J., Tichy, M., Prasil, O., Eichacker, L. A., and Nixon, P. J. (2008). The cyanobacterial homologue of HCF136/YCF48 is a component of an early photosystem II assembly complex and is important for both the efficient assembly and repair of photosystem II in *Synechocystis* sp. PCC 6803. *J. Biol. Chem.* 283, 22390–22399. doi: 10.1074/jbc.M801917200

Komenda, J., Reisinger, V., Muller, B. C., Dobakova, M., Granvogl, B., and Eichacker, L. A. (2004). Accumulation of the D2 protein is a key regulatory step for assembly of the photosystem II reaction center complex in *Synechocystis* PCC 6803. *J. Biol. Chem.* 279, 48620–48629. doi: 10.1074/jbc.M405725200

Komenda, J., Tichy, M., Prasil, O., Knoppova, J., Kuvikova, S., De Vries, R., et al. (2007). The exposed N-terminal tail of the D1 subunit is required for rapid D1 degradation during photosystem II repair in *Synechocystis* sp PCC 6803. *Plant Cell* 19, 2839–2854. doi: 10.1016/j.bbabio.2007.01.005

Kopf, M., Klahn, S., Scholz, I., Matthiessen, J. K., Hess, W. R., and Voss, B. (2014). Comparative analysis of the primary transcriptome of *Synechocystis* sp. PCC 6803. *DNA Res.* 21, 527–539. doi: 10.1093/dnares/dsu018

Kubota, H., Sakurai, I., Katayama, K., Mizusawa, N., Ohashi, S., Kobayashi, M., et al. (2010). Purification and characterization of photosystem I complex from *Synechocystis* sp. PCC 6803 by expressing histidine-tagged subunits. *Biochim. Biophys. Acta* 1, 98–105. doi: 10.1016/j.bbabio.2009.09.001

Kupitz, C., Basu, S., Grotjohann, I., Fromme, R., Zatsepin, N. A., Rendek, K. N., et al. (2014). Serial time-resolved crystallography of photosystem II using a femtosecond X-ray laser. *Nature* 513, 261–265. doi: 10.1038/nature13453

Mabbitt, P. D., Wilbanks, S. M., and Eaton-Rye, J. J. (2014). Structure and function of the hydrophilic Photosystem II assembly proteins: Psb27, Psb28 and Ycf48. *Plant Physiol. Biochem.* 81, 96–107. doi: 10.1016/j.plaphy.2014.02.013

Mulo, P., Laakso, S., Maenpaa, P., and Aro, E. M. (1998). Stepwise photoinhibition of photosystem II. Studies with *Synechocystis* species PCC 6803 mutants with a modified D-E loop of the reaction center polypeptide D1. *Plant Physiol.* 117, 483–490. doi: 10.1104/pp.117.2.483

Mulo, P., Sakurai, I., and Aro, E. M. (2012). Strategies for psbA gene expression in cyanobacteria, green algae and higher plants: from transcription to PSII repair. *Biochim. Biophys. Acta* 1, 247–257. doi: 10.1016/j.bbabio.2011.04.011

Nickelsen, J., and Rengstl, B. (2013). Photosystem II assembly: from cyanobacteria to plants. *Annu. Rev. Plant Biol.* 64, 609–635. doi: 10.1146/annurev-arplant-050312-120124

Nickelsen, J., and Zerges, W. (2013). Thylakoid biogenesis has joined the new era of bacterial cell biology. *Front. Plant Sci.* 4:458. doi: 10.3389/fpls.2013.00458

Nixon, P. J., Trost, J. T., and Diner, B. A. (1992). Role of the carboxy terminus of polypeptide D1 in the assembly of a functional water-oxidizing manganese cluster in photosystem II of the cyanobacterium *Synechocystis* sp. PCC 6803: assembly requires a free carboxyl group at C-terminal position 344. *Biochemistry* 31, 10859–10871. doi: 10.1093/aob/mcq059

Nowaczyk, M. M., Hebeler, R., Schlodder, E., Meyer, H. E., Warscheid, B., and Rogner, M. (2006). Psb27, a cyanobacterial lipoprotein, is involved in the repair cycle of photosystem II. *Plant Cell* 18, 3121–3131. doi: 10.1105/tpc.106.042671

Ossenbühl, F., Inaba-Sulpice, M., Meurer, J., Soll, J., and Eichacker, L. A. (2006). The *Synechocystis* sp PCC 6803 Oxa1 homolog is essential for membrane integration of reaction center precursor protein pD1. *Plant Cell* 18, 2236–2246. doi: 10.1105/tpc.106.043646

Prasil, O., Adir, N., and Ohad, I. (1992). Dynamics of photosystem II: mechanism of photoinhibition and recovery process. *Top. Photosynth.* 11, 295–348.

Rachel, R., Meyer, C., Klingl, A., Gurster, S., Heimerl, T., Wasserburger, N., et al. (2010). Analysis of the ultrastructure of archaea by electron microscopy. *Methods Cell Biol.* 96, 47–69. doi: 10.1016/S0091-679X(10)96003-2

Rast, A., Heinz, S., and Nickelsen, J. (2015). Biogenesis of thylakoid membranes. *Biochim. Biophys. Acta* 9, 821–830. doi: 10.1016/j.bbabio.2015.01.007

Rengstl, B., Knoppova, J., Komenda, J., and Nickelsen, J. (2013). Characterization of a *Synechocystis* double mutant lacking the photosystem II assembly factors YCF48 and Sll0933. *Planta* 237, 471–480. doi: 10.1007/s00425-012-1720-0

Rengstl, B., Oster, U., Stengel, A., and Nickelsen, J. (2011). An intermediate membrane subfraction in cyanobacteria is involved in an assembly network for photosystem II biogenesis. *J. Biol. Chem.* 286, 21944–21951. doi: 10.1074/jbc.M111.237867

Reynolds, E. S. (1963). The use of lead citrate at high pH as an electron-opaque stain in electron microscopy. *J. Cell Biol.* 17, 208–212. doi: 10.1083/jcb.17.1.208

Sacharz, J., Bryan, S. J., Yu, J., Burroughs, N. J., Spence, E. M., Nixon, P. J., et al. (2015). Sub-cellular location of FtsH proteases in the cyanobacterium *Synechocystis* sp. PCC 6803 suggests localised PSII repair zones in the thylakoid membranes. *Mol. Microbiol.* 96, 448–462. doi: 10.1111/mmi.12940

Schottkowski, M., Gkalympoudis, S., Tzekova, N., Stelljes, C., Schunemann, D., Ankele, E., et al. (2009a). Interaction of the periplasmic PratA factor and the PsbA (D1) protein during biogenesis of photosystem II in *Synechocystis* sp. PCC 6803. *J. Biol. Chem.* 284, 1813–1819. doi: 10.1074/jbc.M806116200

Schottkowski, M., Ratke, J., Oster, U., Nowaczyk, M., and Nickelsen, J. (2009b). Pitt, a novel tetratricopeptide repeat protein involved in light-dependent chlorophyll biosynthesis and thylakoid membrane biogenesis in *Synechocystis* sp. PCC 6803. *Mol. Plant* 2, 1289–1297. doi: 10.1093/mp/ssp075

Silva, P., Thompson, E., Bailey, S., Kruse, O., Mullineaux, C. W., Robinson, C., et al. (2003). FtsH is involved in the early stages of repair of photosystem II in *Synechocystis* sp PCC 6803. *Plant Cell* 15, 2152–2164. doi: 10.1105/tpc.012609

Singh, A. K., Li, H., and Sherman, L. A. (2004). Microarray analysis and redox control of gene expression in the cyanobacterium *Synechocystis* sp. PCC 6803. *Physiol. Plant.* 120, 27–35. doi: 10.1111/j.0031-9317.2004.0232.x

Stengel, A., Gugel, I. L., Hilger, D., Rengstl, B., Jung, H., and Nickelsen, J. (2012). Initial steps of photosystem II de novo assembly and preloading with manganese take place in biogenesis centers in *Synechocystis*. *Plant Cell* 24, 660–675. doi: 10.1105/tpc.111.093914

Stingaciu, L. R., O'neill, H., Liberton, M., Urban, V. S., Pakrasi, H. B., and Ohl, M. (2016). Revealing the dynamics of thylakoid membranes in living cyanobacterial cells. *Sci. Rep.* 6, 19627. doi: 10.1038/srep19627

Suga, M., Akita, F., Hirata, K., Ueno, G., Murakami, H., Nakajima, Y., et al. (2015). Native structure of photosystem II at 1.95 A resolution viewed by femtosecond X-ray pulses. *Nature* 517, 99–103. doi: 10.1038/nature13991

Toth, T. N., Chukhutsina, V., Domonkos, I., Knoppova, J., Komenda, J., Kis, M., et al. (2015). Carotenoids are essential for the assembly of cyanobacterial photosynthetic complexes. *Biochim. Biophys. Acta* 1847, 1153–1165. doi: 10.1016/j.bbabio.2015.05.020

Umena, Y., Kawakami, K., Shen, J. R., and Kamiya, N. (2011). Crystal structure of oxygen-evolving photosystem II at a resolution of 1.9 A. *Nature* 473, 55–60. doi: 10.1038/nature09913

van de Meene, A. M., Hohmann-Marriott, M. F., Vermaas, W. F., and Roberson, R. W. (2006). The three-dimensional structure of the cyanobacterium *Synechocystis* sp. PCC 6803. *Arch. Microbiol.* 184, 259–270. doi: 10.1007/s00203-005-0027-y

Van de Meene, A. M., Sharp, W. P., Mcdaniel, J. H., Friedrich, H., Vermaas, W. F., and Roberson, R. W. (2012). Gross morphological changes in thylakoid membrane structure are associated with photosystem I deletion in *Synechocystis* sp. PCC 6803. *Biochim. Biophys. Acta* 1818, 1427–1434. doi: 10.1016/j.bbamem.2012.01.019

Wegener, K. M., Welsh, E. A., Thornton, L. E., Keren, N., Jacobs, J. M., Hixson, K. K., et al. (2008). High sensitivity proteomics assisted discovery of a novel operon involved in the assembly of photosystem II, a membrane protein complex. *J. Biol. Chem.* 283, 27829–27837. doi: 10.1074/jbc.M803918200

Wilde, A., Lunser, K., Ossenbuhl, F., Nickelsen, J., and Borner, T. (2001). Characterization of the cyanobacterial ycf37: mutation decreases the photosystem I content. *Biochem. J.* 357, 211–216. doi: 10.1042/bj3570211

Yang, H., Liao, L., Bo, T., Zhao, L., Sun, X., Lu, X., et al. (2014). Slr0151 in *Synechocystis* sp. PCC 6803 is required for efficient repair of photosystem II under high-light condition. *J. Integr. Plant Biol.* 56, 1136–1150. doi: 10.1111/jipb.12275

Zak, E., Norling, B., Maitra, R., Huang, F., Andersson, B., and Pakrasi, H. B. (2001). The initial steps of biogenesis of cyanobacterial photosystems occur in plasma membranes. *Proc. Natl. Acad. Sci. U.S.A.* 98, 13443–13448. doi: 10.1073/pnas.241503898

Zhang, L., Paakkarinen, V., Van Wijk, K. J., and Aro, E. M. (1999). Co-translational assembly of the D1 protein into photosystem II. *J. Biol. Chem.* 274, 16062–16067. doi: 10.1074/jbc.274.23.16062

Zinchenko, V., Piven, I., Melnik, V., and Shestakov, S. (1999). Vectors for the complementation analysis of cyanobacterial mutants. *Russ. J. Genet.* 35, 228–232.

Conflict of Interest Statement: The authors declare that the research was conducted in the absence of any commercial or financial relationships that could be construed as a potential conflict of interest.

The reviewer SJ and handling Editor declared their shared affiliation, and the handling Editor states that the process nevertheless met the standards of a fair and objective review.

frontiers in Plant Science

ORIGINAL RESEARCH
published: 31 March 2016
doi: 10.3389/fpls.2016.00405

Photosystem II Repair and Plant Immunity: Lessons Learned from Arabidopsis Mutant Lacking the THYLAKOID LUMEN PROTEIN 18.3

*Sari Järvi[1], Janne Isojärvi[1], Saijaliisa Kangasjärvi[1], Jarkko Salojärvi[2], Fikret Mamedov[3], Marjaana Suorsa[1] and Eva-Mari Aro[1]**

[1] Molecular Plant Biology, Department of Biochemistry, University of Turku, Turku, Finland, [2] Plant Biology, Department of Biosciences, University of Helsinki, Helsinki, Finland, [3] Molecular Biomimetics, Department of Chemistry—Ångström Laboratory, Uppsala University, Uppsala, Sweden

OPEN ACCESS

Edited by:
Julian Eaton-Rye, University of Otago, New Zealand

Reviewed by:
Masaru Kono, The University of Tokyo, Japan
Tiago Toscano Selão, Nanyang Technological University, Singapore

***Correspondence:**
Eva-Mari Aro
evaaro@utu.fi

Specialty section:
This article was submitted to Plant Cell Biology, a section of the journal Frontiers in Plant Science

Received: *15 December 2015*
Accepted: *16 March 2016*
Published: *31 March 2016*

Citation:
Järvi S, Isojärvi J, Kangasjärvi S, Salojärvi J, Mamedov F, Suorsa M and Aro E-M (2016) Photosystem II Repair and Plant Immunity: Lessons Learned from Arabidopsis Mutant Lacking the THYLAKOID LUMEN PROTEIN 18.3. Front. Plant Sci. 7:405. doi: 10.3389/fpls.2016.00405

Chloroplasts play an important role in the cellular sensing of abiotic and biotic stress. Signals originating from photosynthetic light reactions, in the form of redox and pH changes, accumulation of reactive oxygen and electrophile species or stromal metabolites are of key importance in chloroplast retrograde signaling. These signals initiate plant acclimation responses to both abiotic and biotic stresses. To reveal the molecular responses activated by rapid fluctuations in growth light intensity, gene expression analysis was performed with *Arabidopsis thaliana* wild type and the *tlp18.3* mutant plants, the latter showing a stunted growth phenotype under fluctuating light conditions (Biochem. J, 406, 415–425). Expression pattern of genes encoding components of the photosynthetic electron transfer chain did not differ between fluctuating and constant light conditions, neither in wild type nor in *tlp18.3* plants, and the composition of the thylakoid membrane protein complexes likewise remained unchanged. Nevertheless, the fluctuating light conditions repressed in wild-type plants a broad spectrum of genes involved in immune responses, which likely resulted from shade-avoidance responses and their intermixing with hormonal signaling. On the contrary, in the *tlp18.3* mutant plants there was an imperfect repression of defense-related transcripts upon growth under fluctuating light, possibly by signals originating from minor malfunction of the photosystem II (PSII) repair cycle, which directly or indirectly modulated the transcript abundances of genes related to light perception via phytochromes. Consequently, a strong allocation of resources to defense reactions in the *tlp18.3* mutant plants presumably results in the stunted growth phenotype under fluctuating light.

Keywords: *Arabidopsis thaliana*, defense, photosynthesis, photosystem II repair cycle, thylakoid lumen, transcriptomics

INTRODUCTION

Photosystem II (PSII), embedded in the thylakoid membranes, catalyzes light-dependent water splitting with concomitant oxygen evolution and electron transfer to the plastoquinone pool. PSII consists of the chloroplast-encoded core subunits D1, D2, CP43, and CP47, as well as numerous other subunits, encoded by both the chloroplast and nuclear genomes. Of these proteins, the nuclear-encoded proteins PsbO, PsbP, and PsbQ together with the manganese-calcium cluster form the so called oxygen-evolving complex (OEC), located at the lumenal surface of the PSII complex. In higher plants, the functional PSII complex is formed as a PSII dimer, to which nuclear-encoded light-harvesting complex (LHC) II proteins, Lhcb1-6, are tightly connected forming PSII-LHCII supercomplexes.

Photosynthetic water splitting and evolution of one oxygen molecule require four sequential excitations and subsequent charge separations in the reaction center chlorophyll (Chl) P680, thus producing extremely oxidizing, and potentially hazardous reactive oxygen species (ROS), which enhance oxidative damage to PSII as well as to other thylakoid proteins (Krieger-Liszkay et al., 2008; Pospísil, 2009). Despite the existence of detoxification systems for scavenging of ROS, damage to PSII is unavoidable (Aro et al., 1993; Tyystjärvi and Aro, 1996; Takahashi and Badger, 2011). In particular, the PSII core protein D1 is prone to light-induced damage, and thus an efficient repair cycle has evolved for PSII, which includes proteolytic degradation of damaged D1 protein and its replacement with a newly-synthetized D1 copy (reviewed in Baena-Gonzalez and Aro, 2002; Edelman and Mattoo, 2008; Nixon et al., 2010). These processes involve reversible monomerization of the PSII-LHCII supercomplexes (Danielsson et al., 2006), as well as dynamic changes in grana diameter and in lumen volume (Kirchhoff et al., 2011; Herbstova et al., 2012). A vast number of auxiliary proteins, such as kinases, phosphatases, proteases, transporters, and chaperones have been shown to assist the PSII repair cycle (reviewed in Mulo et al., 2008; Chi et al., 2012; Nickelsen and Rengstl, 2013; Järvi et al., 2015). One of these, the THYLAKOID LUMEN PROTEIN OF 18.3 kDa (TLP18.3) has been shown to be required for efficient degradation of the damaged D1 protein and dimerization of the PSII complex (Sirpiö et al., 2007). Notably, high light treatment challenging the PSII repair cycle triggered only a moderate damage of PSII in *tlp18.3* plants (Sirpiö et al., 2007), which suggest that TLP18.3 is not a crucial component of the repair cycle but instead plays a role in fine tuning the repair cycle. Based on structural data, TLP18.3 has been suggested to be an acidic phosphatase, but only low phosphatase activity was measured for TLP18.3 (Wu et al., 2011). Recently, the regulatory role of the PSII repair cycle has been extended to include the maintenance of photosystem I (PSI) and indeed, insufficient regulation of the PSII repair cycle seems to exert an effect also on the function of PSI (Tikkanen et al., 2014). Moreover, PSII is crucial for plant immunity through production of ROS, which are not only damaging the components of the photosynthetic electron transfer chain, but also act as important retrograde signaling molecules (Rodríguez-Herva et al., 2012; de Torres Zabala et al., 2015). In line with this, a functional connection between PSII repair and regulation of cell death in tobacco leaves infected by tobacco mosaic virus has been established (Seo et al., 2000).

While the exact role of photosynthetic components in sensing and signaling the pathogen infection is only emerging, a wealth of information has accumulated during the past few years on the consequences of fluctuating light on the activity of the photosynthetic machinery (Grieco et al., 2012; Suorsa et al., 2012; Allahverdiyeva et al., 2013; Kono and Terashima, 2014). Nevertheless, we still lack knowledge on how the rapid fluctuations in growth light intensity affect the acclimation processes at the level of nuclear gene expression, and even less is known about potential cross-talk between light acclimation, the PSII repair cycle and disease resistance under fluctuating light. Here, we investigated how the constantly fluctuating growth light intensity modulates the transcript profile of wild-type *Arabidopsis thaliana* (hereafter Arabidopsis) plants, and how such an acclimation response is further affected by the deficiency of the thylakoid lumen protein TLP18.3. Five-week old plants grown either under constant or fluctuating light conditions for their entire life span were used as material to study the late stage of the acclimation process.

MATERIALS AND METHODS

Plant Material and Growth Conditions

Arabidopsis, ecotype Columbia 0, wild-type and *tlp18.3* (GABI-Kat 459D12) plants (Sirpiö et al., 2007) were used in all experiments. Plants were grown in 8 h light regime at 23°C either under a photon flux density of 120 μmol photons m^{-2} s^{-1} or under fluctuating light intensities, in which plants were exposed to 50 μmol photons m^{-2} s^{-1} for 5 min and subsequently to high-light of 500 μmol photons m^{-2} s^{-1} for 1 min (Tikkanen et al., 2010), the cycles being repeated during the entire photoperiod. Osram HQI-BT 400 W/D Metal Halide lamps with spectral power distribution from 350 to 800 nm were used as a light source. Five-week-old plants were used for all experiments.

Gene Expression Analyses

Microarray analyses of wild-type and *tlp18.3* plants were performed essentially as in Konert et al. (2015). In short, leaf material was harvested 4 h after the onset of the light period in order to be sure that the plants were in a photosynthetically active state and that the PSII repair cycle was properly ongoing and immediately frozen in liquid nitrogen. RNA was isolated using an Agilent Plant RNA isolation mini kit according to manufacturer's instructions. Cy-3 labeled RNA samples were hybridized to Agilent Arabidopsis Gene Expression Microarrays, 4 × 44 K (Design ID 021169) and scanned with Agilent Technologies Scanner G2565CA with a profile AgilentHD _GX_1Color. Numeric data were produced with Agilent Feature Extraction program, version 10.7.3.

Pre-processing of microarrays was performed using Limma's normexp background correction method to avoid negative or zero corrected intensities, followed by between-array normalization using the quantile method to make all array distributions to have the same empirical distribution. Control probes were filtered and then within-array replicate spots were

replaced with their average. Pair-wise comparisons between groups were conducted using the Linear Models for Microarray Data (Limma) package Version 3.26.1 from Bioconductor (http://www.bioconductor.org/). The false discovery rate of differentially expressed genes for treatment/control and between-treatment comparisons was based on the Benjamini and Hochberg (BH) procedure. Genes with a score below an adjusted *p*-value threshold of 0.01 and which also showed a minimum of twofold change in expression between conditions or genotype were selected as significantly differentially expressed genes. Gene annotations were obtained from the Arabidopsis Information Resource (TAIR; http://www.arabidopsis.org/). Functional clustering and analysis was performed using the Database for Annotation, Visualization and Integrated Discovery (DAVID) (http://david.abcc.ncifcrf.gov/home.jsp) version 6.7. Differentially expressed genes were compared against gene sets collected from various sources such as publications using the Plant GeneSet Enrichment Analysis Toolkit (PlantGSEA) (http://structuralbiology.cau.edu.cn/PlantGSEA/).

To detect co-regulated gene sets, a cluster analysis of the differentially expressed genes was carried out using data from (Georgii et al., 2012), consisting of microarray data downloaded from NASCArrays (ftp://uiftparabid.nottingham.ac.uk/NASCarrays/By_Experiment_ID/), ArrayExpress (http://www.ebi.ac.uk/microarrayas/ae/), Gene Expression Omnibus (http://www.ncbi.nlm.nih.gov/geo/), and The Integrated Microarray Database System (http://ausubellab.mgh.harvard.edu/). Arrays were normalized with Robust Multi-array Average (RMA), and log2 ratio of the mean of treatment and control expressions across biological replicates was computed. Bayesian Hierarchical Clustering was carried out using R package BHC (Cooke et al., 2011) using log2 fold change ± 1 as discretization threshold. Gene set enrichment analysis of the co-regulated gene clusters was carried out using StringDB (http://string-db.org/; Szklarczyk et al., 2015).

Isolation of the Thylakoid Membrane and Separation of Protein Complexes

Thylakoid isolation and blue native (BN)-PAGE were performed essentially as described in Järvi et al. (2011). Sodium fluoride was included in thylakoid isolation buffers for samples intended for BN-PAGE, whilst excluded from thylakoids used for spectroscopy analyses (see below). For BN-PAGE, the thylakoid membrane (4 μg Chl) was resuspended into ice-cold 25BTH20G buffer [25 mM BisTris/HCl (pH 7.0), 20% (w/v) glycerol and 0.25 mg ml^{-1} Pefabloc] to a Chl concentration of 1.0 mg ml^{-1}. An equal volume of 2.0% (w/v) detergent (n-dodecyl β-D-maltoside, Sigma) solution (diluted in 25BTH20G) was added to the sample and thylakoid membrane was solubilized in darkness for 5 min on ice. Traces of insoluble material were removed by centrifugation at 18,000 g at 4°C for 20 min. Prior to loading, the samples were supplemented with a one-tenth volume of Serva Blue G buffer [100 mM BisTris/HCl (pH 7.0), 0.5 M ACA, 30% (w/v) sucrose, and 50 mg ml^{-1} Serva Blue G].

Spectroscopic Quantitation of PSI and PSII

Room temperature continuous wave electron paramagnetic resonance (EPR) spectroscopy was performed essentially as described in Danielsson et al. (2004) and Suorsa et al. (2015). Measurements were performed at the Chl concentration of 2 mg ml^{-1}.

Photosynthetic Activity Measurements

The Dual-PAM-100 (Walz, http://www.walz.com/) was used for the measurement of PSII quantum yields. Quantum yields of PSII (F_V/F_M, Φ_{II}, Φ_{NPQ}, and Φ_{NO}) were determined from leaves dark adapted for 30 min before the measurements. Saturating pulse (800 ms, 6000 μmol photons $m^{-2}s^{-1}$) was applied to determine the maximal fluorescence. Measurements were done in actinic red light of 50, 120, or 500 μmol photons $m^{-2}s^{-1}$.

Statistical Analyses

The numerical data were subjected to statistical analysis by Student's *t*-test with statistical significance at the $p < 0.05$.

RESULTS

Fluctuating Growth Light Only Slightly Modified the Photosynthetic Light Reactions

Accumulating evidence during recent years has demonstrated that sudden, abrupt changes in light intensity threaten particularly PSI, not PSII (Grieco et al., 2012; Suorsa et al., 2012; Allahverdiyeva et al., 2013; Kono and Terashima, 2014). Indeed, quantitation of the functional PSI/PSII ratios from wild-type plants with EPR revealed a PSI/PSII ratio of 1.12 for plants grown under constant light conditions (Suorsa et al., 2015), whereas plants grown under fluctuating light conditions exhibited a clearly lower value, 1.02.

The *tlp18.3* plants showed a distinct stunted phenotype upon growth under fluctuating white light and the dry weight of the *tlp18.3* plants (12.2 ± 5.7 mg) was markedly decreased as compared to wild type (29.9 ± 4.7 mg; $n = 6$). This observation prompted us to monitor whether the oligomeric structure of the thylakoid membrane protein complexes of wild-type and *tlp18.3* plants grown either under constant or fluctuating light conditions is altered. Malfunction of the PSII repair cycle is often evidenced by a low amount of the most active PSII complexes, the PSII-LHCII complexes, accompanied by a high amount of PSII monomers, which are under the repair cycle (Danielsson et al., 2006). To that end, the BN-PAGE separation of thylakoid protein complexes according to their molecular mass was applied. In line with earlier results (Sirpiö et al., 2007), the *tlp18.3* thylakoids accumulated slightly less of the PSII-LHCII complexes under constant light (**Figure 1**). Similar result was also evident under fluctuating light intensities, the amount of PSII-LHCII being somewhat lower in *tlp18.3* plants as compared to wild type. However, no significant differences were observed in heterogeneity of the photosynthetic protein complexes, when wild-type and mutant plants grown either under constant or fluctuating light were compared (**Figure 1**). A previous report has shown that the maximal PSII quantum yield is not changed

in *tlp18.3* plants grown under constant growth light conditions as compared to wild type (Sirpiö et al., 2007). In line with this, the maximum quantum yield and effective quantum yields of PSII remained rather similar, when the *tlp18.3* and wild-type plants grown their entire life span under fluctuating light were compared (**Table 1**). Indeed, the PSII activity was only slightly down-regulated in *tlp18.3* plants as compared to wild type. Thus, the growth defect shown by the *tlp18.3* plants under fluctuating light intensities does not originate from the diminished pool of active PSII complexes.

Consequences of Fluctuating Growth Light Intensity on Gene Expression

To further characterize plant acclimation to fluctuating light, we performed transcript profiling of the wild-type and *tlp18.3* plants grown under constant and fluctuating light intensities and compared the four datasets: (*i*) wild-type plants grown under fluctuating vs. constant growth light, (*ii*) *tlp18.3* plants grown under fluctuating vs. constant growth light, (*iii*) *tlp18.3* vs. wild-type plants grown under fluctuating light, and (*iv*) *tlp18.3* vs. wild-type plants grown under constant light. Gene enrichment analysis and functional annotation clustering of differentially expressed genes were performed using the DAVID bioinformatic resource (the cutoff was set to logFC > 1 and the adjusted *p*-value threshold to a minimum of 0.01).

Wild-type plants grown under fluctuating light showed significantly different transcript abundance for 406 genes as compared to wild type grown under constant light, whereas in the *tlp18.3* mutant, 321 genes responded differentially to fluctuating light as compared to growth light (**Figure 2**). When the transcript abundances between the genotypes was compared, 237 genes showed significantly different transcript abundance in *tlp18.3* plants compared to wild type when grown under fluctuating light conditions, whereas under constant growth light the number of differentially expressed genes between wild type and the *tlp18.3* mutant was 102 (**Figure 2**). Thus, it can be concluded that the growth light condition altered the number of differentially regulated genes more pronouncedly than the genotype. Moreover, the wild-type plants showed more profound changes at their gene expression level as a response to fluctuating growth light than the *tlp18.3* plants.

TABLE 1 | PSII quantum yields of wild-type and *tlp18.3* plants grown under fluctuating light.

Photosynthetic parameter	Wild type	*tlp18.3*
EFFECTIVE PSII QUANTUM YIELD, Φ_{II}		
50 μmol photons $m^{-2}s^{-1}$	0.50 ± 0.02	0.47 ± 0.04
120 μmol photons $m^{-2}s^{-1}$	0.28 ± 0.06	0.26 ± 0.03
500 μmol photons $m^{-2}s^{-1}$	0.04 ± 0.01	0.03 ± 0.01
NON-PHOTOCHEMICAL ENERGY DISSIPATION, Φ_{NPQ}		
50 μmol photons $m^{-2}s^{-1}$	0.13 ± 0.02	0.15 ± 0.04
120 μmol photons $m^{-2}s^{-1}$	0.48 ± 0.07	0.47 ± 0.03
500 μmol photons $m^{-2}s^{-1}$	0.68 ± 0.01	0.66 ± 0.01*
YIELD OF NON-REGULATED NON-PHOTOCHEMICAL ENERGY LOST, Φ_{NO}		
50 μmol photons $m^{-2}s^{-1}$	0.37 ± 0.01	0.38 ± 0.03
120 μmol photons $m^{-2}s^{-1}$	0.24 ± 0.01	0.27 ± 0.00*
500 μmol photons $m^{-2}s^{-1}$	0.28 ± 0.00	0.31 ± 0.02
MAXIMAL QUANTUM YIELD OF PSII, F_V/F_M		
	0.78 ± 0.01	0.76 ± 0.02*

The values are the means ± SD, n = 4–5, except for F_V/F_M n = 12. Statistically significant differences comparing the mutant plants to that of the corresponding wild type are marked with asterix (*). See text for details.

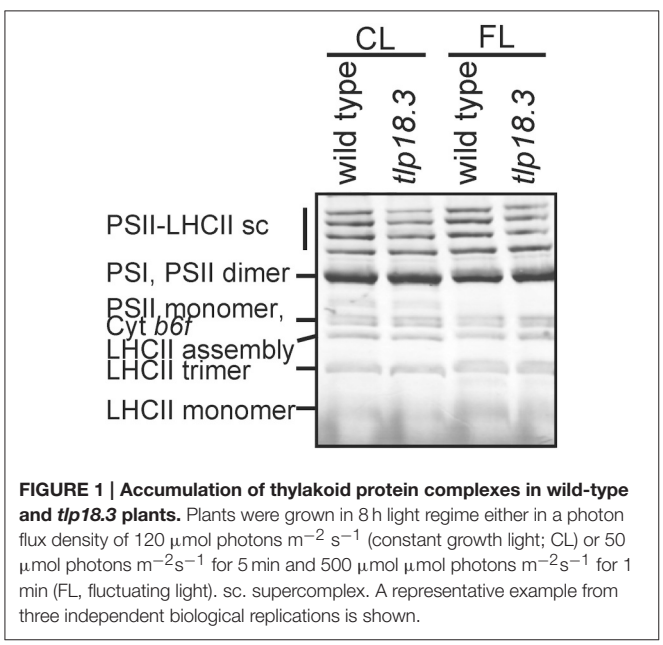

FIGURE 1 | Accumulation of thylakoid protein complexes in wild-type and *tlp18.3* plants. Plants were grown in 8 h light regime either in a photon flux density of 120 μmol photons m^{-2} s^{-1} (constant growth light; CL) or 50 μmol photons $m^{-2}s^{-1}$ for 5 min and 500 μmol μmol photons $m^{-2}s^{-1}$ for 1 min (FL, fluctuating light). sc. supercomplex. A representative example from three independent biological replications is shown.

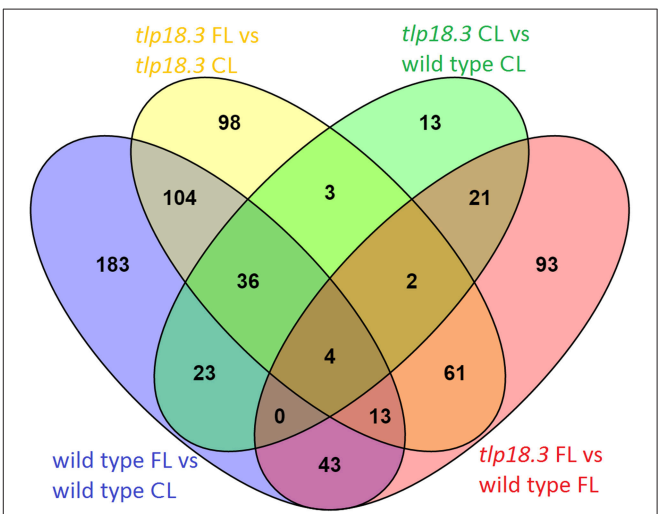

FIGURE 2 | Venn diagram showing the overlap of significantly differentially regulated genes (logFC > 1) in response to either fluctuating light (FL) as compared to constant growth light (CL) or deficient function of the TLP18.3 protein.

Plants Grown under Fluctuating Light did not Show Differential Abundance of Photosynthesis Related Transcripts

Examination of differentially expressed genes revealed no photosynthesis-related gene ontologies in any of the four datasets analyzed (**Tables 2, 3**). Indeed, no gene ontologies related to photosynthetic light reactions, Calvin-Benson-Bassham cycle, or biosynthesis of photosynthetic pigments was observed in the gene enrichment analysis. Presumably, regulation of the photosynthetic machinery at transcriptional level does not play an important role during acclimation to relatively mild light intensity fluctuations, being designed such that the total amount of photons hitting the leaf remained nearly unchanged during the 8 h light period, when constant and fluctuating light conditions were compared. Likewise, deficient function of the TLP18.3 protein had only minor effects on transcript abundance of various photosynthesis genes.

Fluctuating Light Conditions Induced Transcriptional Adjustments in Immunity Related Genes Both in Wild-Type and *tlp18.3* Plants

Bioinformatic analysis revealed that the majority of differentially expressed gene ontologies between plants grown under fluctuating and constant light conditions were linked to biotic or abiotic stress responses (**Tables 2A,B**). In wild type, growth under fluctuating light resulted in decreased transcript abundance within numerous gene ontologies related to plant immunity, as compared to wild type grown under constant light (**Table 2A**). These genes included mitogen-activated protein kinases (MAPKs) involved in early defense signaling, Toll/Interleukin-1 receptor-nucleotide binding site (TIR-NBS) class resistance (R) proteins mediating effector-triggered immunity (ETI) as well as pathogen related defense proteins, such as plant defensins (Supplementary Table 1). In contrast, the *tlp18.3* mutant showed both decreased and increased transcript abundance within gene ontologies related to plant immunity, when fluctuating and constant light grown plants were compared to each other (**Table 2B**). For example, ankyrin *BDA1* (*AT5G54610*), which is induced by salicylic acid (SA) and is involved in innate immunity (Blanco et al., 2005; Yang et al., 2012) showed cumulative repression in the transcript abundance in response to fluctuating light and deficient function of the TLP18.3 protein. In contrast, plant defensin *PDF2.1* (*AT2G02120*) and defensin-like (*AT2G43535*) genes, which are activated in response to fungal infection, were induced in *tlp18.3* plants under fluctuating light.

With respect to abiotic stress, gene ontologies "response to UV" and "response to light stimulus" were enriched in the transcriptome of *tlp18.3* leaves, when plants grown under fluctuating and constant light were compared (**Table 2B**). For example, increased abundance of transcripts for *EARLY LIGHT-INDUCED PROTEIN2* (*ELIP2*; *AT4G14690*), which modulates Chl biosynthesis to prevent photo-oxidative stress (Tzvetkova-Chevolleau et al., 2007; Hayami et al., 2015), was observed in the fluctuating-light-grown *tlp18.3* plants (Supplementary Table 1). In contrast, no gene ontologies related to light perception showed differential expression in the wild-type plants as a

TABLE 2 | Classification of significantly differently expressed genes base on gene enrichment analysis of plants grown either under fluctuating light (FL) or constant growth light (CL): (A) Gene enrichment analysis of wild-type plants grown either under fluctuating or constant light; (B) Gene enrichment analysis of *tlp18.3* plants grown either under fluctuating or constant light.

Term		Count	*P*-value
(A) WILD TYPE FL vs. WILD TYPE CL			
Increased Transcript Abundance			
GOTERM_MF_FAT	GO:0005507 copper ion binding	5	0.0055
GOTERM_CC_FAT	GO:0031225 anchored to membrane	6	0.0076
Decreased Transcript Abundance			
GOTERM_BP_FAT	GO:0006952 defense response	43	3.26E-14
GOTERM_MF_FAT	GO:0004672 *protein kinase activity*	40	7.91E-12
GOTERM_BP_FAT	GO:0010033 *response to organic substance*	42	1.18E-11
GOTERM_BP_FAT	GO:0006468 *protein amino acid phosphorylation*	39	4.18E-11
GOTERM_BP_FAT	GO:0009751 *response to salicylic acid stimulus*	16	8.69E-11
GOTERM_BP_FAT	GO:0006955 immune response	20	4.62E-10
GOTERM_BP_FAT	GO:0016310 *phosphorylation*	39	7.75E-10
GOTERM_BP_FAT	GO:0010200 response to chitin	14	1.24E-09
GOTERM_MF_FAT	GO:0004674 *protein serine/threonine kinase activity*	33	4.75E-09
GOTERM_BP_FAT	GO:0006796 *phosphate metabolic process*	39	6.76E-09
GOTERM_BP_FAT	GO:0006793 *phosphorus metabolic process*	39	6.91E-09
GOTERM_BP_FAT	GO:0045087 innate immune response	18	8.31E-09
GOTERM_BP_FAT	GO:0009617 *response to bacterium*	17	1.02E-08
GOTERM_BP_FAT	GO:0009611 *response to wounding*	13	7.11E-08
GOTERM_BP_FAT	GO:0042742 *defense response to bacterium*	14	1.10E-07
GOTERM_BP_FAT	GO:0009743 response to carbohydrate stimulus	14	2.74E-07
GOTERM_MF_FAT	GO:0032559 *adenyl ribonucleotide binding*	49	1.85E-06
GOTERM_MF_FAT	GO:0030554 *adenyl nucleotide binding*	50	5.06E-06
GOTERM_MF_FAT	GO:0001883 *purine nucleoside binding*	50	5.06E-06
GOTERM_MF_FAT	GO:0001882 *nucleoside binding*	50	5.54E-06
GOTERM_MF_FAT	GO:0005524 ATP binding	47	7.74E-06
GOTERM_BP_FAT	GO:0009814 defense response, incompatible interaction	9	9.97E-06
GOTERM_BP_FAT	GO:0009873 ethylene mediated signaling pathway	11	1.73E-05
GOTERM_BP_FAT	GO:0009723 response to ethylene stimulus	13	2.44E-05
GOTERM_MF_FAT	GO:0032555 purine ribonucleotide binding	49	3.11E-05
GOTERM_MF_FAT	GO:0032553 ribonucleotide binding	49	3.11E-05

(Continued)

TABLE 2 | Continued

Term		Count	*P*-value
(A) WILD TYPE FL vs. WILD TYPE CL			
GOTERM_BP_FAT	GO:0009753 response to jasmonic acid stimulus	10	5.35E-05
GOTERM_BP_FAT	GO:0009719 response to endogenous stimulus	26	5.38E-05
GOTERM_MF_FAT	GO:0017076 purine nucleotide binding	50	7.16E-05
GOTERM_BP_FAT	GO:0000160 two-component signal transduction system	11	1.41E-04
GOTERM_MF_FAT	GO:0005529 sugar binding	8	3.13E-04
GOTERM_MF_FAT	GO:0000166 nucleotide binding	52	0.0016
GOTERM_MF_FAT	GO:0004713 protein tyrosine kinase activity	11	0.0016
GOTERM_BP_FAT	GO:0009725 response to hormone stimulus	21	0.0021
GOTERM_BP_FAT	GO:0009816 defense response to bacterium	4	0.0028
GOTERM_BP_FAT	GO:0009620 *response to fungus*	13	0.0031
GOTERM_MF_FAT	GO:0005509 calcium ion binding	12	0.0034
GOTERM_BP_FAT	GO:0009863 salicylic acid mediated signaling pathway	4	0.0038
GOTERM_BP_FAT	GO:0006979 response to oxidative stress	10	0.0043
GOTERM_BP_FAT	GO:0043900 regulation of multi-organism process	3	0.0050
GOTERM_CC_FAT	GO:0005618 cell wall	15	0.0057
GOTERM_BP_FAT	GO:0009867 jasmonic acid mediated signaling pathway	4	0.0065
GOTERM_CC_FAT	GO:0030312 external encapsulating structure	15	0.0065
GOTERM_BP_FAT	GO:0016265 death	9	0.0068
GOTERM_BP_FAT	GO:0008219 cell death	9	0.0068
GOTERM_CC_FAT	GO:0012505 endomembrane system	59	0.0073
GOTERM_MF_FAT	GO:0030246 carbohydrate binding	8	0.0073
GOTERM_BP_FAT	GO:0009625 response to insect	3	0.0099
(B) *tlp18.3* FL vs. *tlp18.3* CL			
Increased Transcript Abundance			
GOTERM_BP_FAT	GO:0009611 *response to wounding*	8	1.33E-04
GOTERM_BP_FAT	GO:0010224 response to UV-B	5	4.47E-04
GOTERM_MF_FAT	GO:0080030 methyl indole-3-acetate esterase activity	3	0.0013
GOTERM_BP_FAT	GO:0009628 response to abiotic stimulus	20	0.0017
GOTERM_BP_FAT	GO:0009411 response to UV	5	0.0022
GOTERM_MF_FAT	GO:0030414 peptidase inhibitor activity	4	0.0032
GOTERM_BP_FAT	GO:0009620 *response to fungus*	10	0.0064
GOTERM_MF_FAT	GO:0004857 enzyme inhibitor activity	6	0.0081
GOTERM_BP_FAT	GO:0009416 response to light stimulus	10	0.0094
GOTERM_MF_FAT	GO:0005385 zinc ion transmembrane transporter activity	3	0.0099
Decreased Transcript Abundance			
GOTERM_BP_FAT	GO:0009751 *response to salicylic acid stimulus*	8	4.23E-06
GOTERM_BP_FAT	GO:0009617 *response to bacterium*	9	1.14E-05
GOTERM_MF_FAT	GO:0004672 *protein kinase activity*	15	8.88E-05
GOTERM_MF_FAT	GO:0004674 *protein serine/threonine kinase activity*	13	3.89E-04
GOTERM_BP_FAT	GO:0006468 *protein amino acid phosphorylation*	14	6.61E-04
GOTERM_BP_FAT	GO:0006793 *phosphorus metabolic process*	15	0.0011
GOTERM_BP_FAT	GO:0042742 *defense response to bacterium*	6	0.0013
GOTERM_BP_FAT	GO:0016310 *phosphorylation*	14	0.0017
GOTERM_BP_FAT	GO:0006796 *phosphate metabolic process*	14	0.0033
GOTERM_BP_FAT	GO:0006869 lipid transport	5	0.0041
GOTERM_BP_FAT	GO:0010033 *response to organic substance*	13	0.0049
GOTERM_BP_FAT	GO:0010876 lipid localization	5	0.0061
GOTERM_MF_FAT	GO:0030554 *adenyl nucleotide binding*	19	0.0078
GOTERM_MF_FAT	GO:0001883 *purine nucleoside binding*	19	0.0078
GOTERM_MF_FAT	GO:0001882 *nucleoside binding*	19	0.0081
GOTERM_MF_FAT	GO:0032559 *adenyl ribonucleotide binding*	18	0.0092

Categories, which co-exist in (A) and (B), are italicized.
Gene enrichment analysis was performed using DAVID (adjusted p-value threshold minimum 0.01). % indicates the percentage of genes differentially regulated over the number of total genes within the term. BP, biological process; CC, cellular component; GO, gene ontology; MF, molecular function.

response to fluctuating light (**Table 2A**). Decreased transcript abundance of gene ontologies associated with lipid localization and lipid transport were also observed as response to fluctuating light specifically in *tlp18.3* leaves. Several genes encoding lipid-transfer proteins such as *LIPID TRANSFER PROTEIN 3* (*LTP3*; *AT5G59320*), which mediates freezing and drought stress in Arabidopsis (Guo et al., 2013), were down-regulated in the *tlp18.3* mutant, when plants were grown under fluctuating light as compared to constant growth light (Supplementary Table 1).

When fluctuating-light-grown *tlp18.3* and wild-type plants were compared to each other, increased transcript abundance of genes related to the defense mechanisms in the *tlp18.3* mutant was again the most prominent result (**Table 3A**). Enrichment analysis and functional annotation clustering of the differentially expressed gene ontologies in *tlp18.3* and wild-type plants also revealed that several gene clusters related to abiotic stresses were

TABLE 3 | Classification of significantly differentially expressed genes base on gene enrichment analysis in wild-type and *tlp18.3* plants: (A) Gene enrichment analysis of in *tlp18.3* plants as compared to wild-type plants grown under fluctuating light (FL); (B) Gene enrichment analysis of in *tlp18.3* plants as compared to wild-type plants grown under constant light (CL).

Term		Count	*P*-value
(A) *tlp18.3* FL vs. WILD TYPE FL			
Increased Transcript Abundance			
GOTERM_BP_FAT	GO:0009611 response to wounding	12	1.75E-10
GOTERM_BP_FAT	GO:0010033 response to organic substance	24	7.66E-09
GOTERM_BP_FAT	GO:0010200 response to chitin	10	1.45E-08
GOTERM_BP_FAT	GO:0009743 response to carbohydrate stimulus	11	5.85E-08
GOTERM_BP_FAT	GO:0009719 response to endogenous stimulus	18	5.33E-06
GOTERM_BP_FAT	GO:0009725 response to hormone stimulus	16	4.05E-05
GOTERM_BP_FAT	GO:0009723 response to ethylene stimulus	9	4.41E-05
GOTERM_BP_FAT	GO:0006952 defense response	16	1.66E-04
GOTERM_BP_FAT	GO:0000160 two-component signal transduction system	7	8.21E-04
GOTERM_BP_FAT	GO:0009628 response to abiotic stimulus	16	8.28E-04
GOTERM_BP_FAT	GO:0009409 response to cold	7	0.0012
GOTERM_BP_FAT	GO:0009873 ethylene mediated signaling pathway	6	0.0017
GOTERM_BP_FAT	GO:0009612 response to mechanical stimulus	3	0.0029
GOTERM_BP_FAT	GO:0009631 cold acclimation	3	0.0045
GOTERM_BP_FAT	GO:0006869 lipid transport	5	0.0066
GOTERM_BP_FAT	GO:0009620 response to fungus	8	0.0066
GOTERM_CC_FAT	GO:0012505 endomembrane system	29	0.0072
GOTERM_BP_FAT	GO:0009753 response to jasmonic acid stimulus	5	0.0081
GOTERM_BP_FAT	GO:0009266 response to temperature stimulus	7	0.0090
GOTERM_BP_FAT	GO:0010876 lipid localization	5	0.0098
Decreased Transcript Abundance			
GOTERM_BP_FAT	GO:0009642 response to light intensity	5	5.96E-05
GOTERM_BP_FAT	GO:0006979 response to oxidative stress	7	1.73E-04
GOTERM_MF_FAT	GO:0004784 superoxide dismutase activity	3	2.66E-04
GOTERM_MF_FAT	GO:0016721 oxidoreductase activity.	3	2.66E-04
GOTERM_BP_FAT	GO:0009628 response to abiotic stimulus	12	4.88E-04
GOTERM_BP_FAT	GO:0000302 response to reactive oxygen species	5	7.28E-04
GOTERM_BP_FAT	GO:0006801 superoxide metabolic process	3	7.45E-04
GOTERM_BP_FAT	GO:0010035 response to inorganic substance	8	8.78E-04
GOTERM_MF_FAT	GO:0005507 copper ion binding	5	0.0013
GOTERM_BP_FAT	GO:0009416 response to light stimulus	7	0.0022
GOTERM_BP_FAT	GO:0009314 response to radiation	7	0.0026
GOTERM_BP_FAT	GO:0009617 response to bacterium	5	0.0055
GOTERM_BP_FAT	GO:0009063 cellular amino acid catabolic process	3	0.0073
GOTERM_BP_FAT	GO:0009644 response to high-light intensity	3	0.0073
GOTERM_BP_FAT	GO:0009310 amine catabolic process	3	0.0083
(B) *tlp18.3* CL vs. WILD TYPE CL			
Increased Transcript Abundance			
GOTERM_MF_FAT	GO:0030614 oxidoreductase activity.	5	1.92E-09
GOTERM_MF_FAT	GO:0008794 arsenate reductase (glutaredoxin) activity	5	1.92E-09
GOTERM_MF_FAT	GO:0030613 oxidoreductase activity.	5	1.92E-09
GOTERM_MF_FAT	GO:0030611 arsenate reductase activity	5	2.62E-09
GOTERM_MF_FAT	GO:0015035 protein disulfide oxidoreductase activity	6	5.97E-09
GOTERM_MF_FAT	GO:0015036 disulfide oxidoreductase activity	6	1.21E-08
GOTERM_MF_FAT	GO:0016667 oxidoreductase activity	6	1.84E-07
GOTERM_BP_FAT	GO:0045454 cell redox homeostasis	6	8.27E-07
GOTERM_BP_FAT	GO:0022900 electron transport chain	6	2.05E-06
GOTERM_BP_FAT	GO:0019725 cellular homeostasis	6	8.08E-06
GOTERM_BP_FAT	GO:0042592 homeostatic process	6	2.07E-05
GOTERM_BP_FAT	GO:0006091 generation of precursor metabolites and energy	6	1.23E-04
GOTERM_MF_FAT	GO:0009055 electron carrier activity	6	0.0012
Decreased Transcript Abundance			
GOTERM_BP_FAT	GO:0009751 response to salicylic acid stimulus	5	4.07E-04
GOTERM_MF_FAT	GO:0004672 protein kinase activity	8	0.0038
GOTERM_BP_FAT	GO:0010033 response to organic substance	9	0.0050
GOTERM_MF_FAT	GO:0004674 protein serine/threonine kinase activity	7	0.0086

Gene enrichment analysis was performed using DAVID (adjusted p-value threshold minimum 0.01). % indicates the percentage of genes differentially regulated over the number of total genes within the term. BP, biological process; CC, cellular component; GO, gene ontology; MF, molecular function.

differentially expressed in *tlp18.3* plants as compared to wild type under fluctuating light. Decreased transcript abundance of gene ontologies "response to light stimulus" and "response to oxidative stress" was observed in the *tlp18.3* mutant as compared to wild type. Closer look at the genes among these categories pinpointed that the transcript abundance for cytosolic and chloroplastic *COPPER/ZINC SUPEROXIDE DISMUTASES 1* (*AT1G08830*) and 2 (*AT2G28190*), respectively, was repressed in *tlp18.3* plants as compared to wild type under fluctuating light conditions (Supplementary Table 1).

Finally, when constant-light-grown *tlp18.3* and wild-type plants were compared, only a few gene ontologies related to biotic or abiotic stresses were identified (**Table 3B**). This result is consistent with the postulated role of TLP18.3 specifically during the dynamic light acclimation process, as evidenced by the distinct growth phenotype of the mutant plants under fluctuating light.

Adjustments in Immunity-Related Genes under Fluctuating Light are Linked to Plant Hormones

Plant acclimation to various stresses, including light stress, is regulated by signaling cascades, which include plant hormones as central components (Karpinski et al., 2013; Müller and Munné-Bosch, 2015). In wild-type plants, growth under fluctuating light as compared to constant light resulted in reduced transcript abundance of several genes related to SA signaling cascades (**Table 2A**). For example, expression of a gene encoding SYSTEMIC ACQUIRED RESISTANCE DEFICIENT 1 (SARD1; AT1G73805), a key regulator of ISOCHORISMATE SYNTHASE 1, a rate-limiting enzyme in pathogen-induced SA biosynthesis (Zhang et al., 2010), was shown to be down-regulated in wild-type plants grown under fluctuating light. Also expression of a gene encoding BENZOIC ACID/SA CARBOXYL METHYLTRANSFERASE 1 (BSMT1; AT3G11480), which synthetizes methyl salicylate (a mobile signal molecule for plant systemic acquired resistance) from SA (Park et al., 2007), was down-regulated in fluctuating light. In line with these results, *WALL-ASSOCIATED KINASE 2* (*WAK2; AT1G21270*) and *L-TYPE LECTIN RECEPTOR KINASE IV.1* (*LecRK-IV.1; AT2G37710*), which are both induced by SA, showed reduced transcript abundance in wild-type plants as response to fluctuating light (He et al., 1999; Blanco et al., 2005) (Supplementary Table 1). Also the *tlp18.3* plants grown under fluctuating light showed decreased abundance of gene transcripts related to SA signaling as compared to plants grown under constant light (**Table 2B**). However, the number of repressed genes was lower in the *tlp18.3* mutant as compared to wild type and no differential expression of SARD1 or BSMT1 were observed in *tlp18.3* plants as response to fluctuating light (**Table 2**, Supplementary Table 1). Decreased amount of transcripts related to SA signaling was also evident when *tlp18.3* plants grown under constant light were compared to wild type (**Table 3B**), while no difference in SA signaling was observed between *tlp18.3* and wild-type plants grown under fluctuating light (**Table 3A**). To that end, the fluctuating light condition and to a lesser extent deficient function of the TLP18.3 protein repressed the SA responsive genes.

Similarly, ethylene (ET)- and jasmonate (JA)-related defense pathways showed reduced transcript abundance in wild-type plants grown under fluctuating light as compared to constant light (**Table 2A**), while in the *tlp18.3* mutant no difference was observed in ET/JA defense reactions between the light conditions (**Table 2B**). It seems that the repression of ET/JA responsive gene expression under fluctuating light is blocked in the *tlp18.3* mutants, which became apparent when ET/JA responses between fluctuating light grown *tlp18.3* and wild-type plants were compared (**Table 3A**).

The most prominent alteration in the gene ontology level, when the transcript abundances of constant light grown *tlp18.3* and wild-type plants were compared, was an increase in transcripts of six genes encoding CC-type glutaredoxins (*ROXY 5, ROXY 11-15*) and two of those, *ROXY 5* and *ROXY 13*, were up-regulated in *tlp18.3* as compared to wild type also under fluctuating light (**Tables 3, 4**, Supplementary Table 1). As CC-type glutaredoxins have been suggested to be capable of suppressing the JA and ET-induced defense genes (Zander et al., 2012), a causal connection might exist between expression of JA and ET-responsive genes and differential expression of *ROXY* genes. It can be concluded that alteration in the gene expression patterns of SA, ET, and JA signaling are taking place during plant acclimation to fluctuating light and that these alterations are strongly affected by the deficient function of the TLP18.3 protein.

Phytochrome-Mediated Light Signaling is Likely to be Altered in *tlp18.3* Plants

Next, we wanted to further explore which Arabidopsis genes showed a differential expression pattern in the *tlp18.3* plants both under constant and fluctuating light conditions. In addition to ROXY5 and ROXY13 located in the endomembrane system, genes encoding cold (DELTA-9 DESATURASE 1)

TABLE 4 | List of genes which are significantly differentially expressed in *tlp18.3* plants as compared to wild type both under fluctuating (FL) and constant light (CL) conditions (logFC > 1).

Gene		logFC FL	logFC CL
Drought-repressed 4	AT1G73330	2.06	1.15
ELF4	AT2G40080	1.72	1.60
Major facilitator superfamily protein	AT5G62730	1.46	1.25
Major facilitator superfamily protein	AT2G16660	1.32	1.18
Monothiol glutaredoxin-S4/ROXY 13	AT4G15680	1.21	1.57
Putative glutaredoxin-C12/ROXY 5	AT2G47870	1.18	1.23
Delta-9 acyl-lipid desaturase 1	AT1G06080	−1.35	−1.01
HAD superfamily, subfamily IIIB acid phosphatase	AT4G29270	−1.94	−1.54
Transcription factor PIL1	AT2G46970	−2.23	−1.37
Transcription factor HFR1	AT1G02340	−2.31	−1.29
TLP18.3	AT1G54780	−7.13	−7.07

and drought-repressed (DROUGHT-REPRESSED 4) proteins, acid phosphatase (AT4G29270), and two putative membrane transporters (AT5G62730, AT2G16660) showed differential expression in the *tlp18.3* mutant. Interestingly, two genes encoding bHLH class phytochrome A-signaling components, LONG HYPOCOTYL IN FAR-RED 1 (HFR1; AT1G02340) and PHYTOCHROME INTERACTING FACTOR 3-LIKE 1 (PIL1; AT2G46970; Fairchild et al., 2000; Salter et al., 2003), showed decreased transcript abundance in *tlp18.3* plants as compared to wild type (**Table 4**). Instead, expression of the gene encoding EARLY FLOWERING 4 (ELF4; AT2G40080), a phytochrome-controlled regulator of circadian clock was induced in the *tlp18.3* mutant as compared to wild type. Taken together, the deficient function of TLP18.3 is likely to change the phytochrome-mediated light signaling both under constant and fluctuating light intensities.

Decreased Transcript Abundance of Dark-Induced Genes Suggest that Nitrogen to Carbon and/or Phosphorus to Carbon Ratios Might be Altered in *tlp18.3* Plants under Fluctuating Light

Nutrient availability plays an important regulatory role in growth and development of plants, but also cross-talk between nutrient availability and disease resistance exist (Huber, 1980; Hermans et al., 2006). Interestingly, *GLUTAMINE-DEPENDENT ASPARAGINE SYNTHASE 1/DARK-INDUCED 6* (*ASN1/DIN6; AT3G47340)* and *DARK-INDUCED 1/SENESCENCE 1* (*DIN1/SEN1; AT4G35770*) genes showed strong down-regulation in fluctuating light grown *tlp18.3* plants as compared to either fluctuating light grown wild type or constant light grown *tlp18.3* plants (Supplementary Table 1). ASN1/DIN6 regulates the flow of nitrogen into asparagine, which acts as a nitrogen storage and transport compound in darkness and its gene expression is regulated by the nitrogen to carbon ratio (Lam et al., 1994). DIN1/SEN1, which has been suggested to contribute to enhanced susceptibility to plant viruses, is induced by phosphate starvation and repressed by sugars (Fernández-Calvino et al., 2015). The differential expression of *ASN1/DIN6* and *DIN1/SEN1* is linked to deficient function of TLP18.3 under fluctuating light but the exact mechanism behind transcriptional repression of these two genes remains to be verified.

Cluster Analysis of Genes whose Expression in Fluctuating Light Requires Functionality of TLP18.3

Finally, to shed light on gene expression changes that depend on the functionality of TLP18.3 under fluctuating light, the expression profiles of genes differentially expressed in wild type but not in *tlp18.3* upon growth under fluctuating light were clustered using publicly available datasets (**Figure 3**). These wild-type specific genes grouped into 13 co-expression clusters, which were further analyzed for enrichment of gene ontology categories (Supplementary Table 2). Clusters 3-13 contained genes with increased transcript abundance in different abiotic stress conditions including salinity and drought as well as methyl viologen (Paraquat; PQ) and the SA analog BTH (**Figure 3**). Under UV-B stress, in contrast, the expression of these genes was generally down-regulated (**Figure 3**). This pattern of gene expression was particularly evident within the gene clusters 5, 6, and 9, which showed significant enrichment of gene ontology categories related to plant immunity, such as "response to chitin," "ethylene-activated signaling pathway," or "systemic acquired resistance" (Supplementary Table 2). In wild type the genes belonging to clusters 5, 6, and 9 were generally down-regulated, showing a similar pattern to UV-B stress.

DISCUSSION

During the past few years evidence has been accumulated concerning the role of photosynthesis in plant immunity. Here, we have provided new insights into the linkage between light acclimation and plant immunity at the level of gene expression as well as addressed the role of the TLP18.3 protein within these processes. Chloroplasts, in addition to their main task in conversion of solar energy into chemical energy, participate in a number of other reactions like biosynthesis of amino acids, hormones, and secondary metabolites as well as cellular sensing of abiotic and biotic stress signals. Indeed, signals originating from the photosynthetic light reactions such as redox state of the electron transfer chain, accumulation of stromal metabolites as well as ROS and reactive electrophilic species are key components of chloroplast retrograde signaling (Fey et al., 2005; Piippo et al., 2006; Queval and Foyer, 2012; Szechyńska-Hebda and Karpiński, 2013; Bobik and Burch-Smith, 2015; Gollan et al., 2015). These signals respond rapidly to changes in perception of light by the two photosystems.

Here, we focused on plants grown under either constant or fluctuating light conditions for their entire life span in order to unravel how the rapid fluctuations in the growth light intensity affect the acclimation processes at the level of nuclear gene expression. In short, neither photosynthesis-related genes nor the photosynthetic protein complexes showed significant alterations as a response to fluctuating light (**Figure 1**, **Tables 1**–**3**). Instead, EPR spectroscopy revealed that the relative amount of functional PSI complexes was lowered in fluctuating light as compared to plants grown under constant light. Most prominently, in wild-type plants fluctuations in growth light suppressed the expression of genes related to defense reactions (**Table 2A**). Despite the high-light peaks of 1 min, the low-light phase is dominant in our fluctuating light setup. Hence, it is highly likely that decreased transcript abundance of the defense genes in wild-type Arabidopsis under fluctuating light is linked to shade-avoidance and is mediated by plant hormones (Vandenbussche et al., 2005; Wit et al., 2013). The experimental setup, in which the gene expression was studied from plants grown their entire life span either under constant or fluctuating light did not allow us to identify specific immune responses activated by the fluctuations in the growth light intensity. Instead, this experimental setup shed light into late stages of the plant acclimation process, in which a vast number of defense pathways were affected.

Contrary to wild type, in the *tlp18.3* mutant the alterations in the overall gene expression pattern, as a response to fluctuating light, were less evident and indeed, the *tlp18.3* plants were less capable of turning off the gene expression

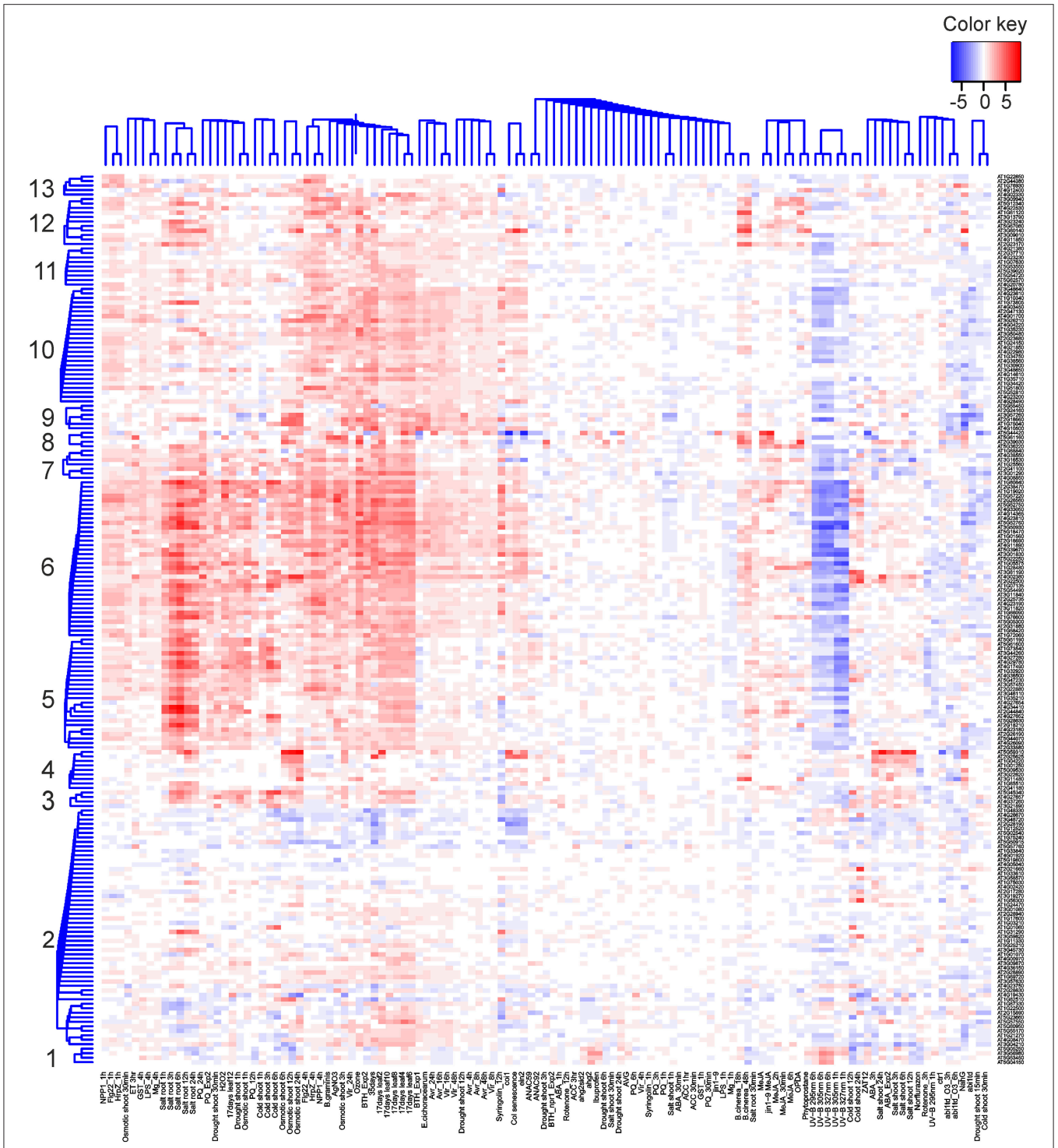

FIGURE 3 | Cluster analysis of genes differentially expressed in the wild-type but not in *tlp18.3* plants in response to fluctuating light as compared to constant growth light. Bayesian hierarchical clustering of genes, which are significantly differentially regulated (logFC > 1) in wild type under fluctuating light as compared to constant light, is presented. Data sets used include abiotic and biotic stress experiments. Blue and red indicate decreased and increased expression as compared to untreated plants, respectively.

related to plant immunity under fluctuating light conditions (**Table 2B**, **Figures 2**, **3**). It is known that the photoreceptor-derived signals activate the shade-avoidance responses and reduce the defense reactions against pathogens and pests to save resources for the growth of the plant (Ballare, 2014). Interestingly, the gene expression of two components

of phytochrome-mediated light signaling, *HFR1* and *PIL1*, was shown to be altered in *tlp18.3* leaves (**Table 4**). *HFR1* and *PIL1* genes are involved in transcriptional regulation pathways downstream of phytochromes, which integrate light and hormonal signals and play a role in shade-avoidance responses (Jiao et al., 2007). Of these, HFR1 also contributes to the crosstalk between light signaling and plant innate immunity (Tan et al., 2015). Based on these results, it is evident that the functionality of TLP18.3 protein modifies the light perception and/or signaling network, and possibly also the signaling related to nutrient availability (Supplementary Table 1). Allocation of resources to defense reactions in the *tlp18.3* mutant is likely associated with the lower biomass of mutant plants as compared to wild-type plants under low-light dominant fluctuating light. It should be noted that the *tlp18.3* plants also had lower biomass as compared to wild type when grown under high-light dominant fluctuating light with longer, 1 h light pulses (Sirpiö et al., 2007). It remains to be studied whether the growth phenotype of *tlp18.3* plants under high-light dominant fluctuating light originates directly from the diminished pool of active PSII complexes. Indeed, duration, frequency, and intensity of fluctuating light regimes have been shown to affect the acclimation responses in Arabidopsis (Alter et al., 2012). To that end, it would be interesting to compare how the gene expression patterns of low-light and high-light dominant fluctuating light conditions differ from each other.

Defective degradation of the D1 core protein of PSII in *tlp18.3* plants is a promising system for the search of chloroplast-derived retrograde signals which affect gene expression related to plant immunity. In line with this, low amount of the D1 degrading protease FtsH has been earlier observed to accelerate the hypersensitive reaction in tobacco (Seo et al., 2000). Recently, a link between PsbS-mediated photoprotection and pathogen resistance has also been shown to exist (Göhre et al., 2012; Johansson Jänkänp et al., 2013). Further, as the PSII repair cycle and maintenance of PSI are interconnected (Tikkanen et al., 2014), also PSI and/or PSI electron acceptors might act as a source of retrograde signaling components under fluctuating light. It should be noted that the pool of active PSII was not changed in *tlp18.3* plants as compared to wild type under low-light dominant fluctuating light (**Table 1**) and thus the effect might be indirect. We postulate that the compensation mechanisms activated in the *tlp18.3* mutant are likely to alter the chloroplast-derived retrograde signals. Taken together, our results demonstrate that light acclimation and plant immunity are interconnected and the proper repair cycle of PSII plays a key role in the process.

AUTHOR CONTRIBUTORS

SJ, JI, SK, JS, and FM contributed to acquisition, analysis, and drafting the work, while MS and EA designed the work and contributed to acquisition, analysis, and drafting the work.

FUNDING

Our research was financially supported by the Academy of Finland (project numbers 272424, 271832, and 273870), TEKES LIF 40128/14, the Swedish Research Council, the Swedish Energy Agency, the Knut and Alice Wallenberg Foundation and the Initial Training Networks (ITN) CALIPSO (607607), and PHOTOCOMM (317184).

ACKNOWLEDGMENTS

Microarray and sequencing unit of the Turku Centre for Biotechnology is thanked for assistance with microarray hybridizations. Kurt Ståle, Mika Keränen, Virpi Paakkarinen, Marjaana Rantala, Sanna Rantala, Ville Käpylä, and Saara Mikola are acknowledged for their excellent technical assistance.

SUPPLEMENTARY MATERIAL

The Supplementary Material for this article can be found online at: http://journal.frontiersin.org/article/10.3389/fpls.2016.00405

REFERENCES

Allahverdiyeva, Y., Mustila, H., Ermakova, M., Bersanini, L., Richaud, P., Ajlani, G., et al. (2013). Flavodiiron proteins Flv1 and Flv3 enable cyanobacterial growth and photosynthesis under fluctuating light. *Proc. Natl. Acad. Sci. U.S.A.* 110, 4111–4116. doi: 10.1073/pnas.1221194110

Alter, P., Dreissen, A., Luo, F. L., and Matsubara, S. (2012). Acclimatory responses of Arabidopsis to fluctuating light environment: comparison of different sunfleck regimes and accessions. *Photosynth. Res.* 113, 221–237. doi: 10.1007/s11120-012-9757-2

Aro, E. M., Virgin, I., and Andersson, B. (1993). Photoinhibition of Photosystem II. Inactivation, protein damage and turnover. *Biochim. Biophys. Acta* 1143, 113–134. doi: 10.1016/0005-2728(93)90134-2

Baena-Gonzalez, E., and Aro, E. M. (2002). Biogenesis, assembly and turnover of photosystem II units. *Philos. Trans. R. Soc. Lond. B. Biol. Sci.* 357, 1451–1459. discussion: 1459–1460. doi: 10.1098/rstb.2002.1141

Ballare, C. L. (2014). Light regulation of plant defense. *Annu. Rev. Plant. Biol.* 65, 335–363. doi: 10.1146/annurev-arplant-050213-040145

Blanco, F., Garreton, V., Frey, N., Dominguez, C., Perez-Acle, T., Van der Straeten, D., et al. (2005). Identification of NPR1-dependent and independent genes early induced by salicylic acid treatment in Arabidopsis. *Plant Mol. Biol.* 59, 927–944. doi: 10.1007/s11103-005-2227-x

Bobik, K., and Burch-Smith, T. M. (2015). Chloroplast signaling within, between and beyond cells. *Front. Plant Sci.* 6:781. doi: 10.3389/fpls.2015.00781

Chi, W., Sun, X., and Zhang, L. (2012). The roles of chloroplast proteases in the biogenesis and maintenance of photosystem II. *Biochim. Biophys. Acta* 1817, 239–246. doi: 10.1016/j.bbabio.2011.05.014

Cooke, E. J., Savage, R. S., Kirk, P. D., Darkins, R., and Wild, D. L. (2011). Bayesian hierarchical clustering for microarray time series data with replicates and outlier measurements. *BMC Bioinformatics* 12:399. doi: 10.1186/1471-2105-12-399

Danielsson, R., Albertsson, P. A., Mamedov, F., and Styring, S. (2004). Quantification of photosystem I and II in different parts of the thylakoid membrane from spinach. *Biochim. Biophys. Acta* 1608, 53–61. doi: 10.1016/j.bbabio.2003.10.005

Danielsson, R., Suorsa, M., Paakkarinen, V., Albertsson, P. A., Styring, S., Aro, E. M., et al. (2006). Dimeric and monomeric organization of photosystem II. Distribution of five distinct complexes in the different domains of the thylakoid membrane. *J. Biol. Chem.* 281, 14241–14249. doi: 10.1074/jbc.M600634200

de Torres Zabala, M., Littlejohn, G., Jayaraman, S., Studholme, D., Bailey, T., Lawson, T., et al. (2015). Chloroplasts play a central role in plant defence and are targeted by pathogen effectors. *Nat. Plants* 1:15074. doi: 10.1038/nplants.2015.74

Edelman, M., and Mattoo, A. K. (2008). D1-protein dynamics in photosystem II: the lingering enigma. *Photosynth. Res.* 98, 609–620. doi: 10.1007/s11120-008-9342-x

Fairchild, C. D., Schumaker, M. A., and Quail, P. H. (2000). HFR1 encodes an atypical bHLH protein that acts in phytochrome A signal transduction. *Genes Dev.* 14, 2377–2391. doi: 10.1101/gad.828000

Fernández-Calvino, L., Guzmán-Benito, I., Toro, F. J., Donaire, L., Castro-Sanz, A. B., Ruíz-Ferrer, V., et al. (2015). Activation of senescence-associated Dark-inducible (DIN) genes during infection contributes to enhanced susceptibility to plant viruses. *Mol. Plant. Pathol.* 17, 3–15. doi: 10.1111/mpp.12257

Fey, V., Wagner, R., Brautigam, K., Wirtz, M., Hell, R., Dietzmann, A., et al. (2005). Retrograde plastid redox signals in the expression of nuclear genes for chloroplast proteins of *Arabidopsis thaliana*. *J. Biol. Chem.* 280, 5318–5328. doi: 10.1074/jbc.M406358200

Georgii, E., Salojärvi, J., Brosche, M., Kangasjärvi, J., and Kaski, S. (2012). Targeted retrieval of gene expression measurements using regulatory models. *Bioinformatics* 28, 2349–2356. doi: 10.1093/bioinformatics/bts361

Göhre, V., Jones, A. M., Sklenár, J., Robatzek, S., and Weber, A. P. (2012). Molecular crosstalk between PAMP-triggered immunity and photosynthesis. *Mol. Plant Microbe Interact.* 25, 1083–1092. doi: 10.1094/MPMI-11-11-0301

Gollan, P. J., Tikkanen, M., and Aro, E. M. (2015). Photosynthetic light reactions: integral to chloroplast retrograde signalling. *Curr. Opin. Plant Biol.* 27, 180–191. doi: 10.1016/j.pbi.2015.07.006

Grieco, M., Tikkanen, M., Paakkarinen, V., Kangasjärvi, S., and Aro, E. M. (2012). Steady-state phosphorylation of light-harvesting complex II proteins preserves photosystem I under fluctuating white light. *Plant Physiol.* 160, 1896–1910. doi: 10.1104/pp.112.206466

Guo, L., Yang, H., Zhang, X., and Yang, S. (2013). Lipid transfer protein 3 as a target of MYB96 mediates freezing and drought stress in Arabidopsis. *J. Exp. Bot.* 64, 1755–1767. doi: 10.1093/jxb/ert040

Hayami, N., Sakai, Y., Kimura, M., Saito, T., Tokizawa, M., Iuchi, S., et al. (2015). The responses of Arabidopsis early light-induced protein2 to ultraviolet B, high light, and cold stress are regulated by a transcriptional regulatory unit composed of two elements. *Plant Physiol.* 169, 840–855. doi: 10.1104/pp.15.00398

He, Z., Cheeseman, I., He, D., and Kohorn, B. D. (1999). A cluster of five cell wall-associated receptor kinase genes, Wak1–5, are expressed in specific organs of Arabidopsis. *Plant Mol. Biol.* 39, 1189–1196. doi: 10.1023/A:1006197318246

Herbstova, M., Tietz, S., Kinzel, C., Turkina, M. V., and Kirchhoff, H. (2012). Architectural switch in plant photosynthetic membranes induced by light stress. *Proc. Natl. Acad. Sci. U.S.A.* 109, 20130–20135. doi: 10.1073/pnas.1214265109

Hermans, C., Hammond, J. P., White, P. J., and Verbruggen, N. (2006). How do plants respond to nutrient shortage by biomass allocation? *Trends Plant Sci.* 11, 610–617. doi: 10.1016/j.tplants.2006.10.007

Huber, D. (1980). "The role of mineral nutrition in defense," in *Plant Disease: An Advanced Treatise: How Plants Defend Themselves*, ed J. G. Horsfall (New York, NY: Academic Press), 381–406. doi: 10.1016/B978-0-12-356405-4.50028-9

Järvi, S., Suorsa, M., and Aro, E.M, (2015). Photosystem II repair in plant chloroplasts—regulation, assisting proteins and shared components with photosystem II biogenesis. *Biochim. Biophys. Acta* 1847, 900–909. doi: 10.1016/j.bbabio.2015.01.006

Järvi, S., Suorsa, M., Paakkarinen, V., and Aro, E. M. (2011). Optimized native gel systems for separation of thylakoid protein complexes: novel super- and mega-complexes. *Biochem. J.* 439, 207–214. doi: 10.1042/BJ20102155

Jiao, Y., Lau, O. S., and Deng, X. W. (2007). Light-regulated transcriptional networks in higher plants. *Nat. Rev. Genet.* 8, 217–230. doi: 10.1038/nrg2049

Johansson Jänkänpää, H., Frenkel, M., Zulfugarov, I., Reichelt, M., Krieger-Liszkay, A., Mishra, Y., et al. (2013). Non-photochemical quenching capacity in *Arabidopsis thaliana* affects herbivore behaviour. *PLoS ONE* 8:e53232. doi: 10.1371/journal.pone.0053232

Karpinski, S., Szechynska-Hebda, M., Wituszynska, W., and Burdiak, P. (2013). Light acclimation, retrograde signalling, cell death and immune defences in plants. *Plant Cell Environ.* 36, 736–744. doi: 10.1111/pce.12018

Kirchhoff, H., Hall, C., Wood, M., Herbstova, M., Tsabari, O., Nevo, R., et al. (2011). Dynamic control of protein diffusion within the granal thylakoid lumen. *Proc. Natl. Acad. Sci. U.S.A.* 108, 20248–20253. doi: 10.1073/pnas.1104141109

Konert, G., Rahikainen, M., Trotta, A., Durian, G., Salojärvi, J., Khorobrykh, S., et al. (2015). Subunits B'gamma and B'zeta of protein phosphatase 2A regulate photo-oxidative stress responses and growth in *Arabidopsis thaliana*. *Plant Cell Environ.* 38, 2641–2651. doi: 10.1111/pce.12575

Kono, M., and Terashima, I. (2014). Long-term and short-term responses of the photosynthetic electron transport to fluctuating light. *J. Photochem. Photobiol. B.* 137, 89–99. doi: 10.1016/j.jphotobiol.2014.02.016

Krieger-Liszkay, A., Fufezan, C., and Trebst, A. (2008). Singlet oxygen production in photosystem II and related protection mechanism. *Photosynth. Res.* 98, 551–564. doi: 10.1007/s11120-008-9349-3

Lam, H. M., Peng, S. S., and Coruzzi, G. M. (1994). Metabolic regulation of the gene encoding glutamine-dependent asparagine synthetase in *Arabidopsis thaliana*. *Plant Physiol.* 106, 1347–1357. doi: 10.1104/pp.106.4.1347

Müller, M., and Munné-Bosch, S. (2015). Ethylene response factors: a key regulatory hub in hormone and stress signaling. *Plant Physiol.* 169, 32–41. doi: 10.1104/pp.15.00677

Mulo, P., Sirpiö, S., Suorsa, M., and Aro, E. M. (2008). Auxiliary proteins involved in the assembly and sustenance of photosystem II. *Photosynth. Res.* 98, 489–501. doi: 10.1007/s11120-008-9320-3

Nickelsen, J., and Rengstl, B. (2013). Photosystem II assembly: from cyanobacteria to plants. *Annu. Rev. Plant Biol.* 64, 609–635. doi: 10.1146/annurev-arplant-050312-120124

Nixon, P. J., Michoux, F., Yu, J., Boehm, M., and Komenda, J. (2010). Recent advances in understanding the assembly and repair of photosystem II. *Ann Bot.* 106, 1–16. doi: 10.1093/aob/mcq059

Park, S. W., Kaimoyo, E., Kumar, D., Mosher, S., and Klessig, D. F. (2007). Methyl salicylate is a critical mobile signal for plant systemic acquired resistance. *Science* 318, 113–116. doi: 10.1126/science.1147113

Piippo, M., Allahverdiyeva, Y., Paakkarinen, V., Suoranta, U. M., Battchikova, N., and Aro, E. M. (2006). Chloroplast-mediated regulation of nuclear genes in *Arabidopsis thaliana* in the absence of light stress. *Physiol. Genomics* 25, 142–152. doi: 10.1152/physiolgenomics.00256.2005

Pospísil, P. (2009). Production of reactive oxygen species by photosystem II. *Biochim. Biophys. Acta* 1787, 1151–1160. doi: 10.1016/j.bbabio.2009.05.005

Queval, G., and Foyer, C. H. (2012). Redox regulation of photosynthetic gene expression. *Philos. Trans. R. Soc. Lond. B. Biol. Sci.* 367, 3475–3485. doi: 10.1098/rstb.2012.0068

Rodríguez-Herva, J. J., González-Melendi, P., Cuartas-Lanza, R., Antúnez-Lamas, M., Río-Alvarez, I., Li, Z., et al. (2012). A bacterial cysteine protease effector protein interferes with photosynthesis to suppress plant innate immune responses. *Cell. Microbiol.* 14, 669–681. doi: 10.1111/j.1462-5822.2012.01749.x

Salter, M. G., Franklin, K. A., and Whitelam, G. C. (2003). Gating of the rapid shade-avoidance response by the circadian clock in plants. *Nature* 426, 680–683. doi: 10.1038/nature02174

Seo, S., Okamoto, M., Iwai, T., Iwano, M., Fukui, K., Isogai, A., et al. (2000). Reduced levels of chloroplast FtsH protein in tobacco mosaic virus-infected tobacco leaves accelerate the hypersensitive reaction. *Plant Cell* 12, 917–932. doi: 10.1105/tpc.12.6.917

Sirpiö, S., Allahverdiyeva, Y., Suorsa, M., Paakkarinen, V., Vainonen, J., Battchikova, N., et al. (2007). TLP18.3, a novel thylakoid lumen protein regulating photosystem II repair cycle. *Biochem. J.* 406, 415–425. doi: 10.1042/BJ20070460

Suorsa, M., Järvi, S., Grieco, M., Nurmi, M., Pietrzykowska, M., Rantala, M., et al. (2012). PROTON GRADIENT REGULATION5 is essential for proper acclimation of Arabidopsis photosystem I to naturally and artificially fluctuating light conditions. *Plant Cell* 24, 2934–2948. doi: 10.1105/tpc.112.097162

Suorsa, M., Rantala, M., Mamedov, F., Lespinasse, M., Trotta, A., Grieco, M., et al. (2015). Light acclimation involves dynamic re-organization of the pigment-protein megacomplexes in non-appressed thylakoid domains. *Plant J.* 84, 360–373. doi: 10.1111/tpj.13004

Szechyńska-Hebda, M., and Karpiński, S. (2013). Light intensity-dependent retrograde signalling in higher plants. *J. Plant Physiol.* 170, 1501–1516. doi: 10.1016/j.jplph.2013.06.005

Szklarczyk, D., Franceschini, A., Wyder, S., Forslund, K., Heller, D., Huerta-Cepas, J., et al. (2015). STRING v10: protein-protein interaction networks, integrated over the tree of life. *Nucleic Acids Res.* 43, D447–D452. doi: 10.1093/nar/gku1003

Takahashi, S., and Badger, M. R. (2011). Photoprotection in plants: a new light on photosystem II damage. *Trends Plant Sci.* 16, 53–60. doi: 10.1016/j.tplants.2010.10.001

Tan, C. M., Li, M. Y., Yang, P. Y., Chang, S. H., Ho, Y. P., Lin, H., et al. (2015). Arabidopsis HFR1 is a potential nuclear substrate regulated by the Xanthomonas type III effector XopD(Xcc8004). *PLoS ONE* 10:e0117067. doi: 10.1371/journal.pone.0117067

Tikkanen, M., Grieco, M., Kangasjärvi, S., and Aro, E. M. (2010). Thylakoid protein phosphorylation in higher plant chloroplasts optimizes electron transfer under fluctuating light. *Plant Physiol.* 152, 723–735. doi: 10.1104/pp.109.150250

Tikkanen, M., Mekala, N. R., and Aro, E. M. (2014). Photosystem II photoinhibition-repair cycle protects Photosystem I from irreversible damage. *Biochim. Biophys. Acta* 1837, 210–215. doi: 10.1016/j.bbabio.2013.10.001

Tyystjärvi, E., and Aro, E. M. (1996). The rate constant of photoinhibition, measured in lincomycin-treated leaves, is directly proportional to light intensity. *Proc. Natl. Acad. Sci. U.S.A.* 93, 2213–2218. doi: 10.1073/pnas.93.5.2213

Tzvetkova-Chevolleau, T., Franck, F., Alawady, A. E., Dall'Osto, L., Carrière, F., Bassi, R., et al. (2007). The light stress-induced protein ELIP2 is a regulator of chlorophyll synthesis in *Arabidopsis thaliana*. *Plant J.* 50, 795–809. doi: 10.1111/j.1365-313X.2007.03090.x

Vandenbussche, F., Pierik, R., Millenaar, F. F., Voesenek, L. A., and Van Der Straeten, D. (2005). Reaching out of the shade. *Curr. Opin. Plant Biol.* 8, 462–468. doi: 10.1016/j.pbi.2005.07.007

Wit, M., Spoel, S. H., Sanchez-Perez, G. F., Gommers, C. M., Pieterse, C. M., Voesenek, L. A., et al. (2013). Perception of low red: far-red ratio compromises both salicylic acid-and jasmonic acid-dependent pathogen defences in Arabidopsis. *Plant J.* 75, 90–103. doi: 10.1111/tpj.12203

Wu, H. Y., Liu, M. S., Lin, T. P., and Cheng, Y. S. (2011). Structural and functional assays of AtTLP18.3 identify its novel acid phosphatase activity in thylakoid lumen. *Plant Physiol.* 157, 1015–1025. doi: 10.1104/pp.111.184739

Yang, Y., Zhang, Y., Ding, P., Johnson, K., Li, X., and Zhang, Y. (2012). The ankyrin-repeat transmembrane protein BDA1 functions downstream of the receptor-like protein SNC2 to regulate plant immunity. *Plant Physiol.* 159, 1857–1865. doi: 10.1104/pp.112.197152

Zander, M., Chen, S., Imkampe, J., Thurow, C., and Gatz, C. (2012). Repression of the *Arabidopsis thaliana* jasmonic acid/ethylene-induced defense pathway by TGA-interacting glutaredoxins depends on their C-terminal ALWL motif. *Mol. Plant.* 5, 831–840. doi: 10.1093/mp/ssr113

Zhang, Y., Xu, S., Ding, P., Wang, D., Cheng, Y. T., He, J., et al. (2010). Control of salicylic acid synthesis and systemic acquired resistance by two members of a plant-specific family of transcription factors. *Proc. Natl. Acad. Sci. U.S.A.* 107, 18220–18225. doi: 10.1073/pnas.1005225107

Conflict of Interest Statement: The authors declare that the research was conducted in the absence of any commercial or financial relationships that could be construed as a potential conflict of interest.

frontiers in Plant Science

ORIGINAL RESEARCH
published: 18 February 2016
doi: 10.3389/fpls.2016.00157

Critical Assessment of Protein Cross-Linking and Molecular Docking: An Updated Model for the Interaction Between Photosystem II and Psb27

*Kai U. Cormann†, Madeline Möller and Marc M. Nowaczyk**

Plant Biochemistry, Ruhr University Bochum, Bochum, Germany

OPEN ACCESS

Edited by:
Julian Eaton-Rye,
University of Otago, New Zealand

Reviewed by:
Conrad Mullineaux,
Queen Mary University of London, UK
Peter Mabbitt,
Australian National University, Australia

****Correspondence:***
Marc M. Nowaczyk
marc.m.nowaczyk@rub.de

†Present address:
Kai U. Cormann,
Institute of Bio- and Geosciences, IBG-1: Biotechnology, Forschungszentrum Jülich, Jülich D-52425, Germany

Specialty section:
This article was submitted to Plant Cell Biology, a section of the journal Frontiers in Plant Science

Received: *25 November 2015*
Accepted: *30 January 2016*
Published: *18 February 2016*

Citation:
Cormann KU, Möller M and Nowaczyk MM (2016) Critical Assessment of Protein Cross-Linking and Molecular Docking: An Updated Model for the Interaction Between Photosystem II and Psb27. Front. Plant Sci. 7:157. doi: 10.3389/fpls.2016.00157

Photosystem II (PSII) is a large membrane-protein complex composed of about 20 subunits and various cofactors, which mediates the light-driven oxidation of water and reduction of plastoquinone, and is part of the photosynthetic electron transfer chain that is localized in the thylakoid membrane of cyanobacteria, algae, and plants. The stepwise assembly of PSII is guided and facilitated by numerous auxiliary proteins that play specific roles in this spatiotemporal process. Psb27, a small protein localized in the thylakoid lumen, appears to associate with an intermediate PSII complex that is involved in assembly of the Mn_4CaO_5 cluster. Its precise binding position on the PSII intermediate remains elusive, as previous approaches to the localization of Psb27 on PSII have yielded contradictory results. This was our motivation for a critical assessment of previously used methods and the development of an improved analysis pipeline. The combination of chemical cross-linking and mass spectrometry (CX-MS) with isotope-coded cross-linkers was refined and validated with reference to the PSII crystal structure. Psb27 was localized on the PSII surface adjacent to the large lumenal domain of CP43 on the basis of a cross-link connecting Psb27-K91 to CP43-K381. Additional contacts associating Psb27 with CP47 and the C-termini of D1 and D2 were detected by surface plasmon resonance (SPR) spectroscopy. This information was used to model the binding of Psb27 to the PSII surface in a region that is occupied by PsbV in the mature complex.

Keywords: cyanobacteria, photosystem II, assembly, CX-MS, SPR, Psb27

INTRODUCTION

Photosystem II (PSII) catalyzes the light-driven oxidation of water (McEvoy and Brudvig, 2006; Cox et al., 2013). It is the only known enzymatic system that is able to use water as a universal source of electrons for the reduction of plastoquinone, the initial reaction of photosynthetic electron transport (PET). PSII is a large membrane-protein complex that is localized in the thylakoid membrane of all organisms that perform oxygenic photosynthesis, including cyanobacteria, algae, and plants. Cyanobacterial PSII has been successfully characterized by X-ray crystallography, and detailed structural models with a resolution down to 1.9 Å are

available (Ferreira et al., 2004; Guskov et al., 2009; Umena et al., 2011). These PSII structures reveal the spatial disposition of up to 20 protein subunits and multiple cofactors, such as chlorophylls, carotenoids, and lipids. In particular, a comprehensive analysis of the water-oxidizing complex (WOC), which is composed of an inorganic Mn_4O_5Ca cluster and its coordinating amino acid residues, has been facilitated by the atomic level of resolution of the latest structures (Umena et al., 2011; Suga et al., 2015). The core complex is a heterodimer of the D1 and D2 subunits (PsbA and PsbD), which coordinate most of the cofactors involved in electron transfer. Two domains of the adjacent light-harvesting proteins CP43 and CP47 protrude out of the plane of the membrane into the thylakoid lumen, and act as anchoring points for the soluble extrinsic subunits PsbO, PsbV, and PsbU, which shield the WOC on the lumenal face of the thylakoid membrane (Roose et al., 2007). The remaining 13 small (<10 kDa) and hydrophobic (with 1–2 transmembrane helices) subunits play various roles during PSII assembly and in the mature complex, but the exact functions of many of them remain obscure (Shi et al., 2012). However, assembly of the different components during PSII biogenesis is an intricate process that is coordinated by a network of auxiliary proteins (Mulo et al., 2008; Nixon et al., 2010; Becker et al., 2011; Nickelsen and Rengstl, 2013). These accessory factors direct the spatiotemporal formation and distribution of precursor complexes in a coordinated assembly process, including a series of distinct, metastable assembly intermediates. Structural analysis of these intermediate PSII complexes is severely hampered by their low abundance and transient nature, with the consequence that none of these complexes has been successfully analyzed by X-ray crystallography so far.

One of the best studied proteins involved in PSII biogenesis is the auxiliary factor Psb27 (Nowaczyk et al., 2010; Fagerlund and Eaton-Rye, 2011; Mabbitt et al., 2014), which forms part of several distinct PSII assembly intermediates and plays a role in both PSII biogenesis and repair (Nowaczyk et al., 2006; Roose and Pakrasi, 2008; Grasse et al., 2011; Liu et al., 2011b; Komenda et al., 2012).

Psb27 has been shown to stabilize unassembled CP43 in a precomplex that is composed of the membrane-embedded subunits CP43, PsbK, PsbZ, and Psb30 (Komenda et al., 2012). After formation of a stable (inactive) monomeric PSII intermediate including Psb27, but not the extrinsic proteins PsbO, PsbV, and PsbU, it might facilitate assembly of the WOC, as this step is followed by the release of Psb27, photoactivation of the cluster and association of the extrinsic proteins (Roose and Pakrasi, 2008). In cyanobacteria, Psb27 is modified by an N-terminal lipid modification and attached to the lumenal side of the thylakoid membrane (Nowaczyk et al., 2006). Moreover, it is involved in acclimation to fluctuating light conditions in higher plants (Hou et al., 2015). Notably, isolation of the monomeric PSII-Psb27 complex revealed species- or preparation-dependent differences. Whereas a complex isolated from *Thermosynechococcus elongatus* via two-step chromatography is devoid of all three extrinsic proteins (Nowaczyk et al., 2006), a similar complex isolated from *Synechocystis* sp. PCC6803 via one-step chromatography still contains considerable amounts of PsbO, but not PsbV or PsbU (Liu et al., 2011b).

The structure of recombinant Psb27 has been solved by NMR spectroscopy (Cormann et al., 2009; Mabbitt et al., 2009) and by X-ray crystallography (Michoux et al., 2012), which reveal a four-helix bundle with a dipolar charge distribution. Part of the surface that is formed by helices III and IV is highly conserved and might facilitate binding to PSII. Several approaches have been used in attempts to localize the Psb27 binding site on the lumenal surface of PSII. *In silico* docking experiments suggested a location for Psb27 that partly overlaps the PsbO binding site (Cormann et al., 2009; Fagerlund and Eaton-Rye, 2011), whereas experimental results based on mass spectrometry (Liu et al., 2011a, 2013) support the localization of Psb27 on the opposite side of CP43 Loop E, pointing toward transmembrane helices III and IV. These conflicting results may be attributed to limitations of the methods used, and this motivated us to undertake a critical assessment of both. We made use of the high-resolution PSII crystal structure for validation of the methods and to define critical parameters for the evaluation of mass spectrometry (MS) data. An optimized workflow involving a combination of isotope-coded cross-linking and MS based on a previous study (Rexroth et al., 2014), as well as surface plasmon resonance (SPR)-based mapping (Cormann et al., 2014) pinpointed a Psb27 binding position in the vicinity of CP43 at the PsbV binding site on the lumenal PSII surface.

RESULTS

Identification of Correct Models Derived by Ab Initio Docking Requires Experimental Data

To check the ability of *ab initio* docking algorithms to predict the correct position of soluble subunits at the PSII surface, we made use of the CAPRI protocol for 'Critical Assessment of PRedicted Interactions' (Janin et al., 2003). In this method, the three-dimensional structures of free interaction partners are used to model the configuration of the complex of interest, and the results are compared to the experimentally derived coordinates of the assembled proteins. The fraction of native or non-native contacts discovered and the root mean square deviations (RMSD) between the predicted and the experimentally determined positions serve as criteria for classifying the quality of the models obtained as high, medium, acceptable, or incorrect. In the case of PSII, PsbV is the only soluble subunit whose structure is available in both unbound (Kerfeld et al., 2003) and bound (Umena et al., 2011) forms. As no PSII crystal structure without the extrinsic subunits PsbO, PsbV, and PsbU is available, we removed them from the PDB file and docked the unbound PsbV structure to the membrane-intrinsic portion of PSII. This structure served as the reference standard for the following analysis.

The ClusPro server 2.0 (Comeau et al., 2004a,b; Kozakov et al., 2006), which has been employed in most modeling studies due to its top ranking performance in the latest comparative docking experiments (Kozakov et al., 2013; Lensink and Wodak, 2013),

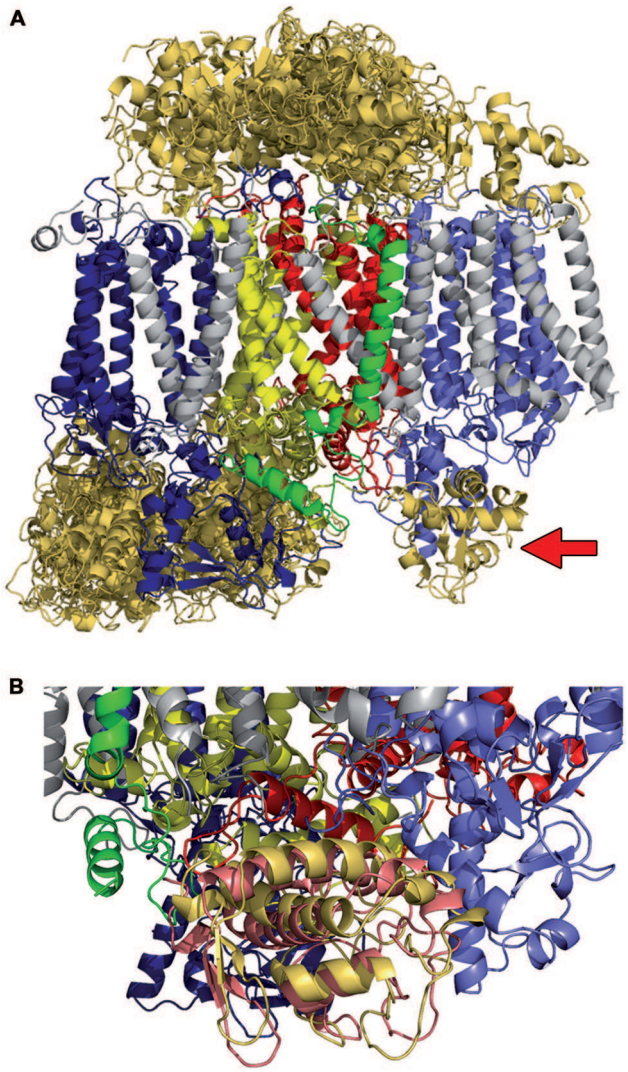

FIGURE 1 | *Ab initio* docking of PsbV (orange) to monomeric Photosystem II using ClusPro server 2.0. (A) Summary representation of 29 models that were generated on the basis of monomeric PSII without the extrinsic subunits PsbU, PsbO, PsbV (PDB: 3ARC) and the crystal structure of free PsbV (PDB: 1MZ4): 15 models show PsbV on the cytoplasmic side, 14 on the lumenal side. The calculation is based on van der Waals forces and electrostatic interactions. Only one model (red arrow) essentially reproduces the native position of PsbV, but it was ranked 24th of the 29 structures predicted by ClusPro 2.0. **(B)** Overlay of the native (salmon) and modeled (yellow) PsbV binding positions.

distinguishes between four subgroups of PSII models that differ in the energy parameters for contacts, based on hydrophobicity, charge or shape. Whereas three subgroups place PsbV in clearly erroneous positions with contacts to the membrane-embedded residues of PSII, PsbV is exclusively localized at the solvent-accessible interfaces in models favoring interactions based on charge and shape. Within this second group of 29 models, 15 place PsbV on the cytoplasmic side of PSII and 14 assign it to the lumenal side (**Figure 1A**). One of the latter models closely approximates the native position of PsbV adjacent to the CP43 and D1 subunits (**Figure 1B**). With a calculated fraction of 60% of the native interaction site and an RMSD of 5.2 Å relative to its position in the PSII crystal structure, this model is classified as acceptable. However, the software ranks it in position 24 out of 29, based on its cluster size, and thus obviously incorrect models are suggested to represent the native structure. In light of such limitations, only experimental data can distinguish the correct model from the majority of false-positive results.

Reliable Assignment of Cross-Linked Peptides is Facilitated by Isotopic Labeling

The analysis of cross-linking MS (CX-MS) data is especially challenging owing to the fact that structurally meaningful interpeptide cross-links are obscured by the vastly greater number of non-informative intrapeptide cross-links, dead-end cross-links, and free peptides. Moreover, mass spectrometric analysis of PSII samples is even more difficult, as this protein complex consists of around 20, mostly hydrophobic, subunits per monomer. However, the major problem lies in the overwhelming number of theoretically possible peptides, in particular if post-translational modifications other than the cross-link itself are included in the analysis. Furthermore, the experimental data set may include spectra of copurifying impurities, which are not included in the database used for CX-MS analyses. Hence, careful inspection of the results for false-positive MS2 assignments is mandatory. Thus, we used the high-resolution crystal structure of PSII (Umena et al., 2011) to test and validate our CX-MS approach.

Two PSII samples (inactive, monomeric Psb27-PSII and active, dimeric PSII) were incubated with the isotope-coded cross-linker bis(sulfosuccinimidyl)suberate (BS3, spacer length: 11.4 Å), then digested with trypsin and analyzed by LC-ESI tandem mass spectrometry. Data analysis was performed with StavroX v. 3.1.19 (Götze et al., 2012).

As the false discovery rate represents one of the main difficulties in the identification of cross-linked peptides, most software tools provide a scoring function that estimates the probability of a false positive assignment. StavroX calculates a score based on the identified fragment ions for each precursor mass (Götze et al., 2012). To establish a correlation between the score and the false discovery rate, the dataset is searched analogously against a decoy database consisting of reversed protein sequences. Previous validation of the software based on model systems yielded a false discovery rate of 2% for scores >100 (Götze et al., 2012).

We first attempted to identify only H_{12}-BS3 cross-links in the two PSII data sets, in order to test the reliability of the software. When scores ≤ 100 were considered, the number of hits in the decoy database equaled the number of possible cross-linked peptides identified with the native database. For scores >100 the number of peptide identifications for the native sequences clearly exceeded that for the decoy database, but StavoX still reported 9 and 10 decoy hits compared to 65 and 80 hits for the native database in the two datasets, respectively. In addition,

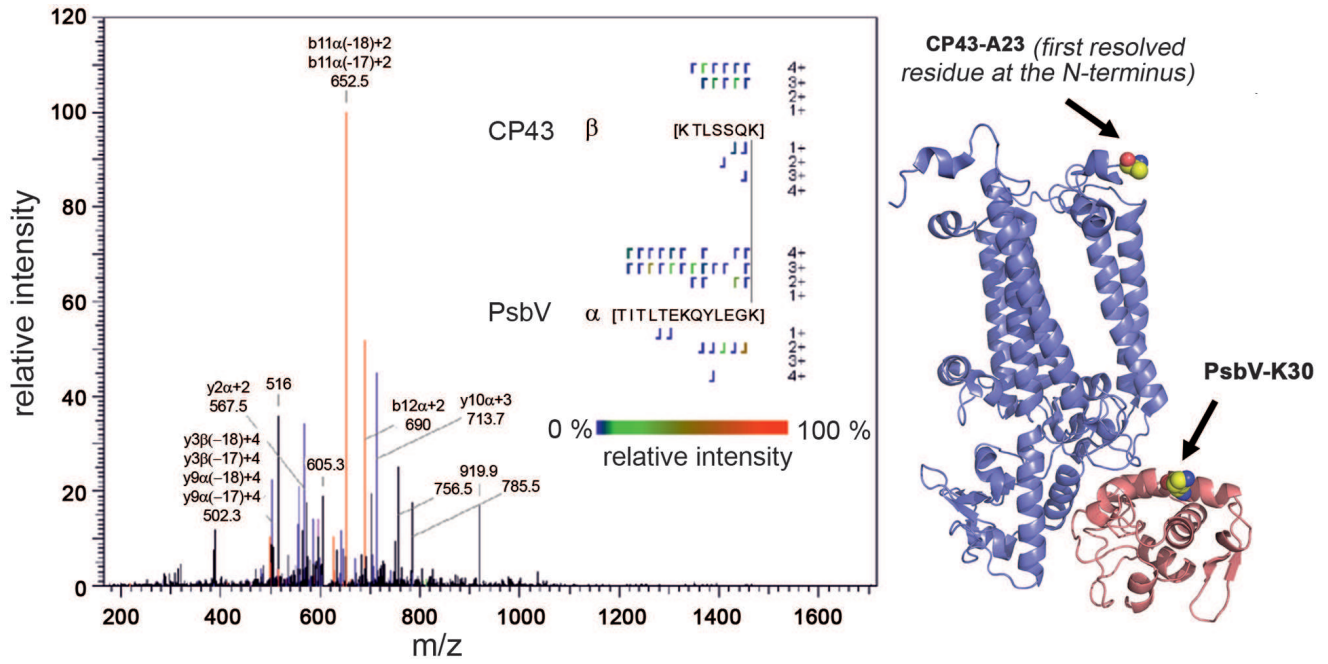

FIGURE 2 | Example of the identification of false-positive cross-links by StavroX. Identified b-ions (red), y-ions (blue), and unidentified signals (black) are indicated in the spectrum. Purple signals represent either b- or y-ions. A cross-link between the N-terminal part of CP43 and PsbV was identified by the software (Score: 137), although the domains are located on different sides of the membrane. Furthermore, trypsin should not recognize a BS3-modified lysine.

the results obtained with the native database contained false-positive discoveries with scores >100, although these "cross-links" clearly contradict the PSII crystal structure. Thus, despite the fact that it is based on nearly complete assignment of the entire fragment ion series, the result shown in **Figure 2** suggests that the N-terminal portion of CP43 is cross-linked to PsbV, although these sequences are located on different sides of the membrane. Even though the number of false discoveries is clearly lower than that of true hits, it might nevertheless account for the contradictory and artefactual structural models, since each suggested assignment is the basis for a structural constraint.

Moreover, assignments that are based only on the identification of H_{12}-BS3 cross-linked peptides might be ambiguous, even though the score calculated for each identification is above the threshold. **Figure 3** shows an MS2 fragment pattern that was assigned to cross-linked peptides of PsbL and CP47 (score 136) and PsbL and PsbX (score 100). Most of the observed fragments were assigned to the α-peptide (PsbL), whereas the identity of the β-peptide is ambiguous. In the upper spectrum only two (b-)ions of the β-peptide (CP47, red arrows) were found, and in the lower spectrum none of the PsbX-specific fragments were identified. Although the identification of the PsbL/CP47 cross-link is more reasonable – also from the structural perspective – there is still considerable uncertainty about the correct assignment.

Hence, to avoid ambiguous assignments and to reduce the false discovery rate further, we included the deuterated cross-linker (D_{12}-BS3) in our analysis. For each peptide containing a H_{12}-BS3 modification the dataset should then include a second peptide with the same amino acid sequence modified by D_{12}-BS3. The mass difference of 12 Da between the two versions of the cross-linker should be matched by the corresponding precursor ions and, due to the nearly identical chemical properties of H_{12}-BS3 and D_{12}-BS3, both peptides are expected to exhibit a very similar retention time and the same pattern of fragment ions. So, we considered only those peptides that fulfilled the following three criteria: (1) identification in the H_{12}-BS3 and D_{12}-BS3 modified form, (2) simultaneous elution, and (3) similarity of fragment-ion patterns. Using this more stringent approach, we identified 10 intermolecular and five intramolecular cross-links (Supplementary Table S1 and Supplementary Figures S1–S19). In addition to the similar fragment *patterns* of the peptides cross-linked with H_{12}-BS3 and D_{12}-BS3, the fragment *masses* in both spectra provide additional information which strengthens the validity of the assignment: While ions that do not include the cross-linking BS3 molecule exhibit identical masses in both spectra (e.g., y6α/β + 1), fragments containing the cross-linker show the predicted mass shift of 12 Da/z (e.g., b10α/β + 2, b12α/β + 2, and b13α/β + 2) as illustrated for the PsbU–PsbU cross-link (**Figure 4**).

Finally, it is noteworthy that the number of identified peptides exceeds the number of cross-links because, as a result of missed cleavages and methionine oxidation, some of the peptides included the same cross-link (e.g., a cross-link was identified in the oxidized and the reduced form of a methionine-containing peptide). Moreover, highly abundant

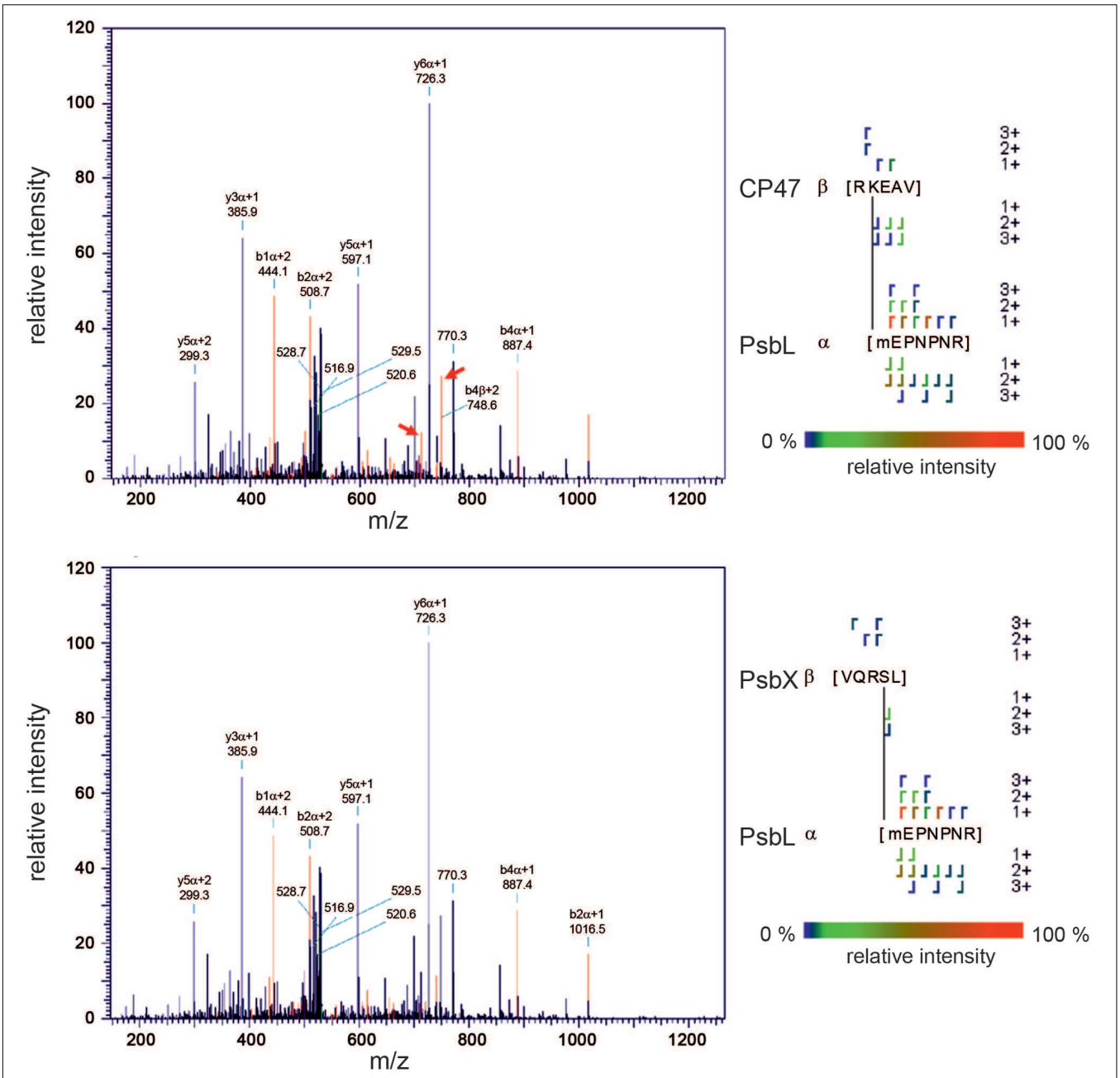

FIGURE 3 | Example of an ambiguous assignment. MS2 fragmentation pattern that was either assigned to H_{12}-BS3 cross-linked peptides of PsbL and CP47 (upper spectrum, Score: 136) or PsbL and PsbX (lower spectrum, Score: 100). In the case of PsbL and CP47 only two (b-)ions were assigned to the β-peptide (red arrows), whereas for PsbX no specific ions were found.

peptides showed broad elution peaks and were identified several times.

Flexible Termini are the Preferred Cross-Linking Sites

The high-resolution crystal structure of mature PSII should facilitate an *in silico* approach to the prediction of potential cross-links in the protein complex. We used the Xwalk algorithm (Kahraman et al., 2011) to calculate solvent-accessible surface distances between lysine residues in PSII. Potential cross-links were limited to a maximum distance of 35 Å, as the distance constraint for BS3 is 11.4 Å and the size of two lysine side-chains is 13 Å. The additional 10 Å was added to allow for conformational dynamics. Interestingly, Xwalk did not predict the majority of cross-links that were identified by the MS approach. The reason for this unexpected result becomes obvious on closer inspection of the crystal structure of PSII (Umena

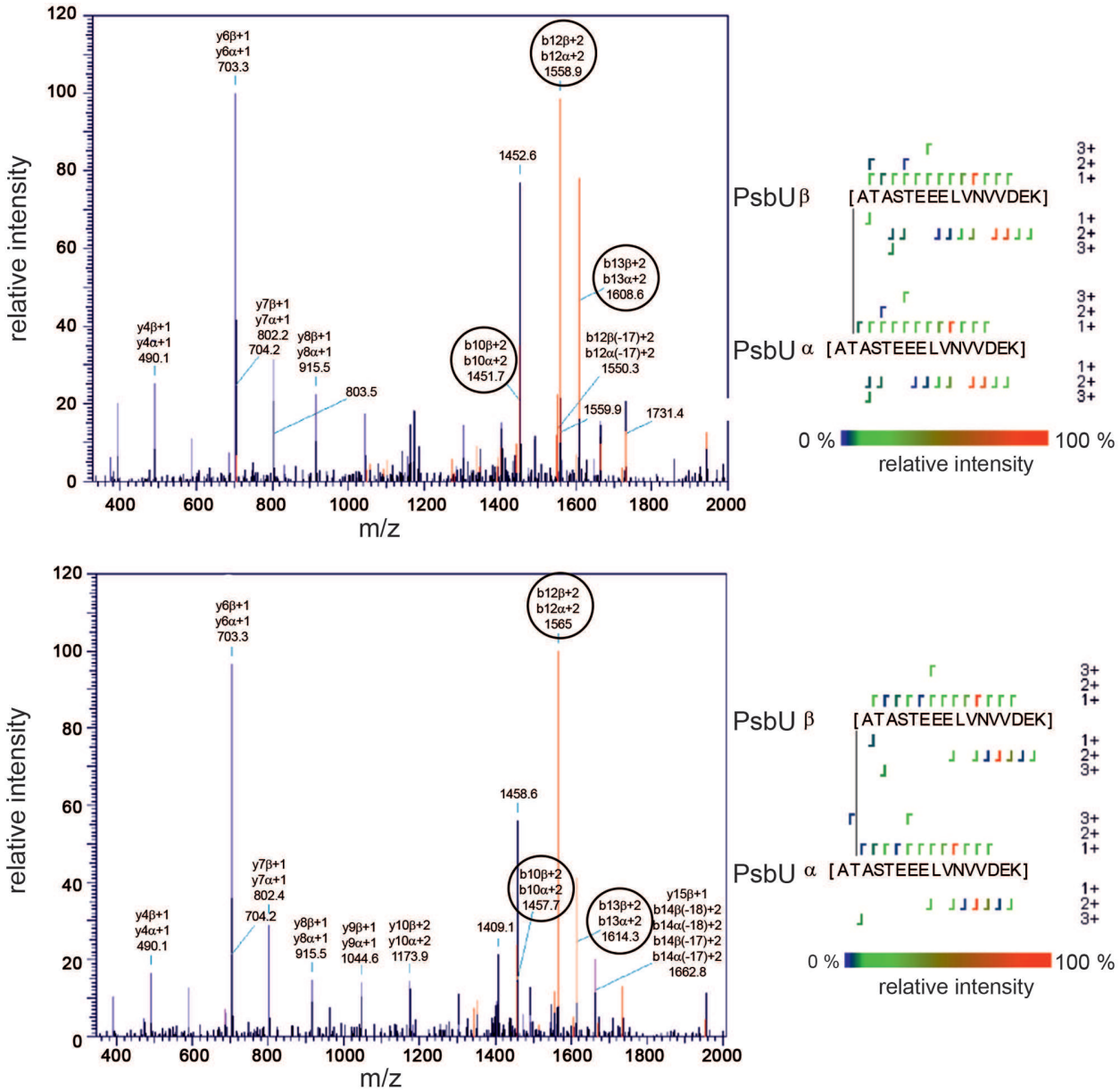

FIGURE 4 | Example of a correct assignment. A cross-link between the N-termini of two PsbU subunits was identified unambiguously by two independent assignments for the light (H_{12}-BS3, Score: 232; upper spectrum) and heavy (D_{12}-BS3, Score: 238; lower spectrum) forms of the cross-linker. That the two fragmentation patterns are almost identical is obvious, but for some ions that contain the cross-linker (in this case only b-ions), the 12-Da mass shift between the light and heavy form is clearly discernible (black circles).

et al., 2011). Although the structure was solved with a high resolution of 1.9 Å, many of the protein termini are not resolved at all, due to their enhanced flexibility. On the other hand, in 14 of 15 cross-links a protein N-terminus provided at least one primary amine. This leads to the model of easy accessible and flexible cross-linking hotspots, like the N-termini of PsbO and PsbL (**Figure 5**), that readily react with the cross-linker. As a consequence, the partly fixed cross-linker scans the surface within a 35-Å radius for a second reactive side-chain (preferably lysine, but also serine or threonine). Thus, we never observed cross-links between protein–protein interfaces that are hidden in the complex. Instead, surface-exposed, flexible parts of PSII are the preferred cross-linking sites.

Psb27 is Cross-Linked to the Center of the Lumenal CP43 Domain

To probe the interaction of Psb27 with PSII, the corresponding monomeric intermediate complex without the extrinsic proteins PsbO, PsbU, and PsbV (Nowaczyk et al., 2006) was treated

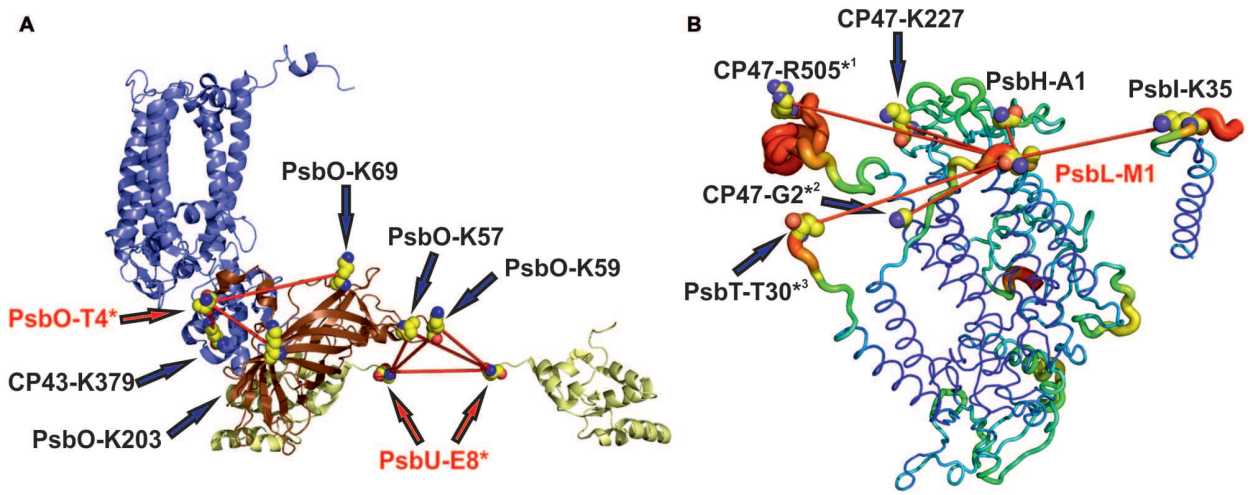

FIGURE 5 | Examples of cross-linking hotspots on the surface of PSII. Of 15 experimentally derived cross-links, 14 involve protein N-termini, which are not resolved in the PSII crystal structure (PDB: 3ARC) due to their enhanced flexibility. **(A)** The N-termini of PsbO and PsbU are cross-linked to different amino acids at the lumenal PSII surface. **(B)** The N-terminus of PsbL is an example for a cross-linking hotspot on the cytoplasmic PSII surface. It is involved in six cross-links between PsbL and the adjacent subunits. Protein chains are labeled according to their B-factor with PyMOL (DeLano, 2002) from red (highest flexibility) to blue (rigid), and amino acids that are involved in a cross-link but are not resolved in the crystal structure are marked by an asterisk.

with the isotopically coded cross-linker and analyzed by mass spectrometry. Only one cross-link involving Psb27 was found, based on the three criteria for a reliable cross-link defined previously by our validation approach. The results shown in **Figure 6** clearly demonstrate the presence of a cross-link between Psb27-K91 and CP43-K381. The precursor ions of the light and heavy peptides (2388.329/2400.404 Da, $z = 4$) elute at the same time, and show a mass difference of 12 Da. Fragmentation of both precursor ions leads to high-quality MS2 spectra and reliable assignment of the fragmentation pattern (Score: 234/178). Some of the fragment ions exhibit identical masses (e.g., y5α/y6α), whereas others differ in m/z due to the presence of the cross-linker (e.g., y5β, b6α). In general, the intensity of assigned fragment ions is comparable between the two spectra, while unassigned fragments (e.g., 974.6) are mainly present in only one of the two spectra.

CP43-K381 is localized at the tip of the large lumenal domain of CP43, which hampers the identification of the exact Psb27 binding position. Being the only structural constraint within a radius of 35 Å, the cross-link allows for localization of Psb27 at the PsbO binding site, but also on the opposite side of the CP43 domain at the PsbV binding position. Interestingly, two other cross-links involving CP43-K381 (CP43-K323, CP43-K339) that are not present in the dataset for the mature PSII complex were identified in the Psb27-PSII dataset (Supplementary Table S2, Supplementary Figures S20–S29). This may indicate that CP43-K381 forms a cross-linking hotspot unless positions K323/K339 are shielded by PsbO/PsbU, and the whole domain might also be more flexible without the extrinsic proteins. Nevertheless, more structural constraints are necessary for the secure localization of Psb27 in order to distinguish at least between its binding to the PsbO or PsbV binding site onthe PSII surface.

Psb27 Interacts with the Lumenal Domains of CP43, D1, D2, and CP47

For further analysis of the interaction between PSII and Psb27, recombinant Psb27 was probed for binding to various lumenal PSII domains (CP43, CP47, D2, mD1, D1a, PsbE) and a cytoplasmic control (Psb28) in an *in vitro* approach that is based on SPR spectroscopy (Cormann et al., 2014). The screening resulted in reproducible, concentration-dependent binding responses for CP43, CP47, D2, and the mature D1 C-terminus (mD1), each of which was fitted to a one-site binding isotherm (**Figure 7**). The highest affinities were measured between Psb27 and CP43 (21 ± 2 μM) and Psb27 and mD1 (34 ± 4 μM), whereas binding to CP47 and D2 occurred with considerably lower affinities ($K_D \approx 100$ μM). No binding or very low binding responses were observed for PsbE, the D1 a-loop (D1a), or Psb28. These results support a localization of Psb27 at the PsbV-binding position, mainly driven by contacts to CP43 and D1, rather than by binding to the D2/D1a site. Finally, the ClusPro server 2.0 was used to predict the binding position of Psb27 on the PSII surface in an *ab initio* modeling approach and to compare the results with the experimentally derived constraints. Models were calculated based on the crystal structures of Psb27 (PDB code: 2Y6X) and PSII (PDB code: 3ARC) after removal of the extrinsic proteins, but none of the deduced models explains the simultaneous contacts to D1, D2, CP43, and CP47 (data not shown) detected by SPR spectroscopy.

DISCUSSION

The combination of chemical cross-linking with mass spectrometry is a very powerful tool for the structural analysis of intact protein complexes, but it is also challenging to

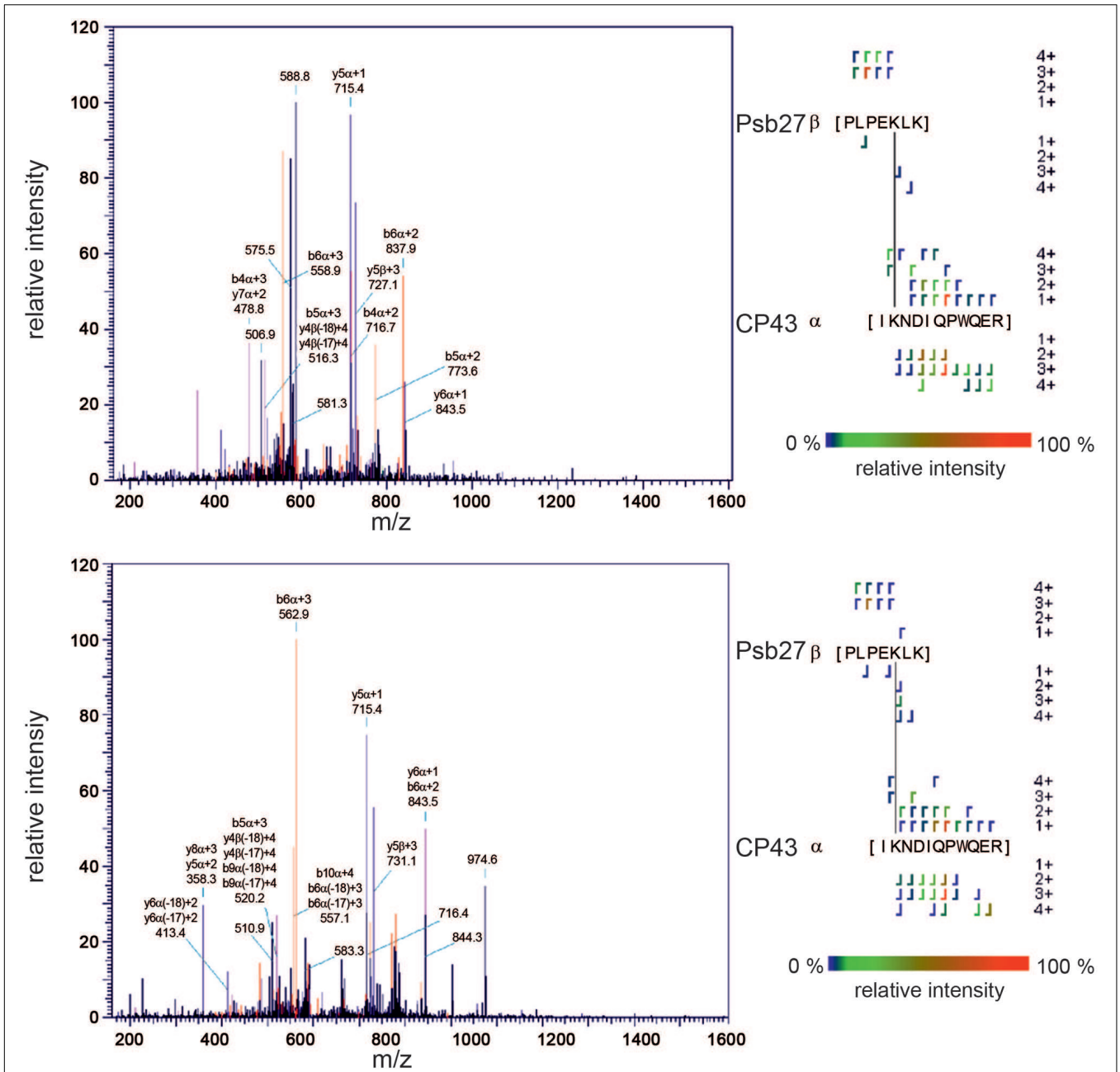

FIGURE 6 | Identification of a cross-link between Psb27 and CP43. An intermediate Psb27-PSII complex (Nowaczyk et al., 2006) was labeled with isotopically coded BS3 and analyzed by MS. The MS2 fragmentation patterns for a peptide that includes a cross-link between Psb27-K91 and CP43-K381 formed by the light (upper spectrum, Score: 234) and the heavy (lower spectrum, Score: 178) form of the cross linker are shown. Masses of the precursor ions: 2388.329 and 2400.404 ($z = 4$); Examples of identical ions: y5α, y6α; Examples of ions that contain the cross-linker: y5β, b6α.

use (Seebacher et al., 2006; Sinz, 2006; Petrotchenko and Borchers, 2010; Stengel et al., 2012; Bricker et al., 2015). Careful analysis of the results is necessary to avoid misinterpretation of the data, as the number of possible assignments for cross-linked peptides increases exponentially with the number of peptides in the database, and the complexity of the sample. If multiple post-translational modifications are additionally allowed for in the database search, the proportion of false positives will increase dramatically (Chen et al., 2009; Baker et al., 2010).

Therefore, to reduce the complexity of the samples as much as possible, we chose to work with highly purified PSII particles and restricted the data analysis to only one common post-translational modification (methionine oxidation) and one cross-link per peptide, and we employed an isotopically coded cross-linker that permits further validation of the assignments

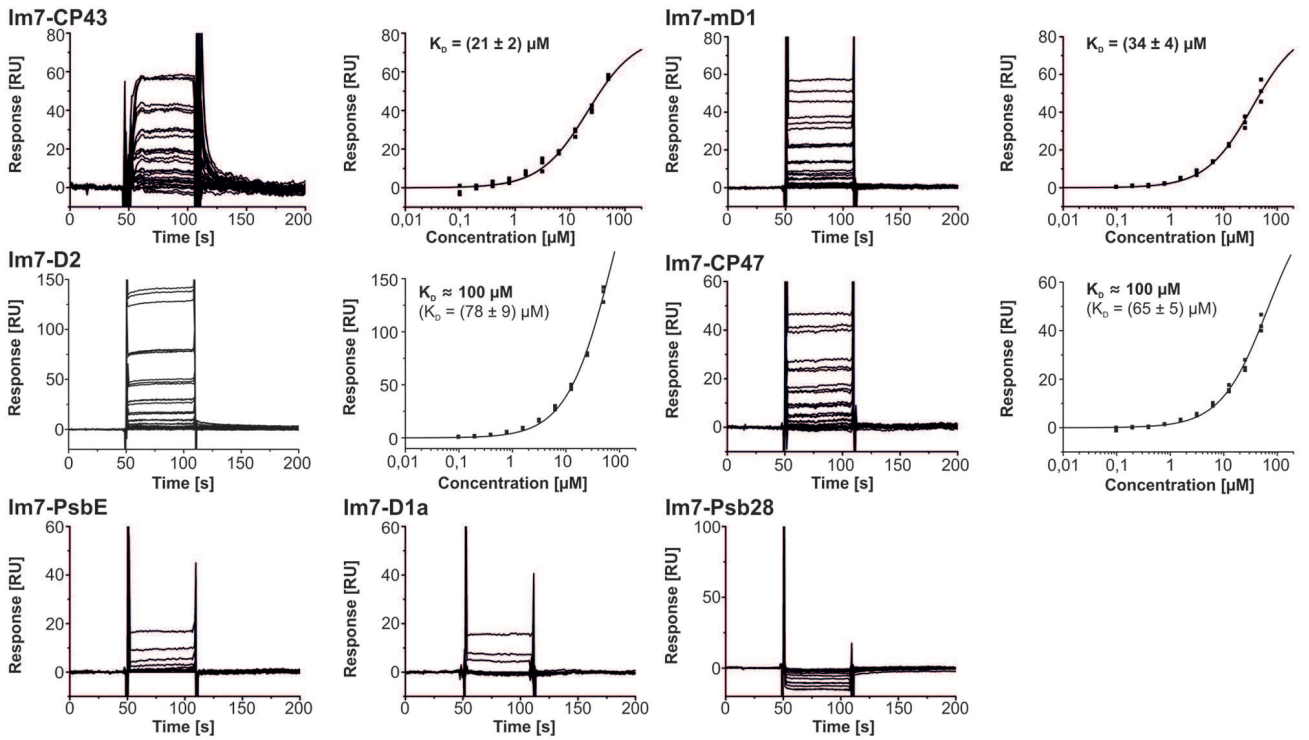

FIGURE 7 | SPR interaction analysis of Psb27. Recombinant Psb27 was probed for binding to various lumenal PSII domains (CP43, CP47, D2, mD1, D1a, and PsbE) and cytoplasmic Psb28 as negative control. In the case of CP43, mD1, D2, and CP47, triplicate sensograms for each analyte concentration reveal reproducible, concentration-dependent steady-state binding responses that can be fitted to a one-site binding isotherm (K_D given with SEs). The highest affinities were measured for CP43 (21 ± 2 µM) and mD1 (34 ± µM), whereas lower affinities were determined for CP47 and D2 (~100 µM). Analysis of D1a, PsbE, and the Psb28 control detected only weak binding at the highest concentrations.

(Seebacher et al., 2006; Petrotchenko and Borchers, 2010). This required the use of two runs of StavroX for each dataset to independently identify cross-linked peptides with light and heavy forms of the cross-linker, which were added in a 1:1 ratio to each sample analyzed. Only peptides that were identified with high confidence in both runs, eluted at the same time in each case, and exhibited comparable fragmentation patterns, were considered as positive identifications. This workflow was further validated by correlation of the results with the known crystal structure of the mature PSII complex. Cross-links that matched our criteria were mapped to the high-resolution crystal structure of PSII, and inspected for plausible reaction partners within range of the cross-linker (<35 Å) and for steric hindrance. Moreover, all identified cross-links were examined for cleavage at the cross-link site, as trypsin, the most commonly used protease in proteomic studies, is unable to cleave C-terminal to modified lysine residues (Hitchcock et al., 2003; Prudova et al., 2010). All identified cross-links appeared feasible and consistent with the PSII structure.

Interestingly, almost all identified cross-links included at least one natural N-terminus as a cross-linking site, which is not unreasonable, as termini are usually the most flexible parts of proteins. This enhanced flexibility may increase the probability that the cross-linker will attach and, once fixed, can scan the surface within the distance accessible to it for a reaction partner, which might be located in a less flexible part of the protein. The preference of the BS3 cross-linker for flexible regions of proteins has previously been observed in a cross-linking and mass spectrometry study of chloroplast ATP synthase (Schmidt et al., 2013). Interestingly, MassMatrix, another commonly used software package for the analysis of cross-linked peptides (Xu and Freitas, 2009), does not consider cross-linked protein termini (Sriswasdi et al., 2014).

The validated workflow was then used for analysis of the intermediate Psb27-PSII complex. One cross-link between Psb27-K91 and CP43-K381 was identified with high confidence, and restricts the binding site of Psb27 to the vicinity of the lumenal CP43 domain. This result also points to one limitation of the cross-linking approach. Although the cross-link was identified with high confidence, its impact on the probabilistic determination of the binding site is relatively low. One structural constraint is not sufficient to fix the binding site, but even with more cross-links, it might still be difficult – depending on their positions – to localize the protein, since the long spacer length of BS3 introduces an inherent fuzziness. From a structural point of view, a zero-length cross-linker like EDC would be more appropriate, but interpretation of zero-length cross-linking MS data and application of differential isotopic labeling is also a much more complex undertaking (Rivera-Santiago et al., 2015).

Therefore, we turned to SPR-based mapping for more precise identification of the Psb27 binding site on PSII – an approach

that has been used successfully to localize the PSII assembly factor CyanoP on the lumenal PSII surface (Cormann et al., 2014). This method relies on PSII peptides and domains that are expressed by *in vitro* translation, captured via the strong binding of the Im7 fusion partner to its cognate binding partner DNaseE7 and probed individually for interaction with the protein of interest (Cormann et al., 2014). Although, it is unknown if the PSII domains adopt native structures, this approach has been validated similarly using the high-resolution PSII crystal structure (Umena et al., 2011). In our previous study, we have shown that the extrinsic subunits PsbV and PsbO only bind to the lumenal domains which provide a broad interaction interface in the complex structure, whereas the other domains showed no or very weak binding responses (Cormann et al., 2014).

Here, we observed binding of Psb27 to lumenal domains of CP43 and CP47, as well as to the C-termini of D1 and D2, which is consistent with the CX-MS result. Moreover, binding to CP43 and D1 seems to be the main driving force for the interaction with the PSII surface, as the binding affinities for both are considerably higher than those for CP47 and D2. These results would favor a localization of Psb27 at the PsbV binding position on PSII (**Figures 8A,B**), which is consistent with biochemical data. It has been shown previously that highly purified Psb27-PSII complexes from *T. elongatus* are devoid of PsbO, PsbV, and PsbU, and that *in vitro* reconstitution of the Psb27-PSII complex with the isolated extrinsic proteins is apparently impossible under the conditions tested (Nowaczyk et al., 2006). However, purified PSII complexes isolated from *Synechocystis* sp. PCC6803 via His-tagging of Psb27 have been found to contain considerable amounts of PsbO, but not PsbV or PsbU (Liu et al., 2011b). These data suggest that simultaneous binding of PsbO and Psb27 is possible, albeit with less stable association of PsbO relative to the mature complex, but simultaneous binding of Psb27 and PsbV or PsbU seems rather unlikely.

Moreover, we have demonstrated a direct interaction of Psb27 with mD1, which argues against the more distal binding position previously proposed for Psb27 on the basis of cross-linking data (Liu et al., 2011a), even if the whole CP43 domain were more flexible in the intermediate PSII complex lacking the adjacent extrinsic proteins. Interestingly, we observed that the CP43-K381 residue involved in the cross-link with Psb27 acts as a cross-linking hotspot on the lumenal surface of the PSII intermediate, but not in the mature complex (**Figure 8A**). The accessibility of CP43-K381/K323/K339 in the Psb27-PSII complex is also inconsistent with the localization of Psb27 based on a chemical footprinting approach (Liu et al., 2013). These authors reported that several residues in the CP43 loop domain (Glu367, Asp376, Asp378, and Asp383) became inaccessible to the solvent upon binding of Psb27, whereas they should be solvent-accessible according to our model (**Figure 8C**). We cannot explain the specific factors that have led to three different experimentally derived models for binding of Psb27 to PSII, but the problems may be related to the experimental conditions used, as mentioned earlier (Mabbitt et al., 2014)

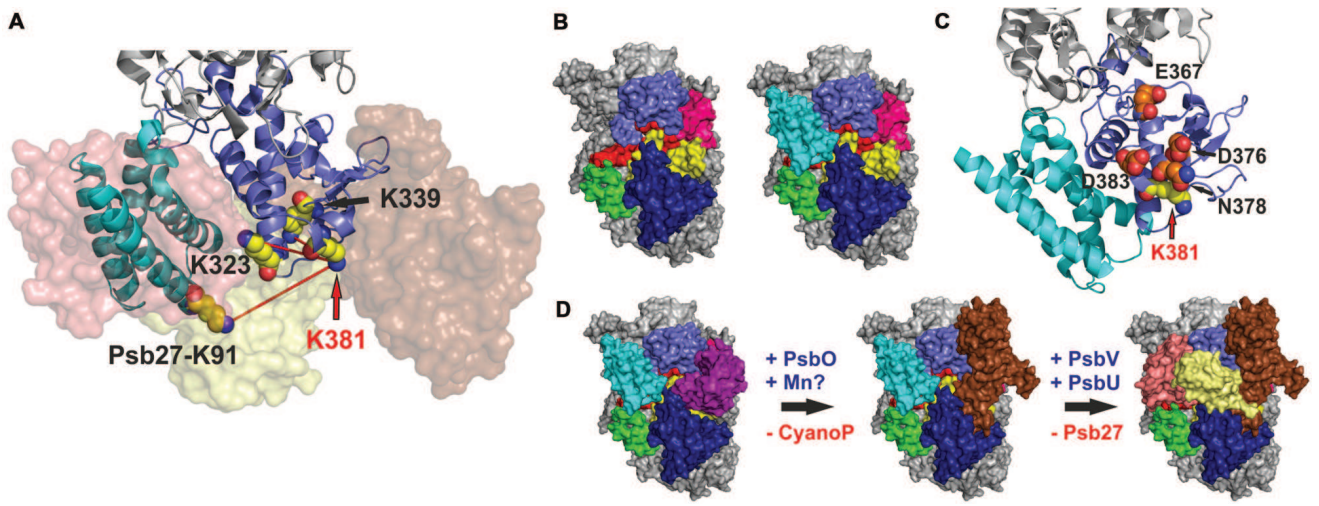

FIGURE 8 | Localization of Psb27 at the PsbV binding position on PSII. (A) CP43-K381 becomes a cross-linking hotspot (CP43-K232, CP43-K339, and Psb27-K91) in the Psb27-PSII intermediate complex, whereas in the mature complex the whole CP43 domain (light blue) is masked and fixed by attachment of the extrinsic proteins PsbO (brown), PsbV (salmon), and PsbU (pale yellow). **(B)** Left: Lumenal PSII surface (CP43 domain: light blue; CP47 domain: dark blue; mD1: red; D1a: pink; D2: yellow; PsbE: green) without the extrinsic proteins. Right: The position of Psb27 (cyan) was modeled based on the cross-link between Psb27-K91 and CP43-K381, the results of the SPR analysis and the membrane attachment of its N-terminus. The position differs from that in a previous model, which localizes Psb27 more distally and partially overlapping the PsbO binding position (Liu et al., 2011a). **(C)** Amino-acid residues of CP43 (D383, E367, D376, and N378) that are in close proximity to CP43-K381 and are protected from chemical modification after binding of Psb27, according to the results of a footprinting approach (Liu et al., 2013). This model appears both incompatible with the previous model (Liu et al., 2011a) and inconsistent with the position of Psb27 in our model. **(D)** Proposed scheme for assembly of the extrinsic part of PSII. The interaction of Psb27 with the C-terminus of D1 in an intermediate PSII complex, and the simultaneous binding of CyanoP – which is speculative but possible (Cormann et al., 2014) – might imply a function for Psb27 during assembly and photoactivation of the manganese cluster. Subsequently, PsbO replaces CyanoP after incorporation of manganese and afterward Psb27 is replaced by PsbV and PsbU in the proposed scheme.

or to the interpretation of MS data. Strikingly, one of the cross-linked peptides (Psb27K63↔CP43D321) identified by Liu et al. (2011a) is apparently cleaved by trypsin C-terminal to Psb27K63, although it should be protected by the cross-link. Furthermore, both presented cross-links (Psb27K58↔CP43D215 and Psb27K63↔CP43D321) are supposed to contain post-translational modifications (triple methylation, deamidation, formation of methyl esters) that have not otherwise been reported for cyanobacterial samples to the best of our knowledge, and which cannot be explained as by-products of sample preparation (Liu et al., 2011a). One reason for these contradictions could be a false positive identification by MassMatrix (Xu et al., 2008; Xu and Freitas, 2009), the software which was used in the 2011 study. The probability of false positive identifications is given by the pp-value, which is calculated by the software for each identification (Xu et al., 2008; Xu and Freitas, 2009). Liu et al. (2011a) used a minimal pp-score of 5 for the cross-link analysis, which might be compatible with a high proportion of false positive identifications (Xu et al., 2008; Xu and Freitas, 2009).

However, localization of Psb27 at the PsbV binding position is in agreement with concurrent binding of CyanoP, which is localized at the PsbO binding site (Cormann et al., 2014). Both proteins are able to bind simultaneously to an intermediate PSII complex that plays a role in PSII biogenesis/repair and both interact with the C-terminus of D1 (Cormann et al., 2014), which suggest a cooperative role in manganese cluster assembly (**Figure 8D**). It has been shown previously that Psb27 facilitates assembly of the manganese cluster (Roose and Pakrasi, 2008) and plays a role in the structural integrity of the manganese binding site (Grasse et al., 2011), but the model and the sequence of events (**Figure 8D**) are speculative, as it is not clear whether the complexes depicted are actually formed *in vivo*. Binding of Psb27 to PSII is further constrained by its N-terminal lipid modification (Nowaczyk et al., 2006), which is difficult to consider by an *in vitro* approach. Integration of additional *in vivo* data and in particular crystallization of – in case of Psb27 – relatively stable intermediate complexes would further reveal the structural and functional relationships between Psb27 and PSII during biogenesis and repair.

CONCLUSION

We have shown that *in silic*o molecular docking does not seem to be suitable for the localization of auxiliary proteins on the lumenal PSII surface, at least with the tested software and where no further experimental data are available. False positive results are also an important issue in the identification of cross-links by mass spectrometry. Therefore, we have developed a CX-MS approach for the structural analysis of intermediate PSII complexes that is based on high-resolution mass spectrometry and isotope-coded cross-linkers. Validation of the method by comparison with the PSII crystal structure identified only cross-links that are consistent with the structure, and analysis of an intermediate Psb27-PSII complex corroborated binding of Psb27 adjacent to the lumenal CP43 domain and the C-terminus of D1. In particular the combination of the two complementary methods – CX-MS and SPR based mapping – facilitates a detailed structural characterization of unstable intermediate complexes that are part of the intricate life cycle of PSII.

MATERIALS AND METHODS

PCR and Molecular Cloning

The coding sequence of the *psb27* gene (*tll2462*) of *T. elongatus* (without the segment encoding the signal peptide and the N-terminal cysteine) was amplified by PCR, using the primer oligonucleotides: GAAGATGGTCTCTGCGCCGCCAATGTGC CTACGG (forward) and GAATAAGGTCTCCTATCAGGACTT CGCTTCGCG (reverse). After digestion with *Eco31*I, the product was inserted into the pASK-IBA35plus vector (IBA).

To generate an expression vector for Psb28 fused to the ColE7 immunity protein (Im7), the *psb28* gene of *T. elongatus* (*tlr0493*) was amplified by PCR using the primers GGAATTCCATATG GGTGCAATGGCAGAAATTC (forward) and CGAATTCCCC GAGAGTTCTCAGACTTCTG (reverse). Subsequently, the gene sequence was inserted into the plasmid pIVEX24IN (Cormann et al., 2014) via the *Nde*I and *Sma*I restriction sites. Construction of expression templates for Im7 fusions to the lumenal PSII domains is described elsewhere (Cormann et al., 2014).

Cell-Free Protein Expression

For cell-free expression of Im7-tagged domains of CP43 (residues 293 – 424), CP47 (271 – 446) D1 (D1a: 54 – 113; mD1: 295 – 344), D2 (294 – 352), and PsbE (48 – 84), we used the RTS100 system (5Prime) as described by Cormann et al. (2014).

Heterologous Protein Overexpression and Purification

Heterologous overexpression of Psb27 was performed in *Escherichia coli* Overexpress C43 cells (Lucigen). After transformation of C43 cells with the Psb27 plasmid, an overnight starter culture (50 ml LB medium supplemented with 1 % (w/v) glucose and 100 μg/ml ampicillin) was inoculated with a single colony. The culture was grown in vigorously shaken (200 rpm) flasks at 37°C. Then two flasks with 500 ml were each inoculated with a 5-ml aliquot of the overnight preculture and incubated at 200 rpm and 37°C. Psb27 expression was induced by the addition of anhydrotetracycline (200 μg/l) when the cultures had reached an OD_{600} of 0.6. After additional 16 h of incubation, the cells were harvested (4000 rpm, 20 min, 4°C, GSA rotor), resuspended in IMAC equilibration buffer (20 mM MES, 500 mM NaCl, 20 mM imidazole; pH 6.5) and disrupted by sonification. For purification of Psb27, the ÄKTA system (GE, Healthcare) was used. In the first step, the supernatant was applied to an equilibrated IMAC column (His Trap crude FF 5 ml, GE Healthcare) and washed with ten column volumes (CV) of IMAC equilibrating buffer. For elution, a linear gradient from 0 to 66% of IMAC elution buffer (20 mM MES, 500 mM NaCl, 500 mM imidazole; pH 6.5) was applied at a flow rate of 2 ml/min over four CV, and this was followed by five CV of 100% IMAC elution buffer. Fractions containing Psb27 were pooled

and dialyzed twice against 1 l of IEC equilibration buffer (20 mM MES, pH 6.5). For the second purification step a ResourceS column ($CV = 1$ ml, GE Healthcare) was equilibrated with five CV of IEC equilibration buffer at a flow rate of 4 ml/min to reduce the conductivity to ≤4.5 mS/cm. A sample volume equivalent to the yield of protein from 1 l of expression culture was applied to the column, which was then washed with five CV of IEC equilibration buffer. For elution a linear gradient from 0 to 50% of IEC elution buffer (20 mM MES, 1 M NaCl; pH 6.5) was applied over 20 CV, followed by 100% elution buffer over 10 CV. The purified protein was dialyzed overnight against 1 l of MBS (20 mM MES, 150 mM NaCl; pH 6.5) and stored at –80°C.

The expression and purification of Psb28 fused to Im7 was performed according to Cormann et al. (2014).

Isolation of PSII from *T. elongatus*

Isolation of PSII complexes from wild-type *T. elongatus* was carried out according to Kuhl et al. (2000).

4.5 Cross-Linking in Combination with Mass Spectrometry (CX-MS)

Isolated PSII complexes (2.4 μM) were incubated with a 1:1 mixture of BS3-H12/D12 (Creative Molecules Inc.) in buffer (20 mM MES/NaOH, 10 mM $CaCl_2$, 0.03% (w/v) dodecyl-β-D-maltoside; pH 6.5) containing the cross-linker at a final concentration of 5 mM. After a 30-min incubation on ice, NH_4HCO_3 (100 mM) was added, and the reaction mixture was incubated for 15 min at room temperature to terminate the cross-linking reaction. Tryptic digestion and sample preparation were performed after protein precipitation by addition of cold acetone (Nowaczyk et al., 2011). Tryptic peptides were desalted with ZipTips (Millipore) and resuspended in buffer A (0.1% (v/v) formic acid in water). Samples were applied to an UPLC Symmetry C_{18} trapping column (5 μm, 180 μm × 20 mm) and subsequently transferred to an UPLC BEH C_{18} column (1.7 μm, 75 μm × 150 mm). Both columns (Waters, Milford, MA, USA) were driven by the nanoACQUITY gradient UPLC pump system (Waters) coupled to an Orbitrap Elite Velos Pro Hybrid FTMS mass spectrometer (Thermo Fisher Scientific Inc., Waltham, MA, USA) via a PicoTip Emitter (SilicaTip, 30 μm, New Objective, Woburn, MA, USA). The column oven was set to a temperature of 45°C and the spray voltage to 1.5–1.8 kV. Peptides were eluted with a multistep gradient of buffer A to buffer B (0.1% formic acid in acetonitrile) at a flow rate of 0.4 μl/min (0–5 min: 1% buffer B; 5–10 min: 5% buffer B; 10–175 min: 40% buffer B; 175–200 min: 99% buffer B; 200–210 min: 1% buffer B). The linear ion trap and orbitrap were operated in parallel, i.e., during a full MS scan on the orbitrap in the range of 300–2000 m/z at a resolution of 240,000. Tandem MS (MS/MS) spectra of the 20 most intense precursors were detected in the ion trap. The heated desolvation capillary was set to 200°C. The relative collision energy for collision-induced dissociation was set to 35%. Dynamic exclusion was enabled, with a repeat count of one and a 1-min exclusion duration window. Singly or doubly charged ions, as well as ions with an unassigned charge state, were rejected from MS/MS. StavroX v. 3.1.19 was used for MS/MS data interpretation (Götze et al., 2012) with the following settings: Protease cleavage sites: K, R; missed cleavages: K:3, R:1; Variable modifications: methionine oxidation (max. 2); cross-linker: BS3-H12/D12; cross-linked amino acids: 1. K, N-term.; 2. K, S, T, Y, N-term; precursor precision: 3.0 ppm; fragment ion precision: 0.8 Da; lower mass limit: 200 Da; upper mass limit: 5000 Da; S/N ratio: 2.0; ion types: b-and y-ions; neutral loss: only of identified fragments.

Surface Plasmon Resonance Spectroscopy

Surface plasmon resonance measurements were performed with a Biacore 3000 instrument and CM5 sensor chips (GE Healthcare). Covalent binding of DNase E7 to the gold surface was done according to Hosse et al. (2009). The Gentle Elution Buffer (Thermo Scientific) was used for surface conditioning, with two consecutive 1-min injections and a flow rate of 60 μl/min. Details of the on-chip purification of the Im7 fusion proteins and the preparation of the reference surface are given in Cormann et al. (2014). For SPR interaction analysis with the lumenal PSII domains a dilution series from 50 μM to 100 nM of Psb27 in running buffer MBS-EP (20 mM MES, 150 mM NaCl, 3 mM EDTA, 0,05% (v/v) Surfactant P20; pH 6.5) was applied for 60 s to the reference and the active surface. Dissociation was monitored for 120 s, and afterward the surface was cleaned with a 1-minute injection of 1 M NaCl in MBS-EP. Each experiment was performed at a constant flow rate of 30 μl/min and at a temperature of 298 K.

Ab Initio Docking

The Cluspro 2.0 Server (Comeau et al., 2004a,b) was used for *ab initio* docking calculations. It calculates various structures of the protein complex on the basis of protein structures in pdb files. In this case, monomeric PSII without the extrinsic subunits PsbU, PsbO, PsbV (PDB: 3ARC) (Umena et al., 2011) and the crystal structures of PsbV (PDB: 1MZ4) (Kerfeld et al., 2003) and Psb27 (PDB: 2Y6X) (Michoux et al., 2012) were used. The models of docked PsbV were then compared to the crystal structure.

Cross-Link Prediction with Xwalk

The Xwalk algorithm (Kahraman et al., 2011) was used for the calculation of distances between solvent-accessible primary amines in the PSII crystal structure (Umena et al., 2011). These models were calculated without additional distance information.

AUTHOR CONTRIBUTIONS

KC designed and carried out most of the experiments, analyzed the data, and prepared the figures. MP was involved in surface plasmon resonance experiments and data analysis. MN conceived and supervised the project, analyzed the data, and wrote the manuscript, with contributions of all authors.

FUNDING

This work was supported by grants from the Ruhr University Research School and the Greif-Stiftung (to KC) and by DFG Research Group FOR 2092 (NO 836/3-1, MN).

ACKNOWLEDGMENTS

Ansgar Poetsch, Christian Trötschel, and Sascha Rexroth are gratefully acknowledged for support with the MS analysis. We thank Melanie Völkel, Claudia König, Regina Oworah-Nkruma, and Tanja Bojarzyn for excellent technical assistance and Paul Hardy for critical reading of the manuscript.

SUPPLEMENTARY MATERIAL

The Supplementary Material for this article can be found online at: http://journal.frontiersin.org/article/10.3389/fpls.2016.00157

REFERENCES

Baker, P. R., Medzihradszky, K. F., and Chalkley, R. J. (2010). Improving software performance for peptide electron transfer dissociation data analysis by implementation of charge state- and sequence-dependent scoring. *Mol. Cell. Proteom.* 9, 1795–1803. doi: 10.1074/mcp.M110.000422

Becker, K., Cormann, K. U., and Nowaczyk, M. M. (2011). Assembly of the water-oxidizing complex in photosystem II. *J. Photochem. Photobiol. B* 104, 204–211. doi: 10.1016/j.jphotobiol.2011.02.005

Bricker, T. M., Mummadisetti, M. P., and Frankel, L. K. (2015). Recent advances in the use of mass spectrometry to examine structure/function relationships in photosystem II. *J. Photochem. Photobiol. B* 152, 227–246. doi: 10.1016/j.jphotobiol.2015.08.031

Chen, Y., Chen, W., Cobb, M. H., and Zhao, Y. (2009). PTMap–a sequence alignment software for unrestricted, accurate, and full-spectrum identification of post-translational modification sites. *Proc. Natl. Acad. Sci. U.S.A.* 106, 761–766. doi: 10.1073/pnas.0811739106

Comeau, S. R., Gatchell, D. W., Vajda, S., and Camacho, C. J. (2004a). ClusPro: a fully automated algorithm for protein-protein docking. *Nucleic Acids Res.* 32, W96–W99. doi: 10.1093/nar/gkh354

Comeau, S. R., Gatchell, D. W., Vajda, S., and Camacho, C. J. (2004b). ClusPro: an automated docking and discrimination method for the prediction of protein complexes. *Bioinformatics* 20, 45–50. doi: 10.1093/bioinformatics/btg371

Cormann, K. U., Bangert, J. A., Ikeuchi, M., Rögner, M., Stoll, R., and Nowaczyk, M. M. (2009). Structure of Psb27 in solution: implications for transient binding to photosystem II during biogenesis and repair. *Biochemistry* 48, 8768–8770. doi: 10.1021/bi9012726

Cormann, K. U., Bartsch, M., Rögner, M., and Nowaczyk, M. M. (2014). Localization of the CyanoP binding site on photosystem II by surface plasmon resonance spectroscopy. *Front. Plant Sci.* 5:595. doi: 10.3389/fpls.2014.00595

Cox, N., Pantazis, D. A., Neese, F., and Lubitz, W. (2013). Biological water oxidation. *Acc. Chem. Res.* 46, 1588–1596. doi: 10.1021/ar3003249

DeLano, W. L. (2002). *The PyMOL Molecular Graphics System*. Palo Alto, CA: DeLano Scientific.

Fagerlund, R. D., and Eaton-Rye, J. J. (2011). The lipoproteins of cyanobacterial photosystem II. *J. Photochem. Photobiol. B* 104, 191–203. doi: 10.1016/j.jphotobiol.2011.01.022

Ferreira, K. N., Iverson, T. M., Maghlaoui, K., Barber, J., and Iwata, S. (2004). Architecture of the photosynthetic oxygen-evolving center. *Science* 303, 1831–1838. doi: 10.1126/science.1093087

Götze, M., Pettelkau, J., Schaks, S., Bosse, K., Ihling, C. H., Krauth, F., et al. (2012). StavroX–a software for analyzing crosslinked products in protein interaction studies. *J. Am. Soc. Mass Spectrom.* 23, 76–87.

Grasse, N., Mamedov, F., Becker, K., Styring, S., Rögner, M., and Nowaczyk, M. M. (2011). Role of novel dimeric photosystem II (PSII)-Psb27 protein complex in PSII repair. *J. Biol. Chem.* 286, 29548–29555. doi: 10.1074/jbc.M111.238394

Guskov, A., Kern, J., Gabdulkhakov, A., Broser, M., Zouni, A., and Saenger, W. (2009). Cyanobacterial photosystem II at 2.9-A resolution and the role of quinones, lipids, channels and chloride. *Nat. Struct. Mol. Biol.* 16, 334–342. doi: 10.1038/nsmb.1559

Hitchcock, A. L., Auld, K., Gygi, S. P., and Silver, P. A. (2003). A subset of membrane-associated proteins is ubiquitinated in response to mutations in the endoplasmic reticulum degradation machinery. *Proc. Natl. Acad. Sci. U.S.A.* 100, 12735–12740. doi: 10.1073/pnas.2135500100

Hosse, R. J., Tay, L., Hattarki, M. K., Pontes-Braz, L., Pearce, L. A., Nuttall, S. D., et al. (2009). Kinetic screening of antibody-Im7 conjugates by capture on a colicin E7 DNase domain using optical biosensors. *Anal. Biochem.* 385, 346–357. doi: 10.1016/j.ab.2008.11.026

Hou, X., Fu, A., Garcia, V. J., Buchanan, B. B., and Luan, S. (2015). PSB27: a thylakoid protein enabling *Arabidopsis* to adapt to changing light intensity. *Proc. Natl. Acad. Sci. U.S.A.* 112, 1613–1618. doi: 10.1073/pnas.1424040112

Janin, J., Henrick, K., Moult, J., Eyck, L. T., Sternberg, M. J., Vajda, S., et al. (2003). CAPRI: a critical assessment of PRedicted interactions. *Proteins* 52, 2–9. doi: 10.1002/prot.10381

Kahraman, A., Malmstrom, L., and Aebersold, R. (2011). Xwalk: computing and visualizing distances in cross-linking experiments. *Bioinformatics* 27, 2163–2164. doi: 10.1093/bioinformatics/btr348

Kerfeld, C. A., Sawaya, M. R., Bottin, H., Tran, K. T., Sugiura, M., Cascio, D., et al. (2003). Structural and EPR characterization of the soluble form of cytochrome c-550 and of the psbV2 gene product from the cyanobacterium *Thermosynechococcus elongatus*. *Plant Cell Physiol.* 44, 697–706. doi: 10.1093/pcp/pcg084

Komenda, J., Knoppova, J., Kopecna, J., Sobotka, R., Halada, P., Yu, J., et al. (2012). The Psb27 assembly factor binds to the CP43 complex of photosystem II in the cyanobacterium *Synechocystis* sp. PCC 6803. *Plant Physiol.* 158, 476–486. doi: 10.1104/pp.111.184184

Kozakov, D., Beglov, D., Bohnuud, T., Mottarella, S. E., Xia, B., Hall, D. R., et al. (2013). How good is automated protein docking? *Proteins* 81, 2159–2166. doi: 10.1002/prot.24403

Kozakov, D., Brenke, R., Comeau, S. R., and Vajda, S. (2006). PIPER: an FFT-based protein docking program with pairwise potentials. *Proteins* 65, 392–406. doi: 10.1002/prot.21117

Kuhl, H., Kruip, J., Seidler, A., Krieger-Liszkay, A., Bunker, M., Bald, D., et al. (2000). Towards structural determination of the water-splittinge enzyme. Purification, crystallization, and preliminary crystallographic studies of photosystem II from a thermophilic cyanobacterium. *J. Biol. Chem.* 275, 20652–20659. doi: 10.1074/jbc.M001321200

Lensink, M. F., and Wodak, S. J. (2013). Docking, scoring, and affinity prediction in CAPRI. *Proteins* 81, 2082–2095. doi: 10.1002/prot.24428

Liu, H., Chen, J., Huang, R. Y., Weisz, D., Gross, M. L., and Pakrasi, H. B. (2013). Mass spectrometry-based footprinting reveals structural dynamics of loop E of the chlorophyll-binding protein CP43 during photosystem II assembly in the cyanobacterium *Synechocystis* 6803. *J. Biol. Chem.* 288, 14212–14220. doi: 10.1074/jbc.M113.467613

Liu, H., Huang, R. Y., Chen, J., Gross, M. L., and Pakrasi, H. B. (2011a). Psb27, a transiently associated protein, binds to the chlorophyll binding protein CP43 in photosystem II assembly intermediates. *Proc. Natl. Acad. Sci. U.S.A.* 108, 18536–18541. doi: 10.1073/pnas.1111597108

Liu, H., Roose, J. L., Cameron, J. C., and Pakrasi, H. B. (2011b). A genetically tagged Psb27 protein allows purification of two consecutive photosystem II (PSII) assembly intermediates in *Synechocystis* 6803, a cyanobacterium. *J. Biol. Chem.* 286, 24865–24871. doi: 10.1074/jbc.M111.246231

Mabbitt, P. D., Rautureau, G. J., Day, C. L., Wilbanks, S. M., Eaton-Rye, J. J., and Hinds, M. G. (2009). Solution structure of Psb27 from cyanobacterial photosystem II. *Biochemistry* 48, 8771–8773. doi: 10.1021/bi901309c

Mabbitt, P. D., Wilbanks, S. M., and Eaton-Rye, J. J. (2014). Structure and function of the hydrophilic photosystem II assembly proteins: Psb27, Psb28 and Ycf48. *Plant Physiol. Biochem.* 81, 96–107. doi: 10.1016/j.plaphy.2014.02.013

McEvoy, J. P., and Brudvig, G. W. (2006). Water-splitting chemistry of photosystem II. *Chem. Rev.* 106, 4455–4483. doi: 10.1021/cr0204294

Michoux, F., Takasaka, K., Boehm, M., Komenda, J., Nixon, P. J., and Murray, J. W. (2012). Crystal structure of the Psb27 assembly factor at 1.6 A: implications for binding to photosystem II. *Photosynth. Res.* 110, 169–175. doi: 10.1007/s11120-011-9712-7

Mulo, P., Sirpiö, S., Suorsa, M., and Aro, E.-M. (2008). Auxiliary proteins involved in the assembly and sustenance of photosystem II. *Photosynth. Res.* 98, 489–501. doi: 10.1007/s11120-008-9320-3

Nickelsen, J., and Rengstl, B. (2013). Photosystem II assembly: from cyanobacteria to plants. *Annu. Rev. Plant Biol.* 64, 609–635. doi: 10.1146/annurev-arplant-050312-120124

Nixon, P. J., Michoux, F., Yu, J., Boehm, M., and Komenda, J. (2010). Recent advances in understanding the assembly and repair of photosystem II. *Ann. Bot.* 106, 1–16. doi: 10.1093/aob/mcq059

Nowaczyk, M. M., Hebeler, R., Schlodder, E., Meyer, H. E., Warscheid, B., and Rögner, M. (2006). Psb27, a cyanobacterial lipoprotein, is involved in the repair cycle of photosystem II. *Plant Cell* 18, 3121–3131. doi: 10.1105/tpc.106.042671

Nowaczyk, M. M., Sander, J., Grasse, N., Cormann, K. U., Rexroth, D., Bernat, G., et al. (2010). Dynamics of the cyanobacterial photosynthetic network: communication and modification of membrane protein complexes. *Eur. J. Cell Biol.* 89, 974–982. doi: 10.1016/j.ejcb.2010.08.008

Nowaczyk, M. M., Wulfhorst, H., Ryan, C. M., Souda, P., Zhang, H., Cramer, W. A., et al. (2011). NdhP and NdhQ: two novel small subunits of the cyanobacterial NDH-1 complex. *Biochemistry* 50, 1121–1124. doi: 10.1021/bi102044b

Petrotchenko, E. V., and Borchers, C. H. (2010). Crosslinking combined with mass spectrometry for structural proteomics. *Mass Spectrom. Rev.* 29, 862–876. doi: 10.1002/mas.20293

Prudova, A., Auf Dem Keller, U., Butler, G. S., and Overall, C. M. (2010). Multiplex N-terminome analysis of MMP-2 and MMP-9 substrate degradomes by iTRAQ-TAILS quantitative proteomics. *Mol. Cell. Proteom.* 9, 894–911. doi: 10.1074/mcp.M000050-MCP201

Rexroth, S., Rexroth, D., Veit, S., Plohnke, N., Cormann, K. U., Nowaczyk, M. M., et al. (2014). Functional characterization of the small regulatory subunit PetP from the cytochrome b_6f complex in *Thermosynechococcus elongatus*. *Plant Cell* 26, 3435–3448. doi: 10.1105/tpc.114.125930

Rivera-Santiago, R. F., Sriswasdi, S., Harper, S. L., and Speicher, D. W. (2015). Probing structures of large protein complexes using zero-length cross-linking. *Methods* 89, 99–111. doi: 10.1016/j.ymeth.2015.04.031

Roose, J. L., and Pakrasi, H. B. (2008). The Psb27 protein facilitates manganese cluster assembly in photosystem II. *J. Biol. Chem.* 283, 4044–4050. doi: 10.1074/jbc.M708960200

Roose, J. L., Wegener, K. M., and Pakrasi, H. B. (2007). The extrinsic proteins of photosystem II. *Photosynth. Res.* 92, 369–387. doi: 10.1007/s11120-006-9117-1

Schmidt, C., Zhou, M., Marriott, H., Morgner, N., Politis, A., and Robinson, C. V. (2013). Comparative cross-linking and mass spectrometry of an intact F-type ATPase suggest a role for phosphorylation. *Nat. Commun.* 4:1985. doi: 10.1038/ncomms2985

Seebacher, J., Mallick, P., Zhang, N., Eddes, J. S., Aebersold, R., and Gelb, M. H. (2006). Protein cross-linking analysis using mass spectrometry, isotope-coded cross-linkers, and integrated computational data processing. *J. Proteome Res.* 5, 2270–2282. doi: 10.1021/pr060154z

Shi, L. X., Hall, M., Funk, C., and Schröder, W. P. (2012). Photosystem II, a growing complex: updates on newly discovered components and low molecular mass proteins. *Biochim. Biophys. Acta* 1817, 13–25. doi: 10.1016/j.bbabio.2011.08.008

Sinz, A. (2006). Chemical cross-linking and mass spectrometry to map three-dimensional protein structures and protein-protein interactions. *Mass Spectrom. Rev.* 25, 663–682. doi: 10.1002/mas.20082

Sriswasdi, S., Harper, S. L., Tang, H. Y., and Speicher, D. W. (2014). Enhanced identification of zero-length chemical cross-links using label-free quantitation and high-resolution fragment ion spectra. *J. Proteome Res.* 13, 898–914. doi: 10.1021/pr400953w

Stengel, F., Aebersold, R., and Robinson, C. V. (2012). Joining forces: integrating proteomics and cross-linking with the mass spectrometry of intact complexes. *Mol. Cell. Proteom.* 11, R1110.14027. doi: 10.1074/mcp.R111.014027

Suga, M., Akita, F., Hirata, K., Ueno, G., Murakami, H., Nakajima, Y., et al. (2015). Native structure of photosystem II at 1.95 Å resolution viewed by femtosecond X-ray pulses. *Nature* 517, 99–103. doi: 10.1038/nature13991

Umena, Y., Kawakami, K., Shen, J. R., and Kamiya, N. (2011). Crystal structure of oxygen-evolving photosystem II at a resolution of 1.9Å. *Nature* 473, 55–60. doi: 10.1038/nature09913

Xu, H., and Freitas, M. A. (2009). MassMatrix: a database search program for rapid characterization of proteins and peptides from tandem mass spectrometry data. *Proteomics* 9, 1548–1555. doi: 10.1002/pmic.200700322

Xu, H., Zhang, L., and Freitas, M. A. (2008). Identification and characterization of disulfide bonds in proteins and peptides from tandem MS data by use of the MassMatrix MS/MS search engine. *J. Proteome Res.* 7, 138–144. doi: 10.1021/pr070363z

Conflict of Interest Statement: The authors declare that the research was conducted in the absence of any commercial or financial relationships that could be construed as a potential conflict of interest.

frontiers in Plant Science

REVIEW
published: 10 May 2016
doi: 10.3389/fpls.2016.00617

The Use of Advanced Mass Spectrometry to Dissect the Life-Cycle of Photosystem II

Daniel A. Weisz[1,2], *Michael L. Gross*[2] *and Himadri B. Pakrasi*[1]*

[1] Department of Biology, Washington University in St. Louis, St. Louis, MO, USA, [2] Department of Chemistry, Washington University in St. Louis, St. Louis, MO, USA

Photosystem II (PSII) is a photosynthetic membrane-protein complex that undergoes an intricate, tightly regulated cycle of assembly, damage, and repair. The available crystal structures of cyanobacterial PSII are an essential foundation for understanding PSII function, but nonetheless provide a snapshot only of the active complex. To study aspects of the entire PSII life-cycle, mass spectrometry (MS) has emerged as a powerful tool that can be used in conjunction with biochemical techniques. In this article, we present the MS-based approaches that are used to study PSII composition, dynamics, and structure, and review the information about the PSII life-cycle that has been gained by these methods. This information includes the composition of PSII subcomplexes, discovery of accessory PSII proteins, identification of post-translational modifications and quantification of their changes under various conditions, determination of the binding site of proteins not observed in PSII crystal structures, conformational changes that underlie PSII functions, and identification of water and oxygen channels within PSII. We conclude with an outlook for the opportunity of future MS contributions to PSII research.

Keywords: Photosystem II, Photosystem II life-cycle, mass spectrometry, post-translational modification, chemical cross-linking, protein footprinting

OPEN ACCESS

Edited by:
Julian Eaton-Rye, University of Otago, New Zealand

Reviewed by:
Jian-Ren Shen, Okayama University, Japan
Julian Whitelegge, University of California, Los Angeles, USA

***Correspondence:**
Himadri B. Pakrasi
pakrasi@wustl.edu

Specialty section:
This article was submitted to Plant Cell Biology, a section of the journal Frontiers in Plant Science

Received: *05 February 2016*
Accepted: *22 April 2016*
Published: *10 May 2016*

Citation:
Weisz DA, Gross ML and Pakrasi HB (2016) The Use of Advanced Mass Spectrometry to Dissect the Life-Cycle of Photosystem II. Front. Plant Sci. 7:617. doi: 10.3389/fpls.2016.00617

INTRODUCTION

Since the late 1990s, mass spectrometry (MS) has become a central tool for the study of proteins and their role in biology. The advent of electrospray ionization (ESI) and matrix-assisted laser desorption ionization (MALDI) permits the ionization of peptides and proteins and their introduction into the gas phase, enabling their analysis by MS. The typical "bottom-up" workflow that emerged in the wake of these breakthroughs involves: (1) enzymatic digestion (often by trypsin) of a protein to produce peptides of small enough size (typically 1–3 kDa) to be ionized

Abbreviations: *A.thaliana*, *Arabidopsis thaliana*; BS^3, (bis(sulfosuccinimidyl)suberate); *C. reinhardtii*, *Chlamydomonas reinhardtii*; DSP, dithiobis(succinimidyl propionate); DTSSP, 3,3′-dithiobis(sulfosuccinimidyl propionate); EDC, 1-ethyl-3-(3-dimethylaminopropyl)carbodiimide; ESI, electrospray ionization; FAB, fast atom bombardment; FTICR, Fourier transform ion cyclotron resonance; GEE, glycine ethyl ester; LC, liquid chromatography; LHCII, Light-harvesting complex II; LMM, low-molecular-mass; LTQ, linear ion trap quadrupole; MALDI, matrix-assisted laser desorption ionization; MS, mass spectrometry; *N. tabacum*, *Nicotiana tabacum*; NHS, N-hydroxysuccinimide; OCP, orange carotenoid protein; PBS, phycobilisome; PSII, Photosystem II; PC, plastocyanin; PTM, post-translational modification; QqQ, triple-quadrupole; SCP, small CAB-like protein; *Synechococcus* 7002, *Synechococcus* sp. PCC 7002; *Synechocystis* 6803, *Synechocystis* sp. PCC 6803; *T. elongatus, Thermosynechococcus elongatus*; TOF, time-of-flight; WOC, water-oxidizing complex.

and fragmented efficiently in a mass spectrometer; (2) liquid chromatographic (LC) separation of the peptides; and (3) online (or offline) injection of the separated peptides into a mass spectrometer. The "top-down" approach is an attractive alternative that eliminates the protein digestion step, but the subsequent steps are generally more difficult for intact proteins than peptides, and this approach is currently best-suited for small, soluble proteins. After injection of the peptides, a typical tandem MS analysis consists of: (1) ionization of the peptide sample by ESI or MALDI and introduction into the gas phase; (2) measurement of the mass-to-charge (m/z) ratio of the intact peptide (also referred to as "MS^1" analysis); and (3) fragmentation of the precursor ion and measurement of its "product-ion" spectrum ("MS/MS" or "MS^2" analysis), which provides information about the peptide's amino acid sequence. When genomic information is available to predict the sequence of all proteins in the organism, computer analysis of the peptide masses and product-ion spectra can determine the highest-scoring match for each peptide from the protein database. This highest-scoring match is taken as the identity of the peptide, assuming data quality meets certain statistical criteria. A given protein is then determined to have been present in the sample if the quality and number of its peptide hits meet an additional set of statistical criteria. The ability to identify many proteins in a sample at once by MS has become the cornerstone of the field of proteomics.

Protein identification is only the most basic application of MS-based proteomics, and it has traditionally been described as the first "pillar" of the field. The second pillar is characterization of the many proteoforms that exist for each protein, arising, e.g., from splice variants and post-translational modifications (PTMs). These two pillars address questions about the *composition* of a protein sample. The third pillar is quantification—either absolute or relative—of proteins using isotopic labeling or label-free approaches. This pillar is typically used to address questions about the *dynamics* of a system—how composition of proteins or proteoforms changes over time, space, or under different environmental conditions or perturbations. A proposed fourth pillar focuses on the emerging area of structural proteomics that uses MS-based techniques to address questions about the three-dimensional *structure* of proteins and protein complexes in a cell.

These four pillars of proteomics have each become indispensable tools for gleaning information about photosynthesis (Battchikova et al., 2015; Bricker et al., 2015; Heinz et al., 2016) and, in particular for this review, the life-cycle of PSII. A search for publications containing both "Photosystem II" and "mass spectrometry" in the article title, abstract, and/or keywords was performed on the Scopus database. The results, displayed in **Figure 1**, show that prior to the advent of ESI and MALDI in the late 1980s, publications were nearly zero per year. Starting in the early 1990s and continuing through 2015, publications have risen steadily, with around 20–30 publications per year in the last several years. The rise can be attributed to method and instrument development, and to increasing accessibility of MS instrumentation to biology researchers. An overview of how MS-based tools are typically applied to PSII life-cycle research is given in **Table 1**. This review focuses on MS of proteins. However, it should be noted that another widely used application of MS in PSII research is the analysis of the isotopic composition of evolved oxygen by membrane-inlet mass spectrometry. This technique has yielded significant insight into the mechanistic aspects of water oxidation by PSII (reviewed in Shevela and Messinger, 2013).

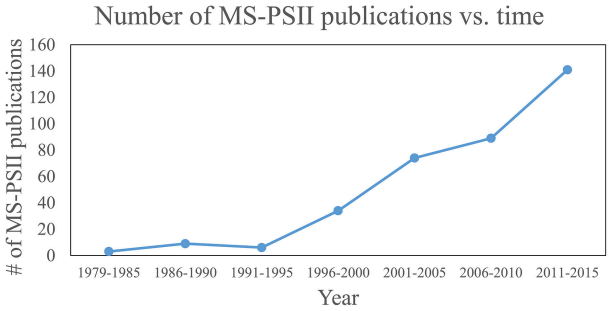

FIGURE 1 | Plot of publications that use MS for PSII research over time. Publications that contain "Photosystem II" and "mass spectrometry" in their article title, abstract, or keywords were searched on the Scopus database. Each data point represents the total number of publications for that range of years.

In the sections that follow, we consider questions of PSII composition, dynamics, and structure separately. For each area, a brief overview of the relevant MS-based tools is given, followed by examples of several PSII life-cycle research areas that have benefitted from these techniques. In the final section, the outlook for future contributions of MS techniques to PSII life-cycle research is discussed.

COMPOSITION OF PSII COMPLEXES

MS-Based Methods to Study the Composition of PSII Complexes

PSII Subunits with Soluble Domains

The bottom-up MS workflow is highly effective at identifying soluble proteins or proteins with soluble domains. It is, therefore, the main MS strategy that has been used to detect the core PSII proteins D1, D2, CP43, and CP47, which are transmembrane proteins but have multiple soluble domains, the extrinsic (soluble) PSII proteins, or unknown PSII-bound proteins. Bottom-up MS analysis can be preceded by either in-gel or in-solution digestion of the protein, each with advantages. Gel electrophoresis serves as a one- or two-dimensional fractionation step, simplifying the mixture to be analyzed by MS. Using this approach to remove interferences can improve instrument sensitivity toward proteins in the band of interest. Native PAGE, either alone or followed by denaturing SDS-PAGE (2D-BN-PAGE), is a common choice for resolving multiple protein complexes in a thylakoid membrane or purified PSII preparation; unknown bands can be excised and analyzed by MS to identify components of specific complexes (Granvogl et al., 2008; Pagliano et al., 2014; Gao et al., 2015). However, targeted band excision can miss potentially important proteins that migrated at

TABLE 1 | Overview of the role of MS in PSII life-cycle research.

Kind of information	Information desired	MS-based technique
Composition	PSII subunits present in a complex	Bottom-up MS (intact or top-down MS for LMM subunits)
	Accessory proteins that associate with PSII	Bottom-up MS
	PTMs	Bottom-up MS
Dynamics	Protein and PTM changes between samples	Label-free or isotopic-label-based relative quantification
	PSII subunit lifetime	Rate of unlabeled protein disappearance after isotopic label exposure
	Relative position of subcomplexes in PSII life-cycle	Relative isotopic label incorporation after pulse
Structure	Binding site of proteins not found in PSII crystal structures	Cross-linking, footprinting
	Conformational changes	Footprinting, quantify changes in modification extent
	Water and oxygen channel detection	Footprinting

positions not selected for in-gel digestion. In theory, native PAGE can remove unbound proteins from complexes, simplifying MS analysis; however, disruption of certain relevant protein-protein interactions in complexes cannot ever be fully excluded. Alternatively, in-solution digestion allows a more comprehensive analysis of the protein components in a sample, but without the sample simplification or complex-specific resolution provided by prior SDS-PAGE or native PAGE.

MS instrumentation, as well as membrane-protein sample preparation (Whitelegge, 2013; Battchikova et al., 2015; Heinz et al., 2016) and bioinformatics capabilities, has improved over the last two decades to facilitate PSII life-cycle research (**Table 2** summarizes the kinds of experiments that have been performed and the main MS instrumentation and features that enable them). Early mass spectrometers that were applied to PSII research, especially triple-quadrupole (QqQ) and MALDI-time-of-flight (MALDI-TOF) instruments, had relatively low sensitivity, resolving power, and mass accuracy (on the order of 100-several hundred ppm; Michel et al., 1988; Sharma et al., 1997a,b,c; Frankel et al., 1999). Scarcity of genomic sequence data combined with low instrument sensitivity, mass accuracy, and fragmentation efficiency meant that sample analysis was mainly restricted to highly purified PSII complexes or individual subunits, with poor capability for novel protein identification. The mid-2000s saw the appearance of higher-performing instruments, especially the hybrid quadrupole-TOF (Q-TOF) and increasing availability of genomic sequence data for commonly studied photosynthetic organisms. These enabled routine bottom-up identification of the main subunits of PSII complexes (those with soluble domains) from more complex starting mixtures and identification of novel PSII-associated proteins (Kashino et al., 2002; Heinemeyer et al., 2004; Komenda et al., 2005). The fragmentation efficiency of the Q-TOF, however, still limited sequence coverage of proteins. The development and distribution of Fourier transform instruments (ion cyclotron resonance and orbitraps) sometimes interfaced with ion traps provided improved fragmentation efficiency and enabled analysis of highly complex mixtures with higher sequence coverage than ever before. These instruments allow proteome-wide experiments, enable routine confident PTM site identification, and have opened the door for bottom-up MS experiments on photosynthetic systems not before feasible (see **Table 2** and sections below).

The Low-Molecular-Mass (LMM) Subunits

Fully assembled PSII contains around 13 low-molecular-mass (LMM) proteins (<10 kDa) whose transmembrane domains account for around 40–85% of the sequence. Identification of these very hydrophobic proteins by bottom-up LC-MS/MS is challenging, with typically four or fewer LMM proteins detected (Granvogl et al., 2008; Haniewicz et al., 2013; Pagliano et al., 2014). Difficulties are associated with the proteins' hydrophobicity and lack of soluble domains, which lead to sample losses during preparation, poor tryptic digestion due to infrequent arginines and lysines, slow elution during chromatography, and poor ionization efficiency due to lack of abundant proton-accepting residues. Fractionation by gel electrophoresis carries the additional challenge of extracting the protein from the gel, made more difficult because tryptic digestion sites are infrequent (Granvogl et al., 2008).

To circumvent these difficulties, intact-mass measurement (no MS/MS fragmentation of the protein) and more recently top-down MS strategies have been employed, both of which avoid protein digestion and are able to identify nearly all the LMM subunits in a purified complex (summarized in **Table 3**). Intact-mass measurement of the LMM subunits was demonstrated by both ESI and MALDI methods, using QqQ and MALDI-TOF instruments (see references cited in **Table 3**). Both methods achieve roughly 50–200 ppm mass accuracy; especially without fragmentation data, this would typically not be enough for confident identification of an unknown protein. However, because there are only approximately 13 LMM subunits, predicted masses, which are available from genomic sequences in many organisms, are distinctive, and because the starting sample is typically a purified PSII complex, these intact-mass measurements are routinely accepted as confident identifications.

MS/MS fragmentation of intact LMM subunits, however, can be induced using both ESI and MALDI, although ESI has been more successful (see **Table 3** and references cited therein). Whitelegge and co-workers (Thangaraj et al., 2010) identified 11 LMM proteins in purified PSII from *G. sulphuraria* with a linear ion trap quadrupole-Fourier transform ion cyclotron resonance (LTQ-FTICR) instrument after offline LC and confirmed several modifications. They employed both collisional-activated dissociation (CAD) and electron-capture dissociation (ECD) to fragment the proteins, but CAD gave better results for all

TABLE 2 | MS instruments and instrument features for PSII life-cycle research applications.

Biological application	Mass accuracy (MS^1)	Mass accuracy (MS^2)	Sensitivity/Good sequence coverage	QqQ	TOF	Q-TOF	LTQ-Orbitrap	Q-Exactive[a]	LTQ-FT-ICR
ID proteins-purified PSII complex/simple mixture/gel band	Med	Low	Low	+	+	++	++	++	++
ID LMM subunits-purified PSII complex-intact/top-down	Med	Low	Low	+	+	++	++	++	++
ID proteins-membranes/complex mixture/unknown protein search	High	Med	Med	–	–	+	++	++	++
ID modifications-targeted search	High	Med	Med	+	+	+	++	++	++
ID modifications-non-targeted search (PTMs, footprinting)	High	Med	High	–	–	–	+	++	+
Quantification of proteins/modifications[b]-targeted search	High	Med	Med	+	+	+	++	++	++
Quantification of proteins/modifications[b]-non-targeted search	High	Med	High	–	–[c]	–	+	++	+
Cross-linking	High	Med-High	High	–	–	–	+	++	+

High: high priority; Med: medium priority; Low: low priority. "–," undesirable instrument choice; "+," acceptable instrument choice; "++," desirable instrument choice.

[a] *The Q-Exactive is the most sensitive instrument listed. For experiments where it is given an equal rating as other instruments, high sensitivity was not deemed absolutely critical to the experiment. However, if a Q-Exactive is readily accessible, it is generally the preferred choice of the instruments listed. Other high-performing instruments have been released recently and are expected to be highly useful for PSII research as well.*

[b] *Ratings are assuming precursor-ion-based quantification, as has been used in the large majority of studies focused on the PSII life-cycle. Product-ion-based quantification is relevant for studies that use iTRAQ and some forms of spectral counting.*

[c] *As an exception, rough quantification of relative LMM subunit stoichiometry between samples has been performed by intact-mass measurement on a MALDI-TOF (Sugiura et al., 2010a).*

LMM proteins. Eichacker and co-workers (Granvogl et al., 2008) demonstrated top-down analysis on a Q-TOF with sequence coverage ranging from 14 to 82%. This method has been used in several other recent studies (Plöscher et al., 2009; Boehm et al., 2011, 2012). Notably, Eichacker and co-workers (Granvogl et al., 2008) developed a protocol to perform in-gel extraction of intact LMM proteins prior to top-down analysis (capable of extracting all but the PsbZ protein from the gel matrix). This technique can be used to analyze individual BN-PAGE bands and, thus, identify the LMM components specific to individual types of PSII complexes in heterogeneous mixtures such as a thylakoid membrane proteome or affinity-tagged PSII complexes.

PSII Life-Cycle Application: Composition of Subcomplexes

Many subcomplexes form during the PSII life-cycle, and MS has played a critical role, in combination with gel electrophoresis, immunoblotting, crystallography, electron microscopy and other biochemical techniques, in identifying their components (Heinz et al., 2016). A schematic of the life-cycle is shown in **Figure 2** (for reviews of the life-cycle and the subcomplexes that form, see Baena-González and Aro, 2002; Aro et al., 2005; Nixon et al., 2010; Shi et al., 2012; Komenda et al., 2012b; Nickelsen and Rengstl, 2013; Järvi et al., 2015; Heinz et al., 2016). A summary of the main subcomplexes whose composition has been studied by MS is found in **Table 4** (for completeness, several other subcomplexes are also included). MS analysis generally allows more rapid, comprehensive, and definitive profiling of PSII subunits than other methods, and is especially useful for the LMM subunits that tend to stain poorly on gels. However, owing to the high sensitivity of MS and because relative quantification by MS is not straightforward, it can be difficult to distinguish a trace component of a complex from one that is stoichiometric. Immunoblotting, therefore, complements MS for characterizing composition of subcomplexes.

At the start of *de novo* PSII assembly, each of the four core subunits D1, D2, CP47, and CP43, forms a pre-complex with specific LMM components. Using a ΔD1 mutant in *Synechocystis* sp. PCC 6803 (hereafter *Synechocystis* 6803) and top-down ESI-MS on a Q-TOF, Nixon and co-workers (Boehm et al., 2011) showed that the CP47 pre-complex contains the LMM subunits

TABLE 3 | Identification of LMM subunits by MS.

MS technique	Ionization method	Number of LMM subunits identified	Instrument	Mass accuracy (MS^1)	References
Bottom-up	ESI, MALDI	0–4	Variety	~1–100 ppm (peptides)	Many, e.g., Kereïche et al., 2008; Plöscher et al., 2011; Haniewicz et al., 2013; Pagliano et al., 2014
Intact	ESI	9–11	QqQ	~50–200 ppm	Sharma et al., 1997a; Gómez et al., 2002; Laganowsky et al., 2009; Thangaraj et al., 2010
	MALDI	9–13	MALDI-TOF	~50–200 ppm	Sugiura et al., 2010a; Pagliano et al., 2011; Nowaczyk et al., 2012; Nakamori et al., 2014; Pagliano et al., 2014
Top-down	ESI	8–13	Q-TOF, LTQ-FTICR	3–30 ppm (Q-TOF), <1–5 ppm (LTQ-FTICR)	Granvogl et al., 2008; Plöscher et al., 2009; Thangaraj et al., 2010; Boehm et al., 2011, 2012
	MALDI	5	MALDI-TOF/TOF	~50–200 ppm	Pagliano et al., 2014

PsbH, PsbL, and PsbT, whereas the CP43 pre-complex contains the LMM subunits PsbK and Psb30. In this study, it was not possible by MS alone to demonstrate fully stoichiometric binding, just co-purification, of those LMM subunits to CP47 and CP43. However, these results are consistent with the PSII crystal structures and other non-MS-based results (Boehm et al., 2011 and references cited therein). Previous evidence implies PsbZ could also associate with the CP43 pre-complex (Iwai et al., 2007; Guskov et al., 2009; Takasaka et al., 2010), but it was not detected by MS in this study. As determined by affinity purification and immunoblotting, the D1 pre-complex contains PsbI and possibly Ycf48 (Dobáková et al., 2007). It was suggested that a Ycf39-ScpB-ScpE complex may also associate as early as this stage to insert chlorophyll into D1 (Knoppová et al., 2014). The D2 pre-complex contains PsbE and PsbF (Müller and Eichacker, 1999; Komenda et al., 2008).

The D1 and D2 pre-complexes merge to form the reaction center (RC) complex, the earliest subcomplex capable of charge separation (Baena-González and Aro, 2002; Dobáková et al., 2007). The RC complex, initially isolated from spinach and wheat by detergent solubilization of thylakoid membranes, was characterized by gel electrophoresis and immunoblotting to contain D1, D2, PsbE, PsbF, and PsbI (Nanba and Satoh, 1987; Ikeuchi and Inoue, 1988). Intact-mass and bottom-up MS studies later confirmed this composition (Sharma et al., 1997a,b,c). Several biochemical studies detected the 10-kDa PsbW subunit, which is found in green algae and higher plants but not in cyanobacteria, as an additional component (Irrgang et al., 1995; Lorković et al., 1995; Shi and Schröder, 1997). Subsequently, more specific studies (including an MS-based one, Granvogl et al., 2008) showed that PsbW associates later, to dimers during formation of PSII-Light-harvesting complex II (LHCII) supercomplexes (see below; Shi et al., 2000; Thidholm et al., 2002; Rokka et al., 2005; Granvogl et al., 2008). Despite attaching to PSII at a late stage of assembly, PsbW may bind tightly to the D1/D2 surface and, thus, remain partially attached to the RC complex during solubilization, while other peripheral PSII subunits are removed, explaining the controversy (Rokka et al., 2005). This case highlights that subcomplexes obtained from detergent solubilization, a technique used especially in early PSII subcomplex studies, do not necessarily represent subcomplexes that form *in vivo*. An alternative major method for isolating PSII subcomplexes is purifying them from mutant strains that are "blocked" at a particular stage of assembly. Such complexes are indeed formed *in vivo*, but it is possible that the altered relative quantity of PSII subunits in the thylakoid membrane arising from the mutation may lead to artefactual binding of certain subunits to some subcomplexes (Thidholm et al., 2002). In cyanobacteria, two slightly different forms of the RC complex were observed, labeled RCII* and RCIIa, which differ slightly in accessory protein content (see **Table 3** and the section below). MS was critical in RCII* component characterization, and was indirectly used for RCIIa characterization as well by gel and immunoblot comparison (Knoppová et al., 2014).

The next complex formed during PSII assembly is the RC47 intermediate, also called the CP43-less core monomer in plants, formed by attachment of the CP47 pre-complex to the RC complex. In 1998, Barber and co-workers (Zheleva et al., 1998) showed by MS that the monomeric RC47 complex from spinach contains the D1, D2, CP47, PsbE, PsbF, PsbI, $PsbT_c$, and PsbW proteins, and the dimeric form contains, in addition, PsbK and PsbL. From the later studies on PsbW cited above, PsbW presence may arise from a tight binding to the D1/D2 surface, not *in vivo* presence in the RC47 complex during assembly. Based on Nixon and co-workers' study (Boehm et al., 2011) on the CP47 pre-complex in *Synechocystis* 6803, it would be expected that RC47 also contains PsbH. Indeed, a more recent MS-based study of the RC47 complex from *Synechocystis* 6803 identified all the proteins found by Barber and co-workers (Zheleva et al., 1998) in their monomeric RC47 complex (except PsbW which is not found in cyanobacteria), plus PsbH, PsbM, PsbX, PsbY, and Psb28 (Boehm et al., 2012).

Attachment of the CP43 pre-complex to RC47 forms the inactive PSII monomer (Nickelsen and Rengstl, 2013). Active monomeric PSII is formed upon D1 processing (Liu et al., 2013a), dissociation of Psb27 (Liu et al., 2013a), assembly of the water-oxidizing manganese-calcium cluster and photoactivation (Dasgupta et al., 2008), and binding of PsbO, PsbU, and PsbV (cyanobacteria) or PsbO, PsbP, and PsbQ (algae and higher plants; Bricker et al., 2012). Active monomers dimerize and can attach to the phycobilisome antenna complex (cyanobacteria)

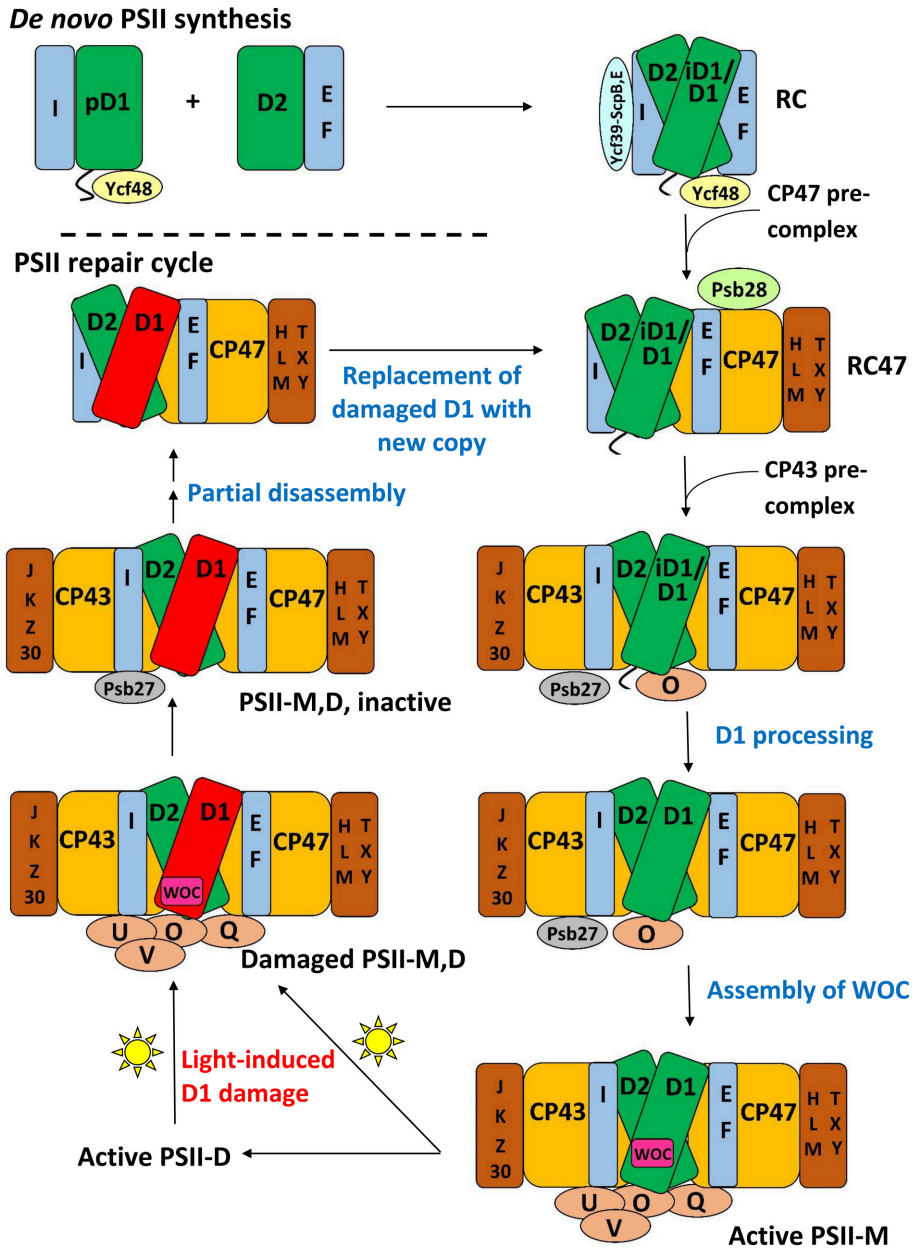

FIGURE 2 | A schematic of the PSII life-cycle. Refer to the text for description of each step. This schematic represents the cyanobacterial PSII life-cycle. The subcomplex progression is similar in algae and higher plants, though several homologous subunits are named differently in these species than in cyanobacteria, and certain subunits are unique to each group (see Rokka et al., 2005; Shi et al., 2012; Nickelsen and Rengstl, 2013; Järvi et al., 2015; Heinz et al., 2016). In algae and higher plants, damaged complexes migrate from thylakoid grana to stromal lamellae for repair and the first steps of reassembly (Tikkanen and Aro, 2014; Järvi et al., 2015). In cyanobacteria, chloroplasts and such inter-thylakoid structure are absent, and repair is not believed to require spatial migration of damaged complexes. *De novo* PSII synthesis through RC formation appears to begin in specialized membrane subfractions in cyanobacteria, algae, and higher plants before PSII migration to the general thylakoid membrane space, though the details of this process in the various species classes remains to be resolved (Zak et al., 2001; Nickelsen et al., 2011; Nickelsen and Rengstl, 2013; Rast et al., 2015). E, F, H, I, J, K, L, M, O, Q, T, U, V, X, Y, Z, and 30 refer to the PsbE, PsbF, PsbH, etc. proteins, respectively. PSII-M, PSII monomer; PSII-D, PSII dimer.

(Mullineaux, 2008) or various oligomeric states of LHCII complexes (algae and higher plants) (Kouřil et al., 2012).

Although, crystal structures of active PSII dimers from cyanobacteria are available, several MS studies of fully-assembled cyanobacterial PSII have provided independent confirmation of the subunits present in purified complexes under more native conditions (Sugiura et al., 2010a; Nowaczyk et al., 2012). Using native conditions has even helped discover a component (PsbQ) that was lost during crystallization (Kashino et al., 2002; Roose et al., 2007). The majority of PSII from algae and higher plants

is found in several PSII dimer-LHCII supercomplexes (for a review see Kouřil et al., 2012). MS studies (in concert with other techniques) have identified their subunit compositions, even in the absence of crystal structures of the complexes from these organisms. Eichacker and co-workers (Granvogl et al., 2008) showed that the four PSII-LHCII supercomplexes in *Nicotiana tabacum* contain identical PSII core and LMM subunits (of the eight LMM subunits identified), and that only PSII-LHCII supercomplexes contain the PsbW protein. These results support previous studies that suggest that PsbW may facilitate linkage of LHCII trimers to PSII (Shi et al., 2000; Thidholm et al., 2002; Rokka et al., 2005). Using both bottom-up and top-down MS techniques, Pagliano et al. (2014) found that the various supercomplexes in pea contain identical core and LMM subunits, but that the $C_2S_2M_2$ supercomplex contains the PsbQ, PsbR, PsbP, Lhcb3, and Lhcb6 proteins whereas the C_2S_2 supercomplex does not. In light of the stabilizing effect of the PsbQ and PsbP proteins on oxygen evolution, this finding raises interesting questions about the role of the C_2S_2 supercomplex. Another recent study used MS to characterize PSII-LHCII supercomplexes in *N. tabacum* and found a few differences in subunit composition; in particular, the C_2S_2 supercomplex contained Lhcb1 isoform CB25, while the $C_2S_2M_2$ supercomplex did not (Haniewicz et al., 2015).

Several studies indicate that PSII-PSI-antenna megacomplexes can form in both cyanobacteria and higher plants. Using *in vivo* cross-linking, Blankenship and co-workers (Liu et al., 2013b) captured a PSII-PSI-phycobilisome megacomplex in *Synechocystis* 6803. The authors used MS to demonstrate presence of subunits from each complex in the preparation (**Tables 3, 5**), and identified cross-links revealing specific inter-complex subunit interactions. Aro and co-workers (Tikkanen et al., 2008b, 2010) showed that LHCII can transfer excitation energy to PSI in grana margins of higher plants as a means of balancing energy flux under varying light conditions. In support of this hypothesis, two PSII-PSI-LHCII megacomplexes from *Arabidopsis thaliana* were observed by a novel large-pore BN-PAGE system (Järvi et al., 2011), and more recently, a PSII-PSI-LHCII megacomplex was identified by MS from the macroalga *Ulva* sp. under drought stress conditions (Gao et al., 2015).

PSII Life-Cycle Application: Identification of Accessory Proteins

Many accessory proteins bind transiently to PSII subcomplexes during the PSII life-cycle, serving key regulatory roles, but are not present in the crystal structure owing to their absence in fully assembled PSII. For reviews of the accessory proteins of PSII (see Shi et al., 2012; Komenda et al., 2012b; Nickelsen and Rengstl, 2013; Mabbitt et al., 2014; Järvi et al., 2015; Heinz et al., 2016). Bottom-up MS has played a key role in identifying some of the known ones, and others likely remain to be identified. Identifying a previously unknown PSII-associated protein in this manner, however, is not straightforward because the mass spectrometers used for bottom-up analysis are so sensitive that dozens of contaminant proteins are often detected even in "purified" complexes. Low signal intensity of a peptide compared to those of known PSII peptides does not necessarily indicate a contaminant at low abundance because different peptides have different intrinsic ionization efficiencies, and many accessory proteins bind sub-stoichiometrically to PSII. Certain contaminant proteins such as NDH-1 complex subunits (Nowaczyk et al., 2012), ATP synthase subunits (Komenda et al., 2005), phycobilisome subunits (Kufryk et al., 2008), certain ribosomal proteins (Liu et al., 2011b), and several carbon dioxide-concentrating mechanism proteins (Kufryk et al., 2008; Liu et al., 2011b) are frequently observed. Careful examination of the full list and consideration of the experimental conditions are needed to distinguish plausible PSII-interaction candidates from contaminant proteins (Kashino et al., 2002). Although, different MS search software packages use different algorithms for scoring protein hits, a strict statistical confidence threshold should be employed and reported. Overall, although a simple bottom-up experiment is a powerful tool to suggest new candidate proteins that associate with PSII, subsequent targeted experiments on each one are needed to confirm the interaction.

This strategy has proven successful many times for identifying new PSII interaction partners. An early example (Kashino et al., 2002) analyzed SDS-PAGE bands by MALDI-TOF MS from a highly purified PSII preparation and identified several novel proteins, Sll1638 (PsbQ), Sll1252, and Sll1398 (Psb32), that appeared to be plausible PSII interaction partners. Follow-up biochemical studies targeting these proteins confirmed their role in the PSII life-cycle and elucidated functional aspects of each (Inoue-Kashino et al., 2011; Wegener et al., 2011; Bricker et al., 2012). A later proteomic study of purified PSII complexes revealed that the Slr0144-Slr-0152 proteins, all part of one operon, associate with PSII, leading to further characterization of their role in PSII assembly (Wegener et al., 2008). In other cases, specific subcomplexes were isolated before MS analysis and identification of accessory proteins. For example, analysis of a gel band from Δ*ctpA*-HT3-PSII revealed that the Psb27 protein binds specifically to a PSII subcomplex that accumulates before D1 processing (Roose and Pakrasi, 2004), initiating the studies that ultimately elucidated its role in PSII assembly (Nowaczyk et al., 2006; Roose and Pakrasi, 2008; Grasse et al., 2011; Liu et al., 2011a,b; Komenda et al., 2012a). MS analysis showed that the Ycf39, ScpB (HliC), and ScpE (HliD) proteins bind specifically to the RCII* form of the reaction center complex, but not the related RCIIa form (Knoppová et al., 2014). The specific binding of the accessory proteins Psb28 (Dobáková et al., 2009; Boehm et al., 2012) and Psb28-2 (Boehm et al., 2012) to the RC47 complex, and of Ycf48 to RCII* and RCIIa (Knoppová et al., 2014), was initially discovered by immunoblotting, but the proteins' presence was confirmed by MS, strengthening the finding.

PSII Life-Cycle Application: Identification of PTMs

Identification of Processing Events to Form Mature PSII Proteins

The D1 protein is synthesized as a precursor protein (pD1) with a C-terminal extension that gets cleaved during PSII

TABLE 4 | Composition of complexes in the PSII life-cycle by MS and other methods.

Sub-complex	Composition by MS	Species[a]	References	Composition by other methods	Species[a]	References
D1 pre-complex	ND	–	–	pD1, I, (Ycf48[c])	*Syn.* 6803	Dobáková et al., 2007
D2 pre-complex	ND	–	–	D2, E, F	*Syn.* 6803	Komenda et al., 2008
CP47 pre-complex	CP47, H, L, T	*Syn.* 6803	Boehm et al., 2011	CP47, H	*Syn.* 6803	Komenda et al., 2005
CP43 pre-complex	CP43, K, Psb30	*Syn.* 6803	Boehm et al., 2011	CP43, K, Z, Psb30[c]	*C. reinhardtii*, *T. elongatus*	Sugimoto and Takahashi, 2003; Iwai et al., 2007
RC	D1, D2, E, F, I	Pea	Sharma et al., 1997a,b	D1, D2, E, F, I, (W[d])	Spinach	Nanba and Satoh, 1987; Ikeuchi and Inoue, 1988; Irrgang et al., 1995
RCII*	D1/iD1, D2, E, F, I, Ycf48, Ycf39, ScpB, ScpE	*Syn.* 6803	Knoppová et al., 2014	D1/iD1, D2, E, F, I, Ycf48, Ycf39, ScpE	*Syn.* 6803	Komenda et al., 2004; Dobáková et al., 2007; Komenda et al., 2008; Knoppová et al., 2014
RCIIa	ND	–	–	D1/iD1, D2, E, F, I, Ycf48	*Syn.* 6803	Dobáková et al., 2007; Komenda et al., 2008; Knoppová et al., 2014
RC47 monomer	D1, D2, CP47, E, F, I, L, M, T, X, Y, Psb28, Psb28-2	*Syn.* 6803	Boehm et al., 2012	D1, D2, CP47, E, F, H, Psb28, Psb28-2	*Syn.* 6803	Komenda et al., 2004; Dobáková et al., 2009; Boehm et al., 2012
RC47 monomer	D1, D2, CP47, E, F, I, T_C, W	Spinach	Zheleva et al., 1998	D1, D2, CP47, E, F, H, I, M, R, T_C	Spinach	Rokka et al., 2005
RC47 dimer	D1, D2, CP47, E, F, I, K, L, T_C, W	Spinach	Zheleva et al., 1998	ND	–	–
PSII monomer, inactive	Psb27	*Syn.* 6803, *T. elongatus*	Grasse et al., 2011; Liu et al., 2013a	RC47 components + CP43, Psb27	*Syn.* 6803, *T. elongatus*	Roose and Pakrasi, 2008; Grasse et al., 2011; Liu et al., 2013a
PSII monomer/dimer, active	D1, D2, CP47, CP43, E, F, H, I, J, K, L, M, O, Q, U, V, T, X, Y, Z, Psb30	*Syn.* 6803, *T. elongatus*	Kashino et al., 2002; Nowaczyk et al., 2012	Crystal structure shows all components as by MS except PsbQ	*Syn.* 6803, *T. elongatus*	Roose et al., 2007; Umena et al., 2011
PSII monomer/dimer, active	D1, D2, CP47, CP43, E, F, H, I, K, L, M, O, R, T_C, X	*N. tabacum*	Granvogl et al., 2008; Haniewicz et al., 2015	D1, D2, CP47, CP43, O, P, S; R, W (pea)	*A. thaliana*	Caffarri et al., 2009; Pagliano et al., 2011
PSII-LHCII supercomplexes[b]	D1, D2, CP47, CP43, E, F, H, I, K, L, M, O,R, T_C, W, X; Lhcb1-4, 6	*N. tabacum*	Granvogl et al., 2008; Haniewicz et al., 2015	D1, D2, CP47, CP43, O, P, Q, S; Lhcb1-6; W (pea)	*A. thaliana*	Thidholm et al., 2002; Caffarri et al., 2009; Kouřil et al., 2012
PSII-PSI-PBS megacomplex	D1, D2, CP47, CP43, O, U, V; PsaA, B, C, D, E, F, L, Slr0172, Ycf4, PC; ApcA, B, C, D, E, F, CpcA, B, D, G1, G2	*Syn.* 6803	Liu et al., 2013b	ND	–	–
PSII-PSI-LHCII megacomplex	D1, D2, CP47, CP43, E; PsaA,B,L; LhcbM1, LhcbM10, Lhca2	*Ulva* sp.	Gao et al., 2015	D1, D2, CP47, CP43; PsaB,D,F,G, K,L; unspecified LHCII subunits	*A. thaliana*	Järvi et al., 2011

ND, not determined.

[a] *When two species are listed in the same subcomplex entry, the protein components are the union of those found in the individual studies.*

[b] *Characterization of specific PSII-LHCII supercomplexes.*

[c] *Uncertain; evidence is suggestive.*

[d] *Subsequent studies indicate PsbW presence in this complex may be an artifact of solubilization conditions (discussed in the text).*

TABLE 5 | Summary of MS-based PSII cross-linking studies[a].

Species	Cross-linked subunit 1	Cross-linked subunit 2	Cross-linker	Method notes	References
Syn. 6803	Psb27	CP43	EDC, DTSSP	• Cross-linked species enriched on gel • In-gel digestion; trypsin or chymotrypsin • LTQ-Orbitrap XL • MassMatrix search software	Liu et al., 2011a
Syn. 6803	PsbQ	CP47, PsbO	EDC, DTSSP	• No cross-link enrichment • In-solution digestion; trypsin • LTQ-Orbitrap XL • MassMatrix search software	Liu et al., 2014b
Syn. 6803	D2, CP43, CP47	ApcE	DSP	• No pre-MS cross-link enrichment • In-solution digestion; trypsin + LysC • LTQ-Orbitrap XL • $\geq +3$ charge states selected for MS^2 to maximize cross-link selection • MassMatrix search software	Liu et al., 2013b
T. elongatus	Psb27	CP43	BS^3 d0/d12	• Isotope-encoded cross-linker • No cross-link enrichment • In-solution digestions; trypsin • Orbitrap Elite Velos Pro • StavroX search software	Cormann et al., 2016
C. reinhardtii	PsbP	PsbQ	EDC	• Wash step isolates extrinsic proteins after cross-linking • Cross-linked species enriched on gel • In-gel digestion; trypsin or Asp-N • Ultraflex MALDI-TOF • MS^1 only; trypsin and Asp-N samples independently indicate the same cross-linked residues	Nagao et al., 2010
Spinach	PsbP	PsbQ	BS^3	• Wash step isolates extrinsic proteins after cross-linking • Cross-linked species enriched on gel • In-gel digestion; trypsin ± LysC • LTQ-FTICR • MassMatrix search software	Mummadisetti et al., 2014
Spinach	PsbP	PsbE	EDC	• Biotin-tagged PsbP isolates the free protein + its cross-linked partners • Cross-linked species enriched on gel • In-gel digestion; trypsin • LTQ-Orbitrap XL • MassMatrix search software	Ido et al., 2012
Spinach	PsbP	PsbR, CP26	EDC	• Biotin-tagged PsbP isolates the free protein + its cross-linked partners • Cross-linked species enriched on gel • In-gel digestion; trypsin • LTQ-Orbitrap XL • MassMatrix search software	Ido et al., 2014

[a] *Only inter-protein cross-links that reveal interactions not detectable in the available PSII crystal structures are shown here.*

assembly (Takahashi et al., 1988). An early study using peptide sequencing showed that in spinach, cleavage occurs after Ala-344, removing nine C-terminal residues (Takahashi et al., 1988). Several years later, it was found that, in *Synechocystis* 6803, cleavage also occurs after Ala-344, removing 16 C-terminal residues (Nixon et al., 1992). In this study, peptide sequencing as well as fast atom bombardment (FAB)-MS (a predecessor for ESI and MALDI) were used to pinpoint this cleavage site. Ala-344 serves as a ligand for a Mn ion in the water oxidation cluster (Umena et al., 2011) so that without cleavage, PSII remains incapable of oxygen evolution (Roose and Pakrasi, 2004). The extension, thus, protects early assembly intermediates from harmful premature water oxidation activity. Interestingly, although D1 in higher plants is cleaved in a single step, cyanobacterial D1 is cleaved in two steps, and an intermediate D1 (iD1) is formed transiently (Inagaki et al., 2001). Although, the iD1 cleavage site remained unknown for two decades, in 2007, MS and biochemical evidence demonstrated that the CtpA protease cleaves after Ala-352 to form iD1, which is then cleaved again after Ala-344 to form mature D1 (Komenda et al., 2007). The significance of the two-step cleavage remains unknown, although iD1 may serve as a signal for transferring an early PSII assembly intermediate from the cytoplasmic to the thylakoid membrane (Komenda et al., 2007).

The CP43 protein also appears to be cleaved before, or during an early stage of, PSII assembly. Tandem MS analysis identified a CP43 peptide in spinach starting with a modified form of Thr-15 (Michel et al., 1988). Based on the genomic sequence, the preceding residue is a leucine, so this peptide would not be a predicted trypsin cleavage product. It was also found that the N-terminus of CP43 is blocked from analysis by Edman degradation, likely owing to N-terminal modification. Taken together, these results show that the first 14 residues of CP43 are cleaved, leaving Thr-15 as the mature protein's N-terminus (Michel et al., 1988). Subsequent studies identified the corresponding CP43 peptide in *A. thaliana* (Vener et al., 2001) and *Synechocystis* 6803 (Wegener et al., 2008), suggesting that this cleavage is conserved. Crystal structures of cyanobacterial PSII were not able to resolve the most N-terminal portion of CP43, so those structures do not address this question of CP43 cleavage (Loll et al., 2005; Umena et al., 2011).

Cyanobacterial Psb27, PsbQ, and PsbP have unusually hydrophobic properties for soluble lumen-localized proteins and contain a lipoprotein signal motif and conserved cysteine in their N-terminal regions (Thornton et al., 2004; Nowaczyk et al., 2006; Fagerlund and Eaton-Rye, 2011). This led to the suggestion that they are N-terminally lipid-modified and, thus, anchored to the lumenal surface of the thylakoid membrane. Using lipase treatment and MALDI-TOF MS, Rögner and co-workers (Nowaczyk et al., 2006) showed that Psb27 from *Thermosynechococcus elongatus* does indeed contain such a modification. Also using MALDI-TOF MS, Wada and co-workers (Ujihara et al., 2008) confirmed this finding with Psb27 from *Synechocystis* 6803 and also found that *Synechocystis* 6803 PsbQ, recombinantly expressed in *E. coli*, is also N-terminally lipid modified. Notably, this group developed a method to extract lipid-modified peptides from a gel matrix after in-gel digestion, enabling downstream MS analysis (Ujihara et al., 2008). During PSII assembly, it is important that Psb27 binds to the lumenal surface before the other extrinsic proteins (Liu et al., 2013a), and the lipid anchor may facilitate this sequence by keeping Psb27 in close proximity at all times. A similar role for the lipid anchor of PsbQ was proposed recently (Liu et al., 2015). A lipid modification on PsbP has not yet been demonstrated although strong suggestive evidence indicates its presence (Fagerlund and Eaton-Rye, 2011).

Identification of Phosphorylation Sites

In the early 1980s, phosphorylation of the four PSII subunits that later came to be known as D1, D2, CP43, and PsbH, was observed. These studies were conducted *in vivo* and *in vitro* using ^{32}P labeling of whole cells and thylakoid membranes from *Chlamydomonas reinhardtii* and pea, with detection of phosphoproteins by autoradiography (Owens and Ohad, 1982, 1983; Steinback et al., 1982). Immunoblotting with antibodies that recognize phosphorylated residues was introduced later and became another popular detection method (Rintamäki et al., 1997). Neither of these methods, however, reveal the modified residue. This information was first obtained by gas-phase sequencing using Edman degradation, which demonstrated that the PsbH phosphorylation site is Thr-2, its N-terminus, in spinach (Michel and Bennett, 1987) and *C. reinhardtii* (Dedner et al., 1988). Since then, MS analysis has replaced Edman degradation and become the dominant method for phosphorylation-site determination, as it is higher-throughput, more definitive, more sensitive, and not limited by N-terminal blockage (e.g., acetylation). The main sites identified are presented below (for reviews, see Vener, 2007; Pesaresi et al., 2011; Puthiyaveetil and Kirchhoff, 2013).

Tandem MS demonstrated phosphorylation of D1-Thr-2, D2-Thr-2, and CP43-Thr-15, the mature proteins' N-termini, in spinach (Michel et al., 1988), *A. thaliana* (Vener et al., 2001), and *C. reinhardtii* (Turkina et al., 2006). Phosphorylation of CP43 was also observed at Thr-20, Thr-22, and Thr-346 in spinach (Rinalducci et al., 2006), and at Thr-346 and Ser-468 in *A. thaliana* (Sugiyama et al., 2008; Reiland et al., 2009). MS analysis showed that PsbH is phosphorylated at its N-terminus in *A. thaliana*, supporting the Edman degradation data from spinach and *C. reinhardtii*, and additionally demonstrated phosphorylation of Thr-4 (Vener et al., 2001). Intact-mass MS evidence also indicates double PsbH phosphorylation in spinach and pea (Gómez et al., 1998, 2002). More recently, phosphorylation of the extrinsic proteins PsbP, PsbQ, and PsbR was observed in phosphoproteomic studies of *A. thaliana* (Sugiyama et al., 2008; Lohrig et al., 2009; Reiland et al., 2009). Although, not discussed here, phosphorylation of LHCII is well-documented, and it regulates state transitions in green algae and higher plants (for reviews see Lemeille and Rochaix, 2010; Minagawa, 2011; Schönberg and Baginsky, 2012; Tikkanen and Aro, 2014; Tikhonov, 2015).

Phosphorylation of PSII subunits is not absolutely required for PSII repair (Bonardi et al., 2005) but assists in transferring damaged PSII complexes from the stacked thylakoid grana to

stromal lamellae, where repair occurs. Phosphorylation appears to induce architectural changes in the stacked grana and increase membrane fluidity in such a way as to promote mobility of damaged PSII centers to the stromal lamellae for repair (Tikkanen et al., 2008a; Fristedt et al., 2009, 2010; Herbstová et al., 2012; Järvi et al., 2015). For many of the PSII phosphorylation sites, light intensity and/or other environmental conditions affect the phosphorylation extent, with implications for the functional significance of these modifications. MS analysis has played a critical role in these quantitative studies, and methodology for such measurements is discussed in the dynamics section below. For reviews that discuss the role of PSII phosphorylation (see Pesaresi et al., 2011; Mulo et al., 2012; Schönberg and Baginsky, 2012; Järvi et al., 2015).

PSII phosphorylation may not be needed in cyanobacteria owing to the lack of spatial organization of thylakoids (Mulo et al., 2012). However, a recent global proteomics study of the cyanobacterium *Synechococcus* sp. PCC 7002 (hereafter *Synechococcus* 7002) found that a portion of D1 copies are phosphorylated at their N-terminus, Thr-2 (Yang et al., 2014), as in higher plants. This finding opens the possibility for a role of phosphorylation in PSII turnover in cyanobacteria.

Identification of Oxidative and Other Modifications

Light is necessary for PSII function, but even low light intensities can lead to PSII damage, particularly of the D1 protein. Damage triggers partial PSII disassembly, D1 degradation, insertion of a new D1 copy, and PSII re-assembly (Nickelsen and Rengstl, 2013). When the rate of damage exceeds that of repair, photosynthesis is inhibited, referred to as photoinhibition. Photodamage can be initiated in several ways, but a common result of each mechanism is production of highly oxidizing species (e.g., singlet O_2, other reactive oxygen species (ROS), or radical PSII cofactors). These species rapidly oxidize PSII subunits, ultimately rendering the complex non-functional. For reviews of the photoinhibition process (see Barber and Andersson, 1992; Adir et al., 2003; Pospíšil, 2009; Allahverdiyeva and Aro, 2012; Tyystjärvi, 2013).

Although oxidative damage of PSII was long believed to be responsible for photoinhibition (Telfer et al., 1994), MS studies provided the first concrete evidence for specific oxidative modifications of PSII. Bottom-up MS analysis of the D1 and D2 subunits from pea PSII found up to three +16 oxidative modifications (each representing incorporation of an oxygen atom) on certain peptides (Sharma et al., 1997c). Interestingly, not all peptides were oxidized, but the oxidized ones were all located near the predicted D1 and D2 redox cofactor sites, supporting the idea that radical redox cofactors themselves, or ROS produced by reaction with them, cause oxidative damage to PSII. More recently, Bricker and co-workers (Frankel et al., 2012, 2013b) used tandem MS to identify oxidized residues on spinach D1, D2, and CP43 that are located near the Q_A, $Pheo_{D1}$, and manganese cluster sites, all reasonable sources of oxidizing species. Additionally, tryptophan oxidation products in spinach were identified on CP43-Trp-365 and D1-Trp-317, which are located near the manganese cluster (17 and 14 Å, respectively, in the crystal structure from *T. elongatus*; Anderson et al., 2002; Dreaden et al., 2011; Kasson et al., 2012). By monitoring the digested peptides' absorption at 350 nm, the authors found that these tryptophan oxidations are correlated with increased light intensity and decreased oxygen evolution. Other modifications to PSII subunits were also detected by MS (Gómez et al., 2002, 2003; Anderson et al., 2004; Rexroth et al., 2007; Sugiura et al., 2013). Notably, a recent global proteomics study of *Synechococcus* 7002 identified many new PSII PTMs (Yang et al., 2014), but the functional significance of these modifications remains to be determined.

DYNAMICS: QUANTITATIVE OR SEMI-QUANTITATIVE CHANGES IN PSII PROTEINS AND PTMS

MS-Based Methods to Study PSII Dynamics

Most MS-based quantification experiments seek the relative, not absolute quantity of a protein or PTM in one sample compared to another. We focus here on relative quantification methods because nearly all the work on PSII dynamics fell into that category.

Gel-Based Quantification

Perhaps the most basic MS-based semi-quantitative method is in-gel digestion at the same band in two different sample lanes, prompted by a significant staining-intensity difference between the two bands. This approach was used frequently when analyzing different purified PSII complexes (Liu et al., 2011b; Knoppová et al., 2014), yielding information about accessory proteins that bind specifically to certain subcomplexes. A proper loading control (typically equal chlorophyll) must be used to ensure a meaningful comparison. Multiple proteins are typically identified by MS in both bands, however, so it may not be immediately apparent which protein is the main component (Liu et al., 2011b). Confirmation may be necessary by western blotting or one of the more quantitative MS-based techniques described below.

The accuracy of gel-based quantification can be improved by introducing a second electrophoretic separation dimension before in-gel digestion and LC-MS/MS. Semi-quantitative two-dimensional denaturing gel electrophoresis (2DE) (distinct from 2D BN-PAGE described above), a popular technique especially in early proteomics studies, usually first separates proteins by size and then on the basis of pI (Rabilloud et al., 2010). The difference in staining intensity indicates the relative content of that protein in each sample. Because two proteins migrate less often together in two dimensions than in one, separation and quantification accuracy are improved. 2DE is useful for large-scale studies such as whole-cell or whole-organelle proteome profiling that require higher-resolution separation than a 1D gel provides. However, in recent years, 2DE has declined in popularity owing to its numerous drawbacks (reviewed in Rabilloud et al., 2010) and the improvements in other more versatile quantitative MS methods. Such large-scale proteomics studies have detected expression-level changes in several PSII proteins in response to a variety of

stress conditions (e.g., Ingle et al., 2007; Aryal et al., 2011; Li et al., 2011; Guerreiro et al., 2014). However, insights into the PSII life-cycle have mainly emerged from more focused studies on purified PSII complexes.

Label-Free Quantification

Some MS-based relative quantification methods use a so-called label-free approach, but the better approach, when feasible, is to introduce a stable isotope into the sample. For label-free quantification, the samples to be compared are analyzed by LC-MS/MS separately. A variety of software tools can then be used to obtain an extracted ion chromatogram (EIC) of any peptide. The EIC displays the total intensity (peak area) of that peptide. Comparing the intensities of the same peptide from two different samples indicates the relative content of that peptide in those samples. Although the concept is simple, accurate label-free quantification depends on a number of factors: equal sample loading (on a relevant basis, e.g., chlorophyll concentration), reproducible LC runs, lack of ion suppression, and appropriate normalization during data analysis. For quantification of proteins, data from component peptides must be merged in a statistically sound way (Bantscheff et al., 2012; Nahnsen et al., 2013). Thorough mass spectral sampling of possible precursors—not as crucial in non-quantitative experiments—is necessary for accurate peak definition, but that typically diverts instrument time from obtaining product-ion spectra that give information for peptide identification and sequence coverage (Bantscheff et al., 2012). Various strategies have been designed to address this challenge (e.g., data-independent acquisition approaches such as MS^E (Silva et al., 2006; Grossmann et al., 2010) and "all-ion fragmentation" (Geiger et al., 2010) especially when combined with Ultra-Performance LC (UPLC) (Bantscheff et al., 2012). Label-free quantification by spectral counting, which involves comparing the total number of product-ion (MS/MS) spectra obtained for a given peptide or protein, is a common approach (Lundgren et al., 2010), although that has been used in fewer PSII-related studies (Fristedt and Vener, 2011; Stöckel et al., 2011). Label-free quantification of intact proteins is more direct than comparing peptides, but best applied for small proteins. Intact-mass spectra (MALDI and ESI) of the LMM PSII proteins indeed have been used in a number of instances for label-free quantification between states (Laganowsky et al., 2009; Sugiura et al., 2010a).

Isotope Label-Based Quantification

The alternative to label-free quantification is introduction of a stable isotope label into one of the two samples being compared (certain methods also allow greater multiplexing, see below). In contrast to the label-free approach, the labeled and unlabeled samples (often called "heavy" and "light") are mixed and analyzed in a single LC-MS/MS run. The mass spectra of the light and heavy peptide show two peaks shifted slightly in mass. Comparison of their peak areas, just as in label-free quantification, indicates the relative amount of that peptide in each sample (Bantscheff et al., 2012). Although, comparing peak areas from a single LC-MS/MS run eliminates the concerns of label-free LC reproducibility and ion suppression, labeling introduces additional sample preparation steps and often involves costly reagents.

Isotopic labeling (with ^2H,^{13}C, ^{15}N, or ^{18}O) of all proteins can be accomplished during cell growth (metabolic labeling), or by labeling a subset of proteins or peptides at various stages after cell lysis (chemical or enzymatic labeling). In the SILAC method ("stable isotope labeling by amino acids in cell culture"; reviewed in Chen et al., 2015), addition of labeled arginine or lysine to the growth medium results in incorporation of only the labeled form of that amino acid into all proteins. Hippler and co-workers (Naumann et al., 2007) used a SILAC-based method to measure changes in expression of PSII subunits and other proteins in *C. reinhardtii* under iron deficiency, and Jacobs and co-workers (Aryal et al., 2011) used this method to measure light-dark diurnal cycles in *Cyanothece* sp. ATCC 51142. A more common approach in PSII life-cycle research, however, has been ^{15}N metabolic labeling (see "Measuring the temporal dynamics of life-cycle events using isotopic labeling" below), in which the growth medium is modified so that the only nitrogen source is a labeled salt such as potassium nitrate or ammonium chloride (Gouw et al., 2010).

Isotopic labeling at the peptide or protein level during downstream processing after cell lysis is an alternative to metabolic labeling. Tandem mass tags (TMT) (Thompson et al., 2003), isotope tags for relative and absolute quantification (iTRAQ) (Ross et al., 2004), enzymatic ^{18}O labeling, and isotope-coded affinity tags (ICAT) can be used in proteomics experiments in photosynthetic organisms (Thelen and Peck, 2007). TMT and iTRAQ are related approaches that have become popular recently (Bantscheff et al., 2012). Both modify peptides with one of several possible isobaric tags that produce reporter ions during MS/MS fragmentation. Each sample is labeled with a different tag, but owing to the tags' isobaric nature, identical peptides from each sample are observed together chromatographically and as a single peak in a low-resolving power mass spectrum. Each tag, however, contains a unique reporter ion that appears as a distinct peak in the product-ion (MS/MS) spectra, and the ratio of these ions reveals the relative amounts of that peptide in each sample. The iTRAQ reagent modifies primary amines, and TMT tags are available that modify primary amines, thiols, or carbonyl groups. Advantages of these labeling approaches include the ability to multiplex up to 8 or 10 samples, greater than with metabolic and other chemical labeling methods, and the isobaric nature of the same peptide across all samples reduces both LC separation demands and MS data complexity (Bantscheff et al., 2012). Although, many proteomics studies on photosynthetic organisms have used these chemical labeling methods, most have not focused on PSII life-cycle issues (Thelen and Peck, 2007; Battchikova et al., 2015). Two relevant examples include the detection of elevated PsbO cysteine oxidation under DCMU and dark conditions (Guo et al., 2014), and intriguing evidence that PSII thermotolerance in *Synechocystis* 6803 may arise in part from antenna trimming and an increased rate of electron transfer to the cytochrome b_6/f complex (Rowland et al., 2010).

PSII Life-Cycle Application: Measuring Changes in Phosphorylation Levels

As mentioned in the composition section above, phosphorylation of PSII subunits affects membrane fluidity and inter-thylakoid dynamics, thus playing a role in facilitating PSII turnover in green algae and higher plants (see the reviews cited in that section for in-depth treatment of this topic). Many of the studies that have contributed to our current understanding of this process used MS quantification techniques to compare phosphorylation levels between samples and under different environmental conditions.

When using peak-area-based label-free quantification to determine the change in a modified peptide between samples, it is crucial that the peak area of the unmodified peptide be taken into account as well, to distinguish a true change in modification *extent* from simply an increased level of protein expression in one of the states. This method is demonstrated in a study of phosphorylation and nitration in *A. thaliana* grown under low and high light regimes (Galetskiy et al., 2011b). The authors first normalized each modified-peptide peak area in each sample to that of its unmodified counterpart and then compared the modified peptides' normalized peak area to each other. This method can reveal *fold-changes in modification extent* between the two states, but not the absolute percentage of that peptide that contains the modification (the "*modification stoichiometry*").

To find the modification stoichiometry, it is necessary to know in addition the relative "flyability" (ionization efficiency) of the modified and unmodified peptides. Vierstra and co-workers (Vener et al., 2001) showed that the relative flyabilities of six synthetic phosphopeptides and their non-phosphorylated counterparts are nearly identical. Suggesting this as a general phenomenon for phosphorylated peptides, they estimated the modification stoichiometry for the phosphorylated peptides of D1, D2, CP43, PsbH, and an LHCII protein. In 2010, Vener and co-workers (Fristedt et al., 2010) calculated the actual relative flyability ratio for these PSII peptide pairs, and reported reliable modification stoichiometry for these proteins for the first time under the various conditions in their study. Interestingly, the flyability ratios were indeed close to 1 for each pair (ranging from 0.89 to 1.23), supporting the earlier suggestion that this may be the case for most phosphorylated/non-phosphorylated peptide pairs (Vener et al., 2001). Other studies have since used those flyability ratios to determine changes in the modification stoichiometry of those same phosphorylation sites under other growth conditions (Fristedt and Vener, 2011; Romanowska et al., 2012; Samol et al., 2012). Knowledge of modification stoichiometry under different conditions is quite valuable; it enabled, for example, a greater level of confidence and detail in the model proposed for how phosphorylation affects thylakoid membrane stacking than would have been possible with fold-change data alone (Fristedt et al., 2010).

Chemical isotopic labeling of peptides has also been applied fruitfully to the study of PSII phosphorylation. Immobilized metal-ion affnity chromatography (IMAC) is a standard protocol for enrichment of phosphopeptides, taking advantage of the interaction between phosphoryl groups and a Fe^{3+}-agarose matrix (Andersson and Porath, 1986). Given that free carboxyl groups can also interact with the resin, it has become common to convert free carboxylates to methyl esters after digestion and prior to IMAC, to avoid this interaction (Ficarro et al., 2002). Vener and co-workers (Vainonen et al., 2005) modified this approach by using deuterated methanol (CD_3) as the esterification reagent for one sample, and unlabeled methanol for a second sample to quantify by "isotope encoding." After mixing the samples and analyzing by LC-MS/MS, the relative amount of each phosphorylated peptide in the two samples is quantified by comparison of their mass spectral peak areas. It should be noted that this approach does not reveal the modification stoichiometry of any phosphorylation site; rather the techniques described above still need to be performed to gain that information. Instead, as with other isotope-labeling strategies, it enables more confident and straightforward comparisons of the level of any given peptide between samples. This labeling method was used to study phosphorylation of PSII under a variety of conditions and genetic backgrounds (Vainonen et al., 2005; Lemeille et al., 2010; Fristedt and Vener, 2011; Samol et al., 2012).

PSII Life-Cycle Application: Measuring Changes in Oxidation Levels

As discussed above, oxidation of PSII subunits is a well-documented phenomenon, and occurs, at least partially, from oxidizing species generated during the electron transfer reactions of PSII, especially under stress. However, relatively few studies have quantified changes in PSII subunit oxidation under different controlled conditions. Adamska and co-workers (Galetskiy et al., 2011a) used label-free quantification to compare oxidation and nitration (also associated with oxidative stress) levels of thylakoid membrane protein complexes from *A. thaliana* grown under low and high light. They found significantly more modified sites in PSII than in the PSI, cytochrome b_6/f, and ATP synthase complexes. Interestingly, the modified D1, D2, and PsbO sites increased around 2-5-fold, whereas CP47, CP43, PsbE, and PsbR oxidation levels remained roughly constant. D1 and D2 bind most of the redox-active cofactors of PSII, so the increased oxidation especially of these two proteins is not surprising. Similarly, by measuring the increase in 350 nm absorption, Barry and co-workers (Dreaden et al., 2011; Kasson et al., 2012) found that two tryptophan oxidation products increase after exposure to high light, with a corresponding decrease in oxygen evolution activity. Adamska and co-workers (Galetskiy et al., 2011b) found that nitration levels in assembled PSII complexes decrease after exposure to high light, but increase in PSII subcomplexes. This may imply that once nitrated, PSII complexes are damaged and targeted for disassembly and repair.

PSII Life-Cycle Application: Measuring the Temporal Dynamics of Life-Cycle Events using Isotopic Labeling

Measurement of PSII subunit lifetimes has focused mainly on D1, using immunodetection following addition of a protein-synthesis inhibitor or by radioisotope pulse-chase labeling with detection by autoradiography or phosphorimaging (Aro et al., 1993; Mullet and Christopher, 1994; Ohnishi and Murata, 2006). Recently, several studies used ^{15}N labeling pulses and quantified the disappearance of unlabeled PSII subunits using MS. This method

enables simultaneous detection of a larger number of PSII subunits and eliminates any concern of overlapping signal from proteins with similar electrophoretic mobility (Yao et al., 2012b). From surveying nine PSII subunits from *Synechocystis* 6803, Vermaas and co-workers (Yao et al., 2012a) found that protein half-lives range from 1.5 to 33 h in a PSI-less mutant grown under low light (4 μmol $m^{-2}s^{-1}$ photon flux). In WT *Synechocystis* 6803 grown under 75 μmol $m^{-2}s^{-1}$ photon flux, half-lives of D1, D2, CP47, and CP43 ranged from <1 to 11 h (Yao et al., 2012b). In both studies, D1 exhibited the shortest half-life. These studies highlight the wide range in PSII subunit lifetime and the tight regulation of protein synthesis and PSII assembly that must occur to ensure constant proper stoichiometric availability of all subunits. Interestingly, the chlorophyll half-life was several times longer than that of the core chlorophyll-binding proteins, but the half-life was reduced in the absence of the small CAB-like proteins (SCPs), implying that SCPs play a role in chlorophyll recycling during PSII turnover (Yao et al., 2012a).

Rögner, Nowaczyk, and co-workers demonstrated an elegant application of ^{15}N labeling by purifying several subcomplexes in the PSII life-cycle after a pulse with ^{15}N (from $^{15}NH_4Cl$). Comparing extents of incorporation of ^{15}N in different subcomplexes (e.g., monitoring D1 and D2 peptides) reveals the subcomplexes' position in the PSII life-cycle. Using this method, the authors demonstrated that in *T. elongatus*, Psb27 binds to a monomeric subcomplex early in the PSII assembly process (Nowaczyk et al., 2006), and that Psb27 binds again during disassembly to inactive dimers (Grasse et al., 2011). This information fits well with the current understanding of Psb27 as a gatekeeper preventing manganese cluster assembly in immature complexes (Liu et al., 2013a; Mabbitt et al., 2014).

Cyanobacteria contain multiple versions of the *psbA* gene, and the resulting versions of the D1 protein have some different properties and are expressed preferentially under different environmental conditions (for reviews see Mulo et al., 2009; Sugiura and Boussac, 2014). For example, the *psbA1* gene product in *T. elongatus* is dominant under standard growth conditions, but expression of the *psbA3* gene product, which differs from the PsbA1 copy by ∼21 residues, increases under high light conditions (Clarke et al., 1993; Kós et al., 2008; Mulo et al., 2009). Characterization of PSII from mutants that express only specific versions of the gene has shown differences in electron-transfer properties, with the implication that PsbA3 assists in photoprotection of PSII under light stress conditions (Sander et al., 2010; Sugiura et al., 2010b). D1-copy expression was mainly monitored on the transcript level (Golden et al., 1986; Komenda et al., 2000; Kós et al., 2008; Sugiura et al., 2010b). However, using ^{15}N labeling and MS-based quantification, Rögner and co-workers showed that PsbA3 incorporation on the protein level could be monitored unambiguously in *T. elongatus* under high light conditions (Sander et al., 2010) and in the Δ*psbJ* mutant (Nowaczyk et al., 2012). Those studies used ^{15}N-labeled PSII from a strain that only expresses the PsbA3 copy as a standard for 100% incorporation; relative peak area of the unlabeled PsbA3 peptides compared to this standard is a measure of the incorporation. Such definitive monitoring should allow further detailed studies of *psbA* gene incorporation dynamics.

Progress has also recently been made on the role of the PsbA4 D1 copy; an iTRAQ labeling study found elevated expression of PsbA4 in *Cyanothece* sp. PCC 7822 in the dark (Welkie et al., 2014), providing complementary evidence to that of Pakrasi and co-workers (Wegener et al., 2015) who found that PsbA4 incorporation into PSII renders the complex non-functional. PsbA4 replaces PsbA1 at night in cyanobacterial species that fix nitrogen during this time, protecting against even the trace levels of oxygen evolution that could occur and damage the nitrogenase enzyme (Wegener et al., 2015).

STRUCTURE: DETERMINING PROTEIN-PROTEIN INTERACTIONS IN PSII COMPLEXES

MS-Based Methods to Study PSII Structure

X-ray crystallography remains the benchmark for determining the structure of protein complexes, but besides fully-assembled active PSII, many complexes that form during the PSII life-cycle are too transient and low in abundance to be easily amenable to crystallography. Valuable information about protein-protein interactions within PSII was obtained from immunogold labeling (Tsiotis et al., 1996; Promnares et al., 2006) and yeast two-hybrid assays (Schottkowski et al., 2009; Komenda et al., 2012a; Rengstl et al., 2013), but the former is primarily suitable for large PSII complexes (Dobáková et al., 2009), and the latter is time-consuming and low-throughput. Both provide relatively low-resolution structural information. Recently, advanced structural proteomics techniques bypass the limitations of the above techniques and offer higher-resolution structural data (although still lower than X-ray crystallography). Either chemical cross-linking or protein footprinting followed by MS detection of these modifications are enabled by MS instruments with high sensitivity, resolving power, and <1–5 ppm mass accuracy on orbitrap- and FTICR-based instruments (**Table 2**). These methods allow not only identification of the binding partners of a specific protein but also a low-resolution mapping of the binding site.

Chemical Cross-Linking

Briefly, the chemical cross-linking technique (reviewed in Sinz, 2014) uses a small molecule with two functional groups on either end that can react with protein residues, separated by a spacer arm (typically less than 14 Å). Many types of cross-linkers are available (Paramelle et al., 2013). The ones most commonly used in PSII research (Bricker et al., 2015) can react with either the primary amine of a lysine and protein N-terminus (and under certain conditions, to a lesser extent with the hydroxyl group of a serine, threonine, or tyrosine, Mädler et al., 2009), or with the carboxylate of aspartate and glutamate side chains and protein C-termini. After both sides of the cross-linker react with neighboring proteins, digestion, LC-MS/MS, and specialized data analysis can identify cross-linked peptides. Inter-protein cross-linked peptides provide structural information about the complex because the two linked residues are constrained to the spacer arm-length distance from each other.

Cross-linking has been used for decades to study protein-protein interactions (Clegg and Hayes, 1974; Wetz and Habermehl, 1979; Walleczek et al., 1989; Back et al., 2003; Sinz, 2014), but its power was limited until modern MS instrumentation and the proteomics platform enabled high-throughput analysis and confident identification of linked peptides (Rappsilber, 2011). Identification of cross-linked peptides by MS is more challenging than for a typical protein digest, especially for large complexes, because the candidate peptide database increases roughly with the square of the number of peptides. As a result, false positives based on the mass spectrum are common even with high mass accuracy instruments, making high-quality product-ion spectra critical for a confident assignment. Despite powerful and constantly improving cross-link search algorithms (Rinner et al., 2008; Xu and Freitas, 2009; Petrotchenko and Borchers, 2010; Götze et al., 2012, 2015; Yang et al., 2012; Hoopmann et al., 2015), manual verification of the product-ion spectra of hits is highly recommended. Successful cross-linking requires high sequence coverage and high mass accuracy as is now practical with orbitrap- and FTICR-based instruments (**Table 2**).

Because cross-linked peptides give typically low-intensity signals compared to those of unlinked peptides, they are often not selected for fragmentation by the instrument's traditional "highest-abundance ion" selection criteria. Several strategies have been developed to improve cross-link selection and/or reduce false positives. They include various methods to enrich for cross-linked peptides before LC-MS/MS (Chu et al., 2006; Kang et al., 2009; Fritzsche et al., 2012; Leitner et al., 2012); use of isotope-coded linkers whose "fingerprint" increases confidence in an identification and can enable real-time guided selection of cross-links for fragmentation (Müller et al., 2001; Pearson et al., 2002; Seebacher et al., 2006; Petrotchenko et al., 2014); and MS-cleavable linkers that simplify data analysis by cleaving a cross-linked peptide into its component peptides before fragmentation (Kao et al., 2011; Petrotchenko et al., 2011; Weisbrod et al., 2013; Buncherd et al., 2014).

Protein Footprinting

Protein footprinting is another MS-based structural technique that has been used to study PSII. Its principle is that a protein residue's solvent accessibility determines its susceptibility to modification by a reagent in the solution; residues buried in a protein-protein interface are less susceptible to modification than surface-exposed residues. These modifications are then detected by MS. Instruments with high sensitivity, resulting in high sequence coverage, are critical so that footprinting experiments yield maximal information (**Table 2**). A common approach is hydroxyl radical footprinting using the well-established technique of synchrotron radiolysis of water to generate the radicals (Takamoto and Chance, 2006; Wang and Chance, 2011). Fast photochemical oxidation of proteins (FPOP) is a more recent hydroxyl radical fooptrinting technique that uses a laser pulse to generate the radicals and can probe protein dynamics that occur on a faster timescale, down to microseconds (Gau et al., 2011). Hydroxyl radical footprinting can modify 14 of the 20 amino acid side chains (Wang and Chance, 2011). Another technique, glycine ethyl ester (GEE) labeling, adapts a long-standing method for modifying and cross-linking carboxylate groups in proteins (Hoare and Koshland, 1967; Swaisgood and Natake, 1973) for protein footprinting (Wen et al., 2009; Gau et al., 2011). It is easier to implement than hydroxyl radical footprinting, and data interpretation is simpler, but it can only probe changes on aspartate, glutamate, and protein C-termini.

PSII Life-Cycle Application: Cross-Linking and Footprinting to Determine Interactions among PSII Subunits

Early cross-linking studies on PSII provided information about subunit connectivity before PSII crystal structures were available. Many studies focused on the lumenal extrinsic proteins (Enami et al., 1987; Bricker et al., 1988; Odom and Bricker, 1992; Han et al., 1994), which are more easily accessible to soluble cross-linkers, but interactions involving the transmembrane subunits can also be detected (Tomo et al., 1993; Seidler, 1996; Harrer et al., 1998). In the absence of the MS-based platforms currently available, gel electrophoresis and immunoblotting identify cross-linked products and their likely component proteins. Those methods are still helpful today as confirmation and when cross-linked peptides are not detected by MS (Hansson et al., 2007; Nagao et al., 2010; Liu et al., 2011a, 2014b), but MS provides much greater confidence in the identification and pinpoints the exact cross-linked residues. Notably, Satoh and co-workers (Enami et al., 1998) used FAB-MS to identify intramolecular cross-linked peptides in PsbO, and deduced the linked residues even without MS/MS capability.

Since these early studies, crystal structures have elucidated the connectivity between the components of active cyanobacterial PSII. As a result, more recent cross-linking studies have focused on accessory proteins that bind only to subcomplexes and/or that are not found in the crystal structures, though work has continued on the lumenal extrinsic PSII subunits from algae and higher plants, PsbP and PsbQ, which differ significantly from their cyanobacterial counterparts (Bricker et al., 2012; results are summarized in **Table 5**). Cross-linking-MS has also been recently applied to study interactions within the phycobilisome (Tal et al., 2014) and between the phycobilisome and the photoprotective orange carotenoid protein (OCP) (Zhang et al., 2014; Liu et al., 2016), reviewed in Bricker et al. (2015).

With complementary use of the cross-linkers EDC and DTSSP, Pakrasi and co-workers (Liu et al., 2011a) demonstrated that the accessory protein Psb27 binds on the lumenal surface of CP43. Because this interaction is transient and occurs in only a small fraction of PSII centers in the cell at a given time, the authors purified PSII complexes from the Δ*ctp*A mutant strain of *Synechocystis* 6803 that accumulates such complexes (Liu et al., 2011b), maximizing chances of capturing and observing Psb27 inter-protein cross-links. The two cross-linked species detected were used to map Psb27 onto the PSII crystal structure, showing how Psb27 accomplishes its role as a gatekeeper, protecting partially assembled PSII complexes from gaining premature harmful water oxidation activity (Roose and Pakrasi, 2008). Recently, Nowaczyk and co-workers (Cormann et al., 2016)

identified a different cross-link between Psb27 and CP43 in *T. elongatus* using an isotope-encoded version of the BS^3 cross-linker. Despite the different cyanobacterial species used in the two studies, and the different Psb27 residues that were cross-linked, both cross-links localize Psb27 to the same domain on CP43 (Liu et al., 2011a; Cormann et al., 2016).

Cyanobacterial PsbQ is a component of active PSII (Roose et al., 2007), but is not found in any of the crystal structures, presumably because it is destabilized under crystallization conditions. Pakrasi and co-workers (Liu et al., 2014b) again used EDC and DTSSP in parallel and detected a PsbQ-CP47 and two PsbQ-PsbO cross-links by MS. A PsbQ-PsbQ cross-link that appears to arise from two different copies of the protein was also detected. Taken together, these results position PsbQ along the lumenal PSII dimer interface, consistent with evidence that PsbQ stabilizes the PSII dimer (Liu et al., 2014b). In this study, in-solution digestion was used instead of in-gel digestion to avoid losses of large cross-linked peptides that are difficult to extract from the gel matrix.

Several recent studies have probed the binding sites of the higher plant lumenal extrinsic proteins PsbP and PsbQ, which help optimize Ca^{2+} and Cl^{-} binding properties at the oxygen-evolving center (Bricker et al., 2012). Ifuku and co-workers (Ido et al., 2012, 2014) identified cross-links in spinach PSII between PsbP and PsbE, PsbR, and CP26 by MS and provided MS-based evidence for PsbP-CP43, PsbQ-CP43 and PsbQ-CP26 cross-links. The suggestive evidence arose from MS identification of CP43 or CP26 in individual cross-linked gel bands after affinity pull-downs using biotin-tagged PsbP or PsbQ (Ido et al., 2014). Their binding model for PsbP is different than that proposed by Bricker and co-workers (Mummadisetti et al., 2014), who identified nine intra-protein cross-links between the N-terminal and C-terminal regions of spinach PsbP that constrain significantly its binding conformation. The authors also identified a PsbP-PsbQ cross-link, consistent with that observed in *C. reinhardtii* by Enami and co-workers (Nagao et al., 2010).

The PsbQ-CP43 interaction in spinach PSII suggested by Ifuku and co-workers (Ido et al., 2014) contrasts with the PsbQ-CP47 cross-link identified in *Synechocystis* 6803 by Pakrasi and co-workers (Liu et al., 2014b) and their evidence for a PsbQ-PsbQ interaction at the PSII dimer interface. Significant sequence differences between cyanobacterial and plant PsbQ may explain this discrepancy. Bricker and co-workers (Mummadisetti et al., 2014) also found cross-linking evidence for a PsbQ-PsbQ interaction in spinach that may require a position at the dimer interface, consistent with the Pakrasi group's results in *Synechocystis* 6803. However, they suggest that that interaction could in theory arise from an inter-PSII-dimer interaction, and, thus, the results could alternatively be consistent with the Ifuku group's positioning of spinach PsbQ near CP43. Interestingly, the recently published crystal structure of PSII from the eukaryotic red alga *Cyanidium caldarium* indeed shows PsbQ′ binding to the lumenal surface of CP43 (Ago et al., 2016). PsbQ′ shares relatively low sequence homology to green algal or higher plant PsbQ; and though PsbQ′ can functionally replace PsbQ at least partially in *C. reinhardtii*, it cannot bind to spinach PSII (Ohta et al., 2003). Therefore, the red algal PsbQ′-CP43 interaction supports Ifuku and co-workers' (Ido et al., 2014) similar conclusion in spinach, but at the same time it does not necessarily contradict the alternate PsbQ-CP47 interaction observed by the other groups in spinach and *Synechocystis* 6803. The recent characterization of an active PSII complex from *Synechocystis* 6803 with multiple copies of the PsbQ protein (Liu et al., 2015) hints at one possible reconciliation of these findings, if such a complex is present in other species as well. Despite some discrepancies, these results begin to elucidate the binding orientation of the higher plant lumenal extrinsic proteins, suggesting a mechanism for stabilization of PSII-LHCII supercomplexes (Ido et al., 2014), and paving the road for further structural studies.

Although the advanced techniques for improving cross-link identification described in the methods section above have largely not yet been applied to PSII studies (with the exception of the recent use of isotope-encoded BS^3 by Nowaczyk and co-workers, Cormann et al., 2016), several other creative approaches have been used. Enami and co-workers (Nagao et al., 2010) improved identification confidence by detecting the same cross-linked residues in peptides from two separate digestion experiments, one with trypsin and one with Asp-N. Pakrasi and co-workers (Liu et al., 2011a) provided strong evidence, using the thiol-cleavable cross-linker DTSSP and 2D gel electrophoresis, that Psb27 and CP43 cross-link to each other, allowing targeted data analysis and providing higher confidence in the subsequent MS cross-link identification. Ifuku and co-workers (Ido et al., 2012, 2014) used a biotin-tagged PsbP or PsbQ to purify only those cross-linked proteins. Although this method is not as efficient as purifying only cross-linked peptides by means of a tagged linker, because following digestion many non-linked peptides from the tagged protein will be present, it does simplify sample complexity and focuses on cross-links containing a particular protein of interest. Notably, Blankenship and co-workers (Liu et al., 2013b) demonstrated that *in-vivo* cross-linking of thylakoid membrane complexes is possible and can capture interactions between protein complexes that are otherwise difficult to preserve after cell lysis. Using the membrane-permeable cross-linker DSP, they captured a PSII-PSI-phycobilisome megacomplex and identified five cross-links between PSII subunits and the PBS, and five between PSI subunits and the PBS, providing the first molecular-level description of the interface of these complexes.

Like cross-linking, protein footprinting is a technique that has long been used in PSII structural studies but that has become significantly more powerful in combination with modern MS. Early studies using N-hydroxysuccinimidobiotin (NHS-biotin) and other modification reagents investigated the binding site of higher plant PsbO to PSII. In the absence of MS detection, specific modification sites could either not be identified (Bricker et al., 1988) or were localized to particular protein domains by N-terminal sequencing of peptides (Frankel and Bricker, 1992). With the rise of protein MS in the mid-1990s, MALDI-TOF and FAB-MS were used to identify modified peptides; lack of MS/MS capability, however, produced lower-confidence peptide identification than is achievable today, and meant that specific modified residues could only be pinpointed in favorable cases (Frankel and Bricker, 1995; Miura et al., 1997; Frankel

et al., 1999). Nonetheless, these pioneering footprinting studies demonstrated, e.g., that PsbO interacts with Loop E of CP47 (Frankel and Bricker, 1992), and that charged residues on the surface of PsbO are involved in its interaction with PSII (Miura et al., 1997; Frankel et al., 1999).

Recently, hydroxyl radical footprinting using synchrotron radiolysis of water was used to study the binding surfaces of spinach PsbP and PsbQ to PSII, with detection of modified residues by MS (Mummadisetti et al., 2014). The results reveal buried regions on the surface of these proteins that complement the authors' cross-linking data and suggest these proteins' binding interfaces to other PSII subunits. The data also confirm and elaborate on the binding region identified by this group in a previous study using NHS-biotin as footprinting reagent (Meades et al., 2005).

Although the above footprinting studies detected whether or not a residue was modified in a given state, it is also possible to analyze footprinting data quantitatively to detect a conformational change in a complex in two different states. The label-free approaches described above can be used to monitor the relative change in modification, normalized to the unmodified peptide, in different PSII complexes. The utility of this approach was demonstrated in a study of the role of Psb27 in PSII assembly (Liu et al., 2013a) using GEE labeling. The authors monitored the relative changes in aspartate and glutamate modification of three PSII complexes representing different stages of PSII assembly, not only extending previous information about the Psb27 binding site (Liu et al., 2011a; Komenda et al., 2012a), but also demonstrating a conformational change upon D1 processing that prompts Psb27 dissociation and permits assembly of the oxygen evolving complex (Liu et al., 2013a). Blankenship and co-workers have also used quantitative GEE labeling to detect a light-dependent conformational change in the OCP protein that appears to underlie its photoprotective function (Liu et al., 2014a). The recent implementation of isotopically-labeled GEE (iGEE) footprinting (Zhang et al., 2016) will streamline, and increase confidence in, quantitative comparisons of modification extent between states.

Hydroxyl radical footprinting has also been used to identify putative water and oxygen channels in PSII (Frankel et al., 2013a), a topic that has been explored previously through computational studies (Murray and Barber, 2007; Ho and Styring, 2008; Gabdulkhakov et al., 2009; Vassiliev et al., 2012). This study provides general experimental support for the existence of such channels, confirms specific channel identifications from computational work (Ho and Styring, 2008; Vassiliev et al., 2012), and proposes a previously unidentified putative oxygen/ROS exit channel (see Bricker et al., 2015 for a discussion of the MS-based and computational results).

FUTURE DIRECTIONS

MS technology and associated sample preparation techniques are evolving rapidly. Increasing sensitivity and speed of instruments for bottom-up proteomics allows better coverage of transmembrane PSII proteins; for example, coverage of the core D1, D2, CP47, and CP43 proteins is routinely ∼50–85% on a Thermo Q-Exactive Plus instrument, whereas ∼20–40% coverage was reported on LTQ-Orbitrap, LTQ-FTICR, and MALDI-TOF instruments (Aro et al., 2005; Frankel et al., 2012; Liu et al., 2013a,b). This increased coverage will mean that more PTMs and cross-linked peptides can be identified, and a larger portion of the PSII complex can be mapped by footprinting. PTM analysis, especially using quantitative techniques to compare complexes exposed to different conditions, may help elucidate signals (largely unknown in cyanobacteria) that trigger D1 degradation. The increasing availability of high-sensitivity instruments that can achieve high sequence coverage is enabling detailed quantitative and non-quantitative global proteomic studies. The new challenge is to reduce the large amounts of information becoming available into specific testable hypotheses for targeted follow-up studies.

Improvements at all stages of the cross-linking workflow are occurring, from linker design to linked-peptide enrichment and software analysis. Specifically, isotope-labeled and MS-cleavable linkers are powerful tools that are just beginning to be applied to PSII research. *In-vivo* cross-linking is a promising approach to detect transient or unstable interactions that are difficult to capture after cell lysis. Cross-linking may enable binding site identification for at least some of the approximately 30 accessory proteins now known or believed to associate with PSII during its life-cycle (Nickelsen and Rengstl, 2013; Järvi et al., 2015). Detecting interactions between PSII subcomplexes and, e.g., D1 degradation proteases or proteins involved in chlorophyll loading would also be of prime interest.

Intact-mass measurements of the large core PSII proteins D1, D2, CP47, and CP43 were reported in several studies (Sharma et al., 1997b; Whitelegge et al., 1998; Huber et al., 2004; Thangaraj et al., 2010), with detection of the phosphorylated form of D1 as well in some cases (Whitelegge et al., 1998; Huber et al., 2004). However, their top-down analysis has not yet been achieved. Top-down technology is continuously developing, especially methods for increased product-ion sequence coverage (Frese et al., 2012; Shaw et al., 2013; Brunner et al., 2015) and analysis of larger integral membrane proteins and their PTMs (Ryan et al., 2010; Howery et al., 2012). Such analysis will make it easier to identify nearly-stoichiometric (and potentially important) PTM events from trace ones under different conditions, not an easy task using bottom-up MS. Native MS is capable of analyzing certain intact membrane protein complexes, although the technology is still developing, and no one approach works for all protein complexes (reviewed in Mehmood et al., 2015). Native MS analysis of PSII has not yet been demonstrated, but the technique could in theory serve as a complementary method to native gels to characterize the distribution of PSII subcomplexes under various conditions, and their components. This might be particularly useful to address the stoichiometry of accessory proteins and cofactors, and could add a new tool to address the long-standing question of chlorophyll loading in PSII.

CONCLUSION

The use of MS has been fueled by improvements in sample preparation methods for analysis of membrane proteins, increasing availability of MS instrumentation, and significant advances in instrument sensitivity, speed, and mass accuracy.

Techniques from each of the four pillars of proteomics will continue to be employed to study the PSII life cycle. These techniques have addressed a wide range of questions regarding the composition of PSII complexes, the time-dependent dynamic changes of individual subunits and complexes under different environmental conditions, and the tertiary and quaternary structure of PSII complexes.

Modern MS techniques provide a higher level of detail and confidence than previous methods; examples are identification of a protein's phosphorylation site instead of mere detection of a phosphorylated protein, and identification of specific cross-linked residues instead of only suggestive evidence that two particular proteins are cross-linked to each other. For other applications, the use of MS permits entirely new questions to be asked (e.g., what proteins are present on a proteome-wide scale for a purified PSII complex).

The new information has opened up new questions about function. For example, what are the physiological roles of the many new PTMs that have been identified? What purpose does an accessory protein serve by binding at this particular location on a PSII complex? In some cases, the sensitivity of MS is a potential pitfall: identification of a protein in a PSII sample does not necessarily mean it is a stoichiometric component, or that it associates specifically with the complex at all. Thus, information from MS should be a starting point for more targeted genetic and biochemical studies, and MS is one component of an expanding toolbox for PSII life-cycle research. Rapidly developing MS technology promises continued contributions to this field, which has a wide range of fascinating questions about membrane protein complex composition, dynamics, and structure yet to be answered.

AUTHOR CONTRIBUTIONS

HP, MG conceived of the article. DW collected data from the literature and drafted the manuscript. HP, MG, and DW revised the manuscript.

ACKNOWLEDGMENTS

The authors thank Dr. Hao Zhang (Washington University) and Dr. Phil Jackson (University of Sheffield) for helpful discussions. This work was supported by the Photosynthetic Antenna Research Center, an Energy Frontier Research Center funded by the U.S. Department of Energy (DOE), Office of Basic Energy Sciences (Grant DE-SC 0001035 to MG and HP), by the Chemical Sciences, Geosciences, and Biosciences Division, Office of Basic Energy Sciences, Office of Science, U.S. Department of Energy (grant no. DE-FG02-99ER20350 to HP), and by the NIH (Grant P41GM103422) to MG.

REFERENCES

Adir, N., Zer, H., Shochat, S., and Ohad, I. (2003). Photoinhibition - a historical perspective. *Photosynth. Res.* 76, 343–370. doi: 10.1023/A:1024969518145

Ago, H., Adachi, H., Umena, Y., Tashiro, T., Kawakami, K., Kamiya, N., et al. (2016). Novel features of eukaryotic Photosystem II revealed by its crystal structure analysis from a red alga. *J. Biol. Chem.* 291, 5676–5687. doi: 10.1074/jbc.M115.711689

Allahverdiyeva, Y., and Aro, E. M., (2012). "Photosynthetic responses of plants to excess light: Mechanisms and conditions for photoinhibition, excess energy dissipation, and repair," in *Photosynthesis: Plastid Biology, Energy Conversion and Carbon Assimilation. Advances in Photosynthesis and Respiration,* eds J. J. Eaton-Rye, B. C. Tripathy and T. D. Sharkey (Dordrecht: Springer), 275–297.

Anderson, L. B., Maderia, M., Ouellette, A. J. A., Putnam-Evans, C., Higgins, L., Krick, T., et al. (2002). Posttranslational modifications in the CP43 subunit of photosystem II. *Proc. Natl. Acad. Sci. U.S.A.* 99, 14676–14681. doi: 10.1073/pnas.232591599

Anderson, L. B., Ouellette, A. J. A., Eaton-Rye, J., Maderia, M., MacCoss, M. J., Yates, J. R., et al. (2004). Evidence for a post-translational modification, aspartyl aldehyde, in a photosynthetic membrane protein. *J. Am. Chem. Soc.* 126, 8399–8405. doi: 10.1021/ja0478781

Andersson, L., and Porath, J. (1986). Isolation of phosphoproteins by immobilized metal (Fe^{3+}) affinity chromatography. *Anal. Biochem.* 154, 250–254. doi: 10.1016/0003-2697(86)90523-3

Aro, E. M., McCaffery, S., and Anderson, J. M. (1993). Photoinhibition and D1 protein degradation in peas acclimated to different growth irradiances. *Plant Physiol.* 103, 835–843.

Aro, E.-M., Suorsa, M., Rokka, A., Allahverdiyeva, Y., Paakkarinen, V., Saleem, A., et al. (2005). Dynamics of photosystem II: a proteomic approach to thylakoid protein complexes. *J. Exp. Bot.* 56, 347–356. doi: 10.1093/jxb/eri041

Aryal, U. K., Stöckel, J., Krovvidi, R. K., Gritsenko, M. A., Monroe, M. E., Moore, R. J., et al. (2011). Dynamic proteomic profiling of a unicellular cyanobacterium *Cyanothece* ATCC51142 across light-dark diurnal cycles. *BMC Syst. Biol.* 5:194. doi: 10.1186/1752-0509-5-194

Back, J. W., de Jong, L., Muijsers, A. O., and de Koster, C. G. (2003). Chemical cross-linking and mass spectrometry for protein structural modeling. *J. Mol. Biol.* 331, 303–313. doi: 10.1016/S0022-2836(03)00721-6

Baena-González, E., and Aro, E.-M. (2002). Biogenesis, assembly and turnover of photosystem II units. *Phil. Trans. R. Soc. Lond. B.* 357, 1451–1459. doi: 10.1098/rstb.2002.1141

Bantscheff, M., Lemeer, S., Savitski, M. M., and Kuster, B. (2012). Quantitative mass spectrometry in proteomics: critical review update from 2007 to the present. *Anal. Bioanal. Chem.* 404, 939–965. doi: 10.1007/s00216-012-6203-4

Barber, J., and Andersson, B. (1992). Too much of a good thing—light can be bad for photosynthesis. *Trends Biochem. Sci.* 17, 61–66. doi: 10.1016/0968-0004(92)90503-2

Battchikova, N., Angeleri, M., and Aro, E.-M. (2015). Proteomic approaches in research of cyanobacterial photosynthesis. *Photosynth. Res.* 126, 47–70. doi: 10.1007/s11120-014-0050-4

Boehm, M., Romero, E., Reisinger, V., Yu, J., Komenda, J., Eichacker, L. A., et al. (2011). Investigating the early stages of Photosystem II assembly in *Synechocystis* sp. PCC 6803: Isolation of CP47 and CP43 complexes. *J. Biol. Chem.* 286, 14812–14819. doi: 10.1074/jbc.M110.207944

Boehm, M., Yu, J., Reisinger, V., Beckova, M., Eichacker, L. A., Schlodder, E., et al. (2012). Subunit composition of CP43-less photosystem II complexes of *Synechocystis* sp. PCC 6803: implications for the assembly and repair of photosystem II. *Phil. Trans. R. Soc. B* 367, 3444–3454. doi: 10.1098/rstb.2012.0066

Bonardi, V., Pesaresi, P., Becker, T., Schleiff, E., Wagner, R., Pfannschmidt, T., et al. (2005). Photosystem II core phosphorylation and photosynthetic acclimation require two different protein kinases. *Nature* 437, 1179–1182. doi: 10.1038/nature04016

Bricker, T. M., Mummadisetti, M. P., and Frankel, L. K. (2015). Recent advances in the use of mass spectrometry to examine structure/function relationships in photosystem II. *J. Photochem. Photobiol. B* 152, 227–246. doi: 10.1016/j.jphotobiol.2015.08.031

Bricker, T. M., Odom, W. R., and Queirolo, C. B. (1988). Close association of the 33-kDa extrinsic protein with the apoprotein of CPa1 in photosystem II. *FEBS Lett.* 231, 111–117. doi: 10.1016/0014-5793(88)80713-0

Bricker, T. M., Roose, J. L., Fagerlund, R. D., Frankel, L. K., and Eaton-Rye, J. J. (2012). The extrinsic proteins of Photosystem II. *Biochim. Biophys. Acta* 1817, 121–142. doi: 10.1016/j.bbabio.2011.07.006

Brunner, A. M., Lossl, P., Liu, F., Huguet, R., Mullen, C., Yamashita, M., et al. (2015). Benchmarking multiple fragmentation methods on an Orbitrap Fusion for top-down phospho-proteoform characterization. *Anal. Chem.* 87, 4152–4158. doi: 10.1021/acs.analchem.5b00162

Buncherd, H., Roseboom, W., de Koning, L. J., de Koster, C. G., and de Jong, L. (2014). A gas phase cleavage reaction of cross-linked peptides for protein complex topology studies by peptide fragment fingerprinting from large sequence database. *J. Proteomics* 108, 65–77. doi: 10.1016/j.jprot.2014.05.003

Caffarri, S., Kouřil, R., Kereiche, S., Boekema, E. J., and Croce, R. (2009). Functional architecture of higher plant photosystem II supercomplexes. *EMBO J.* 28, 3052–3064. doi: 10.1038/emboj.2009.232

Chen, X., Wei, S., Ji, Y., Guo, X., and Yang, F. (2015). Quantitative proteomics using SILAC: principles, applications, and developments. *Proteomics* 15, 3175–3192. doi: 10.1002/pmic.201500108

Chu, F., Mahrus, S., Craik, C. S., and Burlingame, A. L. (2006). Isotope-coded and affinity-tagged cross-linking (ICATXL): An efficient strategy to probe protein interaction surfaces. *J. Am. Chem. Soc.* 128, 10362–10363. doi: 10.1021/ja0614159

Clarke, A. K., Soitamo, A., Gustafsson, P., and Öquist, G. (1993). Rapid interchange between two distinct forms of cyanobacterial photosystem II reaction center protein D1 in response to photoinhibition. *Proc. Natl. Acad. Sci. U.S.A.* 90, 9973–9977. doi: 10.1073/pnas.90.21.9973

Clegg, C., and Hayes, D. (1974). Identification of neighboring proteins in ribosomes of *Escherichia coli*- Topographical study with crosslinking reagent dimethyl suberimidate. *Eur. J. Biochem.* 42, 21–28. doi: 10.1111/j.1432-1033.1974.tb03309.x

Cormann, K. U., Möller, M., and Nowaczyk, M. M. (2016). Critical assessment of protein cross-linking and molecular docking: an updated model for the interaction between Photosystem II and Psb27. *Front. Plant Sci.* 7:157. doi: 10.3389/fpls.2016.00157

Dasgupta, J., Ananyev, G., and Dismukes, G. C. (2008). Photoassembly of the water-oxidizing complex in photosystem II. *Coord. Chem. Rev.* 252, 347–360. doi: 10.1016/j.ccr.2007.08.022

Dedner, N., Meyer, H. E., Ashton, C., and Wildner, G. F. (1988). N-terminal sequence analysis of the 8 kDa protein in *Chlamydomonas reinhardii*: localization of the phosphothreonine. *FEBS Lett.* 236, 77–82. doi: 10.1016/0014-5793(88)80288-6

Dobáková, M., Sobotka, R., Tichý, M., and Komenda, J. (2009). Psb28 protein is involved in the biogenesis of the Photosystem II inner antenna CP47 (PsbB) in the cyanobacterium *Synechocystis* sp. PCC 6803. *Plant Physiol.* 149, 1076–1086. doi: 10.1104/pp.108.130039

Dobáková, M., Tichý, M., and Komenda, J. (2007). Role of the PsbI protein in photosystem II assembly and repair in the cyanobacterium *Synechocystis* sp. PCC 6803. *Plant Physiol.* 145, 1681–1691. doi: 10.1104/pp.107.107805

Dreaden, T. M., Chen, J., Rexroth, S., and Barry, B. A. (2011). N-formylkynurenine as a marker of high light stress in photosynthesis. *J. Biol. Chem.* 286, 22632–22641. doi: 10.1074/jbc.M110.212928

Enami, I., Kamo, M., Ohta, H., Takahashi, S., Miura, T., Kusayanagi, M., et al. (1998). Intramolecular cross-linking of the extrinsic 33-kDa protein leads to loss of oxygen evolution but not its ability of binding to Photosystem II and stabilization of the manganese cluster. *J. Biol. Chem.* 273, 4629–4634. doi: 10.1074/jbc.273.8.4629

Enami, I., Satoh, K., and Katoh, S. (1987). Crosslinking between the 33 kDa extrinsic protein and the 47 kDa chlorophyll-carrying protein of the PSII reaction center core complex. *FEBS Lett.* 226, 161–165. doi: 10.1016/0014-5793(87)80571-9

Fagerlund, R. D., and Eaton-Rye, J. J. (2011). The lipoproteins of cyanobacterial photosystem II. *J. Photochem. Photobiol. B* 104, 191–203. doi: 10.1016/j.jphotobiol.2011.01.022

Ficarro, S. B., McCleland, M. L., Stukenberg, P. T., Burke, D. J., Ross, M. M., Shabanowitz, J., et al. (2002). Phosphoproteome analysis by mass spectrometry and its application to *Saccharomyces cerevisiae*. *Nat. Biotechnol.* 20, 301–305. doi: 10.1038/nbt0302-301

Frankel, L. K., and Bricker, T. M. (1992). Interaction of CPa-1 with the manganese-stabilizing protein of Photosystem II: identification of domains on CPa-1 which are shielded from N-hydroxysuccinimide biotinylation by the manganese-stabilizing protein. *Biochemistry* 31, 11059–11064. doi: 10.1021/bi00160a015

Frankel, L. K., and Bricker, T. M. (1995). Interaction of the 33-kDa extrinsic protein with Photosystem II: identification of domains on the 33-kDa protein that are shielded from NHS-biotinylation by Photosystem II. *Biochemistry* 34, 7492–7497. doi: 10.1021/bi00022a024

Frankel, L. K., Cruz, J. A., and Bricker, T. M. (1999). Carboxylate groups on the manganese-stabilizing protein are required for its efficient binding to Photosystem II. *Biochemistry* 38, 14271–14278. doi: 10.1021/bi991366v

Frankel, L. K., Sallans, L., Bellamy, H., Goettert, J. S., Limbach, P. A., and Bricker, T. M. (2013a). Radiolytic mapping of solvent-contact surfaces in Photosystem II of higher plants: experimental identification of putative water channels within the photosystem. *J. Biol. Chem.* 288, 23565–23572. doi: 10.1074/jbc.M113.487033

Frankel, L. K., Sallans, L., Limbach, P. A., and Bricker, T. M. (2013b). Oxidized amino acid residues in the vicinity of Q_A and $Pheo_{D1}$ of the Photosystem II reaction center: putative generation sites of reducing-side reactive oxygen species. *PLoS ONE* 8:e58042. doi: 10.1371/journal.pone.0058042

Frankel, L. K., Sallans, L., Limbach, P., and Bricker, T. M. (2012). Identification of oxidized amino acid residues in the vicinity of the Mn_4CaO_5 cluster of Photosystem II: implications for the identification of oxygen channels within the photosystem. *Biochemistry* 51, 6371–6377. doi: 10.1021/bi300650n

Frese, C. K., Altelaar, A. F. M., van den Toorn, H., Nolting, D., Griep-Raming, J., Heck, A. J. R., et al. (2012). Toward full peptide sequence coverage by dual fragmentation combining electron-transfer and higher-energy collision dissociation tandem mass spectrometry. *Anal. Chem.* 84, 9668–9673. doi: 10.1021/ac3025366

Fristedt, R., Granath, P., and Vener, A. V. (2010). A protein phosphorylation threshold for functional stacking of plant photosynthetic membranes. *PLoS ONE* 5:e10963. doi: 10.1371/journal.pone.0010963

Fristedt, R., and Vener, A. V. (2011). High light induced disassembly of Photosystem II supercomplexes in *Arabidopsis* requires STN7-dependent phosphorylation of CP29. *PLoS ONE* 6:e24565. doi: 10.1371/journal.pone.0024565

Fristedt, R., Willig, A., Granath, P., Crevecoeur, M., Rochaix, J.-D., and Vener, A. V. (2009). Phosphorylation of Photosystem II controls functional macroscopic folding of photosynthetic membranes in *Arabidopsis*. *Plant Cell* 21, 3950–3964. doi: 10.1105/tpc.109.069435

Fritzsche, R., Ihling, C. H., Götze, M., and Sinz, A. (2012). Optimizing the enrichment of cross-linked products for mass spectrometric protein analysis. *Rapid Commun. Mass Spectrom.* 26, 653–658. doi: 10.1002/rcm.6150

Gabdulkhakov, A., Guskov, A., Broser, M., Kern, J., Mueh, F., Saenger, W., et al. (2009). Probing the accessibility of the Mn_4Ca cluster in Photosystem II: channels calculation, noble gas derivatization, and cocrystallization with DMSO. *Structure* 17, 1223–1234. doi: 10.1016/j.str.2009.07.010

Galetskiy, D., Lohscheider, J. N., Kononikhin, A. S., Popov, I. A., Nikolaev, E. N., and Adamska, I. (2011a). Mass spectrometric characterization of photooxidative protein modifications in *Arabidopsis thaliana* thylakoid membranes. *Rapid Commun. Mass Spectrom.* 25, 184–190. doi: 10.1002/rcm.4855

Galetskiy, D., Lohscheider, J. N., Kononikhin, A. S., Popov, I. A., Nikolaev, E. N., and Adamska, I. (2011b). Phosphorylation and nitration levels of photosynthetic proteins are conversely regulated by light stress. *Plant Mol. Biol.* 77, 461–473. doi: 10.1007/s11103-011-9824-7

Gao, S., Gu, W., Xiong, Q., Ge, F., Xie, X., Li, J., et al. (2015). Desiccation enhances phosphorylation of PSII and affects the distribution of protein complexes in the thylakoid membrane. *Physiol. Plant.* 153, 492–502. doi: 10.1111/ppl.12258

Gau, B., Garai, K., Frieden, C., and Gross, M. L. (2011). Mass spectrometry-based protein footprinting characterizes the structures of oligomeric apolipoprotein E2, E3, and E4. *Biochemistry* 50, 8117–8126. doi: 10.1021/bi200911c

Geiger, T., Cox, J., and Mann, M. (2010). Proteomics on an Orbitrap benchtop mass spectrometer using all-ion fragmentation. *Mol. Cell. Proteomics* 9, 2252–2261. doi: 10.1074/mcp.M110.001537

Golden, S. S., Brusslan, J., and Haselkorn, R. (1986). Expression of a family of *psbA* genes encoding a photosystem II polypeptide in the cyanobacterium *Anacystis nidulans* R2. *EMBO J.* 5, 2789–2798.

Gómez, S. M., Bil', K. Y., Aguilera, R., Nishio, J. N., Faull, K. F., and Whitelegge, J. P. (2003). Transit peptide cleavage sites of integral thylakoid membrane proteins. *Mol. Cell. Proteomics* 2, 1068–1085. doi: 10.1074/mcp.M300062-MCP200

Gómez, S. M., Nishio, J. N., Faull, K. F., and Whitelegge, J. P. (2002). The chloroplast grana proteome defined by intact mass measurements from liquid chromatography mass spectrometry. *Mol. Cell. Proteomics* 1, 46–59. doi: 10.1074/mcp.M100007-MCP200

Gómez, S. M., Park, J. J., Zhu, J., Whitelegge, J. P., and Thornber, J. P. (1998). "Isolation and characterization of a novel xanthophyll-rich pigment-protein complex from spinach," in *Photosynthesis: Mechanisms and Effects, Vol. 1*," ed G. Garab (Dordrecht: Kluwer Academic Publishers), 353–356.

Gouw, J. W., Krijgsveld, J., and Heck, A. J. R. (2010). Quantitative proteomics by metabolic labeling of model organisms. *Mol. Cell. Proteomics* 9, 11–24. doi: 10.1074/mcp.R900001-MCP200

Granvogl, B., Zoryan, M., Plöscher, and Eichacker, L. A. (2008). Localization of 13 one-helix integral membrane proteins in Photosystem II subcomplexes. *Anal. Biochem*. 383, 279–288. doi: 10.1016/j.ab.2008.08.038

Grasse, N., Mamedov, F., Becker, K., Styring, S., Rögner, M., and Nowaczyk, M. M. (2011). Role of novel dimeric Photosystem II (PSII)-Psb27 protein complex in PSII repair. *J. Biol. Chem.* 286, 29548–29555. doi: 10.1074/jbc.M111.238394

Grossmann, J., Roschitzki, B., Panse, C., Fortes, C., Barkow-Oesterreicher, S., Rutishauser, D., et al. (2010). Implementation and evaluation of relative and absolute quantification in shotgun proteomics with label-free methods. *J. Proteomics* 73, 1740–1746. doi: 10.1016/j.jprot.2010.05.011

Götze, M., Pettelkau, J., Fritzsche, R., Ihling, C. H., Schaefer, M., and Sinz, A. (2015). Automated assignment of MS/MS cleavable cross-links in protein 3D-structure analysis. *J. Am. Soc. Mass. Spectrom.* 26, 83–97. doi: 10.1007/s13361-014-1001-1

Götze, M., Pettelkau, J., Schaks, S., Bosse, K., Ihling, C., Krauth, F., et al. (2012). StavroX-A Software for analyzing crosslinked products in protein interaction studies. *J. Am. Soc. Mass. Spectrom.* 23, 76–87. doi: 10.1007/s13361-011-0261-2

Guerreiro, A. C. L., Benevento, M., Lehmann, R., van Breukelen, B., Post, H., Giansanti, P., et al. (2014). Daily rhythms in the cyanobacterium *Synechococcus elongatus* probed by high-resolution mass spectrometry-based proteomics reveals a small defined set of cyclic proteins. *Mol. Cell. Proteomics* 13, 2042–2055. doi: 10.1074/mcp.M113.035840

Guo, J., Nguyen, A. Y., Dai, Z., Su, D., Gaffrey, M. J., Moore, R. J., et al. (2014). Proteome-wide light/dark modulation of thiol oxidation in cyanobacteria revealed by quantitative site-specific redox proteomics. *Mol. Cell. Proteomics* 13, 3270–3285. doi: 10.1074/mcp.M114.041160

Guskov, A., Kern, J., Gabdulkhakov, A., Broser, M., Zouni, A., and Saenger, W. (2009). Cyanobacterial photosystem II at 2.9-Å resolution and the role of quinones, lipids, channels and chloride. *Nat. Struct. Mol. Biol.* 16, 334–342. doi: 10.1038/nsmb.1559

Han, K. C., Shen, J. R., Ikeuchi, M., and Inoue, Y. (1994). Chemical cross-linking studies of extrinsic proteins in cyanobacterial photosystem II. *FEBS Lett.* 355, 121–124. doi: 10.1016/0014-5793(94)01182-6

Haniewicz, P., De Sanctis, D., Büchel, C., Schröder, W. P., Loi, M. C., Kieselbach, T., et al. (2013). Isolation of monomeric photosystem II that retains the subunit PsbS. *Photosynth. Res.* 118, 199–207. doi: 10.1007/s11120-013-9914-2

Haniewicz, P., Floris, D., Farci, D., Kirkpatrick, J., Loi, M. C., and Büchel, C. (2015). Isolation of plant Photosystem II complexes by fractional solubilization. *Front. Plant Sci.* 6:1100. doi: 10.3389/fols.2015.01100

Hansson, M., Dupuis, T., Stromquist, R., Andersson, B., Vener, A. V., and Carlberg, I. (2007). The mobile thylakoid phosphoprotein TSP9 interacts with the light-harvesting complex II and the peripheries of both photosystems. *J. Biol. Chem.* 282, 16214–16222. doi: 10.1074/jbc.M605833200

Harrer, R., Bassi, R., Testi, M. G., and Schäfer, C. (1998). Nearest-neighbor analysis of a photosystem II complex from *Marchantia polymorpha* L. (liverwort), which contains reaction center and antenna proteins. *Eur. J. Biochem.* 255, 196–205. doi: 10.1046/j.1432-1327.1998.2550196.x

Heinemeyer, J., Eubel, H., Wehmhoner, D., Jansch, L., and Braun, H. P. (2004). Proteomic approach to characterize the supramolecular organization of photosystems in higher plants. *Phytochemistry* 65, 1683–1692. doi: 10.1016/j.phytochem.2004.04.022

Heinz, S., Liauw, P., Nickelsen, J., and Nowaczyk, M. (2016). Analysis of photosystem II biogenesis in cyanobacteria. *Biochim. Biophys. Acta* 1857, 274–287. doi: 10.1016/j.bbabio.2015.11.007

Herbstová, M., Tietz, S., Kinzel, C., Turkina, M., and Kirchhoff, H. (2012). Architectural switch in plant photosynthetic membranes induced by light stress. *Proc. Natl. Acad. Sci. U.S.A.* 109, 20130–20135. doi: 10.1073/pnas.1214265109

Ho, F. M., and Styring, S. (2008). Access channels and methanol binding site to the $CaMn_4$ cluster in Photosystem II based on solvent accessibility simulations, with implications for substrate water access. *Biochim. Biophys. Acta* 1777, 140–153. doi: 10.1016/j.bbabio.2007.08.009

Hoare, D. G., and Koshland, D. E. (1967). A method for quantitative modification and estimation of carboxylic acid groups in proteins. *J. Biol. Chem.* 242, 2447–2453.

Hoopmann, M. R., Zelter, A., Johnson, R. S., Riffle, M., MacCoss, M. J., Davis, T. N., et al. (2015). Kojak: efficient analysis of chemically cross-linked protein complexes. *J. Proteome Res.* 14, 2190–2198. doi: 10.1021/pr501321h

Howery, A. E., Elvington, S., Abraham, S. J., Choi, K. H., Dworschak-Simpson, S., Phillips, S., et al. (2012). A designed inhibitor of a CLC antiporter blocks function through a unique binding mode. *Chem. Biol.* 19, 1460–1470. doi: 10.1016/j.chembiol.2012.09.017

Huber, C. G., Walcher, W., Timperio, A. M., Troiani, S., Porceddu, A., and Zolla, L. (2004). Multidimensional proteomic analysis of photosynthetic membrane proteins by liquid extraction-ultracentrifugation-liquid chromatography-mass spectrometry. *Proteomics* 4, 3909–3920. doi: 10.1002/pmic.200400823

Ido, K., Kakiuchi, S., Uno, C., Nishimura, T., Fukao, Y., Noguchi, T., et al. (2012). The conserved His-144 in the PsbP protein is important for the interaction between the PsbP N-terminus and the Cyt b_{559} subunit of Photosystem II. *J. Biol. Chem.* 287, 26377–26387. doi: 10.1074/jbc.M112.385286

Ido, K., Nield, J., Fukao, Y., Nishimura, T., Sato, F., and Ifuku, K. (2014). Cross-linking evidence for multiple interactions of the PsbP and PsbQ proteins in a higher plant Photosystem II supercomplex. *J. Biol. Chem.* 289, 20150–20157. doi: 10.1074/jbc.M114.574822

Ikeuchi, M., and Inoue, Y. (1988). A new 4.8-kDa polypeptide instrinsic to the PS II reaction center, as revealed by modified SDS-PAGE with improved resolution of low-molecular-weight proteins. *Plant Cell Physiol.* 29, 1233–1239.

Inagaki, N., Yamamoto, Y., and Satoh, K. (2001). A sequential two-step proteolytic process in the carboxyl-terminal truncation of precursor D1 protein in *Synechocystis* sp. PCC6803. *FEBS Lett*. 509, 197–201. doi: 10.1016/S0014-5793(01)03180-5

Ingle, R. A., Schmidt, U. G., Farrant, J. M., Thomson, J. A., and Mundree, S. G. (2007). Proteomic analysis of leaf proteins during dehydration of the resurrection plant *Xerophyta viscosa*. *Plant Cell Environ.* 30, 435–446. doi: 10.1111/j.1365-3040.2006.01631.x

Inoue-Kashino, N., Kashino, Y., Orii, H., Satoh, K., Terashima, I., and Pakrasi, H. B. (2011). S4 protein Sll1252 is necessary for energy balancing in photosynthetic electron transport in *Synechocystis* sp. PCC 6803. *Biochemistry* 50, 329–339. doi: 10.1021/bi101077e

Irrgang, K. D., Shi, L. X., Funk, C., and Schröder, W. P. (1995). A nuclear-encoded subunit of the Photosystem II reaction center. *J. Biol. Chem.* 270, 17588–17593.

Iwai, M., Suzuki, T., Dohmae, N., Inoue, Y., and Ikeuchi, M. (2007). Absence of the PsbZ subunit prevents association of PsbK and Ycf12 with the PSII complex in the thermophilic cyanobacterium *Thermosynechococcus elongatus* BP-1. *Plant Cell Physiol.* 48, 1758–1763. doi: 10.1093/pcp/pcm148

Järvi, S., Suorsa, M., and Aro, E.-M. (2015). Photosystem II repair in plant chloroplasts - Regulation, assisting proteins and shared components with photosystem II biogenesis. *Biochim. Biophys. Acta* 1847, 900–909. doi: 10.1016/j.bbabio.2015.01.006

Järvi, S., Suorsa, M., Paakkarinen, V., and Aro, E.-M. (2011). Optimized native gel systems for separation of thylakoid protein complexes: novel super- and mega-complexes. *Biochem J.* 439, 207–214. doi: 10.1042/BJ20102155

Kang, S., Mou, L., Lanman, J., Velu, S., Brouillette, W., Prevelige, P. E., et al. (2009). Synthesis of biotin-tagged chemical cross-linkers and their applications for mass spectrometry. *Rapid Commun. Mass Spectrom.* 23, 1719–1726. doi: 10.1002/rcm.4066

Kao, A., Chiu, C.-l., Vellucci, D., Yang, Y., Patel, V. R., Guan, S., et al. (2011). Development of a novel cross-linking strategy for fast and accurate

identification of cross-linked peptides of protein complexes. *Mol. Cell. Proteomics* 10:002212. doi: 10.1074/mcp.M110.002212

Kashino, Y., Lauber, W. M., Carroll, J. A., Wang, Q. J., Whitmarsh, J., Satoh, K., et al. (2002). Proteomic analysis of a highly active photosystem II preparation from the cyanobacterium *Synechocystis* sp. PCC 6803 reveals the presence of novel polypeptides. *Biochemistry* 41, 8004–8012. doi: 10.1021/bi026012+

Kasson, T. M. D., Rexroth, S., and Barry, B. A. (2012). Light-induced oxidative stress, N-formylkynurenine, and oxygenic photosynthesis. *PLoS ONE* 7:42220. doi: 10.1371/journal.pone.0042220

Kereïche, S., Kouřil, R., Oostergetel, G. T., Fusetti, F., Boekema, E. J., Doust, A. B., et al. (2008). Association of chlorophyll a/c_2 complexes to photosystem I and photosystem II in the cryptophyte *Rhodomonas* CS24. *Biochim. Biophys. Acta* 1777, 1122–1128. doi: 10.1016/j.bbabio.2008.04.045

Knoppová, J., Sobotka, R., Tichý, M., Yu, J., Konik, P., Halada, P., et al. (2014). Discovery of a chlorophyll binding protein complex involved in the early steps of Photosystem II assembly in *Synechocystis*. *Plant Cell* 26, 1200–1212. doi: 10.1105/tpc.114.123919

Komenda, J., Hassan, H. A. G., Diner, B. A., Debus, R. J., Barber, J., and Nixon, P. J. (2000). Degradation of the Photosystem II D1 and D2 proteins in different strains of the cyanobacterium *Synechocystis* PCC 6803 varying with respect to the type and level of *psbA* transcript. *Plant Mol. Biol.* 42, 635–645. doi: 10.1023/A:1006305308196

Komenda, J., Knoppová, J., Kopečná, J., Sobotka, R., Halada, P., Yu, J., et al. (2012a). The Psb27 assembly factor binds to the CP43 complex of Photosystem II in the cyanobacterium *Synechocystis* sp. PCC 6803. *Plant Physiol.* 158, 476–486. doi: 10.1104/pp.111.184184

Komenda, J., Kuviková, S., Granvogl, B., Eichacker, L. A., Diner, B. A., and Nixon, P. J. (2007). Cleavage after residue Ala352 in the C-terminal extension is an early step in the maturation of the D1 subunit of Photosystem II in *Synechocystis* PCC 6803. *Biochim. Biophys. Acta* 1767, 829–837. doi: 10.1016/j.bbabio.2007.01.005

Komenda, J., Nickelsen, J., Tichý, M., Prášil, O., Eichacker, L., and Nixon, P. J. (2008). The cyanobacterial homologue of HCF136/YCF48 is a component of an early Photosystem II assembly complex and is important for both the efficient assembly and repair of Photosystem II in Synechocystis sp. PCC 6803. *J. Biol. Chem.* 283, 22390–22399. doi: 10.1074/jbc.M801917200

Komenda, J., Reisinger, V., Müller, B. C., Dobáková, M., Granvogl, B., and Eichacker, L. A. (2004). Accumulation of the D2 protein is a key regulatory step for assembly of the Photosystem II reaction center complex in *Synechocystis* PCC 6803. *J. Biol. Chem.* 279, 48620–48629. doi: 10.1074/jbc.M405725200

Komenda, J., Sobotka, R., and Nixon, P. J. (2012b). Assembling and maintaining the Photosystem II complex in chloroplasts and cyanobacteria. *Curr. Opin. Plant Biol.* 15, 245–251. doi: 10.1016/j.pbi.2012.01.017

Komenda, J., Tichý, M., and Eichacker, L. A. (2005). The PsbH protein is associated with the inner antenna CP47 and facilitates D1 processing and incorporation into PSII in the cyanobacterium *Synechocystis* PCC 6803. *Plant Cell Physiol.* 46, 1477–1483. doi: 10.1093/pcp/pci159

Kós, P. B., Deák, Z., Cheregi, O., and Vass, I. (2008). Differential regulation of *psbA* and *psbD* gene expression, and the role of the different D1 protein copies in the cyanobacterium *Thermosynechococcus elongatus* BP-1. *Biochim. Biophys. Acta* 1777, 74–83. doi: 10.1016/j.bbabio.2007.10.015

Kouřil, R., Dekker, J. P., and Boekema, E. J. (2012). Supramolecular organization of photosystem II in green plants. *Biochim. Biophys. Acta* 1817, 2–12. doi: 10.1016/j.bbabio.2011.05.024

Kufryk, G., Hernandez-Prieto, M. A., Kieselbach, T., Miranda, H., Vermaas, W., and Funk, C. (2008). Association of small CAB-like proteins (SCPs) of *Synechocystis* sp. PCC 6803 with Photosystem II. *Photosynth. Res.* 95, 135–145. doi: 10.1007/s11120-007-9244-3

Laganowsky, A., Gómez, S. M., Whitelegge, J. P., and Nishio, J. N. (2009). Hydroponics on a chip: analysis of the Fe deficient *Arabidopsis* thylakoid membrane proteome. *J. Proteomics* 72, 397–415. doi: 10.1016/j.jprot.2009.01.024

Leitner, A., Reischl, R., Walzthoeni, T., Herzog, F., Bohn, S., Förster, F., et al. (2012). Expanding the chemical cross-linking toolbox by the use of multiple proteases and enrichment by size exclusion chromatography. *Mol. Cell. Proteomics* 11:M111.014126. doi: 10.1074/mcp.M111.014126

Lemeille, S., and Rochaix, J.-D. (2010). State transitions at the crossroad of thylakoid signalling pathways. *Photosynth. Res.* 106, 33–46. doi: 10.1007/s11120-010-9538-8

Lemeille, S., Turkina, M., Vener, A. V., and Rochaix, J.-D. (2010). Stt7-dependent phosphorylation during state transitions in the green alga *Chlamydomonas reinhardtii*. *Mol. Cell. Proteomics* 9, 1281–1295. doi: 10.1074/mcp.M000020-MCP201

Li, X.-J., Yang, M.-F., Zhu, Y., Liang, Y., and Shen, S.-H. (2011). Proteomic analysis of salt stress responses in rice shoot. *J. Plant Biol.* 54, 384–395. doi: 10.1007/s12374-011-9173-8

Liu, H., Chen, J., Huang, R.-C., Weisz, D., Gross, M. L., and Pakrasi, H. B. (2013a). Mass spectrometry-based footprinting reveals structural dynamics of Loop E of the chlorophyll-binding protein CP43 during Photosystem II assembly in the cyanobacterium *Synechocystis* 6803. *J. Biol. Chem.* 288, 14212–14220. doi: 10.1074/jbc.M113.467613

Liu, H., Huang, R. Y.-C., Chen, J., Gross, M. L., and Pakrasi, H. B. (2011a). Psb27, a transiently associated protein, binds to the chlorophyll binding protein CP43 in photosystem II assembly intermediates. *Proc. Natl. Acad. Sci. U.S.A.* 108, 18536–18541. doi: 10.1073/pnas.1111597108

Liu, H., Roose, J. L., Cameron, J. C., and Pakrasi, H. B. (2011b). A genetically tagged Psb27 protein allows purification of two consecutive Photosystem II (PSII) assembly intermediates in *Synechocystis* 6803, a cyanobacterium. *J. Biol. Chem.* 286, 24865–24871. doi: 10.1074/jbc.M111.246231

Liu, H., Weisz, D. A., and Pakrasi, H. B. (2015). Multiple copies of the PsbQ protein in a cyanobacterial photosystem II assembly intermediate complex. *Photosynth. Res.* 126, 375–383. doi: 10.1007/s11120-015-0123-z

Liu, H., Zhang, H., King, J., Wolf, N., Prado, M., Gross, M. L., et al. (2014a). Mass spectrometry footprinting reveals the structural rearrangements of cyanobacterial orange carotenoid protein upon light activation. *Biochim. Biophys. Acta* 1837, 1955–1963. doi: 10.1016/j.bbabio.2014.09.004

Liu, H., Zhang, H., Niedzwiedzki, D., Prado, M., He, G., Gross, M. L., et al. (2013b). Phycobilisomes supply excitations to both photosystems in a megacomplex in cyanobacteria. *Science* 342, 1104–1107. doi: 10.1126/science.1242321

Liu, H., Zhang, H., Orf, G. S., Lu, Y., Jiang, J., King, J. D., et al. (2016). Dramatic domain rearrangements of the cyanobacterial orange carotenoid protein upon photoactivation. *Biochemistry* 55, 1003–1009. doi: 10.1021/acs.biochem.6b00013

Liu, H., Zhang, H., Weisz, D. A., Vidavsky, I., Gross, M. L., and Pakrasi, H. B. (2014b). MS-based cross-linking analysis reveals the location of the PsbQ protein in cyanobacterial photosystem II. *Proc. Natl. Acad. Sci. U.S.A.* 111, 4638–4643. doi: 10.1073/pnas.1323063111

Lohrig, K., Mueller, B., Davydova, J., Leister, D., and Wolters, D. A. (2009). Phosphorylation site mapping of soluble proteins: bioinformatical filtering reveals potential plastidic phosphoproteins in *Arabidopsis thaliana*. *Planta* 229, 1123–1134. doi: 10.1007/s00425-009-0901-y

Loll, B., Kern, J., Saenger, W., Zouni, A., and Biesiadka, J. (2005). Towards complete cofactor arrangement in the 3.0 Å resolution structure of photosystem II. *Nature* 438, 1040–1044. doi: 10.1038/nature04224

Lorković, Z. J., Schröder, W. P., Pakrasi, H. B., Irrgang, K. D., Herrmann, R. G., and Oelmüller, R. (1995). Molecular characterization of PsbW, a nuclear-encoded component of the Photosystem II reaction center complex in spinach. *Proc. Natl. Acad. Sci. U.S.A.* 92, 8930–8934. doi: 10.1073/pnas.92.19.8930

Lundgren, D. H., Hwang, S.-I., Wu, L., and Han, D. K. (2010). Role of spectral counting in quantitative proteomics. *Expert Rev. Proteomics* 7, 39–53. doi: 10.1586/EPR.09.69

Mabbitt, P. D., Wilbanks, S. M., and Eaton-Rye, J. J. (2014). Structure and function of the hydrophilic Photosystem II assembly proteins: Psb27, Psb28 and Ycf48. *Plant Physiol. Bioch.* 81, 96–107. doi: 10.1016/j.plaphy.2014.02.013

Mädler, S., Bich, C., Touboul, D., and Zenobi, R. (2009). Chemical cross-linking with NHS esters: a systematic study on amino acid reactivities. *J. Mass Spectrom.* 44, 694–706. doi: 10.1002/jms.1544

Meades, G. D., McLachlan, A., Sallans, L., Limbach, P. A., Frankel, L. K., and Bricker, T. M. (2005). Association of the 17-kDa extrinsic protein with Photosystem II in higher plants. *Biochemistry* 44, 15216–15221. doi: 10.1021/bi051704u

Mehmood, S., Allison, T. M., and Robinson, C. V. (2015). Mass spectrometry of protein complexes: from origins to applications. *Annu. Rev. Phys. Chem.* 66, 453–474. doi: 10.1146/annurev-physchem-040214-121732

Michel, H., Hunt, D. F., Shabanowitz, J., and Bennett, J. (1988). Tandem mass spectrometry reveals that three Photosystem II proteins of spinach chloroplasts contain *N*-acetyl-*O*-phosphothreonine at their NH_2 termini. *J. Biol. Chem.* 263, 1123–1130.

Michel, H. P., and Bennett, J. (1987). Identification of the phosphorylation site of an 8.3 kDa protein from photosystem II of spinach. *FEBS Lett.* 212, 103–108. doi: 10.1016/0014-5793(87)81565-X

Minagawa, J. (2011). State transitions-The molecular remodeling of photosynthetic supercomplexes that controls energy flow in the chloroplast. *Biochim. Biophys. Acta* 1807, 897–905. doi: 10.1016/j.bbabio.2010.11.005

Miura, T., Shen, J. R., Takahashi, S., Kamo, M., Nakamura, E., Ohta, H., et al. (1997). Identification of domains on the extrinsic 33-kDa protein possibly involved in electrostatic interaction with Photosystem II complex by means of chemical modification. *J. Biol. Chem.* 272, 3788–3798.

Müller, B., and Eichacker, L. A. (1999). Assembly of the D1 precursor in monomeric Photosystem II reaction center precomplexes precedes Chlorophyll *a*-triggered accumulation of Reaction Center II in barley etioplasts. *Plant Cell* 11, 2365–2377. doi: 10.1105/tpc.11.12.2365

Müller, D. R., Schindler, P., Towbin, H., Wirth, U., Voshol, H., Hoving, S., et al. (2001). Isotope tagged cross linking reagents. A new tool in mass spectrometric protein interaction analysis. *Anal. Chem.* 73, 1927–1934. doi: 10.1021/ac001379a

Mullet, J. E., and Christopher, D. A. (1994). Separate photosensory pathways coregulate blue-light/ultraviolet-A-activated *psb*D-*psb*C transcription and light-induced D2 and CP43 degradation in barley (*Hordeum vulgare*) chloroplasts. *Plant Physiol.* 104, 1119–1129. doi: 10.1104/pp.104.4.1119

Mullineaux, C. W. (2008). Phycobilisome-reaction centre interaction in cyanobacteria. *Photosynth. Res.* 95, 175–182. doi: 10.1007/s11120-007-9249-y

Mulo, P., Sakurai, I., and Aro, E.-M. (2012). Strategies for *psbA* gene expression in cyanobacteria, green algae and higher plants: from transcription to PSII repair. *Biochim. Biophys. Acta* 1817, 247–257. doi: 10.1016/j.bbabio.2011.04.011

Mulo, P., Sicora, C., and Aro, E.-M. (2009). Cyanobacterial *psbA* gene family: optimization of oxygenic photosynthesis. *Cell. Mol. Life Sci.* 66, 3697–3710. doi: 10.1007/s00018-009-0103-6

Mummadisetti, M., Frankel, L. K., Bellamy, H. D., Sallans, L., Goettert, J. S., Brylinski, M., et al. (2014). Use of protein cross-linking and radiolytic footprinting to elucidate PsbP and PsbQ interactions within higher plant Photosystem II. *Proc. Natl. Acad. Sci. U.S.A.* 111, 16178–16183. doi: 10.1073/pnas.1415165111

Murray, J. W., and Barber, J. (2007). Structural characteristics of channels and pathways in photosystem II including the identification of an oxygen channel. *J. Struct. Biol.* 159, 228–237. doi: 10.1016/j.jsb.2007.01.f016

Nagao, R., Suzuki, T., Okumura, A., Niikura, A., Iwai, M., and Dohmae, N. (2010). Topological analysis of the extrinsic PsbO, PsbP and PsbQ proteins in a green algal PSII complex by cross-linking with a water-soluble carbodiimide. *Plant Cell Physiol.* 51, 718–727. doi: 10.1093/pcp/pcq042

Nahnsen, S., Bielow, C., Reinert, K., and Kohlbacher, O. (2013). Tools for label-free peptide quantification. *Mol. Cell. Proteomics* 12, 549–556. doi: 10.1074/mcp.R112.025163

Nakamori, H., Yatabe, T., Yoon, K.-S., and Ogo, S. (2014). Purification and characterization of an oxygen-evolving photosystem II from *Leptolyngbya* sp. strain O-77. *J. Biosci. Bioeng.* 118, 119–124. doi: 10.1016/j.jbiosc.2014.01.009

Nanba, O., and Satoh, K. (1987). Isolation of a photosystem II reaction center consisting of D-1 and D-2 polypeptides and cytochrome *b*-559. *Proc. Natl. Acad. Sci. U.S.A.* 84, 109–112. doi: 10.1073/pnas.84.1.109

Naumann, B., Busch, A., Allmer, J., Ostendorf, E., Zeller, M., Kirchhoff, H., et al. (2007). Comparative quantitative proteomics to investigate the remodeling of bioenergetic pathways under iron deficiency in *Chlamydomonas reinhardtii*. *Proteomics* 7, 3964–3979. doi: 10.1002/pmic.200700407

Nickelsen, J., and Rengstl, B. (2013). Photosystem II assembly: from cyanobacteria to plants. *Annu. Rev. Plant Biol.* 64, 609–635. doi: 10.1146/annurev-arplant-050312-120124

Nickelsen, J., Rengstl, B., Stengel, A., Schottkowski, M., Soll, J., and Ankele, E. (2011). Biogenesis of the cyanobacterial thylakoid membrane system - an update. *FEMS Microbiol. Lett.* 315, 1–5. doi: 10.1111/j.1574-6968.2010.02096.x

Nixon, P. J., Michoux, F.,Yu, J., Boehm, M., and Komenda, J. (2010). Recent advances in understanding the assembly and repair of photosystem II. *Ann. Bot.* 106, 1–16. doi: 10.3389/fols.2075.07700

Nixon, P. J., Trost, J. T., and Diner, B. A. (1992). Role of the carboxy terminus of polypeptide D1 in the assembly of a functional water-oxidizing manganese cluster in Photosystem II of the cyanobacterium *Synechocystis* sp. PCC 6803: assembly requires a free carboxyl group at C-terminal position 344. *Biochemistry* 31, 10859–10871. doi: 10.1021/bi00159a029

Nowaczyk, M. M., Hebeler, R., Schlodder, E., Meyer, H. E., Warscheid, B., and Rögner, M. (2006). Psb27, a cyanobacterial lipoprotein, is involved in the repair cycle of Photosystem II. *Plant Cell* 18, 3121–3131. doi: 10.1105/tpc.106.042671

Nowaczyk, M. M., Krause, K., Mieseler, M., Sczibilanski, A., Ikeuchi, M., and Rögner, M. (2012). Deletion of *psbJ* leads to accumulation of Psb27-Psb28 photosystem II complexes in *Thermosynechococcus elongatus*. *Biochim. Biophys. Acta* 1817, 1339–1345. doi: 10.1016/j.bbabio.2012.02.017

Odom, W. R., and Bricker, T. M. (1992). Interaction of CPa-1 with the manganese-stabilizing protein of Photosystem II: identification of domains cross-linked by 1-ethyl-3-[3-(dimethylamino)propyl]carbodiimide. *Biochemistry* 31, 5616–5620. doi: 10.1021/bi00139a027

Ohnishi, N., and Murata, N. (2006). Glycinebetaine counteracts the inhibitory effects of salt stress on the degradation and synthesis of D1 protein during photoinhibition in *Synechococcus* sp. PCC 7942. *Plant Physiol.* 141, 758–765. doi: 10.1104/pp.106.076976

Ohta, H., Suzuki, T., Ueno, M., Okumura, A., Yoshihara, S., Shen, J. R., et al. (2003). Extrinsic proteins of photosystem II - An intermediate member of the PsbQ protein family in red algal PSII. *Eur. J. Biochem.* 270, 4156–4163. doi: 10.1046/j.1432-1033.2003.03810.x

Owens, G. C., and Ohad, I. (1982). Phosphorylation of *Chlamydomonas reinhardi* chloroplast membrane proteins *in vivo* and *in vitro*. *J. Cell. Biol.* 93, 712–718. doi: 10.1083/jcb.93.3.712

Owens, G. C., and Ohad, I. (1983). Changes in thylakoid polypeptide phosphorylation during membrane biogenesis in *Chlamydomonas reinhardii* y-1. *Biochim. Biophys. Acta* 722, 234–241. doi: 10.1016/0005-2728(83)90179-2

Pagliano, C., Chimirri, F., Saracco, G., Marsano, F., and Barber, J. (2011). One-step isolation and biochemical characterization of a highly active plant PSII monomeric core. *Photosynth. Res.* 108, 33–46. doi: 10.1007/s11120-011-9650-4

Pagliano, C., Nield, J., Marsano, F., Pape, T., Barera, S., Saracco, G., et al. (2014). Proteomic characterization and three-dimensional electron microscopy study of PSII-LHCII supercomplexes from higher plants. *Biochim. Biophys. Acta* 1837, 1454–1462. doi: 10.1016/j.bbabio.2013.11.004

Paramelle, D., Miralles, G., Subra, G., and Martinez, J. (2013). Chemical cross-linkers for protein structure studies by mass spectrometry. *Proteomics* 13, 438–456. doi: 10.1002/pmic.201200305

Pearson, K. M., Pannell, L. K., and Fales, H. M. (2002). Intramolecular cross-linking experiments on cytochrome c and ribonuclease A using an isotope multiplet method. *Rapid Commun. Mass Spectrom.* 16, 149–159. doi: 10.1002/rcm.554

Pesaresi, P., Pribil, M., Wunder, T., and Leister, D. (2011). Dynamics of reversible protein phosphorylation in thylakoids of flowering plants: the roles of STN7, STN8 and TAP38. *Biochim. Biophys. Acta* 1807, 887–896. doi: 10.1016/j.bbabio.2010.08.002

Petrotchenko, E. V., and Borchers, C. H. (2010). ICC-CLASS: isotopically-coded cleavable crosslinking analysis software suite. *BMC Bioinformatics* 11:64. doi: 10.1186/1471-2105-11-64

Petrotchenko, E. V., Makepeace, K. A. T., Serpa, J. J., and Borchers, C. H. (2014). Analysis of protein structure by cross-linking combined with mass spectrometry. *Methods Mol. Biol.* 1156, 447–463. doi: 10.1007/978-1-4939-0685-7_30

Petrotchenko, E. V., Serpa, J. J., and Borchers, C. H. (2011). An isotopically coded CID-cleavable biotinylated cross-linker for structural proteomics. *Mol. Cell. Proteomics* 10:M110.001420. doi: 10.1074/mcp.M110.001420.

Plöscher, M., Granvogl, B., Zoryan, M., Reisinger, V., and Eichacker, L. A. (2009). Mass spectrometric characterization of membrane integral low molecular weight proteins from photosystem II in barley etioplasts. *Proteomics* 9, 625–635. doi: 10.1002/pmic.200800337

Plöscher, M., Reisinger, V., and Eichacker, L. A. (2011). Proteomic comparison of etioplast and chloroplast protein complexes. *J. Proteomics* 74, 1256–1265. doi: 10.1016/j.jprot.2011.03.020

Pospíšil, P. (2009). Production of reactive oxygen species by photosystem II. *Biochim. Biophys. Acta* 1787, 1151–1160. doi: 10.1016/j.bbabio.2009.05.005

Promnares, K., Komenda, J., Bumba, L., Nebesarova, J., Vacha, F., and Tichy, M. (2006). Cyanobacterial small chlorophyll-binding protein ScpD (HliB) is located on the periphery of Photosystem II in the vicinity of PsbH and CP47 subunits. *J. Biol. Chem.* 281, 32705–32713. doi: 10.1074/jbc.M606360200

Puthiyaveetil, S., and Kirchhoff, H. (2013). A phosphorylation map of the photosystem II supercomplex C2S2M2. *Front. Plant Sci.* 4: 459. doi: 10.3389/fpls.2013.00459

Rabilloud, T., Chevallet, M., Luche, S., and Lelong, C. (2010). Two-dimensional gel electrophoresis in proteomics: Past, present and future. *J. Proteomics* 73, 2064–2077. doi: 10.1016/j.jprot.2010.05.016

Rappsilber, J. (2011). The beginning of a beautiful friendship: cross-linking/mass spectrometry and modelling of proteins and multi-protein complexes. *J. Struct. Biol.* 173, 530–540. doi: 10.1016/j.jsb.2010.10.014

Rast, A., Heinz, S., and Nickelsen, J. (2015). Biogenesis of thylakoid membranes. *Biochim. Biophys. Acta* 1847, 821–830. doi: 10.1016/j.bbabio.2015.01.007

Reiland, S., Messerli, G., Baerenfaller, K., Gerrits, B., Endler, A., Grossmann, J., et al. (2009). Large-scale Arabidopsis phosphoproteome profiling reveals novel chloroplast kinase substrates and phosphorylation networks. *Plant Physiol.* 150, 889–903. doi: 10.1104/pp.109.138677

Rengstl, B., Knoppová, J., Komenda, J., and Nickelsen, J. (2013). Characterization of a *Synechocystis* double mutant lacking the photosystem II assembly factors YCF48 and Sll0933. *Planta* 237, 471–480. doi: 10.1007/s00425-012-1720-0

Rexroth, S., Wong, C. C. L., Park, J. H., Yates, J. R. III, and Barry, B. A. (2007). An activated glutamate residue identified in Photosystem II at the interface between the manganese-stabilizing subunit and the D2 polypeptide. *J. Biol. Chem.* 282, 27802–27809. doi: 10.1074/jbc.M704394200

Rinalducci, S., Larsen, M. R., Mohammed, S., and Zolla, L. (2006). Novel protein phosphorylation site identification in spinach stroma membranes by titanium dioxide microcolumns and tandem mass spectrometry. *J. Proteome Res.* 5, 973–982. doi: 10.1021/pr050476n

Rinner, O., Seebacher, J., Walzthoeni, T., Mueller, L., Beck, M., Schmidt, A., et al. (2008). Identification of cross-linked peptides from large sequence databases. *Nat. Methods* 5, 315–318. doi: 10.1038/NMETH.1192

Rintamäki, E., Salonen, M., Suoranta, U. M., Carlberg, I., Andersson, B., and Aro, E.-M. (1997). Phosphorylation of Light-harvesting Complex II and Photosystem II core proteins shows different irradiance-dependent regulation *in vivo*: application of phosphothreonine antibodies to analysis of thylakoid phosphoproteins. *J. Biol. Chem.* 272, 30476–30482. doi: 10.1074/jbc.272.48.30476

Rokka, A., Suorsa, M., Saleem, A., Battchikova, N., and Aro, E. M. (2005). Synthesis and assembly of thylakoid protein complexes: multiple assembly steps of photosystem II. *Biochem. J.* 388, 159–168. doi: 10.1042/BJ20042098

Romanowska, E., Wasilewska, W., Fristedt, R., Vener, A. V., and Zienkiewicz, M. (2012). Phosphorylation of PSII proteins in maize thylakoids in the presence of Pb ions. *J. Plant Physiol.* 169, 345–352. doi: 10.1016/j.jplph.2011.10.006

Roose, J. L., Kashino, Y., and Pakrasi, H. B. (2007). The PsbQ protein defines cyanobacterial Photosystem II complexes with highest activity and stability. *Proc. Natl. Acad. Sci. U.S.A.* 104, 2548–2553. doi: 10.1073/pnas.0609337104

Roose, J. L., and Pakrasi, H. B. (2004). Evidence that D1 processing is required for manganese binding and extrinsic protein assembly into Photosystem II. *J. Biol. Chem.* 279, 45417–45422. doi: 10.1074/jbc.M408458200

Roose, J. L., and Pakrasi, H. B. (2008). The Psb27 protein facilitates manganese cluster assembly in Photosystem II. *J. Biol. Chem.* 283, 4044–4050. doi: 10.1074/jbc.M708960200

Ross, P. L., Huang, Y. L. N., Marchese, J. N., Williamson, B., Parker, K., Hattan, S., et al. (2004). Multiplexed protein quantitation in *Saccharomyces cerevisiae* using amine-reactive isobaric tagging reagents. *Mol. Cell. Proteomics* 3, 1154–1169. doi: 10.1074/mcp.M400129-MCP200

Rowland, J. G., Simon, W. J., Nishiyama, Y., and Slabas, A. R. (2010). Differential proteomic analysis using iTRAQ reveals changes in thylakoids associated with Photosystem II-acquired thermotolerance in *Synechocystis* sp. PCC 6803. *Proteomics* 10, 1917–1929. doi: 10.1002/pmic.200900337

Ryan, C. M., Souda, P., Bassilian, S., Ujwal, R., Zhang, J., Abramson, J., et al. (2010). Post-translational modifications of integral membrane proteins resolved by top-down Fourier transform mass spectrometry with collisionally activated dissociation. *Mol. Cell. Proteomics* 9, 791–803. doi: 10.1074/mcp.M900516-MCP200

Samol, I., Shapiguzov, A., Ingelsson, B., Fucile, G., Crevecoeur, M., Vener, A. V., et al. (2012). Identification of a Photosystem II phosphatase involved in light acclimation in *Arabidopsis*. *Plant Cell* 24, 2596–2609. doi: 10.1105/tpc.112.095703

Sander, J., Nowaczyk, M., Buchta, J., Dau, H., Vass, I., Deák, Z., et al. (2010). Functional characterization and quantification of the alternative PsbA copies in *Thermosynechococcus elongatus* and their role in photoprotection. *J. Biol. Chem.* 285, 29851–29856. doi: 10.1074/jbc.M110.127142

Schönberg, A., and Baginsky, S. (2012). Signal integration by chloroplast phosphorylation networks: an update. *Front. Plant Sci.* 3:256. doi: 10.3389/fpls.2012.00256

Schottkowski, M., Gkalympoudis, S., Tzekova, N., Stelljes, C., Schuenemann, D., Ankele, E., et al. (2009). Interaction of the periplasmic PratA factor and the PsbA (D1) protein during biogenesis of Photosystem II in *Synechocystis* sp. PCC 6803. *J. Biol. Chem.* 284, 1813–1819. doi: 10.1074/jbc.M806116200

Seebacher, J., Mallick, P., Zhang, N., Eddes, J., Aebersold, R., and Gelb, M. H. (2006). Protein cross-linking analysis using mass spectrometry, isotope-coded cross-linkers, and integrated computational data processing. *J. Proteome Res.* 5, 2270–2282. doi: 10.1021/pr060154z

Seidler, A. (1996). Intermolecular and intramolecular interactions of the 33-kDa protein in photosystem II. *Eur. J. Biochem.* 242, 485–490. doi: 10.1111/j.1432-1033.1996.0485r.x

Sharma, J., Panico, M., Barber, J., and Morris, H. R. (1997a). Characterization of the low molecular weight photosystem II reaction center subunits and their light-induced modifications by mass spectrometry. *J. Biol. Chem.* 272, 3935–3943.

Sharma, J., Panico, M., Barber, J., and Morris, H. R. (1997b). Purification and determination of intact molecular mass by electrospray ionization mass spectrometry of the photosystem II reaction center subunits. *J. Biol. Chem.* 272, 33153–33157.

Sharma, J., Panico, M., Shipton, C. A., Nilsson, F., Morris, H. R., and Barber, J. (1997c). Primary structure characterization of the photosystem II D1 and D2 subunits. *J. Biol. Chem.* 272, 33158–33166. doi: 10.1074/jbc.272.52.33158

Shaw, J. B., Li, W., Holden, D. D., Zhang, Y., Griep-Raming, J., Fellers, R. T., et al. (2013). Complete protein characterization using top-down mass spectrometry and ultraviolet photodissociation. *J. Am. Chem. Soc.* 135, 12646–12651. doi: 10.1021/ja4029654

Shevela, D., and Messinger, J. (2013). Studying the oxidation of water to molecular oxygen in photosynthetic and artificial systems by time-resolved membrane-inlet mass spectrometry. *Front. Plant Sci.* 4:473. doi: 10.3389/fpls.2013.00473

Shi, L.-X., Hall, M., Funk, C., and Schröder, W. (2012). Photosystem II, a growing complex: updates on newly discovered components and low molecular mass proteins. *Biochim. Biophys. Acta* 1817, 13–25. doi: 10.1016/j.bbabio.2011.08.008

Shi, L.-X., Lorković, Z. J., Oelmüller, R., and Schröder, W. P. (2000). The low molecular mass PsbW protein is involved in the stabilization of the dimeric Photosystem II complex in *Arabidopsis thaliana*. *J. Biol. Chem.* 275, 37945–37950. doi: 10.1074/jbc.M006300200

Shi, L.-X., and Schröder, W. P. (1997). Compositional and topological studies of the PsbW protein in spinach thylakoid membrane. *Photosynth. Res.* 53, 45–53. doi: 10.1023/A:1005830405809

Silva, J. C., Gorenstein, M. V., Li, G. Z., Vissers, J. P. C., and Geromanos, S. J. (2006). Absolute quantification of proteins by LCMS^{E} - A virtue of parallel MS acquisition. *Mol. Cell. Proteomics* 5, 144–156. doi: 10.1074/mcp.M500230-MCP200

Sinz, A. (2014). The advancement of chemical cross-linking and mass spectrometry for structural proteomics: from single proteins to protein interaction networks. *Expert Rev. Proteomics* 11, 733–743. doi: 10.1586/14789450.2014.960852

Stöckel, J., Jacobs, J. M., Elvitigala, T. R., Liberton, M., Welsh, E. A., Polpitiya, A. D., et al. (2011). Diurnal rhythms result in significant changes in the cellular protein complement in the cyanobacterium *Cyanothece* 51142. *PLoS ONE* 6:e16680. doi: 10.1371/journal.pone.0016680

Steinback, K. E., Bose, S., and Kyle, D. J. (1982). Phosphorylation of the light-harvesting chlorophyll-protein regulates excitation energy distribution between Photosystem II and Photosystem I. *Arch. Biochem. Biophys.* 216, 356–361. doi: 10.1016/0003-9861(82)90221-1

Sugimoto, I., and Takahashi, Y. (2003). Evidence that the PsbK polypeptide is associated with the Photosystem II core antenna complex CP43. *J. Biol. Chem.* 278, 45004–45010. doi: 10.1074/jbc.M307537200

Sugiura, M., and Boussac, A. (2014). Some Photosystem II properties depending on the D1 protein variants in Thermosynechococcus elongatus. *Biochim. Biophys. Acta* 1837, 1427–1434. doi: 10.1016/j.bbabio.2013.12.011

Sugiura, M., Iwai, E., Hayashi, H., and Boussac, A. (2010a). Differences in the interactions between the subunits of Photosystem II dependent on D1 protein variants in the thermophilic cyanobacterium *Thermosynechococcus elongatus*. *J. Biol. Chem.* 285, 30008–30018. doi: 10.1074/jbc.M110.136945

Sugiura, M., Kato, Y., Takahashi, R., Suzuki, H., Watanabe, T., Noguchi, T., et al. (2010b). Energetics in Photosystem II from *Thermosynechococcus elongatus* with a D1 protein encoded by either the $psbA_1$ or $psbA_3$ gene. *Biochim. Biophys. Acta* 1797, 1491–1499. doi: 10.1016/j.bbabio.2010.03.022

Sugiura, M., Koyama, K., Umena, Y., Kawakami, K., Shen, J.-R., Kamiya, N., et al. (2013). Evidence for an unprecedented histidine hydroxyl modification on D2-His336 in Photosystem II of *Thermosynechoccocus vulcanus* and *Thermosynechoccocus elongatus*. *Biochemistry* 52, 9426–9431. doi: 10.1021/bi401213m

Sugiyama, N., Nakagami, H., Mochida, K., Daudi, A., Tomita, M., Shirasu, K., et al. (2008). Large-scale phosphorylation mapping reveals the extent of tyrosine phosphorylation in *Arabidopsis*. *Mol. Syst. Biol.* 4, 193. doi: 10.1038/msb.2008.32

Swaisgood, H., and Natake, M. (1973). Effect of carboxyl group modification on some of the enzymatic properties of L-glutamate dehydrogenase. *J. Biochem.* 74, 77–86.

Takahashi, M., Shiraishi, T., and Asada, K. (1988). COOH-terminal residues of D1 and the 44 kDa CPa-2 at spinach photosystem II core complex. *FEBS Lett.* 240, 6–8. doi: 10.1016/0014-5793(88)80330-2

Takamoto, K., and Chance, M. R. (2006). Radiolytic protein footprinting with mass spectrometry to probe the structure of macromolecular complexes. *Annu. Rev. Biophys. Biomol. Struct.* 35, 251–276. doi: 10.1146/annurev.biophys.35.040405.102050

Takasaka, K., Iwai, M., Umena, Y., Kawakami, K., Ohmori, Y., Ikeuchi, M., et al. (2010). Structural and functional studies on Ycf12 (Psb30) and PsbZ-deletion mutants from a thermophilic cyanobacterium. *Biochim. Biophys. Acta* 1797, 278–284. doi: 10.1016/j.bbabio.2009.11.001

Tal, O., Trabelcy, B., Gerchman, Y., and Adir, N. (2014). Investigation of phycobilisome subunit interaction interfaces by coupled cross-linking and mass spectrometry. *J. Biol. Chem.* 289, 33084–33097. doi: 10.1074/jbc.M114.595942

Telfer, A., Bishop, S. M., Phillips, D., and Barber, J. (1994). Isolated photosynthetic reaction center of Photosystem II as a sensitizer for the formation of singlet oxygen: detection and quantum yield determination using a chemical trapping technique. *J. Biol. Chem.* 269, 13244–13253.

Thangaraj, B., Ryan, C. M., Souda, P., Krause, K., Faull, K. F., Weber, A. P. M., et al. (2010). Data-directed top-down Fourier-transform mass spectrometry of a large integral membrane protein complex: Photosystem II from *Galdieria sulphuraria*. *Proteomics* 10, 3644–3656. doi: 10.1002/pmic.201000190

Thelen, J. J., and Peck, S. C. (2007). Quantitative proteomics in plants: choices in abundance. *Plant Cell* 19, 3339–3346. doi: 10.1105/tpc.107.053991

Thidholm, E., Lindström, V., Tissier, C., Robinson, C., Schröder, W. P., and Funk, C. (2002). Novel approach reveals localisation and assembly pathway of the PsbS and PsbW proteins into the photosystem II dimer. *FEBS Lett.* 513, 217–222. doi: 10.1016/S0014-5793(02)02314-1

Thompson, A., Schäfer, J., Kuhn, K., Kienle, S., Schwarz, J., Schmidt, G., et al. (2003). Tandem mass tags: a novel quantification strategy for comparative analysis of complex protein mixtures by MS/MS. *Anal. Chem.* 75, 1895–1904. doi: 10.1021/ac0262560

Thornton, L. E., Ohkawa, H., Roose, J. L., Kashino, Y., Keren, N., and Pakrasi, H. B. (2004). Homologs of plant PsbP and PsbQ proteins are necessary for regulation of Photosystem II activity in the cyanobacterium *Synechopystis* 6803. *Plant Cell* 16, 2164–2175. doi: 10.1105/tpc.104.023515

Tikhonov, A. N. (2015). Induction events and short-term regulation of electron transport in chloroplasts: an overview. *Photosynth. Res.* 125, 65–94. doi: 10.1007/s11120-015-0094-0

Tikkanen, M., and Aro, E.-M. (2014). Integrative regulatory network of plant thylakoid energy transduction. *Trends Plant Sci.* 19, 10–17. doi: 10.1016/j.tplants.2013.09.003

Tikkanen, M., Grieco, M., Kangasjarvi, S., and Aro, E.-M. (2010). Thylakoid protein phosphorylation in higher plant chloroplasts optimizes electron transfer under fluctuating light. *Plant Physiol.* 152, 723–735. doi: 10.1104/pp.109.150250

Tikkanen, M., Nurmi, M., Kangasjarvi, S., and Aro, E.-M. (2008a). Core protein phosphorylation facilitates the repair of photodamaged photosystem II at high light. *Biochim. Biophys. Acta* 1777, 1432–1437. doi: 10.1016/j.bbabio.2008.08.004

Tikkanen, M., Nurmi, M., Suorsa, M., Danielsson, R., Mamedov, F., Styring, S., et al. (2008b). Phosphorylation-dependent regulation of excitation energy distribution between the two photosystems in higher plants. *Biochim. Biophys. Acta* 1777, 425–432. doi: 10.1016/j.bbabio.2008.02.001

Tomo, T., Enami, I., and Satoh, K. (1993). Orientation and nearest-neighbor analysis of *psb*I gene product in the photosystem II reaction center complex using bifunctional cross-linkers. *FEBS Lett.* 323, 15–18. doi: 10.1016/0014-5793(93)81438-6

Tsiotis, G., Walz, T., Spyridaki, A., Lustig, A., Engel, A., and Ghanotakis, D. (1996). Tubular crystals of a Photosystem II core complex. *J. Mol. Biol.* 259, 241–248. doi: 10.1006/jmbi.1996.0316

Turkina, M. V., Kargul, J., Blanco-Rivero, A., Villarejo, A., Barber, J., and Vener, A. V. (2006). Environmentally modulated phosphoproteome of photosynthetic membranes in the green alga *Chlamydomonas reinhardtii*. *Mol. Cell Proteomics* 5, 1412–1425. doi: 10.1074/mcp.M600066-MCP200

Tyystjärvi, E. (2013). Photoinhibition of Photosystem II. *Int. Rev. Cell. Mol. Biol.* 300, 243–303. doi: 10.1016/B978-0-12-405210-9.00007-2

Ujihara, T., Sakurai, I., Mizusawa, N., and Wada, H. (2008). A method for analyzing lipid-modified proteins with mass spectrometry. *Anal. Biochem.* 374, 429–431. doi: 10.1016/j.ab.2007.11.014

Umena, Y., Kawakami, K., Shen, J., and Kamiya, N. (2011). Crystal structure of oxygen-evolving photosystem II at a resolution of 1.9 Å. *Nature* 473, 55–60. doi: 10.1038/nature09913

Vainonen, J. P., Hansson, M., and Vener, A. V. (2005). STN8 protein kinase in *Arabidopsis thaliana* is specific in phosphorylation of Photosystem II core proteins. *J. Biol. Chem.* 280, 33679–33686. doi: 10.1074/jbc.M505729200

Vassiliev, S., Zaraiskaya, T., and Bruce, D. (2012). Exploring the energetics of water permeation in photosystem II by multiple steered molecular dynamics simulations. *Biochim. Biophys. Acta* 1817, 1671–1678. doi: 10.1016/j.bbabio.2012.05.016

Vener, A. V. (2007). Environmentally modulated phosphorylation and dynamics of proteins in photosynthetic membranes. *Biochim. Biophys. Acta* 1767, 449–457. doi: 10.1016/j.bbabio.2007.11.007

Vener, A. V., Harms, A., Sussman, M. R., and Vierstra, R. D. (2001). Mass spectrometric resolution of reversible protein phosphorylation in photosynthetic membranes of *Arabidopsis thaliana*. *J. Biol. Chem.* 276, 6959–6966. doi: 10.1074/jbc.M009394200

Walleczek, J., Martin, T., Redl, B., Stofflermeilicke, M., and Stoffler, G. (1989). Comparative cross-linking study on the 50S ribosomal subunit from *Escherichia coli*. *Biochemistry* 28, 4099–4105. doi: 10.1021/bi00435a071

Wang, L. W., and Chance, M. R. (2011). Structural mass spectrometry of proteins using hydroxyl radical based protein footprinting. *Anal. Chem.* 83, 7234–7241. doi: 10.1021/ac200567u

Wegener, K. M., Bennewitz, S., Oelmüller, R., and Pakrasi, H. B. (2011). The Psb32 protein aids in repairing photodamaged Photosystem II in the cyanobacterium *Synechocystis* 6803. *Mol. Plant* 4, 1052–1061. doi: 10.1104/pp.114.253336

Wegener, K. M., Nagarajan, A., and Pakrasi, H. B. (2015). An atypical *psbA* gene encodes a sentinel D1 protein to form a physiologically relevant inactive Photosystem II complex in cyanobacteria. *J. Biol. Chem.* 290, 3764–3774. doi: 10.1074/jbc.M114.604124

Wegener, K. M., Welsh, E. A., Thornton, L. E., Keren, N., Jacobs, J. M., Hixson, K. K., et al. (2008). High sensitivity proteomics assisted discovery of a novel operon involved in the assembly of Photosystem II, a membrane protein complex. *J. Biol. Chem.* 283, 27829–27837. doi: 10.1074/jbc.M803918200

Weisbrod, C. R., Chavez, J. D., Eng, J. K., Yang, L., Zheng, C., and Bruce, J. E. (2013). *In vivo* protein interaction network identified with a novel real-time cross-linked peptide identification strategy. *J. Proteome Res.* 12, 1569–1579. doi: 10.1021/pr3011638

Welkie, D., Zhang, X., Markillie, M. L., Taylor, R., Orr, G., Jacobs, J., et al. (2014). Transcriptomic and proteomic dynamics in the metabolism of a diazotrophic cyanobacterium, *Cyanothece* sp. PCC 7822 during a diurnal light-dark cycle. *BMC Genomics* 15:1185. doi: 10.1186/1471-2164-15-1185

Wen, J. Z., Zhang, H., Gross, M. L., and Blankenship, R. E. (2009). Membrane orientation of the FMO antenna protein from *Chlorobaculum tepidum* as determined by mass spectrometry-based footprinting. *Proc. Natl. Acad. Sci. U.S.A.* 106, 6134–6139. doi: 10.1073/pnas.0901691106

Wetz, K., and Habermehl, K.-O. (1979). Topographical studies on poliovirus capsid proteins by chemical modification and cross-linking with bifunctional reagents. *J. Gen. Virol.* 44, 525–534. doi: 10.1099/0022-1317-44-2-525

Whitelegge, J. P. (2013). Integral membrane proteins and bilayer proteomics. *Anal. Chem.* 85, 2558–2568. doi: 10.1021/ac303064a

Whitelegge, J. P., Gundersen, C. B., and Faull, K. F. (1998). Electrospray-ionization mass spectrometry of intact intrinsic membrane proteins. *Protein Sci.* 7, 1423–1430.

Xu, H., and Freitas, M. A. (2009). MassMatrix: a database search program for rapid characterization of proteins and peptides from tandem mass spectrometry data. *Proteomics* 9, 1548–1555. doi: 10.1002/pmic.200700322

Yang, B., Wu, Y.-J., Zhu, M., Fan, S.-B., Lin, J., Zhang, K., et al. (2012). Identification of cross-linked peptides from complex samples. *Nat. Methods* 9, 904–909. doi: 10.1038/nmeth.2099

Yang, M.-K., Yang, Y.-H., Chen, Z., Zhang, J., Lin, Y., Wang, Y., et al. (2014). Proteogenomic analysis and global discovery of posttranslational modifications in prokaryotes. *Proc. Natl. Acad. Sci. U.S.A.* 111, E5633–E5642. doi: 10.1073/pnas.1412722111

Yao, D. C. I., Brune, D. C., Vavilin, D., and Vermaas, W. F. J. (2012a). Photosystem II component lifetimes in the cyanobacterium *Synechocystis* sp. strain PCC 6803: Small Cab-like proteins stabilize biosynthesis intermediates and affect early steps in chlorophyll synthesis. *J. Biol. Chem.* 287, 682–692. doi: 10.1074/jbc.M111.320994

Yao, D. C. I., Brune, D. C., and Vermaas, W. F. J. (2012b). Lifetimes of photosystem I and II proteins in the cyanobacterium *Synechocystis* sp. PCC 6803. *FEBS Lett.* 586, 169–173. doi: 10.1016/j.febslet.2011.12.010

Zak, E., Norling, B., Maitra, R., Huang, F., Andersson, B., and Pakrasi, H. B. (2001). The initial steps of biogenesis of cyanobacterial photosystems occur in plasma membranes. *Proc. Natl. Acad. Sci. U.S.A.* 98, 13443–13448. doi: 10.1073/pnas.241503898

Zhang, H., Liu, H., Blankenship, R. E., and Gross, M. L. (2016). Isotope-encoded carboxyl group footprinting for mass spectrometry-based protein conformational studies. *J. Am. Soc. Mass Spectrom.* 27, 178–181. doi: 10.1007/s13361-015-1260-5

Zhang, H., Liu, H., Niedzwiedzki, D. M., Prado, M., Jiang, J., Gross, M. L., et al. (2014). Molecular mechanism of photoactivation and structural location of the cyanobacterial orange carotenoid protein. *Biochemistry* 53, 13–19. doi: 10.1021/bi401539w

Zheleva, D., Sharma, J., Panico, M., Morris, H. R., and Barber, J. (1998). Isolation and characterization of monomeric and dimeric CP47-reaction center Photosystem II complexes. *J. Biol. Chem.* 273, 16122–16127. doi: 10.1074/jbc.273.26.16122

Conflict of Interest Statement: The authors declare that the research was conducted in the absence of any commercial or financial relationships that could be construed as a potential conflict of interest.

frontiers in Plant Science

ORIGINAL RESEARCH
published: 21 June 2016
doi: 10.3389/fpls.2016.00844

Testing the Role of the N-Terminal Tail of D1 in the Maintenance of Photosystem II in Tobacco Chloroplasts

Franck Michoux[1†], Niaz Ahmad[1†], Zheng-Yi Wei[1†], Erica Belgio[2†], Alexander V. Ruban[2] and Peter J. Nixon[1]*

[1] Sir Ernst Chain Building-Wolfson Laboratories, Department of Life Sciences, Imperial College London, London, UK, [2] School of Biological and Chemical Sciences, Queen Mary University of London, London, UK

A key step in the repair of photoinactivated oxygen-evolving photosystem II (PSII) complexes is the selective recognition and degradation of the damaged PSII subunit, usually the D1 reaction center subunit. FtsH proteases play a major role in D1 degradation in both cyanobacteria and chloroplasts. In the case of the cyanobacterium *Synechocystis* sp. PCC 6803, analysis of an N-terminal truncation mutant of D1 lacking 20 amino-acid residues has provided evidence that FtsH complexes can remove damaged D1 in a processive reaction initiated at the exposed N-terminal tail. To test the importance of the N-terminal D1 tail in higher plants, we have constructed the equivalent truncation mutant in tobacco using chloroplast transformation techniques. The resulting mutant grew poorly and only accumulated about 25% of wild-type levels of PSII in young leaves which declined as the leaves grew so that there was little PSII activity in mature leaves. Truncating D1 led to the loss of PSII supercomplexes and dimeric complexes in the membrane. Extensive and rapid non-photochemical quenching (NPQ) was still induced in the mutant, supporting the conclusion that PSII complexes are not required for NPQ. Analysis of leaves exposed to high light indicated that PSII repair in the truncation mutant was impaired at the level of synthesis and/or assembly of PSII but that D1 could still be degraded. These data support the idea that tobacco plants possess a number of back-up and compensatory pathways for removal of damaged D1 upon severe light stress.

Keywords: photosystem II, photoinhibition, PSII repair, chloroplast transformation, d1, D1 degradation

OPEN ACCESS

Edited by:
Julian Eaton-Rye, University of Otago, New Zealand

Reviewed by:
Byung-Ho Kang, Chinese University of Hong Kong, Hong Kong
Wataru Sakamoto, Okayama University, Japan

***Correspondence:**
Peter J. Nixon
p.nixon@imperial.ac.uk

***Present Address:**
Franck Michoux, Alkion Biopharma SAS, Evry, France;
Niaz Ahmad, Agricultural Biotechnology Division, National Institute for Biotechnology and Genetic Engineering, Faisalabad, Pakistan;
Zheng-Yi Wei, Laboratory of Plant Bioreactor and Genetics Engineering, Agro-Biotechnology Research Institute and Jilin Provincial Key Laboratory of Agricultural Biotechnology, Jilin Academy of Agricultural Science, Changchun, China
Erica Belgio, Institute of Microbiology, Academy of Sciences of the Czech Republic, Třeboň, Czech Republic

Specialty section:
This article was submitted to Plant Cell Biology, a section of the journal Frontiers in Plant Science

Received: *27 January 2016*
Accepted: *30 May 2016*
Published: *21 June 2016*

Citation:
Michoux F, Ahmad N, Wei Z-Y, Belgio E, Ruban AV and Nixon PJ (2016) Testing the Role of the N-Terminal Tail of D1 in the Maintenance of Photosystem II in Tobacco Chloroplasts. Front. Plant Sci. 7:844. doi: 10.3389/fpls.2016.00844

INTRODUCTION

The multisubunit oxygen-evolving photosystem II (PSII) complex of the thylakoid membrane is susceptible to irreversible damage by light and is considered a weak link in the light reactions of photosynthesis (reviewed by Vass, 2012). PSII activity is maintained through the operation of a PSII repair cycle in which inactivated PSII complexes are partially disassembled and irreversibly damaged PSII subunits, notably the D1 reaction center subunit, are degraded and replaced by newly synthesized subunits; followed by reactivation of PSII activity through light-driven assembly of the inorganic Mn_4CaO_5 cluster involved in water oxidation (reviewed by Komenda et al., 2012).

Degradation of photodamaged D1 in the cyanobacterium *Synechocystis* sp. PCC 6803 (hereafter *Synechocystis* 6803) is mediated predominantly by a hexameric FtsH heterocomplex consisting of the FtsH2 and FtsH3 subunits (Silva et al., 2003; Komenda et al., 2006; Boehm et al., 2012). Previous studies on *Escherichia coli* FtsH have concluded that FtsH-catalyzed degradation of membrane proteins is a highly processive reaction usually initiated at the N- or C-terminal tail of a target protein (Chiba et al., 2000, 2002), with efficient degradation at the N-terminus requiring a tail of at least 20 amino-acid residues (Chiba et al., 2000). The observation that shortening the N-terminal tail of D1 to just 12 residues in *Synechocystis* 6803 inhibited D1 degradation during PSII repair provided important evidence that the main pathway for FtsH-mediated proteolysis of damaged D1 proceeded from the N-terminus (Komenda et al., 2007).

Given that FtsH complexes have also been assigned a major role in D1 degradation in chloroplasts (Bailey et al., 2002; Kato et al., 2012), processive N-terminal D1 degradation has likewise been considered a possible mechanism (Nixon et al., 2005; Komenda et al., 2007). Here we have begun to test this hypothesis by using chloroplast transformation technology to generate a tobacco mutant lacking 20 amino-acid residues at the N-terminus of D1. In contrast to the equivalent cyanobacterial mutant, we observe a substantial decrease in PSII accumulation in the mutant. However, D1 could still be degraded in the mutant upon exposure to high light, consistent with the current view that higher plant chloroplasts are able to efficiently remove damaged D1 via multiple pathways depending on the environmental and cellular context.

MATERIALS AND METHODS

Growth of Plants

Seeds of *Nicotiana tabacum* (cv Petit Havana) were germinated in magenta boxes on Murashige and Skoog (MS) medium containing 8 g L^{-1} agar and 30 g L^{-1} sucrose as described by Ahmad et al. (2012) and plants grown at 25°C, under a day/night cycle of 16 h light/8 h dark, a photon flux density of 50 μmol photons m^{-2} s^{-1} supplied by white fluorescent bulbs and 30% humidity. After 3 or 4 weeks, plants were transferred from MS medium to plastic pots filled with Levington F2 + S seed and modular compost pH 5.3–5.7 (www.scotts.com) supplemented with medium sized Vermiculite pH 6.0 (2–5 mm, density 100 kgm^{-3}) (Sinclair, UK) at a ratio of 4:1 and then grown in a greenhouse at 25/20°C (day/night) in a 16 h photoperiod at a photosynthetic photon flux of 120 μmol photons m^{-2} s^{-1} and 40% humidity. The same procedure was adopted for the regeneration of transplastomic mutant plants except that the MS medium contained spectinomycin.

Generation of Transforming Plasmids

Total genomic DNA was extracted from tobacco leaves using a DNeasy Plant Mini Kit (PEQLAB, Germany) following the manufacturer's protocol. The transforming plasmid was constructed in four steps using the primers described in **Table 1**: (1) PCR was performed to amplify a 3-kb genomic fragment between *trnH* and *trnK* (with primers 1 and 2), which was cloned into pGEMT-easy vector (Promega, UK); (2) the *aadA* spectinomycin-resistance cassette was amplified by PCR (using primers 3 and 4) from a modified version of the pHK40 plasmid (Kuroda and Maliga, 2001) in which the tobacco *psbA* promoter from the original pHK40 cassette was replaced by a coffee Prrn16S promoter linked to a T7g10 5′UTR (Michoux, 2008). This modification was performed to avoid any unwanted homologous recombination–mediated rearrangements between the chloroplast transformation vector and the tobacco chloroplast *psbA* or *Prrn* 16S RNA. Construction details are described in Michoux (2008) and are available on request; (3) the amplified *aadA* cassette was inserted into the unique BglII restriction site located at the start of the *psbA* promoter, which had been blunted using Mung Bean nuclease (NEB, UK); (4) the wild-type (WT) BssHII/MfeI fragment encompassing part of the *aadA* and *psbA* genes was replaced by a mutated version lacking 20 codons of *psbA* and now containing a unique NdeI site, generated by overlap extension PCR using primers 5, 6, 7, and 8 (see **Table 1** for sequence information). Amplification reactions were performed using Phusion DNA polymerase (Finnzymes, Finland) and the final vector was sequenced to ensure no unwanted DNA mutations have been introduced during the cloning process.

Generation of Tobacco Transplastomic Mutants

Plastid transformation was performed using the biolistic protocol described by Svab and Maliga (1993). The transformation vector was immobilized onto 550 nm gold particles following the manufacturer's protocol (Seashell Technology, USA). Young leaves of aseptically grown *N. tabacum* were bombarded under sterile conditions on RMOP medium (Svab and Maliga, 1993) using a biolistic device (Bio-Rad Laboratories, UK). Bombarded leaves were then kept in the dark for 48 h at room temperature, before being cut into small pieces and placed on RMOP plates containing spectinomycin (500 mg L^{-1}) for regeneration and selection of transformants.

Evaluation of Homoplastomy

After three (03) rounds of selection and regeneration on spectinomycin-containing medium, the putative transformed lines were transferred to compost to evaluate homoplastomy by Southern hybridization using a *psbA*-specific probe and the methods described previously (Ahmad et al., 2012).

Protein Extraction, Gel Electrophoresis, and Immunoblotting

Isolation of thylakoid membrane proteins, quantification of chlorophyll, SDS-PAGE, and Blue-native PAGE (BN-PAGE) were performed as described in Ahmad et al. (2012). Anti-peptide antibodies specific for the C-terminal region of D1 and D2 and antibodies specific for CP43, CP47, and PsaD (Komenda et al., 2007) plus NdhI (Burrows et al., 1998) were used in immunoblotting experiments as described by Ahmad et al. (2012). For relative quantification of D1, signal intensities obtained using ImageJ for 25, 50, and 100% of the untreated sample were used to generate a standard curve (Abramoff

TABLE 1 | Sequence of primers used during PCR reactions.

Primer	Sequence (5′-3′)	Location
1. B19	AAATCGAATTAAATTCTTCGTTTTTACAAA	27 bp after *trnH*
2. B03	GGGTATCGAACTTCTTAATTGCA	449 bp from end of *matK*
3. aadA-AclI-F	ATCCAACGTTATCGATTTGCTCCCTCAATGAGAATGGAT	5′ start of Prrn16S promoter
4. aadA-AclI-R	TAGAAACGTTACTAGTGGATCGCACTCTACCGATTGA	3′ end of 3′ UTR *rbcL*
5. aadA-BssHII	AGCTAGACAGGCTTATCTTGGACAAGAAGA	116 bp before 3′ end of *aadA* gene
6.PsbA-A20-NdeI-F	AAGATTTTCATATGACTAGCACTGAAAACCGTCTTTACATTGGA	Start codon of *psbA*. New NdeI site shown as underlined
7.PsbA-A20-NdeI-R	TCCAATGTAAAGACGGTTTTCAGTGCTAGTCATATGAAAATCTT	Start codon of *psbA*. New NdeI site shown as underlined
8. PsbA-MfeI	TCCTAGAGGCATACCATCAGAAAAACTTCCT	525 bp after 5′ start of *psbA*

et al., 2004). The signal intensities of treated samples were then calculated as a percentage value (of the untreated sample) using this standard curve.

Fluorescence Measurements

For all low temperature fluorescence measurements, leaf homogenates were carefully prepared and diluted to avoid reabsorption (Weis, 1985) in 10 mM Hepes buffer, pH 7.6. Low-temperature (77 K) fluorescence emission spectra were recorded on a Jobin Yvon FluoroMax-3 spectrophotometer equipped with a liquid-nitrogen cooled cryostat. Excitation was defined at 435 nm with a 5-nm spectral bandwidth. The fluorescence spectral resolution was kept at 1 nm. Spectra were normalized at their absolute maximum. The spectral manipulations were performed using GRAMS/AI software (Thermo Fisher Scientific Inc., Waltham, USA).

Chlorophyll fluorescence induction was performed with a DUAL PAM 100 chlorophyll fluorometer (Heinz Walz, Effeltrich, Germany). Plants were adapted in the dark for 30 min before the measurements. Actinic illumination of 100 and 700 μmol photons m^{-2} s^{-1}, respectively (see the Results Section), was provided by arrays of 635-nm LEDs illuminating both the adaxial and abaxial surfaces of the leaf. The F_o (the fluorescence level with open PSII reaction centers) was excited by a measuring beam of 10 μmol photons m^{-2} s^{-1}. Maximum fluorescence at the level of all closed reaction centers (F_m) was determined by using a 0.8 s saturating light pulse (10,000 μmol photons m^{-2} s^{-1}). The quantum yield of PSII (F_v/F_m) was calculated as $[(F_m - F_o)/F_m]$ and NPQ as $[(F_m - F'_m)/F'_m]$, where F'_m is the maximum fluorescence level attained at the end of actinic light illumination. *qP* was calculated as $[(F'_m - F_s)/F_o]$, where F_s is the steady-state fluorescence level at the end of actinic light illumination.

Time-resolved fluorescence spectroscopy was performed using a time-correlated single photon counting (TCSPC) principle on a FluoTime 200 fluorometer (PicoQuant, Berlin, Germany). Detached leaves were vacuum-infiltrated with 50 mM nigericin to completely inhibit NPQ. Excitation at a 10 MHz repetition rate was provided by a 470 nm laser diode, which was carefully adjusted to completely close all PSII reaction centers without causing photoinhibitory quenching of F_m, and to be far below the onset of singlet-singlet exciton annihilation. Fluorescence was detected at 682 nm on leaves with a 2-nm slit width. The instrumental response function was in the range of 50 ps. For lifetime analysis, FluoFit software (PicoQuant, Berlin, Germany) was used. The quality of the fits was judged by the χ^2 parameter.

Transmission Electron Microscopy

Leaf samples obtained from plants growing on sucrose-containing medium were fixed in 2% glutaraldehyde in 0.1 M sodium cacodylate buffer pH 7.2, post-fixed in 1% osmium tetroxide in the same buffer then embedded in epoxy resin. Ultrathin sections were cut and stained with uranyl acetate followed by lead citrate before observation at 120 kV in a FEI Tecnai T12 transmission electron microscope.

High-Light Stress Experiments

Leaves of mutant and WT plants grown in the greenhouse were placed in darkness overnight, floating in the presence of H_2O or 5 mM lincomycin in individual petri dishes, with the petiole immersed. The leaves were then exposed to fluorescent light of 1000 μmol photons m^{-2} s^{-1} for up to 4 h, before incubating overnight at 30 μmol photons m^{-2} s^{-1} to test for recovery.

RESULTS

Construction of Tobacco D1 Mutants with Truncated N-Terminal Tail

Previous work has shown that deletion of 20 amino-acid residues from the N-terminal tail of the D1 subunit of the cyanobacterium *Synechocystis* 6803, leaving a predicted tail of 12 residues rather than 32 found in WT, still permitted accumulation of oxygen-evolving complexes. Importantly this *Synechocystis* 6803 mutant (termed A20) was severely impaired in the degradation of D1 during PSII repair. To test whether a similar phenotype would be observed in higher plants, we used chloroplast transformation technology to generate the equivalent mutant in tobacco in which residues D1-T2 to D1-I21, inclusive, were deleted (**Figure 1A**). Two independent lines, designated A20-G and A20-H, were recovered. Southern blotting indicated that the mutants were homoplastomic (**Figure 1B**) and immunoblotting experiments confirmed that the D1 protein had a higher electrophoretic mobility in denaturing gels consistent with its smaller size (**Figure 1C**).

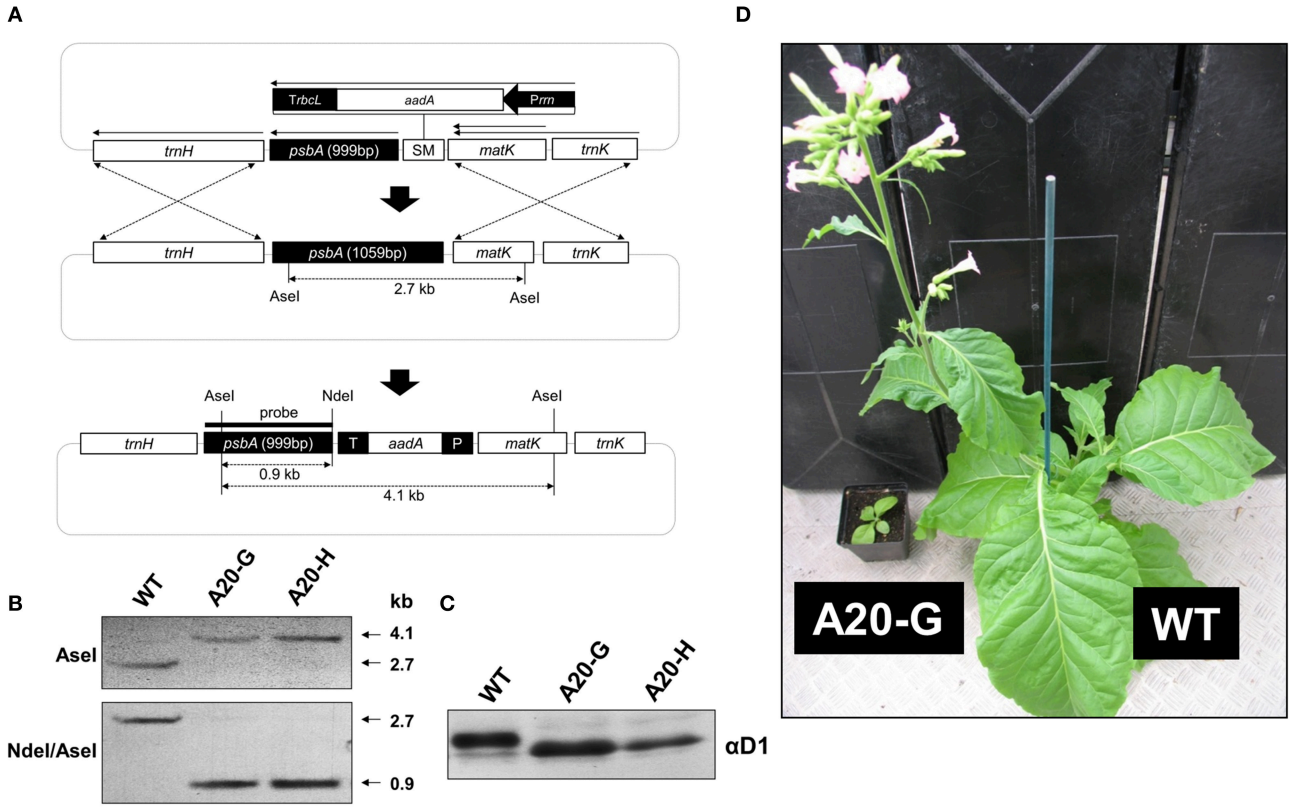

FIGURE 1 | Construction of tobacco D1 truncation mutants. (A) Structure of shooting vector showing location of the *aadA* selectable marker (SM) upstream of the *psbA* gene and position of the *psbA* probe. **(B)** Southern hybridization analysis of WT and A20-G and A20-H lines. **(C)** Immunoblot of D1 in WT, A20-G, and A20-H thylakoid membranes carried out on sucrose-grown plants. **(D)** Growth of WT and A20-G in the greenhouse after 4 months.

Tobacco A20 Plants Accumulate Less PSII and Grow Poorly

The tobacco A20 mutants showed a clear growth defect when grown photoautotrophically on compost in the greenhouse and were unable to flower and set seed (see **Figure 1D** for a comparison of A20-G and WT). Determination of the chlorophyll fluorescence parameter (F_v/F_m) in dark-adapted leaves from 6 to 8-week-old plants revealed reduced levels of PSII activity in the A20-G mutant, chosen for further study, with the effect most clearly seen in older leaves (**Figures 2A,B**). A reduction in the levels of accumulated PSII complex was confirmed by immunoblotting using D1- and D2-specific antibodies (**Figure 2C**). On an equal chlorophyll basis the mutants only accumulated about 25% of WT levels of PSII whereas levels of photosystem I (PSI) and NADH dehydrogenase-like (NDH) complex were close to that of WT levels as deduced from the PsaD and NdhI immunoblots, respectively. In contrast, control homoplastomic plants containing the spectinomycin-resistance cassette upstream of the intact *psbA* gene contained WT levels of D1 (Supplementary Figure 1) and gave an F_v/F_m value indistinguishable from WT (data not shown). Transmission electron microscopy provided evidence that grana could still form in the A20-G mutant but that overall the thylakoid system was less organized than in the WT (Supplementary Figure 2). Analysis of 3-month-old greenhouse-grown material by BN-PAGE revealed that the A20-G mutant only accumulated monomeric PSII complexes and that the PSII-LHCII supercomplexes (PSII SCs) and dimeric PSII complexes observed in WT were undetectable (**Figure 3**). An intense chlorophyll-containing band corresponding to unassembled LHCII trimers was observed at similar levels in both mutant and WT whereas the mutant extract contained less PSI than WT based on protein staining (**Figure 3**).

Tobacco A20 Mutant Shows Enhanced Non-Photochemical Chlorophyll Fluorescence Quenching

Figure 4 shows the 77K fluorescence emission spectra of WT and A20-G leaf homogenates isolated from 3-month-old greenhouse-grown plants normalized to the PSI fluorescence band at 735 nm. The PSII emission band region at 670–700 nm of the mutant revealed strong differences to that of WT. Instead of the two typical bands at 685 and 695 nm originating from the CP43 and CP47 complexes of PSII, respectively (Andrizhiyevskaya et al., 2005), the A20-G mutant possessed one strong band around 681 nm. This emission, which is clearly defined in the A20-G-minus-WT difference spectrum (dotted line), is dominated by the LHCII antenna (Ruban and Horton, 1992). Hence, these data are

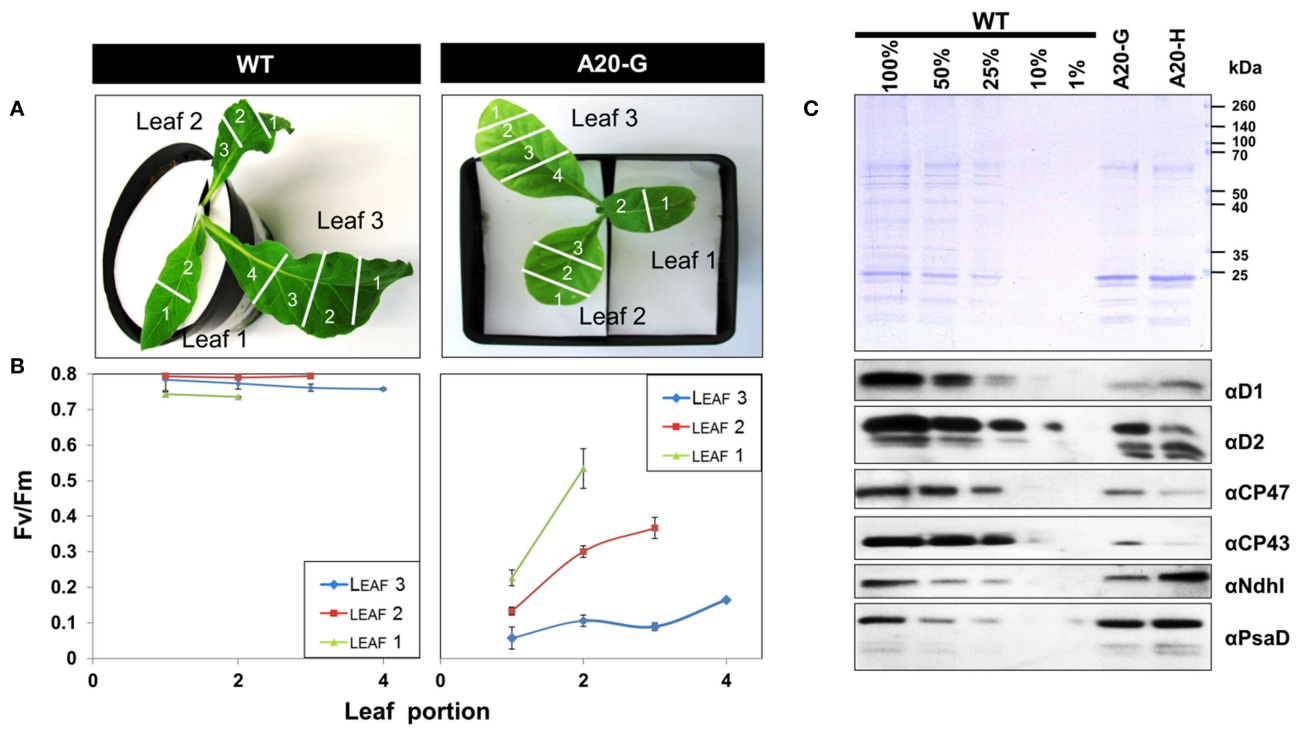

FIGURE 2 | Reduced photosystem II activity in the mutants. (A,B) F_v/F_m values for various leaf segments of plants grown in compost. **(C)** Immunochemical detection of the D1, D2, CP43, and CP47 subunits of PSII, the NdhI subunit of the NDH complex and the PsaD subunit of PSI. Coomassie-stained gel shows protein loading. Immunoblots were normalized by equal chlorophyll loading and all leaves were pooled for analysis. Plants were ~4–8 weeks old.

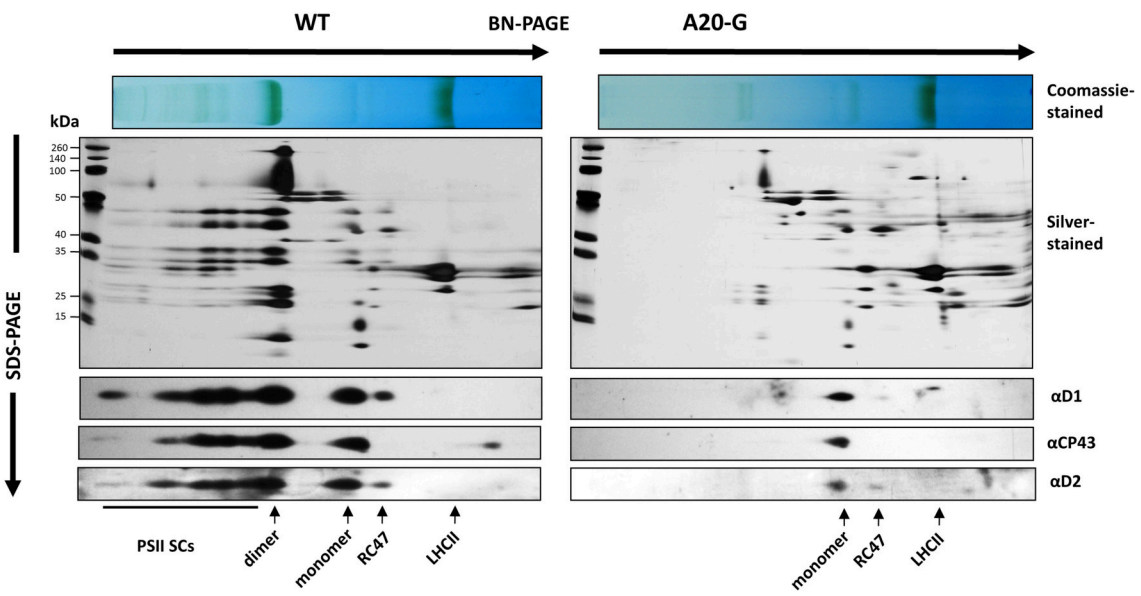

FIGURE 3 | 2D gel analysis of thylakoid proteins. Detergent-solubilised membrane proteins from either WT or A20-G were separated by BN-PAGE in the first dimension then by denaturing SDS-PAGE in the second dimension followed by immunoblotting using antibodies specific for D1, D2, or CP43 or silver staining. Positions of PSII supercomplexes (PSII SCs), dimeric PSII (dimer), monomeric PSII (monomer), PSII complexes lacking CP43 (RC47), and trimeric LHCII (LHCII) are indicated.

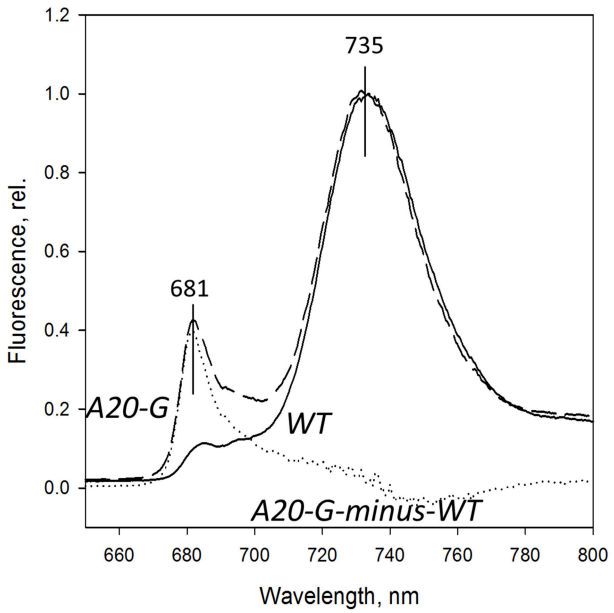

FIGURE 4 | 77K fluorescence emission spectra. Spectra from chloroplasts of the WT (solid line) and A20-G mutant (dashed line) were normalized at 735 nm. Dashed line is A20-G*minus*-wild type difference spectrum. Chloroplasts were isolated from 3-month-old plants grown in the greenhouse.

consistent with the biochemical analysis presented in **Figures 2**, **3** showing depletion of PSII in the mutant but retention of LHCII.

The strong increase of LHCII emission indicated that the LHCII complex was not coupled to any reaction center and hence that excitation was not being quenched. Indeed, the PAM fluorescence induction traces in **Figure 5** show that the mutant possessed a strongly elevated F_o in comparison to that of the WT and decreased F_v/F_m ratio (**Table 2**). Interestingly, despite vastly reduced levels of PSII in the mutant, illumination induced even more extensive non-photochemical quenching (NPQ) of chlorophyll fluorescence in the mutant than in WT and with much faster kinetics (**Figure 5**). Relaxation of NPQ in the mutant was, however, slower than in the WT and in the plants illuminated with 700 μmol photons m^{-2} s^{-1} NPQ recovered to only 40% after 30 min in the dark (**Table 2**). Time-resolved spectroscopy also revealed that the state of LHCII antenna in the A20-G mutant was not affected by the presence of closed reaction centers since the average fluorescence lifetime at F_m of the mutant plants was almost the same as WT (**Figure 6**).

D1 is Still Degraded in the A20 Mutant

To test the effect of truncating D1 on the degradation of D1, WT, and A20-G leaves were exposed to high light either in the absence or presence of lincomycin, an inhibitor of protein synthesis in the chloroplast, and levels of D1 and CP47 were determined immunochemically. As anticipated from previous work, D1 levels declined in WT leaves in the presence of lincomycin due to light-induced degradation of D1 whereas net loss of D1 was significantly less in the absence of lincomycin due to PSII repair (**Figure 7**; Kato et al., 2009). In contrast, the low levels of D1 detected in the A20-G leaves declined in both the presence or absence of lincomycin, indicating that degradation of truncated D1 still occurred in the mutant under these illumination conditions; instead the mutant was impaired in the ability to maintain levels of D1 in the absence of lincomycin, most likely due to a defect in the synthesis of D1 and/or its insertion into PSII during the repair process (**Figure 7**).

DISCUSSION

We describe here the construction and initial characterization of tobacco mutants designed to test the role of the N-terminal tail of D1 on selective D1 degradation during PSII repair. The mutants were severely impaired in their ability to grow photoautotrophically on compost and there was a loss of PSII activity in leaves as they matured so that mature leaves contained little PSII activity. Loss of PSII subunit expression in older leaves has also been reported in studies on tobacco null mutants lacking low-molecular-mass subunits of PSII and has been ascribed to developmental effects on gene expression (Suorsa et al., 2004). In the case of the tobacco A20 mutants described here, specific effects on the accumulation of *psbA* mRNA, translation efficiency, targeting of D1 to the thylakoid membrane, and assembly into PSII must also be considered. Cyclic electron flow (CEF) around PSI presumably still produced ATP to maintain cellular function in older leaves, although the level of PSI also seemed to decline in the mutant compared to WT as leaves became older (compare **Figures 2**, **3**), possibly in response to reduced levels of PSII activity or differences in chloroplast development.

A dramatic effect seen in the tobacco A20 mutant is the loss of PSII SCs in the membrane as deduced from BN-PAGE (**Figure 3**) and fluorescence emission spectroscopy (**Figure 4**), despite the retention of LHCII complexes and some residual PSII. Current structural models of the abundant $C_2M_2S_2$ PSII SC, which consists of a dimeric PSII core complex surrounded by monomeric (CP29, CP26, and CP29) and trimeric LHCII complexes (Caffarri et al., 2009) place the N-terminal tail of D1 in one PSII monomer in the vicinity of the N-terminal tail of PsbH and CP29 in the opposing monomer of the dimer (Puthiyaveetil and Kirchoff, 2013). Consequently it is possible that truncation of the N-terminal tail might have a direct effect on assembly of dimeric core complexes and larger PSII SCs. However, loss of PSII SCs has been observed in many types of mutant so indirect effects of truncating D1 such as long range effects on the binding of lumenal extrinsic proteins (Ido et al., 2009), low-molecular-mass PSII subunits (Suorsa et al., 2004), or assembly factors such as PsbN (Torabi et al., 2014) are possible. Given the impaired PSII assembly displayed by the mutant, downregulation of PSII activity to minimize damage to PSII or the accumulation of disassembled damaged complexes could also lead to fewer PSII SCs.

A clear phenotype displayed by the tobacco A20 mutants is the ability to perform effective NPQ despite severe depletion of PSII complexes; this phenotype is consistent with energy-dependent qE quenching being a phenomenon of unassembled

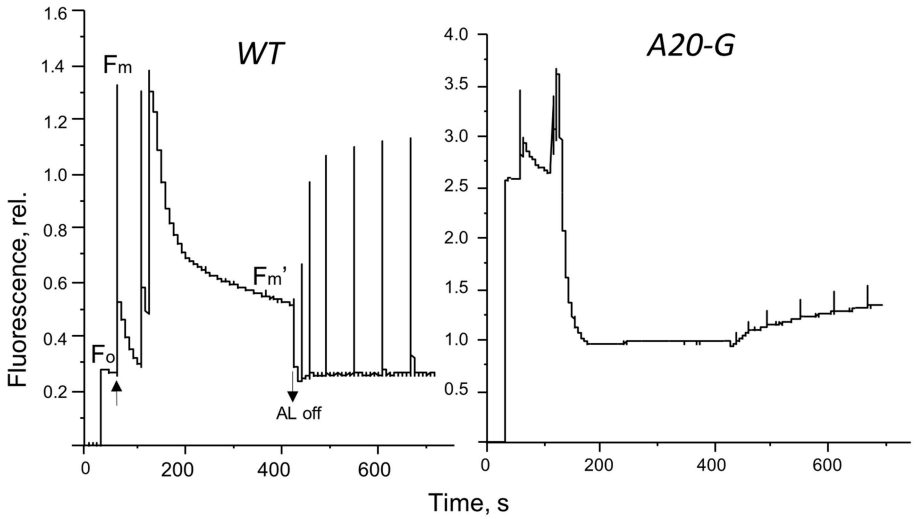

FIGURE 5 | Fluorescence induction. Pulse amplitude modulated fluorescence induction traces of leaves from the WT and A20-G mutant of tobacco. Arrows indicate actinic light switched on/off.

TABLE 2 | Fluorescence induction parameters of leaves from WT and A20-G tobacco mutant exposed to two different light intensities.

Sample	Light Intensity (μmol photons m^{-2} s^{-1})	F_v/F_m	*qP*	NPQ
WT	100	0.8	0.4	0.96
A20-G	100	0.19	0.07	3.7
WT	700	0.78	0.2	2.1
A20-G	700	0.25	0.003	5.6

F_v/F_m is the PSII fluorescence yield, qP is a photochemical quenching coefficient, and NPQ a measure of non-photochemical quenching.

LHCII complexes as advocated by Ruban and co-workers from analysis of lincomycin-poisoned plant leaves (Belgio et al., 2012).

Our data clearly show that D1 can still be effectively degraded in the A20-G mutant (**Figure 7**) despite having an N-terminal tail of 12 residues, which is considered too short to engage productively with FtsH complexes in the membrane (Chiba et al., 2000; Lee et al., 2011). Assuming that N-terminal FtsH-mediated D1 degradation is blocked in the A20-G mutant, which is reasonable given the currently accepted mechanism of FtsH, our data support the existence of additional and/or compensatory pathways for D1 degradation. In the literature, discussion has focused on Deg protease-mediated cleavage of D1 coupled to FtsH proteolysis as a supplementary escape pathway that becomes more important at high light intensities (Kato et al., 2012). Kato and colleagues have also provided evidence that depletion of FtsH in the chloroplast leads to the up-regulation of other chloroplast proteases such as Clp and SppA that might compensate for the loss of FtsH-mediated degradation of D1 (Kato et al., 2012). Adam and colleagues have proposed that proper post-translational maturation of the N-terminal tail of D1 is important for recognition by

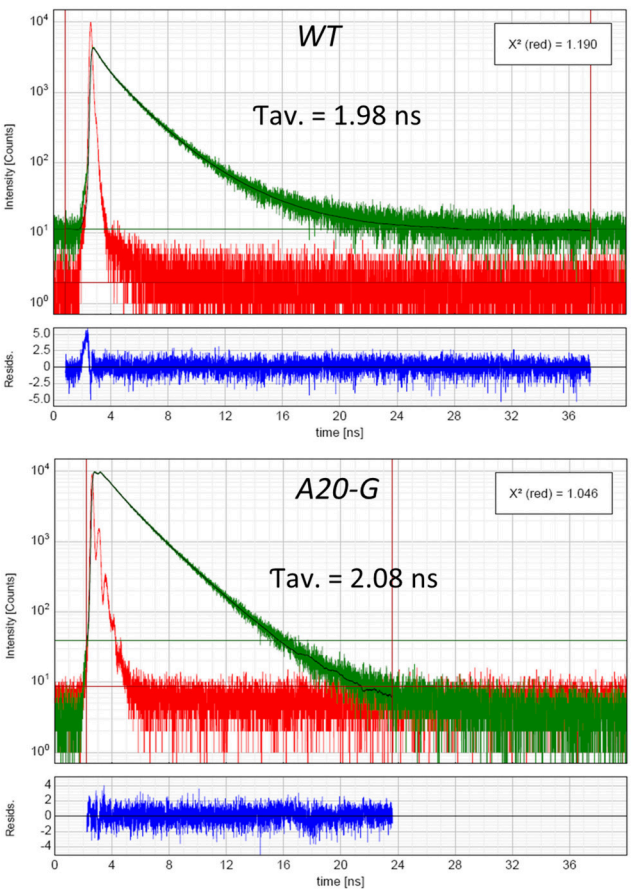

FIGURE 6 | Lifetime of excited states. Time-resolved fluorescence analysis of WT and A20-G tobacco leaves measured in F_m state. For more technical details see the Materials and Methods.

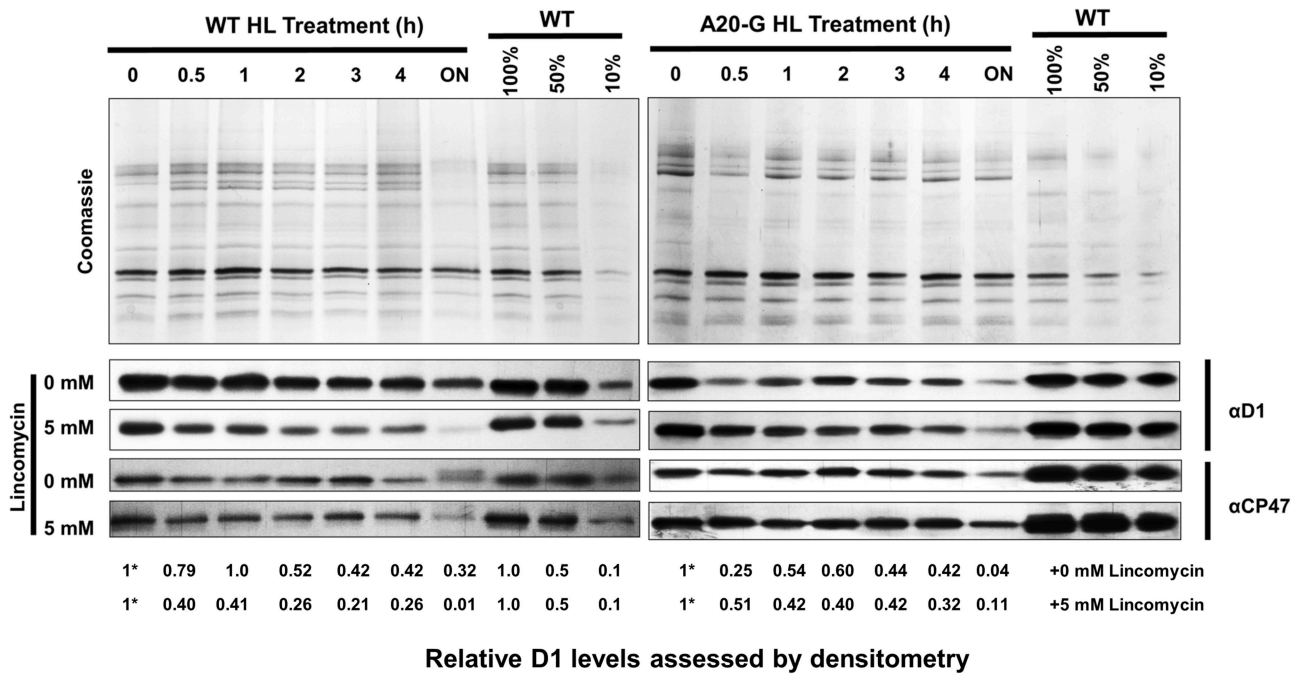

FIGURE 7 | Analysis of D1 degradation in mutant and WT. Leaves of WT and A20-G were exposed to high light (HL; 1000 μmol photons m^{-2} s^{-1}) for a period of 4 h either in the absence or presence of 5 mM lincomycin then exposed to growth light overnight (ON; 30 μmol photons m^{-2} s^{-1}). At each time point, thylakoids were harvested for immunoblotting analysis using D1 and CP47-specific antibodies. Coomassie-stained gels of untreated samples are shown to confirm loading. Relative levels of D1 were determined by densitometry with the initial amount normalized to a value of 1 indicated by asterisk. 3-month-old greenhouse-grown plants were used.

FtsH and that if the N-terminal Met is no longer excised damaged D1 is degraded by an alternative protease(s) (Adam et al., 2011). Additional proteases might also be present at different stages of chloroplast development, such as during senescence.

In the case of *Synechocystis* 6803, D1 degradation in WT appears to occur primarily via the N-terminal FtsH-mediated route (Komenda et al., 2007). However, it must be emphasized that this conclusion is based on the study of D1 degradation under largely non-photoinhibitory conditions when the rates of PSII damage and repair are balanced (Komenda et al., 2007), rather than under the more extreme photoinhibitory conditions usually used to study D1 degradation in plants, that could lead to more extensive photooxidative damage and trigger additional alternative "back-up" pathways to FtsH for D1 degradation. Indeed detailed experiments by Kato et al. (2009) have shown that an Arabidopsis mutant depleted in FtsH is impaired in D1 degradation at low (20 μmol photons m^{-2} s^{-1}) to medium irradiances (100 μmol photons m^{-2} s^{-1}) but less so at high irradiances (1200 μmol photons m^{-2} s^{-1}). Likewise, in the case of *Synechocystis* 6803, it is likely that when FtsH-mediated PSII repair alone cannot cope with the rates of damage to PSII, other proteases might also contribute to D1 degradation as discussed by Nixon et al. (2005). In support of this concept, analysis of cyanobacterial PSII mutants that are more susceptible to photodamage has provided evidence that other proteases can indeed partially compensate for the loss of the FtsH2/FtsH3 complex (Komenda et al., 2010).

AUTHOR CONTRIBUTIONS

FM, AR, and PN designed the research; FM, NA, ZW, and EB performed the research; All authors analyzed the data FM, NA, AR, and PN wrote the manuscript.

FUNDING

We are grateful to the Biotechnology and Biological Science Research Council (grant BB/E006388/1) for supporting this work.

ACKNOWLEDGMENTS

We are grateful to Dr. Tony Brain (Kings College London) for performing the transmission electron microscopy, Professor Pal Maliga for providing plasmids and Shengxi Shao for help with the densitometry analysis.

SUPPLEMENTARY MATERIAL

The Supplementary Material for this article can be found online at: http://journal.frontiersin.org/article/10.3389/fpls.2016.00844

REFERENCES

Abramoff, M. D., Magelhaes, P. J., and Ram, S. J. (2004). Image processing with image. *J. Biophotonics Int.* 11, 36–42.

Adam, Z., Frottin, F., Espagne, C., Meinnel, T., and Giglione, C. (2011). Interplay between N-terminal methionine excision and FtsH protease is essential for normal chloroplast development and function in Arabidopsis. *Plant Cell* 23, 3745–3760. doi: 10.1105/tpc.111.087239

Ahmad, N., Michoux, F., and Nixon, P. J. (2012). Investigating the production of foreign membrane proteins in tobacco chloroplasts: expression of an algal plastid terminal oxidase. *PLoS ONE* 7:*e*41722. doi: 10.1371/journal.pone.0041722

Andrizhiyevskaya, E. G., Chojnicka, A., Bautista, J. A., Diner, B. A., van Grondelle, R., and Dekker, J. P. (2005). Origin of the F685 and F695 fluorescence in photosystem II. *Photosynth. Res.* 84, 173–180. doi: 10.1007/s11120-005-0478-7

Bailey, S., Thompson, E., Nixon, P. J., Horton, P., Mullineaux, C. W., Robinson, C., et al. (2002). A critical role for the Var2 FtsH homologue of *Arabidopsis thaliana* in the photosystem II repair cycle *in vivo*. *J. Biol. Chem.* 277, 2006–2011. doi: 10.1074/jbc.M105878200

Belgio, E., Johnson, M. P., Juric, S., and Ruban, A. V. (2012). Higher plant photosystem II light-harvesting antenna, not the reaction center, determines the excited-state lifetime – both the maximum and the non-photochemically quenched. *Biophys. J.* 102, 2761–2771. doi: 10.1016/j.bpj.2012.05.004

Boehm, M., Yu, J., Krynicka, V., Barker, M., Tichy, M., Komenda, J., et al. (2012). Subunit organisation of a *Synechocystis* hetero-oligomeric thylakoid FtsH complex involved in photosystem II repair. *Plant Cell* 24, 3669–3683. doi: 10.1105/tpc.112.100891

Burrows, P. A., Sazanov, L. A., Svab, Z., Maliga, P., and Nixon, P. J. (1998). Identification of a functional respiratory complex in chloroplasts through analysis of tobacco mutants containing disrupted plastid *ndh* genes. *EMBO J.* 17, 868–876. doi: 10.1093/emboj/17.4.868

Caffarri, S., Kouril, R., Kereïche, S., Boekema, E. J., and Croce, R. (2009). Functional architecture of higher plant photosystem II supercomplexes. *EMBO J.* 28, 3052–3063. doi: 10.1038/emboj.2009.232

Chiba, S., Akiyama, Y., and Ito, K. (2002). Membrane protein degradation by FtsH can be initiated from either end. *J. Bacteriol.* 184, 4775–4782. doi: 10.1128/JB.184.17.4775-4782.2002

Chiba, S., Akiyama, Y., Mori, H., Matsuo, E.-I., and Ito, K. (2000). Length recognition at the N-terminal tail for the initiation of FtsH-mediated proteolysis. *EMBO Rep.* 1, 47–52. doi: 10.1093/embo-reports/kvd005

Ido, K., Ifuku, K., Yamamoto, Y., Ishihara, S., Murakami, A., Takabe, K., et al. (2009). Knockdown of the PsbP protein does not prevent assembly of the dimeric PSII core complex but impairs accumulation of photosystem II supercomplexes in tobacco. *Biochim. Biophys. Acta* 1787, 873–881. doi: 10.1016/j.bbabio.2009.03.004

Kato, Y., Miura, E., Ido, K., Ifuku, K., and Sakamoto, W. (2009). The variegated mutants lacking chloroplastic FtsHs are defective in D1 degradation and accumulate reactive oxygen species. *Plant Physiol.* 151, 1790–1801. doi: 10.1104/pp.109.146589

Kato, Y., Sun, X., Zhang, L., and Sakamoto, W. (2012). Cooperative D1 degradation in the photosystem II repair mediated by chloroplastic proteases in Arabidopsis. *Plant Physiol.* 159, 1428–1439. doi: 10.1104/pp.112.199042

Komenda, J., Barker, M., Kuviková, S., de Vrie, R., Mullineaux, C. W., Tichy, M., et al. (2006). The FtsH protease slr0228 is important for quality control of photosystem II in the thylakoid membrane of *Synechocystis* sp. PCC 6803. *J. Biol. Chem.* 281, 1145–1151. doi: 10.1074/jbc.M503852200

Komenda, J., Knoppová, J., Krynická, V., Nixon, P. J., and Tichy, M. (2010). Role of FtsH2 in the repair of photosystem II in mutants of the cyanobacterium *Synechocystis* PCC 6803 with impaired assembly or stability of the CaMn(4) cluster. *Biochim. Biophys. Acta* 1797, 566–575. doi: 10.1016/j.bbabio.2010.02.006

Komenda, J., Sobotka, R., and Nixon, P. J. (2012). Assembling and maintaining the photosystem II complex in chloroplasts and cyanobacteria. *Curr. Opin. Plant Biol.* 15, 245–251. doi: 10.1016/j.pbi.2012.01.017

Komenda, J., Tichy, M., Prásil, O., Knoppova, J., Kuvikova, S., de Vries, R., et al. (2007). The exposed N-terminal tail of the D1 subunit is required for rapid D1 degradation during photosystem II repair in *Synechocystis* sp PCC 6803. *Plant Cell* 19, 2839–2854. doi: 10.1105/tpc.107.053868

Kuroda, H., and Maliga, P. (2001). Complementarity of the 16S rRNA penultimate stem with sequences downstream of the AUG destabilizes the plastid mRNAs. *Nucl. Acids Res.* 29, 970–975. doi: 10.1093/nar/29.4.970

Lee, S., Augustin, S., Tatsuta, T., Gerdes, F., Langer, T., and Tsai, F. T. F. (2011). Electron cryomicroscopy structure of a membrane–anchored mitochondrial AAA protease. *J. Biol. Chem.* 286, 4404–4411. doi: 10.1074/jbc.M110.158741

Michoux, F. (2008). *Developing New Strategies for the Production of Foreign Proteins in Higher Plant Chloroplasts*. Ph.D. Thesis, Imperial College London.

Nixon, P. J., Barker, M., Boehm, M., de Vrie, R., and Komenda, J. (2005). FtsH-mediated repair of the photosystem II complex in response to light stress. *J. Exp. Bot.* 56, 357–363. doi: 10.1093/jxb/eri021

Puthiyaveetil, S., and Kirchoff, H. (2013). A phosphorylation map of the photosystem II supercomplex C2S2M2. *Front. Plant Sci.* 4:459. doi: 10.3389/fpls.2013.00459

Ruban, A. V., and Horton, P. (1992). Mechanism of ΔpH-dependent dissipation of absorbed excitation energy by photosynthetic membranes. *I. Spectroscopic analysis of isolated light harvesting complexes. Biochim. Biophys. Acta* 1102, 30–38. doi: 10.1016/0005-2728(92)90061-6

Silva, P., Thompson, E., Bailey, S., Kruse, O., Mullineaux, C. W., Robinson, C., et al. (2003). FtsH is involved in the early stages of repair of photosystem II in *Synechocystis* sp PCC 6803. *Plant Cell* 15, 2152–2164. doi: 10.1105/tpc.012609

Suorsa, M., Regel, R. E., Paakkarinen, V., Battchikova, N., Herrmann, R. G., and Aro, E.-M. (2004). Protein assembly of photosystem II and accumulation of subcomplexes in the absence of low molecular mass subunits PsbL and PsbJ. *Eur. J. Biochem.* 271, 96–107. doi: 10.1046/j.1432-1033.2003.03906.x

Svab, Z., and Maliga, P. (1993). High-frequency plastid transformation in tobacco by selection for a chimeric *aadA* gene. *Proc. Natl. Acad. Sci. U.S.A.* 90, 913–917. doi: 10.1073/pnas.90.3.913

Torabi, S., Umate, P., Manavski, N., Plöchinger, M., Kleinknecht, L., Bogireddi, H., et al. (2014). PsbN is required for assembly of the photosystem II reaction center in *Nicotiana tabacum*. *Plant Cell* 26, 1183–1199. doi: 10.1105/tpc.113.120444

Vass, I. (2012). Molecular mechanisms of photodamage in the photosystem II complex. *Biochim. Biophys. Acta* 1817, 209–217. doi: 10.1016/j.bbabio.2011.04.014

Weis, E. (1985). Chlorophyll fluorescence at 77 K in intact leaves: characterization of a technique to eliminate artefacts related to self absorption. *Photosynth. Res.* 6, 73–86. doi: 10.1007/BF00029047

Conflict of Interest Statement: The authors declare that the research was conducted in the absence of any commercial or financial relationships that could be construed as a potential conflict of interest.

frontiers in Plant Science

PERSPECTIVE
published: 24 May 2016
doi: 10.3389/fpls.2016.00694

Insights into the Cyanobacterial Deg/HtrA Proteases

Otilia Cheregi†, Raik Wagner† and Christiane Funk†*

Department of Chemistry, Umeå University, Umeå, Sweden

Proteins are the main machinery for all living processes in a cell; they provide structural elements, regulate biochemical reactions as enzymes, and are the interface to the outside as receptors and transporters. Like any other machinery proteins have to be assembled correctly and need maintenance after damage, e.g., caused by changes in environmental conditions, genetic mutations, and limitations in the availability of cofactors. Proteases and chaperones help in repair, assembly, and folding of damaged and misfolded protein complexes cost-effective, with low energy investment compared with neo-synthesis. Despite their importance for viability, the specific biological role of most proteases *in vivo* is largely unknown. Deg/HtrA proteases, a family of serine-type ATP-independent proteases, have been shown in higher plants to be involved in the degradation of the Photosystem II reaction center protein D1. The objective of this review is to highlight the structure and function of their cyanobacterial orthologs. Homology modeling was used to find specific features of the SynDeg/HtrA proteases of *Synechocystis* sp. PCC 6803. Based on the available data concerning their location and their physiological substrates we conclude that these Deg proteases not only have important housekeeping and chaperone functions within the cell, but also are needed for remodeling the cell exterior.

Keywords: cyanobacteria, serine proteases, phylogeny, PSII degradation, chaperone, secretion, cell surface

OPEN ACCESS

Edited by:
Roman Sobotka,
Czech Academy of Sciences,
Czech Republic

Reviewed by:
Martin Hagemann,
University of Rostock, Germany
Tina Summerfield,
University of Otago, New Zealand

****Correspondence:***
Christiane Funk
christiane.funk@umu.se

†All authors have contributed equally to this work.

Specialty section:
This article was submitted to Plant Cell Biology, a section of the journal Frontiers in Plant Science

Received: *11 January 2016*
Accepted: *05 May 2016*
Published: *24 May 2016*

Citation:
Cheregi O, Wagner R and Funk C (2016) Insights into the Cyanobacterial Deg/HtrA Proteases. Front. Plant Sci. 7:694. doi: 10.3389/fpls.2016.00694

INTRODUCTION

Proteolysis, associated with nutrient uptake, processing and activation of proteins, or removal of damaged proteins, is vital for every cell. Cells therefore have developed a sophisticated system of molecular chaperones and proteases to reduce the amount of unfolded or aggregated proteins (Wickner et al., 1999). Proteases belonging to the Deg (for *deg*radation of periplasmic proteins) or HtrA (for *h*igh *t*emperature *r*equirement *A*) family are known in all kingdoms, in Bacteria, Eukarya, and even some Archaea (Koonin and Aravind, 2002; Page and Di Cera, 2008). These serine proteases belong, according to the MEROPS nomenclature, to the S1C subfamily of the clan PA (Rawlings et al., 2012), consisting of endopeptidases with the catalytic residues histidine, aspartate, and with serine or cysteine as nucleophile. Families are assigned to the S1 subfamily when they are similar to chymotrypsin; S1C contains Deg peptidases and their homologs. Degs are ATP-independent serine endopeptidases, which besides the trypsin-type protease domain possess 0–4 PDZ or PDZ-like domains toward their C-terminus (Pallen and Wren, 1997; Clausen et al., 2002). PDZ domains mediate protein–protein interactions and are important for substrate recognition and/or for the regulation of proteolytic activity (Krojer et al., 2002; Wilken et al., 2004), the PDZ domains of Deg/HtrA proteases even have been shown to act as enzymatic co-factors

(see Clausen et al., 2011). While commonly serine proteases consist of monomers, members of the Deg/HtrA family form homotrimers. One distinctive property of Deg/HtrAs is their ability to self-compartmentize and assemble into complex oligomers. The assembly and disassembly of higher-order oligomers allows for precise regulation of protease activity.

Eukaryotic Deg proteases take care of damaged cellular components, act as tumor repressors, or protect the cell from the accumulation of toxic protein aggregates responsible for neurodegeneration in, e.g., Alzheimer's and Parkinson's diseases. Most prokaryotic Deg/HtrA proteases play critical roles in protein quality control within the periplasmic compartment. Several members of the family even have explicit functions in bacterial pathogenicity and are involved in biofilm formation (Biswas and Biswas, 2005), secretion of virulence factors (Baud et al., 2009) and/or remodeling of cell–cell contacts within the host organisms (Hoy et al., 2010). *Escherichia coli* possesses three Deg/HtrA proteases, EcDegP (or EcHtrA), EcDegQ (or EcHhoA) and DegS (or EcHhoB). EcDegP seems to be responsible for maintaining the periplasmic protein homeostasis and thus is crucial for survival under stress conditions such as higher temperatures (Lipinska et al., 1988); EcDegS cleaves the transmembrane RseA protein in the cytoplasmic membrane, which binds and inhibits the σ^E factor (Walsh et al., 2003). EcDegQ of *E. coli* is a periplasmic protease with similar functions to EcDegP (Pallen and Wren, 1997). Contrary to *E. coli* many prokaryotes encode only a DegQ homolog, stressing the importance of this protease (Kim and Kim, 2005).

Less information is available on Deg proteases from photosynthetic organisms. In the genome of *Arabidopsis thaliana*, 16 *DEG* protease genes have been identified (reviewed in Huesgen et al., 2009; Schuhmann et al., 2012), 15 in *Oryza sativa* (Tripathi and Sowdhamini, 2006), and 20 in *Populus trichocarpa* (Garcia-Lorenzo et al., 2006). In *A. thaliana* (hereafter *Arabidopsis*) at least five AtDeg proteases (AtDeg1, AtDeg2, AtDeg5, AtDeg7, and AtDeg8) are located in the chloroplast (Schuhmann et al., 2012; Tanz et al., 2014). Of those, the Deg proteases located in the thylakoid lumen (AtDeg1, AtDeg5, and AtDeg8), as well as the mitochondrion-located AtDeg14 (Tanz et al., 2014), share high homology to cyanobacterial Deg proteases (Schuhmann et al., 2012).

For detailed information on human, bacterial and plant Deg proteases the reader is referred to the excellent review by Clausen et al. (2011). In this review, we will focus on cyanobacterial Deg proteases, which generally have been neglected in other reviews. Special focus will be on the three Deg proteases SynHhoA, SynHhoB, and SynHtrA of *Synechocystis sp.* PCC 6803 (hereafter *Synechocystis* 6803). These SynDeg proteases relate more to each other than to their homologs in *E. coli* (see Kieselbach and Funk, 2003), making it impossible to assign functions based on homology studies. They are encoded by *sll1679* (SynHhoA), *sll1427* (SynHhoB), and *slr1204* (SynHtrA), but their function within the cyanobacterial cell still is not known. Even the subcellular location of the three cyanobacterial SynDeg proteases remains enigmatic. In the following sections, we will review the current knowledge of the *Synechocystis* 6803 SynDeg proteases and compare these data with Deg proteases of other organisms.

THE FAMILY OF DEG PROTEASES IN CYANOBACTERIA – A PHYLOGENETIC COMPARISON

Within cyanobacteria biochemical or molecular biological information is available only on the SynDeg proteases of *Synechocystis* 6803. The cyanobacterial phylogeny has been recently re-determined based on new data obtained using modern techniques, e.g., comparative mass genomics, comparison of conserved proteins and resulting secondary metabolites; more than 200 cyanobacterial genomes have been sequenced (Micallef et al., 2015). A subset of those, stretching over the whole phylum, was here investigated in the search for Deg proteases (InterPro domain IPR001940[1]). The majority of the cyanobacterial strains contain three to five genes encoding members of the Deg family, however, up to seven genes are present in, e.g., *Cyanothece sp*. PCC 7425 or *Nostoc punctiforme* ATCC 29133, while several *Prochlorococcus* strains only contain two genes. Based on the analyzed species it seems that cyanobacterial Deg proteases only contain one PDZ domain.

Using the maximum likelihood method to generate a bootstrap consensus tree it becomes obvious that Deg proteases do not cluster in their phylogenetic subclades (**Figure 1**, name abbreviations are explained in **Supplementary Table S1**; Calteau et al., 2014). Looking at a wide variety of species, orthologs to SynHhoB and SynHtrA of *Synechocystis* 6803 form one cluster, while SynHhoA-homologs form a distinct, different one. Notably, genes encoding Deg peptidases in the *Prochlorococcus* and *Synechococcus* branch highlight the evolutionary development within this group. *Deg* genes of *Prochlorococcus* have common ancestors with the low-light adapted *Synechococcus* strains, i.e., *Synechococcus* sp. RCC307. RCC307 and several early species contain three genes encoding Deg proteases: one of a HhoB/HtrA type and two distinct ones, forming the base of the *Prochlorococcus/Synechococcus* clade. *Synechococcus* sp. CC9311 contains additionally a gene coding for a modified Deg lacking its PDZ domain. Its protease domain is similar to the "specialized" Degs of the *Synechococcus* branch. Some low-light adapted *Prochlorococcus* strains like *Prochlorococcus marinus* SS120 or NATL1A have lost their HhoB/HtrA type peptidase. Even the high-light adapted strains underwent massive genetic restructuring (Kettler et al., 2007), which affected the Deg peptidases. Strains like *Prochlorococcus marinus* MED4, MIT9215, and MIT9301 lost the PDZ domain of their HhoB/HtrA type Deg, while this HhoB/HtrA type is lacking completely in MIT9312, MIT9215, and AS9601. Genes encoding Deg peptidases of *Prochlorococcus marinus* lacking a PDZ domain cluster with "unusual" *deg* genes of very ancient species like *Gloeobacter* but also evolutionary young *Nostocales*. Even *deg* genes with additional unknown, or mutated peptidase domains, rendering the gene product proteolytically inactive (*Nostoc punctiforme* ATCC 29133, *Anabaena variabilis* ATCC 29413) are within this cluster. These enzymes might have undergone neo-functionalization.

[1]http://www.ebi.ac.uk/interpro/

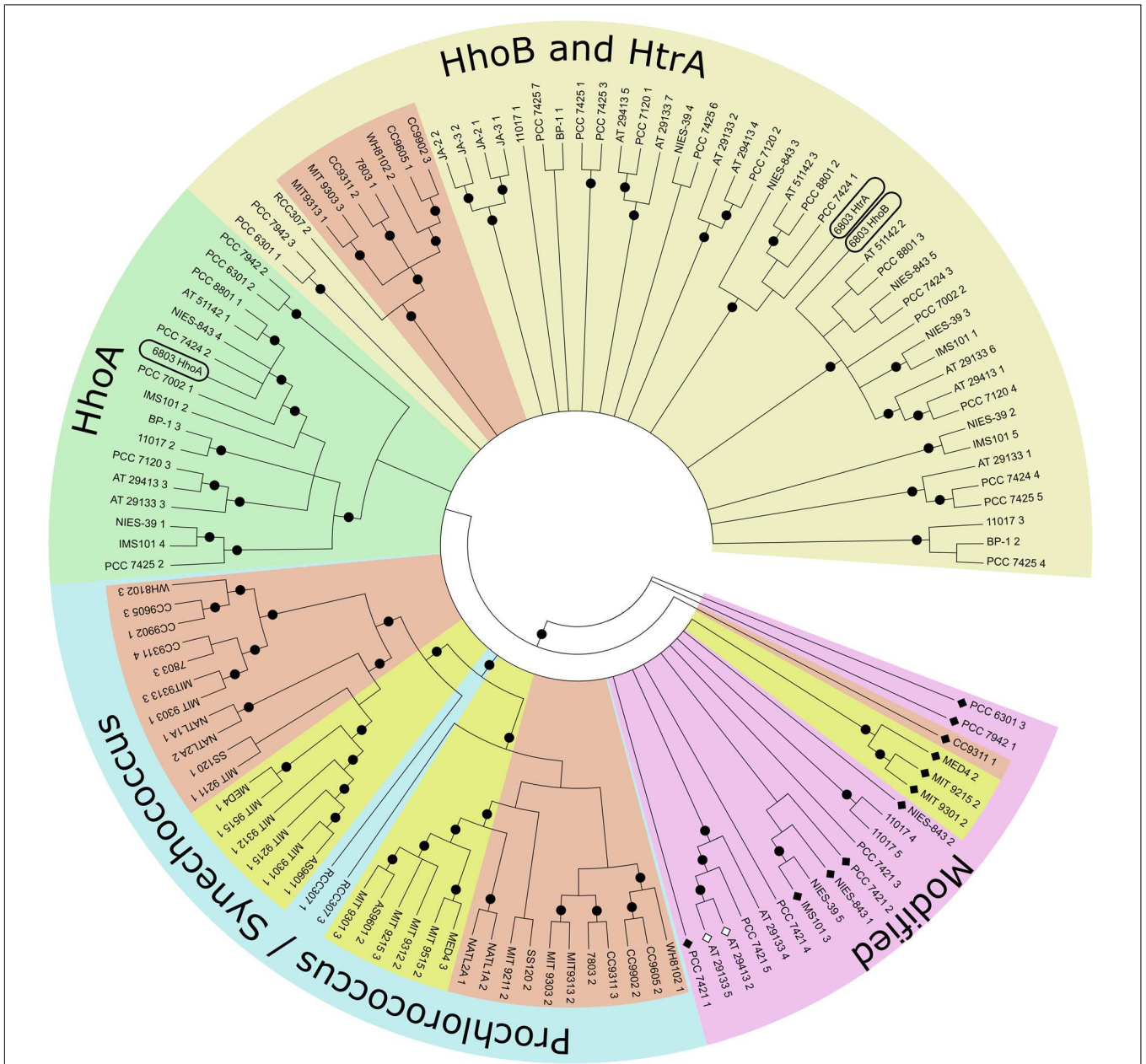

FIGURE 1 | Topological bootstrap consensus tree of cyanobacterial Deg proteases. Phylogenetic tree built using the Maximum Likelihood method from predicted mature protein sequences. The bootstrap consensus tree was inferred from 1000 replicates. Full taxonomic names can be found in **Supplementary Table S1**. The last number of each taxon indicates the gene copy of the Deg peptidase of that species. Light yellow: cluster containing *Synechocystis* 6803 HhoB and HtrA. Light green section contains HhoA of *Synechocystis* 6803. Light blue circle section contains species of the evolutionary distinct monophyletic groups *Prochlorococcus* and *Synechococcus*. Species of *Prochlorococcus* are known to be high light (yellow) or low light (red) adapted. Also low light adapted *Synechococcus* are marked in red. In the light purple circle section cluster proteins that are (a) very ancient like *Gloeobacter* sequences, (b) Deg peptidases without a PDZ domain (black diamonds), (c) inactive Deg peptidases (white diamonds, ATCC 29133, ATCC 29413), or (d) peptidases with additional elements for unknown reasons. Black circles indicate branches with a frequency of 70% and more.

STRUCTURAL IMPLICATIONS OF DEGS FROM PHOTOSYNTHETIC ORGANISMS

Of all photosynthetic organisms only the structures of recombinant *Arabidopsis* AtDeg1, AtDeg2, AtDeg5, and AtDeg8 have been published. The domain architectures of all Deg proteases are well conserved (Kieselbach and Funk, 2003; Page and Di Cera, 2008). Most family members contain either an amino terminal transit peptide or a transmembrane-spanning helix followed by the structurally conserved peptidase domain (see **Supplementary Table S1**). This peptidase domain consists of two β-barrels perpendicular to each other, build by twelve

β-strands connected by loops. Usually two longer α-helices enclose the barrel structure, additional smaller helices and β-strands can be found in the available crystal structures of Deg peptidases. The amino acids of the catalytic triad, His, Asp and Ser, are placed within the cleft between the β-barrels. Three of the five loops of the peptidase domain are needed to form the active site: the LD loop is the activation loop, L1 contains the serine residue of the catalytic triad and forms the oxyanion hole, while L2 forms a substrate specific pocket. Loops L3 and LA are regulatory loops for activation via oligomerization (Clausen et al., 2011). L3 is called sensor loop, it is important to initiate the activation cascade. The LA loop is involved in hexamer formation of the soluble Deg peptidases. Additionally regulatory elements can be found; AtDeg1 of *Arabidopsis*, for example, sense the pH via a special histidine residue in its peptidase domain, while human HTRA1, HTRA3, and HTRA4 contain fragments of an insulin growth factor binding protein (Clausen et al., 2002).

The Deg proteases of photosynthetic organisms contain up to two PDZ domains, which are connected via a short linker to the C-terminal end of the peptidase domain (Kim and Sheng, 2004). PDZ domains set apart the Deg subfamily from other members of the MEROPS S1 family; they are able to bind to the carboxyl-termini of proteins or they can dimerize with other PDZ domains. Cyanobacterial Degs as well as AtDeg1 and AtDeg8 of *Arabidopsis* contain only one PDZ domain; AtDeg2 has two PDZ domains. Its second PDZ domain (PDZ2) is not able to bind substrate due to a conserved internal ligand occupying the peptide binding site, instead this internal ligand is part of the docking site for the LA loop to form a stable hexamer (Sun et al., 2012). AtDeg15 and AtDeg5 of *Arabidopsis* do not contain any PDZ domains. AtDeg15 acts as glyoxysomal processing peptidase (Helm et al., 2007), while AtDeg5 forms peptidase-substrate complexes together with AtDeg8 (Sun et al., 2007). PDZ domains are compact globular domains made up canonical by six β-sheets and two α-helices (Clausen et al., 2011). The first element of PDZ domains in Deg peptidases is the carboxylate-binding loop, which interacts with the C-termini of substrate proteins and presents those to the proteolytic active site. This loop usually is composed of a GLGF motif, but in cyanobacteria the first position often is replaced by phenylalanine or tyrosine, while positions two and four are either isoleucine or valine. The motif is followed by the peptide-binding site formed of a β-strand and an α-helix. PDZ domains of cyanobacteria contain at least one interaction clamp (IC1) for protein-protein interaction (Clausen et al., 2002; Krojer et al., 2008). Plant Deg1 even contains a second interaction clamp (IC2), four of its residues seem to be involved in interaction (Kley et al., 2011). Sequence alignments highlight that this motif is only found in higher plants. However, other residues might be important for oligomerization of cyanobacterial Deg proteases. IC1s of cyanobacteria seem to contain additional residues resulting in a varying structure after homology modeling (see **Figure 2**).

The basic unit of Deg proteases in their tertiary structure is a homotrimer formed by hydrophobic interactions and hydrogen bonds of the peptidase domains. The trimeric form resembles a meniscus lens or a shallow funnel with the active sites located at the center of the concave site, while the PDZ domains are on the rim of the trimer. Depending on the activation mechanism, the organism, and the functional state Deg peptidases can oligomerize into larger structures via intramolecular PDZ–PDZ interactions (for a review, see Hansen and Hilgenfeld, 2013). Hexamers, nonamers, dodecamers, octodecamers, and 24-mers were detected using size exclusion chromatography or crystallography (Krojer et al., 2008; Huesgen et al., 2011). For AtDeg1 a pH-dependent oligomerization has been observed; inactive monomers oligomerize into trimers at acidic pH. These trimers furthermore assemble into hexamers by interaction of IC1 and IC2 with the closest LA loop of the opposing trimer. By formation of these hexamers the PDZ domains are fixed; the PDZ–L3–LD interaction network establishes a defined opening of the hexameric cage and stabilizes the active site (Kley et al., 2011). Reorientation of LD by L3 of the neighboring protomer allosterically activates the Deg peptidase and is ubiquitous among this subfamily (Clausen et al., 2011). The resting state of AtDeg2 is suggested to be a hexamer, incubation with the substitute-substrate β-casein then leads to the formation of higher oligomeric states. The first PDZ domain (PDZ1) binds the substrate and presents it to the active site, while PDZ2 becomes fixed and forms an LA-docking surface. Interactions of PDZ2 with PDZ1 of the opposing trimer lead to trimer-dimerization. It is suggested that PDZ2 can also unlock the hexameric state to re-assemble into an active dodecamer in the presence of substrate (Sun

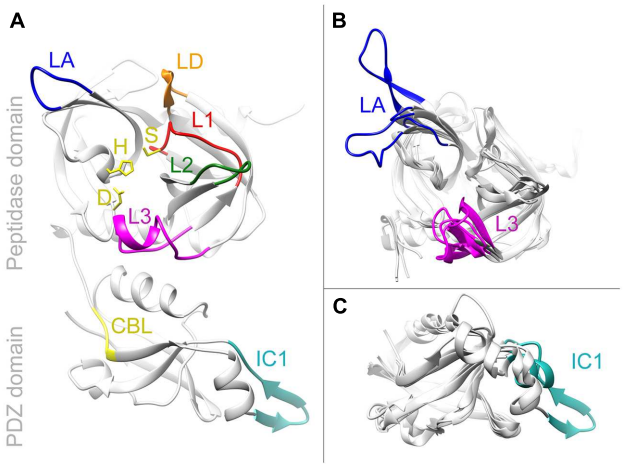

FIGURE 2 | Homology models of HhoB. Models were obtained by Phyre2. **(A)** SynHhoB modeled after 3STJ, the crystal structure derived of *E. coli* DegQ. Side chains of the catalytic triad (H151, D181, and S258) are shown in yellow. They are surrounded by loops forming the active site: activation loop LD in orange, loop for the oxyanion hole L1 in red, and the substrate specific loop L2 in green. The regulator loops are LA (blue) and L3 (magenta). Of the PDZ domain the carboxylate binding loop (CBL) is given in yellow and the interaction clamp one (IC1) in cyan. **(B,C)** Superposition of peptidase domain **(B)** or PDZ domain **(C)** using different HhoB models. These models were formed using information of the crystal structures of DegQ, Deg1, Deg2, and Deg8. Color coding is the same as in **(A)**. Only varying elements were colored.

et al., 2012). AtDeg5, lacking any PDZ domains, forms trimers in solution that bind two calcium ions along the channel between the protomers. These calcium ions are dispensable for trimer formation (Sun et al., 2013). AtDeg8 exists as monomer and trimer at pH 6.0, while hexamers are formed at pH 8.0. The crystal structure of hexameric AtDeg8 shows flattened PDZ domains resulting in a flatter funnel formation and a narrower cavity of the hexamer compared to other structures, substrate access to its active site seems to be prevented (Sun et al., 2013). Furthermore, in the resolved crystal structures of AtDeg5 and AtDeg8 the histidines of the catalytic triad are rotated and the L2 loop seems to be differently formed pointing to a different activation mechanism (Sun et al., 2013). AtDeg5 and AtDeg8 are so far the only Deg proteases known to form hetero-oligomers out of homo-trimers (Sun et al., 2007).

The PDZ domain of the three SynDeg proteases of *Synechocystis* 6803 is needed for oligomerization beyond homotrimers (Huesgen et al., 2011). While recombinant SynHhoB does not form higher oligomers, SynHhoA aggregates into 12–24-mers, and SynHtrA into 9–12 protomers. Interestingly, recombinant SynDegs lacking their PDZ domains were still proteolytically active, implying that in *Synechocystis* 6803 the PDZ domain is not needed as signal for L3 reorientation to form the active site (Huesgen et al., 2011). So far no crystallographic structures of cyanobacterial Deg peptidases have been published. Homology modeling was performed using *Thermotoga maritima* HtrA and *E. coli* EcDegS as template (Jansén et al., 2005); today many more Deg structures of various organisms are known. We used the intense mode of Phyre2 (Kelley et al., 2015) for homology modeling of *Synechocystis* 6803 SynHhoB (Sll1427). Phyre2 returned several models with high confidence, from those SynHhoB modeled after *E. coli* EcDegQ, RSCB-ID 3STJ, chain C (Sawa et al., 2011) was picked as template, because this protein has been crystallized in its trimeric form and *Synechocystis* 6803 SynHhoB forms trimers in solutions (Huesgen et al., 2011), (**Figure 2**). Superposition of SynHhoB modeled after AtDeg1 (3qo6), AtDeg2 (4fln), and AtDeg8 (4ic6) using EcDegQ as template (Kley et al., 2011; Sun et al., 2012, 2013) is shown in **Figures 2B,C**. Due to different positioning of the PDZ domains in the known Deg structures the peptidase domain was independently modeled from the PDZ domain. The basic Deg peptidase elements, perpendicular β-barrels with the active site consisting of the catalytic triad and loops LD, L1, and L2 are conserved in the model of *Synechocystis* 6803 SynHhoB. Sterical variations can be observed in loops LA and L3 of the peptidase domain, as well as in IC1 and the substrate binding helix. In *Synechocystis* SynHhoB LA loop and IC1 motif seem to be longer compared to *Arabidopsis* AtDegs. The Phyre2s method includes prediction and modeling of secondary structures, the variety of IC1 therefore could induce the observed changes in the substrate binding helix at the N-terminus. Differences in the activation state of the template Deg proteases explains the observed variation of the *Synechocystis* 6803 L3 loop. For more detailed structural comparisons of cyanobacterial Deg proteases we have to await the resolution of their crystal structures.

REGULATION OF THE DEG PROTEASES

Transcriptional Regulation

The three *Syn-deg* genes are found in the *Synechocystis* 6803 genome at distinct locations and belong to transcriptional units (TU) including 1–3 genes (Kopf et al., 2014). *SynHhoA* is part of an operon with *sll1680* and *sll1681,* encoding a hypothetical protein and a protein of unknown function. Its mRNA is transcribed with a length of 3800 bp. Antisense RNA (aRNA) overlapping the 3′ end of *Syn-hhoA* is expressed at higher levels than *Syn-hhoA* itself, in all conditions tested (Kopf et al., 2014). mRNA of *Syn-hhoB* has a length of 1510 bp with extra 239 bp at the 3′ end and 21 bp at the 5′ end. Even within *Syn-hhoB* antisense RNA is located on the complementary strand, toward the 3′ end, which is expressed at lower levels than *Syn-hhoB* (Kopf et al., 2014). *Syn-htrA* is part of a TU of 1500 bp, with a short 3′ UTR (47 bp) and a longer 5′ UTR end of 122 bp. The antisense RNA located complementary to this gene, *ncr0370*, is, similar to aRNA of *Syn-hhoB*, overlapping the 3′ end of the gene and its 3′ UTR. *Ncr0370* has maximal reads in the exponential phase, about 10 times higher than *Syn-htrA*. In the nine stress conditions investigated (Kopf et al., 2014), *Syn-htrA* is induced in each experiment about eight times, while the expression of the non-coding RNA declines, pointing to possible functional correlations. Contrary to the strong up-regulation of *Syn-htrA* in all investigated stress conditions (cold, Fe limitation, high light stress, darkness, heat shock, stationary phase, C depletion, N depletion and P depletion, Kopf et al., 2014), the expression of *Syn-hhoA* and *Syn-hhoB* are low. According to the study of Mrázek et al. (2001), which predicts gene expression level from relative codon usage bias, all three *Syn-deg* genes are predicted to be lower expressed than other members of the chaperone/degradation machinery such as the genes encoding DnaK, ClpC, FtsH, and CtpA proteases. Microarray analyses, taking different stress conditions and different genetic backgrounds in consideration, support these results (Hernandez-Prieto and Futschik, 2012; Kopf et al., 2014) (**Supplementary Table S2**). Only few abiotic stresses significantly induce *Syn-deg* genes: 2 h treatment of UV-B light combined with high light intensity (Huang et al., 2002b) and 30 min growth in salt (0.5 M NaCl) or hyperosmotic stress (0.5 M sorbitol; Kanesaki et al., 2002). Stressing *Synechocystis* 6803 cells with high concentrations of Cd^{2+} affects primarily the level of all protease-encoding genes, *Syn-htrA* being among the most strongly induced already after 30 min of stress (Houot et al., 2007). *Syn-htrA* and *Syn-hhoA* genes were found to be induced in a Δ*psbO*:Δ*psbU* pseudorevertant that is able to grow photoautotrophically at pH ∼7.5 (Summerfield et al., 2007). In this work, *Syn-hhoA* and *Syn-htrA* seem to be part of a stress-response network, which balances the instability of PSII caused by the deletion of *psbO* and *psbV* (Summerfield et al., 2007). Co-expression analysis has demonstrated that *Syn-hhoA*, *Syn-hhoB,* and *Syn-htrA* belong to distinct co-expression clusters suggesting unique physiological functions (Miranda et al., 2013), besides their proposed overlapping functions (Barker et al., 2006). *Syn-htrA* is co-expressed with genes coding for enzymes involved in iron- and nitrogen-metabolism, *Syn-hhoA* with genes coding for

enzymes involved in response to heat shock and high light stress, cellular responses (chaperones, proteases) and transcription, while *Syn-hhoB* displays a similar expression pattern with genes encoding enzymes involved in carbohydrate metabolism and periplasmic processes, most probably peptidoglycan and S-layer biosynthesis (Miranda et al., 2013).

Regulation of Protein Level

Investigations on the whole proteome can be performed using 2D DIGE (Difference in Gel Electrophoresis), in which labeling with different fluorescent dyes allows detection of differences in protein expression between a control and a mutant strain, or between standard and stress conditions. Investigations on the proteome of *Synechocystis* 6803 grown under standard conditions or after exposure to stress have revealed proteins, which are part of a general stress response, as well as proteins specific to a certain stress condition. Expression of the SynDeg proteases of *Synechocystis* 6803 was affected only by stresses having a direct impact on the membrane system, such as heat shock (Slabas et al., 2006; Suzuki et al., 2006) and salt stress (Fulda et al., 2006; Huang et al., 2006). It is interesting to note that pH stress, either acidic or basic pH, has a remarkable effect on the periplasmic proteome, but seems not to affect general stress proteins such as proteases and chaperones, including SynDeg proteases (Kurian et al., 2006; Zhang et al., 2009). This is a puzzling piece of information, since SynHhoA has been localized in the periplasm (Fulda et al., 2000) and its activity is increased at high pH, especially in the presence of divalent cations (Huesgen et al., 2011). This result correlates well with the expression study of Ohta et al. (2005), where none of the *Syn-deg* genes was found to be significantly affected by acid stress.

Gene expression and proteomics data are consistently overlapping: heat shock, salt stress, and high light stress affect the level of mRNAs and their corresponding SynDeg proteins. A more focused approach, testing the presence and the induction of SynDeg proteases using antibodies (Lam et al., 2015) has revealed that, while SynHhoA and SynHhoB are present in equimolar ratios under normal growth conditions, SynHtrA is barely detectable. SynHtrA is strongly up-regulated under high light and heat stress. In agreement with their supposed overlapping functions, upon high light stress SynHhoA accumulated significantly in mutants depleted of either SynHhoB (Δ*hhoB*) or SynHtrA (Δ*htrA*) compared to WT (Lam et al., 2015). Under high light and heat stress SynHtrA showed the highest up-regulation in Δ*hhoB*, however, the amount of SynHhoB decreased in a Δ*htrA* mutant exposed to heat stress. This indicates that their function is not complementary, but rather inversely regulated (Lam et al., 2015). *Synechocystis* 6803 mutant strains lacking any of the three SynDeg proteases compensate for the missing one by up-regulating other serine endopeptidases, such as Clp and Lon proteases (Lam et al., 2015). Using different strategies for the fractionation of cell compartments the SynDeg proteases have been detected in thylakoid membrane (SynHhoA and SynHtrA; Roberts et al., 2012), plasma membrane (SynHhoA, SynHhoB, and SynHtrA; Huang et al., 2006; Roberts et al., 2012), in the outer membrane (SynHtrA; Huang et al., 2004) and in the periplasmic space (SynHhoA; Fulda et al., 2000). The Deg proteases therefore might be active in different metabolons, however, they also might be located within specific membrane patches connecting plasma membrane and thylakoid membrane (thylakoid centers, Nickelsen and Rengstl, 2013). Probing the secretome of *Synechocystis* 6803 with SynDeg specific antibodies it was possible to show that all three proteases are secreted to the exterior of the cells, the secretion being enhanced with culture age (Cheregi et al., 2015), even though none of the SynDeg proteins contains targeting sequences for export.

SUBSTRATE IDENTIFICATION

Substrate preference can be analyzed by the resulting cleavage sites of a protein library. EcDegP and EcDegQ from *E. coli* were found to prefer valine or isoleucine, β-branching residues, at P1 of their cleavage sites (Kolmar et al., 1996) or even threonine and isoleucine (Krojer et al., 2008). Further factors like disulfide-bridges might determine the specificity due to accessibility (Kolmar et al., 1996). Recent studies in *Streptococcus pneumoniae* showed higher frequencies of non-polar residues at the P1 site (Cassone et al., 2012). Recombinant SynHhoA from *Synechocystis* 6803 cleaved PsbO from spinach on two sites: between valine (R1) and lysine (R1′) and between methionine on R1 and threonine on R1′ (Roberts et al., 2012). N-terminal combined fractional diagonal chromatography (COFRADIC) was used to identify the preferred cleavage sites of the three *Synechocystis* 6803 proteases (Lam et al., 2015). Analysis of the neo N-termini produced by the single recombinant peptidases resulted in about 3000 cleavage sites for SynHhoA or SynHtrA, while SynHhoB only produced circa 700 cleavage sites. Statistical analysis of neo N-termini and their proteins showed that all three peptidases prefer to cleave sites with hydrophobic residues. The cleavage sites varied by one to two amino acids within one target showing a low cleavage site specificity of *Synechocystis* 6803 SynDeg peptidases. Highest probability for a cleavage of all three SynDeg proteases was between valine or alanine at P1, and alanine or serine at P1′. Hydrophobic residues were also preferred at positions P2–P4, while glycine and negatively charged amino acids at P1 and arginine at R1′ were unfavored. While analyses of cleavage sites specificities give insights to substrate preference, real substrates cannot be predicted by this information, several thousands of proteins would fit the profile. Furthermore, compartmentation, proximity of substrate and peptidase, activity state of peptidase, and folding state of a protein determine its fate as a possible substrate.

Identifying a protease substrate is fundamental for understanding its biological role. Using proteomics, two types of strategies are employed: gel-based strategies that rely on visual detection of accumulating protein spots in a protease-depleted mutant background (Ünlü et al., 1997; Miranda et al., 2013; Cheregi et al., 2015; Lam et al., 2015) and gel-free strategies that rely on the identification of cleavage products from complex mixtures of proteins that are digested in a solution (Gevaert and Vandekerckhove, 2004; Lam et al., 2015). The 2D DIGE method has been used to identify protein

substrates both in single SynDeg deletion mutants (Lam et al., 2015) and in a triple SynDeg deletion mutant (Miranda et al., 2013; Cheregi et al., 2015). Interpretation of the results is complicated because proteomic changes can be caused by secondary effects of the missing protease. Proteins therefore can accumulate in the deletion mutant as possible substrates or they could diminish/disappear due to activation of other proteases in an *in vivo* system. Applying the 2D DIGE method to single and triple *Syn-deg* mutants, several proteins were detected to be possible targets of the proteases. The following proteins were observed to accumulate: a GTP cyclohydrolase (Miranda et al., 2013; Cheregi et al., 2015), the pyruvate kinase 2 (Pyk2), two phosphate ABC transporters (SphX and PstB1'), a serine hydroxymethyltransferase (GlyA) and a guanylate (GMP) synthetase (GuaA; Lam et al., 2015) (**Table 1**). Proteins involved in twitching and motility (PilO, PilA) are down-regulated both in single and triple deletion mutants. The triple *Syn-deg* mutant showed defects in its cell wall, consistent with a decreased amount of proteins (RfbD, Slr1534) involved in cell structure (Cheregi et al., 2015). Increased amounts of neo N-termini for type 1 secretion mechanism components and elements for peptidoglycan and outer membrane lipopolysaccharide biosynthesis were also found in the Δ*hhoB* single mutant using COFRADIC (Lam et al., 2015). More in-depth experiments are needed to confirm these hypothetical substrates, however, for one protein there is experimental evidence being a physiological target of *Synechocystis* 6803 SynDegs (Miranda et al., 2013; Lam et al., 2015): the extrinsic PsbO protein of PSII, which is degraded by a recombinant SynDeg protease after reduction by thioredoxin (Roberts et al., 2012).

Secondary effects of protease deletion led to down-regulation of many proteins, with functions in energy metabolism and carbon fixation, photosynthesis, amino acid biosynthesis, stress response and protein quality control (Miranda et al., 2013; Cheregi et al., 2015; Lam et al., 2015). The enzymes Gap2 (Lam et al., 2015), phosphoglycerate kinase, enolase and glpX (Miranda et al., 2013; Cheregi et al., 2015) of the Calvin–Bensson–Basham are down-regulated and negatively affect the production of NADPH. Also, subunits of the ATP synthase (AtpA, AtpD) are down-regulated. Furthermore in the absence of one SynDeg protease other protein quality control factors were differentially regulated (Lam et al., 2015).

Absence of a single SynDeg protease caused opposite effects on the accumulation of some proteins compared to the triple *Syn-deg*-deletion mutant. Pyruvate kinase (Pyk2) and fructose biphosphate aldolase (FbaII) are upregulated in single mutants, while FbaII has been found to be down-regulated in the triple *Syn-deg* mutant, both under normal growth and under stress conditions (Miranda et al., 2013; Cheregi et al., 2015; Lam et al., 2015) pointing to intricate regulatory mechanisms that sense the absence of one or more SynDeg proteases. Sll1306, a putative chitooligosaccharide deacetylase, and ArgC, an enzyme involved in amino acid biosynthesis, are other proteins which are differentially regulated in the single and the triple *Syn-deg* mutant: down-regulated in all single mutants (Lam et al., 2015) and accumulated in the triple mutant (Miranda et al., 2013; Cheregi et al., 2015), while GlyA, a serine hydroxymethyltransferase, with a primary role in folate metabolism, is accumulating in all single *Syn-deg* mutants and is down-regulated in the triple *Syn-deg* mutant.

To identify possible substrates of the *Synechocystis* 6803 SynDeg proteases, a gel-free approach, N-terminal COFRADIC, was performed on *in vivo* and *in vitro* whole cells proteome (Lam et al., 2015). The *in vivo* screening is based on comparing the labeled N-termini of each single *Syn-deg* mutant and WT, while in the *in vitro* approach the N-termini isolated from WT whole cells extracts were compared with and without the addition of one of the recombinant SynDeg proteases (Lam et al., 2015).

Comparing the N-terminal proteome of single *Syn-deg* deletion mutants to wild-type neo N-termini putative substrates should be detectable in wild-type, but not in the mutants. Of the eleven proteins with neo N-termini only in wild-type three proteins also were detected in an *in vitro* COFRADIC approach and therefore might be native substrates of the *Synechocystis* 6803 SynDeg peptidases (Lam et al., 2015): RbcS for SynHhoA, PsbO for SynHhoB as well as for SynHtrA, and Pbp8 for SynHtrA. Comparing the proteomes of single mutants with wild type, deletion of SynHhoA had impact on CO_2 fixation, while the proteomes of Δ*hhoB* and Δ*htrA* pointed to changes in the photosystems, accumulating PsbO, PsaC, and PsaD (Lam et al., 2015). The SynHhoB single mutant seems to be impaired in its ability to take up phosphate as its PstS1 levels are strongly reduced resulting in defective phosphate sensing (Pitt et al., 2010; Lam et al., 2015). Beside the impact of SynHtrA on photosynthetic proteins its deletion also affects a member of a penicillin-binding protein Pbp8 (Lam et al., 2015), which has been shown to be important in the final step of cell division together with Pbp5 (Marbouty et al., 2009).

PSII DEGRADATION

Photosystem II is vulnerable to various abiotic stresses such as light or heat. Most likely triggered by reactive oxygen species the most critical damage occurs in the reaction center protein D1 (PsbA). In higher plants the acceptor-side photoinhibition of PSII induces cleavage of the DE-loop of D1, producing a 23- and a 9 kDa fragment (Aro et al., 1993). However, D1 damage occurs even under low light intensity (Tyystjärvi and Aro, 1996). Weak illumination of PSII is enough to produce cationic radicals at the donor side. Furthermore iron–sulfur centers of cytochrome (Jung and Kim, 1990) or more recently the disruption of the Mn-cluster were suggested to contribute to photoinhibition (Hakala et al., 2005; Ohnishi et al., 2005). Two protease families, FtsH and Deg proteases, contribute to the degradation of photo-damaged D1 in plants. The membrane-bound ATP-dependent metallo-proteases FtsH1 and FtsH5 (type A) and FtsH2 and FtsH8 (type B; Zaltsman et al., 2005) form a hexameric complex to degrade their substrate progressively from the terminal end (Lindahl et al., 1996).

Besides FtsH, Deg1, Deg5, Deg7, and Deg8 are major players in the catabolism of Photosystem II in plants. Cooperative D1 degradation by Deg and FtsH has been observed under photoinhibitory conditions (Kato et al., 2012). AtDeg1 is the

TABLE 1 | Differentially regulated proteins identified by gel based assay (DIGE; Cheregi et al., 2015; Lam et al., 2015) and gel free assay (COFRADIC; Lam et al., 2015) comparing WT *Synechocystis* 6803 with the single mutants Δ*hhoA*, Δ*hhoB,* and Δ*htrA* or the triple Deg mutant (Δ*deg*), grown at normal conditions.

Method	ΔHhoA		ΔHhoB		ΔHtrA		Δdeg	
	Up	down	Up	Down	Up	Down	Up	Down
Gel based assay (DIGE)	Pyk2 Slr0105	UtrA Gap2 Sll1358 LexA Sll1306	Pyk2 SphX PstP1 **GlyA**	**PstS1** UtrA LexA PilA1 **PilO**	Pyk2 **GlyA** AhcY GuA ClpC Slr0105	UrtA Sll1358 LexA Sll1306 **PilO**	NdhI FolE Sll1306 PrsA Gst1 Sll1530	RfbD GlpX Slr1534
Gel-free Assay (COFRADIC)	SucD CpcB Slr1410		Sll0180 **PstS1** **PsbO**	**Sll0141** HlyD PilJ FutA2 LpxA HlyA FrpC Gua Pds **FabF**	PilQ Pbp8 **PsbO** CcmM Sll0274	**Sll0141** MrgA **FabF**	-	-

Underlined are proteins found to be differentially regulated in at least three mutant strains; proteins differentially regulated in at least two mutant strains are shown bold. Only those proteins were considered that were at least two times up- or down-regulated. In the COFRADIC assay, only proteins with more than 100 N-termini were included.

best characterized HtrA-family member. The protease activity of AtDeg1 leads to the specific cleavage of an exposed loop of photodamaged D1 by the concerted action of other thylakoid proteases (Kapri-Pardes et al., 2007), for reviews, see (Edelman and Mattoo, 2008; Huesgen et al., 2009). D1 fragmentation generated by AtDeg1 was found to be enhanced in mutants lacking FtsH2 in *Arabidopsis* (Kato et al., 2015) and *Chlamydomonas* (Malnoë et al., 2014). Interestingly, AtDeg1 protease is selectively activated under light-stress conditions, during which acidification of the thylakoid lumen occurs and photosynthetic proteins are damaged (Ströher and Dietz, 2008). The importance of AtDeg1 in PSII repair was supported by the finding that this protein also acts as chaperone, assisting in the assembly and biogenesis of PSII by interacting with the PSII reaction center protein D2 (Sun et al., 2010). AtDeg5 and AtDeg8 were shown to form hetero-oligomeric complexes with a 1:1 stoichiometry (Sun et al., 2007). *At-deg5*, *At-deg8*, and even stronger *At-deg5*/*At-deg8* knock-out mutants of *Arabidopsis* displayed growth inhibition under high light conditions. Pulse-chase experiments visualized the D1 turnover to be impaired in these mutants. AtDeg5 was further shown to be involved in plant development and degradation of PsbF (Cyt b_{559}) after wounding (Lucínski et al., 2011). Even recombinant AtDeg7 was able to degrade D1, D2, CP43, and CP47 after high light pre-treatment of *Arabidopsis* thylakoids. Analysis of *At-deg7* knock-out plants revealed that they were impaired in growth compared to wild-type plants. This effect was even more pronounced in *At-deg7*/*At-deg5* and *At-deg7*/*At-deg8*, but not in *At-deg7*/*At-deg2* mutants (Sun et al., 2010).

Despite indirect evidence for an involvement of SynDeg proteases in D1 degradation in *Synechocystis* 6803 (Silva et al., 2002; Kanervo et al., 2003), the D1 degradation mechanism seems to differ in plants and cyanobacteria (Nixon et al., 2005; Komenda et al., 2007; Yamamoto et al., 2008). Instead, SynHhoA might be involved in the degradation of D1 protein cross-links (Funk and Adamska, unpublished). Damaged D1 protein aggregates with nearby polypeptides, such as D2, Cyt b_{559}, and/or CP43 (Lupínková and Komenda, 2004; Komayama et al., 2007) for review, see (Yamamoto et al., 2008). Binding of the extrinsic PsbO protein to Photosystem II has shown to play a regulatory role in directing the damaged D1 protein to degradation or aggregation (Yamamoto et al., 2008). Earlier studies have shown that aggregates of the D1 protein are digested by a stromal serine-type protease (Ishikawa et al., 1999; Ferjani et al., 2001). In pull-down assays all three SynDeg proteases were co-isolated with Photosystem II in sub-stoichiometric amounts (Roberts et al., 2012). Alternatively, the plasma membrane of cyanobacteria may also be a site for D1 degradation and PSII repair (Huang et al., 2002a).

Proteomic comparisons of wild-type *Synechocystis* 6803 cells with single or multiple SynDeg deletion mutants grown under normal (Cheregi et al., 2015; Lam et al., 2015) or stress (Miranda et al., 2013) conditions did not point to an involvement of the SynDeg proteases in D1 degradation, however, the hydrophobic D1 protein might have escaped detection. Instead, biochemical studies showed PsbO to be a substrate of the combined action of SynHhoB/SynHtrA (Lam et al., 2015, see previous paragraph) or under reduced conditions of SynHhoA (Roberts et al., 2012). Even AtDeg1 from *Arabidopsis* was able to degrade this thylakoid lumen protein *in vitro* (Chassin et al., 2002) and *in vivo* (Li et al., 2010). The extrinsic PsbO, PsbP, and PsbQ proteins as well as Mn are released from their binding sites by heat stress (Yamamoto and Nishimura, 1983). Even though PsbO is a highly stable protein (Hashimoto et al., 1996), it is oxidatively damaged under light stress (Henmi et al., 2004).

SynHhoA and SynHtrA Deg proteases have further been shown to be able to degrade *in vitro* the cyanobacterial phycobilisome (Diao et al., 2011) as well as plant light harvesting antenna proteins. AtDeg1 stimulated cleavage of the minor light-harvesting proteins CP26 (Lhcb5) and CP29 (Lhcb4) as well as PsbS (Zienkiewicz et al., 2012). Degradation of CP24 (Lhcb6) was impaired in *Arabidopsis At-deg2* knock-out mutants under short-term stress (salt, wounding, high temperature, and high irradiance; Lucínski et al., 2011).

CYANOBACTERIAL DEG PROTEASES HAVE IMPACT ON THE CELL SURFACE AND MIGHT BE INVOLVED IN SECRETION

The roles of Deg proteases in quality control in the periplasm and at the cell surface are well documented for *E. coli* and many strains of pathogenic bacteria. Also in cyanobacteria, their emerging functions are related to the modification of the outer cell layers (Barker et al., 2006; Cheregi et al., 2015; Lam et al., 2015) and even to the modification of secreted compounds (Cheregi et al., 2015). The triple *Syn-deg*-deletion mutant (Δ*deg*) is affected in phototaxis, probably due to disturbances in pilus biogenesis or in the phototaxis sensory pathways (Barker et al., 2006). Our recent investigation has shown that the intactness of the outermost cell layer, the S-layer, is compromised in this mutant. This hydrophilic layer apparently is absent in Δdeg, consistent with the observed down-regulation of the enzyme GDP-D mannose dehydratase, which affects the synthesis of fucose, mannose and talose (Mohamed et al., 2005; Cheregi et al., 2015). These sugars are components of the glycoproteins of the S-layer and they are also components of secreted exopolysaccharides. Additional evidence supporting the role of SynDeg proteases in the maintenance of extracytoplasmatic properties was obtained in proteomics experiments, demonstrating many proteins related to motility (PilA1, PilJ, PilN, PilO, PilT, and PilQ; Miranda et al., 2013; Cheregi et al., 2015; Lam et al., 2015) and outer cell layer composition (HlyA, Pbp8, Sll1306, Slr1534; Miranda et al., 2013; Cheregi et al., 2015; Lam et al., 2015) to be affected by the deletion of one or all *Syn-deg* genes. As mentioned above, Pbp8, a probable D-alanyl-D-alanine carboxypeptidase with a role in peptidoglycan biosynthesis, is a potential physiological substrate of HtrA (Lam et al., 2015). Two of the most abundant secreted proteins in *Synechocystis* 6803, the hemolysin HlyA and an iron (III) transporter FutA2 (Gao et al., 2014) are much stronger degraded in Δ*hhoB* compared to wild type. In general an increased degradation of secreted proteins was observed in the absence of SynDeg proteases (Cheregi et al., 2015; Lam et al., 2015). Inefficient secretion might induce the higher degradation rate by other proteases in the mutant. Similar to pathogenic strains (Biswas and Biswas, 2005), in *Synechocystis* 6803 SynHhoB (and even SynHtrA and/or SynHhoA) might work as chaperones in the periplasm protecting the cell from aggregated proteins (Lam et al., 2015).

Few glycolytic enzymes with altered expression in the single or triple *Syn-deg* deletion mutants are known to be secreted both, in cyanobacteria (Hahn et al., 2014; Vilhauer et al., 2014; Cheregi et al., 2015) and pathogenic bacteria (reviewed by Henderson and Martin, 2011). Despite lacking any identifiable secretion signal these glycolytic enzymes (enolase, phosphoglycerate kinase, fructose-biphosphate aldolase) have been found to be associated with the surface of bacteria where they exhibit non-glycolytic functions (Henderson and Martin, 2011; Mani et al., 2015). The ability of a protein to have more than one biological function has been termed "moonlighting." Moonlighting activity depends on the presence of more than one biochemical active site on a protein and may occur only at a cellular location different from the one where the protein is commonly found (Henderson and Martin, 2011). Besides the described impact on metabolism, deletion of one or all SynDeg protease(s) could affect moonlighting functions of other enzymes, e.g., these glycolytic enzymes.

Our hypothesis that the *Synechocystis* 6803 SynDeg proteases function in remodeling the cell exterior is emphasized by the finding that all three proteases are secreted into the media from cells growing in stationary phase. Secretion of SynDeg proteases is part of the virulence mechanism in many pathogenic, Gram-negative bacteria (Biswas and Biswas, 2005; Hoy et al., 2012). However, proteolytic activity in the extracellular media is not an exclusive feature of pathogenic strains: production of extracellular material and acquisition of nutrients require remodeling based on proteolysis (Havarstein et al., 1995).

CHAPERONE ACTIVITY

Intracellular protein concentrations are high leading easily to protein aggregation. Molecular chaperones primarily work as cellular defense factors preventing and averting mutation- and stress-induced accumulation of misfolded and aggregated proteins. These quality control factors distinguish between substrates that can be refolded and damaged proteins that have to be degraded. Deg proteases are of particular interest as many family members combine the dual activities of chaperones and proteases. While other enzymes with combined protease/chaperone function contain special subunits or domains for their chaperone activity (e.g., ClpAP of the Clp protease or the AAA-domain of Lon or FtsH proteases), Deg proteases are ATP-independent and combine their antagonistic functions in the same protein. Their PDZ domains act as gatekeepers (see paragraph above) and in this way permit a direct coupling of substrate-binding and subsequent translocation into the inner chamber, which seems to be highly important for the chaperone activity.

In *E. coli* this dual function as chaperone and protease has been shown to be tightly regulated (Spiess et al., 1999; Clausen et al., 2002). *In vitro* studies demonstrated a temperature-switch between the two functions (Spiess et al., 1999); EcDegP acts as a chaperone at temperatures below 28°C, whereas it has protease activity at higher temperatures. The switch in activity should mainly depend on the interplay of loops LA and L2. Especially, an extended L2 loop seems to be required for protease inhibition (Clausen et al., 2002). The physiological relevance of EcDegP acting as chaperone has been supported *in vivo* (Clausen et al., 2002). Tight control of chaperone and protease function is of pivotal importance in preventing deleterious HtrA protease activity (for review, see Hansen and Hilgenfeld, 2013). The chaperone/protease regulation therefore is archived not only by temperature: Since the expression of *Ec-deg*P is regulated by σ^E, which in turn is activated by EcDegS, the concerted action of EcDegS and EcDegP permits recognition and relief of periplasmic protein-folding stress. Under non-stressed

conditions, EcDegP encapsulates folded monomers of outer-membrane proteins and participates in guiding them through the periplasm protecting them from proteolytic degradation during their passage through the periplasm (Sawa et al., 2011). It further promotes folding of proteins (Spiess et al., 1999) and prevents aggregation of misfolded ones (Shen et al., 2009).

Even EcDegQ is combining chaperone and protease activities (Wrase et al., 2011). Single particle cryo-EM data visualized up to six substrates densely bound inside a EcDegQ 12-mer, their PDZ-domains located adjacent to substrate density (Malet et al., 2012). The EcDegQ cage assembly is triggered by substrate binding. Chaperone activity has further been shown for HtrA of yeast (Ynm3 or Nma111; Padmanabhan et al., 2009), of *Chlamydia trachomatis* (Huston et al., 2011) and plant AtDeg1 (Sun et al., 2010), while human HtrA2/Omi has been shown to display protease activity at room temperature (Savopoulos et al., 2000).

In *Synechocystis* 6803 a temperature switch between chaperone- and protease function has not been observed (Huesgen et al., 2011). However, recombinant SynHhoB, which has very low proteolytical activity (Huesgen et al., 2011; Lam et al., 2015), was able to assist folding of denatured MalS at normal temperature (Lam et al., 2015). Absence of HhoB in a *Synechocystis* 6803 mutant leads to different expression of several periplasmic proteins, especially transporters or signaling components (Lam et al., 2015). Chaperones are known to be important for protein secretion (Gottesman, 1996). The location of SynHhoB in the plasma membrane (Roberts et al., 2012) and the co-expression of its corresponding gene with a wide range of periplasmic proteins (Miranda et al., 2013) support its function within secretion. SynHhoB itself is secreted in cultures growing in the stationary phase (Cheregi et al., 2015). Notably, many proteins differentially regulated in a *Syn-hhoB*-deletion mutant are predicted to enter the periplasm in an unfolded state through the general secretory (SEC) pathway (Lam et al., 2015). Interesting is the fact that during stress *in vivo* SynHhoB activity seems to be tightly connected to SynHtrA activity. The down-regulation of the chaperone SynHhoB accompanied by an up-regulation of the protease SynHtrA (Lam et al., 2015) during stress make it tempting to speculate about a hetero-oligomeric unit of SynHhoB/SynHtrA, which switches function from chaperone to protease similar to the temperature switch observed for the homo-oligomeric EcDegP in *E. coli* or HtrA in *Thermotoga maritima* (Spiess et al., 1999; Kim et al., 2003). A similar thermal shift even was observed between two forms of SynHhoA with slightly different molecular mass (Lam et al., 2015); the amount of SynHhoA with higher molecular mass increased, whereas the lower molecular mass form decreased during heat stress. Further studies on the chaperone functions of the three cyanobacterial SynDeg proteases are necessary to gain more insight.

FUTURE PERSPECTIVES

Deg proteases are important ATP-independent quality-control factors. Members from the Deg family in *H. sapiens* were associated with different cancer types, Parkinson's and Alzheimer's diseases. Many pathogenic bacteria strains lacking the Deg/HtrA function lose virulence or their virulence is decreased due to an increased vulnerability to stresses or to a decrease in secretion of virulence factors. In some prokaryotes, including *Synechocystis* 6803, Deg proteases are secreted outside the cell. Thus, the HtrA proteases of bacterial pathogens are relevant targets for new therapeutic approaches as they promote the pathogen's invasiveness. Their ability to control the cell surface in *Synechocystis* 6803 might be usefull for the production of green energy and higher value products in cyanobacteria. In photosynthetic organisms, the Deg proteases have been shown to be important for quality control of Photosystem II and thereby in biomass production.

To fully understand the function of cyanobacterial Deg proteases it is important to unambiguously identify their subcellular localization. Visualizing the Deg proteases *in vivo* by GFP-tagging unfortunately was not successful in our hands (Lam et al., unpublished results). Other approaches, e.g., gold immuno labeling, therefore will be necessary to localize SynHhoA, SynHhoB, and SynHtrA. An important property of *E. coli* Deg proteases is their ability to discriminate between polypeptides that still can be refolded or need to be degraded. This chaperone/proteases switch might even be present in *Synechocystis* 6803, performed by a SynHhoB/SynHtrA heteromer. More work on the chaperone activity of the SynDeg proteases is necessary to understand this phenomenon. For this even structural details of cyanobacterial homo- or hetero-oligomers will be needed. Finally, the search for additional native substrates and regulators will contribute to our understanding of this fascinating protease family.

METHODS

Alignment

All analyzed sequences derived from CyanoBase (Nakamura et al., 1998). Mature sequences from *Synechocystis* sp. PCC 6803 SynDeg proteases were obtained, the predicted signal peptides according to Pred-Tat (Bagos et al., 2010) was excluded. Sequences of mature SynHtrA, SynHhoB, and SynHhoA then were blasted against the Cyanobase database using blastp 2.2.26 (Altschul et al., 1997; Altschul et al., 2005). Candidate sequences with high similarity to the Deg proteases of *Synechocystis* 6803 were screened for the Interproscan domain PR00834 indicating a member of the MEROPS subfamily S1C[2] (Rawlings et al., 2012). The focus was set on species designated as cyanobacteria, gene products lacking PDZ domains were included. The resulting protein list was analyzed via Pred-Tat (Bagos et al., 2010) and predicted signal peptides were excluded. Mature protein sequences were aligned via MUSCLE (Edgar, 2004), gap open -2.9, gap extend 0, hydrophobicity multiplier 1.2, clustering method UPGMP, lambda 24.

[2]http://www.ebi.ac.uk/interpro/interproscan.html

Molecular Phylogenetic Analysis by Maximum Likelihood Method

The evolutionary relationship was inferred by using the Maximum Likelihood method with software PhyML 3.1 (Guindon et al., 2010) based on the Le_Gascuel_2008 model (Le and Gascuel, 2008). The bootstrap consensus tree was inferred from 1000 replicates (Felsenstein, 1985). The initial tree for the heuristic search was obtained by applying the Bio-Neighbor-Joining method. A discrete Gamma distribution was used to model evolutionary rate differences among sites [four categories (gamma shape parameter 0.729)], the analysis involved 124 amino acid sequences. Tree visualization was done in MEGA6 (Tamura et al., 2013). Full taxon names are described in **Supplementary Table S1**. Branches with frequencies equal or higher than 70% were labeled with a black circle.

Homology Modeling

The sequence of mature SynHhoB of *Synechocystis sp.* PCC 6803 or sequences of its domains were analyzed via the Phyre2 web portal for protein modeling, prediction and analysis (Kelley et al., 2015). For modeling the intense mode of Phyre2 was chosen. The *in silico* SynHhoB model formed after the DegQ trimer was chosen (RCSB designator 3STJ; Sawa et al., 2011) to visualize the domain elements. The same model was taken as a template to overlay the SynHhoB models formed after Deg1 (3qo6), Deg2 (4fln), and Deg8 (4ic6). Resulting superpositions were visualized with software Chimera 1.10.2 (Pettersen et al., 2004).

AUTHOR CONTRIBUTIONS

All authors listed, have made substantial, direct and intellectual contribution to the work, and approved it for publication.

ACKNOWLEDGMENTS

This work was supported by grants from the Swedish Energy Agency (Project Number 36641-1 and 38239-1) and the strong research environment "Solar Fuel", Umeå University. RW would like to thank the Sven and Lilli Lawskis foundation for his fellowship.

SUPPLEMENTARY MATERIAL

The Supplementary Material for this article can be found online at: http://journal.frontiersin.org/article/10.3389/fpls.2016.00694

TABLE S1 | Nomenclature information of cyanobacterial strains used in the phylogenetic tree in Figure 1.

TABLE S2 | Summary of Deg genes expression in microarray and RNA sequencing experiments extracted from the Cyanoexpress (Hernandez-Prieto and Futschik, 2012).

REFERENCES

Altschul, S. F., Madden, T. L., Schäffer, A. A., Zhang, J., Zhang, Z., Miller, W., et al. (1997). Gapped BLAST and PSI-BLAST: a new generation of protein database search programs. *Nucleic Acids Res.* 25, 3389–3402. doi: 10.1093/nar/25.17.3389

Altschul, S. F., Wootton, J. C., Gertz, E. M., Agarwala, R., Morgulis, A., Schäffer, A. A., et al. (2005). Protein database searches using compositionally adjusted substitution matrices. *FEBS J.* 272, 5101–5109. doi: 10.1111/j.1742-4658.2005.04945.x

Aro, E.-M., Virgin, I., and Andersson, B. (1993). Photoinhibition of Photosystem II. Inactivation, protein damage and turnover. *Biochim. Biophys. Acta* 1143, 113–134. doi: 10.1016/0005-2728(93)90134-2

Bagos, P. G., Nikolaou, E. P., Liakopoulos, T. D., and Tsirigos, K. D. (2010). Combined prediction of Tat and Sec signal peptides with hidden Markov models. *Bioinformatics* 26, 2811–2817. doi: 10.1093/bioinformatics/btq530

Barker, M., de Vries, R., Nield, J., Komenda, J., and Nixon, P. J. (2006). The Deg proteases protect *Synechocystis* sp. PCC 6803 during heat and light stresses but are not essential for removal of damaged D1 protein during the photosystem two repair cycle. *J. Biol. Chem.* 281, 30347–30355. doi: 10.1074/jbc.M601064200

Baud, C., Hodak, H., Willery, E., Drobecq, H., Locht, C., Jamin, M., et al. (2009). Role of DegP for two-partner secretion in *Bordetella*. *Mol. Microbiol.* 74, 315–329. doi: 10.1111/j.1365-2958.2009.06860.x

Biswas, S., and Biswas, I. (2005). Role of HtrA in surface protein expression and biofilm formation by *Streptococcus mutans*. *Infect. Immun.* 73, 6923–6934. doi: 10.1128/iai.73.10.6923-6934.2005

Calteau, A., Fewer, D., Latifi, A., Coursin, T., Laurent, T., Jokela, J., et al. (2014). Phylum-wide comparative genomics unravel the diversity of secondary metabolism in cyanobacteria. *BMC Genomics* 15:977. doi: 10.1186/1471-2164-15-977

Cassone, M., Gagne, A. L., Spruce, L. A., Seeholzer, S. H., and Sebert, M. E. (2012). The HtrA protease from *Streptococcus pneumoniae* digests both denatured proteins and the competence-stimulating peptide. *J. Biol. Chem.* 287, 38449–38459. doi: 10.1074/jbc.M112.391482

Chassin, Y., Kapri-Pardes, E., Sinvany, G., Arad, T., and Adam, Z. (2002). Expression and characterization of the thylakoid lumen protease DegP1 from *Arabidopsis*. *Plant Physiol.* 130, 857–864. doi: 10.1104/pp.007922

Cheregi, O., Miranda, H., Gröbner, G., and Funk, C. (2015). Inactivation of the Deg protease family in the cyanobacterium *Synechocystis* sp. PCC 6803 has impact on the outer cell layers. *J. Photochem. Photobiol. B Biol.* 152, 383–394. doi: 10.1016/j.jphotobiol.2015.05.007

Clausen, T., Kaiser, M., Huber, R., and Ehrmann, M. (2011). HTRA proteases: regulated proteolysis in protein quality control. *Nat. Rev. Mol. Cell Biol.* 12, 152–162. doi: 10.1038/nrm3065

Clausen, T., Southan, C., and Ehrmann, M. (2002). The HtrA family of proteases: implications for protein composition and cell fate. *Mol. Cell* 10, 443–455. doi: 10.1016/S1097-2765(02)00658-5

Diao, H., Ting, Z., Juang, Z., Kaihong, Z., Ming, Z., and Cheng, Y. (2011). Heterogenous expression of *Synechocystis* sp. PCC 6803 Deg proteases and their possible roles on phycobiliprotein degradation in vitro Journal of Wuhan University of Technology-Matter. *Sci. Ed. Dec.* 2011, 1049–1059.

Edelman, M., and Mattoo, A. (2008). D1-protein dynamics in photosystem II: the lingering enigma. *Photosyn. Res.* 98, 609–620. doi: 10.1007/s11120-008-9342-x

Edgar, R. C. (2004). MUSCLE: multiple sequence alignment with high accuracy and high throughput. *Nucleic Acids Res.* 32, 1792–1797. doi: 10.1093/nar/gkh340

Felsenstein, J. (1985). Confidence limits on phylogenies: an approach using the bootstrap. *Evolution (N. Y.)* 39, 783–791. doi: 10.2307/2408678

Ferjani, A., Abe, S., Ishikawa, Y., Henmi, T., Yuka, T., Nishi, Y., et al. (2001). Characterization of the stromal protease(s) degrading the cross-linked products of the D1 protein generated by photoinhibition of photosystem II. *Biochim. Biophys. Acta* 1503, 385–395. doi: 10.1016/S0005-2728(00)00233-4

Fulda, S., Huang, F., Nilsson, F., Hagemann, M., and Norling, B. (2000). Proteomics of *Synechocystis* sp. strain PCC 6803. *Eur. J. Biochem.* 267, 5900–5907. doi: 10.1046/j.1432-1327.2000.01642.x

Fulda, S., Mikkat, S., Huang, F., Huckauf, J., Marin, K., Norling, B., et al. (2006). Proteome analysis of salt stress response in the cyanobacterium *Synechocystis* sp. strain PCC 6803. *Proteomics* 6, 2733–2745. doi: 10.1002/pmic.200500538

Gao, L., Huang, X., Ge, H., Zhang, Y., Kang, Y., Fang, L., et al. (2014). Profiling and compositional analysis of the exoproteome of *Synechocystis* Sp. *PCC* 6803. *J. Metabol. Sys. Biol.* 1:8.

Garcia-Lorenzo, M., Sjodin, A., Jansson, S., and Funk, C. (2006). Protease gene families in *Populus* and *Arabidopsis*. *BMC Plant Biol.* 6:30. doi: 10.1186/1471-2229-6-30

Gevaert, K., and Vandekerckhove, J. (2004). COFRADIC^{TM}: the Hubble telescope of proteomics. *Drug Discov. Today* 3, 16–22. doi: 10.1016/S1741-8372(04)02416-8

Gottesman, S. (1996). Proteases and their targets in *Escherichia coli*. *Annu. Rev. Genet.* 30, 465–506. doi: 10.1146/annurev.genet.30.1.465

Guindon, S., Dufayard, J.-F., Lefort, V., Anisimova, M., Hordijk, W., and Gascuel, O. (2010). New algorithms and aethods to estimate maximum-likelihood phylogenies: assessing the performance of PhyML 3.0. *Syst. Biol.* 59, 307–321. doi: 10.1093/sysbio/syq010

Hahn, A., Stevanovic, M., Brouwer, E., Bublak, D., Tripp, J., Schorge, T., et al. (2014). Secretome analysis of *Anabaena* sp. PCC 7120 and the involvement of the TolC-homologue HgdD in protein secretion. *Environ. Microbiol.* 17, 767–780. doi: 10.1111/1462-2920.12516

Hakala, M., Tuominen, I., Keränen, M., Tyystjärvi, T., and Tyystjärvi, E. (2005). Evidence for the role of the oxygen-evolving manganese complex in photoinhibition of Photosystem II. *Biochim. Biophys. Acta* 1706, 68–80. doi: 10.1016/j.bbabio.2004.09.001

Hansen, G., and Hilgenfeld, R. (2013). Architecture and regulation of HtrA-family proteins involved in protein quality control and stress response. *Cell. Mol. Life Sci.* 70, 761–775. doi: 10.1007/s00018-012-1076-4

Hashimoto, A., Yamamoto, Y., and Steven, T. M. (1996). Unassembled subunits of the photosynthetic oxygen-evolving complex present in the thylakoid lumen are long-lived and assembly-competent. *FEBS Lett.* 391, 29–34. doi: 10.1016/0014-5793(96)00686-2

Havarstein, L. S., Diep, D. B., and Nes, I. F. (1995). A family of bacteriocin ABC transporters carry out proteolytic processing of their substrates concomitant with export. *Mol. Microbiol.* 16, 229–240. doi: 10.1111/j.1365-2958.1995.tb02295.x

Helm, M., Lück, C., Prestele, J., Hierl, G., Huesgen, P. F., Fröhlich, T., et al. (2007). Dual specificities of the glyoxysomal/peroxisomal processing protease Deg15 in higher plants. *Proc. Natl. Acad. Sci. U.S.A.* 104, 11501–11506. doi: 10.1073/pnas.0704733104

Henderson, B., and Martin, A. (2011). Bacterial virulence in the moonlight: multitasking bacterial moonlighting proteins are virulence determinants in infectious disease. *Infect. Immun.* 79, 3476–3491. doi: 10.1128/IAI.00179-11

Henmi, T., Miyao, M., and Yamamoto, Y. (2004). Release and reactive-oxygen-mediated damage of the oxygen-evolving complex subunits of PSII during photoinhibition. *Plant Cell Physiol.* 45, 243–250. doi: 10.1093/pcp/pch027

Hernandez-Prieto, M. A., and Futschik, M. E. (2012). CyanoEXpress: a web database for exploration and visualisation of the integrated transcriptome of cyanobacterium *Synechocystis* sp. PCC 6803. *Bioinformation* 8, 634–638. doi: 10.6026/97320630008634

Houot, L., Floutier, M., Marteyn, B., Michaut, M., Picciocchi, A., Legrain, P., et al. (2007). Cadmium triggers an integrated reprogramming of the metabolism of *Synechocystis* PCC 6803, under the control of the Slr1738 regulator. *BMC Genomics* 8:350. doi: 10.1186/1471-2164-8-350

Hoy, B., Geppert, T., Boehm, M., Reisen, F., Plattner, P., Gadermaier, G., et al. (2012). Distinct roles of secreted HtrA proteases from gram-negative pathogens in cleaving the junctional protein and tumor suppressor E-cadherin. *J. Biol. Chem.* 287, 10115–10120. doi: 10.1074/jbc.C111.333419

Hoy, B., Löwer, M., Weydig, C., Carra, G., Tegtmeyer, N., Geppert, T., et al. (2010). *Helicobacter* pylori HtrA is a new secreted virulence factor that cleaves E-cadherin to disrupt intercellular adhesion. *EMBO Rep.* 11, 798–804. doi: 10.1038/embor.2010.114

Huang, F., Fulda, S., Hagemann, M., and Norling, B. (2006). Proteomic screening of salt-stress-induced changes in plasma membranes of *Synechocystis* sp. strain PCC 6803. *Proteomics* 6, 910–920. doi: 10.1002/pmic.200500114

Huang, F., Hedman, E., Funk, C., Kieselbach, T., Schröder, W. P., and Norling, B. (2004). Isolation of outer membrane of Synechocystis sp. PCC 6803 and its proteomic characterization. *Mol. Cell. Proteomics* 3, 586–595. doi: 10.1074/mcp.M300137-MCP200

Huang, F., Parmryd, I., Nilsson, F., Persson, A. L., Pakrasi, H. B., Andersson, B., et al. (2002a). Proteomics of *Synechocystis* sp. strain PCC 6803: Identification of plasma membrane proteins. *Mol. Cell. Proteomics* 1, 956–966. doi: 10.1074/mcp.M200043-MCP200

Huang, L., McCluskey, M. P., Ni, H., and LaRossa, R. A. (2002b). Global gene expression profiles of the cyanobacterium *Synechocystis* sp. strain PCC 6803 in response to irradiation with UV-B and white light. *J. Bacteriol.* 184, 6845–6858. doi: 10.1128/jb.184.24.6845-6858.2002

Huesgen, P. F., Miranda, H., Lam, X., Perthold, M., Schuhmann, H., Adamska, I., et al. (2011). Recombinant Deg/HtrA proteases from *Synechocystis* sp. PCC 6803 differ in substrate specificity, biochemical characteristics and mechanism. *Biochem. J.* 435, 733–742. doi: 10.1042/BJ20102131

Huesgen, P. F., Schuhmann, H., and Adamska, I. (2009). Deg/HtrA proteases as components of a network for photosystem II quality control in chloroplasts and cyanobacteria. *Res. Microbiol.* 160, 726–732. doi: 10.1016/j.resmic.2009.08.005

Huston, W. M., Tyndall, J. D. A., Lott, W. B., Stansfield, S. H., and Timms, P. (2011). Unique residues involved in activation of the multitasking protease/chaperone HtrA from *Chlamydia trachomatis*. *PLoS ONE* 6:e24547. doi: 10.1371/journal.pone.0024547

Ishikawa, Y., Nakatani, E., Henmi, T., Ferjani, A., Harada, Y., Tamura, N., et al. (1999). Turnover of the aggregates and cross-linked products of the D1 protein generated by acceptor-side photoinhibition of photosystem II. *Biochim. Biophys. Acta* 1413, 147–158. doi: 10.1016/S0005-2728(99)00093-6

Jansén, T., Kidron, H., Taipaleenmäki, H., Salminen, T., and Mäenpää, P. (2005). Transcriptional profiles and structural models of the *Synechocystis* sp. PCC 6803 Deg proteases. *Photosynth. Res.* 84, 57–63. doi: 10.1007/s11120-005-0475-x

Jung, J., and Kim, H.-S. (1990). The *Chromophores as endogenous* sensitizers involved in the photogeneration of singlet oxygen in spinach thylakoids. *Photochem. Photobiol.* 52, 1003–1009. doi: 10.1111/j.1751-1097.1990.tb01817.x

Kanervo, E., Spetea, C., Nishiyama, Y., Murata, N., Andersson, B., and Aro, E.-M. (2003). Dissecting a cyanobacterial proteolytic system: efficiency in inducing degradation of the D1 protein of photosystem II in cyanobacteria and plants. *Biochim. Biophys. Acta* 1607, 131–140. doi: 10.1016/j.bbabio.2003.09.007

Kanesaki, Y., Suzuki, I., Allakhverdiev, S. I., Mikami, K., and Murata, N. (2002). Salt stress and hyperosmotic stress regulate the expression of different sets of genes in *Synechocystis* sp. PCC 6803. *Biochem. Biophys. Res. Commun.* 290, 339–348. doi: 10.1006/bbrc.2001.6201

Kapri-Pardes, E., Naveh, L., and Adam, Z. (2007). The thylakoid lumen protease Deg1 is involved in the repair of photosystem II from photoinhibition in *Arabidopsis*. *Plant Cell* 19, 1039–1047. doi: 10.1105/tpc.106.046573

Kato, Y., Ozawa, S.-I., Takahashi, Y., and Sakamoto, W. (2015). D1 fragmentation in photosystem II repair caused by photo-damage of a two-step model. *Photosyn. Res.* 126, 409–416. doi: 10.1007/s11120-015-0144-7

Kato, Y., Sun, X., Zhang, L., and Sakamoto, W. (2012). Cooperative D1 degradation in the photosystem II repair mediated by chloroplastic proteases in *Arabidopsis*. *Plant Physiol.* 159, 1428–1439. doi: 10.1104/pp.112.199042

Kelley, L. A., Mezulis, S., Yates, C. M., Wass, M. N., and Sternberg, M. J. E. (2015). The Phyre2 web portal for protein modeling, prediction and analysis. *Nat. Protoc.* 10, 845–858. doi: 10.1038/nprot.2015.053

Kettler, G. C., Martiny, A. C., Huang, K., Zucker, J., Coleman, M. L., Rodrigue, S., et al. (2007). Patterns and implications of gene gain and loss in the evolution of *Prochlorococcus*. *PLoS Genet.* 3:e231. doi: 10.1371/journal.pgen.0030231

Kieselbach, T., and Funk, C. (2003). The family of Deg/HtrA proteases: from *Escherichia coli* to *Arabidopsis*. *Physiol. Plant.* 119, 337–346. doi: 10.1034/j.1399-3054.2003.00199.x

Kim, D. Y., Kim, D. R., Ha, S. C., Lokanath, N. K., Lee, C. J., Hwang, H.-Y., et al. (2003). Crystal structure of the protease domain of a heat-shock protein HtrA from *Thermotoga maritima*. *J. Biol. Chem.* 278, 6543–6551. doi: 10.1074/jbc.M208148200

Kim, D. Y., and Kim, K. K. (2005). Structure and function of HtrA family proteins, the key players in protein quality control. *BMB Rep.* 38, 266–274.

Kim, E., and Sheng, M. (2004). PDZ domain proteins of synapses. *Nat. Rev. Neurosci.* 5, 771–781. doi: 10.1038/nrn1517

Kley, J., Schmidt, B., Boyanov, B., Stolt-Bergner, P. C., Kirk, R., Ehrmann, M., et al. (2011). Structural adaptation of the plant protease Deg1 to repair photosystem II during light exposure. *Nat. Struct. Mol. Biol.* 18, 728–731. doi: 10.1038/nsmb.2055

Kolmar, H., Waller, P. R., and Sauer, R. T. (1996). The DegP and DegQ periplasmic endoproteases of *Escherichia coli*: specificity for cleavage sites and substrate conformation. *J. Bacteriol.* 178, 5925–5929.

Komayama, K., Khatoon, M., Takenaka, D., Horie, J., Yamashita, A., Yoshioka, M., et al. (2007). Quality control of Photosystem II: cleavage and aggregation of heat-damaged D1 protein in spinach thylakoids. *Biochim. Biophys. Acta* 1767, 838–846. doi: 10.1016/j.bbabio.2007.05.001

Komenda, J., Tichý, M., Prášil, O., Knoppová, J., Kuviková, S., de Vries, R., et al. (2007). The exposed N-terminal tail of the D1 subunit is required for rapid D1 degradation during photosystem II repair in *Synechocystis* sp PCC 6803. *Plant Cell* 19, 2839–2854. doi: 10.1105/tpc.107.053868

Koonin, E. V., and Aravind, L. (2002). Origin and evolution of eukaryotic apoptosis: the bacterial connection. *Cell Death Differ.* 9, 394–404. doi: 10.1038/sj.cdd.4400991

Kopf, M., Klähn, S., Scholz, I., Matthiessen, J. K. F., Hess, W. R., and Voss, B. (2014). Comparative analysis of the primary transcriptome of *Synechocystis* sp. *PCC* 6803. *DNA Res.* 21, 527–539. doi: 10.1093/dnares/dsu018

Krojer, T., Garrido-Franco, M., Huber, R., Ehrmann, M., and Clausen, T. (2002). Crystal structure of DegP (HtrA) reveals a new protease-chaperone machine. *Nature* 416, 455–459. doi: 10.1038/416455a

Krojer, T., Pangerl, K., Kurt, J., Sawa, J., Stingl, C., Mechtler, K., et al. (2008). Interplay of PDZ and protease domain of DegP ensures efficient elimination of misfolded proteins. *Proc. Natl. Acad. Sci. U.S.A.* 105, 7702–7707. doi: 10.1073/pnas.0803392105

Kurian, D., Phadwal, K., and Maenpaa, P. (2006). Proteomic characterization of acid stress response in *Synechocystis* sp PCC 6803. *Proteomics* 6, 3614–3624. doi: 10.1002/pmic.200600033

Lam, X. T., Aigner, H., Timmerman, E., Gevaert, K., and Funk, C. (2015). Proteomic approaches to identify substrates of the three Deg/HtrA proteases of the cyanobacterium *Synechocystis* sp. *PCC* 6803. *Biochem. J.* 468, 373–384. doi: 10.1042/BJ20150097

Le, S. Q., and Gascuel, O. (2008). An improved general amino acid replacement matrix. *Mol. Biol. Evol.* 25, 1307–1320. doi: 10.1093/molbev/msn067

Li, J., Sun, X., and Zhang, L. (2010). Deg1 is involved in the degradation of the PsbO oxygen-evolving protein of photosystem II in *Arabidopsis*. *Chin. Sci. Bull.* 55, 3145–3148. doi: 10.1007/s11434-010-4042-2

Lindahl, M., Tabak, S., Cseke, L., Pichersky, E., Andersson, B., and Adam, Z. (1996). Identification, characterization, and molecular cloning of a homologue of the bacterial FtsH protease in chloroplasts of higher plants. *J. Biol. Chem.* 271, 29329–29334. doi: 10.1074/jbc.271.46.29329

Lipinska, B., Sharma, S., and Georgopoulos, C. (1988). Sequence analysis and regulation of the htrA gene of *Escherichia coli*: a σ32-independent mechanism of heat-inducible transcription. *Nucleic Acids Res.* 16, 10053–10067. doi: 10.1093/nar/16.21.10053

Lucínski, R., Misztal, L., Samardakiewicz, S., and Jackowski, G. (2011). Involvement of Deg5 protease in wounding-related disposal of PsbF apoprotein. *Plant Physiol. Biochem.* 49, 311–320. doi: 10.1016/j.plaphy.2011.01.001

Lupínková, L., and Komenda, J. (2004). Oxidative modifications of the photosystem II D1 protein by reactive oxygen species: from isolated protein to cyanobacterial cells. *Photochem. Photobiol.* 79, 152–162. doi: 10.1111/j.1751-1097.2004.tb00005.x

Malet, H., Canellas, F., Sawa, J., Yan, J., Thalassinos, K., Ehrmann, M., et al. (2012). Newly folded substrates inside the molecular cage of the HtrA chaperone DegQ. *Nat. Struct. Mol. Biol.* 19, 152–157. doi: 10.1038/nsmb.2210

Malnoë, A., Wang, F., Girard-Bascou, J., Wollman, F.-A., and de Vitry, C. (2014). Thylakoid FtsH protease contributes to photosystem II and cytochrome b6f remodeling in *Chlamydomonas reinhardtii* under stress conditions. *Plant Cell* 26, 373–390. doi: 10.1105/tpc.113.120113

Mani, M., Chen, C., Amblee, V., Liu, H., Mathur, T., Zwicke, G., et al. (2015). MoonProt: a database for proteins that are known to moonlight. *Nucleic Acids Res.* 43, D277–D282. doi: 10.1093/nar/gku954

Marbouty, M., Mazouni, K., Saguez, C., Cassier-Chauvat, C., and Chauvat, F. (2009). Characterization of the *Synechocystis* strain PCC 6803 penicillin-binding proteins and cytokinetic proteins FtsQ and FtsW and their network of interactions with ZipN. *J. Bacteriol.* 191, 5123–5133. doi: 10.1128/jb.00620-09

Micallef, M. L., D'Agostino, P. M., Al-Sinawi, B., Neilan, B. A., and Moffitt, M. C. (2015). Exploring cyanobacterial genomes for natural product biosynthesis pathways. *Mar. Genomics* 21, 1–12. doi: 10.1016/j.margen.2014.11.009

Miranda, H., Cheregi, O., Netotea, S., Hvidsten, T. R., Moritz, T., and Funk, C. (2013). Co-expression analysis, proteomic and metabolomic study on the impact of a Deg/HtrA protease triple mutant in *Synechocystis* sp. PCC 6803 exposed to temperature and high light stress. *J. Proteomics* 78, 294–311. doi: 10.1016/j.jprot.2012.09.036

Mohamed, H. E., van de Meene, A. M. L., Roberson, R. W., and Vermaas, W. F. J. (2005). Myxoxanthophyll is required for normal cell wall structure and thylakoid organization in the cyanobacterium *Synechocystis* sp. *strain PCC* 6803. *J. Bacteriol.* 187, 6883–6892. doi: 10.1128/jb.187.20.6883-6892.2005

Mrázek, J., Bhaya, D., Grossman, A. R., and Karlin, S. (2001). Highly expressed and alien genes of the *Synechocystis* genome. *Nucleic Acids Res.* 29, 1590–1601. doi: 10.1093/nar/29.7.1590

Nakamura, Y., Kaneko, T., Hirosawa, M., Miyajima, N., and Tabata, S. (1998). CyanoBase, a www database containing the complete nucleotide sequence of the genome of *Synechocystis* sp. strain PCC 6803. *Nucleic Acids Res.* 26, 63–67. doi: 10.1093/nar/26.1.63

Nickelsen, J., and Rengstl, B. (2013). Photosystem II assembly: from cyanobacteria to plants. *Annu. Rev. Plant Biol.* 64, 609–635. doi: 10.1146/annurev-arplant-050312-120124

Nixon, P. J., Barker, M., Boehm, M., de Vries, R., and Komenda, J. (2005). FtsH-mediated repair of the photosystem II complex in response to light stress. *J. Exp. Bot.* 56, 357–363. doi: 10.1093/jxb/eri021

Ohnishi, N., Allakhverdiev, S. I., Takahashi, S., Higashi, S., Watanabe, M., Nishiyama, Y., et al. (2005). Two-step mechanism of photodamage to photosystem II: step 1 occurs at the oxygen-evolving complex and step 2 occurs at the photochemical reaction center. *Biochemistry* 44, 8494–8499. doi: 10.1021/bi047518q

Ohta, H., Shibata, Y., Haseyama, Y., Yoshino, Y., Suzuki, T., Kagasawa, T., et al. (2005). Identification of genes expressed in response to acid stress in *Synechocystis* sp. PCC 6803 using DNA microarrays. *Photosynth. Res.* 84, 225–230. doi: 10.1007/s11120-004-7761-x

Padmanabhan, N., Fichtner, L., Dickmanns, A., Ficner, R., Schulz, J. B., and Braus, G. H. (2009). The yeast HtrA orthologue Ynm3 is a protease with chaperone activity that aids survival under heat stress. *Mol. Biol. Cell* 20, 68–77. doi: 10.1091/mbc.E08-02-0178

Page, M. J., and Di Cera, E. (2008). Evolution of peptidase diversity. *J. Biol. Chem.* 283, 30010–30014. doi: 10.1074/jbc.M804650200

Pallen, M. J., and Wren, B. W. (1997). The HtrA family of serine proteases. *Mol. Microbiol.* 26, 209–221. doi: 10.1046/j.1365-2958.1997.5601928.x

Pettersen, E. F., Goddard, T. D., Huang, C. C., Couch, G. S., Greenblatt, D. M., Meng, E. C., et al. (2004). UCSF Chimera–a visualization system for exploratory research and analysis. *J. Comput. Chem.* 25, 1605–1612. doi: 10.1002/jcc.20084

Pitt, F. D., Mazard, S., Humphreys, L., and Scanlan, D. J. (2010). Functional characterization of *Synechocystis* sp. strain PCC 6803 pst1 and pst2 gene clusters reveals a novel strategy for phosphate uptake in a freshwater cyanobacterium. *J. Bacteriol.* 192, 3512–3523. doi: 10.1128/JB.00258-10

Rawlings, N. D., Barrett, A. J., and Bateman, A. (2012). MEROPS: the database of proteolytic enzymes, their substrates and inhibitors. *Nucleic Acids Res.* 40, D343–D350. doi: 10.1093/nar/gkr987

Roberts, I. N., Lam, X. T., Miranda, H., Kieselbach, T., and Funk, C. (2012). Degradation of PsbO by the Deg protease HhoA is thioredoxin dependent. *PLoS ONE* 7:e45713. doi: 10.1371/journal.pone.0045713

Savopoulos, J. W., Carter, P. S., Turconi, S., Pettman, G. R., Karran, E. H., Gray, C. W., et al. (2000). Expression, purification, and functional analysis of the human serine protease HtrA2. *Protein Exp. Purificat.* 19, 227–234. doi: 10.1006/prep.2000.1240

Sawa, J., Malet, H., Krojer, T., Canellas, F., Ehrmann, M., and Clausen, T. (2011). Molecular adaptation of the DegQ protease to exert protein quality control in the bacterial cell envelope. *J. Biol. Chem.* 286, 30680–30690. doi: 10.1074/jbc.M111.243832

Schuhmann, H., Huesgen, P., and Adamska, I. (2012). The family of Deg/HtrA proteases in plants. *BMC Plant Biol.* 12:52. doi: 10.1186/1471-2229-12-52

Shen, Q.-T., Bai, X.-C., Chang, L.-F., Wu, Y., Wang, H.-W., and Sui, S.-F. (2009). Bowl-shaped oligomeric structures on membranes as DegP's new functional forms in protein quality control. *Proc. Natl. Acad. Sci. U.S.A.* 106, 4858–4863. doi: 10.1073/pnas.0811780106

Silva, P., Choi, Y. J., Hassan, H. A. G., and Nixon, P. J. (2002). Involvement of the HtrA family of proteases in the protection of the cyanobacterium *Synechocystis* PCC 6803 from light stress and in the repair of photosystem II. *Philos. Trans. R. Soc. Lond. B Biol. Sci.* 357, 1461–1468. doi: 10.1098/rstb.2002.1146

Slabas, A. R., Suzuki, I., Murata, N., Simon, W. J., and Hall, J. J. (2006). Proteomic analysis of the heat shock response in *Synechocystis* PCC 6803 and a thermally tolerant knockout strain lacking the histidine kinase 34 gene. *Proteomics* 6, 845–864. doi: 10.1002/pmic.200500196

Spiess, C., Beil, A., and Ehrmann, M. (1999). A temperature-dependent switch from chaperone to protease in a widely conserved heat shock protein. *Cell* 97, 339–347. doi: 10.1016/S0092-8674(00)80743-6

Ströher, E., and Dietz, K.-J. (2008). The dynamic thiol–disulphide redox proteome of the *Arabidopsis thaliana* chloroplast as revealed by differential electrophoretic mobility. *Physiol. Plant.* 133, 566–583. doi: 10.1111/j.1399-3054.2008.01103.x

Summerfield, T., Eaton-Rye, J., and Sherman, L. (2007). Global gene expression of a ΔPsbO:ΔPsbU mutant and a spontaneous revertant in the cyanobacterium *Synechocystis* sp. strain PCC 6803. *Photosynth. Res.* 94, 265–274. doi: 10.1007/s11120-007-9237-2

Sun, R., Fan, H., Gao, F., Lin, Y., Zhang, L., Gong, W., et al. (2012). Crystal structure of *Arabidopsis* Deg2 protein reveals an internal PDZ ligand locking the hexameric resting state. *J. Biol. Chem.* 287, 37564–37569. doi: 10.1074/jbc.M112.394585

Sun, W., Gao, F., Fan, H., Shan, X., Sun, R., Liu, L., et al. (2013). The structures of *Arabidopsis* Deg5 and Deg8 reveal new insights into HtrA proteases. *Acta Crystallogr. Sect. D* 69, 830–837. doi: 10.1107/S0907444913002023

Sun, X., Ouyang, M., Guo, J., Ma, J., Lu, C., Adam, Z., et al. (2010). The thylakoid protease Deg1 is involved in photosystem-II assembly in *Arabidopsis thaliana*. *Plant J.* 62, 240–249. doi: 10.1111/j.1365-313X.2010.04140.x

Sun, X., Peng, L., Guo, J., Chi, W., Ma, J., Lu, C., et al. (2007). Formation of DEG5 and DEG8 complexes and their involvement in the degradation of photodamaged photosystem II reaction center D1 protein in *Arabidopsis*. *Plant Cell* 19, 1347–1361. doi: 10.1105/tpc.106.049510

Suzuki, I., Simon, W. J., and Slabas, A. R. (2006). The heat shock response of *Synechocystis* sp. PCC 6803 analysed by transcriptomics and proteomics. *J. Exp. Bot.* 57, 1573–1578. doi: 10.1093/jxb/erj148

Tamura, K., Stecher, G., Peterson, D., Filipski, A., and Kumar, S. (2013). MEGA6: molecular evolutionary genetics analysis eersion 6.0. *Mol. Biol. Evol.* 30, 2725–2729. doi: 10.1093/molbev/mst197

Tanz, S. K., Castleden, I., Hooper, C. M., Small, I., and Millar, A. H. (2014). Using the SUBcellular database for *Arabidopsis* proteins to localize the Deg protease family. *Front. Plant Sci.* 5:396. doi: 10.3389/fpls.2014.00396

Tripathi, L., and Sowdhamini, R. (2006). Cross genome comparisons of serine proteases in *Arabidopsis* and rice. *BMC Genomics* 7:200. doi: 10.1186/1471-2164-7-200

Tyystjärvi, E., and Aro, E. M. (1996). The rate constant of photoinhibition, measured in lincomycin-treated leaves, is directly proportional to light intensity. *Proc. Natl. Acad. Sci. U.S.A.* 93, 2213–2218. doi: 10.1073/pnas.93.5.2213

Ünlü, M., Morgan, M. E., and Minden, J. S. (1997). Difference gel electrophoresis. A single gel method for detecting changes in protein extracts. *Electrophoresis* 18, 2071–2077. doi: 10.1002/elps.1150181133

Vilhauer, L., Jervis, J., Ray, W. K., and Helm, R. (2014). The exo-proteome and exo-metabolome of Nostoc punctiforme (*Cyanobacteria*) in the presence and absence of nitrate. *Arch. Microbiol.* 196, 357–367. doi: 10.1007/s00203-014-0974-2

Walsh, N. P., Alba, B. M., Bose, B., Gross, C. A., and Sauer, R. T. (2003). OMP peptide signals initiate the envelope-stress response by activating DegS protease via relief of inhibition mediated by its PDZ domain. *Cell* 113, 61–71. doi: 10.1016/S0092-8674(03)00203-4

Wickner, S., Maurizi, M. R., and Gottesman, S. (1999). Posttranslational quality control: folding, refolding, and degrading proteins. *Science* 286, 1888–1893. doi: 10.1126/science.286.5446.1888

Wilken, C., Kitzing, K., Kurzbauer, R., Ehrmann, M., and Clausen, T. (2004). Crystal structure of the DegS stress sensor: how a PDZ domain recognizes misfolded protein and activates a protease. *Cell* 117, 483–494. doi: 10.1016/S0092-8674(04)00454-4

Wrase, R., Scott, H., Hilgenfeld, R., and Hansen, G. (2011). The Legionella HtrA homologue DegQ is a self-compartmentizing protease that forms large 12-meric assemblies. *Proc. Natl. Acad. Sci. U.S.A.* 108, 10490–10495. doi: 10.1073/pnas.1101084108

Yamamoto, Y., Aminaka, R., Yoshioka, M., Khatoon, M., Komayama, K., Takenaka, D., et al. (2008). Quality control of photosystem II: impact of light and heat stresses. *Photosyn. Res.* 98, 589–608. doi: 10.1007/s11120-008-9372-4

Yamamoto, Y., and Nishimura, M. (1983). *The Oxygen Evolving System of Photosynthesis*. Tokyo: Academic Press.

Zaltsman, A., Ori, N., and Adam, Z. (2005). Two types of FtsH protease subunits are required for chloroplast biogenesis and photosystem II repair in *Arabidopsis*. *Plant Cell* 17, 2782–2790. doi: 10.1105/tpc.105.035071

Zhang, L.-F., Yang, H.-M., Cui, S.-X., Hu, J., Wang, J., Kuang, T.-Y., et al. (2009). Proteomic analysis of plasma membranes of cyanobacterium *Synechocystis* sp. strain PCC 6803 in response to high pH stress. *J. Proteome Res.* 8, 2892–2902. doi: 10.1021/pr900024w

Zienkiewicz, M., Ferenc, A., Wasilewska, W., and Romanowska, E. (2012). High light stimulates Deg1-dependent cleavage of the minor LHCII antenna proteins CP26 and CP29 and the PsbS protein in *Arabidopsis thaliana*. *Planta* 235, 279–288. doi: 10.1007/s00425-011-1505-x

Conflict of Interest Statement: The authors declare that the research was conducted in the absence of any commercial or financial relationships that could be construed as a potential conflict of interest.

frontiers in Plant Science

ORIGINAL RESEARCH
published: 14 June 2016
doi: 10.3389/fpls.2016.00828

The RNA Structure of *cis*-acting Translational Elements of the Chloroplast *psbC* mRNA in *Chlamydomonas reinhardtii*

*Mir Munir A. Rahim[1], Frederic Vigneault[2] and William Zerges[3]**

[1] Department of Microbiology and Immunology, Dalhousie University, Halifax, NS, Canada, [2] Synthetic Biology Platform, Wyss Institute for Biologically Inspired Engineering, Harvard University, Boston, MA, USA, [3] Biology Department and Centre for Structural and Functional Genomics, Concordia University, Montreal, QC, Canada

Photosystem II is the first of two light-driven oxidoreductase complexes in oxygenic photosynthesis. The biogenesis of photosystem II requires the synthesis of polypeptide subunits encoded by the genomes in the chloroplast and the nucleus. In the chloroplast of the green alga *Chlamydomonas reinhardtii*, the synthesis of each subunit requires interactions between the 5′ UTR of the mRNA encoding it and gene-specific translation factors. Here, we analyze the sequences and structures in the 5′ UTR of the *psbC* mRNA, which are known to be required to promote translation and genetic interaction with *TBC1*, a nuclear gene required specifically for *psbC* translation. Results of enzymatic probing *in vitro* and chemical probing *in vivo* and *in vitro* support three secondary structures and reveal that one participates in a pseudoknot structure. Analyses of the effects of mutations affecting pseudoknot sequences, by structural mapping and thermal gradient gel electrophoresis, reveal that flexibility at the base of the major stem-loop is required for translation and higher order RNA conformation, and suggest that this conformation is stabilized by *TBC1*. This RNA pseudoknot tertiary structure is analogous to the internal ribosome entry sites that promote translation of certain viruses and cellular mRNAs in the nuclear-cytoplasmic systems of eukaryotes.

Keywords: photosystem II, secondary structure, stem-loop, dimethyl sulfate, 5′ UTR

OPEN ACCESS

Edited by:
Roman Sobotka,
The Czech Academy of Sciences,
Czech Republic

Reviewed by:
Kateřina Bišová,
Institute of Microbiology of the Czech Academy of Sciences,
Czech Republic
Yves Choquet,
Centre National de la Recherche Scientifique, France

****Correspondence:***
William Zerges
william.zerges@concordia.ca

Specialty section:
This article was submitted to Plant Cell Biology, a section of the journal Frontiers in Plant Science

Received: *30 January 2016*
Accepted: *26 May 2016*
Published: *14 June 2016*

Citation:
Rahim MMA, Vigneault F and Zerges W (2016) The RNA Structure of cis-acting Translational Elements of the Chloroplast psbC mRNA in Chlamydomonas reinhardtii. Front. Plant Sci. 7:828. doi: 10.3389/fpls.2016.00828

INTRODUCTION

In the semiautonomous organelles chloroplasts and mitochondria, the translation of mRNAs, encoding polypeptide subunits of the photosynthetic and respiratory complexes, respectively, requires interactions between their 5′ UTRs and organelle gene-specific translation factors encoded by the nuclear genome. For example, in the chloroplast of the unicellular green alga *Chlamydomonas reinhardtii*, translation of the *psbC* mRNA, encoding the CP43 subunit of photosystem II (PSII), is controlled by interactions between its 547 base 5′ UTR and three nuclear genes: *TBC1*, *TBC2,* and *TBC3*. These *trans*-acting functions were identified from *psbC* translation defects in *tbc1* and *tbc2* mutants, and the ability of a suppressor *tbc3* allele to bypasses the requirement for *TBC1* and *TBC1*-interacting sequences in the *psbC* 5′ UTR (Rochaix et al., 1989; Zerges and Rochaix, 1994; Zerges et al., 1997, 2003). These results support a model in which *TBC1* and *TBC3* conjointly interact with sequences in the *psbC* 5′ UTR to activate translation,

while *TBC2* appears to operate via a distinct mechanism, since mutant *tbc2* alleles do not show these genetic interactions.

Random and site-directed mutagenesis previously allowed the identification of *cis*-acting sequences in the *psbC* 5′ UTR that are required to drive translation and are involved in the *trans*-interactions with *TBC1*, *TBC2,* and *TBC3* (Rochaix et al., 1989; Zerges and Rochaix, 1994; Zerges et al., 1997, 2003). Translation absolutely requires a 100 nt sequence in the center of the 5′ UTR (223–320) and the translation initiation region, including a predicted Shine–Dalgarno sequence and the initiation codon (which is GUG rather than the common AUG) (Zerges et al., 2003). The requirement for this 100 nt central sequence supports its role in translational activation, contrasting the repressive role of most *cis*-acting translational regulatory sequences in diverse model organisms (Zerges and Hauser, 2009). The 100 nt sequence in this central region is predicted to form a large stem-loop (SL) structure *in silico* (Rochaix et al., 1989). *TBC1*, *TBC2,* and *TBC3* act via sequences in the *psbC* 5′ UTR, either directly or indirectly through unknown translation factors (Zerges and Rochaix, 1994; Zerges et al., 1997, 2003). The *TBC1* interaction involves the 100 nt central region because a spontaneous suppressor point mutation therein, *psbC-F34suI*, restores *psbC* translation in the *tbc1* mutant background, and is predicted to destabilize this SL in simulations using the mfold server (Zuker, 2003). The *TBC1* interaction also involves the 200 nt region (positions 321–529) between the predicted SL and the Shine–Dalgarno initiation region (533–538), based on *TBC1*-independence of the low level of translation of 5′ UTR deletion mutant screen of this region (Zerges et al., 2003). *TBC3* acts via two regions of the *psbC* 5′ UTR: one is within the interval 27–222; located 5′ to the central region with the predicted SL, and the other is in the translation initiation region. Two bulges on the stem of this SL are also required, since a mutant lacking them, *psbC-FuD34*, is completely defective of *psbC* translation. The absence of these bulges is predicted *in silico* to stabilize the SL structure (Rochaix et al., 1989). Together, these genetic results support a model in which complete or partial melting of the SL is required for *psbC* translation, and the *TBC1* and *TBC3* interactions are required therein. There is currently no biochemical evidence of this SL or the effects of the mutations in *psbC-F34suI* and *psbC-FuD34* on the structure of the *psbC* 5′ UTR.

TBC2 activates translation of the *psbC* mRNA via 5′ UTR sequences in the interval 391–519 (Zerges et al., 2003) and does not show genetic interactions with *TBC1, TBC3* and the predicted SL (as described above for the latter three). Therefore, *TBC2* appears to function in a distinct step in the activation of *psbC* translation from that involving *TBC1, TBC3*, and the predicted SL (Zerges and Hauser, 2009).

Here we characterize the RNA structure of the *psbC* 5′ UTR by enzymatic probing *in vitro* and chemical probing both *in vitro* and *in vivo*. The results support the formation of the central SL structure with several differences from the structure previously described (Rochaix et al., 1989). These included a smaller apical loop, and additional internal loop and bulge in the stem, and the melting of base-pairs at the base of the stem. In addition, we provide evidence for the formation of a pseudoknot tertiary structure involving the base-pairing of the apical loop of this SL structure with a 3′ sequence element. Finally, we extend our results by *in vivo* chemical probing of the *psbC* mRNA for secondary structure and bound factors in wild-type, *tbc1* and *tbc2* mutant strains. This work begins to extend one of the most extensive genetic analyses of translational control to the biochemical level by revealing experimental evidence in support of a *cis*-acting translational element in the *psbC* 5′ UTR.

MATERIALS AND METHODS

Culture Conditions

Chlamydomonas reinhardtii strains (Supplementary Table S1) were grown in Tris-acetate-phosphate (TAP) medium (Gorman and Levine, 1965) under a light intensity of 50–75 microeinsteins (μE) m^{-2} s^{-1}.

Dimethyl Sulfate (DMS) Treatments and Analyses

Dimethyl sulfate (DMS) treatments of cells and total RNA samples were performed as described previously (Zaug and Cech, 1995; Higgs et al., 1999). RNA was extracted with Tri-Reagent (Sigma) following the manufacturer's protocol. Modified A and C residues were revealed by primer extension reactions from the 5′ end-labeled [^{32}P] oligonucleotide primers (Supplementary Table S2), which had been purified from a 12% non-denaturing polyacrylamide gel, and hybridized to the *psbC* mRNA in total RNA samples in 0.5 M HEPES pH 7.0, 3.0 M NaCl, 3.0 mM EDTA and extended by Superscript II (Invitrogen). Hybridizations were carried out during 5 min at 85°C and the subsequent 90 min when samples cooled to room temperature. During the reverse transcription reactions, the temperature was increased as follows: 25°C, 10 min; 35°C, 10 min, 45°C, 40 min; 55°C, 10 min; 75°C, 15 min. Products were resolved on 8% (w/v) denaturing polyacrylamide gels and visualized by autoradiography. Positions of pause sites were determined from sequencing ladders derived from each [^{32}P]-labeled primer and the *psbC* 5′ UTR in a plasmid vector. The *psbC* 5′ UTR plasmid was constructed by PCR amplification using Primers 1 and 7 (Supplementary Table S2), followed by cloning in pBluescribe at the *Bam*HI and *Sac*I restriction sites (Sambrook and Russell, 2001).

Generation of RNA Substrates for Enzymatic Probing Reactions and Thermal Gradient Gel Electrophoresis (TGGE)

RNAs were transcribed with T7 RNA polymerase from cloned wild-type and mutant *psbC* 5′ UTRs that had been amplified by PCR by the upstream Primer 1 (Supplementary Table S2) and the downstream Primer 5 (Supplementary Table S2). The T7 promoter was introduced 5′ to the UTR and fragments were cloned into pUC19. Similarly, the RNA corresponding to 225 bp of the 3′ UTR was transcribed from a cloned fragment that had been PCR amplified with upstream Primer 2 (Supplementary Table S2) which also contains the T7 promoter and the downstream Primer 3 (Supplementary Table

S2). All DNA fragment inserts were sequenced to exclude the possibility of mutations introduced during PCR. For the enzymatic probing experiments, RNAs were either 5′ end-labelled using T4 polynucleotide kinase (Fermentas) or 3′ end-labeled with T4 phage RNA ligase (Fermentas) and cytidine 3′,5′-(^{32}P)bisphosphate (^{32}P-pCp, Amersham). For TGGE, RNAs were uniformly labeled during synthesis with [α-^{32}P]CTP. Each RNA was purified from an 8% (w/v) denaturing polyacrylamide gel with 8 M urea (Sambrook and Russell, 2001).

A homemade TGGE apparatus was built based on a model described previously (Wartell et al., 1990). The gel had 6% acrylamide/N,N′methylene-bis-acrylamide (60:1) and the running buffer was Tris-borate-EDTA buffer (Sambrook and Russell, 2001). Temperature melting points were measured as previously described by plotting the slope (baseline of each structural states) between two structural transition and identifying the equidistant point (Szewczak et al., 1998).

Digestions with RNase T1 (Fermentas) and RNase V1 (Ambion) were performed with approximately 3×10^5cpm RNA in 10 μl 10 mM Tris [pH 7], 100 mM KCl, 10 mM $MgCl_2$ [Ambion] and either 1μg sheared yeast RNA (10 mg/ml, Ambion) and 1 mU of RNase V1 (1 U/μl, Ambion) for 5 min at 24°C, or 4 μg sheared yeast RNA (Sigma Chemicals) and 500 mU of RNase T1 (100 U/μl, Fermentas) for 2 min at 24°C. Reactions were terminated by addition of 20 μl of precipitation/inactivation buffer (Ambion) and incubation at −20°C for at least 1 h. Products (and undigested substrate) were precipitated with ethanol and resolved by electrophoresis on a 6% denaturing polyacrylamide gel and visualized by autoradiography.

As a molecular weight standard, the 100 bp RNA ladder (Fermentas) was labeled with ^{32}P using T4 polynucleotide kinase and [γ -^{32}P] ATP, and a molecular weight ladder was prepared by heat-treating ^{32}P-labeled RNA (10,000 cpm) with 1.0 μg sheared yeast RNA (Sigma–Aldrich) in 5 μl alkaline hydrolysis buffer (50 mM sodium carbonate/sodium bicarbonate [pH 9.2], 1.0 mM EDTA) for 2 min.

RESULTS

Chemical and Enzymatic Probing *in vitro* Reveals the Base-pairing Status of Nucleotide Residues in the *psbC* 5′ UTR

RNA molecules corresponding to the *psbC* 5′ UTR, with either the wild-type sequence or carrying the mutations *psbC-FuD34* and *psbC-F34suI* (Introduction), were probed *in vitro* for unpaired G residues and base-paired nucleotide residues, using RNase T1 and RNase V1, respectively (Knapp, 1989). Treatment of ^{32}P-labeled RNA substrates with each RNase results in site-specific cleavages, which were resolved by denaturing PAGE and revealed by autoradiography (**Figure 1**). In addition, A and C residues of 5′ UTR and beginning of the coding sequence of the endogenous *psbC* mRNA, were probed for base-pairing with DMS *in vitro* in total RNA preparations. A and C residues that are not base-paired are methylated by DMS, while base-pairing prevents their methylation. DMS-methylated A and C residues were revealed by their ability to block reverse transcription (RT) in primer extension reactions from a ^{32}P-labeled oligonucleotide primer. Seven primers that hybridize to sites across the 5′ UTR were used for this analysis (Primers 4–10, Supplementary Table S2). RNase cleavage sites and DMS methylated bases were mapped using the length of RNase digestion and primer extension products, which correspond to the distance between them and the ^{32}P-labeled end. RNase probing data were obtained between U55 and A523 (**Figure 1**). The mapped sites are shown relative to the sequence in **Figure 2**. RNase V1 cleavage sites were mapped at high resolution at the extremities of this region (A482–A523 and U55–A100) and to within 2–3 nt for the central region (positions G101–A522). RNase T1 cleavages were mapped more precisely because most G residues are sufficiently dispersed in the 5′ UTR to assign each cleavage product to one G. All results were reproducible in at least two independent biological replicate experiments. RNA structures that are supported by these results are presented below, after the description of the DMS mapping results.

DMS accessibility of A and C residues could be obtained for three regions and located in the intervals A14–A44 (**Figure 3A**), A120–A295 (**Figures 3B,C**), and C502–A581 (**Figure 3D**). These regions are bracketed in **Figure 2**. Mapping of DMS accessibility was hampered outside these regions by DMS-independent RT pause sites, which generated primer extension products on the non-DMS-treated RNA (**Figure 4**). These RT pauses probably occur at RNA structures that block the enzyme and are not due to naturally modified bases because the same pattern of stops was observed on an RNA that had been synthesized from a plasmid template *in vitro*. These RT pauses were particularly strong and frequent between positions 369 to 416 (**Figure 4C**) and may reflect a stable RNA structure involving positions within this interval (see below).

Results of Enzymatic and Chemical Mapping Reveal RNA Secondary and Tertiary Structures Formed by the *psbC* 5′ UTR

The A and C residues in the 525–580 interval, including those flanking the GUG initiation codon (549–551), were modified by DMS *in vitro*, indicating that this region is unstructured (**Figure 3D**, summarized in **Figure 2**). This is consistent with a previous report that ribosome subunits are directed to the initiation codon of chloroplast mRNAs by the absence of local secondary structure (Scharff et al., 2011). Although, the A and C residues in the 500–525 interval were modified by DMS *in vitro*, this region was also cleaved by RNase V1 (**Figure 1C**), indicating base-pairing. These seemingly contradictory results could be explained by the concurrent existence of distinct conformations involving these bases. Additional work is required to resolve this issue.

The *psbC* 5′ UTR forms several SL structures in simulations using the mfold server (Zuker, 2003). These structures are of various sizes and involve localized sequences. Three of these SLs are supported by our data and named SL1, SL2, and SL3 (**Figures 5A–C**). SL1 (54–86) is supported by multiple RNase

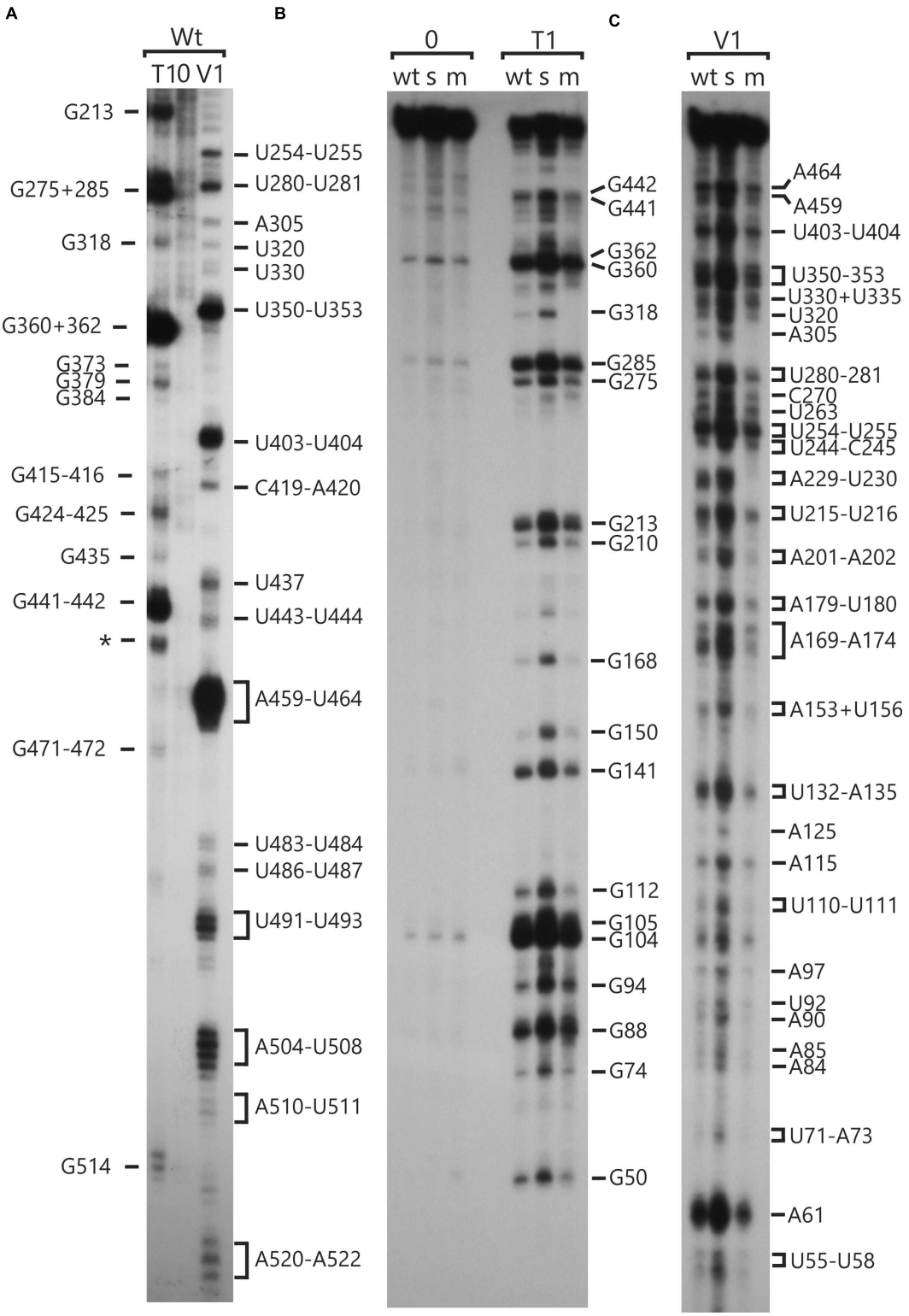

FIGURE 1 | RNA structure analyses of the *psbC* 5′ UTR by enzymatic probing. *In vitro* transcribed RNA corresponding to the wild-type and mutant *psbC* 5′ UTR were untreated (0) or digested with RNase T1 (T1) or RNase V1 (V1), which cleave unpaired G residues or RNA helices, respectively. Digestion products were resolved by denaturing PAGE and revealed by autoradiography. The positions of cleavage sites are indicated with respect to their positions on the 5′ UTR, based on the motilities of molecular size markers (not shown). **(A)** The substrate RNA was 3′-^{32}P-labeled wild-type *psbC* 5′ UTR. **(B,C)** The substrates were 5′-^{32}P-end-labeled RNAs corresponding to the *psbC* 5′ UTR with wild-type sequence (wt), or carrying one of the mutations; *psbC-FuD34* (m), or *psbC-F34sul* (s). The exact position of certain digestion products could not be determined with certainty (*).

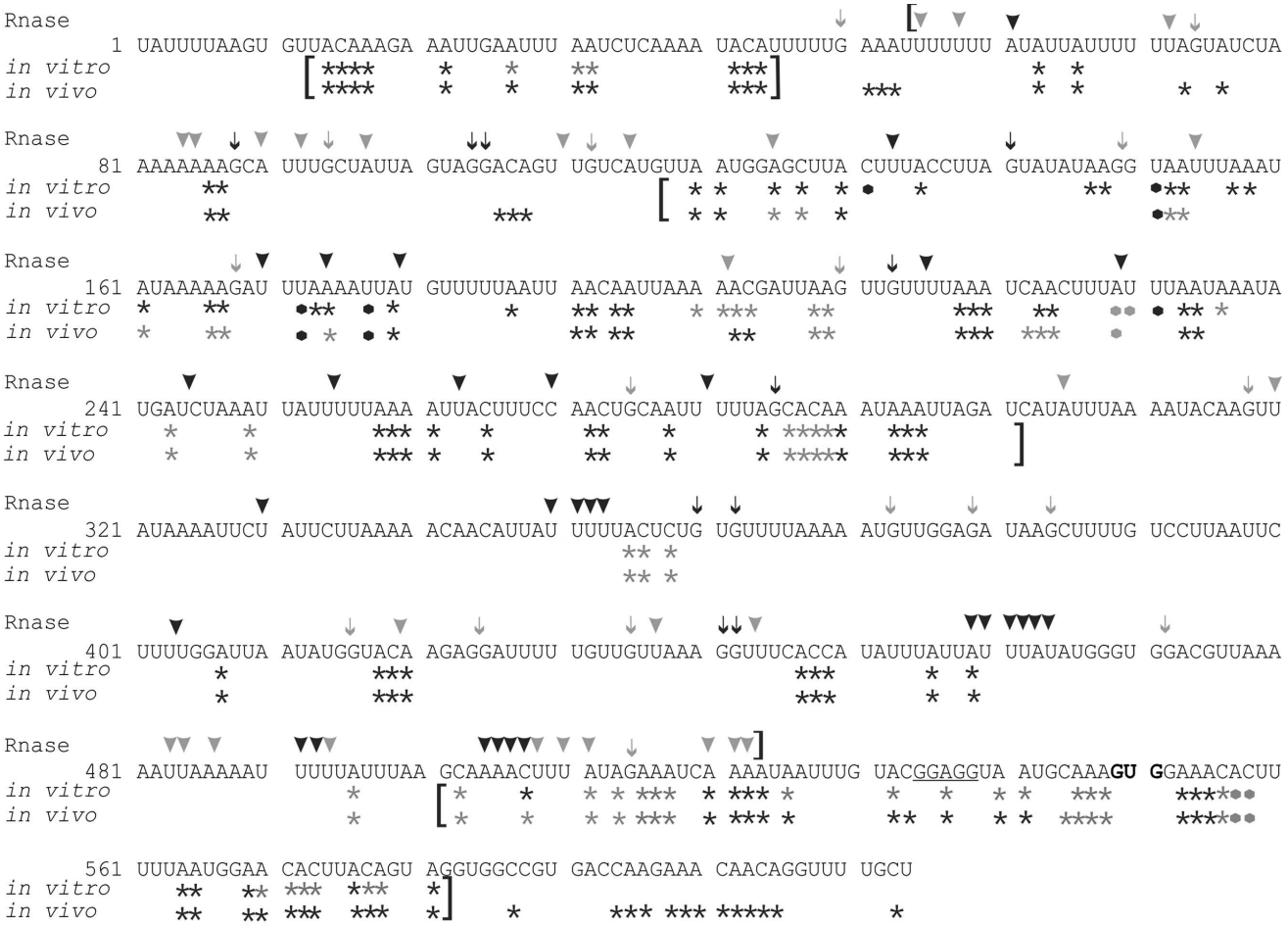

FIGURE 2 | RNA structure mapping results are shown with respect to the *psbC* 5′ UTR sequence. Asterisks indicate bases methylated by DMS *in vitro* and *in vivo*. Arrowheads indicate residues that were cleaved by RNase V1. Arrows indicate G residues that were cleaved by RNase T1. Most frequently methylated or cleaved positions are indicated by black asterisks, arrows and arrowheads. Less frequently methylated or cleaved sites are indicated in gray. Brackets indicate results with high accuracy and resolution. The 5′ terminal residue is designated +1, the translation initiation codon (GUG) is in bold, and the predicted Shine–Dalgarno sequence is underlined. Black and gray dots represent strong and weak RT pause sites, respectively.

V1 cleavage sites in the stem; at U55, U58, A61, U72, A84, and A85 (**Figures 1B** and **5A**). The SL3 supported by an RNase V1 cleavage site at U351 in the stem and RNase T1 accessibility of G360 and G362, and DMS-accessibility of A355, C356, and C358 in the apical loop (**Figure 4B**). A weak RNase T1 cleavage site is also present at G373, which is located at the base of the stem suggesting transient melting of its base-pairing with U348 (**Figure 1A**). It should be noted that the nucleotides 368–374 in the stem of SL3 are also predicted to be involved in the formation of a pseudoknot structure described below. SL1 and SL3 were not studied further.

The largest stem-loop structure, SL2, was given particular attention because, as was stated in the Introduction, it is formed by sequences that are required for translation from the *psbC* 5′ UTR and which interact with *TBC1* (Rochaix et al., 1989; Zerges and Rochaix, 1994; Zerges et al., 2003). SL2 is predicted to be formed by sequences in the 220–320 interval, in the center of the *psbC* 5′ UTR (**Figures 2** and **5C**). Results of our DMS methylation and RNase susceptibility analyses provide the first experimental evidence of this structure: (i) The base-pairing of residues in the stem of this structure is supported by strong RNase V1 cleave sites at A229–U230, U244–C245, U254–U255, and a weaker site at A305 (**Figure 1C**). (ii) DMS-accessibility could be determined for 22 of the 35 A and C residues, that are predicted to form the stem structure, due to RT-pause sites in the 300–320 interval (**Figure 4B**). Consequently, the base-pairing status of the predicted bulged residue C315 could not be determined. Nevertheless, the predicted bulge of A233 and A234 from the stem is supported by the DMS-accessibility of these residues (**Figures 3B,C**). (iii) The apical loop of SL2 is supported by DMS-accessibility of A258-261, C265, A272, C273, A278, A284, C286, A287, C288, and A289 (**Figure 3C**), and RNase T1 cleavage sites at G275and G285 (**Figure 1B**).

Our results also reveal that SL2 has features that were not predicted *in silico*, or described previously (Rochaix et al., 1989). Instead of the previous 47 nt apical loop, additional base-pairing

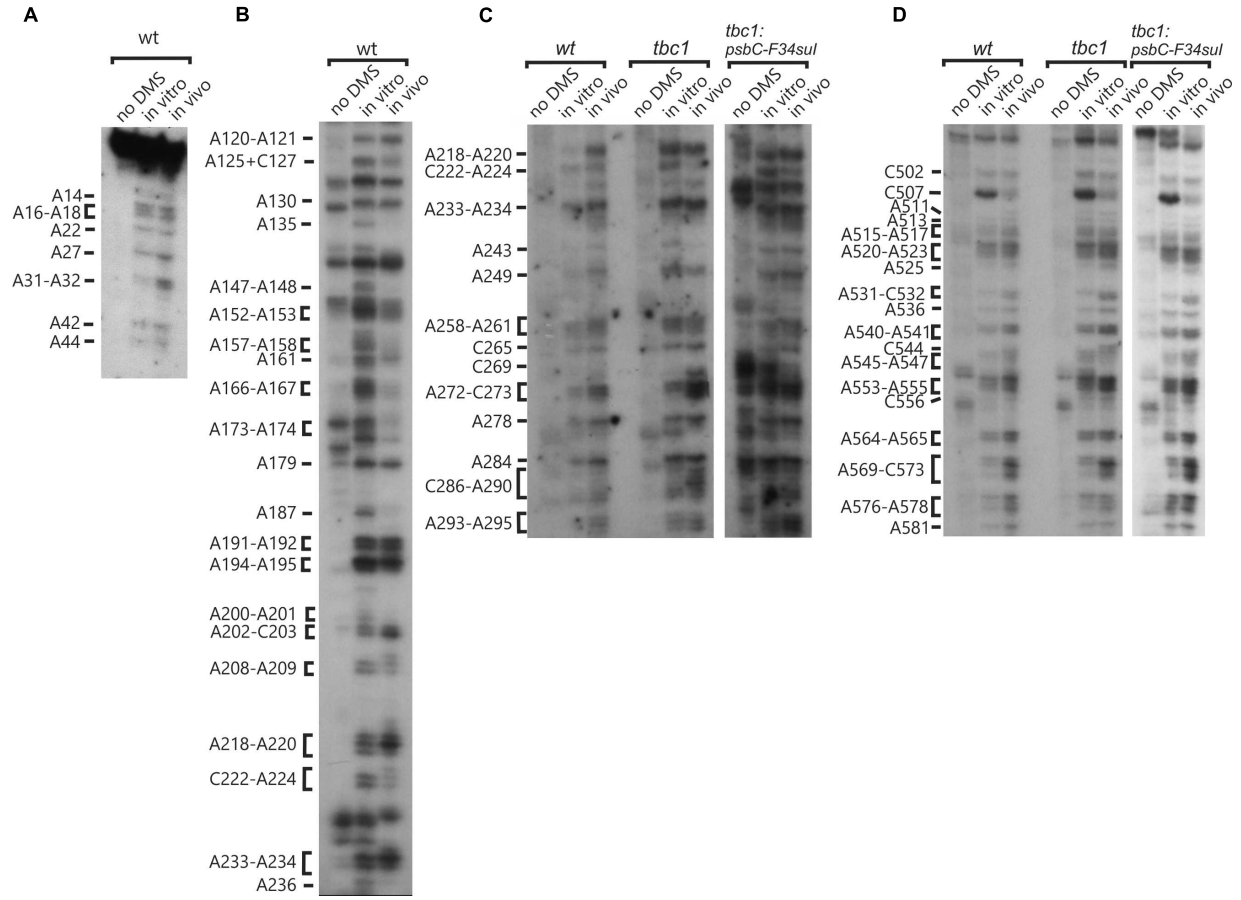

FIGURE 3 | High accuracy and resolution DMS mapping of A and C residues of the *psbC* 5′ UTR. DMS-treated (*in vitro* and *in vivo*) and untreated (no DMS) total RNA was analyzed by primer extension reactions using [^{32}P] primers specific for the *psbC* 5′ UTR. cDNAs generated by termination of RT at methylated bases were resolved on denaturing PAGE and revealed by autoradiography. **(A)** Methylated A and C residues between positions 14 and 44 of the WT *psbC* 5′ UTR. **(B)** Methylated A and C residues between positions 120 and 236 of the WT *psbC* 5′ UTR. **(C)** Methylated A and C residues between positions 218 and 295 of *psbC* 5′ UTR from the wild-type (WT), the *tbc1* mutant, and *psbC-F34sul*. **(D)** Methylated A and C residues between positions 502 and 581 of *psbC* 5′ UTR from the wild-type (WT), the *tbc1* mutant, and *psbC-F34sul*. Bases methylated by DMS are indicated on the left margin of each autoradiograph.

was revealed between sequences near the base of the loop; between U251–U254 and A290–A293, such that the apical loop is 35 nt and the apical extremity of the stem has an internal loop composed of A249–U250 and A294–A295 on opposing strands. In addition, four residues that were predicted to be base-paired in the stem showed evidence of transient melting; A223, A224, and A243 were weakly assessable to DMS (**Figure 3C**), and G318 was weakly accessible to cleavage by RNase T1 (**Figure 1**). A223, A224, and G318 are close to the base of the stem where transient melting could be expected. The weak DMS-accessibility of A243 suggests that base-pairing of A243–U244 with U300–A301 transiently melts to create an internal loop (**Figure 5C**).

A Pseudoknot Tertiary Structure Involves SL2

In the apical loop of SL2 non-paired residues were revealed by strong DMS-methylation sites at A258–A261, C265, A278, A284–A290 and weaker sites at A272 and C273 (**Figure 3C**), by a strong RNase T1 cleavage site at G285, and by a weak site at G275 (**Figure 1**). However, we also found evidence that residues in the apical-most region of the loop are involved in base-pairing, based on strong RNase V1 cleavage sites at U263, C270, and U280–U281 (**Figure 1C**), and the absence of DMS-modification of residues at positions A264, C269, C270, A271, C276, and A277 (**Figure 3C**). Because we could not detect complementarity sequence elements within the apical loop, whose hybridization would explain these base-paired residues, we explored the possibility that the apical loop base-pairs with a complementary sequence in the regions flanking SL2 to form a tertiary structure called a pseudoknot (Draper et al., 1998). When we searched sequences flanking this stem-loop structure for complementarity to the paired sequences in the loop, one such sequence was detected in the interval A367–A385 (**Figure 5D**), beginning 45 nt 3′ to the base of SL2. The data support hybridization of A367–A383 in this interval with U263–U283 in the SL2 apical loop to form the second stem of a pseudoknot (**Figure 5E**). The loop between these two stems would be 45 bases; sufficiently long

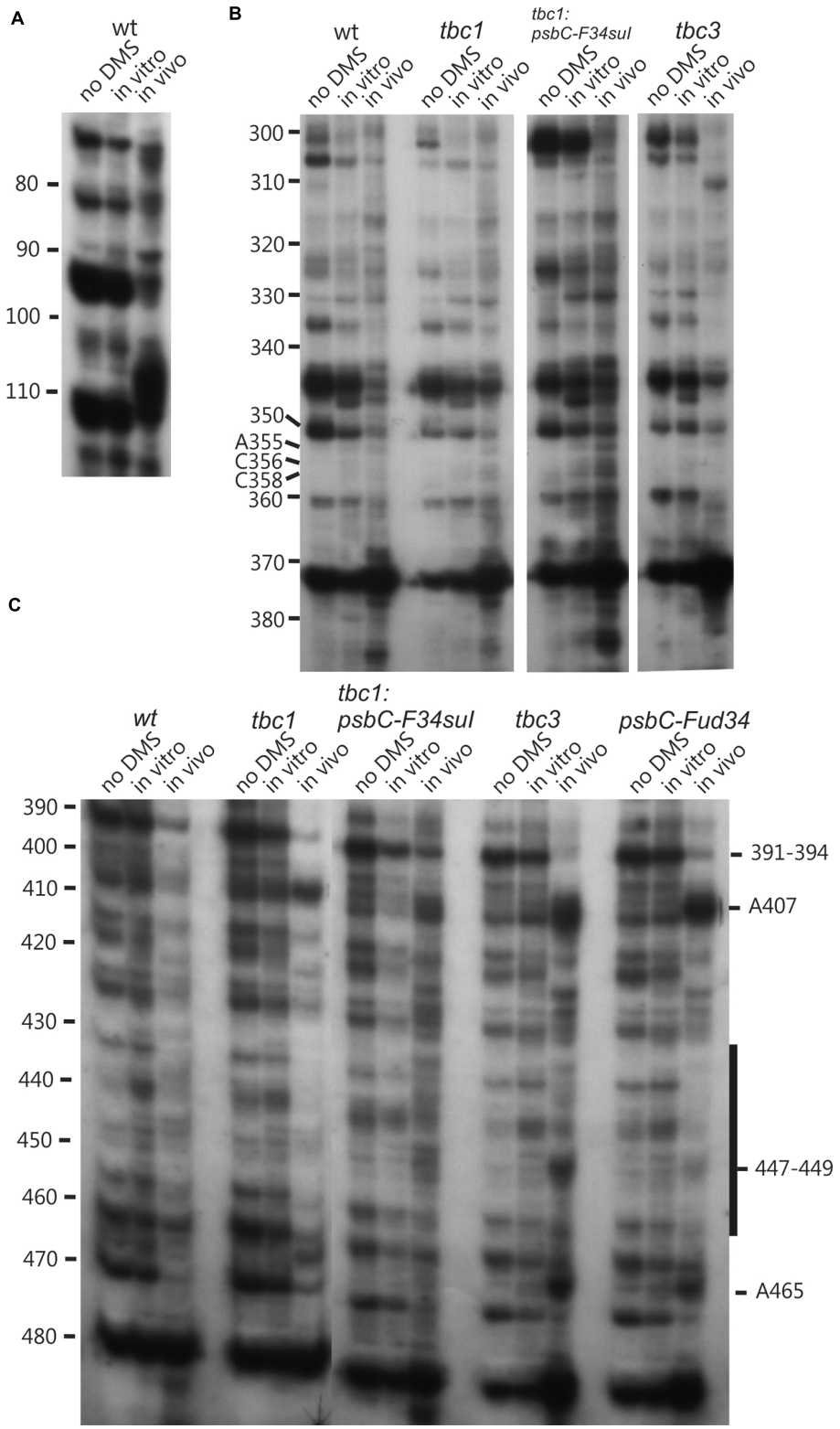

FIGURE 4 | Lower accuracy DMS mapping of A and C residues of the *psbC* 5′ UTR. DMS-treated (*in vitro and in vivo*) and untreated (no DMS) total RNA was analyzed by primer extension reactions using [^{32}P]-labeled primers specific for the *psbC* 5′ UTR, as described for **Figure 3**. **(A–C)** Regions showing multiple RT stop sites in the untreated as well as DMS-treated RNA from WT and various mutants. Note the strong RT stop sites **(A)**, hypermethylated residues A407 and A465, and hypomethylated residues between positions 430–450 **(C)**, and hypermethylated residues close the position 110 **(A)**.

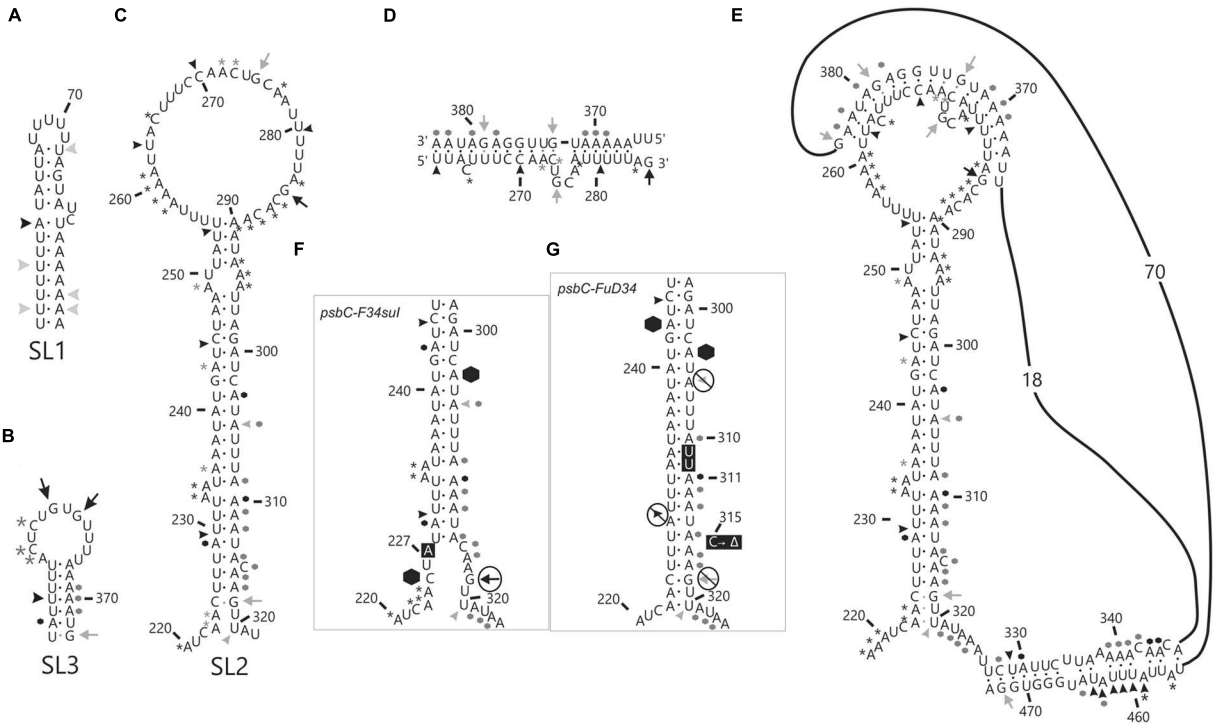

FIGURE 5 | *In vitro* analysis of stem-loop (SL) structures in the *psbC* 5′ UTR. Asterisks (*) indicate A and C residues that are methylated by DMS *in vitro*. Arrows indicate G residues that are substrates for RNase T1 and arrowheads indicated cleavage sites for RNase V1. Most frequently methylated or cleaved positions are indicated by black asterisks, arrows and arrowheads. Less frequently methylated or cleaved sites are indicated in gray. Hexagons indicate locations of strong premature RT stops. Black dots indicate base-pairs that are strongly supported by the data, while gray dots are partially supported and could be present in a subpopulation of RNA substrate molecules. **(A–C)** DMS methylation and RNase cleavage sites on the three stem-loop structures (SL1, 2 and 3), which were seen in simulations using the *mfold* server (Zuker, 2003). **(D)** Base-pairing of the nucleotides in the loop structure of SL2 to the sequences (367–383) 3′ to the SL2 structure giving rise to **(E)** pseudoknot tertiary structure. **(F,G)** DMS methylation, RNase cleavage and premature RT stop sites on the stem structure of SL2 from *FuD34* and *F34su1* mutant *psbC* 5′ UTR are shown. Note that DMS methylation could not be determined for the *psbC-FuD34* mutant 5′ UTR and the absence of asterisks is due to this, not inaccessibility. **(F,G)** Mutant residues are shown in black boxes with white text.

to extend length of the major stem (28–30 bp). This secondary stem has 16 base-pairs and two bulges (C265 and U274–A277) (**Figure 5D**). Transient melting of the base-pairing between A272–C273 and G373–U374 is supported by weak T1 cleavage and DMS methylation sites (**Figures 1B,C**). The data also support a third stem involving pairing of a sequence located immediately 3′ to SL2 (positions 327–346) with another located 3′ to the secondary stem (positions 455–473) (**Figure 5E**). Finally, this pseudoknot structure is the only one identified by the pseudoknot prediction program KineFold (Xayaphoummine et al., 2005).

Chemical Probing of A and C Residues *In Vivo* Validates the *In Vitro* Results

Dimethyl sulfate rapidly enters live cells and methylate A and C residues that are neither base-paired nor bound by protein factors (Wells et al., 2000). Therefore, we treated live cells with DMS, prepared total RNA from them, and then mapped DMS methylated A and C residues by RT-mediated primer extension, as was described above for the analyses of DMS-induced methylation *in vitro* (**Figures 3** and **4**, summarized in **Figure 2**). Of the approximately 100 A and C residues that were DMS-accessible *in vitro* in the 548 nt 5′ UTR, only eleven were inaccessible *in vivo* (A135, A147–148, A157–158, A173, A187, A200–201, C222, A236). In addition, DMS-accessibility of C507 was reduced *in vivo*. Only two of these differences involved a residue in SL2 (C222 and A236) and complete consistency was found between the *in vitro* and *in vivo* results supporting second stem of the pseudoknot. C222 was weakly accessible and is part of the base of the stem where transient melting could be expected. A236 is predicted to be paired in the SL2 and, therefore, its DMS inaccessibility *in vivo* provides further experimental support of this structure. The eleven residues accessible only *in vitro* might, *in vivo*, be bound by protein factors or paired in RNA structures that require conditions that were not present in our *in vitro* experiments. Together, the chemical and enzymatic probing data provide evidences for many residues within the *psbC* 5′ UTR that are base-paired and, therefore, involved in the formation of secondary and tertiary structures. The general correspondence of the *in vitro* and *in vivo* mapping results provide confidence that our *in vitro* mapping experiments were performed on RNA structures that are relevant *in vivo*.

A few bases were accessible to both RNase V1 and DMS (e.g., residues at positions 125, 174, 420, 459, 457, see **Figure 2**). This seemingly contradictory evidence for paired and non-paired

status, respectively, could represent the concurrent existence of alternative structural features, which we have not identified in these analyses.

The *psbC-F34suI* Mutation Destabilizes the Major Stem-Loop Structure SL2

In order to determine whether the *psbC-F34suI* suppressor mutation alleviates the requirement for the *trans*-acting *TBC1* function by altering the structure of SL2 (see Introduction), we characterized the structure of this mutant 5′ UTR by enzymatic and DMS probing experiments, as described above for the wild-type 5′ UTR (**Figures 1, 3, 4,** and summarized in **5F**). This mutation corresponds to a U to A transition at position 227 in the 3′ strand of the stem and near the base of SL2 (**Figure 5F**). Because this mutation reduces the complementarity between the strands by one base-pair, it was predicted to destabilize the stem (Rochaix et al., 1989). Indeed, relative to the results with the wild-type 5′ UTR, we detected enhanced cleavage by RNase T1 at G318 (**Figures 1B** and **5F**) supporting the enhanced melting of the proximal-most base-pairs of SL2. This mutation also restored *in vivo* DMS accessibility of C222–A224 and of the residues between positions 430 and 460, which showed reduced methylation in *tbc1* mutant (described below), to wild-type levels (**Figures 3C** and **4D**). In addition, *psbC-F34suI* generates strong RT pause sites within the stem (A303) and the apical loop (∼C270) providing further support that it alters SL2 structure (**Figures 3C** and **4B**).

The *psbC-FuD34* Mutation Stabilizes the Major Stem-Loop Structure SL2

The *psbC* 5′ UTR mutation, *psbC-Fud34,* abolishes translation of the *psbC* mRNA and was predicted to stabilize SL2 (Rochaix et al., 1989) by removing the two bulges in the stem. The A233–A234 bulge is eliminated by base-pairing of these residues with two inserted U residues, between A309 and A310 and the C315 bulge is eliminated by the deletion of this position (**Figure 5G**). Results of *in vitro* enzymatic probing experiments on an RNA corresponding to the *psbC-Fud34* 5′ UTR revealed the evidence for the stabilization of the base of SL2 as the absence of the RNase T1 cleavages at G318 (**Figure 1B**). This mutant 5′ UTR also lacked two of the three RNase V1 cleavage sites in the SL2 stem; at A229–U230 and A305 (**Figure 1C**). While this could be interpreted as partial melting of the SL2 stem in this mutant, the preponderance of evidence suggests that a higher order structure involving SL2 sterically blocks access of RNase V1 to these base-paired sequences. This evidence includes the results of enzymatic and chemical probing experiments supporting SL2 formation and the enhanced complementarity of the strands of the stem in the *psbC-Fud34* 5′ UTR, meaning that SL2 is more thermodynamically stable than in *wild-type*. On the *psbC-FuD34* mutant 5′ UTR, we detected striking blocks to primer extension by reverse transcription on each strand of the central stem-loop; at 241–245 and 301–305, which, on the wild-type 5′ UTR, were detected as weaker RT pause sites (**Figure 6**). These blocks were so potent that most RT reactions stopped at them and they precluded determinations of base-pairing status based on DMS accessibility. Nevertheless, these potent RT-pause sites, and TGGE results presented in the next subsection, provide additional support of a highly stabilized structure of SL2 relative to the wild-type (Ehresmann et al., 1987). We also detected alteration of DMS accessibility downstream of SL2, which were also detected in *tbc* mutants, described later. These alterations included hypermethylation of A407 and A465, and hypomethylation of residues between positions 430 and 460 (**Figure 4C**).

TGGE profiles can complement RNA structure probing by chemicals and ribonucleases (Szewczak et al., 1998), and has been used to study the structure of the 5′ UTR of a chloroplast RNA (Klaff et al., 1997). In this technique, a homogeneous sample of an RNA molecule is incubated across a linear temperature gradient from 65 to 25°C. The sample is incubated in a single long well, across the origin of a polyacrylamide gel which has this temperature gradient oriented perpendicular to the direction of electrophoresis. In this temperature gradient, the RNA forms a gradient of structures, ranging from unfolded at the 65°C extreme, to folded at the 25°C extreme, with folding intermediates in the interim. During subsequent electrophoresis, while the temperature gradient maintains the RNA in its adopted conformation, the electrophoretic mobility reveals the degree of structure, which is detected as retarded mobility. As seen in **Figure 7A**, the wild-type *psbC* 5′ UTR showed a linear structural transition in TGGE analysis. In contrast, the *psbC-FuD34* mutant 5′ UTR exhibited a dramatically altered melting profile (**Figures 7B,C**). The conformation(s) adopted by this mutant UTR between 50 and 55°C are less hydrodynamic, and show retarded mobility. Retarded electrophoretic mobility is especially pronounced for RNA molecules with internal loops, such as a spliced intron lariat (Domdey et al., 1984). *In silico* simulations using the mfold server (Zuker, 2003) show SL2 of the wild-type and *psbC-F34suI* mutant 5′ UTRs unfold by melting of the base of the stem beginning at 48°C and 43°C, respectively. By contrast, the SL2 with the *psbC-FuD34* mutation is predicted to unfold by melting of the stem beginning at the apical loop and at 54°C. The *psbC-FuD34* 5′ UTR probably has retarded mobility at 50–55°C because it has an enlarged apical loop, which is not the case for the melting wild-type and *psbC-F34suI* 5′ UTRs (**Figure 7D**). At the 25°C temperature extreme, the wild-type and *psbC-FuD34* 5′ UTRs do not detectably differ in electrophoretic mobility and therefore, within the limits of detection of TGGE, do not differ in structure. Therefore, these results provide further evidence that the SL2 structure in the *psbC-FuD34* 5′ UTR is stabilized, suggesting this may be the basis of its inability to promote translation.

DMS Probing of the *psbC* mRNA in the *tbc2* Mutant Shows a Footprint on the Coding Region, Which Was Not Detected in Wild-Type, or the *tbc1* or *tbc3* Mutants

We also used *in vivo* DMS probing experiments to characterize effects of mutations at the *TBC1*, *TBC2* and *TBC3* loci on the *in vivo* status of A and C residues with respect to base-pairing and bound protein. The mutant *tbc2* strain had no reproducible

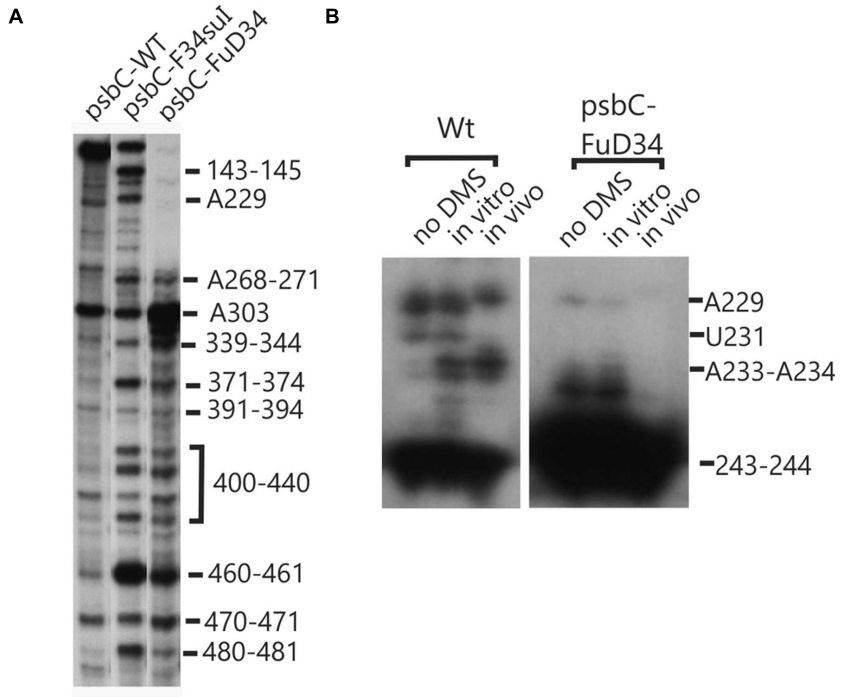

FIGURE 6 | Structural analyses of the *FuD34 and F34su1* mutant *psbC* 5′ UTRs. Structure of mutant *FuD34* and *F34su1psbC* 5′ UTRs were probed by primer extension reactions without **(A)** of with DMS treatment **(B)**. Note the strong RT stop sites in *FuD34* and *F34su1* mutant *psbC* 5′ UTRs without DMS-treatment, at positions 229, 241–245, and 301–305, which correspond with each strands of the central stem-loop. A more proximal primer (Primer 8, hybridizing 279–263) was used in **(B)** compared with the more distal primer (Primer 5, hybridizes (549–532) in **(A)**, in order to pass the 301–305 block in *FuD34*.

alterations of the DMS methylation pattern relative to the wild-type 5′ UTR. However, drastically reduced DMS accessibility in the *tbc2* mutant was detected in the coding sequence in the interval 600–620, which is downstream of the initiation codon (549–551) (**Figure 8**). This is probably the footprint of a bound protein factor because it is too short to represent a stalled ribosome, which should be at least 30 nt (Zoschke et al., 2013) and it is unlikely to represent an RNA structure, based on *in silico* predictions (with the program mfold) and the DMS-accessibility of the same A and C residues in the wild-type and *psbC-F34suI* mRNAs, both *in vitro* and *in vivo* (**Figures 3D** and **8**). This could be the footprint of proteins that were previously detected by UV-crosslinking in extracts of non-membrane proteins from the *tbc2* mutant, but not in equivalent extracts of wild-type and *tbc1* mutant strains (Zerges and Rochaix, 1994).

The DMS Methylation Pattern of the 5′ UTR is Altered in the *tbc1* and *tbc3* Mutants

Enhanced DMS accessibility was detected at many of A and C residues upstream from SL2 (**Supplementary Figure S1**). Alterations of the DMS methylation pattern were observed dispersed across the 5′ UTR of the wild-type *psbC* mRNA in the *tbc1* mutant, relative to the wild-type strain for *TBC1* (**Figures 3** and **4**). Within SL2, several alterations were also detected. We detected enhanced *in vivo* DMS accessibility of C269, A272, and C273 within the apical loop (**Figure 3C**) and a reduced DMS accessibility of C222–A224, and A243. Downstream of SL2, a cluster of reduced DMS-accessible residues between positions 426 and 460 was detected (**Figure 4C**). Lastly, C544, located close to the initiation codon, showed enhanced *in vivo* DMS accessibility in the *tbc1* mutant, relative to the wild-type strain (**Figure 3D**). These residues could be involved in the trans-acting translational activation by *TBC1*.

As another criterion for residues in the *psbC* 5′ UTR that are involved in the *trans*-acting translational activation by *TBC1*, we asked whether any of the residues that showed altered DMS-accessibility in the *tbc1* mutant were reversed to the wild-type accessibility by the *psbC-F34suI* suppressor mutation in SL2. When we examined the DMS methylation pattern in the suppressed double mutant strain (*tbc1* mutant and *psbC-F34suI*) certain effects of the *tbc1* mutant on DMS accessibility of the wild-type *psbC* 5 UTR were reversed, while others were not. For example, reduced DMS-accessibility of residues in the 426–489 interval (**Figure 4C**) were restored to the higher accessibility seen in wild-type. The enhanced DMS-accessibility in the stem of SL2 (C269, A271, A272, and C273) also appeared to be restored to the accessibility in wild-type, however, *psbC-F34suI* also resulted in a strong RT pauses which obscured these results (**Figures 3C** and **6A**). Finally, the enhanced DMS accessibility of the C544, near the initiation codon, in the tbc1 mutant was also reversed to the wild-type level, suggesting a role of this residue mediating the transacting *TBC1* function (**Figure 3D**). Additional work

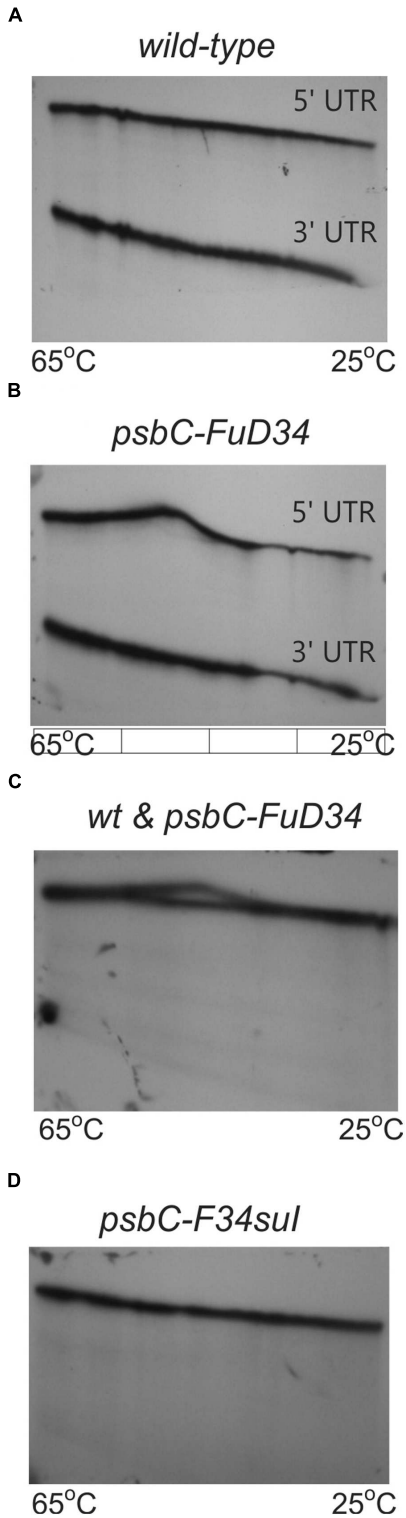

FIGURE 7 | TGGE melting profile of the *FuD34 and F34su1* mutant *psbC* 5′ UTRs. TGGE analysis of *psbC* 5′ UTRs from WT **(A)**, *FuD34* **(B,C)** and *F34su1* **(D)** mutants. The *psbC* 3′ UTR RNA was used as control. Note the alteration of electrophoretic mobility in the mutant *FuD34* compared to the WT *psbC* 5′ UTR, while the *F34suI* mutation does not appear to alter the TGGE profile.

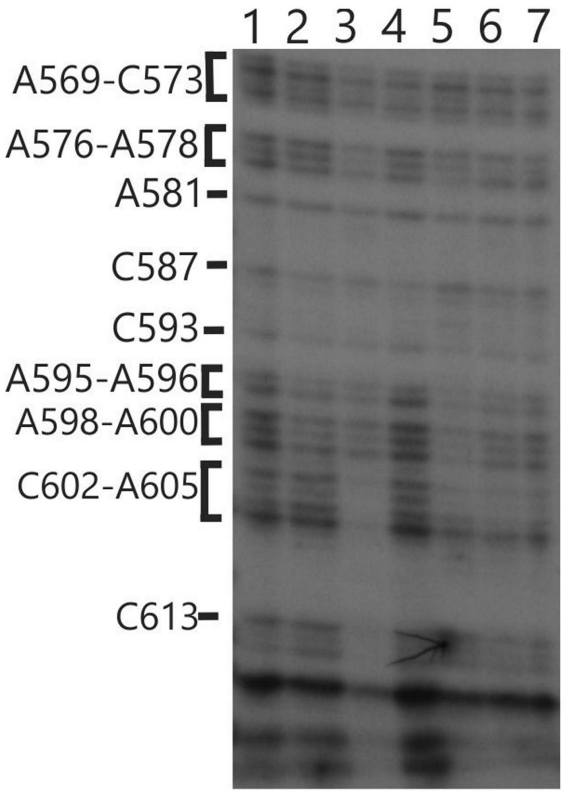

FIGURE 8 | *In vivo* DMS mapping of the 5′ region of the coding sequence from WT and various mutants. Hypomethylated bases were detected downstream of position 602 on the *psbC* 5′ UTR in the *tbc2* mutant (lane 3). Lane (1) wild-type, Lane (2) *tbc1* mutant, Lane (3) *tbc2* mutant, Lane (4) the *psbC-F34suI* suppressor mutation, Lane (5) tbc3 mutant, Lane (6) *FuD34* mutant, Lane (7) double mutant for *tbc3* and *psbC-FuD34*.

is required to understand the structural and mechanistic roles of these residues in mediating translational activation by *TBC1*. In SL2, near the base, we found enhanced DMS-accessibility of residues A309–312 in the *tbc3* mutant, suggesting that an internal loop is present in the stem at this position in this mutant which is not present in the wild-type or other mutant stains (**Figure 4B**). In a region that is not required for translation (Zerges and Rochaix, 1994; Zerges et al., 1997, 2003), located between the pseudoknot and the GUG initiation codon, we observed enhanced DMS accessibility in mutant(s) relative to in wild-type. These include A407 and A465 in the *tbc1* and *tbc3* mutants, and A449–C450 in the *tbc3* mutant (**Figure 4C**). Additional work is required to understand the significance of these results with regards to RNA structure or bound trans-acting factors.

DISCUSSION

This work extends one of the most extensive genetic analyses of translational control in any system to the biochemical level by revealing experimental evidence for a *cis*-acting translational element in the *psbC* 5′ UTR, named here SL2. We also provide

evidence that the apical loop of SL2 hybridizes with a downstream sequence located between it and the GUG initiation codon, to form a pseudoknot. The translational activator function of SL2 was demonstrated previously by effects of site-directed mutagenesis on expression of a chimeric reporter transcript in chloroplast transformants (Zerges et al., 2003).

The SL2-containing pseudoknot structure has features of internal ribosome entry sites (IRESs). IRESs in certain eukaryotic viral and a minority of cellular mRNAs, promote 5′-methylguanosine cap-independent translation initiation (Lozano and Martínez-Salas, 2015). IRES elements have diverse structures and promote translation initiation by different mechanisms and some form pseudoknot tertiary structures (Costantino et al., 2008). Involvement of pseudoknot structures in the regulation of translation initiation has also been demonstrated in bacteria (Brantl, 2007; Haentjens-Sitri et al., 2008; Babitzke et al., 2009; Wu et al., 2014). IRES elements have not been found in bacterial genetic systems, although eukaryotic viral IRES can function in bacteria (Colussi et al., 2015). Therefore, our results raise the possibility of a natural IRES-like structure in a "bacterial" genetic system, considering that chloroplast genetic systems are essentially bacterial in most regards.

SL3 and the pseudoknot (**Figures 5B,E**) appear to be mutually incompatible structures because each requires base-pairing interactions by the sequence interval 365–373 (**Figures 5B,D,E**). This could mean that one or the other of these *in silico* predicted structures does not form. Alternatively, SL3 and the pseudoknot could be alternative structures, with populations of each existing concurrently. It is also possible that SL2 and SL3 could, together, be involved in a RNA triple helix. RNA pseudoknot triple helix structures have been described recently (Cash et al., 2013) and involve low complexity sequences (e.g., A and U homopolymers in our case). RNA triple helices are involved in various biological process including translational regulation (Conrad, 2014).

The translation defects in the mutants lacking SL2 sequences were not due to the removal of one or more essential translational elements because they can be reversed by suppressor mutations in *tbc3* or SL2 (*psbC-F34suI*). A potential inhibitory function of the SL2 pseudoknot is revealed by the effect of SL2 structure bearing the *psbC-FuD34* mutation, which is defective in translation (Rochaix et al., 1989). These results are consistent with a regulatory function of the SL2-pseudoknot as a translational switch.

Flexibility at the base of SL2 is critical for its translational activation function based on the following. The *psbC-FuD34* mutation stabilizes the base of SL2 stem, as revealed by results of chemical and enzymatic probing (**Figure 5G**), the potent blocks to RT-mediated primer extension at the mutant SL2 (**Figure 6**), and results of TGGE (**Figures 7B,C**). This mutation also appears to stabilize a higher-order structure which blocks the access of RNase V1 to SL2 stem (**Figures 5C,G**).

Our results suggest that *TBC1* promotes an RNA conformation that requires flexibility of SL2 with respect to the flanking sequences because the *psbC-F34suI* mutation abolishes base-pairing in this region (**Figure 5F**). This RNA conformation could be the SL2-containing pseudoknot because *TBC1* was shown to functionally interact with SL2 and sequences including the 3′ strand of the second stem (interval 320–390) (Zerges et al., 2003). A few other observations suggest that the many dispersed newly methylated sites detected upstream of SL2 in the *tbc1* mutant are due to an effect of *TBC3*. First, none of these methylations are restored by *the psbC-F34suI* suppressor mutation (**Supplementary Figure S1**). Second, the region upstream SL2 was previously shown to be required for the interaction with *TBC3*, but not with *TBC1* (Zerges and Rochaix, 1994; Zerges et al., 1997, 2003). Third, many of these methylations in the *tbc1* mutant are shared with the *tbc3* mutant. Thus, in the *tbc1* mutant, a hypothetical *TBC3*-dependent translational factor might be prevented from binding to this region of the leader, or it might bind constitutively.

Finally, we found in the *tbc2* mutant that a region in the beginning of the coding region is protected from *in vivo* methylation by DMS. These results suggest that the translational block in this mutant is associated with one or more stalled ribosomes or a bound protein factor in this region, which generate this footprint. These sequences, however, are not required for trans-acting *TBC2* function because it can be conferred to translation of a heterologous reporter gene (Zerges and Rochaix, 1994; Zerges et al., 1997). If this footprint is relevant to the translational block in the tbc2 mutant, then it would have to result somehow from effects of *TBC2* on sequences in the 5′ UTR.

AUTHOR CONTRIBUTIONS

MR and FV performed the research. MR, FV, and WZ designed the research, analyzed the data and wrote the paper. WZ managed the project.

FUNDING

This work was funded entirely by a Discovery Grant from the Natural Sciences and Engineering Council of Canada (217566) to WZ.

ACKNOWLEDGMENT

We thank the staff of the Science Technical Center (Concordia University) for constructing the TGGE apparatus.

SUPPLEMENTARY MATERIAL

The Supplementary Material for this article can be found online at: http://journal.frontiersin.org/article/10.3389/fpls.2016.00828

FIGURE S1 | Dimethyl sulfate (DMS) mapping of A and C residues of the *psbC* 5′ UTR. DMS-treated (*in vitro and in vivo*) and untreated (no DMS) total RNA was analyzed by primer extension reactions using [^{32}P] primers specific for the *psbC* 5′ UTR. cDNAs generated by termination of RT at methylated bases were resolved on denaturing PAGE and revealed by autoradiography. Methylated A and C residues between positions 140 and 195 of *psbC* 5′ UTR from the wild-type (WT), mutants *tbc3* and *tbc1*:*psbC-F34sul*.

REFERENCES

Babitzke, P., Baker, C. S., and Romeo, T. (2009). Regulation of translation initiation by RNA binding proteins. *Annu. Rev. Microbiol.* 63, 27–44. doi: 10.1146/annurev.micro.091208.073514

Brantl, S. (2007). Regulatory mechanisms employed by cis-encoded antisense RNAs. *Curr. Opin. Microbiol.* 10, 102–109. doi: 10.1016/j.mib.2007.03.012

Cash, D. D., Cohen-Zontag, O., Kim, N.-K., Shefer, K., Brown, Y., Ulyanov, N. B., et al. (2013). Pyrimidine motif triple helix in the *Kluyveromyces lactis* telomerase RNA pseudoknot is essential for function in vivo. *Proc. Natl. Acad. Sci. U.S.A.* 110, 10970–10975. doi: 10.1073/pnas.1309590110

Colussi, T. M., Costantino, D. A., Zhu, J., Donohue, J. P., Korostelev, A. A., Jaafar, Z. A., et al. (2015). Initiation of translation in bacteria by a structured eukaryotic IRES RNA. *Nature* 519, 110–113. doi: 10.1038/nature14219

Conrad, N. K. (2014). The emerging role of triple helices in RNA biology. *Wiley Interdiscip. Rev. RNA* 5, 15–29. doi: 10.1002/wrna.1194

Costantino, D. A., Pfingsten, J. S., Rambo, R. P., and Kieft, J. S. (2008). tRNA-mRNA mimicry drives translation initiation from a viral IRES. *Nat. Struct. Mol. Biol.* 15, 57–64. doi: 10.1038/nsmb1351

Domdey, H., Apostol, B., Lin, R. J., Newman, A., Brody, E., and Abelson, J. (1984). Lariat structures are in vivo intermediates in yeast pre-mRNA splicing. *Cell* 39, 611–621. doi: 10.1016/0092-8674(84)90468-9

Draper, D. E., Gluick, T. C., and Schlax, P. J. (1998). "Pseudoknots, RNA folding, and translational regulation," in *RNA Structure and Function*, eds R. W. Simons and M. Grunberg-Manago (Plainview, NY: Cold Spring Harbor Laboratory Press), 415–436.

Ehresmann, C., Baudin, F., Mougel, M., Romby, P., Ebel, J. P., and Ehresmann, B. (1987). Probing the structure of RNAs in solution. *Nucleic Acids Res.* 15, 9109–9128. doi: 10.1093/nar/15.22.9109

Gorman, D. S., and Levine, R. P. (1965). Cytochrome f and plastocyanin: their sequence in the photosynthetic electron transport chain of *Chlamydomonas reinhardii*. *Proc. Natl. Acad. Sci. U.S.A.* 54, 1665–1669. doi: 10.1073/pnas.54.6.1665

Haentjens-Sitri, J., Allemand, F., Springer, M., and Chiaruttini, C. (2008). A competition mechanism regulates the translation of the *Escherichia coli* operon encoding ribosomal proteins L35 and L20. *J. Mol. Biol.* 375, 612–625. doi: 10.1016/j.jmb.2007.10.058

Higgs, D. C., Shapiro, R. S., Kindle, K. L., and Stern, D. B. (1999). Small cis-acting sequences that specify secondary structures in a chloroplast mRNA are essential for RNA stability and translation. *Mol. Cell. Biol.* 19, 8479–8491. doi: 10.1128/MCB.19.12.8479

Klaff, P., Mundt, S. M., and Steger, G. (1997). Complex formation of the spinach chloroplast psbA mRNA 5′ untranslated region with proteins is dependent on the RNA structure. *RNA* 3, 1468–1479.

Knapp, G. (1989). Enzymatic approaches to probing of RNA secondary and tertiary structure. *Methods Enzymol.* 180, 192–212. doi: 10.1016/0076-6879(89)80102-8

Lozano, G., and Martínez-Salas, E. (2015). Structural insights into viral IRES-dependent translation mechanisms. *Curr. Opin. Virol.* 12, 113–120. doi: 10.1016/j.coviro.2015.04.008

Rochaix, J. D., Kuchka, M., Mayfield, S., Schirmer-Rahire, M., Girard-Bascou, J., and Bennoun, P. (1989). Nuclear and chloroplast mutations affect the synthesis or stability of the chloroplast psbC gene product in *Chlamydomonas reinhardtii*. *EMBO J.* 8, 1013–1021.

Sambrook, J., and Russell, D. W. (2001). *Molecular Cloning: A Laboratory Manual*. Cold Spring Harbor, NY: Cold Spring Harbor Laboratory Press.

Scharff, L. B., Childs, L., Walther, D., and Bock, R. (2011). Local absence of secondary structure permits translation of mRNAs that lack ribosome-binding sites. *PLoS Genet.* 7:e1002155. doi: 10.1371/journal.pgen.1002155

Szewczak, A. A., Podell, E. R., Bevilacqua, P. C., and Cech, T. R. (1998). Thermodynamic stability of the P4-P6 domain RNA tertiary structure measured by temperature gradient gel electrophoresis. *Biochemistry* 37, 11162–11170. doi: 10.1021/bi980633e

Wartell, R. M., Hosseini, S. H., and Moran, C. P. Jr. (1990). Detecting base pair substitutions in DNA fragments by temperature-gradient gel electrophoresis. *Nucleic Acids Res.* 18, 2699–2705. doi: 10.1093/nar/18.9.2699

Wells, S. E., Hughes, J. M., Igel, A. H., Ares, M. Jr., (2000). Use of dimethyl sulfate to probe RNA structure in vivo. *Methods Enzymol.* 318, 479–493. doi: 10.1016/S0076-6879(00)18071-1

Wu, Y. J., Wu, C. H., Yeh, A. Y., and Wen, J. D. (2014). Folding a stable RNA pseudoknot through rearrangement of two hairpin structures. *Nucleic Acids Res.* 42, 4505–4515. doi: 10.1093/nar/gkt1396

Xayaphoummine, A., Bucher, T., and Isambert, H. (2005). Kinefold web server for RNA/DNA folding path and structure prediction including pseudoknots and knots. *Nucleic Acids Res.* 33, W605–W610. doi: 10.1093/nar/gki447

Zaug, A. J., and Cech, T. R. (1995). Analysis of the structure of *Tetrahymena* nuclear RNAs in vivo: telomerase RNA, the self-splicing rRNA intron, and U2 snRNA. *RNA* 1, 363–374.

Zerges, W., Auchincloss, A. H., and Rochaix, J. D. (2003). Multiple translational control sequences in the 5′ leader of the chloroplast psbC mRNA interact with nuclear gene products in *Chlamydomonas reinhardtii*. *Genetics* 163, 895–904.

Zerges, W., Girard-Bascou, J., and Rochaix, J. D. (1997). Translation of the chloroplast psbC mRNA is controlled by interactions between its 5′ leader and the nuclear loci TBC1 and TBC3 in *Chlamydomonas reinhardtii*. *Mol. Cell. Biol.* 17, 3440–3448. doi: 10.1128/MCB.17.6.3440

Zerges, W., and Hauser, C. (eds) (2009). "Protein synthesis in the chloroplast," in *The Chlamydomonas Sourcebook: Organellar and Metabolic Processes* (Amsterdam: Elsevier).

Zerges, W., and Rochaix, J. D. (1994). The 5′ leader of a chloroplast mRNA mediates the translational requirements for two nucleus-encoded functions in *Chlamydomonas reinhardtii*. *Mol. Cell. Biol.* 14, 5268–5277. doi: 10.1128/MCB.14.8.5268

Zoschke, R., Watkins, K. P., and Barkan, A. (2013). A rapid ribosome profiling method elucidates chloroplast ribosome behavior in vivo. *Plant Cell* 25, 2265–2275. doi: 10.1105/tpc.113.111567

Zuker, M. (2003). Mfold web server for nucleic acid folding and hybridization prediction. *Nucleic Acids Res.* 31, 3406–3415. doi: 10.1093/nar/gkg595

Conflict of Interest Statement: The authors declare that the research was conducted in the absence of any commercial or financial relationships that could be construed as a potential conflict of interest.

The reviewer KB and handling Editor declared their shared affiliation, and the handling Editor states that the process nevertheless met the standards of a fair and objective review.

frontiers in Plant Science

MINI REVIEW
published: 12 January 2016
doi: 10.3389/fpls.2015.01261

The Roles of Cytochrome b_{559} in Assembly and Photoprotection of Photosystem II Revealed by Site-Directed Mutagenesis Studies

Hsiu-An Chu and Yi-Fang Chiu*

Institute of Plant and Microbial Biology – Academia Sinica, Taipei, Taiwan

Cytochrome b_{559} (Cyt b_{559}) is one of the essential components of the Photosystem II reaction center (PSII). Despite recent accomplishments in understanding the structure and function of PSII, the exact physiological function of Cyt b_{559} remains unclear. Cyt b_{559} is not involved in the primary electron transfer pathway in PSII but may participate in secondary electron transfer pathways that protect PSII against photoinhibition. Site-directed mutagenesis studies combined with spectroscopic and functional analysis have been used to characterize Cyt b_{559} mutant strains and their mutant PSII complex in higher plants, green algae, and cyanobacteria. These integrated studies have provided important *in vivo* evidence for possible physiological roles of Cyt b_{559} in the assembly and stability of PSII, protecting PSII against photoinhibition, and modulating photosynthetic light harvesting. This mini-review presents an overview of recent important progress in site-directed mutagenesis studies of Cyt b_{559} and implications for revealing the physiological functions of Cyt b_{559} in PSII.

Keywords: photosynthesis, photosystem II, cytochrome b_{559}, site-directed mutagenesis, photoprotection, photoinhibition

OPEN ACCESS

Edited by:
Julian Eaton-Rye,
University of Otago, New Zealand

Reviewed by:
Pavel Pospíšil,
Palacký University, Czech Republic
Gary Brudvig,
Yale University, USA

****Correspondence:***
Hsiu-An Chu
chuha@gate.sinica.edu.tw

Specialty section:
This article was submitted to Plant Cell Biology, a section of the journal Frontiers in Plant Science

Received: *03 November 2015*
Accepted: *24 December 2015*
Published: *12 January 2016*

Citation:
Chu H-A and Chiu Y-F (2016) The Roles of Cytochrome b_{559} in Assembly and Photoprotection of Photosystem II Revealed by Site-Directed Mutagenesis Studies. Front. Plant Sci. 6:1261. doi: 10.3389/fpls.2015.01261

INTRODUCTION

Cytochrome b_{559} is one of the essential components of Photosystem II in all oxygenic photosynthetic organisms (Whitmarsh and Pakrasi, 1996; Stewart and Brudvig, 1998; Guskov et al., 2009; Umena et al., 2011). Cyt b_{559} is a heme-bridged heterodimer protein comprising one α- and one β- subunit (encoded by the *psbE* and *psbF* genes) of 9 and 4 kDa, respectively (see **Figure 1**). Each subunit provides a His ligand (His-22 residue of the α- or β-subunit of Cyt b_{559} in *Synechocystis* sp. PCC 6803, corresponding to His-23 residue of α- or His-24 residue of the β-subunit of Cyt b_{559} in *Thermosynechococcus elongatus*) for the non-covalently bound heme, which is located near the stromal side of PSII. In addition, Cyt b_{559} has different redox potential forms depending on the type of PSII preparations and treatments: a HP form with a midpoint redox potential of about +400 mV, an IP form of about +200 mV, and a LP form with a midpoint redox potential of about 0–80 mV (Stewart and Brudvig, 1998; Roncel et al., 2001 and references therein). In intact PSII preparations, Cyt b_{559} is mostly in the reduced HP form under

Abbreviations: APC, allophycocyanin; Car, β-carotene; Cyt b_{559}, cytochrome b_{559}; HP, high potential; IP, intermediate potential; LP, low potential; NPQ, non-photochemical fluorescences quenching; PQ, plastoquinone; PQH_2, plastoquinol; PSII, Photosystem II; Q_A, primary quinone electron acceptor in PSII; Q_B, the secondary quinone electron acceptor in PSII; Q_C, the third plastoquinone-binding site in PSII.

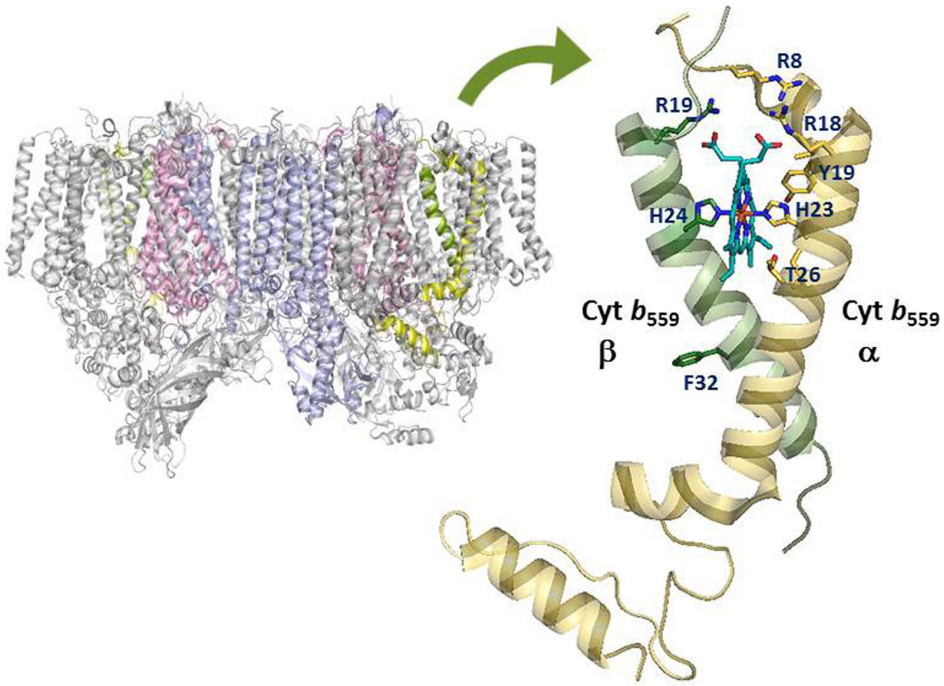

FIGURE 1 | Structural model of the cytochrome b_{559} in Photosystem II. Amino acid residues of cytochrome b_{559} targeted by recent site-directed mutagenesis work are labeled by using amino acid sequences of cytochrome b_{559} from *Thermosynechococcus elongatus*. The figure was created using PyMol and the PDB file 4UB8.

ambient conditions. In inactive or less intact PSII preparations, Cyt b_{559} is typically in the LP or IP form and mostly oxidized (presumably by molecular oxygen) under ambient conditions (Barber and De Las Rivas, 1993; Poulson et al., 1995; Pospíšil et al., 2006).

Several studies have proposed that Cyt b_{559} participates in secondary electron transfer pathways that protect PSII against photoinhibition (see **Figure 2**; Heber et al., 1979; Falkowski et al., 1986; Thompson and Brudvig, 1988; Barber and De Las Rivas, 1993; Poulson et al., 1995; Magnuson et al., 1999; Faller et al., 2001; Tracewell and Brudvig, 2008 and references therein). In these models, the HP form of Cyt b_{559} is thought to donate its electron, via a β-carotene molecule (Car_{D2}), to reduce highly oxidized chlorophyll radicals in PSII under donor-side photoinhibitory conditions (e.g., the oxygen-evolving complex is impaired or under assembly). Oxidized Cyt b_{559} may accept an electron from the acceptor side of PSII (Q_B^-, or reduced PQH_2 from the pool), thus forming a cyclic pathway of electron transfer within PSII. On the other hand, when the electron transfer on the acceptor side of PSII is inhibited (e.g., under high-light conditions), the oxidized Cyt b_{559} might accept an electron from the acceptor side of PSII to prevent the formation of damaging singlet oxygen species (Nedbal et al., 1992; Vass et al., 1992; Barber and De Las Rivas, 1993; Bondarava et al., 2010). In addition, several different enzymatic functions of Cyt b_{559} have been proposed, such as superoxide dismutase (Ananyev et al., 1994) and PQH_2 oxidase in intact PSII (Kruk and Strzałka, 1999, Kruk and Strzalka, 2001; Bondarava et al., 2003, 2010) and superoxide oxidase and reductase in tris-washed PSII (Tiwari and Pospísil, 2009; Pospíšil, 2011). Moreover, a novel quinone-binding site (Q_C) was identified close (about 15 Å) to the heme of Cyt b_{559} in the 2.9-Å PSII crystal structure from *T. elongatus* (Guskov et al., 2009). The occupancy of this Q_C site with PQ (or PQH_2) has been proposed to modulate the redox equilibration between Cyt b_{559} and the PQ pool (Kaminskaya et al., 2006, 2007; Kaminskaya and Shuvalov, 2013) or be involved in the exchange of PQ on the Q_B site from the pool (Guskov et al., 2009). However, the Q_C site was not detected in the more recent 1.9-Å PSII crystal structure (Umena et al., 2011). Despite the recent remarkable progress in understanding the structure and function of PSII, the exact function of Cyt b_{559} in PSII remains unclear.

This mini-review gives an overview of important progress in recent site-directed mutagenesis studies performed to reveal the physiological function(s) of Cyt b_{559} in PSII. More comprehensive reviews on the structure and functions of Cyt b_{559} are available (Whitmarsh and Pakrasi, 1996; Stewart and Brudvig, 1998; Faller et al., 2005; Pospíšil, 2011; Shinopoulos and Brudvig, 2012).

FUNCTION IN ASSEMBLY AND STABILITY OF PSII REACTION CENTERS

Prior mutagenesis studies with *Synechocystis* sp. PCC 6803, *Chlamydomonas reinhardtii* or *Nicotiana tabacum* showed no

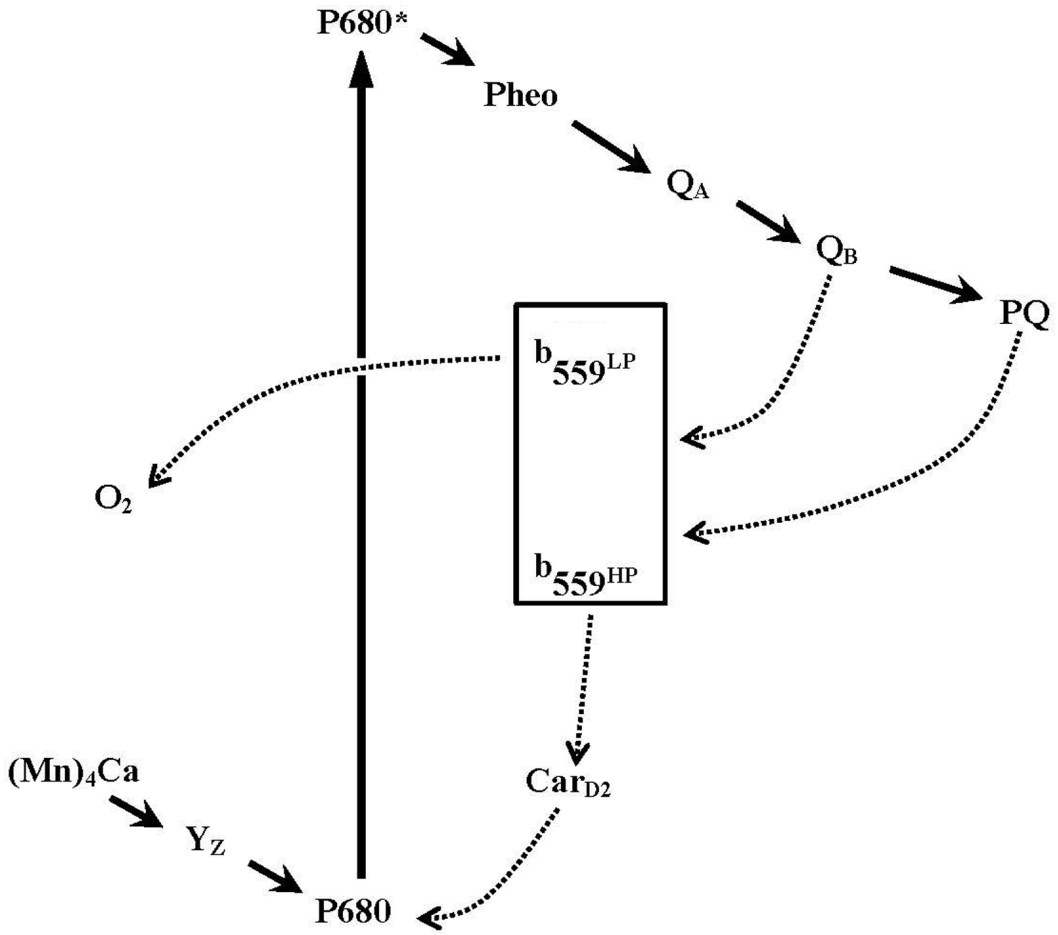

FIGURE 2 | A simplified scheme for electron transfer pathways within Photosystem II reaction centers. Primary electron transfer pathway (bold solid lines with arrows) and possible secondary electron transfer pathways involving cytochrome b_{559} (dotted line with arrows) are shown. The scheme is modified from Whitmarsh and Pakrasi (1996).

stable PSII reaction centers assembled in the absence of either Cyt b_{559} subunit (Pakrasi et al., 1988, 1989, 1990; Morais et al., 1998; Swiatek et al., 2003; Suorsa et al., 2004). Several authors proposed that Cyt b_{559} plays an important structural role, such as being a nucleating factor, during the early stage of PSII assembly (Pakrasi et al., 1988; Morais et al., 1998; Komenda et al., 2004).

In addition, mutagenesis studies with *Synechocystis* sp. PCC 6803 showed that substituting either of the heme axial ligands (His22 of the α-subunit or His22 of the β-subunit of Cyt b_{559} in *Synechocystis* sp. PCC 6803) with Leu, Met, Glu, Gln, Tyr, Lys, Arg, or Cys abolished the photoautotrophic growth and severely diminished the assembly or stability of PSII in the mutant cells, except for H22Kα mutant cells, which were able to grow photoautotrophically and accumulated stable PSII reaction centers (∼81% as compared with wild-type cells; Pakrasi et al., 1991; Hung et al., 2007, 2010). Electron paramagnetic resonance results indicated the displacement of one of the two axial ligands to the heme of Cyt b_{559} in H22Kα mutant reaction centers, at least in isolated reaction centers (Hung et al., 2010). In addition, H22Kα and Y18Sα (corresponding to Y19Sα in *T. elongatus*) in mutant PSII core complexes contained predominately the LP form of Cyt b_{559}. The findings support the concept that the redox properties of Cyt b_{559} are strongly influenced by the hydrophobicity and ligation environment of the heme (Krishtalik et al., 1993; Gadjieva et al., 1999; Roncel et al., 2001; Pospíšil and Tiwari, 2010).

Spectroscopic and functional characterizations of the cyanobacterium *Synechocystis* sp. PCC 6803 with mutation of charged residues on the cytoplasmic side of Cyt b_{559} in PSII have been reported (Chiu et al., 2013). All mutant cells grew photoautotrophically and assembled stable PSII. However, R7Eα, R17Eα, and R17Lβ mutant cells grew significantly slower and were more susceptible to photoinhibition as compared with wild-type cells. In addition, the PSII core complexes from R7Eα and R17Lβ cells contained predominantly the LP form of Cyt b_{559}. Electron paramagnetic resonance results indicated the displacement of one of the two axial ligands to the heme of Cyt b_{559} in the reaction centers of the R7Eα and R17Lβ mutants. In recent PSII crystal structural models (Guskov et al., 2009; Umena et al., 2011), the side chains of

these Arg residues of Cyt b_{559} (corresponding to Arg8 and Arg18 residues of the α-subunit and Arg19 residue of the β-subunit of Cyt b_{559} in *T. elongatus*) are in close contact with the heme propionates of Cyt b_{559} (see **Figure 1**). Thus, the electrostatic interactions between these Arg residues and the heme propionates of Cyt b_{559} may affect the ligation structure and redox properties of the heme in Cyt b_{559} (Chiu et al., 2013).

Furthermore, mutagenesis studies of *C. reinhardtii* showed that the H23Yα, H23Mα, and H23Cα mutant cells were unable to grow photoautotrophically, were sensitive to photoinhibition, accumulated 10–20% of the PSII (compared to wild-type cells), and contained a disrupted heme pocket while still retaining significant O_2 evolution activity (Morais et al., 2001; Hamilton et al., 2014). Thus, the heme of Cyt b_{559} was not required for photosynthetic water oxidation by PSII (Morais et al., 2001). A recent study also presented evidence to ascribe the photoinhibition phenotype of H23Cα mutant cells to a faster rate of photodamage and an impaired PSII repair cycle (Hamilton et al., 2014). Hence, Cyt b_{559} may play important roles in the assembly, repair and maintenance of the PSII complex *in vivo*.

In the other recent mutant study of *T. elongatus* that took advantage of the robustness of the PSII variant with PsbA3 as the D1 subunit, the four constructed Cyt b_{559} mutants (H23Aα, H23Mα, Y19Fα, and T26Pα) grew photoautotrophically (*T. elongatus* is an obligate photoautotroph; Sugiura et al., 2015). Although the H23Aα and H23Mα mutants assembled only an apo-Cyt b_{559}, the steady-state level of active PSII was comparable to that in the wild-type control. The results suggest that the heme has no structural role in the assembly of PSII in the presence of α- and β-subunits of Cyt b_{559}. This finding is in strong contrast to the *Synechocystis* sp. PCC 6803 mutant showing that proper coordination of the heme cofactor in Cyt b_{559} is important to the assembly or stability of PSII (Pakrasi et al., 1991; Hung et al., 2007). In addition, Cyt b_{559} mutant cells of *T. elongatus* showed no correlation between the rate of photoinhibition and the redox potential of the heme. However, the recovery of the oxygen-evolving activity of PSII after photoinhibition was significantly slower in these mutant cells. PsbA3 is the D1 isoform expressed in *T. elongatus* under high-light conditions (Nakamura et al., 2002; Kós et al., 2008). The high-light D1 isoform in cyanobacteria has a Glu instead of a Gln residue (for the low-light D1 isoform) at position 130 in the D1 protein sequence (for a review, see Mulo et al., 2009) and this Glu residue forms hydrogen-bonding interactions with pheophytinD1 (Dorlet et al., 2001; Shibuya et al., 2010). Cyanobacterial PSIIs with the high-light D1 isoform showed increased photo-tolerance and accelerated non-radiative charge recombination (Tichy et al., 2003). This phototolerant property has been attributed to a photoprotection mechanism involving the redox potential of pheophytinD1, which enhances the probability for non-radiative recombination of the singlet radical pair and prevents the formation of potentially damaging ^{3}P680 and singlet oxygen species (Vass and Cser, 2009; Sugiura et al., 2014). Further investigation could determine whether PsbA3 may compensate the photoprotective function of Cyt b_{559} in the assembly and stability of PSII in these Cyt b_{559} mutant cells.

FUNCTION IN PROTECTING PSII AGAINST PHOTOINHIBITION

Numerous site-directed mutagenesis studies have investigated the role of Cyt b_{559} in protecting PSII against photoinhibition under high light. In the photoprotective models, oxidized Cyt b_{559} may accept an electron from the acceptor side of PSII (Q_B^-, Q_C, or reduced PQH_2 from the pool). Previous mutant studies of dark-adapted leaves of the F26Sβ Cyt b_{559} tobacco mutant showed a greatly reduced PQ pool, conversion of the redox-potential form of Cyt b_{559} to the LP form, and photosynthetic activities sensitive to high light (Bondarava et al., 2003, 2010). In addition, R7Eα and R17Lβ Cyt b_{559} mutant cells of *Synechocystis* sp. PCC 6803 and R18Sα Cyt b_{559} mutant cells of *T. elongatus* showed markedly reduced PQ pools, altered redox-potential forms of Cyt b_{559}, and high susceptibility to light stress (Chiu et al., 2013; Guerrero et al., 2014). A defect in PQH_2 oxidase activity of Cyt b_{559} due to altered redox-potential forms of Cyt b_{559} in these mutant strains could explain their high susceptibility to strong light and greatly reduced PQ pools. Therefore, Cyt b_{559} may function as a PQH_2 oxidase to keep the PQ pool and the acceptor side of PSII oxidized in the dark, thereby preventing PSII from acceptor-side photoinhibition (Kruk and Strzałka, 1999, Kruk and Strzalka, 2001; Bondarava et al., 2003, 2010). However, one recent study reported no defect in PQH_2 oxidation in the dark in H23Cα mutant cells of *C. reinhardtii*, even though H23Cα mutant cells contained a disrupted heme-binding pocket of Cyt b_{559} and were sensitive to photoinhibition (Hamilton et al., 2014). Further studies are required to clarify this discrepancy. In addition, study of the 2.9-Å resolution PSII crystal structure reported the binding of Q_C at a hydrophobic cavity near Cyt b_{559} (Guskov et al., 2009). Several spectroscopic studies have provided evidence that the occupancy of the Q_C site by PQ (or PQH_2) may modulate the redox potential of Cyt b_{559} and mediate the redox equilibration between Cyt b_{559} and the PQ pool (Kaminskaya et al., 2006, 2007; Kaminskaya and Shuvalov, 2013). A recent study provided evidence of a possible one-electron oxidation of PQH_2 by Cyt b_{559} at the Q_C site involved in the formation of a superoxide anion radical (Yadav et al., 2014). The above results are consistent with Cyt b_{559} possibly accepting an electron from PQH_2 via the Q_C site in PSII. However, the Q_C site was not present in the more recent 1.9-Å PSII crystal structure (Umena et al., 2011). Further investigations are needed to solve this important issue.

Spectroscopic and functional characterization of the H22Kα and Y18Sα Cyt b_{559} mutant cells of *Synechocystis* sp. PCC 6803 showed that both mutants have functional PSII and exhibited the normal period-four oscillation in oxygen yield (Hung et al., 2010). However, both mutants were more susceptible to photoinhibition than the wild type under high-light conditions. In addition, PSII core complexes from the H22Kα and Y18Sα

mutants predominantly contained the oxidized LP form of Cyt b_{559} (∼79 and 86%, respectively). A defect in the photoprotective function of Cyt b_{559} in H22Kα and Y18Sα mutants could explain their high susceptibility to strong light. Furthermore, H22Kα and Y18Sα Cyt b_{559} mutants in a D1-D170A genetic background that prevented assembly of the Mn cluster showed almost completely abolished accumulation of PSII even under normal-growth-light conditions. The data support an important redox role of Cyt b_{559} in protecting PSII under donor-side photoinhibition conditions (Hung et al., 2010).

Furthermore, under low light, the H23Cα Cyt b_{559} mutant showed more rapid assembly of the Mn_4CaO_5 cluster than the wild-type control in *C. reinhardtii* (Hamilton et al., 2014). However, the photoactivation of oxygen-evolving PSII in the H23Cα mutant was inhibited under high light. The results suggest that reduction of $P680^+$ via cyclic electron flow within PSII (via Cyt b_{559} and Car_{D2}, **Figure 2**) may compete with the photoactivation process and provides important *in vivo* evidence for a photoprotective role of Cyt b_{559} in photo-assembly of the Mn_4CaO_5 cluster in PSII (Hamilton et al., 2014).

A recent mutant study involving *T. elongatus* showed that the midpoint redox potential of the HP form of Cyt b_{559} was significantly destabilized (converted to the IP form) in mutant PSII core complexes of Cyt b_{559} mutant strains (I14Aα, I14Sα, R18Sα, I27Aα, I27Tα, and F32Yβ; Guerrero et al., 2014). When the oxygen-evolving complex was inactive, the yield of dark-reduction of Cyt b_{559} was lower and the kinetics was slower in the R18Sα mutant than in wild-type cells. The results support the concept that the HP form of Cyt b_{559} may function as a PQH_2 oxidase to keep the PQ pool oxidized and also as an electron reservoir for the cyclic electron flow within PSII when the donor-side of PSII is impaired (Guerrero et al., 2014).

Moreover, a previous spectroscopic study showed that different spectral forms of Car were oxidized in PSII samples containing different redox forms of Cyt b_{559} (Tracewell and Brudvig, 2008). The authors proposed that the quenching properties of PSII may be controlled by the redox form of Cyt b_{559} by modulating the different type of oxidized Car species (radical cation or neutral radical) formed in PSII. Future study could investigate the quenching properties of PSII in the wild type versus Cyt b_{559} mutant strains of cyanobacteria with different redox forms of Cyt b_{559} to validate this proposal.

EFFECTS ON PHOTOSYNTHETIC LIGHT HARVESTING

Recent mutant studies revealed a novel role of Cyt b_{559} in modulating photosynthetic light harvesting in PSII reaction centers. A spontaneously generated mutant from *Synechocystis* sp. PCC 6803 wild-type cells grown in BG-11 agar plates containing 5 mM Glu and 10 μM DCMU carried an Arg7 to Leu mutation on the alpha-subunit of Cyt b_{559} in PSII (Chiu et al., 2009). Results of 77-K fluorescence and room-temperature chlorophyll *a* fluorescence spectra indicated that the energy transfer from phycobilisomes to PSII reaction centers was partially inhibited or uncoupled in this mutant. In addition, the cytoplasmic side of Cyt b_{559} is located within the predicted contact sites in PSII for the APC core complex of the phycobilisome (Barber et al., 2003). The Arg7 to Leu mutation of Cyt b_{559} may alter the interaction between the APC core complex and PSII reaction centers, thereby reducing energy delivery from the antenna to the reaction center and protecting mutant cells against DCMU-induced photo-oxidative stress (Rutherford and Krieger-Liszkay, 2001).

Many cyanobacteria including *Synechocystis* sp. PCC 6803 have a novel blue-green light-induced NPQ mechanism to protect PSII reaction centers against photodamage under high-light stress (Kirilovsky and Kerfeld, 2012). Under high-light conditions, a soluble orange carotenoid protein is able to absorb blue–green light and undergoes photo-conversion into the active red form, which interacts with the APC core of the phycobilisome and dissipates excess excitation energy from the phycobilisome as heat. Interestingly, several *Synechocystis* sp. PCC 6803 mutant cells (e.g., R7Lα and R17Lβ) with mutations on the cytoplasmic side of Cyt b_{559} in PSII showed significant inhibition of the effects of blue–green light-induced NPQ and apparent acceleration on its recovery (Chiu et al., 2013). These results are consistent with the proposal that the mutations on Cyt b_{559} may alter the interaction between the phycobilisome and PSII reaction centers, thereby affecting the regulation of photosynthetic light harvesting in *Synechocystis* sp. PCC 6803.

CONCLUSION AND PERSPECTIVES

Site-directed mutagenesis studies combined with spectroscopic and functional characterization have revealed multiple roles of Cyt b_{559} in the assembly and photoprotection of PSII reaction centers. The findings provide convincing evidence for the physiological role(s) of Cyt b_{559} in a photoprotective secondary electron transfer pathway within PSII reaction centers, as was suggested from earlier studies of isolated PSII complexes (reviews in Whitmarsh and Pakrasi, 1996; Stewart and Brudvig, 1998; Shinopoulos and Brudvig, 2012). In the near future, site-directed mutagenesis studies combined with advanced high-resolution protein crystallography and spectroscopic and functional analysis will provide further new insights (e.g., structure and function relationships for different redox forms of Cyt b_{559}) and possibly the final proof of the molecular mechanisms of Cyt b_{559} in PSII.

AUTHOR CONTRIBUTIONS

H-AC wrote the major part of the manuscript. Y-FC wrote the minor part of the manuscript, contributed the **Figure 1** and edited the references.

ACKNOWLEDGMENT

This work is supported by the Ministry of Science and Technology in Taiwan (104-2311-B-001-035 and 104-2627-M-001-001) and Academia Sinica to H-AC.

REFERENCES

Ananyev, G., Renger, G., Wacker, U., and Klimov, V. (1994). The photoproduction of superoxide radicals and the superoxide dismutase activity of Photosystem II. The possible involvement of cytochrome b559. *Photosynth. Res.* 41, 327–338. doi: 10.1007/BF00019410

Barber, J., and De Las Rivas, J. (1993). A functional model for the role of cytochrome b559 in the protection against donor and acceptor side photoinhibition. *Proc. Natl. Acad. Sci. U.S.A.* 90, 10942–10946. doi: 10.1073/pnas.90.23.10942

Barber, J., Morris, E. P., and da Fonseca, P. C. A. (2003). Interaction of the allophycocyanin core complex with Photosystem II. *Photochem. Photobiol. Sci.* 2, 536–541. doi: 10.1039/b300063j

Bondarava, N., De Pascalis, L., Al-Babili, S., Goussias, C., Golecki, J. R., Beyer, P., et al. (2003). Evidence that cytochrome b559 mediates the oxidation of reduced plastoquinone in the dark. *J. Biol. Chem.* 278, 13554–13560. doi: 10.1074/jbc.M212842200

Bondarava, N., Gross, C. M., Mubarakshina, M., Golecki, J. R., Johnson, G. N., and Krieger-Liszkay, A. (2010). Putative function of cytochrome b559 as a plastoquinol oxidase. *Physiol. Plant.* 138, 463–473. doi: 10.1111/j.1399-3054.2009.01312.x

Chiu, Y.-F., Chen, Y.-H., Roncel, M., Dilbeck, P. L., Huang, J.-Y., Ke, S.-C., et al. (2013). Spectroscopic and functional characterization of cyanobacterium *Synechocystis* PCC 6803 mutants on the cytoplasmic-side of cytochrome b559 in Photosystem II. *Biochim. Biophys. Acta* 1827, 507–519. doi: 10.1016/j.bbabio.2013.01.016

Chiu, Y.-F., Lin, W.-C., Wu, C.-M., Chen, Y.-H., Hung, C.-H., Ke, S.-C., et al. (2009). Identification and characterization of a cytochrome b559 *Synechocystis* 6803 mutant spontaneously generated from DCMU-inhibited photoheterotrophical growth conditions. *Biochim. Biophys. Acta* 1787, 1179–1188. doi: 10.1016/j.bbabio.2009.05.007

Dorlet, P., Xiong, L., Sayre, R. T., and Un, S. (2001). High field EPR study of the pheophytin anion radical in wild type and D1-E130 mutants of Photosystem II in *Chlamydomonas reinhardtii*. *J. Biol. Chem.* 276, 22313–22316. doi: 10.1074/jbc.M102475200

Falkowski, P. G., Fujita, Y., Ley, A., and Mauzerall, D. (1986). Evidence for cyclic electron flow around Photosystem II in *Chlorella pyrenoidosa*. *Plant Physiol.* 81, 310–312. doi: 10.1104/pp.81.1.310

Faller, P., Fufezan, C., and Rutherford, A. W. (2005). "Side-path electron donors: cytochrome b559, chlorophyll Z and β-Carotene," in *Photosystem II*, eds T. J. Wydrzynski and K. Satoh (Dordrecht: Springer), 347–365.

Faller, P., Pascal, A., and Rutherford, A. W. (2001). Beta-carotene redox reactions in Photosystem II: electron transfer pathway. *Biochemistry* 40, 6431–6440. doi: 10.1021/bi0026021

Gadjieva, R., Mamedov, F., Renger, G., and Styring, S. (1999). Interconversion of low- and high-potential forms of cytochrome b559 in tris-washed Photosystem II membranes under aerobic and anaerobic conditions. *Biochemistry* 38, 10578–10584. doi: 10.1021/bi9904656

Guerrero, F., Zurita, J. L., Roncel, M., Kirilovsky, D., and Ortega, J. M. (2014). The role of the high potential form of the cytochrome b559: study of *Thermosynechococcus elongatus* mutants. *Biochim. Biophys. Acta* 1837, 908–919. doi: 10.1016/j.bbabio.2014.02.024

Guskov, A., Kern, J., Gabdulkhakov, A., Broser, M., Zouni, A., and Saenger, W. (2009). Cyanobacterial Photosystem II at 2.9-Å resolution and the role of quinones, lipids, channels and chloride. *Nat. Struct. Mol. Biol.* 16, 334–342. doi: 10.1038/nsmb.1559

Hamilton, M. L., Franco, E., Deák, Z., Schlodder, E., Vass, I., and Nixon, P. J. (2014). Investigating the photoprotective role of cytochrome b559 in Photosystem II in a mutant with altered ligation of the haem. *Plant Cell Physiol.* 55, 1276–1285. doi: 10.1093/pcp/pcu070

Heber, U., Kirk, M. R., and Boardman, N. K. (1979). M.R. Kirk a, N.K. BoardmanPhotoreactions of cytochrome b559 and cyclic electron flow in Photosystem II of intact chloroplasts. *Biochim. Biophys. Acta* 546, 292–306. doi: 10.1016/0005-2728(79)90047-1

Hung, C.-H., Huang, J.-Y., Chiu, Y.-F., and Chu, H.-A. (2007). Site-directed mutagenesis on the heme axial-ligands of cytochrome b559 in Photosystem II by using cyanobacteria *Synechocystis* PCC 6803. *Biochim. Biophys. Acta* 1767, 686–693. doi: 10.1016/j.bbabio.2007.02.016

Hung, C.-H., Hwang, H.-J., Chen, Y.-H., Chiu, Y.-F., Ke, S.-C., Burnap, R. L., et al. (2010). Spectroscopic and functional characterizations of cyanobacterium *Synechocystis* PCC 6803 mutants on and near the heme axial ligand of cytochrome b559 in Photosystem II. *J. Biol. Chem.* 285, 5653–5663. doi: 10.1074/jbc.M109.044719

Kaminskaya, O., Shuvalov, V. A., and Renger, G. (2006). Evidence for a novel quinone-binding site in the Photosystem II (PS II) complex that regulates the redox potential of cytochrome b559. *Biochemistry* 46, 1091–1105. doi: 10.1021/bi0613022

Kaminskaya, O., Shuvalov, V. A., and Renger, G. (2007). Two reaction pathways for transformation of high potential cytochrome b559 of PS II into the intermediate potential form. *Biochim. Biophys. Acta* 1767, 550–558. doi: 10.1016/j.bbabio.2007.02.005

Kaminskaya, O. P., and Shuvalov, V. A. (2013). Biphasic reduction of cytochrome b559 by plastoquinol in Photosystem II membrane fragments: evidence for two types of cytochrome b559/plastoquinone redox equilibria. *Biochim. Biophys. Acta* 1827, 471–483. doi: 10.1016/j.bbabio.2013.01.007

Kirilovsky, D., and Kerfeld, C. A. (2012). The orange carotenoid protein in photoprotection of Photosystem II in cyanobacteria. *Biochim. Biophys. Acta* 1817, 158–166. doi: 10.1016/j.bbabio.2011.04.013

Komenda, J., Reisinger, V., Muller, B. C., Dobakova, M., Granvogl, B., and Eichacker, L. A. (2004). Accumulation of the D2 protein is a key regulatory step for assembly of the Photosystem II reaction center complex in *Synechocystis* PCC 6803. *J. Biol. Chem.* 279, 48620–48629. doi: 10.1074/jbc.M405725200

Kós, P. B., Deák, Z., Cheregi, O., and Vass, I. (2008). Differential regulation of psbA and psbD gene expression, and the role of the different D1 protein copies in the cyanobacterium *Thermosynechococcus elongatus* BP-1. *Biochim. Biophys. Acta* 1777, 74–83. doi: 10.1016/j.bbabio.2012.04.010

Krishtalik, L. I., Tae, G.-S., Cherepanov, D. A., and Cramer, W. A. (1993). The redox properties of cytochromes b imposed by the membrane electrostatic environment. *Biophys. J.* 65, 184–195. doi: 10.1016/S0006-3495(93)81050-6

Kruk, J., and Strzałka, K. (1999). Dark reoxidation of the plastoquinone-pool is mediated by the low-potential form of cytochrome b559 in spinach thylakoids. *Photosynth. Res.* 62, 273–279. doi: 10.1023/a:1006374319191

Kruk, J., and Strzalka, K. (2001). Redox changes of cytochrome b559 in the presence of plastoquinones. *J. Biol. Chem.* 276, 86–91. doi: 10.1074/jbc.M003602200

Magnuson, A., Rova, M., Mamedov, F., Fredriksson, P.-O., and Styring, S. (1999). The role of cytochrome b559 and tyrosineD in protection against photoinhibition during in vivo photoactivation of Photosystem II. *Biochim. Biophys. Acta* 1411, 180–191. doi: 10.1016/s0005-2728(99)00044-4

Morais, F., Barber, J., and Nixon, P. J. (1998). The chloroplast-encoded α subunit of cytochrome b559 is required for assembly of the Photosystem Two complex in both the light and the dark in *Chlamydomonas reinhardtii*. *J. Biol. Chem.* 273, 29315–29320. doi: 10.1074/jbc.273.45.29315

Morais, F., Kuhn, K., Stewart, D. H., Barber, J., Brudvig, G. W., and Nixon, P. J. (2001). Photosynthetic water oxidation in cytochrome b559 mutants containing a disrupted heme-binding pocket. *J. Biol. Chem.* 276, 31986–31993. doi: 10.1074/jbc.M103935200

Mulo, P., Sicora, C., and Aro, E.-M. (2009). Cyanobacterial psbA gene family: optimization of oxygenic photosynthesis. *Cell. Mol. Life Sci.* 66, 3697–3710. doi: 10.1007/s00018-009-0103-6

Nakamura, Y., Kaneko, T., Sato, S., Ikeuchi, M., Katoh, H., Sasamoto, S., et al. (2002). Complete genome structure of the thermophilic cyanobacterium *Thermosynechococcus elongatus* BP-1. *DNA Res.* 9, 123–130. doi: 10.1093/dnares/9.4.123

Nedbal, L., Samson, G., and Whitmarsh, J. (1992). Redox state of a one-electron component controls the rate of photoinhibition of Photosystem II. *Proc. Natl. Acad. Sci. U.S.A.* 89, 7929–7933. doi: 10.1073/pnas.89.17.7929

Pakrasi, H. B., Ciechi, P. D., and Whitmarsh, J. (1991). Site directed mutagenesis of the heme axial ligands of cytochrome b559 affects the stability of the Photosystem II complex. *EMBO J* 10, 1619–1627.

Pakrasi, H. B., Diner, B. A., Williams, J. G. K., and Arntzen, C. J. (1989). Deletion mutagenesis of the cytochrome b559 protein inactivates the reaction center of Photosystem II. *Plant Cell* 1, 591–597. doi: 10.2307/3868946

Pakrasi, H. B., Nyhus, K. J., and Granok, H. (1990). Targeted deletion mutagenesis of the beta subunit of cytochrome b559 protein destabilizes the reaction center of Photosystem II. *Z. Naturforsch. C* 45, 423–429.

Pakrasi, H. B., Williams, J. G., and Arntzen, C. J. (1988). Targeted mutagenesis of the psbE and psbF genes blocks photosynthetic electron transport: evidence for a functional role of cytochrome b559 in Photosystem II. *EMBO J.* 7, 325–332.

Pospíšil, P. (2011). Enzymatic function of cytochrome b559 in Photosystem II. *J. Photochem. Photobiol. B* 104, 341–347. doi: 10.1016/j.jphotobiol.2011.02.013

Pospíšil, P., Šnyrychová, I., Kruk, J., Strzałka, K., and Nauš, J. (2006). Evidence that cytochrome b559 is involved in superoxide production in Photosystem II: effect of synthetic short-chain plastoquinones in a cytochrome b559 tobacco mutant. *Biochem. J.* 397, 321–327. doi: 10.1042/BJ20060068

Pospíšil, P., and Tiwari, A. (2010). Differential mechanism of light-induced and oxygen-dependent restoration of the high-potential form of cytochrome b559 in Tris-treated Photosystem II membranes. *Biochim. Biophys. Acta* 1797, 451–456. doi: 10.1016/j.bbabio.2009.12.023

Poulson, M., Samson, G., and Whitmarsh, J. (1995). Evidence that cytochrome b559 protects Photosystem II against photoinhibition. *Biochemistry* 34, 10932–10938. doi: 10.1021/bi00034a027

Roncel, M., Ortega, J. M., and Losada, M. (2001). Factors determining the special redox properties of photosynthetic cytochrome b559. *Eur. J. Biochem.* 268, 4961–4968. doi: 10.1046/j.0014-2956.2001.02427.x

Rutherford, A. W., and Krieger-Liszkay, A. (2001). Herbicide-induced oxidative stress in Photosystem II. *Trends Biochem. Sci.* 26, 648–653. doi: 10.1016/S0968-0004(01)01953-3

Shibuya, Y., Takahashi, R., Okubo, T., Suzuki, H., Sugiura, M., and Noguchi, T. (2010). Hydrogen bond interaction of the pheophytin electron acceptor and its radical anion in Photosystem II as revealed by Fourier transform infrared difference spectroscopy. *Biochemistry* 49, 493–501. doi: 10.1021/bi9018829

Shinopoulos, K. E., and Brudvig, G. W. (2012). Cytochrome b559 and cyclic electron transfer within Photosystem II. *Biochim. Biophys. Acta* 1817, 66–75. doi: 10.1016/j.bbabio.2011.08.002

Stewart, D. H., and Brudvig, G. W. (1998). Cytochrome b559 of Photosystem II. *Biochim. Biophys. Acta* 1367, 63–87. doi: 10.1016/s0005-2728(98)00139-x

Sugiura, M., Azami, C., Koyama, K., Rutherford, A. W., Rappaport, F., and Boussac, A. (2014). Modification of the pheophytin redox potential in *Thermosynechococcus elongatus* Photosystem II with PsbA3 as D1. *Biochim. Biophys. Acta* 1837, 139–148. doi: 10.1016/j.bbabio.2013.09.009

Sugiura, M., Nakamura, M., Koyama, K., and Boussac, A. (2015). Assembly of oxygen-evolving Photosystem II efficiently occurs with the apo-Cyt b559 but the holo-Cyt b559 accelerates the recovery of a functional enzyme upon photoinhibition. *Biochim. Biophys. Acta* 1847, 276–285. doi: 10.1016/j.bbabio.2014.11.009

Suorsa, M., Regel, R. E., Paakkarinen, V., Battchikova, N., Herrmann, R. G., and Aro, E.-M. (2004). Protein assembly of Photosystem II and accumulation of subcomplexes in the absence of low molecular mass subunits PsbL and PsbJ. *Eur. J. Biochem.* 271, 96–107. doi: 10.1046/j.1432-1033.2003.03906.x

Swiatek, M., Regel, R. E., Meurer, J., Wanner, G., Pakrasi, H. B., Ohad, I., et al. (2003). Effects of selective inactivation of individual genes for low-molecular-mass subunits on the assembly of Photosystem II, as revealed by chloroplast transformation: the psbEFLJ operon in *Nicotiana tabacum*. *Mol. Genet. Genomics* 268, 699–710. doi: 10.1007/s00438-002-0791-1

Thompson, L. K., and Brudvig, G. W. (1988). Cytochrome b559 may function to protect Photosystem II from photoinhibition. *Biochemistry* 27, 6653–6658. doi: 10.1021/bi00418a002

Tichy, M., Lupinkova, L., Sicora, C., Vass, I., Kuvikova, S., Prasil, O., et al. (2003). *Synechocystis* 6803 mutants expressing distinct forms of the Photosystem II D1 protein from *Synechococcus* 7942: relationship between the psbA coding region and sensitivity to visible and UV-B radiation. *Biochim. Biophys. Acta* 1605, 55–66. doi: 10.1016/S0005-2728(03)00064-1

Tiwari, A., and Pospísil, P. (2009). Superoxide oxidase and reductase activity of cytochrome b559 in Photosystem II. *Biochim. Biophys. Acta* 1787, 985–994. doi: 10.1016/j.bbabio.2009.03.017

Tracewell, C. A., and Brudvig, G. W. (2008). Characterization of the secondary electron-transfer pathway intermediates of Photosystem II containing low-potential cytochrome b559. *Photosynth. Res.* 98, 189–197. doi: 10.1007/s11120-008-9360-8

Umena, Y., Kawakami, K., Shen, J. R., and Kamiya, N. (2011). Crystal structure of oxygen-evolving Photosystem II at a resolution of 1.9 *Å*. *Nature* 473, 55–60. doi: 10.1038/nature09913

Vass, I., and Cser, K. (2009). Janus-faced charge recombinations in Photosystem II photoinhibition. *Trends Plant Sci.* 14, 200–205. doi: 10.1016/j.tplants.2009.01.009

Vass, I., Styring, S., Hundal, T., Koivuniemi, A., Aro, E., and Andersson, B. (1992). Reversible and irreversible intermediates during photoinhibition of Photosystem II: stable reduced QA species promote chlorophyll triplet formation. *Proc. Natl. Acad. Sci. U.S.A.* 89, 1408–1412. doi: 10.1073/pnas.89.4.1408

Whitmarsh, J., and Pakrasi, H. (1996). "Form and function of cytochrome b559," in *Oxygenic Photosynthesis: The Light Reactions*, eds D. Ort and C. Yocum (Dordrecht: Springer), 249–264.

Yadav, D. K., Prasad, A., Kruk, J., and Pospíšil, P. (2014). Evidence for the involvement of loosely bound plastosemiquinones in superoxide anion radical production in Photosystem II. *PLoS ONE* 9:e115466. doi: 10.1371/journal.pone.0115466

Conflict of Interest Statement: The authors declare that the research was conducted in the absence of any commercial or financial relationships that could be construed as a potential conflict of interest.

frontiers in Plant Science

REVIEW
published: 18 August 2016
doi: 10.3389/fpls.2016.01223

Iron–Nutrient Interactions within Phytoplankton

Hanan Schoffman[1†], Hagar Lis[2†], Yeala Shaked[2,3] and Nir Keren[1]*

[1] Department of Plant and Environmental Sciences, Institute of Life Sciences, The Hebrew University of Jerusalem, Jerusalem, Israel, [2] The Freddy and Nadine Herrmann Institute of Earth Sciences, Hebrew University of Jerusalem, Jerusalem, Israel, [3] Interuniversity Institute for Marine Sciences in Eilat, Eilat, Israel

Iron limits photosynthetic activity in up to one third of the world's oceans and in many fresh water environments. When studying the effects of Fe limitation on phytoplankton or their adaptation to low Fe environments, we must take into account the numerous cellular processes within which this micronutrient plays a central role. Due to its flexible redox chemistry, Fe is indispensable in enzymatic catalysis and electron transfer reactions and is therefore closely linked to the acquisition, assimilation and utilization of essential resources. Iron limitation will therefore influence a wide range of metabolic pathways within phytoplankton, most prominently photosynthesis. In this review, we map out four well-studied interactions between Fe and essential resources: nitrogen, manganese, copper and light. Data was compiled from both field and laboratory studies to shed light on larger scale questions such as the connection between metabolic pathways and ambient iron levels and the biogeographical distribution of phytoplankton species.

Keywords: nutrient, co-limitation, limitation, manganese, iron, nitrogen, photosynthesis, phytoplankton

OPEN ACCESS

Edited by:
Julian Eaton-Rye, University of Otago, New Zealand

Reviewed by:
Tom Bibby, University of Southampton, UK
Douglas Andrew Campbell, Mount Allison University, Canada

****Correspondence:***
Nir Keren
nir.ke@mail.huji.ac.il

† These authors have contributed equally to this work.

Specialty section:
This article was submitted to Plant Cell Biology, a section of the journal Frontiers in Plant Science

Received: *16 March 2016*
Accepted: *02 August 2016*
Published: *18 August 2016*

Citation:
Schoffman H, Lis H, Shaked Y and Keren N (2016) Iron–Nutrient Interactions within Phytoplankton. Front. Plant Sci. 7:1223. doi: 10.3389/fpls.2016.01223

INTRODUCTION

Of all the trace metals, iron (Fe) is especially prominent in biochemical catalysis (Morel and Price, 2003; Shcolnick and Keren, 2006). Most life forms are heavily dependent on iron (for interesting exceptions see Archibald, 1983 and Aguirre et al., 2013) and phytoplankton, with their Fe-rich photosynthetic apparatus, have significantly higher Fe demands as opposed to their heterotrophic counterparts (Raven et al., 1999). The intracellular Fe content of these phototrophic microorganisms is 4–6 orders of magnitude greater than the Fe concentrations in their surroundings (Morel and Price, 2003), necessitating a substantial energetic investment in Fe uptake. Indeed, iron availability limits primary production in approximately one third of the world's oceans (Martin, 1990; Boyd et al., 2007; Breitbarth et al., 2010) as well as some fresh water environments (McKay et al., 2004; North et al., 2007, 2008). For more on iron limitation and iron chemistry, see **Box 1**.

Thanks to its flexible redox chemistry, iron is well suited for electron transfer reactions and therefore serves a wide range of catalytic functions. One of the most prominent Fe-dependent processes in phytoplankton is the photosynthetic transport chain. Iron is found within the reaction center of both photosystems, with 2–3 Fe atoms in photosystem II (PSII) and 12 Fe atoms in photosystem I (PSI) (Raven et al., 1999). PSI is likely the greatest iron sink in phytoplankton. Cytochrome *c* and cytochrome b_6f are two Fe-containing electron carriers within the photosynthetic and respiratory electron transfer chains. In addition, iron is a structural component of nitrate assimilation enzymes as well as in nitrogenase, the nitrogen fixing enzyme

BOX 1 | Why does iron limit primary productivity in aquatic environments? Iron limits primary productivity in up to one third of the world's oceans. This may be surprising in light of the fact that not only is Fe the fourth most abundant element in the Earth's crust (Taylor, 1964; Martin et al., 1989), but it is also required in trace amounts (extended Redfield ratios C:N:P is 106:16:1 as opposed to C:Fe 1:0.001; Sunda et al., 1991; Quigg et al., 2003). Unfortunately, for phytoplankton, readily bioavailable iron in aquatic environments is vanishingly scarce. Fe is found in two environmentally relevant oxidation states – Fe(II) and Fe(III). Of the pair, Fe(II) is the more soluble and reactive while Fe(III) has very low solubility and tends to precipitate as ferric oxyhydroxides (Millero, 1998; Liu and Millero, 2002). Under the oxic conditions and near neutral pH characterizing most aquatic habitats in which phytoplankton are found, iron is present in its ferric form – Fe (III). This means that dissolved Fe concentrations are low, reaching sub-nanomolar levels in open ocean waters (Johnson et al., 1997; McKay et al., 2004). In addition, over 99% of dissolved iron is bound by strong organic ligands (Gledhill and Van den Berg, 1994; Rue and Bruland, 1995; Wu and Luther, 1995), which may render the iron less bioavailable (see Shaked and Lis, 2012 and Lis et al., 2015b for discussion of this topic).

and in superoxide dismutase (Fe-SOD) which is involved in the processing of the reactive oxygen species superoxide.

Above are just some examples of iron's essential roles and, as can be seen, Fe influences a wide range of metabolic pathways, be it directly or indirectly. Iron metabolism is thus intertwined with the metabolism of other macro and micronutrients within the cell. In this review, we explore the interactions between iron and other nutrients within phytoplankton cells, assessing iron-limiting and iron-sufficient scenarios. It should be noted that we use the term iron "limitation" to define a physiological status in which Fe is in short supply but not completely absent within the cell. The understanding of Fe–nutrient interactions at the cellular level serves to elucidate larger scale questions such as elemental stoichiometry within cells, phytoplankton community composition and interactions within natural waters and the biogeographic distribution of different phytoplankton species.

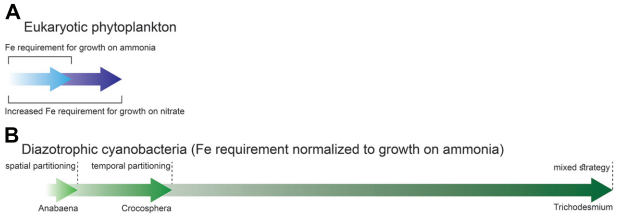

FIGURE 1 | Phytoplankton iron requirements vary as a function of the nitrogen species acquired. (A) In eukaryotic phytoplankton nitrate assimilation requires roughly 1.8 times more iron than ammonia utilization (Raven, 1988). **(B)** In nitrogen-fixing cyanobacteria iron requirement differs as a function of the strategy utilized by the organism to partition N_2 fixation from oxygen evolution during photosynthesis. The data in this figure is based on Raven (1988) and Berman-Frank et al. (2007).

SELECTED EXAMPLES OF IRON INTERACTION WITH MACRO AND MICRONUTRIENTS

Iron/Nitrogen

Iron metabolism intersects with a range of macronutrients, including phosphorous (Mills et al., 2004), nitrogen and silica in diatoms (Armbrust, 2009). Here we focus on nitrogen, where interaction with iron has been extensively studied as compared to the other nutrients listed above. Theoretical calculations (Raven, 1988; Morel et al., 1991), laboratory (Maldonado and Price, 1996; Wang and Dei, 2001) and field experiments (Price et al., 1991) show that the iron requirements of phytoplankton are strongly influenced by their nitrogen source. This is because ammonia (NH_4^+) can be directly incorporated into amino acids, but nitrate (NO_3) and nitrogen (N_2) must be reduced to ammonia prior to assimilation. Phytoplankton growing on ammonia have lower Fe requirements than the same cells growing on nitrate or those which are able to convert N_2 to NH_4^+ via nitrogen fixation (**Figure 1**).

The link between iron and nitrogen fixation has received much attention: while enrichment experiments show that nitrogen may be limiting in certain marine environments over short time scales, nitrogen fixation increases the N inventory of the ocean over geological time scales (Falkowski, 1997; Mills et al., 2004). The "ultimate" limiting nutrient in large areas of the world's oceans is thus the one that limits nitrogen fixation.

Examples from Eukaryotic Phytoplankton: Fe and Nitrate Assimilation

Growth on nitrate requires more iron than does growth on ammonia (**Figure 1A**). The extra iron is needed for nitrate assimilation. Firstly, the two NO_3^--reducing enzymes (nitrate and nitrite reductase) contain Fe cofactors. Secondly, the reducing power for NO_3^- reduction is produced by the photosynthetic electron transport chain. Field experiments performed by Price et al. (1991) and Ditullio et al. (1993) suggest that iron availability may limit nitrate uptake in natural waters. These studies observed increased NO_3^- uptake rates by phytoplankton following addition of iron to waters from the Equatorial Pacific and North Pacific Ocean, respectively. Indeed, the nitrate and nitrite reductase activities of eukaryotic phytoplankton decrease when cells are iron limited (Timmermans et al., 1994; Milligan and Harrison, 2000). Transcriptional analysis of *Phaeodactylum* diatoms under Fe limitation revealed a reduced capacity for nitrate uptake – genes associated with nitrate assimilation were downregulated, including the aforementioned reductase enzymes (Allen et al., 2008). Despite lowered enzyme activity, the cellular nitrogen requirement of the diatoms was still fully met and intracellular carbon to nitrogen ratios did not increase under these conditions, as would be expected under nitrogen stress. Therefore, Fe limitation will probably not lead to nitrogen limitation of the cell. Having said this, when cellular iron levels are low, phytoplankton cells do not take up nitrate as efficiently as they would under Fe-sufficient conditions. The major reason for this is an energy constraint. Iron limitation induces a decrease in

the photosynthetic activity, thereby decreasing the reductive power available for NO_3 assimilation (Morel et al., 1991; Milligan and Harrison, 2000). Therefore, iron limits nitrate acquisition primarily through its role in the photosynthetic transport chain rather than its role in nitrate-reducing enzymes. Interestingly, phytoplankton cultures grown on NO_3 demonstrate a greater light dependency than those grown on NH_4 under both Fe sufficient and deficient conditions (Larsson et al., 1985; Rueter and Ades, 1987; Li et al., 2004). Like iron, low light levels induce an energy constraint on nitrate assimilation because of lower photosynthetic activity. Therefore, low light can greatly aggravate the effect of Fe limitation on nitrate acquisition, a situation which may be of environmental relevance in high latitude, low iron waters.

Examples from Cyanobacteria: Fe and Nitrogen Fixation

Nitrogen fixation places an additional Fe burden on diazotrophic organisms on top of their routine cellular Fe requirements (Raven, 1988; Kustka et al., 2002). The N_2-fixing enzyme nitrogenase contains 38 Fe atoms per holoenzyme (Raven, 1988; Whittaker et al., 2011). Adding to the Fe burden are the facts that: (a) nitrogenase is characterized by slow reaction rates, necessitating a relatively large intracellular pool of this enzyme and (b) N_2 fixation requires a large amount of photosynthetically derived energy and reducing power (Raven, 1988). Nitrogenase is irreversibly inhibited by molecular oxygen (Postgate, 1998; Bergman, 2001; Gallon, 2001; Berman-Frank et al., 2003). Therefore, N_2 fixation in diazotrophic cyanobacteria presents a unique constraint – conducting an oxygen sensitive process within an O_2 evolving organism. This has led to the temporal and/or spatial partitioning of N_2 fixation from photosynthetic processes within these organisms. Each partitioning strategy has its particular Fe costs (**Figure 1B**).

Unicellular marine diazotrophs, like *Cyanothece*, exhibit temporal separation of photosynthesis and N_2 fixation with the former being performed during the day and the latter at night (Reddy et al., 1993; Colón-López et al., 1997; Welkie et al., 2014). Some filamentous cyanobacteria such as *Anabaena* implement spatial partitioning of N_2 fixation within specialized heterocyst cells (Haselkorn, 1978; Kumar et al., 2010). The photosynthetic transport chain within heterocysts has been modified to minimize O_2 concentrations. The oxygen evolution capacity of PSII is eliminated – some studies report the complete absence of PSII while others describe modified PSII which lack water-splitting capabilities (for further details on this fascinating subject see Wolk et al., 1994 and references therein and Cardona et al., 2009). A further modification of the photosynthetic transport chain within heterocysts is the abundance of PSI and ATP synthase (Cardona et al., 2009). PSI is situated at a bioenergetics crossroad: electrons leaving PSI can be used for linear electron flow producing ATP and NADPH or to the cyclic or pseudo-cyclic Mehler reaction which produces only ATP (Asada, 2006). The Mehler pathway may also serve as a sink for molecular oxygen within heterocysts (Berman-Frank et al., 2001b; Milligan et al., 2007). Light induced a threefold increase in O_2 consumption by purified heterocysts cells from *Anabaena* (Milligan et al., 2007). The Mehler reaction also plays an important role in the prominent non-heterocystous marine diazotroph *Trichodesmium*. Milligan et al. (2007) show that the Mehler reaction can consume as much as 75% of gross O_2 production when grown on N_2 as opposed to 10% when the cells are grown on NO_3. This can be put down to the fact that *Trichodesmium* perform both N_2 fixation and oxygenic photosynthesis within the same cell. Both processes occur in different regions of the same cell (spatial separation) and their respective activities peak at different times during the photoperiod (temporal separation) (Berman-Frank et al., 2003). N_2 fixation peaks around mid-day and concurs with a depression in carbon fixation, lowered photosynthetic quantum yield, decreased net oxygen evolution and an increase in the Mehler reaction (Berman-Frank et al., 2001b). The high iron content of *Trichodesmium* have been confirmed by several laboratory studies (e.g., Rueter et al., 1992; Berman-Frank et al., 2001a; Webb et al., 2001; Fu and Bell, 2003; Chappell and Webb, 2010). However, as will be discussed below, applying theoretical calculations to the question of whether iron limits nitrogen fixation the field may prove to be tricky.

The environmental distribution of the N_2-fixation strategies described above is strongly influenced by ambient iron concentrations. Heterocystous strains such as *Anabaena* are generally found in high Fe environments such as fresh, brackish or coastal waters. These organisms are filamentous and large and are thus likely to practice luxury iron uptake and storage. However, because of their size and iron requirements, heterocystous cyanobacteria are prone to iron limitation in environmental and laboratory settings. In comparison, smaller unicellular diazotrophs such as *Cyanothece* have the advantage of a large surface area to volume ratio and can be found in open ocean waters where Fe concentration are considerably lower (Zehr et al., 2001). *Cyanothece* practices a cost-efficient method of diurnal separation of N_2 from photosynthesis (Reddy et al., 1993; Stöckel et al., 2008) which allows for Fe recycling between photosynthetic apparatus during the day and nitrogenase at night (Tuit et al., 2004; Berman-Frank et al., 2007). The non-heterocystous open ocean diazotroph *Trichodesmium* may inhabit Fe-poor waters despite high iron demands. This is by virtue of their high Fe use efficiency (Berman-Frank et al., 2007), symbiotic association with bacteria which may aid in iron acquisition (Achilles et al., 2003; Roe et al., 2012) and the ability to access unconventional iron sources such as the colloidal and particulate pools (Rueter et al., 1992; Rubin et al., 2011; Bergman et al., 2013).

The extent of Fe limitation of environmental N_2 fixation is still under debate. Both iron and phosphorous may limit nitrogen fixation. A recent study by Snow et al. (2015) highlights the complexity of the interactions between iron, phosphorous and diazotrophs within the Northern Atlantic. Enrichment experiments in natural environments give contrasting results: Moore et al. (2009) suggest that large-scale patterns of N_2 fixation in the north and south Atlantic correlate primarily with Fe availability. On the other hand, Sañudo-Wilhelmy et al. (2001) showed that N fixation rates of *Trichodesmium* species in the central Atlantic Ocean are independent of dissolved

iron concentrations and are rather limited by phosphate. To complicate matters further, Mills et al. (2004) report on Fe–P co-limitation of N fixation in the eastern tropical North Atlantic while Bonnet et al. (2008) observed no response to Fe and P additions in the southern subtropical Pacific Gyre.

Iron/Manganese

The crucial roles of manganese in photosynthesis and growth of autotrophic organisms have long been recognized (Raven, 1990; Merchant and Sawaya, 2005; Nelson and Junge, 2015). Four manganese atoms form the core of the water-splitting catalytic site of PSII. Aside from this, Mn and Fe may act as cofactors in the scavenging of reactive oxygen species (ROS), with phytoplankton typically containing both Fe and Mn forms of the superoxide-disproportionating enzyme superoxide dismutase (SOD) (see Wolfe-Simon et al., 2005 for a review). Although both Fe and Mn play major roles in photosynthesis, the consequences of Fe limitation on growth and photosynthetic activity of phytoplankton are more severe than those induced by Mn limitation (Brand et al., 1983; Bruland et al., 1991; Salomon and Keren, 2011, 2015; Hernandez-Prieto et al., 2012; Fraser et al., 2013; Sharon et al., 2014; Rudolf et al., 2015). Indeed, Fe is more commonly a limiting factor on growth and photosynthetic activity of phytoplankton in natural environments. Insufficient Fe in the cell may lead to a shortage in electron carriers within the photosynthetic chain. This, in turn, results in a lack of sinks for the electrons generated by PSII activity. "Stray" electrons then leak out and reduce molecular oxygen molecules leading to the formation of the ROS – superoxide (Asada, 2006).

Examples from Eukaryotic Phytoplankton: Mn and Fe SOD

Studies conducted on the fresh water *Chlamydomonas reinhardtii* (Allen et al., 2006) and marine *Thalassiosira* diatom species (Peers and Price, 2004) show an increased Mn requirement and concurrent increase of Mn-SOD activity under Fe-limiting conditions. This phenomenon can be appreciated on two levels. First, Mn-SOD is necessary to deal with the ROS induced by iron limitation. Second, Mn-SOD may replace Fe-SOD. The two SOD isoforms are typically found in one of two organelles – Mn-SODs serve in the mitochondria while Fe-SODs are generally found in the chloroplast. Interestingly, Allen and coworkers (Allen et al., 2006) report the localization of Mn-SOD in both the chloroplast and mitochondria under Fe-limitation, indicating an Mn-mediated compensation for Fe limitation.

Peers and Price (2004) observed a unique photosynthetic and growth response upon addition of either Fe or Mn to cultures limited by both nutrients and a synergistic effect when adding both trace elements together. This suggests that Mn–Fe interaction extends beyond simple substitution within the SOD enzyme. Both manganese and iron limitation reduce photosynthetic yield. However, their influence is mediated via different molecular routes. While Mn availability determines the photochemical activity of the overall pool of PSII, Fe availability affects all of the membrane complexes involved in photosynthetic and respiratory electron transport. Therefore, addition of either trace metal will increase photosynthetic yield and growth but only the addition of both will result in maximal growth rates and photosynthetic activity observed in non-limited cultures.

Examples from Cyanobacteria: Mn Mediation of Fe Stress Response and Fe/Mn Transport

The model cyanobacterium *Synechocystis* sp. PCC 6803 show reduced photosynthetic yield under both Fe and Mn limitation (Sandstrom et al., 2002; Singh and Sherman, 2007; Shcolnick et al., 2009; Salomon and Keren, 2011). Interestingly, the study of Mn/Fe co-limitation introduced a temporal element into the interactions of these two metals (Salomon and Keren, 2015). *Synechocystis* cells acclimated to Mn deficiency prior to Fe limitation showed an atypical response to iron stress. While these cells were able to respond to iron insufficiency by inducing specific Fe transporters, other physiological responses to Fe limitation were not observed, including loss of additional PSI activity and induction of *isiAB* transcription – a hallmark of iron stress in cyanobacteria. This suggests that acclimation to environmentally relevant Mn concentrations, much lower than those employed in laboratory experiments suggest, modulates iron stress responses. At low extracellular Mn concentrations the number of functional PSII units decreases and with it the electron flux generated by water splitting activity. This may protect photosynthetic organisms from the deleterious effects of oxidative damage during Fe-limiting conditions in environments prone to fluctuations in iron concentrations.

Sharon et al. (2014) report reduced intracellular Mn content under iron limitation in *Synechocystis* sp. PCC 6803. The cause of this is hypothesized to be reduced transport of Mn into the cell. Since Mn^{2+} and Fe^{3+} have very similar coordination spheres (Williams and Frausto da Silva, 2001), it is reasonable to assume that Fe^{3+} transporters will serve as a low affinity Mn^{2+} transport system. Examination of the changes in Fe transporter expression during transition into Fe limitation show little changes in the transcription of Fe(III) permeases and an upregulation of genes encoding for proteins involved in Fe^{2+} uptake via reduction (Kranzler et al., 2014). Strong support for this hypothesis is provided by radioactive Fe transport assays (Kranzler et al., 2011) where Fe limited cells exhibit a ∼7 fold increase in the rate of reduction and a two order of magnitude increase in the rate of Fe^{2+} uptake, as compared to replete cells. Fe^{2+}configuration differs from that of Fe^{3+} and Mn^{2+}. Therefore, Fe^{3+} but not Fe^{2+} transport, will be able to support non-specific Mn^{2+} transport. Mn transport via Fe^{3+} transporters may account for the unidentified low affinity Mn transport system detected by Bartsevich and Pakrasi (1996). Such "promiscuity" of metal binding proteins has been demonstrated for Mn/Cu/Zn and Cu/Co (Tottey et al., 2008; Foster and Robinson, 2011).

Iron/Copper: Plastocyanin/Cytochrome c_6 and Copper Dependent Iron Uptake

Enrichment experiments conducted by Coale (1991) and Peers et al. (2005) in the Fe-limited Bering Sea showed that Fe addition elicited the greatest growth response, and addition of Cu induced a lower, yet significant, increase of phytoplankton growth. The addition of both trace metals had a synergistic effect on growth rates (Peers et al., 2005). Copper, like iron, plays a role in

photosynthetic and respiratory electron transfer reactions. In the exploration of Cu–Fe interactions within the cell, we will consider the following biochemical intersections: (1) interchangeability between the copper-based electron carrier plastocyanin and its functionally equivalent iron based homologue – cytochrome c_6 within the photosynthetic electron transfer chain and (2) the role of copper in high affinity iron transport systems.

Both cytochrome c_6 (Fe based) and plastocyanin (Cu based) transfer electrons between the cytochrome b_6f complex (hereafter cytochrome b_6f) and PSI. In both cyanobacteria and green algae the expression of these proteins was found to be dependent on the Cu status of the cell with plastocyanin being replaced by cytochrome c_6 under Cu-deplete conditions (Wood, 1978 and review in Merchant and Helmann, 2012). The expression of these two electron carriers is regulated as a function of copper and iron availability. For example, oceanic diatoms constitutively express the Cu-based carrier plastocyanin in lieu of the Fe-based cytochrome c_6 (Peers and Price, 2006). The selective pressure favoring plastocyanin is a result of continual exposure to Fe limitation in open ocean environments. While lowering Fe dependency, this apparent tradeoff elevates Cu demand by 10-fold and leaves open ocean diatoms more susceptible to Cu limitation than their coastal counterparts (Peers et al., 2005). These findings could account for the dual limitation by Cu and Fe observed in the Bering Sea (Peers et al., 2005; Peers and Price, 2006; Annett et al., 2008).

Cu–Fe interactions can also take the form of biochemical dependence in certain organisms – when one nutrient is required in the other's acquisition. A multi-copper oxidase-permease complex plays a role in high affinity Fe transport in iron-stressed eukaryotic phytoplankton, among them *C. reinhardtii* (La Fontaine et al., 2002; Merchant et al., 2006; Blaby-Haas and Merchant, 2013) and several marine diatoms (Maldonado et al., 2006). As with plastocyanin expression, this system also leads to an increased cellular Cu demand under Fe limitation. Since copper supports increased iron uptake, the addition of both trace metals to co-limited cells induces a synergistic growth response. Interestingly, a second well-characterized high affinity iron transport system within phytoplankton also features Cu–Fe interplay. Some Fe-limited cyanobacteria produce low-molecular-weight Fe-specific chelators known as siderophores. Along with their high specificity for binding iron, siderophores are also able to bind copper, a potentially harmful trace metal (Sunda, 1975). Several studies have suggested that siderophores may mitigate copper toxicity (the Cu-siderohore complex is not toxic to cells and cannot be transported into the cell); however, this is a benefit second to their primary role in iron acquisition (Clarke et al., 1987; Nicolaisen et al., 2010).

Iron/Light

Light energy imposes a fundamental constraint on primary productivity; and given the strong coupling between iron and photosynthetic electron transfer, Fe-light interactions are inevitable (**Figure 2**). Sub-optimal light conditions need not be confined to low light intensities but can also include damaging high light intensities. Both have been shown to inhibit the photosynthetic activity and the growth of phytoplankton (Adir et al., 2003; Hakala et al., 2005; Komenda et al., 2012; Tyystjärvi, 2013; Roach and Krieger-Liszkay, 2014; Järvi et al., 2015). The definition of low, high and excess light is organism dependent, with different strains exhibiting unique responses to a range of light intensities. These can be described by the photosynthesis vs. irradiation (PI) curve under defined conditions (Hassidim et al., 1997; Eisenstadt et al., 2008).

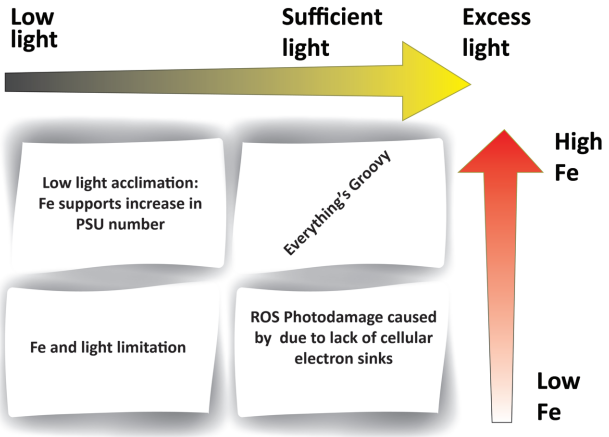

FIGURE 2 | Iron–light interactions within phytoplankton. The figure outlines different combinations of iron and light availability. Low iron (e.g., in HNLC regions) results in insufficient Fe-containing electron carriers within the photosynthetic electron transport chain. Low light levels (e.g., high latitudes) induce an increase in Fe requirements in order to support greater PSU number. A lack in both Fe and light (e.g., high latitude HNLC regions) results in the dual limitation of photosynthesis.

Examples from Eukaryotic Phytoplankton: PSI and Cytochrome b_6f

Studies of phytoplankton cultures have long shown a discrepancy in the iron requirements and use efficiencies (expressed as mol assimilated C per mol cellular Fe) of coastal as opposed to open ocean eukaryotic phytoplankton (Sunda and Huntsman, 1995, 1997) and cyanobacteria (Sunda and Huntsman, 2015). This phenomenon may be explained by differences in the photosynthetic architecture of organisms residing in these two environments. Oceanic diatoms contain several fold less PSI and cytochrome b_6f as compared to coastal diatoms (Strzepek and Harrison, 2004). Both these components of the photosynthetic apparatus are major sinks of cellular iron (Raven et al., 1999), resulting in lower Fe requirements of open ocean as compared to coastal diatoms. Such differences most likely reflect the evolution of oceanic phytoplankton under Fe-poor but relatively uniform light conditions. Strzepek and Harrison (2004) show that while oceanic isolates have a much lower Fe requirement due to a lowered PSI:PSII and cytochrome b_6f:PSII ratios, this also causes a reduced tolerance to rapid changes in irradiance as compared to coastal isolates. On the other hand, coastal diatoms have a greater Fe requirement but are equipped to handle the fluctuating light intensities which characterize dynamic and turbid coastal waters. This is because PSI and cytochrome b_6f can participate in cyclic

electron transport processes, which alleviate excitation pressure (Takahashi et al., 2013).

The capture of photons by any single photosystem can be considered as a statistical event. Therefore one way of acclimating to sub-saturating light conditions, is to increase the number of active photosynthetic units (PSU). This, in turn, increases the iron requirement of cells (Falkowski et al., 1981; Raven, 1990). Culture experiments show increased Fe requirements of phytoplankton grown under low light intensities (e.g., Sunda and Huntsman, 1997, 2011, 2015). Therefore, environments characterized by both low light intensities and paucity of iron very likely foster the dual limitation of photosynthetic organisms by iron and light. One striking example relates to high latitude High Nutrient Low Chlorophyll (HNLC) regions distinguished by low Fe concentrations in ambient waters and seasonally low light conditions. Incubation experiments in these areas show that the increase of irradiance and addition of Fe elicited a growth response independently while a concomitant increase in both factors acted synergistically to produce the greatest growth response (Maldonado and Price, 1999). These results can be explained by a biochemical dependence of light on iron – a situation in which one resource in required in order to acquire another resource efficiently. A recent study on Southern Ocean diatoms uncouples the traditional association between low light and high iron demand (Strzepek et al., 2012). These organisms were able to increase their light use efficiency without increasing their iron demands significantly. This is accomplished by increasing PSU size rather than the number of PSUs, a strategy that is not as costly in iron.

Examples from Cyanobacteria: *isiAB*

Typical cyanobacterial Fe-stress responses include a decrease in both PSI abundance (Fraser et al., 2013) and phycobillisome cross-section (Sherman and Sherman, 1983; Sandmann, 1985; Salomon and Keren, 2015) and, in certain strains, the expression of *isiAB* (Laudenbach and Straus, 1988; Ghassemian and Straus, 1996; Park et al., 1999; Dühring et al., 2006). Lowering the number of PSI complexes reduces Fe requirements as does the induction of *isiB* coding for a flavodoxin that can replace ferredoxin within the electron transport chain (Laudenbach et al., 1988). The function of IsiA, on the other hand, remains ambiguous (Singh and Sherman, 2007; Behrenfeld and Milligan, 2013). IsiA bears a strong structural similarity to the PSII chlorophyll binding CP43 protein (reviewed in Singh and Sherman, 2007). IsiA binds chlorophyll and forms a ring around photosystem I (Bibby et al., 2001b; Boekema et al., 2001). However, it can also form aggregates in the total absence of PSI (Yeremenko et al., 2004; Ihalainen et al., 2005; Wilson et al., 2007; Berera et al., 2009). This protein has been suggested to offset either of the following possible outcomes of iron-light limitation in photosynthetic organisms: (1) a decrease in photosynthetic activity and (2) potential oxidative damage under high light conditions arising from a shortage in Fe electron carriers.

It has been suggested that IsiA increases the PSU size and PSI cross-section under Fe deficiency in order to compensate for the lowering of phycobilisome and PSI levels (Bibby et al., 2001a; Fromme et al., 2003; Ryan-Keogh et al., 2012; Sun and Golbeck, 2015). On the other hand, during iron starvation electron flux originating from PSII is likely to cause oxidative

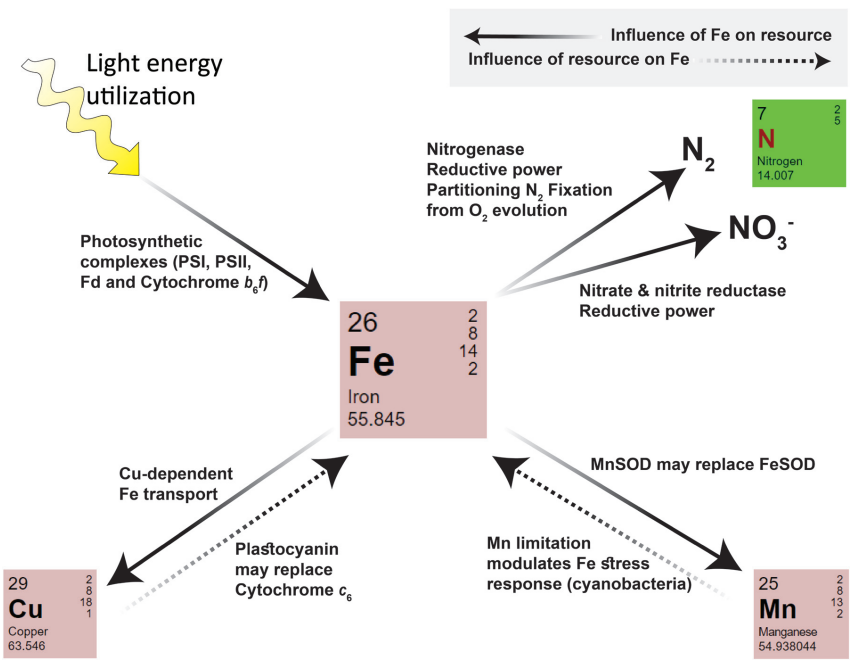

FIGURE 3 | A summary of intracellular interactions between iron and N, Mn, Cu, and light within phytoplankton. Iron influences the requirement and uptake/utilization of a given resource (indicated by arrows with solid lines). The Fe requiring processes and enzymes of each pathway are indicated next to the arrow. Iron itself may also be influenced by other resources (indicated by arrows with dashed lines).

TABLE 1 | Tradeoffs and co-limitation scenarios for iron-nitrogen, manganese, copper, and light interactions.

Resource	Description of interaction	Type of interaction/s with iron	Trade offs	Adaptations to low [Fe]	Co-limitation scenarios
Nitrogen	Photochemically produced reductive energy (NADPH) requires Fe based electron carriers. Fe dependent enzymes: Nitrate and nitrite reductases (NO_3) Nitrogenase (N_2)	Biochemical dependence	Ambient Fe concentrations constrain biogeographic distribution of diazotrophic/non-diazotrophic phytoplankton in accordance with their partitioning strategy.	Temporal partitioning of N_2 fixations allows for smaller cells and Fe recycling.	While iron limitation lowers the efficiency of NO_3 uptake, nitrogen demands of Fe-limited cells can still be fully met. Nitrogen fixation may be Fe limited.
Manganese	Mn-SOD may replace Fe-SOD Transporter promiscuity – Mn may enter cell via specific Fe transporters.	Substitution Indirect		Mn-SOD compensates for decreased levels of Fe-SOD under limitation.	Mn concentrations in most natural waters are above limiting levels (see Brand et al., 1983 and Hecky and Kilham, 1988).
Copper	Plastocyanin is a Cu based electron carrier which may substitute for the Fe containing cytochrome c_6. Cu dependent high affinity Fe transporters.	Substitution Biochemical dependence	Fe demands decreased but greater Cu demands of open ocean diatoms leave them more prone to Cu limitation.	Plastocyanin is constitutively expressed in open ocean diatoms in lieu of cytochrome c_6.	Ambient Cu concentrations are mostly sufficient (see Peers et al., 2005 and Peers and Price, 2006).
Light	Iron is essential to photosynthesis, the greatest cellular Fe sink.	Biochemical dependence	Species with lowered PSI:PSII and Cytochrome b_6f:PSII ratios have lower Fe demands but smaller dynamic range for handling fluctuating light intensities.	Open ocean strains have less PSI and Cytochrome b_6f. Southern Ocean diatoms increase PSU size rather than number, increasing light capture without inflating Fe costs.	Low iron waters at high latitudes.

damage due to lack of Fe-based electron carriers. Indeed, several reports suggests that IsiA functions in the quenching of excitation energy that cannot be utilized by the organism under Fe stress, thereby protecting PSII from oxidative damage (Park et al., 1999; Sandstrom et al., 2002; van der Weij-de Wit et al., 2007; Berera et al., 2009; Wahadoszamen et al., 2015). A third, but not exclusive, role for IsiA is as a reservoir for chlorophyll which may balance the degradation of PSI during iron recycling when cells are iron limited (Riethman and Sherman, 1988). Chlorophyll life-time may exceed that of the proteins which bind it (Vavilin et al., 2005). In such cases when the binding proteins are degraded chlorophyll must be bound in a way that would prevent photodynamic damages.

SUMMARY

Iron plays a central role in energy production and biochemical catalysis within phytoplankton cells, being involved in multiple metabolic pathways either directly, via its catalytic role in enzymes, or indirectly via its part in the production of energy rich molecules such as NADPH and ATP. Fe thus influences the requirements, acquisition and utilization of essential resources within phytoplankton cells. These same resources, in turn, modulate iron requirements, acquisition and use efficiency (summarized in **Figure 3** and **Table 1**). Considering the core functions iron fulfills in cell metabolism and its relative scarcity in aquatic environments, it is little wonder that the availability of this trace metal exerts strong selective pressure on phytoplankton. Under iron-limiting conditions, phytoplankton must find a way to increase cellular iron on the one hand and decrease their Fe demands on the other. Both types of adaptation are closely tied in to light utilization and the metabolic pathways of different nutrients within the cell. **Table 1** summarizes adaptations to low Fe and the tradeoffs which may occur within organisms from the perspective of nitrogen, manganese and copper metabolisms as well as light utilization.

One of the most prominent characteristics of iron-limited cells is a decrease in size – not only do smaller cells have smaller nutrient requirements but the resultant increase in surface area to volume ratio is of great advantage under Fe-deficient conditions (see Sunda and Huntsman, 1995; and Lis et al., 2015a for a discussion of this). Under iron limitation phytoplankton also express high affinity transport systems (Maldonado et al., 1999; Maldonado and Price, 2001; Kustka et al., 2007; Allen et al., 2008; Kranzler et al., 2014). Both these strategies aid in the acquisition of Fe when it is a limiting resource. In addition, cells can reduce their iron requirements within different metabolic pathways. This may include substitution of Fe with other catalytically active trace metals, a decrease in Fe-rich cellular components or dependence on alternative biochemical pathways. Such changes may be temporary or even permanent if a species has evolved under constant Fe stress.

A possible outcome of iron's interaction with light and nutrients is co-limitation. Co-limitation is the synchronous limitation of growth and/or productivity by iron together with one or more resources (see Arrigo, 2005). Saito et al. (2008)

describe three co-limitation scenarios, each of which is based on the mode of interaction between the two resources: (1) Independent nutrient co-limitation where two nutrients are each drawn down to a point which limits growth. (2) Biochemical substitution co-limitation where one nutrient can replace another in a bioactive molecule and (3) Biochemically dependent co-limitation where one nutrient is needed for the uptake of another nutrient. This can also be extended to the utilization of a given resource (e.g., light). It should be noted that the spatial patterns and significance of co-limitation within natural environments remain unclear (Moore et al., 2013). These depend on a great deal of factors such as nutrient supply, biological nutrient demand and community interactions including competition, symbiosis, parasitism and predation. Nonetheless, the study of Fe-nutrient/light interactions on a single cell level in a laboratory setting defines the conceptual limits for the environmental relevance of co-limitation. **Table 1** lists the iron-light/nutrient interactions discussed in this review and their potential for co-limitation within environmental setting.

The question of nutrient requirement and usage by phytoplankton is multifaceted. Nutrient supply and demand are dictated by a wide range of factors. When looking at supply, we must consider abiotic factors such as nutrient influx, chemical speciation and chemical interactions and photochemistry as well as biotic factors such as competition, symbiosis and physiological uptake systems. Demand is influenced by factors such as cell size, nutrient use efficiency, luxury uptake or storage, symbiosis, and of course, the nutrient interactions within the cell. Moreover, at both the single cell and the community level, nutrient demands are not static. They are influenced by the dynamics between cell physiology, biochemistry and environmental cues such as light. This results in distinct requirements amongst phytoplankton leading to diverse limitation patterns in different environments and the differential limitation of different phytoplankton species found within the same environment (Moore et al., 2013). As research progresses in the mapping out of the intricate network of nutrient interactions within the cell, so will our ability to understand phytoplankton dynamics within their natural environments, including nutrient limitations and growth patterns.

AUTHOR CONTRIBUTIONS

All authors listed, have made substantial, direct and intellectual contribution to the work, and approved it for publication.

ACKNOWLEDGMENT

The authors would like to acknowledge the support of the Israel Science Foundation grant (806/11).

REFERENCES

Achilles, K. M., Church, T. M., Wilhelm, S. W., Luther, G. W. I., and Hutchins, D. A. (2003). Bioavailability of iron to *Trichodesmium* colonies in the western subtropical Atlantic Ocean. *Limnol. Oceanogr.* 48, 2250–2255. doi: 10.4319/lo.2003.48.6.2250

Adir, N., Zer, H., Shochat, S., and Ohad, I. (2003). Photoinhibition – a historical perspective. *Photosynth. Res.* 76, 343–370. doi: 10.1023/A:1024969518145

Aguirre, J. D., Clark, H. M., McIlvin, M., Vazquez, C., Palmere, S. L., Grab, D. J., et al. (2013). A manganese-rich environment supports superoxide dismutase activity in a Lyme disease pathogen, *Borrelia burgdorferi*. *J. Biol. Chem.* 288, 8468–8478. doi: 10.1074/jbc.M112.433540

Allen, A. E., Laroche, J., Maheswari, U., Lommer, M., Schauer, N., Lopez, P. J., et al. (2008). Whole-cell response of the pennate diatom *Phaeodactylum tricornutum* to iron starvation. *Proc. Natl. Acad. Sci. U.S.A.* 105, 10438–10443. doi: 10.1073/pnas.0711370105

Allen, M. D., Kropat, J., Tottey, S., Del Campo, J. A., and Merchant, S. S. (2006). Manganese deficiency in *Chlamydomonas* results in loss of photosystem II and MnSOD function, sensitivity to peroxides, and secondary phosphorus and iron deficiency. *Plant Physiol.* 143, 263–277. doi: 10.1104/pp.106.088609

Annett, A. L., Lapi, S., Ruth, T. J., and Maldonado, M. T. (2008). The effects of Cu and Fe availability on the growth and Cu: C ratios of marine diatoms. *Limnol. Oceanogr.* 53, 2451–2461. doi: 10.4319/lo.2008.53.6.2451

Archibald, F. (1983). *Lactobacillus plantarum*, an organism not requiring iron. *FEMS Microbiol. Lett.* 19, 29–32. doi: 10.1111/j.1574-6968.1983.tb00504.x

Armbrust, E. V. (2009). The life of diatoms in the world's oceans. *Nature* 459, 185–192. doi: 10.1038/nature08057

Arrigo, K. R. (2005). Marine microorganisms and global nutrient cycles. *Nature* 437, 349–355. doi: 10.1038/nature04159

Asada, K. (2006). Production and scavenging of reactive oxygen species in chloroplasts and their functions. *Plant Physiol.* 141, 391–396. doi: 10.1104/pp.106.082040

Bartsevich, V. V., and Pakrasi, H. B. (1996). Manganese transport in the cyanobacterium *Synechocystis* sp. PCC 6803. *J. Biol. Chem.* 271, 26057–26061. doi: 10.1074/jbc.271.42.26057

Behrenfeld, M. J., and Milligan, A. J. (2013). Photophysiological expressions of iron stress in phytoplankton. *Annu. Rev. Mar. Sci.* 5, 217–246. doi: 10.1146/annurev-marine-121211-172356

Berera, R., Van Stokkum, I. H. M., D'Haene, S., Kennis, J. T. M., Van Grondelle, R., and Dekker, J. P. (2009). A mechanism of energy dissipation in cyanobacteria. *Biophys. J.* 96, 2261–2267. doi: 10.1016/j.bpj.2008.12.3905

Bergman, B. (2001). Nitrogen-fixing cyanobacteria in tropical oceans, with emphasis on the Western Indian Ocean. *S. Afr. J. Bot.* 67, 426–432. doi: 10.1016/S0254-6299(15)31159-5

Bergman, B., Sandh, G., Lin, S., Larsson, J., and Carpenter, E. J. (2013). *Trichodesmium* - a widespread marine cyanobacterium with unusual nitrogen fixation properties. *FEMS Microbiol. Rev.* 37, 286–302. doi: 10.1111/j.1574-6976.2012.00352.x

Berman-Frank, I., Cullen, J. T., Shaked, Y., Sherrell, R. M., and Falkowski, P. G. (2001a). Iron availability, cellular iron quotas, and nitrogen fixation in *Trichodesmium*. *Limnol. Oceanogr.* 46, 1249–1260. doi: 10.4319/lo.2001.46.6.1249

Berman-Frank, I., Lundgren, P., Chen, Y. B., Küpper, H., Kolber, Z., Bergman, B., et al. (2001b). Segregation of nitrogen fixation and oxygenic photosynthesis in the marine cyanobacterium *Trichodesmium*. *Science* 294, 1534–1537. doi: 10.1126/science.1064082

Berman-Frank, I., Lundgren, P., and Falkowski, P. (2003). Nitrogen fixation and photosynthetic oxygen evolution in cyanobacteria. *Res. Microbiol.* 154, 157–164. doi: 10.1016/S0923-2508(03)00029-9

Berman-Frank, I., Quigg, A., Finkel, Z. V., Irwin, A. J., and Haramaty, L. (2007). Nitrogen-fixation strategies and Fe requirements in cyanobacteria. *Limnol. Oceanogr.* 52, 2260–2269. doi: 10.4319/lo.2007.52.5.2260

Bibby, T. S., Nield, J., and Barber, J. (2001a). Iron deficiency induces the formation of an antenna ring around trimeric photosystem I in cyanobacteria. *Nature* 412, 743–745. doi: 10.1038/35089098

Bibby, T. S., Nield, J., and Barber, J. (2001b). Three-dimensional model and characterization of the iron stress-induced CP43'-photosystem I supercomplex isolated from the cyanobacterium *Synechocystis* PCC 6803. *J. Biol. Chem.* 276, 43246–43252. doi: 10.1074/jbc.M106541200

Blaby-Haas, C. E., and Merchant, S. S. (2013). Iron sparing and recycling in a compartmentalized cell. *Curr. Opin. Microbiol.* 16, 677–685. doi: 10.1016/j.mib.2013.07.019

Boekema, E. J., Hifney, A., Yakushevska, A. E., Piotrowski, M., Keegstra, W., Berry, S., et al. (2001). A giant chlorophyll-protein complex induced by iron deficiency in cyanobacteria. *Nature* 412, 745–748. doi: 10.1038/35089104

Bonnet, S., Guieu, C., Bruyant, F., Prášil, O., Van Wambeke, F., Raimbault, P., et al. (2008). Nutrients limitation of primary productivity in the Southeast Pacific (BIOSOPE cruise). *Biogeosci. Discuss.* 4, 2733–2759. doi: 10.5194/bgd-4-2733-2007

Boyd, P. W., Jickells, T., Law, C. S., Blain, S., Boyle, E. A., Buesseler, K. O., et al. (2007). Mesoscale iron enrichment experiments 1993-2005: synthesis and future directions. *Science* 315, 612–617. doi: 10.1126/science.1131669

Brand, L. E., Sunda, W. G., and Guillard, R. R. L. (1983). Limitation of marine phytoplankton reproductive rates by zinc, manganese and iron. *Limnol. Oceanogr.* 28, 1182–1198. doi: 10.4319/lo.1983.28.6.1182

Breitbarth, E., Achterberg, E. P., Ardelan, M. V., Baker, A. R., Bucciarelli, E., Chever, F., et al. (2010). Iron biogeochemistry across marine systems – progress from the past decade. *Biogeosciences* 7, 1075–1097. doi: 10.5194/bg-7-1075-2010

Bruland, K. W., Donat, J. R., and Hutchins, D. A. (1991). Interactive influences of bioactive trace metals on biological production in oceanic waters. *Limnol. Oceanogr.* 36, 1555–1577. doi: 10.4319/lo.1991.36.8.1555

Cardona, T., Battchikova, N., Zhang, P., Stensjö, K., Aro, E.-M., Lindblad, P., et al. (2009). Electron transfer protein complexes in the thylakoid membranes of heterocysts from the cyanobacterium *Nostoc punctiforme*. *Biochim. Biophys. Acta* 1787, 252–263. doi: 10.1016/j.bbabio.2009.01.015

Chappell, P. D., and Webb, E. A. (2010). A molecular assessment of the iron stress response in the two phylogenetic clades of *Trichodesmium*. *Environ. Microbiol.* 12, 13–27. doi: 10.1111/j.1462-2920.2009.02026.x

Clarke, S. E., Stuart, J., and Sanders-Loehr, J. (1987). Induction of siderophore activity in *Anabaena* spp. and its moderation of copper toxicity. *Appl. Environ. Microbiol.* 53, 917–922.

Coale, K. H. (1991). Effects of iron, manganese, copper, and zinc enrichments on productivity and biomass in the subarctic Pacific. *Limnol. Oceanogr.* 36, 1851–1864. doi: 10.4319/lo.1991.36.8.1851

Colón-López, M. S., Sherman, D. M., and Sherman, L. A. (1997). Transcriptional and translational regulation of nitrogenase in light-dark- and continuous-light-grown cultures of the unicellular cyanobacterium *Cyanothece* sp. strain ATCC 51142. *J. Bacteriol.* 179, 4319–4327.

Ditullio, G. R., Hutchins, D. A., and Bruland, K. W. (1993). Interaction of iron and major nutrients controls phytoplankton growth and species composition in the tropical North Pacific Ocean. *Limnol. Oceanogr.* 38, 495–508. doi: 10.4319/lo.1993.38.3.0495

Dühring, U., Axmann, I. M., Hess, W. R., and Wilde, A. (2006). An internal antisense RNA regulates expression of the photosynthesis gene isiA. *Proc. Natl. Acad. Sci. U.S.A.* 103, 7054–7058. doi: 10.1073/pnas.0600927103

Eisenstadt, D., Ohad, I., Keren, N., and Kaplan, A. (2008). Changes in the photosynthetic reaction centre II in the diatom *Phaeodactylum tricornutum* result in non-photochemical fluorescence quenching. *Environ. Microbiol.* 10, 1997–2007. doi: 10.1111/j.1462-2920.2008.01616.x

Falkowski, P. G. (1997). Evolution of the nitrogen cycle and its influence on the biological sequestration of CO2 in the ocean. *Nature* 387, 272–275. doi: 10.1038/387272a0

Falkowski, P. G., Owens, T. G., Ley, A. C., and Mauzerall, D. C. (1981). Effects of growth irradiance levels on the ratio of reaction centers in two species of marine phytoplankton. *Plant Physiol.* 68, 969–973. doi: 10.1104/pp.68.4.969

Foster, A. W., and Robinson, N. J. (2011). Promiscuity and preferences of metallothioneins: the cell rules. *BMC Biol.* 9:25. doi: 10.1186/1741-7007-9-25

Fraser, J. M., Tulk, S. E., Jeans, J. A., Campbell, D. A., Bibby, T. S., and Cockshutt, A. M. (2013). Photophysiological and photosynthetic complex changes during iron starvation in *Synechocystis* sp. PCC 6803 and *Synechococcus elongatus* PCC 7942. *PLoS ONE* 8:e59861. doi: 10.1371/journal.pone.0059861

Fromme, P., Melkozernov, A., Jordan, P., and Krauss, N. (2003). Structure and function of photosystem I: interaction with its soluble electron carriers and external antenna systems. *FEBS Lett.* 555, 40–44. doi: 10.1016/S0014-5793(03)01124-4

Fu, F. X., and Bell, P. R. F. (2003). Growth, N2 fixation and photosynthesis in a cyanobacterium, *Trichodesmium* sp., under Fe stress. *Biotechnol. Lett.* 25, 645–649. doi: 10.1023/A:1023068232375

Gallon, J. R. (2001). N_2 fixation in photorophs: adaptation to a specialized way of life. *Plant Soil* 230, 39–48. doi: 10.1023/A:1004640219659

Ghassemian, M., and Straus, N. A. (1996). Fur regulates the expression of iron-stress genes in the cyanobacterium *Synechococcus* sp. strain PCC 7942. *Microbiology* 142, 1469–1476. doi: 10.1099/13500872-142-6-1469

Gledhill, M., and Van den Berg, C. M. G. (1994). Determination of complexation of iron (III) with natural organic complexing ligands in seawater using cathodic stripping voltammetry. *Mar. Chem.* 47, 41–54. doi: 10.1016/0304-4203(94)90012-4

Hakala, M., Tuominen, I., Keränen, M., Tyystjärvi, T., and Tyystjärvi, E. (2005). Evidence for the role of the oxygen-evolving manganese complex in photoinhibition of Photosystem II. *Biochim. Biophys. Acta* 1706, 68–80. doi: 10.1016/j.bbabio.2004.09.001

Haselkorn, R. (1978). Heterocysts. *Annu. Rev. Plant Physiol.* 29, 319–344. doi: 10.1146/annurev.pp.29.060178.001535

Hassidim, M., Keren, N., Ohad, I., Reinhold, L., and Kaplan, A. (1997). Acclimation of *Synechococcus* strain WH7803 to ambient CO_2 concentration and to elevated light intensity. *J. Phycol.* 33, 811–817. doi: 10.1111/j.0022-3646.1997.00811.x

Hecky, R. E., and Kilham, P. (1988). Nutrient limitation of phytoplankton in freshwater and marine environments: a review of recent evidence on the effects of enrichment. *Limnol. Oceanogr.* 33, 796–822. doi: 10.4319/lo.1988.33.4part2.0796

Hernandez-Prieto, M. A., Schon, V., Georg, J., Barreira, L., Varela, J., Hess, W. R., et al. (2012). Iron deprivation in *Synechocystis*: inference of pathways, non-coding RNAs, and regulatory elements from comprehensive expression profiling. *G3 (Bethesda)* 2, 1475–1495. doi: 10.1534/g3.112.003863

Ihalainen, J. A., D'Haene, S., Yeremenko, N., Van Roon, H., Arteni, A. A., Boekema, E. J., et al. (2005). Aggregates of the chlorophyll-binding protein IsiA (CP43') dissipate energy in cyanobacteria. *Biochemistry* 44, 10846–10853. doi: 10.1021/bi0510680

Järvi, S., Suorsa, M., and Aro, E. M. (2015). Photosystem II repair in plant chloroplasts–Regulation, assisting proteins and shared components with photosystem II biogenesis. *Biochim. Biophys. Acta* 1847, 900–909. doi: 10.1016/j.bbabio.2015.01.006

Johnson, K. S., Gordon, R. M., and Coale, K. H. (1997). What controls dissolved iron concentrations in the world ocean? *Mar. Chem.* 57, 137–161. doi: 10.1016/S0304-4203(97)00043-1

Komenda, J., Sobotka, R., and Nixon, P. J. (2012). Assembling and maintaining the Photosystem II complex in chloroplasts and cyanobacteria. *Curr. Opin. Plant Biol.* 15, 245–251. doi: 10.1016/j.pbi.2012.01.017

Kranzler, C., Lis, H., Finkel, O. M., Schmetterer, G., Shaked, Y., and Keren, N. (2014). Coordinated transporter activity shapes high-affinity iron acquisition in cyanobacteria. *ISME J.* 8, 409–417. doi: 10.1038/ismej.2013.161

Kranzler, C., Lis, H., Shaked, Y., and Keren, N. (2011). The role of reduction in iron uptake processes in a unicellular, planktonic cyanobacterium. *Environ. Microbiol.* 13, 2990–2999. doi: 10.1111/j.1462-2920.2011.02572.x

Kumar, K., Mella-Herrera, R. A., and Golden, J. W. (2010). Cyanobacterial heterocysts. *Cold Spring Harb. Perspect. Biol.* 2, 1–19. doi: 10.1101/cshperspect.a000315

Kustka, A. B., Allen, A. E., and Morel, F. M. (2007). Sequence analysis and transcriptional regulation of iron acquisition genes in two marine diatoms. *J. Phycol.* 43, 715–729. doi: 10.1111/j.1529-8817.2007.00359.x

Kustka, A. B., Carpenter, E. J., and Sanudo-Wilhelmy, S. (2002). Iron and marine fixation: progress and future directions. *Res. Microbiol.* 153, 255–262. doi: 10.1016/S0923-2508(02)01325-6

La Fontaine, S., Quinn, J. M., Nakamoto, S. S., Dudley Page, M., Göhre, V., Moseley, J. L., et al. (2002). Copper-dependent iron assimilation pathway in the model photosynthetic eukaryote *Chlamydomonas reinhardtii*. *Eukaryot. Cell* 1, 736–757. doi: 10.1128/EC.1.5.736-757.2002

Larsson, M., Olsson, T., and Larsson, C. (1985). Distribution of reducing power between photosynthetic carbon and nitrogen assimilation in *Scenedesmus*. *Planta* 164, 246–253. doi: 10.1007/BF00396088

Laudenbach, D. E., Reith, M. E., and Straus, N. A. (1988). Isolation, sequence analysis, and transcriptional studies of the flavodoxin gene from *Anacystis nidulans* R2. *J. Bacteriol.* 170, 258–265.

Laudenbach, D. E., and Straus, N. A. (1988). Characterization of a cyanobacterial iron stress-induced gene similar to psbC. *J. Bacteriol.* 170, 5018–5026.

Li, D., Cong, W., Cai, Z., Shi, D., and Ouyang, F. (2004). Effect of iron stress, light stress, and nitrogen source on physiological aspects of marine red tide alga. *J. Plant Nutr.* 27, 29–41. doi: 10.1081/PLN-120027545

Lis, H., Kranzler, C., Keren, N., and Shaked, Y. (2015a). A comparative study of iron uptake rates and mechanisms amongst marine and fresh water cyanobacteria: prevalence of reductive iron uptake. *Life (Basel)* 5, 841–860. doi: 10.3390/life5010841

Lis, H., Shaked, Y., Kranzler, C., Keren, N., and Morel, F. M. M. (2015b). Iron bioavailability to phytoplankton: an empirical approach. *ISME J.* 9, 1003–1013. doi: 10.1038/ismej.2014.199

Liu, X., and Millero, F. J. (2002). The solubility of iron in seawater. *Mar. Chem.* 77, 43–54. doi: 10.1016/S0304-4203(01)00074-3

Maldonado, M. T., Allen, A. E., Chong, J. S., Lin, K., Leus, D., Karpenko, N., et al. (2006). Copper-dependent iron transport in coastal and oceanic diatoms. *Limnol. Oceanogr.* 51, 1729–1743. doi: 10.4319/lo.2006.51.4.1729

Maldonado, M. T., Boyd, P. W., Harrison, P. J., and Price, N. M. (1999). Co-limitation of phytoplankton growth by light and Fe during winter in the NE subarctic Pacific Ocean. *Deep. Sea Res. Part II Top. Stud. Oceanogr.* 46, 2475–2485. doi: 10.1016/S0967-0645(99)00072-7

Maldonado, M. T., and Price, N. M. (1996). Influence of N substrate on Fe requirements of marine centric diatoms. *Mar. Ecol. Prog. Ser.* 141, 161–172. doi: 10.3354/meps141161

Maldonado, M. T., and Price, N. M. (1999). Utilization of Fe bound to strong organic ligands by phytoplankton communities in the subarctic Pacific Ocean. *Deep. Sea Res. Part II Top. Stud. Oceanogr.* 46, 2447–2473. doi: 10.1016/S0967-0645(99)00071-5

Maldonado, M. T., and Price, N. M. (2001). Reduction and transport of organically bound iron by *Thalassiosira oceanica* (Bacillariophyceae). *J. Phycol.* 37, 298–310. doi: 10.1046/j.1529-8817.2001.037002298.x

Martin, J. H. (1990). Glacial-interglacial CO_2 change: the iron hypothesis. *Paleoceanography* 5, 1–13. doi: 10.1029/PA005i001p00001

Martin, J. H., Gordon, R. M., Fitzwater, S., and Broenkow, W. W. (1989). Vertex: phytoplankton/iron studies in the Gulf of Alaska. *Deep Sea Res. A* 36, 649–680. doi: 10.1016/0198-0149(89)90144-1

McKay, R. M. L., Bullerjahn, G. S., Porta, D., Brown, E. T., Sherrell, R. M., Smutka, T. M., et al. (2004). Consideration of the bioavailability of iron in the North American Great Lakes: development of novel approaches toward understanding iron biogeochemistry. *Aquat. Ecosyst. Health Manag.* 7, 475–490. doi: 10.1080/14634980490513364

Merchant, S., and Sawaya, M. R. (2005). The light reactions: a guide to recent acquisitions for the picture gallery. *Plant Cell* 17, 648–663. doi: 10.1105/tpc.105.030676

Merchant, S. S., Allen, M. D., Kropat, J., Moseley, J. L., Long, J. C., Tottey, S., et al. (2006). Between a rock and a hard place: trace element nutrition in *Chlamydomonas*. *Biochim. Biophys. Acta* 1763, 578–594. doi: 10.1016/j.bbamcr.2006.04.007

Merchant, S. S., and Helmann, J. D. (2012). Elemental economy: microbial strategies for optimizing growth in the face of nutrient limitation. *Adv. Microb. Physiol.* 60, 91–210. doi: 10.1016/B978-0-12-398264-3.00002-4

Millero, F. J. (1998). Solubility of Fe(III) in seawater. *Earth Planet. Sci. Lett.* 154, 323–329. doi: 10.1016/S0012-821X(97)00179-9

Milligan, A. J., Berman-Frank, I., Gerchman, Y., Dismukes, G. C., and Falkowski, P. G. (2007). Light-dependent oxygen consumption in nitrogen-fixing cyanobacteria plays a key role in nitrogenase protection. *J. Phycol.* 43, 845–852. doi: 10.1111/j.1529-8817.2007.00395.x

Milligan, A. J., and Harrison, P. J. (2000). Effects of non-steady-state iron limitation on nitrogen assimilation in the marine diatom *Thalassiosira weissflogii* (Bacillariophyceae). *J. Phycol.* 36, 78–86. doi: 10.1046/j.1529-8817.2000.99013.x

Mills, M. M., Ridame, C., Davey, M., La Roche, J., and Geider, R. J. (2004). Iron and phosphorus co-limit nitrogen fixation in the eastern tropical North Atlantic. *Nature* 429, 232–292. doi: 10.1038/nature02550

Moore, C. M., Mills, M. M., Achterberg, E. P., Geider, R. J., LaRoche, J., Lucas, M. I., et al. (2009). Large-scale distribution of Atlantic nitrogen fixation controlled by iron availability. *Nat. Geosci.* 2, 867–871. doi: 10.1038/ngeo667

Moore, C. M., Mills, M. M., Arrigo, K. R., Berman-Frank, I., Bopp, L., Boyd, P. W., et al. (2013). Processes and patterns of oceanic nutrient limitation. *Nat. Geosci.* 6, 701–710. doi: 10.1038/ngeo1765

Morel, F. M. M., Hudson, R. J. M., and Price, N. M. (1991). Limitation of productivity by trace metals in the sea. *Limnol. Oceanogr.* 36, 1742–1755. doi: 10.4319/lo.1991.36.8.1742

Morel, F. M. M., and Price, N. M. (2003). The biogeochemical cycles of trace metals in the oceans. *Science* 300, 944–947. doi: 10.1126/science.1083545

Nelson, N., and Junge, W. (2015). Structure and energy transfer in photosystems of oxygenic photosynthesis. *Annu. Rev. Biochem.* 84, 659–683. doi: 10.1146/annurev-biochem-092914-041942

Nicolaisen, K., Hahn, A., Valdebenito, M., Moslavac, S., Samborski, A., Maldener, I., et al. (2010). The interplay between siderophore secretion and coupled iron and copper transport in the heterocyst-forming cyanobacterium *Anabaena* sp. PCC 7120. *Biochim. Biophys. Acta* 1798, 2131–2140. doi: 10.1016/j.bbamem.2010.07.008

North, R. L., Guildford, S. J., Smith, R. E. H., Havens, S. M., and Twiss, M. R. (2007). Evidence for phosphorus, nitrogen, and iron colimitation of phytoplankton communities in Lake Erie. *Limnol. Oceanogr.* 52, 315–328. doi: 10.4319/lo.2007.52.1.0315

North, R. L., Guildford, S. J., Smith, R. E. H., Twiss, M. R., and Kling, H. J. (2008). Nitrogen, phosphorus, and iron co-limitation of phytoplankton communities in the nearshore and offshore regions of the African Great Lakes. *Int. Vereinigung Theor. Angew. Limnol.* 30, 259–264.

Park, Y. I., Sandström, S., Gustafsson, P., and Oquist, G. (1999). Expression of the *isiA* gene is essential for the survival of the cyanobacterium *Synechococcus* sp. PCC 7942 by protecting photosystem II from excess light under iron limitation. *Mol. Microbiol.* 32, 123–129. doi: 10.1046/j.1365-2958.1999.01332.x

Peers, G., and Price, N. M. (2004). A role for manganese in superoxide dismutases and growth of iron-deficient diatoms. *Limnol. Oceanogr.* 49, 1774–1783. doi: 10.4319/lo.2004.49.5.1774

Peers, G., and Price, N. M. (2006). Copper-containing plastocyanin used for electron transport by an oceanic diatom. *Nature* 441, 341–344. doi: 10.1038/nature04630

Peers, G., Quesnel, S. A., and Price, N. M. (2005). Copper requirements for iron acquisition and growth of coastal and oceanic diatoms. *Limnol. Oceanogr.* 50, 1149–1158. doi: 10.4319/lo.2005.50.4.1149

Postgate, J. (1998). *Nitrogen Fixation*, 3rd Edn. Cambridge: Cambridge university press.

Price, N. M., Andersen, L. F., and Morel, F. M. M. (1991). Iron and nitrogen nutrition of equatorial Pacific plankton. *Deep Sea Res. A* 38, 1361–1378. doi: 10.1016/0198-0149(91)90011–90014

Quigg, A., Finkel, Z. V., Irwin, A. J., Rosenthal, Y., Ho, T. Y., Reinfelder, J. R., et al. (2003). The evolutionary inheritance of elemental stoichiometry in marine phytoplankton. *Nature* 425, 291–294. doi: 10.1038/nature01953

Raven, J. A. (1988). The iron and molybdenum use efficiencies of plant growth with different energy, carbon and nitrogen sources. *New Phytol.* 109, 279–288. doi: 10.1111/j.1469-8137.1988.tb04196.x

Raven, J. A. (1990). Predictions of Mn and Fe use efficiencies of phototrophic growth as a function of light availability for growth and of C assimilation pathway. *New Phytol.* 116, 1–18. doi: 10.1111/j.1469-8137.1990.tb00505.x

Raven, J. A., Evans, M. C. W., and Korb, R. E. (1999). The role of trace metals in photosynthetic electron transport in O_2-evolving organisms. *Photosynth. Res.* 60, 111–150. doi: 10.1023/A:1006282714942

Reddy, K. J., Haskell, J. B., Sherman, D. M., and Sherman, L. A. (1993). Unicellular, aerobic nitrogen-fixing cyanobacteria of the genus *Cyanothece*. *J. Bacteriol.* 175, 1284–1292.

Riethman, H. C., and Sherman, L. A. (1988). Purification and characterization of an iron stress-induced chlorophyll-protein from the cyanobacterium *Anacystis nidulans* R2. *Biochim. Biophys. Acta* 935, 141–151. doi: 10.1016/0005-2728(88)90211-3

Roach, T., and Krieger-Liszkay, A. (2014). Regulation of photosynthetic electron transport and photoinhibition. *Curr. Protein Pept. Sci.* 15, 351–362. doi: 10.2174/1389203715666140327105143

Roe, K. L., Barbeau, K., Mann, E. L., and Haygood, M. G. (2012). Acquisition of iron by *Trichodesmium* and associated bacteria in culture. *Environ. Microbiol.* 14, 1681–1695. doi: 10.1111/j.1462-2920.2011.02653.x

Rubin, M., Berman-Frank, I., and Shaked, Y. (2011). Dust- and mineral-iron utilization by the marine dinitrogen-fixer *Trichodesmium*. *Nat. Geosci.* 4, 529–534. doi: 10.1038/ngeo1181

Rudolf, M., Kranzler, C., Lis, H., Margulis, K., Stevanovic, M., Keren, N., et al. (2015). Multiple modes of iron uptake by the filamentous, siderophore-producing cyanobacterium, *Anabaena* sp. PCC 7120. *Mol. Microbiol.* 97, 577–588. doi: 10.1111/mmi.13049

Rue, E. L., and Bruland, K. W. (1995). Complexation of iron(lll) by natural organic ligands in the Central North Pacific as determined by a new competitive ligand equilibration/adsorptive cathodic stripping voltammetric method. *Mar. Chem.* 5, 117–138. doi: 10.1016/0304-4203(95)00031-L

Rueter, J. G., and Ades, D. R. (1987). The role of iron nutrition in photosynthesis and nitrogen assimilation in *Scenedesmus quadricauda* (Chlorophyceae). *J. Phycol.* 23, 452–457. doi: 10.1111/j.1529-8817.1987.tb02531.x

Rueter, J. G., Hutchins, D. A., Smith, R. W., and Unsworth, N. L. (1992). "Iron nutrition of *Trichodesmium*," in *Marine Pelagic Cyanobacteria: Trichodesmium and Other Diazotrophs*, eds E. J. Carpenter and D. G. Capone (Dordrecht: Springer), 289–306.

Ryan-Keogh, T. J., Macey, A. I, Cockshutt, A. M., Moore, C. M., and Bibby, T. S. (2012). The cyanobacterial chlorophyll-binding protein isiA acts to increase the in vivo effective absorption cross-section of PSI under iron limitation. *J. phycol.* 48, 145–154. doi: 10.1111/j.1529-8817.2011.01092.x

Saito, M. A., Goepfert, T. J., and Ritt, J. T. (2008). Some thoughts on the concept of colimitation: three definitions and the importance of bioavailability. *Limnol. Oceanogr.* 53, 276–290. doi: 10.4319/lo.2008.53.1.0276

Salomon, E., and Keren, N. (2011). Manganese limitation induces changes in the activity and in the organization of photosynthetic complexes in the cyanobacterium *Synechocystis* sp. strain PCC 6803. *Plant Physiol.* 155, 571–579. doi: 10.1104/pp.110.164269

Salomon, E., and Keren, N. (2015). Acclimation to environmentally relevant Mn concentrations rescues a cyanobacterium from the detrimental effects of iron limitation. *Environ. Microbiol.* 17, 2090–2098. doi: 10.1111/1462-2920.12826

Sandmann, G. (1985). Consequences of iron deficiency on photosynthetic and respiratory electron transport in blue-green algae. *Photosynth. Res.* 6, 261–271. doi: 10.1007/BF00049282

Sandstrom, S., Ivanov, A. G., Park, Y.-I., Oquist, G., and Gustafsson, P. (2002). Iron stress responses in the cyanobacterium *Synechococcus* sp. PCC7942. *Physiol. Plant.* 116, 255–263. doi: 10.1034/j.1399-3054.2002.1160216.x

Sañudo-Wilhelmy, S. A., Kustka, A. B., Gobler, C. J., Hutchins, D. A., Yang, M., Lwiza, K., et al. (2001). Phosphorus limitation of nitrogen fixation by *Trichodesmium* in the central Atlantic Ocean. *Nature* 411, 66–69. doi: 10.1038/35075041

Shaked, Y., and Lis, H. (2012). Disassembling iron availability to phytoplankton. *Front. Microbiol.* 3:123. doi: 10.3389/fmicb.2012.00123

Sharon, S., Salomon, E., Kranzler, C., Lis, H., Lehmann, R., Georg, J., et al. (2014). The hierarchy of transition metal homeostasis: iron controls manganese accumulation in a unicellular cyanobacterium. *Biochim. Biophys. Acta* 1837, 1990–1997. doi: 10.1016/j.bbabio.2014.09.007

Shcolnick, S., and Keren, N. (2006). Metal homeostasis in cyanobacteria and chloroplasts. Balancing benefits and risks to the photosynthetic apparatus. *Plant Physiol.* 141, 805–810. doi: 10.1104/pp.106.079251

Shcolnick, S., Summerfield, T. C., Reytman, L., Sherman, L. A., and Keren, N. (2009). The mechanism of iron homeostasis in the unicellular cyanobacterium *Synechocystis* sp. PCC 6803 and its relationship to oxidative stress. *Plant Physiol.* 150, 2045–2056. doi: 10.1104/pp.109.141853

Sherman, D. M., and Sherman, L. A. (1983). The effects of iron deficiency and iron restoration on the ultrastructure of the cyanobacterium *Anacystis nidulans*. *J. Bacteriol.* 156, 393–401.

Singh, A. K., and Sherman, L. A. (2007). Reflections on the function of IsiA, a cyanobacterial stress-inducible, Chl-binding protein. *Photosynth. Res.* 93, 17–25. doi: 10.1007/s11120-007-9151-7

Snow, J. T., Schlosser, C., Woodward, E. M. S., Mills, M. M., Achterberg, E. P., Mahaffey, C., et al. (2015). Environmental controls on the biogeography of diazotrophy and *Trichodesmium* in the Atlantic Ocean. *Global Biogeochem. Cycles* 29, 865–884. doi: 10.1002/2015GB005090

Stöckel, J., Welsh, E. A., Liberton, M., Kunnvakkam, R., Aurora, R., and Pakrasi, H. B. (2008). Global transcriptomic analysis of *Cyanothece* 51142 reveals robust diurnal oscillation of central metabolic processes. *Proc. Natl. Acad. Sci. U.S.A.* 105, 6156–6161. doi: 10.1073/pnas.0711068105

Strzepek, R. F., and Harrison, P. J. (2004). Photosynthetic architecture differs in coastal and oceanic diatoms. *Nature* 431, 689–692. doi: 10.1038/nature02954

Strzepek, R. F., Hunter, K. A., Frew, R. D., Harrison, P. J., and Boyd, P. W. (2012). Iron-light interactions differ in Southern Ocean phytoplankton. *Limnol. Oceanogr.* 57, 1182–1200. doi: 10.4319/lo.2012.57.4.1182

Sun, J., and Golbeck, J. H. (2015). The presence of the IsiA-PSI supercomplex leads to enhanced photosystem I electron throughput in iron-starved cells of *Synechococcus* sp. PCC 7002. *J. Phys. Chem. B* 119, 13549–13559. doi: 10.1021/acs.jpcb.5b02176

Sunda, W. (1975). *The Relationship between Cupric Ion Activity and the Toxicity of Copper to Phytoplankton*. Woods Hole, MA: Massachusetts Institute of Technology and Woods Hole Oceanographic Institution.

Sunda, W. G., and Huntsman, S. A. (1995). Iron uptake and growth limitation in oceanic and coastal phytoplankton. *Mar. Chem.* 50, 189–206. doi: 10.1016/0304-4203(95)00035-P

Sunda, W. G., and Huntsman, S. A. (1997). Interrelated influence of iron, light and cell size on marine phytoplankton growth. *Nature* 390, 389–392. doi: 10.1038/37093

Sunda, W. G., and Huntsman, S. A. (2011). Interactive effects of light and temperature on iron limitation in a marine diatom: implications for marine productivity and carbon cycling. *Limnol. Oceanogr.* 56, 1475–1488. doi: 10.4319/lo.2011.56.4.1475

Sunda, W. G., and Huntsman, S. A. (2015). High iron requirement for growth, photosynthesis, and low-light acclimation in the coastal cyanobacterium *Synechococcus bacillaris*. *Front. Microbiol.* 6:561. doi: 10.3389/fmicb.2015.00561

Sunda, W. G., Swift, D. G., and Huntsman, S. A. (1991). Low iron requirement for growth in oceanic phytoplankton. *Nature* 351, 55–57. doi: 10.1038/351055a0

Takahashi, H., Clowez, S., Wollman, F.-A., Vallon, O., and Rappaport, F. (2013). Cyclic electron flow is redox-controlled but independent of state transition. *Nat. Commun.* 4:1954. doi: 10.1038/ncomms2954

Taylor, S. R. (1964). Abundance of chemical elements in the continental crust: a new table. *Geochim. Cosmochim. Acta* 28, 1273–1285. doi: 10.1016/0016-7037(64)90129-2

Timmermans, K. R., Stolte, W., and Baar, H. J. W. (1994). Iron-mediated effects on nitrate reductase in marine phytoplankton. *Mar. Biol.* 121, 389–396. doi: 10.1007/BF00346749

Tottey, S., Waldron, K. J., Firbank, S. J., Reale, B., Bessant, C., Sato, K., et al. (2008). Protein-folding location can regulate manganese-binding versus copper- or zinc-binding. *Nature* 455, 1138–1142. doi: 10.1038/nature07340

Tuit, C., Waterbury, J., and Ravizza, G. (2004). Diel variation of molybdenum and iron in marine diazotrophic cyanobacteria. *Limnol. Oceanogr.* 49, 978–990. doi: 10.4319/lo.2004.49.4.0978

Tyystjärvi, E. (2013). Photoinhibition of Photosystem II. *Int. Rev. Cell Mol. Biol.* 300, 243–303. doi: 10.1016/B978-0-12-405210-9.00007-2

van der Weij-de Wit, C. D., Ihalainen, J. A., van de Vijver, E., D'Haene, S., Matthijs, H. C. P., van Grondelle, R., et al. (2007). Fluorescence quenching of IsiA in early stage of iron deficiency and at cryogenic temperatures. *Biochim. Biophys. Acta* 1767, 1393–1400. doi: 10.1016/j.bbabio.2007.10.001

Vavilin, D., Brune, D. C., and Vermaas, W. (2005). ^{15}N-labeling to determine chlorophyll synthesis and degradation in *Synechocystis* sp. PCC 6803 strains lacking one or both photosystems. *Biochim. Biophys. Acta* 1708, 91–101. doi: 10.1016/j.bbabio.2004.12.011

Wahadoszamen, M., D'Haene, S., Ara, A. M., Romero, E., Dekker, J. P., Grondelle, R. v., et al. (2015). Identification of common motifs in the regulation of light harvesting: the case of cyanobacteria IsiA. *Biochim. Biophys. Acta* 1847, 486–492. doi: 10.1016/j.bbabio.2015.01.003

Wang, W. X., and Dei, R. C. H. (2001). Biological uptake and assimilation of iron by marine plankton: influences of macronutrients. *Mar. Chem.* 74, 213–226. doi: 10.1016/S0304-4203(01)00014-7

Webb, E. A., Moffett, J. W., and Waterbury, J. B. (2001). Iron stress in open-ocean cyanobacteria (*Synechococcus*, *Trichodesmium*, and *Crocosphaera* spp.): identification of the IdiA protein. *Appl. Environ. Microbiol.* 67, 5444–5452. doi: 10.1128/AEM.67.12.5444-5452.2001

Welkie, D., Zhang, X., Markillie, M. L., Taylor, R., Orr, G., Jacobs, J., et al. (2014). Transcriptomic and proteomic dynamics in the metabolism of a diazotrophic

cyanobacterium, *Cyanothece* sp. PCC 7822 during a diurnal light–dark cycle. *BMC Genomics* 15:1185. doi: 10.1186/1471-2164-15-1185

Whittaker, S., Bidle, K. D., Kustka, A. B., and Falkowski, P. G. (2011). Quantification of nitrogenase in *Trichodesmium* IMS 101: implications for iron limitation of nitrogen fixation in the ocean. *Environ. Microbiol. Rep.* 3, 54–58. doi: 10.1111/j.1758-2229.2010.00187.x

Williams, R., and Frausto da Silva, J. J. (2001). *The Biological Chemistry of the Elements: The Inorganic Chemistry of Life*, 2nd Edn. New York, NY: Oxford University Press.

Wilson, A., Boulay, C., Wilde, A., Kerfeld, C. A., and Kirilovsky, D. (2007). Light-induced energy dissipation in iron-starved cyanobacteria: roles of OCP and IsiA proteins. *Plant Cell* 19, 656–672. doi: 10.1105/tpc.106.045351

Wolfe-Simon, F., Grzebyk, D., Schofield, O., and Falkowski, P. G. (2005). The role and evolution of superoxide dismutases in algae. *J. Phycol.* 41, 453–465. doi: 10.1111/j.1529-8817.2005.00086.x

Wolk, C. P., Ernst, A., and Elhai, J. (1994). "Heterocyst metabolism and development," in *The Molecular Biology of Cyanobacteria*, ed. D. A. Bryant (Dordrecht: Springer), 769–823.

Wood, P. M. (1978). Interchangeable copper and iron proteins in algal photosynthesis. Studies on plastocyanin and cytochrome c_{552} in *Chlamydomonas*. *Eur. J. Biochem.* 87, 9–19. doi: 10.1111/j.1432-1033.1978.tb12346.x

Wu, J., and Luther, G. W. (1995). Complexation of Fe(III) by natural organic ligands in the Northwest Atlantic Ocean by a competitive ligand equilibration method and a kinetic approach. *Mar. Chem.* 50, 159–177. doi: 10.1016/0304-4203(95)00033-N

Yeremenko, N., Kouřil, R., Ihalainen, J. A., D'Haene, S., van Oosterwijk, N., Andrizhiyevskaya, E. G., et al. (2004). Supramolecular organization and dual function of the IsiA chlorophyll-binding protein in cyanobacteria †. *Biochemistry* 43, 10308–10313. doi: 10.1021/bi048772l

Zehr, J. P., Waterbury, J. B., Turner, P. J., Montoya, J. P., Omoregie, E., Steward, G. F., et al. (2001). Unicellular cyanobacteria fix N_2 in the subtropical North Pacific Ocean. *Nature* 412, 635–638. doi: 10.1038/35088063

Conflict of Interest Statement: The authors declare that the research was conducted in the absence of any commercial or financial relationships that could be construed as a potential conflict of interest.

frontiers in Plant Science

ORIGINAL RESEARCH
published: 12 February 2016
doi: 10.3389/fpls.2016.00137

A Two-Component Regulatory System in Transcriptional Control of Photosystem Stoichiometry: Redox-Dependent and Sodium Ion-Dependent Phosphoryl Transfer from Cyanobacterial Histidine Kinase Hik2 to Response Regulators Rre1 and RppA

Iskander M. Ibrahim[1], *Sujith Puthiyaveetil*[2] *and John F. Allen*[3]*

[1] Faculty of Engineering and Science, University of Greenwich, Chatham Maritime, Kent, UK, [2] Institute of Biological Chemistry, Washington State University, Pullman, WA, USA, [3] Research Department of Genetics, Evolution and Environment, University College London, London, UK

OPEN ACCESS

Edited by:
Julian Eaton-Rye,
University of Otago, New Zealand

Reviewed by:
Iwane Suzuki,
University of Tsukuba, Japan
Lou Sherman,
Purdue University, USA

***Correspondence:**
John F. Allen
j.f.allen@ucl.ac.uk

Specialty section:
This article was submitted to Plant Cell Biology, a section of the journal Frontiers in Plant Science

Received: *21 October 2015*
Accepted: *26 January 2016*
Published: *12 February 2016*

Citation:
Ibrahim IM, Puthiyaveetil S and Allen JF (2016) A Two-Component Regulatory System in Transcriptional Control of Photosystem Stoichiometry: Redox-Dependent and Sodium Ion-Dependent Phosphoryl Transfer from Cyanobacterial Histidine Kinase Hik2 to Response Regulators Rre1 and RppA. Front. Plant Sci. 7:137. doi: 10.3389/fpls.2016.00137

Two-component systems (TCSs) are ubiquitous signaling units found in prokaryotes. A TCS consists of a sensor histidine kinase and a response regulator protein as signal transducers. These regulatory systems mediate acclimation to various environmental changes by coupling environmental cues to gene expression. Hik2 is a sensor histidine kinase and its gene is found in all cyanobacteria. Hik2 is the homolog of Chloroplast Sensor Kinase (CSK), a protein involved in redox regulation of chloroplast gene expression during changes in light quality in plants and algae. Here we describe biochemical characterization of the signaling mechanism of Hik2 and its phosphotransferase activity. Results presented here indicate that Hik2 undergoes autophosphorylation on a conserved histidine residue, and becomes rapidly dephosphorylated by the action of response regulators Rre1 and RppA. We also show that the autophosphorylation of Hik2 is specifically inhibited by sodium ions.

Keywords: redox sensor, redox regulator, photosystem stoichiometry, transcriptional control, Histidine Kinase 2, Chloroplast Sensor Kinase (CSK), *Synechocystis sp.* PCC 6803, salt stress

INTRODUCTION

Bacteria are found in almost every habitable environment, and successfully adapt to environmental change in a wide range of different ecological niches. One reason for the ecological success of bacteria is their remarkable ability to sense and respond to changing environmental conditions. For this environmental acclimation, bacteria mostly utilize sensor-response circuits known as two-component systems (TCSs). TCSs mediate acclimatory responses by changing bacterial cellular physiology, which is accomplished in most cases by regulation of gene expression at transcriptional and post-transcriptional levels. Each TCS consists of two proteins, a sensor histidine kinase (component 1) and a response regulator (component 2) (Stock et al., 2000). Upon environmental stimulus, the sensor histidine kinase undergoes autophosphorylation on the conserved histidine

residue, receiving the γ-phosphate from ATP. The phosphoryl group from the histidine is subsequently transferred to a conserved aspartate residue in the response regulator to cause a structural change that elicits a change in target gene expression (Stock et al., 2000).

Although TCSs are ubiquitous in bacteria, in eukaryotes they are found only in plants, fungi, and protists. Cyanobacterial genomes typically encode a large number of two-component systems, ranging from as many as 146 histidine kinases and 168 response regulators in the filamentous cyanobacterium *Nostoc punctiforme* to as few as five histidine kinases and six response regulators in the small genome of the marine unicellular cyanobacterium *Prochlorococcus* MED4 (Mary and Vaulot, 2003). Three histidine kinases are fully conserved in all cyanobacterial genomes. One of these is Histidine kinase 2 (Hik2) (Ashby and Houmard, 2006). Interestingly, a homolog of Hik2 is also found in chloroplasts of nearly all algae and plants as Chloroplast Sensor Kinase (CSK). This wide distribution of Hik2 and CSK suggests important functional roles for these sensors in cyanobacteria and chloroplasts, respectively (Puthiyaveetil et al., 2008). In chloroplasts of the model plant *Arabidopsis thaliana*, CSK regulates transcription of chloroplast genes in response to changes in reduction-oxidation (redox) potential of the photosynthetic electron transport chain (Puthiyaveetil et al., 2008). *csk* knockout plants are unable to link changes in light quality to the expression of photosynthetic reaction center genes in chloroplast DNA. Therefore, the CSK-signaling pathway has been suggested to underlie the acclimatory process of adjustment of the stoichiometry of chloroplast photosystem I and photosystem II (Puthiyaveetil et al., 2008).

A yeast two-hybrid analysis of cyanobacterial two-component systems demonstrates interaction of Hik2 with Response regulator 1 (Rre1) (Sato et al., 2007). A homolog of Rre1 also occurs in chloroplasts of non-green algae as Ycf29 (hypothetical chloroplast open reading frame 29; Puthiyaveetil et al., 2008; Puthiyaveetil and Allen, 2009). In non-green algae, CSK is likely to regulate chloroplast genes through Ycf29 by means of the His-to-Asp phosphotransfer mechanism. However, in green algae and higher plants, Ycf29 has been lost, and CSK regulates transcription of chloroplast genes through phosphorylation of chloroplast sigma factor 1 (SIG1) in a catalytic mechanism similar to that of serine/threonine kinases (Puthiyaveetil et al., 2010, 2012, 2013). This rewiring of the CSK signaling pathway may have accompanied replacement of the original, conserved histidine residue in plant and green algal CSKs.

Hik2, in contrast to CSK, contains all motifs characteristic of bacterial histidine kinases, including the conserved histidine residue. Hik2 also has a clearly identifiable GAF sensor domain at its N-terminus (**Figure 1A**). Hik2, like CSK, does not contain transmembrane helices and is probably a soluble sensor kinase. However, little is known about the precise functional role of Hik2 and its signaling mechanism. Interestingly, in addition to Rre1, a second response regulator RppA (Regulator of photosynthesis and photopigment-related gene expression A) also interacts with Hik2 in a yeast two-hybrid assay (Sato et al., 2007). RppA is a redox response regulator that regulates photosynthesis genes (Li and Sherman, 2000). In cyanobacteria, photosynthesis genes are also regulated by a paralogous group of response regulators known as RpaA and RpaB (Regulator of phycobilisome association; Ashby and Mullineaux, 1999; Kato et al., 2011; Majeed et al., 2012). Homologs of RpaB are also found in the chloroplasts of some non-green algae (Ashby et al., 2002; Puthiyaveetil and Allen, 2009). It has been unclear whether Hik2 interacts with RpaA or RpaB. Hik2 has also been implicated in osmosensing, raising the possibility that it is a multi-sensor kinase (Paithoonrangsarid et al., 2004). However, direct evidence for signals affecting Hik2 activity has been lacking thus far.

In laboratory conditions, most genes coding for two-component regulatory proteins can be inactivated in cyanobacteria without adverse effect on cell growth. However, the *Hik2* gene seems to be indispensable (Paithoonrangsarid et al., 2004). In order to understand the signaling and functional properties of Hik2, we employed an *in vitro* approach. The sensory mechanism of Hik2 and its interaction with its putative response regulators are explored in this study. Here, we demonstrate autophosphorylation of Hik2 on a conserved histidine residue, and show that this autophosphorylation depends on the presence of glycine residues in the protein's ATP-binding domain. We also find that autophosphorylation is specifically inhibited in the presence of NaCl. Furthermore, we show rapid and specific phosphotransfer activity from Hik2 to both Rre1 and RppA, thus identifying them as genuine response regulators and functional interaction partners of Hik2 in cyanobacteria. The interaction of Hik2 with Rre1 and RppA is further confirmed by a pull-down assay. Our results suggest that a Hik2-based signaling pathway integrates acclimatory responses to light and salt stresses in cyanobacteria.

MATERIALS AND METHODS

Construction of Recombinant Plasmids

Coding sequences corresponding to the full-length *Synechocystis sp.* PCC 6803 Hik2 (slr1147), Rre1 (slr1783), RppA (sll0797), RpaA (sll0797), and to the receiver domains of response regulators Rre1 and RppA were amplified from *Synechocystis* sp. PCC 6803 genomic DNA using the primer pairs listed in **Table 1**. PCR products of full-length Hik2 (Hik2_F) was digested with *NdeI* and *XhoI* or *BamH* and *XhoI* endonucleases (New England BioLabs) and cloned into a pET-21b (Invitrogen) or pETG-30A (EMBL) expression vectors. PCR products of full-length Rre1, RppA, RpaA, and RpaB were digested with *KpnI* and *XhoI* endonucleases (New England BioLabs) and cloned into pETG-41A (EMBL) expression vector. PCR products of receiver domains of Rre1 and RppA were digested with *BamHI* and *XhoI* and cloned into pET-30a(+) expression vector (Invitrogen). The identities of the recombinant clones were confirmed by sequencing (results not shown).

Site-Directed Mutagenesis of the Conserved Motifs within H, G1, G2, Boxes of Hik2

Mutagenesis of the conserved histidine residue of the H-box (His^{185}) to glutamine, and of the conserved glycine residues of

TABLE 1 | Primer pairs used for cloning *Hik2, Rre1, RppA, RpaA*, and *RpaB*.

– Hik2F_His_6 (cloned in pET-21b)
Forward: GCGCGCcatatgGCCGGTTCCATCTCA
Reverse: GCGCGCctcgagCACTTGTTCTCCAGAGCG
– Hik2F_GST (cloned in pETG-30A)
Forward: TTGGCGggtaccATGGCCGGTTCCATCTCA
Reverse: GCGCGCctcgagCACTTGTTCTCCAGAGCG
– Rre1F_MBP (cloned into pETG-41A)
Forward: GCGCGCggtaccGTGGGCTTGAGTTTGCTG
Reverse: GCGGCGctcgagCTAGACGATCGCCTCCAATTC
– RppAF_MBP (cloned into pETG-41A)
Forward: GCGCGCggtaccCGAATTTTGCTGGTGGAA
Reverse: GCGGCGctcgagCTACAGTCTTGCTAATAGCTC
– RpaAF_MBP (cloned into pETG-41A)
Forward GCGCggtaccATGCCTCGAATACTGATC
Reverse: GCGCGCctcgagCTACGTTGGACTACCGCC
– RpaBF_MBP (cloned into pETG-41A)
Forward: GCGCGCggtaccGTGGTCGATGACGAGGCC
Reverse: GCGGCGctcgagCTAGATTCTAGCTTCCAATTC
– Rre1_Receiver_His_6 (cloned into pET-30a+)
Forward: GCGGCGggatccATGGTGGGCTTGAGTTTG
Reverse: GCGGCGctcgagCTAGACGATCGCCTCCAATTC
– RppA_Receiver_His_6 (cloned into pET-30a+)
Forward: GCGGCGggatccATGCGAATTTTGCTGGTG
Reverse: GCGGCGctcgagCTACAGTCTTGCTAATAGCTC
For H-box
–$His^{185}Q$
Forward: CTGACCTCTTGCAGCAACTCCGCAATC
Reverse: GATTGCGGAGTTGCTGCAAGAGGTCAG
For G1-box
– $Gly^{359}A$
Forward: CGCCGACACGGCTTATGGCATTC
Reverse: GAATGCCATAAGCCGTGTCGGCG
– $Gly^{361}A$
Forward:
GATCGCCGACACGGGTTATGCGATTCCCCCGGAGGATCAAC
Reverse:
GTTGATCCTCCGGGGGAATTGCATAACCCGTGTCGGCGATC
For G2-box
– $Gly^{386}A$
Forward: CGAGGCTCCATTAATGCGACTGGTTTGGGTTTG
Reverse: CAAACCCAAACCAGTCGCATTAATGGAGCCTCG
– $Gly^{388}A$
Forward: CATTAATGGCACTGCGTTGGGTTTGGCGATC
Reverse: GATCGCCAAACCCAACGCAGTGCCATTAATG
– $Gly^{390}A$
Forward: CACTGGTTTGGCATTGGCGATCGTG
Reverse: CACGATCGCCAATGCCAAACCAGTG

Sequences in lower case are restriction site overhangs. Sequences underlined are codons for glutamine or alanine.

the G1 box (Gly^{359} and Gly^{361}), and G2-box (Gly^{386}, Gly^{388}, and Gly^{390}) to alanine was made using Stratagene QuickChange site-directed mutagenesis kit. The primer pairs used are listed in **Table 1**. Mutagenesis was confirmed by sequencing (results not shown).

Expression and Purification of Recombinant Hik2 and Response Regulators

Recombinant plasmids were transformed into *E. coli* BL21(DE3) chemically competent cells (Stratagene). Transformed bacterial colonies, grown on agar plates, were used to inoculate starter cultures (10 mL each) in Luria Broth (LB) growth media (Sambrook et al., 1989) with 100 $\mu g\,mL^{-1}$ ampicillin for the Hik2 and full-length response regulator clones, or with 35 $\mu g\,mL^{-1}$ kanamycin for clones containing receiver domain response regulators, as the selectable marker. Each culture was grown overnight, then diluted 1:100 in 1 L LB media and grown at 37°C to an optical density at 600 nm of ∼0.55, before inducing protein expression with 0.5 mM IPTG (Melford). Bacterial cultures were grown for a further 16 h at 16°C. Cells were harvested by centrifugation at 6000 rpm for 10 min. The pellet was re-suspended in a buffer containing 300 mM NaCl, 20 mM Tris-HCl, pH 7.4, 25 mM imidazole, and 1 mM PMSF, and the cells lysed with an EmulsiFlex-C3 homogenizer (Avestin). Lysate was separated by centrifugation at 18,000 rpm for 20 min. The supernatant was applied to a Ni^{2+} affinity chromatography column (GE Healthcare) and the C-terminally poly-histidine tagged Hik2 protein, the N-terminally poly-histidine tagged receiver domain of response regulators, and also the full-length response regulators obtained from a pETG-41A vector containing an N-terminal poly-histidine tag followed by a MPB tag were all purified using a Ni^{2+} affinity chromatography column according to the column manufacturer's instructions. For the salt treatment assay, full-length Hik2 protein was desalted into Tris-HCl (10 mM final, pH 7.4) using PD-10 desalting column (Amersham Biosciences) and used in the autophosphorylation assay immediately.

Pull-Down Assay

The bait and prey proteins were overexpressed as described above. Bacterial pellets containing the overexpressed proteins were re-suspended in 5 mL of phosphate-buffered saline (PBS) (140 mM NaCl, 2.7 mM KCl, 1.8 mM $KHPO_4$, and 8.1 mM $NaHPO_4$ at pH 7.3) and lysed by several freeze-thaw cycles, followed by sonication three times for 15 s at maximum power. The lysate was clarified by centrifugation at 18,000 rpm for 20 min. The supernatant containing bait proteins (Hik2-GST or GST) was incubated with Protino Glutathione Agarose 4B particles (Promega) and washed six times with 10-bead volume of ice-cold PBS. Prey (Rre1_Rec-His_6 and RppA_Rec-His_6) and bait (Hik2-GST or GST) proteins were then mixed together and incubated for 2 h at 19°C on a rotating platform. The supernatant was removed and the pelleted-beads were washed 3–4 times and eluted according to the manufacturer's instructions.

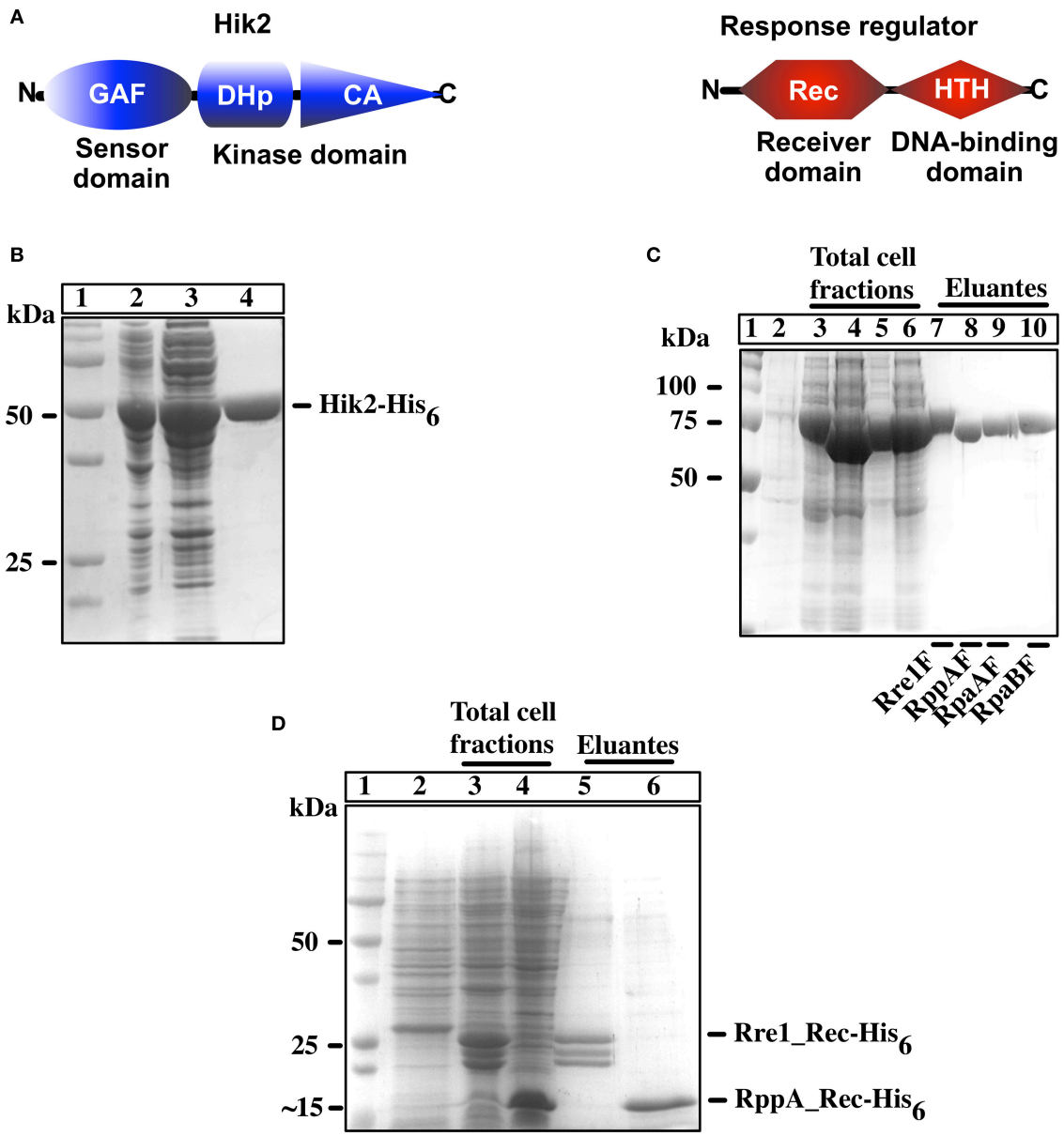

FIGURE 1 | Overexpression and purification of recombinant Hik2 and response regulators. (A) Schematic representation of domain architecture of full-length Hik2 and its putative response regulators as predicted by the SMART database (Chenna et al., 2003). The GAF (named after its presence in cGMP-specific phosphodiesterases, in certain Adenylyl cyclases, and in transcription factor FhlA) domain and the conserved DHp (dimerization and phosphoacceptor) and CA (Catalytic and ATP-binding) domains of Hik2 are depicted by blue oval, cylinder, and triangle, respectively. The conserved receiver (Rec) and the helix-turn-helix (HTH) DNA-binding domains of response regulator are depicted in red hexagon and parallelogram, respectively. **(B)** Protein overexpression and purification for Hik2F. Different cell fractions separated on a 12% SDS-PAGE and stained with Coomassie brilliant blue are shown. Lane 1 shows protein molecular weight standards in kDa; in lane 2 is total cell fraction after IPTG induction; lane 3 is soluble cell fraction; lane 4 is purified Hik2 protein. **(C)** Full-length response regulators: protein overexpression and purification. In lane 1 are protein molecular weight standards identified numerically in kDa; in lane 2 is the total cell fraction before IPTG induction; lanes 3–6 are total cell fractions containing N-terminus MBP-tagged Rre1F (lane 3), RppAF (lane 4), RpaAF (lane 5), RpaB (lane 6); lanes 7–10 are purified proteins; Rre1F (lane 7), RppAF (lane 8), RpaAF (lane 9), and RpaBF (lane 10). **(D)** Receiver domain of Rre1 and RppA: lane 1 shows molecular weight marker; lane 2 is total cell fraction before IPTG induction; lanes 2 and 3 are total cell fraction after IPTG induction containing receiver domain of Rre1 (Rre1_Rec, lane 3), and RppA (RppA_Rec, lane 4); lanes 5 and 6 are purified proteins; Rre1_Rec (lane 5) and RppA_Rec (lane 6). The positions of molecular weight markers are indicated on the left and their values given in kDa.

In vitro Autophosphorylation Assay

Autophosphorylation was performed with 2 μM of purified recombinant Hik2 protein in a kinase reaction buffer (50 mM Tris-HCl (pH 7.5), 50 mM KCl, 10% glycerol, and 10 mM $MgCl_2$) in a final reaction volume of 25 μL. The autophosphorylation reaction was initiated by the addition of 5 μL of five-fold concentrated ATP solution containing 2.5 mM disodium ATP (Sigma) with 2.5 μCi [γ-^{32}P]-ATP (6000 Ci mmol^{-1})

(PerkinElmer) or with 5 μCi [α-^{32}P]-ATP (3000 Ci mmol^{-1}) as a control. Reactions were incubated for 15 s at 22°C. The autophosphorylation reaction was terminated by addition of 6 μL of five-fold concentrated Laemmli sample buffer (Laemmli, 1970). Reaction products were resolved on a 12% SDS-PAGE (sodium dodecyl sulfate polyacrylamide gel electrophoresis) gel. The gel was rinsed with SDS running buffer and transferred into a polyethylene bag. The sealed bag was exposed to a phosphor plate overnight. The incorporated γ-^{32}P was visualized using autoradiography and the band intensity from the autoradiograph was quantified using ImageJ version 1.44 (Schneider et al., 2012).

Autophosphorylation Assay in the Presence of Salt

2 μM recombinant Hik2 protein was pre-equilibrated with 5 μL of five-fold concentrated, low potassium reaction buffer [250 mM Tris-HCl (pH 7.5), 25 mM KCl, 50% glycerol, and 50 mM $MgCl_2$] and with water, as a control, or with the following salts: NaCl (0.3 M final concentration), Na_2SO_4 (0.25 M final concentration), $NaNO_3$ (0.3 M final concentration), or KCl (0.375 M final concentration) in a total reaction volume of 20 μL. Reaction mixtures were then incubated at room temperature (22°C) for 30 min. Autophosphorylation was assayed as above. Hik2 was titrated with varying concentrations of NaCl and autophosphorylation was performed for 15 s. The incorporated γ-^{32}P was visualized and the band intensity quantified as described earlier. The concentration-dependent inhibition curve for Hik2 was plotted from data points representing at least three independent experiments, using Prism 6 (Motulsky and Christopoulos, 2003).

Acid-Base Stability Assay

Four replicates of autophosphorylation reactions of Hik2 were performed as above. Proteins were then resolved on a 12% SDS-PAGE gel and blotted onto a PVDF membrane. Each lane containing the autophosphorylated Hik2 protein was excised and incubated in 50–100 mL of 50 mM Tris-HCl (pH 7.4; neutral conditions), 1 M HCl (acidic conditions), or 3 M NaOH (basic conditions) for 2.5 h at 55°C with agitation. The extent of γ-^{32}P hydrolysis was analyzed using autoradiography.

Phosphotransfer Analysis

The autophosphorylation reaction was carried out by mixing 30 μM Hik2 in a total reaction volume of 375 μL containing kinase reaction buffer [50 mM Tris-HCl (pH 7.5), 50 mM KCl, 10% glycerol, 25 mM $MgCl_2$, and 2 mM DTT] and ATP [2.5 mM disodium ATP and 37.5 μCi [γ-^{32}P]ATP (6000 Ci mmol^{-1})]. The reaction mixture was incubated at 30°C for 10 min. In the meantime, 25 μM of each of the response regulators Rre1, RppA, RpaA, or RpaB were diluted with the kinase reaction buffer to give a total volume of 62.5 μL. A control lacking response regulator was prepared in the same way, except that response regulator protein solution was replaced with an equal volume of water. For each phosphotransfer reaction, 62.5 μL of autophosphorylated radiolabeled Hik2 protein was mixed with 62.5 μL of the response regulator or with the water control. Kinase and response regulator were present at a concentration of 1 and 5 μM, respectively. Reactions were mixed and incubated at 30°C. Twenty-five microliter samples were removed at 0, 20, 40, 60, and 90 min, and the reactions stopped by the addition of Laemmli sample buffer. Proteins were resolved on 15% SDS-PAGE and the presence of γ-^{32}P was analyzed using autoradiography. The incorporated γ^{32-}P was visualized and quantified as before.

RESULTS

Overexpression and Purification of Full-Length Hik2 and Response Regulators Recombinant Proteins

In order to examine the autophosphorylation activity of full-length Hik2 protein and its interaction with its putative response regulator(s), we cloned the coding sequences of full-length *Synechocystis* sp. PCC 6803 *Hik2, Rre1, RppA*, and *RpaA and RpaB* genes. **Figure 1** shows the purified C-terminally His_6 tagged full-length Hik2 (**Figure 1B**); N-terminally His_6-MBP tagged full-length response regulators (**Figure 1C**) and N-terminally His_6 tagged receiver domains (**Figure 1D**) separated on a reducing SDS-PAGE gel. The apparent molecular weights are: Hik2, 50 kDa (**Figure 1B**, lane 4); Rre1F, 75 kDa (**Figure 1C**, lane 7); RppAF, 70 kDa (**Figure 1C**, lane 8); RpaAF, 72 kDa (**Figure 1C**, lane 9); and RpaBF, 72 kDa (**Figure 1C**, lane 10); Rre1_Rec, 25 kDa (**Figure 1D**, lane 5); and RppA_Rec 15 kDa, (**Figure 1D**, lane 6). Theoretical molecular weights are: Hik2, 49 kDa; Rre1F, 75 kDa; RppAF, 70 kDa; RpaAF, 71 kDa; and RpaBF, 70 kDa; Rre1_Rec, 20 kDa; and RppA_Rec 14 kDa.

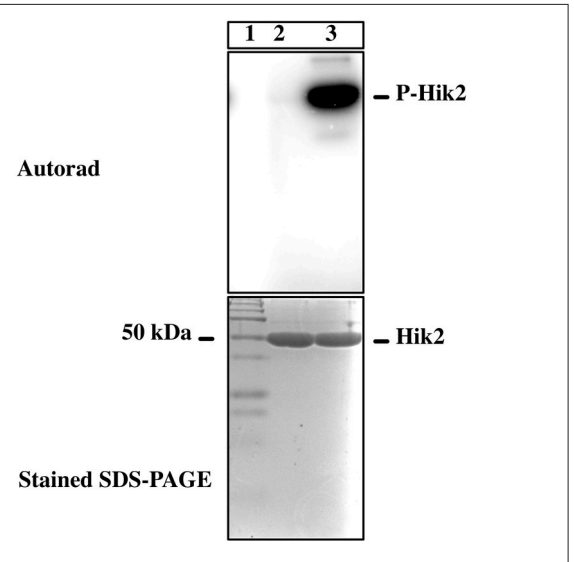

FIGURE 2 | Autophosphorylation activity of Hik2. An autoradiograph of the reaction product is presented. Lane 1 is protein molecular weight marker in kDa; in lane 2 Hik2 was incubated with [α-^{32}P]-ATP; lane 3, with [γ-^{32}P]-ATP.

The Full-Length Hik2 Autophosphorylates *In vitro;* Na^+ Ions Inhibit its Autophosphorylation Activity

Histidine kinases catalyze transfer of only the γ-phosphate from an ATP molecule to their conserved histidine residue. To test whether Hik2 autophosphorylates as a typical histidine kinase, the recombinant and purified Hik2 was assayed for autokinase activity in the presence of [γ-^{32}P]ATP and [α-^{32}P]ATP. **Figure 2**, lane 2 shows that Hik2 remained unlabeled when incubated with [α-^{32}P], however, it was heavily labeled with ^{32}P upon incubation with [γ-^{32}P]ATP (**Figure 2**, lane 3), suggesting robust autophosphorylation activity in Hik2. Hik2 has been suggested to act as an osmosensor (Paithoonrangsarid et al., 2004). We therefore tested whether Hik2 could directly sense salts. Hik2 was incubated with water (control), NaCl, Na_2SO_4, $NaNO_3$, or KCl (at final concentrations of 0.3, 0.25, 0.3, and 0.375 M, respectively) in the presence of 2.5 μCi of [γ-^{32}P]ATP. **Figure 3A**, lane 1 shows that Hik2, in the absence of salt, is autokinase active. However, when it was treated with NaCl (lane 2), Na_2SO_4 (lane 3) or with $NaNO_3$ (lane 4), the autophosphorylation activity of Hik2 was decreased by up to 75% compared to the untreated protein. Interestingly, KCl did not inhibit the autophosphorylation activity of Hik2 (lane 5). This suggests that the Na^+ ion, but not the Cl^- ion, is responsible for suppressing the autokinase activity of Hik2. In a dose-response curve, inhibition of 50% autophosphorylation activity of Hik2 was seen at 0.25 M of NaCl (**Figure 3B**). It has been found that treatment of *Synechocystis* sp. PCC 6803 in 0.5 M NaCl reduced its growth rate by 50%, and 0.3 M NaCl was sufficient to elicit induction of salt tolerance genes that are under the control of Rre1 (Marin et al., 2003). Therefore, our result of 0.3 M NaCl inhibiting the activity of Hik2 (**Figures 3A,B**) is likely to be physiologically relevant.

Characterization of the Nature of Phosphoamino Group of Hik2

In order to understand the nature of phosphoamino acid in Hik2, we used an acid-base stability assay and mutagenesis studies. Phosphorylations on serine and threonine residues are stable in acidic condition, but are labile under alkaline

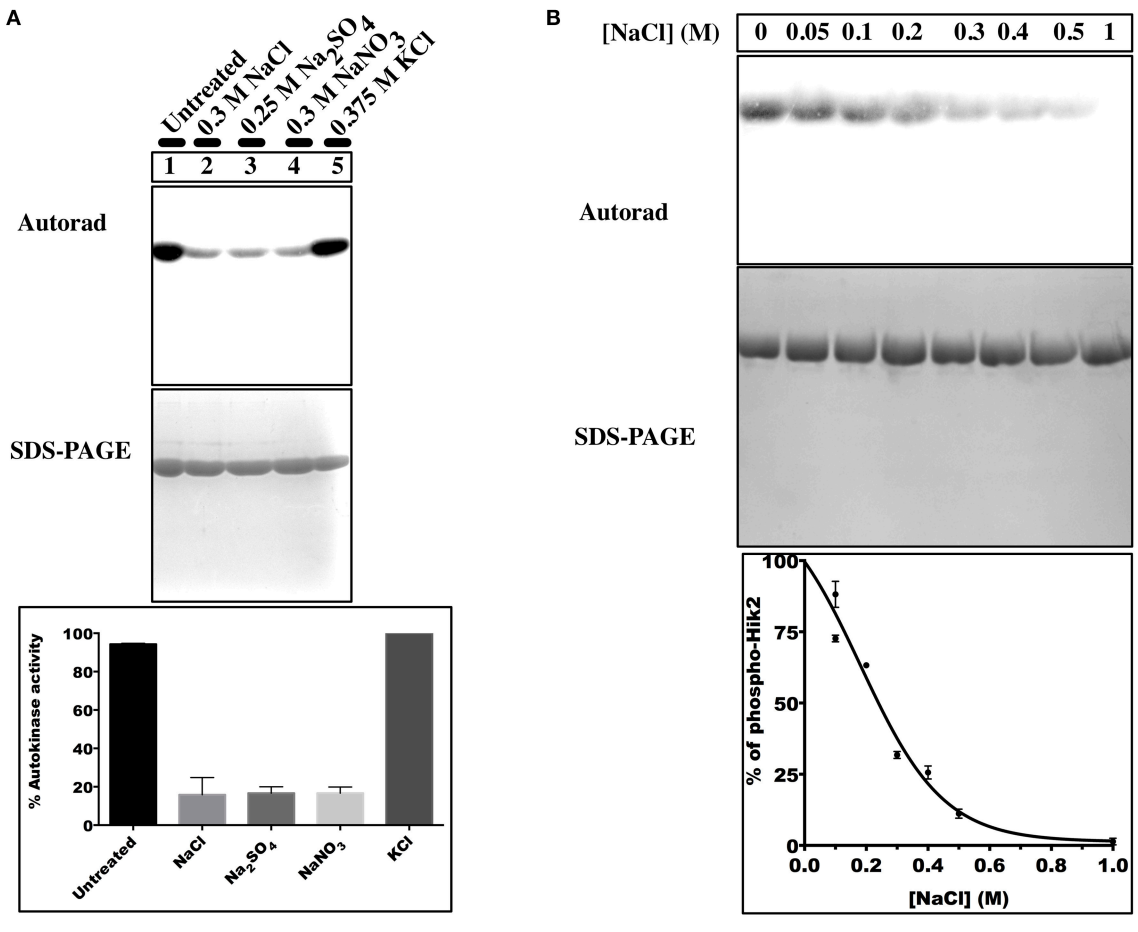

FIGURE 3 | Effects of different salts on the autophosphorylation activity of Hik2. (A) Lane 1, untreated sample; lane 2, treated with 0.3 M NaCl; lane 3, treated with 0.25 M Na_2SO_4; lane 4, treated with 0.3 M $NaNO_3$; lane 5, treated with 0.375 M KCl. **(B)** Concentration-dependent inhibition of Hik2. Data points represent intensity of ^{32}P labeling quantified by ImageJ. Each data point is the mean of three measurements ± S.E.

condition. Conversely, phosphorylation on basic residues (histidine, arginine, or lysine), as in histidine kinases, are acid labile but stable under basic condition (Attwood et al., 2007). Phosphorylations on acidic residues, such as aspartate or glutamate, are susceptible to both acid and base hydrolysis (Attwood et al., 2011). We therefore employed an acid-base stability assay to confirm the nature of phosphoamino acid in Hik2. **Figure 4A**, lane 1 shows that the ^{32}P on untreated Hik2 (control) was relatively stable. **Figure 4A**, lane 2 shows that the ^{32}P on Hik2 was relatively stable at pH 7.4 (neutral), at 55°C for 2.5 h. **Figure 4A**, lane 3 shows that the ^{32}P on Hik2 was completely hydrolysed upon incubation in 1 M HCl, (acidic condition) at 55°C for 2.5 h. **Figure 4A**, lane 4 shows that the ^{32}P on Hik2 was relatively stable when incubated in 3 M NaOH (basic condition), at 55°C for 2.5 h. This behavior of the Hik2 phosphoamino acid is consistent with phosphorylation on a histidine residue, as in sensor histidine kinases. We next mutated the conserved histidine (His^{185}) to glutamine. **Figure 4B**, lane 2 shows that the His^{185}Q mutation completely abolished ^{32}P labeling of Hik2. Our results are consistent with the single autophosphorylation site of Hik2 being His^{185}.

The ATP-binding domain of histidine kinases contains conserved motifs essential for autokinase activity. These include G1 and G2 boxes, which have the characteristic glycine signatures "DxGxG" and "GxGxG," respectively. The conserved glycine residues in G1 and G2 boxes of Hik2 were identified by sequence alignment; they were then individually substituted to alanine residues in order to establish their role in the autokinase activity of Hik2. **Figure 4C** shows that the wild-type protein becomes autophosphorylated; however, substitution of the first or second conserved glycine residues in the G1-box abolished the autophosphorylation activity of Hik2 (**Figure 4C**, lanes 2 and 3). Similarly, substitution of any of the conserved glycine residues within the G2-box completely abolished the autophosphorylation activity of Hik2 (**Figure 4C**, lanes 4, 5, and 6).

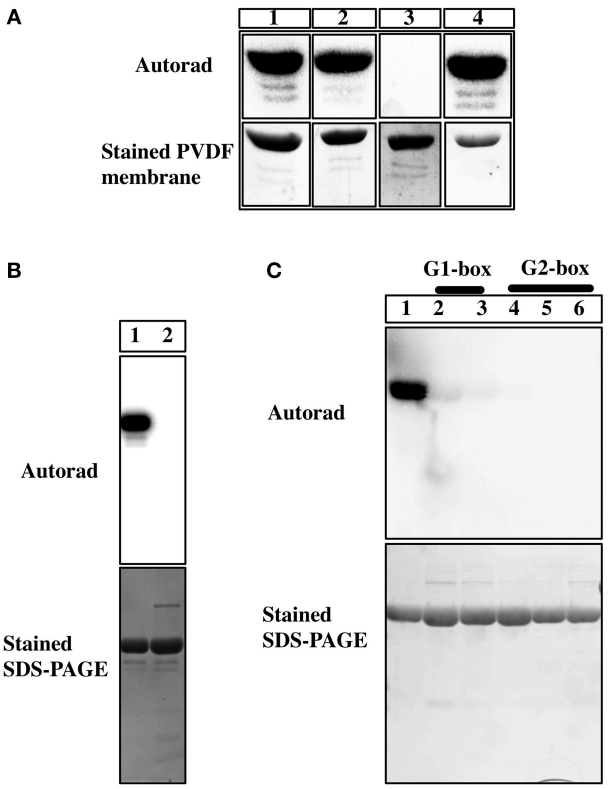

FIGURE 4 | Characterization of phosphoamino group of Hik2. (A) Autoradiograph of the Acid-base stability assay. Lane 1, untreated Hik2; lane 2, treated with 50 mM Tris-HCl (pH 7.4); lane 3, with 1 M HCl; lane 4, with 3 M NaOH. **(B)** Effects of His^{185}Q mutagenesis on the autokinase activity of Hik2. Autoradiograph of the autokinase assay is presented. Lane 1 shows the wild-type Hik2 protein. Lane 2, His^{185}Q mutant protein. **(C)** Effects of G1 or G2 box mutations on the autokinase activity of Hik2. Autoradiograph of the protein gel from the phosphorylation assay. Lane 1, wild type Hik2 protein; lane 2, G1-box mutant Gly^{359}A; lane 3, G1-box mutant Gly^{361}A; lane 4, G2-box mutant Gly^{386}A; lane 5, G2-box mutant Gly^{388}A; lane 6, G2-box mutant Gly^{390}A.

Pull-Down Assay Shows that Hik2 Interacts with Rre1 and RppA

A GST-based pull-down assay was performed to validate the earlier report (Sato et al., 2007) of Hik2 interactions with Rre1 and RppA in a yeast two-hybrid assay. The result in **Figure 5** shows that the bait Hik2 protein pulls down prey proteins Rre1 and RppA (**Figure 5**, lanes 8 and 9, respectively). However, in the control pull-down assay, where GST was used as bait, prey proteins Rre1 and RppA were not co-purified with Hik2 (**Figure 5**, lanes 6 and 7, respectively), suggesting specific Hik2-Rre1 and Hik2-RppA interactions.

Phosphotransfer Kinetics of Hik2 Reveals Preferential Phosphotransfer to Rre1 and RppA Response Regulators

In bacteria, individual two-component systems are insulated from each other for minimal cross-talk and faithful signal transmission (Skerker et al., 2008). Co-evolving amino acid residues in sensor kinases and response regulators establish this separation, which is manifested as preferential phosphotransfer kinetics from the sensor kinase to its cognate response regulator. Cognate kinase-response regulator pairs therefore exhibit faster phosphotransfer kinetics than non-cognate pairs (Skerker et al., 2008). The phosphotransfer analysis of Hik2 was performed with the full-length response regulators (**Figures 6A,B**) as in (Laub et al., 2007; experimental section). Results in **Figures 6A,B** showing kinetics of dephosphorylation of phospho-Hik2 indicate that Rre1 dephosphorylates phospho-Hik2 the fastest when compared to RppA, RpaA, and RpaB. Hik2-RppA exhibited the second fastest phosphotransfer kinetics. Furthermore, when Rre1 and RppA were mixed together, they dephosphorylated phospho-Hik2 at a much higher rate than each on its own. Moreover, the result presented in **Figures 6A,B** shows differences in the stabilities of the phosphoryl groups on Rre1 and RppA. The phosphate group on Rre1 is relatively stable, while RppA loses its phosphate group rapidly. We therefore could not detect phosphate groups on RppA in our experimental condition. Our inability to detect a phosphoryl group on RppA is likely

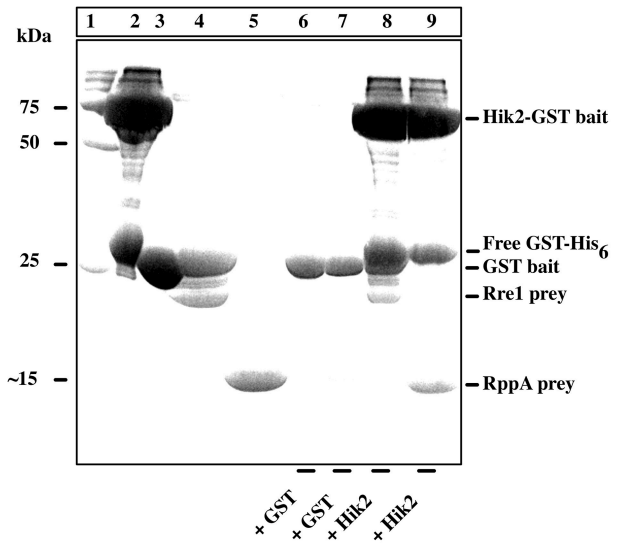

FIGURE 5 | Interaction of Hik2 with Rre1 and RppA in a GST-based pull-down assay. Coomassie-stained SDS-PAGE. Lane 1, protein molecular weight markers in kDa; lane 2, over-expressed and purified Hik2-GST bait; lane 3, over-expressed and purified control GST bait; lane 4, over-expressed and purified Rre1 prey; lane 5, over-expressed and purified RppA prey; lanes 6–9 show the products of the pull-down assay. The bait used in each assay is indicated at bottom of the lane. Hik2-GST bait pulls down Rre1 (lane 8) and RppA (lane 9), while the control bait GST does not pull-down either response regulator (lanes 6 and 7, respectively). The positions of the molecular weight markers are indicated on the left. The positions of bait and prey proteins are indicated on the right.

to be the result of a rapid autodephosphorylation reaction in RppA, such as in some response regulators (Laub et al., 2007). The phosphotransfer kinetics toward RppA (**Figures 6A,B**) were therefore inferred from the loss of phosphates from the sensor kinase, Hik2. RpaA and RpaB exhibited slower kinetics comparing to Rre1 and RppA, suggesting that they are less likely to be response regulators of Hik2 under this experimental condition. Phosphoryl group on Rre1 is less stable in the presence of RppA (**Figure 6C**).

DISCUSSION

The work presented in this study shows that the full-length recombinant Hik2 protein of *Synechocystis* sp. PCC 6803 purified from *E. coli* becomes autophosphorylated *in vitro*, as predicted on the basis of sequence information and comparison with other histidine sensor kinases. Interestingly, when Hik2 was treated with NaCl (**Figure 3A**, lane 2), its autophosphorylation activity was inhibited. Further examination of salt sensing activity of Hik2 led us to determine that it responds specifically to Na^+ ions (**Figure 3A**). We found that Cl^- ions do not affect the autokinase activity of Hik2 (**Figure 3A**, lane 5). Interestingly, a chimeric sensor kinase, made up of the sensor domain of Hik2 and the kinase domain of Hik7, has been reported to respond to Cl^- ions *in vivo* (Kotajima et al., 2013). Our finding, in contrast, shows that the kinase activity of full-length Hik2 protein is modulated by Na^+ ions (**Figure 3**), and not by Cl^- ions. The reason for an apparent inconsistency between the results presented here with purified proteins (**Figure 3**) and those reported for whole cells (Kotajima et al., 2013) may be that additional, unspecified interactions occur *in vivo*.

Bacterial cells exposed to high salt concentrations have to cope with lower water potential and higher ionic potential, which can otherwise be toxic to cellular metabolism (Los et al., 2010). Sodium ions, when present in excess in the cytoplasm, compete for potassium-binding sites in proteins and lead to the malfunction of proteins by destabilizing their tertiary structure. In cyanobacteria, an increase of sodium ion concentration in the cell is linked to an efflux of potassium ions. Furthermore, salt stress has a marked inhibitory effect on photosynthesis. Treatment of cyanobacteria with high concentrations of NaCl results a 40% decrease in the amount of the D1 protein of the photosystem II reaction center complex, thus leading to a decrease in the rate of photosystem II mediated oxygen evolution (Sudhir et al., 2005). It is therefore vital that cyanobacteria contain robust regulatory system(s) to achieve salt and osmotic homeostasis. Indeed, to date, four multi-functional sensor histidine kinases—Hik10, Hik16, Hik33, Hik34—have been proposed to sense salt, while Hik2 has been suggested to function as an osmosensor (Paithoonrangsarid et al., 2004). The inhibitory effect of salt on Hik2 autophosphorylation (**Figure 3**) supports the possibility that Hik2's osmosensing properties are a direct result of its sensitivity to salt. It is therefore likely that Hik2 is a genuine salt sensor, and that this has been overlooked in the earlier study on Hik2 salt sensing (Paithoonrangsarid et al., 2004). We do not yet know how Hik2 senses salt. The GAF sensor domain in Hik2 may bind Na^+, as in the case of some Na^+ sensors (Cann, 2007; Biswas and Visweswariah, 2011). Na^+ ions directly modulating the kinase domain, as in the case of the bacterial osmosensor EnvZ (Wang et al., 2012), is another possibility.

It remains to be determined whether Hik2 senses and responds to other regulatory signals. The Hik2 homolog in chloroplasts, CSK, binds quinone (Puthiyaveetil et al., 2013). This raises the prospect of Hik2 also sensing plastoquinone (PQ) redox state, and thereby regulating photosynthesis genes. If this is indeed the case, Hik2 would qualify as a multi-sensor kinase.

Histidine kinases contain a conserved kinase domain, consisting of DHp and CA subdomains. The phosphorylation site of a histidine kinase is located within the first helix of the DHp domain. We confirmed the phosphorylation site of Hik2 to be His^{185} by using an acid-base stability assay and site-directed mutagenesis (**Figures 4A,B**). The CA domain contains conserved motifs, G1 and G2 boxes, which are characterized by "DxGxG" and "GxGxG" respectively. The CA domain is essential for binding the ATP molecule and for priming the γ-phosphate of ATP for a nucleophilic attack by the conserved histidine residue that is located within the H-box (Conley et al., 1994). In particular, conserved glycine residues in the G2-box facilitate the flexibility of the ATP-lid, which controls the entry and the release of the ATP-Mg^{2+} complex and the ADP-Mg^{2+} complex, respectively (Marina et al., 2001). Consequently, mutations within the G1 or G2 boxes disrupt the

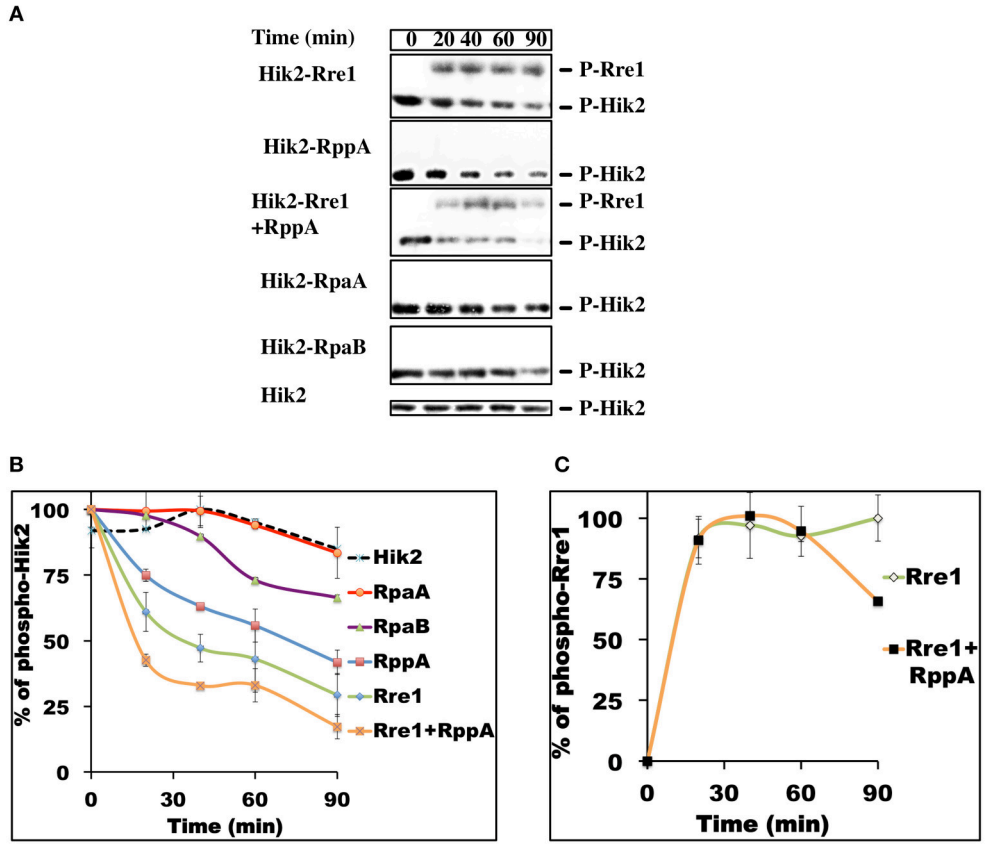

FIGURE 6 | Time-course of phosphotransfer from Phospho-Hik2 to full-length Rre1, RppA, and RpaA response regulators. (A) Autoradiograph of ^{32}P labeling. **(B)** Kinetics of phosphotransfer from P-Hik2 to response regulators. **(C)** Phosphorylation of Rre1F. The assay was repeated at least three times, with similar results obtained in each case. Each data point is calculated from band intensity from the autoradiograph, using ImageJ, and the percentage of activity was plotted as a function of time, in minutes. Error bars indicate standard error of the mean value from three experiments.

structure of the nucleotide-binding pocket, and thereby impair the autophosphorylation of histidine kinases. Indeed, mutation within the G1 or G2 box for several histidine kinases abolishes their autokinase activity (Gamble et al., 1998; Chen et al., 2009). Along these lines, substitution of any of the conserved glycine residues with alanine in the G1 or G2 box of Hik2 abolishes its autophosphorylation activity (**Figure 4C**).

The second step in a TCS is the phosphotransfer reaction from the conserved histidine residue of the histidine kinase to an aspartic acid residue in the response regulator. The phosphotransfer reaction between cognate sensor-response regulator pairs has favored kinetics, and these can be used to identify functional partners (Laub et al., 2007; Skerker et al., 2008). The phosphotransfer kinetics shown in **Figure 6** illustrate that Hik2 has the highest phosphotransfer activity toward Rre1, followed by RppA (**Figures 6A,B**). These findings are consistent with the earlier yeast-two hybrid study (Sato et al., 2007) and with the pull-down assay results presented in **Figure 5**, and further confirm that Rre1 and RppA are cognate response regulators of Hik2. Our results (**Figure 6**) also rule out RpaA and RpaB as functional partners of Hik2 in cyanobacteria.

The precise functional role and target genes of Rre1 in cyanobacteria are not yet clear, though Rre1 has been suggested to regulate osmotic responsive genes (Paithoonrangsarid et al., 2004). The homolog of Rre1 in red algal plastids, Ycf29, binds to phycobiliprotein genes in low light, where it is then likely to activate their expression (Minoda and Tanaka, 2005). The notion that Rre1 can have different effects at salt/osmotic/light-stress-responsive target genes is consistent with the fact that it is a NarL-type response regulator. NarL-type response regulators can act as activators as well as repressors of transcription depending on the nature and location of their binding sites in their target genes (Maris et al., 2002).

In cyanobacteria and chloroplasts, the redox state of the PQ pool controls transcription of chloroplast genes that encode reaction-center proteins of photosystem II and I, initiating a long-term acclimatory process known as photosystem stoichiometry adjustment (Pfannschmidt et al., 1999). In cyanobacteria, this process has been suggested to involve the RppA response regulator (Li and Sherman, 2000). Our phosphotransfer analysis (**Figure 6**) further supports this possibility. Interestingly the sensor kinase RppB, found in

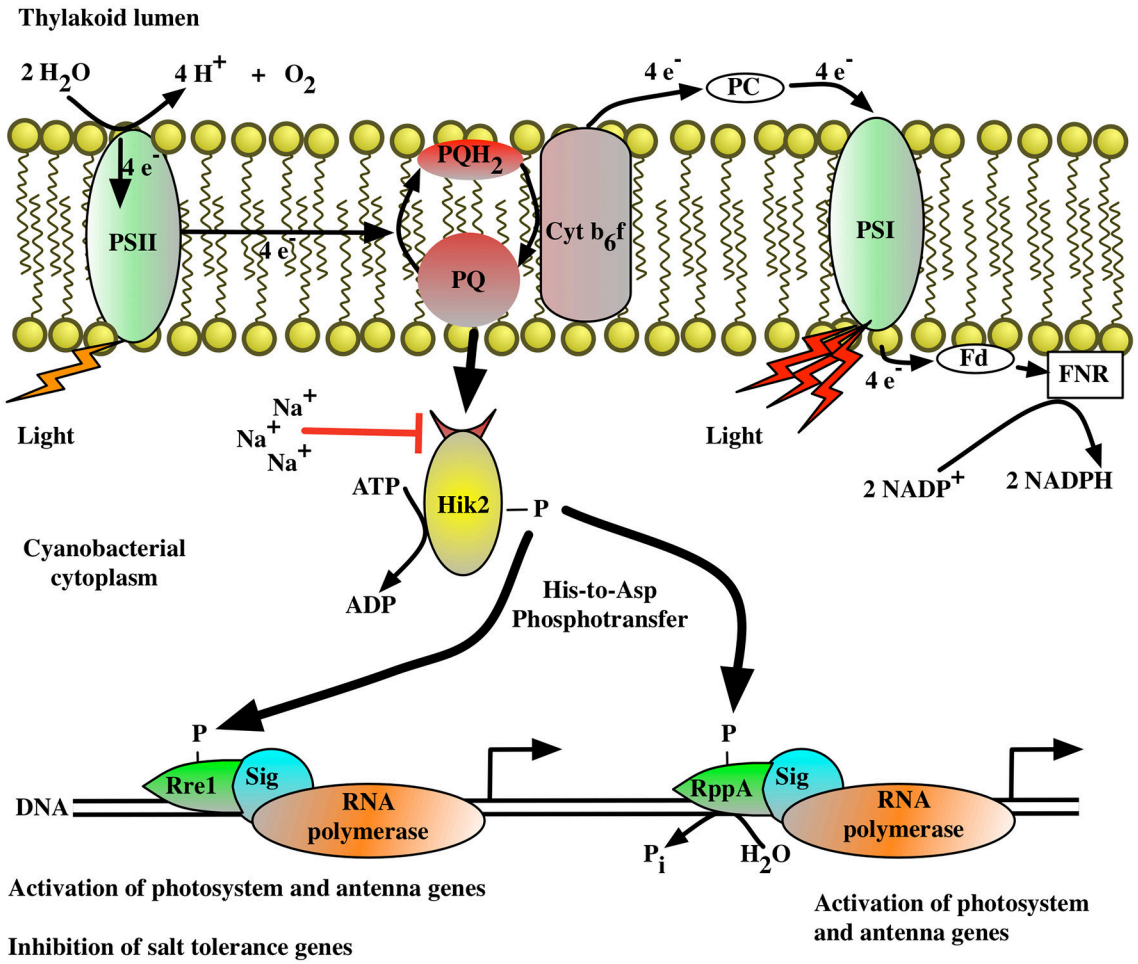

FIGURE 7 | The proposed signal transduction pathway for the Hik2-based two-component system in cyanobacteria. The autophosphorylation activity of Hik2 is regulated by signals from the photosynthetic electron transport chain and by sodium ions (Na^{2+}). The red arrow indicates an inhibitory effect. A black arrow indicates activation. Autophosphorylated (active) Hik2 transfers phosphoryl groups to Rre1 and RppA. Phosphorylated Rre1 and RppA activate genes encoding the photosynthetic machinery. In addition, the phosphorylated form of Rre1 acts as a negative regulator for salt/osmotic tolerance genes. Under high salt/osmotic condition, Na^{2+} inhibits the autophosphorylation of Hik2. Phospho-Rre1 becomes dephosphorylated, which in turn removes the repression of salt/osmotic tolerance genes.

the same operon as RppA, turned out to have no role in the regulation of photosynthesis genes (Li and Sherman, 2000). Sensor kinases other than RppB have therefore been proposed to work with RppA in photosystem stoichiometry adjustment in cyanobacteria (Li and Sherman, 2000). We suggest Hik2 is the cognate sensor of RppA in this regulatory pathway. Since the number of sensor kinases tends to be lower than that of response regulators in bacteria, more than one response regulator is likely to partner with a given kinase (Laub and Goulian, 2007). The functional role of CSK, the chloroplast homolog of Hik2 (Puthiyaveetil et al., 2008), together with the results presented here and elsewhere (Sato et al., 2007), supports Hik2 being the sensor that acts on Rre1 and RppA transcription factors to regulate photosynthesis genes as part of the mechanism of photosystem stoichiometry adjustment in cyanobacteria. The same Hik2-Rre1 system acting on a different set of target genes may also underlie the salt/osmotic tolerance in cyanobacteria. Salt stress, like light quality changes, induces photosystem stoichiometry adjustment in cyanobacteria, and a common sensory system has been suggested to govern these two responses (Murakami et al., 1997). Our work identifies this shared signaling system, with the Hik2 sensor kinase as the hub integrating both salt and redox signals and the Rre1 and RppA response regulators forming its bifurcated arms. A similar, bifurcated quinone redox signaling pathway has been proposed to connect regulation of photosynthetic reaction center stoichiometry with regulation of the relative light-harvesting antenna size of photosystem I (PS I) and photosystem II (PS II) during light state 1-state 2 transitions(Allen, 1995; Allen and Nilsson, 1997; Li and Sherman, 2000).

Figure 7 presents a working model of transcriptional control by the Hik2-based two-component signal transduction system

in cyanobacteria. In this model (**Figure 7**), the activated Hik2 autophosphorylates and transfers phosphoryl groups to Rre1 and RppA. Phospho-Rre1 activates genes coding for phycobilisomes. Phospho-RppA regulates genes for photosystems, thereby balancing the distribution of excitation energy driving electron transfer between PS II and PS I by means of photosystem stoichiometry adjustment. Our scheme also posits that phospho-Rre1 represses salt/osmotic tolerance genes, a suggestion consistent with the fact that Rre1 belongs to the NarL-type family of response regulators, which act as both activators and repressors of transcription at different target genes (Maris et al., 2002). Upon salt and/or hyperosmotic signal, the activity of Hik2 is inhibited (**Figure 3**, lanes 2–4); Rre1 and RppA therefore remain in their unphosphorylated states. As a result, Rre1 can no longer act as a repressor of salt/osmotic tolerance genes, in turn releasing the repression on their transcription.

While our results demonstrate that Hik2 is a multifunctional sensor histidine kinase, they do not rule out the possibility of Hik2 having additional inputs and outputs, as yet uncharacterized. A central and co-ordinating position of Hik2 in diverse cellular control circuits would be consistent with the indispensability of the *Hik2* gene for cyanobacterial growth and viability (Li and Sherman, 2000; Paithoonrangsarid et al., 2004; Ashby and Houmard, 2006).

AUTHOR CONTRIBUTIONS

IMI performed the experimental work and devised experimental strategies; SP advised and supervised; JFA posed questions and outlined the investigation; all three authors contributed to interpretation of the data, discussion, conclusions, and to writing the manuscript.

ACKNOWLEDGMENTS

We thank D. Nuernberg for the gift of *Synechocystis* sp. PCC 6803 genomic DNA; W. de Paula and S. J. L. Rowden for discussion; and two anonymous referees for comments on the manuscript. IMI thanks Queen Mary University of London for a graduate teaching studentship. SP held a Leverhulme Trust early career postdoctoral research fellowship. JA acknowledges the support of a research grant F/07 476/AQ and fellowship EM-2015-068 of the Leverhulme Trust.

REFERENCES

Allen, J. F. (1995). Thylakoid protein phosphorylation, state 1-state 2 transitions, and photosystem stoichiometry adjustment - redox control at multiple levels of gene expression. *Physiol. Plant.* 93, 196–205. doi: 10.1034/j.1399-3054.1995.930128.x

Allen, J. F., and Nilsson, A. (1997). Redox signalling and the structural basis of regulation of photosynthesis by protein phosphorylation. *Physiol. Plant.* 100, 863–868. doi: 10.1111/j.1399-3054.1997.tb00012.x

Ashby, M. K., and Houmard, J. (2006). Cyanobacterial two-component proteins: structure, diversity, distribution, and evolution. *Microbiol. Mol. Biol. Rev.* 70, 472–509. doi: 10.1128/MMBR.00046-05

Ashby, M. K., Houmard, J., and Mullineaux, C. W. (2002). The ycf27 genes from cyanobacteria and eukaryotic algae: distribution and implications for chloroplast evolution. *FEMS Microbiol. Lett.* 214, 25–30. doi: 10.1016/s0378-1097(02)00834-0

Ashby, M. K., and Mullineaux, C. W. (1999). Cyanobacterial ycf27 gene products regulate energy transfer from phycobilisomes to photosystems I and II. *FEMS Microbiol. Lett.* 181, 253–260. doi: 10.1111/j.1574-6968.1999.tb08852.x

Attwood, P. V., Besant, P. G., and Piggott, M. J. (2011). Focus on phosphoaspartate and phosphoglutamate. *Amino Acids* 40, 1035–1051. doi: 10.1007/s00726-010-0738-5

Attwood, P. V., Piggott, M. J., Zu, X. L., and Besant, P. G. (2007). Focus on phosphohistidine. *Amino Acids* 32, 145–156. doi: 10.1007/s00726-006-0443-6

Biswas, K. H., and Visweswariah, S. S. (2011). Distinct allostery induced in the cyclic GMP-binding, cyclic GMP-specific phosphodiesterase (PDE5) by cyclic GMP, sildenafil, and metal ions. *J. Biol. Chem.* 286, 8545–8554. doi: 10.1074/jbc.M110.193185

Cann, M. (2007). A subset of GAF domains are evolutionarily conserved sodium sensors. *Mol. Microbiol.* 64, 461–472. doi: 10.1111/j.1365-2958.2007.05669.x

Chen, T., Liu, J., Lei, G., Liu, Y. F., Li, Z. G., Tao, J. J., et al. (2009). Effects of Tobacco Ethylene Receptor mutations on receptor kinase activity, plant growth and stress responses. *Plant Cell Physiol.* 50, 1636–1650. doi: 10.1093/pcp/pcp107

Chenna, R., Sugawara, H., Koike, T., Lopez, R., Gibson, T. J., Higgins, D. G., et al. (2003). Multiple sequence alignment with the Clustal series of programs. *Nucleic Acids Res.* 31, 3497–3500. doi: 10.1093/nar/gkg500

Conley, M. P., Berg, H. C., Tawa, P., Stewart, R. C., Ellefson, D. D., and Wolfe, A. J. (1994). pH dependence of CheA autophosphorylation in *Escherichia coli*. *J. Bacteriol.* 176, 3870–3877.

Gamble, R. L., Coonfield, M. L., and Schaller, G. E. (1998). Histidine kinase activity of the ETR1 ethylene receptor from Arabidopsis. *Proc. Natl. Acad. Sci. U.S.A.* 95, 7825–7829. doi: 10.1073/pnas.95.13.7825

Kato, H., Kubo, T., Hayashi, M., Kobayashi, I., Yagasaki, T., Chibazakura, T., et al. (2011). Interactions between histidine kinase NblS and the response regulators RpaB and SrrA are involved in the bleaching process of the cyanobacterium *Synechococcus elongatus* PCC 7942. *Plant Cell Physiol.* 52, 2115–2122. doi: 10.1093/pcp/pcr140

Kotajima, T., Shiraiwa, Y., and Suzuki, I. (2013). Functional analysis of the N-terminal region of an essential histidine kinase, Hik2, in the cyanobacterium *Synechocystis* sp. PCC 6803. *FEMS Microbiol. Lett.* 351, 88–94. doi: 10.1111/1574-6968.12346

Laemmli, U. K. (1970). Cleavage of structural proteins during assembly of the head of bacteriophage-T4. *Nature* 227, 680–685. doi: 10.1038/227680a0

Laub, M. T., Biondi, E. G., and Skerker, J. M. (2007). Phosphotransfer profiling: systematic mapping of two-component signal transduction pathways and phosphorelays. *Meth. Enzymol.* 423, 531–548. doi: 10.1016/S0076-6879(07)23026-5

Laub, M. T., and Goulian, M. (2007). Specificity in two-component signal transduction pathways. *Annu. Rev. Genet.* 41, 121–145. doi: 10.1146/annurev.genet.41.042007.170548

Li, H., and Sherman, L. A. (2000). A redox-responsive regulator of photosynthesis gene expression in the cyanobacterium *Synechocystis* sp strain PCC 6803. *J. Bacteriol.* 182, 4268–4277. doi: 10.1128/JB.182.15.4268-4277.2000

Los, D. A., Zorina, A., Sinetova, M., Kryazhov, S., Mironov, K., and Zinchenko, V. V. (2010). Stress sensors and signal transducers in cyanobacteria. *Sensors (Basel)* 10, 2386–2415. doi: 10.3390/s100302386

Majeed, W., Zhang, Y., Xue, Y., Ranade, S., Blue, R. N., Wang, Q., et al. (2012). RpaA regulates the accumulation of monomeric photosystem I and PsbA under high light conditions in *Synechocystis* sp. PCC 6803. *PLoS ONE* 7:e45139. doi: 10.1371/journal.pone.0045139

Marin, K., Suzuki, L., Yamaguchi, K., Ribbeck, K., Yamamoto, H., Kanesaki, Y., et al. (2003). Identification of histidine kinases that act as sensors in the perception of salt stress in *Synechocystis* sp. PCC 6803. *Proc. Natl. Acad. Sci. U.S.A.* 100, 9061–9066. doi: 10.1073/pnas.1532302100

Marina, A., Mott, C., Auyzenberg, A., Hendrickson, W. A., and Waldburger, C. D. (2001). Structural and mutational analysis of the PhoQ histidine kinase catalytic domain. Insight into the reaction mechanism. *J. Biol. Chem.* 276, 41182–41190. doi: 10.1074/jbc.M106080200

Maris, A. E., Sawaya, M. R., Kaczor-Grzeskowiak, M., Jarvis, M. R., Bearson, S. M., Kopka, M. L., et al. (2002). Dimerization allows DNA target site recognition by the NarL response regulator. *Nat. Struct. Biol.* 9, 771–778. doi: 10.1038/nsb845

Mary, I., and Vaulot, D. (2003). Two-component systems in Prochlorococcus MED4: genomic analysis and differential expression under stress. *FEMS Microbiol. Lett.* 226, 135–144. doi: 10.1016/S0378-1097(03)00587-1

Minoda, A., and Tanaka, K. (2005). "Roles of the transcription factors encoded in the plastid genome of Cyanidioschyzon merolae," in *Photosynthesis: Fundamental Aspects to Global Perspectives,* eds A. V. D. Est and D. Bruce (Lawrence, KS: Alliance Communications Group), 728–729.

Motulsky, H., and Christopoulos, A. (2003). *Fitting Models to Biological Data Using Linear and Nonlinear Regression. A Practical Guide to Curve Fitting.* San Diego, CA: GraphPad Software Inc. Available online at: http://www.graphpad.com

Murakami, A., Kim, S.-J., and Fujita, Y. (1997). Changes in photosystem stoichiometry in response to environmental conditions for cell growth observed with the cyanophyte *Synechocystis* PCC 6714. *Plant Cell Physiol.* 38, 392–397. doi: 10.1093/oxfordjournals.pcp.a029181

Paithoonrangsarid, K., Shoumskaya, M. A., Kanesaki, Y., Satoh, S., Tabata, S., Los, D. A., et al. (2004). Five histidine kinases perceive osmotic stress and regulate distinct sets of genes in *Synechocystis*. *J. Biol. Chem.* 279, 53078–53086. doi: 10.1074/jbc.M410162200

Pfannschmidt, T., Nilsson, A., and Allen, J. F. (1999). Photosynthetic control of chloroplast gene expression. *Nature* 397, 625–628. doi: 10.1038/17624

Puthiyaveetil, S., and Allen, J. F. (2009). Chloroplast two-component systems: evolution of the link between photosynthesis and gene expression. *Proc. Biol. Sci.* 276, 2133–2145. doi: 10.1098/rspb.2008.1426

Puthiyaveetil, S., Ibrahim, I. M., and Allen, J. F. (2012). Oxidation-reduction signalling components in regulatory pathways of state transitions and photosystem stoichiometry adjustment in chloroplasts. *Plant Cell Environ.* 35, 347–359. doi: 10.1111/j.1365-3040.2011.02349.x

Puthiyaveetil, S., Ibrahim, I. M., and Allen, J. F. (2013). Evolutionary rewiring: a modified prokaryotic gene-regulatory pathway in chloroplasts. *Philos. Trans. R. Soc. Lond. B Biol. Sci.* 368:20120260. doi: 10.1098/rstb.2012.0260. Available online at: http://rstb.royalsocietypublishing.org/content/368/1622/20120260

Puthiyaveetil, S., Ibrahim, I. M., Jelicic, B., Tomasic, A., Fulgosi, H., and Allen, J. F. (2010). Transcriptional control of photosynthesis genes: the evolutionarily conserved regulatory mechanism in plastid genome function. *Genome Biol. Evol.* 2, 888–896. doi: 10.1093/gbe/evq073

Puthiyaveetil, S., Kavanagh, T. A., Cain, P., Sullivan, J. A., Newell, C. A., Gray, J. C., et al. (2008). The ancestral symbiont sensor kinase CSK links photosynthesis with gene expression in chloroplasts. *Proc. Natl. Acad. Sci. U.S.A.* 105, 10061–10066. doi: 10.1073/pnas.0803928105

Sambrook, J., Fritsch, E. F., and Maniatis, T. (1989). *Molecular Cloning a Laboratory Manual, 2nd Edn.* Cold Spring Harbor, NY: Cold Spring Laboratory Press.

Sato, S., Shimoda, Y., Muraki, A., Kohara, M., Nakamura, Y., and Tabata, S. (2007). A large-scale protein protein interaction analysis in *Synechocystis* sp. PCC 6803. *DNA Res.* 14, 207–216. doi: 10.1093/dnares/dsm021

Schneider, C. A., Rasband, W. S., and Eliceiri, K. W. (2012). NIH Image to ImageJ: 25 years of image analysis. *Nat. Methods* 9, 671–675. doi: 10.1038/nmeth.2089

Skerker, J. M., Perchuk, B. S., Siryaporn, A., Lubin, E. A., Ashenberg, O., Goulian, M., et al. (2008). Rewiring the specificity of two-component signal transduction systems. *Cell* 133, 1043–1054. doi: 10.1016/j.cell.2008.04.040

Stock, A. M., Robinson, V. L., and Goudreau, P. N. (2000). Two-component signal transduction. *Annu. Rev. Biochem.* 69, 183–215. doi: 10.1146/annurev.biochem.69.1.183

Sudhir, P. R., Pogoryelov, D., Kovacs, L., Garab, G., and Murthy, S. D. S. (2005). The effects of salt stress on photosynthetic electron transport and thylakoid membrane proteins in the cyanobacterium Spirulina platensis. *J. Biochem. Mol. Biol.* 38, 481–485. doi: 10.5483/BMBRep.2005.38.4.481

Wang, L. C., Morgan, L. K., Godakumbura, P., Kenney, L. J., and Anand, G. S. (2012). The inner membrane histidine kinase EnvZ senses osmolality via helix-coil transitions in the cytoplasm. *EMBO J.* 31, 2648–2659. doi: 10.1038/emboj.2012.99

Conflict of Interest Statement: The authors declare that the research was conducted in the absence of any commercial or financial relationships that could be construed as a potential conflict of interest.

frontiers in Plant Science

PERSPECTIVE
published: 09 August 2016
doi: 10.3389/fpls.2016.01135

Environmental pH and the Requirement for the Extrinsic Proteins of Photosystem II in the Function of Cyanobacterial Photosynthesis

*Jaz N. Morris[1], Julian J. Eaton-Rye[2] and Tina C. Summerfield[1]**

[1] Department of Botany, University of Otago, Dunedin, New Zealand, [2] Department of Biochemistry, University of Otago, Dunedin, New Zealand

In one of the final stages of cyanobacterial Photosystem II (PS II) assembly, binding of up to four extrinsic proteins to PS II stabilizes the oxygen-evolving complex (OEC). Growth of cyanobacterial mutants deficient in certain combinations of these thylakoid-lumen-associated polypeptides is sensitive to changes in environmental pH, despite the physical separation of the membrane-embedded PS II complex from the external environment. In this perspective we discuss the effect of environmental pH on OEC function and photoautotrophic growth in cyanobacteria with reference to pH-sensitive PS II mutants lacking extrinsic proteins. We consider the possibilities that, compared to pH 10.0, pH 7.5 increases susceptibility to PS II-generated reactive oxygen species (ROS) causing photoinhibition and reducing PS II assembly in some mutants, and that perturbations to channels in the lumenal regions of PS II might alter the accessibility of water to the active site as well as egress of oxygen and protons to the thylakoid lumen. Reduced levels of PS II in these mutants, and reduced OEC activity arising from the disruption of substrate/product channels, could reduce the *trans*-thylakoid pH gradient (ΔpH), leading to the impairment of photosynthesis. Growth of some PS II mutants at pH 7.5 can be rescued by elevating CO_2 levels, suggesting that the pH-sensitive phenotype might primarily be an indirect result of back-pressure in the electron transport chain that results in heightened production of ROS by the impaired photosystem.

Keywords: assembly, extrinsic proteins, oxygen-evolving complex, pH, photosystem II, reactive oxygen species, thylakoid lumen

OPEN ACCESS

Edited by:
Christine Helen Foyer, University of Leeds, UK

Reviewed by:
Conrad Mullineaux, Queen Mary University of London, UK
John Frederick Allen, University College London, UK

****Correspondence:***
Tina C. Summerfield
tina.summerfield@otago.ac.nz

Specialty section:
This article was submitted to Plant Cell Biology, a section of the journal Frontiers in Plant Science

Received: *27 February 2016*
Accepted: *18 July 2016*
Published: *09 August 2016*

Citation:
Morris JN, Eaton-Rye JJ and Summerfield TC (2016) Environmental pH and the Requirement for the Extrinsic Proteins of Photosystem II in the Function of Cyanobacterial Photosynthesis. Front. Plant Sci. 7:1135. doi: 10.3389/fpls.2016.01135

INTRODUCTION

Photosystem II (PS II) is a thylakoid membrane-bound protein complex that functions as a water-plastoquinone oxidoreductase in oxygenic phototrophs (Vinyard et al., 2013). In cyanobacteria, the mature PS II monomer contains at least 17 membrane-spanning subunits, of which seven are essential for PS II function, as well as up to four extrinsic, thylakoid-lumen-associated subunits (PsbO, PsbU, PsbV, and possibly CyanoQ), which are necessary for maximal rates of oxygen evolution (Shen, 2015; Heinz et al., 2016; Roose et al., 2016). The PS II extrinsic proteins, along with the lumenal domains of the intrinsic reaction center proteins D1 and D2 and the adjacent

chlorophyll-binding core antenna proteins CP43 and CP47, form a protective environment around the site of the Mn_4CaO_5 cluster or oxygen-evolving complex (OEC) that catalyzes the water-splitting reaction (Shen, 2015).

The extrinsic proteins bind to the PS II monomer subsequent to assembly and photoactivation of the Mn_4CaO_5 cluster (Dasgupta et al., 2008; Nickelsen and Rengstl, 2013). Based on their locations in the X-ray-derived structure of PS II from *Thermosynechococcus vulcanus* (Umena et al., 2011; Suga et al., 2015), and extensive biochemical studies (reviewed in Bricker et al., 2012; Ifuku, 2015; Ifuku and Noguchi, 2016; Roose et al., 2016), it seems likely that PsbO and PsbV bind first: PsbO binds via interactions with loop E of CP47, loop E of CP43 and the C-terminus of both D1 and D2; PsbV binds via loop E of CP43 and the C-terminus of both D1 and D2. Subsequently, PsbU binds via PsbO, PsbV, loop E of CP47, loop E of CP43 as well as the C-terminus of both D1 and D2; finally, CyanoQ is predicted to bind via associations with PsbO and loop E of CP47. Although none of the extrinsic proteins provide direct ligands to the Mn_4CaO_5 cluster, they protect this site from the reductive environment of the lumen, and increase the affinity for the Ca^{2+} and Cl^- co-factors (reviewed in Bricker et al., 2012).

During light-driven photosynthetic electron transport, electrons are extracted in a series of oxidative 'S' state transitions (S_0–S_4) of the Mn_4CaO_5 cluster, resulting in the oxidation of two waters; in this process four electrons are transferred sequentially to the PS II reaction center P_{680} via Y_Z (D1:Tyr161), and one dioxygen molecule and four protons are released to the thylakoid lumen (Shen, 2015; Najafpour et al., 2016). The X-ray-derived structures of PS II from *T. vulcanus* and *T. elongatus* have revealed that extensive hydrophilic regions and hydrogen bond networks in both extrinsic and intrinsic proteins in the vicinity of the OEC may allow water transport to, and proton and molecular oxygen transport from, the catalytic center (Linke and Ho, 2014; Lorch et al., 2015; Vogt et al., 2015).

The buildup of protons in the lumen from PS II water-splitting contributes to the pH gradient (ΔpH) and membrane potential ($\Delta\psi$) across the thylakoid membrane, which creates a proton electrochemical potential that is used to drive the ATP synthase catalyzed production of ATP. Additionally, protons are pumped into the lumen independently of PS II via NADPH dehydrogenase complexes involved in cyclic electron flow (CEF) around Photosystem I (PS I), respiration, and carbon uptake (Battchikova et al., 2011), and via plastoquinol oxidation by the cytochrome b_6f complex (Kallas, 2012). As a consequence, the cyanobacterial thylakoid lumen pH is acidified in the light, by around two pH units, relative to the cytosolic pH (Belkin et al., 1987; Belkin and Packer, 1988). Although the pH microenvironment in the vicinity of PS II would be expected to be independent of environmental pH, changes in environmental pH do affect PS II. A number of mutants in the model strain *Synechocystis* sp. PCC 6803 (hereafter *Synechocystis* 6803), which are deficient in extrinsic proteins that stabilize the OEC, are obligate photoheterotrophs or photomixotrophs in pH 7.5-buffered growth media, but were observed to grow photoautotrophically at pH 10.0 (Eaton-Rye et al., 2003).

Despite ongoing interest in the transcriptomic and proteomic response to pH in cyanobacteria (Ohta et al., 2005; Kurian et al., 2006; Summerfield and Sherman, 2008; Zhang et al., 2009; Li et al., 2014; Matsuhashi et al., 2015), relatively few studies have investigated the role of environmental pH on the assembly of PS II, or on the photochemical and redox processes of the photosystem. Here, we offer a perspective regarding the effects of environmental pH on the function of PS II in cyanobacterial cells and propose a mechanism by which some mutations in the lumenal regions of PS II prevent photoautotrophic growth at pH 7.5.

GROWTH OF pH-SENSITIVE PS II MUTANTS

Environmental pH Affects PS II

Many cyanobacterial species are able to grow photoautotrophically across a neutral to alkaline pH range, and oxygen evolution and PS II-specific variable chlorophyll fluorescence emission from *Synechocystis* 6803 wild-type cells was similar from pH 7.5–10.0 (Summerfield et al., 2013; Touloupakis et al., 2016). Across this pH range, the internal pH of cyanobacterial cells is well buffered by pH homeostasis mechanisms (Krulwich et al., 2011). For example, a relatively large change in external pH from pH 10.0 to 8.0 decreased cytosolic pH from 7.2 to 6.8 in *Synechocystis* 6803 (Jiang et al., 2013). In cyanobacteria, excluding thylakoid-deficient *Gloeobacter* spp., PS II extrinsic proteins and the oxygen-evolving machinery face the more acidic thylakoid lumen (pH = ∼5, Belkin et al., 1987) and are thus further protected from the environmental pH compared to the cytosol. Considering that the cytosol and thylakoid lumen are well-buffered with respect to environmental pH, and the fact that PS II oxygen evolution is known to function optimally when the lumen pH is relatively low, between pH 5.0 and 6.5 (Kramer et al., 1999; Najafpour et al., 2016), it was surprising that a number of *Synechocystis* 6803 PS II mutants were unable to grow photoautotrophically at environmental pH 7.5, whereas growth was possible at pH 10.0 (**Table 1**; **Figures 1D,E**) (Eaton-Rye et al., 2003; Summerfield et al., 2005a,b, 2007).

PS II Mutants Lacking Extrinsic Proteins

The loss of extrinsic proteins has multiple effects on PS II (Bricker et al., 2012). By destabilizing the binding of Ca^{2+} and Cl^- the function of the Mn_4CaO_5 catalytic site might be directly affected (Ifuku and Noguchi, 2016). In addition, the extrinsic proteins, along with the lumenal domains of the intrinsic proteins, maintain channels that allow the access of substrate water to the catalytic site, and egress of oxygen and protons. The absence of either of the extrinsic PS II proteins PsbO and PsbV reduced growth and oxygen evolution compared to the *Synechocystis* 6803 wild type (Burnap and Sherman, 1991; Shen et al., 1995) but did not affect pH tolerance (Eaton-Rye et al., 2003). Deletion of PsbO or PsbV resulted in decreased oxygen evolution compared to deletion of PsbU or CyanoQ, consistent with the partial dependency of PsbU and

TABLE 1 | Photoautotrophic growth, and relative level of PS II assembly of strains of *Synechocystis* sp. PCC 6803 carrying mutations in PS II extrinsic proteins, and lumenal domains of intrinsic proteins[1].

Strain	pH 7.5		pH 10.0	
	Photoautotrophic growth	Number of PS II centers[5]	Photoautotrophic growth	Number of PS II centers[5]
ΔPsbO[2]	Yes	0.57	Yes	0.91
ΔPsbO:ΔPsbU[2]	No	0.55	Yes	0.90
ΔPsbO:ΔPsbU:ΔCyanoQ[3]	No	0.40	Yes	0.64
ΔPsbO:ΔPsbU:ΔCyanoP[4]	No	n.a.	Yes	n.a.
ΔPsbO:ΔPsbV[2]	No	0.34	No	n.d.
ΔPsbV[2]	Yes	0.50	Yes	0.51
ΔPsbV:ΔCyanoQ[3]	No	0.24	Yes	0.37
ΔPsbV:ΔPsbU[2]	Yes	0.54	Yes	0.54
ΔCyanoQ[3]	Yes	0.80	Yes	0.91
CP47 F363R:ΔPsbV[2]	No	n.d.	No	n.d.
CP47 E364Q:ΔPsbV[2]	No	0.35	Yes	0.58
CP47 E364Q:ΔPsbV:ΔCyanoQ[3]	No	0.22	Yes	0.46
CP47 Δ(R384-V392):ΔPsbO[2]	Yes	0.59	Yes	0.59
CP47 Δ(R384-V392):ΔPsbO:ΔPsbU[2]	No	0.38	Yes	0.38
CP47 Δ(R384-V392):ΔPsbV[2]	No	0.37	Yes	0.37
CP47 Δ(R384-V392):ΔPsbV:ΔCyanoQ[3]	No	0.22	No	0.26
CP47 Δ(G429-T436):ΔPsbO[2]	No	n.a.	Yes	n.a.
CP47 Δ(G429-T436):ΔPsbV[2]	No	0.29	No	0.57

[1]*White rows: strains capable of photoautotrophic growth at pH 7.5 and pH 10.0; partially shaded rows: strains displaying the pH 7.5 sensitive phenotype; shaded rows: strains incapable of photoautotrophic growth at either pH.* [2] *Eaton-Rye et al., 2003.* [3]*Summerfield et al., 2005a.* [4]*Summerfield et al., 2005b; n.a., data not available; n.d., no PS II could be detected.* [5]*Number of PS II centers normalized to relative wild-type values in the same study and was determined using [^{14}C] atrazine binding (Morgan et al., 1998).*

CyanoQ binding on the presence of PsbO or PsbV (Shen et al., 1998; Thornton et al., 2004). Deletion of PsbU or CyanoQ in ΔPsbO or ΔPsbV backgrounds, respectively, revealed the pH-sensitive phenotype (**Table 1**, **Figures 1D,E**); ΔPsbO:ΔPsbU and ΔPsbV:ΔCyanoQ strains do not grow photoautotrophically at pH 7.5, whereas photoautotrophic growth at pH 10.0 is possible (Eaton-Rye et al., 2003; Summerfield et al., 2005a). Another extrinsic PS II protein, CyanoP, was also putatively assigned a role in the PS II dimer (Thornton et al., 2004; Nickelsen and Rengstl, 2013) but evidence suggests it may be a PS II assembly factor rather than a stoichiometric OEC subunit (Cormann et al., 2014; Jackson and Eaton-Rye, 2015). Deletion of CyanoP from other extrinsic protein mutants did not affect pH sensitivity (Summerfield et al., 2005b).

PS II Mutants with Deletions and Amino Acid Substitutions in Intrinsic Proteins

Mutations in the large, lumenal loop E of the PS II intrinsic protein CP47 (loop E: residues ∼260–450) also resulted in a loss of photoautotrophic growth and reduction in PS II center assembly at pH 7.5 in some strains also lacking PsbV (**Table 1**). Alkaline pH 10.0 restored photoautotrophic growth (compared to pH 7.5) in ΔPsbV mutants carrying a CP47 Glu364 to Gln substitution or a deletion from Arg384 to Val392; however, ΔPsbV strains with either Phe363 of CP47 changed to Arg, or a deletion from Gly429 to Thr436, could not grow photoautotrophically at either pH level (Morgan et al., 1998; Clarke and Eaton-Rye, 1999; Eaton-Rye et al., 2003).

Mutations in loop E of CP47 are likely to contribute to a loss of growth in *Synechocystis* 6803 ΔPsbV strains by affecting assembly of the further extrinsic proteins to PS II. The C-terminal half of loop E of CP47 crosslinks with amino acids in the N-terminal region of PsbO and interacts with PsbU and possibly CyanoQ. Analysis of analogous amino acid residues from the *T. vulcanus* PS II crystal structure (Protein Data Base accession 4UB6) (Suga et al., 2015) using PyMOL^{TM} (Schrodinger, LLC; DeLano, 2002) show that the Arg384 to Val392 (Arg385-Val393 in *T. vulcanus*) region is within 4 Å of *T. vulcanus* PsbO Leu164-Gly167 and PsbU Asn11-Gly18; furthermore, a CP47 Δ(R384-V392):ΔPsbV mutant could not grow photoautotrophically at pH 7.5, possibly due to perturbation of PsbO and PsbU assembly to PS II. However, as noted above, the deletion of Gly429 to Thr436 in the ΔPsbV mutant resulted in a strain unable to grow at pH 7.5 or pH 10.0 – this more severe phenotype might result from impaired CyanoQ binding, in addition to perturbed PsbO binding. The Gly429-Thr436 (Gly427-Thr434 in *T. vulcanus*) residues are in close proximity (∼5.8 Å) to CP47 Asp440, and within 4 Å of *T. vulcanus* PsbO Gln176 and Lys178. CP47 Asp440 and PsbO Lys178 in *T. vulcanus* correspond to CP47 Asp440 and PsbO Lys180 in *Synechocystis* 6803, which were suggested to be important crosslinking sites for CyanoQ (Liu et al., 2014). Consistent with the hypothesis that impaired CyanoQ binding caused the loss of all photoautotrophic growth in the CP47 Δ(G429-T436):ΔPsbV strain, deletion of

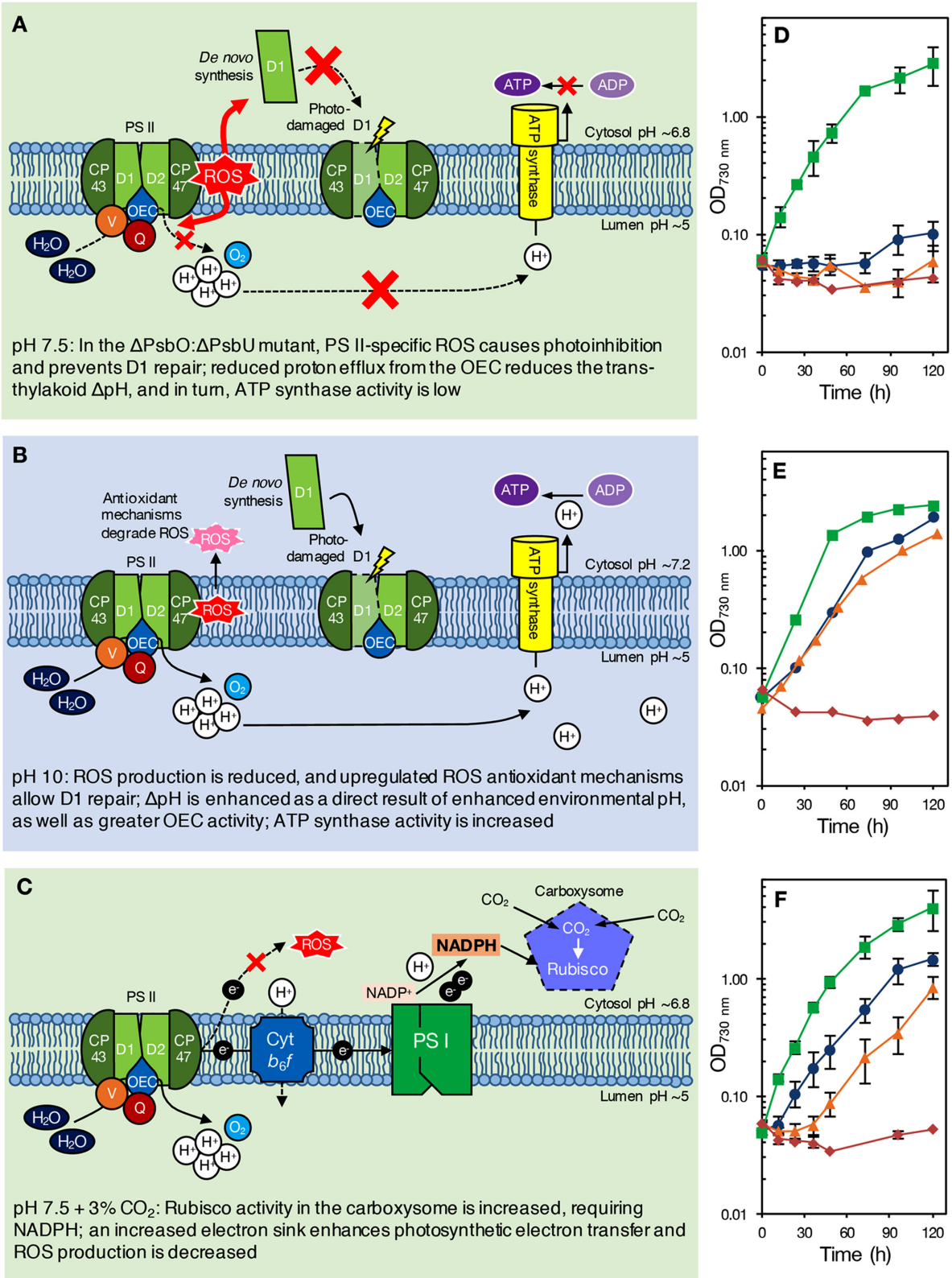

FIGURE 1 | Continued

FIGURE 1 | (A–C) Proposed model of pH effects on a ΔPsbO:ΔPsbU strain of *Synechocystis* 6803 at pH 7.5 **(A)**, green background; pH 10.0 **(B)**, blue background; and pH 7.5 with 3% CO_2 **(C)**, green background. The ΔPsbO:ΔPsbU strain was chosen for illustrative purposes only; we would expect a similar response from other pH 7.5-sensitive strains, such as ΔPsbV:ΔCyanoQ. **(A)** At pH 7.5, ROS formation from an impaired OEC prevents PS II repair, causing photoinhibition and reducing PS II levels. Additionally, reduced delivery of protons to the thylakoid lumen results in low ΔpH and insufficient ATP synthase activity [alternatively, growth may be retarded via sensing of the reduced ΔpH (not shown)]. **(B)** At pH 10.0, however, upregulation of oxidative stress response genes induces the synthesis of antioxidant defense compounds, allowing PS II repair and photoautotrophic growth. Increased environmental pH naturally enhances ΔpH, increasing ATP synthase activity [or activating other ΔpH-dependent processes that promote photoautotrophic growth (not shown)]. **(C)** With 3% CO_2, enhanced Rubisco activity in the carboxysome requires NADPH, drawing electrons from PS II that would otherwise lead to ROS production and photoinhibition. The internal pH values indicated are based on those determined for wild-type cells by Belkin et al. (1987) and Jiang et al. (2013), and might be different in PS II mutants. **(D–F)** Photoautotrophic growth of *Synechocystis* 6803 wild type, ΔPsbO:ΔPsbU, ΔPsbV:ΔCyanoQ, and ΔPsbO:ΔPsbV PS II mutants at **(D)** pH 7.5, ambient (~0.04%) CO_2 conditions; **(E)** pH 10.0, ambient (~0.04%) CO_2 conditions; and **(F)** pH 7.5, high (3%) CO_2 conditions. Green, squares: wild type; blue, circles: ΔPsbO:ΔPsbU cells; orange, triangles: ΔPsbV:ΔCyanoQ cells; red, diamonds: ΔPsbO:ΔPsbV cells. Data in **(D,F)** are the mean of 3–7 independent experiments (±SEM, error bars not visible are smaller than the markers) and were carried out as described previously (Morris et al., 2014). Data in **(E)** (averages only) are derived from Eaton-Rye et al. (2003) and Summerfield et al. (2005a).

CyanoQ in the CP47 Δ(R384-V392):ΔPsbV background resulted in a strain that could not be rescued by pH 10.0. In the CP47 Δ(R384-V392) mutant, loss of PsbO did not cause pH sensitivity (**Table 1**): potentially these cells were already impaired in PsbO binding; therefore, deletion of PsbV in this strain might have resulted in a phenotype similar to the obligate photoheterotrophic ΔPsbO:ΔPsbV mutant (Shen et al., 1995).

PROPOSED EFFECTS OF ENVIRONMENTAL pH ON PS II MUTANTS

Cells Deficient in Extrinsic Proteins Are More Susceptible to Photoinhibition and Exhibit Reduced PS II Assembly at pH 7.5

The number of PS II centers was reduced by the loss of extrinsic proteins, particularly at pH 7.5 (**Table 1**). The extrinsic proteins stabilize the OEC and PS II dimer (Bricker et al., 2012), therefore, reduced PS II levels could be a result of altered PS II assembly processes. The external pH appears to have little impact on the lumenal pH in cyanobacteria (Belkin et al., 1987). However, a model describing connection between the thylakoid membrane and cytoplasmic membrane in cyanobacteria has been proposed to be via thylakoid centers that are involved in PS II biogenesis (Rast et al., 2015). Through their connection with the cytoplasmic membrane (Van de Meene et al., 2012) these thylakoid centers may be affected by the pH of the periplasm and this may alter PS II biogenesis.

Alternatively, or additionally, low levels of PS II centers in these mutants might be a consequence of the production of reactive oxygen species (ROS) by an impaired OEC; ROS cause photoinhibition by affecting PS II repair following photodamage, as well as by targeting PS II directly (Murata et al., 2007; Nixon et al., 2010; Vass, 2012). However, PS II centers lacking all, or specific combinations of extrinsic proteins are probably natural assembly and repair intermediates in the cyanobacterial cell. Assuming that PsbO and PsbV attach to PS II first, centers lacking PsbO and PsbU but retaining PsbV and CyanoQ (or lacking PsbV and CyanoQ, but retaining PsbO and PsbU) might not ordinarily occur, and could result in excess ROS leading to photoinhibition and a loss of photoautotrophic growth at low pH (**Figure 1A**). Some lines of evidence support this theory. Dissociation of the extrinsic proteins from spinach PS II-enriched membrane fragments resulted in increased hydrogen peroxide production (Hillier and Wydrzynski, 1993). In addition, a strain of *Synechococcus* sp. PCC 7942 lacking PsbU exhibited increased resistance to oxidative stress and this has been suggested to be due to increased ROS production associated with impaired PS II centers (Balint et al., 2006). Furthermore, although ΔPsbO:ΔPsbU cells, for example, cannot grow photoautotrophically at pH 7.5, cells supplemented with 5 mM glucose can grow and evolve oxygen from PS II when assayed with actinic light at 2.0 mE m^{-2} s^{-1} (Summerfield et al., 2005a). However, when 6.5 mE m^{-2} s^{-1} light is applied, rapid and total inactivation of oxygen evolution occurs in the same strains (Eaton-Rye et al., 2003). This implies that light dosage, as well as pH, causes the loss of PS II activity in these mutants. Additionally, cyanobacteria appear to be more sensitive to ROS at low pH; photomixotrophic growth of both the *Synechocystis* 6803 wild type and PS II mutants showed increased sensitivity to the $^1O_2$ ROS generator Rose Bengal at pH 7.5 compared to pH 10.0 (Summerfield et al., 2013). ΔPsbO:ΔPsbU and ΔPsbV:ΔCyanoQ cells were also more sensitive to the O_2^- generator methyl viologen than wild-type cells at either pH (Summerfield et al., 2013). At pH 10.0, cells may be able to better resist oxidative damage (**Figure 1B**); a suite of general oxidative stress-responsive genes were downregulated in ΔPsbO:ΔPsbU cells at pH 7.5 compared to pH 10.0, or compared to wild-type cells at either pH (Summerfield et al., 2013). Interestingly, a similar set of stress-responsive genes was upregulated in a ΔPsbO:ΔPsbU pseudorevertant capable of pH 7.5 growth (Summerfield et al., 2007), implying that antioxidant defense is involved in pH 7.5 recovery. Considering that total PS II levels are already reduced in these mutants, any photoinhibition by ROS at pH 7.5 might further reduce the number of effective PS II centers to levels that cannot sustain sufficient oxygen evolution and growth, especially in high light conditions. However, it must be considered that the relative level of PS II in these mutants does not correlate well with the capacity for photoautotrophic growth (**Table 1**) or oxygen evolution, indicating that more factors underpin the pH-sensitive phenotype than the capacity for PS II assembly alone.

Reduced *Trans*-thylakoid pH Gradient at pH 7.5

During photosynthesis, the *trans*-thylakoid ΔpH is enhanced by proton release from light-driven oxidation of water by PS II. In PS II mutants, a reduction in assembled PS II centers, or a perturbation of water, oxygen and proton channels in the OEC would be likely to result in reduced proton delivery to the lumen. In cyanobacteria, ΔpH between the lumen and cytosol is as much as 2–3 pH units, and ΔpH increases with increasing environmental pH (Belkin et al., 1987). Therefore, reduced proton egress from PS II might be more harmful at pH 7.5 than pH 10.0, since ΔpH would already be reduced by environmental pH, potentially leading to ATP levels insufficient for cellular requirements (**Figure 1A**). While this theory is inconsistent with data on the pH-optimum for oxygen-evolving activity in extrinsic-protein deficient PS II centers isolated from higher plants (Commet et al., 2012), the function of isolated PS II in experimental conditions would be independent of cellular ATP and NADPH requirements. PS II mutants can grow in the presence of glucose at pH 7.5; respiration of added glucose could permit growth in these mutants by favoring CEF, allowing generation of ATP independently of PS II function. In *Synechococcus* Y-7c-s, a reduction in total cellular ATP, and the ATP:(ATP+ADP) ratio, was observed when external pH was reduced from pH 8 to growth-limiting pH 6 (Kallas and Castenholz, 1982). However, overall internal pH (the average of cytosol and thylakoid pH) across the same external pH range was only somewhat affected, suggesting that the observed limitation of energy supply might not be due to ΔpH alone. In support of the hypothesis that ATP supply might limit growth as pH is reduced, two strains of *Synechocystis* 6803 cells acclimated to pH 5.5 growth over 3 months independently acquired mutations in genes encoding F_1–F_0 ATP synthase components (Uchiyama et al., 2015), although these mutations are, as yet, functionally uncharacterized. Furthermore, experimental investigation of this hypothesis would require greater investigation of internal pH changes within the cell during photosynthesis and respiration, which to date has proven difficult (Berry et al., 2005).

As highlighted earlier, channels that surround the PS II OEC are likely to be perturbed by the loss of extrinsic proteins. Mutants with Phe363Arg and Glu364Gln substitutions in loop E of CP47 (**Table 1**) might also harbor impaired channels to the OEC. The *T. vulcanus* PS II crystal structure (*T. vulcanus* numbering is used throughout this paragraph) shows that CP47 Phe363 and Glu364 are adjacent to PsbO and D2 in a probable channel that might allow substrate water access to the OEC active site (Bricker et al., 2015). Additionally, Phe363 is implicated in the formation of a hydrophobic region around Y_D (D2 Tyr160), with the side-chain carboxyl group on Glu364 contributing to an H-bond network with Y_D via D2 Arg294 (Glu364-Arg294 distance: 2.8 Å; Ferreira et al., 2004; Saito et al., 2013; Suga et al., 2015). A perturbed hydrophobic pocket in the obligate photoheterotrophic F363R mutant might affect Y_D oxidation, altering the dark redox-state of Mn_4CaO_5 and resulting in a more deleterious phenotype than in the pH 7.5-sensitive E364Q mutant, where the carboxyl group on the substituted Gly might be able to partially contribute to H-bonding with D2 Arg294. Such speculation is only possible because of advances in the resolution of the PS II structure; experimental manipulation of putative channels in PS II in variable pH conditions has not been investigated as yet.

Enhancement of Rubisco Activity by CO_2 Draws Electrons from PS II and Reduces ROS Formation at pH 7.5

NADPH generated by photosynthetic electron transport is used to energize carbon uptake via Rubisco in the Calvin-Benson-Bassham (CBB) cycle; at pH 7.5, inorganic carbon is predominantly in the form of CO_2 (for review, see Price, 2011; Kupriyanova et al., 2013). We observed that 3% CO_2 supported photoautotrophic growth of ΔPsbO:ΔPsbU and ΔPsbV:ΔCyanoQ cells at pH 7.5, but had little impact on growth of the *Synechocystis* 6803 wild type, ΔPsbO:ΔPsbV cells (**Figures 1C,F**), or a ΔPsbO:ΔPsbU pseudorevertant (data not shown). In these conditions, increased Rubisco activity might require a large flux of NADPH, causing a build-up of $NADP^+$; this major electron sink might accelerate photosynthetic electron transport, even where OEC function is impaired by the loss of extrinsic proteins in PS II mutants. Inhibitors of CBB cycle activity prevent repair of photodamaged PS II (Takahashi and Murata, 2005, 2008), therefore it is possible that enhanced CBB cycle activity at 3% CO_2 has the opposite effect in ΔPsbO:ΔPsbU and ΔPsbV:ΔCyanoQ cells at pH 7.5, allowing efficient PS II repair and photoautotrophic growth (**Figure 1C**). In ambient CO_2 conditions, without such a high demand for electrons from PS II, altered electron transfer in these mutants might otherwise result in production of ROS, and subsequently, photoinhibition (**Figure 1A**). At pH 10.0, total inorganic carbon and bicarbonate are somewhat higher compared to pH 7.5 (Price, 2011): hence the growth of some PS II mutants at pH 10.0 might also partially be a result of carbon fixation increasing the sink for electrons from PS II.

CONCLUSION

A number of pH-sensitive *Synechocystis* 6803 PS II extrinsic protein mutants demonstrate that changes in environmental pH affect the function of the OEC and lumen-exposed PS II proteins. This is despite the presence of pH homeostasis mechanisms that buffer cytosolic pH and thylakoid lumen pH in cyanobacterial cells. Growth of these mutants at pH 10.0 appears to result in decreased ROS production, or increased oxidative stress responses; accordingly, light dosage appears to enhance the deleterious effects of pH 7.5 on oxygen evolution. Therefore, testing growth in pH 7.5 conditions is a useful investigative tool to reveal the relative stringency for different PS II proteins or protein regions; pH 10.0 conditions, in contrast, can be used to rescue some partially obligate photoheterotrophs carrying PS II mutations. The effects of environmental pH on PS II may arise through its impact on the requirement for substrate/product channels to and from the OEC that are dependent upon the

extrinsic proteins. The environmental pH may also influence the extent of any destabilizing effect on PS II assembly that results from the absence or mutation of the PS II extrinsic proteins or lumenal regions of the transmembrane subunits. Increasing demand for NADPH, and hence photosynthetic electron transport, by elevated Rubisco activity might be a sink for excess energy captured by PS II with impaired function, thus allowing the recovery of some pH-sensitive strains by excess CO_2. Understanding the causes of pH-sensitivity in such mutants may well elucidate the physiological mechanisms for maintaining an appropriate chemical environment for the shuttling of water, protons and oxygen to and from the Mn_4CaO_5 catalytic center.

AUTHOR CONTRIBUTIONS

JM wrote the first draft of the manuscript and all authors contributed to completing the manuscript.

ACKNOWLEDGMENTS

The authors are supported by funding from the University of Otago to the laboratories of TS and JE-R; JM is a recipient of the University of Otago Senior Smeaton Scholarship in Experimental Science.

REFERENCES

Balint, I., Bhattacharya, J., Perelman, A., Schatz, D., Moskovitz, Y., Keren, N., et al. (2006). Inactivation of the extrinsic subunit of Photosystem II, PsbU, in *Synechococcus* PCC 7942 results in elevated resistance to oxidative stress. *FEBS Lett.* 580, 2117–2122. doi: 10.1016/j.febslet.2006.03.020/epdf

Battchikova, N., Eisenhut, M., and Aro, E.-M. (2011). Cyanobacterial NDH-1 complexes: novel insights and remaining puzzles. *Biochim. Biophys. Acta* 1807, 935–944. doi: 10.1016/j.bbabio.2010.10.017

Belkin, S., Mehlhorn, R. J., and Packer, L. (1987). Proton gradients in intact cyanobacteria. *Plant Physiol.* 84, 25–30. doi: 10.1104/pp.84.1.25

Belkin, S., and Packer, L. (1988). Determination of pH gradients in intact cyanobacteria by electron spin resonance spectroscopy. *Methods Enzymol.* 167, 677–685. doi: 10.1016/0076-6879(88)67078-9

Berry, S., Fischer, J. H., Kruip, J., Hauser, M., and Wildner, G. F. (2005). Monitoring cytosolic pH of carboxysome-deficient cells of *Synechocystis* sp. PCC 6803 using fluorescence analysis. *Plant Biol.* 7, 342–347. doi: 10.1055/s-2005-837710

Bricker, T. M., Mummadisetti, M. P., and Frankel, L. K. (2015). Recent advances in the use of mass spectrometry to examine structure/function relationships in Photosystem II. *J. Photochem. Photobiol. B Biol.* 152, 227–246. doi: 10.1016/j.jphotobiol.2015.08.031

Bricker, T. M., Roose, J. L., Fagerlund, R. D., Frankel, L. K., and Eaton-Rye, J. J. (2012). The extrinsic proteins of Photosystem II. *Biochim. Biophys. Acta* 1817, 121–142. doi: 10.1016/j.bbabio.2011.07.006

Burnap, R. L., and Sherman, L. A. (1991). Deletion mutagenesis in *Synechocystis* sp. PCC 6803 indicates that the Mn-stabilizing protein of Photosystem II is not essential for oxygen evolution. *Biochemistry* 30, 440–446. doi: 10.1021/bi00216a020

Clarke, S. M., and Eaton-Rye, J. J. (1999). Mutation of Phe-363 in the Photosystem II protein CP47 impairs photoautotrophic growth, alters the chloride requirement, and prevents photosynthesis in the absence of either PSII-O or PSII-V in *Synechocystis* sp. PCC 6803. *Biochemistry* 38, 2707–2715. doi: 10.1021/bi981981j

Commet, A., Boswell, N., Yocum, C. F., and Popelka, H. (2012). pH optimum of the Photosystem II H_2O oxidation reaction: effects of PsbO, the manganese-stabilizing protein, Cl^- retention, and deprotonation of a component required for O_2 evolution activity. *Biochemistry* 51, 3808–3818. doi: 10.1021/bi201678m

Cormann, K. U., Bartsch, M., Rögner, M., and Nowaczyk, M. M. (2014). Localization of the CyanoP binding site on Photosystem II by surface plasmon resonance spectroscopy. *Front. Plant Sci.* 5:595. doi: 10.3389/fpls.2014.00595

Dasgupta, J., Ananyev, G. M., and Dismukes, G. C. (2008). Photoassembly of the water-oxidizing complex in Photosystem II. *Coord. Chem. Rev.* 252, 347–360. doi: 10.1016/j.ccr.2007.08.022

DeLano, W. L. (2002). *The PyMOL Molecular Graphics System*. San Carlos, CA: DeLano Scientific.

Eaton-Rye, J. J., Shand, J. A., and Nicoll, W. S. (2003). pH-dependent photoautotrophic growth of specific Photosystem II mutants lacking lumenal extrinsic polypeptides in *Synechocystis* PCC 6803. *FEBS Lett.* 543, 148–153. doi: 10.1016/s0014-5793(03)00432-0

Ferreira, K. N., Iverson, T. M., Maghlaoui, K., Barber, J., and Iwata, S. (2004). Architecture of the photosynthetic oxygen-evolving complex. *Science* 303, 1831–1838. doi: 10.1126/science.1093087

Heinz, S., Liauw, P., Nickelsen, J., and Nowaczyk, M. (2016). Analysis of Photosystem II biogenesis in cyanobacteria. *Biochim. Biophys. Acta* 1857, 272–287. doi: 10.1016/j.bbabio.2015.11.007

Hillier, W., and Wydrzynski, T. (1993). Increases in peroxide formation by the Photosystem II oxygen evolving reactions upon removal of the extrinsic 16, 22 and 33 kDa proteins are reversed by $CaCl_2$ addition. *Photosynth. Res.* 38, 417–423. doi: 10.1007/BF00046769

Ifuku, K. (2015). Localization and functional characterization of the extrinsic subunits of Photosystem II: an update. *Biosci. Biotechnol. Biochem.* 8451, 1–9. doi: 10.1080/09168451.2015.1031078

Ifuku, K., and Noguchi, T. (2016). Structural coupling of extrinsic proteins with the oxygen-evolving center in Photosystem II. *Front. Plant Sci.* 7:84. doi: 10.3389/fpls.2016.00084

Jackson, S. A., and Eaton-Rye, J. J. (2015). Characterization of a *Synechocystis* sp. PCC 6803 double mutant lacking the CyanoP and Ycf48 proteins of Photosystem II. *Photosynth. Res.* 124, 217–229. doi: 10.1007/s11120-015-0122-0

Jiang, H.-B., Cheng, H.-M., Gao, K.-S., and Qiu, B.-S. (2013). Inactivation of Ca^{2+}/H^+ exchanger in *Synechocystis* sp. strain PCC 6803 promotes cyanobacterial calcification by upregulating CO_2-concentrating mechanisms. *Appl. Environ. Microbiol.* 79, 4048–4055. doi: 10.1128/AEM.00681-13

Kallas, T. (2012). "Cytochrome b_6f complex at the heart of energy transduction and redox signaling," in *Photosynthesis: Plastid Biology, Energy Conversion, and Carbon Assimilation*, eds J. J. Eaton-Rye, B. C. Tripathy, and T. D. Sharkey (Dordrecht: Springer), 501–560. doi: 10.1007/978-94-007-1579-0_21

Kallas, T., and Castenholz, R. W. (1982). Internal pH and ATP-ADP pools in the cyanobacterium *Synechococcus* sp. during exposure to growth-inhibiting low pH. *J. Bacteriol.* 149, 229–236.

Kramer, D. M., Sacksteder, C. A., and Cruz, J. A. (1999). How acidic is the lumen? *Photosynth. Res.* 60, 151–163. doi: 10.1023/A:1006212014787

Krulwich, T. A., Sachs, G., and Padan, E. (2011). Molecular aspects of bacterial pH sensing and homeostasis. *Nat. Rev. Microbiol.* 9, 330–343. doi: 10.1038/nrmicro2549

Kupriyanova, E. V., Sinetova, M. A., Cho, S. M., Park, Y. I., Los, D. A., and Pronina, N. A. (2013). CO_2-concentrating mechanism in cyanobacterial photosynthesis: organization, physiological role, and evolutionary origin. *Photosynth. Res.* 117, 133–146. doi: 10.1007/s11120-013-9860-z

Kurian, D., Phadwal, K., and Mäenpää, P. (2006). Proteomic characterization of acid stress response in *Synechocystis* sp. PCC 6803. *Proteomics* 6, 3614–3624. doi: 10.1002/pmic.200600033

Li, Y., Rao, N., Yang, F., Zhang, Y., Yang, Y., Liu, H., et al. (2014). Biocomputional construction of a gene network under acid stress in *Synechocystis* sp. PCC 6803. *Res. Microbiol.* 165, 420–428. doi: 10.1016/j.resmic.2014.04.004

Linke, K., and Ho, F. M. (2014). Water in Photosystem II: structural, functional and mechanistic considerations. *Biochim. Biophys. Acta* 1837, 14–32. doi: 10.1016/j.bbabio.2013.08.003

Liu, H., Zhang, H., Weisz, D. A., Vidavsky, I., Gross, M. L., and Pakrasi, H. B. (2014). MS-based cross-linking analysis reveals the location of the PsbQ protein in cyanobacterial Photosystem II. *Proc. Natl. Acad. Sci. U.S.A.* 111, 4638–4643. doi: 10.1073/pnas.1323063111

Lorch, S., Capponi, S., Pieront, F., and Bondar, A.-N. (2015). Dynamic carboxylate/water networks on the surface of the PsbO subunit of Photosystem II. *J. Phys. Chem. B* 119, 12172–12181. doi: 10.1021/acs.jpcb.5b06594

Matsuhashi, A., Tahara, H., Ito, Y., Uchiyama, J., Ogawa, S., and Ohta, H. (2015). Slr2019, lipid A transporter homolog, is essential for acidic tolerance in *Synechocystis* sp. PCC 6803. *Photosynth. Res.* 125, 267–277. doi: 10.1007/s11120-015-0129-6

Morgan, T. R., Shand, J. A., Clarke, S. M., and Eaton-Rye, J. J. (1998). Specific requirements for cytochrome *c*-550 and the manganese-stabilizing protein in photoautotrophic strains of *Synechocystis* sp. PCC 6803 with mutations in the domain Gly-351 to Thr-436 of the chlorophyll-binding protein CP47. *Biochemistry* 37, 14437–14449. doi: 10.1021/bi980404s

Morris, J. N., Crawford, T. S., Jeffs, A., Stockwell, P. A., Eaton-Rye, J. J., and Summerfield, T. C. (2014). Whole genome re-sequencing of two "wild-type" strains of the model cyanobacterium *Synechocystis* sp. PCC 6803. *New Zeal. J. Bot.* 52, 36–47. doi: 10.1080/0028825x.2013.846267

Murata, N., Takahashi, S., Nishiyama, Y., and Allakhverdiev, S. I. (2007). Photoinhibition of Photosystem II under environmental stress. *Biochim. Biophys. Acta* 1767, 414–421. doi: 10.1016/j.bbabio.2006.11.019

Najafpour, M. M., Renger, G., Moghaddam, A. N., Aro, E.-M., Carpentier, R., Nishihara, H., et al. (2016). Manganese compounds as water-oxidizing catalysts: from the natural water-oxidizing complex to nanosized manganese oxide structures. *Chem. Rev.* 116, 2886–2936. doi: 10.1021/acs.chemrev.5b00340

Nickelsen, J., and Rengstl, B. (2013). Photosystem II assembly: from cyanobacteria to plants. *Annu. Rev. Plant Biol.* 64, 609–635. doi: 10.1146/annurev-arplant-050312-120124

Nixon, P. J., Michoux, F., Yu, J., Boehm, M., and Komenda, J. (2010). Recent advances in understanding the assembly and repair of Photosystem II. *Ann. Bot.* 106, 1–16. doi: 10.1093/aob/mcq059

Ohta, H., Shibata, Y., Haseyama, Y., Yoshino, Y., Suzuki, T., Kagasawa, T., et al. (2005). Identification of genes expressed in response to acid stress in *Synechocystis* sp. PCC 6803 using DNA microarrays. *Photosynth. Res.* 84, 225–230. doi: 10.1007/s11120-004-7761-x

Price, G. D. (2011). Inorganic carbon transporters of the cyanobacterial CO_2 concentrating mechanism. *Photosynth. Res.* 109, 47–57. doi: 10.1007/s11120-010-9608-y

Rast, A., Heinz, S., and Nickelsen, J. (2015). Biogenesis of thylakoid membranes. *Biochim. Biophys. Acta* 1847, 821–830. doi: 10.1016/j.bbabio.2015.01.007

Roose, J. L., Frankel, L. K., Mummadisetti, M. P., and Bricker, T. M. (2016). The extrinsic proteins of Photosystem II: update. *Planta* 243, 889–908. doi: 10.1007/s00425-015-2462-6

Saito, K., Rutherford, A. W., and Ishikita, H. (2013). Mechanism of tyrosine D oxidation in Photosystem II. *Proc. Natl. Acad. Sci. U.S.A.* 110, 7690–7695. doi: 10.1073/pnas.1300817110

Shen, J.-R. (2015). The structure of Photosystem II and the mechanism of water oxidation in photosynthesis. *Annu. Rev. Plant Biol.* 66, 23–48. doi: 10.1146/annurev-arplant-050312-120129

Shen, J.-R., Burnap, R. L., and Inoue, Y. (1995). An independent role of cytochrome *c*-550 in cyanobacterial Photosystem II as revealed by double-deletion mutagenesis of the *psbO* and *psbV* genes in *Synechocystis* sp. PCC 6803. *Biochemistry* 34, 12661–12668. doi: 10.1021/bi00039a023

Shen, J.-R., Qian, M., Inoue, Y., and Burnap, R. L. (1998). Functional characterization of *Synechocystis* sp. PCC 6803 Δ*psbU* and Δ*psbV* mutants reveals important roles of cytochrome *c*-550 in cyanobacterial oxygen evolution. *Biochemistry* 37, 1551–1558. doi: 10.1021/bi971676i

Suga, M., Akita, F., Hirata, K., Ueno, G., Murakami, H., Nakajima, Y., et al. (2015). Native structure of Photosystem II at 1.95 Å resolution viewed by femtosecond X-ray pulses. *Nature* 517, 99–103. doi: 10.1038/nature13991

Summerfield, T. C., Crawford, T. S., Young, R. D., Chua, J. P., Macdonald, R. L., Sherman, L. A., et al. (2013). Environmental pH affects photoautotrophic growth of *Synechocystis* sp. PCC 6803 strains carrying mutations in the lumenal proteins of PSII. *Plant Cell Physiol.* 54, 859–874. doi: 10.1093/pcp/pct036

Summerfield, T. C., Eaton-Rye, J. J., and Sherman, L. A. (2007). Global gene expression of a ΔPsbOΔPsbU mutant and a spontaneous revertant in the cyanobacterium *Synechocystis* sp. strain PCC 6803. *Photosynth. Res.* 94, 265–274. doi: 10.1007/s11120-007-9237-2

Summerfield, T. C., Shand, J. A., Bentley, F. K., and Eaton-Rye, J. J. (2005a). PsbQ (Sll1638) in *Synechocystis* sp. PCC 6803 is required for Photosystem II activity in specific mutants and in nutrient-limiting conditions. *Biochemistry* 44, 805–814. doi: 10.1021/bi048394k

Summerfield, T. C., and Sherman, L. A. (2008). Global transcriptional response of the alkali-tolerant cyanobacterium *Synechocystis* sp. strain PCC 6803 to a pH 10 environment. *Appl. Environ. Microbiol.* 74, 5276–5284. doi: 10.1128/AEM.00883-08

Summerfield, T. C., Winter, R. T., and Eaton-Rye, J. J. (2005b). Investigation of a requirement for the PsbP-like protein in *Synechocystis* sp. PCC 6803. *Photosynth. Res.* 84, 263–268. doi: 10.1007/s11120-004-6431-3

Takahashi, S., and Murata, N. (2005). Interruption of the Calvin cycle inhibits the repair of Photosystem II from photodamage. *Biochim. Biophys. Acta* 1708, 352–361. doi: 10.1016/j.bbabio.2005.04.003

Takahashi, S., and Murata, N. (2008). How do environmental stresses accelerate photoinhibition? *Trends Plant Sci.* 13, 178–182. doi: 10.1016/j.tplants.2008.01.005

Thornton, L. E., Ohkawa, H., Roose, J. L., Kashino, Y., Keren, N., and Pakrasi, H. B. (2004). Homologs of plant PsbP and PsbQ proteins are necessary for regulation of Photosystem II activity in the cyanobacterium *Synechocystis* 6803. *Plant Cell* 16, 2164–2175. doi: 10.1105/tpc.104.023515

Touloupakis, E., Cicchi, B., Benavides, A. M. S., and Torzillo, G. (2016). Effect of high pH on growth of *Synechocystis* sp. PCC 6803 cultures and their contamination by golden algae (*Poterioochromonas* sp.). *Appl. Microbiol. Biotechnol.* 100, 1333–1341. doi: 10.1007/s00253-015-7024-0

Uchiyama, J., Kanesaki, Y., Iwata, N., Asakura, R., Funamizu, K., Tasaki, R., et al. (2015). Genomic analysis of parallel-evolved cyanobacterium *Synechocystis* sp. PCC 6803 under acid stress. *Photosynth. Res.* 125, 243–254. doi: 10.1007/s11120-015-0111-3

Umena, Y., Kawakami, K., Shen, J. R., and Kamiya, N. (2011). Crystal structure of oxygen-evolving Photosystem II at a resolution of 1.9 Å. *Nature* 473, 55–60. doi: 10.1038/nature09913

Van de Meene, A. M. L., Sharp, W. P., McDaniel, J. M., Friedrich, H., Vermaas, W., and Roberson, R. W. (2012). Gross morphological changes in thylakoid membrane structure are associated with Photosystem I deletion in *Synechocystis* sp. PCC6803. *Biochim. Biophys. Acta* 1818, 1427–1434. doi: 10.1016/j.bbamem.2012.01.019

Vass, I. (2012). Molecular mechanisms of photodamage in the Photosystem II complex. *Biochim. Biophys. Acta* 1817, 209–217. doi: 10.1016/j.bbabio.2011.04.014

Vinyard, D. J., Ananyev, G. M., and Dismukes, C. G. (2013). Photosystem II: the reaction center of oxygenic photosynthesis. *Annu. Rev. Biochem.* 82, 577–606. doi: 10.1146/annurev-biochem-070511-100425

Vogt, L., Vinyard, D. J., Khan, S., and Brudvig, G. W. (2015). Oxygen-evolving complex of Photosystem II: an analysis of second-shell residues and hydrogen-bonding networks. *Curr. Opin. Chem. Biol.* 25C, 152–158. doi: 10.1016/j.cbpa.2014.12.040

Zhang, L.-F., Yang, H.-M., Cui, S.-X., Hu, J., Wang, J., Kuang, T.-Y., et al. (2009). Proteomic analysis of plasma membranes of cyanobacterium *Synechocystis* sp. strain PCC 6803 in response to high pH stress. *J. Proteome Res.* 8, 2892–2902. doi: 10.1021/pr900024w

Conflict of Interest Statement: The authors declare that the research was conducted in the absence of any commercial or financial relationships that could be construed as a potential conflict of interest.

frontiers in Plant Science

ORIGINAL RESEARCH
published: 17 February 2016
doi: 10.3389/fpls.2016.00105

Effect of Light Acclimation on the Organization of Photosystem II Super- and Sub-Complexes in *Arabidopsis thaliana*

*Ludwik W. Bielczynski, Gert Schansker and Roberta Croce**

Biophysics of Photosynthesis/Energy, Faculty of Sciences, Department of Physics and Astronomy, VU University Amsterdam, Amsterdam, Netherlands

To survive under highly variable environmental conditions, higher plants have acquired a large variety of acclimation responses. Different strategies are used to cope with changes in light intensity with the common goal of modulating the functional antenna size of Photosystem II (PSII). Here we use a combination of biochemical and biophysical methods to study these changes in response to acclimation to high light (HL). After 2 h of exposure, a decrease in the amount of the large PSII supercomplexes is observed indicating that plants are already acclimating to HL at this stage. It is also shown that in HL the relative amount of antenna proteins decreases but this decrease is far less than the observed decrease of the functional antenna size, suggesting that part of the antenna present in the membranes in HL does not transfer energy efficiently to the reaction center. Finally, we observed LHCII monomers in all conditions. As the solubilization conditions used do not lead to monomerization of purified LHCII trimers, we should conclude that a population of LHCII monomers exists in the membrane. The relative amount of LHCII monomers strongly increases in plants acclimated to HL, while no changes in the trimer to monomer ratio are observed upon short exposure to stress.

Keywords: ***Arabidopsis thaliana*, light intensity acclimation, BN-PAGE, 2D-PAGE, PSII**

OPEN ACCESS

Edited by:
Julian Eaton-Rye, University of Otago, New Zealand

Reviewed by:
Alexander Ruban, Queen Mary University of London, UK
Gyozo Garab, Biological Research Center, Hungary

****Correspondence:***
Roberta Croce
r.croce@vu.nl

Specialty section:
This article was submitted to Plant Cell Biology, a section of the journal Frontiers in Plant Science

Received: *11 December 2015*
Accepted: *20 January 2016*
Published: *17 February 2016*

Citation:
Bielczynski LW, Schansker G and Croce R (2016) Effect of Light Acclimation on the Organization of Photosystem II Super- and Sub-Complexes in Arabidopsis thaliana. Front. Plant Sci. 7:105. doi: 10.3389/fpls.2016.00105

INTRODUCTION

Land plants appeared on Earth around 568–815 million years ago (Clarke et al., 2011). On an evolutionary time scale, this is enough time to evolve highly sophisticated acclimation responses to allow survival as a sessile organism under variable environmental conditions. As photoautotrophs, the acclimation responses to different light conditions are essential adaptations. They provide balance between the harvesting of enough energy for metabolic and anabolic processes and the protection against excess excitation energy (EEE). EEE represents a risk associated with the light-harvesting systems as it increases the probability of reactive oxygen species (ROS) generation, which can be highly destructive for the photosynthetic apparatus and the cell (reviewed in Asada, 2006).

As light interception occurs in the chloroplast, it is there that the first steps and coordination of the light intensity acclimation take place. From all the complexes involved in the light phase of photosynthesis, Photosystem II (PSII) is the major target of acclimation. Its composition, functionality and amount are dynamically adjusted in response to changes in light conditions (Ballottari et al., 2007; Betterle et al., 2009; Johnson et al., 2011; Belgio et al., 2014; Kono and Terashima, 2014; Dietz, 2015; Suorsa et al., 2015).

Upon exposure to HL, short term responses are activated in a range from seconds to minutes. This time is only sufficient for rearrangement of the chloroplast components, without an influence of biosynthesis or degradation. Protonation and phosphorylation of different components (Allen, 1992; Fristedt and Vener, 2011; Wientjes et al., 2013a,b; Pietrzykowska et al., 2014) trigger the processes known as non-photochemical quenching (NPQ; Ruban et al., 2012) and state transitions (Tikkanen and Aro, 2012).

Long-term acclimation occurs in a range from hours to weeks and involves selective synthesis and degradation of chloroplast components. It also involves phosphorylation of some of the components (Fristedt and Vener, 2011). As a consequence of PSII antenna size adjustments, the chlorophyll (Chl) *a*/*b* ratio decreases in increasing light intensities (Park et al., 1997; Ballottari et al., 2007; Wientjes et al., 2013c) and the density of PSII supercomplexes in the thylakoid membrane is modified (Kouřil et al., 2013).

The current model of PSII comes from the crystal structure of PSII from the cyanobacterium *Thermosynechococcus vulcanus* (Umena et al., 2011). In combination with other methods, up to 40 protein subunits that compose PSII were identified (reviewed Shi et al., 2012). More than half have a molecular mass below 15 kDa and are expressed under specific environmental conditions (Plöscher et al., 2009). The reaction center (RC) complex is a heterodimer composed of the products of the genes PsbA (D1) and PsbD (D2), binding in total six Chl *a* and two pheophytins (Umena et al., 2011). Associated to the RC are the internal antennae CP47 (PsbB) and CP43 (PsbC) binding 16 and 13 Chl *a,* respectively, and a number of small subunits (Shi et al., 2012). In higher plants this complex is called the PSII core (C).

In plants the core is supplemented with an outer antenna system, composed of Chl *a*/*b* binding proteins known as light-harvesting complexes (LHC), forming supercomplexes (Dekker and Boekema, 2005). PSII supercomplexes exist in different configurations, containing a variable number of LHCIIs (heterotrimers of Lhcb1-3) and minor antennae (Caffarri et al., 2009). LHCII has two possible docking sites on the core, where it can bind with different affinities: strongly (S) through CP43 and CP26 (Lhcb5), and with moderate affinity (M) on the CP47 side through CP24 (Lhcb6) and CP29 (Lhcb4). Most of the PSII complexes are in dimeric form (C_2) and can bind several LHCIIs, forming C_2S, C_2M, C_2S_2, C_2SM, C_2S_2M, and $C_2S_2M_2$ supercomplexes. In addition two complexes containing monomeric core were observed: the naked core (C) and the core with a strongly bound LHCII (CS).

Photosystem II heterogeneity is partially a result of the repair cycle of the D1 protein (Aro et al., 2005). Photodamage of PSII due to radicals and oxygen species formation is an intrinsic property of PSII. As a consequence, plants constantly replace PSII in the light. The process is multiphasic involving (i) phosphorylation of different subunits, (ii) monomerization and migration to the stroma lamellae, (iii) partial disassembly of PSII core, (iv) proteolysis of damaged proteins, (v) replacement of the damaged D1 protein, and (vi) reassembly, dimerization and photoactivation of PSII.

Besides the structural and functional heterogeneity due to the balance between photoinhibition and repair cycle, the PSII supercomplexes are rearranged during light acclimation (Ballottari et al., 2007; Kouřil et al., 2013). The adjustment is achieved through regulation of the expression levels of Lhcb1-3 and Lhcb6 proteins. In plants, most of the PSII supercomplexes are randomly distributed surrounded by an extra pool of LHCII loosely associated with them (called "extra" LHCII). In HL the decrease in the antenna size mainly affects the size of this extra LHCII pool (Wientjes et al., 2013c) leading to a denser PSII packing (Kouřil et al., 2013). The PSII supercomplexes in some parts of the grana are also organized in semicrystaline arrays. The most common semicrystaline structure under all light conditions is composed of $C_2S_2M_2$ supercomplexes. However, in the thylakoids from HL acclimated plants, due to the decrease of M trimers, some C_2S_2 semi-crystalline structures were also observed (Kouřil et al., 2013).

Upon a short light stress treatment, plants switch on a series of mechanisms known as NPQ. The main NPQ component (qE) reflects a process by which EEE is dissipated as heat. The process is triggered by low lumenal pH that activates the PsbS protein (Li et al., 2000) and the xanthophyll cycle (Demmig-Adams et al., 1990; reviewed in Jahns and Holzwarth, 2012). It was suggested that the pH dependent NPQ is induced by allosteric conformational changes and aggregation of peripheral LHCII (Horton and Ruban, 2005; Horton et al., 2008). Changes in the PSII antenna size were also suggested based on biochemical (Betterle et al., 2009), and functional (Holzwarth et al., 2009) data and supported by structural evidence (Johnson et al., 2011). However, more recently it was proposed that the effective antenna size of PSII is even increasing during NPQ (Belgio et al., 2014).

In this work, we have studied the structural changes of PSII during short HL stress and long-term acclimation to different light intensities by combining quantitative biochemical analysis with functional measurements performed on the same plants. This has allowed us to get a more complete picture of the effect of light acclimation on the composition and functional organization of the photosynthetic complexes.

MATERIALS AND METHODS

Plant Material

Arabidopsis thaliana (ecotype Col-0) WT seeds were sown on Murashige and Skoog (MS) medium agar plates. After 5–7 days the seedlings were transplanted to final pots. Plants were grown for 7 weeks in growth chambers (AR-36L, Plant Climatics Percival) at 70% RH, 21°C, a photoperiod of 8/16 h (day/night) and under 200 or 600 μmol photons*m^{-2*}s^{-1}. After 3 weeks, a batch of plants grown under 200 μmol photons*m^{-2*}s^{-1} was transferred and grown for an additional 3 weeks at 1800 μmol photons*m^{-2*}s^{-1} (FytoScope FS 3400, Photon Systems Instruments). For the short HL stress experiment the plants were grown as previously described under 200 μmol photons*m^{-2*}s^{-1} and then after 6 weeks of growth, transferred for 0.5, 2 and 6 h to 1800 μmol photons*m^{-2*}s^{-1}. Plants

illuminated with growth light (200 μmol photons*m^{-2}*s^{-1}) for 6 h were used as a control.

Thylakoid Isolation

If not stated otherwise the plants were harvested after a night in darkness. The plants from short-term HL stress were harvested and immediately transferred to an ice bath, where they stayed until thylakoid isolation. The isolation procedure was described in Robinson et al. (1980), and modified according to Caffarri et al. (2009). Isolated thylakoid membranes were resuspended in the storage buffer (20 mM HEPES, pH 7.5, 0.4 M sorbitol, 15 mM NaCl and 5 mM $MgCl_2$). The samples were rapidly frozen in liquid nitrogen and stored at −80°C.

Pigment Isolation

The amount of chlorophylls on a leaf fresh weight basis, Chl *a*/*b* ratio and chlorophyll/carotenoid (Chl/Car) ratio were determined from absorption spectra of 80% acetone extracts measured with a Carry 4000 spectrophotometer (Varian). The absorption spectra were fitted with the spectra of individual pigments in the same solvent, as described in Croce et al. (2002). The quantification of different carotenoids was performed by HPLC using a System Gold 126 Solvent module and 168 Detector (Beckman Coulter) as described by Gilmore and Yamamoto (1991) with the modification reported in Xu et al. (2015).

2D-PAGE Analysis

For thylakoid membrane complex quantification a BN-PAGE was performed in a gel (4% stacking and 4–12.5% resolving gel) polymerized from a bisacrylamide/acrylamide mixture with a ratio of 32:1 (Järvi et al., 2011). The gels were cast from the bottom, in batch to decrease the mixing of the top layer using a Mini-PROTEAN 3 Multi-Casting Chamber (Bio-Rad). To prevent the mixing of butanol (used to get a straight gel top) with the top layers of the resolving gel the glycerol gradient in the gel was modified from 0–20% to 5–20% and a cushion of water was put on the top before casting. The gels were left overnight at room temperature (RT) to assure good polymerization of the low-acrylamide concentration layers. Before loading, an aliquot corresponding to 8 μg of Chl was taken from each sample, resuspended in 25BTH20G buffer [25 mM BisTris/HCl (pH 7.0), 20% (w/v) glycerol] to a final Chl concentration of 0.5 mg/ml and to a selected final n-dodecyl α-D-maltopyranoside (α-DDM) concentration. Second dimensions were performed in a Tricine-SDS PAGE system (Schägger, 2006). Gels after 2D were stained with the Serva Blue G Coomassie stain (SERVA Electrophoresis), subsequently, the gels were digitized with ImageQuant LAS4000 (GE, Healthcare). The data were preprocessed in ImageJ and analyzed with an R-project homemade script based on the workflow from Natale et al. (2011) with the modifications described in the section "Results." The statistical analysis was performed using R-project and all the graphs were plotted using the ggplot2 package. After Coomassie staining the gels showed a fluctuating background drift, which necessitated a broad region of interest (ROI) selection and a constant background exclusion based on a threshold from local minima (see **Figure 2C**). To adjust for the variation in the staining/destaining and digitization steps during the gel processing (if not mentioned otherwise), a second normalization to total protein content (sum of the Integrated Optical Densities, IODs of all measured ROIs in a gel) was applied.

Sucrose Gradients

Sucrose gradients were prepared according to Caffarri et al. (2009). Before loading on the sucrose gradient, thylakoid samples corresponding to 500 μg of Chl were solubilized in a final concentration of 0.6% α-DDM.

Functional Antenna Size of PSII

To estimate the functional antenna size the measuring protocol was adapted from Dinç et al. (2012). The fluorescence induction curves (OJIPs) were measured with HandyPea (Hansatech) on dark acclimated (>1 h) intact leaves. A 1 s pulse of red light (650 nm) was given in the intensity range of 200–3500 μmol photons*m^{-2}*s^{-1} (200, 300, 450, 600, 750, 900, 1200, 1500, 2000, 2500, 3000, and 3500 μmol photons*m^{-2}*s^{-1}). The leaf clips assured that the measurements for each light intensity were on the same spot of the first fully developed leaf, from 10 different plants. The dark acclimation periods between measurements of different light intensities were at least 10 min long. The fluorescence intensity is a function of the light intensity and to correct for this, measured fluorescence was normalized to the Photosynthetic Photon Flux Density (PPFD). Linear regression was performed to get the slope and the slope error of the in growth of the fluorescence intensity as a function of the light intensity at 300 μs.

RESULTS

Long-Term Acclimation

General Plant Characterization

To investigate the long-term light acclimation of *A. thaliana,* plants were grown under three different light intensities: 200 (GL200), 600 (GL600), and 1800 μmol photons*m^{-2}*s^{-1} (GL1800). As shown in **Figure 1A**, rosette and leaf morphology differed. Under GL200, plants had elongated petioles, the leaves were thin and had small oval leaf blades (Keller et al., 2011; Hersch et al., 2014). Under GL600, they grew faster, developed thicker leaves (Weston et al., 2000) with longer and broader leaf blades, and almost no petioles. Under GL1800, the rosettes were smaller, the older leaves brownish (Page et al., 2012), leathery thick, and the younger smaller, in larger number and concentrated around the central meristem.

The quenching analysis gives the possibility to observe time-related changes of energy partitioning between different pathways in PSII during light and dark acclimation (see **Figure 1B**). The parameter related with linear electron flow (LEF), Φ_{PSII}, was higher when the plants were grown under higher light intensities (see **Figure 1B**, Left panel). As for the NPQ (see **Figure 1B**, Right panel), in steady state, Φ_{NPQ} was lower in plants grown in higher light intensities, but during the fast NPQ induction phase the HL grown plants were reaching the maximum faster than the other plants. The maximum efficiency of PSII (F_V/F_M) was also

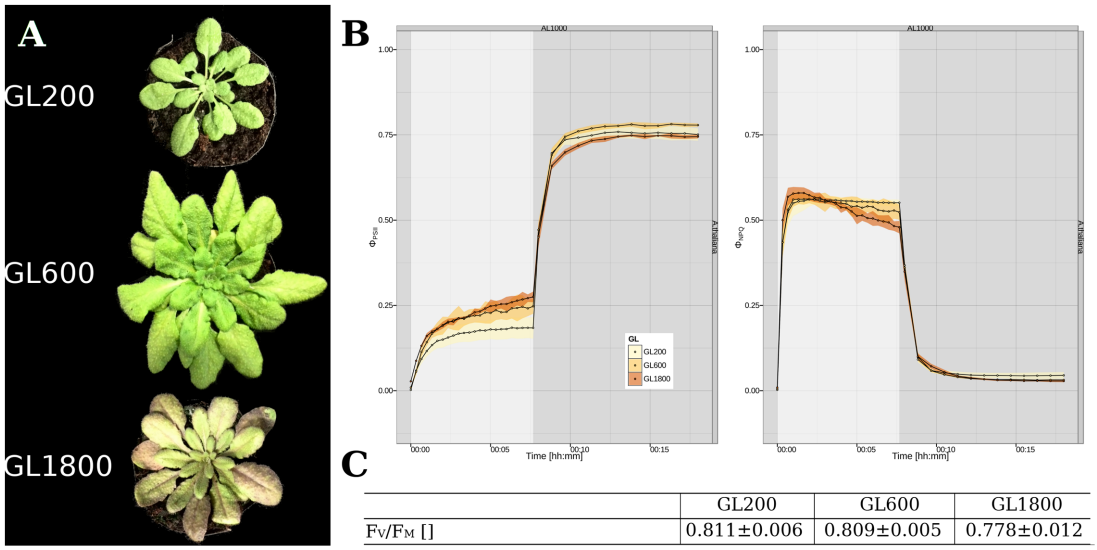

	GL200	GL600	GL1800
F_V/F_M []	0.811±0.006	0.809±0.005	0.778±0.012

FIGURE 1 | General characterization of plants long-term acclimated to different light intensities. (A) Visual appearance of the *Arabidopsis thaliana* plants grown under 200 (GL200), 600 (GL600), and 1800 μmol photons*m^{-2}*s^{-1} (GL1800). **(B)** Parameters from the quenching analysis related with the energy distribution in PSII, Φ_{PSII} (Left panel) and Φ_{NPQ} (Right panel) during an 8 min illumination with 1000 μmol photons*m^{-2}*s^{-1} and 10 min of darkness for plants grown under 200, 600, and 1800 μmol photons*m^{-2}*s^{-1}, respectively, as a yellow, orange and brown trace, ($n = 4$). The illumination and dark periods are marked, respectively, as gray and white background. **(C)** Dark fluorescence parameter F_V/F_M of plants grown at all three light intensities ($n = 4$).

dependent on the light conditions and especially in HL, showed a lower value (see **Figure 1C**).

All these data show that our plants have the characteristics of plants acclimated to different light intensities covering a large range of light acclimation responses between shade-avoidance (GL200) and high-light acclimation responses (GL1800), with an intermediate light intensity (GL600).

Pigment Analysis

To characterize the range of changes in pigment composition, pigment analysis was performed after a night of darkness (see **Table 1**). In plants grown under GL1800 the Chl content on a fresh leaf weight basis was almost half that under GL200. The Chl *a*/*b* ratio increased under higher light intensities, in agreement with a reduction of the antenna size (Andersson, 1996; Ballottari et al., 2007; Kouřil et al., 2013). The chlorophyll/carotenoid (Chl/Car) ratio decreased in plants grown at higher light intensities. As for the carotenoid composition, increased levels were observed for all of them under HL. In the thylakoids, Zeaxanthin (Zea) was observed in very small amounts in plants grown under GL200 and increased in plants grown at higher light intensities, indicating that Zea is not completely re-converted to violaxanthin in darkness.

Structural Antenna Size

To determine the composition of the thylakoid membranes, 2D-PAGE was performed. The isolated thylakoid membranes were solubilized with α-DDM (1% final concentration), a mild detergent that preserves the PSII supercomplexes (see **Figure 2A**). In the second dimension, the proteins of which these complexes are composed, were separated in a denaturing gel (Tricine-SDS PAGE; see **Figure 2B**) allowing a relative quantification of the proteins in each complex. To test and ensure the reproducibility of the results, three repetitions per condition were performed. A workflow from Natale et al. (2011) was adapted to perform a half-automated, qualitative and quantitative analysis of the most abundant thylakoid membrane proteins.

TABLE 1 | Pigment analysis of plants grown under different light conditions.

	GL200	GL600	GL1800
Chls/fresh weight [mg/g]	0.8621 ± 0.1156	0.7821 ± 0.0354	0.3893 ± 0.0986
Chl a/b	3.235 ± 0.022	3.249 ± 0.006	3.562 ± 0.047
Chl/Car	3.905 ± 0.024	3.698 ± 0.015	3.228 ± 0.054
Neo/100 Chls	3.424 ± 0.048	3.743 ± 0.031	4.004 ± 0.178
Vio/100 Chls	2.753 ± 0.033	3.035 ± 0.005	4.106 ± 0.183
Ant/100 Chls	0.196 ± 0.023	0.381 ± 0.010	0.621 ± 0.030
Lut/100 Chls	12.364 ± 0.0125	12.900 ± 0.041	13.981 ± 0.284
Zea/100 Chls	0.195 ± 0.005	0.296 ± 0.027	0.678 ± 0.018
β-Car/100 Chls	6.677 ± 0.017	6.688 ± 0.069	7.592 ± 0.176
Cars/100 Chls	25.609 ± 0.157	27.044 ± 0.108	30.98 ± 0.513
(Z + 0.5 × A)/(Z + A + V)	0.0932 ± 0.002	0.131 ± 0.007	0.183 ± 0.003

Total chlorophylls (Chls) were quantified by fitting the 80% acetone extracts from a leaf from five different plants (n = 5) grown under GL200, 600, and 1800 and normalized to the fresh weight. The chlorophyll a/b (Chl a/b) ratio and chlorophyll/carotenoid (Chl/Car) ratio was determined in the same way from isolated thylakoid membranes in three repetitions (n = 3). The same extracts were used for the quantification by HPLC of the carotenoids: neoxanthin (Neo), violaxanthin (Vio), anteraxanthin (Ant), zeaxanthin (Zea), lutein (Lut) and β-carotene (β-car). All carotenoids were calculated per 100 Chls.

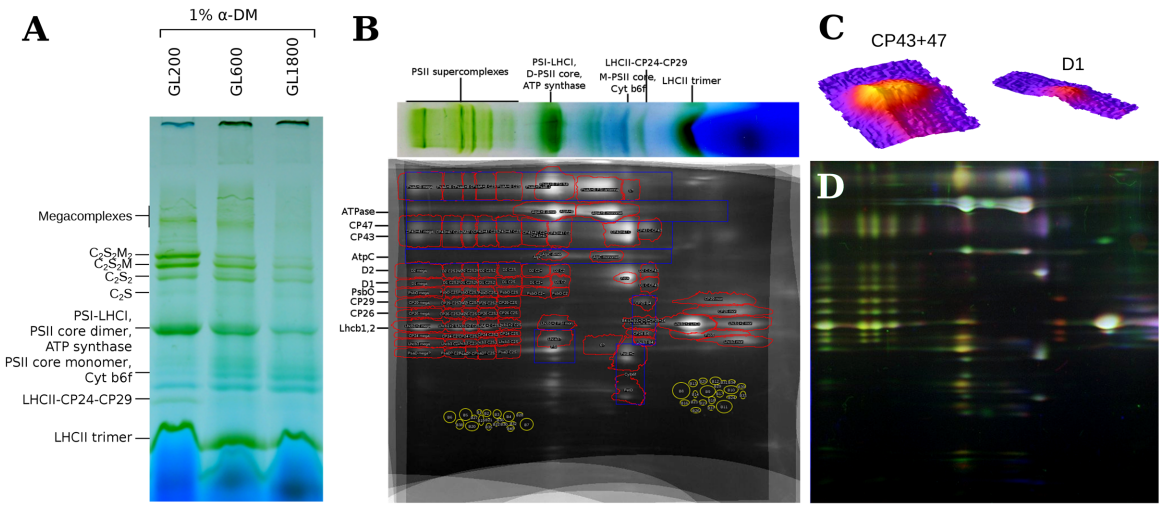

FIGURE 2 | 2D-PAGE of thylakoids isolated from plants grown under different light intensities. (A) The BN-PAGE of thylakoids isolated from plants grown under GL200, 600, and 1800, solubilized with 1% α-DDM. **(B)** Sum of nine 2D-PAGE gels of isolated thylakoids from plants grown under all light conditions. The red contours represent ROIs of selected proteins in specific complexes. The blue contours represent the integrated areas for quantification of a selected protein independent of the complex. On the top, a lane from the BN-PAGE is shown. **(C)** Overlap of the gels of thylakoids from plants grown under GL200, 600, and 1800, that are shown in the red, green, and blue channels, respectively. **(D)** 3D surface plots of CP43 + 47 and D1 megacomplex ROIs, respectively.

After the warping step, the alignment of the gels was accurate enough for a qualitative analysis (see **Figure 2D**). The dot patterns on the 2D-gel were the same for plants grown under all light conditions, which suggests that there are no qualitative differences in the protein composition of the most abundant thylakoid proteins. The identification of specific proteins on 2D-gels was performed based on previous work (Aro et al., 2005; Andaluz et al., 2006; Caffarri et al., 2009; Takabayashi et al., 2013).

To automate the quantification of proteins from the 2D-PAGE gels a ROI map (see **Figure 2B**) was created based on an averaged image of nine, warped 2D gels. For the quantification of the (super)complexes, multiple proteins representative of each complex were selected.

To determine if changes in the PSII antenna size occur, antenna proteins have to be quantified relative to a PSII core protein that is present in each PSII complex. Candidates were: D1, D2, CP43, and CP47. The dots on the gel of CP43 and CP47 were more pronounced than the dots of D1 and D2 (see **Figure 2C**). Since the small MW-difference of CP43 and CP47 led to an incomplete separation, the averaged IOD of the CP43 and CP47 dots was chosen (besides the C-CP43 fraction where only CP47 is present). This reference was shown to follow changes in D1 and D2 closely, under all light conditions (see **Figure 3A**), confirming that it accurately reflected the amount of PSII core. The small differences in stoichiometry between conditions and the quite pronounced standard deviation in **Figure 3** were due to the low signal from D1 and D2. Looking at the other components of the PSII core, we observed, for plants grown under higher light intensities, a decrease in the amount of PsbO per core, which could be due to the dissociation of PsbO during photoinactivation of PSII complexes (Hundal et al., 1990).

Antennae of PSII

The minor antennae CP24, CP26, and CP29 and Lhcb1,2 (major components of LHCII trimers) were quantified from the sum of the corresponding dots from all PSII complexes and normalized to the amount of the PSII core (see **Figure 3B**). Because of the sequence specific affinity of Coomassie for the proteins, a second normalization was performed using as reference the plants grown under GL200. When the plants grew under higher light intensities, the amount of CP24 decreased, whereas the amounts of CP26 and CP29 were maintained at a similar level, in agreement with previous results (Ballottari et al., 2007; Kouřil et al., 2013). Under GL1800, the amount of LHCII per PSII decreased to ∼80% of the value observed under GL200. Note that at GL200 the antenna size of *A. thaliana* is already reduced compared to the values observed when lower light intensities were used: 100 μmol photons*m^{-2*}s^{-1} in Ballottari et al. (2007) and Kouřil et al. (2013).

PSII Antenna Size Heterogeneity

Previous work has indicated that the differences in antenna size, observed upon light acclimation, lead to changes not only in the amount of "extra" LHCII but also in the relative amount of the PSII (super)complexes (Wientjes et al., 2013a). To quantify these changes we estimated the core protein distribution of PSII in PSII supercomplexes (megacomplexes, $C_2S_2M_2$, C_2S_2M, C_2S_2, C_2S, CS) and core complexes (core dimers, C_2; core monomers C; core monomers without CP43, C-CP43). The amount of CP43 and CP47 was normalized to the total amount of these proteins for each condition (see **Figure 4C**). When the plants were grown under GL200, PSII was observed mostly in the form of megacomplexes, C_2S_2M, C_2S_2 and core monomers. At higher light intensities, the fraction of large supercomplexes decreased

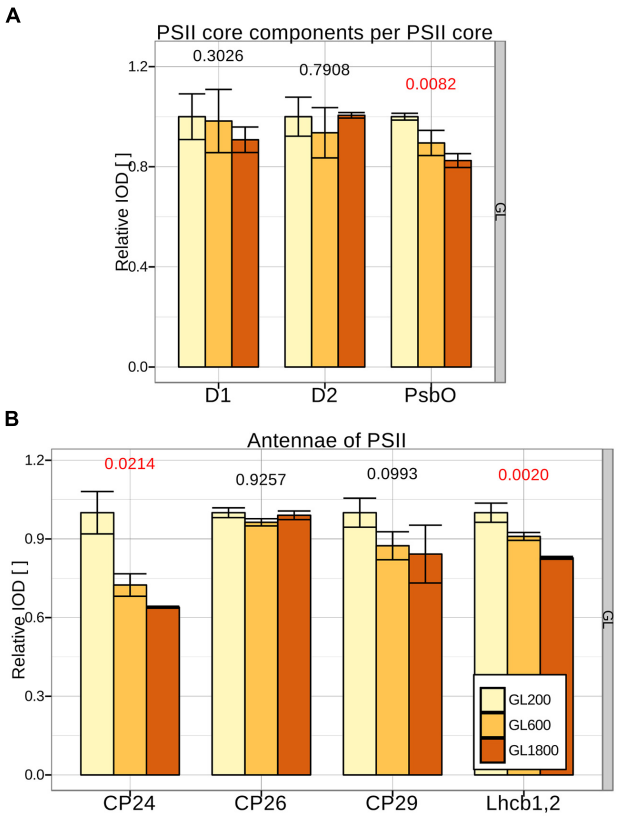

FIGURE 3 | Changes in the PSII composition during long-term acclimation to different light intensities. (A) The amount of PSII core proteins: D1, D2, and PsbO per CP43, 47 was quantified in isolated thylakoids from plants grown under GL200, 600, and 1800 (respectively, yellow, orange, and brown fill) separated during 2D-PAGE in three different repetitions ($n = 3$). **(B)** The amount of minor PSII antennae: CP24, CP26, CP29, and Lhcb1,2 per PSII core was quantified in isolated thylakoids from the same samples. Numbers below the bars are the *p*-values of ANOVA's *F*-test on a specific group. Red color signifies rejection of the null hypothesis that the response to all growth lights is the same ($\alpha < 0.05$), black its acceptance.

(from megacomplexes to C_2S_2M), while the amount of smaller complexes increased (C_2S, C, C-CP43).

A similar trend was observable when looking at Lhcb1,2 distributed between the different fractions (see **Figure 4A**). Under all conditions the trimeric fraction was the most abundant containing 35–45% of the LHCII pool. The monomeric fraction was, however, also large, representing approximately 20% of the LHCII population in GL200 and increasing to 35% in HL. The rest of LHCII was associated with the supercomplexes. During acclimation to higher light intensities, there was a relative decrease in the amount of Lhcb1,2 associated with the large PSII supercomplexes ($C_2S_2M_2$, C_2S_2M). Accumulation of core proteins did not correlate with the accumulation of LHCII trimers, but with the increase of Lhcb1,2 monomers.

To rule out the possibility of solubilization artifacts, the results were validated by performing the same 2D-PAGE analysis on thylakoids from the plants grown under GL200, solubilized with 0.6 and 1.5% of α-DDM (see **Figures 4B,D**). The results show that an almost threefold increase in detergent to protein ratio did not influence the core distribution of PSII (see **Figure 4D**). Similarly, in the case of the antenna, only the amount of LHCII-CP24-CP29 (B4) slightly decreased when using a high detergent concentration, while no changes were observed for the other complexes (see **Figure 4B**).

To further verify if the presence of LHCII monomers could be the result of solubilization (see **Figure 4E**), purified LHCII trimers were directly solubilized with different detergent concentrations and loaded on a BN-PAGE. No monomerization was observed under any of the solubilization conditions, confirming the high stability of the trimers to detergent treatment. It is interesting to observe that LHCII trimers loaded on the BN gel without the addition of detergent (**Figure 4E**, most right lane) form dimers, trimers, tetramers, and higher assemblies, indicating that complexes can aggregate in the gel, contrary to what was previously assumed (Ilioaia et al., 2008).

Functional Antenna Size of PSII

In the next step, we determined the changes in the functional antenna size (the antenna that is able to transfer the absorbed energy to the PSII Reaction Center, RC), by measuring the fluorescence rise, at different light intensities, on leaves (see **Figure 5A**). The slope of the normalized fluorescence at 300 μs vs. the light intensity (see **Figure 5B**) is proportional to the absorption cross-section of PSII and is then used to determine the functional antenna size of PSII (Dinç et al., 2012). The data show that in plants grown under GL600 and GL1800, the functional antenna size dropped to 73 and 59%, respectively, of the value of plants grown under GL200 (see **Figure 5C**).

The discrepancy between the functional and structural antenna size measurements may be caused by several factors. The protein quantification was performed on thylakoid membranes isolated from the whole leaf and represents thus an averaged population. This can be important because during growth a light gradient within a leaf, with cell layers deeper in the leaf being exposed to lower light intensities, leads to a range of differently acclimated chloroplasts. In the top layers PSII can have smaller antennae than in the bottom layer (Nishio et al., 1993; Vogelmann and Han, 2000; Evans and Vogelmann, 2003). For the functional measurements, fluorescence is emitted in response to excitation with red light, which is absorbed strongly by the top cell layers causing a strong light gradient inside the leaf and the measured fluorescence emission is derived mainly from chloroplasts in the top cell layers (Terashima et al., 2009). To check if this is the case here as well, we measured the PSII functional antenna size from the axial and abaxial sides of the leaves of plants grown under GL1800 (see **Figure 6**), where the leaves are thickest and the anticipated effect should be most pronounced. We did not observe any significant differences in the antenna sizes measurements between the axial and abaxial side. The smaller antenna size observed in this experiment, when compared to the previous batch (see **Figures 5** and **6**) should be ascribed to the biological variation between the rounds of growth, as the standard errors within each set were small. This leads to the conclusion that the

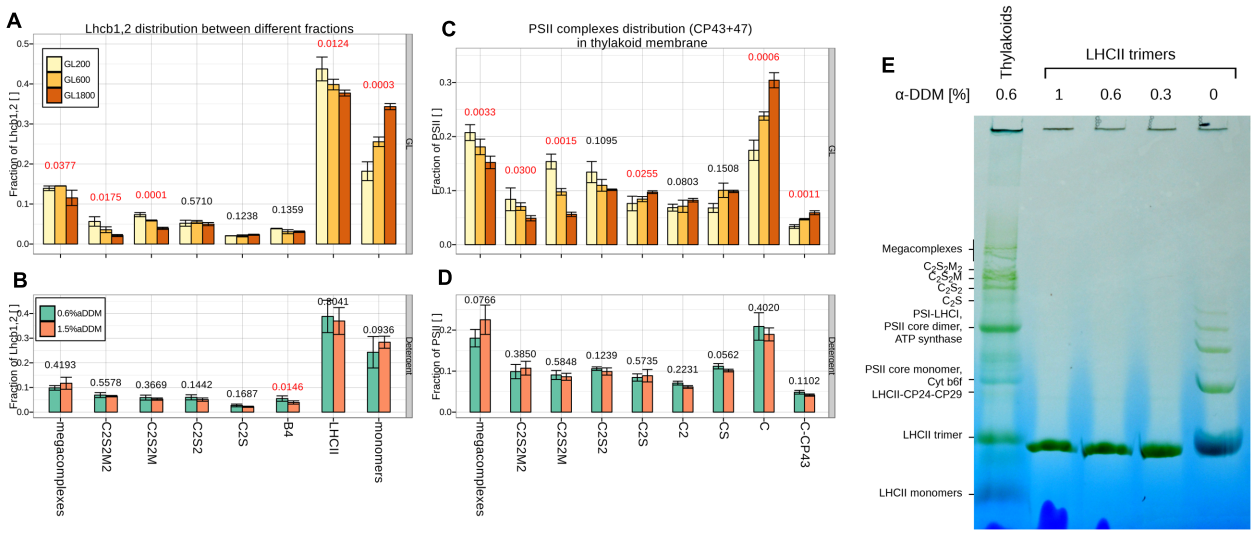

FIGURE 4 | Growth light (GL) and detergent influence on PSII complexes and Lhcb1, 2 distribution. The distribution of PSII between different PSII complexes according to the Lhcb1,2 **(A,B)**: supercomplexes (megacomplexes, $C_2S_2M_2$, C_2S_2M, C_2S_2, C_2S), different complexes (CP29 + LHCII + CP24 complex, B4; Light Harvesting complex of PSII, LHCII) and monomers or CP43 and CP47 **(C,D)**: supercomplexes (megacomplexes, $C_2S_2M_2$, C_2S_2M, C_2S_2, C_2S, CS) or different core complexes (core dimers, C_2; core monomers, C; core monomers without CP43, C-CP43) in isolated thylakoids separated during 2D-PAGE and quantified from three different gels ($n = 3$). Thylakoids were taken from plants grown under GL200, 600, and 1800 (respectively, yellow, orange, and brown fill; **A,C** panels) or only GL200, but were solubilized in 0.6 and 1.5% α-DDM (respectively, green and blue cyan fill; **B,D** panels). Numbers above the bars are the *p*-values of ANOVA's *F*-test on a specific group. Red color signifies rejection of the null hypothesis that the response to all GLs is the same ($\alpha < 0.05$), black its acceptance. **(E)** BN-PAGE of thylakoids solubilized in 0.6% α-DDM and LHCII trimers (3 μg of Chl) solubilized in 0, 0.3, 0.6, and 1% of α-DDM.

difference between functional and structural measurements did not originate from the shallow probing during fluorescence measurements. A series of other effects can influence the measurements of the functional antenna size, including changes in the leaf structure, as well as chloroplast and membrane organization. However, the large difference between the protein content and the functional measurements suggests also that in HL, part of the antenna does not transfer the absorbed light efficiently to the RC.

Short-Term Light Stress

Next, we studied the effect of short light stress on the PSII super- and sub-complexes and the possible transition between short- and long-term strategies by following the first 6 h of HL treatment. The thylakoid membranes were isolated from plants grown under GL200 and transferred for 0.5, 2 and 6 h to GL1800. All plants analyzed in this experiment were light adapted and following the treatment the leaves were immediately cooled in an ice/water mixture. To validate if the short-term response was induced properly, pigment analysis was performed (see **Table 2**). The deepoxidation level of xanthophylls increased sharply to around 40% during the first 30 min, and as plants were kept longer under GL1800 the level reached 55% after 6 h.

2D-PAGE analysis was used to determine possible changes in the PSII organization and composition (see **Figure 7**). No changes in the distribution of complexes and supercomplexes were observed upon 30 min of HL. A decrease in the mega and supercomplexes containing trimer M was observed after 2 h of treatment, accompanied by a small relative increase of LHCII-CP24-CP29 and LHCII trimers. The amount of LHCII monomers increased only slightly during the treatment.

DISCUSSION

Differences in the growth light intensity have been shown to lead to changes in the protein composition and in the organization of the thylakoid membrane of plants. Long-term acclimation is known to reduce the number of LHCII (and CP24) subunits present in the membrane (Ballottari et al., 2007; Kouřil et al., 2013), while short-term response is suggested to consist of a reorganization of the membrane with the disconnection of part of the antenna from PSII (Betterle et al., 2009; Holzwarth et al., 2009; Johnson et al., 2011). Both these strategies should then result in a change in the antenna size of PSII. In this work, we have investigated this aspect systematically by studying how short-term light responses and long-term acclimation affect the quaternary structure of PSII super- and sub-complexes.

In Vitro vs. *In Folio*

Native gels are a powerful tool to study the presence and the different aggregation states of photosynthetic complexes and supercomplexes (Aro et al., 2005; Andaluz et al., 2006; Danielsson et al., 2006; Järvi et al., 2011). However, there are several issues that may complicate the extrapolation of the biochemical data to *in folio* systems and we had started

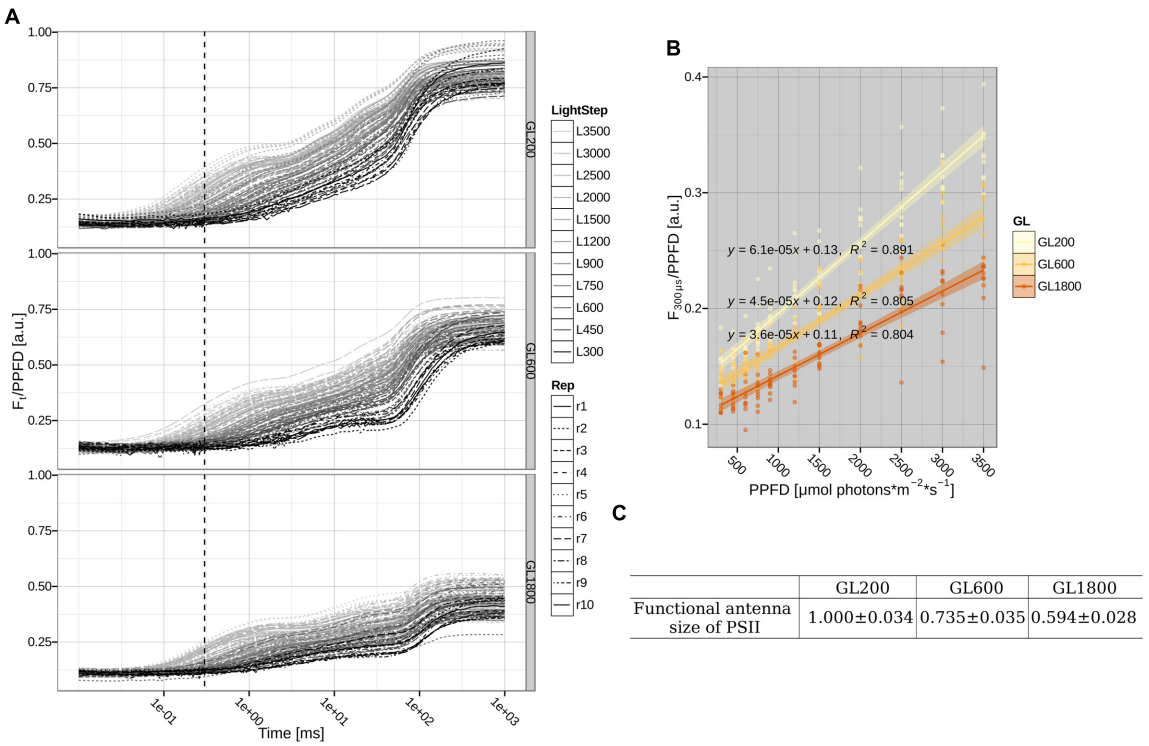

	GL200	GL600	GL1800
Functional antenna size of PSII	1.000±0.034	0.735±0.035	0.594±0.028

FIGURE 5 | Functional antenna size of PSII. (A) Direct measurements of chlorophyll *a* fluorescence *in folio* during a 1 s pulse of 300, 450, 600, 750, 900, 1200, 1500, 2000, 2500, 3000, and 3500 µmol photons*m^{-2}*s^{-1} were normalized to the photosynthetic photon flux density (PPFD). The dotted, vertical line shows the 300 µs time point. Shown traces for 10 different plants (Rep1-10, respectively, represented by different line types) grown under GL200, 600, and 1800 (respectively, Top, Central, and Bottom Left panels). **(B)** Relationship between normalized fluorescence at 300 µs and PPFD fitted with a linear regression. The fitted lines with their standard error are shown as lines with shadows. Individual data points are from the plants grown under GL200, 600, and 1800, yellow, orange, and brown color, respectively. **(C)** The slope and standard error of a fit of the normalized fluorescence at 300 µs against PPFD relationship corresponding to the functional antenna size of PSII on 10 different plants (n = 10) grown under GL200, 600, and 1800.

our investigation by checking the validity of the analysis and answering several questions. Do the differences observed upon solubilization of the membranes reflect the situation *in folio*? Are the results biased by the solubilization steps? To minimize the solubilization artifacts we used low concentrations of a mild detergent (but strong enough to solubilize both grana and lamellae). We also used different amounts of detergent in a range that covers the possible differences in protein/lipids/detergent ratios in the various samples. The results show no influence of the detergent concentration on the PSII supercomplex distribution. Despite the fact that these results indicate that the observed differences are not due to the solubilization, we should keep in mind that the purification procedure has likely an effect on very labile complexes and our analysis gives the lowest threshold for the largest fractions of PSII supercomplexes.

The other essential question is how to analyze the gel and check the reproducibility of the results. To achieve this goal we adapted for our purposes the workflow from Natale et al. (2011). We used only open source or homemade programs based on ImageJ or R. To correct for differences in acrylamide polymerization and electrophoresis we had to warp the gels in ImageJ (UnwarpJ package). To correct for the differences in Coomassie staining between gels (fluctuating background drift) we performed a local normalization to the minimum of a broad ROI. The selectivity of the background exclusion was tested on empty parts of the gel (data not shown) giving satisfactory results. The sample loading (protein content) on a BN-PAGE is often slightly different, especially, if working with plants grown under non-standard conditions, as some pellet is present after solubilization. In this respect it is important to mention that the pellet of samples from plants grown under different conditions has a composition similar to that of the solubilized fraction (data not shown) excluding the possibility that there was selective solubilization. Additionally, when needed, we performed a normalization to total protein content (we had around 97 recognized protein dots) or to a reference protein. It is crucial to remember that the absolute values are difficult to obtain as the binding mechanism of Coomassie is complex (Georgiou et al., 2008). Additionally, we observed an influence of freezing and thawing on the quality of the samples, so each sample was run fresh after isolation or after only one freeze-thaw cycle. It should be kept in mind that all data obtained upon freezing and thawing the membranes multiple times are unreliable.

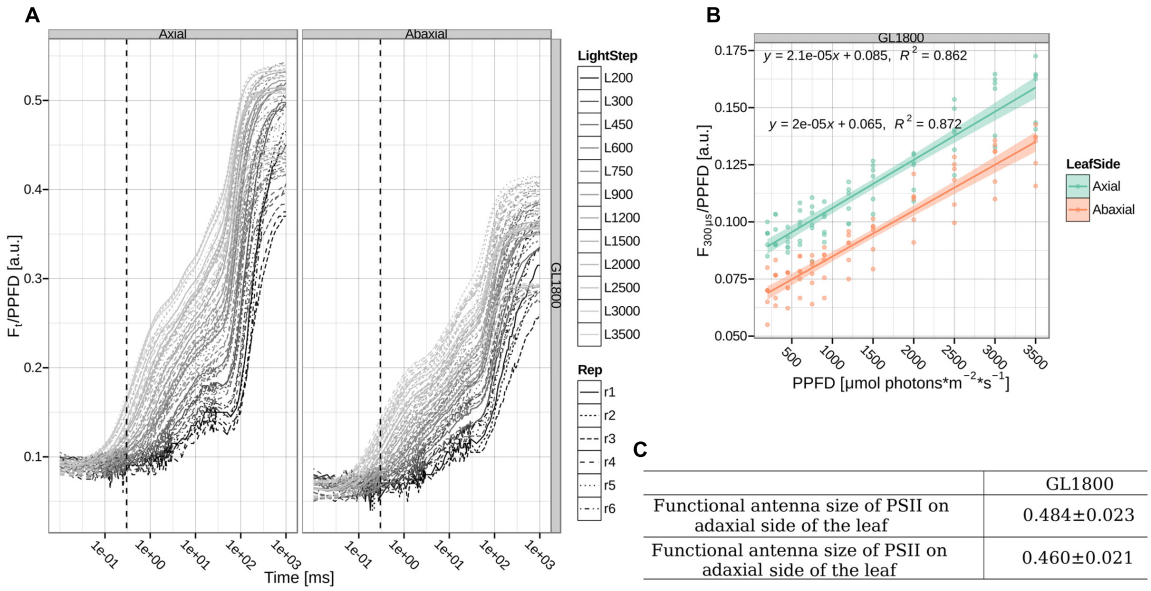

	GL1800
Functional antenna size of PSII on adaxial side of the leaf	0.484±0.023
Functional antenna size of PSII on adaxial side of the leaf	0.460±0.021

FIGURE 6 | Functional antenna size of PSII. (A) Direct measurements of chlorophyll *a* fluorescence *in folio* during a 1 s pulse in the range of 200–3500 µmol photons*m^{-2}*s^{-1} were normalized to the PPFD. The dotted, vertical line shows the 300 µs time point. Shown traces for six different plants (Rep1-6, respectively, represented by different line types) grown under GL1800 and measured on the axial or abaxial side of the leaf (respectively, Left and Right panel). **(B)** Normalized fluorescence at 300 µs as a function of PPFD on plants from GL1800 measured on axial and abaxial side of the leaf (cyan and orange points, respectively). The linear regression fit and its error are shown as a line with a shadow. **(C)** The relative slope and standard error of a fit of the normalized fluorescence at 300 µs against PPFD relationship corresponding to the functional antenna size of PSII on six different plants ($n = 6$) grown under GL1800. Data normalized to GL200 measurements performed on adaxial side of the leaves.

TABLE 2 | Pigment analysis during the first 6 h of HL.

	0 h	0.5 h	2 h	6 h
Chl a/b	3.210 ± 0.014	3.231 ± 0.005	3.240 ± 0.020	3.241 ± 0.006
Chl/Car	4.193 ± 0.007	4.036 ± 0.019	3.981 ± 0.017	3.740 ± 0.013
Neo/100 Chls	3.269 ± 0.139	3.440 ± 0.095	3.416 ± 0.080	3.613 ± 0.193
Vio/100 Chls	3.157 ± 0.181	1.930 ± 0.067	1.804 ± 0.081	1.822 ± 0.101
Ant/100 Chls	0.416 ± 0.015	0.634 ± 0.021	0.725 ± 0.017	1.001 ± 0.042
Lut/100 Chls	14.989 ± 0.654	15.921 ± 0.257	15.772 ± 0.338	16.218 ± 0.643
Zea/100 Chls	0.274 ± 0.015	1.129 ± 0.053	1.599 ± 0.154	2.296 ± 0.129
β-Car/100 Chls	1.739 ± 0.939	1.720 ± 0.372	1.797 ± 0.619	1.781 ± 1.125
Cars/100 Chls	23.846 ± 0.041	24.776 ± 0.118	25.116 ± 0.109	26.734 ± 0.096
(Z + 0.5 × A)/(Z + A + V)	0.125 ± 0.003	0.391 ± 0.004	0.474 ± 0.010	0.546 ± 0.002

Pigments were extracted from thylakoids from plants grown under GL200 and transferred for 0.5, 2 and 6 h. The chlorophyll a/b (Chl a/b) ratio and chlorophyll/carotenoid (Chl/Car) ratio was determined the same way from isolated thylakoid membranes in three different repetitions (n = 3). The same extracts were used for the quantification by HPLC of the carotenoids: neoxanthin (Neo), violaxanthin (Vio), anteraxanthin (Ant), zeaxanthin (Zea), lutein (Lut) and β-carotene (β-car). All carotenoids were calculated per 100 Chls.

Acclimation of PSII (Super)Complexes

Upon HL acclimation a reduction in the relative amount of PSII mega and supercomplexes containing trimer M at increasing light intensities was observed. This was expected on the basis of the reduction of CP24 and Lhcb3 (Ballottari et al., 2007; Kouřil et al., 2013), which are essential for the stabilization of trimer M (Kovács et al., 2006; Caffarri et al., 2009). Under the same conditions, the relative amount of core monomers significantly increased. This is in agreement with the idea that the source of the PSII core monomers is the constant activity of the repair cycle, which is higher in HL (Aro et al., 2005).

No significant changes in any of the PSII supercomplexes could be observed during the first 30 min, when the amount of zeaxanthin is already high, while a relative decrease in the supercomplexes containing trimer M started to be observed only after 2 h of HL exposure. Although we cannot exclude that during the fast phase of NPQ the antenna is disconnected and then it reconnects again during the preparation, we can conclude that the presence of zeaxanthin does not have an effect on the organization of the supercomplexes and that the long term acclimation is already active after 2 h of HL.

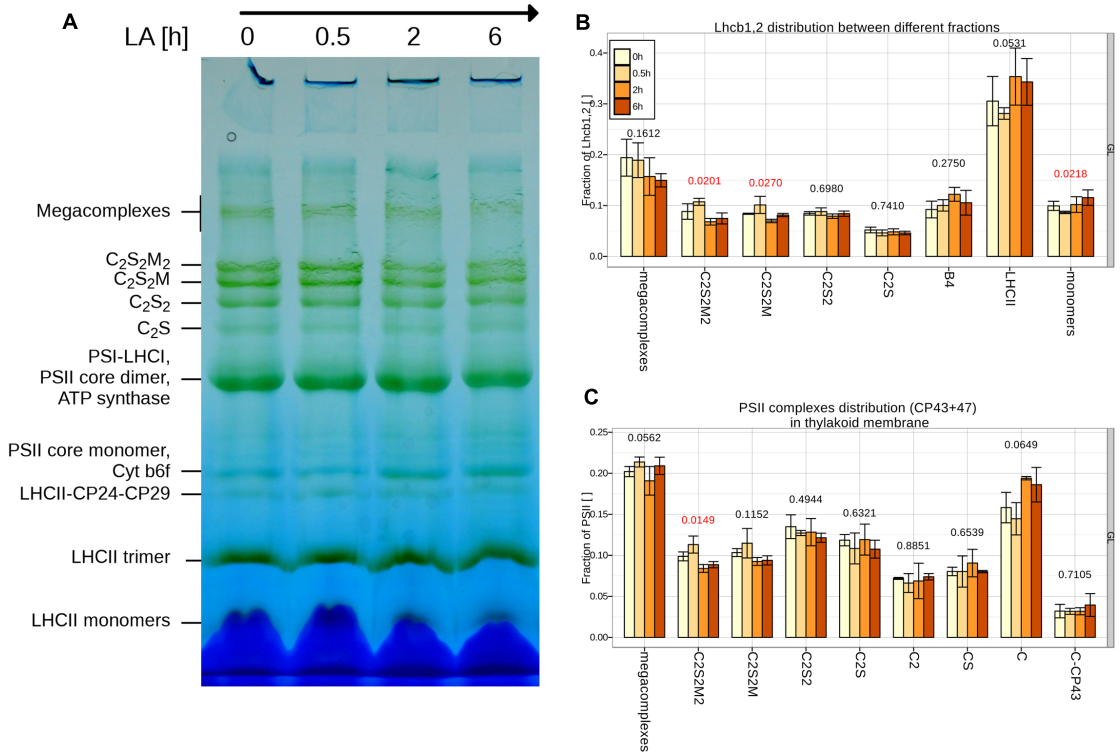

FIGURE 7 | Changes in the distribution of PSII complexes during the first 6 h of HL. (A) BN-PAGE of thylakoids from plants grown under GL200 and transferred for 0.5, 2 and 6 h. **(B)** The distribution of PSII between different PSII complexes according to Lhcb1,2: supercomplexes (megacomplexes, $C_2S_2M_2$, C_2S_2M, C_2S_2, C_2S), different complexes (CP29 + LHCII + CP24 complex, B4; Light Harvesting complex of PSII, LHCII) and monomers; or CP43 + 47 **(C)**: core dimers, C_2; core monomers, C; core monomers without CP43, C-CP43 in isolated thylakoids separated during 2D-PAGE and quantified from three different gels ($n = 3$). Thylakoids were obtained from plants grown under GL200 and transferred for 0.5, 2 and 6 h to GL1800. Red color signifies rejection of the null hypothesis that the response to all growth light is the same ($\alpha < 0.05$), black its acceptance.

LHCII Monomers vs. Trimers

It is interesting to see that no changes are observed in the ratio between LHCII trimers and monomers in the first hours of HL, while an increase in LHCII monomers is visible upon long-term acclimation to HL. The data suggest that a population of LHCII monomers exists in the membrane as the high stability of LHCII trimers to detergent treatment seems to exclude that their presence is an artifact of the purification. It has been proposed that the LHCII monomer can be partially responsible for the irreversible part of the quenching (Garab et al., 2002). More recently it was shown that LHCII in the membrane of the green alga *Chlamydomonas reinhardtii* exists in different quenching states and that the ratio between these states depends on the growth light conditions (Tian et al., 2015). Here, we observed that the PSII maximum efficiency is lower in HL than in LL indicating that a larger part of the absorbed energy is not used for photochemistry. Moreover, a large difference between the antenna size at the protein and at the functional level is observed in HL. It is thus tempting to speculate that LHCII monomers observed in high amount in HL are less efficient in transferring energy to the RC and act as a reservoir of LHCII.

AUTHOR CONTRIBUTIONS

RC conceived the research. LB, GS, and RC designed the research. LB, performed most of the experimental work. GS performed the antenna size measurements. LB and RC wrote the paper. All the authors contributed to the final version.

FUNDING

This research is financed by the BioSolar Cells open innovation consortium, supported by the Dutch Ministry for Economic Affairs, Agriculture and Innovation by the Dutch Organization for Scientific research (NWO), division Earth and Life Science via a Vici grant and by the European Research council (Consolidator grant 281341).

ACKNOWLEDGMENTS

The authors thank Pengqi Xu for providing the LHCII trimers. Dr. Jeremy Harbinson is thanked for helpful discussions.

REFERENCES

Allen, J. F. (1992). Protein phosphorylation in regulation of photosynthesis. *Biochim. Biophys. Acta* 1098, 275–335. doi: 10.1016/S0005-2728(09)91014-3

Andaluz, S., López-Millán, A.-F., De las Rivas, J., Aro, E.-M., Abadía, J., and Abadía, A. (2006). Proteomic profiles of thylakoid membranes and changes in response to iron deficiency. *Photosynth. Res.* 89, 141–155. doi: 10.1007/s11120-006-9092-6

Andersson, I. (1996). Large structures at high resolution: the 1.6 Å crystal structure of spinach ribulose-1,5- bisphosphate carboxylase/oxygenase complexed with 2-carboxyarabinitol bisphosphate. *J. Mol. Biol.* 259, 160–174. doi: 10.1006/jmbi.1996.0310

Aro, E.-M., Suorsa, M., Rokka, A., Allahverdiyeva, Y., Paakkarinen, V., Saleem, A., et al. (2005). Dynamics of photosystem II: a proteomic approach to thylakoid protein complexes. *J. Exp. Bot.* 56, 347–356. doi: 10.1093/jxb/eri041

Asada, K. (2006). Production and scavenging of reactive oxygen species in chloroplasts and their functions. *Plant Physiol.* 141, 391–396. doi: 10.1104/pp.106.082040

Ballottari, M., Dall'Osto, L., Morosinotto, T., and Bassi, R. (2007). Contrasting behavior of higher plant photosystem I and II antenna systems during acclimation. *J. Biol. Chem.* 282, 8947–8958. doi: 10.1074/jbc.M606417200

Belgio, E., Kapitonova, E., Chmeliov, J., Duffy, C. D. P., Ungerer, P., Valkunas, L., et al. (2014). Economic photoprotection in photosystem II that retains a complete light-harvesting system with slow energy traps. *Nat. Commun.* 5, 1–8. doi: 10.1038/ncomms5433

Betterle, N., Ballottari, M., Zorzan, S., de Bianchi, S., Cazzaniga, S., Dall'Osto, L., et al. (2009). Light-induced dissociation of an antenna hetero-oligomer is needed for non-photochemical quenching induction. *J. Biol. Chem.* 284, 15255–15266. doi: 10.1074/jbc.M808625200

Caffarri, S., Kouřil, R., Kereïche, S., Boekema, E. J., and Croce, R. (2009). Functional architecture of higher plant photosystem II supercomplexes. *EMBO J.* 28, 3052–3063. doi: 10.1038/emboj.2009.232

Clarke, J. T., Warnock, R. C. M., and Donoghue, P. C. J. (2011). Establishing a time-scale for plant evolution. *New Phytol.* 192, 266–301. doi: 10.1111/j.1469-8137.2011.03794.x

Croce, R., Canino, G., Ros, F., and Bassi, R. (2002). Chromophore organization in the higher-plant photosystem II antenna protein CP26. *Biochemistry* 41, 7334–7343. doi: 10.1021/bi0257437

Danielsson, R., Suorsa, M., Paakkarinen, V., Albertsson, P.-A., Styring, S., Aro, E.-M., et al. (2006). Dimeric and monomeric organization of photosystem II. Distribution of five distinct complexes in the different domains of the thylakoid membrane. *J. Biol. Chem.* 281, 14241–14249. doi: 10.1074/jbc.M600634200

Dekker, J. P., and Boekema, E. J. (2005). Supramolecular organization of thylakoid membrane proteins in green plants. *Biochim. Biophys. Acta* 1706, 12–39. doi: 10.1016/j.bbabio.2004.09.009

Demmig-Adams, B., Adams, W. W., Heber, U., Neimanis, S., Winter, K., Krüger, A., et al. (1990). Inhibition of zeaxanthin formation and of rapid changes in radiationless energy dissipation by dithiothreitol in spinach leaves and chloroplasts. *Plant Physiol.* 92, 293–301. doi: 10.1104/pp.92.2.293

Dietz, K.-J. (2015). Efficient high light acclimation involves rapid processes at multiple mechanistic levels. *J. Exp. Bot.* 66, 2401–2414. doi: 10.1093/jxb/eru505

Dinç, E., Ceppi, M. G., Tóth, S. Z., Bottka, S., and Schansker, G. (2012). The chl a fluorescence intensity is remarkably insensitive to changes in the chlorophyll content of the leaf as long as the chl a/b ratio remains unaffected. *Biochim. Biophys. Acta* 1817, 770–779. doi: 10.1016/j.bbabio.2012.02.003

Evans, J. R., and Vogelmann, T. C. (2003). Profiles of C-14 fixation through spinach leaves in relation to light absorption and photosynthetic capacity. *Plant Cell Environ.* 26, 547–560. doi: 10.1046/j.1365-3040.2003.00985.x

Fristedt, R., and Vener, A. V. (2011). High light induced disassembly of photosystem II supercomplexes in *Arabidopsis* requires STN7-dependent phosphorylation of CP29. *PLoS ONE* 6:e24565. doi: 10.1371/journal.pone.0024565

Garab, G., Cseh, Z., Kovács, L., Rajagopal, S., Várkonyi, Z., Wentworth, M., et al. (2002). Light-induced trimer to monomer transition in the main light-harvesting antenna complex of plants: thermo-optic mechanism. *Biochemistry* 41, 15121–15129. doi: 10.1021/bi026157g

Georgiou, C. D., Grintzalis, K., Zervoudakis, G., and Papapostolou, I. (2008). Mechanism of *Coomassie brilliant* blue G-250 binding to proteins: a hydrophobic assay for nanogram quantities of proteins. *Anal. Bioanal. Chem.* 391, 391–403. doi: 10.1007/s00216-008-1996-x

Gilmore, A. M., and Yamamoto, H. Y. (1991). Resolution of lutein and zeaxanthin using a non-endcapped, lightly carbon-loaded C18 high-performance liquid chromatographic column. *J. Chromatogr. A* 543, 137–145. doi: 10.1016/S0021-9673(01)95762-0

Hersch, M., Lorrain, S., de Wit, M., Trevisan, M., Ljung, K., Bergmann, S., et al. (2014). Light intensity modulates the regulatory network of the shade avoidance response in *Arabidopsis*. *Proc. Natl. Acad. Sci. U.S.A.* 111, 6515–6520. doi: 10.1073/pnas.1320355111

Holzwarth, A. R., Miloslavina, Y., Nilkens, M., and Jahns, P. (2009). Identification of two quenching sites active in the regulation of photosynthetic light-harvesting studied by time-resolved fluorescence. *Chem. Phys. Lett.* 483, 262–267. doi: 10.1016/j.cplett.2009.10.085

Horton, P., Johnson, M. P., Perez-Bueno, M. L., Kiss, A. Z., and Ruban, A. V. (2008). Photosynthetic acclimation: does the dynamic structure and macro-organisation of photosystem II in higher plant grana membranes regulate light harvesting states? *FEBS J.* 275, 1069–1079. doi: 10.1111/j.1742-4658.2008.06263.x

Horton, P., and Ruban, A. (2005). Molecular design of the photosystem II light-harvesting antenna: photosynthesis and photoprotection. *J. Exp. Bot.* 56, 365–373. doi: 10.1093/jxb/eri023

Hundal, T., Virgin, I., Styring, S., and Andersson, B. (1990). Changes in the organization of photosystem II following light-induced D1-protein degradation. *Biochim. Biophys. Acta* 1017, 235–241. doi: 10.1016/0005-2728(90)90190-F

Ilioaia, C., Johnson, M. P., Horton, P., and Ruban, A. V. (2008). Induction of efficient energy dissipation in the isolated light-harvesting complex of photosystem II in the absence of protein aggregation. *J. Biol. Chem.* 283, 29505–29512. doi: 10.1074/jbc.M802438200

Jahns, P., and Holzwarth, A. R. (2012). The role of the xanthophyll cycle and of lutein in photoprotection of photosystem II. *Biochim. Biophys. Acta* 1817, 182–193. doi: 10.1016/j.bbabio.2011.04.012

Järvi, S., Suorsa, M., Paakkarinen, V., and Aro, E.-M. (2011). Optimized native gel systems for separation of thylakoid protein complexes: novel super- and mega-complexes. *Biochem. J.* 439, 207–214. doi: 10.1042/BJ20102155

Johnson, M. P., Goral, T. K., Duffy, C. D. P., Brain, A. P. R., Mullineaux, C. W., and Ruban, A. V. (2011). Photoprotective energy dissipation involves the reorganization of photosystem II light-harvesting complexes in the grana membranes of spinach chloroplasts. *Plant Cell* 23, 1468–1479. doi: 10.1105/tpc.110.081646

Keller, M. M., Jaillais, Y., Pedmale, U. V., Moreno, J. E., Chory, J., and Ballaré, C. L. (2011). Cryptochrome 1 and phytochrome B control shade-avoidance responses in *Arabidopsis* via partially independent hormonal cascades. *Plant J.* 67, 195–207. doi: 10.1111/j.1365-313X.2011.04598.x

Kono, M., and Terashima, I. (2014). Long-term and short-term responses of the photosynthetic electron transport to fluctuating light. *J. Photochem. Photobiol. B Biol.* 137, 89–99. doi: 10.1016/j.jphotobiol.2014.02.016

Kouřil, R., Wientjes, E., Bultema, J. B., Croce, R., and Boekema, E. J. (2013). High-light vs. low-light: effect of light acclimation on photosystem II composition and organization in *Arabidopsis thaliana*. *Biochim. Biophys. Acta* 1827, 411–419. doi: 10.1016/j.bbabio.2012.12.003

Kovács, L., Damkjaer, J., Kereïche, S., Ilioaia, C., Ruban, A. V., and Boekema, E. J. (2006). Lack of the light-harvesting complex CP24 affects the structure and function of the grana membranes of higher plant chloroplasts. *Plant Cell* 18, 3106–3120. doi: 10.1105/tpc.106.045641

Li, X. P., Björkman, O., Shih, C., Grossman, A. R., Rosenquist, M., Jansson, S., et al. (2000). A pigment-binding protein essential for regulation of photosynthetic light harvesting. *Nature* 403, 391–395. doi: 10.1038/35000131

Natale, M., Maresca, B., Abrescia, P., and Bucci, E. (2011). Image analysis workflow for 2-D electrophoresis gels based on ImageJ. *Proteomics Insights* 4, 37–49. doi: 10.4137/PRI.S7971

Nishio, J., Sun, J., and Vogelmann, T. (1993). Carbon fixation gradients across spinach leaves do not follow internal light gradients. *Plant Cell* 5, 953–961. doi: 10.1105/tpc.5.8.953

Page, M., Sultana, N., Paszkiewicz, K., Florance, H., and Smirnoff, N. (2012). The influence of ascorbate on anthocyanin accumulation during high light acclimation in *Arabidopsis thaliana*: further evidence for redox control of anthocyanin synthesis. *Plant Cell Environ.* 35, 388–404. doi: 10.1111/j.1365-3040.2011.02369.x

Park, Y., Chow, W. S., and Anderson, J. M. (1997). Antenna size dependency of photoinactivation of photosystem II in light-acclimated pea leaves. *Plant Physiol.* 115, 151–157. doi: 10.1104/pp.115.1.151

Pietrzykowska, M., Suorsa, M., Semchonok, D. A., Tikkanen, M., Boekema, E. J., Aro, E.-M., et al. (2014). The light-harvesting chlorophyll a/b binding proteins Lhcb1 and Lhcb2 play complementary roles during state transitions in *Arabidopsis*. *Plant Cell* 26, 3646–3660. doi: 10.1105/tpc.114.127373

Plöscher, M., Granvogl, B., Zoryan, M., Reisinger, V., and Eichacker, L. A. (2009). Mass spectrometric characterization of membrane integral low molecular weight proteins from photosystem II in barley etioplasts. *Proteomics* 9, 625–635. doi: 10.1002/pmic.200800337

Robinson, H., Sharp, R., and Yocum, C. (1980). Effect of manganese on the nuclear magnetic relaxivity of water protons in chloroplast suspensions. *Biochem. Biophys. Res. Commun.* 93, 755–761. doi: 10.1016/0006-291X(80)91141-9

Ruban, A. V., Johnson, M. P., and Duffy, C. D. P. (2012). The photoprotective molecular switch in the photosystem II antenna. *Biochim. Biophys. Acta* 1817, 167–181. doi: 10.1016/j.bbabio.2011.04.007

Schägger, H. (2006). Tricine–SDS-PAGE. *Nat. Protoc.* 1, 16–22. doi: 10.1038/nprot.2006.4

Shi, L.-X., Hall, M., Funk, C., and Schröder, W. P. (2012). Photosystem II, a growing complex: updates on newly discovered components and low molecular mass proteins. *Biochim. Biophys. Acta* 1817, 13–25. doi: 10.1016/j.bbabio.2011.08.008

Suorsa, M., Rantala, M., Mamedov, F., Lespinasse, M., Trotta, A., Grieco, M., et al. (2015). Light acclimation involves dynamic re-organization of the pigment-protein megacomplexes in non-appressed thylakoid domains. *Plant J.* 84, 360–373. doi: 10.1111/tpj.13004

Takabayashi, A., Kadoya, R., Kuwano, M., Kurihara, K., Ito, H., Tanaka, R., et al. (2013). Protein co-migration database (PCoM -DB) for *Arabidopsis* thylakoids and Synechocystis cells. *Springerplus* 2:148. doi: 10.1186/2193-1801-2-148

Terashima, I., Fujita, T., Inoue, T., Chow, W. S., and Oguchi, R. (2009). Green light drives leaf photosynthesis more efficiently than red light in strong white light: revisiting the enigmatic question of why leaves are green. *Plant Cell Physiol.* 50, 684–697. doi: 10.1093/pcp/pcp034

Tian, L., Dinç, E., and Croce, R. (2015). LHCII Populations in different quenching states are present in the thylakoid membranes in a ratio that depends on the light conditions. *J. Phys. Chem. Lett.* 6, 2339–2344. doi: 10.1021/acs.jpclett.5b00944

Tikkanen, M., and Aro, E.-M. (2012). Thylakoid protein phosphorylation in dynamic regulation of photosystem II in higher plants. *Biochim. Biophys. Acta.* 1817, 232–238. doi: 10.1016/j.bbabio.2011.05.005

Umena, Y., Kawakami, K., Shen, J.-R., and Kamiya, N. (2011). Crystal structure of oxygen-evolving photosystem II at a resolution of 1.9?Å. *Nature* 473, 55–60. doi: 10.1038/nature09913

Vogelmann, T. C., and Han, T. (2000). Measurement of gradients of absorbed light in spinach leaves from chlorophyll fluorescence profiles. *Plant Cell Environ.* 23, 1303–1311. doi: 10.1046/j.1365-3040.2000.00649.x

Weston, E., Thorogood, K., Vinti, G., and López-Juez, E. (2000). Light quantity controls leaf-cell and chloroplast development in *Arabidopsis thaliana* wild type and blue-light-perception mutants. *Planta* 211, 807–815. doi: 10.1007/s004250000392

Wientjes, E., van Amerongen, H., and Croce, R. (2013a). LHCII is an antenna of both photosystems after long-term acclimation. *Biochim. Biophys. Acta* 1827, 420–426. doi: 10.1016/j.bbabio.2012.12.009

Wientjes, E., Van Amerongen, H., and Croce, R. (2013b). Quantum yield of charge separation in photosystem II: Functional effect of changes in the antenna size upon light acclimation. *J. Phys. Chem. B* 117, 11200–11208. doi: 10.1021/jp401663w

Wientjes, E., Drop, B., Kouril, R., Boekema, E. J., and Croce, R. (2013c). During state 1 to state 2 transition in *Arabidopsis thaliana*, the photosystem II supercomplex gets phosphorylated but does not disassemble. *J. Biol. Chem.* 288, 32821–32826. doi: 10.1074/jbc.M113.511691

Xu, P., Tian, L., Kloz, M., and Croce, R. (2015). Molecular insights into zeaxanthin-dependent quenching in higher plants. *Sci. Rep.* 5:13679. doi: 10.1038/srep13679

Conflict of Interest Statement: The authors declare that the research was conducted in the absence of any commercial or financial relationships that could be construed as a potential conflict of interest.

frontiers in Plant Science

OPINION
published: 12 January 2016
doi: 10.3389/fpls.2015.01234

Photosystem II Assembly from Scratch

Thilo Rühle[1] *and Dario Leister*[1,2]*

[1] *Plant Molecular Biology, Department of Biology, Ludwig-Maximilians-University Munich, Munich, Germany,* [2] *Department of Plant and Environmental Sciences, Copenhagen Plant Science Centre, University of Copenhagen, Copenhagen, Denmark*

Keywords: PSII assembly, PSII, PSII complex, assembly factor, synthetic bacterium, forward genetic screen, reverse genetic, chloroplast

Construction of a functional Photosystem II (PSII) in cyanobacteria and chloroplasts depends on the action of auxiliary factors, which transiently interact with PSII intermediates during assembly. In addition to a common PSII structure and a conserved set of PSII assembly factors, cyanobacteria, and higher plants have evolved additional, clade-specific assembly factors. Most such factors in cyanobacteria and chloroplasts have been identified by "top-down" approaches (forward and reverse genetics), which involved genetic disruption of individual components in the assembly process and subsequent characterization of the ensuing phenotypic effects on the respective mutant lines/strains. In contrast, a "bottom-up" strategy, based on the engineering of a synthetic bacterium with a plant-type PSII, has the potential to identify all assembly factors sufficient to make a functional plant PSII.

OPEN ACCESS

Edited by:
Julian Eaton-Rye, University of Otago, New Zealand

Reviewed by:
Eva-Mari Aro, University of Turku, Finland
Johnna Roose, Louisiana State University, USA

****Correspondence:***
Dario Leister
leister@lmu.de

Specialty section:
This article was submitted to Plant Cell Biology, a section of the journal Frontiers in Plant Science

Received: *28 October 2015*
Accepted: *19 December 2015*
Published: *12 January 2016*

Citation:
Rühle T and Leister D (2016) Photosystem II Assembly from Scratch. Front. Plant Sci. 6:1234. doi: 10.3389/fpls.2015.01234

Photosystem II (PSII) is a water-plastoquinone photo-oxidoreductase, which is found in cyanobacteria and their endosymbiotic descendants, the chloroplasts. Light-driven water splitting and subsequent electron transfer steps are carried out with the assistance of non-proteinaceous cofactors. Thus, the PSII monomer harbors a Mn_4CaO_5 cluster, chloride, bicarbonate, 1-2 hemes, 1 nonheme iron, 35 chlorophyll *a* molecules, 2 pheophytins, 11 β-carotenes, and 2 plastoquinones (Umena et al., 2011), all of which are embedded in a shell made up of at least 20 proteins (Shen, 2015) that determine their correct positioning and relative orientation. Several PSII-associated lipids have been identified in crystal structures and might also be important for functionality (Mizusawa and Wada, 2012; Kansy et al., 2014). The structural core of PSII is conserved between chloroplasts and cyanobacteria (Allen et al., 2011). However, the oxygen-evolving complex in cyanobacteria contains subunits U and V, which are replaced by Q, R, P, and Tn in higher plants (Bricker et al., 2012). Furthermore, in contrast to the soluble, peripherally attached phycobilisomes found in cyanobacteria, green photosynthetic eukaryotes have evolved integrated light-harvesting complexes and lack phycobilisomes (Hohmann-Marriott and Blankenship, 2011; **Figure 1A**).

In accordance with its structural complexity, the assembly of PSII is an elaborate and highly coordinated process, which depends on the action of a network of assembly factors and the fabrication of distinct metastable modules during the course of assembly (see for reviews on this topic: Nixon et al., 2010; Nickelsen and Rengstl, 2013; and papers in this special issue of Frontiers in Plant Science). Several modules common to cyanobacterial and chloroplast PSII assembly processes have been described and are characterized by transient binding of specific assembly factors. An additional level of complexity arises from the fact that PSII is susceptible to photodamage, with subunit D1 being the primary target (Kato and Sakamoto, 2009), as replacement of damaged D1 entails partial disassembly of PSII and reassembly of a functional complex. This repair mechanism features some distinct intermediates, but otherwise involves steps and assembly factors that are shared with the *de novo* assembly pathway (Järvi et al., 2015).

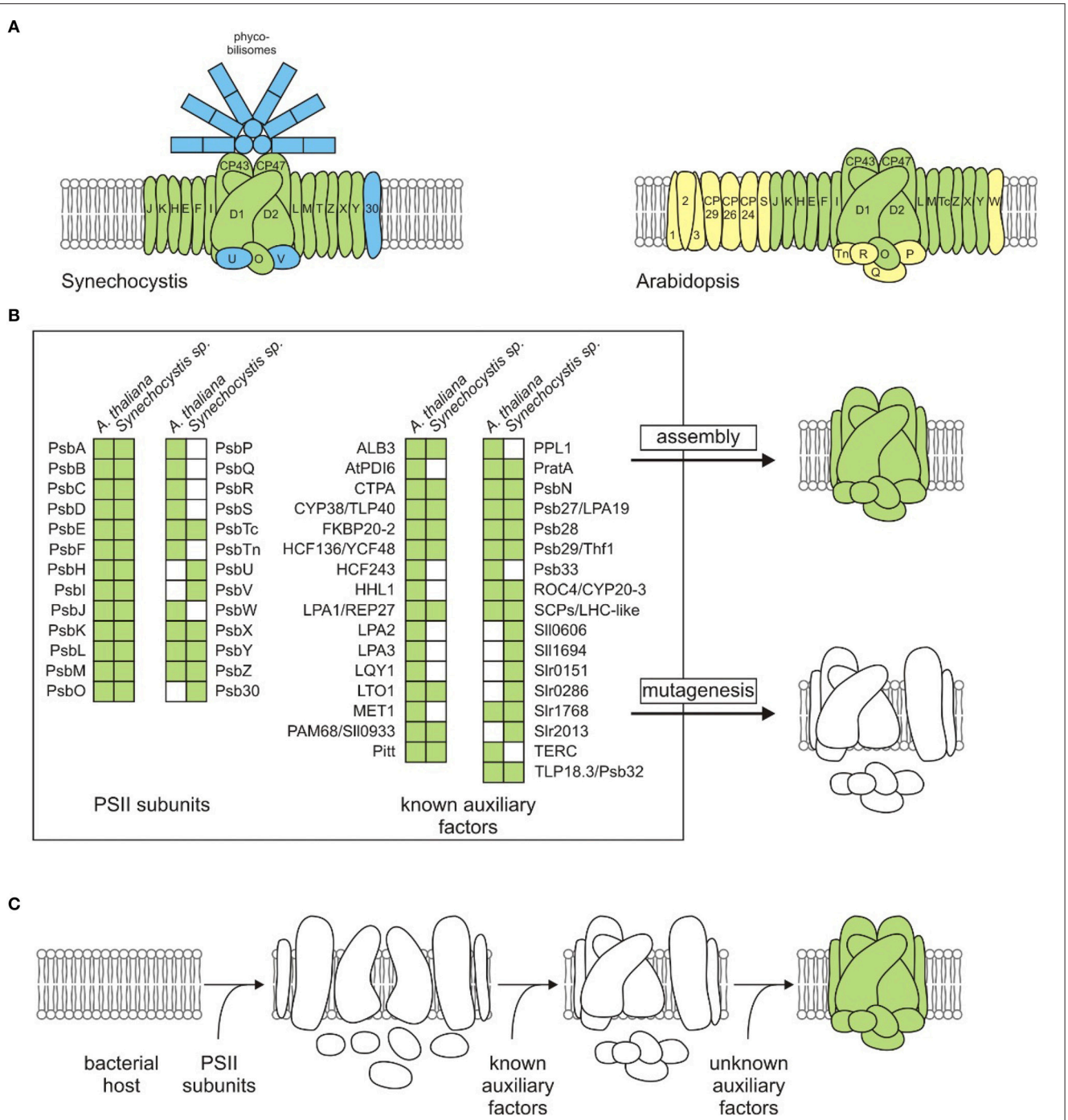

FIGURE 1 | Strategies for identifying auxiliary factors in PSII assembly. (A) Subunit compositions of cyanobacterial (*Synechocystis*) and plant thylakoid (*Arabidopsis*) PSII complexes. Components shown in blue or yellow are only found in *Synechocystis* or *Arabidopsis*, respectively. Light-harvesting proteins Lhcb1, 2 and 3 are labeled with numbers (1, 2, and 3). **(B)** PSII subunits and known PSII auxiliary factors. The list of auxiliary factors has been adapted from Nickelsen and Rengstl (2013) and Järvi et al. (2015), and the recently identified auxiliary factors MET1 (Bhuiyan et al., 2015) and Slr0151 (Yang et al., 2014) have been added. Note that for simplicity, no distinction has been made between factors necessary for assembly, repair or supercomplex formation, and Deg/FtsH proteases are not listed. The classical strategy for study of the assembly process is based on mutagenesis of single components in an intact system. Subsequent analyses focus on the identification of a specific loss of function in a photosynthetic organism. Green and white squares indicate presence and absence of a component listed for each organism, respectively. **(C)** Generation of a synthetic, bacterial host strain carrying a functional plant-type PSII. The design of the synthetic approach largely depends on the choice of the host organism. In the case of a cyanobacterial host, endogenous PSII subunits or auxiliary factors must be deleted or replaced by the plant-type subunits/factors, whereas the presence of essential cofactors (see text), in addition to subunits and auxiliary factors, must be assured for the assembly of a functional, plant-type PSII in a non-photosynthetic bacterium. White and green PSII cartoons in **(B,C)** indicate un- or partially assembled and fully assembled PSII complexes, respectively.

It has become increasingly clear in recent years that the set of assembly factors is largely conserved between cyanobacteria and chloroplasts (Nickelsen and Rengstl, 2013). However, higher plants have extended their inventory during evolution, giving rise to new, plant-specific factors, such as the D1 stabilization factor HCF243 (Zhang et al., 2011) or the repair factors PPL1 and LQY1 (Ishihara et al., 2007; Lu et al., 2011; **Figure 1B**). Furthermore, the consequences of disruption of conserved auxiliary factors sometimes differ between the two systems. For instance, *Arabidopsis* PAM68 and its cyanobacterial counterpart (Armbruster et al., 2010), as well as HCF136 (Meurer et al., 1998) and the cyanobacterial homolog YCF48 (Komenda et al., 2008), participate in the early steps of PSII assembly, but their absence has more severe effects on photosynthesis in plants. Thus, to understand the evolutionary diversification of assembly factors, it is crucial to study chloroplast and cyanobacterial PSII assembly in parallel.

CLASSICAL OR "TOP-DOWN" METHODS OF IDENTIFYING PSII ASSEMBLY FACTORS

Extensive efforts have been made over the past several decades to identify auxiliary factors involved in PSII assembly, and a large number have been found by screening *Synechocystis* sp. PCC 6803 (hereafter *Synechocystis*), *Chlamydomonas reinhardtii*, or *Arabidopsis thaliana* (hereafter *Arabidopsis*) mutant collections for PSII-defective mutants. This type of genetic approach has emerged as a powerful strategy, since single components of an initially intact system can be functionally deleted without directly altering other elements in the assembly process. Subsequent studies then allow the in-depth characterisation of the effects of the loss of a specific function in the assembly process.

Forward Genetic Screens

A classical way to screen for mutants defective in PSII is based on the observation of a high-chlorophyll fluorescence (HCF) phenotype in mutagenized *Arabidopsis* plants, which can be recognized when leaves are exposed to UV light in the dark (Meurer et al., 1996). Several assembly factors, including HCF136 and HCF243 (stabilization of D1 and assembly of the reaction center), LPA1 (D1 integration), LPA2 and LPA3 (integration of CP43) were identified in this manner (Meurer et al., 1998; Peng et al., 2006; Ma et al., 2007; Cai et al., 2010; Zhang et al., 2011). The sensitivity of this screening method for PSII mutants can be further increased by measuring photosynthetic parameters of large mutant collections under varying growth conditions using automatic pulse-amplitude modulation (PAM) of chlorophyll fluorescence (Varotto et al., 2000) or imaging PAM technologies (Ajjawi et al., 2010). This type of approach has led to the identification of several novel factors such as LPA19, PAM68, LQY1, HHL1, and PSB33 (Armbruster et al., 2010; Wei et al., 2010; Lu et al., 2011; Jin et al., 2014; Fristedt et al., 2015). However, forward screens are both labor-intensive and time-consuming, and more than 90% of nuclear genes in *Arabidopsis* have at least one homolog (Armisén et al., 2008). In many cases, duplicated genes code for proteins with redundant functions, and for that reason are inaccessible to classical forward screening techniques.

Reverse Genetic Screens

The increasing accumulation of information on entire genomes, transcriptomes, and proteomes in public databases, together with the availability of indexed libraries of *Arabidopsis* mutant lines with mutations in almost every gene, and the establishment of efficient methods for gene silencing, and genetic engineering by means of homologous recombination in cyanobacteria, have made it possible to apply reverse genetic strategies to both cyanobacterial and eukaryotic photosynthetic model organisms and selectively knock out whole gene families. In one such case, the *Synechocystis* genome database was searched for TPR (tetratricopeptide repeat) genes (Klinkert et al., 2004) and the ORFs were systematically mutagenized. Of the 22 putative TPR proteins identified, PratA and Pitt were shown to be important for Mn^{2+} transport to D1 (Stengel et al., 2012) and for early steps in photosynthetic pigment-protein complex formation (Schottkowski et al., 2009), respectively. Interestingly, the green lineage-specific TPR-domain-containing protein MET1 was recently shown to assist in PSII supercomplex formation and in PSII repair (Bhuiyan et al., 2015). A further example of the power of reverse genetics is the screen of the lumenal immunophilin family in *Arabidopsis*, which comprises at least 16 FKBP (FK-506 binding proteins) and cyclophilins that are known to function as protein chaperones or foldases. Two of these, CYP38/TLP40 and FKBP20-2, were found to be involved in early PSII biogenesis and PSII-LHCII assembly, respectively (Lima et al., 2006; Fu et al., 2007; Sirpiö et al., 2008).

Potential and Limitations of Top-down Approaches

It is obvious that additional PSII assembly auxiliary factors will be identified in forward as well as reverse genetic screens. But the latter are becoming more important owing to major advances in rates of data generation and data mining brought by "omics" technologies. Additionally, methods for large-scale quantification of transient protein interactions of PSII subunits or known PSII auxiliary factors with unknown proteins (Braun et al., 2013) will provide a more thorough understanding of the components and their function in the assembly process.

However, an inherent limitation of top-down approaches is that they allow only those factors that are *required* for a given process to be identified. To define the suite of assembly factors and additional auxiliary factors *sufficient* for PSII assembly, an entirely different strategy is needed, in which all structural PSII proteins and auxiliary factors are brought together and the final outcome of their interplay (PSII assembly) can be monitored. This "bottom-up" concept cannot be optimally implemented in commonly used model organisms like *Arabidopsis*, maize, barley or tobacco, as "brute force" genetic approaches (like shot-gun complementation) are not feasible in these organisms and non-photosynthetic propagation of mutants is difficult to achieve, if at all. Consequently, new tactics have to be adopted to speed up and complement research on PSII assembly. Such efforts must be

directed at the discovery of the complete set of auxiliary factors sufficient to make a functional plant-type photosystem and are outlined below.

A NOVEL "BOTTOM-UP" APPROACH: GENERATION OF A SYNTHETIC BACTERIUM WITH A FUNCTIONAL PLANT-TYPE PSII

In this context, microbial cell systems possess unsurpassed advantages over plants in several respects. They are fast growing (with doubling times as short as 20 min), they have small genomes that are easy to manipulate, and do not show genetic compartmentalization. The ideal host system for study of the assembly of a plant-type PSII via a "bottom-up" approach should fulfill the following requirements: (i) be able to synthesize such essential non-proteinaceous cofactors as Chl *a*, pheophytin, heme and β-carotene, (ii) possess an appropriate electron acceptor for PSII, and (iii) a lipid composition similar to that found in thylakoids, (iv) be capable of heterotrophic growth, and (v) intermediates should accumulate in mutants that are dysfunctional in the assembly process. Notably several cyanobacteria meet virtually all these criteria, which is a reflection of their evolutionary relationship to chloroplasts. However, in the case of a cyanobacterial host like *Synechocystis* endogenous PSII subunits and known, conserved auxiliary factors must be deleted, because they could interfere with the plant-type PSII subunits or auxiliary factors to be tested. This would entail the use of either a sequential, marker-less deletion strategy (Viola et al., 2014 and references within) or a time-saving, multiplex editing strategy recently described for bacterial strains, but not yet established in polyploid cyanobacteria (Ramey et al., 2015). Alternatively, cyanobacterial PSII genes can be directly replaced by their (appropriately optimized) plant counterparts in order to keep untranslated regulatory regions and operon structures intact (Viola et al., 2014). A plant-type PSII can then be constructed stepwise by mimicking the chloroplast assembly process. Known and normally short-lived assembled modules, for instance the D2-Cyt b_{559} complex, the reaction-center complex lacking both CP47 and CP43 or the reaction-center complex lacking CP43 alone (Müller and Eichacker, 1999; Komenda et al., 2004; Dobáková et al., 2007; Nixon et al., 2010), can serve as checkpoints after introducing known plant-type assembly factors into a cyanobacterial strain expressing the respective plant-type subunits found in each module. As the ultimate goal, unknown factors required for the building of each PSII module can be identified by complementation assays with cDNA libraries derived from higher plants (**Figure 1C**). An initial benchmark for this kind of approach would be the successful assembly of the minimal PSII core of the five subunits D1, D2, α, and β subunits of Cyt b_{559} and PsbI, which is able to perform charge separation (Nanba and Satoh, 1987).

Critical Aspects

The bottom-up strategy is inherently appealing, but there are significant uncertainties. While top-down strategies rely on the disruption of a single component of a complex system followed by the characterisation of the effects attributable to loss of that component, the success of the bottom-up strategy critically depends on the ability to monitor the completion of each step in the assembly process. This is the vital prerequisite for the identification of novel assembly factors introduced by shot-gun complementation approaches by perhaps only incremental advances in the assembly process. Nevertheless, in light of the tremendously fast progress in sequencing, gene-synthesis and gene-editing technologies, such synthetic biology-related approaches will sooner or later enrich the field of thylakoid assembly research.

FUNDING

This work was funded by a grant from the Ludwig-Maximilians-University (LMUexcellent) and by the German Science Foundation (DFG, grant LE 1265/20-1).

ACKNOWLEDGMENTS

We thank Paul Hardy for critical comments on the manuscript.

REFERENCES

Ajjawi, I., Lu, Y., Savage, L. J., Bell, S. M., and Last, R. L. (2010). Large-scale reverse genetics in *Arabidopsis*: case studies from the Chloroplast 2010 Project. *Plant Physiol.* 152, 529–540. doi: 10.1104/pp.109.148494

Allen, J. F., de Paula, W. B. M., Puthiyaveetil, S., and Nield, J. (2011). A structural phylogenetic map for chloroplast photosynthesis. *Trends Plant Sci.* 16, 645–655. doi: 10.1016/j.tplants.2011.10.004

Armbruster, U., Zühlke, J., Rengstl, B., Kreller, R., Makarenko, E., Rühle, T., et al. (2010). The *Arabidopsis* thylakoid protein PAM68 is required for efficient D1 biogenesis and Photosystem II assembly. *Plant Cell* 22, 3439–3460. doi: 10.1105/tpc.110.077453

Armisén, D., Lecharny, A., and Aubourg, S. (2008). Unique genes in plants: specificities and conserved features throughout evolution. *BMC Evol. Biol.* 8:280. doi: 10.1186/1471-2148-8-280

Bhuiyan, N. H., Friso, G., Poliakov, A., Ponnala, L., and Van Wijk, K. J. (2015). MET1 is a thylakoid-associated TPR protein involved in Photosystem II supercomplex formation and repair in *Arabidopsis*. *Plant Cell* 27, tpc.114.132787. doi: 10.1105/tpc.114.132787

Braun, P., Aubourg, S., Van Leene, J., De Jaeger, G., and Lurin, C. (2013). Plant protein interactomes. *Annu. Rev. Plant Biol.* 64, 161–187. doi: 10.1146/annurev-arplant-050312-120140

Bricker, T. M., Roose, J. L., Fagerlund, R. D., Frankel, L. K., and Eaton-Rye, J. J. (2012). The extrinsic proteins of Photosystem II. *Biochim. Biophys. Acta* 1817, 121–142. doi: 10.1016/j.bbabio.2011.7.006

Cai, W., Ma, J., Chi, W., Zou, M., Guo, J., Lu, C., et al. (2010). Cooperation of LPA3 and LPA2 is essential for Photosystem II assembly in *Arabidopsis*. *Plant Physiol.* 154, 109–120. doi: 10.1104/pp.110.159558

Dobáková, M., Tichy, M., and Komenda, J. (2007). Role of the PsbI protein in Photosystem II assembly and repair in the cyanobacterium *Synechocystis* sp. PCC 6803. *Plant Physiol.* 145, 1681–1691. doi: 10.1104/pp.107.107805

Fristedt, R., Herdean, A., Blaby-Haas, C. E., Mamedov, F., Merchant, S. S., Last, R. L., et al. (2015). PHOTOSYSTEM II PROTEIN33, a protein conserved

in the plastid lineage, is associated with the chloroplast thylakoid membrane and provides stability to Photosystem II supercomplexes in *Arabidopsis*. *Plant Physiol.* 167, 481–492. doi: 10.1104/pp.114.253336

Fu, A., He, Z., Cho, H. S., Lima, A., Buchanan, B. B., and Luan, S. (2007). A chloroplast cyclophilin functions in the assembly and maintenance of Photosystem II in *Arabidopsis thaliana*. *Proc. Natl. Acad. Sci. U.S.A.* 104, 15947–15952. doi: 10.1073/pnas.0707851104

Hohmann-Marriott, M. F., and Blankenship, R. E. (2011). Evolution of photosynthesis. *Annu. Rev. Plant Biol.* 62, 515–548. doi: 10.1146/annurev-arplant-042110-103811

Ishihara, S., Takabayashi, A., Ido, K., Endo, T., Ifuku, K., and Sato, F. (2007). Distinct functions for the two PsbP-like proteins PPL1 and PPL2 in the chloroplast thylakoid lumen of *Arabidopsis*. *Plant Physiol.* 145, 668–679. doi: 10.1104/pp.107.105866

Järvi, S., Suorsa, M., and Aro, E.-M. (2015). Photosystem II repair in plant chloroplasts—Regulation, assisting proteins and shared components with Photosystem II biogenesis. *Biochim. Biophys. Acta* 1847, 900–909. doi: 10.1016/j.bbabio.2015.01.006

Jin, H., Liu, B., Luo, L., Feng, D., Wang, P., Liu, J., et al. (2014). HYPERSENSITIVE TO HIGH LIGHT1 Interacts with LOW QUANTUM YIELD OF PHOTOSYSTEM II1 and Functions in Protection of Photosystem II from Photodamage in *Arabidopsis*. *Plant Cell* 26, 1213–1229. doi: 10.1105/tpc.113.122424

Kansy, M., Wilhelm, C., and Goss, R. (2014). Influence of thylakoid membrane lipids on the structure and function of the plant Photosystem II core complex. *Planta* 240, 781–796. doi: 10.1007/s00425-014-2130-2

Kato, Y., and Sakamoto, W. (2009). Protein quality control in chloroplasts: a current model of D1 protein degradation in the Photosystem II repair cycle. *J. Biochem.* 146, 463–469. doi: 10.1093/jb/mvp073

Klinkert, B., Ossenbühl, F., Sikorski, M., Berry, S., Eichacker, L., and Nickelsen, J. (2004). PratA, a periplasmic tetratricopeptide repeat protein involved in biogenesis of Photosystem II in *Synechocystis* sp. PCC 6803. *J. Biol. Chem.* 279, 44639–44644. doi: 10.1074/jbc.M405393200

Komenda, J., Nickelsen, J., Tichı, M., Prášil, O., Eichacker, L. A., and Nixon, P. J. (2008). The cyanobacterial homologue of HCF136/YCF48 is a component of an early Photosystem II assembly complex and is important for both the efficient assembly and repair of Photosystem II in *Synechocystis* sp. PCC 6803. *J. Biol. Chem.* 283, 22390–22399. doi: 10.1074/jbc.M801917200

Komenda, J., Reisinger, V., Müller, B. C., Dobáková, M., Granvogl, B., and Eichacker, L. A. (2004). Accumulation of the D2 Protein is a key regulatory step for assembly of the Photosystem II reaction center complex in *Synechocystis* PCC 6803. *J. Biol. Chem.* 279, 48620–48629. doi: 10.1074/jbc.M405725200

Lima, A., Lima, S., Wong, J. H., Phillips, R. S., Buchanan, B. B., and Luan, S. (2006). A redox-active FKBP-type immunophilin functions in accumulation of the Photosystem II supercomplex in *Arabidopsis thaliana*. *Proc. Natl. Acad. Sci. U.S.A.* 103, 12631–12636. doi: 10.1073/pnas.0605452103

Lu, Y., Hall, D. A., and Last, R. L. (2011). A small zinc finger thylakoid protein plays a role in maintenance of Photosystem II in *Arabidopsis thaliana*. *Plant Cell* 23, 1861–1875. doi: 10.1105/tpc.111.085456

Ma, J., Peng, L., Guo, J., Lu, Q., Lu, C., and Zhang, L. (2007). LPA2 is required for efficient assembly of Photosystem II in *Arabidopsis thaliana*. *Plant Cell* 19, 1980–1993. doi: 10.1105/tpc.107.050526

Meurer, J., Meierhoff, K., and Westhoff, P. (1996). Isolation of high-chlorophyll-fluorescence mutants of *Arabidopsis thaliana* and their characterisation by spectroscopy, immunoblotting and northern hybridisation. *Planta* 198, 385–396. doi: 10.1007/BF00620055

Meurer, J., Plücken, H., Kowallik, K. V., and Westhoff, P. (1998). A nuclear-encoded protein of prokaryotic origin is essential for the stability of Photosystem II in *Arabidopsis thaliana*. *EMBO J.* 17, 5286–5297. doi: 10.1093/emboj/17.18.5286

Mizusawa, N., and Wada, H. (2012). The role of lipids in Photosystem II. *Biochim. Biophys. Acta* 1817, 194–208. doi: 10.1016/j.bbabio.2011.04.008

Müller, B., and Eichacker, L. A. (1999). Assembly of the D1 precursor in monomeric Photosystem II reaction center precomplexes precedes chlorophyll *a*-triggered accumulation of reaction center II in barley etioplasts. *Plant Cell* 11, 2365–2377. doi: 10.1105/tpc.11.12.2365

Nanba, O., and Satoh, K. (1987). Isolation of a Photosystem II reaction center consisting of D-1 and D-2 polypeptides and cytochrome b-559. *Proc. Natl. Acad. Sci. U.S.A.* 84, 109–112. doi: 10.1073/pnas.84.1.109

Nickelsen, J., and Rengstl, B. (2013). Photosystem II assembly: from cyanobacteria to plants. *Annu. Rev. Plant Biol.* 64, 609–635. doi: 10.1146/annurev-arplant-050312-120124

Nixon, P. J., Michoux, F., Yu, J., Boehm, M., and Komenda, J. (2010). Recent advances in understanding the assembly and repair of Photosystem II. *Ann. Bot.* 106, 1–16. doi: 10.1093/aob/mcq059

Peng, L., Ma, J., Chi, W., Guo, J., Zhu, S., Lu, Q., et al. (2006). LOW PSII ACCUMULATION1 is involved in efficient assembly of Photosystem II in *Arabidopsis thaliana*. *Plant Cell* 18, 955–969. doi: 10.1105/tpc.105.037689

Ramey, C. J., Barón-Sola, Á., Aucoin, H. R., and Boyle, N. R. (2015). Genome engineering in cyanobacteria: where we are and where we need to go. *ACS Synth. Biol.* 4, 1186–1196. doi: 10.1021/acssynbio.5b00043

Schottkowski, M., Ratke, J., Oster, U., Nowaczyk, M., and Nickelsen, J. (2009). Pitt, a novel tetratricopeptide repeat protein involved in light-dependent chlorophyll biosynthesis and thylakoid membrane biogenesis in *Synechocystis* sp. PCC 6803. *Mol. Plant* 2, 1289–1297. doi: 10.1093/mp/ssp075

Shen, J.-R. (2015). The structure of Photosystem II and the mechanism of water oxidation in photosynthesis. *Annu. Rev. Plant Biol.* 66, 23–48. doi: 10.1146/annurev-arplant-050312-120129

Sirpiö, S., Khrouchtchova, A., Allahverdiyeva, Y., Hansson, M., Fristedt, R., Vener, A. V., et al. (2008). AtCYP38 ensures early biogenesis, correct assembly and sustenance of Photosystem II. *Plant J.* 55, 639–651. doi: 10.1111/j.1365-313X.2008.03532.x

Stengel, A., Gügel, I. L., Hilger, D., Rengstl, B., Jung, H., and Nickelsen, J. (2012). Initial steps of Photosystem II de novo assembly and preloading with manganese take place in biogenesis centers in *Synechocystis*. *Plant Cell* 24, 660–675. doi: 10.1105/tpc.111.093914

Umena, Y., Kawakami, K., Shen, J.-R., and Kamiya, N. (2011). Crystal structure of oxygen-evolving Photosystem II at a resolution of 1.9Å. *Nature* 473, 55–60. doi: 10.1038/nature09913

Varotto, C., Pesaresi, P., Maiwald, D., Kurth, J., Salamini, F., and Leister, D. (2000). Identification of photosynthetic mutants of *Arabidopsis* by automatic screening for altered effective quantum yield of Photosystem 2. *Photosynthetica* 38, 497–504. doi: 10.1023/A:1012445020761

Viola, S., Rühle, T., and Leister, D. (2014). A single vector-based strategy for marker-less gene replacement in *Synechocystis* sp. PCC 6803. *Microb. Cell Fact.* 13:4. doi: 10.1186/1475-2859-13-4

Wei, L., Guo, J., Ouyang, M., Sun, X., Ma, J., Chi, W., et al. (2010). LPA19, a Psb27 homolog in *Arabidopsis thaliana*, facilitates D1 protein precursor processing during PSII biogenesis. *J. Biol. Chem.* 285, 21391–21398. doi: 10.1074/jbc.M110.105064

Yang, H., Liao, L., Bo, T., Zhao, L., Sun, X., Lu, X., et al. (2014). Slr0151 in *Synechocystis* sp. PCC 6803 is required for efficient repair of Photosystem II under high-light condition. *J. Integr. Plant Biol.* 56, 1136–1150. doi: 10.1111/jipb.12275

Zhang, D., Zhou, G., Liu, B., Kong, Y., Chen, N., Qiu, Q., et al. (2011). HCF243 encodes a chloroplast-localized protein involved in the D1 protein stability of the *Arabidopsis* Photosystem II complex. *Plant Physiol.* 157, 608–619. doi: 10.1104/pp.111.183301

Conflict of Interest Statement: The authors declare that the research was conducted in the absence of any commercial or financial relationships that could be construed as a potential conflict of interest.

frontiers in Plant Science

ORIGINAL RESEARCH
published: 12 May 2016
doi: 10.3389/fpls.2016.00648

Strain of Synechocystis PCC 6803 with Aberrant Assembly of Photosystem II Contains Tandem Duplication of a Large Chromosomal Region

Martin Tichý[1,2], *Martina Bečková*[1,2], *Jana Kopečná*[1], *Judith Noda*[1], *Roman Sobotka*[1,2] *and Josef Komenda*[1,2]*

[1] *Laboratory of Photosynthesis, Institute of Microbiology, Academy of Sciences of the Czech Republic, Center Algatech, Třeboň, Czech Republic,* [2] *Faculty of Science, University of South Bohemia, České Budějovice, Czech Republic*

Cyanobacterium *Synechocystis* PCC 6803 represents a favored model organism for photosynthetic studies. Its easy transformability allowed construction of a vast number of *Synechocystis* mutants including many photosynthetically incompetent ones. However, it became clear that there is already a spectrum of *Synechocystis* "wild-type" substrains with apparently different phenotypes. Here, we analyzed organization of photosynthetic membrane complexes in a standard motile Pasteur collection strain termed PCC and two non-motile glucose-tolerant substrains (named here GT-P and GT-W) previously used as genetic backgrounds for construction of many photosynthetic site directed mutants. Although, both the GT-P and GT-W strains were derived from the same strain constructed and described by Williams in 1988, only GT-P was similar in pigmentation and in the compositions of Photosystem II (PSII) and Photosystem I (PSI) complexes to PCC. In contrast, GT-W contained much more carotenoids but significantly less chlorophyll (Chl), which was reflected by lower level of dimeric PSII and especially trimeric PSI. We found that GT-W was deficient in Chl biosynthesis and contained unusually high level of unassembled D1-D2 reaction center, CP47 and especially CP43. Another specific feature of GT-W was a several fold increase in the level of the Ycf39-Hlip complex previously postulated to participate in the recycling of Chl molecules. Genome re-sequencing revealed that the phenotype of GT-W is related to the tandem duplication of a large region of the chromosome that contains 100 genes including ones encoding D1, Psb28, and other PSII-related proteins as well as Mg-protoporphyrin methylester cyclase (Cycl). Interestingly, the duplication was completely eliminated after keeping GT-W cells on agar plates under photoautotrophic conditions for several months. The GT-W strain without a duplication showed no obvious defects in PSII assembly and resembled the GT-P substrain. Although, we do not exactly know how the duplication affected the GT-W phenotype, we hypothesize that changed stoichiometry of protein components of PSII and Chl biosynthetic machinery encoded by the duplicated region impaired properassembly and functioning of these multi-subunit complexes. The study also emphasizes the crucial importance of a proper control strain for evaluating *Synechocystis* mutants.

Keywords: ***Synechocystis*** **6803, chlorophyll, photosystem I, photosystem II assembly, large tandem duplication**

OPEN ACCESS

Edited by:
John Love,
University of Exeter, UK

Reviewed by:
Alessandro Vitale,
CNR–National Research Council of Italy, Italy
Ben Matthew Abell,
Sheffield Hallam University, UK

***Correspondence:**
Josef Komenda
komenda@alga.cz

Specialty section:
This article was submitted to Plant Cell Biology, a section of the journal Frontiers in Plant Science

Received: *14 December 2015*
Accepted: *28 April 2016*
Published: *12 May 2016*

Citation:
Tichý M, Bečková M, Kopečná J, Noda J, Sobotka R and Komenda J (2016) Strain of Synechocystis PCC 6803 with Aberrant Assembly of Photosystem II Contains Tandem Duplication of a Large Chromosomal Region. Front. Plant Sci. 7:648. doi: 10.3389/fpls.2016.00648

INTRODUCTION

Cyanobacteria represent excellent model organisms for photosynthesis research as they perform oxygenic photosynthesis similar to that in algae and plants while having much simpler cellular organization. Unlike the other photosynthetic bacteria they possess both types of reaction center and oxidize water to molecular oxygen by Photosystem II (PSII) and reduce NADP by Photosystem I (PSI). For both pigment-protein complexes the high resolution crystal structures are available, mostly thanks to thermophilic cyanobacteria with very stable complexes ideal for crystallographic analysis (Jordan et al., 2001; Ferreira et al., 2004; Umena et al., 2011).

PSII is the multi-subunit membrane complex that utilizes light energy to catalyze oxidation of water. For this process to occur the inner symmetrically located antennae CP47 and CP43 containing chlorophyll (Chl) and β-carotene deliver absorbed light energy to a pair of reaction center (RCII) subunits called D1 and D2, which bind the cofactors involved in primary charge separation. There are also around 13 small, mostly single helix trans-membrane subunits mostly bound at the periphery of D1, D2, CP47, and CP43 (Ferreira et al., 2004; Guskov et al., 2009; Umena et al., 2011). The lumenal part of the complex is the binding site for the PsbO, PsbU, and PsbV extrinsic subunits (reviewed in Roose et al., 2007) which optimize the environment for the $CaMn_4O_5$ cluster extracting electrons from water (Ferreira et al., 2004; Guskov et al., 2009; Umena et al., 2011).

Information on the biogenesis of cyanobacterial PSII is less complete and mostly comes from characterization of this process in the cyanobacterium *Synechocystis* PCC 6803 (hereafter *Synechocystis*). This cyanobacterial strain is able to grow in the presence of glucose even without functional PSII and is therefore appropriate for constructing site-directed mutants affected in its assembly (Williams, 1988). Existing data indicate that each large Chl-protein initially forms a pre-complex (module) containing neighboring low-molecular-mass polypeptides plus pigments and cofactors. These modules are afterwards combined in a step-wise fashion initially into the PSII reaction center (RCII) complex consisting of D1 and D2 modules, then CP47 module is attached forming a complex called RC47 (Boehm et al., 2011, 2012). Finally the PSII core complex is completed after binding of the CP43 module (Boehm et al., 2011). The light-driven assembly of the oxygen-evolving $CaMn_4O_5$ cluster occurs afterwards and is assisted by the lumenal extrinsic proteins (Nixon et al., 2010). Accessory factors, such as Ycf39, Ycf48, Psb27, Psb28, and others, associate transiently with PSII at specific stages of assembly but their functions remain unclear (Komenda et al., 2012b).

Availability of high-throughput sequencing techniques allowed genomic sequence comparison among various WT-variants (substrains) of *Synechocystis* used in many laboratories and revealed inherent sequence variability among them. The history of the *Synechocystis* WT-variants has been described recently (Morris et al., 2014). The original motile Pasteur Culture Collection 6803 strain has been used to generate a non-motile, glucose tolerant strain (Williams, 1988). This strain has been disseminated to several laboratories around the world, resulting in many "wild-type" substrains.

In the present study we compared organization of photosynthetic membrane complexes with emphasis on PSII assembly in three *Synechocystis* substrains, two of them variants of the Williams glucose-tolerant strain. The comparison showed that the level and assembly state of PSII (and PSI) in the glucose-tolerant strain obtained from the laboratory at Imperial College London was similar to that in the standard motile Pasteur Culture collection strain (PCC). In contrast, the glucose tolerant strain originating from the strain used in the Arizona lab of Wim Vermaas showed aberrant assembly of PSII, much lower level of PSI related to the decreased synthesis of Chl and high content of carotenoids. Sequencing of the latter strain showed that its genome contains a tandem duplication of a large chromosomal region, most probably responsible for the observed phenotype.

EXPERIMENTAL PROCEDURES

Strains, Their Origin, Construction, and Cultivation

The strains used in this study were the motile, glucose sensitive strain of *Synechocystis* sp. PCC 6803 from the Pasteur collection, and two glucose-tolerant strains (Williams, 1988): GT-P obtained from the laboratory of Prof. Peter Nixon at Imperial College London and GT-W obtained from the laboratory of Prof. Wim Vermaas at Arizona State University. Frozen stocks of GT-P from 2002 and GT-W from 1999 were used for characterization and sequencing. The Psb28-lacking strains were transformed using genomic DNAs isolated from a previously constructed Psb28-less strain (Dobáková et al., 2009). *Synechocystis* strains were grown autotrophically in a rotary shaker under irradiance of 40 μmol photons m^{-2} s^{-1} at 30°C in liquid BG11 medium (Rippka et al., 1979). All experiments and measurements with cells were performed at least in triplicate and typical results are shown in figures.

Cell Absorption Spectra and Determination of Chl Content

Absorption spectra of whole cells were measured at room temperature using a Shimadzu UV-3000 spectrophotometer (Kyoto, Japan). To determine Chl levels, pigments were extracted from cell pellets with 100% methanol and the Chl concentration was determined spectroscopically (Porra et al., 1989).

Determination of Chromosomes Number by Flow Cytometry

Single colonies of GT-P and GT-W strains were inoculated in 50 ml of BG11 medium and grown under standard conditions until they reached a final $OD_{730\,nm}$ value 0.3–0.5. Two milliliters of cells were collected by centrifugation at 8000 × g for 5 min and washed once with fresh media. Collected cells were fixed with 1 ml of 70% ethanol and incubated for 1 h at room temperature. In order to remove residual fixation solution, cells

were washed twice with PBS buffer and resuspended in 100 µl of the same buffer. One microliter of RNAase A was added and samples were incubated for 1 h at 37°C. After enzymatic degradation of RNA, 900 µl of PBS were added, and cells were stained for 20 min in darkness with the cell permeant fluorochrome SYBR Safe (Life Technologies), used in a 1:10,000 dilution of commercial stock. To prepare the reference, with one chromosome per cell a single colony of *Escherichia coli (E. coli)* strain BL-21 was inoculated in 2 ml of M9 minimal media. The culture was grown overnight at 37°C and then supplemented with 20 µg ml^{-1} of chloramphenicol. After 1.5 h of growth in the presence of antibiotic, cells were harvested by centrifugation at 8000 × g for 5 min and fixed and stained by the same method used for *Synechocystis* cells. *Synechocystis* and *E. coli* stained cells were loaded on an APOGEE cytometer (Apogee Flow Systems), and at least 20,000 events were recorded. Samples were excited using a 488 nm laser and the fluorescence emission was collected by a detector with a 530/30 nm filter. The chromosome copy number of *Synechocystis* strains was estimated using the chloramphenicol-treated *E. coli* culture as a standard.

Analysis of Pigments by HPLC

For quantitative determination of Chl precursors, three milliliters of culture at $OD_{750\,nm}$ = 0.5–0.6 was spun down and resuspended in 20 µL of water. Pigments were extracted with an excess of 70% methanol/30% water, filtrated and immediately analyzed via HPLC (Agilent-1200). Separation was carried out on a reverse phase column (ReproSil pur 100, C8, 3 µm particle size, 4 × 150 mm, Watrex) with 35% methanol and 15% acetonitrile in 0.25 M pyridine (solvent A) and 50% methanol in acetonitrile as solvents B. Pigments were eluted with a gradient of solvent B (40%–52% in 5 min) followed by 52–55% of solvent B in 30 min at a flow rate of 0.8 ml min^{-1} at 40°C. Eluted pigments were detected by two fluorescence detectors set at several different wavelengths to detect all Chl precursors from coproporphyrin(ogen) III (Copro III) to monovinyl-chlorophyllide (Chlide); for details see Kopečná et al. (2015)

2D Electrophoresis, Immunodetection, and Protein Radiolabeling

Membrane and soluble protein fractions were isolated from 50 ml of cells at $OD_{750\,nm}$ ~0.4 according to Dobáková et al. (2009) using buffer A (25 mM MES/NaOH, pH 6.5, 5 mM $CaCl_2$, 10 mM $MgCl_2$, 25% glycerol). Isolated membrane complexes (0.25 mg ml^{-1} Chl) were solubilized in buffer A containing 1% n-dodecyl-β-D-maltoside and analyzed either by blue-native (BN) or by clear-native (CN) PAGE at 4°C in a 4–14% gradient polyacrylamide as described in Komenda et al. (2012a). The protein composition of the complexes were analyzed by electrophoresis in a denaturing 12–20% linear gradient polyacrylamide gel containing 7 M urea (Komenda et al., 2012a). Proteins separated in the gel were stained by SYPRO Orange and the gel was either dried and exposed on a Phosphorimager plate or blotted onto a PVDF membrane. Membranes were incubated with specific primary antibodies and then with secondary antibody-horseradish peroxidase conjugate (Sigma, St. Louis, USA). The primary antibodies used in this study were raised in rabbits against: (i) residues 58–86 of the spinach D1 polypeptide; (ii) residues 311-322 of Ycf39 (Knoppová et al., 2014); and (iii) the last 15 residues of *Synechocystis* Psb28 (Dobáková et al., 2009). Antibody against *Synechocystis* ferrochelatase was kindly provided by Prof. Annegret Wilde (Albert Ludwigs Universität, Freiburg) and antibody against barley Mg-protoporphyrin methyl ester oxidative cyclase was kindly provided by Prof. Poul Erik Jensen (University of Copenhagen).

For protein and Chl labeling, the cells were incubated with [^{14}C]glutamate for 30 min as described in Kopečná et al. (2012). After separation of labeled proteins by CN PAGE in the first dimension and by SDS PAGE in the second dimension the 2D 18% polyacrylamide gel was stained by SYPRO Orange, scanned for fluorescence and dried. The gel was exposed on a Phosphorimager plate overnight, scanned by Storm and, for evaluation of Chl labeling, the image was quantified by ImageQuant 5.2 software (all from GE Healthcare, Vienna, Austria).

Genome Re-Sequencing and Mapping

Synechocystis re-sequencing was performed commercially at the Gene Profiling Facility, Princess Margaret Hospital, Toronto. One hundred base paired-end sequencing was performed on a Illumina HiSeq 2000 system (12 samples per lane). Raw paired reads were mapped to the GT-Kazusa sequence using Geneious 7.0 software (http://www.geneious.com; Kearse et al., 2012). Only variants with a higher than 60% frequency were considered. Alternatively, read sequences were assembled *de novo* with the Geneious 7.0 software before mapping to the reference.

RESULTS

Three Variants of the *Synechocystis* Wild Type Strain: Their History and Organization of Photosynthetic Complexes

We compared three *Synechocystis* strains that are used in our laboratory for construction of various, mostly photosynthetic mutants. While the glucose sensitive motile strain, designated here PCC, was directly obtained from Pasteur Culture Collection, the other two strains originated from the glucose-tolerant Williams strain (Williams, 1988). The first one, which we named GT-P, was first grown in the Dupont laboratory of Bruce Diner from which it was transferred to Imperial College (London) and later to our laboratory in Třeboň (Institute of Microbiology, Czech Academy of Sciences). The second one, named GT-W, came from the laboratory of Wim Vermaas (Arizona State University).

Comparison of absorption spectra of the three strains grown autotrophically showed a large similarity between the PCC and GT-P, with the only apparent difference being a higher

phycobilisome content (maximum at 625 nm) in PCC (**Figure 1**). On the other hand, the GT-W strain contained much more carotenoids and less Chl than both previously mentioned strains. Interestingly, when both strains were grown in the presence of 5 mM glucose, in both strains the amount of carotenoids decreased but the level of Chl decreased only in GT-P while in GT-W it increased (Figure S1).

The differences in cellular absorption spectra of autotrophic cultures were also reflected by differences in the content of photosynthetic membrane complexes assessed by 2D blue-native/SDS-PAGE (**Figure 2**). In this respect PCC and GT-P were very similar containing the majority of PSI and PSII as trimers and dimers, respectively, and relatively low levels of the monomeric PSII core complex and CP43-less PSII (RC47). The strains also contained only very low amounts of unassembled CP47 and CP43 and no detectable antenna-less RCII complexes. In contrast, unusually high amounts of unassembled CP47 and especially CP43 were detected in the GT-W strain. Immunoblotting also revealed accumulation of RCII complexes and a concomitant several fold increase in the amount of Ycf39 detected as a component of a larger of two RCII complexes (RCII*) and especially as the unassembled complex with Hlips (Knoppová et al., 2014). Moreover, the levels of PSI trimer and PSII dimers were similar to the levels of their monomeric forms. Finally, cytochrome b_6f complex was present in PCC and GT-P almost exclusively as a monomer while almost equal amounts of dimer and monomer was detected in GT-W. In summary, the strain GT-W showed unusual pigment-protein composition different from the other two strains suggesting aberrant assembly of photosynthetic complexes, namely PSII, and their lower cellular content.

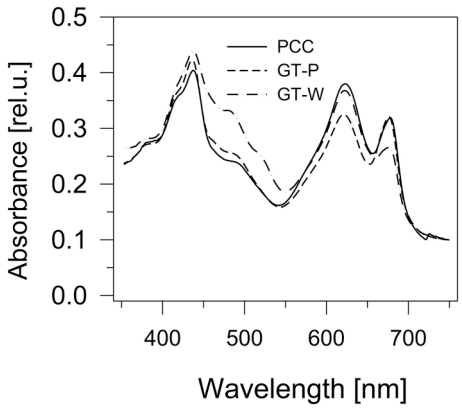

FIGURE 1 | Whole cell absorption spectra of three *Synechocystis* strains PCC, GT-P, and GT-W. The spectra were measured by Shimadzu UV3000 spectrophotometer and were normalized for absorbance of 0.1 at 750 nm.

Chlorophyll Biosynthesis is Strongly Affected in GT-W

As the trimeric PSI complex is the main sink for newly produced Chl molecules in *Synechocystis* (Kopečná et al., 2012), the low PSI level in cells of GT-W should be reflected by changes in Chl metabolism. To assess the rate of *de novo* Chl formation we labeled cells of both GT strains using [^{14}C]glutamate and analyzed Ch-binding membrane complexes using 2D clear-native/SDS-PAGE. In order to separate free pigments from

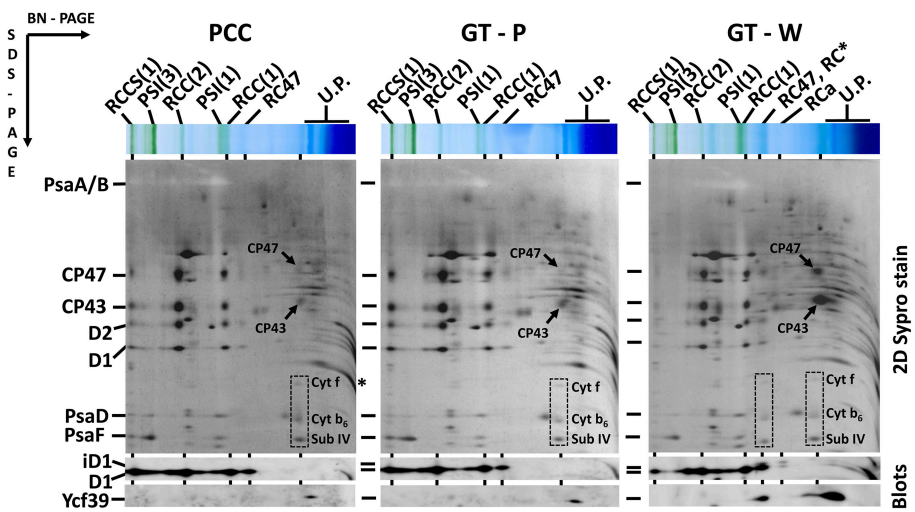

FIGURE 2 | Organization of photosynthetic membrane complexes in PCC, GT-P, and GT-W strains assessed by 2D blue-native/SDS-PAGE in combination with immunoblotting. Membrane proteins of thylakoids isolated from each strain were separated by 4–14% blue-native PAGE, and then in the second dimension by 12–20% SDS-PAGE. The 2D gel was stained by SYPRO Orange and then blotted to a PVDF membrane. The D1 and Ycf39 proteins were detected by specific antibodies (Blots). Unassembled CP47 and CP43 are designated by arrows and subunits of cyt b_6–f complex (Cyt f, cyt b_6, and subunit IV in order from top to bottom) are boxed. Other designations: RCCS1, PSI–PSII supercomplex; RCC(2), and RCC(1), dimeric, and monomeric PSII core complexes; PSI(3) and PSI(1), trimeric and monomeric PSI; RC47, PSII core complex lacking CP43; RC* and RCa, PSII reaction center complexes lacking CP47 and CP43; U.P., unassembled proteins. Arrows indicate unassembled forms of CP47 and CP43 very abundant in GT-W. Each loaded sample contained 5 μg of Chl.

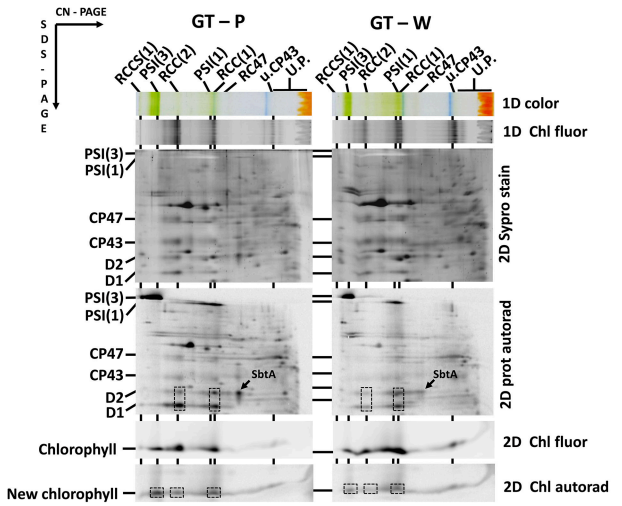

FIGURE 3 | Radiolabeling of membrane proteins and chlorophyll in the GT-P and GT-W strains. Cells of each strain were radiolabeled by [^{14}C]glutamate. Membrane proteins and pigments were then separated by 2D clear-native/SDS-PAGE. Pigment-protein complexes were separated by 2D CN/SDS-PAGE. The first dimension 4-14% native gel was photographed (1D color) and scanned for fluorescence by LAS 4000 (1D Chl fluor). The second dimension 18% SDS PAGE gel was stained with SYPRO (2D SYPRO stain) and scanned for Chl fluorescence (2D Chl fluor). Radioactivity in proteins (2D prot autorad) and in released Chl (2D Chl Autorad) in dried gels was detected by Phosphoimager. The overall signal of the labeled Chl in GT-W quantified by Image Quant software was 37 ± 9% of that in GT-P. The value represents a mean ± SD from three independent measurements. The most important differences between the strains in the amounts of labeled protein (monomeric and dimeric PSII complexes) and Chl (PSI trimer and monomer and PSII dimer) are emphasized by boxes. The labeling of SbtA is also designated by an arrow. Each loaded sample contained 5 μg of Chl. All designations used are described in **Figure 2**.

proteins, we performed 2D protein analysis in the 18% gel, which was briefly stained by SYPRO Orange, scanned for Chl and SYPRO fluorescence and then immediately dried up to retain maximal amounts of free pigments in the gel. In agreement with work of Kopečná et al. (2012) most of the labeled Chl in GT-P was bound to trimeric PSI. However, in GT-W the signals of labeled Chl incorporated into the PSI trimer and PSII dimer were much weaker (**Figure 3**, lower boxes). Labeling in the abundant PSI monomer was also lower in GT-W. Overall, the total signal of labeled Chl in GT-W was <40% of that in GT-P, which demonstrated a significantly reduced rate of *de novo* Chl formation in the GT-W substrain. Since [^{14}C]glutamate also labeled proteins, autoradiogram of the whole gel provided information about synthesis of membrane proteins. GT-W showed a typical protein labeling pattern with intensive labeling of D1 and much lower labeling of D2, CP43, and CP47 in both PSII core monomers and dimers. In contrast, the intensity of D1 and D2 labeling in the PSII core complexes of GT-W was similar but labeling of both proteins in the PSII dimer was much lower than in the monomer and in GT-P (**Figure 3**, middle boxes). Interestingly, the labeling of SbtA, a bicarbonate transporter, was also much lower in GT-W indicating an inability of the strain to actively induce import of anorganic carbon for CO_2 fixation (**Figure 3**, arrows).

To further support the conclusion about inhibition of Chl biosynthesis in GT-W, we compared levels of later Chl biosynthesis precursors in GT-P and GT-W (**Figure 4**). HPLC analysis confirmed that in GT-W the levels of most intermediates were strongly decreased. Only the level of coproporhyrin(ogen) III (copro III) in GT-W was rather similar to that in GT-P suggesting either a block in the subsequent formation of protoporphyrinogen IX and protoporphyrin IX (PP_{IX}) or, alternatively, a fast consumption of PP_{IX} by the heme branch of the tetrapyrrole biosynthesis pathway.

Genomic Sequencing Revealed Duplication of a Large Part of GT-W Chromosome

To explore the genetic basis for the observed aberrant assembly of photosynthetic complexes and decreased Chl biosynthesis, we performed whole genome re-sequencing of both GT strains on a commercial basis, using the Illumina HiSeq platform. Although, the sequence of the original Williams strain is not available, it can be interpolated from the published sequences of the GT strains. Our sequencing supports a common origin of both GT-P and GT-W strains from the Williams GT strain. The GT-P and GT-W strains shared one mutation while containing one and four additional specific mutations respectively (**Table 1**). In addition to the point mutations detected directly by mapping of the reads to the reference sequence, we observed that one part of the GT-W chromosome exhibited approximately twofold coverage of reads. Interestingly, this large 110 kbp region was bordered by ISY100 transposases, sll0431 and sll1397, sharing 100% identity at the DNA level (**Figure 5**, Table S1). It indicates that this part of the genome was duplicated, possibly in the form of a tandem repeat. Indeed, the presence of such tandem duplication was confirmed by PCR with outbound primers from the beginning and end of the duplication (Figure S2). The duplicated region contained 100 genes (Table S1) including those encoding PSII components (D1 protein) and its assembly factors (e.g., Psb28), which could possibly be related to the aberrant PSII assembly observed in the GT-W strain.

Interestingly, the characteristics of the GT-W strain spontaneously changed when repeatedly restreaked on plates without glucose and under moderate light conditions (30 μmol photons s^{-1} m^{-2}) for several months. The strain gradually attained a pigment composition similar to GT-P (**Figure 6**) and also the pattern of membrane protein complexes became similar to that in GT-P with disappearance of most of the unassembled CP43, CP47, and RCII∗ and an increase in the level of PSI trimer (**Figure 7**). This strain also contained lower levels of Ycf39, Psb28, HemH, and Cycl in comparison with GT-W (**Figure 7**). PCR analysis showed that this revertant strain, designated GT-Wrev, lost the duplication (Figure S2) indicating that it is responsible for most of the Chl-deficient phenotype of GT-W.

Since the observed duplication of part of the genome could be a compensatory mechanism for a lower number of genome copies in the GT-W strain, we also compared the number

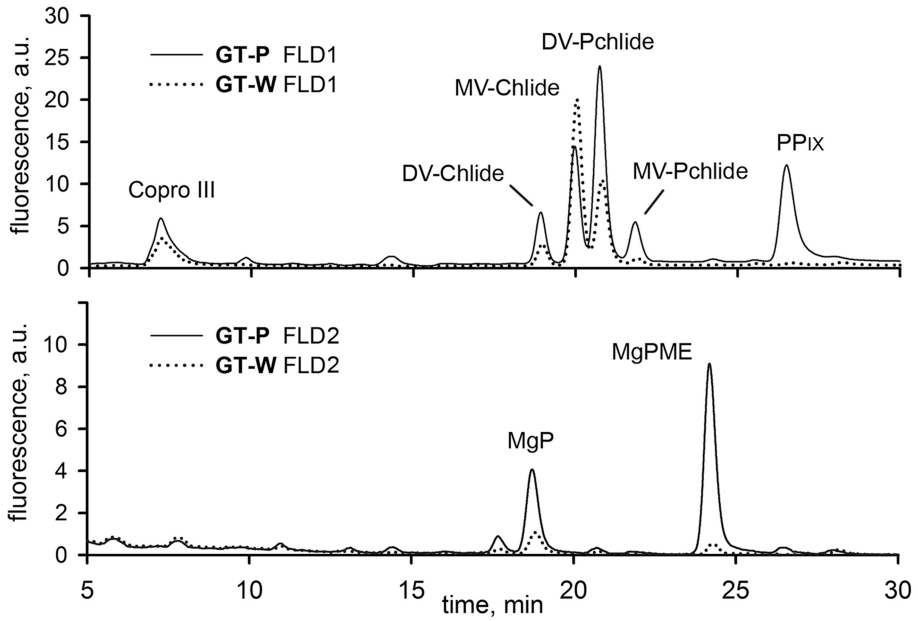

FIGURE 4 | HPLC chromatograms of chlorophyll biosynthesis precursors in GT-P and GT-W strains. Cells of both strains were extracted with 70% methanol and Chl precursors were quantified by HPLC equipped with two fluorescence detectors (FLD1 and FLD2). Each detector was set to wavelengths selected to detect indicated Chl precursors (see Experimental Procedures). Copro III, coproporhyrin(ogen) III; DV-Chlide, divinyl chlorophyllide; DV-Pchlide, divinyl protochlorophyllide; PP_{IX}, protoporphyrin IX; MgP, Mg-protoporphyrin IX; MgPME, Mg-protoporphyrin methylester; MV-Chlide, monovinyl chlorophyllide; MV-Pchlide, monovinyl protochlorophyllide.

TABLE 1 | List of specific mutations in GT-P and GT-W strains.

Base position	Type	Mutated nucleotide	Amino acid change	Gene ID	Annotation	Gene product
GT-P						
488230	SNP	T→G	F255C	*slr1609*	*fadD*	long-fatty-acid CoA ligase
842060	SNP	C→T	R186Q	*sll1799*	*rpl3*	50S ribosomal protein L3
GT-W						
488268	SNP	G→A	V268I	*slr1609*	*fadD*	long-fatty-acid CoA ligase
842060	SNP	G→T	R186Q	*sll1799*	*rpl3*	50S ribosomal protein L3
2354038	Del	5326 bp del	E283Q	*slr0364*	*swmB*	cell surface protein
2780356	SNP	G→C	E283Q	*slr0906*	*psbB*	CP47 protein of PSII
3297450	SNP	C→T	L216 silent	*sll1367*	–	hypothetical protein

Base position refers to the GT-Kazusa sequence.

of chromosomes in both strains. DNA content was assessed using flow cytometry after staining by SYBR Safe and the copy-number calibrated using *E. coli* cells (see Experimental Procedures). **Figure 8** shows that both strains similarly contain 7–11 chromosome copies per cell.

Psb28 Deletion Mutant Constructed in the GT-W Background Shows More Pronounced Phenotype

Previously, Dobáková et al. (2009) has shown a partial Chl deficiency in the Psb28-less strain, causing inhibition of CP47 and PSI synthesis. This strain was constructed in the GT-W background. In contrast, a subsequent study of Sakata et al. (2013) has not confirmed this phenotypic manifestation and the Psb28-less mutant, which has been constructed in WT background closely related to our GT-P strain and has not exhibited lower cellular Chl level. Since the different phenotypes of the mutants could be caused by a different genetic background of the mutants, we tested this possibility by deleting the *psb28* gene in both the GT-P and GT-W strains. *In vivo* absorption spectra of both mutants were then compared with the original control strains (**Figure 9**). The spectrum of the mutant constructed in the GT-P background was indistinguishable from the control, while the GT-W-based mutant showed a lower Chl level as well as much more carotenoids than the control. We also compared the composition of the membrane protein complexes of GT-W and the derived Psb28-less mutant (**Figure 10**). The

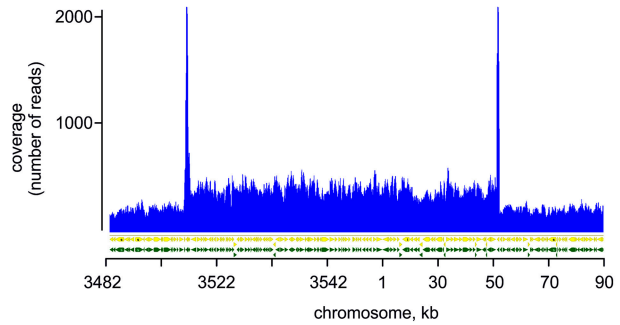

FIGURE 5 | Mapping of reads on the duplicated region of GT-W chromosome. Paired-end reads from Illumina sequencing of the GT-W genome mapped on the reference *Synechocystis* genome (see Experimental Procedures). The read coverage is roughly doubled in the chromosomal region 3520 kb–50 kb; peaks at the border of this region are an artifact of the mapping of reads originating probably from transponase genes located on plasmids.

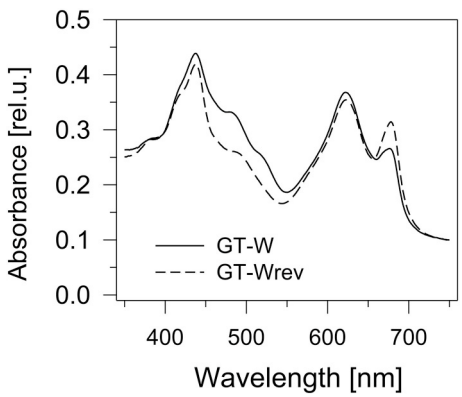

FIGURE 6 | Whole cell absorption spectra of the GT-W strain and its revertant GT-Wrev. The spectra were measured by Shimadzu UV3000 spectrophotometer and normalized for absorbance of 0.1 at 750 nm.

mutant contained higher levels of the RCII complexes and Ycf39, the PSII assembly factor protein which has been proposed to participate in the Chl recycling (Knoppová et al., 2014). The data supported the idea that the differences observed in the two above mentioned studies (Dobáková et al., 2009; Sakata et al., 2013) were caused by the different WT background in which the mutants were constructed.

DISCUSSION

During our previous studies dealing with the biogenesis of photosynthetic membrane complexes in *Synechocystis* we characterized dozens of mutants constructed in different background strains originating from various laboratories. We noticed that mutants constructed in background strains coming from the London laboratory of Peter Nixon and the Arizona laboratory of Wim Vermaas had quite different phenotypes although they both originated from the glucose-tolerant

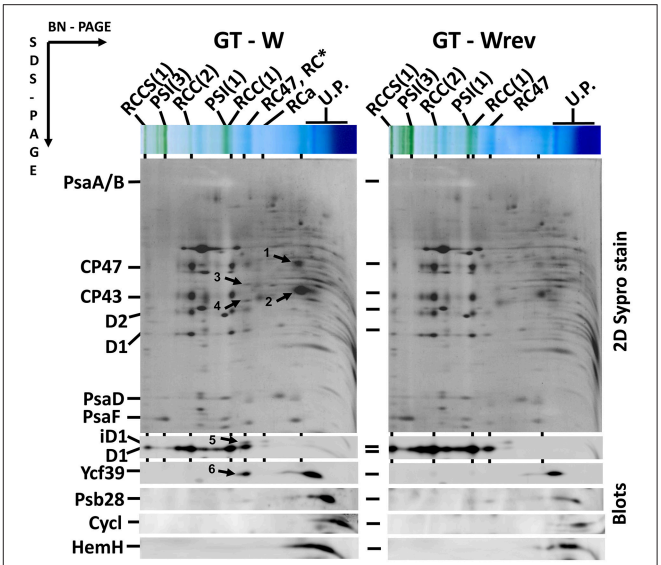

FIGURE 7 | Organization of photosynthetic membrane complexes in the GT-W strain and its revertant GT-Wrev assessed by 2D blue-native/SDS-PAGE in combination with immunoblotting. Membrane proteins of thylakoids isolated from each strain were separated by 4–14% blue-native PAGE, and then in the second dimension by 12–20% SDS-PAGE. The 2D gel was stained by SYPRO Orange and then blotted to a PVDF membrane. The D1, Ycf39, Psb28, Cycl, and HemH proteins were detected by specific antibodies (Blots). Designations as in **Figure 2**. Arrows indicate unassembled forms of CP47(1) and CP43(2), the Ycf48 (3), and Ycf39 (4, 6) assembly factors, and an intermediate form of D1 (5) in RCII* complex, which are all much more abundant than in GT-Wrev. Each loaded sample contained 5 μg of Chl.

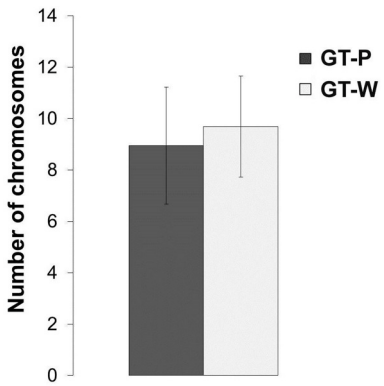

FIGURE 8 | Number of chromosomes detected in the strains GT-P and GT-W. Calculation was done by comparison of the SYBR Safe fluorescence detected by flow cytometry in the both *Synechocystis* strains, using chloramphenicol-treated *E. coli* BL-21 culture as a reference.

Williams substrain (Williams, 1988; Morris et al., 2014). Under photoautotrophic conditions GT-W grew much slower than GT-P (not shown) and the cultures appeared quite different with regard to their cellular spectra, pigment content, and composition of membrane protein complexes. GT-P was in this respect very similar to the glucose sensitive motile PCC strain with minimal amount of unassembled or partially assembled

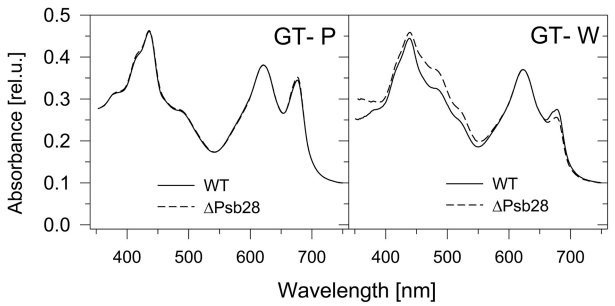

FIGURE 9 | Whole cell absorption spectra of the Psb28-deletion mutants in comparison with their background strains GT-P and GT-W used for their construction. The spectra were measured by Shimadzu UV3000 spectrophotometer and normalized for absorbance of 0.1 at 750 nm.

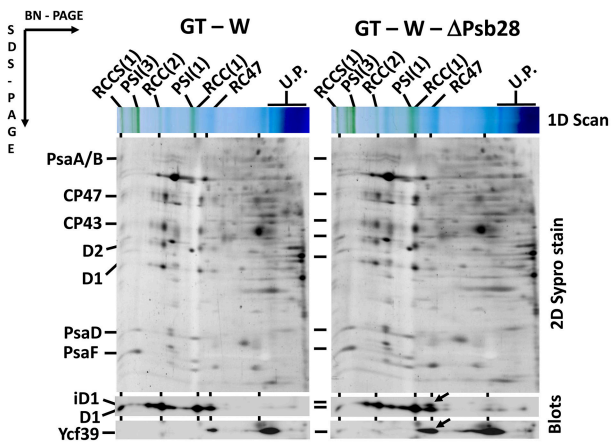

FIGURE 10 | Organization of photosynthetic membrane complexes in the GT-W strain and Psb28-less mutant constructed in this background. Thylakoid proteins isolated from each strain were separated by 4–14% blue-native-PAGE, and then in the second dimension by 12–20% SDS-PAGE. The 2D gel was stained by SYPRO Orange and then blotted to a PVDF membrane. The D1 and Ycf39 proteins were detected by specific antibodies (Blots). Designations as in **Figure 2**. Arrows indicate intermediate forms of the D1 protein and the Yc39 assembly factor present in the RCII* complex, which is more abundant in the Psb28-less strain. Each loaded sample contained 5 μg of Chl.

PSII components. GT-W was much more yellowish and this also corresponded to higher carotenoid and lower Chl levels (**Figure 1**). Moreover, this was also accompanied by aberrant composition of Chl-binding complexes. The strain accumulated a significant level of RCII complexes on the one side and unassembled CP47 and CP43 on the other side indicating that the binding of both PSII antennae to RCII is impaired.

Re-sequencing of the GT-W and GT-P genome revealed one common mutation in a 50S ribosomal protein L3 in comparison with the inferred chromosome sequence of the glucose-tolerant Williams strain. GT-W contained four specific mutations: one silent in the hypothetical protein Sll1367, the second in the PSII protein CP47, the third in the 500 kDa protein Slr0364, and the fourth in the long chain fatty acid coenzyme A-ligase (Slr1609; **Table 1**). The mutation in CP47 was a conservative amino acid change E283Q in the region of a large lumenal loop of the protein important for the assembly of PSII (Haag et al., 1993). A large deletion was found in the huge Slr0364 protein homologous to a protein involved in swimming motility (McCarren and Brahamsha, 2007).

Unexpectedly, no common mutations were found between the GT-W strain and the GT-O strains (Morris et al., 2014) also originating from the Vermaas lab. Although, there is a 5-year difference between the times the strains left the lab, this does not explain why there is no overlap in mutations and why GT-W and GT-P share the *rpl3* mutation while it is absent in GT-O.

The GT-P strain also contained a mutation in the *slr1609* gene. Interestingly, *slr1609* is the most frequently mutated gene—six independent (different) mutations can be found in *Synechocystis* strains sequenced by us and others (Tichý, unpublished data). The reason for this variability is unknown as is the effect of mutations on the activity of the enzyme, which is needed for reuse of fatty acids released from lipids after the action of lipases (Kaczmarzyk and Fulda, 2010). We checked the composition of pigment protein complexes in the *slr1609* deletion mutant but there was no apparent effect of the missing enzyme (Komenda and Tichý, unpublished data).

Apart from the point mutations, the specific feature of the GT-W chromosome was the presence of the large tandem duplication. Genome analysis of eukaryotes revealed that a tandemly arrayed duplicates account for significant proportion of genes and that duplication events are expected to play an important role in evolution of eukaryotes (Rizzon et al., 2006). Although, it is not clear whether gene duplication is a major evolutionary driving force also in prokaryotes compared to horizontal gene transfer, small tandem duplications on a single gene level have been shown previously to complement a non-photosynthetic phenotype of a PSII mutant (Tichy and Vermaas, 2000). In the current experiment we have sequenced 12 *Synechocystis* strains, among them several mutants and their revertants, and we have found one more example of another duplication between two transposases responsible for complementation of a *Synechocystis* mutant (Tichý, unpublished data). It suggests that such genome rearrangements are happening regularly and that under favorable conditions they may get easily selected for.

We have shown that loss of the duplication is accompanied by an increase in the level of PSI and by restoration of proper assembly of PSII (**Figure 7**). This indicates that the impaired autotrophic phenotype of the GT-W strain is related to the duplication and not to the observed specific mutations. We do not know whether the duplication in the GT-W strain is actually segregated or if there are still chromosomes present without the duplication as there is no simple check to confirm the non-duplicated variant. However, from the fact that the growth of GT-W in the absence of glucose easily led to the loss of the duplication it seems that the GT-W strain contains chromosomes both with and without the duplication. We think that the duplication got selected for during prolonged growth on glucose and that the lower level of PSI and impaired assembly of PSII are advantageous under glucose-induced stress. When the

conditions change to photoautotrophy, the ratio of chromosomes with and without the duplication in cells can gradually change, finally leading to complete loss of the duplication.

We do not know how the duplication resulted in low levels of Chl and the inability of CP47 and CP43 to bind to RC in GT-W. Most of the genes present in the duplication code for proteins with unknown function, however, the presence of the gene coding for the PSII structural protein D1 is striking. We believe that the presence of an extra copy of this highly expressed gene could change the stoichiometry of subunits in this multi-subunit complex leading to the observed lower accumulation of PSII and higher accumulation of PSII intermediates. Such gene imbalances and their consequences caused by partial genome duplications have been extensively studied in eukaryotes (Birchler and Veitia, 2012). It has been shown that both under-expression and over-expression of protein complex subunits could lead to similar deleterious effects (Papp et al., 2003). Interestingly, in plants, genes coding for PSII subunits were mostly eliminated from chromosome regions produced by partial genome duplications as opposed to whole-genome duplications (Coate et al., 2011). This is explained by PSII being particularly gene-dosage sensitive (Coate et al., 2011), as incompletely assembled PSII not only impairs photosynthesis but also increase photo-oxidative damage in the cell (Komenda and Masojídek, 1995).

An extra gene copy of Psb28, which has been proposed to affect Chl biosynthesis (Dobáková et al., 2009), and Cycl (Slr1214), cyclase involved in the formation of the fifth ring of Chl, resulted in increased expression and accumulation of these proteins (**Figure 7**). However, this also could lead to an imbalance between individual enzymes of the Chl biosynthesis pathway envisioned to form a multi-enzymatic complex (Sobotka, 2014) Also there was more HemH, which might at least partly explain the low level of PP_{IX} detected in GT-W. Indeed, after the loss of duplication, the GT-Wrev showed a lower level of all of these proteins.

Specifically for prokaryotic cyanobacteria, where transcription is spatially connected to translation, it is also possible that the duplication disturbed the local arrangement in the PSII biogenesis centers further impairing correct and prompt PSII assembly and/or proper interaction with Chl biosynthetic machinery.

It is interesting that the GT-W background is appropriate for complete segregation of mutants in the Chl biosynthesis pathway which cannot segregate in the GT-P background. As an example we can mention the mutant lacking Ycf54, a protein factor needed for the efficient formation of the fifth ring during Chl biosynthesis (this volume of the journal). As mentioned above, the duplication limits the stress imposed on the mutant cells during segregation on glucose media and this helps them to survive mutations, which would be lethal in the other WT variants. On the other hand, rather small phenotypic changes in Chl biosynthesis caused by mutagenesis of GT-P can be enhanced by construction of the mutants in GT-W with already impaired Chl biosynthesis as demonstrated for the Psb28-less strain. As a consequence, the mutants show better detectable phenotypic differences which helps identify the function of proteins encoded by the mutated genes. In conclusion, this study shows that the choice of the proper background strain is not only essential for correct evaluation of mutant phenotypic characteristics but also for successful construction of severely affected mutants that might not survive when made in the inappropriate WT variant.

AUTHOR CONTRIBUTIONS

MT performed experiments, evaluated and interpreted data, wrote the manuscript, MB performed experiments and evaluated data, JKop performed experiments, JN performed experiments, evaluated and interpreted data, wrote the manuscript, RS performed experiments, evaluated, and interpreted data, wrote the manuscript, JK performed experiments, evaluated, and interpreted data, wrote the manuscript.

FUNDING

The work was supported by National Programme of Sustainability I of The Ministry of Education, Youth and Sports, ID: LO1416.

ACKNOWLEDGMENTS

Authors are grateful to Jan Pilný and Lenka Moravcová for excellent technical assistance during protein and pigment analyses.

SUPPLEMENTARY MATERIAL

The Supplementary Material for this article can be found online at: http://journal.frontiersin.org/article/10.3389/fpls.2016.00648

REFERENCES

Birchler, J. A., and Veitia, R. A. (2012). Gene balance hypothesis: connecting issues of dosage sensitivity across biological disciplines. *Proc. Natl. Acad. Sci. U.S.A.* 109, 14746–14753. doi: 10.1073/pnas.1207726109

Boehm, M., Romero, E., Reisinger, V., Yu, J., Komenda, J., Eichacker, L. A., et al. (2011). Investigating the early stages of photosystem II assembly in *Synechocystis* sp. PCC 6803: isolation of CP47 and CP43 complexes. *J. Biol. Chem.* 286, 14812–14819. doi: 10.1074/jbc.M110.207944

Boehm, M., Yu, J., Reisinger, V., Beckova, M., Eichacker, L. A., Schlodder, E., et al. (2012). Subunit composition of CP43-less photosystem II complexes of *Synechocystis* sp PCC 6803: implications for the assembly and repair of photosystem II. *Philos. Trans. R. Soc. Lond. B Biol. Sci.* 367, 3444–3454. doi: 10.1098/rstb.2012.0066

Coate, J. E., Schlueter, J. A., Whaley, A. M., and Doyle, J. J. (2011). Comparative evolution of photosynthetic genes in response to polyploid and nonpolyploid duplication. *Plant Physiol.* 155, 2081–2095. doi: 10.1104/pp.110.169599

Dobáková, M., Sobotka, R., Tichý, M., and Komenda, J. (2009). Psb28 protein is involved in the biogenesis of the Photosystem II Inner Antenna CP47 (PsbB) in the Cyanobacterium *Synechocystis* sp PCC 6803. *Plant Physiol.* 149, 1076–1086. doi: 10.1104/pp.108.130039

Ferreira, K. N., Iverson, T. M., Maghlaoui, K., Barber, J., and Iwata, S. (2004). Architecture of the photosynthetic oxygen-evolving center. *Science* 303, 1831–1838. doi: 10.1126/science.1093087

Guskov, A., Kern, J., Gabdulkhakov, A., Broser, M., Zouni, A., and Saenger, W. (2009). Cyanobacterial photosystem II at 2.9-angstrom resolution and the role of quinones, lipids, channels and chloride. *Nat. Struct. Mol. Biol.* 16, 334–342. doi: 10.1038/nsmb.1559

Haag, E., Eaton-Rye, J. J., Renger, G., and Vermaas, W. F. J. (1993). Functionally important domains of the large hydrophilic loop of CP47 as probed by oligonucleotide-directed mutagenesis in Synechocystis sp. PCC 6803. *Biochemistry* 32, 4444–4454. doi: 10.1021/bi00067a037

Jordan, P., Fromme, P., Witt, H. T., Klukas, O., Saenger, W., and Krauss, N. (2001). Three-dimensional structure of cyanobacterial photosystem I at 2.5 A resolution. *Nature* 411, 909–917. doi: 10.1038/35082000

Kaczmarzyk, D., and Fulda, M. (2010). Fatty acid activation in cyanobacteria mediated by acyl-acyl carrier protein synthetase enables fatty acid recycling. *Plant Physiol.* 152, 1598–1610. doi: 10.1104/pp.109.148007

Kearse, M., Moir, R., Wilson, A., Stones-Havas, S., Cheung, M., Sturrock, S., et al. (2012). Geneious Basic: an integrated and extendable desktop software platform for the organization and analysis of sequence data. *Bioinformatics* 28, 1647–1649. doi: 10.1093/bioinformatics/bts199

Knoppová, J., Sobotka, R., Tichý, M., Yu, J., Konik, P., Halada, P., et al. (2014). Discovery of a chlorophyll binding protein complex involved in the early steps of photosystem II assembly in Synechocystis. *Plant Cell* 26, 1200–1212. doi: 10.1105/tpc.114.123919

Komenda, J., Knoppová, J., Kopečná, J., Sobotka, R., Halada, P., Yu, J. F., et al. (2012a). The Psb27 assembly factor binds to the CP43 complex of photosystem II in the Cyanobacterium *Synechocystis* sp PCC 6803. *Plant Physiol.* 158, 476–486. doi: 10.1104/pp.111.184184

Komenda, J., and Masojídek, J. (1995). Structural changes of Photosystem II complex induced by high irradiance in cyanobacterial cells. *Eur. J. Biochem.* 233, 677–682. doi: 10.1111/j.1432-1033.1995.677_2.x

Komenda, J., Sobotka, R., and Nixon, P. J. (2012b). Assembling and maintaining the Photosystem II complex in chloroplasts and cyanobacteria. *Curr. Opin. Plant Biol.* 15, 245–251. doi: 10.1016/j.pbi.2012.01.017

Kopečná, J., Komenda, J., Bučínská, L., and Sobotka, R. (2012). Long-Term acclimation of the cyanobacterium *Synechocystis* sp PCC 6803 to high light is accompanied by an enhanced production of chlorophyll that is preferentially channeled to trimeric Photosystem I. *Plant Physiol.* 160, 2239–2250. doi: 10.1104/pp.112.207274

Kopečná, J., Pilný, J., Krynická, V., Tomčala, A., Kis, M., Gombos, Z., et al. (2015). Lack of phosphatidylglycerol inhibits chlorophyll biosynthesis at multiple sites and limits chlorophyllide reutilization in *Synechocystis* sp. strain PCC 6803. *Plant Physiol.* 169, 1307–1317. doi: 10.1104/pp.15.01150

McCarren, J., and Brahamsha, B. (2007). SwmB, a 1.12-megadalton protein that is required for nonflagellar swimming motility in Synechococcus. *J. Bacteriol.* 189, 1158–1162. doi: 10.1128/JB.01500-06

Morris, J., Crawford, T., Jeffs, A., Stockwell, P., Eaton-Rye, J., and Summerfield, T. (2014). Whole genome re-sequencing of two 'wild-type'strains of the model cyanobacterium *Synechocystis* sp. PCC 6803. *New Zeal. J. Bot.* 52, 36–47. doi: 10.1080/0028825X.2013.846267

Nixon, P. J., Michoux, F., Yu, J. F., Boehm, M., and Komenda, J. (2010). Recent advances in understanding the assembly and repair of photosystem II. *Ann. Bot.* 106, 1–16. doi: 10.1093/aob/mcq059

Papp, B., Pál, C., and Hurst, L. D. (2003). Dosage sensitivity and the evolution of gene families in yeast. *Nature* 424, 194–197. doi: 10.1038/nature01771

Porra, R. J., Thompson, W. A., and Kriedemann, P. E. (1989). Determination of accurate extinction coefficients and simultaneous equations for assaying chlorophylls *a* and *b* extracted with four different solvents: verification of the concentration of chlorophyll standards by atomic absorption spectroscopy. *BBA-Bioenergetics* 975, 384–394. doi: 10.1016/S0005-2728(89)80347-0

Rippka, R., Deruelles, J., Waterbury, J. B., Herdman, M., and Stanier, R. Y. (1979). Generic assignments, strain histories and properties of pure cultures of cyanobacteria. *J. Gen. Microbiol.* 111, 1–61. doi: 10.1099/00221287-111-1-1

Rizzon, C., Ponger, L., and Gaut, B. S. (2006). Striking similarities in the genomic distribution of tandemly arrayed genes in *Arabidopsis* and rice. *PLoS Comp. Biol.* 2:e115. doi: 10.1371/journal.pcbi.0020115

Roose, J. L., Wegener, K. M., and Pakrasi, H. B. (2007). The extrinsic proteins of photosystem II. *Photosynth. Res.* 92, 369–387. doi: 10.1007/s11120-006-9117-1

Sakata, S., Mizusawa, N., Kubota-Kawai, H., Sakurai, I., and Wada, H. (2013). Psb28 is involved in recovery of photosystem II at high temperature in *Synechocystis* sp. PCC 6803. *BBA-Bioenergetics* 1827, 50–59. doi: 10.1016/j.bbabio.2012.10.004

Sobotka, R. (2014). Making proteins green; biosynthesis of chlorophyll-binding proteins in cyanobacteria. *Photosynth. Res.* 119, 223–232. doi: 10.1007/s11120-013-9797-2

Tichy, M., and Vermaas, W. (2000). Combinatorial mutagenesis and pseudorevertant analysis to characterize regions in loop E of the CP47 protein in *Synechocystis* sp. PCC 6803. *Eur. J. Biochem.* 267, 6296–6301. doi: 10.1046/j.1432-1327.2000.01718.x

Umena, Y., Kawakami, K., Shen, J. R., and Kamiya, N. (2011). Crystal structure of oxygen-evolving photosystem II at a resolution of 1.9 A. *Nature* 473, 55–60. doi: 10.1038/nature09913

Williams, J. G. K. (1988). Construction of specific mutations in Photosystem-II photosynthetic reaction center by genetic-engineering methods in *Synechocystis*-6803. *Method. Enzymol.* 167, 766–778. doi: 10.1016/0076-6879(88)67088-1

Conflict of Interest Statement: The authors declare that the research was conducted in the absence of any commercial or financial relationships that could be construed as a potential conflict of interest.

frontiers in Plant Science

PERSPECTIVE
published: 08 April 2016
doi: 10.3389/fpls.2016.00479

Chloramphenicol Mediates Superoxide Production in Photosystem II and Enhances Its Photodamage in Isolated Membrane Particles

*Ateeq Ur Rehman, Sandeesha Kodru and Imre Vass**

Institute of Plant Biology, Biological Research Centre of the Hungarian Academy of Sciences, Szeged, Hungary

Chloramphenicol (CAP) is an inhibitor of protein synthesis, which is frequently used to decouple photodamage and protein synthesis dependent repair of Photosystem II during the process of photoinhibition. It has been reported earlier that CAP is able to mediate superoxide production by transferring electrons from the acceptor side of Photosystem I to oxygen. Here we investigated the interaction of CAP with Photosystem II electron transport processes by oxygen uptake and variable chlorophyll fluorescence measurements. Our data show that CAP can accept electrons at the acceptor side of Photosystem II, most likely from Pheophytin, and deliver them to molecular oxygen leading to superoxide production. In addition, the presence of CAP enhances photodamage of Photosystem II electron transport in isolated membrane particles, which effect is reversible by superoxide dismutase. It is concluded that CAP acts as electron acceptor in Photosystem II and mediates its superoxide dependent photodamage. This effect has potential implications for the application of CAP in photoinhibitory studies in intact systems.

Keywords: photoinhibition, Photosystem II, chloramphenicol, superoxide

OPEN ACCESS

Edited by:
Roman Sobotka,
Czech Academy of Sciences,
Czech Republic

Reviewed by:
Anja Liszkay,
Centre National de la Recherche Scientifique, France
Esa Tyystjärvi,
University of Turku, Finland

****Correspondence:***
Imre Vass
vass.imre@brc.mta.hu

Specialty section:
This article was submitted to Plant Cell Biology, a section of the journal Frontiers in Plant Science

Received: *04 January 2016*
Accepted: *24 March 2016*
Published: *08 April 2016*

Citation:
Rehman AU, Kodru S and Vass I (2016) Chloramphenicol Mediates Superoxide Production in Photosystem II and Enhances Its Photodamage in Isolated Membrane Particles. Front. Plant Sci. 7:479. doi: 10.3389/fpls.2016.00479

INTRODUCTION

Photosynthesis is a process in which green plants, algae and cyanobacteria utilize energy from sunlight to manufacture carbohydrates from carbon dioxide and water. This process is the ultimate source of energy for all plants to drive their metabolic processes. Too much light reaching the photosynthetic apparatus can cause photodamage and ultimately can lead to the death of a cell. This stress situation is known as photoinhibition (Arntzen et al., 1984; Aro et al., 1993; Vass and Aro, 2008). The major damage of the photosynthetic apparatus under high light conditions is impairment of electron transport in the Photosystem II (PSII) complex, as well as damage of the D1 reaction center subunit (Ohad et al., 1984; Prasil et al., 1992). Important mediators of photodamage in plant cells are the various reactive oxygen species (ROS), such as singlet excited oxygen, free radicals (superoxide and hydroxyl ions) and peroxides, which are produced mainly in the chloroplasts and mitochondria (Apel and Hirt, 2004). The activity of the photodamaged PSII complex can be restored via the so called PSII repair cycle in which *de novo* synthesis of the damaged D1 subunits plays a key role (Aro et al., 1993; Baena-Gonzalez and Aro, 2002; Komenda et al., 2007; Nixon et al., 2010).

Light stress to PSII becomes a problem for photosynthetic capacity when the rate of photodamage exceeds the capacity of repair processes. Therefore, it is important to monitor separately the rates of photodamage and of the protein synthesis dependent repair. Decoupling of photodamage and repair can be achieved by protein synthesis inhibitors, such as lincomycin or chloramphenicol (CAP), which inhibit translation elongation in chloroplasts (Mulo et al., 2003; Chow et al., 2005; Tikkanen et al., 2014) or in cyanobacterial cells (Constant et al., 1997; Nishiyama et al., 2001, 2005; Sicora et al., 2003; Takahashi and Murata, 2005; Takahashi et al., 2009). While there are no reports concerning the participation of lincomycin in photosynthetic electron transport, CAP has been reported to accept electrons from the acceptor side of Photosystem I and to transfer them to molecular oxygen leading to superoxide production (Okada et al., 1991). Superoxide radicals have high reactivity, therefore, it is expected that locally generated superoxide will induce damaging effects in the vicinity of its production. This finding has been considered as a source of potential artifact by several research groups, who used lincomycin instead of CAP in photoinhibition studies (Tyystjarvi and Aro, 1996; Constant et al., 1997; Tyystjarvi et al., 2002; Chow et al., 2005; Campbell and Tyystjärvi, 2012; Miyata et al., 2012; Tikkanen et al., 2014). However, other groups kept using CAP in measurements of PSII photodamage (Nishiyama et al., 2001, 2005; Takahashi and Murata, 2005; Takahashi et al., 2009).

In the present work we investigated whether CAP has the capacity to interact directly with PSII electron transport in isolated membrane particles. Our data show that CAP acts as an electron acceptor to PSII and mediates superoxide production, which enhances photodamage of PSII.

MATERIALS AND METHODS

PSII Membrane Preparation

Photosystem II membrane particles were isolated from fresh spinach leaves as described earlier (Vass et al., 1987) and suspended in buffers containing 40 mM MES-NaOH (pH 6.5), 15 mM $MgCl_2$, 15mM $CaCl_2$ and 1 M betaine, respectively. PSII membranes were stored in −80°C for further use.

Light Induced Oxygen Uptake Measurements

O_2 uptake rates in PSII particles were measured by using a Hansatech DW2 O_2 electrode at 4°C under illumination with 500 μmole $m^{-2}s^{-1}$ light intensity. The total duration of illumination was 1 min. DCMU, which blocks electron transport at the Q_B site of PSII was also added at a concentration of 10 μM when indicated. In order to confirm superoxide formation the rate of oxygen uptake was also measured in the presence of 20 units/mg superoxide dismutase (SOD) that converts O_2^- partly back to O_2, as well as after addition of 1000 units of bovine serum catalase that converts H_2O_2, which is produced by SOD from O_2^-, to H_2O and O_2. One mililiter aliquot of PSII membrane particles at 5 μg Chl mL^{-1} concentration was used in each measurement.

Photoinhibitory Treatment

The PSII particles were resuspended at 5 μg Chl mL^{-1} in 40 mL volume and illuminated with 500 μmole $m^{-2}s^{-1}$ light intensity in the presence and absence of CAP (200 μg/mL). The temperature during illumination was maintained at 4°C. The samples were also illuminated in the presence of SOD (20 units mg^{-1}). For monitoring PSII activity the rate of O_2 evolution was measured at the indicated time points. Photosynthetic activity of irradiated PSII membranes was also assessed by measuring the so called OJIP transient of variable Chl fluorescence during application of a 2 s saturating pulse (Strasser et al., 1995) by using an FL-3000 fluorometer (PSI). F_v/F_m was obtained by calculating $(F_m\text{-}F_o)/F_m$, where F_o and F_m represent the minimum fluorescence in dark adapted sample, and the maximal fluorescence yield under continuous saturating light, respectively.

RESULTS AND DISCUSSION

CAP Acts as Electron Acceptor in PSII

Chloramphenicol has been reported earlier to take up electrons at the acceptor side of PSI (Okada et al., 1991). In order to check if similar phenomenon occurs in PSII, or not, the so

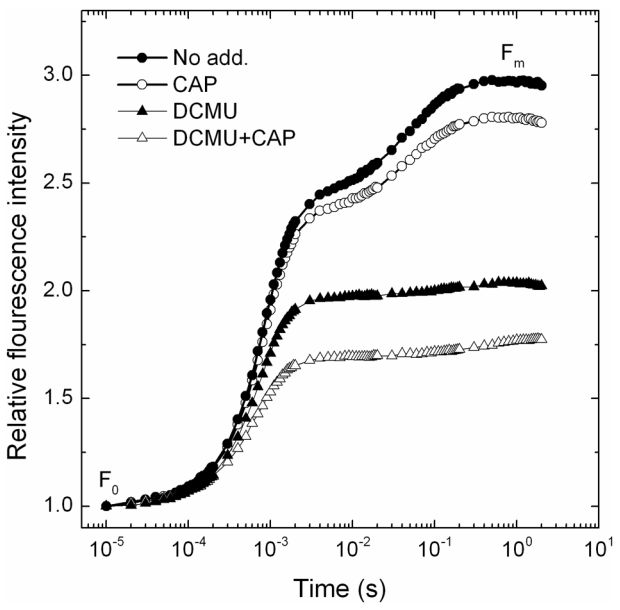

FIGURE 1 | The effect of CAP on PSII activity in PSII membrane particles as quantified by fast chlorophyll fluorescence rise. Photosynthetic activity of spinach PSII membranes was assessed by measuring OJIP transients of chlorophyll fluorescence. The experiments were performed in the absence (closed symbols) and presence of chloramphenicol (open symbols) without further addition (circles) or in the presence of 10 μM DCMU (triangles). The curves are shown after normalization to the same Fo values.

called OJIP Chl fluorescence transient was measured in the absence and presence of CAP. As shown in **Figure 1** the maximal fluorescence level (F_m) was decreased in the presence of CAP (open circles), which is consistent with the presence of an electron acceptor that prevents complete reduction of the Q_A primary quinone electron acceptor. In order to verify if CAP takes up electrons before or after the Q_B binding site we used DCMU, which inhibits electron transport from Q_A^- to Q_B by preventing PQ binding to the Q_B site. Interestingly CAP induced decrease of the F_m level also in the presence of DCMU (**Figure 1**, open triangles), which indicates that CAP takes up electrons from PSII before the DCMU block, i.e., either directly from Q_A^- or from Phe^-. Considering the very negative redox potential of CAP, $E_m(CAP/CAP^-) = -543$ mV (Kapoor and Varshney, 1997), the efficiency of electron transfer from Q_A^- ($E_m(Q_A/Q_A^-) = -120$ to -140 mV, Shibamoto et al., 2009) to CAP should be very low. On the other hand the redox potential of Phe [$E_m(Phe/Pheo^-) = -505$ to -535 mV (Shibamoto et al., 2009; Allakhverdiev et al., 2010)] allows energetically efficient interaction with Phe^-. Therefore, although the lifetime of Phe^- is very short (ca. 200 ps) it is a possible candidate to act as an electron donor for the reduction of CAP. This finding is in agreement with previous suggestions that Phe^- can act as direct electron donor to O_2 and can support superoxide production (Pospísil, 2012).

CAP Induces Superoxide Production in Isolated PSII Particles

It has been reported previously (Okada et al., 1991) that CAP mediates superoxide production in thylakoids by transferring electrons from the PSI acceptor side to oxygen. Since we have shown that CAP functions not only as PSI electron acceptor, but takes up electrons also from PSII it has a potential to produce superoxide in PSII complexes as, well.

In contrast to molecular oxygen superoxide does not produce amperometric signal in Clark-type oxygen electrodes. Therefore, conversion of O_2 to O_2^- leads to oxygen consumption, which can be easily followed by oxygen uptake measurements. In order to investigate CAP mediated superoxide production we measured O_2 uptake under various conditions. The data in **Figure 2A** show that CAP enhances light induced O_2 uptake in PSII particles. This effect is partly reversible by SOD, which converts 1 O_2^- molecule to $^1/_2O_2$ and $^1/_2H_2O_2$. Addition of catalase together with SOD almost completely eliminated the O_2 uptake, which is consistent with the conversion of $^1/_2$ H_2O_2 to $^1/_2$ H_2O + $^1/_2$ O_2. These data demonstrate that CAP can indeed mediate superoxide production in PSII. DCMU had only a minor inhibitory effect on the O_2 uptake, which is consistent with the idea that CAP transfers electrons to oxygen from a PSII acceptor located before the Q_B site.

CAP Enhances Photodamage of PSII in Isolated Membrane Particles

In order to check if CAP mediated superoxide production has any influence on the rate of photodamage PSII membrane particles were exposed to high light treatment in the absence and presence of CAP. According to the data shown in **Figure 2B**, light induced loss of PSII activity, as assessed by variable Chl fluorescence measurements, occurred faster in the presence than in the absence of CAP. Interestingly, the CAP induced enhancement of PSII photodamage was almost completely reversed when SOD was added together with CAP during the photoinhibitory treatment (**Figure 2B**). These data demonstrate that CAP induces

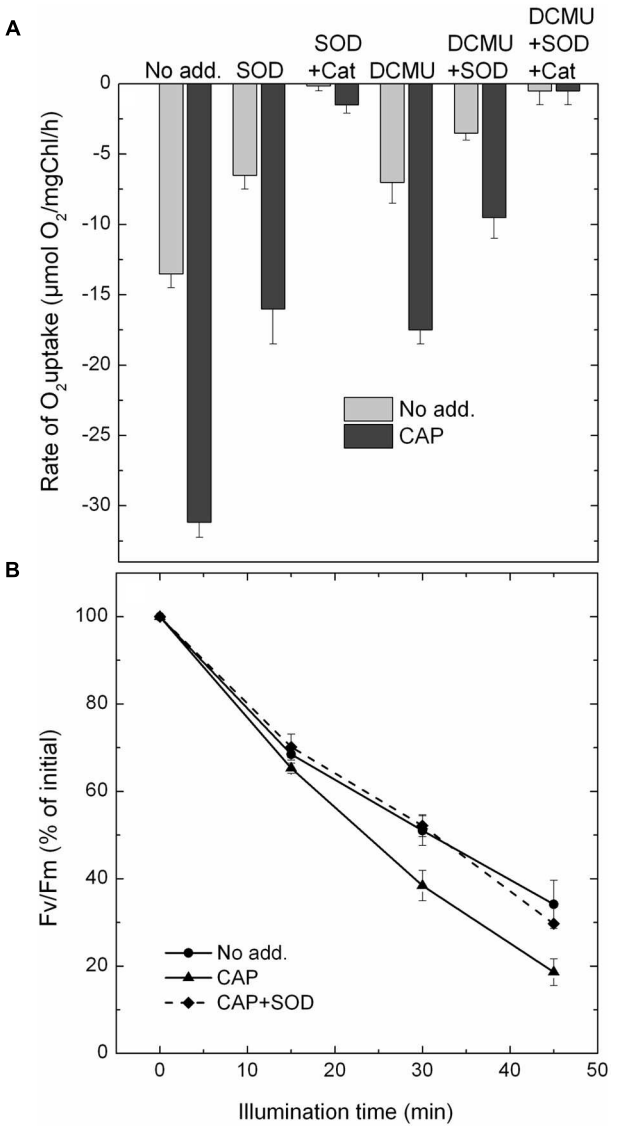

FIGURE 2 | The effect of CAP on superoxide production and photodamage in PSII. (A) CAP mediated oxygen uptake. PSII membrane particles were illuminated, with 500 μmole $m^{-2}s^{-1}$ light intensity, in the chamber of a Clark-type electrode. The rate of O_2 uptake was recorded in the presence and absence of CAP without further addition, in the presence of superoxide dismutase (SOD), and SOD + catalase. Similar series of experiments were also performed in the presence of the electron transport inhibitor DCMU. **(B)** CAP mediated photodamage. PSII membrane particles were exposed to illumination with 500 μmole $m^{-2}s^{-1}$ light intensity without addition, in the presence of CAP and CAP + SOD, and the activity of PSII was monitored by measuring variable Chl fluorescence (Fv/Fm).

enhanced PSII photodamage via production of superoxide in BBY particles.

CONCLUSION

Our data show that CAP accepts electrons from the PSII complex at a site located before the Q_B quinone electron acceptor, most likely from Phe^-. This process leads to superoxide production, which induces enhanced photodamage of PSII in isolated membrane particles. This side effect of CAP has potentially important implications regarding its application as protein synthesis inhibitor in photoinhibitory studies. Besides blocking the repair cycle of PSII CAP may accelerate the rate of photodamage also in intact systems leading to artifacts concerning the mechanism of photoinhibition. The *in vivo* effects of CAP are currently under investigation and will be presented in a forthcoming publication.

AUTHOR CONTRIBUTIONS

IV proposed the research topic, designed part of the experiments and contributed to writing of the manuscript. AUR, designed part of the experiments and contributed to data analysis and writing of the manuscript. SK performed most of the experiments and prepared the figures.

ACKNOWLEDGMENT

This work was supported from a grant by the Hungarian granting agency OTKA (NN-110960).

REFERENCES

Allakhverdiev, S. I., Tomo, T., Shimada, Y., Kindo, H., Nagao, R., and Klimov, V. V. (2010). Redox potential of pheophytin a in photosystem II of two cyanobacteria having the different special pair chlorophylls. *Proc. Natl. Acad. Sci. U.S.A.* 107, 3924–3929. doi: 10.1073/pnas.0913460107

Apel, K., and Hirt, H. (2004). Reactive oxygen species: metabolism, oxidative stress, and signal transduction. *Annu. Rev. Plant Biol.* 55, 373–399. doi: 10.1146/annurev.arplant.55.031903.141701

Arntzen, C. J., Kyle, D. J., Wettern, M., and Ohad, I. (1984). Photoinhibition: a consequence of the accelerated breakdown of the apoprotein of the secondary electron acceptor of Photosystem II. *Biosynth. Photosynth. Apparatus* 82, 313–324.

Aro, E.-M., Virgin, I., and Andersson, B. (1993). Photoinhibition of Photosystem II. Inactivation, protein damage and turnover. *Biochim. Biophys. Acta* 1143, 113–134. doi: 10.1016/0005-2728(93)90134-2

Baena-Gonzalez, E., and Aro, E.-M. (2002). Biogenesis, assembly and turnover of Photosystem II units. *Philos. Trans. R. Soc. Lond. B Biol. Sci.* 357, 1451–1460. doi: 10.1098/rstb.2002.1141

Campbell, D. A., and Tyystjärvi, E. (2012). Parameterization of photosystem II photoinactivation and repair. *Biochim. Biophys. Acta* 4660, 258–265. doi: 10.1016/j.bbabio.2011.04.010

Chow, W. S., Lee, H.-Y., He, J., Hendrickson, L., Hong, Y. -N., and Matsubara, S. (2005). Photoinactivation of Photosystem II in leaves. *Photosynth. Res.* 84, 35–41. doi: 10.1007/s11120-005-0410-1

Constant, S., Perewoska, I., Alfonso, M., and Kirilovsky, D. (1997). Expression of the psbA gene during photoinhibition and recovery in synechocystis PCC 6714: inhibition and adamage of transcritptional and translational machinery prevent the restoration of Photosystem II activity. *Plant Mol. Biol.* 34, 1–13. doi: 10.1023/A:1005754823218

Kapoor, S., and Varshney, L. (1997). Redox reactions of chloramphenicol and some aryl peroxyl radicals in aqueous solutions:? A pulse radiolytic study. *J. Phys. Chem. A* 101, 7778–7782. doi: 10.1021/jp971055z

Komenda, J., Tichy, M., Prasil, O., Knoppová, J., Kuviková, S., de Vries, R., et al. (2007). The exposed N-terminal tail of the D1 subunit is required for rapid D1 degradation during Photosystem II repair in *Synechocystis* sp PCC 6803. *Plant Cell* 19, 2839–2854. doi: 10.1105/tpc.107.053868

Miyata, K., Noguchi, K., and Terashima, I. (2012). Cost and benefit of the repair of photodamaged photosystem II in spinach leaves: roles of acclimation to growth light. *Photosynth. Res.* 113, 165–180. doi: 10.1007/s11120-012-9767-0

Mulo, P., Pursiheimo, S., Hou, C. X., Tyystjarvi, T., and Aro, E.-M. (2003). Multiple effects of antibiotics on chloroplast and nuclear gene expression. *Funct. Plant Biol.* 30, 1097–1103. doi: 10.1071/FP03149

Nishiyama, Y., Allakhverdiev, S. I., and Murata, N. (2005). Inhibition of the repair of Photosystem II by oxidative stress in cyanobacteria. *Photosynth. Res.* 84, 1–7. doi: 10.1007/s11120-004-6434-0

Nishiyama, Y., Yamamoto, H., Allakhverdiev, S. I., Inaba, H., Yokota, A., and Murata, N. (2001). Oxidative stress inhibits the repair of photodamage to the photosynthetic machinery. *EMBO J.* 20, 5587–5594. doi: 10.1093/emboj/20.20.5587

Nixon, P. J., Michoux, F., Yu, J., Boehm, M., and Komenda, J. (2010). Recent advances in understanding the assembly and repair of photosystem II. *Ann. Bot.* 106, 1–16. doi: 10.1093/aob/mcq059

Ohad, I., Kyle, D. J., and Arntzen, C. J. (1984). Membrane protein damage and repair: removal and replacement of inactivated 32-kilodalton polypeptides in chloroplast membranes. *J. Cell Biol.* 99, 481–485. doi: 10.1083/jcb.99.2.481

Okada, K., Satoh, K., and Katoh, S. (1991). Chloramphenicol is an inhibitor of photosynthesis. *FEBS Lett.* 295, 155–158. doi: 10.1016/0014-5793(91)81407-Y

Pospísil, P. (2012). Molecular mechanisms of production and scavenging of reactive oxygen species by photosystem II. *Biochim. Biophys. Acta* 1817, 218–231. doi: 10.1016/j.bbabio.2011.05.017

Prasil, O., Zer, H., Godde, D., and Ohad, I. (1992). Role of the PSII acceptor site in the lihgt induced degradation of D1. *Res. Photosynth.* 4, 501–504.

Shibamoto, T., Kato, Y., Sugiura, M., and Watanabe, T. (2009). Redox potential of the primary plastoquinone electron acceptor QA in photosystem II from *Thermosynechococcus elongatus* determined by spectroelectrochemistry. *Biochemistry* 48, 10682–10684. doi: 10.1021/bi901691j

Sicora, C., Máté, Z., and Vass, I. (2003). The interaction of visible and UV-B light during photodamage and repair of Photosystem II. *Photosynth. Res.* 75, 127–137. doi: 10.1023/A:1022852631339

Strasser, R. J., Srivastava, A., and Govindjee. (1995). Polyphasic chlorophyll a fluorescence transient in plants and cyanobacteria. *Photochem. Photobiol.* 61, 32–42. doi: 10.1111/j.1751-1097.1995.tb09240.x

Takahashi, S., and Murata, N. (2005). Interruption of the Calvin cycle inhibits the repair of Photosystem II from photodamage. *Biochim. Biophys. Acta* 1708, 352–361. doi: 10.1016/j.bbabio.2005.04.003

Takahashi, S., Whitney, S. M., and Badger, M. R. (2009). Different thermal sensitivity of the repair of photodamaged photosynthetic machinery in cultured *Symbiodinium* species. *Proc. Natl. Acad. Sci. U.S.A.* 106, 3237–3242. doi: 10.1073/pnas.0808363106

Tikkanen, M., Mekala, N. R., and Aro, E.-M. (2014). Photosystem II photoinhibition-repair cycle protects Photosystem I from irreversible damage. *Biochim. Biophys. Acta* 1837, 210–215. doi: 10.1016/j.bbabio.2013.10.001

Tyystjarvi, E., and Aro, E. M. (1996). The rate constant of photoinhibition, measured in lincomycin-treated leaves, is directly proportional to light intensity. *Proc. Natl. Acad. Sci. U.S.A.* 93, 2213–2218. doi: 10.1073/pnas.93.5.2213

Tyystjarvi, T., Tuominen, I., Herranen, M., Aro, E.-M., and Tyystjarvi, E. (2002). Action spectrum of psbA gene transcription is similar to that of photoinhibition in *Synechocystis* sp. *PCC* 6803. *FEBS Lett.* 516, 167–171. doi: 10.1016/S0014-5793(02)02537-1

Vass, I., and Aro, E.-M. (2008). "Photoinhibition of Photosystem II electron transport," in *Primary Processes of Photosynthesis: Basic Principles and Apparatus,* ed. G. Renger (Cambridge: Public Royal Society Chemistry), 393–411.

Vass, I., Ono, T. A., and Inoue, Y. (1987). Removal of 33 kDa extrinsic protein sfecifically stabilizes the S2QA- charge paier in Photosystem II. *FEBS Lett.* 211, 215–220. doi: 10.1016/0014-5793(87)81439-4

Conflict of Interest Statement: The authors declare that the research was conducted in the absence of any commercial or financial relationships that could be construed as a potential conflict of interest.

frontiers in Plant Science

ORIGINAL RESEARCH
published: 10 December 2015
doi: 10.3389/fpls.2015.01100

Isolation of Plant Photosystem II Complexes by Fractional Solubilization

*Patrycja Haniewicz[1], Davide Floris[2], Domenica Farci[2], Joanna Kirkpatrick[3], Maria C. Loi[2], Claudia Büchel[4], Matthias Bochtler[1,5] and Dario Piano[1,2]**

[1] Laboratory of Structural Biology, Department of Molecular Biology, International Institute of Molecular and Cell Biology, Warsaw, Poland, [2] Laboratory of Photosynthesis and Photobiology, Department of Life and Environmental Sciences, University of Cagliari, Cagliari, Italy, [3] Proteomics Core Facility, European Molecular Biology Laboratory, Heidelberg, Germany, [4] Laboratory of Plant Cell Physiology, Institute of Molecular Biosciences, Goethe-University Frankfurt, Frankfurt am Main, Germany, [5] Department of Bioinformatics, Institute of Biochemistry and Biophysics, Warsaw, Poland

Photosystem II (PSII) occurs in different forms and supercomplexes in thylakoid membranes. Using a transplastomic strain of *Nicotiana tabacum* histidine tagged on the subunit PsbE, we have previously shown that a mild extraction protocol with β-dodecylmaltoside enriches PSII characteristic of lamellae and grana margins. Here, we characterize residual granal PSII that is not extracted by this first solubilization step. Using affinity purification, we demonstrate that this PSII fraction consists of PSII-LHCII mega- and supercomplexes, PSII dimers, and PSII monomers, which were separated by gel filtration and functionally characterized. Our findings represent an alternative demonstration of different PSII populations in thylakoid membranes, and they make it possible to prepare PSII-LHCII supercomplexes in high yield.

Keywords: photosystem II, PSII-LHCII supercomplex, PSII-LHCII megacomplex, thylakoid membranes, *Nicotiana tabacum*, oligomeric state

OPEN ACCESS

Edited by:
Roman Sobotka, Czech Academy of Sciences, Czech Republic

Reviewed by:
Josef Komenda, Institute of Microbiology of the ASCR, Czech Republic
Bettina Ughy, Biological Research Centre of the Hungarian Academy of Sciences, Hungary

****Correspondence:***
Dario Piano
dario.piano@unica.it

Specialty section:
This article was submitted to Plant Cell Biology, a section of the journal Frontiers in Plant Science

Received: *23 August 2015*
Accepted: *22 November 2015*
Published: *10 December 2015*

Citation:
Haniewicz P, Floris D, Farci D, Kirkpatrick J, Loi MC, Büchel C, Bochtler M and Piano D (2015) Isolation of Plant Photosystem II Complexes by Fractional Solubilization. Front. Plant Sci. 6:1100. doi: 10.3389/fpls.2015.01100

INTRODUCTION

Oxygenic photosynthesis is one of the key processes sustaining the life on our planet by providing the biosphere with oxygen and sugars. Photosystem II (PSII) is a membrane protein complex that plays an essential role in oxygenic photosynthesis. Sunlight drives the splitting of water into oxygen, electrons, and protons (Cardona et al., 2012), but it also causes photodamage, which is minimized by photoprotection in conditions of excess light and repaired by PSII turnover in all conditions. The distribution of PSII in different complexes within the membranes reflects PSII assembly and repair (Pokorska et al., 2009), as well as optimization for efficient usage of light while avoiding or limiting damage (Boekema et al., 1995; Dekker and Boekema, 2005; Takahashi et al., 2009; Watanabe et al., 2009; Pagliano et al., 2011). In lamellae and the marginal grana, PSII is assembled *de novo* or repaired. Exhausted PSII complexes formed in the grana cores migrate to grana margins and lamellae, while being replaced by new and fully functional complexes (Edelman and Mattoo, 2008; Nixon et al., 2010; Puthiyaveetil et al., 2014; Tomizioli et al., 2014). With respect to PSII, lamellae and grana margins may thus be considered as the "nursery", while the grana cores act as the "photochemical plant" of thylakoids.

Five main forms of PSII are thought to occur *in vivo*: the monomeric (PSIIm or C), the dimeric (PSIId or C_2), the incomplete form free of the antenna component CP43 (RC-CP47) and finally the

two PSII complexes, consisting of several combinations of C_2 with the trimeric Light Harvesting Complex II (LHCII), which may bind C_2 strongly (S) or mildly (M) via the so-called minor antenna complexes (CP24, CP26, and CP29). Their assembly leads to higher photosynthetic units called PSII-LHCII supercomplex (PSIIsc or C_2S_2) and megacomplex (PSIImc or $C_2S_2M_2$; Boekema et al., 1999; Eshaghi et al., 1999; de Bianchi et al., 2008; Caffarri et al., 2009). The five PSII types are localized in different regions of the thylakoid membranes (Danielsson et al., 2006). In particular PSIIm and RC-CP47 are typically localized in the lamellae and peripheral part of the grana, being the main constituents of the "nursery" region, whereas PSIId, C_2S_2, $C_2S_2M_2$ are localized in the grana cores, being the main constituents of the functional side of the thylakoid membranes.

We have recently reported the purification of an inactive form of PSIIm that contains the subunit PsbS and appears as one of the main PSII forms associated with the lamellae region of the thylakoid membranes (Haniewicz et al., 2013). In this work, we now describe the fraction that is not solubilized by the mild-extraction protocol. This fraction, that requires harsher extraction conditions, was characterized in order to reveal whether it may contain the grana complexes opening the way for their isolation and characterization. The material solubilized in the second step is characterized by Blue native polyacrylamide gel electrophoresis (BN-PAGE) and mass spectrometry (MS), which together provide information on native molecular mass and subunit composition. After solubilization, granal thylakoids were also subjected to Immobilized-Metal Affinity Chromatography (IMAC) and subsequent Size Exclusion Chromatography (SEC). In the latter step, PSII complexes, supercomplexes, and megacomplexes could be separated, further characterized and compared using several techniques. This procedure allows the chromatography isolation of preparative amounts of highly pure C, C_2, C_2S_2 particles and represents a step further to their structural and functional characterization. The described procedure also provides a direct biochemical probe of PSII organization and distribution in thylakoid membranes.

MATERIALS AND METHODS

Growth of Tobacco Plants

Plant material was obtained from a transplastomic strain of *Nicotiana tabacum* that carries a hexa-histidine tag at the 5′ end of the gene coding for the PsbE subunit (Fey et al., 2008). The plants were grown for 10–12 weeks with a 50% relative humidity at a constant temperature of 25°C and under a light regime of 12 h/day, with a light intensity of 150–200 μmol photons/(s m^2).

Thylakoid Preparation

Thylakoid membranes were purified as reported previously by Fey et al. (2008), but in the last centrifugation step they were resuspended in 20 mM MES–NaOH, pH 6.5; 100 mM NaCl; 5 mM $MgCl_2$; 10 mM $NaHCO_3$; 12.5% (v/v) glycerol.

Thylakoids Solubilization and PSII Core Complex Purification by Affinity Chromatography

Thylakoid fractions were obtained routinely and with high reproducibility. Lamellar fractions were obtained by using the procedure reported in Haniewicz et al. (2013). Minimal modifications were introduced with the aim to ensure a complete removal of the peripheral grana (and lamellae) from the grana cores. Briefly, thylakoids membranes where solubilized for 30 min at 4°C and the final chlorophyll concentration was kept in a range between 2 and 3 mg/ml (SL) without major changes. After solubilization, the supernatant was separated from the unsolubilized fraction by spinning at 45000 × *g*. The unsolubilized granal fraction was homogenized and subsequently solubilized for 10 min at 4°C at a chlorophyll concentration of 1 mg/ml (SG), as reported in Fey et al. (2008) for the isolation of PSII complexes with LHC polypeptides bound. In both cases solubilization was carried out using 20 mM β-dodecylmaltoside (β-DDM).

Photosystem II samples were prepared routinely using Ni affinity chromatography. PSII was isolated following the procedure reported in Piano et al. (2010) with the only difference that the washing buffer was free of glycerol and betaine (20 mM MES–NaOH, pH 6.5; 100 mM NaCl; 10 mM $NaHCO_3$; 15 mM imidazole) and PSII cores were eluted using 40 mM MES–NaOH, pH 6.5; 20 mM NaCl; 5 mM $MgCl_2$; 1 mM $CaCl_2$; 10 mM $NaHCO_3$; 400 mM imidazole. The washing and the elution buffers contained 0.01% instead of 0.03% (w/v) β-DDM.

Size Exclusion Chromatography

The eluted fractions from Ni-NTA chromatography were pooled and concentrated using Vivaspin 20 ultrafiltration membranes with 100 kDa cutoff until a final volume of 200 μl. The protein sample was loaded on a home-made column of 80 ml bed volume Superose 6 resin (GE Healthcare) with a diameter of 10 mm leading to highly reproducible separations of specific protein complexes. Protein separation and column pre-equilibration were performed in gel filtration buffer (40 mM MES–NaOH, pH 6.5; 20 mM NaCl; 5 mM $MgCl_2$; 1 mM $CaCl_2$; 10 mM $NaHCO_3$; 0.01% (w/v) β-DDM).

Absorption Spectroscopy, Chlorophyll Determination, and Yield Calculation

The protein content in thylakoids and purified complexes was calculated referring to the Chl *a* and Chl *b* concentrations from three independent measurements. The analysis was done photometrically in 80% (v/v) acetone using a Pharmacia Biotech Ultrospec 4000 spectrophotometer and Chl concentrations were calculated according to Porra et al. (1989). Yield calculation in thylakoids and PSII complexes was expressed in mg or % of chlorophylls. Measurements were performed on samples from 10 independent purifications starting from different thylakoid stocks. For each of these 10 purifications was calculated the amount of thylakoids and the amounts of the specific PSII complexes isolated (C-PsbS, C, C_2, C_2S_2) expressing them in mg

or % of Chls with respect to the initial thylakoid amount. Finally, the amounts for each of the 5 classes (thylakoids, C-PsbS, C, C_2, C_2S_2) were averaged respect to the 10 independent purifications (**Table 4**). The values were expressed as means ± standard deviations.

Polyacrylamide Gel Electrophoresis

Blue native polyacrylamide gel electrophoresis was routinely used as a reference to cross check the correct SG solubilization, the correct SEC profiles and to select the specific pools to be used for further structural and functional tests. According to Schägger and von Jagow (1991), native electrophoresis was performed using 3–12% (w/v) continuous gradient gels. PSII complexes and thylakoid samples at 0.2 mg Chl/ml were mixed with 0.25 volumes of Coomassie Blue Solution (5% (v/v) serva Blue G, 750 mM aminocaproic acid, 35% (w/v) sucrose). The electrophoresis was carried out at 205 V for 5 h for PSII complexes, while for thylakoids it consisted in a run at 60 V for 12 h. In both cases the run was performed at 4°C. After the electrophoretic run, the gels were stained with Coomassie brilliant blue G250.

Mass Spectrometry

The BN-PAGE gel bands from the SG samples or from the SEC fractions were excised and analyzed. Samples were processed as described in Farci et al. (2014). Protein groups were assigned to bands, and qualitative estimates of protein abundance were based on an "index" obtained by dividing unweighted spectral counts (spectral count) by protein mass (kDa). Proteins were either excluded (index below 0.25), or divided into groups with indices between 0.25 and 0.50 (marked with + in **Table 3**), 0.50 and 0.75 (marked with ++ in **Table 3**) and indices higher than 0.75 (marked with +++ in **Table 3**). Higher indices indicate greater abundance of the protein in the samples.

Oxygen Evolution

Oxygen evolution rates under light saturation were measured using a Clark-type electrode (Hansatech, England) at 20°C. In the reaction mixture the samples were added to gel filtration buffer enriched with freshly prepared electron acceptors (1 mM 2,6-dichloro-*p*-benzoquinone and 1 mM ferricyanide). The measurements were carried out at a Chls concentration of 100 μg/ml for thylakoids and 50 μg/ml for PSII samples. Activity was tested with three independent measurements on the same preparation and the values were expressed as means ± standard deviations.

Electron Microscopy

Size Exclusion Chromatography fractions of different PSII complexes from three independent purifications were checked by Transmission Electron Microscopy (TEM). Samples were diluted in gel filtration buffer and applied on glow-discharged carbon

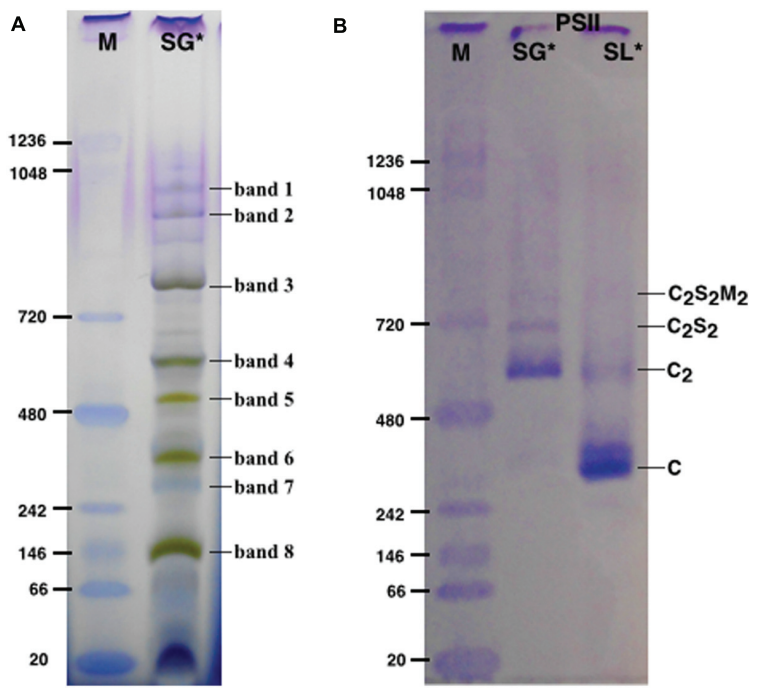

FIGURE 1 | The solubilized grana cores (SG), when resolved by Blue native polyacrylamide gel electrophoresis (BN-PAGE; A) separated into a pattern of bands equivalent to specific thylakoid complexes. The bands were attributed to a given complex on the basis of their mass spectrometry (MS) analysis (see **Table 1**). The PSII pools purified by NiNTA affinity chromatography are resolved by BN-PAGE **(B)**. The lane SG is the PSII pool purified from the solubilized grana fraction, whereas lane SL represents the pool of PSII purified from solubilized lamellae. In lanes M the molecular marker (M) was loaded. $C_2S_2M_2$, C_2S_2, C_2 and C are the PSII-LHCII megacomplexes, PSII-LHCII supercomplexes, PSII dimers and PSII monomers, respectively. *The BN-PAGE used must be considered reliable in the mass range between 66 and 480 kDa according to the molecular marker (M). Above this range, the heaviest bands appear significantly under estimated in weight.

TABLE 1 | Mass spectrometry (MS) analysis performed on the bands of the SG samples resolved by BN-PAGE (see Figure 1A).

Band	PSI (LHCI)	PSII (LHCII)	Cyt b_6f complex	ATP synthase	Complexes
1	PsaB, D, E, F, K CAB4, 7, 40	PsbA, B, C, D, E, O, Q CP29	–	–	PSI and PSII higher complexes
2	PsaA, B, D, F, K CAB40	PsbA, B, C, D, Q	–	–	
3	PsaA, B, D, F, L,H,K CAB4,16, 21, 40, lhca	PsbA, B, C, D, E, O CAB7, 36, 40, CP24, 26, 29	–	atpA, B	PSII megacomplex ($C_2S_2M_2$), PSI-LHCII ATPase
4	PsaA, B, D, E, F, L, CAB4, 25, lhca	PsbA, B, C, D, E, O, S CAB7, 13, 36, 40, CP29, lhcb	–	atpA, B, C, E, F atpα, γ	PSII supercomplex (C_2S_2), PSI-LHCII ATPase
5	PsaB CAB16, 21, 40	PsbA, B, C, D, E, O, S CAB7, 13, 36, 50, CP26, 29	–	–	PSII dimer (C_2) PSI
6	CAB21, 40	PsbA, B, C, D, E, O, Q CAB7, 16, 36, 50, CP26, 29	Cyt. f subunit subunit IV	–	PSII monomer (C), $cytb_6f$ complex
7	CAB40	PsbA, B, C, D CAB7, 36, CP24, 26	–	–	PSII incomplete monomer
8	CAB21, 40	PsbC, D, O, P, Q, S CAB7, 36, 50, CP24, 26, 29	Cyt. f subunit	atpβ	Free subunits

For a more detailed analysis see Supplementary Table S1.

coated copper grids (400 mesh) followed by negative staining using filtered 2% uranyl acetate. Electron microscopy was performed in a CM12 electron microscope (Philips, Eindhoven, Netherlands) operated at 80 kV. Images were recorded under low dose conditions (total dose $\sim 25e\text{-}/Å^2$) with a ES500W camera (Gatan, Pleasanton, CA, USA) at a magnification of 110 kx.

RESULTS

Composition of SL and SG Fractions

In order to characterize PSII species associated to granal thylakoids, we solubilized membranes in two steps. In the first step, we used a previously described mild and long extraction procedure that selectively solubilizes only the peripheral part of the thylakoids (lamellae and grana margins; SL) leading to the chromatography isolation of monomeric PSII that binds the subunit PsbS (see protocol B samples in Table 1 of Haniewicz et al., 2013). The fraction of thylakoids not solubilized during the preparation of SL was pelleted by centrifugation, resuspended and finally subjected to a second solubilization, leading to samples with a PSII content representative for grana cores (SG) that were then subjected to BN-PAGE.

SG samples migrated on BN-PAGE resolving in bands with apparent masses from 1050 to 60 kDa (**Figure 1A**). The content in thylakoid complexes of each band was identified by MS. According to this analysis, PSII was mainly present in the $C_2S_2M_2$, C_2S_2, C_2 and C forms (**Table 1**, Supplementary Table S1). When incubated on ice for more than 6 h, the SL samples, but not the SG, were characterized by a tendency to precipitate, indicating an insufficient solubilization, which led to difficulties in their characterization by BN-PAGE (data not shown). Taken together, these data suggested large differences in the properties of lamellae and grana cores of the thylakoid membranes.

Oxygen Evolving Activity of SL and SG Fractions

The oxygen evolution capacity of SL and SG samples was tested. The SL samples had a minimal activity of 19 μmol O_2/mg Chl h, while the SG samples evolved 10-fold more oxygen (186 μmolO_2/mg Chl h), suggesting the presence of abundant and functional PSII (**Table 2**). These findings are consistent with the accepted view of the lamellae as the assembly and/or repair region of thylakoids in which the PSII particles are mainly inactive, and of the grana in which PSII is in an optimal chemical-physical environment that keeps it very active (Aro et al., 2005).

TABLE 2 | Rates of oxygen evolution of solubilized lamellar (SL) thylakoids, solubilized granal (SG) thylakoids and of PSII-LHCII megacomplexes (C2S2M2), PSII-LHCII supercomplexes (C_2S_2), PSII dimers (C2), and PSII monomers (C).

Thylakoids*		PSII purified samples*			
SL	SG	PSII monomers (C)	PSII dimers(C_2)	PSII-LHCII supercomplexes (C_2S_2)	PSII-LHCII megacomplexes ($C_2S_2M_2$)
19 ± 2	186 ± 5	960 ± 5	1360 ± 12	1030 ± 10	not determined

*For each sample, the activity was tested with three independent measurements and the values obtained were expressed in μmol O2/mg Chl h as means ± standard deviations. The $C_2S_2M_2$ complexes were not characterized because of their low amounts and their C_2S_2 impurities. The activity of the $C_2S_2M_2$ complexes was not determined because of their low amounts and their C_2S_2 impurities. *Values represent means ± standard deviations of three independent measurements.*

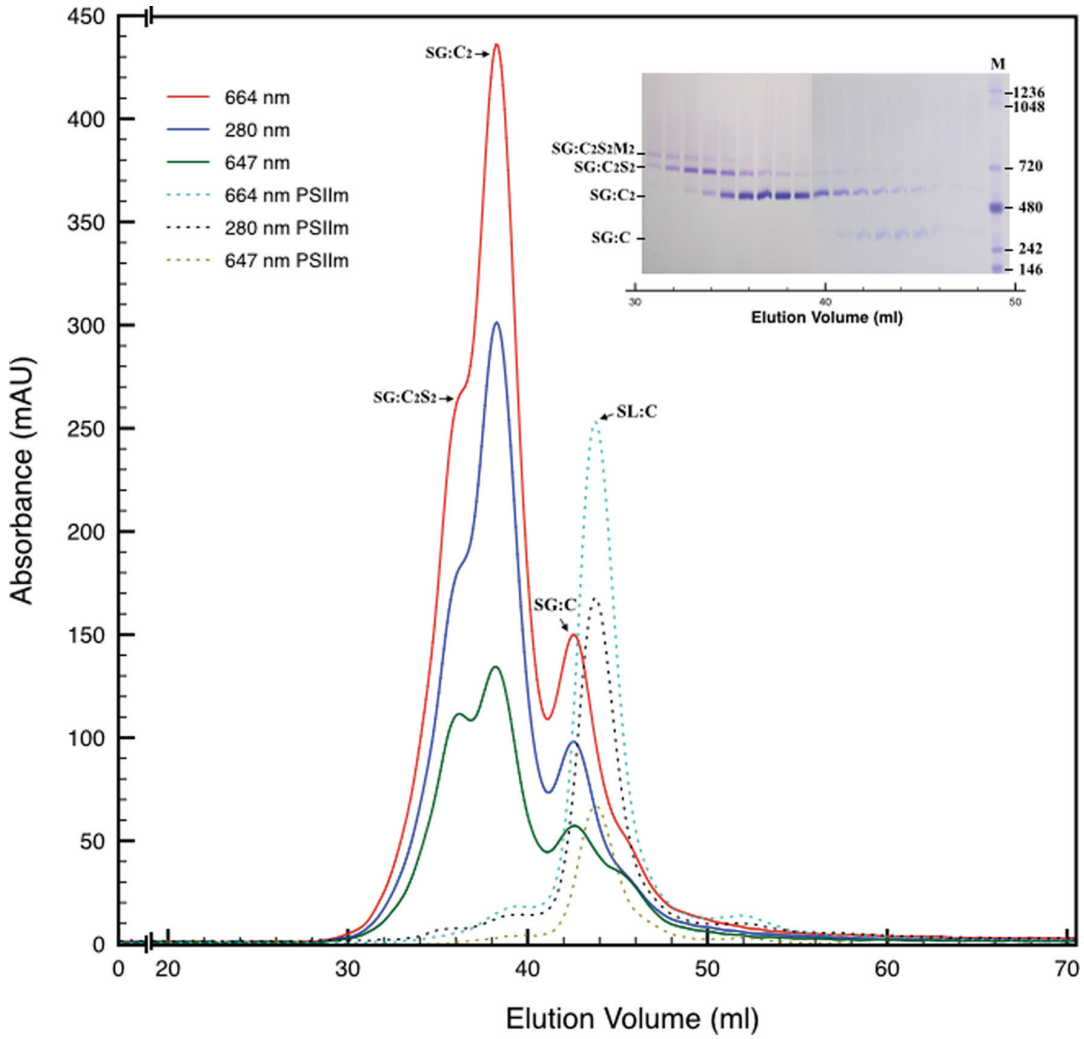

FIGURE 2 | Size exclusion chromatography of the PSII pool isolated from SG thylakoids by affinity chromatography (solid lines). All the measurements were recorded at three different wavelengths: 280 nm (proteins), 664 nm (chlorophyll *a*), 647 nm (chlorophyll *b*). In the inset are shown the elution fractions analyzed by BN-PAGE, confirming the partial separation of several oligomeric states of PSII. M is the molecular marker. The mostly monomeric PSII pool isolated from SL thylakoids by affinity chromatography (dotted lines) was used as a mass reference. In the chromatograms and in the inset SG:$C_2S_2M_2$, SG:C_2S_2, SG:C_2, and SG:C are the PSII-LHCII megacomplexes, PSII-LHCII supercomplexes, PSII dimers, and PSII monomers of grana origin (SG), respectively; SL:C are PSII monomer from lamellae (SL).

Oligomeric States of PSII Complexes from the SG Fraction

The SG and SL samples were subjected to further PSII separation steps after solubilization. The histidine tag on PsbE of the transplastomic plants made it possible to purify PSII by Ni-NTA (Fey et al., 2008). After purification, the oligomeric profile of the obtained SG-PSII was assessed by BN-PAGE and the composition compared with the already characterized SL-PSII (Haniewicz et al., 2013), showing a significant difference between the oligomeric patterns of the two PSII samples (**Figure 1B**). As clearly shown in **Figure 1B**, mainly C and sometimes incomplete PSII forms such as RC-CP47 can be obtained from SL, while SG is a mixture of C_2 and C_2S_2 with the frequent presence of small $C_2S_2M_2$ amounts.

The Different SG-PSII Species can be Separated by Size Exclusion Chromatography

Next, we attempted to separate the different PSII components obtained by the Ni-NTA chromatography from the SG-PSII samples by means of SEC. SG-PSII samples resolved into a characteristic and reproducible profile consisting of a shoulder and two peaks (**Figure 2**). In contrast, the same procedure for the SL-PSII samples led to a single peak corresponding to monomeric PSII confirming the BN-PAGE analysis on the NiNTA pool (**Figures 2** and **1B**) and previous results (Haniewicz et al., 2013). The collected fractions from the SEC analysis on the SG-PSII samples were checked by BN-PAGE and thus divided into four pools corresponding to samples enriched in

TABLE 3 | Mass spectrometry analysis performed on the bands of the SEC fractions resolved by BN-PAGE.

		Name	Accession Number	Mass (kDa)	Qualitative (unweighted subunit presence)				Quantitative* (weighted subunit presence)			
					C	C_2	C_2S_2	$C_2S_2M_2$	C	C_2	C_2S_2	$C_2S_2M_2$
PSII-LHCII (super/megacomplexes)	PSII monomers and dimers	PSB_A (D1)	PSBA_TOBAC	39	+	+	+	+	+++	+++	+++	+++
		PSB_B (CP47)	PSBB_TOBAC	56	+	+	+	+	+++	+++	+++	+++
		PCB_C (CP43)	PSBC_TOBAC	52	+	+	+	+	+++	+++	+++	+++
		PSB_D (D2)	PSBD_TOBAC	40	+	+	+	+	+++	+++	+++	+++
		PSB_E (cytb559)	PSBE_TOBAC	9	+	+	+	+	+++	+++	+++	+
		PSB_H	PSBH_TOBAC	8	+	+	+	+	+++	+++	+++	+++
		PSB_L	PBL_TOBAC	4	−	+	+	−	−	+++	+++	−
		PSB_O (33kDa)	Q84QE8	35	+	+	+	+	−	++	+++	+
		PSB_O (33kDa)	PSBO_TOBAC	35	−	+	+	+	−	++	+++	+
		PSB_R	PSBR_TOBAC	14	−	+	+	+	−	+	+	−
	CAB and LhcII proteins	Lhcb1 (CB24)	CB24_TOBAC	28	+	+	+	+	−	−	+++	+++
		Lhcb1 (CB27)	CB27_TOBAC	28	−	+	+	+	−	−	+++	+++
		Lhcb1 (CB22)	CB22_TOBAC	28	−	−	+	+	−	−	+++	++
		Lhcb1 (CB25)	CB25_TOBAC	28	−	−	+	−	−	−	+++	−
		Lhcb2 (CB23)	CB23_TOBAC (+1)	29	−	+	+	+	−	−	+++	++
		Lhcb3	A0A076L1Y1_TOBAC (+1)	29	−	−	+	+	−	−	−	−
		Lhcb4 (CP29)	Q0PWS7_TOBAC	31	+	+	+	+	−	−	+++	+++
		Lhcb5 (CP26)	Q0PWS5_TOBAC	30	−	+	+	+	−	−	+++	+++
		Lhcb6 (CP24)	Q0PWS6_TOBAC	27	−	+	+	+	−	−	+	+
Plastidial ATP synthase		ATP_A (α-subunit)	ATPA_TOBAC	55	−	+	−	−	−	−	−	−
		ATP_B (β-subunit)	ATPB_TOBAC (+1)	54	−	+	−	−	−	−	−	−
−		37kDa inner membrane polypeptide	Q40501_TOBAC	38	−	+	+	+	−	−	−	−
Vacuolar H^+-ATPase		subunit B	Q9M5Z8_TOBAC	54	−	−	+	+	−	−	−	−

*In the table are shown the protein composition and the relative genes for each of the PSII types separated (**Figure 2** inset). $C_2S_2M_2$, C_2S_2, C_2, C are the PSII-LHCII megacomplexes, PSII-LHCII supercomplexes, PSII dimers, and PSII monomers, respectively. *Unweighted spectrum count/MASS (kDa) = i; + = 0.25 ≤ i ≤ 0.50; ++ = 0.50 ≤ i ≤ 0.75; +++ = i > 0.75 (for details see Materials and Methods).*

a specific complex primarily identified by its apparent size on BN-PAGE (**Figure 2** inset). The identity of each complex was finally confirmed by MS analysis (**Table 3**, Supplementary Table S2). Furthermore, the C_2S_2 and C_2 complexes were also analyzed by TEM (**Figure 3**), demonstrating the sizes reported for C_2 and C_2S_2 (Aro et al., 2005; Nield and Barber, 2006), the latter most easily discernible from the side views (circled in **Figure 3A**). Unfortunately, $C_2S_2M_2$ complexes could not be analyzed by TEM, because they were obtained in low amounts and eluted at the beginning of the C_2S_2 peak in SEC.

The Isolated PSII Types Evolve Oxygen at Very Different Rates

The different PSII complexes obtained by SEC were tested for their oxygen evolving capacity. The pool of $C_2S_2M_2$ was excluded from this analysis since, as mentioned above, it was not perfectly separated from the C_2S_2. Each one of the others pools, represented by a dominant PSII type, were found to be fully functional and characterized by oxygen evolution rates comparable with other reports in literature (Kihara et al., 2014; **Table 2**). As oxygen evolution per Chl is reported, and because C_2S_2 binds about three times more Chls per reaction center than cores (around 210/reaction center as opposed to around 70; Ferreira et al., 2004; Liu et al., 2004; Loll et al., 2005; Barros et al., 2009), the C_2S_2 complexes are characterized by the highest activity.

Mass Spectrometry Analysis on the Four PSII Types Showed Significant Differences in Subunit Composition

The BN-PAGE bands obtained from the SEC fractions (**Figure 2** inset) were excised and directly analyzed by MS to characterize subunit content (**Table 3**, Supplementary Table S2). The main core subunits D1, D2, CP43, CP47, PsbE, PsbH, PsbL, PsbO, and PsbR were found in this analysis. The subunit PsbL, an important dimerization factor (Suorsa et al., 2004), was absent from the C and $C_2S_2M_2$ types. PsbR was identified only in the C_2 and C_2S_2 types, while PsbF was not found. The partial or complete

absence of these three small peptides is most likely due to their small masses, which limit their successful MS identification (Shi et al., 2012). The PsbO subunit was found in both isoforms. The C_2 and C forms appeared to contain lower amounts of this protein, even though they showed a fair water splitting capacity (**Table 2**). PsbP and PsbQ, the other main water splitting subunits, were not identified in the analyzed complexes. Specific subunits were characteristic for a given oligomeric state. As expected, it was found that the subunits CP24, CP26, and CP29 were present just in traces or absent in the C and C_2, while they were found to be characteristic for C_2S_2 and $C_2S_2M_2$. Also the proteins Lhcb1, Lhcb2 and Lhcb3 were found associated with the C_2S_2 and $C_2S_2M_2$ complexes. In particular Lhcb3 was found to be present only in traces and Lhcb1 was present in four different isoforms. One of these, CB25, was specific for the C_2S_2 form.

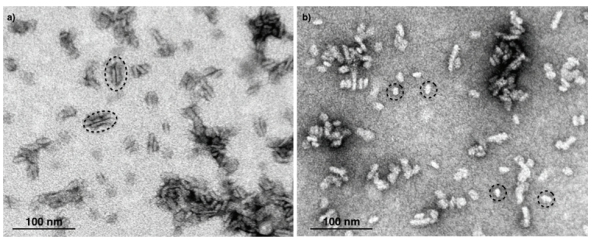

FIGURE 3 | Electron micrographs of negatively stained C_2S_2 complexes (A) and C_2 (B) separated by size exclusion chromatography. The suitable fractions in terms of purity were chosen on the basis of their band pattern on BN-PAGE. Dotted ellipses **(A)** and dotted circles **(B)** surround specific examples of C_2S_2 complex side views and C_2 particles, respectively.

DISCUSSION

The Oxygen Evolving Properties Reflect the PSII Cycle

The distribution of PSII in thylakoid membranes reflects the PSII cycle (Tomizioli et al., 2014). Grana cores sustain water splitting at the highest rates. Lamellae and grana margins are mainly required to recycle and replace PSII, which at these stages is still exposed to light, but requires protection. In agreement with this general picture, PSII isolated from SL samples is inactive, monomeric and retains PsbS. The presence of PsbS and low PSII activity in SL samples fit with the low activity of lamellar PSII reported earlier and with the role of PsbS in non-photochemical quenching (Allen, 2002; Munekage et al., 2002; Gerotto et al., 2015). PsbS may keep PSII in an inactive and protected state for assembly or repair. PSII from the SG samples is a mix of four different types that are very active in oxygen evolution, also in agreement with the current model for the PSII cycle.

PsbP and PsbQ

All active PSII complexes from grana lacked the PsbP and PsbQ subunits, which were found earlier in the SL fractions (Haniewicz et al., 2013). As PsbP and PsbQ are thought to enhance the PSII activity and the Oxygen Evolving Complex (OEC) stability (Bricker and Frankel, 2011), this finding is surprising, but it is not unprecedented. PsbP and PsbQ were also absent after a very mild membrane solubilization in a study on D1 subunit processing (Figure 5B from Che et al., 2013). However, the two subunits were present in several earlier PSII preparations, at least judging from SDS-PAGE gel migration patterns (Boekema et al., 2000; Nield et al., 2000; Caffarri et al., 2009). Mummadisetti et al. (2014) also detected PsbP and PsbQ by Western blotting, but, unfortunately, they did not determine the oligomeric PSII state by BN-PAGE and/or SEC. Boekema et al. (1998) detected PsbP in PSII-LHCII supercomplexes, but other studies did not corroborate this finding (Caffarri et al., 2009; Barera et al., 2012). Thus, PsbP and PsbQ may only be present in some assembly stages of PSII complexes or, more likely, in the very active forms of PSII they may be loosely bound due to their high sensitivity to damage.

Lhcb3 and CP24

Low levels of Lhcb3 and CP24 were detected for both $C_2S_2M_2$ and C_2S_2 complexes. The latter has not been reported to contain these two subunits. However, special hemi-types, intermediate between the C_2S_2 and the $C_2S_2M_2$ types, which retain both extra subunits, have been described and could fit well with the co-presence in our C_2S_2 samples. In Caffarri et al. (2009) is reported a so-called C_2SM complex containing only one S trimer and one M trimer that are bridged through CP29, CP24, and CP26 to the dimeric core. This complex has almost the same mass (1040 kDa) as the C_2S_2 complex (1100 kDa), and therefore co-migrates in

TABLE 4 | Purification yields for the isolated PSII types.

	Thylakoid membranes	Purification				
		Mild solubilization (SL)	Harsh solubilization (SG)			
		C-PsbS	C	C_2	C_2S_2	$C_2S_2M_2$
Mass (mg)	34.97 ± 3.8	0.95 ± 0.11	0.19 ± 0.01	9.55 ± 0.81	1.91 ± 0.18	Not determined
Yield (%)	100	2.73 ± 0.31	0.55 ± 0.04	27.30 ± 2.33	5.45 ± 0.51	Not determined

*$C_2S_2M_2$ yield was not determined because of their low amounts and their C_2S_2 impurities. *Values are expressed in mg or % of chlorophylls and represent means ± standard deviations of 10 independent purifications (see details in Materials and Methods).*

BN-PAGE (and also co-sediments in a sucrose gradient; Caffarri et al., 2009). Another hemi-type, called $C_2S_2^+$, is reported to have similar characteristics (Pietrzykowska et al., 2014). It is likely that these incomplete forms are assembly intermediates on the way to $C_2S_2M_2$, or result from its disintegration, either in membranes or during solubilization or purification.

Isolation of Supercomplexes by Coupling Differential Solubilization and Chromatography

The organization of the thylakoids and in particular the distribution of pigment–protein complexes within are very well characterized (Danielsson et al., 2006). This and other works all demonstrate substantial heterogeneity of the PSII species in the thylakoid membranes (Boekema et al., 1995; Dekker and Boekema, 2005; Danielsson et al., 2006; Takahashi et al., 2009; Watanabe et al., 2009; Pagliano et al., 2011). Here, we present a differential solubilization of the thylakoid membranes, which leads to the isolation of samples with different oligomeric patterns of PSII and other thylakoid complexes (**Figure 1A**). Conceptually, our method to access to the grana cores fraction, in which is found highly active PSII, is similar to the method described by Berthold et al. (1981), the so-called BBY preparation, which also removes lamellae and peripheral granal regions. In contrast to the BBY method, the new method has the advantage to avoid the breakdown of granal PSII core complexes (C and RC-CP47 are found at most in small quantities).

CONCLUSION

It has to be remarked that the mild nature of the solubilization protocol permits a full separation between PSII monomers and dimers, and makes it possible to prepare C_2S_2 in larger quantities without density gradients on sucrose or Percoll (Ghanotakis et al., 1987; Caffarri et al., 2004), (**Table 4**).

AUTHOR CONTRIBUTIONS

DP conceived the study, participated in its design and coordination, carried out the membranes preparation, participated in the biochemical studies, and drafted the manuscript. PH participated in the design of the study, participated the biochemical studies, and participated in the membranes preparation. D. Floris carried out the membranes preparation, participated in the biochemical studies. D. Farci carried out the membranes preparation, participated in the biochemical studies. JK carried out the MS analysis. ML participated in the preparation of membranes. CB contributed to the electron microscopy analysis and helped to draft the manuscript. MB participated in the design of the study and helped to draft the manuscript.

ACKNOWLEDGMENTS

This work was carried out with the support of the program Homing Plus (Foundation for Polish Science) grant No: 2012-6/10 co-financed by the European Union under the European Regional Development Funds; the program PRELUDIUM (National Science Centre) grant number DEC-2012/05/05/N/NZ1/01922; the Marie Curie program "European Reintegration Grant" (PERG05-GA-2009-247789); the program "FSE SARDEGNA 2007-2013, Legge Regionale 7 agosto 2007, n. 7, Promozione della ricerca scientifica e dell'innovazione tecnologica in Sardegna".

SUPPLEMENTARY MATERIAL

The Supplementary Material for this article can be found online at: http://journal.frontiersin.org/article/10.3389/fpls.2015.01100

REFERENCES

Allen, J. (2002). Photosynthesis of ATP—electrons, proton pumps, rotors, and poise. *Cell* 110, 273–276.

Aro, E. M., Suorsa, M., Rokka, A., Allahverdiyeva, Y., Paakkarinen, V., Saleem, A., et al. (2005). Dynamics of photosystem II: a proteomic approach to thylakoid protein complexes. *J. Exp. Bot.* 56, 347–356. doi: 10.1093/jxb/eri041

Barera, S., Pagliano, C., Pape, T., Saracco, G., and Barber, J. (2012). Characterization of PSII-LHCII supercomplexes isolated from pea thylakoid membrane by one-step treatment with α- and β-dodecyl-D-maltoside. *Philos. Trans. R. Soc. Lond. B Biol. Sci.* 367, 3389–3399. doi: 10.1098/rstb.2012.0056

Barros, T., Royant, A., Standfuss, J., Dreuw, A., and Kühlbrandt, W. (2009). Crystal structure of plant light-harvesting complex shows the active, energy-transmitting state. *EMBO J.* 28, 298–306. doi: 10.1038/emboj.2008.276

Berthold, A. D., Babcock, G. T., and Yocum, C. (1981). A highly resolved, oxygen evolving photosystem II preparation from spinach thylakoid membranes. *FEBS Lett.* 134, 231–234. doi: 10.1016/0014-5793(81)80608-4

Boekema, E. J., Hankamer, B., Bald, D., Kruip, J., Nield, J., Boonstra, A. F., et al. (1995). Supramolecular structure of the photosystem II complex from green plants and cyanobacteria. *Proc. Natl. Acad. Sci. U.S.A.* 92, 175–179. doi: 10.1073/pnas.92.1.175

Boekema, E. J., Nield, J., Hankamer, B., and Barber, J. (1998). Localization of the 23-kDa subunit of the oxygen-evolving complex of photosystem II by electron microscopy. *Eur. J. Biochem.* 252, 268–276. doi: 10.1046/j.1432-1327.1998.2520268.x

Boekema, E. J., van Breemen, J. F. L., van Roon, H., and Dekker, J. P. (2000). Conformational changes in photosystem II supercomplexes upon removal of extrinsic subunits. *Biochemistry* 39, 12907–12915. doi: 10.1021/bi0009183

Boekema, E. J., Van Roon, H., Van Breemen, J. F., and Dekker, J. P. (1999). Supramolecular organization of photosystem II and its light-harvesting antenna in partially solubilized photosystem II membranes. *Eur. J. Biochem.* 266, 444–452. doi: 10.1046/j.1432-1327.1999.00876.x

Bricker, T. M., and Frankel, L. K. (2011). Auxiliary functions of the PsbO, PsbP and PsbQ proteins of higher plant Photosystem II: a critical analysis. *J. Photochem. Photobiol. B Biol.* 104, 165–178. doi: 10.1016/j.jphotobiol.2011.01.025

Caffarri, S., Croce, R., Cattivelli, L., and Bassi, R. (2004). A look within LHCII: differential analysis of the Lhcb1-3 complexes building the major trimeric antenna complex of higher-plant photosynthesis. *Biochemistry* 43, 9467–9476. doi: 10.1021/bi036265i

Caffarri, S., Kouril, R., Kereïche, S., Boekema, E. J., and Croce, R. (2009). Functional architecture of higher plant photosystem II supercomplexes. *EMBO J.* 28, 3052–3063. doi: 10.1038/emboj.2009.232

Cardona, T., Sedoud, A., Cox, N., and Rutherford, A. W. (2012). Charge separation in photosystem II: a comparative and evolutionary overview. *Biochim. Biophys. Acta* 1817, 26–43. doi: 10.1016/j.bbabio.2011.07.012

Che, Y., Fu, A., Hou, X., McDonald, K., Buchanan, B. B., Huang, W., et al. (2013). C-terminal processing of reaction center protein D1 is essential for the function and assembly of photosystem II in *Arabidopsis*. *Proc. Natl. Acad. Sci. U.S.A.* 110, 16247–16252. doi: 10.1073/pnas.1313894110

Danielsson, R., Suorsa, M., Paakkarinen, V., Albertsson, P., Styring, S., Aro, E. M., et al. (2006). Dimeric and monomeric organization of photosystem II. *J. Biol. Chem.* 281, 14241–14249. doi: 10.1074/jbc.M600634200

de Bianchi, S., Dall'Osto, L., Tognon, G., Morosinotto, T., and Bassi, R. (2008). Minor antenna proteins CP24 and CP26 affect the interactions between photosystem II subunits and the electron transport rate in grana membranes of *Arabidopsis*. *Plant Cell* 20, 1012–1028. doi: 10.1105/tpc.107.055749

Dekker, J. P., and Boekema, E. J. (2005). Supramolecular organization of thylakoid membrane proteins in green plants. *Biochim. Biophys. Acta* 1706, 12–39. doi: 10.1016/j.bbabio.2004.09.009

Edelman, M., and Mattoo, A. K. (2008). D1-protein dynamic in photosystem II: the lingering enigma. *Photosynth. Res.* 98, 609–620. doi: 10.1007/s11120-008-9342-x

Eshaghi, S., Andersson, B., and Barber, J. (1999). Isolation of a highly active PSII-LHCII supercomplex from thylakoid membranes by a direct method. *FEBS Lett.* 446, 23–26. doi: 10.1016/S0014-5793(99)00149-0

Farci, D., Bowler, M. W., Kirkpatrick, J., McSweeney, S., Tramontano, E., and Piano, D. (2014). New features of the cell wall of the radio-resistant bacterium *Deinococcus radiodurans*. *Biochim. Biophys. Acta* 1838, 1978–1984. doi: 10.1016/j.bbamem.2014.02.014

Ferreira, K. N., Inverson, T. M., Maghlaoui, K., Barber, J., and Iwata, S. (2004). Architecture of the photosynthetic oxygen-evolving center. *Science* 303, 1831–1838. doi: 10.1126/science.1093087

Fey, H., Piano, D., Horn, R., Fischer, D., Schröder, W. P., Bock, R., et al. (2008). Isolation of highly active photosystem II core complexes with a His-tagged Cyt b559 subunit from transplastomic tobacco plants. *Biochim. Biophys. Acta* 1777, 1501–1509. doi: 10.1016/j.bbabio.2008.09.012

Gerotto, C., Franchin, C., Arrigoni, G., and Morosinotto, T. (2015). In vivo identification of Photosystem II Light Harvesting Complexes interacting with Photosystem II Subunit S. *Plant Physiol.* 168, 1747–1761. doi: 10.1104/pp.15.00361

Ghanotakis, D. F., Demetriou, D. M., and Yocum, C. F. (1987). Isolation and characterization of an oxygen-evolving photosystem II reaction center core preparation and a 28 kDa Chl a binding protein. *Biochim. Biophys. Acta* 891, 15–21. doi: 10.1016/0005-2728(87)90078-8

Haniewicz, P., De Sanctis, D., Büchel, C., Schröder, W. P., Loi, M. C., Kieselbach, T., et al. (2013). Isolation of monomeric photosystem II that retains the subunit PsbS. *Photosynth. Res.* 118, 199–207. doi: 10.1007/s11120-013-9914-2

Kihara, S., Hartzler, D. A., and Savikhin, S. (2014). Oxygen concentration inside a functioning photosynthetic cell. *Biophys. J.* 106, 1882–1889. doi: 10.1016/j.bpj.2014.03.031

Liu, Z., Yan, H., Wang, K., Kuang, T., Zhang, J., Gui, L., et al. (2004). Crystal structure of spinach major light-harvesting complex at 2.*72* Å resolution. *Nature* 428, 287–292. doi: 10.1038/nature02373

Loll, B., Kern, J., Saenger, W., Zouni, A., and Biesiadka, J. (2005). Towards complete cofactor arrangement in the 3.0 Å resolution structure of photosystem II. *Nature* 438, 1040–1044. doi: 10.1038/nature04224

Mummadisetti, M. P., Frankela, L. K., Bellamyb, H. D., Sallansc, L., Goettertb, J. S., Brylinskia, M., et al. (2014). Use of protein cross-linking and radiolytic footprinting to elucidate PsbP and PsbQ interactions within higher plant Photosystem II. *Proc. Natl. Acad. Sci. U.S.A.* 111, 16178–16183. doi: 10.1073/pnas.1415165111

Munekage, Y., Hojo, M., Meurer, J., Endo, T., Tasaka, M., and Shikanai, T. (2002). PGR5 is involved in cyclic electron flow around photosystem I and II essential for photoprotection in *Arabidopsis*. *Cell* 110, 361–371. doi: 10.1016/S0092-8674(02)00867-X

Nield, J., and Barber, J. (2006). Refinement of the structural model for the Photosystem II supercomplex of higher plants. *Biochim. Biophys. Acta* 1757, 353–361. doi: 10.1016/j.bbabio.2006.03.019

Nield, J., Orlova, E. V., Morris, E. P., Gowen, B., van Heel, M., and Barber, J. (2000). 3D map of the plant photosystem II supercomplex obtained by cryoelectron microscopy and single particle analysis. *Nat. Struct. Biol.* 7, 44–47. doi: 10.1038/71242

Nixon, P. J., Michoux, F., Yu, J., Boehm, M., and Komenda, J. (2010). Recent advances in understanding the assembly and repair of photosystem II. *Ann. Bot.* 106, 1–16. doi: 10.1093/aob/mcq059

Pagliano, C., Chimirri, F., Saracco, G., Marsano, F., and Barber, J. (2011). Onestep isolation and biochemical characterization of highly active plant PSII monomeric core. *Photosynth. Res.* 108, 33–46. doi: 10.1007/s11120-011-9650-4

Piano, D., El Alaoui, S., Korza, H. J., Filipek, R., Sabala, I., Haniewicz, P., et al. (2010). Crystallization of the photosystem II core complex and its chlorophyll binding subunit CP43 from transplastomic plants of *Nicotiana tabacum*. *Photosynth. Res.* 106, 221–226. doi: 10.1007/s11120-010-9597-x

Pietrzykowska, M., Suorsa, M., Semchonok, D. A., Tikkanen, M., Boekema, E. J., Aro, E. M., et al. (2014). The light-harvesting chlorophyll a/b binding proteins Lhcb1 and Lhcb2 play complementary roles during state transitions in *Arabidopsis*. *Plant Cell* 26, 3646–3660. doi: 10.1105/tpc.114.127373

Pokorska, B., Zienkiewicz, M., Powikrowska, M., Drozak, A., and Romanowska, E. (2009). Differential turnover of the photosystem II reaction centre D1 protein in mesophyll and bundle sheath chloroplast of maize. *Biochim. Biophys. Acta* 1787, 1161–1169. doi: 10.1016/j.bbabio.2009.05.002

Porra, R. J., Thompson, W. A., and Kriedmann, P. E. (1989). Determination of accurate extinction coefficients and simultaneous equations for assaying chlorophylls a and b with four different solvents: verifications of the concentration of chlorophyll standards by atomic absorption spectroscopy. *Biochim. Biophys. Acta* 975, 384–394. doi: 10.1016/S0005-2728(89)80347-0

Puthiyaveetil, S., Tsabari, O., Lowry, T., Lenhert, S., Lewis, R. R., Reich, Z., et al. (2014). Compartmentalization of the protein repair machinery in photosynthetic membranes. *Proc. Natl. Acad. Sci. U.S.A.* 111, 15839–15844. doi: 10.1073/pnas.1413739111

Schägger, H., and von Jagow, G. (1991). Blue native electrophoresis for isolation of membrane protein complexes in enzymatically active form. *Anal. Biochem.* 199, 223–231. doi: 10.1016/0003-2697(91)90094-A

Shi, L. X., Hall, M., Funk, C., and Schröder, W. P. (2012). Photosystem II, a growing complex: updates on newly discovered components and low molecular mass proteins. *Biochim. Biophys. Acta* 1817, 13–25. doi: 10.1016/j.bbabio.2011.08.008

Suorsa, M., Regel, R. E., Paakkarinen, V., Battchikova, N., Herrmann, R. G., and Aro, E. M. (2004). Protein assembly of photosystem II and accumulation of subcomplexes in the absence of low molecular mass subunits PsbL and PsbJ. *Eur. J. Biochem.* 271, 96–107. doi: 10.1046/j.1432-1033.2003.03906.x

Takahashi, T., Inoue-Kashino, N., Ozawa, S., Takahashi, Y., Kashino, Y., and Satoh, K. (2009). Photosystem II complex in vivo is a monomer. *J. Biol. Chem.* 284, 15598–15606. doi: 10.1074/jbc.M109.000372

Tomizioli, M., Lazar, C., Brugière, S., Burger, T., Salvi, D., Gatto, L., et al. (2014). Deciphering thylakoid sub-compartments using a mass spectrometry-based approach. *Mol. Cell. Proteomics* 13, 2147–2167. doi: 10.1074/mcp.M114.040923

Watanabe, M., Iwai, M., Narikawa, R., and Ikeuchi, M. (2009). Is the photosystem II complex a monomer or a dimer? *Plant Cell Physiol.* 50, 1674–1680. doi: 10.1093/pcp/pcp112

Conflict of Interest Statement: The authors declare that the research was conducted in the absence of any commercial or financial relationships that could be construed as a potential conflict of interest.

Advantages of publishing in Frontiers

OPEN ACCESS
Articles are free to read, for greatest visibility

COLLABORATIVE PEER-REVIEW
Designed to be rigorous – yet also collaborative, fair and constructive

FAST PUBLICATION
Average 85 days from submission to publication (across all journals)

COPYRIGHT TO AUTHORS
No limit to article distribution and re-use

TRANSPARENT
Editors and reviewers acknowledged by name on published articles

SUPPORT
By our Swiss-based editorial team

IMPACT METRICS
Advanced metrics track your article's impact

GLOBAL SPREAD
5'100'000+ monthly article views and downloads

LOOP RESEARCH NETWORK
Our network increases readership for your article

Frontiers
EPFL Innovation Park, Building I • 1015 Lausanne • Switzerland
Tel +41 21 510 17 00 • Fax +41 21 510 17 01 • info@frontiersin.org
www.frontiersin.org

Find us on